PHOTOGRAPH THIS SHEET

AD A083439

DTIC ACCESSION NUMBER

III

LEVEL

I

INVENTORY

Maurice Ewing Series 3
Deep Drilling Results in the Atlantic Ocean: Continental Margins and Paleoenvironment

DOCUMENT IDENTIFICATION

19-25 March 1978

DISTRIBUTION STATEMENT A
Approved for public release;
Distribution Unlimited

DISTRIBUTION STATEMENT

| ACCESSION FOR | |
|---|---|
| NTIS | GRA&I |
| DTIC | TAB |
| UNANNOUNCED | |
| JUSTIFICATION | |
| | |
| | |
| | |
| BY | |
| DISTRIBUTION / | |
| AVAILABILITY CODES | |
| DIST | AVAIL AND/OR SPECIAL |
| A | 21 |

DISTRIBUTION STAMP

DTIC
ELECTE
S APR 25 1980 D
D

DATE ACCESSIONED

Price: $18.00 per Volume
Sold by: American Geophysical Union
2000 Florida Ave.,
N.W., Wash., DC 20009

DATE RECEIVED IN DTIC

PHOTOGRAPH THIS SHEET AND RETURN TO DTIC-DDA-2

DOCUMENT PROCESSING SHEET

DTIC FORM OCT 79 70A

Maurice Ewing Series 3

# Deep Drilling Results in the Atlantic Ocean: Continental Margins and Paleoenvironment

Manik Talwani
William Hay
William B. F. Ryan

AMERICAN GEOPHYSICAL UNION

# Deep Drilling Results in the Atlantic Ocean: Continental Margins and Paleoenvironment

*Maurice Ewing Series*

**1 Island Arcs Deep Sea Trenches and Back-Arc Basins,** Manik Talwani and Walter C. Pitman III (editors)

**2 Deep Drilling Results in the Atlantic Ocean: Ocean Crust,** Manik Talwani, Christopher G. Harrison, and Dennis E. Hayes (editors)

**3 Deep Drilling Results in the Atlantic Ocean: Continental Margins and Paleoenvironment,** Manik Talwani, William Hay, and William B. F. Ryan (editors)

Maurice Ewing Series 3

# Deep Drilling Results in the Atlantic Ocean: Continental Margins and Paleoenvironment

**Edited by**
**Manik Talwani**
**William Hay**
**William B. F. Ryan**

American Geophysical Union
Washington, D. C.

# Deep Drilling Results in the Atlantic Ocean: Continental Margins and Paleoenvironment

Published under the aegis of the AGU Geophysical Monograph Board; Bruce Bolt, Chairman; Thomas E Graedel, Rolland L. Hardy, Pearn P. Niiler, Barry E. Parsons, George R Tilton, and William R. Winkler, members.

ISBN: 0-87590-402-5
Library of Congress Catalog Card Number: 79-88753



Printed in the United States of America by
LithoCrafters, Inc.
Chelsea, Michigan

# PREFACE

The second Maurice Ewing Symposium was devoted to the implications of deep drilling results in the Atlantic Ocean. This subject was chosen for two reasons. First, Maurice Ewing was one of the leaders of JOIDES (Joint Oceanographic Institutions For Deep Earth Sampling), the association of oceanographic institutions that was formed to organize and sponsor drilling in the deep ocean, and which has continued to provide scientific advice to the Deep Sea Drilling Project. Second, the first phase of International Program of Ocean Drilling in the Atlantic was finished and it seemed a good time to assess the implications of drilling results in the Atlantic that had been obtained over almost a decade.

During the time this volume was being prepared, discussions were taking place about a new initiative in oceanic drilling, in which a drilling vessel with much enhanced capability might be used. The results presented in this volume thus represent the base on which new drilling plans can be built.

The Maurice Ewing series is based on papers presented at the Maurice Ewing symposia. Two volumes resulted from the second symposium, which was held at Arden House, Harriman, New York on March 19-25, 1978. The symposium was co-sponsored by the Lamont-Doherty Geological Observatory, by JOIDES, and by the Inter-Union Commission in Geodynamics. Financial support for the symposium was provided by the G. Unger Vetlesen Foundation, the U. S. Office of Naval Research, and the U. S. National Science Foundation.

Manik Talwani
William Hay
William B. F. Ryan

# CONTENTS

# MESOZOIC-CENOZOIC SEDIMENTARY FORMATIONS OF THE NORTH AMERICAN BASIN; WESTERN NORTH ATLANTIC

Lubomir F. Jansa

Atlantic Geoscience Centre, Geological Survey of Canada
Bedford Institute of Oceanography, Dartmouth, N. S., Canada

Paul Enos

State University of New York, Binghamton, New York

Brian E. Tucholke

Lamont-Doherty Geological Observatory of Columbia University
Palisades, New York

Felix M. Gradstein

Atlantic Geoscience Centre, Geological Survey of Canada
Bedford Institute of Oceanography, Dartmouth, N. S., Canada

Robert E. Sheridan

Department of Geology, University of Delaware, Newark, Delaware

Abstract. Deep Sea Drilling Project sites in the North American Basin penetrated Mesozoic and Cenozoic sedimentary sequences of similar lithology, age, faunal assemblages and petrographic composition, permitting the definition of six formations. These are in ascending order: the Cat Gap Formation (Oxfordian-Tithonian grey-green limestone, reddish-brown argillaceous limestone, and calcareous claystone); the Blake-Bahama Formation (Tithonian-Barremian light grey limestone and chalk); the Hatteras Formation (Barremian-Cenomanian black and green-grey shale and claystone); the Plantagenet Formation (Late Cenomanian to ?Early Eocene varicolored zeolitic clay); the Bermuda Rise Formation (Paleocene to Middle Eocene chert and siliceous ooze); and the Blake Ridge Formation (Eocene to Holocene hemipelagic grey-green mud with local mass-flow deposits). In addition, the Crescent Peaks Member (Maastrichtian nannofossil marl) of the Plantagenet Formation and the Great Abaco Member (Miocene mass-flow deposits) of the Blake Ridge Formation are defined. The Cat Gap, Blake-Bahama, and Bermuda Rise Formations and the Crescent Peaks and Great Abaco Members are seismically mappable, with the formation boundaries approximately corresponding to major seismic reflectors ($C_o$, B, $A^C$, A*, M, respectively) in the western North Atlantic.

The oldest sedimentary rocks recovered by DSDP in the North American Basin are red or grey-green argillaceous limestones at Sites 99, 100 and 105, which are not older than Oxfordian. These sediments were deposited in a deep bathyal environment, near but above the calcite compensation depth (CCD). Pelagic carbonate deposition above the CCD continued into the Barremian, producing light-grey limestones. The CCD shallowed abruptly in the Barremian, and this was accompanied by stagnation of bottom and intermediate water that developed euxinic conditions which extended through the Cenomanian. Bottom circulation was re-established in the Late Cretaceous, but shallow CCD and lack of terrigenous input to the deep basin resulted in deposition of pelagic multicolored clays. Maastrichtian limestone beds within otherwise carbonate-poor variegated clays indicate temporary deepening of the CCD in the North American Basin in the Late Cretaceous.

Pelagic and hemipelagic clays were deposited in much of the deep basin during the Paleocene, followed by accumulation of dominantly biogenic siliceous deposits in the deep basin in latest Paleocene through Middle Eocene time. Mixed siliceous and calcareous sediments accumulated on the shallower mid-oceanic ridge. Silica diagenesis formed porcelanitic cherts in the upper Lower to lower Middle Eocene sediments, and these correlate with the widespread seismic reflector

Horizon $A^C$. The Upper Eocene and Oligocene are represented by clays with varying amounts of biogenic silica and carbonate, together with locally important mass-flow deposits. Towards the continental margin, sediments of this age are missing because a major pre-Miocene unconformity overlies Lower Cretaceous to Eocene sediments beneath the continental rise. Except for calcareous ridge-flank sediments, deposition of hemipelagic grey-green mud was predominant in the North American Basin throughout the Neogene and continues to the present. The thickest deposits are Miocene and form the continental rise. Mass-flows from the continental shelf and slope deposited a massive blanket of Miocene carbonate breccia (the Great Abaco Member) in the Blake-Bahama Basin, and form flat-lying wedges of dominantly Pleistocene terrigeneous sand, silt, and clay in the present abyssal plains.

## Introduction

The first step toward a lithologic synthesis of the western North Atlantic Basin was undertaken by Lancelot *et al.* (1972) based primarily on Leg 11 sites. More rigorous application of the principles of continental rock stratigraphy to oceanic sediments was demonstrated by Cook (1975) in a study of the stratigraphy of the eastern Equatorial Pacific.

In the present paper, widespread Mesozoic and Cenozoic lithostratigraphic units identified in the North American Basin during Deep Sea Drilling Project (DSDP) Legs 1, 2, 4, 11, 43, 44 are correlated on the basis of sediment characteristics, contacts, regional aspects, physical properties, faunal content, and acoustic characters. The data synthesized here (shipboard descriptions of cores, smear slides, and thin sections; grain size; carbon-carbonate analyses; and X-ray mineralogy) are from site reports and appropriate chapters of the Initial Reports of the Deep Sea Drilling Project (Ewing, Worzel *et al.*, 1969; Peterson, Edgar *et al.*, 1970; Bader, Gerard *et al.*, 1970; Hollister, Ewing *et al.*, 1972; Tucholke, Vogt *et al.*, 1979; and Benson, Sheridan *et al.*, 1978). Data from other, specialized studies are cited in the text. Critical intervals of cores were re-examined at the East Coast Core Repository and studied in thin sections and smear slides. Scanning electron microscopy was used to study composition, diagenetic alteration, and porosity. Comparisons with marginal basins are based on a study of the subsurface Mesozoic of the Scotian Shelf and Grand Banks by Jansa and Wade (1975a,b), on studies of the U.S. Atlantic coastal plain and of the COST B-2 well located off the New Jersey coast (Schlee *et al.*, 1976; Smith *et al.*, 1976), and on brief reconnaissance studies of exposed Mesozoic sections in Morocco, southern Spain, southern France, and northern Italy by Jansa. A complementary study synthesizes lithofacies recovered on DSDP Leg 41 in the eastern North Atlantic (Jansa *et al.*, 1978). The reader also is referred to a complementary study by Tucholke and Mountain (this volume) that synthesizes the depositional history of the North American Basin based on seismic stratigraphy and its correlation with DSDP borehole results.

In studying the western Atlantic lithofacies it is evident that some biostratigraphic data presented in the Initial Reports are not precise, as indicated by differing results of various micropaleontological disciplines. There is a clear need for detailed compilation of the Mesozoic-Cenozoic biostratigraphy of the North Atlantic, but in this report we have limited ourselves to minor revision of the existing biostratigraphic data.

A subcommittee of the American Commission on Stratigraphic Nomenclature (Wilson, 1971) recommended that formal submarine rock-stratigraphic units be named for oceanic topographic features which appear on published charts. They also proposed that the term 'Oceanic' be used in the formal names of submarine formations. Although the latter procedure was followed by Cook (1975) in his pioneering definition of Pacific Basin formations, we omit the term 'Oceanic' for the following reasons. Some deep-sea lithic units extend from the ocean basin onto the continental margin and outcrop on land. Many formations outcropping on land, although not contiguous with deep basin lithofacies, obviously were deposited in an oceanic environment and have strong similarities to known deep-basin lithofacies (Bernoulli, 1972; Jansa *et al.*, 1978). Another possible source of confusion is the prior use of 'Oceanic Formation' for outcropping Tertiary rocks on Barbados (Jukas-Brown and Harrison, 1891). Comparable rocks have been penetrated during drilling in the western central Atlantic (Bader, Gerard *et al.*, 1970). We therefore consider use of a double terminology (land-based and ocean-based) confusing and inappropriate.

## Structural Setting

The North American Basin (Fig. 1) is a large bathymetric depression centered on the Bermuda Rise. The Sohm Abyssal Plain and the Hatteras Abyssal Plain lie north and west of the Bermuda Rise respectively and the Nares Abyssal Plain to the south, with the Blake-Bahama Abyssal Plain adjacent to the basin margin on the southwest. The axis of maximum depth runs northeastward about halfway between Bermuda and the Mid-Atlantic Ridge. The North American Basin is confined on the north by the Newfoundland Ridge and continental margin, on the south by the Antilles and Barracuda Fracture Zone, on the east by the Mid-Atlantic Ridge, and on the west by the North American continental margin. Water depths in the central basin, with the exception of the Bermuda Rise region, generally exceed 5000 m.

The North American Basin, excluding the Mid-Atlantic Ridge and Puerto Rico Trench, is a

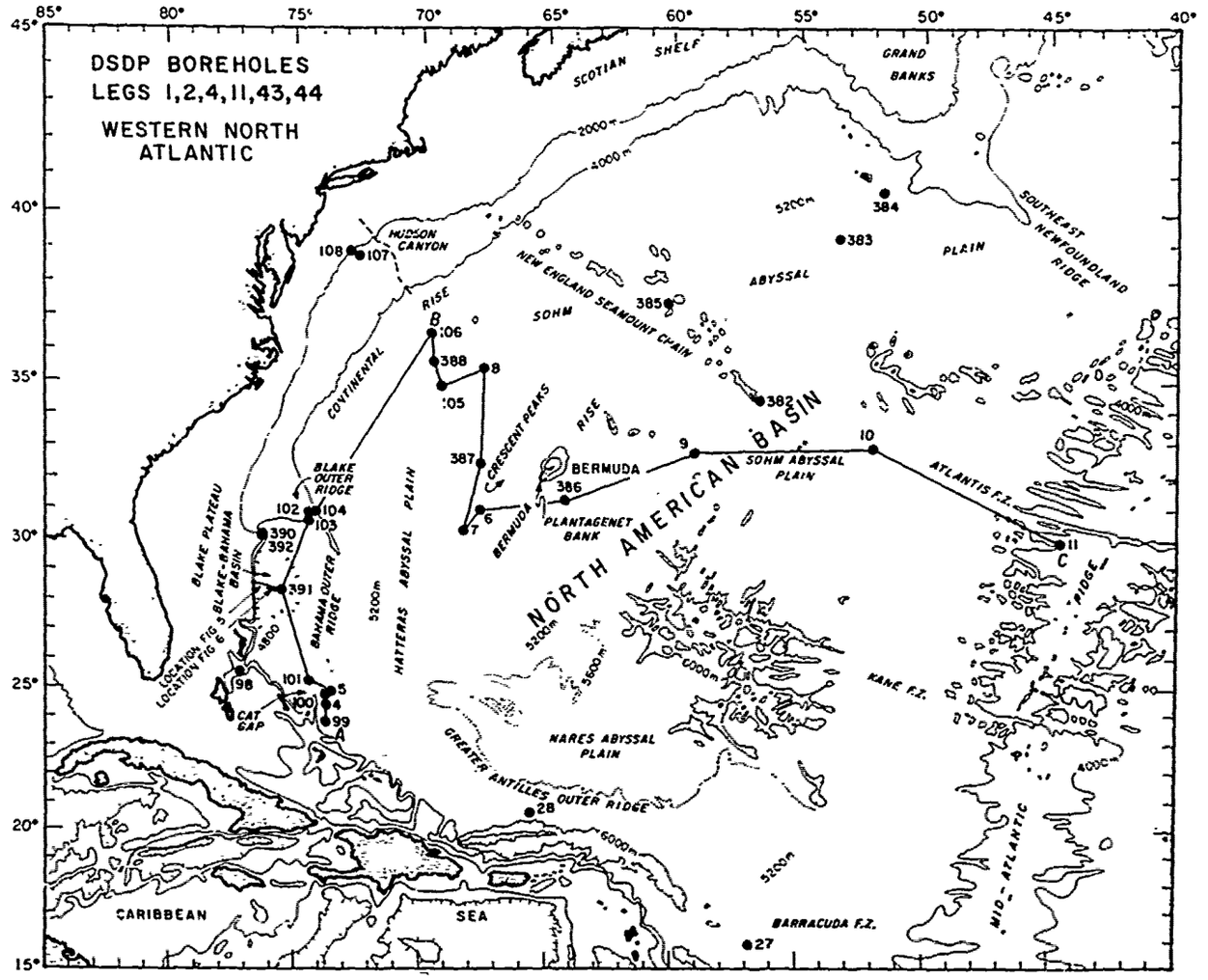


Figure 1. Location map with physiographic features of the North American Basin and location of Deep Sea Drilling Project drill sites (Legs 1, 2, 4, 11, 43, and 44). Bathymetry after Uchupi (1971).

tectonically stable region dominated by subsidence of oceanic basement. Local formation of volcanic peaks such as Bermuda and the New England Seamounts, and regional uplift of the Bermuda Rise occurred during or prior to the Early Cenozoic. Oceanic crust flooring the basin has formed since the initial rifting of North America from Africa about 180 m.y. B.P. (Pitman *et al.*, 1971; Vogt and Einwich, 1978). Magnetic polarity sequences recorded in the crust include the Jurassic quiet zone and Blake Spur Anomaly, the Keathley Sequence (M-series), the Cretaceous quiet zone (Mercanton interval), and anomalies 1 to 34 along the Mid-Atlantic Ridge (Pitman and Talwani, 1972; Schouten and Klitgord, 1977).

The oldest sediments recovered by deep-sea drilling are Oxfordian at Sites 99, 100, and 105 (Hollister, Ewing *et al.*, 1972). Site 100 near Cat Gap was drilled about 25 km west of anomaly M-25, which is the oldest anomaly in the Keathley sequence, and Site 105 was drilled just east of M-25 (Larson and Hilde, 1975). Sedimentary sequences of these two sites are underlain by basalts. Seismic reflection profiles show that the basalts correspond to the top of Layer 2, which can be traced to other DSDP sites throughout the basin. Basal sediments at some drill sites exhibit contact metamorphism, and petrographic evidence indicates that some Layer 2 basalts are sills, but it appears that structural basement in this basin is dominantly basalt with only minor quantities of interlayered sediment (Aumento, Melson, *et al.*, 1974; Bryan, Robinson *et al.*, 1977).

## Methods

The parameters most useful for recognizing and correlating the lithologic sequences are color, inorganic and organic constituents (especially calcium carbonate, silica, and clay mineral content), bedding, sedimentary structures, and bioturbation. The upper and lower contacts of defined lithologic units have been identified in all studied sites. If formation contacts were not cored at the proposed type section, other sites of the same unit are used to define the contact (boundary stratotype). After lithologic units are defined at individual sites, correlation and mapping of units is attempted between sites. This requires enough borehole control and seismic reflection data to establish the continuity of units. Since drill sites are widely separated, the seismic reflection information is especially important in mapping the extent of reflecting horizons. Although seismic sequences do not always correspond to lithostratigraphic units throughout the basin, certain consistent correlations between lithologic changes and major reflectors justify use of seismic data as a mapping tool.

The bulk of the Mesozoic and Cenozoic sediments cored in the North American Basin are subdivided into six formations for which formal stratigraphic names are herein proposed. Data concerning location, thickness, depth of boundaries and core recovery of the stratotypes are summarized in Tables 1 and 2. Some of these units have been recognized by Lancelot *et al.* (1972) as distinct lithofacies. The lithology, age and depositional environments of the formations are summarized in Figure 2. Detailed data concerning lithology of individual cores, age, formation boundaries, correlation of the lithologic units between sites and position of seismic horizons are summarized in Figure 24. The regional distribution of the formations is shown on maps (Figures 3, 8, 10, 12, 15, 18 and 20) and in a schematic cross-section (Figure 22). Sedimentologic parameters for each formation are presented in Tables 4, 6, 8, 10, 12, 14, 17, and 19.

The biostratigraphic framework resulting from detailed analysis of several microfossil groups provides valuable auxilliary information in lithostratigraphic studies of deep sea sediments. In the North American Basin, nannofossils and foraminifers contribute to age determinations for much of the Jurassic through Quaternary; radiolarians are especially helpful in the Tertiary, dinoflagellates are important in the mid-Cretaceous, and crinoids, calpionellids and ammonites are useful for the Upper Jurassic.

A compilation of multiple biostratigraphy based on published literature was made in the North American Basin where lithostratigraphic type sections are defined (Figures 7, 9, 13, 14, 19, and 21). The consensus of ages is broad compared to detailed bio- and chronostratigraphy in some Cretaceous and Cenozoic land sections. A major limitation in oceanic sediments is the relative paucity of the calcareous fossils that result from dissolution of calcareous tests with increasing water depth.

Detailed age interpretation for Jurassic and Lower Cretaceous sediments is hampered by lack of agreement between individual interpretations and this is the main reason that resolution is not to the stage level.

Two factors cause some confusion. These are the equation of Lower Tithonian and Upper Kimmeridgian which results from improved correlation of Boreal and Tethyan ammonite assemblages (e.g. van Hinte, 1976). This necessitates revision of previous Kimmeridgian/Tithonian boundary interpretations, such as those in DSDP Leg 11 sites, but the new

TABLE 1. TYPE LOCALITIES (STRATOTYPES) OF MESOZOIC-CENOZOIC FORMATIONS AND MEMBERS OF THE NORTH AMERICAN BASIN, WESTERN NORTH ATLANTIC

| Unit Name | Dominant Lithology | Type Locality (Stratotype) | | | | Date Drilled | Water Depth (m) | Bottom Hole Depth (m) | Thickness (m) | Core (m) | Core Recovery | |
|---|---|---|---|---|---|---|---|---|---|---|---|---|
| | | Leg | Site | Position Latitude | Position Longitude | | | | | | %Cored | %Recovered |
| Blake Ridge Formation | Hemipelagic Grey-green Mud | 11 | 106 & 106B | 36°26.0'N | 69°27.7'W | 20-26 May 1970 | 4500 | 1012 | 961-1012 | 63.1 | 63.1 | 6.2-6.6 |
| Great Abaco Member | Intraclastic Chalk | 44 | 391A & C | 28°13.7'N | 75°36.9'W | 2-22 Sept 1975 | 4963 | 1412 | 502 | 107.0 | 62.6 | 21.3 |
| Bermuda Rise Formation | Chert and Siliceous Ooze | 43 | 387 | 32°19.2'N | 67°40.0'W | 1-7 Aug 1975 | 5117 | 794.5 | 152.8-220.4 | 29.1-47.7 | 27.9-33.1 | 19.0-21.6 |
| Plantagenet Formation | Variegated Clay | 43 | 386 | 31°11.2'N | 64°14.9'W | 24-31 July 1975 | 4782 | 973.8 | 92.3-311.4 | 46.0 | 72.2 | 41.3-49.8 |
| Crescent Peaks Member | Chalk | 43 | 387 | 32°19.2'N | 67°40.0'W | 1-7 Aug 1975 | 5117 | 794.5 | 25.2 | 6.8 | 43.3 | 27.0 |
| Hatteras Formation | Black Carbonaceous Clay and Shale | 11 | 105 | 34°53.7'N | 69°10.4'W | 13-19 May 1970 | 5251 | 633 | 113.2 | 44.0 | 66.5 | 39.9 |
| Blake-Bahama Formation | Grey and White Limestone | 44 | 391C | 28°13.7'N | 75°36.9'W | 2-22 Sept 1975 | 4963 | 1412 | 325.2-334.7 | 150.4 | 50.9 | 44.9-46.3 |
| Cat Gap Formation | Red Clayey Limestone | 11 | 105 | 34°53.7'N | 69°10.4'W | 13-19 May 1970 | 5251 | 633 | 62.4 | 42.1 | 67.5 | 67.5 |

* Transitional lower boundary

TABLE 2. STRATOTYPE INTERVALS OF TYPE SECTIONS IN THE NORTH AMERICAN BASIN

| Unit Name | Lithology | Stratotype Interval | | | | | | | | | Boundary Stratotype | | | | | | | | | |
|---|---|---|---|---|---|---|---|---|---|---|---|---|---|---|---|---|---|---|---|---|
| | | Top | | | | | | Base | | | Top | | | | | | Base | | | |
| | | Leg | Site | Core | Sec. | cm | Depth (m) | Core | Sec. | cm | Depth* (m) | Leg | Site | Core | Sec. | cm | Depth* (m) | Leg | Site | Core | Sec. | cm | Depth* (m) |
| Blake Ridge Formation | Hemipelagic Grey-green Mud | 11 | 106 | 1 (extends to sea floor) | | | 0 [-4500] | Between 6B and 7B | | | 961-1012 | 11 | 106 | 1 | | | sea floor | 43 | 387 | 12 | 1 | 145 | 223.8 |
| Great Abaco Member | Intraclastic Chalk | 44 | 391 | 3A | 1 | 150 | 147 [-5111] | 20A | | | 649 | 44 | 391 | 3A | 1 | 150 | 147.0 | 44 | 391 | 20A | | | 649 |
| Bermuda Rise | Chert and Siliceous Ooze | 43 | 387 | 12 | 1 | 145 | 223.8 [-5341.8] | 23:2,82● through 27:2,148 | | | 376.6 through 444.2 | 43 | 387 | 12 | 1 | 145 | 223.8 | undefined | | | | | |
| Plantagenet Formation | Variegated Clay | 43 | 386 | between 34 & 35 | | | 612.9-632.0 [-4824] | 41 | 5 | 80 | 724.3 | undefined | | | | | | 43 | 386 | 41 | 5 | 80 | 724.3 |
| Cresecent Peaks Member | Chalk | 43 | 387 | 27 | 2 | 148 | 447 [-556.] | 28 | 1 | 150 | 469.4 | 43 | 387 | 27 | 2 | 148 | 444.2 | 43 | 387 | 28 | 1 | 150 | 469.4 |
| Hatteras Formation | Black Carbonaceous Clay and Shale | 11 | 105 | 9 | 3 | 110 | 290.1 [-5541.1] | 17 | 1 | 30 | 403.3 | 11 | 105 | 9 | 3 | 110 | 290.1 | 11 | 105 | 17 | 1 | 30 | 403.3 |
| Blake-Bahama Formation | Grey and White Limestone | 44 | 391 | between 13C & 14C | | | 991.0-1000.5 [-5955-] [-5964.5] | 45C | ? | 70 | 1325.7 | 11 | 105 | 17 | 1 | 30 | 403.3 | 44<br>11 | 391<br>105 | 45C<br>33 | 2<br>2 | 70<br>27 | 1325.1<br>559 |
| Cat Gap Formation | Red Clayey Limestone | 11 | 105 | 33 | 2 | 27 | 559.8 [-5810.8] | 40 | 1 | 120 | 622.2 (on basalt) | 11 | 105 | 33 | 2 | 27 | 559.8 | undefined | | | | | |

* Meters below sea floor. Range in values denotes interval without coring or recovery.
[ ] Depth below sea level in square brackets.
● Core locations given by: core number:section,depth in centimetres.
' Parastratotype.

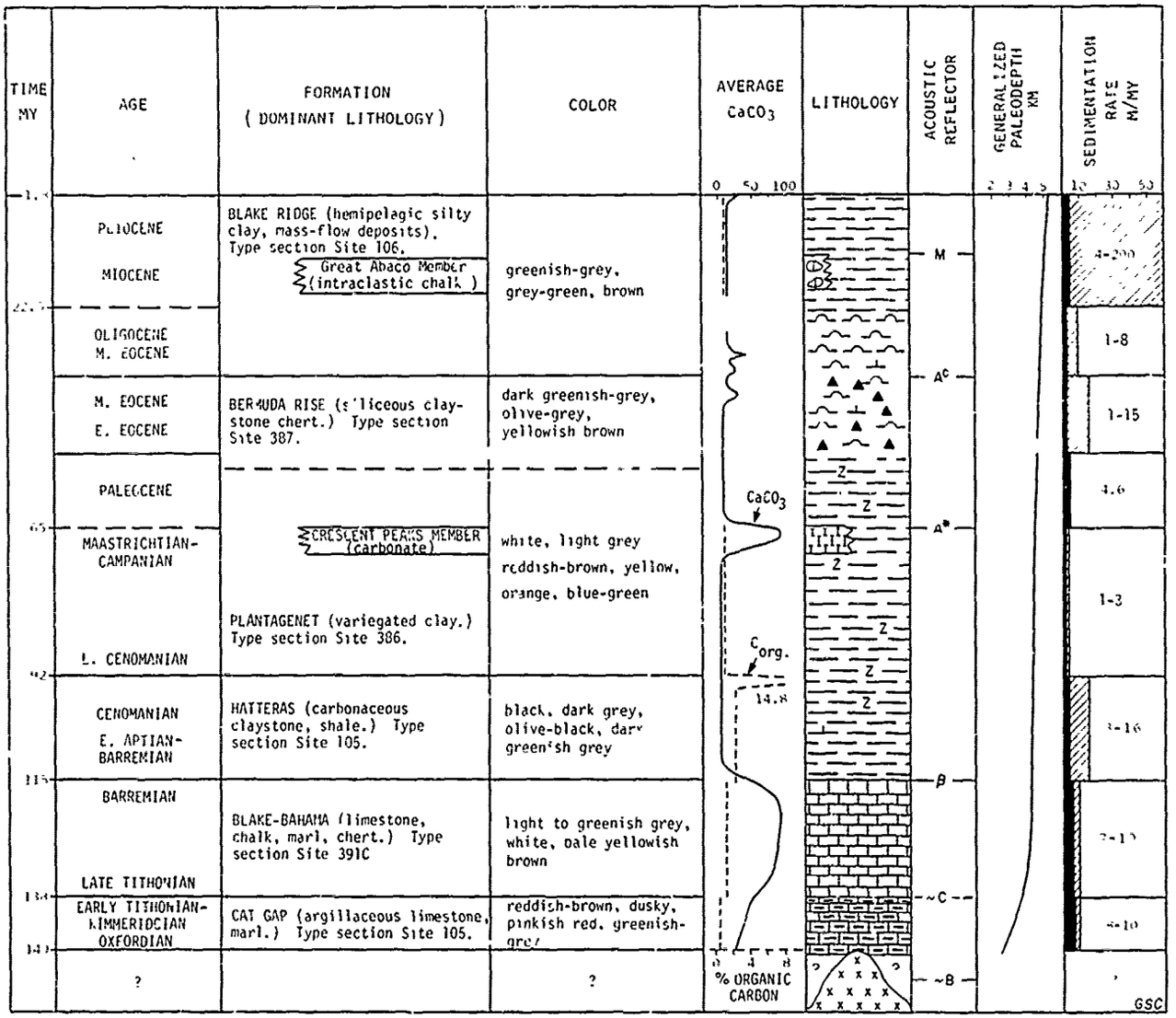


Figure 2. Schematic characteristics of sedimentary formations in the North American Basin, defined in the present paper. For lithologic symbols explanation see Figure 24.

information should be evaluated in the contex of work based on other fossil groups. Second, discrepancies occur between the age interpretations given in the DSDP site reports (basically the result of shipboard studies) and the later biostratigraphic studies of the Initial Reports or other publications. Where discrepancies occur we have favored interpretations in the special paleontologic studies.

Cores from all drill sites in the North American Basin, including type sections, are stored at the DSDP East Coast Core Repository, Lamont-Doherty Geological Observatory, Palisades, New York. The convention used here in discussing DSDP cores is to list core:section, depth within the core (e.g. core 40:1, 120 cm). Sub-seafloor depths are in metres. Occasional discrepancies may occur between our report of core numbers and depths and those listed in the Initial Reports. This results from errors in the Initial Reports, and shifting of cores in liners after shipboard visual descriptions and prior to or after core photography. In each case, we have consulted original data provided by the Deep Sea Drilling Project to obtain accurate information.

## Definition of Formations

Mesozoic-Cenozoic formations of the North American Basin are described below in ascending stratigraphic order.

## Cat Gap Formation

Reddish-brown, brick red, light green, and greenish-grey clayey limestones interbedded with reddish calcareous claystone characterize the Cat Gap Formation. The type section is Site 105 on the lower continental rise southeast of New York (Figures 1 and 3, Tables 1 to 3). The formation also has been sampled at Sites 99A, 100, and 391C. The name is derived from the Cat Gap Channel near Sites 99A and 100, where the formation was first penetrated.

Type Locality. The type section, Site 105, is 62.4 m of clayey limestone and calcareous silty claystone in which the carbonate content decreases downward from 54% (559.8-570 m sub-bottom) through 29% (570-600 m) to 20% or less (600-622.2 m). The clayey limestone is a mixture of neomorphic micrite and clay minerals (mica, montmorillonite, and kaolinite or chlorite traces). Quartz, zeolites, pyrite, and heavy minerals occur in trace quantities in the limestones and as minor components in some of the more clayey beds (Table 4). The organic carbon content averages only 0.11%. Average porosity of sediments is 38%. Colors include dark reddish-brown (10R4/4), pale red (10R6/2), light green, and various shades of grey (5G6/2,N7,N4). The red color characterizes the more clayey beds, grey and greenish the more carbonate-rich beds. Hematite is the main source of red pigmentation (Lancelot *et al.*, 1972). The commonly patchy occurrence of grey-green colors is associated with burrows and bedding planes (Figure 4A) in which the iron is reduced. Much of the claystone and some of the limestone is faintly laminated to fissile. Sometimes the beds are slightly undulatory with development of incipient nodular texture. The current bedding is rare. Elsewhere, burrow mottling is pervasive. Cyclic units containing intraclasts (pebbles) of pelagic red clay or white limestone, overlain by graded sand and silt and burrowed red clay in an upward-fining sequence (Figure 4A) were interpreted as pelagic turbidites by Bernoulli (1972). Deformation ranges from small scale folding and faulting to major disturbances interpreted as slump structures. Beds are typically almost horizontal, and there is no indication of unconformities.

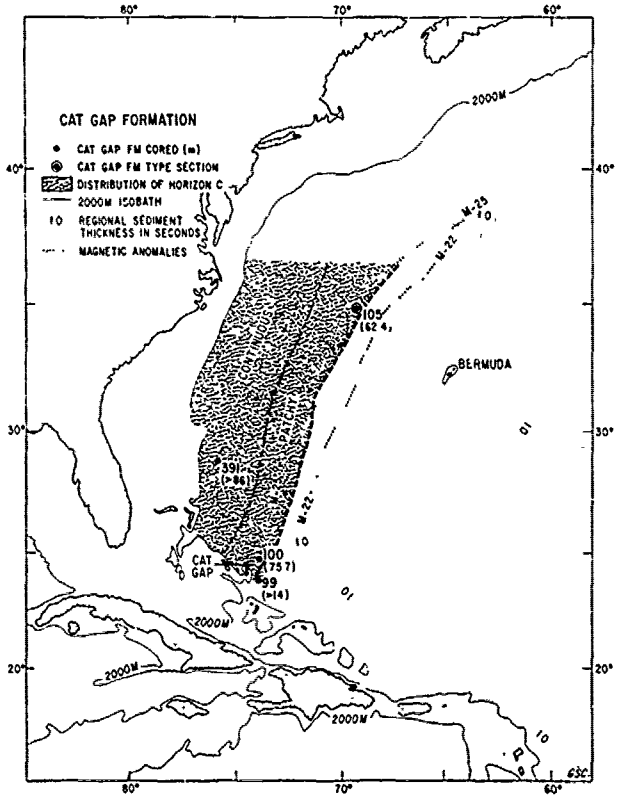


Figure 3. Boreholes that have cored sediments of the Cat Gap Formation. Formation thickness (metres) in parentheses. Seismic Horizon C correlates approximately with the top of the Cat Gap Formation; boundaries indicate mapped pinch-out on basement and easternmost occurrence of Horizon C in basement pockets. The eastern formation boundary lies between magnetic anomalies M-25 and M-22.

Microfossils of the Cat Gap Formation include well preserved nannoplankton, a sparse to rich foraminiferal fauna (simple arenaceous foraminifera, lagenids, epistominids, and primitive miliolids), poorly preserved radiolaria, calcisphaerulids (*Cadosina*), ostracods, and dinoflagellates. Macrofossils include debris of the pelagic crinoid *Saccocoma*, echinoderm fragments, pelagic bivalves (filaments), aptychi, rhyncholites (ammonite beaks), barnacle parts and fish debris (Luterbacher, 1972).

The Cat Gap Formation at Site 105 can be subdivided into a filaments microfacies (cores 40 to 37) and a *Saccocoma* microfacies (core 36 through core 33). The filaments microfacies (Figure 4B), which directly overlies basalt, is a variably argillaceous biomicrite to calcareous claystone containing nannofossils, filament-like pelagic bivalves, foraminifera, ostracods, ammonite aptychi, radiolaria molds, rare *Saccocoma*, and fish fragments. In the upper part of the microfacies, short filaments and the calcisphaerulids (*Cadosina fibrata*) are present. The *Saccocoma*, microfacies (Figure 4C) differs from the underlying filaments microfacies by the occurrence of the pelagic crinoid *Saccocoma*, the rarity or absence of filaments, and somewhat higher average carbonate content (34% vs. 23%).

Contacts. The Cat Gap Formation at Site 105 directly overlies basalt (Table 3, Figure 24). This type of contact is typical only of the eastern pinch-out of the formation against basement. Nearer the continental margin, seismic reflection data indicate that the Cat Gap Formation overlies older sedimentary units not yet drilled (Figure 22). Thus we cannot define a lower boundary stratotype. The upper contact is

TABLE 3. GEOGRAPHIC DISTRIBUTION OF THE CAT GAP FORMATION IN THE NORTH AMERICAN BASIN

| Region | DSDP Location Leg | Site | Top m* | Core@ | Base m* | Core@ | Thickness (m) | Age | Position |
|---|---|---|---|---|---|---|---|---|---|
| Lower Continental Rise | 11 | 105+ | 559,8 [-5810.8] | 33:2,27 | 622.2 B | 40:1,120 | 62.4 | Oxfordian-Tithonian | 34°53.7'N,69°10.4'W |
| Cat Gap Area | 11 | 99 | 234** [-5148] | between 11A & 12A | (248 TD) | 14 | >14 | Oxfordian-Kimmeridgian | 23°41.1'N,73°51.0'W |
| Cat Gap Area | 11 | 100 | 238*** [-5563] | between 1 & 2 | 313.7 B | 10:2,120 | 75.7 | Oxfordian-Kimmeridgian | 24°41.3'N,73°47.9'W |
| Blake-Bahama Basin | 44 | 391 | 1326 [-1258] | 45C:2,70 | (1412 TD) | 54C | >86 | Tithonian-Late Kimmeridgian | 28°13.7'N,75°36.9'W |
| Greenish-grey, carbonate-rich variant: | | | | | | | | | |
| Cat Gap Area | 11 | 100 | 276 [-5601] | between 6 & 7 | 313.7 B | 10:2,130 | 42 | Oxfordian | 24°41.3'N,73°47.9'W |

* metres below sea floor. Range in values denotes interval without coring or recovery.
[ ] depth below sea level in square brackets.
TD denotes total depth penetrated; bottom of formation not cored.
B indicates that the formation rests directly on basement.
@ core locations given by: core number:section,depth in centimetres.
** based on seismic reflector and reduction in drilling rate; interval 202 to 235 m not cored.
*** based on reduction in drilling rate; interval 212 to 238 m not cored.
+ type locality.

TABLE 4. CHARACTERISTICS OF THE CAT GAP FORMATION

| Region | Leg | Site[Δ] | Grain Size N | Sand | Silt | Clay | Carbon/Carbonate N | $CaCO_3$ | Organic | Mineralogy (X-ray Diffraction) N | Quartz (bulk sample) | Quartz | Feldspar | Carbonate (total) | Kaolinite | Mica | Chlorite | Montmorillonite | Zeolite | Porosity N | T |
|---|---|---|---|---|---|---|---|---|---|---|---|---|---|---|---|---|---|---|---|---|---|
| Lower Continental Rise | 11 | 105+ | 1 | 0.6 | 30.4 | 69.1 | 28 | 29.16 ±13.27 | 0.11 ±0.05 | 8* | 22.5 ±6.9 | 30.5 ±11.1 | 0 | | 0.7 ±1.4 | 47.8 ±12.3 | 0.4 ±0.9 | 18.1 ±7.1 | 0 | 2 | 38.0<br>0 |
| Cat Gap Area | 11 | 100 | 8 | 0.5 ±0.43 | 25.29 ±4.31 | 74.21 ±4.63 | 10 | 57.1 ±20.49 | 0.26 ±0.07 | 12* | 11.4 ±12.4 | 24.9 ±23.4 | 0 | | 0.5 ±1.2 | 20.8 ±14.1 | 1.7 ±1.9 | 20.1 ±24.2 | | | |
| Blake-Bahama Basin | 44 | 391C | | | | | 10 | 42.3 | 0.45 | 4b | 15.2 ±1.2 | | 6.0 ±4.1 | 54.0 ±17.1 | 1.7 ±1.7 | 10.2 ±4.9 | 0 | 13.5 ±8.9 | | 4 | 22.3 ±5.9 |

* analysis of less than 2 μm fraction
b analysis of bulk samples
N number of samples. Mean percentage and standard deviation were calculated for each site.
+ type locality
Δ no data available from Site 99A

transitional for about one metre from reddish-brown clayey limestone upward to light-grey chalky limestone with a few pinkish or light-red intervals. The contact is placed at the uppermost occurrence of the dominantly reddish coloration and at a distinct change in lithology and bulk density.

Regional Aspects. Similar reddish-brown marls and limestones were penetrated in the southwestern part of the basin at Sites 99A, 100 (Hollister, Ewing *et al.*, 1972) and 391C (Benson, Sheridan *et al.*, 1978; Figures 3, 22). Compositional variations are summarized in Table 4.

At Site 99A reddish marl alternates with dominant white and greenish limestone and marl, but core recovery was very poor. At Site 100 where the formation overlies basalt, the lower part of the Cat Gap Formation is relatively homogenous greenish-grey argillaceous limestone with some brownish-grey (5G7/1) and pale red laminae in the lower part of the sequence (Table 3). This part of the sequence was designated as a separate unit by shipboard geologists (Lancelot *et al.*, 1972), on the basis of color and high carbonate content averaging 66%.

The upper part of the formation at Site 100 is a reddish, laminated, locally burrowed, clayey limestone with greenish-grey intervals. Current-produced bedding, minor slump structures, and small clasts of lithified white pelagic mud occur near the top, together with several beds of chert. Slumping may be related to the site location on the deep flank of a basement peak, which is evident in a seismic profile across the site (Hollister, Ewing *et al.*, 1972).

The presence of rare pelagic bivalves in the lower greenish-grey subfacies suggests that it is equivalent to the filaments microfacies at Site 105, despite the difference in color. Pelagic bivalves in core 7 resemble "short" filaments. The upper part of the formation at Site 100 (cores 2-6) is a poorly developed *Saccocoma* microfacies, and the microfacies separation is less distinct than at Site 105. Other fossils scattered through the formation include echinoid fragments, plant fragments, ostracods, ammonite aptychi, nannoplankton, silt-sized foraminifera, *Globochaete*, calcisphaerulids, and rare chalcedony-replaced radiolarians.

A somewhat different development of the Cat Gap Formation occurs in the Blake Bahama Basin at Site 391C, as the *Saccocoma* and filaments microfacies were not observed. Here only the uppermost 86 m of the formation was penetrated before the hole was abandoned (Table 3). Seismic data indicate that more than 400 m of sediments lie between the bottom of the hole and basement (Figures 5, 22). The upper 45 m of the cored interval (cores 49 through 45) is alternating greenish-grey (5G4/1) or white (N8) limestone, pale red clayey limestone (25YR6/2), and dark reddish-brown (5YR3/2) and olive-grey (5Y6/1) calcareous claystone. These form a broad transition zone between underlying dark reddish-brown clayey limestone with only a few dark greenish-grey layers (cores 54 through 50) and overlying light-grey limestone. The uppermost occurrence of red clayey limestone at 1326 m (Table 3) is taken as the top of the formation. Fossils and burrows, including *Chondrites*, are more common in the upper part. Radiolarian molds replaced by sparry calcite, calcisphaerulids, chitinous shell debris, and rare foraminifera occur in addition to nannofossils which are fairly well preserved throughout the formation. Calpionellids were observed in thin sections in core 48:1, and Nannoconus is common in core 49. The carbonate content averages 41.6% in the lower part of the cored sequence and 67% in the upper 47 m. Up to 35% aragonite also was detected in the lower part.

Acoustic Character. The top of the Cat Gap Formation is correlated with a reflector below Horizon β at Sites 100 and 391C (Figure 5, Benson, Sheridan *et al.*, 1978). The reflector, named Horizon C by Sheridan *et al.* (1978) shows lateral gradations in reflectivity and is locally more prominent than Horizon β (Figure 6). Associated reflectors occurring within 50 m of Horizon C are highly variable in intensity, perhaps indicating lateral changes in lithology near the contact with the overlying formation. This is supported by similar lateral changes in internal velocity (Figure 5). At Site 105, there is no clearly defined reflector correlating with the top of the Cat Gap Formation. The site was drilled on top of a basement swell, and deep reflectors lap onto the swell and pinch out at the site. The formation is so thin in this region that it might not be resolved by the long wavelength, low frequency (25 Hz) seismic data.

Most of the available seismic reflection data linking drill sites near the continental margin are conventional single-channel, acquired with a 20 inch$^3$ airgun sound source. These records do not clearly define deep reflectors in the thick continental margin sediments so that detailed seismic correlation between these sites is difficult. A few recently obtained multichannel and large airgun reflection profiles in the basin (Grow and Markl, 1977) do show Horizon C over a wide area and this reflector can be traced to sites 100 and 105 from Site 391.

Acoustic basement underlying the Cat Gap Formation at Sites 100 and 105 is oceanic Layer 2. The Cat Gap Formation overlies older crust at Site 391C and a general eastward onlap of reflectors onto acoustic basement throughout this region results in a variety of prominent reflectors appearing within or below the Cat Gap Formation at this site.

*In situ* compressional wave velocities of sediments comprising the Cat Gap Formation are dependent on the thickness of sedimentary overburden as well as the physical character and composition of sediments. At Site 100, where overburden thickness is about 238 m, interval velocity calculated from reflector-borehole correlation is 2.3 km/s

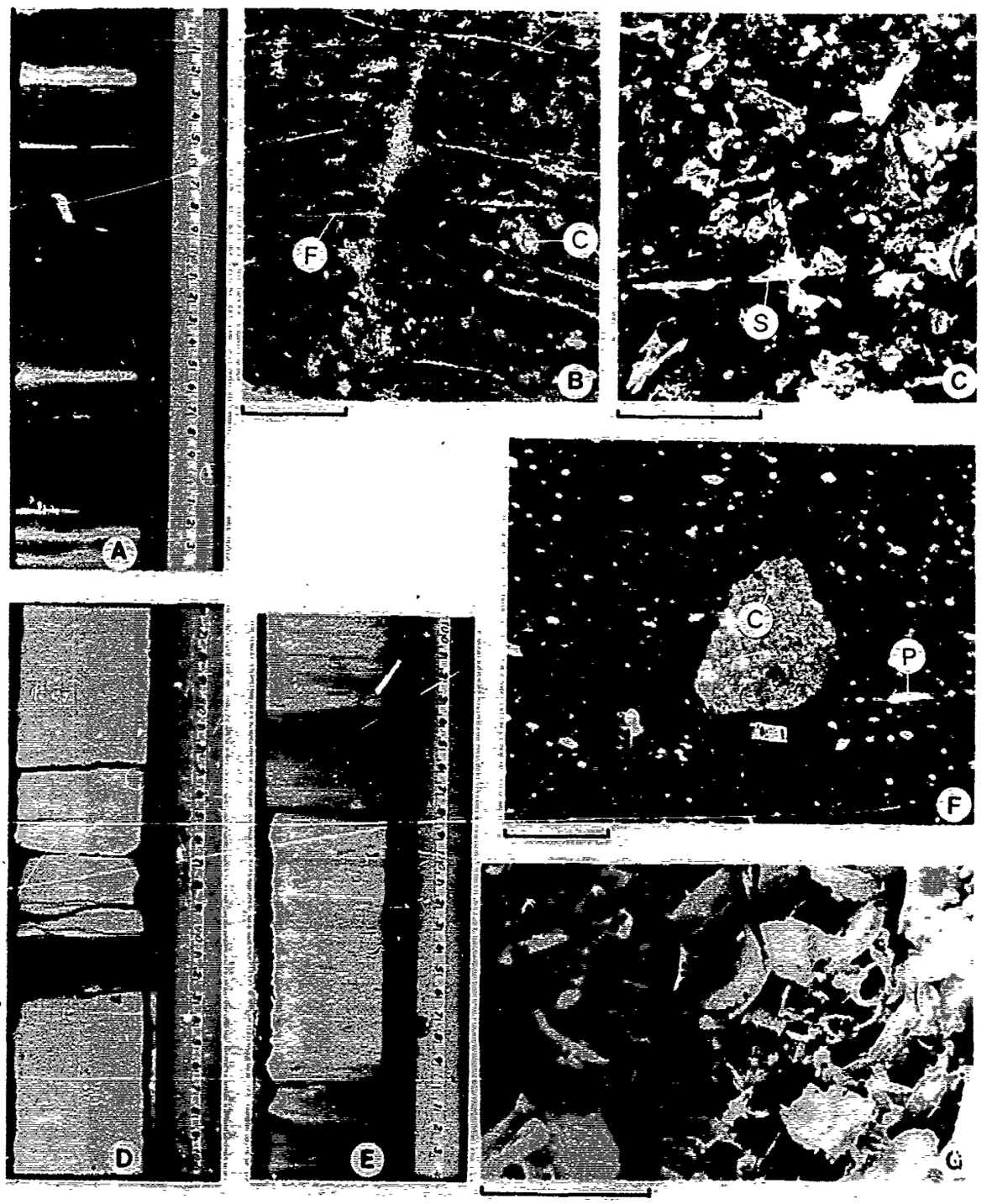
A
F
C
B
S
C
C
P
F
D
E
G

(Hollister, Ewing *et al.*, 1972). At Site 391C the average value of shipboard measurements is 2.8 km/s (Benson, Sheridan *et al.*, 1978), but this figure is lower than *in situ* values of 3.4 to 4.3 km/s (Figure 5) beneath 1326 m of overburden. Cat Gap Formation interval velocity at Site 105 is unknown, but is probably higher than the 1.8 km/s value calculated by Hollister, Ewing *et al.* (1972) for the thicker interval from Horizon β to basement.

Age. The age of the Cat Gap Formation at the type locality (Site 105) was broadly interpreted to span the Oxfordian-Tithonian (Figure 7). An Oxfordian-Kimmeridgian age was established for Sites 99 and 100 (Hollister, Ewing *et al.*, 1972) and at Site 391 the cored part of the formation is Late Kimmeridgian-Tithonian (Figure 9; Benson, Sheridan *et al.*, 1978).

The basal greenish-grey subfacies of the Cat Gap Formation at Site 100 was considered by Hollister, Ewing *et al.* (1972) to be Callovian. The lowest two sedimentary cores (9 and 10) contain Bathonian, Callovian, and Oxfordian dinoflagellates (Habib, 1972). The calcareous nannoplankton in these cores are Callovian or Oxfordian (Hollister, Ewing *et al.*, 1972), but according to Thierstein (1976; see also Larson and Hilde, 1975) the nannoplankton may be restricted to Oxfordian.

The association of pelecypod filaments, protoglobigerinids, *Globochaete*, ammonite aptychi, calcisphaerulids, and minor *Saccocoma* is characteristic of the Oxfordian in the western Mediterranean Jurassic (Azema *et al.*, 1974; Kuhry *et al.*, 1976) and a similar age for the filaments microfacies of the Cat Gap Formation is considered probable. Site 105 was drilled on the eastern side of anomaly M-25, and site 100 is located in the Jurassic magnetic quiet zone just older than anomaly M-25 (Larson and Hilde, 1975; Schouten and Klitgord, 1977). These age data tend to confirm an Oxfordian age for M-25, as suggested by Larson and Hilde (1975) and van Hinte (1976a,b).

Sedimentary rocks with common occurrences of *Saccocoma* in the Mediterranean region are generally assigned to the Kimmeridgian-Early Tithonian (Gonzales-Donoso *et al.*, 1971; Lehman, 1972; Azema *et al.*, 1974; Kuhry *et al.*, 1976). Based on microfossil associations at Site 100, 105 and 391C, an approximate Oxfordian age for the filaments microfacies and a Kimmeridgian-Early Tithonian age for the *Saccocoma* microfacies are indicated.

Depositional Environment. The depositional environment of the Cat Gap Formation can be inferred from sediment composition and texture and from composition and preservation of the fossil assemblages. Coarse terrigeneous detritus is absent. Fine quartz silt, mica, and clay minerals were probably transported in suspension from distant shelf sources. Plant debris and kaolinite at Site 100 suggest contributions from continental sources, possibly by turbidity currents through Cat Gap. Redeposited pelagic sediments at Site 100 and 105 are attributed to slumping from local topographic highs.

Both the foraminiferal and ostracod assemblages suggest a bathyal environment (Luterbacher, 1972; Oertli, 1972), but the environmental significance

Figure 4. Cat Gap and Blake-Bahama Formations.

A. Clayey reddish-brown (10R 4/4) limestone, evenly bedded with thin (light colored) greenish-grey (5G 6/2) laminae, and burrow fillings. Prominent bed of graded detrital carbonate at 117 cm. Note the diffuse boundary between green and reddish-brown zones, Cat Gap Formation (Leg 11-105-38:3, 99-124 cm).

B. Filaments microfacies, with thin shells of pelagic pelecypods (F) and calcisphaerulids (*Stomiosphaera*-C). Thin section, ordinary light, scale bar = 1 mm. Cat Gap Formation (Leg 11-105-37:1, 29 cm).

C. *Saccocoma* microfacies, composed of fragments of pelagic crinoids (S) displaying syntaxial calcite overgrowth, radiolaria replaced by sparry calcite, and hematite-stained argillaceous micrite (thin section, ordinary light, scale bar = 1 mm). Cat Gap Formation (Leg 11-105-33:4, 55 cm).

D. Light-grey (N 7) nannofossil limestone, with thin bed of greenish-grey clay (5G 6/1), indistinctly laminated and bioturbated. Microstylolites are concentrated from 85 to 90 cm. Blake-Bahama Formation (Leg 44-391C-42:3, 76 to 101 cm).

E. Chalky limestone, light greenish-grey (5G 8/1), nonlaminated and heavily burrowed; interbedded with finely and evenly laminated darker zones of olive grey (5Y 4/1), soft clayey limestone. Contacts are gradational. Blake-Bahama Formation (Leg 11-105-28:1, 99 to 124 cm).

F. Intraclast of light-grey micrite containing calpionellids (C) and sparry-calcite-replaced Radiolaria, enclosed in brownish-stained biomicrite (thin section, ordinary light, scale bar = 1 mm). Near base of the Blake-Bahama Formation (Leg 11-105-32:1, 130 cm).

G. Scanning electron micrograph of chalky limestone near the top of the Blake-Bahama Formation (Leg 11-105-17:1, 71 cm). Note fragmented character and corrosion of some of the nannofossils and high porosity of the sediment. Scale bar = 10 μm.

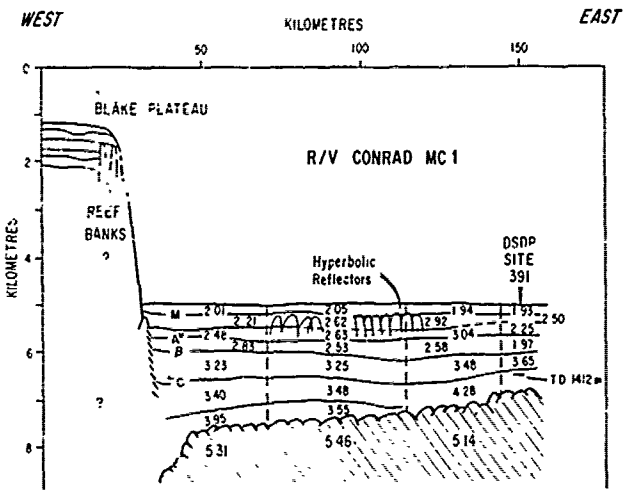


Figure 5. Line tracing of R/V Conrad multichannel profile MC1 through DSDP Site 391 (modified from Sheridan *et al.*, 1978). Location in Figure 1. Reflectors are discussed in text. Hyperbolic reflectors at a shallow depth are diffractions apparently generated from rills created in the M reflector by bottom-current erosion or debris-flow erosion. Interval velocities (km/s) derived from multichannel velocity analyses and averaged in groups separated by dashed lines. Velocities under Site 391 were calculated from reflector/borehole correlation.

of these faunas is still poorly known (Funnel, 1967). The foraminifera are predominantly primitive and arenaceous forms, and the ostracods are dwarf and larval forms. Only isolated protoglobigerinids were found at Sites 100 and 105. Ammonite aptychi are relatively common but phragmocones and casts of shells are exceptionally rare. This suggests that deposition was below the aragonite compensation depth (ACD), but relatively common aragonite at Site 391C indicates that deposition occurred near the ACD. Luterbacher (1972) noted that at Site 105, light-colored clasts of shallower water origin (probably from adjacent highs) were incorporated in the red mudstones (Figure 4F), which were probably deposited near the CCD. Deposition near the CCD (Figure 23) is also indicated by the low carbonate content (14-20%) of cores 38 to 40 at Site 105. Assuming Jurassic ridge-crest elevations similar to those of today, the eastern reaches of the Cat Gap Formation (i.e. that part which has been drilled) were deposited in a bathyal environment. Toward the west deposition may have been on an older, presumably deeper, sea floor, but this has to be proved by future deep drilling in the continental margin.

Sedimentation rates of the Cat Gap Formation (uncorrected for compaction) are about 8 m/m.y. at Site 100, 10 m/m.y. at Site 105, and 14 m/m.y. at 391C. These rates, sediment composition, and sedimentary structures all indicate that the Cat Gap Formation was formed by pelagic deposition, occasionally interrupted by bottom current, slumping and turbidites.

Identifying Features. The Cat Gap Formation is identified by its reddish-brown color, intercalations of pelagic clayey limestone and calcareous claystone, occurrence of incipient nodular texture, and presence of the seismic Horizon C near the top of the formation.

Correlation with Other Units. A lithofacies similar in color, composition and fossil assemblage to the Cat Gap Formation was penetrated in the Cape Verde Basin (Site 367, Lancelot, Seibold *et al.*, 1978), indicating similar development of the Upper Jurassic sequences in the eastern North Atlantic (Jansa *et al.*, 1978). The top of the red marly limestones there forms a widespread reflector which Lancelot, Seibold *et al.* (1978) have designated reflector C.

The lithofacies along the North American outer shelf that are time-synchronous with the Cat Gap Formation are shallow-water carbonate banks of the Abenaki Formation on the Scotian Shelf (Jansa and Wade, 1975), unnamed carbonate sequences of the Great Bahama Bank (Meyerhoff and Hatten, 1974) and seismically identified carbonate banks off the New Jersey coastal plain (Schlee *et al.*, 1976). Possible clastic equivalents are nonmarine deposits on the New Jersey coastal plain and continental shelf (Perry *et al.*, 1975; Smith *et al.*, 1976), and fine-grained marginal-marine clastics (Mic Mac Formation, McIver, 1972) of the Scotian Shelf and Grand Banks (Jansa and Wade, 1975a). Some of the shales of the Mic Mac Formation and an unnamed clastic sequence at the base of the COST B-2 well in the Baltimore Canyon Trough are highly oxidized and reddish colored, but none of the deeper, outer shelf sediments show a similar high oxidation state (Jansa and Wade, 1975a; Jansa *et al.*, 1976).

Bernoulli (1972) compared the reddish-brown argillaceous limestones of the North American Basin with the Alpine Ammonitico Rosso facies and the Rosso ad Aptici variant of the central Apennines and western Greece. The Rosso ad Aptici is a red, green, and grey nodular marly limestone and marl of Toarcian-Aalenian (Early Jurassic) age. The basinal character of this formation is indicated by intercalated slump complexes and turbidites (Bernoulli, 1972) and in this respect it is the closest analogue of the Cat Gap Formation of the North Atlantic. The Ammonitico Rosso facies, indicative of pelagic deposition over topographic highs (the swell facies of Bernoulli and Jenkyns, 1974), differs considerably from the Cat Gap Formation by the condensed nature of these deposits, the presence of nonsequences at the base and within the Ammonitico Rosso, the presence of hard-grounds, ferromanganese crusts and coatings, and the frequent occurrence of worn ammonites.

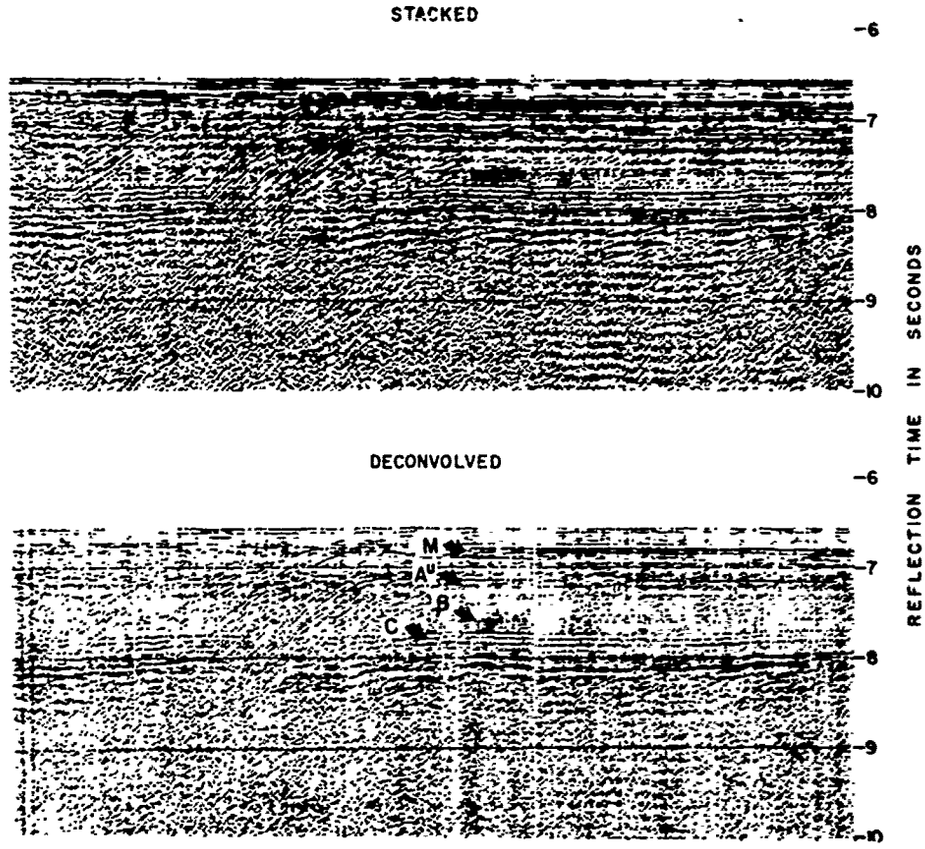


Figure 6. Processed segment of multichannel seismic reflection profile MC1 near Site 391 (from Sheridan *et al.*, 1978). Distance coordinates in kilometres same as in Figure 5. Segment processed with common-depth-point gather, velocity analysis, normal-move-out correction, 24-fold stacking, and time-variable gain. The upper data suffer from ringing that is removed in the lower data by deconvolution. Reflectors are more easily identifiable in deconvolved data.

Blake-Bahama Formation

The light-grey, white and dark grey limestone sequence that overlies the Cat Gap Formation and is overlain by dark grey and black carbonaceous shales (Figure 2) is here named the Blake-Bahama Formation. The type section is at Site 391C (Tables 1, 2 and 5, Figures 8 and 24) in the Blake-Bahama Basin. The lithostratigraphic identity of the Blake-Bahama Formation was recognized by Lancelot *et al.* (1972, p. 918), who described it as "Tithonian-Neocomian white and grey limestone".

Type Locality. At Site 391C, the type locality, 326 m of interlayered lithofacies range from nearly pure limestone (74 to 96% calcite) through marly limestone (45 to 69%) and sandy limestones, to calcareous claystone (16 to 32%). These lithofacies are grouped into three subunits. The basal 107 m is bioturbated clayey limestone with olive-grey (5Y4/1) calcareous clay and greenish (5G6/1 to 5G4/1) calcareous shale in well defined layers 2 to 3 cm thick and in wispy partings spaced about 10 cm apart (Figure 4D). Very thin intervals of millimeter-thick laminated grey calcareous mudstone are interbedded in the upper 40 m. The bioturbated clayey limestones are white (N8) to light bluish-grey (5B7/1) and contain some stylolites and many calcitized and pyritized radiolarians. The middle subunit is 96 m of alternating (1) millimetre-thick laminated light grey to olive grey or very dark grey clayey limestone, (2) light bluish-grey bioturbated clayey limestone, and (3) black to very dark grey calcareous claystone. These three lithologies alternate every 5 to 100 cm without any apparent systematic order. The uppermost subunit, 123 m thick, is characterized by sandy limestone and calcarenite beds up to 1 m thick, with thin interbeds of cross-laminated clayey limestone. Light-grey

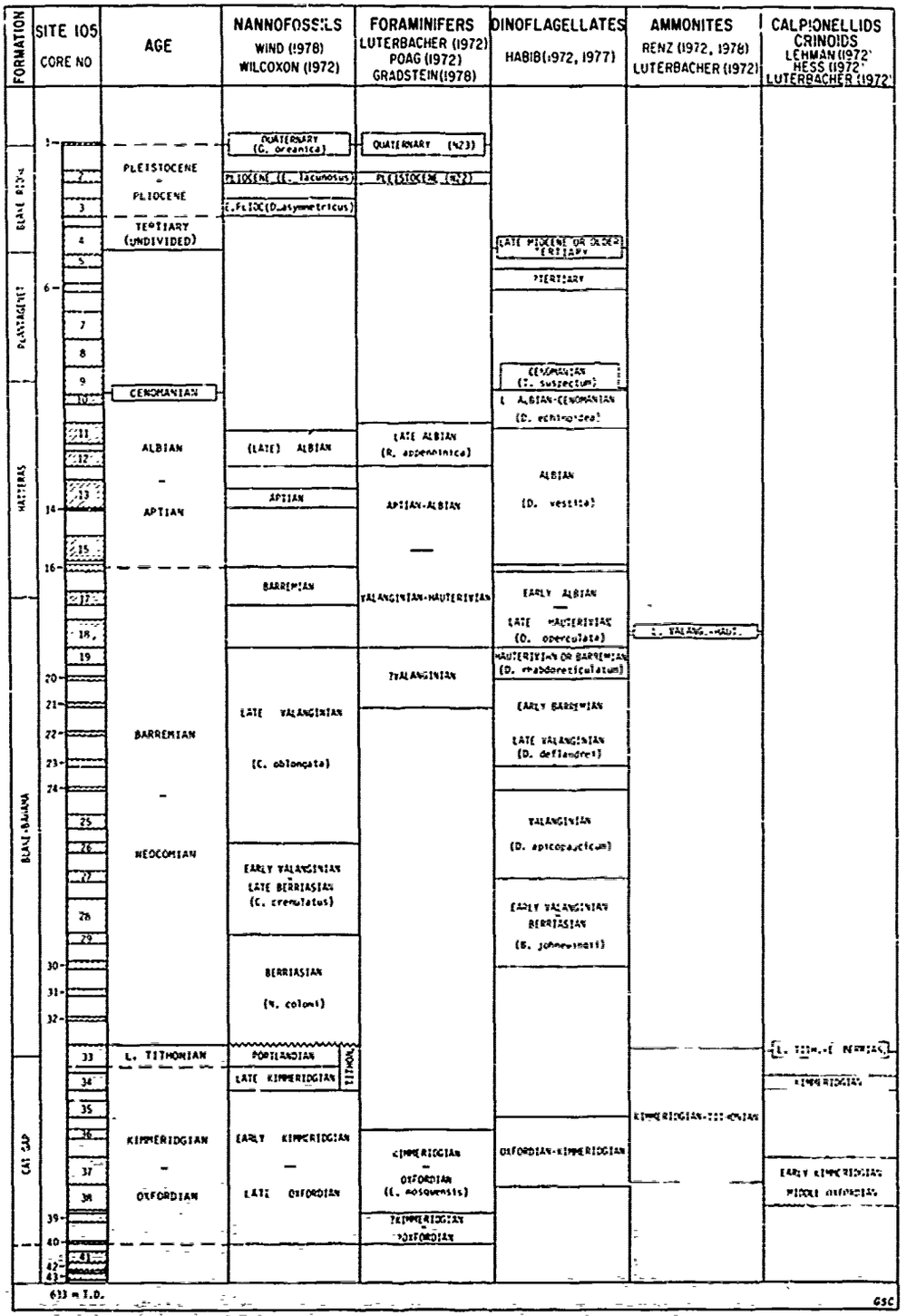


MULTIPLE BIOSTRATIGRAPHY OF LEG 11, SITE 105, LOWER CONTINENTAL RISE HILLS.

Figure 7. Multiple biostratigraphy of Site 105, lower continental rise.

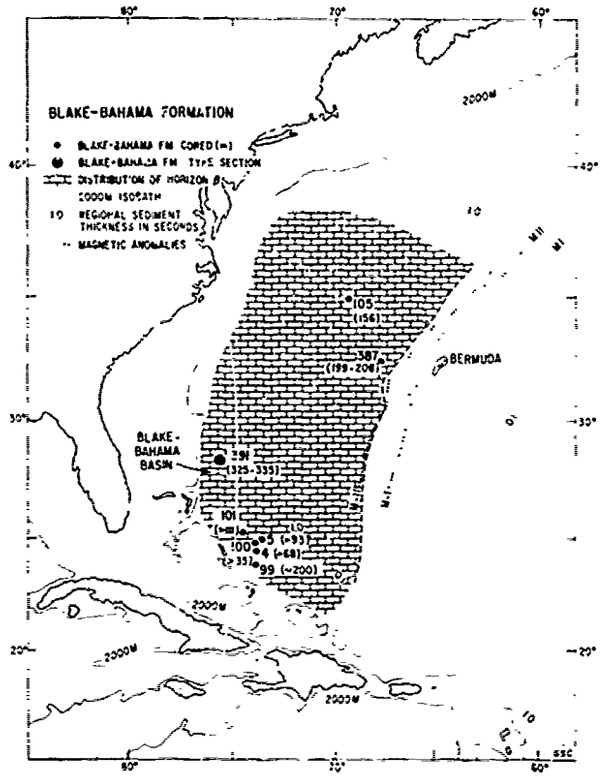


Figure 8. Boreholes that have cored sediments of the Blake-Bahama Formation. Formation thickness (metres) in parentheses. Horizon β correlates approximately with the top of the Blake-Bahama limestones; the eastern boundary indicates mapped pinch-out on basement (after Mountain and Tucholke, 1977), near the magnetic anomaly M-11. This anomaly has been interpreted by van Hinte (1976) to be Valanginian in age.

limestone and dark grey mudstone (several centimetres thick) are interbedded with these clastic lithologies. Scour-and-fill structures are common in this interval.

The Blake-Bahama Formation limestones at the type locality consist of micritic calcite, clay minerals (Table 6), and poorly preserved nannofossils (Figure 4G). They contain abundant casts of radiolarians replaced by calcite or pyrite. Calpionellids and calcisphaerulids are locally common and foraminifers are rare. Ammonite aptychi and fish debris are present in some of the calcareous claystone laminae. Clastic intervals of the upper subunit contain benthic foraminifers and fragments of other benthic fossils. Monocrystalline quartz, microcline, orthoclase, plagioclase, abraded ooids, and wood fragments are components of the clastic limestones (Freeman and Enos, 1978). The dark-grey calcareous claystones contain finely disseminated organic debris, frequent pyrite, and fine quartz silt laminae. The average porosity of the sediments is 22.5%, and the average organic carbon content is 0.3%.

Contacts. Both the lower and upper contacts of the Blake-Bahama Formation are gradational at the type locality. The top of the Cat Gap Formation grades into the Blake-Bahama Formation over an interval of 45 m. As defined earlier, the transition zone occurs within the Cat Gap Formation so that the Cat Gap contains interbeds of light bluish-grey limestone, together with characteristic reddish-brown and greenish-grey clayey limestones and calcareous claystones that increase in abundance downward. The boundary of the Cat Gap and the Blake-Bahama Formations is defined at the first downhole occurrence of reddish-colored beds (Table 5). At Site 105 the lower transitional zone is only a few metres thick, and this is proposed as the Blake-Bahama Formation lower boundary parastratotype (Table 2).

The top of the Blake-Bahama Formation grades into black claystone over an intermittently cored interval about 100 m thick in the type section, at Site 391C. The boundary is placed between cores 13 and 14, above which the limestone is subordinate to dark claystone beds. A boundary parastratotype is defined at Site 105 (Table 2) where although the contact is again transitional over a few metres it is more clearly defined than at Site 391C.

Regional Aspects. The Blake-Bahama Formation was cored at seven other sites in the Cat Gap area, the Bahama Outer Ridge, the lower continental rise, and the Bermuda Rise (Figures 8, 24, Table 5). At Site 387 on the Bermuda Rise the formation rests directly on intrusive basaltic basement (Tucholke, Vogt *et al.*, 1979). At Sites 99A, 100 and 105, as at Site 391C, it directly overlies the Cat Gap Formation (Figure 22). Lithification decreases in the Cat Gap area (Sites 4, 5, 99A, 100) where the formation is near the present sea floor because strong bottom currents have never allowed accumulation of overburden thick enough to cause consolidation of the sediments. The formation is represented here by nannofossil oozes and chalks, containing rare beds of quartzose and porcelanitic chert (Hollister, Ewing *et al.*, 1972).

At Site 387 on the Bermuda Rise the Blake-Bahama Formation consists of alternating layers similar to those described at the type section, except that the darker limestones contain appreciable siderite and dolomite, quartzose chert is common, and no sandy limestones are present. At Sites 101 and 105 the alternating layers are reduced to a simple couplet of (1) hard, white to pale-grey, bioturbated pure micritic limestone (Figure 4E), and (2) soft, dark greenish-grey, laminated clayey limestone. Light-colored limestone layers predominate in the lower part of the formation whereas dark-grey beds with frequent zeolites, became progressively more abundant upwards and are

TABLE 5. GEOGRAPHIC DISTRIBUTION OF THE BLAKE-BAHAMA FORMATION IN THE NORTH AMERICAN BASIN

| Region | DSDP Leg | Location Site | Top m* | Top Core§ | Base m* | Base Core§ | Thickness (m) | Age | Position |
|---|---|---|---|---|---|---|---|---|---|
| Blake-Bahama Basin | 44 | 391+ | 991-1000.5 [-5955 -5964.5] | between 13C & 14C | 1325.7 | 45C:2,70 | 325.2-334.7 | Barremi. Tithonia" | 28°13.7'N,75°36.9'W |
| Bahama Outer Ridge | 11 | 101 | 580** [-6448] | between 8A & 9A | (691 TD) | 10A | >111 | Neccomian | 25°11.9'N,74°26.3'W |
| Lower Continental Rise | 11 | 105 | 403.3 [-5654.3] | 17:1,30 | 559.8 | 33:2,27 | 156.5 | Barremian-Late Tithonian | 34°53.7'N,69°10.4'W |
| Bermuda Rise | 43 | 387 | 583.8-593.1 [-5701.8-5711.1] | between 37 & 38 | 792B | 49 core catcher | 199-208 | ?Barremian-Late Berriasian | 32°19.2'N,67°40'W |
| Unlithified Carbonate Ooze Lithofacies | | | | | | | | | |
| Cat Gap Area | 1 | 4 | 143-191 [-5463 -5511] | between 3 & 4 | (259 TD) | 5 | 68-116 | Neocomian-Tithonian | 24°28.7'N,73°47.5'W |
| Cat Gap Area | 1 | 5 | 154-185 [-5508 -5539] | between 3A & 4A | (281 TD) | 7A | >93-127 | Hauterivian-Tithonian | 24°43.6'N,73°38.5'W |
| Cat Gap Area | 11 | 99 | 32*** [-4946] | between 2A & 3A | 234*** | between 11A & 12A | ~200 | Neocomian-Tithonian | 23°41.1'N,73°51.0'W |
| Cat Gap Area | 11 | 100 | <203 [-5528] | above 1 | 238**** | between 1 & 2 | >35 | Valanginian-Late Tithonian | 24°41.3'N,73°47.9'W |

* Metres below sea floor. Range in values denotes interval without coring or recovery.
[] Depth below sea-level in square brackets.
TD Denotes total depth penetrated; bottom of formation not penetrated.
B Indicates that the formation rests directly on basement.
§ Core locations given by: core number:section,depth in centimetres.
** Based on seismic reflector; interval 543-599 m not cored.
*** Based on reduction in drilling rate; intervals 21-44 m and 202-235 m not cored; reduction in drilling rate 220-240 m.
**** Based on reduction in drilling rate; interval 212-238 m not cored.
+ Type locality.

in transition to the black claystone of the overlying Hatteras Formation. At Site 105, slump units, locally more than a metre thick, are confined to the lower part of the formation (Figure 4F) below 500 m sub-bottom, and only small, minor slumps are present at Site 101 (Lancelot *et al.*, 1972).

At Site 105, calpionellids occur near the base of the formation, but they are rare, poorly preserved, and recrystallized higher in the unit. Calcisphaerulids were found at all sites. Nannoconids are common in some of the cores at Site 99A (Lehman, 1972) and Site 391C (Wind, 1978). In all the sites primitive arenaceous foraminifera are rare, but small planktic foraminifera are even less common (Luterbacher, 1972,. Aptychi are relatively common and echinoderm, mollusc, and ostracod debris occurs locally. The aptychi and nannoplankton are better preserved in the marls due to less diagenetic alteration. The intensity of diagenetic alteration decreases upwards in the sequence.

The terrigeneous component of the clayey limestone is dominated by montmorillonite and mica (Zemmels *et al.*, 1972) at Sites 105, 101A and 99A (Table 6). Other terrigenous components are minor silt-sized quartz, plagioclase, and traces of heavy minerals. Finely disseminated organic matter and quartz silt is common in dark-grey calcareous clays.

Acoustic Character. Horizon β correlates with the impedance contrast between the calcareous sediments of the Blake-Bahama Formation and the overlying dark clays of the Hatteras Formation at six sites where both the reflector and the contact can be identified (Tucholke, 1979). This reflector can generally be traced above basaltic crust older than Barremian age (Figures 6, 17, 24). The eastward pinch-out of Horizon β on Hauterivian to Barremian-age crust (Figure 8) provides rough confirmation for the age of the upper boundary of the formation (Mountain and Tucholke, 1977; Tucholke, 1979). The acoustic character of Horizon β is variable. The reflector is best developed in the Cat Gap region where there is little overburden. Here β is a strong, crisp, fairly smooth reflector capping a zone of acoustically laminated sediments including the Blake-Bahama Formation. The acoustic lamination probably reflects variable impedance of interbedded limestones, cherts, and marls. This acoustic lamination is not always distinct beneath the thicker sediments of the Blake-Bahama Outer Ridge and continental rise, perhaps because of poor signal penetration and because physical property

TABLE 6. CHARACTERISTICS OF THE BLAKE-BAHAMA FORMATION

| Region | Leg | Site | Grain Size | | | | Carbon/Carbonate | | | Mineralogy (X-ray Diffraction) | | | | | | | | Porosity | |
|---|---|---|---|---|---|---|---|---|---|---|---|---|---|---|---|---|---|---|---|
| | | | N | Sand | Silt | Clay | N | $CaCO_3$ | Organic | N | Quartz (bulk sample) | Quartz | Feldspar | Carbonate (total) | Kaolinite | Mica | Chlorite | Montmorillonite | Zeolite | N | % |
| Blake-Bahama Basin | 44 | 391A&C+ | | | | | 5 | | 0.30 ±0.23 | 45b | 9.5 ±8.6 | | 2.4 ±7.1 | 81.0 ±20.5 | 0.3 ±0.7 | 2.0 ±3.5 | 0 | 2.6 ±3.9 | | 72 | 22.5 ±8.0 |
| Cat Gap | 11 | 99A | 3 | 0.27 ±0.15 | 23.63 ±14.51 | 76.10 ±14.65 | 3 | 89.33 ±5.86 | 0.47 ±0.64 | 3* | 1.0 ±0.4 | 15.5 ±14.1 | 0 | | 0.6 ±1.1 | 14.0 ±12.9 | 0 | 49.7 ±3.1 | | 4 | 42.2 ±1.2 |
| Cat Gap | 11 | 100 | 5 | 4.32 ±8.88 | 32.64 ±4.32 | 63.06 ±7.74 | 5 | 88.20 ±14.01 | 0.1 0 | 2* | 3.6 ±1.3 | 44.80 ±5.9 | 0 | | 0 | 23.9 ±9.5 | 1.2 ±1.7 | 14.2 | | | |
| Bahama Ridge | 11 | 101A | | | | | | | | 2* | 3.0 ±0.7 | 50.6 ±19.3 | 0 | | 0 | 20.4 ±3.4 | 0.9 ±1.3 | 28.0 ±24.1 | | | |
| Lower Continental Rise | 11 | 105 | 11 | 0.88 ±0.93 | 29.38 ±5.67 | 69.72 ±5.76 | 40 | 66.43 ±21.30 | 0.72 ±0.85 | 17* | 5.1 ±2.9 | 26.2 ±18.8 | 0 | | 0 | 14.8 ±8.0 | 0 | 58.5 ±15.9 | 0.2 ±1.0 | | |
| Bermuda Rise | 43 | 387 | | | | | 4 | 73.61 ±22.37 | 1.56 ±1.09 | 14b | 3.5 ±2.9 | | 0 | 81.0 ±15.5 | 0.1 ±0.3 | 15.0 ±12.6 | 0.1 ±0.2 | 0.1 ±0.3 | 0 | 19 | 23.4 ±9.7 |

* analysis of less than 2 μm fraction.
b analysis of bulk samples.
\+ type locality.

contrasts are reduced where overburden increases sediment consolidation. Farther east, Horizon β becomes irregular because it more closely overlies rugged altic basement, and at its eastern extremity the reflector is only intermittently observed in basement depressions. The acoustic lamination of sub-β sediments is seldom well developed in this region.

In all areas where Horizon β is observed, it is not uncommon for other, generally weaker reflectors to appear and fade laterally in the interval 50 to 100 m above β. This is particularly evident at Site 391C (Figure 6) and at sites near the Bahama Banks. These reflectors may be carbonate beds within the overlying black clays, probably derived from the adjacent, shallow carbonate provinces (see Hatteras Formation, Site 4). They suggest that Horizon β and the top of the Blake-Bahama Formation is diachronous, reflecting the local persistence of detrital carbonate sedimentation beyond the cessation of pelagic carbonate deposition in the basin.

The base of the Blake-Bahama Formation probably is marked by Horizon C at the top of the Cat Gap Formation (Figure 6) as discussed previously. Where the oceanic crust is younger than about Tithonian, as at Site 387, Horizon C pinches out and the Blake-Bahama Formation rests directly on basaltic basement.

Compressional-wave velocities of the Blake-Bahama Formation vary with overburden thickness. Shipboard velocity measurements on core samples average 2.78 km/s in the top 250 m at Site 391C and 3.31 km/s at the base. At Site 387 measured velocities ranged from 1.8 to 4.7 km/s in various interbeds. These measured values average less than the *in situ* velocities calculated from correlation of the borehole to the seismic record: Site 391C - 3.60 km/s (1000 m overburden); Site 387 - 2.08 km/s (590 m overburden); and Site 100 - (?) 2.05 km/s (presently no overburden). Interval velocities measured by the CDP method in the Blake Bahama Basin are 3.2 to 3.6 km/s, close to the calculated measurements (Figure 5; Sheridan *et al.*, 1978).

Age. The Blake-Bahama Formation has been dated at the type locality by nannofossils, dinoflagellates, foraminifers, and aptychi and appears to be Late Tithonian-Barremian (Figure 9). At Site 105 the formation is also Late Tithonian-Barremian (Figure 7), at Site 99A Tithonian-Hauterivian/Barremian at Site 100 Late Tithonian-Valanginian and at Site 387 Late Berriasian to ?Barremian (Figure 14). At Sites 99A and 100 the upper part of the formation was not cored, and at Sites 4, 5, and 101 the upper boundary is also uncertain due to the scarcity of microfauna and intermittent coring. At these sites the boundary is apparently of Hauterivian to Barremian age.

Depositional Environment. The Blake-Bahama Formation at the type locality is a texturally variable sedimentary sequence of alternating laminated and bioturbated limestone intervals, with graded sandy limestone intervals in the upper part of the formation. The microfossils including common radiolarians, indicate pelagic deposition in an oxygenated deep bathyal environment. The relative paucity of planktic foraminifera and presence of etched nannofossils at the type section suggests deposition near, but above the CCD. Reconstruction of site paleodepth curves indicates water depths possibly as great as 4500 m in the type area, and about 500 m shallower depths, in other sites (Figure 23).

Seismic profiles across the Blake-Bahama Basin show deposition of flat-lying sediments in a basin uninterrupted by basement peaks (Figure 5). The alternately laminated and bioturbated sediments in the lower part of the section at Site 391C may include fine-grained turbidites originating from the Blake Plateau. Some of the laminations may represent reworking by bottom currents that were intensified near the steep marginal escarpment. Marked variations in thickness of the formation observed in profiler records near the Bahama Banks south of the type area led Mountain and Tucholke (1977) to suggest that persistent bottom currents created zones of preferential deposition in the Early Cretaceous.

Turbidity currents were active during deposition of the upper part of the Blake-Bahama Formation at Site 391C, where graded limestone and sandy limestone beds were deposited. The presence of abraded oolites, quartz, and feldspar grains in cross-bedded sandy limestone beds at this site indicate provenance from a mixed terrigenous and carbonate shelf. Oolite banks were probably developed at that time at the outer shelf margin (Enos and Freeman, 1978).

In areas away from the continental margin (Site 387) and on basement rises (Site 105), local slumping of carbonate detritus from highs probably formed 'pelagic turbidites' (Lancelot *et al.*, 1972). However, the Blake-Bahama Formation at these Sites is more characteristic of a pelagic depositional environment.

Sediment accumulation rates average 7 to 10 m/m.y. at all sites, except at Site 101 where the rate may have reached 18 m/m.y.

Identifying Features. Light grey color, micritic limestone composition with abundant calcite replaced radiolarians, occurance of stylolites, presence of seismic reflector β near the upper formation boundary, and the position of the formation between underlying reddish-brown colored limestones of the Cat Gap Formation and overlying dark shales of the Hatteras Formation are identifying features of the Blake-Bahama Formation.

Correlation with Other Units. Deltaic deposition dominated the Late Tithonian-Barremian on the inner and middle North Atlantic shelf north of Cape Hatteras. Shallow-water limestones, locally enclosing hydrozoan-coral - sponge reefs, form a discontinuous belt situated along the more stable

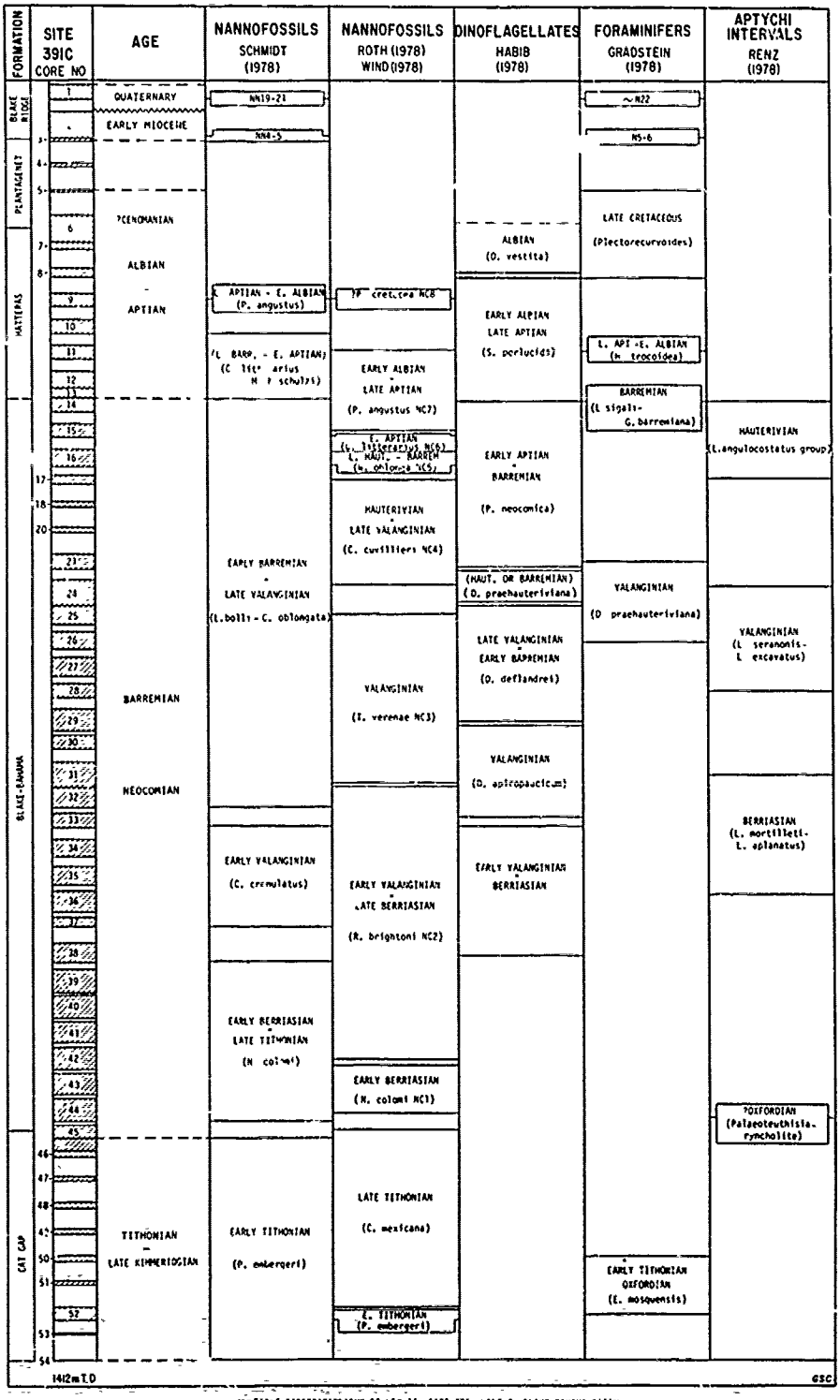


MULTIPLE BIOSTRATIGRAPHY OF LEG 44, SITE 391, HOLE C, BLAKE-BAHAMA BASIN.

Figure 9. Multiple biostratigraphy of Site 391C located in Blake-Bahama Basin.

parts of the outer paleo-shelf and over topographic highs. Fine grained limestones and calcareous clays were deposited at the same time in a deeper outer shelf (Jansa and Wade, 1975a, b; Smith *et al.*, 1976, Perry *et al.*, 1975). The Upper Jurassic-Lower Cretaceous carbonate banks north of the Blake Plateau are identifiable by a strong seismic reflector which is approximately Hauterivian on the Canadian margin (Jansa and Wade 1975a). This seismic reflector is synchronous with the seismic Horizon β in the deep sea and thus both of these seismic reflectors may be correlatable.

Extensive Upper Jurassic and Cretaceous carbonate deposits cover the Blake Plateau and Florida-Bahama region (Meyerhoff and Hatten, 1974), but these shallow-water units cannot be correlated satisfactorily with deposits in the basin. An exception is shallow marine carbonate at the Blake Nose (Sites 390, 392) which can be paleontologically correlated with the top of the Blake-Bahama Formation at the type section (*Gavelinella barremiana-Lenticulina sigali* Zone of Barremian age; Gradstein, 1978).

A lithofacies similar to the Blake-Bahama Formation was cored at Site 367 in the Cape Verde Basin (Jansa *et al.*, 1978) and it outcrops on Maio Island of the Cape Verde Archipelago (Stahlecker, 1933). Thus wide distribution of this lithofacies in the central North Atlantic is indicated.

Bernoulli (1972) compared the lithified portion of the Blake-Bahama Formation with the Late Tithonian-Barremian Maiolica Formation of the southern Alps and Apennines and the unlithified portions of the Blake-Bahama Formation to the Aptian-Albian more argillaceous Marne a Fucoidi and Scaglia Variegata. On the basis of both lithology and age, the Maiolica probably correlates better with the Blake-Bahama Formation.

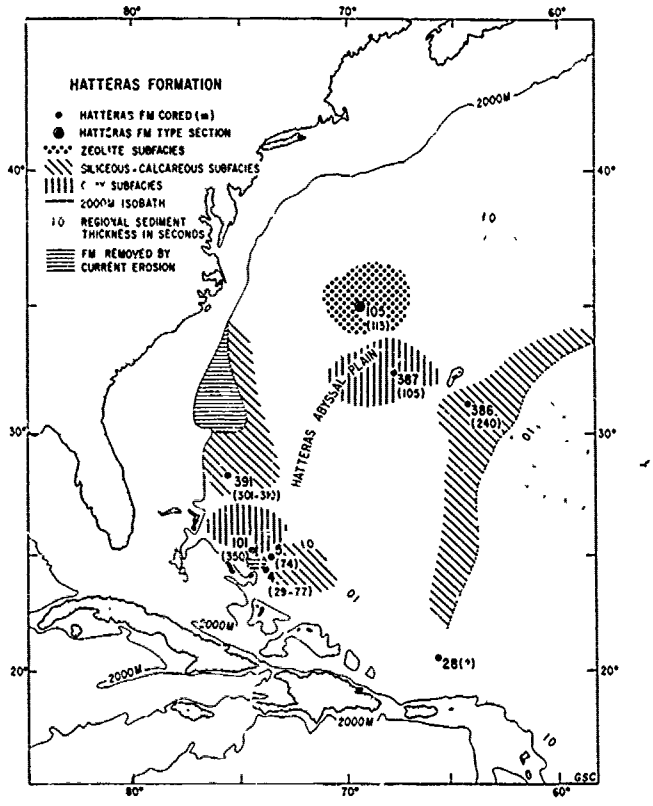


Figure 10. Boreholes that have cored sediments of the Hatteras Formation. Formation thickness (metres) in parentheses. Subfacies are differentiated by indicated patterns. Dashed line shows the approximate eastward limit of black clays.

## Hatteras Formation

The Hatteras Formation as formally defined here is dark greenish-grey to black carbonaceous cla and laminated marl widespread in the North American Basin (Ewing, Worzel *et al.*, 1969; Hollister, Ewing *et al.*, 1972; Tucholke, Vogt *et al.*, 1979). The type section is at Site 105 (Tables 1, 2, and 7) on the lower continental rise adjacent to the Hatteras Abyssal Plain (Figure 1).

This formation was first sampled by piston coring of the outcrop in the Cat Gap area (Saito *et al.*, 1966; Windisch *et al.*, 1968) and first drilled by DSDP at Site 5 (Ewing, Worzel *et al.*, 1969). The continuity of the sequence was recognized by Lancelot *et al.* (1972) who described it from Sites 105 and 101 as "Lower Cretaceous black clays".

Type Locality. At Site 105, the type locality, 113.2 m of dark greenish-grey (5G5/1) to black (N/1) carbonaceous, zeolitic, silty claystones (Figure 11A) alternate with minor, lighter greenish-grey (5Y4/1) claystones. The lower half of the formation is mostly black, but centimetre- to decimetre-thick black beds alternate with dark grey and green-grey beds of comparable thickness at the top of the sequence. Contacts are sharp. Burrows are common in lighter claystone beds, but are lacking in the black claystones. Thin discrete silty laminae containing siderite, pyrite, clinoptilolite, cristobalite, and montmorillonite occur throughout the formation; laminae colors vary through grey, white, and brown (Figure 11A). Silty claystone, the dominant lithology, averages 65% clay-size particles. Clay minerals are dominantly montmorillonite and mica, with less than 2% chlorite and kaolinite (Table 8). Zeolite (clinoptilolite) is an important component (Figure 11C), constituting up to 38% of the bulk mineralogy in X-ray samples. Carbonates, quartz, cristobalite, feldspar, siderite, pyrite, and organic matter particles are minor constituents. Calcium carbonate content is generally less than 2%, but a number of samples show a mode of about 25%. Organic carbon content varies from 0.1 to 4.8% with one value of 14.8% near the top of the formation. Average porosity is about 55%.

Dinoflagellates and rare pyritized radiolaria

are usually the only microfossils present. Foraminifera, mostly primitive agglutinated forms, are rare except in a few intervals near the top of the sequence with well preserved planktic forms (cores 11 and 12, 304 to 322 m; Luterbacher, 1972). Nannofossils are absent except in the uppermost and lowermost portion of the formation. The upper part of the formation is rich in fish scales and teeth.

Contacts. The lower contact with the underlying Blake-Bahama Formation appears sharp (Tables 2, 7), but the core is broken at this point, and some sediment between the juxtaposed black clays and limestones may be missing. Persistence of dark grey colors, clay minerals, and carbonaceous debris into the top of the Blake Bahama limestones suggest that the contact is transitional.

The upper contact is defined at the uppermost occurrence of black clays characteristic of the formation (Table 7). This sharp contact divides black, greenish-grey, and grey sediments of the Hatteras Formation from variegated clays of the overlying Plantagenet Formation. A marked upward decrease in pyrite and zeolite accompanies the color change. A dramatic increase in organic carbon content is found at the top of the type section (core 9:4, 15 cm; 14.8% Corg) and also is reflected in other sites where the upper contact was cored (see below).

Regional Aspects. Dark carbonaceous clays were encountered at six other sites in the North American Basin (Table 7, Figures 10 and 24). Site 28 is omitted from Table 7 because of stratigraphic mixing and poor recovery. Although no major lithologic differences are encountered, varying degrees of induration require designations of clay, claystone, or shale at various sites. Minor differences in composition permit recognition of three regional subfacies characterized by: (1) zeolites (Site 105), (2) radiolarian- and/or nannoplankton-rich beds (Sites 386 and 391C) or radiolarian chert (Site 5A) with only traces of zeolites, (3) clay lacking zeolites or siliceous-calcareous lithofacies (101, 387). Type 2 subfacies probably characterize much of the basin-margin and ridge-flank region of the Hatteras Formation. In these areas, siliceous and calcareous debris were rapidly injected from elevated peaks or banks to the adjacent deep basin below the CCD. An extreme end-member of this process occurs at Site 4 where sediments, although dark grey in color, are dominated by pebbly mudstones with carbonate clasts of shallow-water origin. The type 3 subfacies is probably more typical of the remaining deep-basin Hatteras Formation than is the zeolitic subfacies at Site 105.

The Hatteras Formation overlies limestones and chalks of the Blake-Bahama Formation at all sites except at Site 386 where it rests on basalt. The lower contact of the formation is gradational through intervals which range from a few metres (Site 105) to as much as 100 m (Site 391). The upper contact with variegated clays of the overlying Plantagenet Formation is transitional over a few metres or less at Sites 386, 387, and 391C.

TABLE 7. GEOGRAPHIC DISTRIBUTION OF THE HATTERAS FORMATION IN THE NORTH AMERICAN BASIN

| Region | DSDP Leg | Location Site | Top m* | Top Core§ | Base m* | Base Core§ | Thickness | Age | Position |
|---|---|---|---|---|---|---|---|---|---|
| Lower Continental Rise | 11 | 105+ | 290.1 [-5531] | 9:3,110 | 403.3 | 17:1,30 | 113,2 | Cenomanian-Barremian | 34°53.7'N,69°10.4'W |
| Cat Gap | 1 | 4 | 114 [-5434] | between 2 & 2A | 143-191 | between 3 & 4 | 29-77 | Cenomanian-Aptian | 24°28.7'N,73°47.5'W |
| Cat Gap | 1 | 5 | 71-85.3 [-5425-5439.3] | between 3 & 1A | ∿145.1 | between 3A & 4A | ∿74.1 | ?-Early Albian | 24°43.60'N,73°38.5'W |
| Bahama Outer Ridge | 11 | 101 | 230** [-5098] | between 3A & 4A | 580** | between 8A & 9A | 350 | Albian-Barremian | 25°11.9'N,74°26.3'W |
| Bermuda Rise | 43 | 386 | 724.3 [-5507.3] | 41:5,80 | 965B | between 65 & 66 | 240.7 | Albian-Cenomanian | 31°11.2'N,64°14.9'W |
| Bermuda Rise | 43 | 387 | 478.4-488.5 [5596.4-5606.5] | between 29 & 30 | 583.8-593.1 | between 37 & 38 | ∿105 | Cenomanian-Middle Albian/Hauterivian | 32°19.2'N,67°40'W |
| Blake-Bahama Basin | 44 | 391 | 690 [-5355] | 6C - 3 | 991-1000.5 | between 13C & 14C | 299.5-309 | ?Cenomanian-Aptian/Albian | 28°13.7'N,75°36.9'W |

* Metres below sea floor. Range in values denotes interval without coring or recovery.
[] Depth below sea-level in square brackets.
TD Denotes total depth penetrated; bottom of formation not cored.
B Indicates that the formation rests directly on basement.
§ Core location given by: core number:section,depth in centimetres.
** Based on seismic reflectors; intervals 203-250 m and 543-599 m not cored.
+ Type locality.

TABLE 8. CHARACTERISTICS OF THE HATTERAS FORMATION

| Region | Leg | Site | Grain Size | | | | Carbon/Carbonate | | | Mineralogy (X-ray Diffraction) | | | | | | | | | Porosity | |
|---|---|---|---|---|---|---|---|---|---|---|---|---|---|---|---|---|---|---|---|---|
| | | | N | Sand | Silt | Clay | N | $CaCO_3$ | Organic | N | Quartz (bulk sample) | Quartz | Feldspar | Carbonate (total) | Kaolinite | Mica | Chlorite | Montmorillonite | Zeolite | N | % |
| Lower Continental Rise | 11 | 105+ | 28 | 0.81 ±0.75 | 36.80 ±9.38 | 62.40 ±9.37 | 29 | 7.41 ±11.55 | 1.83 ±2.77 | 8* | 11.9 ±5.1 | 4.0 ±1.9 | 0.6 ±1.1 | | 1.6 ±3.5 | 18.6 ±5.3 | 0.2 ±0.5 | 72.6 ±9.3 | 0.5[c] ±1.0 | 11 | 54.3 ±6.3 |
| Cat Gap | 1 | 4/4A | ? | 21.57 ±30.76 | 12.35 ±9.40 | 65.90 ±40.16 | 1 | 19.80 | 2.7 | 3b | 2.5 ±1.4 | | 0.4 ±0.8 | 89.4 ±12.1 | 0 | 2.1 ±3.7 | 0 | 4.1 ±7.1 | 0 | | |
| Cat Gap | 1 | 5A | | | | | | | | 2b | 8.1 ±7.9 | 61.15 ±51.83 | 0 | 32.5 ±45.9 | 0 | 0 | 0 | 0 | 3.7 ±5.3 | | |
| Bahama Outer Ridge | 11 | 10?A | 10 | 0.07 ±0.13 | 21.89 ±7.76 | 78.06 ±7.74 | 7 | 4.30 ±5.20 | 0.71 ±0.36 | 8* | 22.0 ±3.6 | 11.9 ±5.4 | 0.2 0.7 | | 5.7 ±6.2 | 37.4 ±20.3 | 1.2 ±1.5 | 42.0 ±26.4 | | 2 | 56.0 ±4.2 |
| Bermuda Rise | 43 | 386 | | | | | 57 | 32.96 ±26.60 | 12 1.66 ±2.20 | 44b | 33.7 ±20.3 | | 1.1 ±1.3 | 21.3 ±25.9 | 0.0 ±0.2 | 25.6 ±16.3 | 0.0 ±0.2 | 17.3 ±15.0 | 0 | 24 | 39.0 ±7.4 |
| Bermuda Rise | 43 | 387 | | | | | 3 | 16.0 ±27.71 | 4 5.57 ±5.76 | 13b | 39.3 ±11.6 | | 2.6 ±1.1 | 0 | 0.1 ±0.3 | 22.6 ±4.0 | 0.1 ±0.3 | 34.3 ±10.4 | 0.4 ±1.4 | 14 | 42.4 ±3.9 |
| Blake-Bahama Basin | 44 | 391C | | | | | 7 | | 0.88 ±0.66 | 7b | 33.0 ±13.. | | 13.5 ±9.1 | 14.5 ±31.5 | 2.1 ±1.9 | 35.7 ±8.7 | 0 | 16.7 ±9.8 | | 12 | 41.3 ±7.1 |

a analysis of less than 2μm fractions
b analysis of bulk samples
c in bulk samples recorded Clinoptilolite as abundant, ranging from 0-38.5%
+ type locality

The sediments near the top of the formation at Sites 386 and 387 have organic carbon contents as high as 7.7% and 14.2%, but this was not observed at Site 391C. At this site, the upper boundary of the formation is transitional in the upper 3 metres of core 6 and a disconformity may occur within this transition zone. At Site 101 a major hiatus separates the Hatteras Formation from overlying mid-Tertiary hemipelagic muds. At Sites 4/4A and 5/5A the Hatteras Formation is overlain by graded carbonate debris derived from the adjacent Bahama Banks (Figure 24), and a Late Cenomian to Early Turonian hiatus may be present (Pessagno, 1968).

Acoustic Character. No consistently observed seismic marker correlates with the top of the Hatteras Formation (Figures 6, 17). A weak reflector occurs near the top of the formation at Site 386, but it cannot be definitely correlated with the contact and is of only local extent (Tucholke, Vogt *et al.*, 1979). The absence of a reflector is not surprising because in general the physical-mechanical properties and velocities of the Hatteras and overlying Plantagenet Formations are similar (Demars, 1978).

The interval corresponding to the Hatteras Formation is normally acoustically nonlaminated or very weakly laminated in low-frequency (less than 100 Hz) profiler records. On airgun profiler records near Site 391C deconvolution removes much acoustic reverberation in the interval above Horizon β corresponding to the Hatteras Formation (Figure 6). The remaining internal reflectors probably represent calcareous beds derived from the adjacent Blake Escarpment. Sound velocities in the Hatteras and overlying Plantagenet Formations calculated from borehole-reflectors correlations are about 1.92 km/s at Site 386 (632 m overburden), 1.75 to 1.93 km/s at Site 387 (444 m), 1.75 km/s at Site 101 (230 m), 2.0 km/s at Site 105 (240 m), and 1.97 km/s at Site 391 (649 m). Velocities directly measured on core samples are scattered around these values, some higher measured velocities reflect the preferential recovery of more lithified rocks during the coring process.

Horizon β marks the lower boundary of the Hatteras Formation above Barremian and older crust, as discussed above, and the formation probably closely overlies oceanic layer 2 (basalt) in regions of younger crust.

Age. Ages established for the Hatteras Formation boundaries are variable, both because of diachronism and because of poor control resulting from discontinuous coring and impoverished microfauna (Table 7, Figures 7, 9, 13, 14). At the Site 105 type section the formation is Barremian-Cenomanian (Figure 7). At Site 391C (Figure 9) the formation ranges from Aptian (possibly Barremian) to Albian according to Benson, Sheridan *et al.* (1978). However G. Williams (Geol. Survey of Canada; pers. comm.) has identified dinoflagellates of Cenomanian age at the top of the black clays in core 6. This may result from either uncertainties in the biostratigraphy or the presence of an unrecognized hiatus between the Hatteras and Plantagenet Formations. A similar hiatus may occur at Sites 4 and 5 (Pessagno, 1968). The Hatteras Formation rests on Lower Albian crust at Site 386 and extends into the Late Cenomanian. An Albian-Cenomanian age span has been determined for the Hatteras Formation at Site 386 (Figure 13; Tucholke, Vogt *et al.*, 1979). At Site 387 the formation is dated only by palynomorphs and extends from Late Hauterivian-Middle Albian to Middle Cenomanian-Turonian (Figure 14).

Depositional Environment. The origin of the thick dark carbonaceous claystones in the Atlantic Ocean has been the subject of considerable speculation (Hollister, Ewing *et al.*, 1972; Fischer and Arthur, 1978; Schlanger and Jenkyns, 1976; Dean *et al.*, 1978).

Mineralogic and fossil composition of the formation in North American Basin sites suggest pelagic and hemipelagic deposition in a deep bathyal to abyssal environment below the CCD. The black clay occurrence is not strictly depth-dependent, as is indicated by lateral transitions to shallower, dark-grey bituminous marl lithofacies on the slope off Spanish Sahara (Site 369, Lancelot, Seibold *et al.*, 1978), southern France and England (Schlanger and Jenkyns, 1976), and in Venezuela (Miller *et al.*, 1958) and Columbia (Morales *et al.*, 1958). In the western North Atlantic, the entire basin below about 3200 m was intermittently anoxic (Figure 23).

The development of the black clays has been interpreted to result from a highly stratified water column, with stagnant or oxygen-depleted deep water overlain by oxygenated and circulating water (Schlanger and Jenkyns, 1976; Jansa *et al.*, 1978; Tucholke and Vogt, 1979). Oxygenated shallow water is indicated by deposition of light-colored Aptian-Albian nannofossil oozes at Sites 390 and 392 on the Blake Nose (Benson, Sheridan *et al.*, 1978). Sediments deposited on the continental shelves during the 'black clay event' also show normally oxygenated and current-influenced environments (Jansa and Wade, 1975a; Smith *et al.*, 1976). Indeed, coral-rudist reefs appear to have flourished along the North American continental margin during this period (Douglas *et al.*, 1973). The interbedding of lighter, burrowed sediments in the Hatteras Formation shows that the anoxic conditions were intermittently destroyed and the deep-basin bottom water oxygenated.

Tucholke and Vogt (1979) suggest that the confinement of thick black-clay facies to the Atlantic basins, the Caribbean, and the Indian Ocean indicate that circum-basin barriers to deep flow were responsible for the stagnation. Another hypothesis was proposed by Dean *et al.* (1978), who considered that the black clays were diagenetic facies and that reducing conditions developed within the sediment as a result of increased

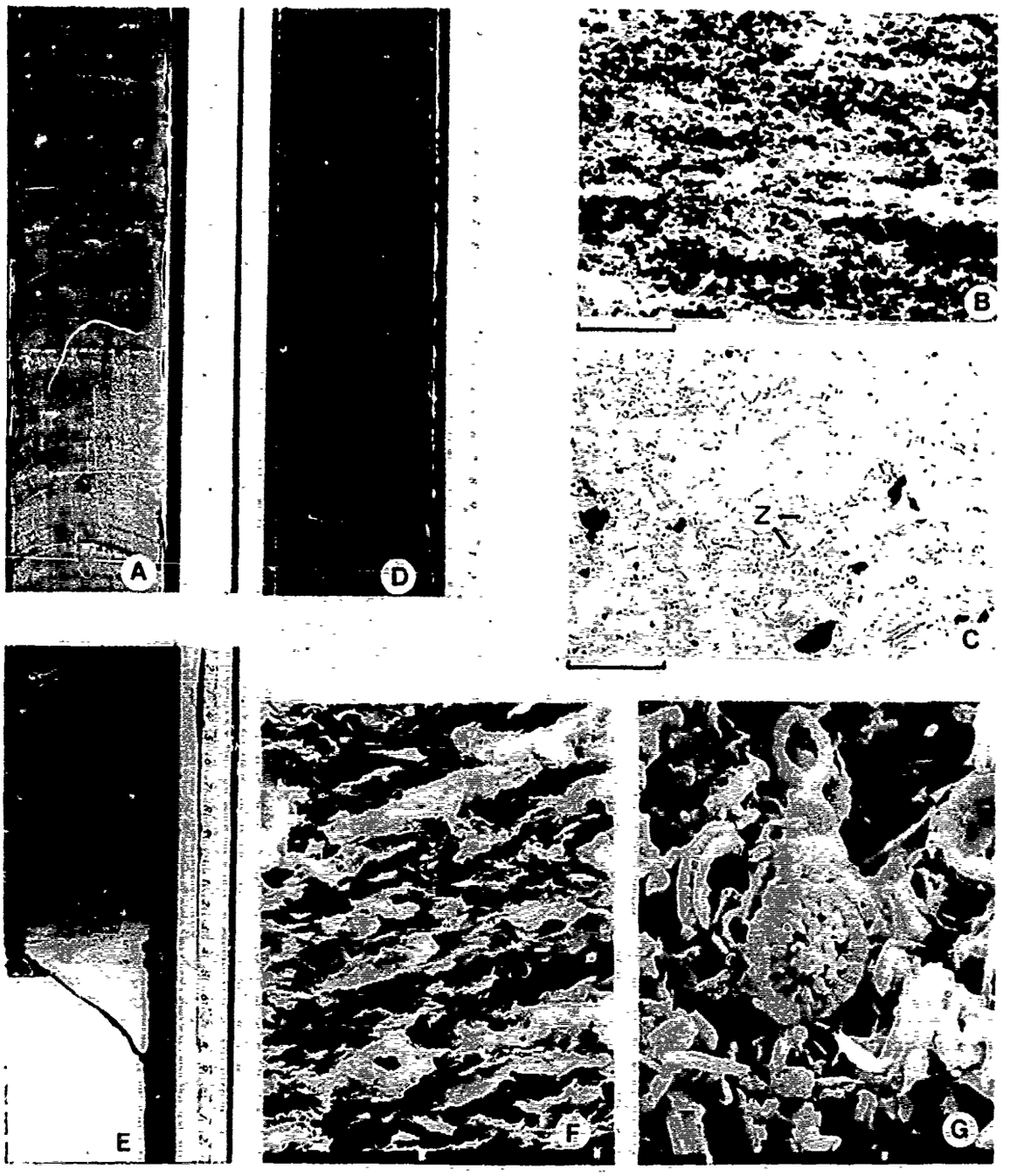
A
D
B
Z
C
E
F
G

organic productivity and subsequent decay of organic matter in the sediment. The reducing conditions may have extended above the water-sediment interface, as indicated by the lack of bioturbation in black clays.

The conditions which caused the black clays to be deposited were geologically rapid but not catastrophic, as is indicated by the commonly transitional contact between the Blake-Bahama and Hatteras Formations. The rise of the CCD at the onset of deposition of the Hatteras Formation (Figure 23) may have resulted from decreased productivity of skeletal carbonate with resulting depletion of calcium carbonate in the bottom water, or from the development of acidic, stagnant bottom water. Sediment accumulation rates of 3 to 5 m/m.y. characterize the deep-basin sites, but higher rates of 12 to 19 m/m.y. occur at Sites 101 and 391 near the continental margin and at Site 386 where local turbidites filled the paleo-ridge-flank fracture valley.

Identifying features. The black and dark grey or greenish-grey colors, clayey composition, lack of bioturbation in the black beds, presence of carbonaceous debris and usual absence of biogenic carbonate are the distinctive features of the Hatteras Formation.

Correlation with Other Units. The period of deep-sea black clay deposition corresponds to a period of transgression on the North American continental margin. On the Scotian Shelf clastic rocks of Upper Missisauga to Logan Canyon Formations enclosing numerous coal beds were deposited in a deltaic and shallow open shelf environment (Jansa and Wade, 1975a). Similar transgressive marginal-marine clastic sequences were penetrated by the Esso Standard Hatteras Gulf Well No. 1 on Cape Hatteras, North Carolina, (Swain, 1952) and by the COST B-2 well located in the Baltimore Canyon Trough (Smith *et al.*, 1976). All these sequences are characterized by the presence of coal seams and coalified plant debris, enclosed in sandstones and shales, but the bottom conditions were generally oxygenated. Even though the shelf sediments contain a high organic matter content, they cannot be correlated with the deep-sea black clay facies on lithologic criteria.

## Plantagenet Formation

Varicoloured, locally zeolitic, noncalcareous claystone forms a thin but widespread unit which overlies the black claystone of the Hatteras Formation throughout the central part of the North American Basin. We propose the name Plantagenet Formation for the variegated claystone. Plantagenet Bank, the southwestern lobe of the Bermuda pedestal, is located near the type locality at Site 386 (Table 1, Figure 1). Deposition at this site appears to have been continuous across the upper boundary of the formation in contrast to a widespread unconformity present at many other sites.

The regional significance of the varicolored zeolitic clays was recognized by Lancelot *et al.* (1972), who described the unit as "Upper Cretaceous to Lower Tertiary(?) multicolored clays". A thin calcareous unit near the top of the variegated claystone is described separately as a member of the Plantagenet Formation.

Type Locality. At Site 386, the type locality, 92.3 m of the claystone is characterized by dusky yellowish-brown (10YR2/2), moderate brown (5YR4/4),

Figure 11. Hatteras and Plantagenet Formations.

A. Black (N 1), zeolitic, silty claystone, with occasional thin silt laminae, but mostly massive. Hatteras Formation (Leg 11-105-15:6, 99-113 cm).

B. Hatteras Formation claystone rich in organic matter. Organic particles are lipids, brownish, elliptical, and circular in shape and 8 µm in average diameter (thin section, ordinary light, scale bar = 100 µm) (Leg 11-105-16:1, 75 cm).

C. Zeolitic silty claystone of the Hatteras Formation. Clay with pods of quartz silt, minor zeolites (Z), and mica; pyrite, organic debris occur in traces (thin section, ordinary light, scale bar = 100 µm, Leg 11-105-11:1, 101 cm).

D. Zeolitic claystone of the Plantagenet Formation, very finely laminated with irregularly banded dusky yellowish-brown (10 YR 2/2), and moderate brown (10 YR 4/4) colors. Note dark color cutting across laminae at 56 and 63 cm (Leg 43-386-38:4, 48-73 cm).

E. Bluish-white (5B 9/1) and light greenish-grey (5G 8/1) limestone of the Crescent Peaks Member in contact with overlying dusky red (10R 3/5) claystone of the Plantagenet Formation (Leg 43-386-35:4, 1-23 cm).

F. Scanning electron micrograph of claystone from the Plantagenet Formation (Leg 43-386-35:2, 98 cm). Note dominantly clay composition and strong lineation of clay particles. Scale bar 30 µm.

G. Scanning electron micrograph of chalk from the Crescent Peaks Member (Leg 43-385-13:2, 53 cm). In contrast to photograph (F), sediment is dominated by nannofossils, some of which are well preserved. Note high interparticle porosity. Scale bar 10 µm.

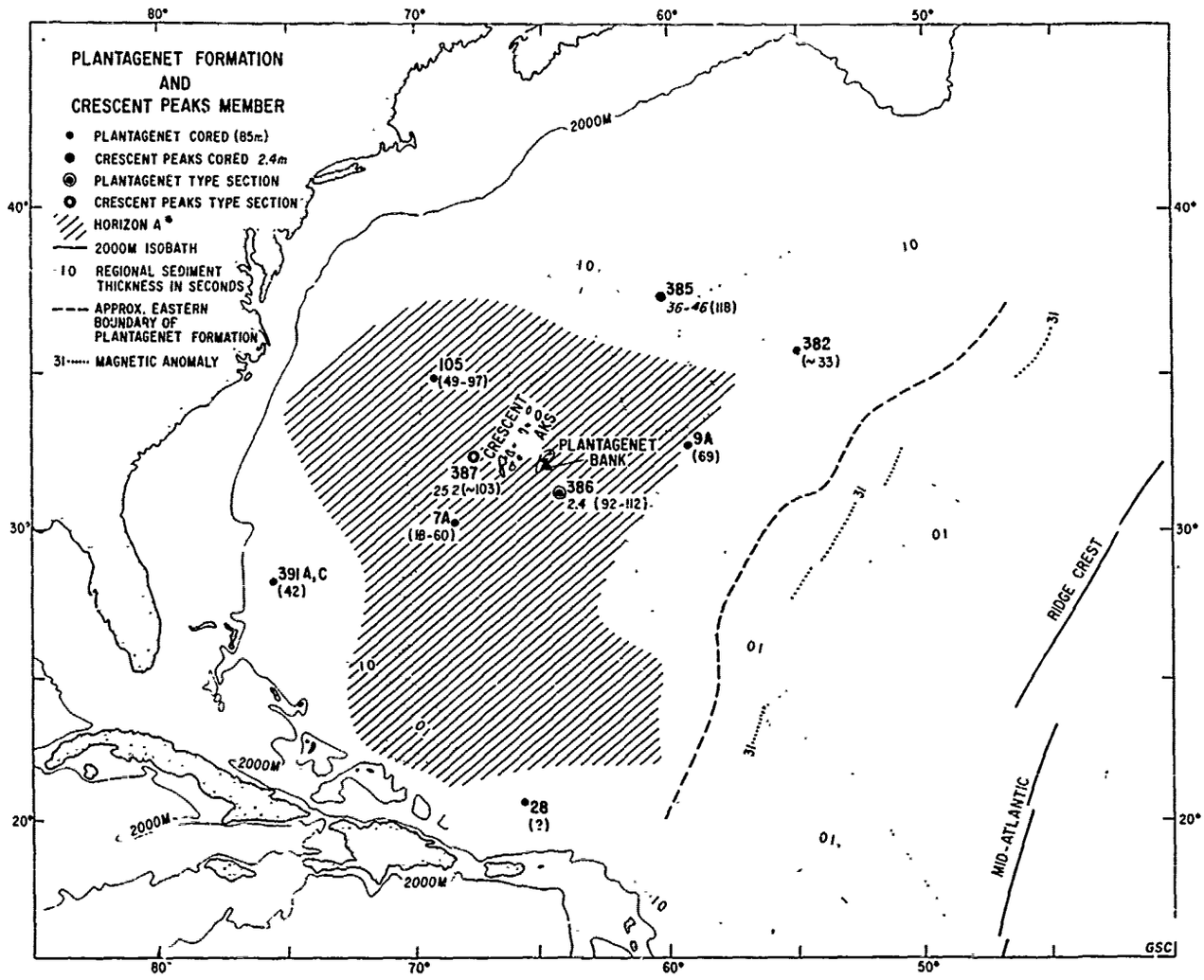


Figure 12. Boreholes that have cored sediments of the Plantagenet Formation and Crescent Peaks Member. Italicized numbers show thickness of Crescent Peaks (metres). Thicknesses in parenthesis are of Plantagenet Formation. Seismic Horizon A* (top of Crescent Peaks Member) and approximate eastern limit of the formation adopted from Tucholke and Mountain (1979).

and dusky dark red (10R315) colors, with some light greenish-grey (5G8/1) beds a few centimetres to decimetres in thickness (Figure 11D). The sequence consists of a reddish-brown interval with increasing green-grey intercalations in the lower part (cores 41, 40), a variegated reddish interval in cores 39 and 38, and a reddish-brown interval (cores 36 to 35). Zeolites (clinoptilolite, phillipsite) form 6 to 20% of the sediment in the central, variegated section; the remaining components are clays (illite and montmorillonite, 60 to 80%) and, in order of decreasing abundance, quartz, disordered cristobalite, and feldspars (Table 10). Iron and manganese oxides including micronodules, and traces of siderite (?) are observed in smear slides. The upper and lower reddish claystones differ in that they contain only traces of zeolites and altered ash, and they have 5 to 15% chlorite and kaolinite. Rare primitive agglutinated foraminifera and poorly preserved radiolarians also are present. Thin, irregular lamination is the only sedimentary structure in this formation. The upper part of the formation contains a distinctive calcareous unit (in Core 35, Crescent Peaks Member; Figure 11E), described later.

Contacts. The Plantagenet Formation overlies the black clays of the Hatteras Formation in a transitional zone of interlaminated red and green-grey claystones a few meters thick. At the type locality, the lower contact of the Plantagenet Formation is defined at the uppermost occurrence of dominantly green-grey and black beds, although

occasional reddish colors recur deeper in the Hatteras Formation. The contact also marks a downward change in mineralogy to more quartz-rich sediment with less clay, consisting entirely of illite and montmorillonite.

The upper contact at Site 386 occurs in a 19 m uncored interval below siliceous claystones of the overlying Bermuda Rise Formation. Low accumulation rates of 2 to 3 m/m.y., calculated for this interval, suggest that the pelagic red clays of the Plantagenet Formation comprise most of the uncored interval.

The contact of the Plantagenet Formation with the overlying Bermuda Rise Formation has been cored at two other sites, 385 and 387 (Figure 24). At Site 385 the contact is placed at 165 m subbottom (between cores 6 and 7) where there is a sharp compositional change from Plantagenet clays rich in zeolites with palagonite and amorphous iron-oxides, to the overlying siliceous, cherty Bermuda Rise Formation. The color change is not sharp; the upper part of the Plantagenet Formation at Site 385 is yellow-brown, brown and green-grey and is locally silty.

At Site 387 the contact is very gradational between 376.6 m and 444.2 m subbottom (Figure 24). Red-brown and greenish variegated clays are found as shallow as 377 m, but cherty siliceous sediments of the overlying Bermuda Rise Formation persist as deep as 413 m subbottom. Picking the upper boundary on color alone is also complicated by the fact that black clays similar to the Hatteras Formation recur in this interval.

At Sites 385 and 387, the Plantagenet Formation above the Crescent Peak Member has very little kaolinite (<5%) or chlorite. This mineralogy may be characteristic of the top of the Plantagenet Formation, up to 19 m of which was uncored at the Site 386 type locality.

An alternative is that the sequence above the Crescent Peak Member at Sites 385 and 387 represents a separate lithologic unit from the Plantagenet Formation as suggested by changes in color and sediment composition. With presently available data, we cannot satisfactorily resolve this question.

Regional Aspects. Variegated claystones were penetrated in seven other sites on the Bermuda Rise (Sites 7A, 9A, 387), New England Seamounts (382, 385), lower continental rise (105), Blake-Bahama Basin (391A,C), and perhaps on the Greater Antilles Outer Ridge (28) where a few fragments of red and variegated claystones were recovered (Table 9, Figures 12, 24). Composition of the claystones is variable. For example, zeolites are not reported from Sites 7A, 387 and 391 (Table 10). Clay minerals comprise the bulk of most

TABLE 9. GEOGRAPHIC DISTRIBUTION OF THE PLANTAGENET FORMATION IN THE NORTH AMERICAN BASIN

| Region | DSDP Location Leg | Site | Top m* | Top Core§ | Base m* | Base Core§ | Thickness (m) | Age | Position |
|---|---|---|---|---|---|---|---|---|---|
| Bermuda Rise | 43 | 386+ | 611.9-632.0 [5394.9 -5415] | between 34 & 35 | 724.3 | 41:5,80 | 92.3-112.0 | Paleocene-Cenomanian | 31°11.2'N,64°14.9'W |
| Bermuda Rise | 1 | 7 | 236-278 [5421 - -5463] | between 2 & 2A** | (296 TD) | 3A | 18-60 | (undated, pre-Eocene) | 30°08.0'N,68°17.8'W |
| Bermuda Rise | 2 | 9 | 682-765** [5663 - -5746] | between 1A & 3A | 834B | between 5A & 6A | 69 | "Cretaceous"-Campanian | 32°46.4'N,59°11.7'W |
| Lower Continental Rise | 11 | 105 | 193-241 [5444 - -5492] | between 4 & 5 | 290.1 | 9:3,110 | 49-97 | Tertiary?-overlies late Cenomanian | 34°53.7'N,69°10.4'W |
| Nashville Seamount | 43 | 382 | 352 [-5879] | 15:5,10 | 385.3 | 19:2,54 | ~33 | Campanian | 34°25.0'N,56°32.3'W |
| Vogel Seamount | 43 | 385 | 165 [-5121] | between 6 & 7 | 283 | 16:3,146 | 118 | early Paleocene-Coniacian? | 37°22.2'N,60°09.5'W |
| Bermuda Rise | 43 | 387 | 376.6-444.2 [-5494.6 -5562.2] | 23:2,82 through 27:2,148*** | 478.4-488.5 | between 29 & 30 | ~103 | overlies early Eocene-Cenomanian | 32°19.2'N,67°40.0'W |
| Blake-Bahama | 44 | 391 | 649 [-5613] | 21A | 691.5 | 6C:3 | 42.5 | overlies Cenomanian | 28°13.7'N,75°36.9'W |

* Metres below sea floor. Range in values denotes interval without coring or recovery.
[] Depth below sea level in square brackets.
*** Transitional boundary.
TD Denotes total depth penetrated; bottom of the formation was not cored.
B Indicates that the formation rests directly on basement.
§ Core location given by: core number:section,depth in centimetres.
** Core 2A appears to contain downhole corings (core catcher contains Upper Cretaceous microfauna).
+ Type locality.

TABLE 10. CHARACTERISTICS OF THE PLANTAGENET FORMATION (EXCLUSIVE CRESCENT PEAKS MEMBER)

| Region | Leg | Site | Grain Size | | | | Carbon/Carbonate | | | Mineralogy (X-ray Diffraction) | | | | | | | | | Porosity | |
|---|---|---|---|---|---|---|---|---|---|---|---|---|---|---|---|---|---|---|---|---|
| | | | N | Sand | Silt | Clay | N | $CaCO_3$ | Organic | N | Quartz (bulk sample) | Quartz | Feldspar | Carbonate (total) | Kaolinite | Mica | Chlorite | Montmorillonite | Zeolite | N | % |
| Bermuda Rise | 43 | 386+ | | | | | 10 | 0 | 3 1.58 ±2.65 | 9b | 14.3 ±5.3 | | 3.0 ±1.2 | 0 | 3.1 ±3.4 | 30.0 ±13.1 | 1.9 ±2.0 | 36.2 ±10.0 | 7.8 ±7.3 | 7 | 47.0 ±4.4 |
| Bermuda Rise | 1 | 7A | 4 | 1.4 ±2.34 | 17.13 ±5.48 | 81.73 ±6.85 | 3 | 16.1 ±14.04 | 0.1 0 | 6b | 29.6 ±4.2 | | 3.3 ±3.3 | 0.7 ±1.9 | 36.1 ±7.2 | 27.5 ±6.4 | 0 | 0 | 0 | | |
| Bermuda Rise | 2 | 9A | 1 | 1.1 | 21.5 | 77.4 | 2 | 0 | 0.1 ±0.14 | 2b | 5.8 ±6.0 | | 4.2 ±3.2 | 0 | 1.2 ±1.7 | 2.6 ±3.7 | 0 | 0 | 24.4 ±26.1 | | |
| Nashville Seamount | 43 | 382 | | | | | 21 | 31.43 ±18.94 | | 13b | 3.1 ±4.6 | | 11.4 ±7.9 | 12.9 ±16.5 | 4.3 ±8.6 | 9.3 ±11.7 | 4.7 ±12.4 | 52.2 ±23.7 | 1.9 ±1.5 | 3 | 61.3 ±0.4 |
| Vogel Seamount | 43 | 385 | | | | | 15 | 18.9 ±16.2 | 2 0.06 ±0.03 | 8b | 13.6 ±3.5 | | 3.9 ±1.4 | 11.1 ±15.7 | 8.9 ±8.3 | 18.5 ±6.0 | 3.1 ±2.9 | 34.8 ±21.0 | 5.5 ±7.5 | 17 | 56.3 ±5.3 |
| Bermuda Rise | 43 | 387 | | | | | | | 1 0.53 | 2b | 15.0 0 | | 3.0 ±1.4 | 15.0 ±21.2 | 14.8 ±10.8 | 33.7 ±18.1 | 9.6 ±6.3 | 8.9 ±12.6 | 0 | 4 | 39.0 ±9.0 |
| | | | (including Crescent Peaks Member) | | | | 3 | 42.0 ±1.73 | 0.53 | 4b | 10.7 ±4.9 | | 1.5 ±1.9 | 30.0 ±21.6 | 9.7 ±9.2 | 25.1 ±16.2 | 6.5 ±5.5 | 16.4 ±14.6 | 0 | 4 | 41.3 ±5.8 |
| Lower Continental Rise | 11 | 105 | 21 | 1.16 ±1.59 | 26.52 ±14.54 | 72.32 ±14.65 | 20 | | 0.1 ±0.02 | 5* | 25.1 ±6.7 | 7.4 ±2.6 | 0 | | 19.1 ±5.3 | 29.7 ±6.1 | 1.2 ±2.6 | 40.6 ±9.2 | 2.0 ±4.5 | 14 | 48.5 ±8.3 |
| Blake-Bahama Basin | 44 | 391A&C | | | | | | | | 3b | 51.6 ±7.1 | | 11.6 ±2.3 | 0 | 5.7 ±1.5 | 21.0 ±3.6 | 0 | 10.0 ±8.9 | 0 | 4 | 42.4 ±3.9 |

\+ type locality
* analysis of less than 2 um fractions
b analysis of bulk samples

samples and kaolinite and chlorite are more abundant than in the Hatteras Formation. Manganese micronodules are present in some claystone beds from the upper part of the formation at Sites 7A and 9A. Volcanic glass is uncommon in claystones at Site 387, but is a persistent, minor component at Sites 382, 385, and 386 which contain volcaniclastic detritus derived from the New England Seamounts. Volcanic glass and shelf-derived quartz silt also form some laminae in the variegated clays in the Blake-Bahama Basin (Site 391C). Limonite (?Fe-Mn) nodules are also present at Site 391A in the uppermost part of the formation (core 21). On the lower continental rise (Site 105) the claystones display color variations with bands of pale brown, red, white, yellow, orange, pink, reddish-brown, purplish, black, and pale green. These claystones are composed of montmorillonite, mica, and kaolinite. Zeolites, principally clinoptilolite, with minor heulandite(?) and phillipsite are present in the upper part of the formation; quartz is common, and feldspars are a minor constituent. A striking feature of the Plantagenet Formation at Site 105 is enrichment of the heavy metals, Mn, Zn, Cu, Pb, Cr, Ni, and V (Lancelot *et al.*, 1972). The resultant mineral assemblage includes sphalerite and todorikite (Mn-oxide) along with a variety of iron minerals (pyrite, siderite, goethite, hematite, and iron montmorillonite). The Plantagenet Formation is almost completely devoid of fossils at all sites, with only occasional traces of primitive agglutinated foraminifera, radiolaria, and phosphatic fish debris. Nannoplankton are only locally common (Sites 386, 387).

At all sites where the Plantagenet Formation was completely penetrated by drilling, it is underlain by the black claystones of the Hatteras Formation or by basaltic basement. The boundary normally is transitional over a few decimetres to a few metres. Thin beds of variegated nonzeolitic clays similar in color to the Plantagenet Formation are locally interbedded in the middle part of the Hatteras Formation at Sites 391C (Core 10) and 386 (Core 46).

The Plantagenet Formation is overlain by chert and siliceous clays of the Bermuda Rise Formation at Sites 7A, 9, 28, 385, 386, and 387, and it is truncated by an erosional unconformity at Sites 105, 382 and 391C (Figure 24).

The Plantagenet facies at Sites 382 and 385 are unusual as they contain volcaniclastic debris up to sand size emplaced during the construction and weathering of Nashville and Vogel Seamounts, respectively (Tucholke, Vogt *et al.*, 1979). At both sites we consider the base of the Plantagenet Formation to lie at the first downhole occurrence of coarse basaltic breccia.

Acoustic Character. The base of the Plantagenet Formation is not marked by a well defined reflector (Figure 17). The upper contact with the Bermuda Rise Formation corresponds approximately to the seismic transition from an acoustically nonlaminated (Plantagenet) to an acoustically laminated sequence of cherty sediments in the Bermuda Rise Formation, but this correlation is not always observed. Nearer the continental margin, at Sites 105 and 391C, the erosional unconformity at the top of the Plantagenet Formation is a well defined reflector, Horizon $A^U$ (Tucholke, 1979). Within the Plantagenet Formation, the top of the Crescent Peaks Member correlates with Horizon A* (discussed below). Sound velocities in the Plantagenet Formation are similar to those in the Hatteras Formation, as noted earlier.

Age. Despite a general lack of fossils in the variegated claystone, several approximate age determinations are now available. At the Site 386 type locality, Middle Paleocene nannoflora overlie Maastrichtian sediments at the top of the formation (core 35). The sediments near the base of the formation (core 44) are Cenomanian in age (Figure 13). At Site 387 (Figure 14) the upper transitional interval above the carbonate member contains nannofossils of Early Eocene (core 23) and Paleocene (cores 24 to 26) age. The lower part of the formation overlies Cenomanian beds and contains a Campanian-Maastrichtian nannoflora. The interval above the carbonate member at Site 385, tentatively assigned to the Plantagenet Formation (cores 7 to 11), contains an Early Paleocene nannoflora at the base. At Site 105 a speculative Tertiary age (Figure 7) from dinoflagellates for the upper part of the formation may result from downhole contamination. At Site 391C the uppermost core in the formation is unfossiliferous, but the underlying core 4C contains palynomorphs not younger than Campanian (G. Williams, pers. comm.). The base of the Plantagenet Formation at this site overlies beds dated Cenomanian (G. Williams, pers. comm.; Figure 9).

Depositional Environment. The Plantagenet Formation is a pelagic deposit which accumulated in an oxygenated environment, in contrast to the underlying Hatteras clays. Accumulation rates were very low (less than a few metres per million years), although local abundance of kaolinite and chlorite suggests some terrigenous influence even on the Bermuda Rise. The lack of calcareous fossils indicates deposition below the CCD and the paucity of siliceous microfossils also suggests minimal surface productivity. Compositionally, the Plantagenet clays are very similar to the mid-plate, mid-gyre 'red clays' presently being deposited in the North Pacific but differ in having greater concentrations of metallic ions. The minerals formed in these clays at Site 105 prompted Lancelot *et al.* (1972) to compare the Plantagenet clays with the Red Sea brine deposits and speculate that the enrichment in metallic ions was due to volcanic hydrothermal exhalations. However, the formation at most sites is not near any recognized spreading centre or active rift,

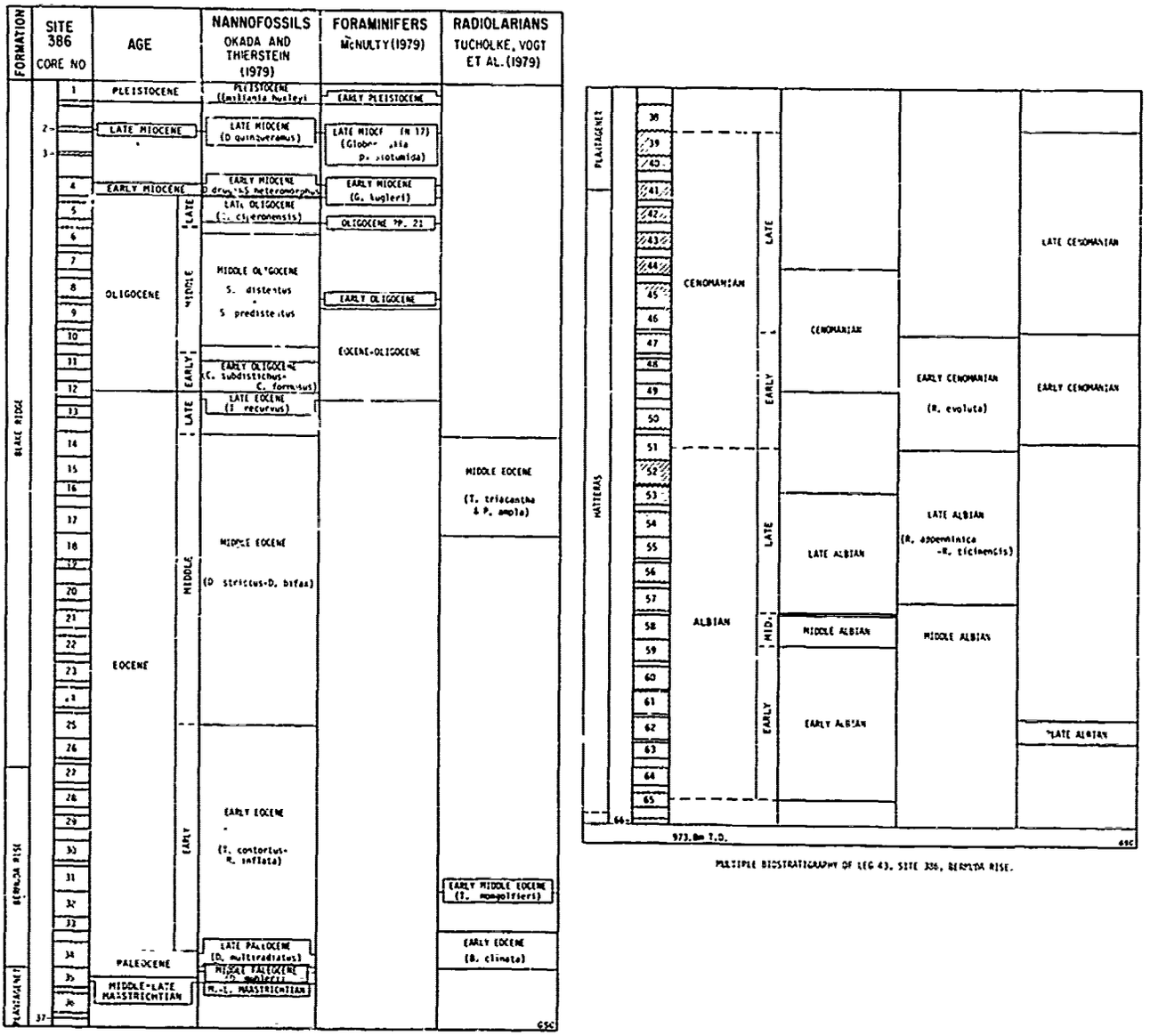


MULTIPLE BIOSTRATIGRAPHY OF LEG 43, SITE 386, BERMUDA RISE.

Figure 13. Multiple biostratigraphy of Site 386 located on Bermuda Rise.

and the widespread distribution of the formation as now recognized makes this comparison even less persuasive. An alternative explanation by Arthur (1979) is that enrichment of metallic ions was caused by upward diffusion and dewatering of the thick underlying black clays. The very long time interval, perhaps 30 m.y., represented by this relatively thin unit also suggests that the Plantagenet Formation either represents an extremely condensed sequence or includes undetected hiatuses. Thus submarine weathering may have played a role in the removal of fossils, the oxidation of iron, and the concentration of heavy metals. The local abundance of zeolites and occurrence of volcanic ash could be related to the volcanic activity of the Kelvin Seamount chain. Near the seamounts the Plantagenet Formation probably intertongues with coarse volcaniclastic debris as suggested by Sites 382 and 385 (Figure 24).

Identifying features. The variegated colors, clayey and locally zeolitic composition, lack of biogenic carbonate, low accumulation rates and presence of seismic Horizon A* in the upper part of the unit are distinctive features of the Plantagenet Formation.

Correlation with Other Units. No lithologic unit similar to the Plantagenet Formation is known on the North American margin. Synchronous, greenish-grey, calcareous glauconitic claystones

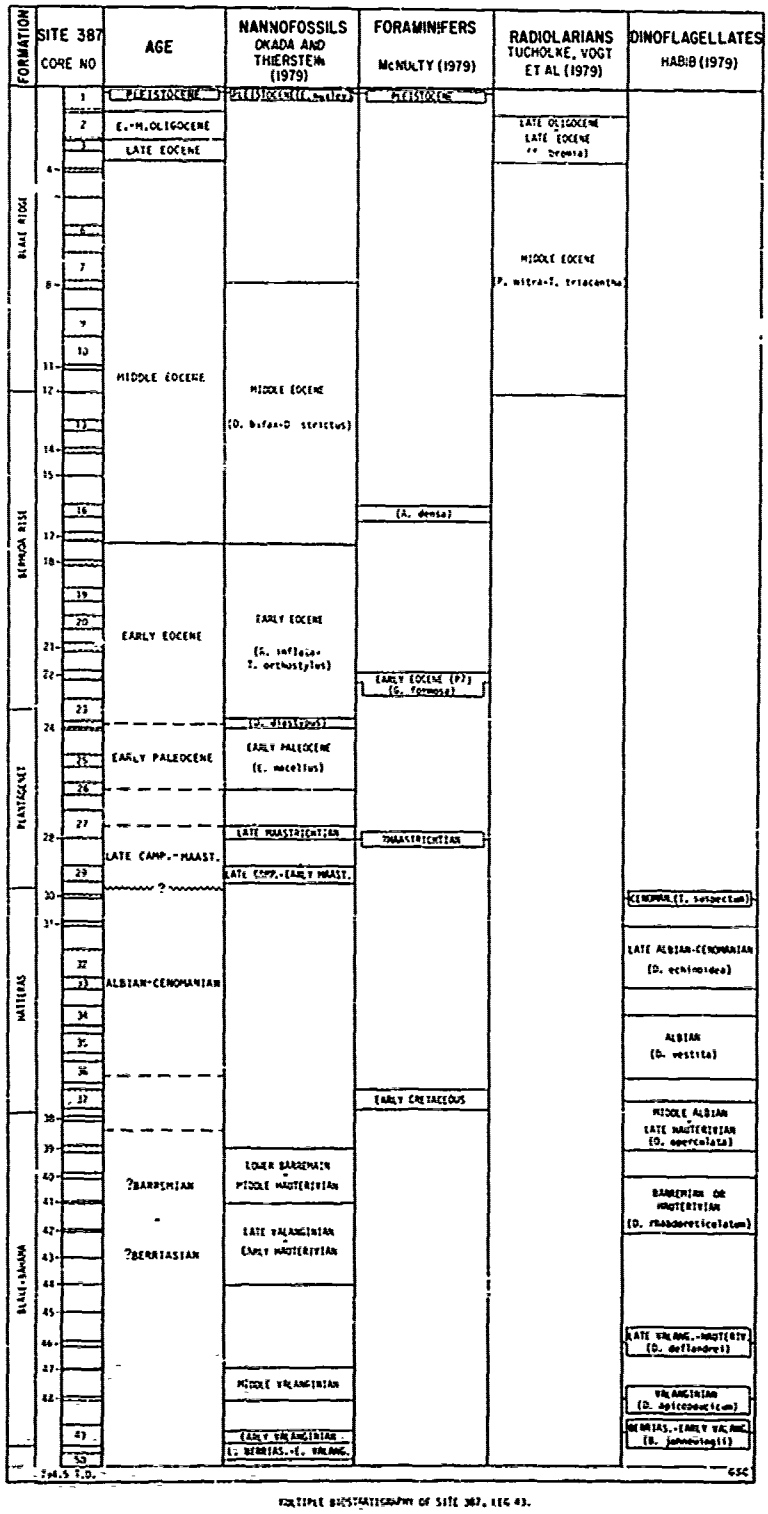


MULTIPLE BIOSTRATIGRAPHY OF SITE 387, LEG 43.

Figure 14. Multiple biostratigraphy of Site 387 located on Bermuda Rise.

and rare sandstones were deposited on the North American margin in a shallow to moderately deep shelf environment (Jansa and Wade, 1975a; Smith *et al.*, 1977). The Plantagenet Formation also lacks a well defined counterpart in the eastern North Atlantic, where mainly greenish-grey clays and marls were widespread at approximately the same time (Lancelot, Siebold *et al.*, 1978). Exceptions are in the Cape Verde Basin, Site 367 (Jansa *et al.*, 1978), and west of the Iberian Peninsula, Site 398 (Ryan, Sibuet *et al.*, 1976) where Upper Cretaceous variegated claystones similar to the Plantagenet Formation occur. The influence of highly oxygenated waters on sedimentation extended into the Tethys region, as suggested by the presence of Upper Cretaceous reddish marls and clays exposed in the Bettic Cordillera and Lombardy Basin in Italy (Jansa, in press).

## Crescent Peaks Member

A relatively thin but lithologically conspicuous unit of nannofossil chalks, marls, and limestones in the upper part of the Plantagenet Formation is named the Crescent Peaks Member. The name is derived from a series of basement peaks west of Bermuda that were originally named by Heezen *et al.* (1959; Figure 1). The type locality is at Site 387 (Table 11, Figure 12) where 25.2 m of homogeneous, moderate olive to light olive-grey marly chalk is intercalated with subsidiary calcareous claystone (Figure 11E). The chalk is composed of micritic carbonate (42%) including nannofossils (10%), and foraminifera (2%); other constituents being montmorillonite, mica, minor kaolinite, chlorite and quartz (Table 12). The contact with the underlying red-brown and green-grey claystone was not recovered, although coring was continuous; the contact probably is sharp like the upper contact with dark greenish-grey claystone (Figure 11E).

Regional Aspects. Comparable carbonates were recovered at Sites 385 at Vogel Seamount and 386 on the Bermuda Rise (Figure 12, Table 11). At Site 386 light greenish-grey, laminated marly limestone 2.4 m thick is enclosed by sharp contacts within reddish claystones of the Plantagenet Formation. At Site 385, 36 to 46 m of light greenish-grey marly nannofossil ooze is intercalated with a few beds of calcareous silty clay containing volcanic glass and zeolites. The unit is underlain by yellowish-red clay with interbeds of greenish-grey vitritic clay but the contact was not cored. It is overlain by brownish-grey zeolitic clay, with a sharp burrow-mottled contact.

Since deposition of the Crescent Peaks Member probably indicates regional depression of the CCD (see Depositional Environment) the unit may be correlative with thicker ridge-flank carbonates cored at Site 10 (Figures 1, 22). The intervening Site 9 did not recover carbonates correlative with the Crescent Peaks Member, but there was a 75 m coring gap at the appropriate level (Figure 24). Seismic mapping of Horizon A* (see below) suggests that the Crescent Peaks Member extends over Mesozoic crust in the entire basin to paleodepths of approximately 5300 m.

Acoustic Character. The top of the Crescent Peaks Member appears to correlate with seismic Horizon A* on the Bermuda Rise (Figure 17; Tucholke, Vogt *et al.*, 1978), but the reflector is not clearly indicated in the seismic section at Site 385. Horizon A* merges with or closely underlies the Horizon $A^U$ unconformity at Site 105; if present at Site 105, the Crescent Peaks Member may have been missed in a 49 m uncored interval above the highest Plantagenet clays recovered in core 5.

The limits of distribution of Horizon A* (Figure 12) probably indicate lateral facies changes in the sedimentary section (Tucholke, 1979). To the west, Horizon A* becomes weaker and is difficult to trace within a thick series of continental margin reflectors. These reflectors may represent progradation of continental margin turbidites and fans in the Late Cretaceous and Early Cenozoic. Horizon A* is truncated by the erosional unconformity marked by Horizon $A^U$,

TABLE 11. GEOGRAPHIC DISTRIBUTION OF THE CRESCENT PEAKS MEMBER OF THE PLANTAGENET FORMATION IN THE NORTH AMERICAN BASIN

| Region | DSDP Location Leg | Site | Top m* | Top Core | Base m* | Base Core | Thickness (m) | Age |
|---|---|---|---|---|---|---|---|---|
| Bermuda Rise | 43 | 387+ | 444.2 [-5562.2] | 27:2,148 | 469.4 | 28:1,150 | 25.2 | Late-Middle Maastrichtian |
| Vogel Seamount | 43 | 385 | 205.8 [-5161.8] | 11:2,125 | 241 through 251 | between 13 & 14 | 36.2-46.2 | Early Paleocene-Middle Maastrichtian |
| Bermuda Rise | 43 | 386 | 636.6 [-5419.6] | 35:4,15 | 639 | 35:5,100 | 2.4 | Middle Maastrichtian |

\+ Type locality.
* Metres below sea floor. Range in values denotes interval without coring or recovery.
[] Depth below sea-level in square brackets.

TABLE 12. CHARACTERISTICS OF THE CRESCENT PEAKS MEMBER*

| Region | Leg | Site | Carbon/Carbonate | | | Mineralogy (X-ray Diffraction) | | | | | | | Porosity | |
|---|---|---|---|---|---|---|---|---|---|---|---|---|---|---|
| | | | N | $CaCO_3$ | Organic | N | Quartz (bulk sample) | Feldspar | Carbonate | Mica | Chlorite | Montmorillonite | Zeolite | N | % |
| Bermuda Rise | 43 | 387+ | 3 | 42.0 ±1.73 | | 2b | 6.5 ±0.7 | 0 | 45.0 ±7.1 | 16.4 ±2.7 | 3.3 ±3.5 | 23.9 ±15.9 | 0 | 2 | 43.5 ±0.2 |
| Vogel Seamount | 43 | 385 | 3 | 42.33 ±4.93 | 0.08 | 3b | 14.0 ±3.4 | 3.0 ±3.4 0 | 29.7 ±6.5 | 20.9 ±3.9 | 5.0 ±1.4 | 13.8 ±3.0 | 0.3 ±0.6 | 3 | 52.1 ±3.3 |
| Bermuda Rise | 43 | 386 | 1 | 57.0 | | 2b | 14.5 ±0.7 | 3.0 0 | 5.5 ±7.8 | 40.6 ±1.2 | 7.7 ±0.8 | 18.4 ±6.9 | 0 | 1 | 22.7 |

b analysis of bulk samples
* no grain size data available
\+ type locality

beneath the continental margin south of Cape Hatteras (Tucholke and Mountain, 1979). Horizon A* also disappears toward the east on the Bermuda Rise, probably because the clay/carbonate impedance contrast creating the reflector is lost in the ridge-flank carbonate province.

Age. Well preserved nannofossils and foraminifera indicate a Middle to Late Maastrichtian age for the unit at Sites 386 and 387 and a Middle Maastrichtian to earliest Paleocene age at Site 385 (Okada and Theirstein, 1979).

Depositional Environment. The composition and homogeneity of the Crescent Peaks Member indicate pelagic deposition in a quiescent, oxygenated environment above the CCD (Figure 23). The cause of the sharp depression and subsequent rise of the CCD in the Maastrichtian is uncertain but may reflect dramatically increased upwelling and productivity in response to changing surface circulation patterns.

Correlation with Other Units. The Crescent Peaks Member is approximately correlative with a lithologically identical foraminiferal-nannofossil chalk (the Wyandot Formation) on the Scotian Shelf and Grand Banks (McIver, 1972). The Wyandot Chalk is associated with the maximum Late Cretaceous transgression and with a sharp decrease of terrigenous-sediment input to the shelf (Jansa and Wade, 1975a,b). Synchronous chalk deposition occurred on the coastal plain in central Alabama (Prairie Bluff Formation, Copeland, 1969). In DSDP boreholes, chalks of this age also occur at Site 4A near Cat Gap, and nannofossil ooze at Site 390A on the Blake Nose, Site 384 on the J-Anomaly Ridge and Site 10 on the mid-ocean ridge flank. These occurrences indicate very widespread chalk deposition in the latest Cretaceous. The chalk on the Scotian Shelf forms a strong seismic reflector which can be followed across the shelf and down the continental slope (Jansa and Wade, 1975a) to the deep basin. Although seismic continuity has not been demonstrated, it is possible that this reflector will prove to be correlative with Horizon A*.

## Bermuda Rise Formation

The Bermuda Rise Formation is a suite of sediments enriched in biogenic silica and chert, generally Early Eocene in age but ranging from Paleocene to early Middle Eocene. The common occurrence of chert within this formation makes it one of the most readily correlatable units lithologically and seismically in the North American Basin, but the most difficult to core. The name is taken from the Bermuda Rise, site of the type locality, where the formation is particularly thick and readily traceable seismically.

Type Locality. Site 387 is designated as the type locality (Tables 1, 2, 13, and Figure 15). Here the formation is about 200 m thick and consists of chert, silicified claystone, radiolarian mudstone, and calcareous mudstone. The claystone and chert are greenish-grey (5V4/2) to olive-grey (5G5/1); the radiolarian mudstone and nannofossil-rich claystones are somewhat lighter. The chert consists largely of porcelanite. The content of siliceous organisms, particularly radiolarians, is high (Table 15). Other constituents are montmorillonite, mica, carbonate, quartz, feldspars, zeolites and up to 18% of cristobalite (Table 14).

At Site 387 primary sedimentary structures and compositional variations define cycles that are reminiscent of Bouma sequences (McCave, 1979). The base of each cycle generally is sharp and consists of (1) a relatively coarse-grained, structureless unit of sponge spicules and large radiolaria followed by (2) a laminated radiolarian mud interval, (3) a structureless interval enriched in carbonate (nannofossils or micrite), and (4) a light-colored mottled interval which grades into (5) a darker mottled radiolarian mud interval. Chert generally is formed in the upper dark mottled interval, but chalcedony replacement of siliceous fossils in the lowermost interval is also common. Coarser rhythmic sequences occur in

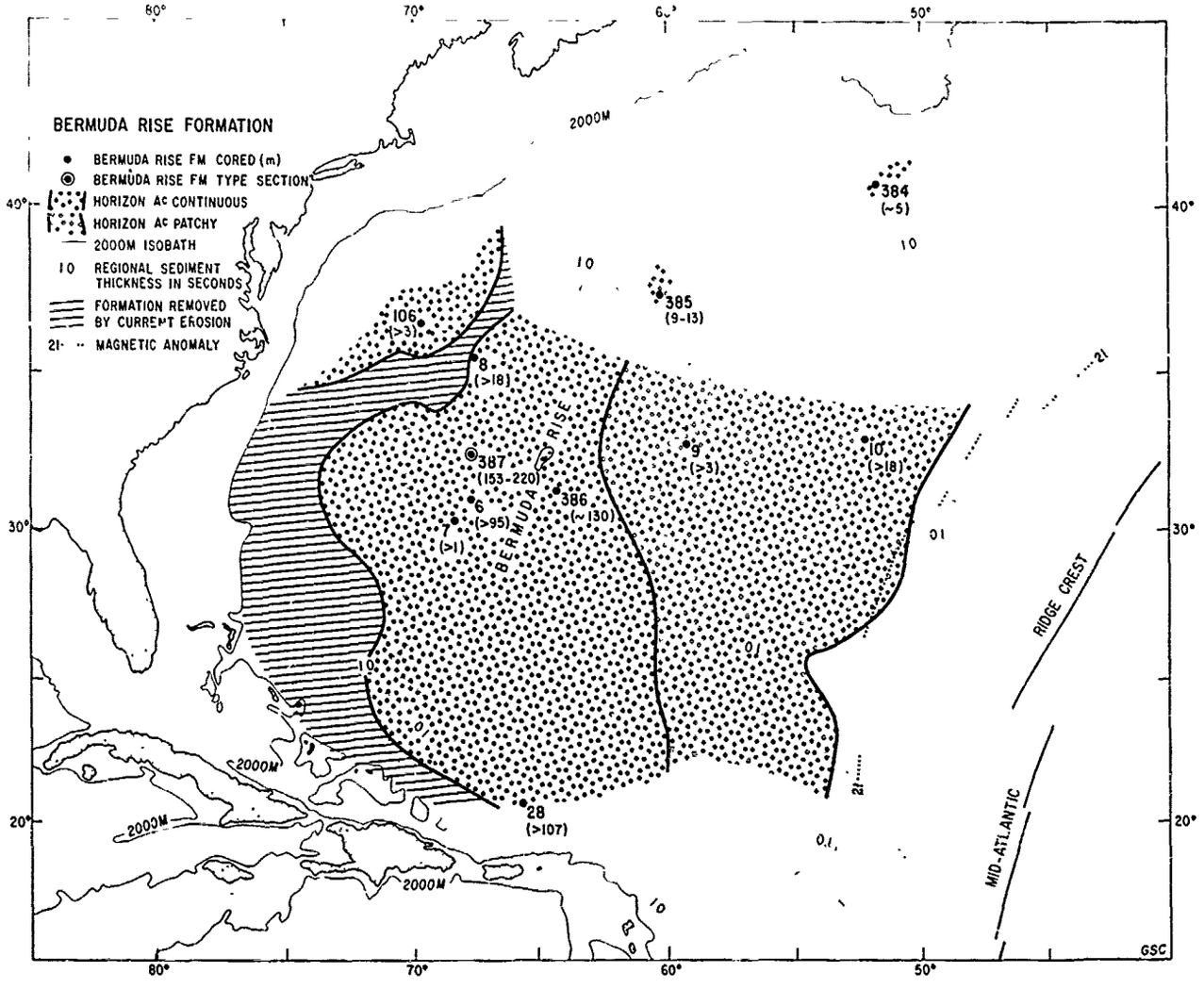


Figure 15. Boreholes that have cored sediments of the Bermuda Rise Formation. Formation thickness (metres) in parentheses. Distribution of Horizon $A^C$ (top of Bermuda Rise cherts) is indicated (not bounded by solid lines where extent is uncertain); based on Tucholke (1978). Horizon $A^C$ is truncated by Horizon $A^U$ (erosional unconformity) along the continental margin.

the Bermuda Rise Formation at Site 6 and possibly at Sites 7 and 8. At Site 386 the sequences are too fine grained to be megascopically observable, but they are cryptically graded (McCave, 1979).

Contacts. The base of the formation at Site 387 is transitional to the Plantagenet Formation over a 31 m interval beneath the lowest porcelanite. The radiolarian content is diminished in this zone (Table 15), although mineralogically the transition interval is indistinguishable from the Bermuda Rise Formation (Table 15; Koch and Rothe, 1979). Color banding is prominent but is in somber shades atypical of the underlying Plantagenet Formation, and it may reflect rhythmic sequences comparable to those noted above (Tucholke, Vogt *et al.*, 1979). The base of this transitional zone coincides with the top of the calcareous Crescent Peaks Member. The upper contact of the Bermuda Rise Formation is placed at the first downhole appearance of chert (Site 387, 223.8 m subbottom), which corresponds to seismic Horizon $A^C$ (Figure 24). It is overlain by graded be.. of biogenic-siliceous clay.

Regional Aspects. The Bermuda Rise Formation has been cored on the Bermuda Rise (Sites 387, 386, 6, 7, and 9) eastward toward the Mid-Atlantic Ridge (Site 10), between the Sohm and Hatteras Abyssal Plains (Site 8), at Vogel Seamount (Site

385) and on the continental rise (Site 106, Figure 15). It is missing beneath a major unconformity under the continental rise and notably in the Blake-Bahama Basin and Cat Gap area but was encountered at Site 28 on the Greater Antilles Outer Ridge north of Puerto Rico (Figures 15, 22, 24 and Table 13). Lithologies include porcelanitic chert, siliceous claystone, radiolarian mud, radiolarian ooze, siliceous calcareous ooze, and some zeolitic clay, silty mudstone, and nannofossil claystone (Figure 16A). The common element is high silica content, except in the three last-named lithologies that are interbedded with siliceous sediment or chert. Chert is characteristic, although it may be small in total volume. Some chert occurs in older units (Blake-Bahama Formation), but these are distinct from the Bermuda Rise Formation. Calcareous oozes with chert beds of equivalent age (Late Paleocene through Middle Eocene) occur at the edge of the Blake Plateau (Site 390), in the Northeast Providence Channel (Site 98), and on the J-Anomaly Ridge south of Grand Banks (Site 384). The Site 384 cherts are probably continuous with those of the Bermuda Rise Formation in the deep basin.

The maximum thickness drilled of the Bermuda Rise Formation is 153 m (exclusive of the transition interval) at the type locality. A similar thickness of about 130 m was encountered at Site 386, also on the Bermuda Rise. Elsewhere coring was too widely spaced and recovery too incomplete to accurately determine the thickness (Figure 24).

Multicolored clays of the Plantagenet Formation underlie the Bermuda Rise Formation at all sites where the appropriate interval was cored (7, 9, 385, 386, 387 and possibly 28), except at Site 10 where carbonates occur (Figure 22). The contact is gradational with a gradual downhole appearance of color banding. Biogenic silica increases and zeolites decrease upward, but details of the transition have not been studied. The upper contact of the Bermuda Rise Formation is defined as the uppermost appearance of chert beds at all sites. This level generally coincides with a seismic reflector and an abrupt decrease in drilling rate. The overlying unit is mainly hemipelagic mud of the Blake Ridge Formation.

Acoustic Character. The top of the Bermuda Rise Formation corresponds to seismic Horizon $A^C$ at most drillsites away from the continental margin (Tucholke, 1979). This reflector has been corre-

TABLE 13. GEOCRAPHIC DISTRIBUTION OF THE BERMUDA RISE FORMATION IN THE NORTH AMERICAN BASIN

| Region | DSDP Location Leg | Site | Top m* | Top Core● | Base m* | Base Core● | Thickness (m) | Age | Position |
|---|---|---|---|---|---|---|---|---|---|
| Bermuda Rise | 43 | 387+ | 223.8 [-5341.8] | 12:1,145 | 376.6 through 444.2 | 23:2,82 through 27:2,148 | 152.8-220.4 | Middle Eocene-Early Eocene | 32°19.2'N,67°40.0'W |
| Bermuda Rise | 1 | 6 | 233-247 [-5538 -5372] | between 4 & 5 | 257 TD | 6 | >10 | Middle Eocene | 30°50.4'N,67°38.9'W |
| Bermuda Rise | 1 | 7 | 9-235 [-5192 -5420] | between 1 & 2 | 236-278 | between 2 & 2A | >1 | Early Middle Eocene | 30°08.0'N,68°17.8'W |
| Lower Continental Rise | 2 | 8 | 287-295 [-5456 -5464] | between 1A & 2A | >305 | below 3A | >18 | Eocene | 35°25.0'N,67°33.2'W |
| Bermuda Rise | 2 | 9 | 492-679 [-5473 -5660] | between 12 & 1A | 682-765 | between 1A & 3A** | >3 | Middle Eocene-?Senonian | 32°46.4'N,59°11.7'W |
| West Flank, Mid-Atlantic Ridge | 2 | 10 | 100-167 [-4812 -4879] | between 7 & 8 | 185-291 | between 9 & 10 | >18 | Early Eocene | 32°51.7'N,52°12.9'W |
| Greater Antilles Outer Ridge | 4 | 28 | 176 [-5697] | 3:1 | between 283 & 345 | ?between 7 & 8 | >107 | Eocene | 20°35.2'N,65°37.3'W |
| Lower Continental Rise | 11 | 106 | 961-1012 [-5461 -5512] | between 6B & 7B | 1015.5 TD | 8B | >3.5 | ?Eocene-Miocene? | 36°26.0'N,69°27.7'W |
| Vogel Seamount | 43 | 385 | 156Δ [-5112] | between 5 & 6 | 165 | between 6 & 7 | 9-13 | Early Eocene | 37°22.2'N,60°09.5'W |
| Bermuda Rise | 43 | 386 | 492 [-5275] | 27:2,20 | 613-632 | between 34 & 35 | ~130 | E. Eocene-?Paleocene | 31°11.2'N,64°14.9'W |

* Metres below sea floor. Range in values denotes interval without coring or recovery.
[] Depth below sea level in square brackets.
TD Denotes total depth penetrated; bottom of formation not cored.
● Core locations given by: core number:section,depth in centimetres.
Δ Drilling brake suggests first chert at 152 m; first chert recovered at 156 m.
\+ Type locality.

TABLE 14. CHARACTERISTICS OF THE BERMUDA RISE FORMATION

| Leg | Site | Grain Size | | | | Carbon/Carbonate | | | Mineralogy (X-ray Diffraction*) | | | | | | | | | | Porosity | | | | Sonic Velocity | | | |
|---|---|---|---|---|---|---|---|---|---|---|---|---|---|---|---|---|---|---|---|---|---|---|---|---|---|---|
| | | | | | | | | | | | | | | | | | | | Chert | | Clay, etc. | | Chert | | Clay, etc. | |
| | | N | Sand | Silt | Clay | N | $CaCO_3$ | Organic | N | Quartz | Feldspar | Carbonate (total) | Kaolinite | Mica | Chlorite | Montmorillonite | Zeolite | Cristobalite | N | % | N | % | N | km/s | N | km/s |
| 48 | 387+ | - | -- | -- | -- | 14 | 11.5 ±9.2 | 0.22 ±0.17 | 14 | 10.9 ±8.9 | 1.9 ±1.7 | 12.5 ±12.6 | 1.0 | 16.5 | 0.4 | 46.9 | 1.1 ±2.8 | 8.8 ±5.6 | 5 | 25.4 ±7.3 | 13 | 45.2 ±7.1 | 5 | 3.34 ±0.41 | 13 | 2.07 ±0.27 |
| | 387 | Transition interval | | | | 4 | 3.0 ±4.4 | 0.63 ±0.62 | 5 | 17.4 ±11.6 | 3.9 ±1.3 | 2.5 ±3.6 | 0.8 | 21.0 | 1.1 | 46.1 | 1.4 ±1.3 | 5.9 ±8.0 | | | 6 | ..3 ±2.7 | | | 6 | 1.76 ±0.12 |
| 1 | 6 | 5 | 20.6 ±31.4 | 24.1 ±21.1 | 55.4 ±31.5 | 4 | 19.8 ±20.2 | 0.2 ±0.1 | 6 | 5.6 ±4.3 | 1.9 ±1.2 | 54.7 ±27.6 | 1.6 ±1.8 | 3.6 ±2.4 | 3.4 ±2.1 | 27.2 ±19.8 | 1.6 ±2.5 | | | | | | | | | |
| 1 | 7 | | -- | -- | -- | | -- | -- | | -- | -- | -- | -- | -- | -- | -- | -- | -- | | | | | | | | |
| 2 | 8 | | -- | -- | -- | | -- | -- | 2 | 5.5 | 0.0 | 0.5 | 0.0 | 0.9 | 0.0 | 0.0 | 5.3 | 87.8 | | | | | | | | |
| 2 | 9 | 3 | 4.7 ±7.1 | 9.7 ±3.2 | 85.6 ±9.7 | 1 | 3.0 | 0.0 | 7 | 10.8 ±10.6 | 3.0 ±4.2 | 2.7 ±4.8 | 5.6 ±9.6 | 3.7 ±5.9 | 0.0 | 0.0 | 12.1 ±12.5 | 62.1 ±43.9 | | | | | | | | |
| 2 | 10 | 3 | 3.6 ±1.3 | 44.1 ±17.5 | 52.3 ±16.3 | 1 | 64.1 | 0.0 | 7 | 3.1 ±1.8 | 0.0 | 88.0 ±18.9 | 0.7 ±1.9 | 0.0 | 0.0 | 0.0 | 1.9 ±5.1 | 6.8 ±18.0 | | | | | | | | |
| 4 | 28 | 1 | 0.1 | 58.6 | 41.3 | 1 | 32.0 | 0.0 | 2 | 6.0 | 0.0 | 63.0 | 0.0 | 0.0 | 7.9 | 20.7 | 2.4 | 0.0 | | | | | | | | |
| 11 | 106 | 1 | 0.6 | 53.0 | 46.4 | 1 | traces | 0.2 | 1 | 4.8 | 0.0 | 0.0 | 0.0 | 8.5 | 0.0 | 31.0 | 0.0 | 55.7 | | -- | | -- | | -- | | -- |
| 43 | 385 | | -- | -- | -- | - | -- | -- | - | -- | -- | -- | -- | -- | -- | -- | -- | -- | 1 | 10.4 | | | 1 | 3.10 | | |
| 43 | 386 | 3 | 0.1 ±0.1 | 19.3 ±0.6 | 80.6 ±0.6 | 13 | 1[illegible] ±11.2 | 0.24 ±0.21 | 13b | 8.9 ±5.4 | 1.8 ±1.7 | 8.3 ±10.7 | 0.3 | 18.9 | 0.2 | 50.2 | 1.4 ±1.9 | 9.9 ±7.7 | 3 | 45.0 ±4.0 | 10 | 47.4 ±5.5 | 4 | 2.40 ±0.26 | 10 | 1.85 ±0.11 |

* analysis of bulk samples
\+ type locality

TABLE 15. COMPOSITION OF THE BERMUDA RISE FORMATION

Based on Smear Slide Estimates (per cent; range in parentheses)

| Component | 387 Top | 387 Base* | 386 Top | 386 Base |
|---|---|---|---|---|
| Clay (includes 'opal') | 70 (57-81) | 89 (82-93) | 82 | 77 |
| Mica | 1 (0-10) | 2 | - | - |
| Altered ash and glass | - | - | 3 | 1 |
| Nannofossils | 6 (0-15) | 1 (0-18) | 5 | 5 |
| Foraminifers | 1 (0-17) | | - | trace |
| Unspecified carbonate | 6 (0-22) | 1 (0-10) | 4 | 2 |
| Radiolarians (includes 'porcelanite') | 12 (0-50) | 2 (0-5) | 3 | 12 |
| Sponge spicules | 2 (0-22) | | - | - |
| Diatoms | 1 (0-9) | | - | - |
| Miscellaneous | 1 | 6 | 3 | 3 |
| N | 31 | 19 | 16 | 20 |
| Interval (m) | 224-377 | 377-444 | 492-539 | 539-613 |

* Transition zone to the Plantagenet Formation.

lated with the shallowest occurrence of cherts at Sites 6, 10, 28, 384, 385, 387; at Site 386 the top of the cherts is seismically masked by an 82 m thick sequence of calcareous turbidites, and Horizon $A^C$ correlates with the top of these turbidites. The distribution of Horizon $A^C$ defines the regional distribution of the Bermuda Rise Formation (Figure 15).

Along the continental margin Horizon $A^C$ is truncated by a major erosional unconformity termed Horizon $A^U$ by Tucholke (1979). Drillsites in this area (Sites 4, 5, 99, 100, 101, 105, 391) show that the Bermuda Rise Formation has been removed and that the Blake Ridge Formation, normally overlying the Bermuda Rise Formation, rests directly on the Plantagenet or older formations.

On the western part of the Bermuda Rise, where siliceous turbidites form the bulk of the unit, the Bermuda Rise Formation is acoustically laminated. This lamination fades out at the contact with the underlying Plantagenet Formation (Figure 17). Elsewhere, the chert(s) form a discrete reflector or reverbatory sequence distinct from the generally non-reflective sediments of the Plantagenet Formation.

Calculated interval velocities in the Bermuda Rise Formation are about 2.01 km/s at Site 387 and 1.91 km/sec at Site 386 (including the overlying calcareous turbidites). Shipboard measured velocities vary considerably, depending on the degree of sample silicification (Table 14).

Age. Radiolarians, foraminifers, and calcareous nannofossils have all yielded Early to early Middle Eocene ages for this formation. The age range at various sites is from latest Paleocene to Middle Eocene (Table 13). A questionable Maastrichtian age at Site 9 may result from mixing during coring. An anomalously young age of the upper boundary at Site 106 (Oligocene-Miocene) is questionable and may result from drilling contamination (Poag, 1977, p. 698).

At the Site 387 type locality, the age of the formation is Middle and Early Eocene (Figure 14). At Site 386 nannofossils indicate latest Paleocene to Middle Eocene ages of the formation, but radiolarian biostratigraphy favours an Early to early Middle Eocene age (Figure 13).

Depositional Environment. Sedimentation during this period is marked by the predominance of biogenic silica over biogenic carbonate in the deep basin below the CCD, and by a significant contribution of biogenic silica in shallower, usually calcareous sediments. This may reflect strong surface circulation, upwelling, and perhaps cooler temperatures. The calcite compensation depth was apparently elevated to less than 4500 m (Figure 23). On the western half of the Bermuda Rise and further west, sedimentation was dominated by fine-grained turbidites probably originating along the North American continental margin. Turbidites on the Bermuda Rise were deposited prior to uplift that formed the Rise in the Middle to Late Eocene, and they include carbonates derived from shallower water (Tucholke and Vogt, 1979).

Sediment accumulation rates as high as 50 m/m.y. are occasionally indicated for the Bermuda Rise Formation at Site 387 where fine turbidites were deposited. Somewhat lower rates of about 20 m/m.y. typify Site 386, where the turbidites are cryptically graded. In pelagic sections (clayey-siliceous and calcareous-siliceous lithofacies) accumulation rates typically were 5 to 8 m/m.y.

Identifying features. The presence of chert, abundance of siliceous organisms, commonly greenish-gray color, and presence of seismic Horizon $A^C$ at the top of the formation are distinctive features of the Bermuda Rise Formation.

Correlations with Other Units. Synchronous facies on the Scotian Shelf and Grand Banks are brownish-grey glauconitic mudstone with minor sand beds, nannofossil marls and zeolitic claystones of the Banquereau Formation (Jansa and Wade, 1975a). In the Baltimore Canyon Trough on the U.S. continental shelf, the Paleocene-Eocene is generally represented by nannofossil marls and chalks with variable biogenic opal content (Smith *et al*, 1976). Dredge hauls and drilling at DSDP Site 108 show that Early and Middle Eocene chalks and limestones rich in silica are prevalent along the continental slope (Gibson, 1970; Hollister, Ewing *et al.*, 1972). Opal-rich sediments of late Early Eocene age are also widespread along the Atlantic Coastal plain (Hathaway *et al.*, 1976) and in Cuba (Gibson and Towe, 1971).

## Blake Ridge Formation

The Blake Ridge Formation is a widespread greenish-grey and brown hemipelagic mud. Its age is Late Cenozoic, with maximum development commonly in the Miocene. In most areas deposition of this mud probably continues to the present. The formation is named for the Blake Ridge, the nor-

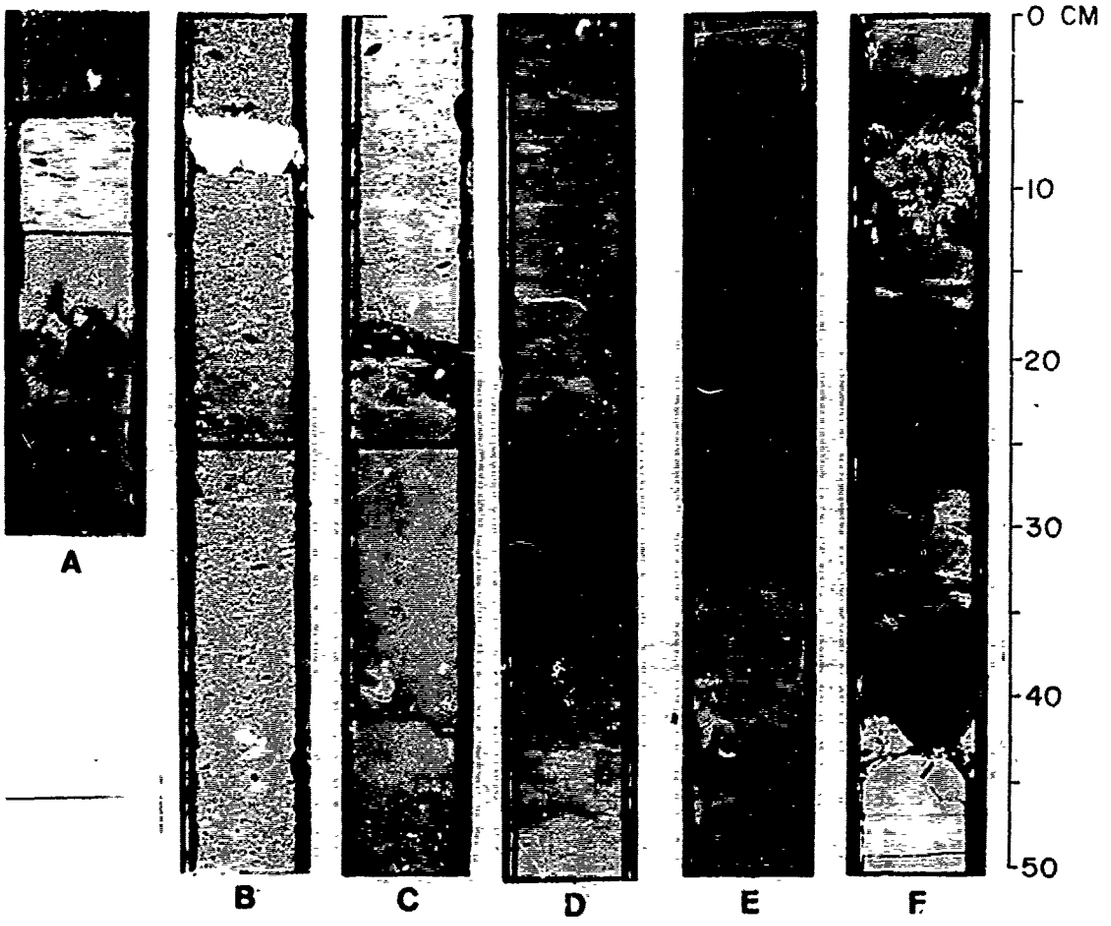


Figure 16. Bermuda Rise and Blake Ridge Formations.

A. Diatom-rich clay of the Bermuda Rise Formation with local chert fragments. Overlying graded bed is calcareous skeletal sand (Leg 1-6-6:1, 113-144 cm; 250 m sub-bottom; early Middle Eocene).

B. Intraclastic chalk of the Great Abaco Member; large clasts near the base are shallow-water limestone lithoclasts (Leg 44-391A-12:4, 25-75 cm).

C. Intraclastic chalk of the Great Abaco Member with intervals of deformed and burrowed, fine-grained, greenish-grey chalk at the top and base. Upper interval contains large clast of the greenish-grey chalk (92 cm) and shallow-water limestone lithoclasts (Leg 44-391A-12:4, 75-125 cm).

D. Very hard hemipelagic mudstone of the Blake Ridge Formation with abundant siliceous organisms. Note bioturbation and faint vertical cracks (e.g. 56-60 cm), probably caused by gas expansion. From type locality, Leg 11-106B-5:4, 25-75 cm, 940 m sub-bottom; Middle Miocene.

E. Blake Ridge Formation turbidites rich in biogenic silica (33% radiolarians, 7% sponge spicules, 1% diatoms from smear-side estimates). Leg 43-386-15:2, 0-98 cm; 349 m below sea floor; Middle Eocene.

F. Blake Ridge Formation volcaniclastic sand; two or three coarse-sand intervals grade up into ripple-laminated fine sand. Contains 16% heavy minerals and 5% volcanic glass from smear-slide estimates (Leg 43-386-13:2, 20-70 cm; 311 m sub-bottom; Middle or Upper Eocene).

thern ridge of the Blake-Bahama Outer Ridge system, which is constructed of this mud (Ewing and Hollister, 1972).

Type Locality. Although this unit has been cored at numerous sites (Table 16) none makes a satisfactory type locality, because of widely spread coring in this monotonous lithology and the consequent failure to core contacts. Site 106, Leg 11, where the maximum thickness was penetrated with reasonable recovery, is designated type locality (Figure 18). The formation was penetrated completely at this site, and cores 7B and 8B at the bottom of the hole (1012-1016 m) recovered cherty mudstone that contains 55% cristobalite (Zemmels *et al.*, 1972) and is referrable to the Bermuda Rise Formation.

At Site 106 nearly 1000 m of predominately dark greenish-grey mud of the Blake Ridge Formation was penetrated (Figures 22, 24). A few intervals are olive-grey, brownish-grey, or greenish-black. The upper three cores, down to 119 m subbottom, contain numerous intervals up to tens of centimeters thick of quartz sand or silt. Minor sandy layers also occur at 343 to 349 m, within the Pleistocene section. Sediments down to this depth are dominantly turbidites, although coring disturbance has obscured primary sedimentary structures. Induration increases progressively with depth from soft plastic mud at the surface, through firm semi-

TABLE 16. GEOGRAPHIC DISTRIBUTION OF THE BLAKE RIDGE FORMATION IN THE NORTH AMERICAN BASIN**

| Region | DSDP Leg | Location Site | Top m* | Top Core§ | Base m* | Base Core§ | Thickness (m) | Age | Position |
|---|---|---|---|---|---|---|---|---|---|
| Lower Continental Rise | 11 | 106**+ | 0 [-4500] | 1 | 961-1012 | between 6B & 7B | 961-1012 | E. Miocene-Holocene | 36°26.0'N,69°27.7'W |
| Bermuda Rise | 1 | 6 | >15 [-5140] | above 1A | 152.1 | 2:1,0 | >137 | overlies Middle Eocene | 30°50.4'N,67°38.9'W |
| Bermuda Rise | 1 | 7 | 0 [-5185] | 1 | 9-235 | between 1 & 2 | <235 | Pliocene & older | 30°08.0'N,68°17.8'W |
| Lower Continental Rise | 2 | 8 | <176 [-5345] | above 1 | 287-293 | between 1A & 2A | >111 | overlies Early Eocene | 35°23.0'N,67°33.2'W |
| Bermuda Rise | 2 | 9 | 202 [-5183] | 7:1,90 | 492-679 | between 12 & 1A | 290-477 | Miocene?-Pliocene? | 32°46.4'N,59°11.7'W |
| Bahama Outer Ridge | 11 | 101 | <32 [-4900] | above 1 | ~230*** | between 3A & 4A | 198-230 | Early Pliocene-Late Miocene | 25°11.9'N,74°26.3'W |
| Blake Outer Ridge | 11 | 102 | 0 [-3426] | 1 | 661 TD | 19 | >661 | Pleistocene/Holocene-Late Miocene | 30°43.9'N,74°27.1'W |
| Blake Outer Ridge | 11 | 103 | 0 [-3964] | 1 | 449 TD | 7 | >449 | Pleistocene/Holocene-Middle Miocene | 30°27.1'N,74°35.0'W |
| Blake Outer Ridge | 11 | 104 | 0 [-3811] | 1 | 617 TD | 10 | >617 | Pleistocene/Holocene-Middle Miocene | 30°49.7'N,74°19.6'W |
| Lower Continental Rise | 11 | 105 | 0 [-5251] | 1 | 193-241 | between 4 & 5 | ~193-241 | Pleistocene/Holocene-Miocene | 34°53.7'N,69°10.4'W |
| Nashville Seamount | 43 | 382** | <51 [-5578] | 1 | 352 | 15:5,22 | 301-352 | Pleistocene-Early Miocene | 34°25.0'N,56°32.3'W |
| Vogel Seamount | 43 | 385 | <22 [-4978] | 1 | 156Δ | between 5 & 6 | 134-156 | Pleistocene-Early Miocene | 37°22.2'N,60°09.5'W |
| Bermuda Rise | 43 | 386** | 60 [-4843] | 1:6,15 | 492 | 27:2,20 | 432 | Late Miocene-Early Eocene | 31°11.2'N,64°14.9'W |
| Bermuda Rise | 43 | 387 | <32 [-5150] | 1 | 224 | 12:1,145 | 188-224 | Pleistocene/Holocene-Middle Eocene | 32°19.2'N,67°40'W |
| Lower Continental Rise | 44 | 388** | 0 [-4920] | 1A | 341 TD | 11A | >341 | Pleistocene-Middle Miocene | 35°31.3'N,69°23.8'W |
| Blake-Bahama Basin | 44 | 391** | 0 [-4964] | 1 | 649 | between 20A & 21A | 649 | Pleistocene/Holocene-Early Miocene | 28°13.7'N,75°36.9'W |

* Metres below sea floor. Range in values denotes interval without coring or recovery.
[] Depth below sea level in square brackets.
TD Denotes total depth penetrated; bottom of formation not cored.
§ Core locations are given by: core number:section,depth in centimetres.
** Includes intervals with appreciable mass-flow deposits; these are also tabulated separately in Table 18.
*** Based on seismic reflector and slight break in drilling rate. Interval 203-250 m not cored; core at 250 m is "intermediate between hemipelagic muds and carbonaceous clays" [Hatteras Formation] (Hollister, Ewing, and others, 1972, p. 109).
Δ Drilling brake in core 5 suggests first chert encountered at 152 m.
+ Type locality.

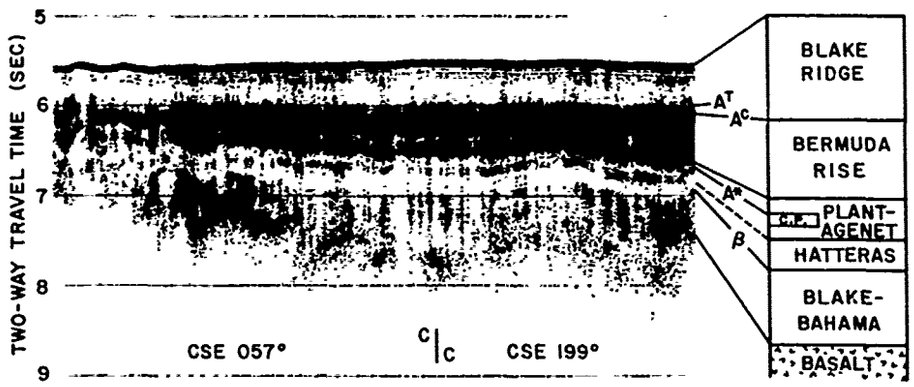


Figure 17. Seismic profiler record just northwest of Site 387 on the western Bermuda Rise, showing major reflectors and correlation with formations described in the text.

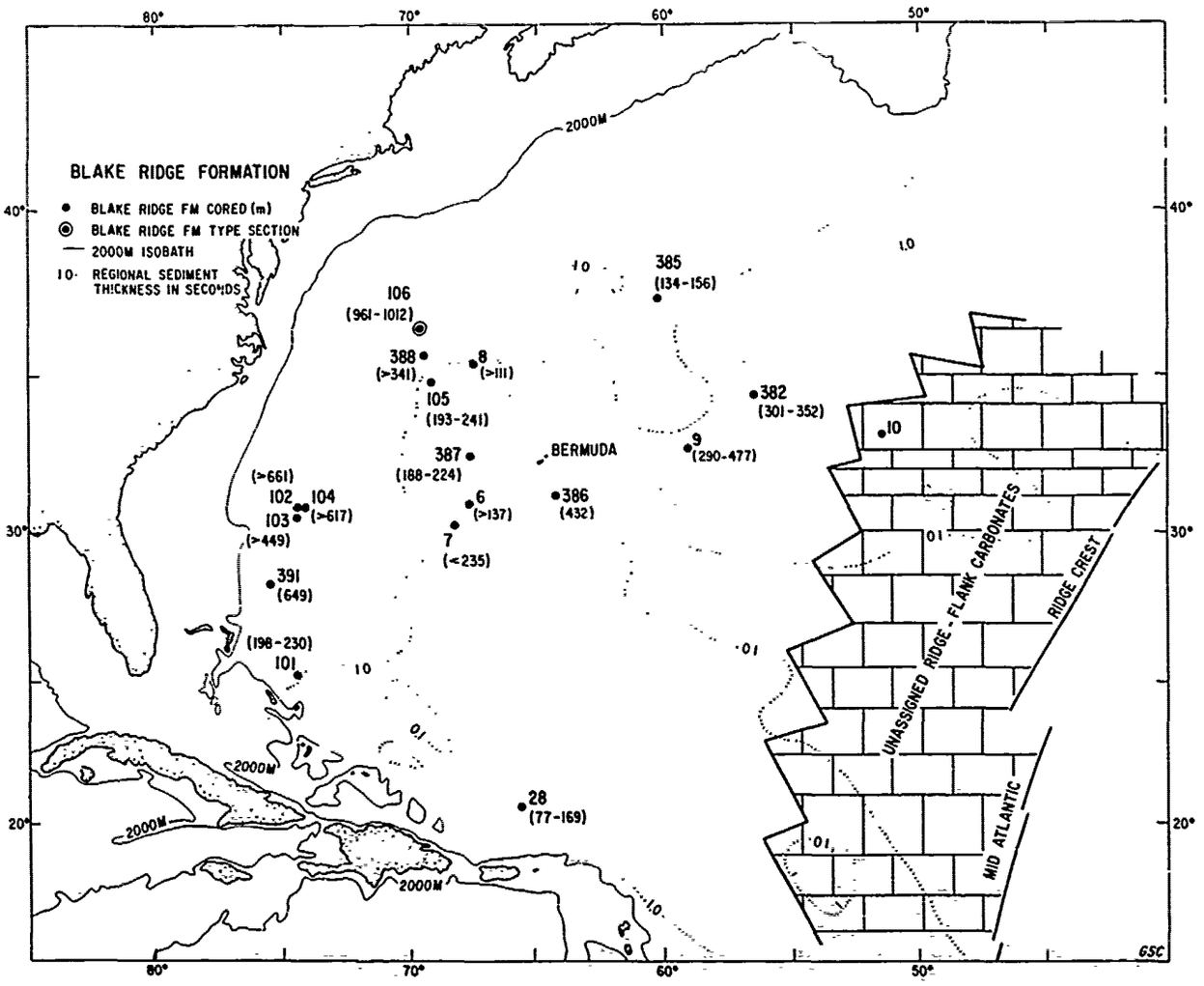


Figure 18. Boreholes that have cored sediments of the Blake Ridge Formation. Formation thickness (metres) in parentheses.

plastic mud at 345 m and very firm, slightly fissile mud at 450 m, to hard mudstone at 940 m. The average mud is silty clay with about 68 per cent clay (Table 17), but the upper part of the formation which contains sand beds has about equal proportions of sand, silt, and clay. Sedimentary components in order of decreasing abundance are mica, quartz, carbonate, kaolinite, montmorillonite, and feldspar (Table 17). Siderite was noted throughout the bottom half of the interval in shipboard descriptions, but was not reported from X-ray mineralogy studies (Zemmels *et al.*, 1972).

Calcareous nannoplankton are common in most cores. Radiolaria, sponge spicules, and dinoflagellates occur sporadically throughout, foraminifera are rare except in the turbidite interval near the top of the formation.

Sedimentary structures include burrows, irregular bedding, and lighter lenses that contain more foraminifers and calcareous nannofossils. Pyrite and siderite line some burrows and form lenses or nodules. The most common structures are burrow-like coalescent spongy voids and vertical fractures which occur in the lower half of the formation and result from gas expansion during core recovery (Hollister, Ewing *et al.*, 1972). Most cores in this interval contained appreciable $CO_2$, $H_2S$, and $CH_4$. However some fractures are lined with siderite suggesting vertical gas migration or expansion *in situ*.

Contacts. The lower contact of the Blake Ridge Formation at Site 106 is within a 50 m uncored interval (961-1012 m). A subtle color change across this interval from dark greenish-grey (5G4/1) to greyish-green (10G4/2), a reduction in terrigenous components (Tables 14 and 17), and appearance of cherty siliceous sediments mark the change to the underlying Bermuda Rise Formation. Two lines of evidence suggest that the Blake Ridge Formation unconformably overlies the Bermuda Rise Formation at Site 106: (1) the Horizon $A^U$ unconformity can be traced to the site at about 1000 m subbottom, and (2) it is likely that cores 7E and 8B from the Bermuda Rise Formation (1012-1015 m) are of Eocene age, thus requiring either severely reduced sedimentation or a hiatus in the internal 961 to 1012 m subbottom. The upper contact of the Blake Ridge Formation at Site 106 is at the sea floor.

Regional Aspects. The Blake Ridge Formation shows little lithologic variation throughout the North American Basin, except where hemipelagic sedimentation was interrupted by debris-flow deposits or turbidites. Color is generally dark greenish-grey but notable differences sometimes occur. At Sites 6 and 7 color is brown, olive, and dark yellowish brown, and at Site where the top 100 m is light brown or yellowish brown and the base is pale olive to yellowish grey. A few yellow-brown bands were encountered at Sites 9 and 386. These lighter colors commonly are found near the Bermuda Rise.

The uniformity in composition of the formation is indicated in Table 17. Quartz content is remarkably uniform despite minor variations in grain size, except at Site 388 which is anomalously quartz rich and at Bermuda Rise Sites 386 and 387 which are clay rich. Feldspar content is fairly uniform, but is consistently high at Site 391 (a high average value at Site 105 reflects a single sample of terrigenous sand). Carbonate content is higher in samples from the relatively shallower Blake Ridge (Sites 102 to 104), Bahama Outer Ridge (Site 101) and Blake-Bahama Basin (Site 391). This may reflect combination of (1) higher productivity of surface waters at the lower latitudes, (2) detrital carbonate input from nearby carbonate platforms, and (3) lack of dilution by terrigenous components. Calcareous nannoplankton are abundant at all sites. Foraminifera are abundant in continental-rise sites but are rare and show the effects of dissolution in cores from the abyssal plains. Mica content generally decreases away from the North American continental shelf, the most likely source area, but chlorite fails to show a parallel trend. Both minerals also are relatively abundant at Bermuda Rise Sites 386 and 387. Montmorillonite is very abundant at Bermuda Rise and New England Seamount sites (382, 385), reflecting local volcanigenic source rocks. It is more abundant in older samples at most sites. Zeolites are common in the upper part of the formation at Sites 386 (above 155 m) and 387 (above 100 m). Siliceous fossils are rare in younger samples at most sites, but increase in abundance with depth, especially at Site 387 below 100 m. Thus, minor variations in composition occur in the formation due to the effect of provenance, productivity and sediment distribution.

Natural gas was detected in cores from all sites on the continental rise (102, 103, 104, 106, 388), but was not noted in abyssal plain and Bermuda Rise sites.

The thickness of the Bermuda Rise Formation is generally 200 to 300 m in the North American Basin (Table 16), but increases markedly on the continental rise to 1000 m (Site 106) and more (Figures 22, 24). Except for local thin units the formation is absent in the Cat Gap area where erosion has exposed rocks as old as Early Cretaceous at or near the sea-floor (Figure 22).

In the central part of the basin the Blake Ridge Formation overlies chert of the Bermuda Rise Formation with no detectable hiatus. Along the continental margin underlying formations are beveled by a regional unconformity (Horizon $A^U$ and the Blake Ridge Formation unconformably overlies older strata. For example at Sites 105 and 391 it rests on the variegated Plantagenet Formation and at Site 101 it overlies the Hatteras Formation.

The top of the formation is at or near the sea floor at all localities. In many places the formation is capped by a unit of Pleistocene and Holocene nannofossil-foraminifera ooze or marl

ranging from a few decimeters to a few meters in thickness. Some exceptions, such as Site 386 where the oozes appear to be 60 m thick, may be due to inadvertent recovery of near sea-floor sediments when spudding in the hole. However, Pliocene-Pleistocene oozes up to 200 m thick probably overlie the Blake Ridge Formation at Site 9.

Mass-Flow Deposits. The most striking regional variants of the Blake Ridge Formation are terrigenous, volcaniclastic, siliceous and calcareous turbidites and carbonate breccias described later as a formal member.

Terrigenous sand and silt are most common at Sites 106 and 388 on the continental rise and at Sites 382 and 383 in the Sohm Abyssal Plain (Tables 18, 19). At Sites 106 and 388 sandy sediments form the top of the formation and contain a mixed foraminiferal fauna indicating Pleistocene age. Individual sand intervals are up to 2.5 m thick. Sedimentary structures and grading were not observed, because of intense drilling disturbance. Graded beds are common at Site 382 and probably at Site 383, where they are Pliocene and Quaternary age. Seismic profiles across all four of these sites show flat-lying, closely spaced reflectors either regionally distributed or in sediment ponds. Near the base of Blake Ridge Formation graded beds of terrigenous silt or sand mixed with calcareous and siliceous debris were cored at Sites 6, 8 and 387, on or near the Bermuda Rise. The beds are mostly less than 10 cm thick. These turbidites are Middle to Late Eocene in age and were deposited prior to uplift of the Bermuda Rise.

Biogenic siliceous and calcareous turbidites with less terrigenous debris also are common at Site 386. Because this site was drilled in the center of a fracture valley, it has accumulated large volumes of debris shed from the adjacent basement peaks, and is likely that this typifies sediments of the Blake Ridge Formation that were deposited in other fracture valleys. The turbidites at Site 386 range in age from Middle Eocene to Early Miocene, and although some are

TABLE 17. CHARACTERISTICS OF THE BLAKE RIDGE FORMATION (EXCLUSIVE OF MASS FLOW INTERVALS - SEE TABLE 18)

| Leg | Site | Grain Size | | | | Carbon/Carbonate | | | Mineralogy (X-ray Diffraction*) | | | | | | | Porosity | | Sonic Velocity | |
|---|---|---|---|---|---|---|---|---|---|---|---|---|---|---|---|---|---|---|---|
| | | N | Sand | Silt | Clay | N | $CaCO_3$ | Organic | N | Quartz | Feldspar | Carbonate (total) | Kaolinite | Mica | Chlorite | Montmorillonite | N | % | N | km/s |
| 1 | 106+ | 16 | 0.3 ±0.4 | 31.5 ±10.0 | 68.2 ±10.1 | 34 | 7.9 ±8.0 | 0.52 ±0.16 | 7 | 26.6 ±2.7 | 5.3 ±0.1 | 6.6 ±7.0 | 5.0 ±2.3 | 37.1 ±5.6 | 2.9 ±0.7 | 17.7 ±12.6 | 5 | 52 ±4.9 | | |
| 1 | 6 | 10 | 0.4 ±0.54 | 8.3 ±3.1 | 91.3 ±3.1 | 12 | 3.7 ±5.2 | 0.14 ±0.13 | 27 | 26.8 ±9.8 | 9.1 ±4.1 | 0.4 ±1.1 | 18.9 ±7.4 | 16.2 ±6.6 | 4.6 ±6.6 | 20.8 ±17.3 | | | | |
| 1 | 7 | 4 | 0.1 ±0.05 | 9.2 ±4.7 | 90.7 ±4.8 | 1 | 1.7 | 0.1 | 8 | 31.4 ±4.1 | 6.9 ±2.0 | 2.2 ±3.3 | 26.6 ±4.3 | 26.1 ±4.3 | 0 | 0 | | | | |
| 2 | 8 | 1 | 0.5 | 48.9 | 50.6 | 0 | - | - | 1 | 25 | 9 | 0 | 15 | 16 | 0 | 34 | | | | |
| 2 | 9 | 18 | 0.1 ±0.3 | 7.8 ±2.8 | 92.1 ±2.8 | 6 | 2.5 ±3.3 | 0.75 ±0.05 | 31 | 24.8 ±4.7 | 3.3 ±3.5 | 0.3 ±1.1 | 18.4 ±5.6 | 14.7 ±4.2 | 0.6 ±2.5 | 37.4 ±13.0 | | | | |
| 11 | 101 | 22 | 1.6 ±4.3 | 34.7 ±4.5 | 63.8 ±5.3 | 22 | 11.6 ±7.5 | 0.64 ±0.13 | 5 | 27.3 ±6.2 | 11.2 ±6.3 | 19.3 ±6.3 | 7.4 ±1.7 | 19.5 ±14.7 | 2.5 ±0.9 | 9.7 ±3.9 | 22 | 60.8 ±5.5 | | |
| 11 | 102 | 41 | 0.9 ±0.9 | 29.3 ±10.5 | 69.8 ±10.4 | 77 | 17.8 ±8.6 | 0.58 ±0.19 | 19 | 22.4 ±2.2 | 9.0 ±4.2 | 22.7 ±6.7 | 5.1 ±2.6 | 31.0 ±6.0 | 2.7 ±1.7 | 6.1 ±6.1 | 67 | 53.9 ±9.4 | | |
| 11 | 103 | 26 | 1.2 ±2.0 | 34.1 ±10.7 | 64.7 ±11.6 | 26 | 15.1 ±13.1 | 0.48 ±0.22 | 10 | 29.4 ±4.6 | 7.9 ±2.7 | 16.8 ±12.0 | 6.1 ±2.6 | 30.4 ±5.8 | 2.9 ±3.4 | 5.9 ±4.4 | 24 | 60.3 ±7.7 | | |
| 11 | 104 | 38 | 0.4 ±0.97 | 23.2 ±18.6 | 76.4 ±19.0 | 42 | 15.2 ±9.8 | 0.65 ±0.27 | 11 | 26.6 ±5.5 | 6.6 ±5.2 | 17.2 ±10.7 | 8.4 ±3.2 | 29.1 ±4.8 | 0.3 ±1.0 | 7.1 ±2.2 | 37 | 64.2 ±6.7 | | |
| 11 | 105 | 12 | 0.4 ±0.5 | 32.4 ±11.6 | 67.2 ±12.0 | 13 | 9.3 ±10.2 | 0.22 ±0.07 | 3 | 25.2 ±1.0 | 19.6 ±19.3 | 8.7 ±7.5 | 3.4 ±3.0 | 31.2 ±14.2 | 3.2 ±6.9 | 7.5 ±6.9 | 13 | 53.3 ±8.2 | | |
| 43 | 382 | | | | | 16 | 8.7 ±9.0 | 0.25 ±0.13 | 22 | 26.6 ±11.2 | 8.6 ±6.2 | 1.9 ±3.7 | 3.9 ±1.6 | 19.2 ±11.5 | 3.4 ±2.0 | 36.4 ±25.1 | 15 | 53.7 ±6.4 | 15 | 1.64 ±0.03 |
| 43 | 385 | | | | | 5 | 1.2 ±1.8 | 0.24 ±0.08 | 6 | 18.8 ±7.9 | 5.8 ±1.7 | 0 | 4.9 ±1.8 | 9.6 ±4.8 | 1.4 ±0.9 | 58.8 ±9.2 | 8 | 74.8 ±4.5 | 1 | 1.53 |
| 43 | 386 | 3 | 2.4 ±4.0 | 16.8 ±17.0 | 80.8 ±21.2 | 5 | 7.8 ±13.8 | 0.14 ±0.05 | 5 | 12.2 ±5.2 | 3.6 ±2.3 | 19.3 ±15.7 | 2.76 ±4.3 | 16.7 ±7.7 | 1.3 ±2.3 | 49.2 ±14.4 | 3 | 62.4 ±4.6 | 2 | 1.55 |
| 43 | 387 | 2 | 4.8 | 13.0 | 82.2 | 9 | 0.4 ±0.3 | 0.17 ±0.07 | 9 | 9.8 ±4.0 | 2.9 ±1.9 | 3.2 ±6.6 | 4.9 ±5.0 | 19.8 ±7.5 | 1.5 ±1.8 | 57.9 ±11.3 | 10 | 69.4 ±4.4 | 3 | 1.57 ±0.04 |
| 44 | 388 | 12 | 0.45 ±0.61 | 24.8 ±5.0 | 74.8 ±5.0 | 26 | 1.5 ±1.1 | 0.38 ±0.10 | 12 | 46.5 ±10.5 | 14.8 ±2.6 | 4.6 ±9.2 | 6.9 ±1.3 | 18.3 ±3.4 | 0.7 ±1.2 | 7.1 ±2.3 | 14 | 53.9 ±6.2 | 22 | 1.59 ±0.17 |
| 44 | 391 | 8 | 0.4 ±0.3 | 26.4 ±6.4 | 73.2 ±6.3 | 12 | 13.8 ±7.4 | 0.33 ±0.06 | 9 | 29.8 ±6.0 | 23.2 ±8.0 | 24.9 ±13.6 | 5.0 ±2.4 | 13.6 ±6.4 | 1.8 ±2.4 | 0.8 ±1.2 | 4 | 46.5 ±8.0 | 8 | 1.50 ±0.02 |

* analysis of bulk samples
\+ type locality

TABLE 18. GEOGRAPHIC DISTRIBUTION OF THE GREAT ABACO MEMBER AND OTHER DEBRIS-FLOW AND TURBIDITE DEPOSITS WITHIN THE BLAKE RIDGE FORMATION IN THE NORTH AMERICAN BASIN

| Region | DSDP Location Leg | Site | Top m* | Top Core$^{\Delta}$ | Base m* | Base Core$^{\Delta}$ | Thickness (m) | Age |
|---|---|---|---|---|---|---|---|---|
| Blake-Bahama Basin | 44$^{+}$ | 391A | 147 [-5111] | 3:1,150 | 649 | between 20 & 21 | 502 | Early-Late Miocene |
| Bermuda Rise | 1 | 6 | 161-190 [-5286- -5315] | between 2 & 3 | 250 | 6:2 | >60 | Middle Eocene |
| Lower Continental Rise | 2 | 8 | 177-254 [-5346- -5423] | between 1 & 2 | 286 | between 1A & 2A | - | Eocene |
| Lower Continental Rise | 11 | 106 | 0 [-4500] | 1 | 119-187 | between 3 & 4 | >119 | Pleistocene |
| Nashville Seamount | 43 | 382 | 0-51 [-5527- -5578] | 1 | 232 | 5:1,130 | 181-232 | Pleistocene |
| Bermuda Rise | 43 | 386 | 155 [-4938] | 4:5,110 | 490 | 27:2,20 | 335 | Late Oligocene-Early Eocene |
| Bermuda Rise | 43 | 387 | 178 [-5296] | 7:3,20 | 224 | 12:1,145 | 46 | Middle Eocene |
| Lower Continental Rise | 44 | 388A | 0 [-4920] | 1 | 53-208 | between 3 & 4 | >53 | Pleistocene |

* Metres below sea floor. Range in value denotes an interval without coring or recovery.
[] Depth below sea-level.
$\Delta$ Core locations are given by: core number:section,depth in centimetres.
+ Great Abaco Member type locality.

cryptically graded they commonly exhibit the rhythmic progression of sedimentary structures previously described for the Bermuda Rise Formation at Site 387.

Site 386 also cored a 160+ m sequence of Late Eocene to Oligocene volcaniclastic-sand turbidites derived from weathering of the Bermuda volcanic pedestal. Although cored at only one site, these deposits can be traced in seismic profiles within a radius of about 150 km around Bermuda (Horizon $A_V$; Tucholke and Mountain, 1979), and they eventually may merit formal member status. Site 386 is the hypostratotype for this variant of the Blake Ridge Formation.

Acoustic Character. Along the continental margin Horizon $A^U$ marks the base of the Blake Ridge Formation. Farther seaward where this

TABLE 19. CHARACTERISTICS OF THE GREAT ABACO MEMBER AND OTHER INTERVALS OF TURBIDITES AND DEBRIS-FLOW DEPOSITS WITHIN BLAKE RIDGE FORMATION

| Leg | Site | Interval Top | Interval Base | Grain Size N | Sand | Silt | Clay | Carbon N | $CaCO_3$ | Organic | Mineralogy (X-ray Diffraction*) N | Quartz | Feldspar | Carbonate (total) | Kaolinite | Mica | Chlorite | Montmorillonite | Porosity N | % | Velocity N | km/s |
|---|---|---|---|---|---|---|---|---|---|---|---|---|---|---|---|---|---|---|---|---|---|---|
| 44 | 391A$^{+}$ | 147 | 649 | 20 | 5.0 ±2.0 | 44.0 ±14.5 | 51.0 ±0.51 | 42 | 60.3 ±32.8 | 0.5 ±0.05 | 24$^{\Delta}$ | 1.75 ±1.0 | | 98.25 ±1.0 | | | | | 27 | 50.3 ±9.8 | 32 | 2.03 ±0.5 |
| | | | | | | | | | | | 10$^{\dagger}$ | 28.5 ±13.5 | 2.5 ±5.3 | 27.7 ±27.5 | 3.5 ±2.4 | & 8 ±8.4 | 1.0 ±3.2 | 15 ±17.8 | | | | |
| 1 | 6 | 190 | 250 | 10 | 14.1 ±23.2 | 26.0 ±14.8 | 59.9 ±23.3 | 9 | 22.6 ±14.3 | 0.2 ±0.1 | | | | | | | | | | | | |
| 2 | 8 | 254 | 288 | 6 | 3.4 ±1.9 | 50.5 ±16.0 | 46.1 ±15.0 | 1 | 3.4 | 0.1 | | | | | | | | | | | | |
| 11 | 106 | 0 | 119 | 8 | 33.4 ±31.2 | 27.6 ±9.3 | 39.0 ±23.7 | 11 | 12.4 ±11.8 | 0.4 ±0.2 | | | | | | | | | 10 | 56.6 ±11.4 | | |
| 43 | 382 | 51 | 232 | | | | | 1 | 9.7 | 0.4 | NO DATA AVAILABLE | | | | | | | | 7 | 55.6 ±9.2 | 5 | 1.58 ±0.06 |
| 43 | 386 | 155 | 490 | 15 | 22.9 28.7 | 39.5 14.9 | 37.6 19.5 | 33 | 18.1 16.1 | 0.3 0.26 | | | | | | | | | 39 | 50.9 ±13.9 | 36 | 1.88 ±0.26 |
| 43 | 387 | 178 | 224 | 4 | 2.2 1.6 | 37.4 5.0 | 60.4 4.2 | 9 | 6.7 8.6 | 0.1 0.1 | | | | | | | | | 7 | 65.8 ±6.9 | 7 | 1.63 ±0.10 |
| 44 | 388 | 0 | 53 | 6 | 6.58 ±10.37 | 33.5 ±6.93 | 59.9 ±15.16 | 6 | 20.2 ±13.0 | 0.2 ±0.11 | | | | | | | | | 5 | 61.34 ±5.01 | 4 | 1.55 ±0.667 |

\+ type locality
$\Delta$ chalk intraclast
$\dagger$ clayey matrix

unconformity does not cut into the Bermuda Rise Formation, the base of the Blake Ridge Formation correlates with Horizon $A^C$. One exception occurs at Site 386; here Horizon $A^C$ is within the base of the Blake Ridge Formation and at the top of a sequence of calcareous turbidites overlying the Bermuda Rise cherts.

The general acoustic character of the Blake Ridge Formation in seismic profiles is highly variable. The formation ranges from acoustically non-laminated (Site 9) through laminated (e.g., Sites 102, 103, 104) to very strongly laminated, flat lying beds (e.g., Site 106, 383). The acoustic character is a direct indicator of vertical and lateral lithologic inhomogeniety of the formation. Sound velocities in these sediments range upward from about 1.5 km/sec, average about 1.7 km/sec, and may reach as high as 2.5 km/sec depending upon formation thickness.

Age. Most of the Blake-Ridge Formation recovered from sites to date is of Miocene age, largely because sampling has been biased toward the continental margin where Upper Eocene and Oligocene sediments have been eroded. At the Site 106 type locality, the formation ranges from Early Miocene to Holocene (Figure 19). Farther seaward the formation overlies the Bermuda Rise cherts and therefore is Middle Eocene and younger (e.g., Sites 386 and 387; Figures 13, 14). At most of these sites the top of the formation is Pleistocene and is capped by Quaternary calcareous oozes, but at Site 9 the formation extends only to the Early Pliocene and is capped by Upper Pliocene and Quaternary oozes.

Depositional Environment. The greenish-grey mud of the Blake Ridge Formation was probably deposited under conditions similar to those which now prevail in the North American Basin, particularly since turbidite deposition appears to have been sharply reduced since the Pleistocene. Deeper areas lay below the CCD and only rapid deposition

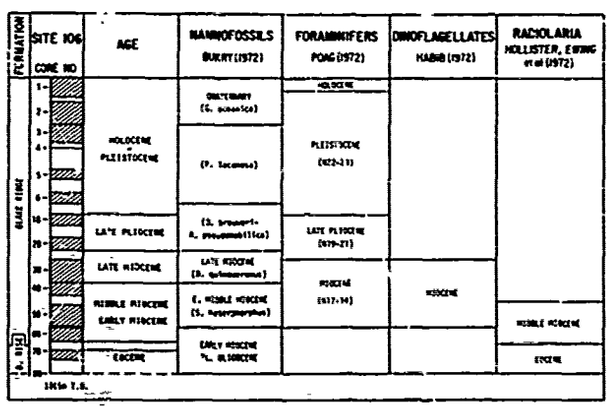


Figure 19. Multiple biostratigraphy of Site 106 upper continental rise.

permitted the preservation of calcareous fossils. Abyssal currents have had a strong effect in transporting, eroding, and depositing sediments of the Blake Ridge Formation, in contrast to their limited role in deposition of older formations. The effect of currents is most pronounced along the deeper part of the continental margin, as indicated by variations in sediment accumulation rates at Sites 101 to 106 (Table 20), marked thickness variations (Table 16), and the formation of depositional outer ridges (Heezen *et al.*, 1966; Ewing and Hollister, 1972; Tucholke and Ewing, 1974).

The Blake Ridge Formation comprises the bulk of the present continental rise and therefore is extremely thick (2-3 km) in this region (see Figure 5 of Grow and Markl, 1977). The large thicknesses result from proximity to terrigenous sources and from the activity of contour following bottom currents. These currents have pirated sediment from cross-contour debris flows and turbidity currents and have transported it laterally, along contours (Hollister and Heezen, 1972). Thus a large volume of sediment has been deposited on the continental rise that otherwise would have been transported beyond the rise to the deep basin.

Much of the sediment in the Blake Ridge Formation was deposited directly from turbidity currents. At the Site 106 type locality, ponded turbidites derived from the continental shelf during Pleistocene low stand of sea level form the upper part of the formation (see Figure 20 of Tucholke and Mountain, 1979). Similar turbidites occur in the Sohm, Hatteras, Nares and Silver Abyssal Plains. The mixed terrigenous and biogenic graded beds of Eocene age at the base of the Blake Ridge Formation also were deposited from turbidity currents presumably originating along the continental margin, but they entrained large volumes of pelagic material enroute to their depositional locality. Turbidite deposition on the western Bermuda Rise ceased when uplift formed the rise in the Middle to Late Eocene. Locally redeposited or "pelagic" turbidites probably were common in areas with irregular morphology. Facies variants were also introduced by locally significant sediment sources (i.e., the volcaniclastic turbidites surrounding Bermuda).

Sediment accumulation rates (Table 20) varied by an order of magnitude in different time intervals at individual sites, and equally large between-site variations occur among sediments deposited during the same time interval. These variations reflect changing patterns of provenance, productivity, bottom currents and sea level fluctuations. Fluctuations in turbidity-current activity are of prime importance at Sites 106, 386, 387 and 388, but equally large variations in accumulation rate at Site 102 to 104 are attributed to interactions of contour currents with their own depositional topography (Ewing and Hollister, 1972). The maximum accumulation rates

TABLE 20. SEDIMENT ACCUMULATION RATES FOR BLAKE RIDGE FORMATION

| Leg | Site | Rate ($m/10^6$ yrs) | Interval (m sub-bottom) | Age | Remarks |
|---|---|---|---|---|---|
| 11 | 106 | 200 | 1-366 | Pleistocene | Terrigenous turbidites |
| | | 43 | 366-961 | Pliocene-Middle Miocene | |
| 2 | 8 | 11-17 | 0-177 | Middle Miocene(?) and younger | Recalculated |
| 2 | 9 | 21 | 200-679 | Pliocene?-Late Miocene? | Includes underlying chert |
| 11 | 101 | 23 | 32-230 | Early Pliocene-Late Miocene | |
| 11 | 102 | 137 | 0-224 | Pleistocene | |
| | | 90 | 224-585 | Pliocene | |
| | | 25 | 585-661 | Late Miocene | |
| 11 | 103 | 26 | 2-47 | Early-Middle Pliocene | |
| | | 193 | 47-449 | Middle-Late Miocene | |
| 11 | 104 | 18 | 5-71 | Late Miocene | |
| | | 95 | 71-315 | Middle-Late Miocene | |
| | | 195 | 315-617 | Middle Miocene | |
| 11 | 105 | 17 | 0-193 | Miocene-Holocene | |
| 43 | 382 | 120 | 0-232 | Quaternary | Terrigenous turbidites |
| | | 6-8 | 232-352 | Miocene-Pliocene | Probable hiatuses in sequence |
| 43 | 385 | 6 | 0-134 | Pleistocene-Late Miocene | |
| 43 | 386 | 3 | <53-157 | Miocene | |
| | | 45 | 157-? | Late Oligocene-Late Eocene | Calcareous and volcanic turbidites |
| | | 19 | 166-319 | Late Oligocene-Late Eocene | Volcanic turbidites |
| | | 47 | 319-409 | Middle-Late Eocene | Biogenic siliceous turbidites |
| | | 26 | 409-492 | Middle Eocene | Calcareous turbidites |
| 43 | 387 | 4 | 0-100 | Pleistocene-Oligocene | |
| | | 8 | 100-178 | Late Eocene | |
| | | >100 | 178-224 | Early Eocene | Biogenic siliceous turbidites |
| 44 | 388 | 45 | 0-53 | Pleistocene | Terrigenous turbidites (in part) |
| | | 30 | 208-341 | Middle-Late Miocene | |
| 44 | 391 | 90 | 0-147 | Quaternary | |
| | | 9 | 147-204 | Late Miocene | Intraclastic chalk |
| | | 43 | 204-400 | Middle Miocene | Intraclastic chalk |
| | | 39 | 400-649 | Early Miocene | Intraclastic |

calculated for turbidity-current and bottom-current deposition (Sites 106 and 104, respectively) are nearly identical at 200 m/m.y.

Identifying features. The predominantly dark greenish-gray color of the hemipelagic mud, common terrigenous components, low induration, and frequent occurrence of turbidites and mass-flow deposits are the most characteristic features of the Blake Ridge Formation.

Correlation with Other Units. The Upper Tertiary sediments marginal to the North American Basin are terrigenous, siliceous, and calcareous deposits more strongly variable in composition than the Blake Ridge Formation. On the Scotian Shelf and Grand Banks, the Oligocene and Miocene rocks are dark yellowish-brown and brownish-grey siliceous mudstones of the Banquereau Formation (Jansa and Wade, 1975a), commonly with diatoms, radiolarians, and sponge spicules. The mudstones are lithologically similar to Eocene-Oligocene radiolarian mud of the Blake Ridge Formation at Site 387, but unlike the more common hemipelagic mud. The Upper Tertiary siliceous mudstones on the shelf reflect cooling of the shelf water. This did not influence the eastern margin of the North American basin where yellowish-brown nannofossil and foraminiferal oozes were deposited contemporaneously (lower flank of the Mid-Atlantic Ridge, Site 10 and 11, Peterson, Edgar *et al.*, 1970). In the Baltimore Canyon Trough region on the continental shelf (COST B-2 well) the Oligocene-Miocene section is 1000 m of fine-grained sandstone interlayered with clay which increases with depth from about 25 percent to 60 percent (Rhodehamel, 1977). Diatoms are abundant in the lower 400 m of the interval (Poag, 1977). Facies that are coeval with the Blake Ridge Formation elsewhere along the U.S. continental shelf include such diverse lithologies as terrigenous gravels, sands, silts, clays and calcareous sands; admixtures of biogenic calcite and silica are highly variable (Hathaway *et al.*, 1976).

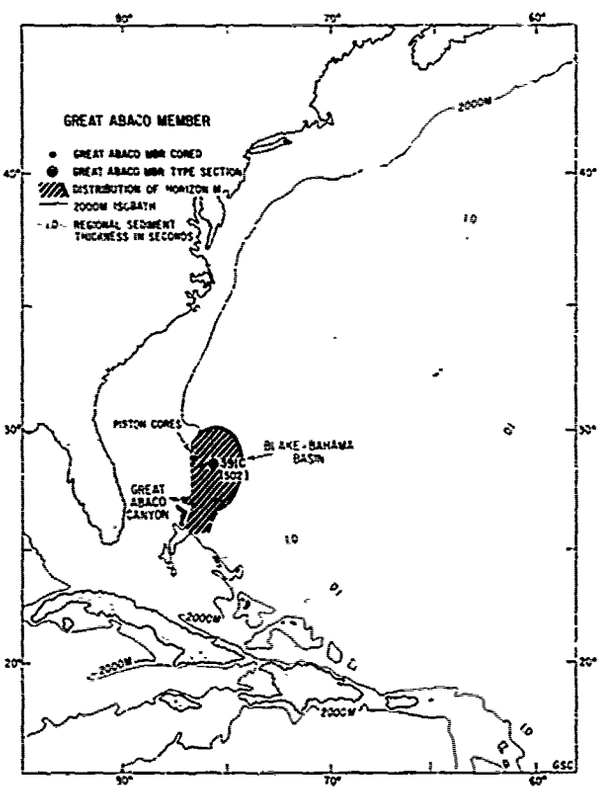


Figure 20. Location of borehole and piston cores that have cored Great Abaco Member, and the distribution of seismic Horizon M which occurs near the top of the Great Abaco Member (thickness in metres in parentheses).

## Great Abaco Member

Massive intervals of intraclastic chalk characterize the Great Abaco Member of the Blake Ridge Formation. Great Abaco Canyon, which leads from the Blake Plateau into the Blake-Bahama Basin, may have served as a conduit for debris flows which deposited the intraclastic chalk and related sediments.

Type Locality. This member has been drilled only at Site 391 which is necessarily the type locality (Table 18), but it constitutes a mappable unit because it can be traced seismically throughout the Blake-Bahama Basin. The validity of seismic correlations has been verified by piston cores at several localities where the unit is near the surface (Figure 20; Sheridan *et al.*, 1974).

Light-grey nannofossil chalk containing intraclasts of dark greenish-grey, olive-grey, or bluish-grey radiolarian mudstone is the characteristic lithology of the Great Abaco Member (Figure 16C). A few intervals of intraclastic chalk also contain lithoclasts of shallow-water limestone (Figure 16B). Interlayered with the massive chalk are several contrasting lithologies: (1) white, uniform carbonate silt (at the top of the member), (2) dark olive-grey radiolarian mudstone identical to intraclasts in the chalk, and (3) thin, graded beds of claystone intraclasts with erosional bases and partial Bouma sequences.

Nannofossils occur in most of these lithologies. Radiolarians and diatoms are abundant in the mudstone layers and intraclasts. Foraminifers were found in the chalk matrix and the carbonate silt and include both planktic and benthic forms from shallow and deep-water environments ranging in age from Cretaceous to Miocene.

Sedimentary structures in the intraclastic chalk include a few cut-and-fill surfaces, low-angle inclined laminae, graded intervals and rare burrows. The carbonate silt and radiolarian mudstone are structureless.

Contacts. The upper contact of the member is at 147 m subbottom where the green-grey mud of the Blake Ridge Formation is underlain by white, uniform carbonate silt (97 percent $CaCO_3$). The lower contact is at 649 m subbottom (Table 18). Here light-grey chalk unconformably overlies a thin interval of rusty-colored variegated claystone of the Plantagenet Formation.

Regional Aspects. Seismic profiles indicate that the 500 m thickness of the Great Abaco Member cored at Site 391 is fairly constant throughout the Blake-Bahama Basin. However, the member pinches out abruptly at the margins of the basin, probably against the normal dark greenish-grey muds of the Blake Ridge Formation. Dispersal of debris flows was apparently confined by the Blake-Bahama Outer Ridge.

Acoustic Character. The base of the member at Site 391 corresponds to the Horizon $A^U$, which is an unconformity at this location. A reflector termed M lies 60 m below the top of the member (Figure 6). A second seismic reflector occurs within the member. It correlates with the top of thick intraclastic chalks beneath an interval of radiolarian mudstone at about 355 m sub-bottom. The Abaco Member can be traced through most of the Blake-Bahama Basin by its series of smooth, closely-spaced internal reflectors.

Calculated interval velocities are 2.50 km/s between M and the intermediate reflector and 2.25 km/s between the intermediate reflector and Horizon $A^U$ (Figure 5). The average shipboard velocities measured on cores for these intervals are 1.82 km/s (range 1.66 to 2.24) and 1.87 km/s (range 1.65 to 2.36).

Age. Based on study of radiolarians, nannofossils, and foraminifera, the Great Abaco Member is Early Miocene to Late Miocene (Figure 21). Detailed analysis of both the intraclasts and the matrix show that many intraclasts belong to the same biozones as the matrix which encloses them. The matrix also contains reworked Cretaceous and Eocene foraminifera from contrasting depositional environments (shallow and deep water; Benson, Sheridan *et al.*, 1978).

Depositional Environment. The radiolarian mudstone that forms interbeds and contributes most of the clasts apparently represents the background sedimentation and was deposited under comparable environments to the green-grey mud of the Blake Ridge Formation. The other sedimentary components were probably deposited from turbidity currents and debris flows. The matrix of the intraclastic chalk is predominantly of pelagic origin but was derived from a variety of older unconsolidated units and contemporaneous oozes originally deposited in shallower water. Shallow-water sources also contributed consolidated and unconsolidated clasts. The indicated sources are the Blake Plateau and escarpment for the pelagic components and the Bahama platform for shallow-water carbonates. Flows originating at these sources incorporated unlithified clasts of hemipelagic mud from the basin floor. Sediment accumulation rates of 9 m/m.y., 43 m/m.y., and 39 m/m.y. were calculated for intervals corresponding roughly to late Middle and Early Miocene (Table 20).

## Summary

Six formations and two members are formally defined in the Mesozoic and Cenozoic sediments of the North American Basin. Drill-hole and seismic data are adequate to specify the lithofacies, contacts, regional aspects, acoustic character, physical properties, ages, and depositional environments. In this paper we have compiled these parameters, but have avoided detailed discussion of depositional conditions because of space limitations. The reader is referred to Tucholke and

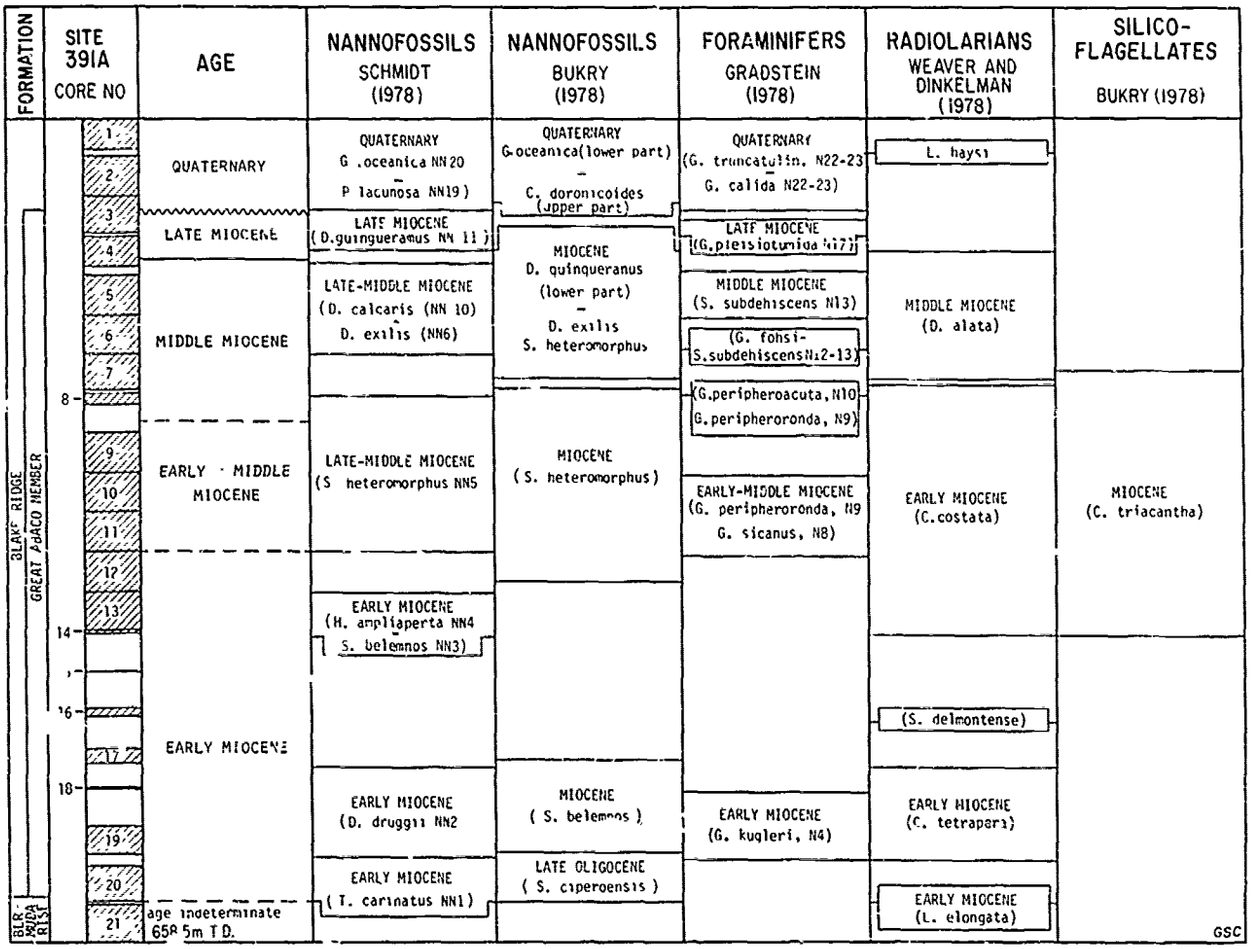


MULTIPLE BIOSTRATIGRAPHY OF THE UPPER CENOZOIC HEMIPELAGIC SEDIMENTS IN SITE 391, HOLE A, BLAKE-BAHAMA BASIN.

Figure 21. Multiple biostratigraphy of Site 391A located in Blake-Bahama Basin.

Mountain (1979) in this volume for broader discussion of paleoenvironments based on both seismic stratigraphy and lithostratigraphy.

The distribution of sedimentary formations within the North American Basin is shown on a schematic geologic cross section, which parallels the continental margin from south to north (A-B on Figure 22) and cuts the basin latitudinally from the North American margin toward the Mid Atlantic Ridge between (B-C). The oldest formation defined in the North American Basin is the Cat Gap Formation. It consists of reddish-brown and greenish-grey pelagic argillaceous limestone of Oxfordian-Tithonian age and occupies the western part of the basin on crust older than about anomaly M-23. It is mappable using seismic Horizon C which may correspond to its upper contact. The overlying Blake-Bahama Formation is light grey pelagic limestone of Tithonian-Barremian age. It is mappable as the acoustic interval between seismic Horizon β and Horizon C, and pinches out eastwards on oceanic crust generally of Hauterivian to Barremian age. The Hatteras Formation consists of green-grey and black shale and claystone of Barremian-Cenomanian age and commonly has a high content of organic carbon derived from terrigeneous and marine sources. The overlying Plantagenet Formation is varicolored, locally zeolitic clay of Late Cenomanian to Paleocene or Early Eocene age. Low accumulation rates and local enrichment in metallic ions are notable characteristics of this unit. Within this formation Middle to Upper Maastrichtian marl and chalk of the Crescent Peaks Member correlate with seismic Horizon A*.

The two formations which comprise most of the Cenozoic sediments are the Bermuda Rise and the Blake Ridge Formations. The Bermuda Rise Formation contains chert and clayey and calcareous sediments enriched in biogenic silica. It is of Late Paleocene to Middle Eocene age. The top of the chert correlates with seismic Horizon $A^C$ which is widespread in the North American Basin. Most of this formation is absent beneath the conti-

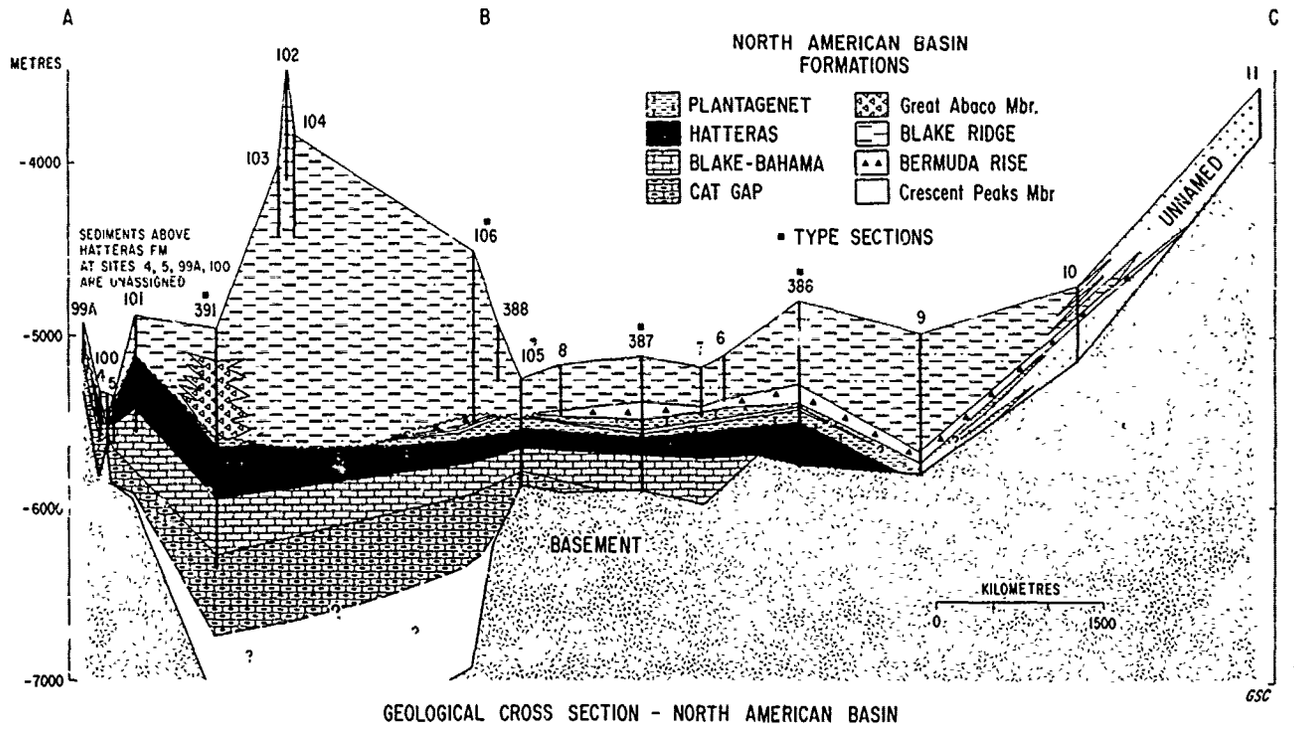


GEOLOGICAL CROSS SECTION - NORTH AMERICAN BASIN

Figure 22. Stratigraphic cross-section of the North American Basin. Location in Figure 1.

nental rise because of Late Paleogene or Early Neogene erosion by bottom currents. The Blake Ridge Formation is a hemipelagic grey-green mud with local debris flow and turbidite deposits of Middle Eocene to Holocene age. Along the continental margin, most of this formation is of Miocene age, and it is the presence of these sediments that is responsible for the present morphologic expression of the continental rise. Within the Blake Ridge Formation, Miocene intraclastic chalks of the Great Abaco Member were deposited by debris flows from the adjacent Blake Plateau and Bahama Banks. This member is confined to the Blake-Bahama Basin and can be mapped using seismic reflector M.

The sedimentary evolution of the basin reflects the interaction of factors including climate, surface and abyssal circulation, biogenic production, sea level changes and tectonic events. The Cat Gap and Blake-Bahama Formations were deposited near or above the CCD, while the Hatteras and Plantagenet Formations were deposited below the CCD, which shallowed significantly during the Barremian. Temporary but sharp deepening, and rise of the CCD resulted in deposition of marl and chalk of the Crescent Peaks Member. In the Tertiary, the Bermuda Rise and Blake Ridge Formations were deposited mostly below the CCD (Figure 23).

Upper Jurassic and Lower Cretaceous sediments (Cat Gap Formation, Blake-Bahama Formation) are primarily pelagic limestone sequences. Local influx of mixed bioclastic and terrigenous debris occur near the continental margin, but most reworked sediment observed in boreholes is the result of local slumping and fine-grained turbidite deposition. Some fine-scale lensing and lamination in these sediments may represent reworking by weak bottom currents. The scarcity of terrigenous sediment in the Oxfordian-Hauterivian sedimentary sequences of the North American Basin reflect low precipitation and low relief of the surrounding land. Extensive carbonate deposition on the shelves, also noticeable by the presence of 'shallow-water' carbonate turbidites, indicates warm climate.

Gradual replacement of carbonate by terrigenous sediment on the North American shelf occurred during Tithonian-Berriasian time, but this change is not reflected in the deep sea basin until the Barremian. Better correlation exists between an approximately Hauterivian termination of carbonate deposition in both the deep sea and on the shelf. The top of the shelf carbonates on the northwestern shelf of the North American Basin is an excellent seismic reflector which may correlate with seismic horizon β of the deep sea basin.

In Valanginian time pulses of anoxic conditions began in the basin with resulting deposition of dark marly chalk and calcareous clay beds at the top of the Blake Bahama Formation. This process culminated approximately in the Barremian, with the establishment of alternating anoxic and low-oxygen conditions in the deep basin. Terrestrial and marine organic carbon were preserved

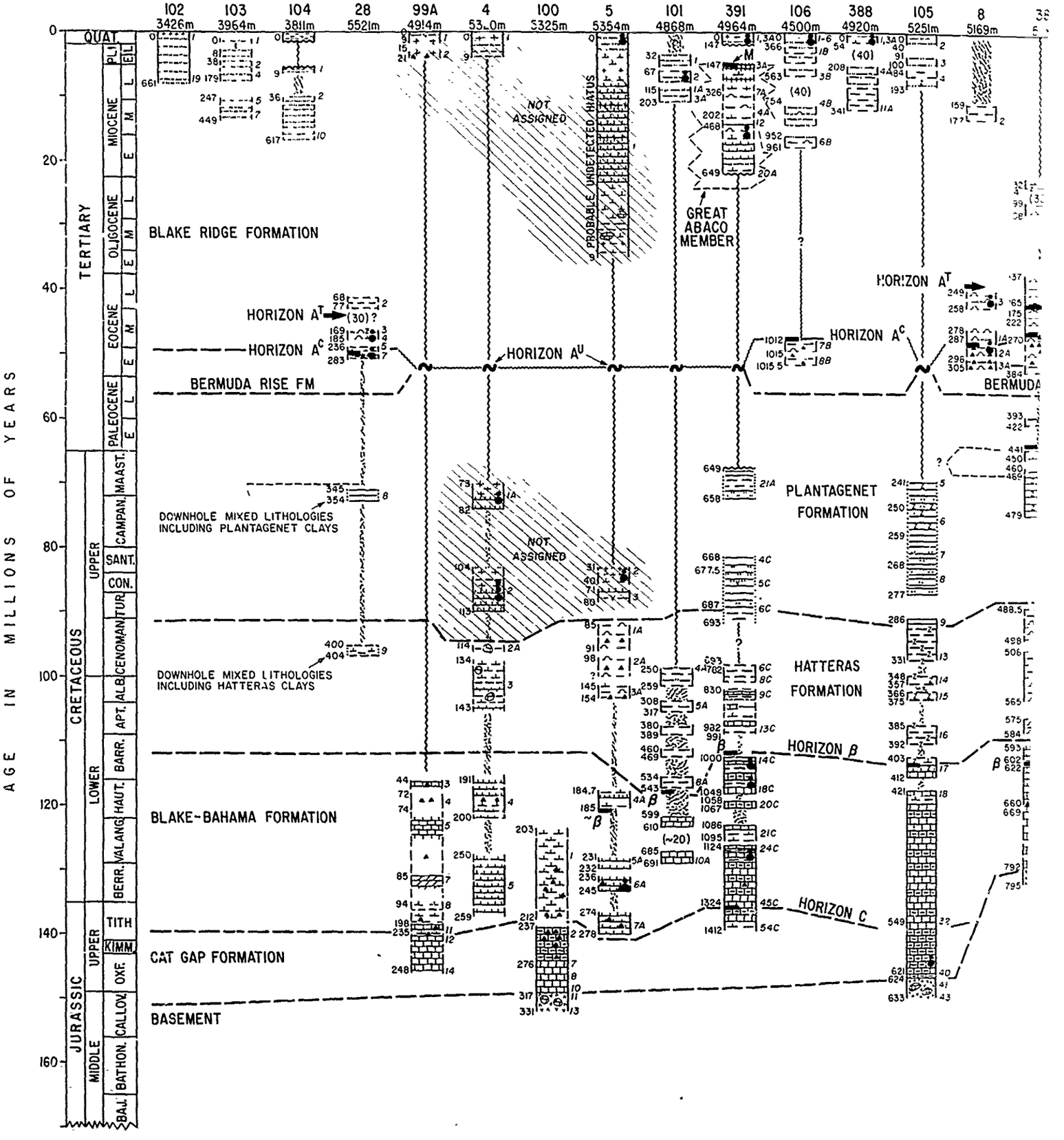


Figure 24. Correlation chart of DSDP sites in the North Atlantic Basin. The chart ...matic ...ers. formation names and boundaries, and stratigraphic position of regionally important se... oozes are not assigned to any formation.

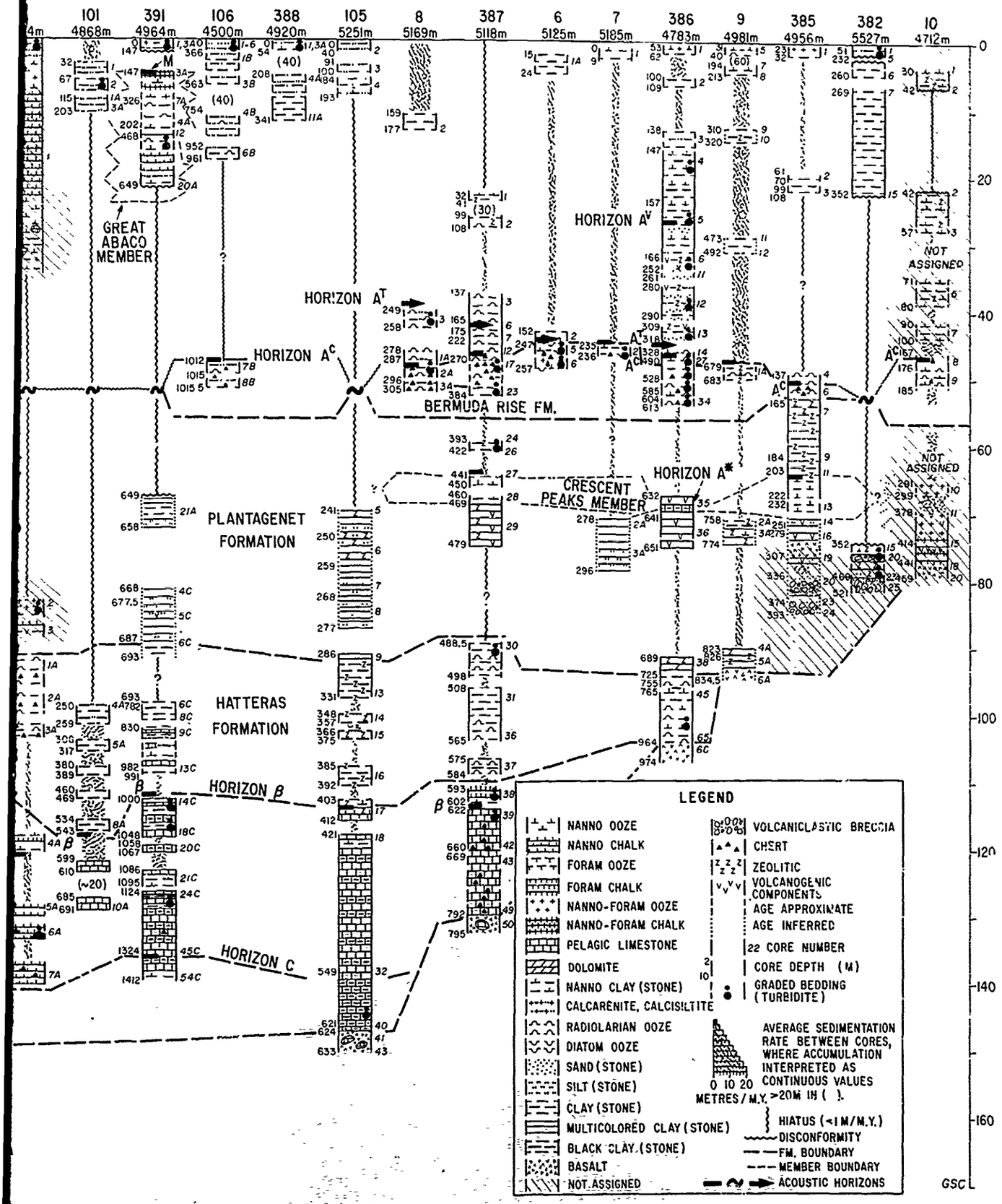


the North Atlantic Basin. The chart shows schematic lithology of individual cores, sub-bottom depth, age, ic position of regionally important seismic markers. Based on Tucholke (1979). Quaternary nanno/ foraminiferal

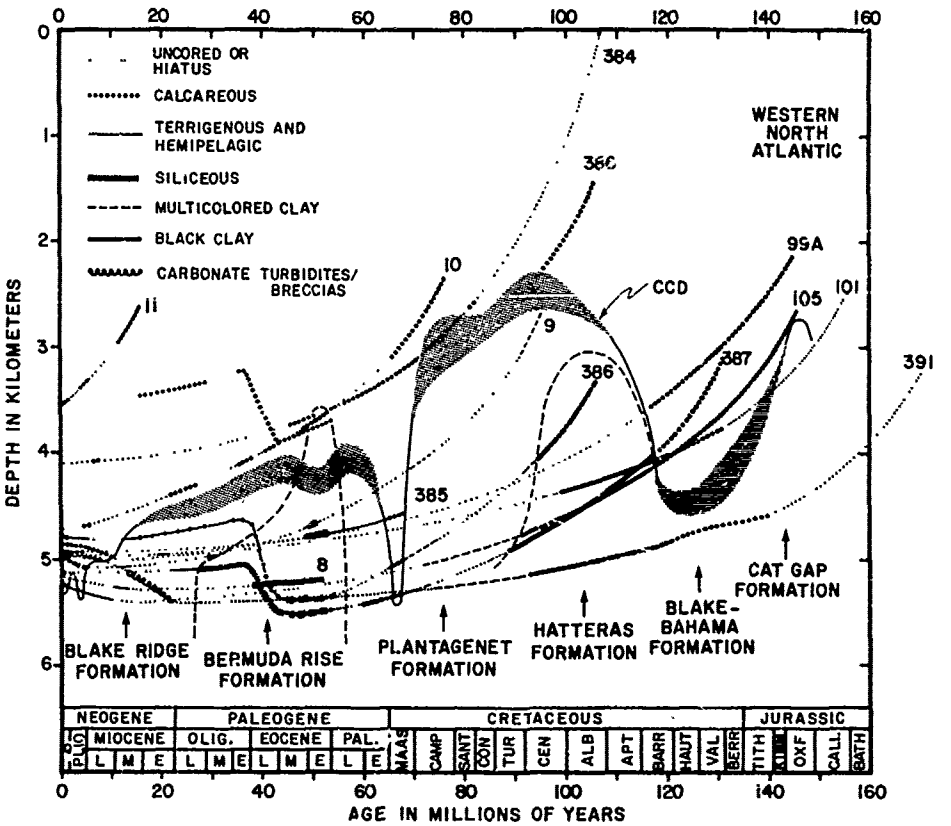


Figure 23. Depth variation of the calcite compensation depth (CCD) through the Mesozoic and Cenozoic in the North American Basin, from Tucholke and Vogt (1979), with Site 391C added. Lithology at each site is plotted along seafloor age versus depth curves for that site. Site 391C may have experienced anomalous subsidence because of its position near the Blake Plateau, and the site paleodepth curve depicted may be too deep. The anomalously deep initial ridge-crest elevation (3300 m), the presence of aragonite in the Jurassic sediments, the early cut-off in reducing (black clay) conditions suggest the Mesozoic part of the curve should be at least 600 m shallower.

beneath stagnant to sluggishly circulating deep water, but surface circulation and organic productivity were well developed. Much of the calcareous and siliceous biogenic debris found locally within the Hatteras Formation probably had intermediate residence on shallow sea floor above the CCD (continental margin, mid-ocean ridge flank, seamounts) before being rapidly emplaced in the deep basin by turbidity currents. Deposits that are synchronous to the Hatteras Formation on the North American Shelf are deltaic, coal-bearing deposits, which may explain the high content of plant debris in the Hatteras Formation. Lack of a similar influence of Lower Cretaceous coal-bearing clastic strata on the deep-sea deposits may be due to trapping of clastic debris behind the shelf edge carbonate platforms.

Increased deep-water oxygenation in the Late Cretaceous (post-Cenomanian) is indicated by the Plantagenet Formation with its varicolored clays and metalliferous deposits. Accumulation rates in the Plantagenet Formation were very low, with the influx of the terrigenous sediment to the basin being minimized by progressing mid-Cretaceous transgression. The North American Basin during Late Cretaceous was sediment starved.

The brief period of chalk deposition during the Maastrichtian was an ocean-wide event which also influenced shelf deposition. The chalks on the shelf are prominent seismic reflectors approximately correlatable with the seismic Horizon A* of the deep North American Basin.

During Late Paleocene through Middle Eocene time, deposition of biogenic silica predominated in the deep North American Basin below the CCD, and mixed calcareous-siliceous sediments were deposited in shallower depth. Increased productivity of siliceous organisms during this time may reflect enhanced circulation and upwelling in response to cooler climates. High productivity

zones were probably well developed along the circum-global 'equatorial' flow through the Tethys, North Atlantic and Pacific Oceans, and biogenic silica production may have been accentuated by Eocene volcanism (Berggren and Hollister, 1974; Gibson and Towe, 1971).

Turbidites originating from the continental margin and deposited on a regional scale first became important in the Paleocene, and by the Eocene they reached the Bermuda Rise region. Turbidites on the Bermuda Rise predate formation of the Rise in the Middle to Late Eocene and they form parts of the Bermuda Rise and Blake Ridge Formations. Volcaniclastic turbidites derived from weathering of the Bermudian volcanic basement were deposited around the pedestal in Late Eocene and Oligocene time. In the Blake-Bahama Basin a series of debris flows incorporated pelagic shelf carbonates and hemipelagic mud, and formed a thick sedimentary sequence spanning most of Miocene. Coarser-grained terrigeneous sediment has been deposited, mostly during the Late Pliocene and Pleistocene, in pockets along the continental rise and in the modern abyssal plains by turbidity currents. These turbidites and debris flow deposits all form facies variations within the Blake Ridge Formation.

Bottom-current activity markedly affected the sedimentary record in the Late Cenozoic. A major unconformity was eroded into the continental rise some time between Late Eocene and the earliest Miocene, excavating Lower Cretaceous sediments. Rapid hemipelagic deposition controlled in large part by bottom currents has dominated the sedimentary record since the Early Miocene. The present continental rise and depositional outer ridges were formed in this regime.

## Acknowledgements

We are indebted to Hollis D. Hedberg, Peter Scholle, John Milliman, Graham Williams, and John Bujak for critical comments on the manuscript and to colleagues at the Atlantic Geoscience Centre and Lamont-Doherty Geological Observatory for lively discussions on problems of Mesozoic-Cenozoic sedimentation in the Atlantic and surrounding continental margins. Critical comments about deep-basin lithostratigraphy were received from numerous colleagues at an informal workshop held at Woods Hole in September 1976; these comments formed the working basis of this report and are gratefully acknowledged. Data and samples for this report were provided by the Deep Sea Drilling Project, supported by the National Science Foundation. Support by the Geological Survey of Canada (L.F.J. and F.H.G.) and National Science Foundation Grants EAR76-12478 (P.E.), DES-75-21594 and OCE-76-82326 (R.E.S.), OCE-76-02038 and ONR Contract N00014-75-C-0210 (B.E.T.), during preparation of this paper is gratefully acknowledged. We thank Gary Cook and Betty Batchelder for drafting the figures. Contribution number 2755 of Lamont-Doherty Geological Observatory.

## References

Arthur, M.A., A model for genesis of Late Cretaceous multicolored claystones of the western Atlantic, *in* Tucholke, B.E., Vogt, P.R. *et al.*, Initial Reports of the Deep Sea Drilling Project, 43, Washington (U.S. Government Printing Office), 1979.

Aubouin, J., Réflexions sur le faciés "ammonitico rosso", Bull. Soc. Géol. Fr., 7, 475-501, 1964.

Aumento, F., W.G. Melson *et al.*, Leg 37 - the volcanic layer, Geotimes, 16-18, 1974.

Azéma, J., R. Bourrouilh, Y. Champetier, Fourcade and Y. Rangheard, Rapports stratigraphiques, paléogéographiques et structuraux entre la chaine Ibérique, les Cordillères Bétiques et les Baléares, Bull. Soc. Géol. Fr. XVI, 101-237, 1976.

Bader, R.G., R.D. Gerard, W.E. Benson, H.M. Bolli, W.W. Hay, W.T. Rothwell, Jr., M.H. Ruef, W.R. Riedel and F.L. Sayles, Initial Reports of the Deep Sea Drilling Project, 4, Washington (U.S. Government Printing Office), 753 p., 1970.

Bathurst, R.G.C., Carbonate sediments and their diagenesis, Dev. Sedimentol., 12, Elsevier, 620 p., 1971.

Benson, W.E., R.E. Sheridan, P. Enos, T. Freeman, F. Gradstein, I.O. Murdmaa, L. Pastouret, R.R. Schmidt, D.H. Stuermer, F.M. Weaver, and P. Worstell, Initial Reports of the Deep Sea Drilling Project, 44, Washington (U.S. Government Printing Office), 1005, 1978.

Berggren, W.A. and C.D. Hollister, Paleogeography, paleobiogeography, and the history of circulation in the Atlantic Ocean, *in* Hay, W.W. (ed.), Studies in Paleo-oceanography, Soc. Econ. Pal. Min. Spec. Publ. 20, 126-186, 1974.

Berggren, W.A., D.P. McKenzie, J.G. Sclater, and J.E. Van Hinte, World-wide correlation of Mesozoic magnetic anomalies and its implications: discussion and reply, Geol. Soc. Amer. Bull., 86, 267-272, 1975.

Bernoulli, D., North Atlantic and Mediterranean Mesozoic Facies: A comparison, *in* Hollister, C.D., Ewing, J.I. *et al.*, eds., Initial Reports of the Deep Sea Drilling Project, 11, Washington (U.S. Government Printing Office), 801-871, 1972.

Bernoulli, D., and H.C. Jenkyns, Alpine, Mediterranean, and Central Atlantic Mesozoic facies in relation to the early evolution of the Tethys, *in* Dott, R.H., Jr., and Shaver, R.H., eds., Modern and Ancient Geosynclinal Sedimentation, Soc. Econ. Pal. Min., Spec. Publ. 19, 129-160, 1974.

Bolli, H., W.B.F. Ryan *et al.*, Basins and margins of the eastern south Atlantic, Geotimes, 22-24, 1975.

Bosellini, A., and E.L. Winterer, Pelagic limestones and radiolarite of the Tethyan Mesozoic: A genetic model, Geology, 279-282, 1975.

Bryan, W.B., Textural and mineralogical relations of basalts from sites 100 and 105, *in* Hollister,

C.D., Ewing, J.I., *et al.*, Initial Reports of the Deep Sea Drilling Project, 11, Washington (U.S. Government Printing Office), 873-876, 1972.

Bryan, W.B., P.T. Robinson *et al.*, Studying oceanic layers, Geotimes, 22-26, 1977.

Bukry, D., Cenozoic coccolith, silicoflagellate, and diatom stratigraphy, Deep Sea Drilling Project, Leg 44, *in* Benson, W.E., Sheridan, R.E. *et al.*, Initial Reports of the Deep Sea Drilling Project, 44, Washington (U.S. Government Printing Office), 807-864, 1979.

Cepek, P., Mesozoic calcareous nannoplankton of the Eastern North Atlantic, Leg 41, *in* Lancelot, Y., Seibold, E. *et al.*, Initial Reports of the Deep Sea Drilling Project, 41, Washington (U.S. Government Printing Office), 1978.

Cook, H.E., North American stratigraphic principles as applied to deep-sea sediments, Amer. Assoc. Petrol. Geol. Bull., 59, 5, 817-837, 1975.

Dabrio, C.J., J.M. Gonzales-Donoso, P. Rivas, and J.A. Vera, Geology of the sub-betic zone, American Geological Institute - Guidebook - X International Field Institute 1971, 171-196, 1971.

Dean, W.E., J.V. Gardner, L.F. Jansa, and P. Cepek, Cyclic sedimentation along the continental margin of Northwest Africa, Leg 41, Deep Sea Drilling Project, *in* Lancelot, Y., Seibold, E. *et al.*, Initial Reports of the Deep Sea Drilling Project, 41, Washington (U.S. Government Printing Office), 965-990, 1979.

Demars, K., Engineering and other physical properties data, Leg 43, *in* Tucholke, B.E., Vogt, P.R. *et al.*, Initial Reports of the Deep Sea Drilling Project, 43, Washington (U.S. Government Printing Office), 1979.

Didon, J., M. Durand-Delga, and J. Kornprobst, Homologies géologiques entre les deux rives du détroit de Gibraltar, Bull. Soc. Géol. Fr., 7, 77-105, 1073.

Douglas, R.G., N. Moullade, and M.E. Nairn, Causes and consequences of continental drift in the South Atlantic, *in* Tarling, D.H., and Runcorn, S.K., eds., Implications of continental drift to the Earth Sciences, 1, Academic Press, London, 517-537, 1973.

Duff, K.L., Paleoecology of a bituminous shale - the Lower Oxfordian clay of central England, Paleontology, 18, Part 3, 443-482, 1975.

Enos, P., and T. Freeman, Shallow-water limestones from the Blake Nose, Sites 390 and 392, *in* Benson, W.E., Sheridan, R.E. *et al.*, Initial Reports of the Deep Sea Drilling Project, 44, Washington (U.S. Government Printing Office), 413-462, 1978.

Ewing, J.I., and C.D. Hollister, Regional aspects of deep sea drilling in the western North Atlantic, *in* Hollister, C.D., Ewing, J.I. *et al.*, Initial Reports of the Deep Sea Drilling Project, 11, Washington (U.S. Government Printing Office), 951-995, 1972.

Ewing, M., J.L. Worzel, A.O. Beall, W.A. Berggren, J.D. Bukry, C.A. Burk, A.G. Fischer, and E.A. Pessagno, Jr., Initial Reports of the Deep Sea Drilling Project, 1, Washington (U.S. Government Printing Office), 672 p., 1969.

Fischer, A.C., and M. Arthur, Secular variation in the pelagic realm, *in* Cook, H.E., and Enos, P., eds., Deep-water carbonate environments, Soc. Econ. Paleontol. Mineral. Spec. Publ. 25, 1978.

Flood, R.D., X-ray mineralogy of DSDP Legs 44 and 44A, western North Atlantic: Lower continental rise hills, Blake Nose, and Blake-Bahama Basin, *in* Benson, W.E., Sheridan, R.E. *et al.*, Initial Reports of the Deep Sea Drilling Project, 44, Washington (U.S. Government Printing Office), 515-522, 1978.

Freeman, T., and P. Enos, Petrology of Upper Jurassic-Lower Cretaceous Limestones, Site 391, *in* Benson, W.E., Sheridan, R.E. *et al.*, Initial Reports of the Deep Sea Drilling Project, 44, Washington (U.S. Government Printing Office), 463-475, 1978.

Funnel, B.M., Foraminifera and Radiolaria as depth indicators in the marine environment, Mar. Geol. 5, 333, 1967.

Garrison, R.E., Pelagic limestones of the Oberalm Beds (Upper Jurassic-Lower Cretaceous), Austrian Alps, Bull. Can. Petrol. Geol., 15, 21-49, 1967.

Gibson, T.G., Late Mesozoic-Cenozic tectonic aspects of the Atlantic coastal margin, Geol. Soc. Amer. Bull., 81, 1813-1822, 1970.

Gibson, T.G., and K.M. Towe, Eocene volcanism and the origin of Horizon A, Science, 172, 153-154, 1971.

Gonzáles-Donoso, J.M., A. Linares, A.C. López-Garrido, and J.A. Vera, Bosquejo estratrigrafico del Jurásico de Las Cordilleras Béticas, Cuad. Geol. Iberica, 2, 55-90, 1971.

Gradstein, F.M., G.L. Williams, W.A.M. Jenkins, and P. Ascoli, Mesozoic and Cenozoic stratigraphy of the Atlantic continental margin, Eastern Canada, *in* Yorath, C.J., Parker, E.R., and Glass, D.J., eds., Canada's Continental Margins and Offshore Exploration, Can. Soc. Petrol. Geol., Memoir 4, 103-131, 1975.

Gradstein, F.M., Biostratigraphy and biogeography of Jurassic Grand Banks Foraminifera, Proceedings of 'Benthonics 75', Halifax (N.S.), Maritime Sed. Spec. Publ. 1, pt. B, 557-583, 1977.

Gradstein, F.M., Biostratigraphy of Lower Cretaceous Blake Nose and Blake-Bahama Basin Foraminifers, DSDP Leg 44, western North Atlantic Ocean, *in* Benson, W.E., Sheridan, R.E. *et al.*, Initial Report Deep Sea Drilling Project, v. 44, Washington (U.S. Government Printing Office), 663-702, 1978.

Gradstein, F.M., D. Bukry, D. Habib, O. Renz, P.H. Roth, R.R. Schmidt, F.M. Weaver, and F.H. Wind, Biostratigraphic summary of DSDP Leg 44 - northwestern Atlantic Ocean, *in* Benson, W.E., Sheridan, R.E. *et al.*, Initial Reports Deep Sea Drilling Project, v. 44, Washington (U.S. Government Printing Office), 657-662, 1978.

Grow, J.A., and R.G. Markl, IPOD-USGS multi-

channel seismic reflection profile from Cape Hatteras to the Mid-Atlantic Ridge, Geology, 6, 625-630, 1977.

Grunau, H.R., Radiolarian cherts and associated rocks in space and time, Eclogae Geol. Helv. 58, 157-208, 1965.

Grunau, J.R., P. Lehner, M.R. Cleintauar, P. Allenbach, and G. Bakker, New radiometric ages and seismic data from Fuerteventura (Canary Islands), Maio (Cape Verde Islands) and Sao Tome (Gulf of Guinea), *in* Prog. Geodynam., Amsterdam, 90-118, 1975.

Habib, D., Dinoflagellate stratigraphy, Leg 11, Deep Sea Drilling Project, *in* Hollister, C.D., Ewing, J.I. *et al.*, Initial Reports of the Deep Sea Drilling Project, 11, Washington (U.S. Government Printing Office), 367-426, 1972.

Habib, D., Comparison of Lower and Middle Cretaceous palynostratigraphic zonations in the western North Atlantic, *in* Stratigraphic Micropaleontology of Atlantic Basin and Borderlands, Elsevier Publishing Co., 341-367, 1977.

Habib, D., Palynostratigraphy of the Lower Cretaceous section at Deep Sea Drilling Project Site 391, Blake-Bahama Basin and its correlation in the North Atlantic, *in* Benson, W.E., Sheridan, R.E. *et al.*, Initial Reports of the Deep Sea Drilling Project, 44, Washington (U.S. Government Printing Office), 887-898, 1978.

Habib, D., Cretaceous palynostratigraphy at Site 387, West Bermuda Rise, *in* Tucholke, B.E., Vogt, P.R. *et al.*, Initial Reports of the Deep Sea Drilling Project, 43, Washington (U.S. Government Printing Office), 1979.

Hallam, A., Mesozoic geology and the opening of the North Atlantic, J. Geol., 79, 129-157, 1971.

Hathaway, J.C., and P.L. Sachs, Sepiolite and clinoptilolite from the Mid-Atlantic Ridge, Amer. Mineral., 50, 852, 1965.

Hathaway, J.C., J.S. Schlee, C.W. Poag, P.C. Valentine, E.G.A. Weed, M.H. Bothner, F.A. Kohout, F.T. Manheim, R. Schoen, R.E. Miller, and D.M. Schultz, Preliminary summary of the 1976 Atlantic Margin Coring Project of the U.S. Geological Survey, U.S. Geol. Sur. Open File Report No. 76-844, 217 p., 1976.

Hayes, D.E., A.C. Pimm, W.E. Benson, W.H. Berger, U. von Rad, P.R. Supko, J.P. Beckman, and P.H. Roth, Initial Reports of the Deep Sea Drilling Project, 14, Washington (U.S. Government Printing Office), 975 p., 1972.

Hayes, J.D., and W.C. Pitmann, III, Lithospheric plate motion, sea level changes and climatic and ecological consequences, Nature, 246, 18-22, 1973.

Hayes, D.E., and P.D. Rabinowitz, Mesozoic magnetic lineations and the magnetic quiet zone off northwest Africa, Earth Planet. Sci. Lett., 28, 101-115, 1975.

Hedberg, H.D., ed., International stratigraphic guide: International Subcommittee on Stratigraphic Classification of IUGS Commission on Stratigraphy, New York, John Wiley, 200 p., 1976.

Heezen, B.C., C.D. Hollister, and W.F. Ruddiman, Shaping of the continental rise by deep geostrophic contour currents, Science, 152, 502-508, 1966.

Heezen, B.C., M. Thorp, and M. Ewing, The floors of the oceans. I - North Atlantic, Geol. Soc. Amer. Spec. Paper 65, 122 p., 1959.

Hess, H., Planktonic crinoids of Late Jurassic age from Leg 11, Deep Sea Drilling Project, *in* Hollister, C.D., Ewing, J.I. *et al.*, Initial Reports of the Deep Sea Drilling Project, 11, Washington (U.S. Government Printing Office), 631-644, 1972.

Hollister, C.D. and B.C. Heezen, Geologic effects of ocean bottom currents: western North Atlantic, *in* Gordon, A.L., (ed.), Studies in Physical Oceanography, 2, Gordon and Breach, New York, 37-66, 1972.

Hollister, C.D., J.I. Ewing, D. Habib, J.C. Hathaway, Y. Lancelot, H. Luterbacher, F.J. Paulus, W. Poag, J.A. Wilcoxon, and P. Worstell, Initial Reports of the Deep Sea Drilling Project, 11, Washington (U.S. Government Printing Office), 1077 p., 1972.

Hurley, P.M., The conformation of the continental drift, Sci. Amer. 218, 52-64, 1968.

Jansa, L.F., The central North Atlantic Basin - Its birth and disappearance, Proc. Congr. Int. Sedimentologie, Nice, t. 2, 231-236, 1975.

Jansa, L.F., in press, Le Cretacé au large de la marge Iberique, Cah. Micropaleont.

Jansa, L.F., J. Gardner, and W.E. Dean, Mesozoic sequences of the central North Atlantic, *in* Lancelot, Y., Seibold, E. *et al.*, Initial Reports of the Deep Sea Drilling Project, 41, Washington (U.S. Government Printing Office), 991-1031, 1978.

Jansa, L.F., and J.A. Wade, Geology of the continental margin off Nova Scotia and Newfoundland, *in* Offshore Geology of Eastern Canada, Can. Geol. Surv. Paper 74-30, 2, 51-105, 1975a.

Jansa, L.F., and J.A. Wade, Paleogeography and sedimentation in the Mesozoic and Cenozoic, southeastern Canada, *in* Yorath, C.J., Parker, E.R., and Glass, D.J., eds., Canada's Continental Margins and Offshore Exploration, Can. Soc. Petrol. Geol. Memoir 4, 79-102, 1975b.

Jefferies, R.P.S., and P. Minton, The mode of life of two Jurassic species of "Posidonia" (Bivalve). Paleontology, 8, 156-185, 1965.

Jenkyns, H.C., The genesis of condensed sequences in the Tethyan Jurassic, Lethaia, 4, 327-352, 1971.

Jordan, R., Salz-und Erdöl/Erdgas-Austritt als Fazies bestimmende Faktoren im Mesozoikum Nordwest-Deutschlands, Geol. Jahrb. Reihe A, 13, 64, 1974.

Jukes-Brown, A.J., and J.B. Harrison, Geology of Barbados, Part II: Oceanic deposits. Quart. J. Geol. Soc. London, 48, 170-226, 1891.

Kuhry, B., Observations on filaments from the

Subbetic of SE Spain, Rev. Espan. Micropaleontol., 7, 231-243, 1975.

Kuhry, B., S.W.G. De Clercq, and L. Dekker, Indications of current action in Late Jurassic limestones, radilarian limestones, *Saccocoma* limestones and associated rocks from the Subbetic of SE Spain, Sediment. Geol., 15, 235-258, 1976.

Lancelot, Y., J.C. Hathaway, and C.D. Hollister, Lithology of sediments from the western North Atlantic, Leg 11, Deep Sea Drilling Project, *in* Hollister, C.D., Ewing, J.I. *et al.*, Initial Reports of the Deep Sea Drilling Project, 11, Washington (U.S. Government Printing Office), 901-950, 1972.

Lancelot, Y., E. Seibold, W.E. Dean, L.F. Jansa, V. Eremeev, J. Gardner, P. Cepek, V. Krasheninnikov, V. Pflaumann, D. Johnson, G. Rankin, and P. Trabant, Initial Reports of the Deep Sea Drilling Project, 41, Washington (U.S. Government Printing Office), 1259, 1978.

Larson, R.L., and T.W.C. Hilde, A revised time scale of magnetic reversals for the Early Cretaceous and Late Jurassic, J. Geophys. Res., 80, 2586-2594, 1975.

Laubscher, H.P., Gewegung und Wärme in der alpinen Orogense, Schweiz. Mineral. Petrogr. Mitt. 50, 503, 1970.

Lehman, R., Microfossils in thin sections from the Mesozoic deposits of Leg 11, Deep Sea Drilling Project, *in* Hollister, C.D., Ewing, J.I. *et al.*, Initial Reports of the Deep Sea Drilling Project, 11, Washington (U.S. Government Printing Office), 659-666, 1972.

Luterbacher, H., Foraminifera from the Lower Cretaceous and Upper Jurassic of the Northwestern Atlantic, *in* Hollister, C.D., Ewing, J.I. *et al.*, Initial Reports of the Deep Sea Drilling Project, 11, Washington (U.S. Government Printing Office), 561-594, 1972.

Luterbacher, H.P., and I. Primoli Silva, Note preliminaire sur une revision du proil de Gubbio, Italie, Riv. Ital. Paleontol. Stratigr., 70, 67, 1962.

Luyendyk, B.P., Gondwanaland dispersal and the early formation of the Indian Ocean, *in* Davies, T.A., Luyendyk, B.P. *et al.*, Initial Reports of the Deep Sea Drilling Project, 16, Washington (U.S. Government Printing Office), 945-951, 1974.

McCave, I.N., Diagnosis of turbidites at Sites 386 and 387 by particle-counter size analysis of the silt (2-40 μm) fraction, *in* Tucholke, B.E., Vogt, P.R. *et al.*, Initial Reports of the Deep Sea Drilling Project, 43, Washington (U.S. Government Printing Office), 1979.

McIver, N.L., Cenozoic and Mesozoic stratigraphy of the Nova Scotia Shelf, Can. J. Earth Sci., 9, 54-70, 1972.

McNulty, C., Smaller Cretaceous foraminifers of Leg 43, Deep Sea Drilling Project, *in* Tucholke, B.E., Vogt, P.R. *et al.*, Initial Reports of the Deep Sea Drilling Project, 43, Washington (U.S. Government Printing Office), 1979.

Meyerhoff, A.A., and C.W. Hatten, Bahamas salient of North America: tectonic framework, stratigraphy, and petroleum potential, Amer. Assoc. Petrol. Geol. Bull., 58, 1201-1239, 1974.

Morales, L.G., and the Columbian Petroleum Industry, General geology and oil occurrences of Middle Magdalena Valley, Columbia, *in* Habitat of Oil, Weeks, L.G., ed., Tulsa, 641-695, 1958.

Mountain, G.S., and B.E. Tucholke, Horizon β: Acoustic character and distribution in the western North Atlantic, Trans. Am. Geophys. Union, 58, 406, 1977.

Oertli, H.J., Jurassic ostracods of DSDP Leg 11 (sites 100 and 105) - preliminary account, *in* Hollister, C.D., Ewing, J.I. *et al.*, Initial Reports of the Deep Sea Drilling Project, 11, Washington (U.S. Government Printing Office), 645-668, 1972.

Okada, H., and H. Thierstein, Calcareous nannoplankton - Leg 43, Deep Sea Drilling Project, *in* Tucholke, B.E., Vogt, P.R. *et al.*, Initial Reports of the Deep Sea Drilling Project, 43, Washington (U.S. Government Printing Office), 1979.

Paulus, F.J., Leg 11 measurements of physical properties in sediments of the western North Atlantic and their relationship to sediment consolidation, *in* Hollister, C.D., Ewing, J.I. *et al.*, Initial Reports of the Deep Sea Drilling Project, 11, Washington (U.S. Government Printing Office), 667-721, 1972.

Perry, W.J., J.P. Minard, E.G.A. Weed, E.I. Robins, and E.C. Rhodemhamel, Stratigraphy of the Atlantic continental margin of the United States north of Cape Hatteras - brief survey, Amer. Assoc. Petrol. Geol. Bull., 59, 1529-1548, 1975.

Pessagno, E.A., Jr., Mesozoic Planctonic Foraminifera and Radiolaria, *in* Ewing, M., Worzel, L.J. *et al* , Initial Reports of the Deep Sea Drilling Project, 1, Washington (U.S. Government Printing Office), 607-611, 1969.

Peterson, M.N.A., N.T. Edgar, C. von der Borch, M.B. Cita, S. Gartner, Jr., R. Goll, and C. Nigrini, Initial Reports of the Deep Sea Drilling Project, 2, Washington (U.S. Government Printing Office), 491 p., 1970.

Pitman, W.C.,III, M. Talwani, and J.R. Heirtzler, Age of the North Atlantic from magnetic anomalies, Earth Planet. Sci. Lett. 11, 195-200, 1971.

Poag, C.W., Neogene planktonic foraminiferal biostratigraphy of the western North Atlantic, Deep Sea Drilling Project, Leg 11, *in* Hollister, C.D., Ewing, J.I. *et al.*, Initial Reports of the Deep Sea Drilling Project, 11, Washington (U.S. Government Printing Office), 483-522, 1972.

Poag, C.W., Foraminiferal biostratigraphy, *in* Scholle, P.A., ed., Geological studies on the COST B-2 well, U.S. Mid-Atlantic Outer Continental Shelf areas: U.S. Geol. Surv. Circ. 750, 35-36, 1977.

Renz, O., Aptychi (Ammonoidea) from the Upper Jurassic and Lower Cretaceous of the western

North Atlantic (Site 105, Leg 11, DSDP), *in* Hollister, C.D., Ewing, J.I. *et al.*, Initial Reports of the Deep Sea Drilling Project, 11, Washington (U.S. Government Printing Office), 607-630, 1972.

Renz, O., Aptychi (Ammonoidea) from the Early Cretaceous of the Blake-Bahama Basi Leg 44, Hole 391C, Deep Sea Drilling Project, *in* Benson, W.E., Sheridan, R.E. *et al.*, Initial Reports of the Deep Sea Drilling Project, 44, Washington (U.S. Government Printing Office), 899-910, 1978.

Renz, O., R. Imlay, Y. Lancelot, and B.F. Ryan, Ammonite-rich Oxfordian limestones from the base of the continental slope off Northwest Africa, Eclogae Geol. Helv., 68/2, 431-448, 1975.

Rhodehamel, E.C., Lithologic descriptions, *in* Scholle, P.A., ed., Geological studies on the COST No. B-2 well, U.S. Mid-Atlantic Outer Continental Shelf area, U.S. Geol. Surv. Circ. 750, 15-22, 1977.

Roth, P.H., Cretaceous nannoplankton biostratigraphy and paleoceanography of the northwestern Atlantic, *in* Benson, W.E., Sheridan, R.E. *et al.*, Initial Reports of the Deep Sea Drilling Project, 44, Washington (U.S. Government Printing Office), 731-760, 1978.

Ryan, W.B.F., J.C. Sibuet *et al.*, Passive continental margin, Geotimes, 21-24, 1976.

Saito, T., L.H. Burckle, and M. Ewing, Lithology and paleontology of the reflective layer, Horizon A, Science, 154, 1173, 1966.

Schlanger, S.O., and H.C. Jenkyns, Cretaceous oceanic anoxic events: causes and consequences, Geol. Mijnbouw, 55, 179-184, 1976.

Schlee, J., J.C. Behrendt, J.A. Grow, J.M. Robb, R.E. Mattick, P.T. Taylor, and B.J. Lawson, Regional geologic framework off Northeastern United States, Amer. Assoc. Petrol. Geol. Bull. 60, 926-951, 1976.

Schmidt, R.R., Calcareous nannoplankton from the western North Atlantic of DSDP Leg 44, *in* Benson, W.E., Sheridan, R.E. *et al.*, Initial Reports of the Deep Sea Drilling Project, 44, Washington (U.S. Government Printing Office), 703-730, 1978.

Scholle, P.A., ed., Geological studies on the COST No. B-2 Well, U.S. Mid-Atlantic Outer Continental Shelf area, U.S. Geol. Surv. Circ. 750, 71, 1977.

Schouten, H., and K.D. Klitgord, Mesozoic magnetic anomalies, western North Atlantic, Map MF-915, U.S. Geol. Surv., 1977.

Sclater, J.G., and R. Detrick, Elevation of mid-ocean ridges and the basement age of JOIDES Deep Sea Drilling sites, Geol. Soc. Amer. Bull., 84, 1547-1554, 1973.

Sheridan, R.E., X. Golovchenko, and J.I. Ewing, Late Miocene turbidite horizon in the Blake-Bahama Basin, Amer. Assoc. Petrol. Geol. Bull. 58, 1797-1805, 1974.

Sheridan, R.E., C.C. Windisch, J.I. Ewing, and P.L. Stoffa, Structure and stratigraphy of the Blake Escarpment based on seismic reflection profiles, Amer. Assoc. Petrol. Geol. Spec. Paper on Continental Slopes and Rises, Watkins, J., and Montadest, L., eds.

Smith, M.A., R.V. Amato, M.A. Furbush, D.M. Pert, M.E. Nelson, J.S.Hendrix, L.C. Tamm, G. Wood, Jr., and D.R. Shaw, Geological and operational summary, COST No. B-2 well, Baltimore Canyon Trough area, Mid-Atlantic OCS, U.S. Geol. Surv., Open File Rep. 76-774, 78 p., 1976.

Stahlecker, R., Necom auf der Kapverden-Insel Maio, Neues Jahrb. Miner., 73. B, 265-301, 1934.

Swain, F.M., Ostracoda from wells in North Carolina, Part 2, Mesozoic Ostracods, U.S. Geol. Surv. Prof. Paper 234-B, 59-90, 1952.

Thierstein, H.R., Calcareous nannoplankton biostratigraphy at the Jurassic-Cretaceous boundary, Bur. Recher. Geol. Minier. Mem. 86, 84-94, 1975.

Thierstein, H.R., Mesozoic calcareous nannoplankton biostratigraphy of marine sediments, Mar. Micropaleont., 1, 325-362, 1976.

Tucholke, B.E., Relationships between acoustic stratigraphy and lithostratigraphy in the western North Atlantic basin, *in* Tucholke, B.E., Vogt, P.R. *et al.*, Initial Reports of the Deep Sea Drilling Project, 43, Washington (U.S. Government Printing Office), 1979.

Tucholke, B.E., and J.I. Ewing, Bathymetry and sediment geometry of the Greater Antilles Outer Ridge and vicinity, Geol. Soc. Amer. Bull., 85, 1789-1802, 1974.

Tucholke, B.E., P.R. Vogt, K. Demars, J. Galehouse, R.L. Houghton, A.G. Kaneps, J. Kendrick, I.N. McCave, C.L. McNulty, I.O. Murdmaa, H. Okado, and P. Rothe, Initial Reports of the Deep Sea Drilling Project, 43, Washington (U.S. Government Printing Office), 1979.

Tucholke, B.E., and G.S. Mountain, Seismic stratigraphy, lithostratigraphy, and paleosedimentation patterns in the western North Atlantic, Am. Geophys. Union, Maurice Ewing Series, 3 (this volume), 1979.

Uchupi, E., Bathymetric atlas of the Atlantic, Caribbean, and Gulf of Mexico, Woods Hole Oceanogr. Inst. Ref. No. 71-72 (unpublished manuscript), 1971.

van Hinte, J.E., A Jurassic time scale, Amer. Assoc. Petrol. Geol. Bull., 60, 489-497, 1971.

van Hinte, J.E., A Cretaceous time scale, Amer. Assoc. Petrol. Geol. Bull., 60, 498-516.

Veevers, J.J., and J.R. Heirtzler, Tectonic and paleogeographic synthesis of Leg 27, *in* Veevers, J.J., Heirtzler, J.R. *et al.*, Initial Reports of the Deep Sea Drilling Project, Washington (U.S. Government Printing Office), 27, 1049-1054, 1974.

Vogt, P.R., and A.M. Einwich, Magnetic anomalies and sea-floor spreading in the western North Atlantic and a revised calibration of the Keathley (M) geomagnetic reversal chronology, *in* Tucholke, B.E., Vogt, P.R. *et al.*, Initial Reports of the Deep Sea Drilling Project, 43, Washington (U.S. Government Printing Office), 1979.

von Rad, U., and H. Rösch, Mineralogy and origin of clay minerals, silica and authigenic silicates in Leg 14 sediments, *in* Hayes, D.E., Pimm, A.C. *et al.*, Initial Reports of the Deep Sea Drilling Project, 14, Washington (U.S. Government Printing Office), 727-752, 1972.

Walker, R.G., and E. Mutti, Turbidite facies and facies associations, *in* SEPM short course - Turbidites and deep water sedimentation., Anaheim, 119-158, 1973.

Walker, T.R., Formation of red beds in moist climates: a hypothesis, Geol. Soc. Amer. Bull., 85, 633-638, 1974.

Wilcoxon, J.A., Upper Jurassic-Lower Cretaceous calcareous nannoplankton from the western North Atlantic Basin, *in* Hollister, C.D., Ewing, J.I. *et al.*, Initial Reports of the Deep Sea Drilling Project, 11, Washington (U.S. Government Printing Office), 427-457, 1972a.

Wilcoxon, J.A., Calcareous nannoplankton ranges, Deep Sea Drilling Project, *in* Hollister, C.D., Ewing, J.I. *et al.*, Initial Reports of the Deep Sea Drilling Project, 11, Washington (U.S. Government Printing Office), 459-482, 1972b.

Williams, G.L., Palynological biostratigraphy, Deep Sea Drilling Project Sites 367 and 370, *in* Lancelot, Y., Seibold, E. *et al.*, eds., Initial Reports of the Deep Sea Drilling Project 41, Washington (U.S.Government Printing Office), 495, 1978.

Wilson, J.A., Stratigraphic Commission Note 39 - Records of the Stratigraphic Commission for 1968-1970, Amer. Assoc. Petrol. Geol. Bull. 55, 1866-1872, 1971.

Wind, F.H., Western North Atlantic Late Jurassic calcareous nannofossil biostratigraphy *in* Benson, W.E., Sheridan, R.E. *et al.*, Initial Reports of the Deep Sea Drilling Project, 44, Washington (U.S. Government Printing Office), 761-774, 1978.

Zemmels, I., H.E. Cook, and J.C. Hathaway, X-ray mineralogy studies, 11, *in* Hollister, C.D., Ewing, J.I. *et al.*, Initial Reports of the Deep Sea Drilling Project, Washington (U.S. Government Printing Office), 729-790, 1972.

# SEISMIC STRATIGRAPHY, LITHOSTRATIGRAPHY AND PALEOSEDIMENTATION PATTERNS IN THE NORTH AMERICAN BASIN

Brian E. Tucholke and Gregory S. Mountain*

Lamont-Doherty Geological Observatory of Columbia University, Palisades, New York 10964

*Also Department of Geological Sciences, Columbia University, New York, New York 10027

Abstract. Single channel and multichannel seismic profiles together with DSDP borehole results from the North American Basin have been studied to determine the nature and distribution of major seismic reflectors and the implications of their lithologic and age correlations for paleosedimentation. Two reflectors observed west of the Blake Spur magnetic anomaly that have not been sampled by drilling are presumed to be older than 175 m.y. The volume and reflection character of sediments beneath these horizons indicate that the Early Jurassic basin received large amounts of terrigenous and bioclastic sediment from debris flows and turbidity currents. An overlying group of reflectors onlaps and masks progressively younger basaltic basement, constituting Horizon B in the southwest corner of the basin. These reflectors may be high-velocity sediments derived from the south and west and deposited on relatively smooth basaltic basement formed prior to anomaly M-23 (Late Jurassic). The oldest sediments yet cored in the basin immediately overlie Horizon B and are limestones of Oxfordian (Late Jurassic) age. In contrast to the seafloor-leveling nature of pre-Horizon B sediments, these limestones are dominantly pelagic, although seismic mapping shows some evidence of mass-flows and current-controlled deposition. Marly interbeds and chert within the limestones probably cause the acoustic laminae seen in the overlying section, which extends upward to Horizon ß of Hauterivian to Barremian (Early Cretaceous) age. A uniformly thin layer (~ 100 m) of black clay overlies Horizon ß in the deep basin, but thicker accumulations occur near the continental margin. Intermittent deep-basin stagnation with restricted terrigenous input characterized "black-clay" deposition up to the end of the Cenomanian. Sustained deep-water oxygenation resumed in the Late Cretaceous and multicolored pelagic clays were deposited, but no significant seismic reflector separates these sediments from the underlying black clays. A rapid, brief depression of the calcite compensation depth beginning in the middle Maestrichtian allowed carbonate-rich sediments to accumulate in the deepest portions of the basin, and these correlate with the widely distributed Horizon $A^*$.

The reflecting sequence originally termed "Horizon A" actually is a complex series of reflectors, several of which are widespread and have consistent lithologic correlations. Horizon $A^C$ is the lowermost and most prominent reflector; it correlates with upper-lower to lower-middle Eocene cherts that are formed within turbidites beneath the western Bermuda Rise and in variable facies elsewhere. The overlying Horizon $A^T$ marks the top of the acoustically laminated siliceous turbidites that reached the western Bermuda Rise before regional uplift formed the rise in the middle to late Eocene. Above this level, Horizon $A^V$ correlates with volcaniclastic turbidites that were dispersed from Bermuda for distances up to 200 km and that document late Paleogene subaerial erosion of the volcanic pedestal. Horizon $A^U$ is an unconformity along the western margin of the basin that was eroded by bottom currents between late Eocene and early Miocene time. Westward under the continental rise, Horizon $A^U$ progressively truncates Horizons $A^T$, $A^C$, $A^*$ and older sediments down to Horizon ß. Miocene and younger sediments above $A^U$ and above laterally equivalent reflectors have an acoustic character that shows, for the first time in the history of the basin, both marked and widespread control of depositional patterns by deep circulation.

## Introduction

Continuous seismic reflection profiles are one of the most valuable sources of data available to the marine geologist for studying

*Also Department of Geological Sciences, Columbia University, New York, New York 10027

the sedimentary evolution of ocean basins. In the absence of borehole control, the profiles alone yield information on sediment thickness, probable sediment source areas, mode of deposition, and tectonic and erosional events. Deep-sea boreholes provide lithostratigraphic and chronostratigraphic frameworks at points along the profiles, and to a first approximation the profiles extend this stratigraphic information to regional scales.

In 1975 we began an intensive program to correlate the results of JOIDES boreholes in the western North Atlantic with seismic profiler sections across the drillsites (Figures 1 and 2), to map the major seismic reflectors according to character, distribution and intrahorizon thickness, and to determine paleosedimentation patterns in the basin. Preliminary results of these investigations have been given by Tucholke (1976, 1979), Tucholke and Mountain (1977a,b), and Mountain and Tucholke (1977). In this paper we discuss the most extensive seismic reflectors in the North American Basin and the implications of their correlations with JOIDES borehole results. This data is used to determine aspects of the sedimentary history of the basin seaward of the continental slope. The study is limited largely to the basin south of the New England Seamounts because there is no adequate borehole control north of the seamounts and because the geologic significance of most reflectors there still is uncertain.

The seismic data used for this study include Lamont-Doherty (L-DGO) small and large-volume airgun profiles, U.S. Geological Survey open-file multichannel seismic (MCS) lines, the IPOD-USGS MCS line (Grow and Markl, 1977), a University of Texas (UTMSI) MCS line across the Blake Outer Ridge (Buffler and others, 1978) and other miscellaneous single-channel data (Figure 2). Recently acquired L-DGO large-volume-airgun profiles across the Blake Outer Ridge helped confirm our tracing of deeper reflectors there (Bryan and Markl, unpub. data).

Lamont-Doherty records span the time interval from the development of the seismic profiler for use in the deep sea (Ewing and Tirey, 1961) to the present. Early explosion records defined gross sediment structure, sediment distribution, and some of the major reflectors in the basin (Ewing and Ewing, 1962, 1963). In mid-1964 a pneumatic sound source (airgun) replaced the explosives. Since that time airgun sound sources, recording technology, and reflector definition have continually improved. Several of the Lamont-Doherty profiler lines acquired in the western North Atlantic in the last three years are 24-fold common-depth-point MCS data. Our interpretations are based on study of full-size records of the highest quality available in each area. In areas of lower data density, older records of lesser quality were used to help map general sediment distribution patterns. Profiles reproduced in this paper were selected to illustrate the greatest number of major reflector relationships within reasonable size limitations, and they consequently may not represent the best available data.

Partly because of improved record quality and partly because of expanding, world-wide data acquisition, the nomenclature applied to prominent seismic horizons has undergone a somewhat tortuous development (see Tucholke, 1979). In this paper we use a form of the general nomenclatural system that has developed historically (A,β,B, etc.). However, we recognize that any system with an alphabetic or numeric basis is destined to become tediously complex and thus of dubious value as improved recording technology defines more and more geologically significant reflectors between reflectors already named. The development of a non-alphanumeric nomenclatural system and other seismic stratigraphic principles is sorely needed, and we presently are planning a workshop on seismic stratigraphy to deal with these problems.

We have treated the seismic stratigraphy separately from lithostratigraphy and chronostratigraphy. However, as will become evident in succeeding pages, many deep-basin seismic horizons have remarkably consistent age and lithologic correlations, probably because major changes in sedimentation (and thus in acoustic impedance) occurred on a basin-wide scale, especially during the Mesozoic. In the following pages, we discuss the sedimentary evolution of the North American Basin from the Lower Jurassic to the present based on seismic and lithostratigraphic data. Stratigraphic relationships are summarized in Table 1.

## The Deepest Reflectors

The development of large-volume airguns and MCS recording technology has greatly increased our knowledge of the seismic stratigraphy in the oldest, most deeply buried parts of the western basin. In the MCS profiles across the continental rise, there are two major, deep reflectors (solid arrows, Fig. 3) that cannot be tied to existing JOIDES boreholes. On the segment of the MCS line that is illustrated, the deeper reflector caps highly reflective layers that infill basement depressions, and it does not extend seaward much beyond shot point (SP) 2000. Landward along the same profile the sediment thickness beneath the reflector increases markedly to 0.7 sec or more two-way reflection time (1575 m at $V_p$ = 4.5 km/sec) before it is lost in a

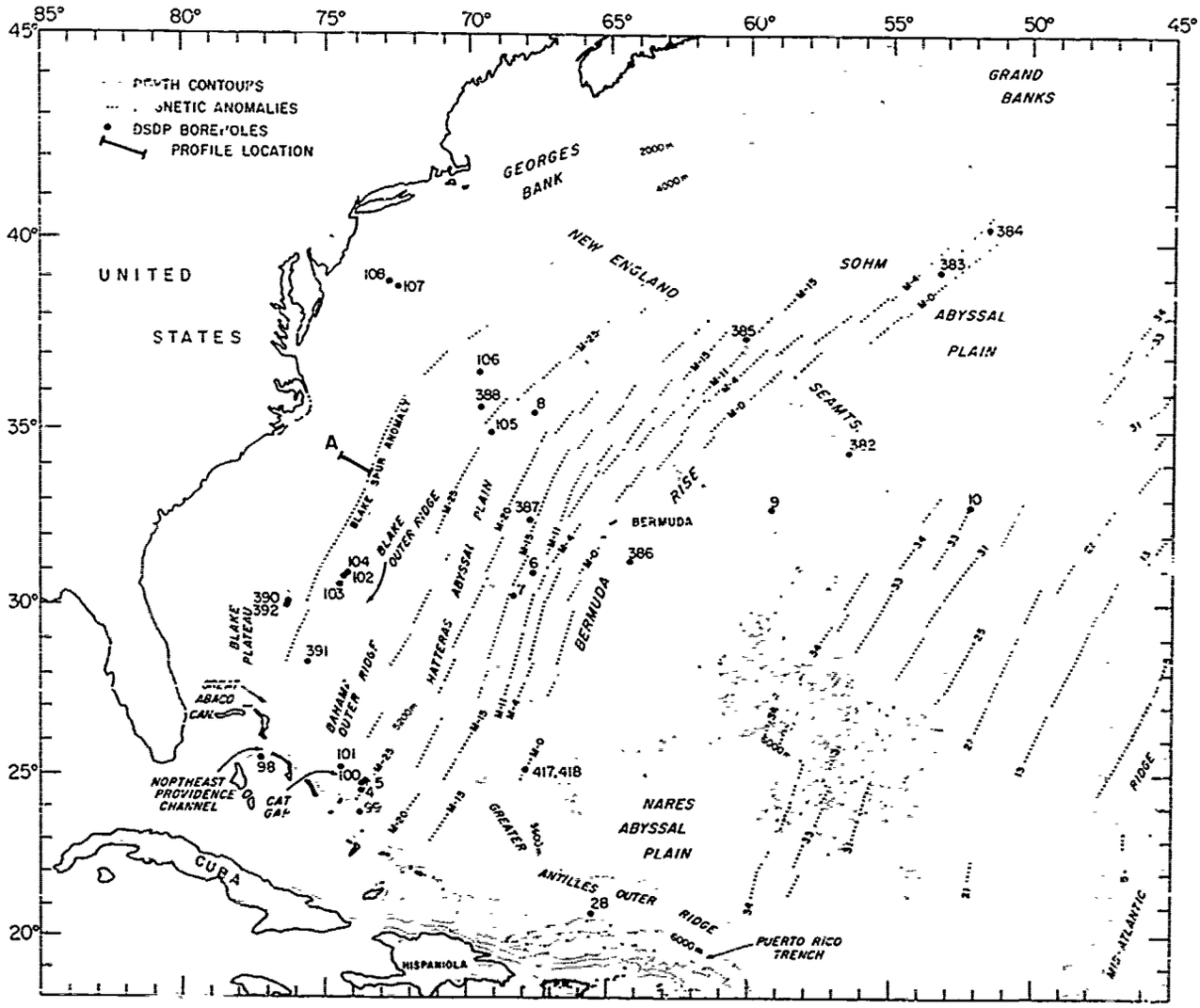


Figure 1. Location of JOIDES boreholes and physiographic provinces in the North American Basin. Bathymetry in corrected meters from Uchupi (1971). M-series magnetic anomalies from Schouten and Klitgord (1977), Bracey (1968), and unpublished L-DGO data. Younger anomalies from Pitman and Talwani (1972), Rabinowitz and Purdy (1976) and Cande and Kristofferson (1977).

diapiric complex beneath the continental slope (see Grow and Markl, 1977).

About 1600 m (0.6 to 0.8 secs) above this deep reflector is another well defined reflector. Toward the west it occurs within an acoustically laminated sequence, but it emerges seaward as the top of a 0.15 sec-thick interval of strong, closely spaced reflectors. It appears to terminate abruptly at a sharp rise in basement (SP 2660), although an intermittently observed, flat-lying reflector just above basement farther seaward could be correlative. This reflector pinches out at a similar basement step observed in other USGS, UTMSI, and LDGO MCS lines across the continental margin and in numerous single channel profiles; in the latter, however, the reflector seldom is well defined. The basement step correlates with the landward edge of the Blake Spur magnetic anomaly (Schouten and Klitgord, 1977), and it appears to be both an original and isochronous feature of the basaltic crust (see Figure 8).

Because the upper reflector pinches out near the Blake Spur Anomaly, underlying sediments probably are older than about 175 m.y. (Shipley and others, 1978). The reverberant character and level attitude of reflectors in this interval indicate that the sediments probably are terrigenous and bio-

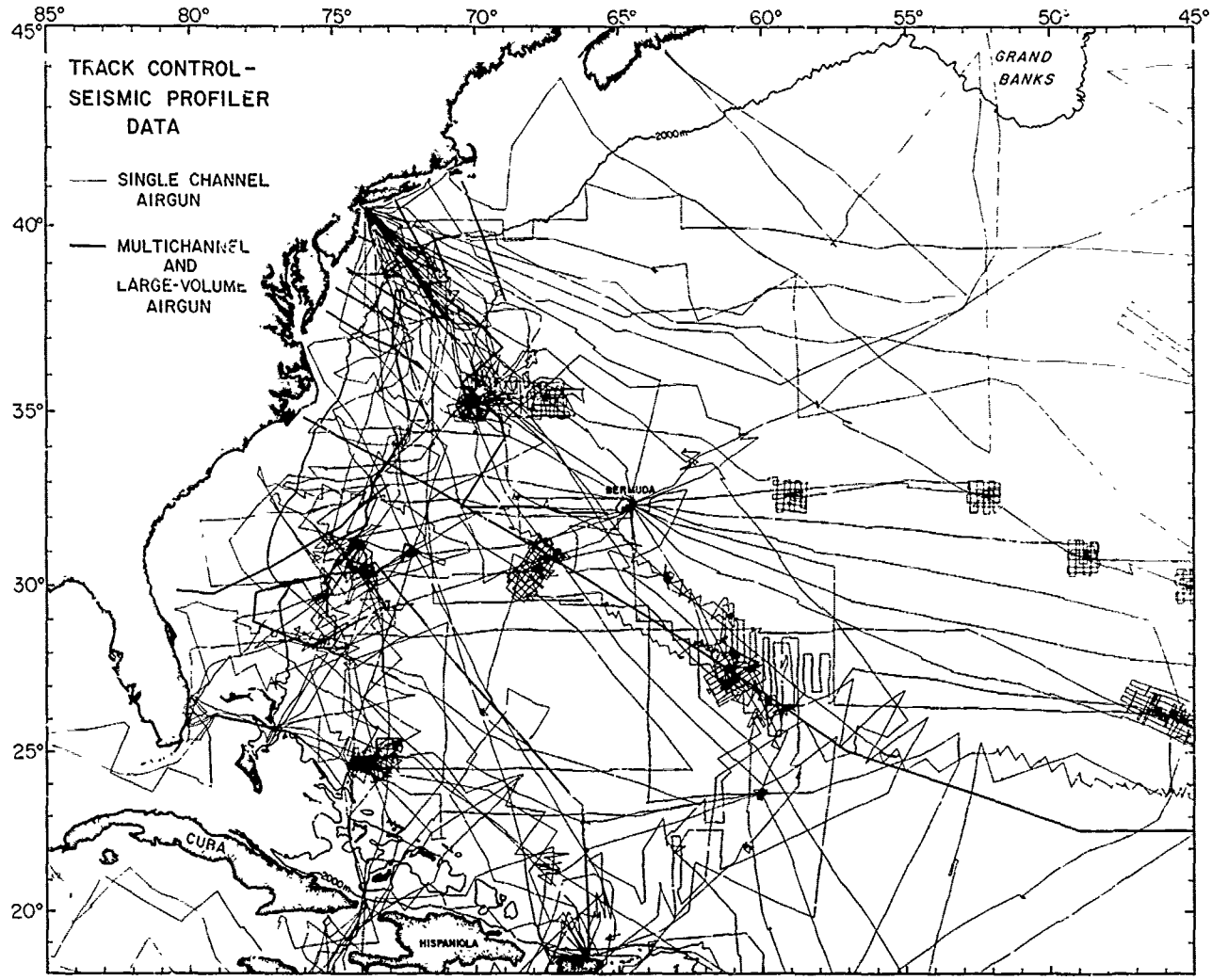


Figure 2. Track control for seismic profiles studied. Tracks for L-DGO explosion records and some non-L-DGO single-channel profiles not shown.

clastic debris derived from the continental margin and deposited by turbidity currents and debris flows. The sediments correlating with the deeper, highly reflective sequence may include relatively coarser clastic debris of Early Jurassic age derived from the youthful continental margin. These inferences are supported by a calculation of sediment accumulation rates. Near the continental slope, more than 3.2 km of sediment underlie the upper reflector. If initial deposition in the basin began about 190 m.y.B.P., then the sediments accumulated at average rates exceeding 210 m/m.y. These rates, even uncorrected for sediment compaction, are an order of magnitude higher than normal pelagic accumulation rates and suggest a large influx of detrital material.

## The Nature of Horizon B

In the region of Cat Gap (Figure 1) Ewing and others (1966) recognized acoustic basement having an unusually smooth surface. To distinguish it from typically rugged volcanic basement, they named it Horizon B. The horizon is easily identified as a strong, prolonged reflector in the vicinity of DSDP Site 100 (Figure 4), where it is as shallow as 5600 m below sea level. Further south, Horizon B is interrupted by a fracture zone and it rises to about 5200 m at Site 99 (Figure 5). To the east and north, Horizon B descends to nearly 6000 m.

On the basis of extensive mapping and cross-correlation of reflectors in this region, it appears that Horizon B actually is

TABLE 1. Stratigraphic Correlations in the Deep North American Basin

| Reflector | Lithologic Correlation (DSDP Site) | Age Correlation (DSDP Site) | Thickness of Subjacent Seismic Interval | Lithology of Subjacent Seismic Interval | Correlation to Formations of Jansa and others (1979) |
|---|---|---|---|---|---|
| $A^V$ | Top of volcaniclastic turbidites around Bermuda (386) | Upper Oligocene (386) | $A^V$ to $A^T$: 168m @ 386 | Volcaniclastic turbidites | Mass-flows within Blake Ridge Fm. |
| $A^U$ | Unconformity (4, 5,99,100,101, 105, 106, 391) | Upper Eocene to ∿ lower Miocene (limited by 8, 104, 106) | Variable; depends on depth of erosion | Variable; depends on depth of erosion | Variable; depends on depth of erosion |
| $A^T$ | Top of turbidites (387) | Middle to ∿ upper Eocene (387,8) | $A^T$ to $A^C$: ≲ 200m (thicker toward margin) | Turbidites of mixed terrigenous, siliceous, calcareous debris | Within Blake Ridge Fm. |
| $A^C$ | Top of cherts (6,7,8,9,10,28, 384,385,387) | Upper lower to lower middle Eocene (6,7,8, 9,10,28,384, 385,387) | $A^C$ to $A^*$: ≲ 300m (thicker toward margin) | Turbidites as above, hemipelagic clays, calcareous oozes in shallow areas | Top of Bermuda Rise Fm. |
| $A^*$ | Marly nannofossil chalk/limestone bed (386,387) | Upper Maestrichtian (386,387) | $A^*$ to β:∿100-200m (up to 700m near margin) | Multicolored pelagic clays above black clays | Crescent Peaks Member of Plantagenet Fm. |
| β | Top of chalk, limestone sequence (5,101, 105,387,391) | Hauterivian to Barremian (5,101, 105,387,391) | β to DRS: up to 1400 m beneath upper rise | Lt. gray limestone, reddish limestone, gray-green limestone | Approximate top of Blake-Bahama Fm. |
| Deep Reflector Sequence (DRS) | Coarse terrigenous-calcareous debris? | ∿ 175 m.y. Toarcian | DRS to DRS: up to 1600 m beneath upper rise | Mixed terrigenous-calcareous debris? | - |
| Deep Reflector Sequence (DRS) | Coarse terrigenous-calcareous debris? | ∿180 m.y. Pliensbachian | DRS to basaltic basement: up to 1600 m beneath upper rise | Mixed coarse terrigenous-calcareous debris? | - |

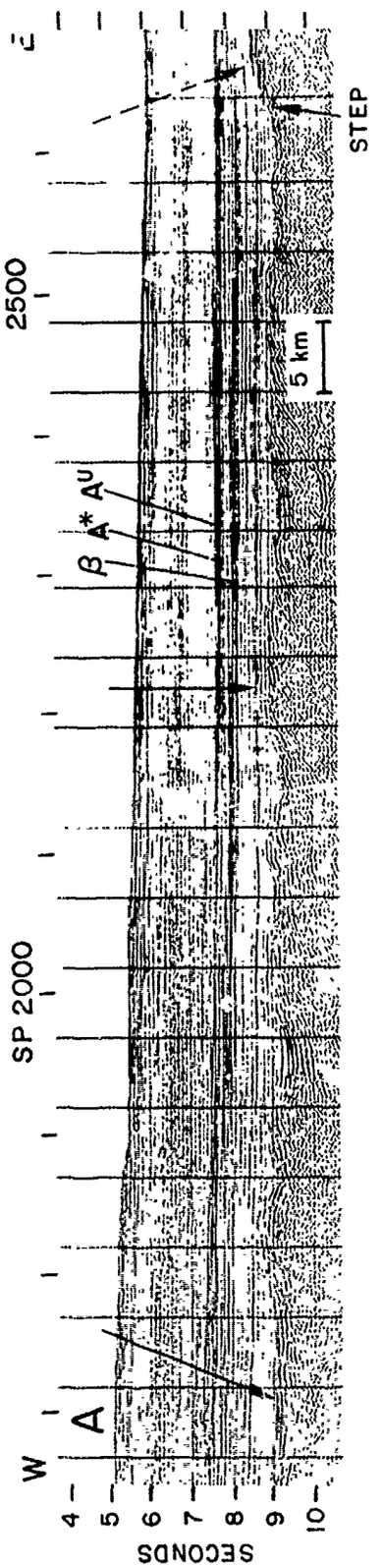


Figure 3. A segment of the IPOD-USGS MCS line (Grow and Markl, 1977) between shot points 1650 and 2690. Location in Figure 1. Solid arrows show deep reflectors discussed in text. Reflector at dashed arrow can be traced seismically to Cat Gap (Figures 4, 6).

formed by several closely spaced deep reflectors that onlap and mask basaltic basement (Figure 4); thus Horizon B is diachronous. In Figure 5 the shaded regions show the known distribution of Horizon B. Farther west, many of the basement-masking reflectors rise far enough that the underlying, more irregular basaltic surface is observed. Because Horizon B is a basement-masking phenomenon, its definition in seismic profiles is largely a function of recording technology; that is, Horizon B often will be penetrated to reveal irregular underlying crust in profiles acquired with high-energy sound sources.

It is important to note, however, that where probable true oceanic basement (layer 2) can be observed west of about anomaly M-23, its surface roughness is subdued compared to that of younger crust. This also is observed in most MCS lines across the continental rise. The subdued irregularity may be related to faster seafloor spreading prior to the time of anomaly M-23, and it probably aided in the formation of smooth acoustic basement by facilitating dispersal of basement-masking sediments.

In the sequence of deep reflectors that approach and in places mask basaltic basement, the uppermost reflector can be traced with reasonable confidence from the Cat Gap area 1000 km north to the IPOD line (dashed arrow, Figures 3, 4,6). In both areas the reflector can be followed eastward to a pinchout on crust of anomaly M-23 age (Oxfordian-Kimmeridgian) or slightly younger. This reflector also was penetrated at DSDP Site 100, where it correlates with Kimmeridgian to Tithonian-age limestones, in good agreement with the pinchout age (Figure 4).

One of the drilling objectives at Site 100 was to determine the nature of Horizon B. Although basalt was recovered at the level of the horizon (Hollister, Ewing, and others, 1972), this unfortunately does not resolve the origin of Horizon B because the site was located on the flank of an acoustic basement high. Had the drillsite been located in an adjacent smooth-basement swale, we suspect that it would have encountered highly reflective sediments directly overlying and seismically masking basalt.

## Carbonate Deposition Below Horizon β

Numerous closely spaced reflectors lie 0.2 to 0.4 secs. (∿ 200 to 400 m) above Horizon B in the Cat Gap region, and these in turn are overlain by an acoustically non-laminated interval. The top of the group of closely spaced reflectors was named Horizon β by Ewing and others (1966) (Figures 4, 6, 7).

Horizon β and the underlying laminated sequence generally are conformable to deeper reflectors. Horizon β can be traced from the

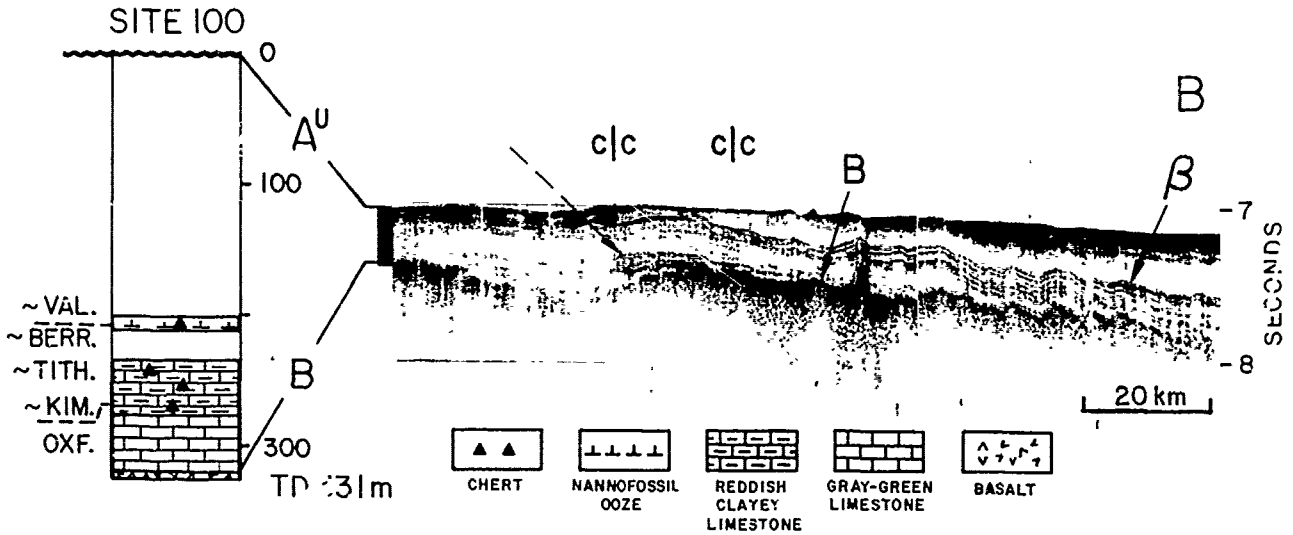


Figure 4. Seismic profile near Site 100; location in Figure 5. Note that deep reflectors onlap and mask probable basaltic basement, compositely forming smooth acoustic basement (Horizon B).

Cat Gap area to the north and west beneath the central continental rise. Landward, it becomes increasingly difficult to distinguish from other flat-lying reflectors that are not observed toward the east. Traced to the east beneath the western Bermuda Rise, Horizon β also is conformable to the underlying basement, suggesting pelagic accumulation of pre-β sediments. The reflector pinches out on crust of anomaly M-11 to M-4 age (late Valanginian-Barremian) near the latitude of Bermuda, but farther south it extends onto crust possibly as young as M-2 (Barremian) age (Figure 8).

The sedimentary section below Horizon β has been drilled at 8 sites (Figure 8). It everywhere corresponds to chalks and limestones of Hauterivian/Barremian age (Early Cretaceous) and older, in good agreement with the β pinchout age. At Site 100, which thus far has penetrated the oldest sediments in the North American Basin, the carbonates below Horizon β continue down at least to the Oxfordian (Hollister, Ewing, and others, 1972). There are three major color and compositional variants in these limestones, consisting of (from the top) light gray limestone, reddish-brown argillaceous limestone, and gray-green limestone. The upper facies has been defined as the Blake-Bahama Formation and the lower two facies as the Cat Gap Formation (Jansa and others, 1979). Benson, Sheridan and others (1978) have correlated the top of the Cat Gap Formation with a reflector termed Horizon C; however, we have not yet satisfied ourselves that contacts between these lithofacies correlate with any of the reflectors below Horizon β. Marly interbeds and high-impedance quartzose cherts are common in the limestones below Horizon β at most drillsites, and they probably account for a majority of the reflectors.

The distribution of sediment thickness below Horizon β (Figure 8) indicates that the continental margin was a major source for sediments up through the Early Cretaceous, and numerous smooth reflectors in the sedimentary sequence suggest that the sediments were deposited from turbidity currents and debris flows. However, the Upper Jurassic to Lower Cretaceous limestones cored from levels beneath Horizon β at most drillsites exhibit sedimentary structures that suggest dominantly pelagic deposition interrupted only by locally derived "pelagic turbidites" (Lancelot and others, 1972). The discrepancy between the seismic and core data can be explained in two ways. First, in the Cat Gap region and probably elsewhere along the continental margin, seafloor-leveling processes such as those that formed Horizon B provided a relatively flat surface for subsequent deposition of pelagic carbonates. Pelagic deposition on this substrate would produce smooth bedding planes suggestive of turbidite deposition in reflection profiles. A second explanation is found in the placement of DSDP boreholes. Site 105, for example, was drilled on one of several basement swells near 35°N (Figure 8), and the pelagic sedimentary record below Horizon β at this site therefore may not be representative of sediments in the surrounding areas. Seismic profiles in this region show that pre-β reflectors lap onto the flanks of the basement swells and suggest that much of the sedimentary section was deposited from turbidity currents.

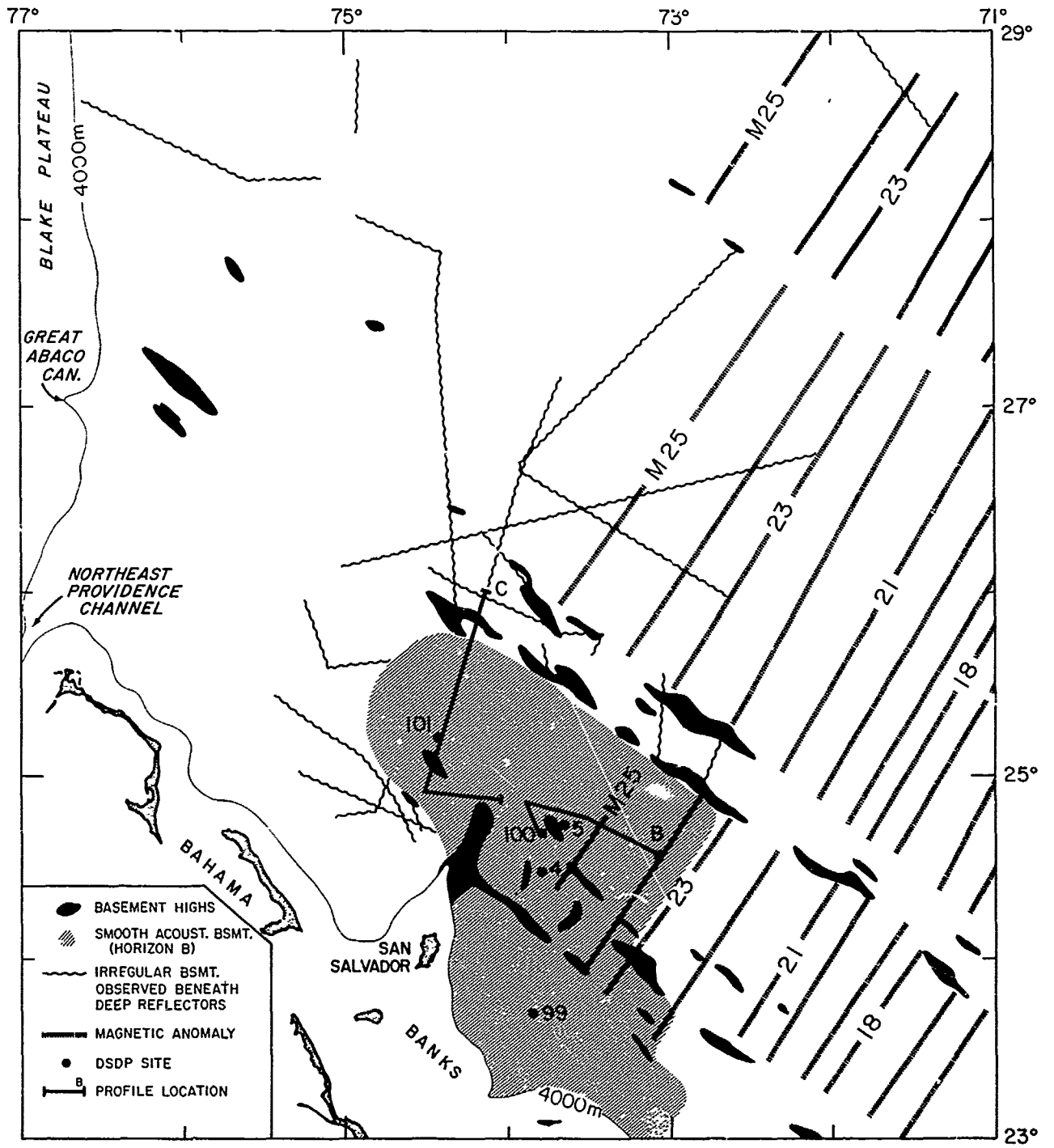


Figure 5. Distribution of smooth acoustic basement (Horizon B, shaded), structural trends, and crustal ages (M-series anomalies) in the southwestern North Atlantic.

In the Cat Gap area, the fact that pelagic sediments in the Horizon B to β interval overlie basement-smoothing deposits below Horizon B indicates that a shift from mass-flow to pelagic deposition occurred in the Late Jurassic. This shift may have been caused by the combined effects of margin subsidence, rising sea level, and growth of reef barriers along the continental margin. Reefs in the Bahamas and along the outer

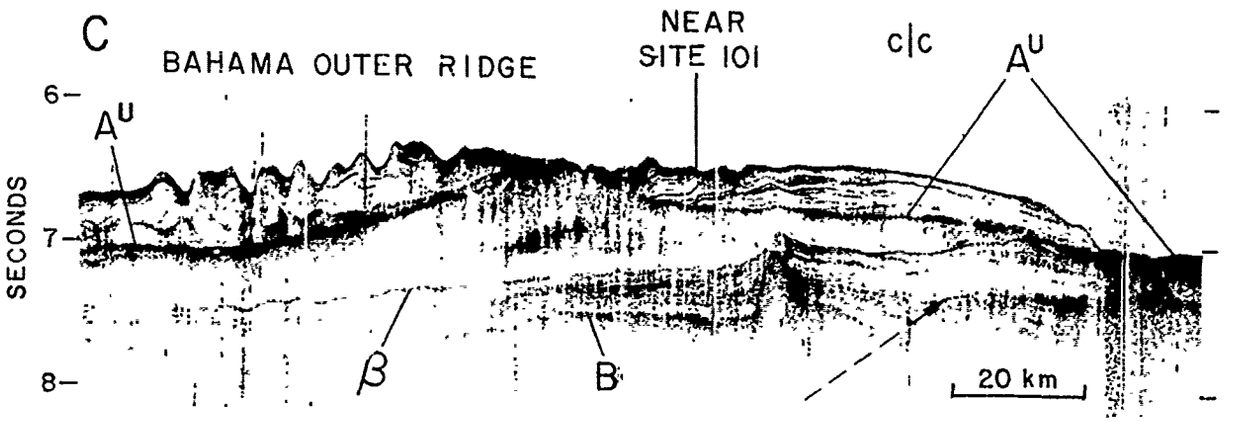


Figure 6. Seismic profile across Site 101 on the southern Bahama Outer Ridge. Location in Figure 5.

Blake Plateau were well established in Late Jurassic to Early Cretaceous time (Meyerhoff and Hatten, 1974; Catalano and others, 1975), and they may have extended much farther north. It is clear that clastic sources only were reduced and not stopped, because the top of the Blake-Bahama Formation at Site 391 (Figure 8) includes abundant sandy turbidites (Jansa and others, 1979). Similar reduction in sediment supply probably occurred farther north along the margin, thus shifting the boundary between dominantly clastic and dominantly pelagic deposition toward the west.

The pelagic accumulation of limestones below Horizon β in the Cat Gap region was interrupted by obvious lensing and differential accumulation (Figures 7, 9). From an apparent source west of the northeast-trending San Salvador basement ridge, sediments were distributed north and east around the end of the ridge in a manner very much like bottom-current-controlled deposition on modern sediment drifts. The drift-like deposit is flanked on the north by a thinned zone of attenuated sedimentation. On the basis of these data, we suggest that bottom currents were active in the Late Jurassic to Early Cretaceous (Neocomian). Although the general deep circulation may have been weak, currents probably were intensified by the steep topography of the San Salvador ridge.

The strong change in acoustic character of sediments observed at the level of Horizon β across most of the basin corresponds to an equally marked change in the composition of the sediments. In contrast to the acoustically laminated limestones below Horizon β, the overlying sediments are acoustically nonlaminated and they correlate with green-gray and black mudstones (hereafter termed black clays) beneath multicolored claystones.

Horizon β resulted from a rise in the calcite compensation depth (CCD), and the overlying black clays were deposited below the CCD in an intermittently anoxic environment (Tucholke and Vogt, 1979). As noted earlier, the location of the eastward pinchout of Horizon β suggests that the reflector becomes younger toward the southern part of the basin. Horizon β cannot be traced eastward as far as Sites 417D and 418A on the southern Bermuda Rise (Figure 8), but drilling results there support the idea that carbonate deposition persisted longer in the southern part of the basin. The sites, located on crust of M-0 (Aptian) age, recovered a few meters of Aptian nannofossil chalk overlying basalt and beneath the black clays (Donnelly, Francheteau, and others, 1977; Bryan, Robinson and others, 1977). Aptian crust has not been drilled farther north so we do not know if carbonates of similar age and paleodepth occur there. However, persistence of carbonate deposition in the south is a distinct possibility, and it could have resulted from either elevated crust or a delayed rise in the CCD. In the latter instance, high surface productivity associated with westerly circum-global equatorial currents through the Tethys, southern North Atlantic and Pacific (Berggren and Hollister, 1974) could have prolonged the rise of the CCD.

### Horizon β To Horizon A*: Black And Multicolored Clays

The weakly or discontinuously reflective sequence of sediments overlying Horizon β is 0.1 to 0.7 sec thick throughout most of the basin. This sequence is capped by one of two regionally important reflectors: 1) Horizon $A^U$, which is an erosional unconformity developed during the mid-Tertiary along the continental margin (Figures 6,7; see later discussion), or 2) Horizon A* which correlates with a bed of Maestrichtian chalks and

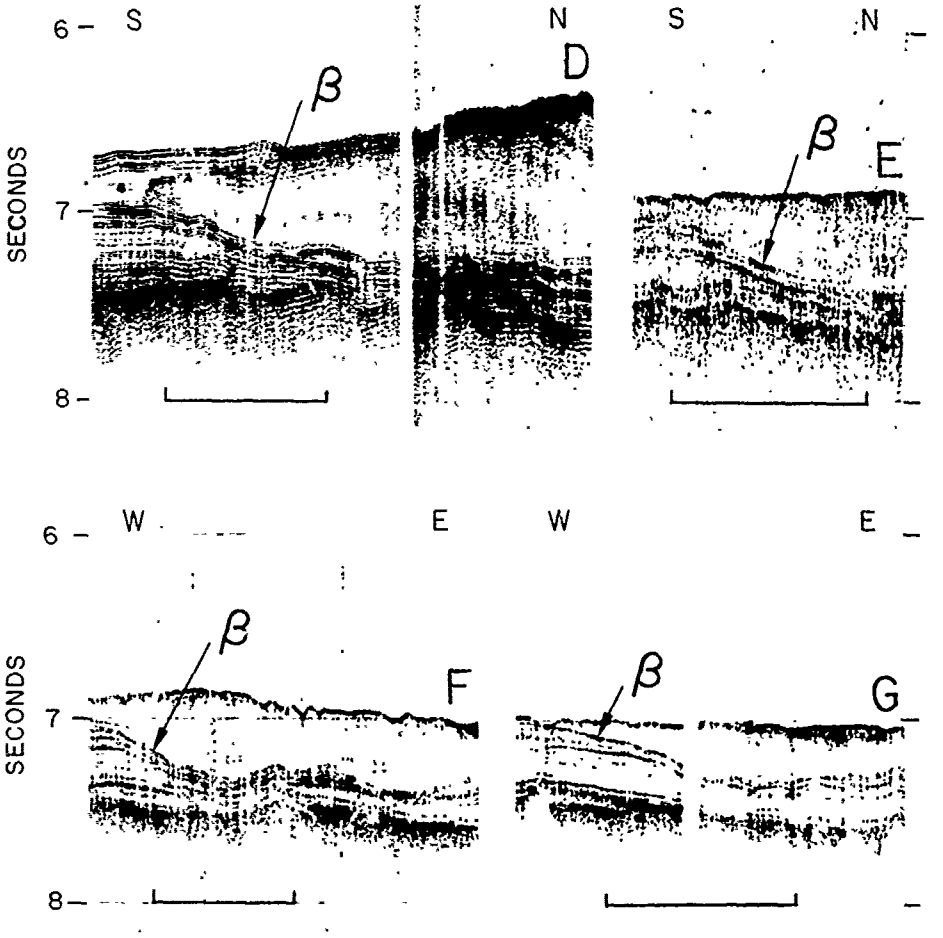


Figure 7. Seismic profiles showing lensing beneath Horizon β in the Cat Gap area. Smooth acoustic basement is Horizon B. Horizon $A^U$ is at seafloor. Scale bars ≈ 20 km. Locations in Figure 9.

limestones east of the continental margin (Figure 10).

The interval between Horizon β (or basaltic basement) and $A^*/A^U$ has been drilled at 12 sites where both seismic boundaries have been identified (Figure 11). The interval contains Hauterivian to Cenomanian/Turonian black clays as well as overlying Upper Cretaceous multicolored clays, and there is no well defined reflector separating these lithofacies (Tucholke, 1979).

The "black clays" (Hatteras Formation; Jansa and others, 1979) consist of finely laminated black mudstones interbedded with moderately burrowed gray-green mudstones, and they were deposited under anoxic to poorly oxygenated deep-basin conditions, respectively. Similar dark gray marly beds locally occur within the limestones below Horizon β, beginning as early as the Valanginian. There continues to be a lively debate about the cause and extent of the anoxic conditions.

By studying the distribution of black-clay deposition along drillsite age/depth curves, Tucholke and Vogt (1979) determined that euxinic sediments were deposited intermittently below 3200 m in the entire North American Basin from Barremian through Cenomanian time. They also argued on the basis of sedimentological and geochemical data that reducing conditions characterized the entire deep water column, not just the subsurface sediments. For these reasons, it was concluded that the North Atlantic deep circulation was severely restricted, possibly because of barriers to deep flow in the Panamanian and Tethyan regions.

Near the beginning of the Turonian, the North American Basin again received oxygenated deep water, but the CCD remained shallow and only pelagic multicolored clays were deposited (Lancelot and others, 1972; Tucholke and Vogt, 1979). These multicolored clays have been defined as the Plantagenet

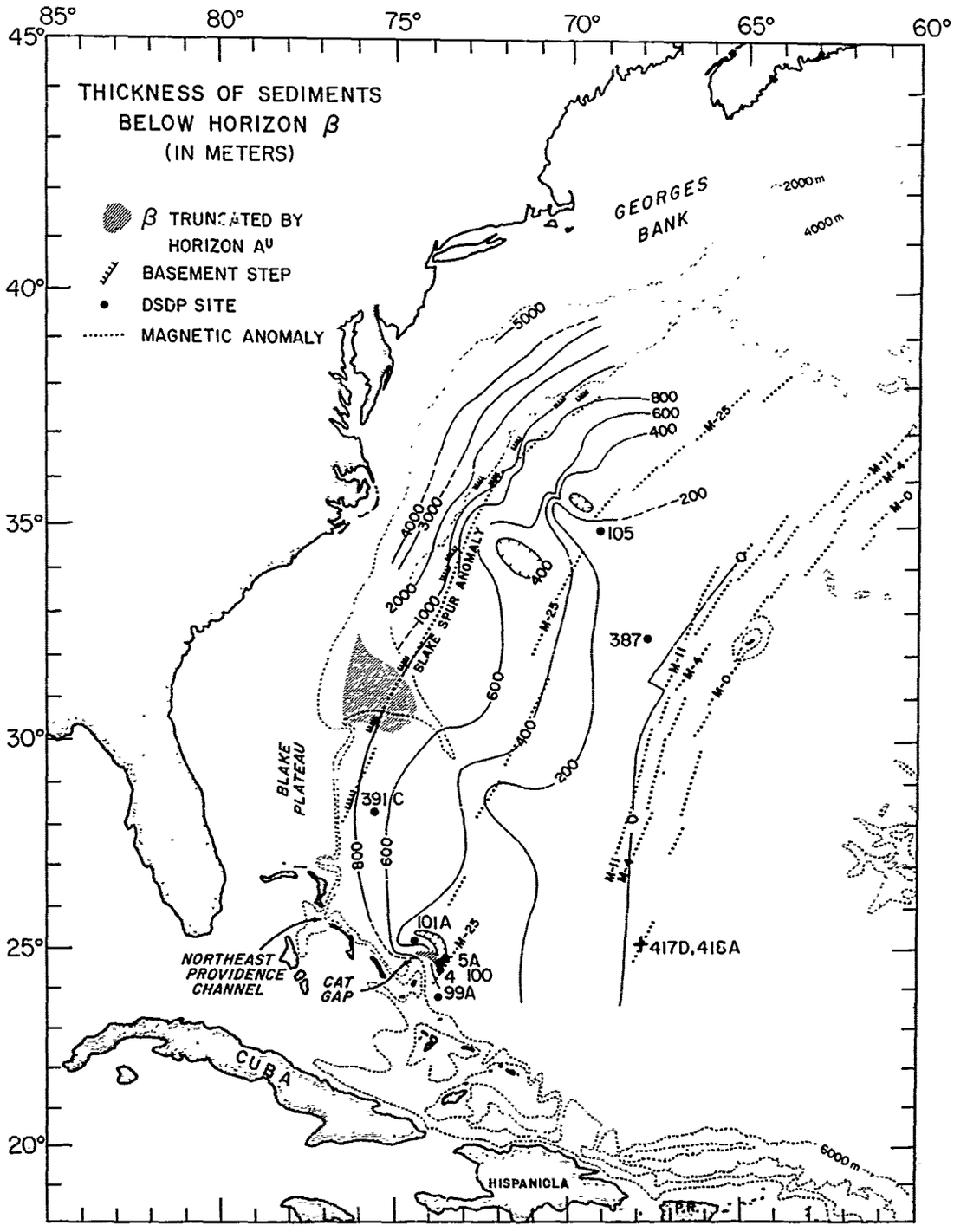


Figure 8. Distribution of Horizon β and thickness of pre-β sediments in meters (determined using velocity regression curves of Houtz [1974]). DSDP boreholes that penetrated Horizon β or recovered pre-β sediments are shown as dots. Shaded areas indicate where Horizon β was eroded by Late Paleogene bottom currents (Horizon $A^U$). Observed basement steps along the Blake Spur Anomaly are indicated.

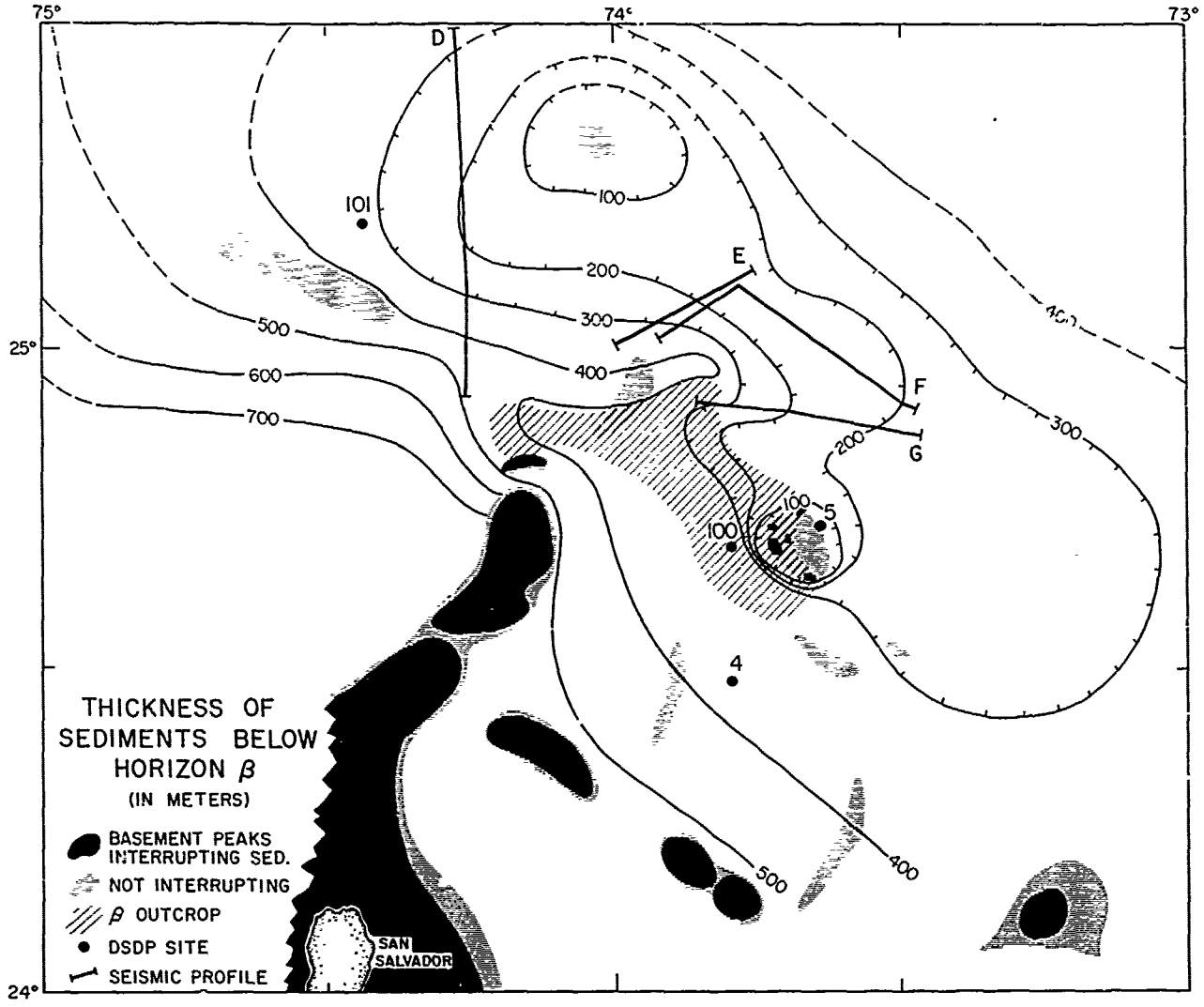


Figure 9. Detail of sediment thickness (in meters) below Horizon β in the Cat Gap area. Horizon β is exposed at the seafloor by Paleogene erosion (Horizon $A^U$) as shown.

Formation by Jansa and others (1979). The thickness generally is small because of their very low accumulation rates (1-2 m/m.y.). Known thickness ranges from about 10-20 m at Site 387 up to a maximum of 90-110 m at Site 386.

In Figure 11 we have mapped the combined thickness of the black and multicolored clays from seismic profiler data. Although the mapped thickness includes multicolored clays, it provides a reasonable approximation of the true distribution of black clays alone because the thickness of the multicolored clays probably is small (< 100 m) and fairly uniform in the basin.

A striking observation is that away from the continental margin the black clays are of relatively uniform thickness (100-200 m) implying that they accumulated evenly and slowly (< 6 m/my). Pockets of thick sediments accumulated in local topographic depressions because of slumping and turbidity currents from adjacent highs (e.g. Site 386, Figure 11). A majority of the basin probably received only pelagic detritus with admixtures of terrigenous debris borne by winds and surface currents. This is in marked contrast to the deposition of abundant terrigenous detritus in the eastern North Atlantic in Early and middle Cretaceous time (Lancelot, Siebold, and others, 1978; Montadert, Roberts, and others, 1976).

Near the western Atlantic continental margin several lobes of thick black-clay sequences are developed. Two of these lobes, one south of Georges Bank Basin and one southeast of Baltimore Canyon Trough, are separated by a thin black-clay section caused

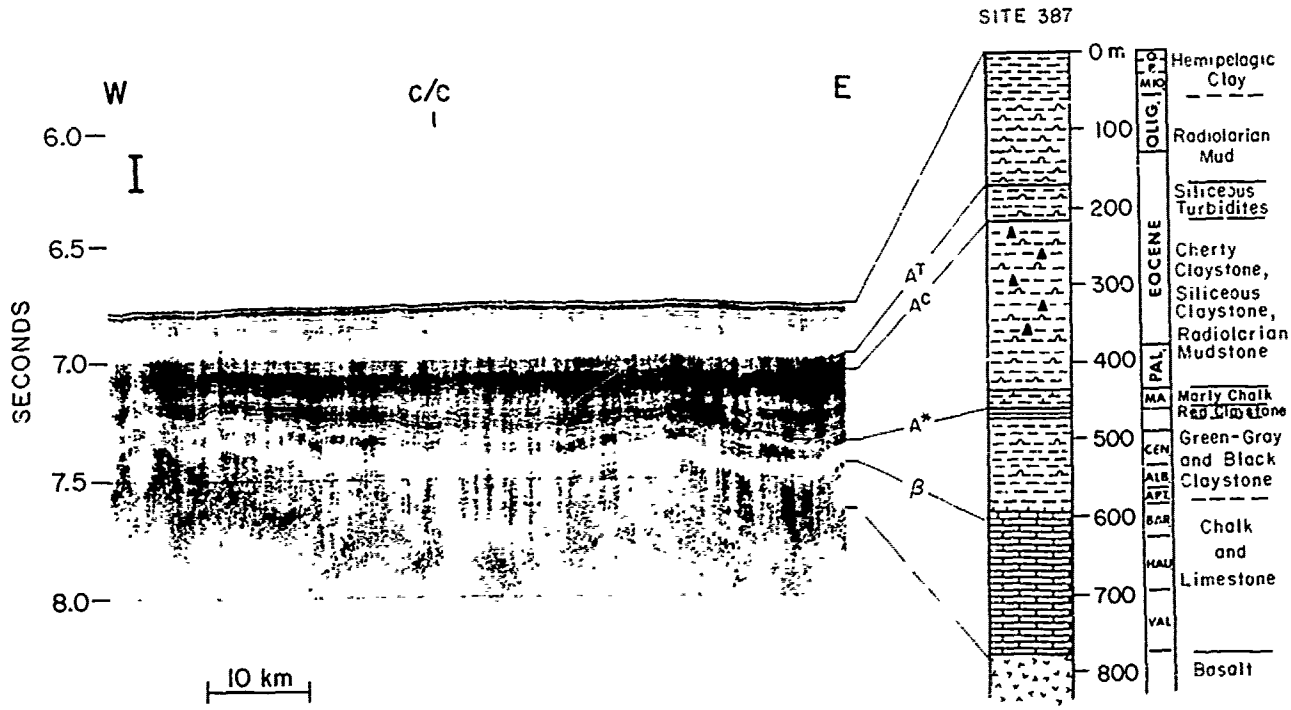


Figure 10. Seismic profile from the western Bermuda Rise showing major reflectors and correlation with lithologic record at nearby Site 387. Location in Figure 12.

primarily by the presence of the basement swell around Site 105. This control by basement topography and the landward thickening indicate that the lobes contain terrigenous debris deposited from turbidity currents and debris flows. Off the Blake Plateau an even thicker sequence (up to 700 m) of black clays is present. In this region Horizon A* has been truncated by mid-Tertiary erosion (Horizon $A^U$, see Figure 11) and the pre-erosion thicknesses during the middle and Late Cretaceous must have been even greater.

Reefs along the edge of the continental shelf may have been important in controlling sediment distribution during the Cretaceous. Reef material has been dredged, drilled, and sampled by submersible at numerous locations along the margin from the Blake Plateau to as far north as Georges Bank and the Grand Banks (Heezen and Sheridan, 1966; Tucholke and Vogt, 1979; Ryan and others, 1978). Deeply buried reef-like structures of unknown age are observed beneath the continental slope on several MCS lines (Figure 11). It is likely that during the Early to middle Cretaceous a reef system extended along the outer shelf of the U.S. east coast and at least intermittently to the Grand Banks. This barrier together with the mid-Cretaceous sea-level transgression (Pitman, 1978; Vail and others, 1977) could have strongly reduced transport of terrigenous sediment to the deep sea (Emery and others, 1970). These factors would account for restriction of thick black-clay sequences to near the continental margin and rather uniform thickness in the deep basin. The marginal reef system probably was breached or overstepped in several places, thus allowing deposition of the observed lobes along the continental margin. In particular, the thickest lobe off the Blake Plateau may have received sediments funnelled through Great Abaco Canyon, which may date to Neocomian time as a reef channel (Sheridan and others, 1969), and through Northeast Providence Channel (Figure 11).

The multicolored pelagic clays that accumulated in the oxygenated deep basin after Cenomanian time (Plantagenet Formation, Jansa and others, 1979) are very fine-grained and barren of biogenic debris. Thus the same factors that prevented sediment dispersal to the anoxic deep basin in the Early Cretaceous must have continued to limit terrigenous input. However, Late Cretaceous lowering of sea level and extinction of the marginal reefs (Pitman, 1978; Douglas and others, 1973) probably resulted in gradually increasing terrigenous influx and further development of the continental rise. At Site 391 near the continental margin, the multicolored clays include terrigenous silt beds that document development of this continental source (Benson, Sheridan and others, 1978). Al-

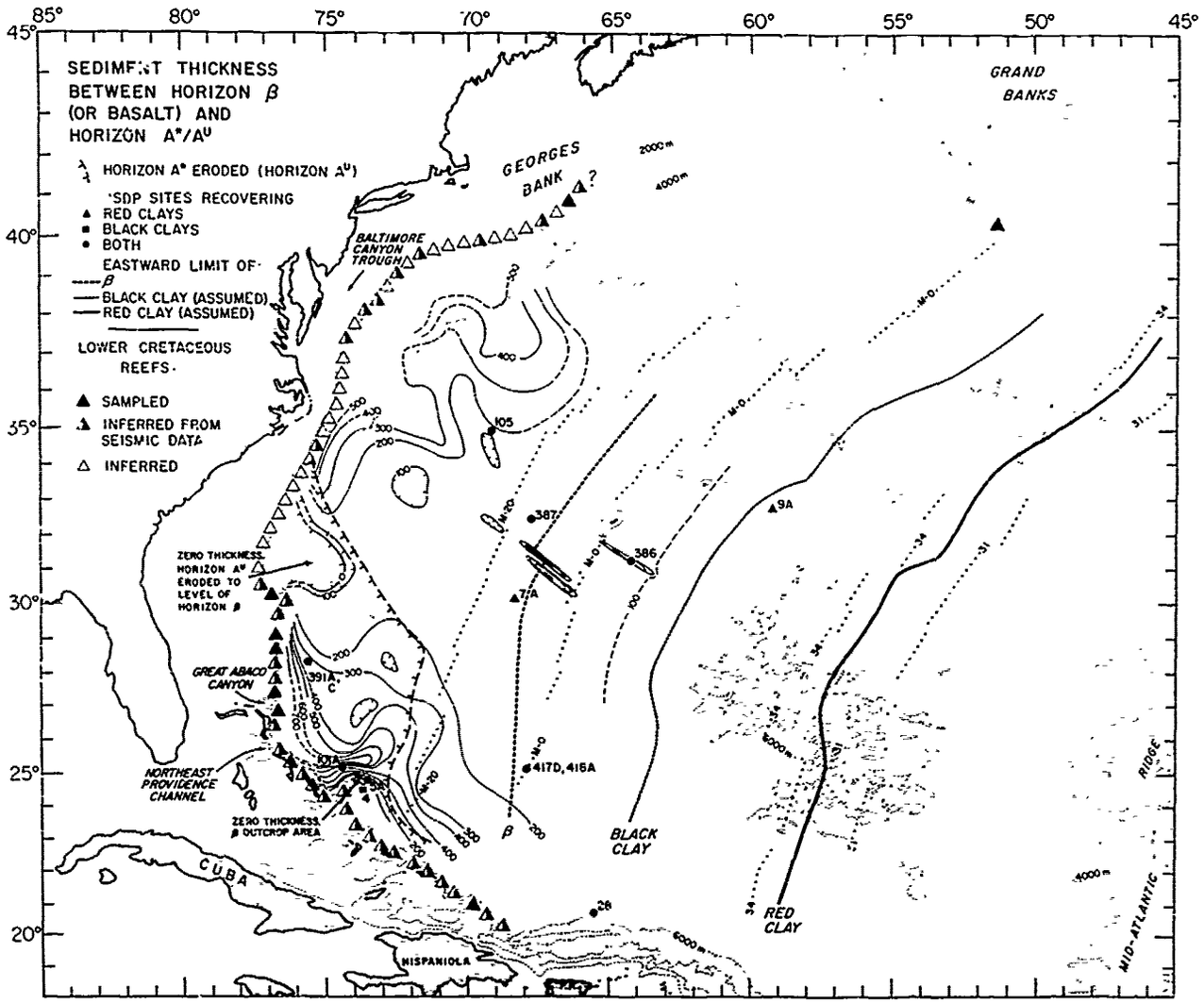


Figure 11. Sediment thickness in meters between Horizon β (or basaltic basement, east of M-2 to M-11) and Horizon $A^*/A^U$. Horizon $A^*$ removed by Paleogene erosion (Horizon $A^U$) west of T's. Conversion of reflection time to thickness is from velocity regression curves of Houtz (1974). Drillsites recovering sediments from this acoustic interval are indicated. Black clays overlie basalt east of the Horizon β limit. "Black Clay" line = estimated late Albian isochron or approximate eastward limit of black clays overlying basalt; black clay deposition persisted to late Cenomanian/Turonian, but ridge-crest basalt of this age probably was above level of anoxic-basin conditions. "Red Clay" line = mid-Campanian isochron or approximate eastward limit of multicolored clays; younger crust was generated mostly above the CCD, but in the deeper basin multicolored clay deposition persisted into the Maestrichtian.

though the multicolored clays were deposited beneath circulating, oxygenated bottom water, we have observed no evidence either in seismic profiles or in primary sedimentary structures of the clays that suggests Late Cretaceous bottom currents were significant in transporting and redistributing sediments.

As noted earlier, where the multicolored clays are in conformity with overlying sediments they are capped by Horizon $A^*$ (Figure 10). Correlation of this seismic marker to the lithostratigraphy is documented only at Sites 386 and 387 on the Bermuda Rise. At these sites $A^*$ matches the level of a bed of middle to upper Maestrichtian pelagic marly chalk and limestone (30-60% $CaCO_3$; Tucholke, Vogt, and others, 1979). At Site 385 near Vogel Seamount, Horizon $A^*$ has not been

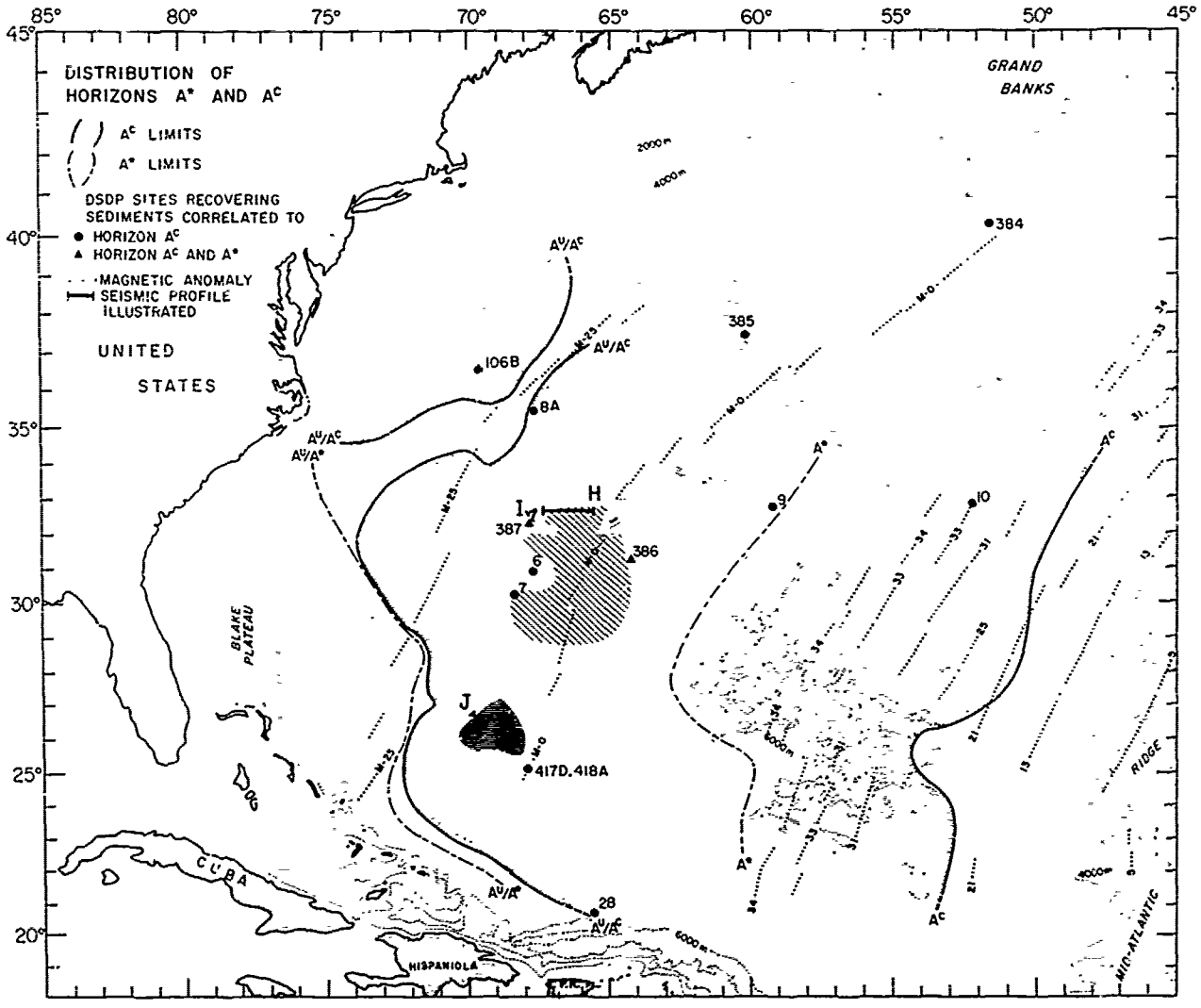


Figure 12. Distribution of Horizons $A^*$ and $A^C$. Western limits show where Paleogene erosion (Horizon $A^U$) removed Horizon $A^*$ and a "channel" in Horizon $A^C$. Horizontally lined area contains unusually thick, non-laminated sediments in the $A^*$-$A^C$ interval (Figure 15). In diagonally hatched area Horizon $A^*$ is very reflective and level (Figure 13).

clearly identified, but the Maestrichtian marly chalks were cored and were interbedded between low-carbonate clays. These data, plus Maestrichtian chalks at other drillsites of shallower paleodepth (Sites 10, 384, 390) indicate a rapid depression of the CCD to more than 5400 m and an equally rapid rise at the end of the Cretaceous (Tucholke and Vogt, 1979). If the correlation of Horizon $A^*$ to this calcareous bed is consistent throughout the basin, then the widespread distribution of Horizon $A^*$ (Figure 12) suggests that the CCD fluctuation was at least a basin-wide event. Jansa and others (1979) formally define the Maestrichtian carbonates as the Crescent Peaks Member of the Plantagenet Formation.

Horizon $A^*$ was first noted to have regional significance by Ewing and others (1970) and it was named by Ewing and Hollister (1972). When this reflector was penetrated at Site 105, it was thought to correlate with the transition from multicolored to black clays (Hollister, Ewing, and others, 1972). However, a later erosional surface (Horizon $A^U$) very closely overlies or truncates Horizon $A^*$ at the site (see Figure 17), and a 40 m interval at this level was not cored. Thus it is possible that $A^*$ does indeed correlate with Maestrichtian carbonates in this region,

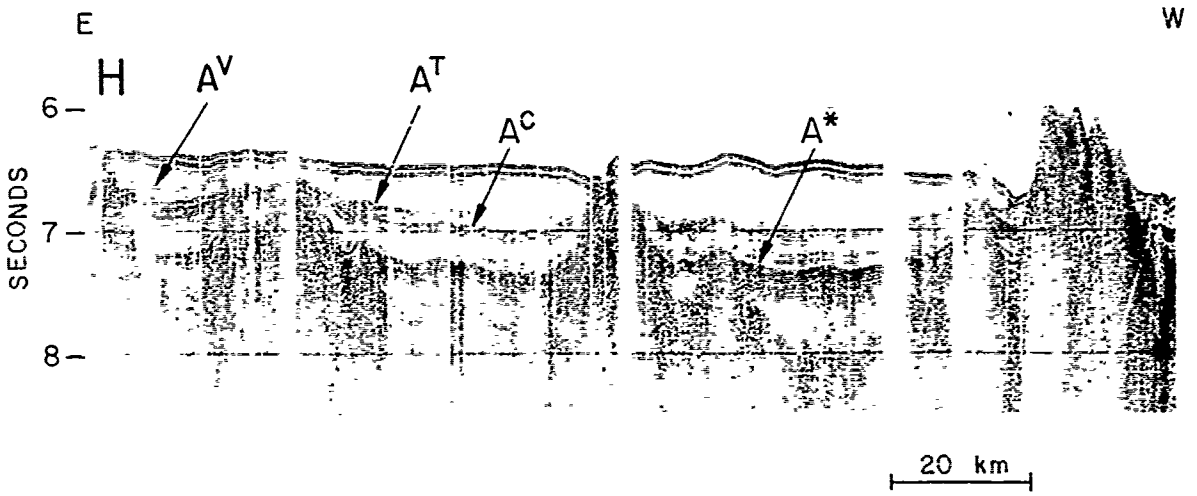


Figure 13. Seismic profile from the western Bermuda Rise showing highly reflective and relatively flat Horizon A*, and reflectors of the overlying "Horizon-A Complex". Location in Figure 12.

but at Site 105 the carbonates either were removed by erosion or were not cored.

Horizon A* exhibits variable acoustic character within the basin. East of Bermuda the reflector is rarely observed, probably for two reasons. First, most of the lower Upper Cretaceous crust in this region probably accumulated only thin sequences of pelagic clay prior to deposition of Maestrichtian chalks, and Horizon A* may overlie basaltic basement so closely that it cannot be resolved (see Figure 19b). Second, on crust younger than about Campanian age, sediment accumulation was above the CCD (e.g. Site 10, Peterson, Edgar, and others, 1970) and Maestrichtian carbonates in this section would not have sufficient impedance contrast to form a reflector.

For three hundred kilometers or more south and west of Bermuda, Horizon A* is a very strong, relatively level reflector that is best developed within topographic lows (Figures 12, 13). The reflector distribution appears to be controlled in part by basement topography, suggesting possible accumulation from turbidity currents and a source area in the vicinity of Bermuda. Until the reflector is drilled in this area, we cannot be certain that it correlates only with Maestrichtian carbonates.

On the southern and westernmost Bermuda Rise, Horizon A* is a distinct reflector that drapes over deeper topographic irregularities in a manner suggesting its pelagic origin (Figure 10). Beneath the westernmost Bermuda Rise, the reflector overrides a basement swell and farther west becomes difficult to distinguish from overlying acoustically laminated sediments. Traced westward beneath the Hatteras Abyssal Plain, Horizon A* becomes interbedded with the base of a series of flat-lying reflectors, and beneath the continental rise it is developed within a thick sequence of reflectors. These reflector relationships suggest that turbidity currents and debris flows were developing the continental rise prior to the deposition of Horizon A* and that turbidity currents later began forming an eastward-encroaching abyssal plain about the same time that Horizon A* was deposited.

## Paleogene Sedimentation and the Horizon-A Complex

Horizon A was first defined by Ewing and Ewing (1962, 1963) in profiler records acquired with explosives north of the Puerto Rico Trench. In this area and in many other parts of the basin the horizon is smooth and strongly reflective, and it was thought to be a fossil abyssal plain (Ewing and Ewing, 1964). Piston cores that recovered turbidites of Maestrichtian age from the "Horizon-A outcrop" north of San Salvador appeared to confirm this idea (Ewing and others, 1966; Saito and others, 1966). Subsequent deep-sea drilling on the Bermuda Rise indicated that high-impedance Eocene cherts were responsible for the reflector (Ewing and others, 1970), and at Site 105 on the lower continental rise Horizon A correlated with an unconformity where some 60 m.y. of sediments were missing (Hollister, Ewing and others, 1972).

These conflicting correlations are resolved when one considers the acoustic character of "Horizon A". It actually is composed of one to several closely spaced, significant reflec-

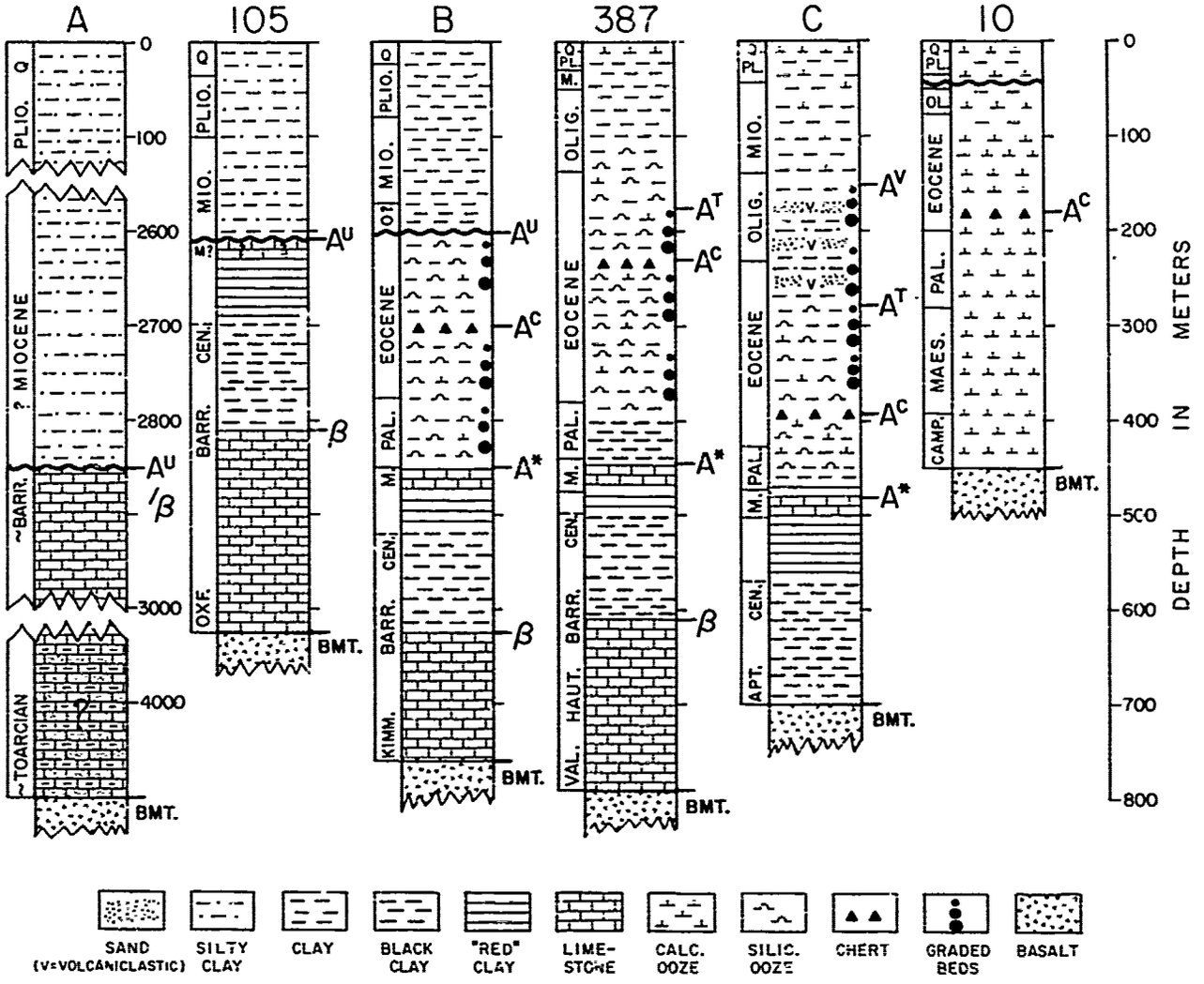


Figure 14. Lithologic columns, generalized at three DSDP drillsites and idealized in three intervening areas, showing correlation with major reflectors from west (left) to east in basin. Idealized sections: A - beneath landward end of Blake Outer Ridge, B - vicinity of DSDP Site 8, C - near Bermuda pedestal, central Bermuda Rise.

tors (Ewing and Ewing, 1964), each of which can be traced laterally on regional scales and each of which has specific geologic correlations. For this reason we use the term "Horizon-A Complex" for the reflector group. Several reflectors in the group ($A^C$, $A^T$, $A^V$ and $A^U$) have been studied separately by Tucholke (1979), and we discuss their geologic significance here.

## Horizon $A^C$

In the series of reflectors that comprise the Horizon-A Complex, Horizon $A^C$ is the deepest known to have a consistent lithologic correlation and it normally is the strongest reflector (Figures 10, 13). Where it has been drilled the reflector correlates with upper-lower to lower-middle Eocene chert, except at Site 386 where it matches middle Eocene chalks overlying the cherts (Tucholke, 1979).

Horizon $A^C$ is widespread in the western North Atlantic (Figure 12), and the chert is developed in a variety of lithofacies (Figure 14). On the western Bermuda Rise, beneath the Hatteras Abyssal Plain, and probably beneath the Sohm Abyssal Plain, the cherts occur within Eocene turbidites that were derived from the North American continental margin. Farther seaward, the cherts are developed within hemipelagic clays deposited

below the Eocene CCD (e.g. Site 9) or within shallower pelagic carbonates along the flank of the Mid-Atlantic Ridge (Site 10) and other shallow regions isolated from terrigenous sources (e.g. Site 384: J-Anomaly Ridge, Site 390: Blake Nose). The charts mark the top of the Bermuda Rise Formation as defined by Mansa and others (1979).

As expected, the eastern pinchout of Horizon $A^C$ is on crust of Eocene age (Figure 12). However, east of Bermuda the reflector generally is observed only in patches within basement depressions (see Figure 19b), and the sedimentary section between Horizon $A^C$ and acoustic basement usually is thinner than 100 m. The thin sedimentary section is expected because this crust was isolated from terrigenous sources and most of the crust of Albian to Santonian age was below the CCD during its entire history (Tucholke and Vogt, 1979).

By considering the character and distribution of Horizon $A^C$, the thickness and acoustic signature of sediments between Horizons $A^C$ and $A^*$, and the lithology of sediments cored from this interval, we can determine several aspects of the Early Paleogene sedimentary environment that led up to the deposition of Horizon $A^C$. As noted earlier, Maestrichtian carbonates correlating with Horizon $A^*$ accumulated in a pelagic environment throughout most of the basin. East of the Hatteras Abyssal Plain the sediments immediately overlying Horizon $A^*$ are mostly acoustically non-laminated and they generally conform to the shape of Horizon $A^*$ suggesting that pelagic deposition continued into the Paleocene. Paleocene deep-basin sediments are poorly represented in JOIDES boreholes, but lithofacies at Site 385 (zeolitic clay) and Site 387 (radiolarian clay) also indicate that pelagic and hemipelagic deposition of clay and biogenic silica below the CCD were dominant (Tucholke, Vogt, and others, 1979). At Site 387 on the western Bermuda Rise, the lower Paleocene section contains black, carbon-rich sediment similar to the Lower Cretaceous black clays, and it probably accumulated in a anoxic environment.

There are some exceptions to these indications of quiescent pelagic deposition. On the southwest Bermuda Rise, the non-laminated sediments above Horizon $A^*$ exhibit marked thickness variations (Figure 15), and it is likely that they were reworked by bottom currents. Considering the early Paleocene anoxic conditions indicated at Site 387, this bottom-current activity must have begun in the latter half of the Paleocene. Climatic cooling began at this time (Boersma and others, 1979), and the deep circulation may have been stimulated by formation of cool bottom water at high latitudes.

Beneath the Hatteras Abyssal Plain and the continental rise, the probable Paleocene sediments overlying Horizon $A^*$ tend to be acoustically laminated. These sediments have not been cored in DSDP boreholes, but they may include admixtures of fine-grained terrigenous debris, biogenic silica, and carbonate displaced from the continental shelf and slope above the CCD. By this time, basin-filling behind shelf-edge barriers and falling sea level probably allowed dispersal of large quantities of such sediments to the deep basin. With time, turbidite dispersal extended farther seaward. Uplift had not yet formed the Bermuda Rise, and distal turbidites flooded the region of both the present Hatteras Abyssal Plain and the western Bermuda Rise. This seafloor-leveling process is clearly demonstrated in seismic profiles from the western Bermuda Rise (Figure 10), and it resulted in marked thickness variations in the Horizon $A^*$ to $A^C$ interval.

The CCD during the Paleocene to middle Eocene probably was 4 to 4.5 km deep (Tucholke and Vogt, 1979). By late Paleocene time, a substantial fraction of biogenic silica was deposited both with carbonates above the CCD and with deeper-basin clays. The implied stimulation of biogenic silica production in surface waters may have been produced by upwelling of cooler, nutrient-rich bottom water; this water is thought to have originated at higher latitudes and surfaced in upwelling zones along a west-flowing circumglobal current through the Tethys, North Atlantic and Pacific Oceans (Berggren and Hollister, 1974).

Biogenic silica production and/or seafloor silica preservation were enhanced most strongly in the late-early and early-middle Eocene. The chert resulting from burial and diagenesis of these sediments now forms Horizon $A^C$. Similar Eocene cherts have been drilled in the eastern North Atlantic (Petersen, Edgar, and others, 1970), the Caribbean (Edgar, Saunders and others, 1973), and the equatorial Pacific (e.g. Tracey, Sutton and others, 1971). Siliceous sediments associated with an authigenic mineral suite indicating alteration of volcanic glass also are observed in shallow-water sediments exposed along the Atlantic coastal plain and Gulf Coast (Gibson and Towe, 1971).

The exact cause of the strongly increased silica content of these sediments still is unclear, although most hypotheses incorporate enhanced deep circulation and upwelling (Jones and others, 1970; Berggren and Phillips, 1971), increased nutrient-phosphorous and silica supply to surface water through subaerial volcanism (Gibson and Towe, 1971; Mattson and Pessagno, 1971), or a combination thereof (Berggren and Hollister, 1974). Herman (1972) suggested that the cherts resulted from coincidence of increased productivity

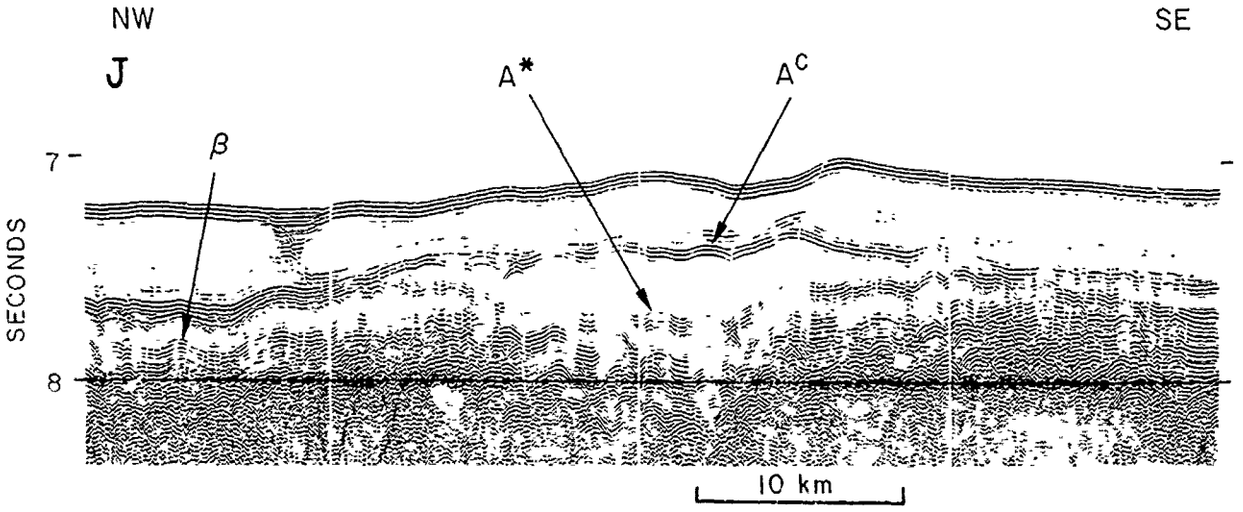


Figure 15. Seismic profile from southwest Bermuda Rise showing differential thickening between Horizons $A^*$ and $A^C$ probably caused by abyssal currents. Location in Figure 12.

(due to cooler climate) and increased seafloor silica preservation (due to increased silica input to bottom water from submarine volcanism). The rapid biogenic silica accumulation in the early to middle Eocene probably cannot be ascribed solely to cooling climates and increased upwelling; although there was a gradual cooling in the early to middle Eocene, temperatures probably remained stable during the remainder of the Eocene (Margolis, 1976), and continued rapid silica accumulation might be expected in contrast to observed decreases. Thus an episode of increased volcanism in conjunction with the cooling climate may best explain the relatively short duration of the enhanced silica accumulation. Significantly increased volcanism in late Paleocene to early Eocene time is known to have occurred in both the Brito-Arctic (Thulean) and Caribbean regions (Jacque and Thouvenin, 1975; Khudoley and Meyerhoff, 1971, among others) and at Bermuda (Tucholke, Vogt, and others, 1979). Major tectonism and volcanicity also occurred throughout most of the Tethyan region during this time (Dewey and others, 1973).

## Horizon $A^T$ and Formation of the Bermuda Rise

Horizon $A^T$ overlies Horizon $A^C$ by about 0.05 to 0.2 seconds reflection time (nominally 45 to 190 m) in the Horizon-A Complex (Figures 10,13). In most of the region between Bermuda and the continental rise it marks the top of the complex. The reflector correlates with the uppermost occurrence of mixed bioclastic/terrigenous turbidites at Sites 386 and 387 on the Bermuda Rise (Tucholke, 1979). Three other drill sites (6,7,8) penetrated the reflector but were too sparsely cored to confirm the correlation between Horizon $A^T$ and the top of the turbidites. However, two of the sites (6,8) cored sediments from the $A^C$-$A^T$ interval and recovered turbidites with abundant calcareous, siliceous, and terrigenous debris. Only minor, locally derived turbidites are present above Horizon $A^T$ in the Bermuda Rise drillsites.

As discussed earlier, these sediments were deposited from turbidity currents that originated along the continental margin of North America. The distribution of Horizon $A^T$ (Figure 16) shows that the distal parts of these currents reached as far as the present central Bermuda Rise, some 1200 km from the source area. At their eastern limit, the turbidites ponded into middle Eocene topographic depressions and fracture zones, much like the Quaternary ponding along the northeast margin of the Nares Abyssal Plain (Shipley, 1978).

The abrupt transition from turbidite to non-turbidite deposition marked by Horizon $A^T$ on the western Bermuda Rise probably resulted from uplift that began to form the rise in the middle Eocene. This timing agrees with the probable age of the main edifice-building volcanism that formed the Bermuda pedestal; drilling results at Site 386, 140 km southeast of Bermuda, show that the Bermuda volcanoes had reached sea level and were being actively eroded by late middle Eocene time (Tucholke and Vogt, 1979). Based on limited biostratigraphic data, the turbidites correlating with Horizon $A^T$ appear to become younger toward the west, ranging from middle Eocene at Site 386 on the central Bermuda rise to late Eocene at Site 8 just west of the rise. Such diachronism is reasonable because turbidites should progressively offlap the Bermuda Rise toward the west as it was uplifted. Farther

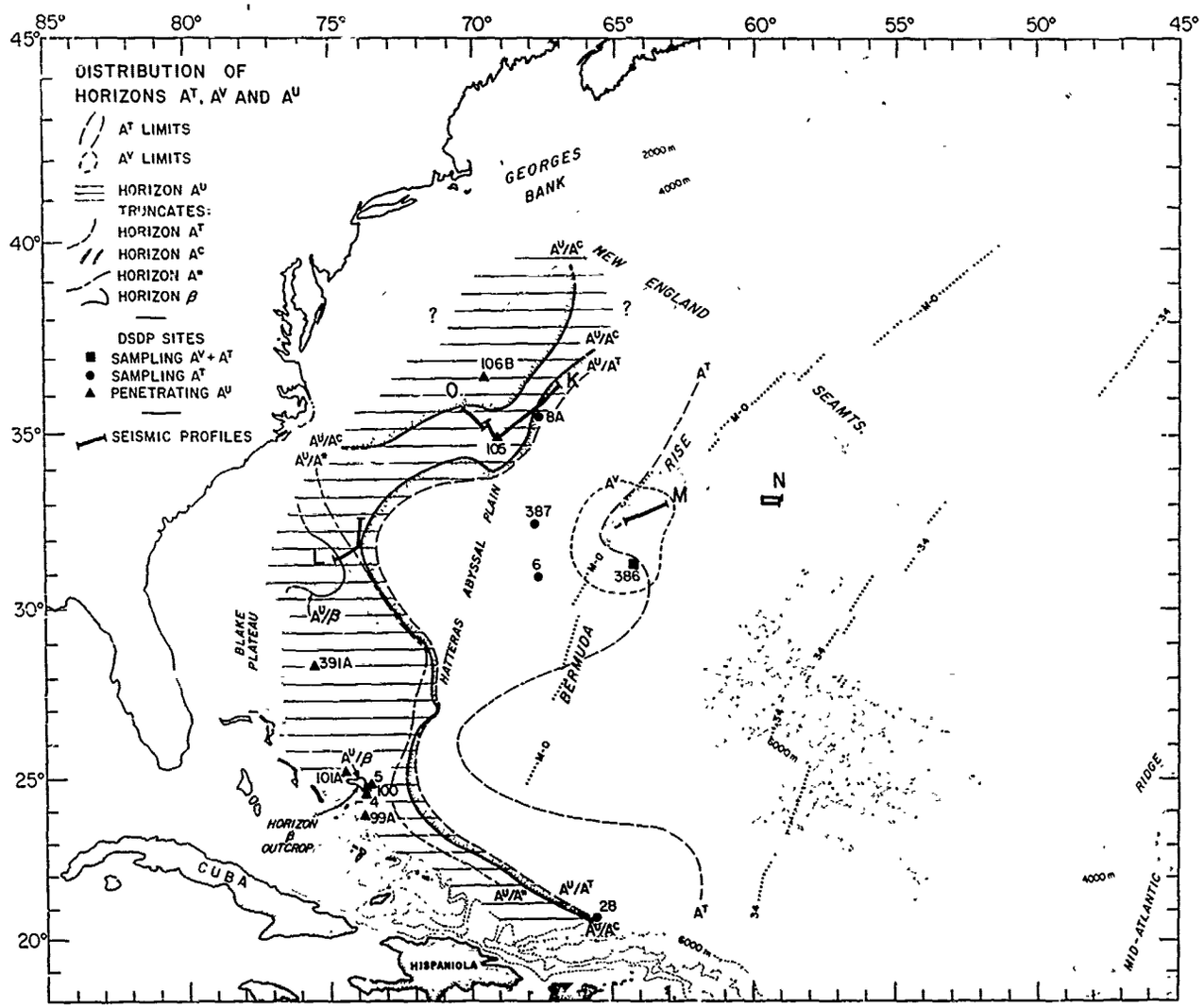


Figure 16. Distribution of Horizons $A^T$, $A^V$, and $A^U$. The Horizon $A^U$ unconformity (horizontal lines) truncates older reflectors beneath the continental margin as shown.

west beneath the Hatteras Abyssal Plain Horizon $A^T$ has not been drilled, but it is likely to be younger than late Eocene. Drilling and dating this horizon at several locations along the western Bermuda rise and Hatteras Abyssal Plain could provide a method for studying the timing and dynamics of uplift that formed the Bermuda Rise. The amount of uplift presently can be estimated at two drillsites; if we assume that Horizon $A^T$ is isochronous and that it was a level (abyssal plain) surface in the middle Eocene, then present depths of the reflector suggest that uplift was about 400 m at Site 387 and 700 m at Site 386, relative to the central Hatteras Abyssal Plain (Tucholke and Vogt, 1979). However, these values are minima because of the possible diachronism of the reflector.

## Late Paleogene Sedimentation, Erosion, and the Origin of Horizon $A^U$

After deposition of Horizon $A^T$ on the Bermuda Rise in the middle to late Eocene, the CCD level remained near 4000-4500 m (Tucholke and Vogt, 1979), and siliceous hemipelagic clays accumulated in most of the deep basin. Deposition of turbidites continued for an unspecified time in the region of the present Hatteras Abyssal Plain, but eventually ceased. Horizon $A^T$ in this area is overlain by acoustically non-laminated sediments that extend upward to the base of the modern (Plio-Pleistocene) Hatteras turbidites. The Paleogene influx of turbidites from the continent may have been stopped because of strong erosion of the Paleogene

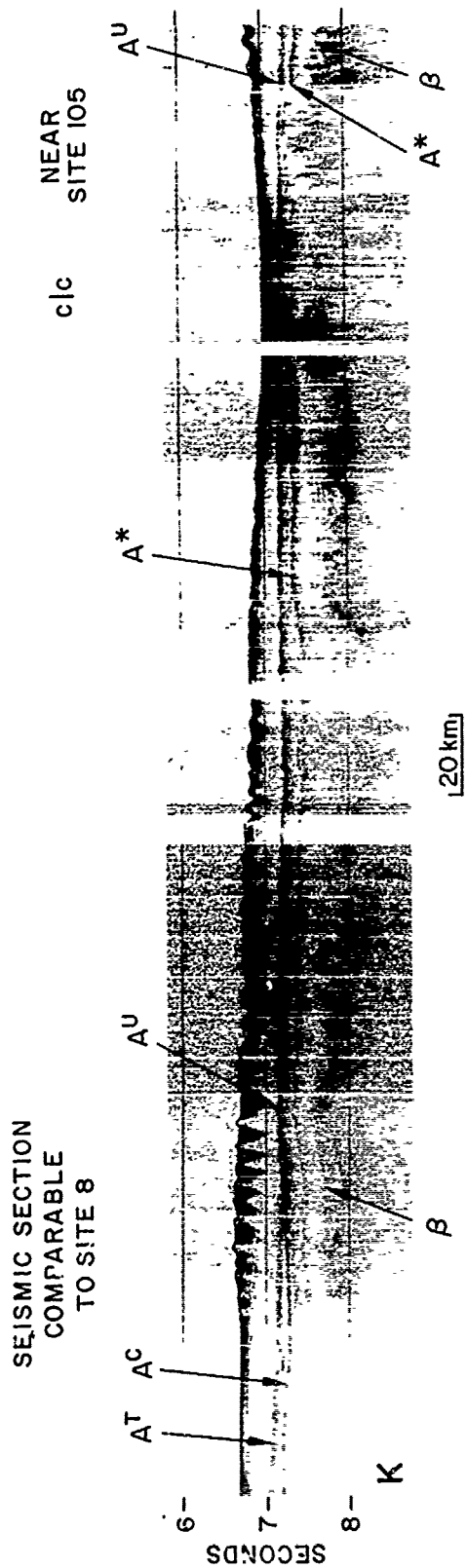


Figure 17. Seismic profile across Site 105 and near Site 8. Note that Horizon $A^*$ at Site 105 rises over the basement swell and is closely approached or truncated by Horizon $A^U$. Location in Figure 16.

continental rise by abyssal currents (see discussion below).

Oligocene sediments are very poorly represented in deep-sea boreholes, but one drillsite (387) on the western Bermuda Rise suggests that deposition of biogenic silica continued in diminishing quantities until middle or late Oligocene time. Younger sediments contain little siliceous debris except for sporadic local occurrences. The cause of the diminuation and cessation of biogenic silica deposition is uncertain. However, because the production of siliceous organisms probably was related to deep and surface circulation patterns and in particular to the westward-flowing circumglobal "equatorial" current, it is likely that circulation changes were responsible. Three factors may have been significant. First is the general climatic cooling that characterized the Eocene and Oligocene (Savin and others, 1975) and its possible effect on the westward flow of the "equatorial" current. If the cooling forced an equatorward compression of global wind belts, then the Tethys Sea north of Africa could gradually have come under the influence of westerly rather than easterly (equatorial) winds. Second, the north coast of Africa in the Eocene probably was near 25°N latitude and slowly drifted north by 5 to 6 degrees by the end of the Oligocene (Berggren and Hollister, 1974). The combination of the northward drift of Africa and the southward shift of the westerlies wind belt could have markedly diminished westward flow through the Tethys. The flow from the Atlantic into the Pacific thus would be reduced and limited more to equatorial latitudes, and it would be accompanied by shifts of high productivity areas from the central to equatorial North Atlantic. A third, complementary factor may have been increased intensity of the deep circulation, probably associated with the cooling Paleogene climate. Sverdrup and others (1942) and Ramsay (1971) have noted that biogenic silica production in the present equatorial Atlantic is limited because necessary nutrients are removed to the South Atlantic and beyond by the southward flowing North Atlantic Deep Water. Therefore, increased deep circulation in the Paleogene actually may have hindered rather than stimulated surface production of biogenic silica.

Deep currents of increased intensity in Paleogene time account for one of the most dramatic changes in abyssal sedimentation that the western North Atlantic has experienced. The deepest seismic expression of these current effects is Horizon $A^U$. This reflector correlates with an erosional unconformity beneath the continental margin and it truncates a variety of deeper reflectors (Figures 14, 16, 17). Both Horizons $A^T$ and $A^C$ are observed near Site 8, but Horizon $A^U$ truncates these

reflectors toward the west, and at Site 105, 160 km southwest of Site 8, the unconformity cuts close to or beneath Horizon A* (Figure 17). To the north at Site 106, Horizon $A^U$ probably immediately overlies the cherts of Horizon $A^C$ (Figure 16).

The most significant erosion of the Paleogene continental rise occurred south of Cape Hatteras (Figures 16, 18) where Horizon $A^U$ merges with, but does not cut significantly below Horizon β. Apparently the carbonates below Horizon β were well lithified beneath a substantial sediment overburden before they were excavated by Paleogene bottom-current erosion. Based on the depths at which erosion-resistant limestones are encountered in other DSDP boreholes with continuous sedimentary records, at least 400 m of overburden were removed. Farther south, in the "Horizon A - Horizon β outcrop" area near San Salvador (Ewing and others, 1966; Windisch and others, 1968), Horizon $A^U$ rises and intersects the present sea floor (Figures 4, 6, 7). At DSDP Sites 5 and 100 in this area, calcareous sediments from below Horizon β are poorly lithified, and it is unlikely that they ever were covered by substantial overburden (Ewing, Worzel and others 1969; Hollister, Ewing and others, 1972).

The distribution of Horizon $A^U$ (Figure 16) clearly suggests that the unconformity was eroded by a southerly flowing, westward-intensified abyssal boundary current, probably a precursor to the modern Western Boundary Undercurrent (WBUC) (Heezen and others, 1966). However, determining the exact timing of the erosion is difficult for two reasons. First, the youngest sediments into which the unconformity is cut mostly are acoustically non-laminated in conventional profiler records (e.g. east of Site 8; Figure 17), and consequently there is no detectable impedance contrast identifying Horizon $A^U$. Where the youngest sediments are laminated, the unconformity intersects them at such a low angle that it is very difficult to determine which beds have been eroded. Second, most DSDP boreholes that have penetrated Horizon $A^U$ were drilled in areas where a major portion of the sedimentary section is missing; for example the Upper Cretaceous to middle Miocene section is missing at Site 105, and the ∿ Cenomanian to upper Miocene section has been eroded at Site 101. Site 8, which was drilled near the eastern edge of Horizon $A^U$, was too sparsely cored to pinpoint the age of erosion. However, seismic profiles in this area do indicate that the unconformity was cut into Horizon $A^T$ (late Eocene turbidites) at or near Site 8. The oldest sediments cored above the unconformity are of middle to late Miocene age (Sites 8, 101, 10[illegible], 106, 388; Hollister, Ewing and others, 1972; Sheridan, Benson and others, 1978). Beneath the Blake Outer Ridge, downward extrapolation of known sedimentation rates at Sites 102, 103 and 104 indicates that sediments as old as lower Miocene may overlie Horizon $A^U$. Thus the erosion probably occurred at some time between the late Eocene and early Miocene.

The apparent difference in depth of erosion north and south of Cape Hatteras (Figure 16) may be due to interaction between the southerly flowing WBUC and the Gulf Stream. The Gulf Stream probably was well developed in Paleogene time (Berggren and Hollister, 1974), and current shear between the base of this flow and the WBUC could have reduced the erosive power of the WBUC north of Cape Hatteras. It also is possible that less sediment originally blanketed Horizon β south of Cape Hatteras, although we do know that massive deposits of Lower Cretaceous black clays covered Horizon β off the southern Blak Plateau (Figure 11).

Tucholke and Vogt (1979) have discussed possible reasons for intensified deep circulation and erosion during this interval. The presently acceptable alternatives seem to be that 1) currents gradually intensified during Late Paleogene time, probably because of cooling climate, and they eroded the continental rise over a period of some 15-20 m.y., 2) after the Greenland-Iceland-Faroe Ridge subsided below sealevel during or following the late Oligocene (Talwani, Udintsev, and others, 1976), cold water from the Norwegian-Greenland Sea flooded the North American Basin and caused erosion on a catastrophic scale within a few million years, or 3) both occurred. Just as puzzling as the cause of the erosion is the mechanism by which current intensity was "suddenly" reduced, allowing rapid deposition of middle (lower?) Miocene and younger sediments. For example, Miocene sediments at Site 104 on the Blake Outer Ridge accumulated as rapidly as 190 m/m.y. (Hollister, Ewing and others, 1972). Possible explanations for this change to depositional conditions include 1) eventual reduction and stabilization of thermohaline gradients responsible for the deep flow, 2) reduction of southward flow of "Arctic"-derived bottom water during Antarctic glaciation, and 3) late Oligocene opening of the Drake Passage to deep circumpolar flow and consequent reduction of southward "draw" on North Atlantic Deep Water by the Antarctic Circumpolar Current east of the Scotia Arc (Tucholke and Vogt, 1979). Other explanations are possible, and there clearly are a host of outstanding questions on the deep circulation that remain to be answered.

Considering the likely morphology of the Paleogene continental rise and probable thickness of sediment that was eroded, we can estimate very roughly that some 2 X $10^5$ $km^3$ of sediment were removed during the erosional

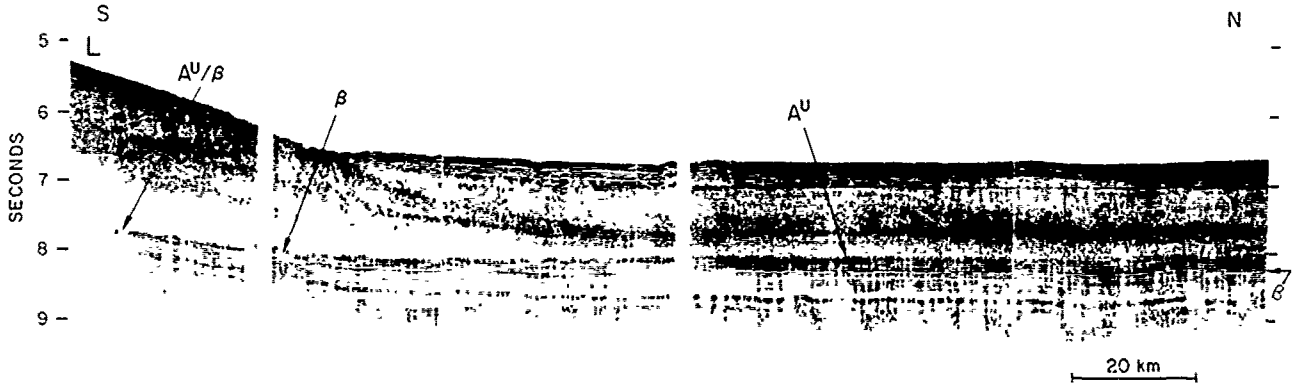


Figure 18. R/V CONRAD 20-12 large-volume-airgun seismic profile approaching the north flank of the Blake Outer Ridge. Horizon $A^U$ approaches and cuts down to Horizon $\beta$ under ridge (partially obscured by bubble pulse). Location in Figure 16.

episode. Beneath the continental rise north of the New England Seamounts, an erosional unconformity of about the same age may be present (Parsons, 1975), and perhaps half as much sediment was eroded from this segment of the continental margin. The fate of this large volume of sediment is uncertain. The sediment would have formed a layer about 50 m thick if spread uniformly throughout the contemporary basin outside the erosional zone. Realistically, some of the sediment probably was transported along paths of other established but less intense abyssal flows to form the cores of major depositional ridges such as the Greater Antilles Outer Ridge north of Puerto Rico (Tucholke and Ewing, 1974). Sedimentation rates on the northern Bermuda Rise also increased dramatically some time after the deposition of Horizon $A^C$ in the middle Eocene, (compare Figures 15, 19b; Ewing and others, 1970; Tucholke and Vogt, 1979), and the massive sediment drifts on the northern rise may contain sediment eroded from the continental margin. The main abyssal boundary current probably carried much of the entrained sediment into the South Atlantic or farther. In the Argentine Basin, thick sediment drifts began to form and sedimentation rates increased sharply during the late Oligocene and early Miocene (Supko, Perch-Nielsen, and others, 1977), but it is not clear that this was caused by increased sediment influx from the North Atlantic.

### Horizon $A^V$ Emergence History of the Bermuda Pedestal

As noted earlier, the volcanic foundation of Bermuda emerged above sea level by late middle Eocene time, although the pedestal probably was intruded by lamprophyre sheets as late as early Oligocene time (Reynolds and Aumento, 1974). The subaerial weathering of the volcanic pedestal is recorded by coarse volcaniclastic turbidites deposited at DSDP Site 386 about 140 km southeast of Bermuda (Tucholke, Vogt, and others, 1979). These turbidites form a strong reflector, termed Horizon AV, that surrounds Bermuda and merges with the acoustically opaque archipelagic apron of the island (Figures 16, 19a). At Site 386, the top of the turbidites dates to the late Oligocene, but Horizon $A^V$ may vary somewhat from this age at other locations, depending upon the complexity of turbidite dispersal paths from the Bermuda pedestal. Horizon $A^V$, although of only local extent, is particularly interesting because it closely overlies Horizons $A^C$ and $A^T$ and is distinguishable from them only upon close examination of high-quality profiler records. Furthermore, because the horizon is highly reflective, it commonly masks the deeper reflectors near the pedestal (Figure 19a). Thus, less than rigorous examination of the seismic stratigraphy near Bermuda could lead to the erroneous conclusion that deposition of "Horizon A" ($A^C$, $A^T$, $A^V$) and the culmination of Bermudan volcanism and denudation were coincident and dated to the middle Eocene.

### Neogene Current-Controlled Sedimentation

Effects of the deep circulation on sedimentation patterns are clearly expressed in middle Miocene and younger sediments deposited above Horizon $A^U$ along the continental rise, and in sediments above Horizon $A^C$ and $A^T$ elsewhere in the basin (Figures 6, 13, 17). Patterns of differential sediment accumulation range

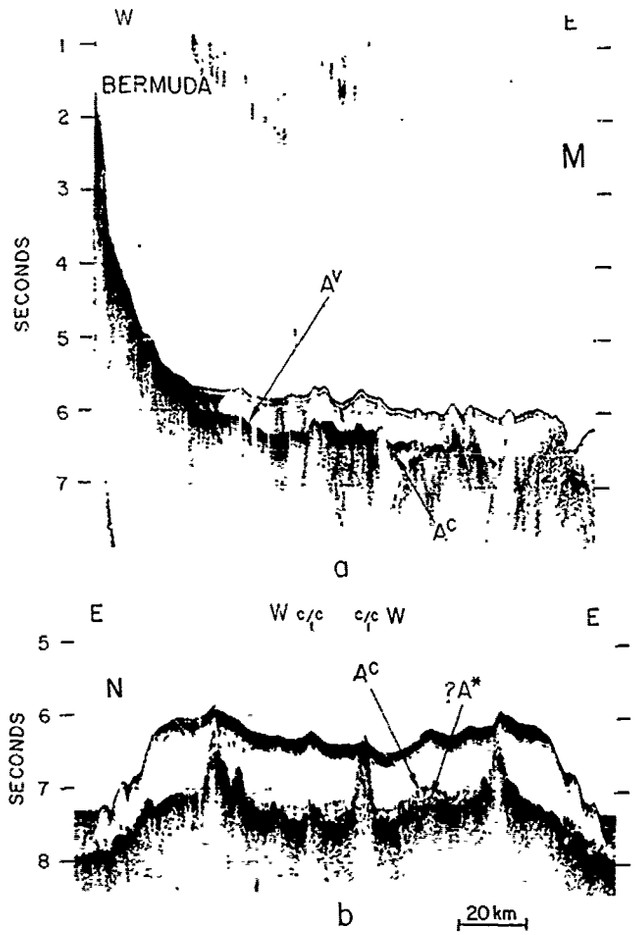


Figure 19. Seismic profiles across the northern Bermuda Rise. In (a) note Horizon $A^V$ merges with the archipelagic apron of Bermuda pedestal and masks deeper reflectors. In (b) note thin sedimentary sections between Horizon $A^C$ and acoustic basement, and massive sediment drifts above. Locations in Figure 16.

in scale from small moats around basement peaks to major depositional ridges such as the Blake-Bahama Outer Ridge. One of the best intermediate-scale examples of deposition controlled by the Western Boundary Undercurrent is seen in a large-volume airgun profile across the "lower continental rise hills" near DSDP Site 105 (Figure 20). The origin of these hills has been a matter of long-standing debate. Explanations have ranged from gravitational sliding (Ballard, 1966; Emery et al., 1970), to current-controlled deposition (Fox, et al., 1968; Rona, 1969; Ewing and Hollister, 1972), and to Pleistocene erosion and sculpting by turbidity currents (Asquith, 1976). The uncertainties resulted primarily from the fact that most seismic profiles do not clearly define the internal structure of the hills (Figure 17). However, the high-energy sound source used to record the profile in Figure 20 shows that the hills are sediment waves containing migrating, differentially deposited beds that are characteristic of current-controlled deposition.

Farther south, the Blake-Bahama Outer Ridge is constructed primarily of Miocene and younger sediments, and it overlies a Horizon $A^U$ unconformity that is relatively flat (Figure 18) or that has sculpted older sediments (Figure 6). Unconformable relationships among seismic reflectors within the Neogene sediments and unconformities encountered in boreholes show that the development of this ridge system is complex and still poorly understood, but the evolution undoubtedly has been dominated by the depositional and erosional activity of the Western Boundary Undercurrent (Markl and others, 1970; Bryan 1970; Ewing and Hollister, 1972). Other depositional ridges such as the Caicos Outer Ridge off the Bahama Banks and the Greater Antilles Outer Ridge north of the Puerto Rico Trench also have formed primarily in the Neogene through current-controlled deposition (Tucholke and Ewing, 1974).

Reflectors within the continental rise above Horizon $A^U$ also show complex interrelationships that probably were controlled by flow of the Western Boundary Undercurrent and by variable sediment influx related to sea level changes. In many locations reflector relationships are complicated further by slumping. We have not traced Horizon $A^U$ unambiguously beneath the upper continental rise nor satisfactorily interpreted the Neogene evolution of this sedimentary prism. However, because Horizon $A^U$ extends westward in a relatively level attitude well below the central continental rise, there can be little doubt that the present rise evolved in response to Neogene processes.

Away from the continental margin, one of the most active regions of late Paleogene and Neogene current-controlled deposition has been the northern Bermuda Rise (Figure 19b). Laine (1978) presented evidence that sediment there has been deposited from a deep, westerly return flow in the clockwise Gulf Stream gyre. If this hypothesis is valid, then most of the sediment deposited on the northern Bermuda Rise could have been entrained by the Gulf Stream from the Western Boundary Undercurrent along the U.S. continental margin.

The marked late Paleogene and Neogene change in sedimentation patterns demonstrated by the seismic stratigraphy also is indicated in the sediment lithology. Sediments deposited throughout the basin during this period consist of gray-green and brown hemipelagic clays and silty clays (Blake Ridge Formation), in contrast to underlying siliceous lithofacies (Jansa and others, 1979). Graded turbidite

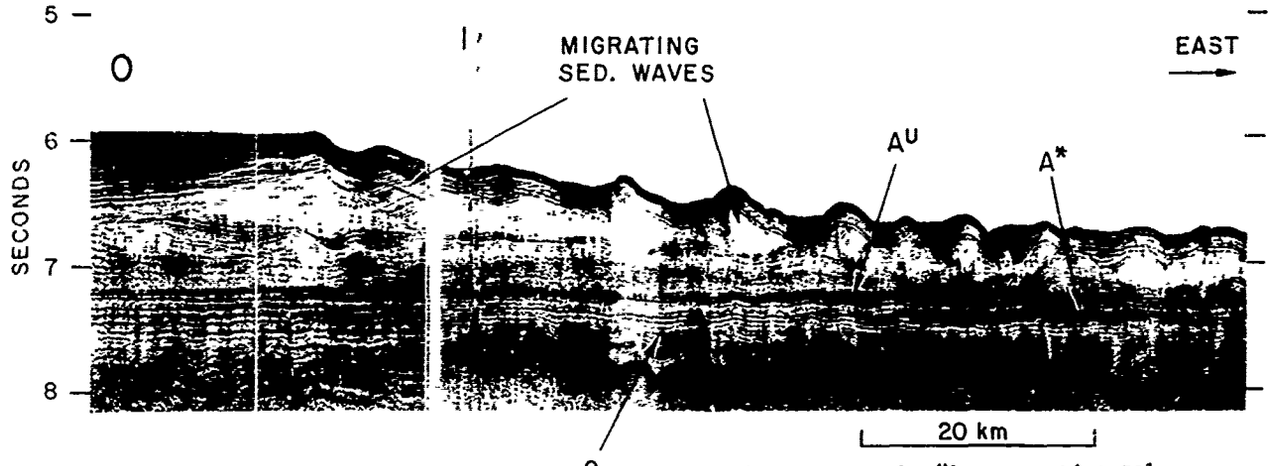


Figure 20. R/V CONRAD 21-01 large-volume airgun profile across the "lower continental rise hills" near Site 105. Note resolution of migrating reflectors within sediment waves above Horizon $A^U$. Location in Figure 16.

deposits have been cored in several boreholes (106, 382, 383) and are traceable as acoustically laminated sequences in seismic profiles across the modern abyssal plains. This latest phase of turbidite deposition and formation of the present abyssal plains probably began near the end of the Pliocene.

## Summary

By mapping the seismic stratigraphy in the North American Basin and correlating reflectors with the lithostratigraphy and biostratigraphic age data at DSDP boreholes, we have been able to interpret major aspects of the sedimentary history of basin. By itself, no one of these stratigraphic studies would be as useful in examining the geological history. Relationships among these stratigraphic elements are summarized in Table 1 and Figure 14.

Deep reflectors beneath the continental rise define relatively smooth, acoustically laminated seismic sequences that pinch out eastward on crust of Early to Late Jurassic age. These sediments have not been drilled, but their acoustic character suggests that they are dominantly terrigenous and bioclastic sediments emplaced by debris flows and turbidity currents. Seafloor smoothing by these sediments is most conspicuous in the southwestern part of the basin where Horizon B (smooth acoustic basement) is formed by highly reflective sediments onlapping and seismically masking upper Middle to Upper Jurassic (anomaly M-23) basaltic crust. Up to this time, sediments transported downslope across the continental margin probably covered most of the Jurassic seafloor. Local basement rises, such as that at Site 105, were notable exceptions.

By Early Cretaceous time, influx of clastic sediment to the deep basin was reduced, probably because of gradually rising sea level and the growth of reef barriers along the edge of the continental shelf. Oxfordian to Hauterivian/ Barremian sediments recovered from the seismic interval between Horizons B and β in the deep basin are dominantly pelagic limestones and marly limestones. The numerous, closely spaced reflectors in this seismic interval generally conform to the shape of underlying depositional surfaces, which also suggests the pelagic nature of the sediments. Thus the reflectors generally are smooth above Jurassic crust, but farther east they drape over irregular basement. The seismically mapped pinchout of Horizon β is on crust of Hauterivian-Barremian age.

Horizon β marks a rise in the CCD near the end of the Neocomian and a change from deposition of carbonates in an oxygenated environment to deposition of black and green-gray clays under alternately anoxic and poorly oxygenated conditions. The black clays are acoustically non-laminated and of relatively uniform thickness (∿ 100 m) in most of the deep basin, indicating dominantly pelagic and hemipelagic deposition with continued restriction of terrigenous sources. Several thick lobes of black clays along the continental margin were deposited seaward of probable breaches in the marginal reef system.

Beginning about Turonian time, bottom water in the western North Atlantic again became oxygenated but the CCD remained shallow, and only a few tens of meters of pelagic multicolored clays were deposited in the deep basin during the Late Cretaceous. However, the contemporary continental rise received a gradually increasing influx of sediment from the continental shelf. Shelf-edge reefs

that became extinct in the middle Cretaceous probably were overstepped by shelf sediments, and lowering Late Cretaceous sea level facilitated sediment dispersal to the deep sea.

A rapid, brief depression of the CCD in the middle to late Maestrichtian resulted in deposition of marly chalks throughout most of the basin. These chalks correlate with Horizon $A^*$. Beneath the continental rise, Horizon $A^*$ is interbedded with numerous reflectors that resulted from terrigenous influx from the continental shelf. Farther seaward, comparable acoustically laminated sediments occur mostly above Horizon $A^*$, suggesting that deposition of turbidites extended gradually seaward during the Paleocene. By early Eocene time distal turbidites were being deposited on the western part of the present Bermuda Rise.

Biogenic silica was an important sedimentary component from late Paleocene probably to late Oligocene time. Silica deposition was especially enhanced during the early part of the Eocene, and diagenesis in upper-lower to lower-middle Eocene sediments formed porcelantic cherts that correlate with Horizon $A^C$. This widespread reflector is observed within siliceous turbidites west of Bermuda and in pelagic clays and ridge-flank carbonates farther east.

Horizon $A^T$ marks the top of the acoustically laminated turbidites within which Horizon $A^C$ is developed west of Bermuda. Horizon $A^T$ ranges in age from middle to late Eocene. The older age documents the time at which uplift began to form the Bermuda Rise, isolating it from turbidite influx. This uplift was accompanied by formation of the Bermuda volcanic pedestal, which reached sea level by late middle Eocene time. Horizon $A^V$ correlates with the top of upper Eocene to upper Oligocene volcaniclastic turbidites that surround Bermuda and record subaerial weathering of the Bermuda volcanoes. The reflector is continuous with the acoustically opaque apron of the Bermuda Pedestal. It extends as much as 200 km away from Bermuda and seismically masks deeper reflectors near the island.

Between late Eocene and early Miocene time, abyssal boundary currents eroded a major unconformity (Horizon $A^U$) along the continental rise. This unconformity truncates Horizons $A^T$, $A^C$, $A^*$, and $\beta$ near and beneath the present continental rise and in the "Horizon A-$\beta$ outcrop" north of San Salvador. The unconformity subsequently was buried beneath rapidly deposited Miocene to Holocene hemipelagic sediments that have shaped the bulk of the present continental rise. There is a striking change in depositional regime above Horizon $A^U$ and laterally time-equivalent levels. Whereas earlier deposition was in the form of pelagic drapes, accretionary prisms, and sediment ponds, the overlying sediments commonly exhibit migrating waves, sediment drifts, local moats, and other patterns of differential deposition. All of these patterns attest to the development of the abyssal circulation as an effective geologic agent after late Eocene time.

## Acknowledgements

We are pleased to acknowledge the long-standing support of the Office of Naval Research (N00014-67-A-0108-0004 and N00014-75-C-0210) and the National Science Foundation (GA550, GA27281, and DES71-00214) for acquisition of seismic profiler records. Without the extensive coverage and cross-correlation of reflectors this data provides, this study would not have been possible. We also thank G. Bryan and R. Markl for allowing us to study large-volume airgun profiles, acquired across the Blake-Bahama Outer Ridge under NSF Grant OCE-76-82326, that confirmed our correlation of pre-$\beta$ reflectors in that region. K. Klitgord provided helpful discussion and kindly allowed us to study profiles recorded along the continental rise on R/V FAY cruises 19, 20, and 21. The National Science Foundation, Grant OCE-76-02038, provided funds specifically for analysis of the seismic and lithostratigraphic data. We thank B. Batchelder for drafting the figures. Critical reviews by W.J. Ludwig, W.C. Pitman III, J.I. Ewing, A.W. Bally, P.R. Vail, and C. Lobo are appreciated. Contribution No. 2756 of Lamont-Doherty Geological Observatory.

## References

Asquith, S., The nature and origin of the lower continental rise hills off the east coast of the United States, unpublished M.S. Thesis, City College of New York, 1976.

Ballard, J.A., Structure of the lower continental rise hills of the western North Atlantic, Geophysics, 31, 506-523, 1966.

Benson, W., R.E. Sheridan, and others, Initial Reports of the Deep Sea Drilling Project, 44, Washington, D.C. (U.S. Government Printing Office) 1978.

Berggren, W.A., and J.D. Phillips, The influence of continental drift on the distribution of Cenozoic benthonic foraminifera in the Mediterranean and Caribbean-Gulf Coast regions, in Symposium on Geology of Libya (Tripoli, 1969), Proc., Beirut (Catholic Press) 263-299, 1971.

Berggren, W.A., and C.D. Hollister, Paleogeography, paleobiogeography, and the history of circulation in the Atlantic Ocean, in Hay, W.W. (ed.), Studies in Paleo-oceanography, Soc. Econ. Pal. Min. Spec. Publ. 20, 126-186, 1974.

Boersma, A., N. Shackleton, M. Hall, and Q. Given, Carbon and oxygen isotope records at DSDP Site 384 (North Atlantic) and some Paleocene paleotemperatures and carbon isotope variations in

the Atlantic Ocean, in Tucholke, B.F., P.R. Vogt, and others, Initial Reports of the Deep Sea Drilling Project, 43, Washington, D.C. (U.S. Government Printing Office) 1978.

Bracey, D.R., Structural implications of magnetic anomalies north of the Bahama-Antilles Islands, Geophysics, 33, 950-961, 1968.

Bryan, G.M., Hydrodynamic model of the Blake Outer Ridge, Jour. Geophys. Res., 75, 4530-4537, 1970.

Bryan, W.B., P.T. Robinson, and others, Studying ocean layers, Geotimes, 22 (7/8), 22-26, 1977.

Buffler, R.T., T.H. Shipley, and J.S. Watkins, Blake continental margin: Am. Assoc. Petrol. Geol. Seismic Sec. 2, 1978.

Cande, S.C., and Y. Kristoffersen, Late Cretaceous magnetic anomalies in the North Atlantic, Earth and Planet. Sci. Letters, 35, 215-224, 1977.

Catalano, R., M. Ranson, and B.C. Heezen, Jurassic algal back reef and Lower Cretaceous rudist limestones from the Bahama Escarpment, Geol. Soc. Amer. Abstr. with Prog., 7, 1023, 1975.

Dewey, J.F., W.C. Pitman III, W.B.F. Ryan, and J. Bonin, Plate tectonics and evaluation of the Alpine system, Geol. Soc. Amer. Bull., 84, 3137-3180, 1973.

Donnelly, T.W., J. Francheteau, and others, Mid-ocean ridge in the Cretaceous, Geotimes, 22(6), 21-23, 1977.

Douglas, R.G., M. Moullade, and A.E.M. Nairn, Causes and consequences of continental drift in the South Atlantic, in Tarling, D.H. and S.K. Runcorn (eds.), Implications of Continental Drift to the Earth Sciences, 1, London (Academic Press) 517-537, 1973.

Edgar, N.T., J.B. Saunders, and others, Initial Reports of the Deep Sea Drilling Project, 15, Washington, D.C. (U.S. Government Printing Office) 1973.

Emery, K.O., E. Uchupi, J.D. Phillips, C.W. Bowin, E.T. Bunce and S.T. Knott, Continental rise off eastern North America, Am. Assoc. Petrol. Geol. Bull., 54, 44-108, 1970.

Ewing, J.I., and G.B. Tirey, Seismic profiler, Jour. Geophys. Res., 66, 2917-2927, 1961.

Ewing, J.I., and M. Ewing, Reflection profiling in and around the Puerto Rico Trench, Jour. Geophys. Res., 67, 4729-4739, 1962.

Ewing, J.I., J.L. Worzel, M. Ewing, and C.C. Windisch, Ages of Horizon A and the oldest Atlantic sediments, Science, 154, 1125-1132, 1966.

Ewing, J.I., C.C. Windisch, and M. Ewing, Correlation of Horizon A with JOIDES borehole results, Jour. Geophys. Res., 75, 5645-5653, 1970.

Ewing, J.I. and C.D. Hollister, Regional aspects of deep-sea drilling in the western North Atlantic, in Hollister, C.D., J.I. Ewing and others, Initial Reports of the Deep Sea Drilling Project, 11, Washington, D.C. (U.S. Government Printing Office) 951-973, 1972.

Ewing, M., and J.I. Ewing, Sediments at proposed LOCO drilling sites, Jour. Geophys. Res., 68, 251-256, 1963.

Ewing, M., and J.I. Ewing, Distribution of oceanic sediments, Studies on Oceanography, Geophysical Institute (Univ. of Tokyo) 525-537, 1964.

Ewing, M., J.L. Worzel, and others, Initial Reports of the Deep Sea Drilling Project, 1, Washington, D.C. (U.S. Government Printing Office) 1969.

Fox, P.J., B.C. Heezen, and A.M. Harian, Abyssal anti-dunes, Nature, 220, 470-472, 1968.

Gibson, T.G., and K.M. Towe, Eocene volcanism and the origin of the Horizon A, Science, 172, 152-154, 1971.

Grow, J.A., and R.G. Markl, IPOD-USGS multichannel seismic reflection profile from Cape Hatteras to the Mid-Atlantic Ridge, Geology, 5, 625-630, 1977.

Heezen, B.C., and R.E. Sheridan, Lower Cretaceous rocks (Neocomian-Albian) dredged from Blake Escarpment, Science, 154, 1644-1647, 1966.

Heezen, B.C., C.D. Hollister, and W.F. Ruddiman, Shaping of the continental rise by deep geostrophic contour currents, Science, 152, 502-508, 1966.

Herman, Y., Origin of deep-sea cherts in the North Atlantic, Nature, 238, 392-393, 1972.

Hollister, C.D., J.I. Ewing, and others, Initial Reports of the Deep Sea Drilling Project, 11, Washington, D.C. (U.S. Government Printing Office) 1972.

Houtz, R., Preliminary study of global sediment sound velocities from sonobuoy data, in Hampton, L. (Ed.), Physics of Sound in Marine Sediments, New York (Plenum Publ. Corp.) 519-535, 1974.

Jansa, L., P. Enos, B.E. Tucholke, F. Gradstein, and R.E. Sheridan, Mesozoic-Cenozoic formations of the North American Basin, western North Atlantic, Am. Geophys. Union, Maurice Ewing Series, 3, (this volume), 1979.

Jacque, M., and M. Thouvenin, Lower Tertiary tuffs and volcanic activity in the North Sea, in Woodland, A.W. (Ed.), Petroleum and the Continental Shelf of Northwest Europe, VI. Geology, London (Applied Science Publ.) 455-465, 1975.

Jones, E.J.W., M. Ewing, J.I. Ewing and S.L. Eittreim, Influences of Norwegian Sea Overflow Water on sedimentation in the northern North Atlantic and Labrador Sea, Jour. Geophys. Res., 75, 1655-1680, 1970.

Khudoley, K.M., and A.A. Meyerhoff, Paleogeography and geological history of Greater Antilles, Geol. Soc. Amer. Mem. 129, 199pp. 1971.

Ladd, J.W., Relative motion of South America with respect to North America and Caribbean tectonics, Geol. Soc. Amer. Bull., 87, 969-976, 1976.

Laine, E., Geological effects of the Gulf Stream system in the North American Basin, unpublished Ph.D. Thesis, Massachusetts Institute of Technology - Woods Hole Oceanographic Institution, W.H.O.I. Ref. No. 78-7, 1978.

Lancelot, Y., J.C. Hathaway, and C.D. Hollister, Lithology of sediments from the Western North Atlantic Leg 11 Deep Sea Drilling Project, in Hollister, C.D., J.I. Ewing, and others, Initial Reports of the Deep Sea Drilling Project, 11, Washington, D.C. (U.S. Government Printing Office) 901-949, 1972.

Lancelot, Y., E. Seibold, and others, Initial Reports of the Deep Sea Drilling Project, 41, Washington, D.C. (U. S. Government Printing Office) 1978.

Margolis, S.V., Cenozoic and Late Mesozoic paleotemperature and paleoglacial history contained in circum-Antarctic deep-sea sediments, 25th Int. Geol. Congr. Abstracts, 3, 885-886, 1976.

Markl, R.G., G.M. Bryan, and J.I. Ewing, Structure of the Blake-Bahama Outer Ridge, Jour. Geophys. Res., 75, 4539-4555, 1970.

Mattson, P.H. and E.A. Pessagno, Jr., Caribbean Eocene volcanism and the extent of Horizon A, Science, 174, 138-139, 1971.

Meyerhoff, A.A., and C.W. Hatten, Bahamas salient of North America, in Burk, C.A., and C.L. Drake (eds.), The Geology of Continental Margins, New York (Springer-Verlag) 429-446, 1974.

Montadert, L., D.G. Roberts and others, Glomar Challenger Sails on Leg 48, Geotimes, 21(12), 19-23, 1976.

Mountain, G.S., and B.E. Tucholke, Horizon β: Acoustic character and distribution in the western North Atlantic (abs.), Trans. Am. Geophys. Union, 58, 406, 1977.

Parsons, M.G., The geology of the Laurentian Fan and the Scotia Rise, in Yorath, C.J., and others (eds.), Canada's Continental Margins and Offshore Petroleum Exploration, Can. Soc. Petrol. Geol. Mem. 4, 155-167, 1975.

Peterson, M.N.A., N.T. Edgar, and others, Initial Reports of the Deep Sea Drilling Project, 2, Washington, D.C. (U.S. Government Printing Office) 1970.

Pitman, W.C. III, and M. Talwani, Sea-floor spreading in the North Atlantic, Geol. Soc. America Bull., 83, 619-646, 1972.

Pitman, W.C. III, Relationship between eustacy and stratigraphic sequences of passive margins, Geol. Soc. Am. Bull., 89, 1389-1403, 1978.

Rabinowitz, P.D. and G.M. Purdy, The Kane Fracture Zone in the western central Atlantic Ocean, Earth and Planet. Sci. Letters, 33, 21-26, 1976.

Ramsay, A.T.S., Occurrence of biogenic siliceous sediments in the Atlantic Ocean, Nature, 233, 115-117, 1971.

Reynolds, P.H., and F. Aumento, Deep Drill 1972. Potassium-argon dating of the Bermuda drill core, Can. Jour. Earth Sci., 11, 1269-1273, 1974.

Rona, P.A., Linear "lower continental rise hills" off Cape Hatteras, Jour. Sed. Petrol., 39, 1132-1141, 1969.

Ryan, W.B.F., M.B. Cita, E.L. Miller, D. Hanselman, W.D. Nesterhoff, B. Hecker and M. Nibbelink, Bedrock geology in New England submarine canyons, Oceanologica Acta, 1, 233-254. 1978.

Saito, T., L.H. Burckle, and M. Ewing, Lithology and paleontology of the reflective layer Horizon A, Science, 154, 1173-1176, 1966.

Savin, S.M., R.G. Douglas, and F.G. Stehli, Tertiary marine paleotemperatures, Geol. Soc. Amer. Bull., 86, 1499-1510, 1975.

Schouten, H., and K. Klitgord, Map showing Mesozoic magnetic anomalies, western North Atlantic, U.S. Geol. Survey Misc. Field Studies, Map MF-915, 1977.

Sheridan, R.E., J.D. Smith, and J. Gardner, Rock dredges from Blake Escarpment near Great Abaco Canyon, Am. Assoc. Petrol. Geol. Bull., 53, 2551-2558, 1969.

Shipley, T.H., Sedimentation and echo character in the abyssal hills of the west-central North Atlantic, Geol. Soc. Amer. Bull., 89, 397-408, 1978.

Shipley, T.H., R.T. Buffler, and J.S. Watkins, Seismic stratigraphy and geologic history of Blake Plateau and adjacent western Atlantic continental margin, Am. Assoc. Petrol. Geol. Bull., 62, 792-812, 1978.

Supko, P.R., K. Perch-Nielsen, and others, Initial Reports of the Deep Sea Drilling Project, 39, Washington, D.C. (U.S. Government Printing Office) 1977.

Sverdrup, H.U., M.W. Johnson, and R.H. Fleming, The Oceans, Englewood Cliffs (Prentice-Hall) 1942.

Talwani, M., G. Udintsev, and others, Initial Reports of the Deep Sea Drilling Project, 38, Washington, D.C. (U.S. Government Printing Office) 1976.

Tracey, J.I. Jr., G.H. Sutton, and others, Initial Reports of the Deep Sea Drilling Project, 8, Washington, D.C. (U.S. Government Printing Office) 1971.

Tucholke, B.E., Jurassic to Recent lithofacies and acoustic facies in the western North Atlantic basin (abs.), Geol. Soc. Amer. Abs. with Prog., 8, 1147-1148, 1976.

Tucholke, B.E., Relationships between acoustic stratigraphy and lithostratigraphy in the western North Atlantic basin, in Tucholke, B.E., Vogt, P.R., and others, Initial Reports of the Deep Sea Drilling Project, 43, Washington, D.C. (U.S. Government Printing Office), in press, 1979.

Tucholke, B.E. and J.I. Ewing, Bathymetry and sediment geometry of the Greater Antilles Outer Ridge and vicinity, Geol. Soc. Amer. Bull., 85, 1789-1802, 1974.

Tucholke, B.E., and G.S. Mountain, The Horizon-A complex: lithostratigraphic correlation and paleoceanographic significance of reflectors in the western North Atlantic (abs.), Trans. Am. Geophys. Union, 58, 406, 1977a.

Tucholke, B.E., and G.S. Mountain, Depositional patterns and depositional environment of Cretaceous black clays in the western North Atlantic (abs.), Geol. Soc. Am. Abs. with Prog., 9, 1207, 1977b.

Tucholke, B.E., and P.R. Vogt, Western North Atlantic: Sedimentary evolution and aspects

of tectonic history, in Tucholke, B.E., P.R. Vogt, and others, Initial Reports of the Deep Sea Drilling Project, 43, Washington, D.C. (U.S. Government Printing Office), in press, 1979.

Tucholke, B.E., P.R. Vogt, and others, Initial Reports of the Deep Sea Drilling Project, 43, Washington, D.C. (U.S. Government Printing Office), in press, 1979.

Uchupi, E., Bathymetric atlas of the Atlantic, Caribbean and Gulf of Mexico: Woods Hole Oceanographic Inst. Ref. No. 71-72, (unpublished manuscript), 1971.

Vail, P.R., R.M. Mitchum,Jr., and S. Thompson III, Global cycles of relative changes of sea level, in Payton, C.E. (Ed.) Seismic Stratigraphy-Application to Hydrocarbon Exploration, Am. Assoc. Petrol. Geol. Mem. 26, 83-97, 1977.

Windisch, C.C., R.J. Leyden, J.L. Worzel, T. Saito, and J. Ewing, Investigation of Horizon β, Science. 162, 1473-1479, 1968.

# EVOLUTION OF THE ATLANTIC CONTINENTAL MARGIN OF THE UNITED STATES

by David W. Folger, William P. Dillon, John A. Grow, Kim D. Klitgord, John S. Schlee

U. S. Geological Survey, Office of Marine Geology,
Woods Hole, Massachusetts 02543

Abstract. Since latest Triassic time, sediments have been accumulating on subsiding continental, transitional, and oceanic crust. The Continental Rise lies on oceanic basement that can be traced by its characteristic hyperbolic acoustic signature and weak lineated magnetic anomalies from the deep sea across the Jurassic magnetic quiet zone as far landward as the East Coast Magnetic Anomaly (ECMA). Fracture zones delineated in the oceanic basement are aligned with displacements in the edge of the adjacent continental crust which appear to control, in part, the geometry of the four major structural basins that underlie the continental margin landward of the ECMA. Transition zones between basins and platforms are often defined by the disruption of gravity and magnetic anomaly trends which parallel the margin. Broad, weak, free-air gravity anomaly lows and long-wavelength, low-amplitude magnetic anomalies characterize these basins while weak gravity highs and high amplitude short wavelength magnetic anomalies are more typical over the intervening platforms.

Following separation of North America from Africa in the Late Triassic and earliest Jurassic, sediments accumulated rapidly on rifted and thinned continental and/or transitional crust, but more slowly on oceanic crust seaward of the ECMA. During Late Cretaceous and Tertiary, subsidence slowed and tectonism was limited to regional warping and minor faulting. As much as 10 km of total sediment were deposited in the Georges Bank basin, 14 km in the Baltimore Canyon Trough, 8 km in the Southeast Georgia Embayment, and 12 km in the Blake Plateau. Upper Triassic and Lower Jurassic continental beds and some evaporite deposits gave way to carbonate deposits of Late Jurassic to Early Cretaceous age; marine sands and clays prograded during the remainder of the Cretaceous. In the early Tertiary, Blake Plateau sedimentation ended or slowed owing to initiation of stronger Gulf Stream flow; off New Jersey and New England, limited deltaic deposition occurred. The shelf edge has shifted 20–30 km landward of the Cretaceous shelf edge, apparently in response to numerous sea level lowerings which may have started in the early Tertiary and culminated in Pliocene and Pleistocene time. Of greatest petroleum potential in the sedimentary basins are traps associated with intrusions, carbonate reefs and banks, pinchouts in the transgressional wedge, drape structures over deeply buried fault blocks, and a few diapirs.

## Introduction

The U. S. Geological Survey has been collecting geological and geophysical data on the Atlantic and Gulf coast continental margins of the United States since 1962. The first six years of this effort involved mainly the mapping of bathymetry, sediment characteristics, and shallow stratigraphy based on single-channel seismic profiles (see Emery and Uchupi, 1972). By 1968 the sediments on the Atlantic shelf had been sampled on a 10-km spacing (Hathaway, 1971) and seismic surveys completed on a 50–75 km spacing. These studies provided an excellent picture of the regional shallow stratigraphy and surficial sediment texture and mineralogy, but were not adequate to assess deep structure and stratigraphy nor to evaluate important environmental phenomena such as sediment dynamics and geotechnical properties.

Partly in response to leasing initiatives, in 1973 new studies were undertaken of the environmental hazards on the Outer Continental Shelf of the Gulf of Mexico and of the resource potential and environmental hazards on the Atlantic Outer Continental Shelf. The new data have included gravity, magnetic, and multichannel seismic

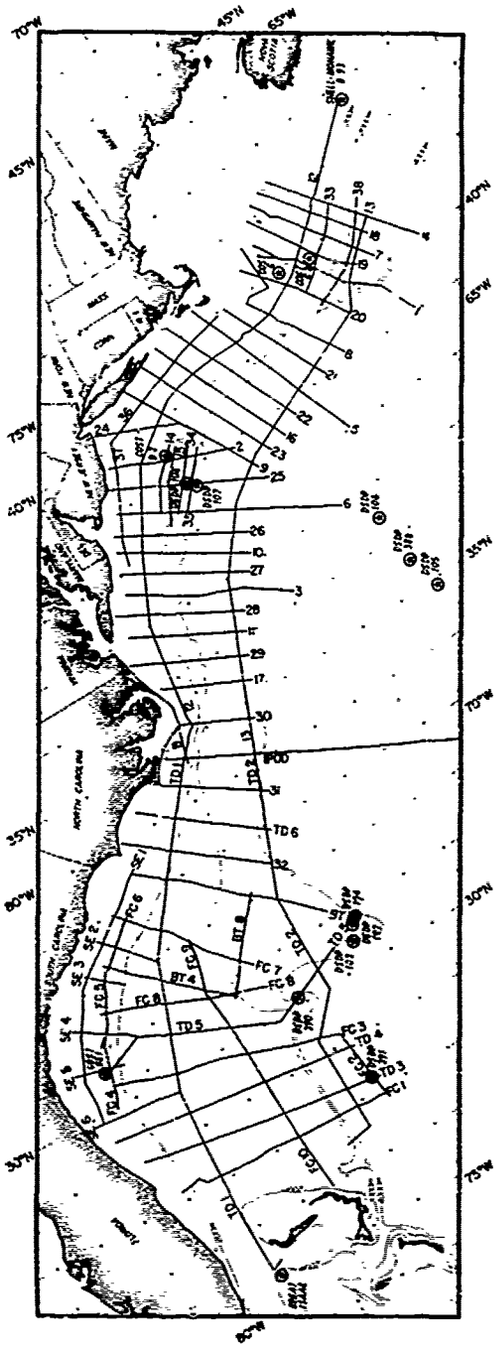

Fig. 1. Tracks along which multichannel seismic data have been collected for the U. S. Geological Survey between 1973 and 1978.

profiles; sediment cores as much as 300-m long; suspended sediment concentrations; and bottom current measurements. This paper presents only those data that provide new information on the structural and stratigraphic evolution of the Atlantic continental margin.

The Atlantic continental margin of the United States is one of the most extensively studied areas of the world. Sediments were sampled in the 19th century (Pourtales, 1872) and some of the earliest marine geophysical surveys were carried out off the mid-Atlantic states (Ewing and others, 1937, 1938, 1940). By the 1950's, syntheses of seismic refraction measurements revealed thick (5 km) sedimentary prisms beneath the shelf that had compressional velocities <4.5 km/s; underlying rocks that had velocities >5.3 km/s were interpreted to be basement (Ewing and Press, 1950; Ewing and Ewing, 1959; Drake and others, 1959). In a classic paper, Drake, Ewing, and Sutton (1959) equated two sedimentary troughs, one beneath the Shelf and another beneath the upper Continental Rise, off the Atlantic margin with the mio- and eugeosynclines of Stille (1936, 1941) and Kay (1951).

Subsequently, single channel seismic reflection profiles (Emery and Uchupi, 1972) revealed horizons on the Continental Slope where water-bottom multiple problems were not as severe as on the Continental Shelf. From these and other data, the high velocities near the Shelf edge in the early refraction studies were reinterpreted and attributed to carbonate rocks (Emery and Uchupi, 1972; Sheridan, 1974; Mattick and others, 1974, 1976a; Schlee and others, 1976, 1977; Grow and others, 1978) instead of basement.

The first Common Depth Point (CDP) seismic reflection profiles to be released to the public were contracted by the U. S. Geological Survey on the Atlantic margin. They revealed that the sedimentary trough beneath the Shelf contained more than 12 km of sediment and the trough beneath the Continental Rise contained less than 8 km of sediment (Schlee and others, 1976; Grow and others, 1978). The troughs were similar in outline to those described by Drake and others (1959) but the CDP profiles showed that the thicker section lay under the Shelf and not under the Slope as previously suggested. The troughs were separated by an acoustically-opaque zone at 3-6 km depth (Behrendt and others, 1974; Schlee and others, 1976; Grow and others, 1979).

Early aeromagnetic and shipboard geomagnetic surveys over the Atlantic continental margin revealed a prominent positive anomaly along the Outer Shelf and Slope which is known as the East Coast Magnetic Anomaly (Keller and others, 1954; Drake and others, 1963; Taylor and others, 1968). Taylor and others (1968) constructed a 100 nT contour magnetic anomaly map of the Atlantic margin which suggested that basement is shallow under the Inner Shelf but is much deeper under the Outer Shelf and Continental Rise. They also inferred that the East Coast Magnetic Anomaly was caused by a vertical intrusive body about 30-km wide only 7 km beneath the Outer Shelf and upper Slope.

Early gravity measurements along the U. S. Atlantic margin were made by means of pendulum systems aboard submarines (Worzel and Shurbet,

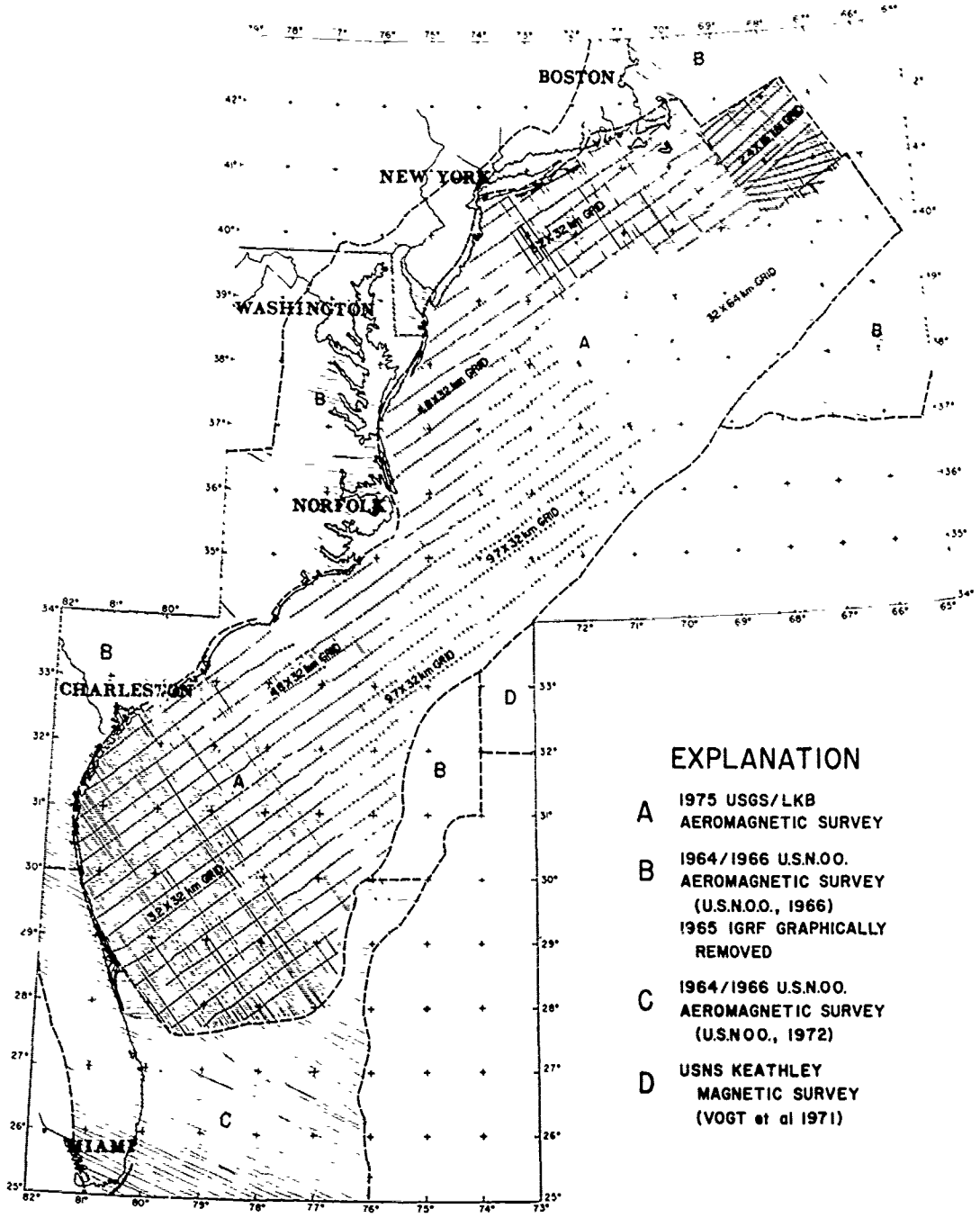


Fig. 2. Tracks along which aeromagnetic data were collected by LKB Resources, Inc. for the U. S. Geological Survey (from Klitgord and Behrendt, 1979).

1955; Worzel, 1965). By the late 1960's, improved surface ship gravimeters increased the quality and quantity of the data collected. Free air gravity anomaly maps of the Atlantic continental margin were published by Emery and others (1970) and Rabinowitz (1974) at contour intervals of 20 and 25 mgal. More recently, U. S. Navy and U. S. Geological Survey data have been compiled to provide a free air gravity anomaly map contoured at an interval of 10 mgal (Grow and others, 1976, in press; Grow and Bowin, 1977; Ewing, 1978).

In addition to these extensive geophysical investigations, several drilling, coring, and dredging programs have provided geological samples

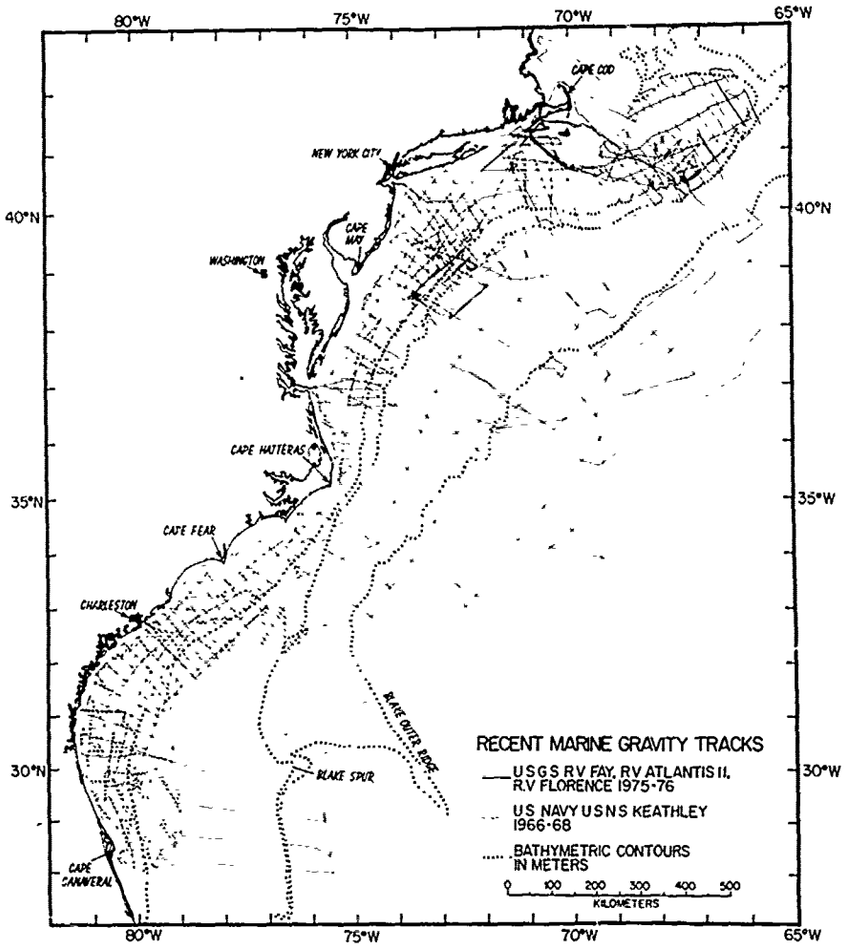


Fig. 3. Tracks along which gravity data have been collected by the U. S. Geological Survey during 1975 and 1976 and by the U. S. Navy between 1966 and 1968 (Grow and Bowin, 1977; Grow and others, in press).

from this region. Published stratigraphic and paleoecologic information includes a study of the COST B-2 well (Scholle, 1977; Poag, 1978); deep-sea drilling sites (JOIDES, 1967; Hollister, Ewing and others, 1972); the Atlantic Slope Project (ASP) of Exxon, Mobil, and Chevron Oil Companies (Poag, 1978); the USGS Atlantic Margin Coring Program (Hathaway and others, 1976; Poag. 1978); dredge hauls from submarine canyons (Stetson, 1936, 1949; Heezen and Sheridan, 1966); and samples collected from submersibles (Gibson and others, 1968; see Weed and others, 1974; Ryan and others, 1978; Valentine, 1978).

## Methods of Investigation

### Common Depth Point (CDP) Seismic Profiles

We now have 20,000 km of CDP profiles collected from 1973 through 1978 (Fig. 1). This gives us a cross-shelf line spacing of about 40 km; in addition, one long line extends continuously along the Shelf from Nova Scotia to the Bahamas, another lies along the base of the Continental Slope from Georges Bank to the Blake basin, and several other short lines parallel the Shelf edge.

Although most of the CDP data presented have been acquired and processed by contract geophysical companies, some of the lines in the Blake Plateau area were obtained in cooperation with the University of Texas and the Institut Français du Petrole. Most data were collected with an array of air guns (volume: 1400-2200 $in^3$ at 1800-2000 psi) fired simultaneously every 50 m; returning signals were received by a 24- to 48-group (50- and 100-m spacing) hydrophone array 2.4 to 3.6 km long. Data were recorded on a 48-channel tape recorder and a single channel analog recorder. Tapes were processed to include true amplitude recovery, normal move-out correction, common depth point gather,

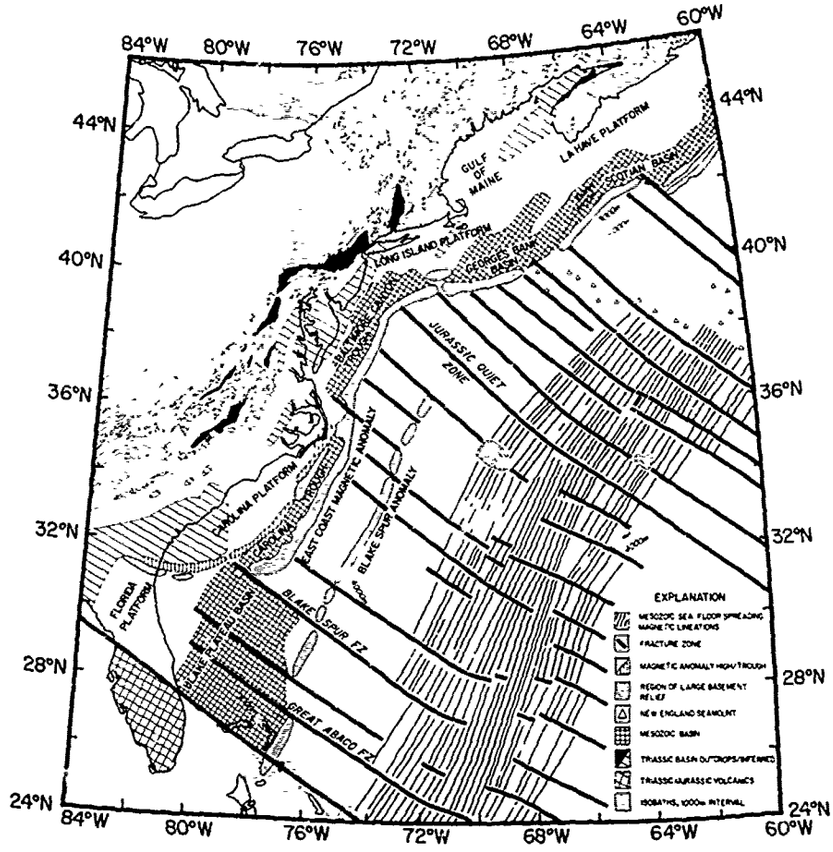


Fig. 4. The major structural elements on the Atlantic continental margin with fracture zones and magnetic anomalies depicted offshore and the distribution of basins and platforms along the margin (from Klitgord and Behrendt, 1979).

velocity analysis, CDP stack and time variant filtering, and horizontal stack.

## Geomagnetic Profiles

A new 185,000 km high-sensitivity aeromagnetic survey (Fig. 2) was acquired through contract in 1975 with LKB Resources, Inc. It was combined with aeromagnetic data collected in 1964-66 by the U. S. Naval Oceanographic Office (published in 1966 and 1972) and with surface ship data published by Vogt and others in 1971. The summarized data have been interpreted by Klitgord and Behrendt (1979). Magnetic anomaly maps were compiled at a scale of 1:250,000 with a contour interval of 2 nT by LKB Resources, Inc. and at a scale of 1:1,000,000 with a contour interval of 50 nT by Klitgord and Behrendt (1977).

The depth-to-basement maps (Klitgord and Behrendt, 1979) and parts of the geologic cross sections presented in this paper are based on depth-to-source estimates derived from a Werner deconvolution-type method (Hartman and others, 1971; Jain, 1976) which assumes that the magnetic sources are either two dimensional dikes or edges of rock bodies. Generally, sediments within a basin have weaker susceptibilities than basement; therefore, the sources of major magnetic anomalies are interpreted to be basement structures, magnetic susceptibility variations within basement rocks, or volcanic rocks within basement or the overlying sediment column. Methods for estimating magnetic source depths require assumptions about the sources. In the interpretations presented, seismic reflection and refraction profiles and borehole data have been used to limit these assumptions and thereby to increase the reliability of the depth estimates.

## Gravity Measurements

During 1975 and 1976, approximately 39,000 km of new gravity data were obtained along the U. S. Atlantic margin on USGS cruises using the Woods

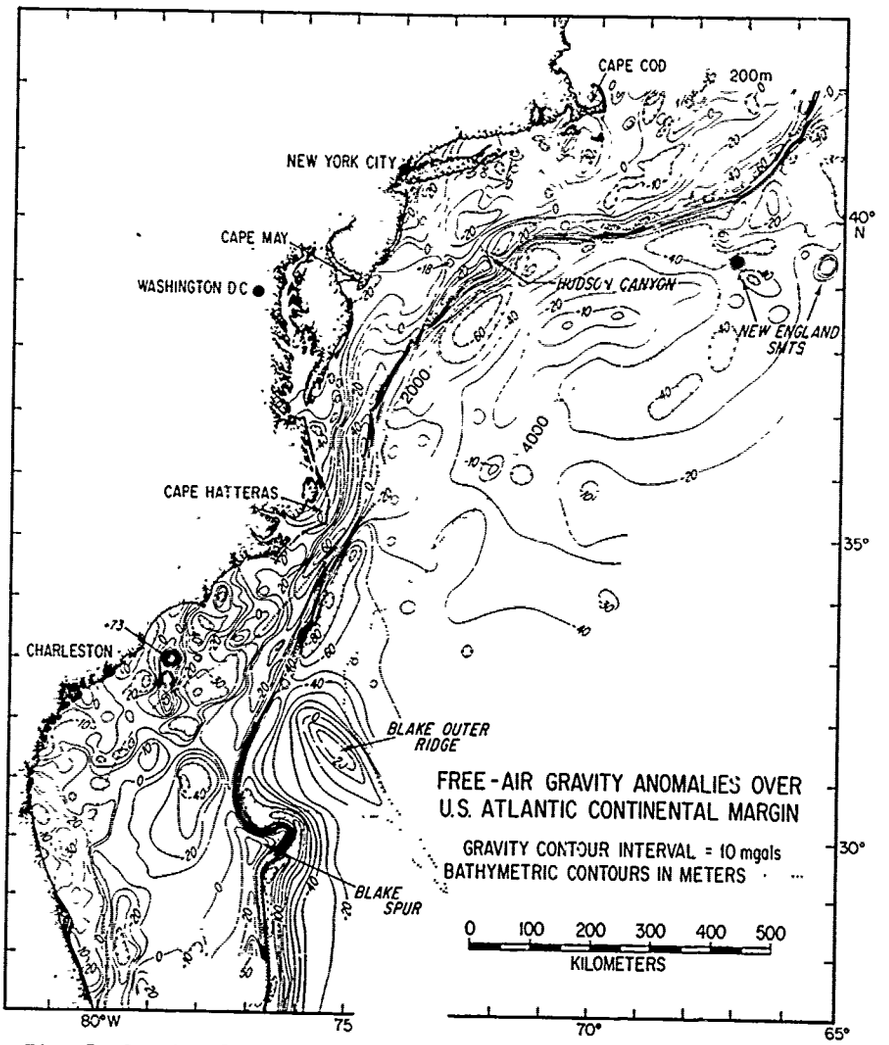


Fig. 5. Gravity field over the U. S. Atlantic continental margin (from Grow and others, in press). Prepared from U. S. Geological Survey and U. S. Navy data (Fig. 3) plus previous data from Emery and others (1970) and Rabinowitz (1974).

Hole Oceanographic Institution's vibrating-string sea gravimeter (Bowin and others, 1972) (Fig. 3). Navigation used satellite and Loran-C systems for positioning; velocity was measured by a combination of doppler sonar, range-range Loran-C, and Chesapeake Speed Log. The root-mean-square of the line cross errors for these cruises are less than 2-1/2 mgal, and the data are satisfactory for contouring at a 10 mgal interval. These data were combined with recently declassified U. S. Navy data and previously published data to provide a preliminary map north of 36°N (Grow and others, 1976); and a revised free-air anomaly map of the entire margin from northern Florida to Maine at a 10-mgal contour interval has been prepared by Grow and others (in press).

## Results of Investigations

### Overview

We now have enough data to recognize the major structural elements of the U. S. Atlantic margin and to construct diagrammatic cross sections of the major basins and platforms. High quality deep seismic reflection data have reduced ambiguities in the interpretation of gravity and magnetic data and conversely, where CDP data are weak, as at the Shelf edge, aeromagnetic data have strengthened the interpretation. Nevertheless, integration of such extensive geophysical measurements is only beginning; thus, this paper is an initial attempt to review it briefly in one place.

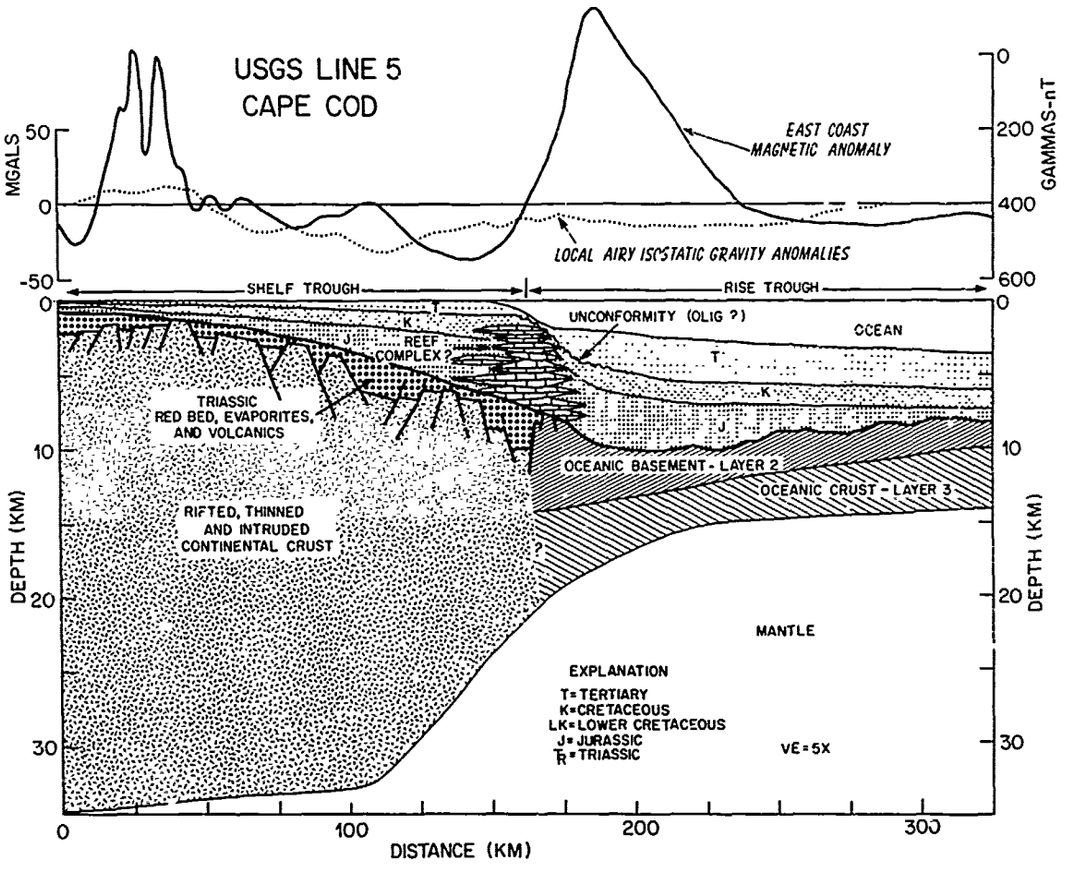


Fig. 6. Interpretative cross section along CDP Line 5 southeast of Cape Cod across the northeastern part of the Long Island platform (0 to 75 km distance) and the southwestern end of the Georges Bank basin (75 to 175 km distance). Line 5 is unique in that the top of oceanic basement can be clearly traced to a depth of 10 km at the axis of the East Coast Magnetic Anomaly (Grow and others, 1979). The Moho configuration is based on gravity modeling (Grow and others, in press).

Clearly, the drilling presently underway in the Baltimore Canyon Trough (Fig. 4) and the Southeast Georgia Embayment will provide a more solid geologic basis for interpretations which now include only the limited core data provided by two Continental Offshore Stratigraphic Test (COST) wells, B-2 and GE-1 (Fig. 1) (Smith and others, 1976; Scholle, 1977) and from 39 shallow (~300 m) stratigraphic holes drilled between 1965 and 1976 (Bunce and others, 1965; Hathaway and others, 1976; Poag, 1978). Data from the two COST wells drilled on Georges Bank (Fig. 1) have not been released at the time of this writing and hence are not available for our interpretation.

The major structural elements of basins, platforms, and fracture zones for the Atlantic continental margin (Klitgord and Behrendt, 1979) are summarized in Figure 4. In solid black are basins that contain exposed red beds and volcanic rocks of probable Triassic and Jurassic age. Extensions of these basins seaward and the presence of other buried Triassic and Jurassic(?) basins have been inferred from magnetic and drillhole data. For example, at Nantucket recent USGS drilling has revealed basalt flows at 459 m below sea level that have a minimum age of 183 ±6 m.y. (Folger and others, 1978). Similar basalts drilled by the USGS near Charleston, S.C., have been dated at 162-204 m.y. (Gohn and others, 1978). The major platforms of shallow pre-Jurassic continental crust along the margin border the syntectonic and post-rift basins that are filled mainly with Mesozoic sediments. These basins are, in order from north to south, the Georges Bank basin, the Baltimore Canyon Trough, the Carolina trough, and the Blake Plateau basin (Fig. 4).

The seaward margin of the Mesozoic shelf basins north of 32°N latitude (Fig. 4) is marked by the

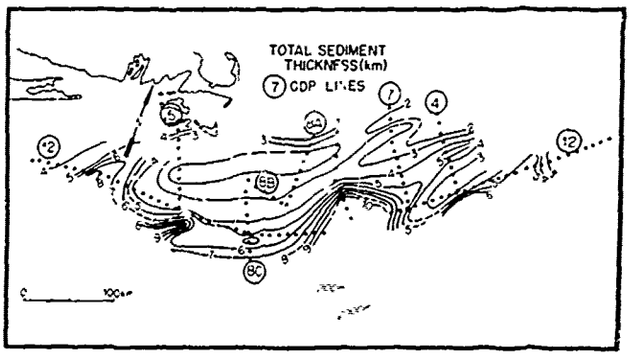


Fig. 7. Isopach map of total sediment overlying basement in the Georges Bank area based on CDP seismic data (from Schlee and others, 1977).

East Coast Magnetic Anomaly (Klitgord and Behrendt, 1979). Most authors (Sheridan, 1974; Mayhew, 1974; Rabinowitz, 1974; Schlee and others, 1976; Grow and Schlee, 1976; Grow and others, 1978) believe that beneath the shelf basins, basement is composed of faulted and thinned blocks of continental(?) crust. Seaward of the ECMA, the seismic-reflection and refraction data and long lineated magnetic anomalies indicate typical oceanic crust (Mayhew, 1974; Schlee and others, 1976; Klitgord and Behrendt, 1977; Sheridan and others, in press). In general, the seismic data indicate a greater depth to basement on the landward side of the ECMA than on the seaward side. Numerous >10-km magnetic depth estimates just landward of the ECMA and a set of 6-8 km depth estimates along the ECMA suggest a basement high in the region. The susceptibility contrasts associated with the shallow (6-8 km) depth estimates suggest that their source is most likely a basement high with a susceptibility contrast >10 X $10^{-4}$ (C.G.S. units) associated with the landward edge of this oceanic crust. The seismic profiles usually do not show coherent reflections deeper than 3-6 km in the vicinity of the magnetic basement high; but in most cases above these highs, a disturbed, acoustically-incoherent zone has been interpreted as carbonate rocks (Schlee and others, 1976; Grow and others, 1978). On the other hand, reflections off oceanic basement can usually be detected to within 50 to 75 km of the ECMA; for example, on CDP Line 5 off Cape Cod (Figs. 1 and 6), oceanic basement was traced to the ECMA where it terminates at a depth of about 10 km (Grow and others, 1979). Thus the ECMA marks the seaward margin of the Mesozoic basins and probably the landward margin of the oceanic crust.

The orientation of fracture zones (Fig. 4) has been determined from the offsets of sea floor spreading anomalies seaward of the Mesozoic quiet zone (Schouten and Klitgord, 1977) and the projection of these fracture zones across the Jurassic quiet zone using the basement relief which clearly marks the trends of the fracture zones (Klitgord and Schouten, 1977). The horizontal offsets in the edge of continental crust, which resulted from the initial rifting of North America from Africa in Early Jurassic, were propagated in the oceanic crust as transform faults which are now preserved in the offshore fracture zone pattern.

A 10-mgal gravity anomaly map (Fig. 5) of the U. S. Atlantic margin has been prepared from recent U. S. Navy and USGS data (Fig. 3) supplemented by earlier data, mainly from the Lamont-Doherty Geological Observatory of Columbia University and the Woods Hole Oceanographic Institution (Grow and others, in press). The most prominent free-air gravity anomalies at continental margins are usually positive along the Shelf edge and negative along the base of the Slope. This is due largely to the edge effects of the changing topography and changing depth to the crust-mantle boundary. However, free-air values change significantly along the length of the U. S. margin and correlate with transitions between shelf basins and platforms and with fracture zones mapped in the oceanic crust (Fig. 4).

The major shelf basins (Fig. 4) are characterized by broad, free-air anomaly gravity lows, usually ranging from 0 to -30 mgal. Areas such as the Cape Cod and Cape Hatteras parts of the Long Island and Carolina platforms are characterized by positive free-air anomalies, usually between 0 and +30 mgal.

The free-air anomaly minimum along the base of the Continental Slope changes abruptly at several locations along the margin. In some cases the free-air positive of the Shelf edge and the negative along the Slope both increase or decrease by 20-30 mgal along strike over a distance of 50 km. The most impressive examples of these abrupt transitions are at the Blake Spur fracture zone, east of Cape Hatteras, near Norfolk Canyon, off Delaware Bay, and south of Cape Cod. The change in free-air anomaly values along strike reflects, in part, significant differences in width and depth of the sedimentary basins and the depth of Moho underlying the crustal blocks. The fact that these abrupt transitions of the Shelf edge positive and the Slope minimums are often concurrent, and

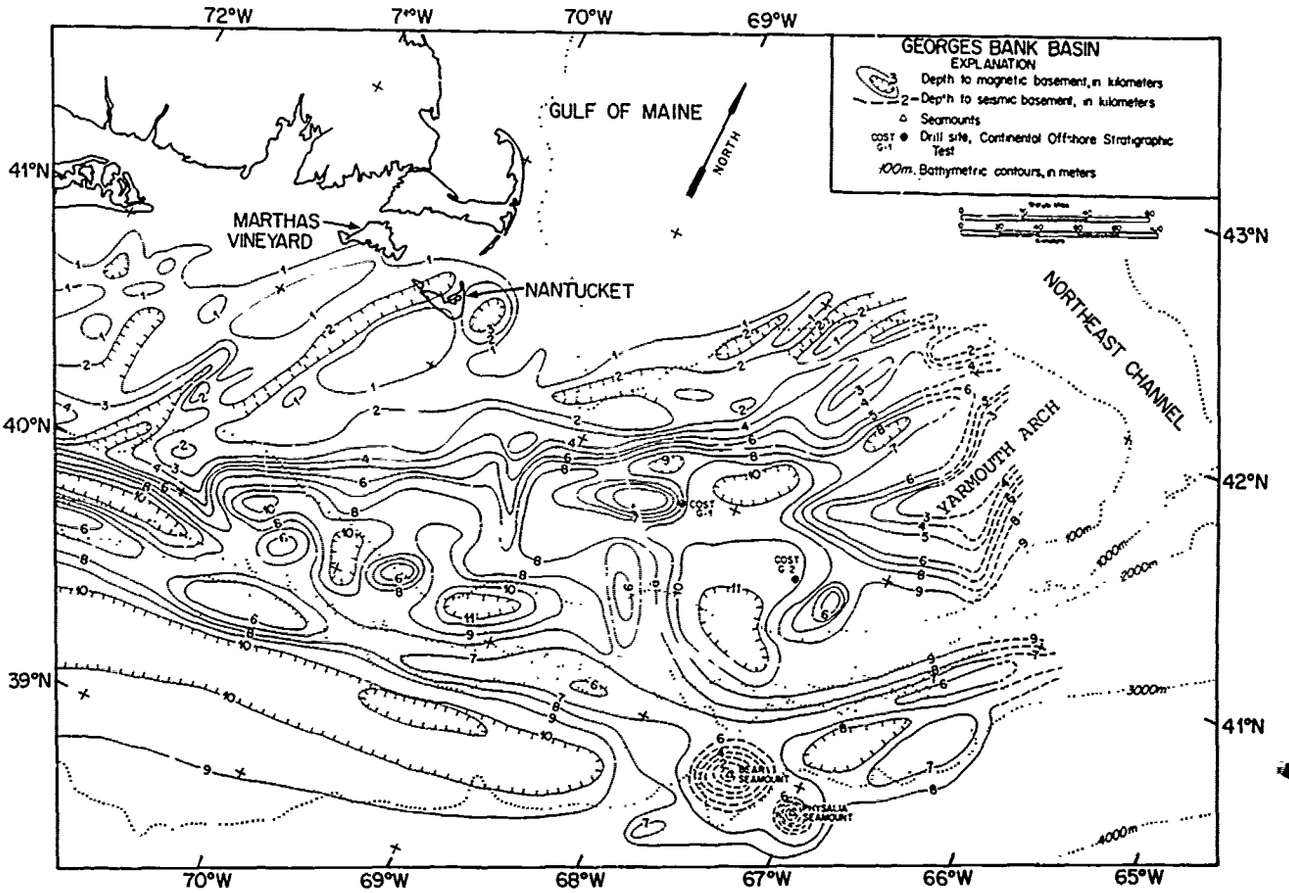


Fig. 8. Depth to basement in the Georges Bank basin based on magnetic depth-to-basement estimates (from Klitgord and Behrendt, 1979).

the fact that they correlate with the early oceanic fracture zones suggest that both the basin distribution and the fracture zones are related to the adjacent continental and transitional crustal blocks beneath the Shelf. A more detailed discussion of the free air anomalies, isostatic anomaly profiles, and several two-dimensional gravity models along multichannel seismic Lines 5 and 6 are given by Grow and others (in press).

The integration of all our geophysical data is depicted in schematics of the crust across the Atlantic continental margin (Grow and others, 1979) and is illustrated by Figure 6. The computations for isostatic anomalies shown in this figure include an assumed water layer density of 1.03 g/cc and a crustal density of 2.7 g/cc, a mantle density of 3.3 g/cc, and a depth of compensation of 30 km at the shoreline. We have ignored sediment corrections which Rabinowitz suggests (1974) are small and do not change the isostatic anomaly greatly.

The stratigraphic system and series boundaries shown within the sedimentary rocks are based on tentative correlations with bore holes to the south (COST B-2) and to the north (Shell-Mohawk B-93, Fig. 1), and on the character of the reflectors. We infer facies changes from the interval velocities, from extrapolation of bore hole data, and from exposures on land, i.e., Triassic basins. The sediment/basement interface is derived from CDP, magnetic, and gravity data. The oceanic crustal layer and mantle boundaries have been determined by seismic refraction data near CDP Lines 2 and 6 off New Jersey (Sheridan and others, in press). The depth to Moho inferred along CDP Lines 5, 6, and IPOD are in agreement with gravity models off Cape Cod and Cape Hatteras (Grow and others, 1979).

## Georges Bank Basin

The structural complexity of the basement underlying Georges Bank is revealed by an isopach map of total sediment thickness based on CDP data (Fig. 7; from Schlee and others, 1977) and a depth-to-magnetic-basement map (Fig. 8; from Klitgord and Behrendt, 1979). On CDP profiles, acoustic basement is lost near the Shelf edge, but the magnetic data indicate that the basement ridge present beneath the ECMA is as shallow as ~6 km below sea level seaward of the basin axis. Within Georges

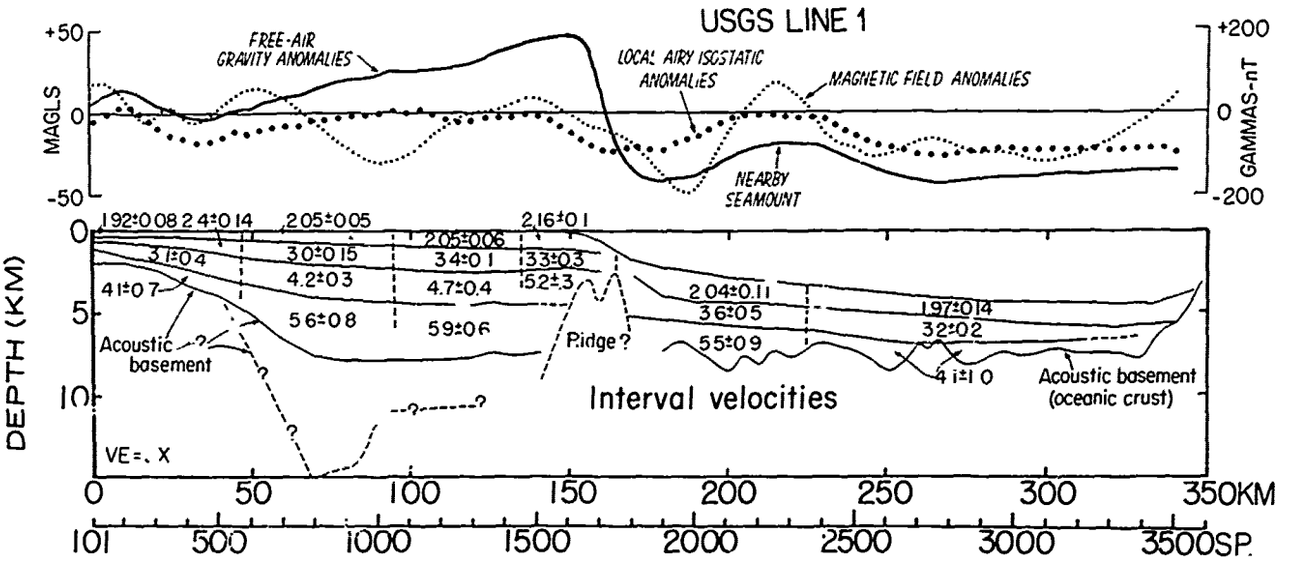


Fig. 9. Cross sections showing seismic interval velocities for CDP seismic Line 1 across the Georges Bank basin (modified from Schlee and others, 1976).

Bank basin, coherent seismic reflectors can be seen only to depths of 7 km (Schlee and others, 1976), but weak reflectors below 7 km combined with magnetic depth solutions indicate that the sedimentary rocks within the Triassic grabens may extend to a depth of 10 to 12 km. Sediments thin to the northeast over block-faulted basement that rise to form the La Have platform. To the northwest, thinning occurs in a somewhat simpler manner on the Long Island platform.

Interpretations of CDP Line 1 (Figs. 1 and 9) across the Georges Bank basin suggests that velocities increase laterally (in a seaward direction) as well as vertically as depth increases. Nearshore, velocities increase with depth from 1.9 km/s (typical of poorly consolidated sand and shales) to 4.1 km/s (typical of consolidated sands and shales. In the basin, they increase from 2.05 km/s (typical of consolidated sands, shales, and carbonate rocks) in the upper kilometer to 5.9 km/s at depth (typical of indurated limestones or dolomites). Seismic refraction data near the seaward edge of Georges Bank also reveal velocities of 5.0 km/s at depths of 1.8 km (Drake and others, 1959; Jaworski and others, 1976). Reflectors along this line are diffuse at the Shelf edge and cannot be traced under the upper Slope. On the basis of these velocities, limited dredge data (Verrill, 1878; Agassiz, 1888; Cushman, 1936; Stetson, 1936, 1949), and submersible observations (Ryan and others, 1978), a lithostratigraphic section has been constructed (Fig. 10).

We have interpreted the high velocities near the Shelf edge as representative of a carbonate bank or reef similar to the one described by Jansa and Wade (1975) and by Given (1977) to the north under the Scotian Shelf, and also inferred off northwest Africa (Bhat and others, 1975). The carbonate platform probably is of Middle Jurassic to Early Cretaceous age (Schlee and others, 1976; Uchupi and others, 1977; Ryan and others, 1978; Poag, 1978). The 5.6-5.9 km/s interval velocity layer indicates that massive carbonate deposits extended across all of Georges Bank during Middle Jurassic time; but the 5.2 km/s zone indicates that carbonate deposits were restricted to the Shelf edge during Late Jurassic and Early Cretaceous time. The section is underlain by probable Triassic and Lower Jurassic red beds and volcanic rocks, and is overlain by a prism of post-Jurassic clastic rocks that is as much as 3-km thick (7-10 km deep?). Thus, the section is similar to, but much thicker than, the one penetrated by the Shell-Mohawk well on the La Have platform (Figs. 1 and 4).

## Long Island Platform

The Long Island platform (Fig. 4) is one of several regions of shallow continental crust buried by only a thin layer of sediments and which lie just landward of the sediment basins. The interpretive section for CDP Line 5 (Fig. 6) crosses the northeastern end of the Long Island platform. Isostatic anomalies along the line of section are low and imply isostatic equilibrium. We infer that the thin sediment cover on the landward part of the profile lies upon nearly normal continental crust, whereas farther seaward, at distances of 100-170 km from the coast (Fig. 6), the continental crust underlying the outer shelf sediments thins gradually to less than 15 km near the ECMA (Grow and others, in press).

The top of oceanic crust can be traced clearly beneath the Continental Rise to a depth of 10 km directly beneath the axis of the ECMA (Grow and others, 1979). The rise of oceanic basement to a

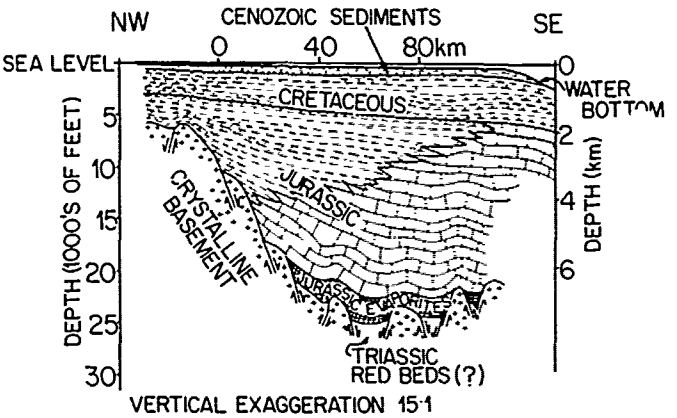


Fig. 10. Cross section showing a thick section of Jurassic and Cretaceous sediment overlying Triassic and Jurassic red beds(?) and faulted crystalline basement (from Schlee, 1978b).

depth of 8 km is inferred from the magnetic depth-to-basement estimates (Klitgord and Behrendt, 1979). This seismic line establishes the clearest correlation between the most landward identifiable oceanic basement and the axis of the high magnetic anomaly (600 nT) that characterizes the ECMA. This line also defines one of the narrowest zones (70 km) of thin continental crust (transitional crust) presently known along the margin.

Baltimore Canyon Trough

A diagrammatic cross section (Fig. 11) along CDP Line 2 (Fig. 1) suggests that the northern part of the Baltimore Canyon Trough is probably built across a zone of rifted, thinned, continental crust (or transitional crust) that lies landward of the thickened edge of oceanic crust (source of the ECMA). The sediments that fill the trough have been penetrated and uplifted by a mafic intrusion of probable Early Cretaceous age; uplift and compaction of strata over this feature have created possible structures for hydrocarbon accumulations (Schlee and others, 1977). Also present is at least one salt(?) diapir (see Line 14, Fig. 1) projected into the line of section (Fig. 11) from 16 km south of Line 2. The top of oceanic basement beneath the ECMA has been defined at 7-8 km depth by magnetic depth-to-source estimates and is overlain by a reef or carbonate bank complex which developed during the Jurassic and Early Cretaceous. This region over the magnetic basement high is the second major area of interest for hydrocarbon accumulation and the site of gas discoveries. The present shelf edge is about 20 km landward of the Cretaceous shelf edge; this change probably resulted mainly from the erosion associated with the major sea level lowering during the Oligocene (Vail and others, 1977) and subsequent redeposition (Grow and others, 1979). The configuration of the basement beneath the Baltimore Canyon Trough based on CDP seismic data is simpler than that beneath the Georges Bank (compare Figs. 7 and 12). The configuration of basement based on magnetic data for the Baltimore Canyon Trough (Fig 13) closely resembles that configuration of basement determined from seismic data, but is more detailed because the magnetic coverage is denser. The axis of the trough extends from the Shelf off Long Island almost to the mouth of Chesapeake Bay. Average axial sediment thickness is 10-12 km. Only the mafic intrusion breaks the continuity of this deep axial depression. The two diagrammatic cross sections of USGS Lines 2 and 6 (Figs. 11 and 14) characterize the sedimentary and crustal structure across the widest part of the Baltimore Canyon Trough. Seismic Line 2 (Fig. 11) crosses the basin where it is widest (150 km) and deepest, containing as much as 14 km of sediment. Block-faulted and thinned continental or transitional crust has been inferred beneath the Continental Shelf as far seaward as the ECMA. The ridge in magnetic basement that forms the seaward edge of the basin rises to an average depth of about 8 km and, in places, comes to within ~6 km of sea level.

The nonmagnetic diapir projected from 16 km south of the line of section, interpreted here as salt, shows that lower Mesozoic evaporite deposits may pierce the overlying carbonate and clastic section (Grow and others, 1979). Some strong reflectors on CDP profile 2 at a depth of 12 km may be due to interbedded evaporite and carbonate deposits. Possible additional evidence for the presence of evaporite deposits in the area was reported by Manheim and Hall (1976): hypersaline (55‰) brines were reported from a depth of 1700 m in ASP holes 15 and 17 off New Jersey. They estimated that saturated brines should exist 3-4 km below bottom, possibly associated with salt diapirs. In addition, off northwest Africa, Aptian and Albian marls with barite were found at DSDP Site 369; Lancelot and others (1972) suggested that the barite indicated upward migration of solutions from Jurassic evaporite deposits. Thus, as suggested by Evans (1978), the accumulation of evaporites may have been common during initial rifting stages of continents because shallow seas were restricted from open ocean waters. The depth of the rift floor and early spreading center is not known, but it may have been shallow similar to that of the East African rift system or the Afar.

The top of oceanic basement Layer 2 has been established on the basis of magnetic depth-to-basement estimates. Our interpretation that oceanic crust is thickest under the ECMA is compatible with the suggestion of Rabinowitz and LeBreque (1976) that abnormally thick ocean crust may be typical of initial rifting stages of sea floor spreading.

CDP Line 6 (Fig. 14) crosses the Baltimore Canyon Trough south of its widest part and is not complicated by the presence of the mafic intrusion. Several diapirs have been inferred here as well as a carbonate-bank buildup over the oceanic basement. The section is compatible with gravity models and shows a wide zone in which thick oceanic crust

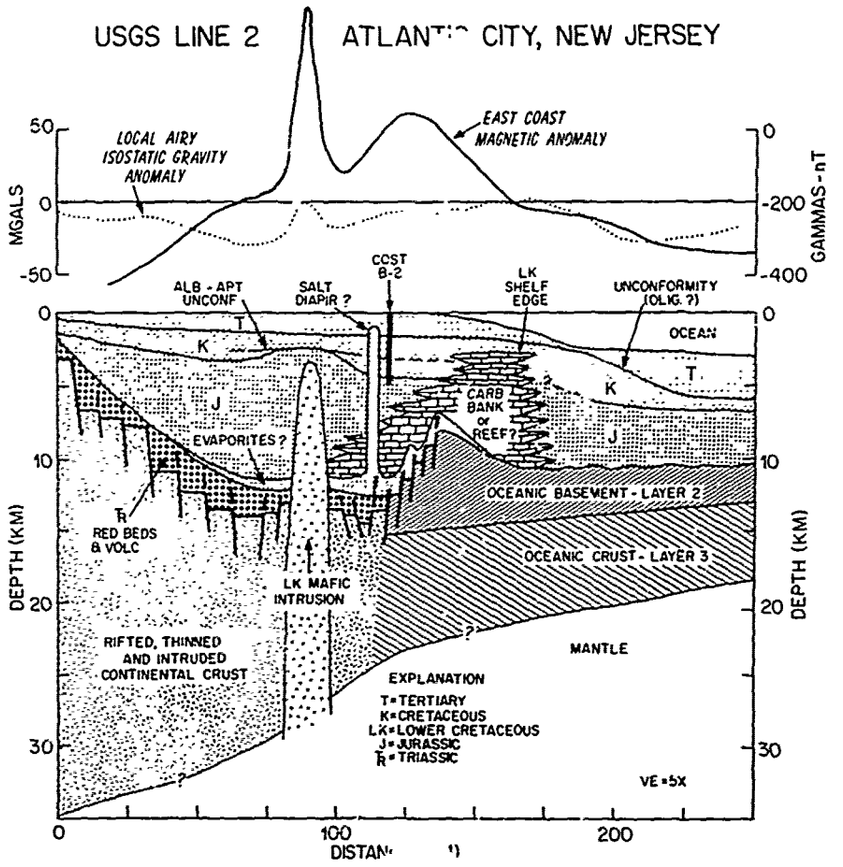


Fig. 11. Interpretative cross se long CDP seismic Line 2 near the widest part of the Baltimore Ca on Trough (from Grow and others, 1979).

extends nearly 80 km seaward of the ECMA (Grow and others, in press).

A seismic refraction profile by Ewing and Ewing (1959) plus two of our refraction profiles close to CDP Line6 (Grow and Schlee, 1976) indicate that a 7.1-7.2 km/s refracting horizon (thought to be the top of oceanic crustal Layer 3B) dips landward from a depth of 13 km beneath the Continental Rise to a depth of 16 km under the Shelf edge (Sheridan and others, in press). One of these refraction profiles indicated that the Moho is at 18-22 km and dips to the northeast. Although no refraction measurements have yet delineated the crustal section beneath the middle Shelf, a gravity model along Line 6 suggests that thinned continental crust (transitional crust) 12-km to 15-km thick underlies the main sedimentary basins in the Baltimore Canyon Trough region (Grow and others, in press).

The Continental Shelf edge crossed by both Profiles 2 and 6 apparently prograded 40-50 km seaward over oceanic crust during Jurassic and Early Cretaceous time whereas to the north, off Cape Cod, and to the south, off Cape Hatteras, little change in the Shelf edge location took place during this time. However, all the profiles show retreat of the Shelf edge by 20-30 km during the Tertiary. According to Vail and others (1977, pt. 4, Fig. 2), many sea level lowerings took place during Mesozoic and Cenozoic time and have left important unconformities along continental margins. Among them, the late Oligocene lowering was perhaps the greatest and is inferred to have caused much of the change in Shelf edge location depicted on these cross sections (Grow and others, 1979). Several other major acoustic units delineated in the Baltimore Canyon Trough and in the Georges Bank basin are bounded by unconformities whose ages, based on the work of Vail and others (1977) and correlation with strata penetrated in wells, are inferred to be late Miocene, late Oligocene, early Paleocene, Coniacian, Albian, Late Jurassic, and Early Jurassic in age.

In Figure 11 we have drawn the main carbonate bank or reef mass close to the area of thickened oceanic basement reflected by the ECMA. Whether the initiation of carbonate accumulation took place directly on basement, on salt that overlay

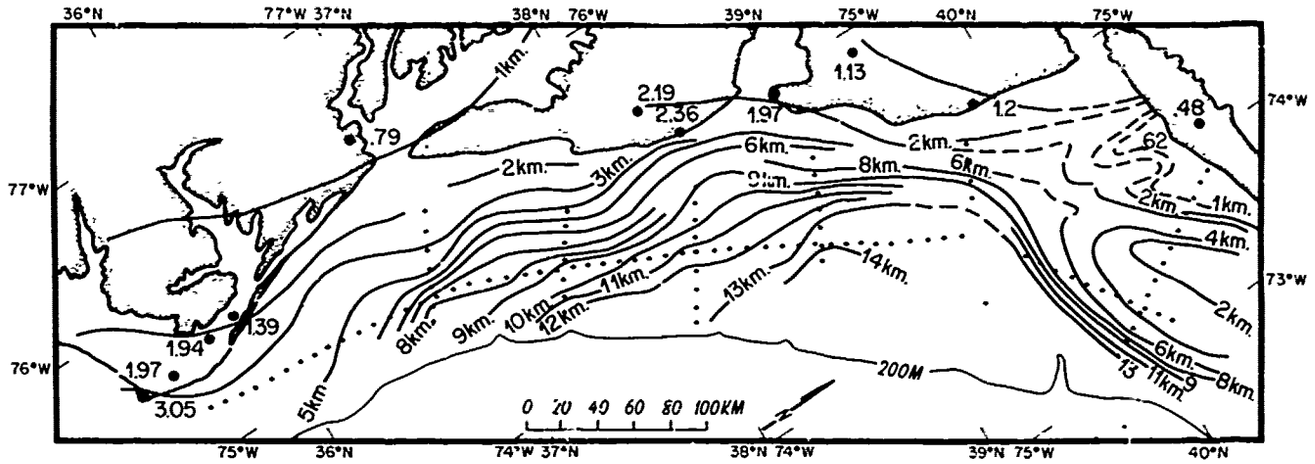


Fig. 12. Depth to basement in the Baltimore Canyon Trough area based on CDP seismic data (from Schlee and others, 1977).

the basement high, or at some later stage over other sediments cannot be deduced with available data. If coastal shelves of the Red Sea are analagous models, then carbonate deposits could directly overlie basalts and older sediments (Ross and Schlee, 1973) and reef buildups could be expected (Carella and Scarpa, 1962; Guilcher, 1955). Of key importance is the relationship between water depth and basement physiography. If the basement high during early rifting stages projected into sufficiently shallow water, given the proper temperature, salinity, and turbidity conditions, carbonate bank growth might have started; if it did, subsidence during the Jurassic and Early

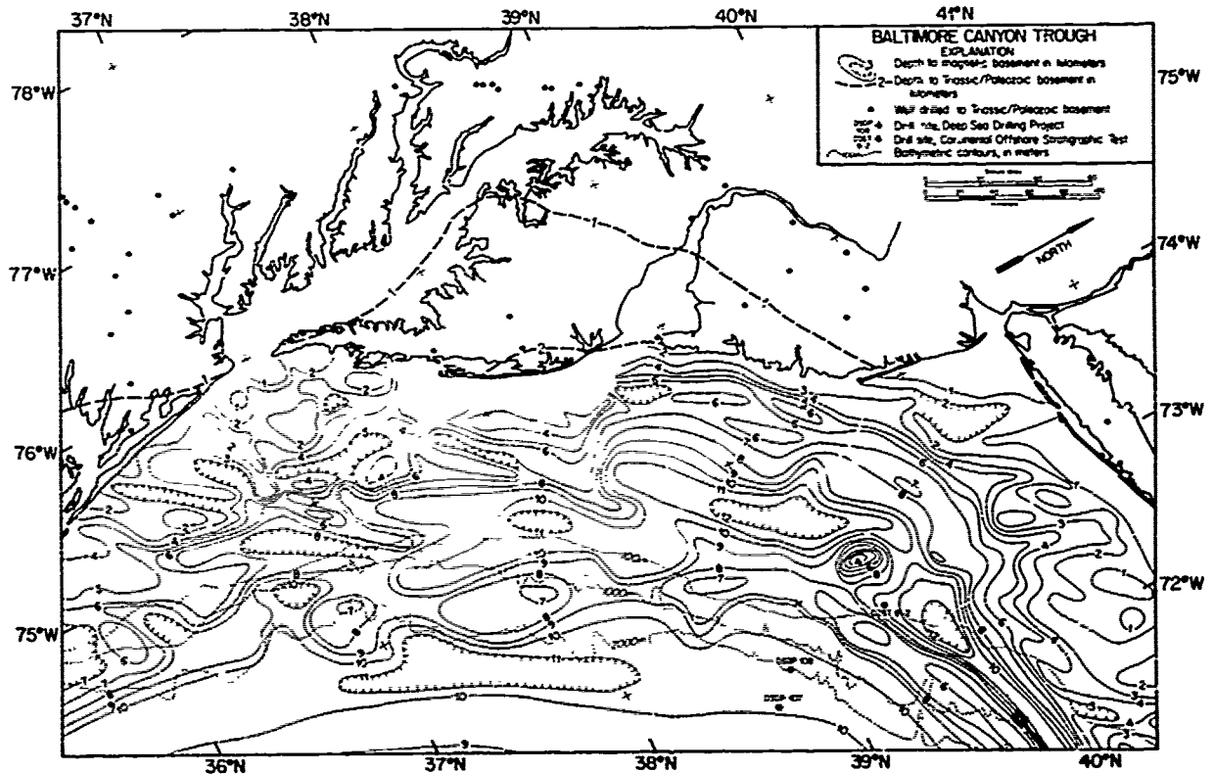


Fig. 13. Depth to basement in the Baltimore Canyon Trough based on magnetic depth-to-source estimates (from Klitgord and Behrendt, 1979).

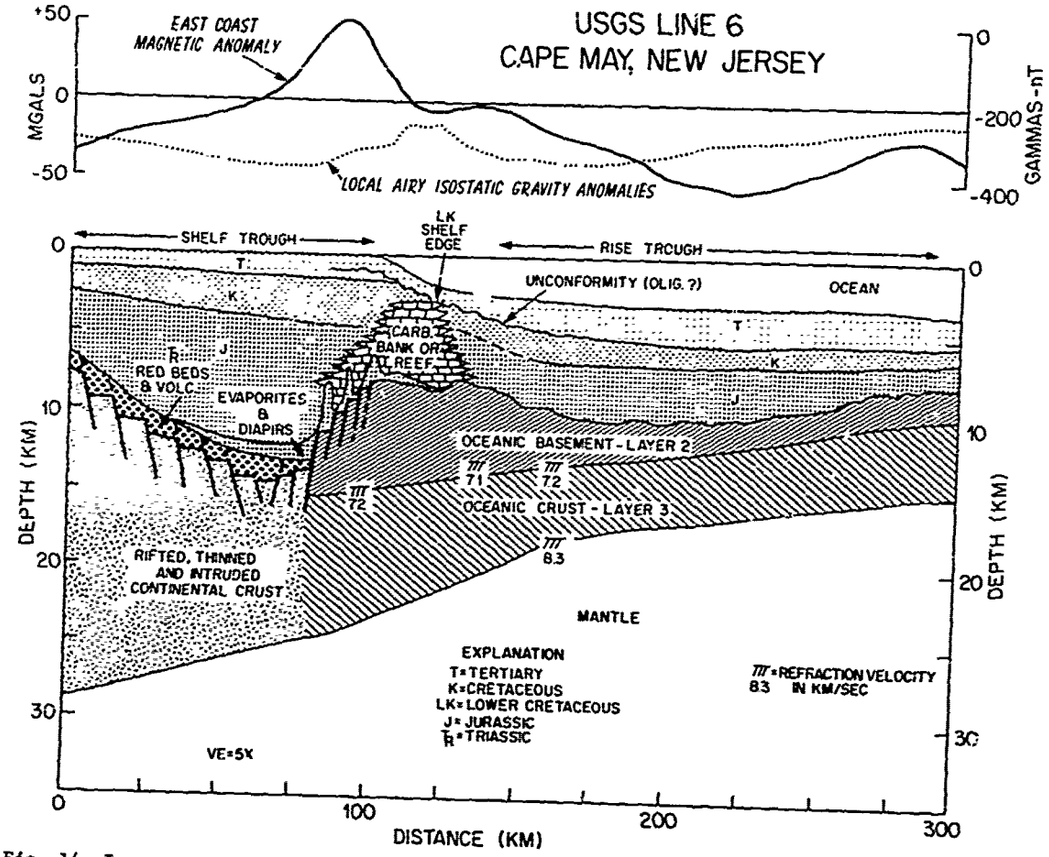


Fig. 14. Interpretative cross section along CDP seismic Line 6 across the south central part of the Baltimore Canyon Trough (Grow and others, 1979). Refraction measurements determine the position of the boundaries between oceanic Layer 3 and mantle (Sheridan and others, in press).

Cretaceous does not appear to have exceeded possible bank buildup or reef growth rates needed to keep the water shallow (Poag, 1978).

A stratigraphic cross section showing the upper 10 km of sediments along CDP line 2 (Fig. 15) depicts the inferred facies change from terrigenous clastic to carbonate deposits. The seismic data can be more accurately interpreted using lithologies drilled by the COST B-2 well (Scholle, 1977; Smith and others, 1976) which is located 10 km northeast of the line of section. About half the 4.8 km of sediment drilled was nonmarine to shallow-marine sands, shales, and limestones of Late Cretaceous and younger age. Lower Cretaceous rocks are mainly terrigenous clastic rocks with some limestone and coal strata. The hole was originally thought to have bottomed in Lower Cretaceous shallow water sediments, but more recent work has revealed Kimmeridgian (Late Jurassic) dinoflagellates near the bottom of the hole that brings the Cretaceous/Jurassic boundary up to ~4.1 km (E. Robbins, personal communication; Poag, 1978). The Upper Jurassic section drilled is mainly alternating sandstone, shale, limestone, and coal. The inferred facies change from terrigenous clastic deposits nearshore to carbonate deposits offshore in the Lower Cretaceous and Upper Jurassic sections is based on interval velocities that increase from 3 to 4 km/s. Refraction velocity data also show 4.8 km/s horizons within the Albian and Aptian strata near the Lower Cretaceous shelf edge (Sheridan and others, in press). Between the depths of 5 and 12 km under most of the Outer Continental Shelf, interval velocity values of 5-6 km/s suggest that carbonate deposits are more extensive in deeper rocks over the entire basin.

Exploratory drilling is now underway in the Baltimore Canyon Trough where hydrocarbon resource estimates are the highest for any of the Atlantic OCS areas (USGS, 1975a, 1975b; Mattick and others, 1976a, 1976b). The largest structural feature in the basin is the mafic intrusion (Great Stone Dome) with 350 m of closure in the Lower Cretaceous. This feature could provide traps for large

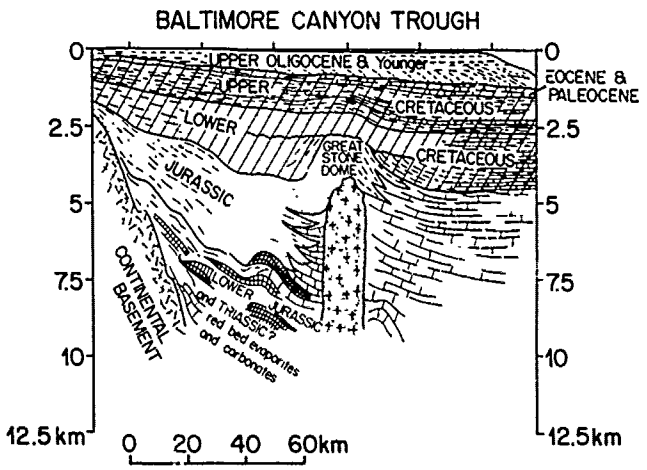


Fig. 15. Interpretative stratigraphic cross section based on CDP seismic Line 2 across the axis of the Baltimore Canyon Trough. The thick section of Jurassic is pierced by a mafic intrusion (the Great Stone Dome) which upwarps the overlying Upper and Lower Cretaceous (Schlee, 1978a).

reserves, most likely gas (Scholle, 1977). Leasing has also taken place on possible diapiric features that may be productive. Some updip pinchouts against continental basement along with drape structures over the horst blocks cannot be ruled out. Some initial results from the exploratory drilling have indicated possible significant gas accumulation associated with the diapirs over the magnetic basement ridge near the shelf edge (Oil & Gas Journal, 8/78).

From analyses of interval velocities, seismic amplitude, and continuity of reflectors within acoustic units, both the Georges Bank basin and the Baltimore Canyon Trough appear: (1) to be built across a zone of deeply buried fault blocks; (2) to show a progression from thick nonmarine strata and evaporite deposits to marine platform and reef carbonate beds (Jurassic and Early Cretaceous in age) in the lower half of the basins, and from nonmarine deposits to broadly prograding marine sandstone and shale (mainly Cretaceous in age) in the upper half; (3) to have undergone extensive erosion of the slope during the Tertiary and Quaternary with intermittent erosion, nondeposition, and deltaic deposition on the shelf; and (4) to have formed a thick continental rise prism when most of the Tertiary sediments bypassed the shelf.

## Carolina Platform and Carolina Trough

The margin east of the Carolinas and south of Cape Hatteras comprises a shallow platform under the Inner Shelf and a narrow, deep trough (Carolina trough) near the Shelf break (Klitgord and Behrendt, 1979; Dillon and others, 1979). Sediments on the Carolina platform are probably less than ~4 km thick. However, the Carolina trough, a narrow feature that is inferred mainly from magnetic and seismic data, extends from Cape Hatteras to Charleston, S.C., and contains more than 10 km of sediment (Dillon and others, 1979). A diagrammatic cross section along the USGS/IPOD line (fig. 16) across the northern end of the Carolina trough reveals several complications not evident in cross sections described previously. The crustal-transition zone is narrow as on the Long Island platform (Fig. 6), but the acoustically diffuse zone not only coincides with the ECMA but extends landward of it. Apparently a carbonate buildup was initiated landward of the transition of oceanic to continental crust. In addition to the 3 diapirs observed on the IPOD line in the region of the ECMA, others were observed along the Continental Slope off Cape Hatteras which extend 50 km north and 200 km south of the IPOD line along the axis of the ECMA (Grow and others, 1977). None have had a detectable magnetic or gravity signature and thus are inferred to be salt or possibly shale. The diapirs off Cape Hatteras and one diapir in the Baltimore Canyon Trough all lie within 20 km of the axis of the ECMA.

Section BT-1 (Fig. 17) across the Carolina platform and trough reveals a smooth, strong reflector at the landward end which correlates with a high velocity refractor (~6 km/s) that was previously thought to be basement (Woollard, 1959; Hersey and others, 1959; Antoine and Henry, 1965; Sheridan and others, 1966; Dowling, 1968). However, correlating reflection and refraction data with recent drilling data from the Charleston area indicates that the strong reflector probably originates from a series of Jurassic basalt flows (Ackerman, 1978; Gohn and others, 1978). On the basis of seismic data along Line BT-1, we infer that Cenozoic and Cretaceous rocks are thin, whereas Jurassic rocks may be as much as 8 km thick. In contrast, seaward of the Slope, Line BT-1 lies along the axis of the Blake Ridge (Markl and others, 1970) where Cenozoic sediments are as much as 5 km thick. Several large faults are shown close to the Shelf edge; one of these is a growth fault that was

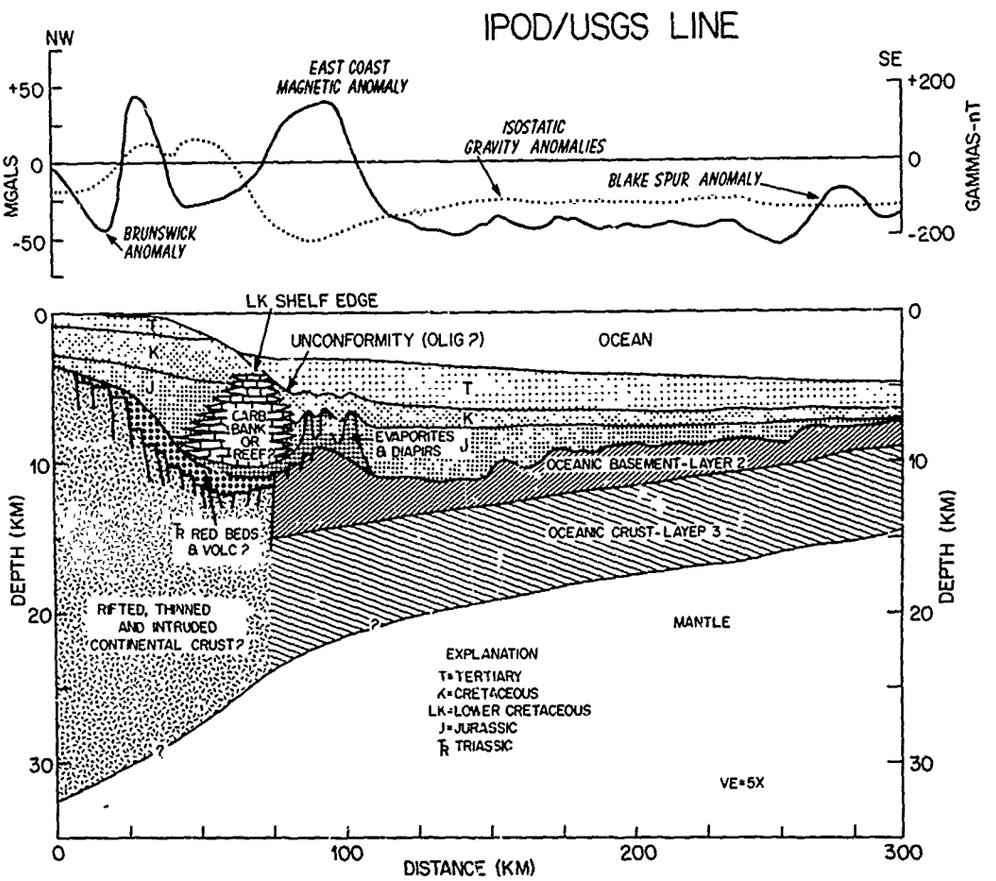


Fig. 16. Interpretative cross section along USGS/IPOD CDP seismic line across the margin southeast of Cape Hatteras (Grow and others, 1979). The transition zone between continental and oceanic crust is narrow and is similar, in this respect, to Line 5 off Cape Cod except for the presence of diapirs (see Grow and Markl, 1977, for additional discussion).

active during Cretaceous and Tertiary time. The area off Georgia and South Carolina is a zone of transition with regard to styles of continental margin subsidence. This change can best be seen in the character of the structure mapped on the post-rift unconformity (Fig. 18) off Cape Fear, N.C., where the Carolina platform is built on continental basement; the unconformity dips gently seaward to 4 km below the Continental Slope and then dips more steeply to about 11 km beneath the Continental Rise. Off Charleston, S.C., an abrupt southward inflection of the unconformity is aligned with the Blake Spur fracture zone that was probably the site of a transform fault, active during early rifting of the continental margin. South of this inflection, the unconformity subsides to >12-km deep in a broad area that includes the eastern two-thirds of the Blake Plateau (Fig.

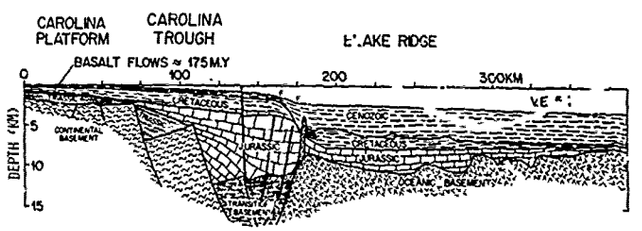


Fig. 17. Diagrammatic cross section along CDP seismic Line BT-1 across the Carolina platform and Carolina trough (Dillon and others, 1979).

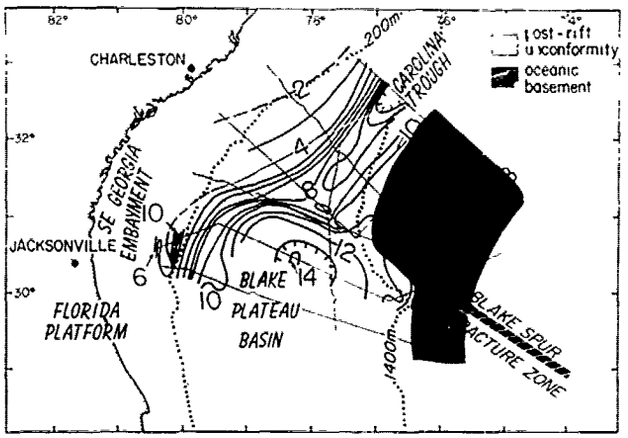


Fig. 18. Depth to a post-rifting unconformity identified in multichannel seismic profiles. The unconformity lies below a strong reflector believed to represent basaltic flows sampled on shore and dated at 160 to 200 m.y. (Dillon and others, 1979).

19). This probably overlies transitional basement. The eastern margin of the Blake Plateau, which formed a shelf edge during most of the region's development, may have been built up by continuous reef growth (Fig. 19). North of the Blake Spur fracture zone, however, where the area of transitional crust is much narrower and input of terrigenous sediments is greater, the shelf edge was formed by a balance of deposition and erosion and, at the same time, some patch reefs and carbonate banks developed.

The diagrammatic cross section along BT-1 (Fig. 17) across the Carolina trough indicates that Triassic rifting produced a rough topography that resulted in a flood of continental deposits during the earliest stages of margin development off the southeastern United States. These strata were tilted seaward and beveled as the newly-forming margin subsided. Basaltic flows covered the landward part of these deposits about 175 m.y. ago; as subsidence proceeded, a transgressive wedge of Upper Jurassic and Cretaceous sediments formed the Continental Shelf.

Southeast Georgia Embayment - Blake Plateau Basin

The area just south of the Carolina platform and trough, marked by the Blake Spur fracture zone, consists of 3 elements: the Southeast Georgia Embayment, the Florida platform, and the Blake Plateau basin. The Embayment extends westward of the coastline south of Charleston (Fig. 18) and is separated from the Blake Plateau basin by a basement high in the vicinity of the COST GE-1 well (Fig. 1). This area is thought to be a Triassic basin on the basis of magnetic inferences similar to those used on the Long Island platform (Klitgord and Behrendt, 1979) and the thick sequence of sediments below the basalt horizon which are thought to be Jurassic in age (Dillon and others, 1979).

The Blake Plateau basin contains more than 10 km of sediments and is probably underlain by transitional crust. The character of the magnetic anomalies suggests a magnetic source which is not typical oceanic crust or large blocks of faulted continental crust. The stratigraphic location of the seismic horizons, inferred to be Jurassic flows (Fig. 18), suggests that a very thick sequence of Jurassic sediments (as much as 6-8 km) are present. The Cretaceous sequence is fairly thin and its uppermost part has been sampled by the DSDP and ASP holes.

Beginning in Tertiary time, the Blake Plateau was affected by erosion or reduced deposition as Gulf Stream flow shifted west. Continental margin subsidence, combined with this reduced sedimentation, resulted in the present physiography of the Blake Plateau—a submerged platform 600-1100 m deep. Landward, the present Continental Shelf edge was formed by sediment progradation against the flank of the fast-flowing Gulf Stream during Cenozoic time. The diagrammatic cross section along FC-3 (Fig. 19) across the Blake Plateau basin shows an evolutionary pattern similar to that to the north (Fig. 17) but one in which the

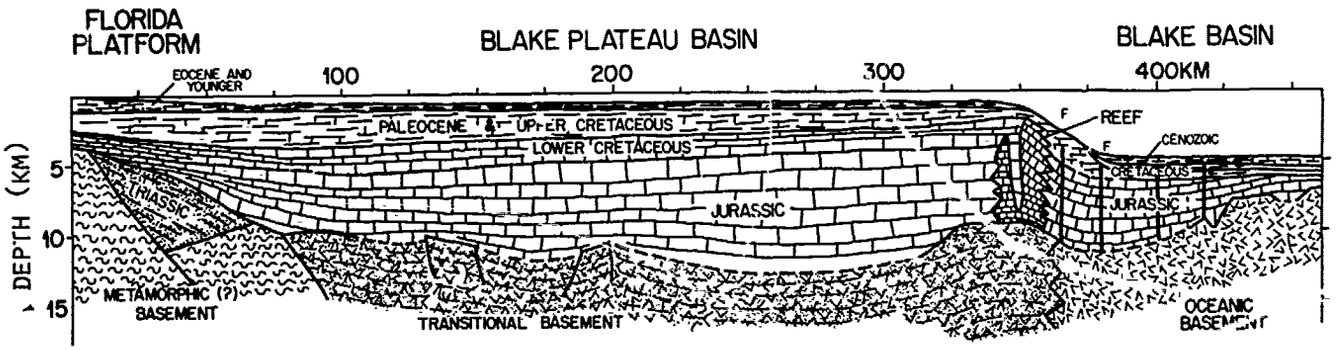


Fig. 19. Diagrammatic cross section based on CDP seismic Line FC-3 (Dillon and others, 1979).

zone of transitional basement was much wider and in which reef growth provided a dam for sediments until approximately the middle of Cretaceous time. Profile FC-3 is located south of the area of inferred Jurassic volcanic flows.

## Discussion

The accumulation of multichannel and single channel seismic reflection data, magnetic anomaly data, gravity anomaly data, refraction data, and drill hole information has enabled us to construct structural and stratigraphic maps and cross sections for the U. S. Atlantic continental margin and to understand better the history of its development. The integration of magnetic, gravity, refraction, and drill hole data with seismic reflection data has been an important part of our studies of the margin, making possible interpolation between the 40-km grid of multichannel seismic profiles.

The general structure of the margin from Florida to Maine is dominated by the basins and platforms (Fig. 4). The platforms have a fairly thin sediment cover and are sites of numerous horsts and grabens which may have been formed during Triassic time. They are the most seaward protrusions of pre-Jurassic continental crust which probably was not greatly affected by subsequent block-faulting and subsidence during Late Triassic and Early Jurassic. Most often the seaward edge of these platforms form the landward edge of the major sedimentary basins while the southwesterly or northeasterly edges probably mark the sites of transform faults during the initial breakup of Africa and North America. However, such platform areas as Cape Hatteras and Long Island extend across the continental margin separating the major basins. The relationship between these initial transform faults and the deep sea fracture zones (Fig. 4) suggests that the original pattern of rifting and transform faults was propagated into the sea floor spreading stage of continental separation. Small offsets also exist in the landward edges of the deep basins (e.g., the Baltimore Canyon Trough, see Figs. 4 and 13) which also persisted into the sea floor spreading phase. The development of the deep sedimentary basins seems to have been partially controlled by this pattern of offsets, resulting in a segmentation of the major basins into a number of smaller basins. For example, the Baltimore Canyon Trough is actually divided into 3 basins with the northernmost being the widest and deepest, and the southernmost being the shallowest and narrowest (Klitgord and Behrendt, 1979). The gravity, magnetic, and multichannel seismic reflection data all suggest this pattern of segmented basin evolution.

The combination of stratigraphic control from drill holes with the multichannel seismic stratigraphy (Schlee and others, 1976; Dillon and others, 1979; Grow and Klitgord, 1978; Mattick and others, 1978) enables us to develop a history for the margin from its initial rifting to the present day.

Following rifting and separation of North America and Africa during the Late Triassic and Early Jurassic, cooling of the lithosphere and high deposition rates resulted in rapid subsidence of the major basins along the U. S. Atlantic shelf. Oldest sediments were probably terrigenous lagoonal, fluvial, and deltaic nearshore but gave way offshore to local evaporites and widespread carbonate deposits. There, a series of carbonate banks built up along much of the continental margin over the oceanic basement high that developed during early stages of rifting. The banks ultimately were overwhelmed by Cretaceous fluvial, deltaic, and shelf sediments. However, these Tertiary and Cretaceous sediments are thinner (<4 km in the Baltimore Canyon Trough) than the Jurassic rocks (8-10 km in the Baltimore Canyon Trough) which filled the basin during the initial, more rapid phase of subsidence. As these Cretaceous sediments prograded seaward over the former carbonate shelf edge, extensive sedimentation was initiated over the slope and rise. During the Cenozoic, a prominent continental rise wedge was deposited along much of the continental margin at the same time that the slope was being cut back in several phases of erosional retreat.

This initial interpretation of the vast amount of geophysical data from the Atlantic continental margin provides a suitable basis for developing a structural and sedimentary history of the United States Atlantic margin and for comparison with other margins. The Outer Continental Shelf is the current frontier for hydrocarbon exploration, and a better understanding of its development history may improve our chances of exploiting the resources of the OCS. The discovery of gas associated with diapirs over the magnetic basement high (along the ECMA) has implication on the potential for similar structures off the Carolina margin and south of Cape Hatteras. Further work is clearly needed, including the development of techniques for looking at the region of the outer basement high. A better understanding of the geologic and tectonic structure of the platforms and their relationship to the offshore Triassic and Jurassic basins is a necessary step in the development of the rifting history of a continental margin.

Acknowledgements. We are indebted to J. C. Behrendt for initiating several facets of this study; to A. Dahl, C. Morse, D. Hutchinson, and C. Paull for technical assistance; to S. Wood for assembling much of the data; to P. Forrestel and L. Sylwester for able drafting; to E. Winget for assembling and typing the manuscript; and to C. W. Poag and E. Uchupi for reviewing the manuscript.

## References

Ackerman, H.D., Exploring the Charleston, South Carolina, earthquake area with seismic refraction - a preliminary study: *in* Rankin, D.W,, ed., Studies related to the Charleston, South Carolina earthquake of 1886, a preliminary report: U.S.

Geol. Survey Prof. Paper 1028, p. 167-175, 1978.
Agassiz, Alexander, Three cruises of the United States Coast and Geodetic Survey steamer BLAKE in the Gulf of Mexico, in the Caribbean sea, and along the Atlantic coast of the United States from 1377 to 1880: 2 vol., Houghton, Mifflin and Co., Boston, Mass., 1888.
Antoine, J.W., and V.J. Henry, Jr., Seismic refraction study of shallow part of continental shelf off Georgia: AAPG Bull., 49, p. 601-609, 1965.
Bhat, H., N.J. McMillan, J. Aubert, B. Parthault, and M. Surin, North American and African drift - the record in Mesozoic coastal plain rocks, Nova Scotia and Morocco: *in* Yorath, C.J., E.R. Parker, and D.J. Glass, eds., Canada's continental margins and offshore petroleum exploration: Memoir 4, Canadian Soc. of Petroleum Geologists, p. 375-389, 1975.
Behrendt, J.C., J. Schlee, and R.Q. Foote, Seismic evidence of a thick section of sedimentary rock in the Atlantic Outer Continental Shelf and Slope of the United States: Eos Trans. AGU, v. 55, p. 278, 1974.
Bowin, C., T.C. Aldrich, and R.A. Folinsbee, VSA gravity meter system: tests and recent developments: J. Geophys. Research, v. 77, p. 2018 - 2033, 1972.
Bunce, E. and others, Ocean drilling on the continental margin: Science, v. 150, no. 3697, p. 709-716, 1965.
Carella, R., and N. Scarpa, Geological results of exploration in Sudan: AGIP Mineraria Ltd., 4th Arabian Petroleum Congress, Beirut, 1962.
Cushman, J.A., Geology and paleontology of the Georges Bank canyon Pt. 4, Cretaceous and late Tertiary foraminifera: GSA Bull. v. 47, no. 3, p. 413-440, 1936.
Dillon, W.P., C.K. Paull, R.T. Buffler, and J.-P. Fail, Structure and development of the Southeast Georgia Embayment and northern Blake Plateau: preliminary analysis: *in* Watkins, J.S., and others, eds., Geological and geophysical investigations of continental margins, AAPG Memoir 29, 1979.
Dowling, J.J., The east coast onshore experiment II: Seismic refraction measurements on the continental shelf between Cape Hatteras and Cape Fear: Seismological Soc. of Amer. Bull. 58, p. 821-834, 1968.
Drake, C.L., M. Ewing, and G.H. Sutton, Continental margins and geosynclines: the east coast of North America north of Cape Hatteras: *in* Ahrens, L.H. et al, eds., Physics and chemistry of the earth, p. 110-198, Pergamon Press, London, 1959.
Drake, C.L., J.R. Heirtzler, and J. Hirshman, Magnetic anomalies off eastern North America: J. Geophys. Res., 63, p. 5259-5275, 1963.
Emery, K.O., and E. Uchupi, Western North Atlantic ocean: topography, rocks, structure, water, life and sediments: AAPG Memoir 17, 1972.
Emery, K.O., E. Uchupi, J.D. Phillips, C.O. Bowin, E.T. Bunce, and S.T. Knott, Continental Rise of eastern North America: AAPG Bull., 54, p. 44-108, 1970.
Evans, Robert, Origin and significance of evaporites in basins around the Atlantic margin: AAPG Bull., 62, p. 223-234, 1978.
Ewing, M., A.P. Crary, and H.M. Rutherford, Geophysical investigations in the emerged and submerged Atlantic coastal plain: Part I, Methods and results: GSA Bull., 48, p. 753-801, 1937.
Ewing, M., G.P. Woollard, and C.A. Vine, Geophysical investigations in the emerged and submerged Atlantic coastal plain: Part III, Barnegat Bay, New Jersey section: GSA Bull., 50, p. 257-296, 1938.
Ewing, M., G.W. Woollard, and C.A. Vine, Geophysical investigations in the emerged and submerged Atlantic coastal plain: Part IV, Cape May, New Jersey section: GSA Bull., 51, p. 1821-1840, 1940.
Ewing, J., and F. Press, Crustal structure and surface wave dispersion: Seismological Soc. of Amer. Bull., 40, p. 271-280, 1950.
Ewing, John, and Maurice Ewing, Seismic refraction measurements in the Atlantic ocean basins, in the Mediterranean Sea, on the mid-Atlantic ridge, and in the Norwegian Sea: GSA Bull., v. 70, no. 3, p. 291-318, 1959.
Ewing, V. Free air gravity map of the U.S. Atlantic margin: Eos Trans, AGU, v. 59, no. 4, p. 378, 1978.
Folger, D.W., J.C. Hathaway, R.A. Christopher, P. C. Valentine, and C.W. Poag, Stratigraphic test well, Nantucket Island, Mass., U.S. Geol. Survey Circ. 773, 28 p., 1978.
Gibson, T.G., J.E. Hazel, and J.E. Mello, Fossiliferous rocks from submarine canyons off northeastern United States: U.S. Geol. Survey Prof. Paper 600-D, p. 222-230, 1968.
Given, M. M., Mesozoic and early Cenozoic geology of offshore Nova Scotia: Canadian Petrol. Geol. Bull., 25, p. 63-91, 1977.
Gohn, G.S., D. Gottfried, R.R. Schneider, and M.A. Lanphere, Preliminary report on the geology of two deep test holes, Clubhouse Crossroads #2 and #3, near Charleston, S.C., GSA, Abs. with Prog. v. 10, no. 4, p. 169, 1978.
Grow, J.A., and J. Schlee, Interpretation and velocity analysis of U. S. Geological Survey multichannel reflection profiles 4, 5, and 6, Atlantic continental margin: U. S. Geol. Survey Misc. Field Series Map MF 808, 1976.
Grow, J.A., C.O. Bowin, and D.R. Hutchinson, The gravity field of the U. S. Atlantic continental margins: Interunion Comm. on Geodynamics Symposium on the Crustal properties across Passive margins Proc., 19-23 June 1978, Halifax, Nova Scotia, Tectonophysics, in press.
Grow, J.A., C.O. Bowin, D.R. Hutchinson, and K.M. Kent, Preliminary free-air gravity anomaly map along the Atlantic continental margin between Virginia and Georges Bank: U.S. Geol. Survey Misc. Field Series Map MF-795, scale 1:1,200,000, 1976.

Grow, J.A., and C.O. Bowin, Free-air gravity anomalies over the U. S. Atlantic continental margin: GSA Abs. with Prog. v. 9, no. 7, p. 999, 1977.

Grow, J.A. and R.G. Markl, IPOD-USGS multichannel seismic reflection profile from Cape Hatteras to the mid-Atlantic ridge: Geology, 5, p. 625-630, 1977.

Grow, J.A., W.P. Dillon, and R.E. Sheridan, Diapirs along the Continental Slope off Cape Hatteras (abs.): SEG Proc. 46th Annual Mtg., p. 192, 1977.

Grow, J.A., R.E. Mattick, and J.S. Schlee, Multichannel seismic depth sections and interval velocities over the Continental Shelf and upper Continental Slope between Cape Hatteras and Cape Cod: *in* Watkins, J.R., L. Montadert, and P.W. Dickerson, eds., Geological and geophysical investigations of continental margins: AAPG Memoir 29, 1979.

Guilcher, André, Geomorphologie de l'extrémité septentrionale du banc corallien Farsan: Institut Océanographiques Annales, 30, p. 55-100, 1955.

Hartman, R.R., D.J. Teskey, and J.L. Friedberg, A system for rapid digital aeromagnetic interpretation: Geophysics, 36, p. 891-918, 1971.

Hathaway, J.C., Data file, continental margin program, east coast of the United States, Vol. 2: Sample collection and analytical data: Woods Hole Oceanographic Institution Ref. 71-15, 496 p, 1971.

Hathaway, J.C., J.S. Schlee, C.W. Poag, P.C. Valentine, E.C.A. Weed, M.H. Bothner, F.A. Kohout, F.T. Manheim, R. Schoen, R.E. Miller, and D.M. Schultz, Preliminary summary of the 1978 Atlantic margin coring project of the U. S. Geological Survey: U. S. Geol. Survey open file report no. 76-844, 217 p., 1976.

Heezen, B.C. and R.E. Sheridan, Lower Cretaceous rocks (Neocomian-Albian) dredged from Blake escarpment: Science, v. 154, p. 1644-1647, 1966.

Hersey, B.C., E.T. Bunce, R.F. Wyrick, and F.T. Dietz, Geophysical investigation of the continental margin between Cape Henry, Va. and Jacksonville, Fl.: GSA Bull. v. 70, p. 437-466, 1959.

Hollister, C.D., J.I. Ewing, et al, Initial report of the Deep Sea Drilling Project, XI, Washington D.C., U. S. Govt. Printing Office, 1972.

Jain, S., An automatic method of direct interpretation of magnetic profiles: Geophysics, v. 41, no. 3, p. 531-541, 1976.

Jansa, L.F. and J.A. Wade, Paleogeography and sedimentation in the Mesozoic and Cenozoic, southeastern Canada: *in* Yorath, C.J., E.R. Parker, and D.J. Glass, eds., Canada's continental margins and offshore petroleum exploration: Canadian Soc. of Petroleum Geol. Memoir 4, p. 79-102, 1975.

Jaworski, B.L., J.A. Grow, and C.A. Meeder, Airgun sonobouy measurements on Georges Bank (abs): Eos Trans. AGU, v. 57, no. 4, p. 265, 1976.

JOIDES, Deep sea drilling project: AAPG Bull. 51, p. 1787-1802, 1967.

Kay, Marshall, North American geosynclines: GSA Memoir 48, p. 143, 1951.

Keller, Fred, J.L. Menschke. and L.R. Alldredge, Aeromagnetic surveys in the Aleutian, Marshall, and Bermuda Islands: Eos Trans. AGU. v. 35, p. 558-572, 1954.

Klitgord, K.D. and J.C. Behrendt, Aeromagnetic anomaly map - U.S. Atlantic continental margin: U.S. Geol. Survey Misc. Field Studies Map MF-913, scale 1:1,000,000, 1977.

Klitgord, K.D., and J.C. Behrendt, Basin structure of the U. S. Atlantic continental margin: *in* Watkins, J.S., L. Montadert, and P.A. Dickerson, eds., Geological and geophysical investigations of continental margins: AAPG Memoir 29, 1979.

Klitgord, K.D., and H. Schouten, The onset of sea floor spreading from magnetic anomalies: Symposium of the geological development of the New York Bight Proc., Lamont-Doherty Geol. Obs., Palisades, N.Y., 1977

Lancelot, Y., J.C. Hathaway, and C.D. Hollister, Lithology of sediments from the western North Atlantic, Leg II, Deep Sea Drilling Project: *in* Kaneps, A.G., ed., Initial reports of the Deep Sea Drilling Project, XI, p. 901-949, US Gov't. Printing Office, Washington, D.C., 1972.

Manheim, F.T., and R.E. Hall, Deep evaporitic strata off New York and New Jersey - evidence from interstitial water chemistry of drill cores: J. Res. U. S. Geol. Survey, v. 4, no. 6, p. 697-702, 1976.

Markl, R.G., G.M. Bryan, and J.I. Ewing, Structure of the Blake-Bahama outer ridge: J. Geophys. Res. v. 75, p. 4539-4555, 1970.

Mattick, R.E., R.Q. Foote, and N.L. Weaver, A preliminary report on U. S. Geological Survey geophysical studies on the northeastern United States Outer Continental Shelf (abs.): Abs. with Prog., NE Sec. GSA, v. 6, p. 52, 1974.

Mattick, R.E., D.W. Folger, N.T. Foley, C.L. Dolton, and K.C. Bayer, Summary reports of the sediments, structural framework, petroleum potential, environmental condition , and operational considerations of the United States mid-Atlantic Continental Shelf: U. S. Geol. Survey open file report no. 76-532, 26 p., 1976a.

Mattick, R.E., P.A. Scholle, K.C. Bayer, and G.L. Dolton, Second Atlantic sale may involve tracts off Virginia and Maryland: Oil and Gas J., v. 74, no. 47, p. 168, 170, 172, 174, 175, 1976b.

Mattick, R.E., O.W. Girard, Jr., P.A. Scholle, and J.A. Grow, Petroleum potential of U. S. Atlantic slope, rise, and abyssmal plain: AAPG v. 62, no. 4, p. 592-607, 1978.

Mayhew, M.A., Geophysics of Atlantic North America: *in* Burke, C.A., and C.L. Drake, eds., The geology of continental margins, p. 409-427, Springer-Verlag, New York, 1974.

Oil and Gas Journal, Texaco logs first discovery off east coast of U.S., Oil and Gas J., 8/21/78, p. 32-33, 1978.

Poag, C.W., Stratigraphy of the Atlantic Continental Shelf and Slope of the United States: Annual Review of Earth and Planetary Sciences, 6, p. 251-280, 1978.

Pourtales, L.F., The characteristics of the Atlantic sea bottom off the coast of the United States: Report by the Supt. of U. S. Coast Survey for 1869, App. II, p. 220-225, 1872.

Rabinowitz, P.D., The boundary between oceanic and continental crust in western North Atlantic: *in* Burke, C.A., and C.L. Drake, eds., The geology of continental margins, p. 67-84, Springer-Verlag, New York, 1974.

Rabinowitz, P.D., and J.L. LaBreque, The isostatic gravity anomaly: key to the evolution of the ocean-continent boundary at passive continental margins: Earth and Planetary Sciences Letters, 35, p. 145-150, 1976.

Ross, D.A., and J.S. Schlee, Shallow structure and geologic development of the southern Red Sea: GSA Bull., 84, p. 3827-3848, 1973.

Ryan, W.B.F., M.B. Cita, E.D. Miller, D. Hanselman, W.D. Nesteroff, B. Hecker, and M. Nillelink: Bedrock geology in New England submarine canyons: Oceanologica Acta, 1, 233-254, 1978.

Schlee, J.S., Stratigraphy and Tertiary development of the continental margin east of Florida: U.S. Geol. Survey Prof. Paper No. 581-F, 25 p., 1977.

Schlee, J.S., Acoustic stratigraphy of the continental margin off the northeastern United States: Prog. and Abs., Symposium on the Crustal Properties across passive margins, Interunion Comm. on Geodynamics, 19-23 June 1978, Halifax, N.S., p. 27, 1978a.

Schlee, J.A., Geology of Georges Bank: *in* Fisher, J.J., ed., New England Marine Geology: new concepts in research and teaching and bibliography of New England marine geology 1870-1970, Proc. New England Sec. Nat'l. Assoc. Geology Teachers, 21-23 April 1978, Kingston, R.I., p. 88, 1978b.

Schlee, J.S., J.C. Behrendt, J.A. Grow, J.M. Robb, R.E. Mattick, P.T. Taylor, and B.J. Lawson, Regional framework off northeastern United States: AAPG Bull., 60, p. 926-951, 1976.

Schlee, J.S., R.G. Martin, R.E. Mattick, W.P. Dillon, and M.M. Ball, Petroleum geology of the United States' Atlantic-Gulf of Mexico margins: Proc. Southwestern Legal Foundation, Exploration and Economics of the Petroleum Industry, 15, p. 47-93, 1977.

Scholle, P.A., Geologic studies on the COST B-2 well, U. S. mid-Atlantic Outer Continental Shelf: U.S. Geol. Survey Circ. 750, p. 71, 1977.

Schouten, H. and K.D. Klitgord, Map showing Mesozoic magnetic lineations, western North Atlantic: U. S. Geol. Survey Misc. Field Studies Map MF-915, scale 1:2,000,000, 1977.

Sheridan, R.E., Conceptual model for the block-fault origin of the North American Atlantic continental margin geosyncline: Geology, 2, p. 465-468, 1974.

Sheridan, R.E., C.L. Drake, J.E. Nafe, and J. Hennion, Seismic refraction study of continental margin east of Florida: AAPG Bull. 50, p. 1972-1991, 1966.

Sheridan, R.E., J.A. Grow, J.C. Behrendt, and K.C Bayer, Seismic refraction study of the continental edge off eastern United States: *in* Interunion Comm. on Geodynamics Symposium on the Crustal properties across passive margins Proc., 19-23 June 1978, Halifax, Nova Scotia, Tectonophysics, in press.

Sheridan, R.E., Older Atlantic crust and the continental edge based on seismic data (abs): Abs. with Prog., Northeastern Sec., GSA, v. 9, no. 3, 1977.

Smith, M.A., R.V. Amato, M.A. Furbish, D.M. Pert, M.E. Nelson, J.S. Hendrix, L.C. Tamm, G. Wood. Jr., and D.R. Shaw, Geological and operational summary, COST No. B-2 well, Baltimore Canyon Trough area, mid-Atlantic OCS: U. S. Geol. Survey open file report 76-774, 9 p., 1976.

Stetson, H.C., Geology and paleontolody of the Georges Bank canyons, 1, Geology: GSA Bull., 47, p. 339-366, 1936.

Stetson, H.C., The sediments and stratigraphy of the east coast continental margin - Georges Bank to Norfolk Canyon: Mass. Inst. of Technology and Woods Hole Oceanographic Inst. Papers in physical oceanography and meteorolgy, 12, p. 1-45, 1949.

Stille, Hans, Wege und ergebnisse der geologisch-tectonischen: *in* Forschung, Festschr. Kaiser Wilhelm Gesellsch Ford. Wiss, Bd. 2, 1936.

Stille, Hans, Einfuhrung: in den bau Amerikas: Borntraeger, Berlin, 1941.

Taylor, P.T., Isidore Zietz, and L.S. Dennis, Geologic implications of aeromagnetic data for the eastern continental margin of the United States: Geophysics, 33, p. 755-780, 1968.

Uchupi, E., R.D. Ballard, and J.P. Ellis, Continental Slope and upper Rise off western Nova Scotia and Georges Bank: AAPG Bull., 61, p. 1483-1492, 1977.

U. S. Geological Survey, Sediments, structural framework, petroleum potential, environmental conditions, and operational considerations of the United States, North Atlantic Continental Shelf: U. S. Geol. Survey open file report 75-353 1975a.

U. S. Geological Survey, Sediments, structural framework, petroleum potential, environmental conditions, and operational considerations of the United States, South Atlantic Outer Continental Shelf: U. S. Geol. Survey open file report 75-411, 1975b.

U. S. Naval Oceanographic Office, Total magnetic intensity aeromagnetic survey 1964-1966 -- U.S. Atlantic coastal region: U. S. Naval Oceanographic Office, Washington D.C., 15 sheets, scale 1:500,000, 1966.

U. S. Naval Oceanographic Office, Residual magnetic intensity contour chart: Gulf of Mexico, environmental and acoustic altas of the Caribbean Sea and Gulf of Mexico, II, Marine Environment: U.S. Naval Oceanographic Office, Washington, D.C., scale: 1": 1° longitude.

Vail, P.R., R.M. Mitchum, Jr., S. Thompson, III, R.G. Todd, J.B. Sangree, J.M. Widmier, J.N. Robb, and W.G. Hatlelid, Seismic stratigraphy and global changes in sea level, *in* Payton, C.E., ed.

Stratigraphic interpretation of seismic data: AAPG Memoir 26, 1977.

Valentine, P.C., Shallow subsurface stratigraphy of the continental margin off southeastern Massachusetts: Abs. with Prog., GSA, v. 10, no. 2, p. 90, 1978.

Verrill, A.E., Occurrence of fossiliferous Tertiary rocks on the Grand Banks and Georges Bank: Amer. J. of Science, 3rd series, no. 16, p. 323-324, 1878.

Vogt, P.R., C.N. Anderson, and D.R. Bracey, Mesozoic magnetic anomalies, sea floor spreading, and geomagnetic reversals in the southwestern North Atlantic: J. Geophys. Res., 76, p. 4796-4823, 1971.

Weed, E.G.A., J.P. Menard, W.J. Perry, Jr., E.C. Rhodehamel, and E.I. Robbins, Generalized pre-Pleistocene geologic map of the northern United States Atlantic continental margin: U. S. Geol. Survey Misc. Inv. Series Map I-861, 1974.

Woollard, G.P., Crustal structre from gravity and seismic measurements: J. Geophys. Res., 64, p. 1521-1544, 1959.

Worzel, J.L., and G.L. Shurbert, Gravity anomalies at continental margins: National Acad. Science Proc., 41, p. 458-467, 1955.

Worzel, J.L., Pendulum gravity measurements at sea, 1936-1959: John Wiley and Sons, Inc., New York, 422 p., 1965.

# STRATIGRAPHIC EVOLUTION OF THE BLAKE PLATEAU AFTER A DECADE OF SCIENTIFIC DRILLING

Robert E. Sheridan

University of Delaware Newark, Delaware 19711

Paul Enos

State University of New York Binghamton, New York 13901

Abstract. The first ocean drilling for purely scientific purposes under JOIDES direction was carried out on the Blake Plateau in 1965. Six shallow-penetration holes (< 330 m) were drilled on the Florida continental shelf, continental slope and Blake Plateau. Bathyal Paleocene sediments were the oldest sediments recovered revealing that the Blake Plateau has been a relatively deep-water environment since at least that time. The continuity of reflectors bounding the Paleocene beneath the shelf and inner plateau rules out the possibility that the Florida slope originated through post-Paleocene faulting.

In 1975 Deep Sea Drilling Project Sites 390 and 392 were drilled on the Blake Nose, a topographic spur of the Black Escarpment. Campanian through Eocene nannofossil oozes were recovered above a pre-Campanian unconformity cut by submarine currents into Aptian-Albian nannofossil oozes. This evidence proves that strong bottom circulation occurred along the Blake Escarpment as early as Campanian. Moreover, the very fossiliferous Aptian-Albian nannofossil ooze indicates that the Blake Plateau was well oxygenated at the time when black shale was being deposited in the adjacent western North Atlantic basin. Very marked water stratification must have persisted during this time.

Below the Barremian nannofossil oozes at Sites 390 and 392, indurated Early Cretaceous shallow-water limestone was penetrated to 349 m. These rocks reveal an upward-shoaling sequence of open-shelf lime muds, oolites, and peritidal sediments followed by emergence and freshwater diagenesis. Subsequently, continued subsidence of the Blake Plateau terminated the shallow carbonate bank deposition and introduced submarine weathering at the edge of the Blake Plateau. A condensed sequence of nannofossil-ooze deposition began in the Barremian.

Chert interlayered with the Middle Paleocene to Middle Eocene nannofossil oozes at Site 390 correlates well with chert recovered at the same stratigraphic position in the globigerina oozes of JOIDES holes J3, J4, and J6 on the plateau proper. Widespread siliceous deposits were being formed across the Blake Plateau at about the same time as cherts were being deposited throughout the western North Atlantic basin.

The U.S.G.S. Atlantic Margin Coring Project in 1976 completed two holes on the Florida shelf and slope. The Late Cretaceous through Oligocene calcareous silt and clay of the continental slope contrasts markedly with the indurated limestone and dolomite of the same age under the shelf. Seismic profiles show that the slope existed during parts of the Late Cretaceous. A major unconformity was discovered which truncates Oligocene to Paleocene sediments and is overlain transgressively by Pliocene and Miocene sediments. Gulf Stream erosion in the Late Tertiary strongly dissected the Florida slope and western edge of the Blake Plateau and controlled the construction of this topography.

The stratigraphy of the Blake Plateau appears to derive mainly from the regional subsidence of the Atlantic margin which occurred at rates similar to those of the New Jersey shelf, for example. The interplay of the intrusion of submarine currents on eustatic sea-level changes with the persistence of carbonate bank-margin facies and the lack of detrital clastic sediments from hinterland sources gave rise to the sedimentary sequence of the Blake Plateau.

## Introduction

In 1965 the first ocean drilling for purely scientific purposes was attempted on the Blake Plateau. The drill ship D/V CALDRILL was transiting the area enroute to Grand Banks for commercial drilling, so part of the cost of the program was supported by Pan American Petroleum Corporation (AMOCO). Seeing an opportunity to begin drilling in the oceans, several marine geologists thought of submitting a modest proposal to NSF (for some $250,000) to have CALDRILL complete some holes on the Blake Plateau. The preliminary seismic refraction and reflection data, piston coring and dredging on the plateau formed a basis for identifying geological problems which could be addressed by drilling, and the intermediate depths of the plateau offered a deep water challenge that was still within the capabilities of the dynamically positioned D/V CALDRILL.

Yet this first scientific drilling program presented other challenges because it was an ambitious task and involved a great deal of money for a single proposal. Also, it was clear that success would lead to further drilling programs which would be competitively pursued by the individual oceanographic institutions. The marine geologists involved, such as Dr. Charles Drake, then of Lamont-Doherty Geological Observatory, fortunately possessed the political sensitivity to develop a consortium of institutions to approach NSF for such an undertaking. Thus, JOIDES (Joint Oceanographic Institutions Deep Earth Sampling) was founded by four oceanographic institutions, including Lamont-Doherty as the operator for the Blake Plateau Program, Woods Hole Oceanographic Institution, Scripps Institute of Oceanography, and the University of Miami (JOIDES, 1965). Now the multimillion dollar offspring of the first drilling program, DSDP (Deep Sea Drilling Project) and IPOD (international Phase of Ocean Drilling), are guided by a much-enlarged JOIDES involving fourteen institutions from six countries.

The CALDRILL program of 1965 completed six shallow-penetration holes (< 330 m), J1 through J6, three being on the Florida shelf and slope and three on the Blake Plateau (Fig. 1) (JOIDES, 1965). Subsequently, as part of Leg 44 of the Deep Sea Drilling Project, D/V GLOMAR CHALLENGER completed two sites in 1975 on the Blake Nose, a topographic spur of the steep Blake Escarpment. These were Sites 390 and 392 (Benson et al., 1976). Finally, as part of the U.S.G.S. Atlantic Margin Coring Project of 1976, D/V GLOMAR CONCEPTION completed two holes (6002 and 6004) on the Florida shelf and slope which contribute to the stratigraphic knowledge of the Blake Plateau (Hathaway et al., 1976). This paper will discuss these available drilling

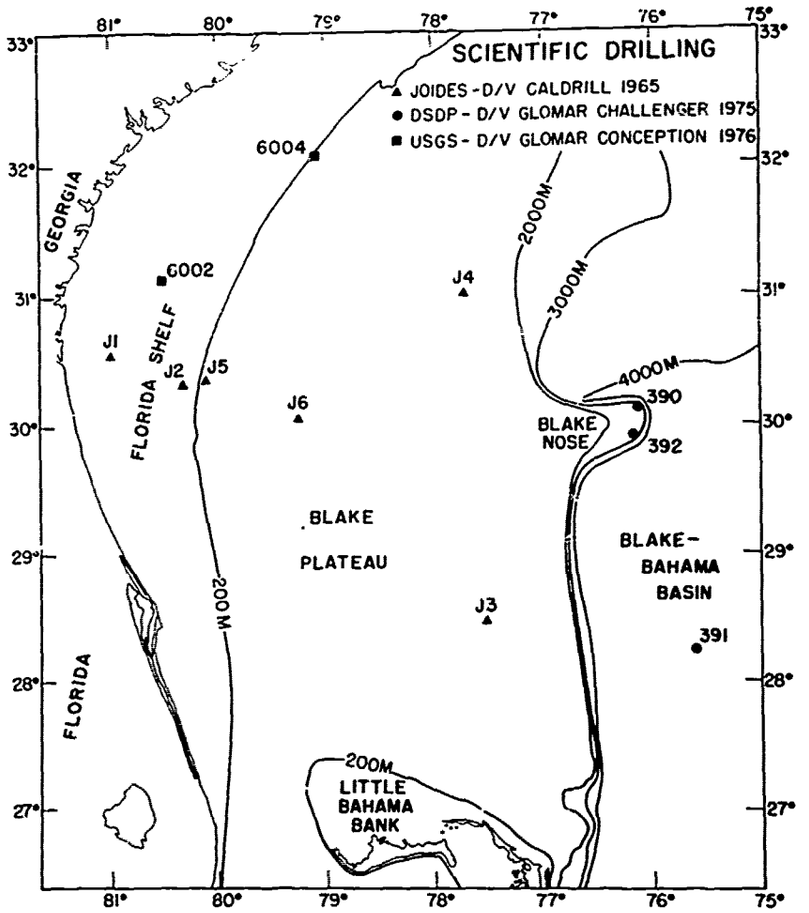


Fig. 1. Location map of the scientific drilling on the Blake Plateau. Sites from cruises of D/V CALDRILL (Schlee, 1977). D/V GLOMAR CHALLENGER (Benson et al., 1976), and D/V GLOMAR CONCEPTION (Hathaway et al., 1976) are shown. Also shown are the major physiographic features. Depths are in meters.

data, especially Sites 390 and 392, which the authors were involved in drilling.

## Drilling Results

Site 390 was selected because the Blake Nose offered a place to spud-in with soft ooze overlying deeper reflectors brought within reach of the drill by erosional unconformities (Fig. 2). The deeper reflectors appeared seismically to be harder rock (Sheridan et al., 1978; Ewing et al., 1966), which was verified by dredging and piston coring of the surficial deposits of the escarpment (Heezen and Sheridan 1966). The drilling proved that Eocene throgh Campanian nannofossil ooze overlies Barremian and older limestones of a neritic facies to a total depth of 206 m subbottom.

Site 392 was selected to calibrate the opaque reflection zone below rough hyperbolic relectors commonly seen at the edge of the Blake Escarpment. This had been interpreted as a "reefal ridge" by Ewing et al. (1966). Again a thin cover of ooze permitted spudding-in, and hard limestone of bank-margin facies was penetrated to 349 m subbottom (Benson et al., 1976) (Fig. 3).

Sites 390 and 392 have recovered the oldest in-place strata under the Blake Plateau, the Barremian or older Early Cretaceous limestone. This datum forms the present base of our direct knowledge of the stratigraphy, although geophysical inferences and correlations indicate that older Jurassic and possibly Triassic sediments should exist at greater depth.

During the Early Cretaceous the Blake Escarpment included environments typical of the present margins of the Bahama Banks (Fig. 4) (Enos and Freeman, 1978). In hole 392A cavernous skelmoldic limestone is a shallow, somewhat restricted, marine limestone with a history of subaerial exposure, fresh water leaching, and karst development. These exposures were probably due to recurring eustatic sea-level fluctuations superimposed on a continually subsiding margin. In drilling over 100 m of this unit the drill bit experienced two sudden drops, one of 4 m and the other a series of small drops totalling 10 m. These drops presumably reflect caverns to be found in the lower half of the unit. Figure 5 shows

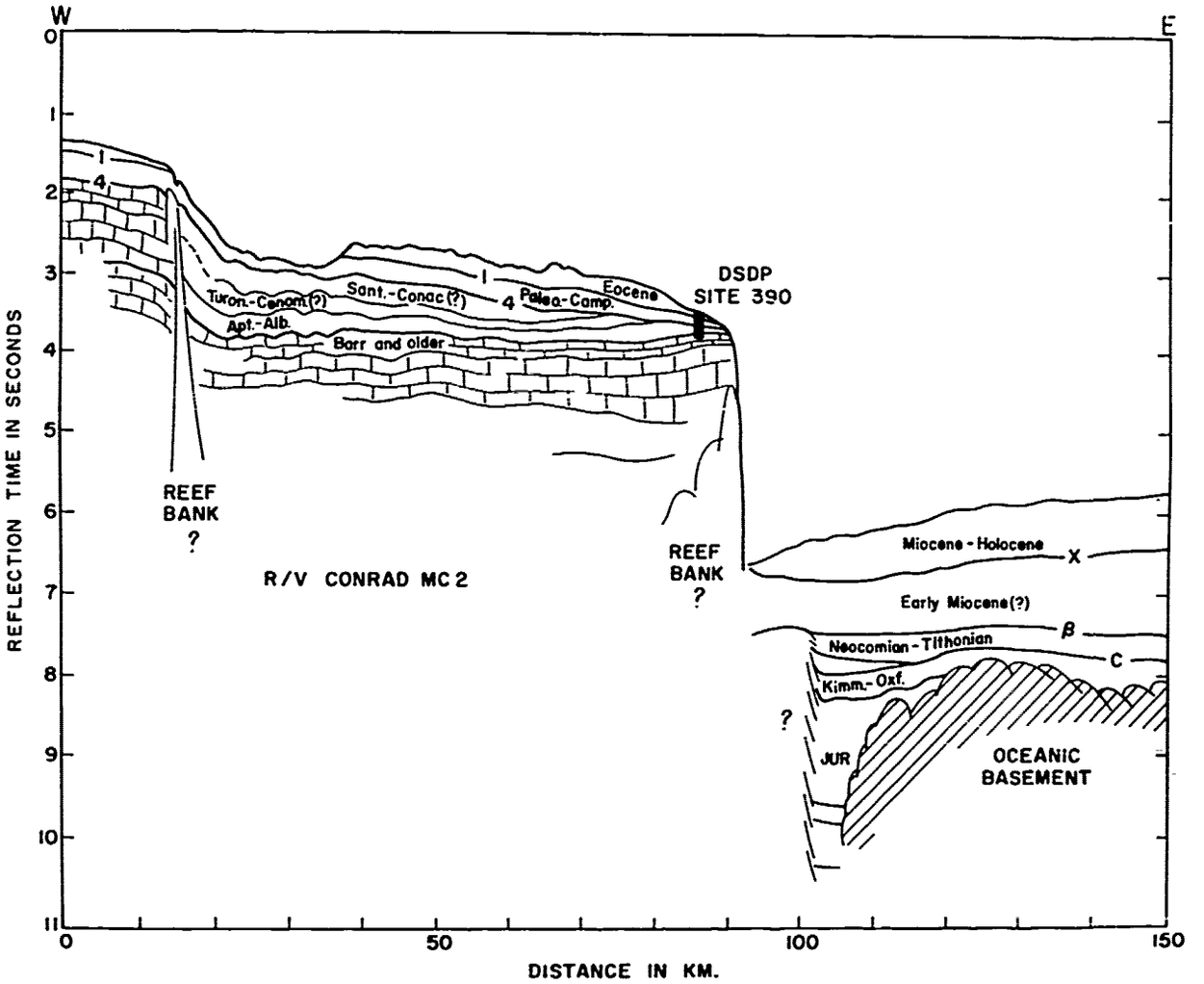


Fig. 2. Line drawing with geologic age correlation of seismic reflection profile MC 2 of R/V CONRAD through Site 390 (Benson et al., 1975; Sheridan et al., in press). Note carbonate bank margin facies identified as hyperbolic reflectors atop an opaque, reflectionless zone.

about the largest cavern we could hope to sample with a core. Calcite schalenohedra projecting into the mini-caverns are probably phreatic-zone cement, not unlike that found in "crystal caverns". Development of this large-scale pore network early in the history could potentially form an excellent petroleum reservoir. However, because of its proximity to the steep Blake Escarpment (about 1 km from the edge) and the lack of effective seals any petroleum was flushed through and out to sea, as noted by Meyerhoff and Hatten (1974) in their evaluation of some Bahamian wells.

Carbonate accumulation at a rate greater than combined subsidence and sea-level rise led to oolite formation at Site 392 in a shallow-water, high-energy environment (Fig. 6a). Dripstone texture in the oolite indicates vertical accretion to form islands with development of a water table (Fig. 6b). The formation of air-water meniscuses in the aerated vadose zone led to differential nourishment of crystals and molding of internal sediment to form the unusual curved surfaces and "bridges" of micrite in the first stage of cementation. Later cementation produced second-generation sparry cement, probably in the phreatic zone, which sealed virtually all the pores (Figure. 6b). Abundant algal fragments intermixed with the ooids (Fig. 7) attest to the presence of organically productive areas, possibly algal reefs.

The topmost limestone has "birds-eye" or fenestral fabric characteristic of many tidal-flat carbonate deposits (Fig. 8). Carbonate muds accumulated behind the oolite shoals and islands along the edge of the Blake Escarpment. Frequent intertidal exposure causes mud cracks (Fig. 9) and promoted expulsion of gas bubbles to create a vein-like appearance (Fig. 10). Burial and freshwater diagenesis cemented the bank-margin limestones into a dense rigid mass with seismic velocities as high as 5.5 km/sec. Subsequent erosion accentuated the bank-margin relief.

Continued subsidence with marine current bypassing allowed the formation of goethitic crusts and pisolites on the exposed limestone surfaces (Fig. 11). The crusts incorporate nannoplankton (Fig. 12) and planktonic foraminifers (Fig. 13), indicating submarine origins. Barremian (?), Aptian, and Albian nannofossil ooze overlie this goethitic crust. The subsidence and sea-level rise resulted in a rapid change in paleoenvironment to deep bathyal levels (Fig. 14), although the deepening that occurred between Barremian and Late Aptian, based on avail-

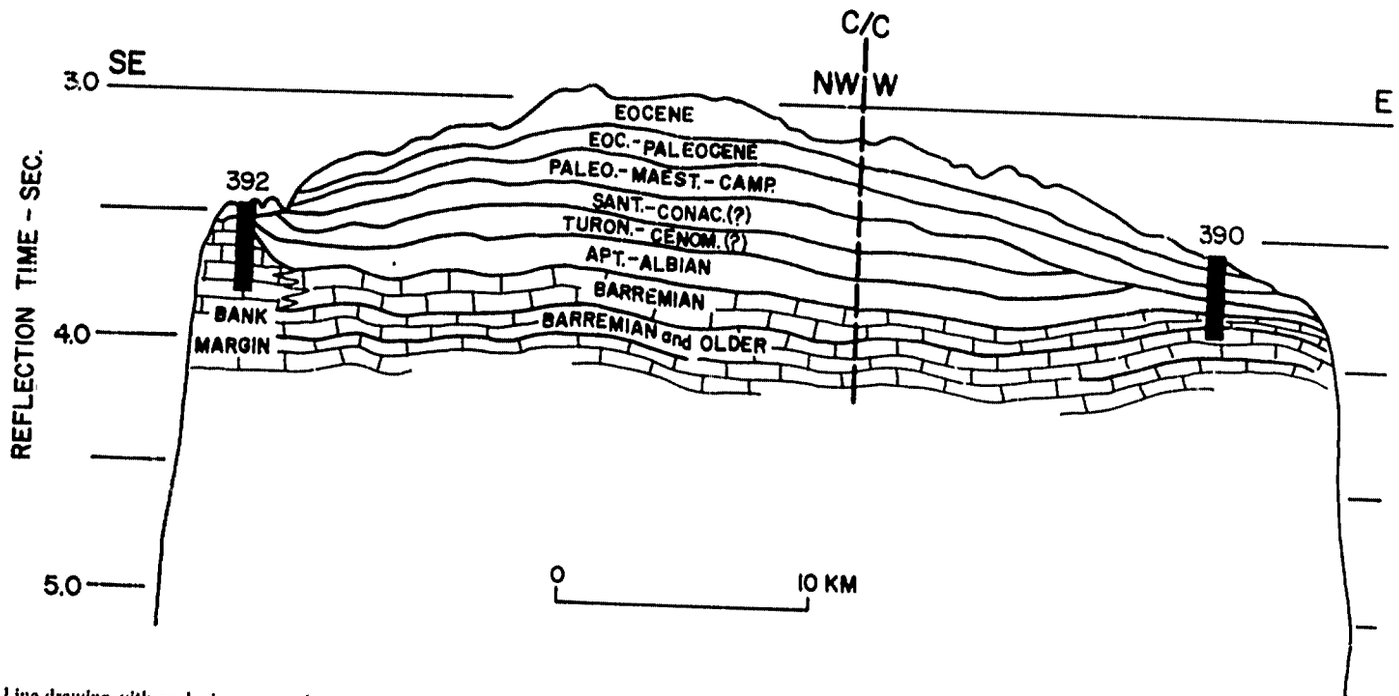


Fig. 3. Line drawing with geologic age correlation of seismic reflection profile of GLOMAR CHALLENGER connecting Site 390 and 392 (Benson et al. 1978). Bank margin at Site 392 gave hyperbolic, opaque reflection pattern.

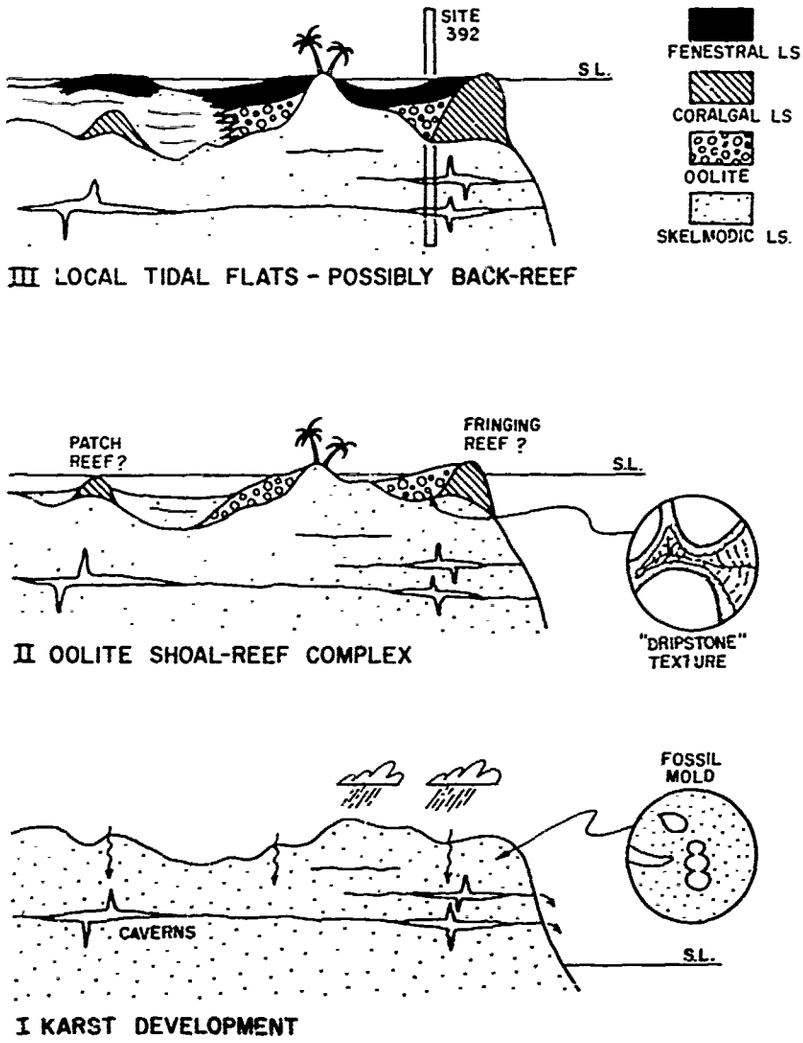


Fig. 4. Sequence of depositional events at Site 392 which produced units of identifiable paleoenvironments of Barremian and older Early Cretaceous age (Benson et al., 1978).

able cores 3 and 4 of hole 392A, did not require subsidence rates appreciably different than those for the rest of the Atlantic margin, 4-5 cm/1000 yrs. Although abrupt increase in subsidence rate is not called for lack of deposition keeping pace with regional subsidence is indicated at Site 392.

Very fossiliferous nannofossil ooze accumulated on the Blake Nose during the Aptian and Albian at the same time that carbonaceous black shale was being deposited in the stagnant deep western North Atlantic basin. Given regional subsidence rates of 4-5 cm/1000 yrs. and the paleobathymetry from 392A (Fig. 14), the Blake Nose was about 1000 m deep by Albian time. Thus somewhere between this intermediate depth of 1000 m and the 3200 to 5000 m depths of deposition of the black shale (Tucholke and Vogt, 1978) of the Hatteras Formation in the deep basin (Jansa et al., 1978) there must have existed a strong oceanic stratification (pycnocline), with oxygenated waters above stagnant anoxic waters. More drilling elsewhere in the Atlantic is needed to better define the exact paleo-depth of this boundary. Some theories, such as that of Schlanger and Jenkyns (1975), suggest that the oceanic oxygen minimum zone was expanded downward to encompass intermediate and abyssal depths during the Cretaceous as an alternate to stagnant, deep anoxic basins confined by local physiography. Sites 390 and 392 put upper limits on the depth of the oxygen minimum zone; it did not extend onto the continental shelf.

Above the lower Albian ooze, a major unconformity spans the late Albian through early Campanian at Sites 390 and 392. This is well documented at Site 390 where continuous coring crossed the boundary. Seismic profiles (Figs. 1 and 2) show low-angle truncation rather than lap-out of the missing Upper Cretaceous section. The nannofossil oozes found above and below the unconformity suggest submarine erosion and bypassing by strong currents at depths of 1000 to 2000 m. Tracing the unconformity landward on the Blake Nose, where it appears conformable with the addition of several layers of Cretaceous sediments, indicates that the currents could have originated just prior to the Campanian, with the Campanian sediments onlapping on the erosional

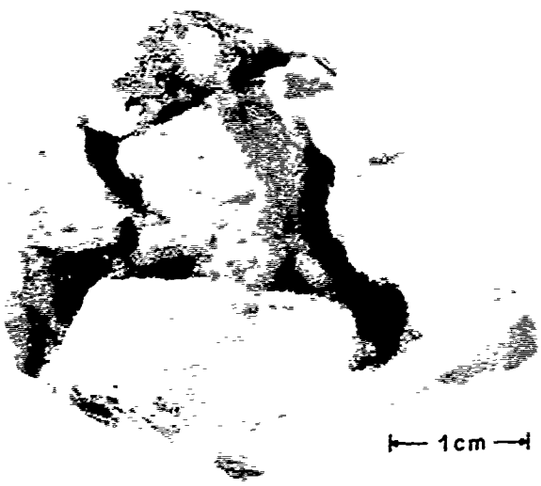


Fig. 5. Cut section of core of cavernous vuggy limestone from Site 392A, subbottom depth 326 m (from Enos and Freeman, 1978).

unconformity after deposition resumed. If these layers of Cretaceous sediments accumulated at reasonable sedimentation rates, this would suggest that the Santonian through Cenomanian sediments exist on the nose beneath the Campanian where these beds are conformable.

The erosive currents must have been deep, bottom-following contour currents rather than surface currents such as the present Antilles Current and Gulf Stream. If these deep currents were part of the Atlantic geostrophic bottom water circulation then such circulation apparently occurred just prior to the Campanian. This may correspond to changes in the deep western North Atlantic circulation in the Late Cretaceous, when the anoxic conditions ended and well oxygenated red and varicolored clays of the Plantagenet Formation (Cenomanian to Paleocene) were deposited (Jansa et al., 1978). The pre-Campanian unconformity can be traced westward under the Blake Plateau (Fig. 2) where it is correlated with Reflector 4 as mapped by Ewing et al. (1966).

During the Paleocene through middle Eocene, sediments rich in biogenic silica were deposited on the Blake Nose with subsequent diagenesis to form chert (Fig. 15). The cherts occur in the lower half of a 90 m interval of nannofossil ooze which is generally rich in siliceous skeletons, particularly sponge spicules and radiolarians (Fig. 15). In the bottom 19 m where the chert and lithified ooze are most abundant, however, siliceous skeletons are rare. This may reflect more complete mobilization of the biogenic silica to form chert. No evidence of volanic activity was noted in this interval. One percent of zeolite is reported in some samples from this interval and from the underlying Lower Paleocene (Danian) ooze, but it is clinoptilolite which probably has a biogenic rather than a volcanogenic source for silica (T. W. Donelly, pers. com.).

The Paleocene and lower Eocene chert of the Blake Nose is correlated with Reflector 1 (Fig. 2), which was traced westward over the wide area of the Blake Plateau by Ewing et al. (1966). The chert at Site 390 correlates well with chert from JOIDES Sites J3, J4, and J6 on the Blake Plateau. Thus the chert is very widespread on the Blake Plateau, as it is in the western North Atlantic basin where Paleocene to middle Eocene chert of the Bermuda Rise Formation (Jansa et al., 1978) forms a prominent seismic Horizon $A^c$ (Tucholke and Moutain, 1978). Silicification and chert are also widespread in the southeastern Atlantic coastal plain rocks of about this age, in units such as the Tallahatta Formation (mid-Eocene) (J. Reinhardt, pers. comm.; Gohn et al., 1976), and the Beaufort Formation (Danian; Gohn et al., 1976). No chert was detected on the continental shelf or Florida-Hatteras slope coring by the JOIDES or U.S.G.S. (although penetration below upper Eocene was limited). A piece of black chert was recovered at Site 6004 (Fig. 1) in the Miocene sediment just above the unconformity with the Paleocene clay (Hathaway, et al., 1976). This chert might be reworked from the widespread Paleocene-Eocene chert layer which was eroded by the Gulf Stream.

The chert on the Blake Plateau implies that the diagenetic conditions for silica mobilization and redeposition from pore waters were prevailing in these intermediate depths (~ 1000 m), as well as in the deep western North Atlantic (4500-5000 m) and on the coastal plain, during the Paleocene to mid-Eocene. Chert formation which produced seismic Horizon $A^c$ was therefore not unique to the deep basin, but was much more widespread.

The controversy over biogenic vs. volcanogenic origin of the silica persists for all these environments as well. The chert is clearly of replacement origin: foraminifera and the carbonate matrix, consisting largely of nannofossils, are replaced quite as readily as available porosity is filled along an irregular but sharp "front" (Fig. 16). In the chert formations of the JOIDES holes, there are abundant radiolarians and sponge spicules to act as the source of silica (Fig. 17), but there are abundant volcanic ash deposits as well. The ash layers extend up into the Miocene well above the Eocene chert (Schlee, 1977; Charm et al., 1969); yet there are no Miocene chert deposits.

## Stratigraphic Cross-Section

Enough seismic refraction and reflection data are available on the Blake Plateau to correlate units between the drill holes and to map them elsewhere on the plateau away from the calibration points. Seismic velocity data from Hersey et al. (1959) and Sheridan et al. (1966) reveal much about the lithofacies variations. Single-channel reflection profiles penetrating the upper 2 seconds of the sediments have been used to map the Upper Cretaceous and Tertiary strata by Ewing et al. (1966) and Emergy and Zarudski (1967). More recently, deeper penetration reflection profiles showing the Lower Cretaceous reflectors have been achieved (Sheridan et al., 1978), and multichannel reflection profiles of good quality show inferred Jurassic and Triassic reflectors as deep as 5 sec (Dillion et al., 1976 and 1977; Shipley et al., 1978). These data have been used to construct a stratigraphic cross-section across the Blake Plateau (Fig. 18).

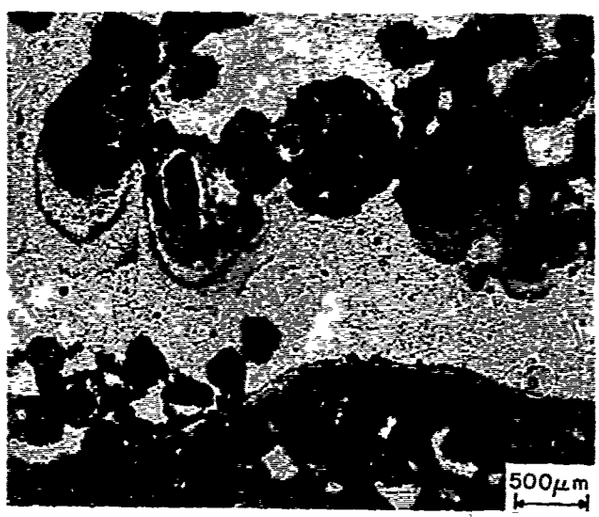


Fig. 6a. Photomicrograph of thin section of oolite from Site 392A (222.3 m subbottom) showing "dripstone" structures and bridges of internal cement (from Enos and Freeman, 1978).

The characteristic opaque or reflector-free zone under hyperbolic reflectors shown at Site 392 to be cemented bank-margin limestone, can be seen beneath Reflector 4 under the plateau edge at 2.0 sec depth on reflection profile MC 2 of R/V CONRAD from Site 390 westward to the Blake Plateau (Fig. 2). Nearby seismic refraction profiles indicate relatively high velocities below Reflector 4, approximately 4 to 4.5 km/sec (Sheridan et al., 1966). These velocities are reasonable for well-cemented shallow-water limestones and suggest a facies change at the Blake Escarpment. Thus it is interpreted that a well-cemented shallow bank margin existed under the edge of the Blake Plateau at present depths of 1500 m. The continuity of reflectors, especially Reflector 4, west of Site 390 (Fig. 2) indicates the bank margin persisted later than the Barremian, perhaps until deposition fo the Campanian oozes above Reflector 4, thus possibly through the Santonian. This margin is interpreted as an Aptian through Santonian reef in Figure 18 although lithofacies details are of course unknown and the margin could be of older Cretaceous age.

The reason for this shift in the bank margin in Barremian to a position of a few km west of the Blake Nose Sites 390 and 392 is not clear. Apparently there was a eustatic lowering of sea-level curing the Valanginian (Vail et al., 1977) with a subsequent eustatic rise in Barremian and this ended the carbonate bank development on the West African margin (Mitchum et al., 197*i*). The termination of the carbonate bank margin at Site 392 may be a response to a similar eustatic cycle, with a still stand in Barremian (Vail et al., 1977) during which shoaling and exposure occurred to terminate the carbonate buildup, and a subsequent resumption in the rise in sea level to cause drowning of the bank margin on the Blake Nose, then islands and tidal flats, and a shifting of the

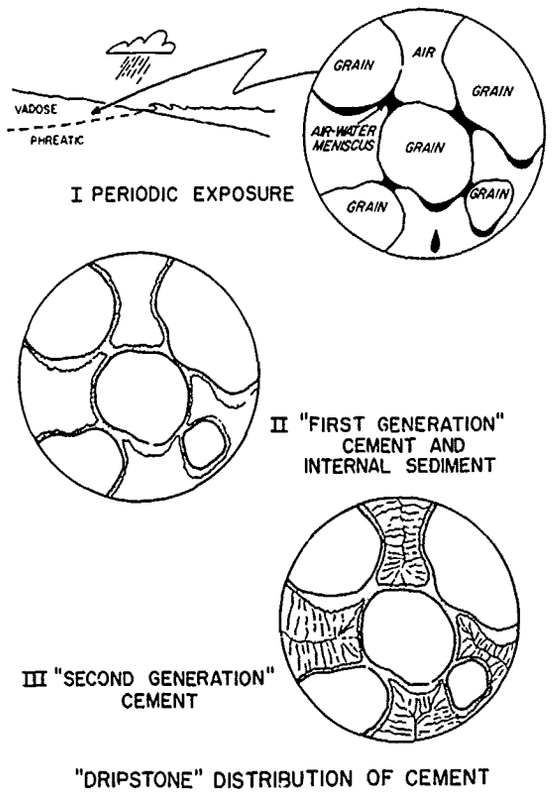


Fig. 6b. Interpretation of "dripstone" structure as indicating periodic exposure to vadose water circulation (Benson et al., 1978).

Fig. 7. Photomicrograph of algal fragment in oolite of Site 392A, 232 m subbottom. Algae is of genus Acroporella, a dasycladacian green algae. Specimen is 2.5 mm across (from Enos and Freeman, 1978).

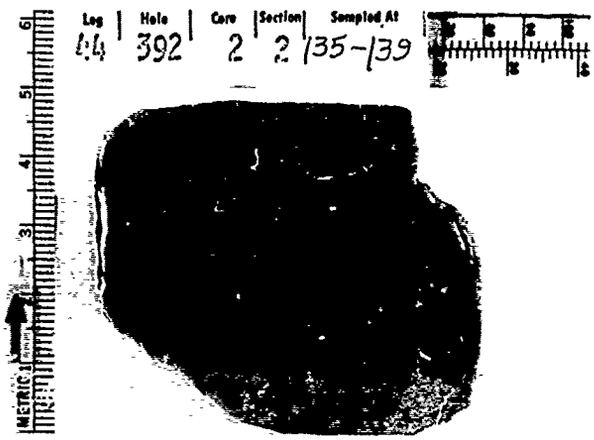


Fig. 8. Cut section of core of fenestral limestone of Site 392A, 141 m subbottom. Note lenticular "birds eye" structures.

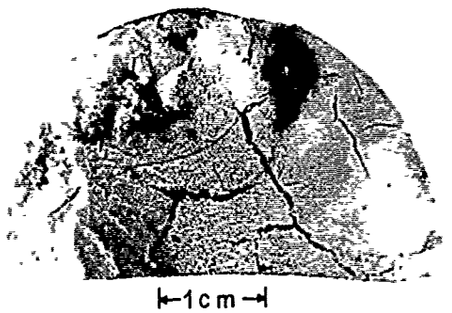


Fig. 9. Core fragment of fenestral limestone showing mud crack on bedding plane. Site 392A, 194 m subbottom (from Enos and Freeman, 1978).

edge of the carbonate buildup farther landward.

The cross-section (Fig. 18) is interpolated from the ocean drilling holes offshore to the stratigraphy from deep wells in Florida and the Bahamas (Applin and Applin, 1965; Maher, 1965; Tator and Hatfield,


Fig. 10. Photomicrograph of fenestral limestone from Site 392A, 108.5 m subbottom. "Veinlet" in fine-grained lime muds produced by gas bubble escape was partially filled with coarser grained bioclastic sand.

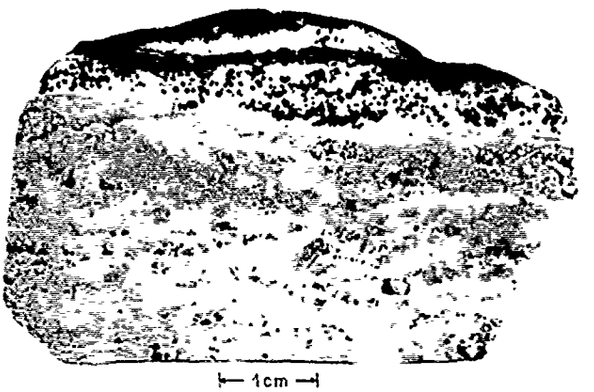


Fig. 11. Cut section of core with crust of red goethitic pisolites in pelagic limestone overlying an erosion surface on fenestral limestone, Site 392, 49 m subbottom (from Enos and Freeman, 1978).

1975). One such well is the Humble Oil and Refining Co. deep test to Paleozoic basement in northern Florida shown on Figure 18 (Maher, 1965). From such drilling data the earlier evolution of the Blake Plateau can be interpreted.

Based on exposed geology of the Atlantic margin to the north, it is a reasonable interpretation that Paleozoic and Precambrian rocks of the Florida-African basement were rifted in the Triassic into fault-bound grabens to form deep sedimentary basins (Dillon et al., 1977; Shipley et al., 1978). Clastics, redbeds, and volcaniclastics of Triassic age are known from the subsurface in Georgia and northern Florida (Murray, 1961) and are reported from a deep test well on Great Isaac Island in the northern Bahamas (Tator and Hatfield, 1975). These clastics probably extend north and east under the inner part of the Blake Plateau.

As rifting proceeded and breakup occurred to initiate seafloor spreading of the early Atlantic Ocean in the Early Jurassic, the pre-breakup unconformity on Triassic clastics and volcanics subsided and

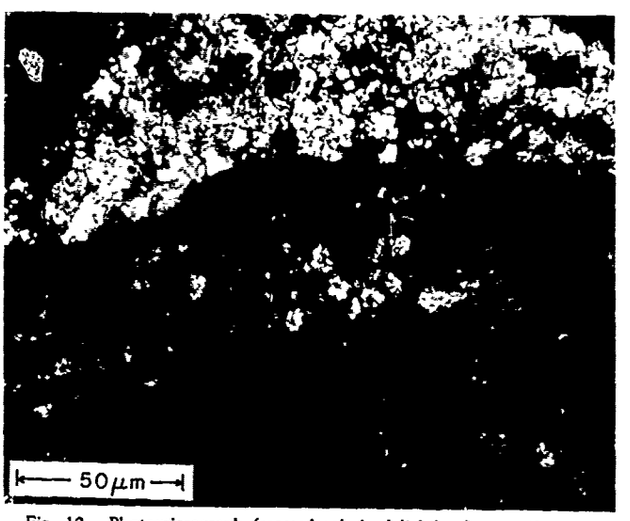


Fig. 12. Photomicrograph (crossed-polarized light) of concretionary growth lamina of geothitic pisolite which includes nannofossils. Site 392, 90 m subbottom, cross-polarized light (from Enos and Freeman, 1978).

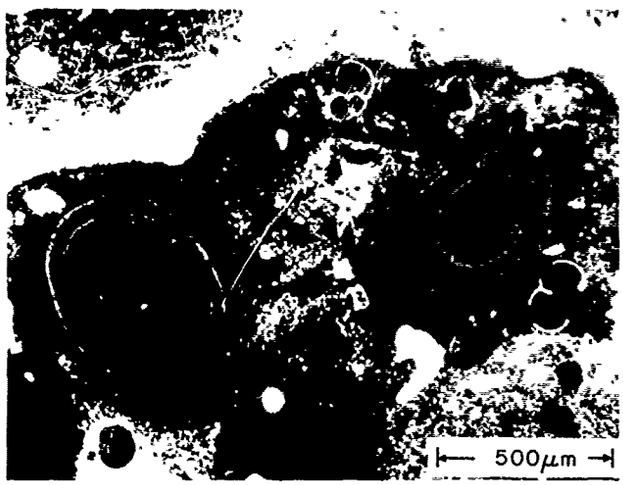


Fig. 13. Photomicrograph pisolitic goethite crust containing planktonic foraminifera from Site 392, 49 m subbottom (from Enos and Freeman, 1978).

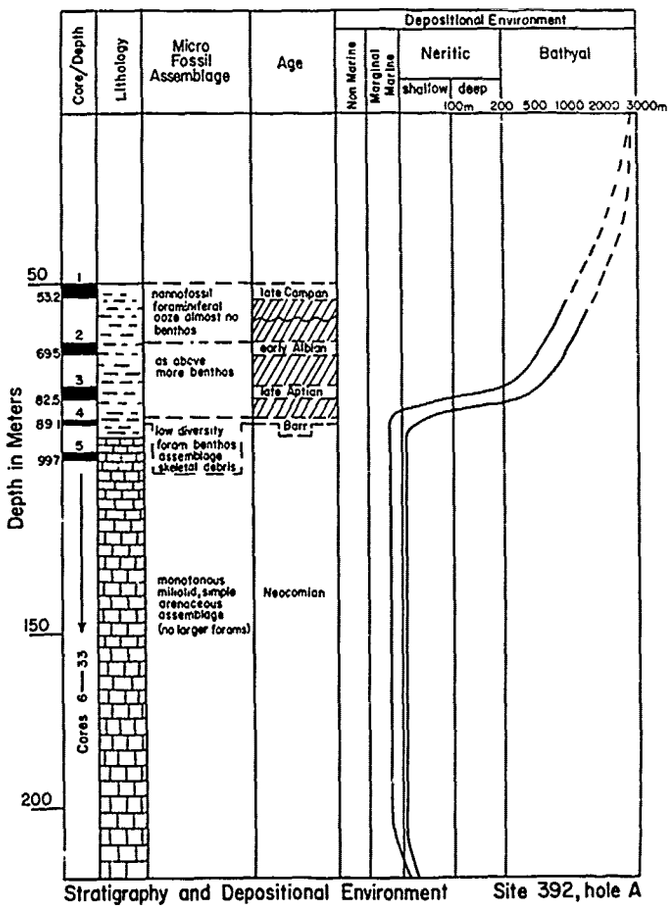


Fig. 14. Paleobathymetry based on facies and microfossils plotted for core samples of Hole 392A (Benson et al., 1978).


Fig. 15. Cut section of core of chert in Eocene cemented limestone of Site 390A, 77.7 m subbottom.

tilted seaward. Soon Jurassic Marine clastics and limestones invaded the Blake Plateau basin and onlapped the Triassic beds. The Great Isaac well penetrated these Jurassic limestones and they very likely continue northward from the Bahamas and underlie the Blake Plateau.

Early Cretaceous terrigenous clastic sands and shales of northern Florida (Applin and Applin, 1965) give way seaward to limestone and dolomite deposited farther offshore under the Blake Plateau in a platform environment behind a typical bank margin complex of oolite shoals, islands, and pertidal mud flats, and possibly organic reefs (Benson et al., 1978). With a decreasing supply of sand and shale to the Florida-Blake Plateau area, the Cretaceous sands and shales grade upward to shelf limestones, such as the Lawson Limestone, in the Late Cretaceous (Maher, 1965). On the Florida platform shelf limestone deposition persisted into the Eocene.

Under the main portion of the plateau, the seismic reflection patterns and interval velocities discussed above (Fig. 2) indicate that the carbonate banks and shallow water limestone deposition may have persisted until the time of Reflector 4, correlated at Site 390 with the pre-Campanian unconformity. Thus shallow water limestone is interpreted to have existed into possibly the Santonian, after which a Campanian transgression occurred and the water on the plateau deepened with continued subsidence in the absence of shelf or bank sedimentation.

The Campanian and Maestrichtian biogenic oozes drilled at Site 390 (Benson et al., 1976) can be traced with seismic continuity up on the plateau (Fig. 2) where the seismic transparency of the interval between Reflectors 1 and 4 (Ewing et al., 1966; Shipley et al., 1978) and

the low interval velocities of 1.7-3.0 km/sec (Hersey et al., 1959; Sheridan et al., 1966) indicate that the pelagic ooze facies persists well westward. Bathyal nannofossil, globigerinid, and pteropod oozes are recovered in the JOIDES core holes J3, J4, and J6, so the bathyal environment is well documented from the Paleocene through "post-Miocene" (Schlee, 1977). The thin Tertiary oozes reflect the low biogenic sedimentation rates, while the sedimentary section was further abbreviated by current erosion and bypassing on the plateau throughout this time.

With continued subsidence coupled with alternating erosion and bypassing to slow pelagic deposition, the Blake Plateau has deepened since the Campanian. As noted earlier, this apparently occurred without any abrupt increase in subsidence rates. No downfaulting of the plateau is necessary to explain the depositional history. The continuity of the Paleocene from Florida to the Blake Plateau precludes any post-Paleocene faulting between the Florida Shelf and Blake Plateau (JOIDES, 1965).

The relief between the Florida Shelf and plateau results from continued regional subsidence, but while the Blake Plateau progressively deepened, shallow-water carbonate deposition in more landward (and presumably less rapidly subsiding) areas kept pace with sea-level. The

Fig. 16. Photomicrograph from JOIDES hole J6 showing boundary of chert (right) and limestone. Foraminiferal test at chert contact is only partly replaced by silica. Subbottom depth 68.6 m, upper Eocene, cross-polarized light.

Fig. 17. Photomicrograph of siliceous limestone from JOIDES hole J4 showing abundant radiolaria (partly replaced by microquartz) and sponge spicules. Subbottom depth 157.6 m, Paleocene.

shelf edge consequently built-up in place slightly west of its present position and at times prograded seaward to near its present location. The major progradation occurred during the Eocene as shown by JOIDES holes J1, J2, and J5. Emery and Zarudski (1967) and Uchupi and Emery (1967) speculated on a Cretaceous "reef" under the inner part of the shelf based on relief observed in single channel reflection profiles, and late Cretaceous prograding seismic reflectors under the Florida slope (Shipley et al., 1978) suggest relief in this area even then. Persistence of deep-water sedimentation under the present Florida-Hatteras slope is proven by the recovery of Maestrichtian bathyal clays at Site 603 (Fig. 1), as reported by Poag (1978). This puts an eastern limit on the extent of shelf progradation during Late Cretaceous. One possible interpretation of the hiatuses at that site is that Gulf Stream current erosion controlled the position of the slope as early as the end of the Cretaceous.

Partially as a result of a slow sedimentation on the Blake Plateau in the Tertiary, several (as many as 9) volcanic ash layers were encountered in the JOIDES cores (Schlee, 1977). Vulcanism in the lesser Antilles and Caribbean is the likely source, thus the ash beds are indicative of

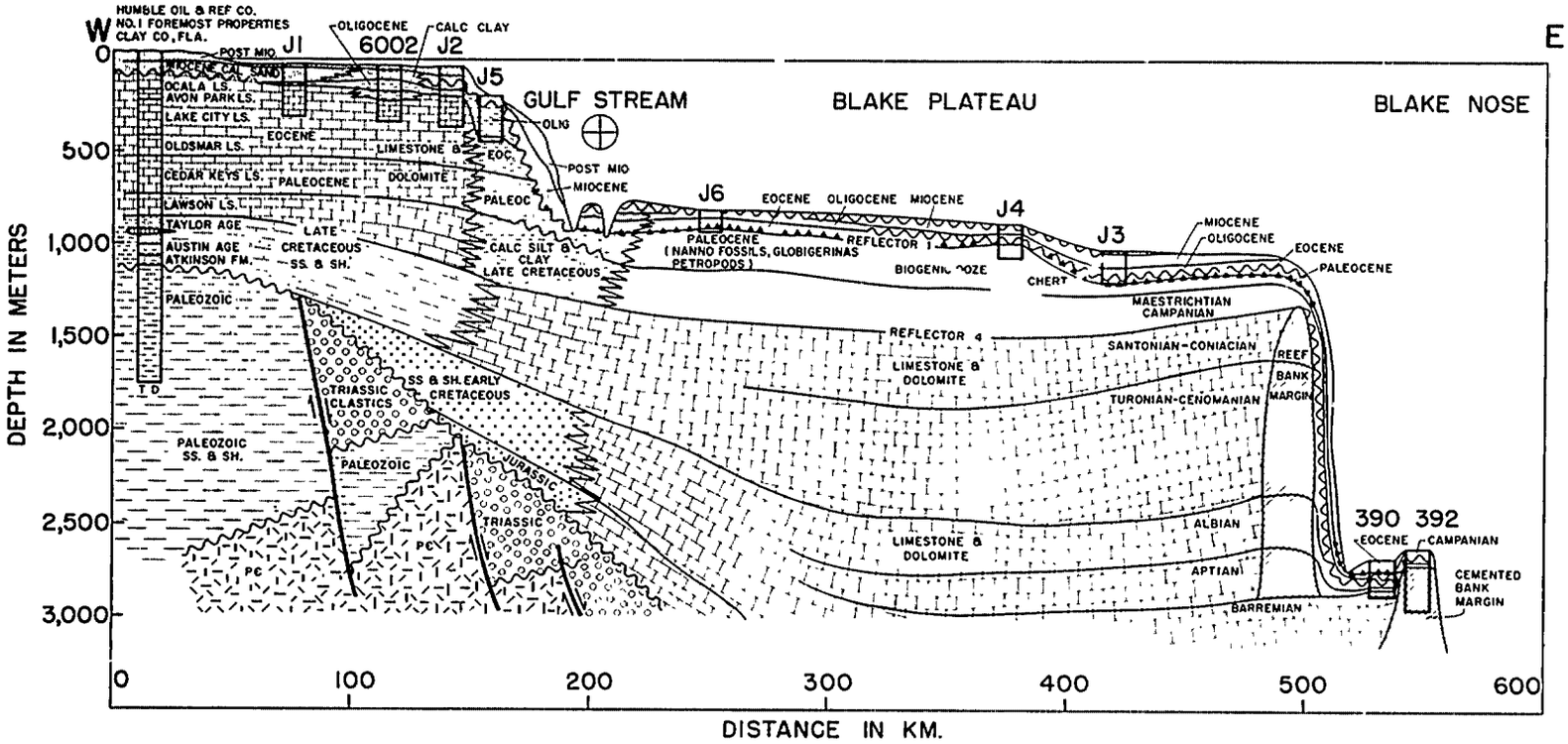


Fig. 18. Diagrammatic stratigraphic cross-section across the Blake Plateau based on the drilling data shown and correlations from wells off-section. The identified seismic reflectors 1 and 4 are used as in (Ewing et al. 1966).

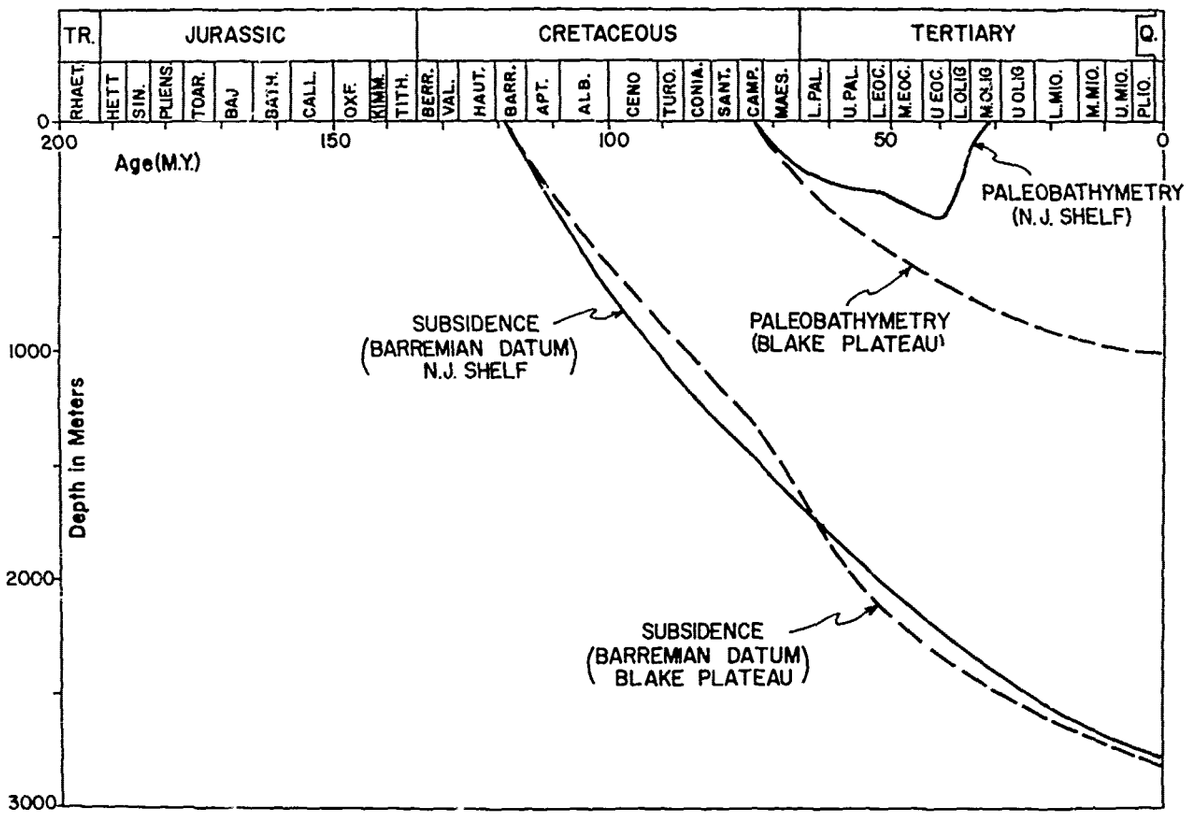


Fig. 19. Subsidence history of Barremian datum of the Blake Plateau compared with subsidence of the same datum on the New Jersey shelf. Also shown are the paleobathymetry plots for the two areas.

the direction of prevailing winds and currents rather than of changes in environment on the Blake Plateau.

The stratigraphic correlations presented here are different than those recently proposed for the Blake area by Shipley et al. (1978). These authors placed their Reflector 4 below the high velocity (3.6-5.1 km/sec) shallow-water limestone of the inner Blake Plateau and tentatively correlated Reflector 4 with the mid-Cenomanian. On the other hand, we correlated Reflector 4 with the pre-Campanian unconformity drilled at Site 390 (Fig. 2), and this reflector as mapped by Ewing et al. (1966) continues to above the high-velocity, shallow-water limestone of the inner and southern Blake Plateau. This pre-Campanian identification of Reflector 4 roughly agrees with that of Ewing et al. (1966) who traced this reflector within 50 km of the coastal wells of Florida where it projects to be equivalent to beds of Taylor (early Campanian) age (Fig. 18). Shipley et al. (1978) identify a reflector of Santonian-Coniacian age above the high velocity (3.6-5.1 km/sec) shallow-water limestone on the inner Blake Plateau, but they have correlated that reflector with Reflector 3 of Ewing et al. (1966) rather than Reflector 4. However, on the inner plateau, Reflector 3 of Ewing et al. (1966) is at 1.6 sec depth, while Reflector 4 is at 1.9 sec; the 1.9 sec reflector of Shipley et al. (1978) is called their Reflector 3. The near merging of Reflectors 3 and 4 seaward on the Blake Plateau and time-transgressive facies changes lead to this confusion between the Ewing et al. (1966) and Shipley et al (1978) terminology.

A deeper reflector of Shipley et al. (1978) which nearly crops out on the Blake Escarpment at 2800 m is tentatively correlated by them as mid-Aptian. This reflector is nearly at the same depth as the deepest reflector cored at Site 390, which correlates with Barremian and older shallow-water limestone. If these are indeed the same reflecting horizons, then these older Barremian and early Aptian sediments are shallower than shown on the Blake Plateau cross-section of Shipley et al. (1978).

In the deep Blake-Bahama Basin, Figure 2 shows the prominent reflector below Horizon $\beta$ which Shipley et al. (1978) tentatively correlated as the top of Oxfordian. Sheridan et al. (1978) now have identified the reflector as Horizon C which was drilled at Site 391 (Benson et al., 1976). At Site 391 Horizon C is correlated with the transition from Upper Tithonian white limestone to the Lower Tithonian (Kimmeridgian) red argillaceous limestone (Fig. 2). This prominent reflector marks the top of the Cat Gap Formation (Jansa et al., 1978).

## Subsidence of Blake Plateau

With the data from Sites 390 and 392 it is possible to deduce the stratigraphy of the Blake Plateau back to the Barremian (Fig. 18). Given this stratigraphy, the subsidence history and paleobathymetry can be plotted, based on the identification of the Barremian reflector and of Reflector 4 as the top of shallow-water limestone, perhaps as young as Santonian, and Reflector 1 as the basal Eocene chert. Using the present depth of these reflectors under the Blake Plateau, the seismically determined sediment thickness, and the interpreted depth of deposition of

the strata of these reflectors, the position of the Barremian datum can be interpolated through geologic time (Fig. 19). The depth of this datum at the end of Santonian is fixed by the thickness of shallow-water limestone above it. Post-Campanian paleobathymetry can be estimated from the drilled Paleocene and younger facies and the thickness of these younger sediments. This paleobathymetry and accumulated sediment thickness above the datum give the depth to the Barremian in the post-Campanian.

As a comparison, the subsidence history and paleobathymetry of a Barremian datum beneath the New Jersey shelf is plotted based on the data from the COST B2 well (Smith et al., 1976). The track of the Barremian datum is very similar in both the Blake Plateau and the New Jersey shelf area, suggesting that both areas were subsiding as part of the same tilt of the Atlantic Margin, at least since Barremian. The regional subsidence rates generally decreased exponentially from 4 to 5 cm/1000 yrs to 1 to 2 cm/1000 yrs since the Barremian for both areas If the pre-reflector 4 rocks are older than the minimum age of Santonian interpreted above, the Blake Plateau curve would be steeper in earlier portions and flatten more markedly. No significant differences in subsidence rates are indicated for the Blake Plateau and New Jersey shelf in Fig. 19. If subsequent dating of the pre-reflector 4 interval introduces an L-shaped rather than a smooth curve, this would suggest down-faulting of the Blake Plateau, which is not indicated by present seismic data. Moreover, some explanation of why the Blake Plateau did not continue to subside at a rate comparable to the rest of the Atlantic Margin would be required. Both Blake Plateau and the New Jersey shelf began to deepen with the Campanian-Maestrichtian transgression which caused bathyal depths on the New Jersey shelf in the Eocene. The Gulf Stream prevented further deposition on the Blake Plateau, while on the New Jersey shelf clastic sands and gravels prograded on the shelf in the Miocene and Pliocene, upbuilding the shelf to a shallow depth. Miocene quartz sands also prograded the Florida shelf edge slightly but apparently never crossed the Gulf Stream barrier to build up the Blake plateau (Fig. 18).

## Summary and Conclusions

In summary, the stratigraphic evolution of the Blake Plateau appears to derive mainly from the regional subsidence of the Atlantic continental margin of North America, with superimposed environmental factors, such as the persistence of carbonate bank margins which supported a carbonate platform, the trapping of terrigenous clastics in deltaic estuaries of inshore shelf areas, the intrusion of currents which eroded and prevented deposition, and the eustatic changes in sea level which may have terminated carbonate bank accretion upon regressions, and shifted the locus of younger bank accretion landward upon transgressions. No major faulting has been identified by the seismic or drilling data which would explain the marginal plateau as down-dropped from the rest of the Atlantic margin.

Acknowledgments. Preparation of this manuscript was supported by funds from the NSF grant DES-76-832326. Much of the carbonate sedimentology was done in cooperation with Tom Freeman, and the paleobathymetry of Site 392 was provided by Felix Gradstein, our colleagues on Leg 44 of the Deep Sea Drilling Project. Seismic reflection data and rock sampling data which provided background for this interpretation were obtained from R/V CONRAD of Lamont-Doherty Geological Observatory and R/V EASTWARD of Duke University. John Schlee provided thin sections of rocks from the JOIDES drill holes and some helpful discussion.

## References

Applin, P.L., and Applin, E.R., The Comanche series associated rocks in the subsurface of central and southern Florida U.S.G.S. Prof. Paper 447, 84 p, 1965.

Benson, W.E., R.E. Sheridan, Paul Enos, Tom Freeman, Felix Gradstein, I.O. Murdmaa, Leo Pastouret, R.R. Schmidt, D.H. Stuermer, F.M. Weaver, and Paula Worstell, Deep Sea Drilling in the North Atlantic. Geotimes, V. 21, No. 2, p. 23-26, 1976.

Benson, W.E., R.E. Sheridan, Paul Enos, Tom Greeman, Felix Gradstein, I.O. Murdmaa, Leo Pastouret, R.R. Schmidt, D.H. Stuermer, F.M. Weaver, and Paula Worstell, Site 392. South rim of Blake Nose, in Benson, W.E., R.E. Sheridan, et al., 1978, Initial Reports of Deep Sea Drilling Project, V. 44, Washingto.. (U.S. Government Printing Office), p. 337-393, 1978.

Charm, W.B., W.D. Nesteroff, and Sylvia Valdes, Detailed stratigraphic description of the JOIDES cores on the continental margin off Florida: U.S.G.S. Prof. Paper 581-D, 13 p. 1969.

Dillon, W.P., R.E. Sheridan, and J.P. Fail, Structure of the western Blake-Bahama Basin as shown by 24 channel CDP profiling. Geology, V. 4, p. 459-462, 1976.

Dillon, W.P., C.K. Paull, and R.T. Buffler, Structure and development of Southeast Georgia Embayment-Blake Plateau (abs.). Amer. Assoc. Petroleum Geologist Bull., V. 61, p. 781, 1977.

Emery, K.O., and E.F.K. Zarudski, Seismic reflection profiles along the drill holes on the continental margins of Florida. U.S.G.S. Prof. Paper 581-A, 8 p, 1967.

Enos, Paul, and Tom Freeman, Shallow-water limestones from the Blake Nose, Sites 390 and 392, in Benson, W.E., R.E. Sheridan, et al., 1978, Initial Reports of the Deep Sea Drilling Project, V. 44. Washington (U.S. Government Printing Office), p. 413-461, 1978.

Ewing, J.I., Maurice Ewing, and Robert Leyden, Seismic profiler survey of Blake Plateau: Amer. Assoc. Petroleum Geologists Bull., V. 50, p 1948-1971, 1966.

Gohn, G.S., B.B. Higgins, J.P. Owens, R. Schneider, and M. Hess, Lithofacies of the Clubhouse Crossroads Core; Charleston Project, South Carolina (abs.): Geol. Soc. Amer. Northeastern Section Meeting Program, V. 8, No. 2, p. 181-182, 1976.

Hathaway, J.C., J. Schlee, C.W. Poag, P.C. Valentine, E.G.A. Weed, M.H. Bothner, F.A. Kohout, F.T. Manheim, R. Schoen, R.E. Miller, and D.M. Schultz, Preliminary summary of the 1976 Atlantic Margin Coring Project of the U.S. Geological Survey. U.S.G.S. Open File Report., 76-844, 217 p, 1976.

Heezen, B.C., and R.E. Sheridan, Lower Cretaceous rocks (Neocomian-Albian) dredged from Blake Escarpment. Science, V. 154, p. 1644-1647, 1966.

Hersey, J.B., E.T. Bunce, R.F. Wyrick, and F.T. Dietz, Geophysical investigation of the continental margin between Cape Henry, Virginia, and Jacksonville, Florida: Geol. Soc. Amer. Bull., V. 70, p. 437-466, 1959.

Jansa, L.F., Paul Enos, B.E. Tucholke, Felix Gradstein, R.E. Sheridan, Mesozoic and Cenozoic Sedimentary Formations of the North American Basin: Western North Atlantic: This Volume (in press). 1978.

JOIDES, Ocean drilling on the continental margin Science, V. 150, p. 709-716, 1965.

Maher, J.C., Correlations of subsurface Mesozoic and Cenozoic rocks along the Atlantic coast: Amer. Assoc. Petroleum Geologists Cross-Section Publ., 18 p, 1965.

Meyerhoff, A.A. and C.W. Hatten, Bahamas salient of North America: Tectonic framework, stratigraphy, and petroleum potential: Amer. Assoc. Petroleum Geologists Bull., V. 58, p. 1201-1239, 1974.

Mitchum, R.M., Jr., P.R. Vail, and S. Thompson III, Seismic stratigraphy and global changes in sea level, Part 2. The depositional sequence as a basic unit for stratigraphic analysis: Amer. Assoc. Petroleum Geologist Mem. 26, p. 53-62. 1977.

Murray, G.M., Geology of the Atlantic and Gulf coastal province of North America: New York, Harper, 692 p. 1961.

Poag, C.W., Stratigraphy of the Atlantic continental shelf and slope of the United States: Ann. Rev. Earth Planet Sciences, V. 6, 251-280, 1978.

Schlanger, S.O., and H.C. Jenkyns, Cretaceous oceanic anoxic events: Causes and consequences: Geologic en Mijnbowv, V. 55, 179-184, 1976.

Schlee, J., Stratigraphy and Tertiary development of the continental margin east of Florida: U.S.G.S. Prof. Paper 581-F, 25 p. 1977.

Sheridan, R.E., C.L. Drake, J.E. Nafe, and J. Hennion, Seismic refraction study on the continental margin east of Florida: Amer. Assoc. Petroleum Geologist Bull., V. 50, p. 1972-1991, 1966.

Sheridan, R.E., C.C. Windisch, J.I. Ewing, and P.L. Stoffa, Stratigraphy and structure across Blake Escarpment based on seismic reflection profiles: in Amer. Assoc. Petroleum Geologist Spec. Paper on Continental Slopes, Watkins, J. and L. Montadent, eds. (in press), 1978

Shipley, T.H., R.T. Buffler, and J.S. Watkins, Seismic stratigraphy and geologic history of Blake Plateau and adjacent western Atlantic continental margin: Amer. Assoc. Petroleum Geologists Bull., V. 62, p. 792-812, 1978.

Smith, M.A. R.B. Amato, M.A. Furbush, D.M. Pert M.E. Nelson, J.S. Hendrix, L.C. Tamm, G. Wood Jr., and D.R. Shaw, Geological and operational summary, COST No. B-2 Well, Baltimore Canyon Trough, Mid-Atlantic OCS: U.S.G.S. Open File Rept., 76-774, 79 p. 1976.

Tator, B.A., and L.E. Hatfield, Bahamas present complex geology: Oil and Gas Jour., V. 73, No. 43, p. 172-176, and No. 44, p. 120-122, 1975.

Tucholke, B.E., and G.S. Mountain, Lithologic correlation and significance of major seismic reflectors in the western North Atlantic: This Volume (in press). 1978.

Tucholke, B.E., and P.R. Vogt, Western North Atlantic: Sedimentary evolution and aspects of tectonic history: in Initial Reports of the Deep Sea Drilling Project, V. 43 Washington (U.S. Gov't. Printing Office.) (in press). 1978.

Uchupi, E., and K.O. Emery, Structure of continental margin off Atlantic coast of United States: Amer. Assoc. Petroleum Geologists Bull. . 51, p. 223-234, 1967.

Vail, P.R., R.M. Mitchum Jr., and S. Thompson III, Seismic stratigraphy and global changes in sea level, Part 4: Global cycles of relative changes of sea level: Amer. Assoc. Petroleum Geologists, Mem. 26, p. 83-97, 1977.

# MAESTRICHTIAN-CAMPANIAN NANNOFLORAL PROVINCES OF THE SOUTHERN ATLANTIC AND INDIAN OCEANS

Frank H. Wind[1]

Antarctic Marine Geology Research Facility, Department of Geology, Florida State University, Tallahassee, Florida 32306

Abstract. During the Maestrichtian and Campanian, southern oceans were inhabited by distinct ecologically-restricted nannofloras whose distribution was limited by water mass boundaries. The most distinctive nannoflora is a diverse high latitude assemblage best typified by the population preserved in DSDP Hole 327A samples from the Falkland Plateau.

Abundant *Biscutum constans* and *(Watznaueria + Cyclagelosphaera)* typified low latitude regions, while higher latitudes were typified by *Biscutum magnum* and *B. coronum*. *Micula staurophora* was extremely abundant in higher latitudes, but south of a pronounced water mass boundary, it was extremely rare. Ratios of low latitude to high latitude species of *Biscutum*, and *Micula staurophora* to *Watznaueria* and *Cyclagelosphaera* are viewed as a valuable tool for determining the deployment of Maestrichtian-Campanian water masses and the regional distribution of the water temperature, salinity, and nutrient levels which distinguished them. Tethyan and Falkland Plateau Provinces were separated by a broad transition zone.

The unusual marine conditions which fostered the development of the Falkland Plateau nannoflora appear to have existed for a short time interval; most forms evolved during th Campanian and nearly all forms disappeared by the middle Maestrichtian.

## Introduction

In 1977, Ciesielski, Sliter, Wind, and Wise reported the existence of significant differences in microplankton composition of Campanian-Maestrichtian samples from two localities on opposite sides of the Maurice Ewing Bank of the east-west trending Falkland Plateau. Although the two sites are separated by just over one-half degree of latitude (62 km), major differences in their respective calcareous nannoplankton assemblages suggested that a major water mass boundary separated the two localities.

The presence of a distinctive high southern latitude nannoflora during the Campanian-Maestrichtian was first revealed during examination of four cores recovered from DSDP Hole 327A on the Falkland Plateau (lat. 50°52'S; long. 46° 47'W). The recovered section contained an exceptionally well-preserved and diverse nannoflora with many previously unreported taxa which Wind and Wise (in Wise and Wind, 1977) placed in eight new genera and nineteen new species. Equally significant was the absence of many species previously considered "cosmopolitan".

Key sites for the delineation of southern hemisphere nannoplankton provinces are DSDP Sites 217, 249, 327, 356, 357, Islas Orcadas Core 07-75-44, and Vema Cores 16-56 and 24-213. Additional southern Atlantic and Indian Ocean sites studied during various stages of this research include DSDP Sites 20, 21 and 216. The present geographic location of each site is listed in Table 1. Paleogeographic positions are shown in Figure 1. Except where noted, the paleogeographic reconstruction used in this paper is from Sliter (1977) modified by data in Matsumoto (1973, Figure 3).

## Biostratigraphy

Low latitude sites were dated using presently recognized zonations proposed or revised by Čepek and Hay (1969), Bukry and Bramlette (1970), Bukry (1973a), and Perch-Nielsen (1972). Key datums for low latitude regions include the first occurrence of *Micula mura*, *Lithraphidites quadratus*, *Tetralithus gothicus*, and *T. trifidus*, and the last occurrences of *T. gothicus*, *T. trifidus*, *Lithraphidites quadratus*, and *Eiffellithus eximius*.

A set of middle and high latitude biostratigraphic datums to supplant tropical biohorizons has been proposed by Martini (1976) and Perch-Nielsen (1977). Martini (1976) notes that the last occurrence of *Broinsonia parca* may be used

[1] Present address:
Texaco, Inc.
3350 Wilshire Boulevard
Los Angeles, California 90010

TABLE 1. Location of Sample Sites

| Sample Site | Latitude | Longitude |
|---|---|---|
| DSDP 20 | 28°32'S | 26°51'W |
| DSDP 21 | 28°35'S | 30°36'W |
| DSDP 216 | 1°28'N | 90°12'E |
| DSDP 217 | 8°56'N | 90°32'E |
| DSDP 249 | 29°57'S | 36°05'E |
| DSDP 327 | 50°52'S | 46°47'W |
| DSDP 354 | 5°54'N | 44°12'W |
| DSDP 355 | 15°43'S | 30°36'W |
| DSDP 356 | 28°17'S | 41°05'W |
| DSDP 357 | 30°00'S | 35°34'W |
| Islas Orcadas 07-75-44 | 50°18'S | 44°32'W |
| Vema 16-56 | 41°21'S | 26°38'E |
| Vema 24-213 | 36°59'S | 25°07'E |

to define the upper boundary of the *Tetralithus trifidus* Zone in high latitudes. Perch-Nielsen (1977) notes that the last-occurrence datum of *Reinhardtites anthophorus* may be similarly applied.

## High-Latitude Nannoplankton

The most common species of the Falkland Plateau (high southern latitude) Province include the following upper Campanian taxa:

*Kamptnerius magnificus* Deflandre, 1959
*Biscutum magnum* Wind and Wise, 1977
*Biscutum coronum* Wind and Wise, 1977
*Biscutum notaculum* Wind and Wise, 1977
*Arkhangelskiella cymbiformis* Vekshina, 1959
*Eiffellithus turriseiffeli* (Deflandre and Fert) Reinhardt, 1965
*Cretarhabdus conicus* Bramlette and Martini, 1964
*Reinhardtites anthophorus* (Deflandre) Perch-Nielsen, 1968
*Monomarginatus pectinatus* Wind and Wise, 1977
*Misceomarginatus pleniporus* Wind and Wise, 1977
*Prediscosphaera cretacea* (Arkhangelsky) Gartner, 1968
*Prediscosphaera spinosa* (Bramlette and Martini) Gartner, 1968
*Prediscosphaera honjoi* Bukry, 1969
*Nephrolithus* sp. (non *N. frequens* Gorka, 1957)
*Acuturris scotus* (Risatti) Wind and Wise, 1977
*Lucianorhabdus cayeuxii* Deflandre, 1959
*Gartnerago obliquum* (Stradner) Reinhardt, 1970
*Gartnerago segmentatum* (Stover) Thierstein, 1974
*Ahmuellerella octoradiata* (Gorka) Reinhardt, 1966
*Broinsonia enormis* (Shumenko) Manivit, 1971
*Zygodiscus diplogrammus* (Deflandre and Fert) Gartner, 1968
*Tranolithus orionatus* Stover, 1966
*Biscutum dissimilis* Wind and Wise, 1977

Lower Maestrichtian: same as above, but with
*Monomarginatus quaternarius* Wind and Wise, 1977
*Cribrosphaerella daniae* Perch-Nielsen, 1973
and without
*Biscutum coronum* Wind and Wise, 1977

Plate 1. All figures phase-contrast illumination, X 2000.

1, 2. *Nephrolithus frequens* Gorka. DSDP 21-208-34 3, 10 cm.
3, 4. *Nephrolithus* n. sp. (low focus, high focus). DSDP 36-327A-11-2, 102 cm.
5, 6. *Biscutum coronum* Wind and Wise. DSDP 36-327A-13-2, 137 cm.
7. *Biscutum magnum* Wind and Wise. DSDP 36-327A-11-2, 102 cm.
8. *Biscutum magnum* Wind and Wise (left) and *B. constans* (Gorka). DSDP 25-249-17-3, 20 cm.
9. *Monomarginatus pectinatus* Wind and Wise. DSDP 36-327A-13-2, 54 cm.
10. *Monomarginatus pectinatus* Wind and Wise (left) and *Misceomarginatus pleniporus* Wind and Wise. DSDP 36-327A-13-2, 54 cm.
11. *Misceomarginatus pleniporus* Wind and Wise. DSDP 36-327A-13-2, 54 cm.
12. *Monomarginatus quaternarius* Wind and Wise. DSDP 36-327A-11-2, 102 cm.
13, 14. *Micula staurophora* (Gardet). DSDP 25-249-17-3, 20 cm.
15. *Watznaueria barnesae* (Black). DSDP 25-249-17-3, 20 cm.
16. *Cyclagelosphaera margareli* Noel. DSDP 25-249-17-3, 20 cm.
17. *Cribrosphaerella ehrenbergii* (Arkhangelsky). DSDP 25-249-17-3, 20 cm.
18. *Cribrosphaerella daniae* Perch-Nielsen. DSDP 36-327A-11-2, 102 cm.
19. *Lithraphidites quadratus* Bramlette and Martini. DSDP 25-249-17-3, 20 cm.
20 *Tetralithus trifidus* (Stradner). Demopolis Chalk, Oktibbeha Co., Mississippi.

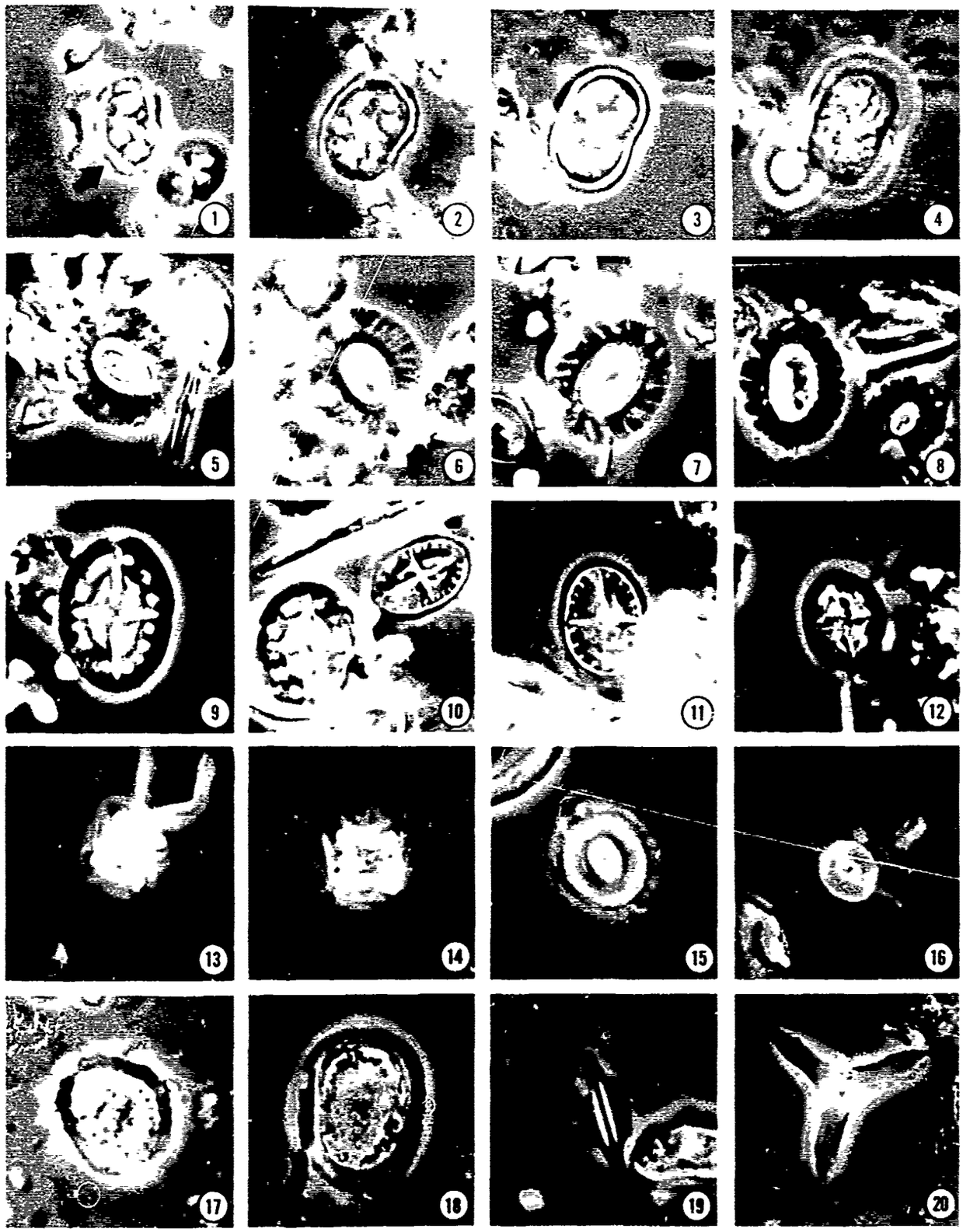
1
2
3
4
5
6
7
8
9
10
11
12
13
14
15
16
17
18
19
20

*Monomarginatus pectinatus* Wind and Wise, 1977
*Misceomarginatus pleniporus* Wind and Wise, 1977
*Broinsonia enormis* (Shumenko) Manivit, 1971
*Zygodiscus diplogrammus* (Deflandre and Fert) Gartner, 1968
*Tranolithus orionatus* Stover, 1966

The specimen described as *Nephrolithus* n. sp. in Plate 1 is not to be confused with *Rhagodiscus reniformis* Perch-Nielsen, 1973. The latter form appears to be an elongate species of *Nephrolithus* with a poorly-defined central area construction. When viewed on the TEM or SEM, specimens of *Nephrolithus* n. sp. such as that illustrated in Plate 1, Figures 3 and 4 are characterized by between approximately 5 and 55 central area perforations defined by rings of 6 inclined calcite laths. Central area perforations of *N. frequens* number between 2 and 15, and are delineated by concentric rings of approximately 10 overlapping calcite rhombs.

Five species named from DSDP Hole 327A serve as valuable biostratigraphic markers in several high and mid-high latitude sites in the southern hemisphere. These species, illustrated in Plate 1, are *Biscutum magnum, B. coronum, Monomarginatus quaternarius, M. pectinatus,* and *Misceomarginatus pleniporus.*

Two Indian Ocean sites (DSDP 217 and DSDP 249) contain sections whose nannofloras incorporate elements of both high- and mid-latitude regions. It is possible, therefore, in these sections to compare the time-stratigraphic relationships of biostratigraphic events of species from both regions.

The stratigraphic placement of cores from DSDP Holes 217, 249, and 327A is illustrated in Figure 2. The bottom portion of Site 249, Core 16 and the top 6.75 meters of Core 17 are placed in the upper Maestrichtian *Nephrolithus frequens* Zone. The remainder of Core 17 and Cores 18 through 22 are placed in the upper Campanian/lower Maestrichtian *Tetralithus trifidus* Zone. The contact between lower and upper Maestrichtian sediments may be represented by a 1 cm clay-bearing limestone present at 17-5, 88 cm. Sediments in the overlying meter or so appear to contain a mixed lower and upper Maestrichtian assemblage. Nannoplankton in the Cretaceous of DSDP Site 249 are discussed in Bukry (1974b). Nannoplankton from DSDP Leg 22 Sites 212, 216 and 217 are reviewed in Gartner (1974) and Bukry (1974a).

The calcareous nannoplankton assemblage in Core 13 of Hole 327A can be dated as either Campanian or earliest Maestrichtian, however, Core 13 is placed in the Campanian based upon an analysis of the planktonic foraminifera by Sliter (1977). Cores 10 through 12 are placed in the early Maestrichtian based upon correlation with the nannofloras in samples from DSDP Sites 217 and 249.

The following species serve as excellent biostratigraphic markers in high southern latitudes.

*Monomarginatus quaternarius:* First occurrence is mid-lower Maestrichtian; highest occurrence is approximately at the boundary between the lower and middle Maestrichtian.

*Misceomarginatus pleniporus:* Age of first occurrence is not known; highest occurrence is mid-lower Maestrichtian.

*Monomarginatus pectinatus:* Known stratigraphic range is the same as for *Misceomarginatus pleniporus.*

*Biscutum coronum:* The known range is the same as for the two preceding species.

*Biscutum magnum:* The point of first occurrence of this species is not known; the highest occurrence appears to be at about the boundary between middle and upper Maestrichtian.

In high latitudes of both southern and northern hemispheres, *Biscutum magnum* and *B. coronum* supplant *Seribiscutum primitivum* (Thierstein) Filewicz, Wind and Wise, a form with similar size and construction, but different central area design. The replacement of *S. primitivum* by *Biscutum magnum* and *B. coronum* took place during the Santonian or Campanian.

## Paleobiogeography

The presence of distinctive latitudinally-restricted nannoplankton species during the Maestrichtian was first reported by Worsley and Martini (1970), who noted a bipolar distribution of *Nephrolithus frequens* and a coeval concentration of *Micula mura* in lower latitudes. Latitudinal and climatological distribution patterns of Maestrichtian nannoplankton are also discussed in Worsley (1974).

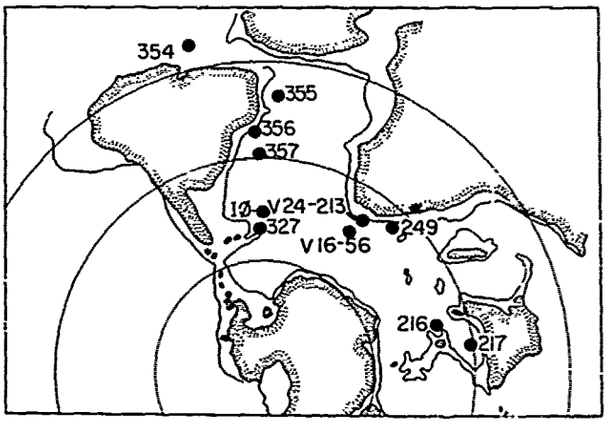


Figure 1. Paleogeographic location of sample sites utilized in the study of Campanian-Maestrichtian southern Atlantic and Indian Ocean nannoplankton provinces. Except for one Islas Orcadas piston core site (IØ 07-75-44) and two Vema piston core sites (Vema 16-56 and 24-213), all localities are Deep Sea Drilling Project (DSDP) sites.

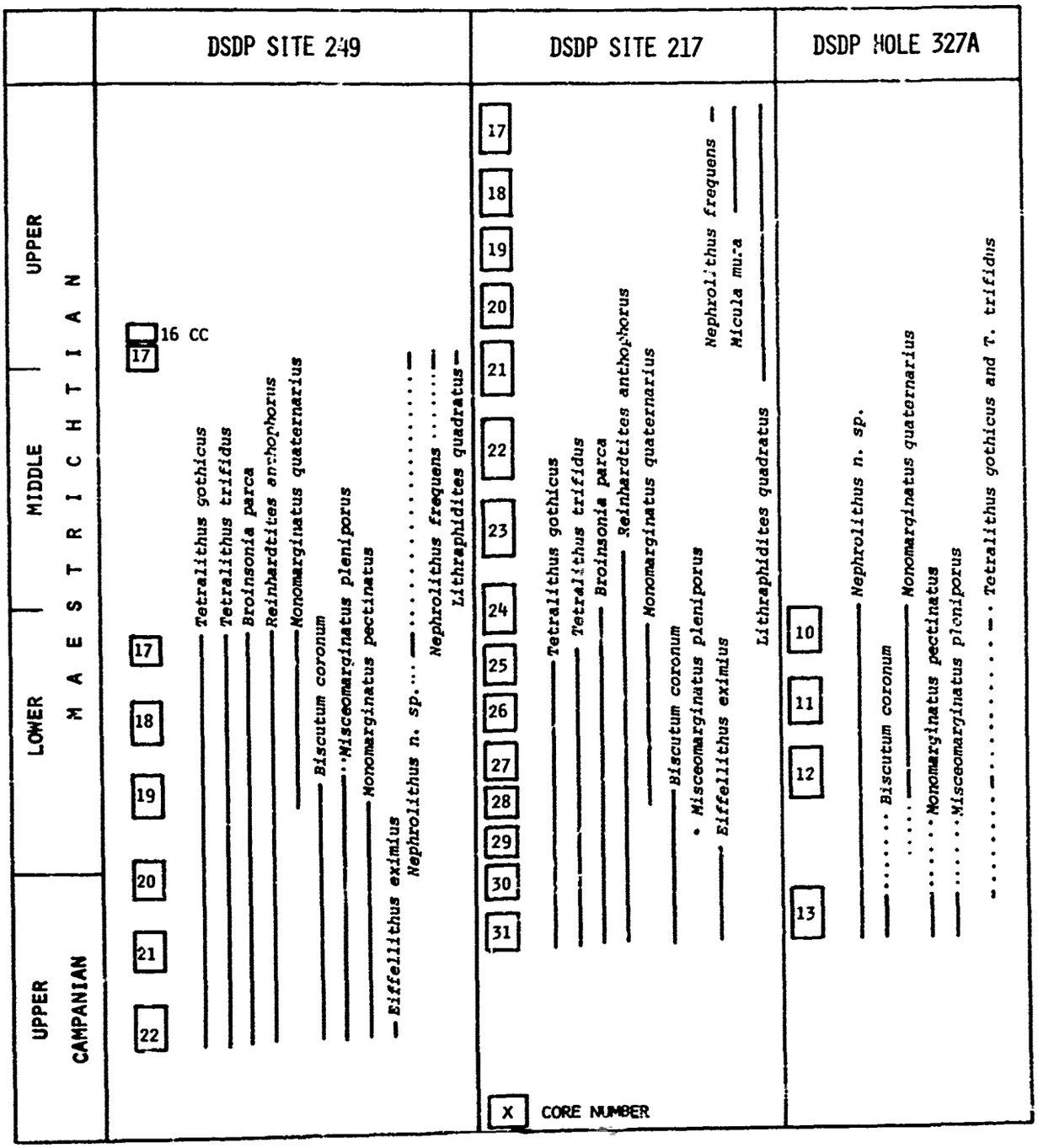


Figure 2. Ranges of key species and correlation of DSDP Sites in the South Atlantic and Indian Oceans. Correlation is based upon an examination of the nannoplankton by the present author, and data from planktonic foraminifera and nannoplankton reports in Initial Report volumes.

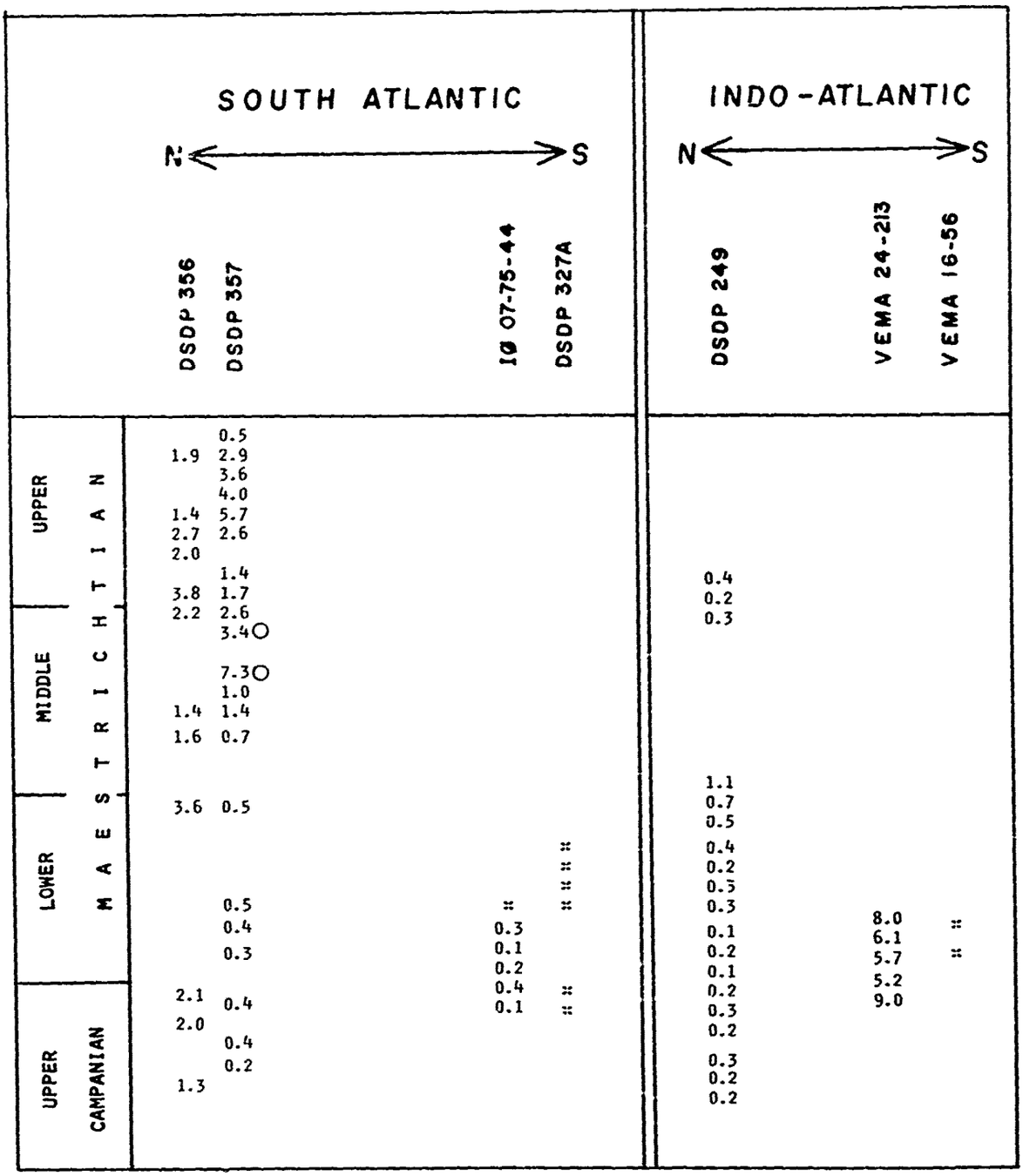


Figure 3. Values of *Micula staurophora/(Watznaueria + Cyclagelosphaera)*. Samples in which all three forms are extremely rare or absent are marked by an asterisk (::). The two circles denote samples from DSDP Site 357 in which specimens of *Biscutum magnum* were observed. Stratigraphic placement of DSDP 356 and 357 cores is based upon planktonic foraminifera data of Premoli Silva and Boersma (1977).

Thierstein (1976) notes that *Kamptnerius magnificus, Lucianorhabdus cayeuxii, Nephrolithus frequens, Gartnerago obliquum, Micula staurophora. Vagalapilla octoradiata, Tetralithus obscurus,* and *Braarudosphaera bigelowi* become more abundant with increasing paleolatitude. The only known report concerning a systematic analysis of Upper Cretaceous calcareous nannoplankton biogeography is an abstract by Thierstein and Haq (1977), in which they conclude that:

(1) Relative abundance distribution at a particular site remains remarkably steady throughout the Maestrichtian, (2) Maestrichtian biogeographic boundaries roughly parallel latitude, (3) Tropical assemblages are characterized by dominance of *Micula staurophora* and *Watznaueria barnesae,* and by common *Micula mura* and *Tetralithus aculeus,* (4) High latitude communities contain abundant *Nephrolithus frequens, Arkhangelskiella cymbiformis, Kamptnerius magnificus, Lucianorhabdus cayeuxii,* and *Zygodiscus anthophorus.*

Few other publications discuss Upper Cretaceous nannoplankton paleobiogeography, and most of these briefly mention the subject when discussing assemblages from a single or closely-grouped set of sample sites.

## Distribution of *Micula staurophora*, *Watznaueria*, and *Cyclagelosphaera*

Both empirical observation and initial examination of the results of Q-mode Varimax Factor Analysis (manuscript in preparation) reveal a generally worldwide inverse relationship in the abundance of *Micula staurophora* and *(Watznaueria barnesae + Cyclagelosphaera margareli).* Representative specimens of these forms are illustrated in Plate 1, Figures 13 through 16. Although the number and arrangement of skeletal elements on the algal cell which is presumed to have secreted the form species *Micula staurophora* is not known *(Watznaueria* and *Cyclagelosphaera* are often preserved as intact coccospheres), the ratio of these forms is still an indicator of the relative number of individuals of each species. Haq and Lohmann (1976) note that population counts are biased in favor of species with large numbers of skeletal elements, and that this bias could be corrected if we knew the average number of coccoliths forming the skeleton of each species. For most fossil forms, this is not known.

One feature of these species argues for the validity of any paleoecological interpretation based upon their distribution and relative abundance. *Micula staurophora, Watznaueria,* and *Cyclagelosphaera* are three of the most dissolution-resistant elements of Campanian and Maestrichtian nannofloras, and consequently, the ratio of these forms as recorded in sediments should be a fairly accurate representation of original phytoplankton skeletal composition. The dominance of tropical assemblages by *Micula staurophora* and *Watznaueria barnesae* cited by Thierstein and Haq (1977) may be due to the enrichment of the former and most dissolution-resistant form by the dissolution of more susceptible taxa. All material referred to in this report consists of well-preserved calcareous nannoplankton assemblages. Samples having been subjected to extensive dissolution and/or calcite overgrowth were not included in the analysis of key species distribution and relative abundance.

Bukry (1973b, p. 889) notes that the coccolith assemblage from Hole 207A in the Tasman Sea (DSDP Leg 21) is remarkable in the common occurrence of *Kamptnerius magnificus* and the absence of *Watznaueria barnesae.* He notes that the reverse is generally true in low latitude oceanic sections, and that in only very few high latitude localities such as those in western Siberia and New Zealand has *W. barnesae* been found to be absent from late Cretaceous samples.

In North Sea samples, *Micula staurophora* is common, while *Watznaueria* and *Cyclagelosphaera* are absent (J. Keany, 1977 personal communication). In Labrador Sea sites, *Micula staurophora* is not only much more common than *Watznaueria* and *Cyclagelosphaera,* but dominates the entire nannoflora, comprising between 49 and 75 percent of all specimens counted. The presence of well-preserved specimens of *Kamptnerius magnificus* and *Lithraphidites quadratus* discounts appreciable preservational enrichment of *Micula staurophora.*

Figure 3 records values of *Micula staurophora* divided by the sum of *Watznaueria* and *Cyclagelosphaera* (M/W+C) for sites in the South Atlantic and Indian Oceans. Values for each sample represent combined counts in excess of 100 specimens. Population percentage of *Micula staurophora* and *(Watznaueria + Cyclagelosphaera)* at key sites in the southern Atlantic and Indian Oceans are listed in Table 2. Trends in these values can be observed both in individual sites, and in relation to paleolatitude.

The most significant differences in M/W+C values between adjacent sites are exhibited by sites on the Agulhas and Mozambique Plateaus. The nannoflora from Vema Core 24-213 is typified by abundant *Micula staurophora* and rare *Watznaueria* and *Cyclagelosphaera.* Coeval samples from DSDP Site 249 to the north contain few specimens of *Micula,* but a much greater concentration of *Watznaueria* and *Cyclagelosphaera.* Samples from Vema Core 16-56, the more southerly site on the Agulhas Plateau, contain only rare specimens of all three forms. Extreme rarity of *Micula staurophora, Watznaueria,* and *Cyclagelosphaera* also characterizes samples from DSDP Hole 327A, and the shallowest sample from Islas Orcadas Core 07-75-44.

The increase in numbers of *Micula staurophora* in younger Maestrichtian nannofloras was first observed by Worsley (1974, p. 123, fig. 21; p. 125, fig. 22), who noted this trend in a sequence of samples from the Braggs section in Alabama. The increase in *Micula staurophora* and decrease in *Watznaueria* and *Cyclagelosphaera* in younger

TABLE 2. Distribution of paleoecological indicator species on the Falkland, Agulhas, and Mozambique Plateaus. Values represent percent of total population based on counts of 300 specimens from each sample.

| Sample Site | *Biscutum constans* | *Biscutum magnum + Biscutum coronum* | *Micula staurophora* | *Watznaueria + Cyclagelosphaera* |
|---|---|---|---|---|
| Vema 16-56 | ----------Lower Maestrichtian---------- | | | |
| 75 cm | 3.33 | 18.67 | 2.00 | 2.33 |
| 100 cm | 3.67 | 23.00 | 1.33 | 1.00 |
| Vema 24-213 | ----------Upper Campanian to Lower Maestrichtian---------- | | | |
| 150 cm | 0.33 | 1.33 | 78.67 | 9.67 |
| 250 cm | 1.00 | 4.33 | 60.33 | 10.67 |
| DSDP Site 249- | ----------Lower Maestrichtian---------- | | | |
| 18-1, 24 cm | 22.33 | 1.00 | 4.33 | 12.00 |
| 19-1, 120 cm | 10.33 | 0.33 | 2.33 | 12.67 |
| 20-1, 20 cm | 8.33 | 0.33 | 5.00 | 8.67 |
| | ----------Upper Campanian---------- | | | |
| 21-2, 20 cm | 10.67 | 0.67 | 5.33 | 12.33 |
| 22-1, 148 cm | 6.67 | 0.00 | 7.67 | 15.67 |
| Islas Orcadas 07-75-44 | ----------Upper Campanian to Lower Maestrichtian---------- | | | |
| 71 cm | 7.33 | 28.67 | 0.00 | 0.33 |
| 75 cm | 18.00 | 8.00 | 2.33 | 6.67 |
| 80 cm | 24.67 | 4.33 | 0.33 | 5.67 |
| 101 cm | 20.00 | 2.00 | 1.67 | 10.33 |
| 150 cm | 21.67 | 1.33 | 4.67 | 11.33 |
| 275 cm | 22.00 | 1.67 | 2.67 | 25.33 |
| 350 cm | 29.00 | 4.33 | 0.67 | 17.67 |
| DSDP Hole 327A- | ----------Lower Maestrichtian---------- | | | |
| 10-3, 14 cm | 0.00 | 9.00 | 0.00 | 0.00 |
| 11-1, 45 cm | 0.00 | 10.00 | 0.33 | 0.00 |
| 11-2, 123 cm | 0.00 | 12.00 | 0.00 | 0.33 |
| 12-1, 67 cm | 0.00 | 13.00 | 0.67 | 0.00 |
| 12-4, 31 cm | 0.00 | 20.33 | 0.00 | 0.00 |
| | ----------Upper Campanian---------- | | | |
| 13-2, 54 cm | 0.00 | 21.33 | 0.33 | 0.33 |
| 13-2, 137 cm | 0.33 | 18.00 | 0.67 | 0.67 |

portions of Maestrichtian sections can be observed in several Atlantic and Indian Ocean sites, and is best illustrated here by the data from DSDP Site 357. The relative abundance distribution of these three forms in the southern oceans is illustrated in Figure 4.

## Distribution of Species of *Biscutum*

During the course of this research, it became evident that it was possible to recognize a second paleolatitudinally-dependant feature of nannofloral composition, i.e., the relative abundance of species of the genus *Biscutum*. During the Late Cretaceous, low and middle latitudes were typified by abundant *B. constans*, while in higher latitudes, this genus was represented by *B. magnum* and *B. coronum*. It was thought that in regions where the distribution of these forms overlapped, it would be possible to analyze the ratios of specimen counts of these species and determine a relative temperature value for isolated samples, and approximate paleotemperature curves (or relative residence time of different water masses over the site) for a sequence of samples. Similar approaches using nannoplankton have been utilized in the study of climatic fluctuation during the Tertiary and Quaternary.

*Biscutum constans* vs. *B. magnum + B. coronum* ratios were determined for all southern hemisphere sites. *Biscutum dissimilis* Wind and Wise (in Wise and Wind, 1977, p. 298, pl. 23, figs. 1-5; pl. 24, figs. 3-6) is a rare nannofloral element and was not included in these counts. Where possible, the number of specimens of *B. magnum + B. coronum* was determined during a count of 100 specimens of the low latitude species.

Low numbers of *Biscutum constans* and extreme abundance of *B. magnum* and *B. coronum* in samples from DSDP Hole 327A and Vema Core 16-56, and in the highest sample from Islas Orcadas Core 07-75-44 generate extraordinarily high *Biscutum* values, which when extrapolated to a count of 100 specimens of *B. constans*, result in as many as 2500 specimens of the high latitude species. In contrast, samples from Vema Core 24-213 and from

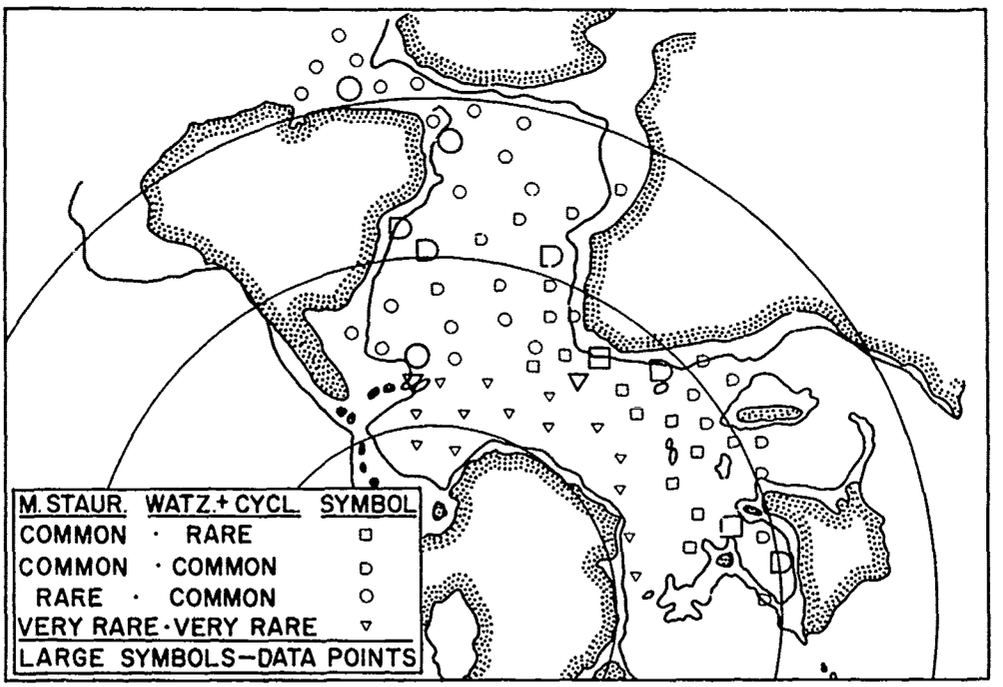


Figure 4. Relative abundance of *Micula staurophora* and *(Watznaueria + Cyclagelosphaera)* in the southern oceans during the late Campanian and early Maestrichtian.

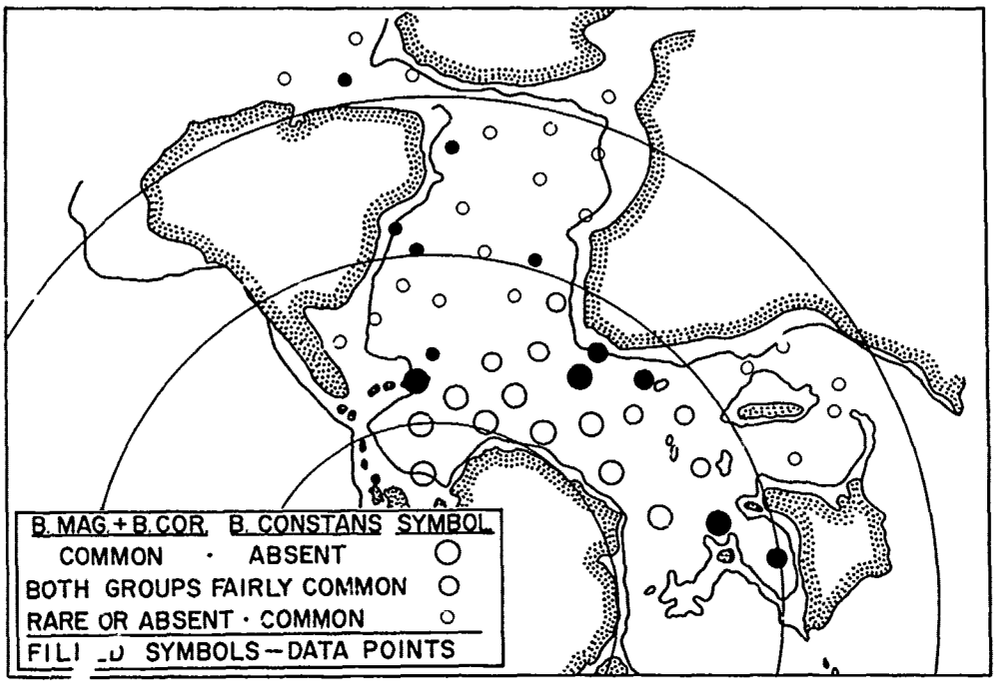


Figure 5. Relative abundance of *Biscutum constans* and *(B. magnum + B. coronum)* in the southern oceans during the late Campanian and early Maestrichtian.

several sites in the Indian Ocean contain relatively few specimens of any species of this genus.

The relative abundance of species of *Biscutum* in samples from several sites is included in Table 2. The paleogeographic distribution in the southern Atlantic and Indian Oceans is illustrated in Figure 5.

## Paleoecological Significance of M/W+C and *Biscutum* Values

The relative abundance of these forms in the southern hemisphere in the upper Campanian through middle Maestrichtian is summarized in Figure 6. *Watznaueria* and *Cyclagelosphaera* were most abundant in low latitudes. *Micula staurophore* increased in abundance with increased latitude, but all three forms rapidly decreased in numbers poleward of a sharp water mass boundary. The low latitude and high latitude species of *Biscutum* occurred in a nearly reciprocal abundance relationship. However, between the area dominated by *B. constans* and the area dominated by *Biscutum magnum* and *B. coronum* existed a zone in which all species of this genus were poorly represented.

At several sites, there appears to be a direct relationship between high counts of *Micula staurophora*, and abundant *Biscutum magnum* and *B. coronum*. Specimens of *B. magnum* were observed in only two samples from DSDP Site 357; the two middle Maestrichtian samples with the highest M/W+C values (see Figure 3). Although high M/W+C values were also calculated for samples in the upper Maestrichtian portion of the section recovered at the site, *Biscutum magnum* was not found. This observation adds support to the determination of an upper-middle Maestrichtian last occurrence datum for this species based upon data from DSDP Sites 217 and 249. Other sites in the southern ocean are typified by high concentrations of the high latitude species of *Biscutum* and an absence or near absence of all of the other species under consideration.

## Possible Causes for Campanian-Maestrichtian Nannoplankton Provinces

Several features of the marine realm are viewed as possible controlling influences on the distribution of Campanian and Maestrichtian nannoplankton assemblages and the species considered herein. A deviation from normal marine salinity, unusually high or low surface water temperatures, or atypical nutrient levels would be expected to in some way alter the assemblage of an indigenous phytoplankton community.

It is probable that abnormally low salinity would be reflected by a high concentration of the pentalith *Braarudosphaera bigelowi* (Gran and Braarud) Deflandre. This species is an excellent paleosalinity monitor; it flourishes in hyposaline conditions, is rare in marine waters of normal salinity, and is not found under hypersaline conditions. The ecology and paleoecology of pentaliths is discussed in Bukry (1974c). Although Thierstein (1976) notes that *B. bigelowi* becomes more abundant with increasing paleolatitude, no pentaliths were observed in the Campanian and Maestrichtian nannofloras in the area of present investigation. In the high southern paleolatitudes, the absence of this form may reflect higher than normal marine salinity.

Unusually cold surface water temperatures are also viewed as a possible limiting factor on the distribution of many Maestrichtian and Campanian taxa. Although surface water temperature is one aspect of the marine realm most easily tied to latitude or paleolatitude, the characterization of the Falkland Plateau assemblage as a cryophyllic population is not supported by the results of distribution studies on Cenozoic and extant populations. Past and present cold water regions support nannoplankton assemblages characterized by greatly reduced abundance and diversity.

Abnormal nutrient levels during the Campanian and Maestrichtian are difficult to detect. The rapid change in paleoecological aspect of the nannoflora in the few centimeters of sediment immediately below a Maestrichtian chert capping the Cretaceous portion of the Islas Orcadas core suggests rapidly altered marine conditions. Upwelling of bottom waters along the Falkland Plateau may have introduced cooler, nutrient-rich water of higher than normal salinity to the southern ocean region. A similar phenomenon may have occurred in the southern portion of the Agulhas Plateau. This altered ecological state would foster a siliceous phytoplankton bloom; a possible source for the chert bed in the Islas Orcadas core and the chert nodules in the section from DSDP Hole 327A.

## Paleobiogeography on the Agulhas and Mozambique Plateaus

Upper Campanian to lower Maestrichtian sediments were recovered in two cores on the Agulhas Plateau (Vema 16-56 and Vema 24-213). Both cores were dated as Maestrichtian by Thierstein (1976) and by Okada (Tucholke and Carpenter, 1977).

The higher latitude site (Vema 16-56) is typified by rare specimens of *Watznaueria, Cyclagelosphaera*, and *Micula staurophora*, abundant *Biscutum magnum*, and rare *B. constans*. The new species of *Nephrolithus* is present, although generally represented only by rims. The high latitude species of *Cribrosphaerella, C. daniae* (see Plate 1, Figure 18) is common and more abundant than *C. ehrenbergi*. All aspects of the nannoflora from this site reflect great similarity of these samples with those from DSDP Hole 327A on the Falkland Plateau.

In contrast, samples from Vema Core 24-213 are typified by high counts of *Micula staurophora*. *Watznaueria* are *Cyclagelosphaera* are present, but to a lesser extent. The remainder of the nannoflora is composed principally of *Kamptnerius mag-*

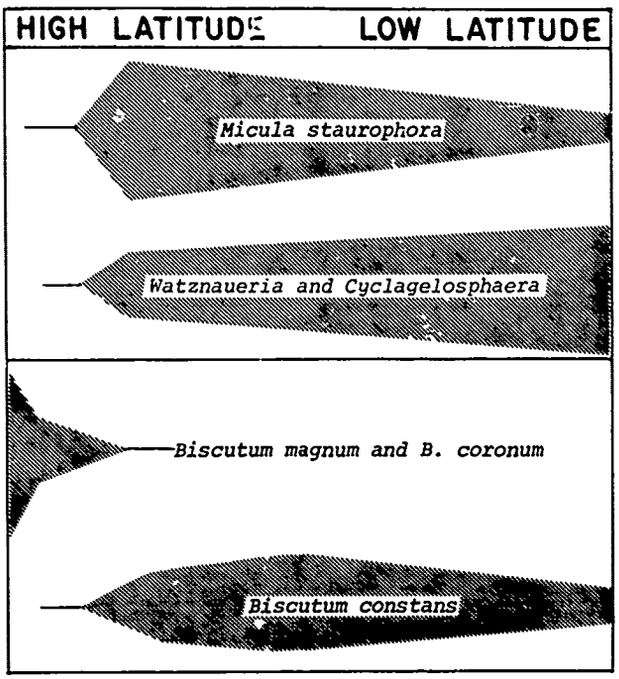


Figure 6. Generalized southern hemisphere distribution of key Campanian-Maestrichtian ecologically sensitive nannoplankton species. Relative abundance of each species or species group at a given paleolatitude is represented by the thickness of the shaded area.

*nificus*, *Reinhardtites* spp., *Arkhangelskiella cymbiformis*, *Gartnerago* spp., *Broinsonia parca*, and *B. enormis*. Although *Biscutum magnum* is more abundant than *B. constans*, this genus as a whole represents no more than approximately five percent of the total population. The assemblage in samples from Vema Core 24-213 closely resembles assemblages from several mid to high latitude sites in the North Atlantic.

Although the two Vema sites are separated by only about 4½ degrees of latitude, their nannofloras are quite different. This condition could indicate that the two sites received phytoplankton remains from assemblages whose composition was dictated by significantly different marine conditions.

In contrast to the ultra-high latitude aspect of the nannoflora from Vema 16-56 and the mid-high latitude character of the assemblage from Vema 24-213, samples from DSDP Site 249 on the Mozambique Plateau contain a coccolith assemblage having middle latitude affinities. The population is typified by low M/W+C values and abundant *Biscutum constans*. *B. magnum and B. coronum* are generally poorly represented.

The trends in nannofloral composition observed in this region south of Africa mirror the situation present in the Indian Ocean. Changes in total numbers and relative abundance of paleoecologically sensitive species coincided with changing latitude of DSDP Site 216 on the Ninetyeast Ridge as the site drifted rapidly northward during the Campanian and Maestrichtian.

## Paleobiogeography on the Falkland Plateau

As discussed in Ciesielski et al. (1977), the nannofloras from Islas Orcadas Core 07-75-44 and DSDP Hole 327A differ greatly in terms of composition and paleoecological indices. The Islas Orcadas Core samples are also radically different from the lower latitude nannofloras in DSDP Sites 20, 21, 356, and 357.

The most contrasting features of the two Falkland Plateau sites are best illustrated by the data in Table 2. While *Biscutum magnum* and *B. coronum* typify samples from the more southerly DSDP site, the most common species of this genus in the Islas Orcadas samples is *B. constans*. *Watznaueria* and *Cyclagelosphaera* are unusually abundant at the Islas Orcadas site when viewed in light of the near-absence of these forms in the adjacent DSDP Hole, or when compared to the general distribution pattern of these species in other mid to high latitude regions.

When the distribution pattern of key elements of the nannofloras of the Falkland Plateau is viewed in light of the generalized latitudinal distribution pattern presented in Figure 6, it appears as if two distinct latitudinal regimes have been brought in close proximity without

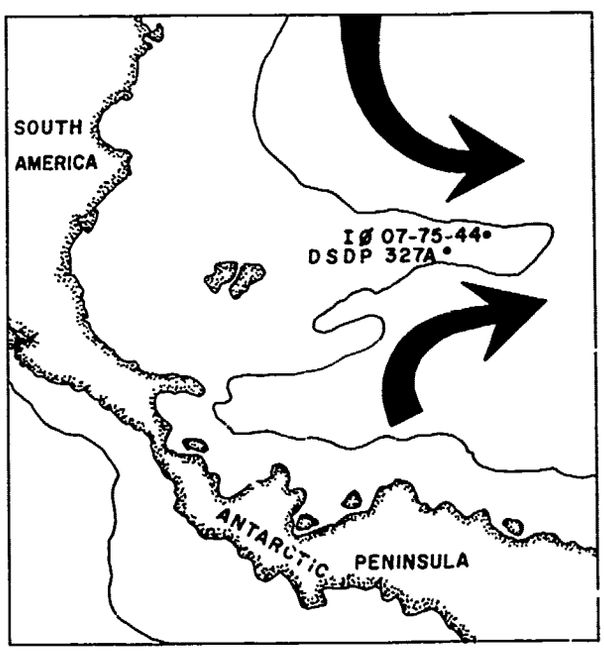


Figure 7. Postulated oceanic circulation in the region of the Falkland Plateau during the Campanian-Maestrichtian. Land and bathymetric configuration is largely conjectural. (from Ciesielski et al., 1977).

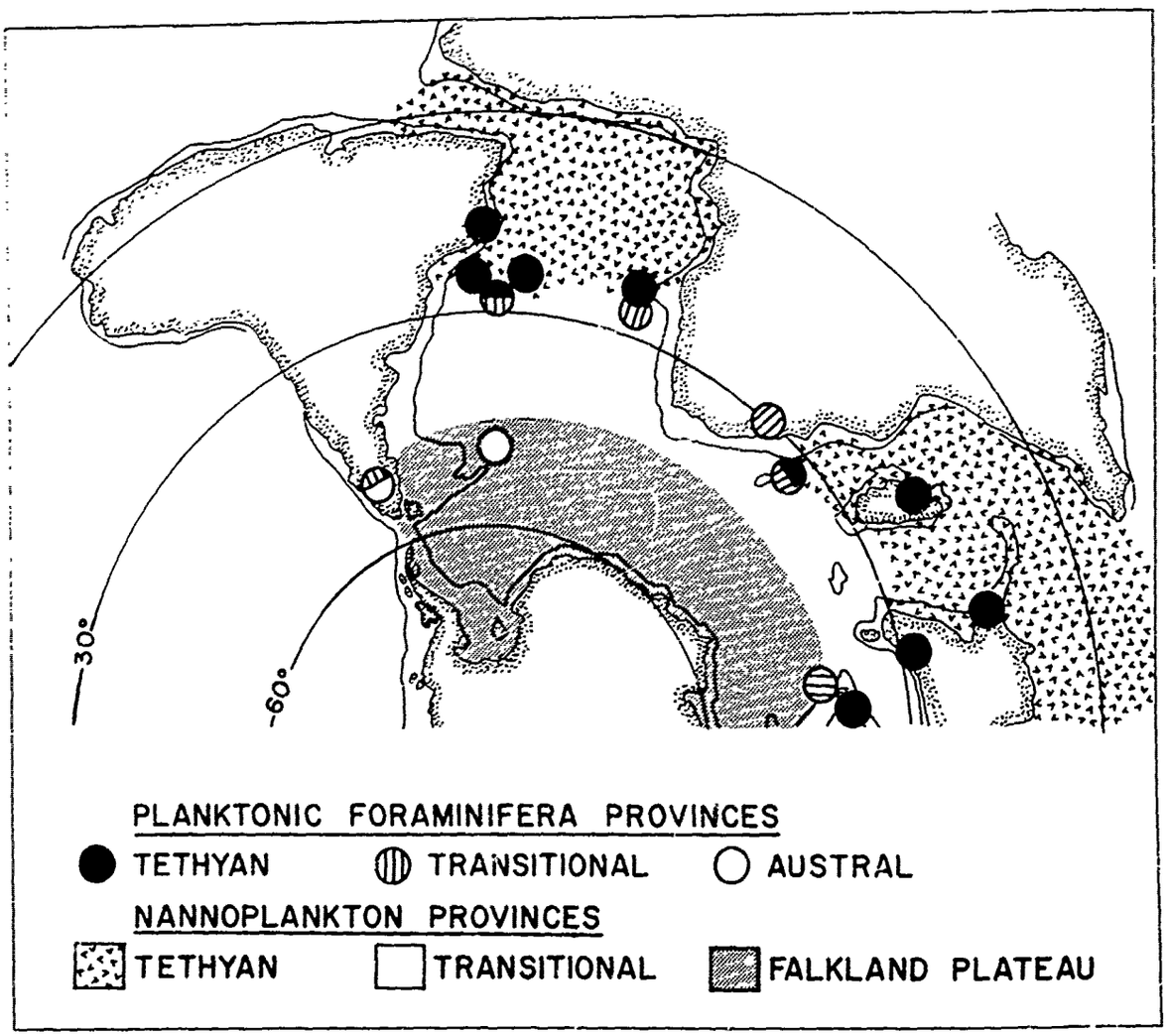


Figure 8. Areal distribution of planktonic foraminifera and calcareous nannoplankton provinces during the late Campanian and early Maestrichtian. Paleogeographic reconstruction and foraminifera data is from Sliter (1977).

benefit of an intervening transition zone. Missing from the Plateau region is the mid-high latitude nannoflora typified by abundant *Micula staurophore* and rare *Watznaueria* and *Cyclagelosphaera*. It is evident that the position of the Falkland Plateau during the Campanian and Maestrichtian coincided with the boundary between two water masses; a warm South Atlantic counterclockwise gyre, and a reciprocal clockwise gyre or region of upwelling between the Antarctic continent and the Falkland Plateau (see Figure 7).

Comparison with Planktonic Foraminifera Paleobiogeography

Sliter (1977) recognized three planktonic foraminifera provinces in the Southern Hemisphere: Tethyan, Transitional, and Austral. The paleogeographic distribution of these faunas is shown in Figure 8. Tethyan assemblages are generally found between 0°and 30°S paleolatitude. Assemblages having Austral affinities are found on the Falkland Plateau (DSDP Hole 327A) and in New Zealand. Ciesielski et al. (1977) and Sliter (1978 personal communication) note that the fauna from the Islas Orcadas Core on the Falkland Plateau belongs in the Austral Province, but that it has a slightly warmer-water aspect than the fauna from DSDP Hole 327A. Sliter has not examined samples from the two sites on the Agulhas Plateau discussed in this paper.

Figure 8 also incorporates the general positions of Tethyan, Transitional, and Falkland Plateau nannoplankton Provinces. Rather than refer-

ring to the region occupied by the high latitude nannoflora as "Austral", I have elected to use the term "Falkland Plateau Province". Sharp differences in nannofloral composition are evident between sites in the southern Atlantic and Indian Oceans and sites in the Tasman Sea (DSDP Sites 207 and 208). It is a distinct possibility that these differences are a result of slight age differences rather than the result of provinciality. The sections recovered in the Atlantic and Indian Oceans are all upper Campanian through middle Maestrichtian, while the two Tasman Sea sites are upper Maestrichtian. Ranges of high latitude species as recorded at DSDP Sites 217 and 249, and to a minor extent, DSDP Site 357, suggests that most if not all of the distinctive species which characterize the Falkland Plateau assemblage died out prior to the upper Maestrichtian. Until upper Maestrichtian samples are obtained from the Falkland Plateau, or older sediments are found in the Tasman Sea or New Zealand, the question as to whether the differences in nannofloral composition between these two regions remains unanswered.

The Tethyan Province is characterized by common to abundant *Biscutum constans* and *Watznaueria + Cyclagelosphaera,* and rare *Micula staurophora.* The Falkland Plateau Province is typified by abundant *Biscutum magnum* and *B. coronum*, and rare *Watznaueria, Cyclagelosphaera,* and *Micula staurophore.* The broad Transition Zone is typified by assemblages in which *Micula staurophora* and *Watznaueria + Cyclagelosphaera* vie for dominance; both *Biscutum constans* and *B. magnum (+ B. coronum)* may be present to some extent, with *B. constans* the most common species of this genus throughout the province.

The southernmost limit of the Tethyan Province is placed at the point of lowest latitude occurrence of the high latitude species of *Biscutum.* The northernmost limit of the Falkland Plateau Province is marked by a line south of which few specimens of *Micula staurophora, Watznaueria* and *Cyclagelosphaera* are present. During the upper Campanian through middle Maestrichtian, this region was also typified by abundant *Biscutum magnum* and *B. coronum.*

Using the criteria outlined here to delineate nannoplankton province boundaries, there appears to be good agreement between the location of a Tethyan-Transitional Province boundary using planktonic foraminifera, and using calcareous nannoplankton. The areal extent of the Austral Foraminifera Province is not precisely known, owing to the paucity of data points in the south Atlantic and Indian Oceans. As a result, it is not possible to compare the limits of the Austral (Planktonic Foraminifera) and Falkland Plateau (Calcareous nannoplankton) Provinces.

## Summary and Conclusions

1. An extremely diverse and well-preserved Campanian-Maestrichtian nannoplankton assemblage typifies samples from DSDP Hole 327A on the Falkland Plateau. The assemblage was not confined to the Falkland Plateau, but also occupied the southern portion of the eastern sector of the Atlantic Ocean and southern Indian Ocean.

2. By comparing the ranges of high, middle, and low latitude nannoplankton species in two Indian Ocean sites (DSDP Sites 217 and 249), it is possible to determine the ages of the cores recovered from DSDP Hole 327A. Core 13 is dated as late Campanian, while cores 10 through 12 are early Maestrichtian. A core from a second site on the Falkland Plateau, Islas Orcadas Core 07-75-44, is dated as latest Campanian to earliest Maestricht-

. Data from DSDP Sites 217 and 249 indicates that nearly all of the distinctive species which characterize the Falkland Plateau Assemblage disappeared before the upper Maestrichtian. It is not known whether this high latitude assemblage was also present in the southern Pacific region.

4. The most obvious difference between well-preserved nannofloras from low, middle, and high latitude regions is the relative abundance of *Micula staurophora* and *Watznaueria barnesae + Cyclagelosphaera margareli. Watznaueria* and *Cyclagelosphaera* were the dominant low-latitude nannofloral components. In higher latitudes, *Micula staurophora* became much more common, and in some regions, its skeletal elements comprised more than half of all elements in the sediment. In the southernmost sites in the Atlantic and Indian Oceans, all three of these forms were extremely rare south of a sharp water mass boundary.

5. In addition to the ratio of *Micula staurophora* to *Watznaueria + Cyclagelosphaera*, the relative abundance of the high latitude species of *Biscutum (B. magnum* and *B. coronum)* appears to be a valid indicator of province affinity and relative paleolatitude. *Biscutum constans* was the dominant low latitude species, while in high latitudes, the genus was represented almost exclusively by species first observed on the Falkland Plateau. The two regimes were separated by a zone in which few specimens of any species of this genus were present.

6. Accelerated flow of the South Atlantic Gyre and the presence of a reciprocal clockwise current or zone of upwelling along the Falkland Plateau resulted in the juxtaposition of nannofloras of radically different composition on the two sides of the plateau during the late Campanian and Maestrichtian.

7. Reasons for the sharp distinction between high and lower latitude assemblages can only be theorized. The definitive explanation awaits additional coring on the northern flank of the Falkland Plateau. However, examination of the nannoflora from Islas Orcadas Core 07-75-44 suggests that the distinctive high latitude Campanian and Maestrichtian nannoflora arose in response to one or more of the following phenomena: extremely cold surface water, reduced salinity, or abnormal nutrient levels.

Acknowledgments. I thank the National Science Foundation for the opportunity to examine the samples utilized in this study. Early drafts of the manuscript were reviewed by S. W. Wise, Jr., R. C. Wright, M. G. Dinkelman, A. L. Odom (F.S.U. Geology), R. Iverson (F.S.U. Oceanography), H. R. Thierstein (Scripps Institution of Oceanography), and P. Roth (Department of Geology and Geophysics; University of Utah).

## References

Bukry, D., 1973a. Low-latitude coccolith biostratigraphic zonation: In Edgar, N. T., Saunders, J. B., et al., Initial Reports of the Deep Sea Drilling Project, v.15, Washington (U. S. Government Printing Office), pp. 685-703.

_____, 1973b. Coccolith and silicoflagellate stratigraphy, Tasman Sea and southwestern Pacific Ocean, Deep Sea Drilling Project Leg 21: In Burns, R. E., Andrews, J. E., et al., Initial Reports of the Deep Sea Drilling Project, v.21, Washington (U. S. Government Printing Office), pp. 885-893.

_____, 1974a. Coccolith and silicoflagellate stratigraphy, eastern Indian Ocean, Deep Sea Drilling Project, Leg 22: In von der Borch, C. C., Sclater, J. G., et al., Initial Reports of the Deep Sea Drilling Project, v.22, Washington (U. S. Government Printing Office), pp. 601-607.

_____, 1974b. Phytoplankton stratigraphy, offshore East Africa, Deep Sea Drilling Project Leg 25: In Simpson, E. S. W., Schlich, R., et al., Initial Reports of the Deep Sea Drilling Project, v.25, Washington (U. S. Government Printing Office), pp. 635-646.

_____, 1974c. Coccoliths as paleosalinity indicators - Evidence from Black Sea: The Black Sea - Geology, Chemistry, and Biology, American Association of Petroleum Geologists Memoir No. 20, pp. 353-363.

_____ and Bramlette, M. N., 1970. Coccolith age determinations Leg 3, Deep Sea Drilling Project: In Maxwell, E., von Herzen, R., et al., Initial Reports of the Deep Sea Drilling Project, v.3, Washington (U. S. Government Printing Office), pp. 589-611.

Čepek, P., and Hay, W. W., 1969. Calcareous nannoplankton and biostratigraphic subdivision of the Upper Cretaceous: Transactions of the Gulf Coast Association of Geological Societies, v.19, pp. 323-336.

Ciesielski, P. F., Sliter, W. V., Wind, F. H., and Wise, Jr., S. W., 1977. Paleoenvironmental analysis and correlation of a Cretaceous Islas Orcadas core from the Falkland Plateau, southwest Atlantic: Marine Micropaleontology, v.2, pp. 27-34.

Ciesielski, P. F., and Wise, Jr., S. W., 1977. Geologic history of the Maurice Ewing Bank of the Falkland Plateau (southwest Atlantic sector of the Southern Ocean) based on piston and drill cores: Marine Geology, v.25, pp. 175-207.

Edwards, A. R., 1966. Calcareous nannoplankton from the uppermost Cretaceous and lowermost Tertiary of the mid-Waipara section, South Island, New Zealand: New Zealand Jour. Geol. Geophys., v.9, pp. 481-490.

Gartner, Jr., S., 1974. Nannofossil biostratigraphy, Leg 22, Deep Sea Drilling Project: In von der Borch, C. C., Sclater, J. G., et al., Initial Reports of the Deep Sea Drilling Project, v.22, Washington (U. S. Government Printing Office), pp. 577-599.

Haq, B. U., and Lohmann, G. P., 1976. Early Cenozoic calcareous nannoplankton biogeography of the Atlantic Ocean: Marine Micropaleontology, v.1, pp. 119-197.

Haq, B. U., Premoli-Silva, I., and Lohmann, G. P., 1977. Calcareous plankton paleobiographic evidence for major climatic fluctuations in the early Cenozoic Atlantic Ocean: Jour. Geophys. Res., v.82, pp. 3861-3876.

McGowran, B., 1974. Foraminifera: In von der Borch, C. C., Sclater, J. G., et al., Initial Reports of the Deep Sea Drilling Project, v.22, Washington (U. S. Government Printing Office), pp. 609-628.

Matsumoto, T., 1973. Late Cretaceous Ammonoidea: In Hallam, A., Atlas of Paleobiogeography, Amsterdam (Elsevier Scientific Publishing Co.), pp. 421-429.

Martini, E., 1976. Cretaceous to Recent calcareous nannoplankton from the central Pacific Ocean (DSDP Leg 33). In Schlanger, S. O., Jackson, E. D., et al., Initial Reports of the Deep Sea Drilling Project, v.33, Washington (U. S. Government Printing Office), pp.439-450.

Perch-Nielsen, K., 1972. Remarks on Late Cretaceous to Pleistocene coccoliths from the North Atlantic: In Laughton, S. A., Berggren, W. W., et al., Initial Reports of the Deep Sea Drilling Project, v.12, Washington (U. S. Government Printing Office), pp. 1003-1069.

_____, 1977. Albian to Pleistocene calcareous nannofossils from the western South Atlantic: In Supko, P. R., Perch-Nielsen, K., et al., 1977. Initial Reports of the Deep Sea Drilling Project, v.39, Washington (U. S. Government Printing Office), pp. 699-823.

Pessagno, Jr., E. A., and Michael, F. Y., 1974. Mesozoic foraminifera, Leg 22, Site 217: In von der Borch, C. C., Sclater, J. G., et al., Initial Reports of the Deep Sea Drilling Project, v.22, Washington (U. S. Government Printing Office), pp. 629-634.

Premoli-Silva, I., and Boersma, A., 1977. Cretaceous planktonic foraminifers - DSDP Leg 39 (South Atlantic): In Supko, P. R., Perch-Nielsen, K., et al., Initial Reports of the Deep Sea Drilling Project, v.39, Washington (U. S. Government Printing Office), pp. 615-642.

Simpson, E. S. W., Schlich, R., et al., 1974. Initial Reports of the Deep Sea Drilling Project, v.25, Washington (U. S. Government Printing Office), 884 pp.

Sliter, W. V., 1977. Cretaceous foraminifers from the southwestern Atlantic Ocean, Leg 36, Deep Sea Drilling Project: In Barker, P. F., Dalziel, I. W. D., et al., Initial Reports of the Deep Sea Drilling Project, v.36, Washington (U. S. Government Printing Office), pp. 519-573.

Thierstein, H. R., 1976. Mesozoic calcareous nannoplankton biostratigraphy of marine sediments: Marine Micropaleontology, v.1, pp. 325-362.

Thierstein, H., and Haq, B. U., 1977. Maestrichtian/Danian biogeographic variations in calcareous nannoplankton (Abstr.): Jour. Paleontology, v.51 Supplement to No. 2, pp.28-29.

Tucholke, B. E., and Carpenter, G. B., 1977. Sediment distribution and Cenozoic sedimentation patterns on the Agulhas Plateau: Geol. Soc. America Bull., v.88, pp. 1337-1346.

Wise, S. W., and Wind, F. H., 1977. Mesozoic and Cenozoic calcareous nannofossils recovered by DSDP Leg 36 drilling on the Falkland Plateau, Atlantic sector of the Southern Ocean. In Barker, P. F., Dalziel, I. W. D., et al., Initial Reports of the Deep Sea Drilling Project, v.36, Washington (U. S. Government Printing Office), pp. 269-492.

Worsley, T. R., 1971. The terminal Cretaceous event: Nature, v.230, pp. 318-320.

_____, 1974. The Cretaceous-Tertiary boundary event in the ocean: In Hay, W. W., ed., Studies in Paleo-oceanography, Society of Economic Paleontologists and Mineralogists Special Publication No. 20, pp. 94-125.

_____, and Martini, E., 1970. Late Maestrichtian nannoplankton provinces: Nature, v.225, pp. 1242-1243.

# THE NORTHWESTERN IBERIAN MARGIN: A CRETACEOUS PASSIVE MARGIN DEFORMED DURING EOCENE ([1])

Gilbert Boillot, Jean-Luc Auxietre, and Jean-Pierre Dunand

Groupe d'Etude de la Marge Conginentale, Laboratoire de Géologie Dynamique
Université Pierre et Marie Curie, 4, place Jussieu, 75230 Paris Cedex 05 France

Pierre-Alain Dupeuble

Laboratoire de Géologie, Faculté des Sciences et Techniques de Rouen, 76130
Mont-Saint-Aignan, France

Alain Mauffret

Groupe d'Etude de la Marge Conginentale, Laboratoire de Géologie Dynamique
Université Pierre et Marie Curie, 4, place Jussieu, 75230 Paris Cedex 05 France

Abstract. The structural evolution of the northwestern Iberian margin has been reconstructed from the results of IPOD drill site 398, as well as from numerous dredgings and a dense network of seismic profiles.

During the Mesozoïc the margin first underwent two consecutive extensional phases interpreted as the result of two episodes of rifting in the Atlantic. Then during Eocene, subsidence was interrupted by compression and related deformation caused by subduction of oceanic sea floor of the Bay of Biscay beneath the Iberian Peninsula. Present day marginal banks are interpreted as blocks of the older passive margin uplifted during early Tertiary as a result of that subduction. Fault escarpments provide opportunities to sample older sediments and basement by dredging.

The northwestern Iberian continental margin is morphologically both complex and anomalous (fig. 1 and 2). The emerged province of Galicia (Spain) is bordered to the West by a narrow (30-40 km) continental shelf adjacent to a wide and deep(350 km long, 100 km wide, and 3 to 4 km deep) U-shaped trough. Seaward, a series of marginal plateaus forms a discontinuous barrier between that trough and the Iberian abyssal plain (Laughton et al., 1975; Auxiètre and Dunand, 1978). These plateaus are, from North to South : Galicia, having its top at -600 m ([2]), Vigo (-2100 m), Vasco da Gama (-1750 m), and Porto (-2200 m).

The origin of these structures has been interpreted in two different manners. According to Montadert et al. (1974), they consist in horsts formed during late Jurassic (?)-early Cretaceous rifting, in connection with the opening of the Atlantic Ocean between Iberia and Newfoundland. For Mauffret et al. (1978), however, these plateaus have appeared only during Eocene times, following compression and deformation of the margin. In this paper we shall try to document the latter interpretation.

Since 1974 the Iberian margin off Galicia has been extensively studied by three french scientific teams joining into the "Groupe Galice" ([3]). Their major objective was to prepare the leg 47b of the "Glomar Challenger" through a detailed geological and geophysical reconnaissance of the area selected for drilling during the IPOD program. The main results have been presented collectively (Groupe Galice, 1978). After the drilling at site 398 (Ryan, Sibuet et al., 1976), we have collected additional data in the same area during the R/V Jean Charcot cruise "Hesperides 76". New seismic profiles together with dredge samples have provided the basis for improved correlations between drilling results and the stratigraphy of the sedimentary basins surrounding the site, previously studied by Black et al. (1974) and Dupeuble et al. (1976).

([1]) Contribution n°90 of the "Groupe d'Etude de la Marge Continentale" (ERA 605) of Université Pierre et Marie Curie, Paris.

([2]) In this paper we make a distinction between Galicia Bank (sensu stricto) with its top at -600 m and the Galicia Plateau which is much larger and includes several isolated highs (the Galicia Bank being one of them).

([3]) Centre Océanologique de Bretagne (CNEXO); Groupe d'Etude de la Marge Continentale (Université Pierre et Marie Curie); Institut Français du Pétrole.

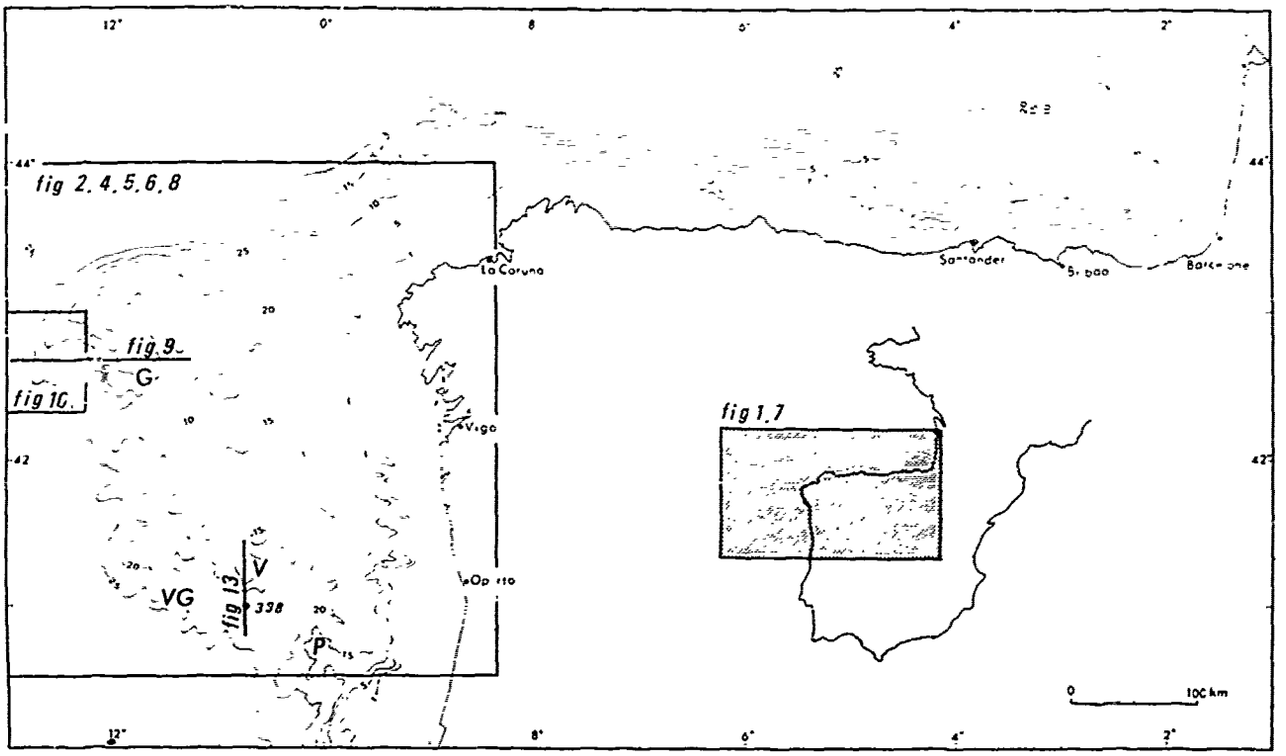


Fig. 1. General location of the region studied and location of figures 2, 4, 5, 6, 8, 10 and 13.
G : Galicia Bank; VG : Vasco da Gama seamount; V : Vigo seamount; P : Porto seamount.

## I - Stratigraphy and sedimentary evolution (tables I and II).

The stratigraphy has been studied through seismic profiles (fig.3), drilling results at site 398, and numerous dredgings (fig.4). Seismic profiles show several units having distinct acoustic characters and often separated by unconformities (table I); drilling results provide the basis for correlation between these units and the lithology; finally the dredge samples complete the picture in particular by yielding information on the older (pre-Cretaceous) formations not reached by drilling. The dense network of seismic profiles (more than 8000 km, fig.5) allows an extension of the stratigraphic results throughout the entire area.

1. The acoustic basement (table II), that was probably not reached by drilling, outcrops along fault escarpments where we dredged several samples. West of Galicia Bank, it consists of metamorphic and plutonic rocks having petrological characteristics comparable to those from the pre-Mesozoïc basement of the Iberian Meseta (Capdevila, personal communication). On the flanks of Vigo, Porto, and Vasco da Gama seamounts, however, dredge hauls yielded limestone fragments, dated late Jurassic to early Cretaceous (mainly Kimmeridgian through Berriasian, possibly Valanginian in some cases).

These limestones show two different facies :

a) Some rocks consist of pelletoïdal to pebbly limestone, and contain various assemblages of benthic foraminifera and calcareous algae. Although faunal assemblages vary from one sample to the other they all indicate the same sedimentary environment : shallow water calcareous sedimentation, often peri-reefal. Some might even suggest brackish conditions.

Identical limestones are present in Portugal (Ramalho, 1971) and on the northern margin of Iberia (Boillot et al., 1978). They have also been found at site 401 on the Armorican margin (Montadert, Roberts et al., 1976).

b) Other samples consist of micritic limestone rich in Calpionellids, dated late Tithonian to Berriasian. These sediments were probably deposited in calm environments in an open sea having good communication with the Tethys where Calpionellids originated (Boillot et al., 1971a). Some micritic fragments have been found intercalated between reefal limestones, and some Calpionellids are also present in the pebbly limestones, suggesting that locally they might have been deposited in relatively shallow water conditions.

2. Cretaceous and Cenozoïc sediments have been sampled by drilling and correlation between lithology and acoustic stratigraphy is straightforward (table I).

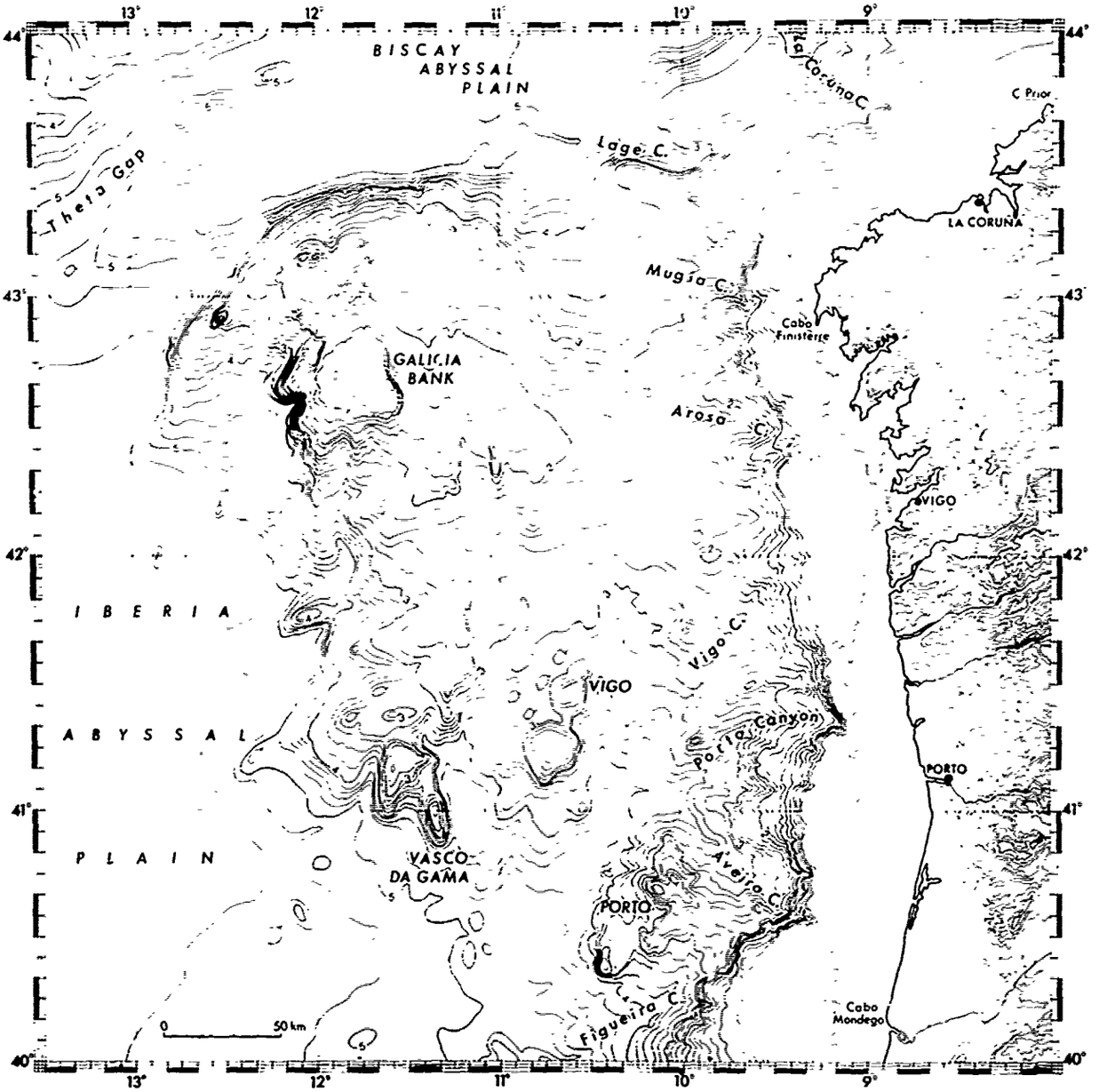


Fig. 2. Bathymetry of the continental margin North-West of the Iberian peninsula (contours drawn in collaboration with J.-R.Vanney), after Berthois et al. and Laughton et al., corrected and reinterpreted with additional data from bathymetric profiles of figure 5.

Intervals sampled by drilling have only rarely been reached by dredging. Black et al. (1964) dredged detrital limestones, rich in Orbitolinas, probably resedimented, on the Galicia Plateau. They might correspond with early Cretaceous sediments of Unit 4 (table I). Upper to uppermost Senonian rocks (unit 2) outcrop on both Vigo seamount and Galicia Plateau (Black et al., 1964; Funnell et al., 1969; Dupeuble et al., 1976). They consist of marls and marly chalks containing pelagic microfauna that suggests deep sea deposition above the CCD. Thus, as far as the Cretaceous is concerned, the redults from dredging compare rather well with the occurrence of calcareous pelagic facies in the uppermost Senonian interval and of detrital limestones in the Neocomian-Aptian layers at the drill site.

Paleocene and Eocene facies, however, show de-

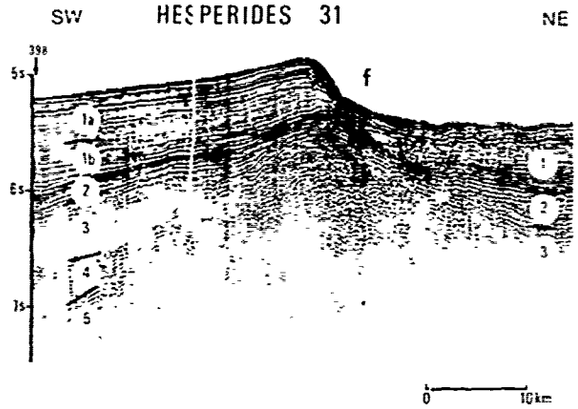


Fig. 3. Acoustic stratigraphy in the vicinity of IPOD Site 398. Location of seismic profile appears on figure 5. Stratigraphy of the sediment section is described in Table I. Units 3 and 4 accumulated in a half graben. F fault was reactivated during Tertiary.

finite local variations. At site 398 and on Vigo seamount (L 258, table II), sedimentation during this interval resembles that of the late Cretaceous. Conversely, a neritic limestone rich in Halimeda and dated from the latest Cretaceous ([4]) has been dredged from Galicia Plateau by Black et al. (1964). Eocene tectonics and associated paleogeographic changes, clearly seen on seismic profiles (§ IV.1), appear also well documented by the rapid shoaling of the Galicia Plateau area toward the end of the Cretaceous ([5]) as interpreted from the sedimentary record.

The influence of the renewed morphology on sedimentation after the Eocene could not be studied because of the scarcity of Oligocene and Neogene samples. Pelagic or hemipelagic conditions seem to have prevailed on the entire margin during this interval.

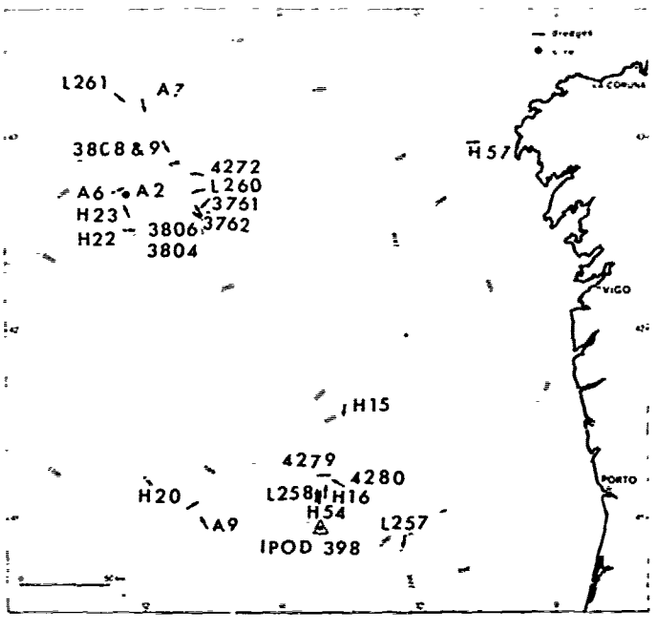


Fig. 4. Dredge samples from the northwestern Iberian margin. Four-digit numbers refer to samples described by Black et al. (1964). Numbers preceded with letters A and L refer to samples studied by Dupeuble et al. (1976). Sample numbers preceded with letter H are from cruise "Hesperides 76". Stratigraphic information from this samples is summarized in Table II.

## II - Structural trends.

Comparison between bathymetry (fig.2) and the schematic structural reconstruction of figure 6, shows that the present day morphology is directly influenced by major structural trends. Shallower areas correspond with horsts, deeper areas with sedimentary basins. Faults show four major directions : N 40°, N 60°, N 340° and N 360°. The first three directions are also apparent on satellite photographs of the nearby continental area (Biju-Duval et al., 1976; fig.7) and are parallel to major strike-slip "tardihercynian" faults that fragmented the Iberian Peninsula at the end of the Paleozoïc (Parga, 1969; Arthaud and Matte, 1975; fig.7). The structure of the margin thus appears to be inherited from that of its pre-Mesozoïc basement where major faults have been re-activated during Mesozoïc and Tertiary times (Boillot et al., 1974). The N 360° faults that are well documented on the margin, however, are barely visible in the basement of the Iberian Meseta (fig.7). They might correspond with early to middle Cretaceous faults contemporaneous with the opening of the adjacent Atlantic.

## III - Extension tectonics during the Mesozoïc.

1. First rifting phase. Although interpretation is sometimes difficult, seismic profiles indicate locations where the acoustic basement shows clear diffraction patterns and corresponds with pre-Mesozoïc basement rocks locally covered with calcareous Jurassic carbonates. They also show other areas where sedimentary basins of late Jurassic and possibly Triassic age are probably incorporated within that basement. In the latter case more

([4]) Age assignment is based on species determination of Halimeda, the occurrence of rounded fragments of Rudistids, and on a comparison with similar facies observed in some Danian layers form the Aquitaine basin.

([5]) Such an interpretation shows a good agreement with other data from Black et al. (1964) (3808, table II) who found on Galicia Plateau a porous and deformed limestone with rare Eocene nannofossils and abundant calcite fragments which, according to the description, could be fragments of Microcodium.

| ACOUSTIC STRATIGRAPHY | ACOUSTIC CHARACTER | CORRELATION WITH DRILLING RESULTS FROM SITE 398 (Ryan, Sibuet et al., 1976) | |
|---|---|---|---|
| | | A g e | Lithology |
| Unit 1 — 1a / 1b | Moderately stratified layers with some evidence of reworking by bottom currents, and progradation | 1a Holocene-late Miocene<br>1b Middle Miocene-late Eocene | Turbidites, contourites and carbonate-poor hemipelagic sediments |
| Unit 2 | Well stratified series | Early Eocene-late Cenomanian<br>(hiatus from mid-Cenomanian through Santonian) | Deep sea pelagic sediments (zeolitic brown clay) with evidence of submarine erosion and hiatuses. High degree of carbonate dissolution except during a short interval dated latest Cretaceous-early Eocene |
| Unit 3 | Acoustically transparent layers | Early Cenomanian-Albian | Black clays and turbidites rich in organic matter, deposited in a deep sea environment |
| Unit 4 | Stratified layers, often showing "fan-shaped" layering that suggests syntectonic filling of grabens and half-grabens | Aptian-Hauterivian | Calcareous series including resedimented uppermost Jurassic neritic limestones |

Table I. Cretaceous and Cenozoïc sediment section on the northwestern Iberian margin from drilling result at site 398 and seismic reflexion profiles.

or less continuous reflectors are visible within the basement, together with diapiric structures (Montadert et al., 1974). It is thus possible to delineate hypothetical contours of Mesozoïc (pre-Cretaceous) sedimentary basins :

- a first trough is located between the marginal plateaus and the coast of Iberia. It is characterized by a thick sediment accumulation and diapirs. It represents probably a submarine extension of the Lusitanian Basin where diapirs correspond with evaporites of Triassic and Liassic age (Zbyszewsky and Berreto de Faria, 1971);
- a second basin apparently lies along the western flank of Galicia Bank ([2]) and Vasco da Gama seamount as suggested by deep reflectors within acoustic basement. The eastern boundary of this basin seems to come closer to the shore South of 41°S (fig.8).

During Triassic and Liassic times a major extensional tectonic phase preceded the separation between the American and the African plates. This rifting phase affected also the Canadian margin (Amoco and Imperial, 1973; Jansa and Wade, 1975), as well as several areas around the North Atlantic and in particular the North Sea, the English Channel and the Aquitaine Basin. We believe that the same event resulted in the formation of a Triassic continental rift at the site of the northwestern Iberian margin, and we interpret the tectonic troughs observed to the East and to the West of the present day marginal banks as a result of the formation of that rift (fig.8). Oceanic crust probably did not form at the time, at least North of 41°N (Le Pichon et al., 1977). To the South, however, the western trough could have evolved into a narrow accretion zone so that Jurassic oceanic crust could be present beneath the Tagus abyssal plain (Olivet, 1978; Auxiètre and Dunand, 1978).

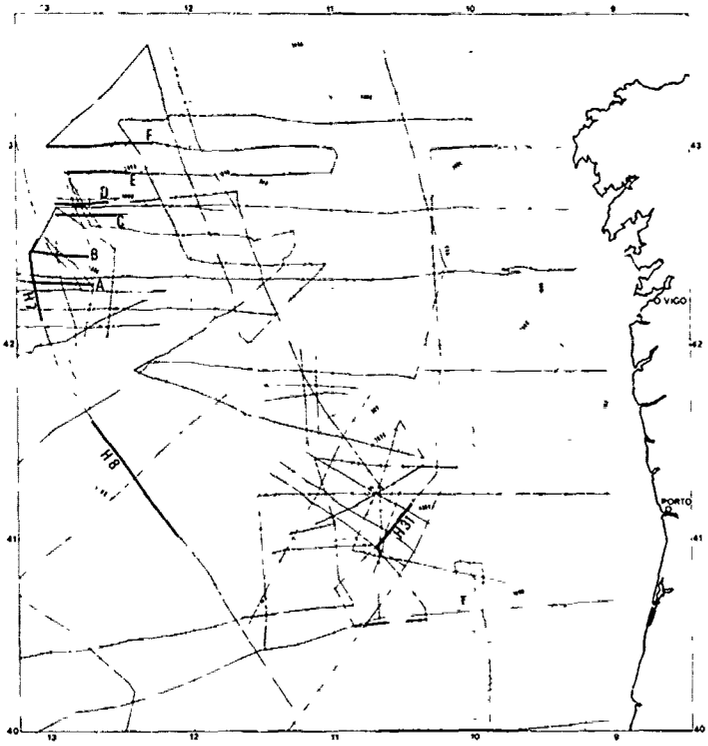


Fig. 5. Location of seismic profiles used for this study (data from Institut Français du Pétrole, Centre Océanologique de Bretagne, and Université Pierre et Marie Curie of Paris). Bold lines represent profiles of figures 3,11, and 15.

2. The late Liassic and Dogger transgression. This transgression has been observed on the continental shelf and in the Portugal Basin. It probably results from the thermally induced detumescence that occurred when activity within the rift died (Baldy et al., 1977). A very thick sedimentary section then accumulated during Jurassic in the Iberian marginal troughs as well as in those of the Canadian margin (Gradstein et al., 1977; Grant, 1977). On this side of the Atlantic, this observation is documented only from seismic profiles, because we could not sample rocks corresponding with that interval.

3. Second rifting phase. On the continental shelf and in the Portugal Basin, the Callovian is characterized by a regression. After the Oxfordian, rapidly subsiding tectonic troughs were invaded by the sea. A generalized regression followed during the latest Jurassic (Wilson, 1975; Mougenot, 1976). In the deeper parts of the margin, the pre-Cretaceous acoustic basement (including late-Jurassic - earliest Cretaceous limestones; § I.1) broke into horsts and grabens (or half-grabens). Tectonic troughs remained active while Neocomian sediments were accumulating, as evidenced by the geometry of these deposits on seismic profiles, where the dip of the sediment layers is seen to decrease from bottom to top (Groupe Galice, 1978).

This activity corresponds to a second rifting phase, during late Jurassic and early Cretaceous, affecting the Northwest Iberian margin and the adjacent continent. Such a rifting phase caused local subsidence within the tectonic troughs, as well as a regional uplift accompanied by erosion of emergent areas. Ancient Triassic fault zones have been rejuvenated at that time. Galicia Bank, which was probably a horst during Triassic times (fig.8), was then uplifted again during the early Cretaceous, as suggested by the direct contact between upper Cretaceous sediments and the underlying pre-Mesozoïc basement of the bank (fig.9; § I.1). Generally, however, the new extensional phase is characterized by a set of fractures oriented along a direction somewhat different from that of the Triassic faults.

The second rifting phase lasted at least from Oxfordian to the end of Aptian. On the margin itself, however, its maximum seems to have occurred only after deposition of the upper Jurassic and lowermost Cretaceous limestones, as these show evidence of fracturation.

The tectonic and sedimentary evolution of the Canadian margin appears quite similar : the latest Jurassic, in particular, is characterized by an unconformity showing erosion of older layers resulting from a major uplift during the classical "late Cimerian" tectonic phase (Gradstein et al., 1977; Grant, 1977; Jansa and Wade, 1975).

4. Subsidence during mid-to late Cretaceous. After the late Jurassic-Neocomian rifting phase, the actual separation of the Newfoundland-Grand Bank area from the margin off Galicia probably occurred during Aptian (Groupe Galice, 1978; Olivet, 1978). The regional subsidence became very rapid while black shales were filling the former grabens and sometimes spilled over some of the horsts (Groupe Galice, 1978). Finally, during the late Cretaceous (while Unit 2 was being deposited), most late Jurassic and Neocomian structures were blanketed by sediment. Cenomanian or Senonian layers, for example, are locally found directly over the pre-Mesozoïc basement. This is observed on the Canadian side on the Avalon high and the La Have platform (Jansa and Wade, 1975) as well as on the Galicia Bank, on the European side. During the same time, the sea spread widely over the neighbouring continent. The area of Galicia Plateau and Vigo seamount was been a deep and monotonous continental rise, covered with a thin veneer of pelagic sediment (fig.9), while the fast drifting of Iberia away from North America (Hays and Pitman, 1973; Hart, 1975) favored the onset of deep water circulation in the newly formed oceanic basin (Rehault and Mauffret, 1978).

## IV - Compression tectonics during Eocene.

### 1. Galicia Plateau.

The flanks of the Galicia Plateau show evidence of a major tectonic event during Eocene times :

| SAMPLE | SEAMONT | FACIES DESCRIPTION | AGE AND PALEOENVIRONMENT | ACOUSTIC STRATIGR. |
|---|---|---|---|---|
| L 260 | Galicia | Marly limestone with corals filled up with planktonics (*Globorotalia truncatulinoides*) | Pleistocene; probably bathyal | |
| A 07 | Galicia | Marly limestone with planktonic assemblage (*Globorotalia truncatulinoides*) and some Pelecypod and Echinid remains | Pleistocene; probably bathyal | |
| L 258<br>A 06 | Vigo<br>Galicia | Marls with *Globorotalia truncatulinoides*, reworking older planktonics mainly from Paleocene and upper Cretaceous | Pleistocene; bathyal | 1 |
| L 261 | | Marl with planktonic assemblage (*Praeorbulina*) | Lower part of Middle Miocene; bathyal | |
| 4279 | Vigo | Foraminiferal limestone and ooze (Black et al.,1964) | Mid-Tertiary; bathyal | |
| A 06 | Galicia | Marl with planktonic assemblage : *Globigerinita dissimilis* and *Globigerina ciperoensis*) | Late Oligocene; bathyal | |
| 3808 | Galicia | Porous and chalky limestone, with *Discoaster aster, Praarudosphaera discula, Coccolithus eopelagicus* etc. and little fragments of calcite crystal (*Microcodium??*) (Black et al., 1964). | Middle Eocene; very shallow water or emersion ?? | |
| L 258 | Vigo | Marl with planktonic assemblage : *Globorotalia aequa, G.velascoensis*<br>Reworked *Globorotalia pusilla* and *G.angulata* in Pleistocene marls (see Pleistocene). | Late Paleocene; bathyal<br>Middle Paleocene; bathyal | 2 |
| 3806 | Galicia | Coarse detrital limestone with rolled fragments of Rudist and *Halimeda* (Black et al., 1964) | Danian? shallow water | |
| 3804<br>3809 | Galicia | Chalk with planctonic assemblage (Black et al., 1964; Funnell et al., 1969). | Uppermost Maestrichtian; bathyal | |
| L 258 | Vigo | Reworked *Globotruncana* and *Heterohelicidae* in Pleistocene marls (see Pleistocene) | Maestrichtian; probably bathyal | |
| L 258 | Vigo | Marls more or less indurated with *Globotruncana arca, G.falsostuarti, Racemigumbelina fructicosa* | Maestrichtian; bathyal | |
| L 260 | Galicia | Marly limestones with *Globotruncana* sp. | Senonian; bathyal | |
| 4272<br>3762 | Galicia | Detrital limestones with broken Foraminifera, Molluscs, Calcareous Algae and *Orbitolina* (probably displaced) (Black et al., 1964) | Lower Cretaceous; shelf environment (resedimented ?) | 4 |
| L 257 | Porto | Micritic limestone with Calpionellids (*Calpionella alpina, Tintinopsella carpathica*) | Late,Early Berriasian Pelagic assemblage | |
| A 09 | Vasco da Gama | Micritic limestones with Calpionellids (*Calpionella alpina, Crassicolaria intermedia, Tintinopsella carpathica-longa, Crassicolaria brevis*) | Late Tithonian; Pelagic assemblage | |
| 4280<br>A 09<br>L 257<br>L 258<br>H 15<br>H 16<br>H 20<br>H 54<br>H 57 | Vigo<br>Vasco da Gama<br>Porto<br>Vigo<br>Vigo<br>Vigo<br>Vasco da Gama<br>Vigo<br>Vasco da Gama | Fine grained to pelletoïdal limestones often with frequent Algae remains such as *Clypeina jurassica, Thaumatoporella parvovesiculifera, Lithocodium aggretatum, Baccinella irregularis* and oncolits of Cyanophycea; Foraminifera are often common:mainly *Trocholina elongata, Neotrocholina* sp., *Pseudocyclammina lituus, Pseudocyclammina parvula-muluchensis, Conicospirillina basiliensis, Nautiloculina oolitica* etc. and Miliolidae | Kimmeridgian to Berriasian or lower Valanginian;<br>Shelf environment often peri-recifal Shallow water. | 5 |
| A 02<br>H 22<br>H 23 | Galicia | Metamorphic and magmatic rocks | Ante-Mesozoic basement | |

Table II. Stratigraphic informations from dredge samples obtained from Galicia Plateau, and Porto, Vigo, and Vasco da Gama seamounts. Location of samples appears on figure 4.

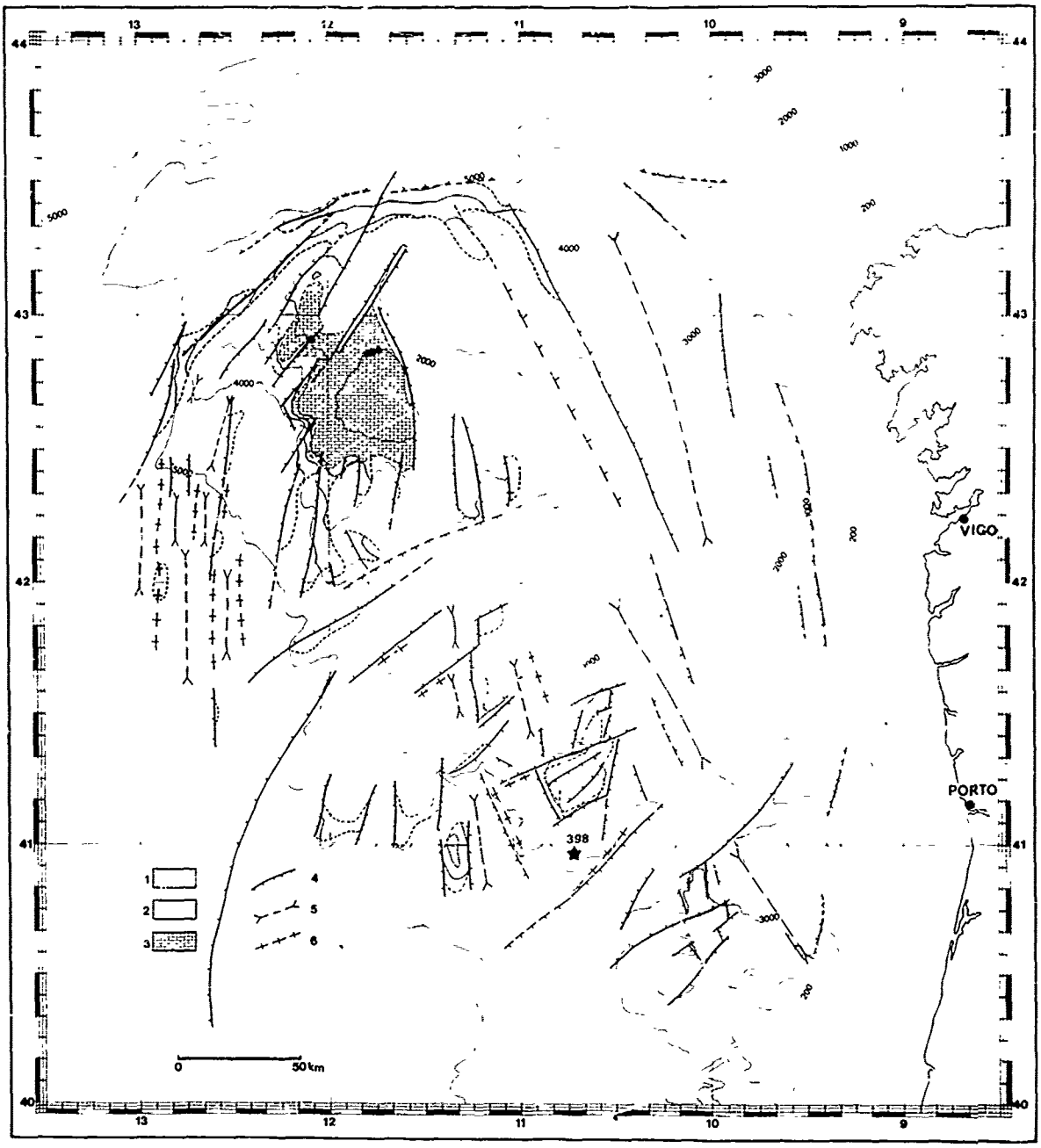


Fig. 6. Schematic structure of the northwestern Iberian margin (slightly modified after Groupe Galice, 1978). 1 : acoustic basement; 2 : Cenozoïc sediment cover; 3 : Cretaceous and Tertiary sediment cover (Galicia Bank); 4 : fault and flexure; 5 : sedimentary basin axis; 6 : structural high axis.

a) To the North, the very steep slope is oriented E-W (fig.2). It turns abruptly toward the SW near 12°W and separates in two branchs. The westernmost escarpment, oriented NE-SW, becomes regularly more gentle when approaching the Iberian abyssal plain (fig.10). Seismic profiles show that the fault zone that corresponds with the escarpment changes laterally to the South-West to a mere flexure in the deeper areas. This flexure is seen to affect the upper Cretaceous - lower Eocene layers (unit 2) whereas upper Eocene-lower Miocene strata seal the structure (fig.11). The age of the flexure is thus believed to be middle Eocene and the faults that extend from the

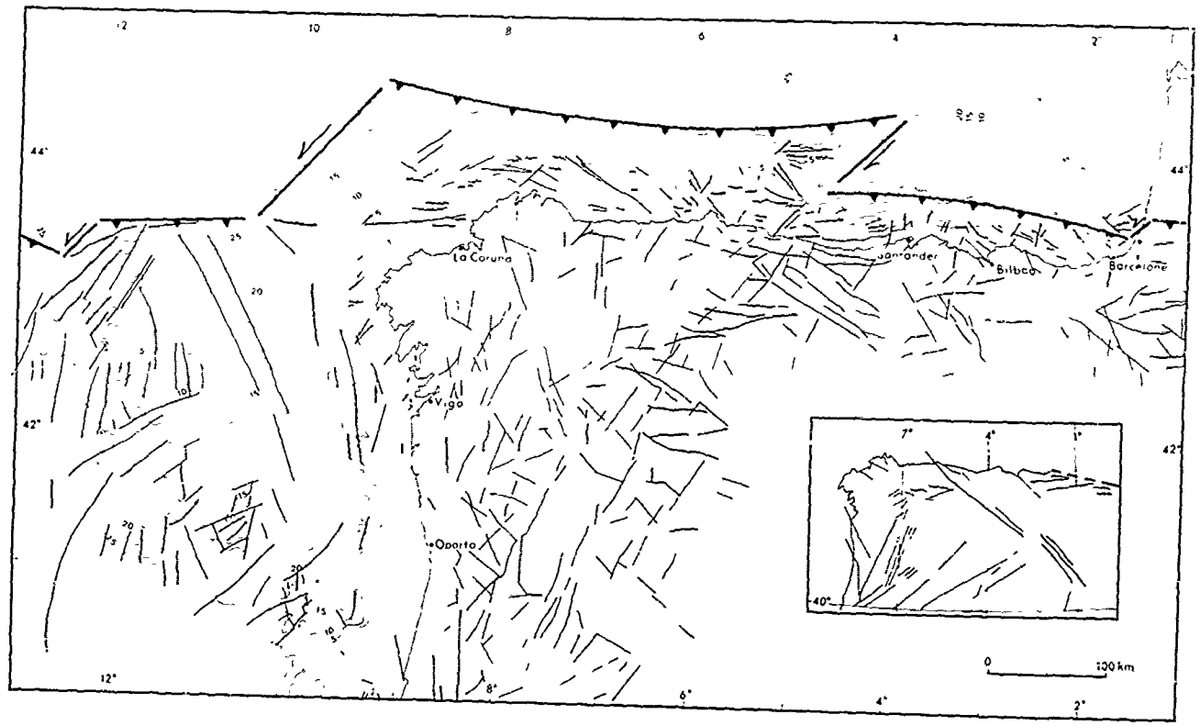


Fig. 7. Orientation of faults observed on the Iberian margin and on the adjacent continent. 1°/ Faults on the margin, from figure 5 and, for the continental shelf, after Boillot et al. (1973, 1975 and 1976) and Lamboy and Dupeuble (1975). 2°/ Orientation of structural trends on the continent from satellite photographs, after Biju-Duval et al. (1976), and tardihercynian strike-slip faults (in the box) from Arthaud and Matte (1975). The northern boundary of the Iberian Plate during Eocene (subduction zone and transform faults) is modified after Le Pichon and Sibuet (1971).

flexure area toward the North-East are probably of the same age. The vertical displacement observed along the fault scarps reaches more than 3000 m so that the Galicia Plateau must have been uplifted of that amount during early Cenozoïc. The same conclusion can be reached by observing faults located to the East of the plateaus where cumulative displacement during the Eocene can be estimated at about 3000 m, with a gradual decrease toward the South.

b) A reconstruction obtained by migrating some of the seismic profiles (profiles B and D, fig.10; Groupe Galice, 1978) shows that the Eocene faults bordering the Galicia Plateau to the North-West are reverse faults. This suggests that the deformation of the margin is indeed the result of a compression. The effect of tectonics increases toward the North where the escarpment reaches a maximum height over the abyssal plain. In that region the base of the slope is characterized by a belt of tectonically deformed sediment (profiles E and F, fig.10).

c) The Galicia Plateau today shows a composite structure. Some of its elements were horsts during the rifting phases, whiles others were active troughs .

- East of 12°W and South of 43°N, Galicia Bank itself ([2]) consists of a metamorphic and cristalline basement covered with a thin layer of upper Cretaceous sediment. This suggests that Eocene tectonics in that area caused uplifting of a Mesozoïc horst.

- Between Galicia Bank sensu stricto, underlain by continental basement (§ I.1), and Albian oceanic crust to the West, lies a "transition zone". That area corresponds with an older Triassic tectonic trough (fig.8) that became reactivated during the second rifting phase. It is probably underlain by continental crust that underwent considerable thinning during the two consecutive extensional phases. South of 42°20 (fig.2), the transition zone lies beneath the abyssal plain and is as deep as 5000 m. To the North-East however, it was uplifted during the Eocene tectonic phase, up to a level of 2000 m below sea surface, and today represents the northwestern part of the Galicia Plateau. During this movement the boundary between the oceanic crust and the transition zone might have acted as a hinge-line.

The area that was uplifted during the Tertiary then does not correspond with the older elevated areas. On the contrary, it represents a newly for-

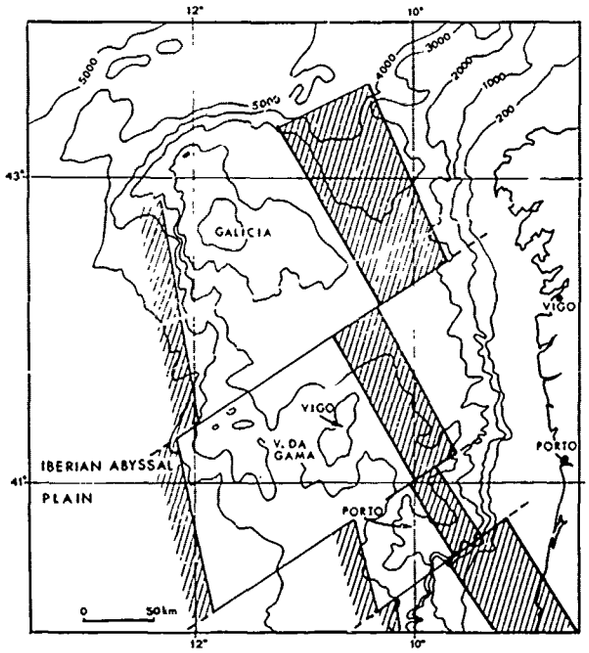


Fig. 8. Schematic distribution of lower Mesozoïc layers (hatched area) North-West of the Iberian peninsula and possible configuration of Triassic and early Liassic continental rifts. During these times, extension appears oriented along a NE-SW direction.

med structure erected during Eocene from the upper Cretaceous continental rise area (fig.9). The erosional surface that truncates Cretaceous layers on top of Galicia Bank suggests that it was emerged and eroded subaerially during Paleogene, and then subsided down to its present depth of 600 m.

d) In the transition zone, the total thickness of unit 2 (upper Cretaceous-lower Eocene) does not show appreciable variation in relation to present day water depth (fig.12 B). This implies homogeneous conditions of sedimentation and thus homogeneous water depths over the entire area. On the contrary, unit 1 (upper Eocene-Recent) increases abruptly in thickness toward the North-West, in the uplifted portion of the transition zone, where the water depth decreases to less than about 4000m (fig.12 A). Such a lateral variation can be explained by the difference in rates of accumulation above and below the CCD. It implies however, that the present day relief was formed after deposition of unit 2 and before that of unit 1, that is during Eocene time.

The above four independant lines of evidence demonstrate beyond any doubt that the Galicia Plateau is a structural high of Cenozoïc age that consists of a part of the Cretaceous margin, uplifted and deformed during a tectonic event.

2. Vigo seamount.

This seamount, which culminates at more than 1500 m above the level of the abyssal plain (fig. 2), is in fact a double horst (fig.6). The acoustic basement outcrops along escarpments where we dredged upper Jurassic and lowermost Cretaceous rocks (§ I.1). In the central area, seismic profiles show the accumulation of thick younger sediments (fig.13).

Comparison between the "acoustic stratigraphy" of this sediment section observed on the top of the seamount and that of the series actually sampled by drilling at site 398 (fig.14), located about 20 km to the South, reveals striking similarities as far as units 2, 3, and 4 (Cretaceous) are concerned. Thicknesses are similar and acoustic facies very comparable. This is particularly evident for unit 3, identified as black shales at the drill site. This facies consists mainly of turbidites characterized by a high rate of deposition (Ryan, Sibuet et al., 1976). Unit 1 (upper Eocene-Holocene) appears different in that it is much thicker in the deeper areas (owing to fast deposition of hemipelagic sediments) than on the top of the seamount. If the relief observed today had existed prior to the Eocene, the Cretaceous sediments, and especially unit 3, observed to consist of turbidites at the drill site, would necessarily present visible differences between the deeper margin and the top of the seamount where only a thin blanket of pelagic sediment would have accumulated. Therefore we conclude that Vigo seamount, like Galicia Bank, is a horst uplifted during the Tertiary as a piece of the Cretaceous continental rise. In our interpretation the perched sedimentary basin on top of Vigo seamount represents an older graben formed during late Jurassic-Neocomian and then uplifted during Eocene. The difference in depth between the Mesozoïc layers from the seamount and those from the adjacent abyssal plain suggests a vertical displacement of about 2000 m.

Our date are not sufficient to discuss the age of the other marginal plateaus (Vasco da Gama, Porto, etc.). We consider, however, that they are equivalent to Galicia and Vigo and that they too result from a Tertiary uplift.

3. The origin of the Eocene tectonics.

The margin off Galicia is not the only part of the Iberian margin where Eocene tectonic activity is recorded. During the latest Cretaceous and the Eocene, the Iberian and European plates have converged during a short period, and some of the oceanic lithosphere that underlies the Bay of Biscay has been subducted beneath the Iberian Peninsula (Sibuet and Le Pichon, 1971). As a result, the entire margin off northern Spain, including the Pyrenean chain, the Basco-Cantabrian ranges, the Le Danois Bank, as well as the continental shelves off the Basque, Asturia, and Galicia provinces, has been highly deformed (Boillot et al., 1971b, 1973, 1977, 1978; Montadert et al., 1971, 1974; Lamboy and Dupeuble, 1975; Lamboy, 1976).

The ancient boundary between the convergent plates is represented by the northern Spain marginal trough, where the pre-Oligocene sediment fill is tectonically deformed, as well as by the negative

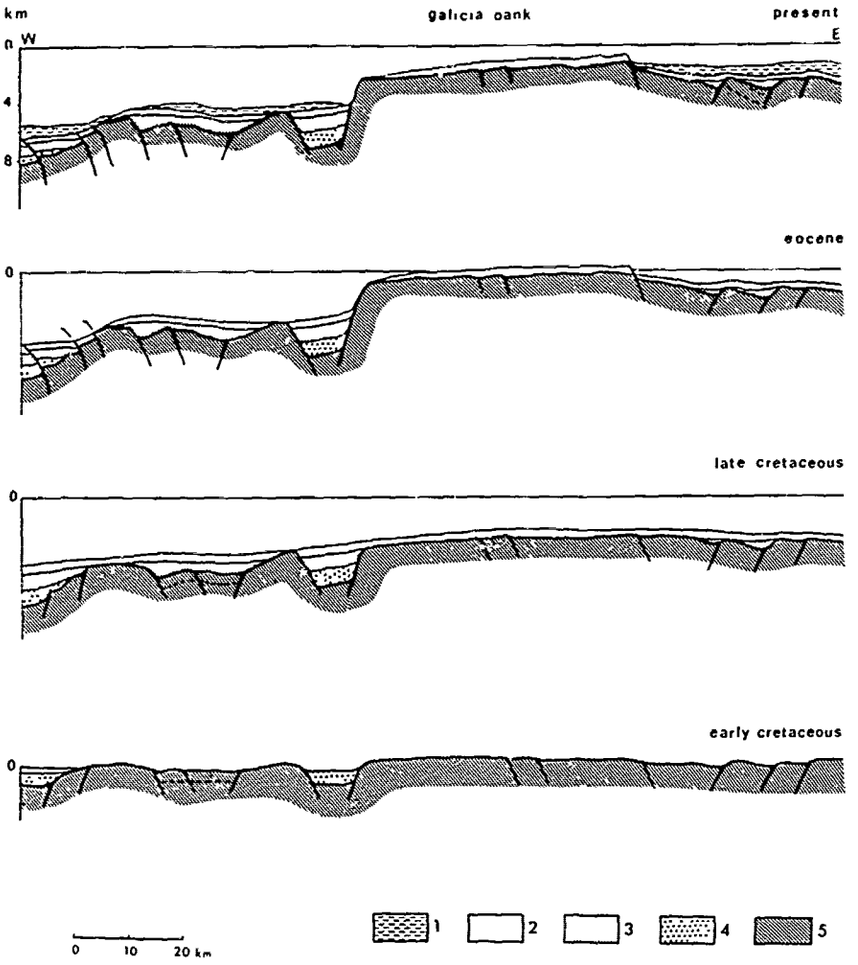


Fig. 9. Structural evolution of Galicia Plateau during Cretaceous and Cenozoïc. Stratigraphy of Units 1 through 4 is described in Table I. 5 : acoustic basement locally including Jurassic or Triassic sediments.

gravity anomalies that extend toward the West to the North of the Galicia Plateau (Groupe Galice, 1978). This allows an extension of the interpretation proposed by Boillot et al. (1973, 1978) for the evolution of the Asturian margin to the region described in this paper. In both cases the stable Cretaceous margin, located at the front of the overriding plate, has been shortened, deformed, and uplifted during Eocene subduction. This subduction, however, seems to have been limited both in time and in amplitude, so that it did not produce other effects such as magmatism and metamorphism. In our reconstruction we have derived the location of plate boundaries from the model proposed by Le Pichon and Sibuet (1971), modified West of Galicia. This model implies a motion of Iberia in a northeasterly direction with respect to a fixed European plate (fig.7).

If our interpretation is correct, there is still a need for further clarification. While Eocene subduction can rather easily explain deformation in the Galicia Plateau area, located quite close to the plate boundary, it is more difficult, however, to explain how the effects of that subduction have caused deformation and uplift in the Vigo, Porto, and Vasco da Gama areas, located more than 200 km South of the thrust zone.

## V - Miocene tectonics.

Neogene tectonic events have been recorded to the South-West of the Iberian Peninsula (Olivet et al., 1976; Olivet, 1978; Bonnin, 1978), and on the Portugal continental shelf (Boillot et al., 1975; Baldy et al., 1977). Deformation appears contemporaneous with a compression in the Betic chains.

In the Galicia and Vigo areas the amplitude of

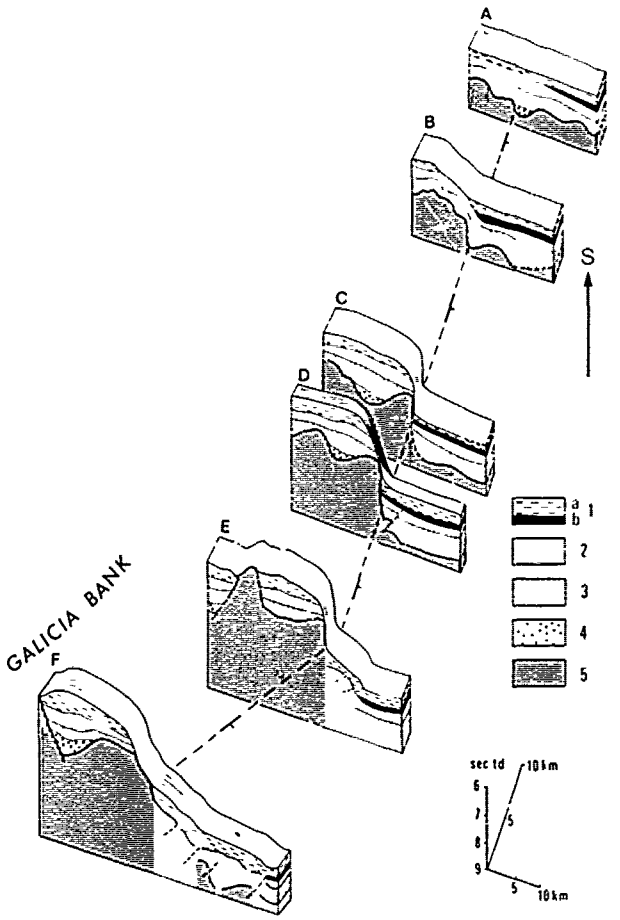


Fig.10. Structure of the northwestern flank of Galicia Bank. The fault bordering Galicia Bank becomes more subdued toward the South-West, and becomes a flexure affecting upper Cretaceous layers (Unit 2) and sealed by Eocene - mid-Miocene sediments (Unit 1b) (fig.11). (Stratigraphy of Units 1 through 4 is described in Table I; location of profiles appears on figure 5).

Neogene tectonics is difficult to estimate. At site 398 the event appears to correspond with a change in the nature of sediments and to the occurrence of hiatuses (Rehault and Mauffret, 1978). Moreover, on seismic profiles, middle Miocene layers locally show flexures which have been sealed by overlying upper Miocene sediments. One of them can be followed over more than 100 km into the Iberian abyssal plain (fig.6 and 15). These younger movements, however, have apparently been much less intense than the Eocene deformation.

## VI - Discussion and Conclusion.

1. The entire western Iberian margin seems to have undergone two distinct rifting phases, well recorded West of Galicia.

The first phase, during Triassic-early Liassic, probably predates the Jurassic opening of the Central Atlantic (Dewey et al., 1973). Apparently no oceanic crust was formed during that time North of 41°N, between Newfoundland and Galicia or in the Bay of Biscay. The result of the extension was therefore probably limited to the formation of a network of continental rifts, characterized by tectonic troughs. Epicontinental sedimentary basins that spread widely during the middle Jurassic lie probably over these buried continental rifts that became inactive and subsided.

The second rifting phase, during late Jurassic-early Cretaceous, preludes to the opening of the Bay of Biscay and of the Atlantic Ocean between North America and Iberia, that probably became effective during Aptian in the area under study. The new rift system may have formed in the same location as the older one, at that time an epicontinental domain. This seems to be the case for the Armorican margin where rifting occurred beneath the sea, without any subaerial erosion (Montadert et al., 1976).

The chronological evolution of the rifting episodes appears rather well established. The kinematics, however, still pose some difficult problems. Off Galicia, transverse faulting hence extension that affected the tectonic troughs during Triassic-Liassic times appears oriented along a N 60° direction (fig.7). According to Boillot et al.(1974, 1975), the same direction prevails during the early Cretaceous phase, whereas Le Pichon et al. (1977), and Auxiètre and Dunand (1978) propose an orientation at exactly 90° from that direction (N 320°).

2. Reconstructing the Eocene motion of the Iberian plate with respect to Europe is also a difficult exercise. We have adopted, with minor modification, the model proposed by Le Pichon and Sibuet (1971) in which the displacement of the Iberian Peninsula is toward the North-East. This model implies that the boundary between converging plates had to extend to the West all the way to King's Trough, and Peake and Freen Deeps. These features would be the remnants of an older intra-oceanic subduction zone. But such an interpretation remains controversial (Searle and Whitmarsh, 1978; Olivet, 1978).

In any case, a strong compression occurred during Eocene to the North and North-West of Spain. With the Paleogene, the passive margin of the Iberian Peninsula became deformed in connection with the subduction of oceanic crust of the Bay of Biscay toward the South. Pre-existing structures became rejuvenated at that time and both the pre-Mesozoïc basement and its Mesozoïc sediment cover underwent considerable uplift leading to the formation of the present day marginal plateaus, interpreted here as Tertiary structures rather than horsts inherited from Mesozoïc rifting phases.

One of the most spectacular consequences of the early Tertiary tectonic event has been to bring old layers, previously deeply buried beneath more

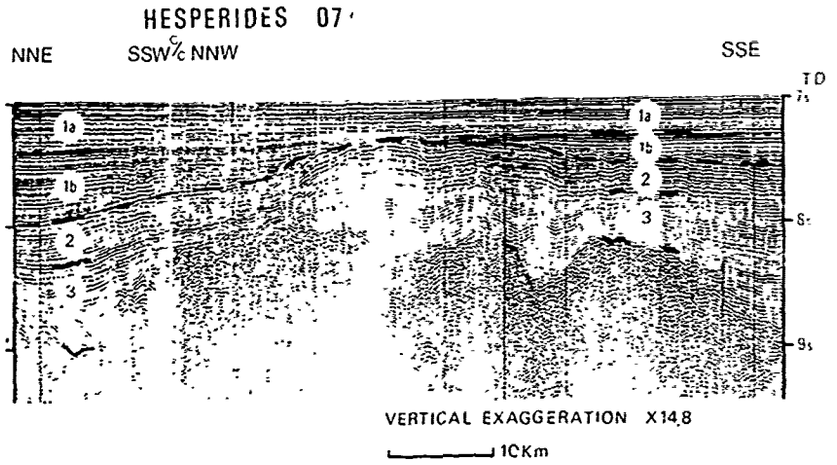


Fig.11. Deformation of the margin during Eocene. A flexure affect Unit 2 (upper Cretaceous) and is sealed by Unit 1b (Eocene - mid-Miocene). Stratigraphy of Units 1 through 3 is described in Table I; location of profiles appears on figure 5.

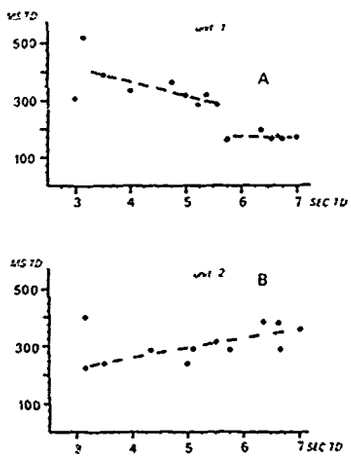


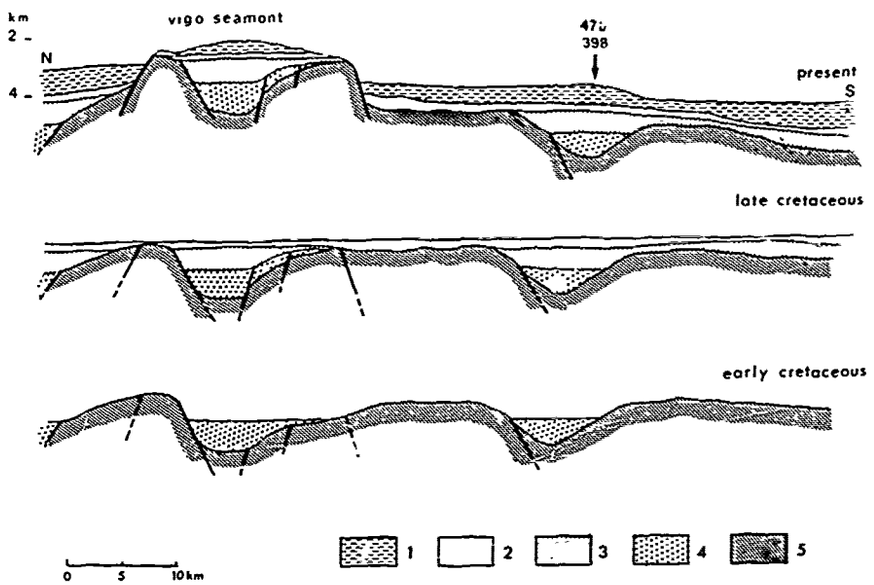


Fig.13. Tectonic and sedimentary evolution of Vigo seamound and site 398 area. (Stratigraphy of Units 1 through 4 is described in Table I). 5 : acoustic basement, including some Jurassic sediments.

Fig.12. Sediment thicknesses (vertical axis) West of Galicia Bank in relation to present day water depth (horizontal axis). A : thickness of Unit 1 (Cenozoïc); B : thickness of Unit 2 (upper Cretaceous-lower Eocene).

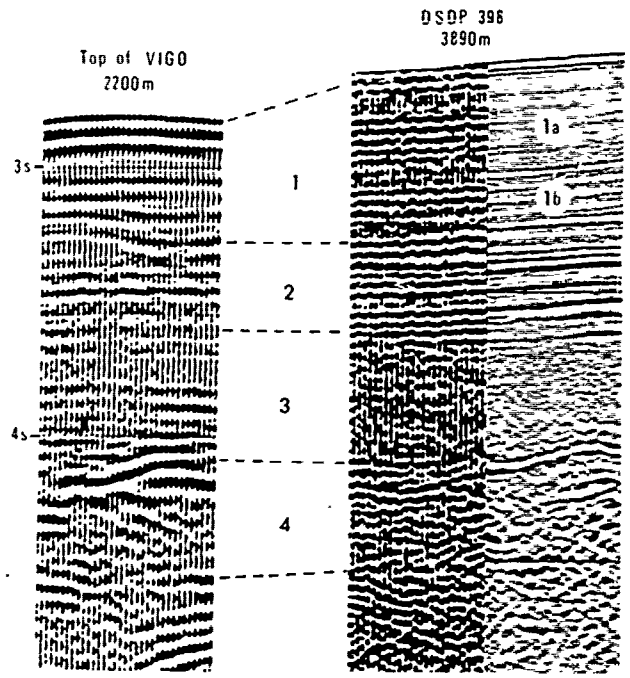


Fig.14. Comparison between acoustic stratigraphy at the top of Vigo seamount (after Montadert et al., 1974) and at site 398 (after Groupe Galice, 1978; to the left : without processing; to the right : with processing). (Stratigraphy of Units 1 through 4 is described in Table I).

recent sediments, to the sea floor along fault escarpments. As a result we could sample by dredging upper Jurassic layers and pre-Mesozoïc basement rocks that could not be reached by drilling at site 398.

Acknowledgements.

We thank :

- The Spanish and Portuguese Governments for permitting the completion of cruises during which data that form the basis for this paper where acquired;
- The crew and scientific parties for these cruises;
- The Centre National pour l'Exploitation des Océans, for providing us with the necessary ship time on board R/V "Le Noroît" and "Jean Charcot";
- The "Centre Océanologique de Bretagne" and "Institut Français du Pétrole" for communication of seismic profiles;
- Yves Lancelot for comments and translation of the French manuscript, and L.Hoinard, for typing the manuscript.

Financial support was provided by Centre National de la Recherche Scientifique, within the framework of ATP, "Géodynamique" and "Soutien à IPOD" under contracts 36-11 and A 12 618.

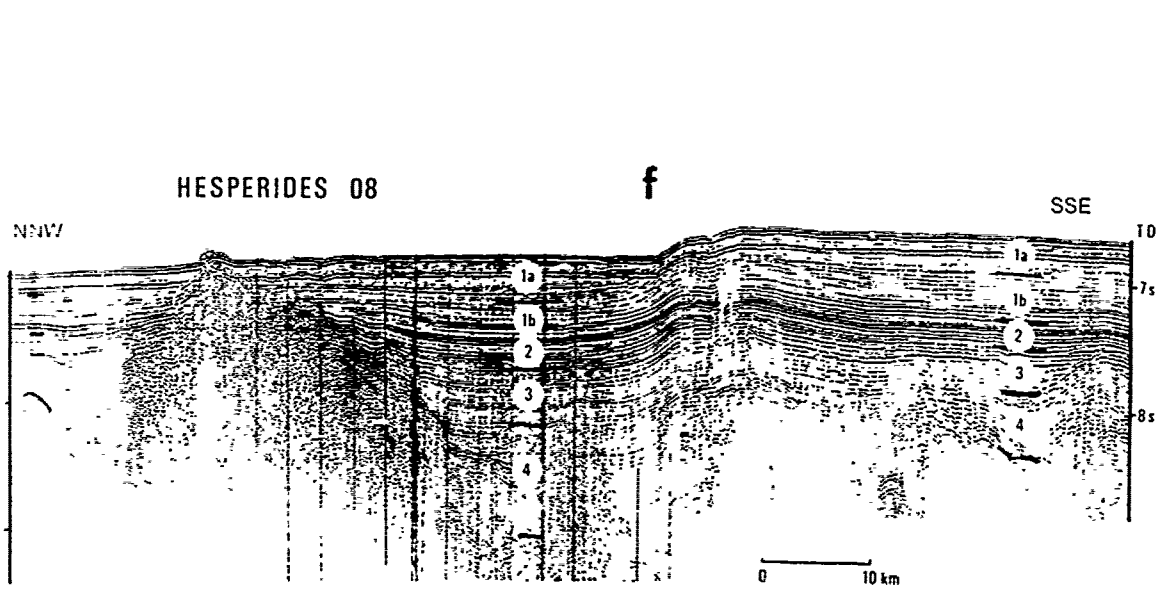


Fig.15. Effects of Miocene tectonics. Unit 1b (Eocene - mid-Miocene) has been deformed and is uncomformably overlain by Unit 1a (upper Miocene-Holocene). (Stratigraphy of Units 1 through 4 is described in Table I; location of profile appears on figure 5).

## References


Amoco Canada Petroleum Company Ltd and Imperial Oil Ltd, Regional geology of the Grand Bank, Bull.Can.Pétrol.Géol., 21, 479-503, 1973.

Arthaud, F., and P.Matte, Les décrochements tardihercyniens du Sud-Ouest de l'Europe. Géométrie et essai de reconstitution des conditions de la déformation, Tectonophysics, 25, 139-171, 1975.

Auxiètre, J.-L., and J.-P.Dunand, Géologie de la marge ouest-ibérique (au Nord de 40°N) : le banc de Galice, les montagnes de Vigo, de Vasco da Gama et de Porto, Thèses de 3è cycle, Université P.et M.Curie, 216 p., 1978.

Baldy, P., G.Boillot, P.-A.Dupeuble, J.Malod, I.Moïta, and D.Mougenot, Carte géologique du plateau continental sud-portugais et sud-espagnol (golfe de Cadix), Bull.Soc.Géol.Fr., (7) XIX, 703-724, 1977.

Berthois, L., R.Brenot, and P.Ailloud, Essai d'interprétation morphologique et géologique de la pente continentale à l'Ouest de la Péninsule Ibérique, Rev.Trav.Inst.Scient.Pêches Maritim., 29, 3, 343-350, 1965.

Biju-Duval, B., J.-C.Rivereau, C.Lamperein, and N.Lopez, Esquisse photogéologique du domaine méditerranéen. Grands traits structuraux à partir des images du satellite Landsat 1, Rev. Inst.Fr.Pétrol., XXI, 3, 365-400, 1976.

Black, M., M.Hill, A.S.Laughton, and D.H.Matthews, Three non magnetic seamounts off the Iberian Coast, Q.J.Geol.Soc.London, 120, 477-517, 1964.

Boillot, G., and R.Capdevila, The Pyrenees:subduction and collision? Earth and Planet.Sci.Letters, 35, 151-160, 1977.

Boillot, G., P.-A.Dupeuble, M.Durand Delga, and L.d'Ozouville, Age minimal de l'Atlantique nord d'après la découverte de calcaire tithonique à Calpionelles dans le Golfe de Gascogne, C.R.Acad.Sc.Paris, D, 273, 671-674, 1971.

Boillot, G., P.-A.Dupeuble, I.Hennequin-Marchand, M.Lamboy, and J.-P.Leprêtre, Carte géologique du plateau continental nord-espagnol entre le canyon de Capbreton et le canyon d'Aviles, Bull.Soc.Géol.Fr., (7) XV, 367-391, 1973.

Boillot, G., P.-A.Dupeuble, I.Hennequin-Marchand, M.Lamboy, J.-P.Leprêtre, and P.Musellec, Le rôle des décrochements "tardihercyniens" dans l'évolution structurale de la marge continentale et dans la localisation des grands canyons sous-marins à l'Ouest et au Nord de la Péninsule Ibérique, Rev.Géogr.Phys.Géol.Dyn., (2) XVI, 75-86, 1974.

Boillot, G., P.-A.Dupeuble, M.Lamboy, L.d'Ozouville, and J.-C.Sibuet, Structure et histoire géologique de la marge continentale au Nord de l'Espagne (entre 4° et 9°W),in "Histoire structurale du golfe de Gascogne", vol.2, Technip, Paris, V/6/1-V/6/52.

Boillot, G., P.-A.Dupeuble, and J.Malod, Subduction and tectonics on the continental margin off Northern Spain, Marine Geology, in press, 1978.

Boillot, G., P.-A.Dupeuble, and P.Musellec, Carte géologique du plateau continental nord-portugais, Bull.Soc.Géol.Fr., (7) XVII, 462-480, 1975.

Boillot, G., J.-P.Lefort, and P.Bouysse, Carte géologique du plateau continental du Golfe de Gascogne et sa notice explicative, Bur.Rech. Géol.et Min. édit., Orléans, 1976.

Bonnin, J., Evolution géodynamique de la ligne Açores-Gibraltar, Thèse, Paris, 144 p., 1978.

Dewey, J.F., W.C.Pitman III, W.B.Ryan, and J.Bonnin, Plate tectonics and the evolution of the Alpine system, Geol.Soc.Amer.Bull., 84, 3137-3180, 1973.

Dupeuble, P.-A., J.-P.Rehault, J.-L.Auxiètre, J.-P.Dunand, and L.Pastouret, Résultats de dragage et essai de stratigraphie des bancs de Galice et des montagnes de Porto et de Vigo (marge occidentale ibérique), Marine Geology, 22, M 37 - M 49, 1976.

Funnell, B.M., J.K.Friend, and A.T.S.Ramsey, Upper Maestrichtian planktonic foraminifera from Galicia bank, West of Spain, Paleontology, 12, part 1, 29-42, 1969.

Grandstein, F.M., A.C.Grant, and J.F.Jansa, Grand Banks and J anomaly ridge : a geological comparison, Science, 197, 1074-1076, 1977.

Grant, A.C., Multichannel seismic reflection profiles of the continental crust beneath the Newfoundland ridge, Nature, 270, 22-25, 1977.

Groupe Galice, The continental margin off Galicia and Portugal : acoustical stratigraphy, dredge stratigraphy and structural evolution, in Ryan, W.B.F., J.-C.Sibuet, et al. "Initial reports of the deep-sea drilling project", Leg 47 B, in press, 1978.

Hart, M.B., The mid-Cretaceous succession of Orphan Knoll (NW Atlantic). Micropaleontology and palaeo-oceanographic implications, Can.J. Earth Sc., 13, 1411-1421, 1975.

Hays, J.D., and W.C.Pitman III, Lithospheric plate motion, sea level changes and climatic and ecological consequence, Nature, 246, 18-22, 1973.

Jansa, L.F., and J.A.Wade, Geology of the continental margin off Nova Scotia and Newfoundland offshore geology of eastern Canada, Geol.Surv. Can. pap. 47-30, 2, 51-105, 1975.

Lamboy, M., Géologie marine et sous-marine du plateau continental au Nord-Ouest de l'Espagne. Genèse des glauconies et des phosphorites. Thèse, Rouen, 285 p., 1976.

Lamboy, M. and P.-A.Dupeuble, Carte géologique du plateau continental nord-ouest espagnol entre le canyon d'Aviles et la frontière portugaise, Bull.Soc.Géol.Fr., (7) XVII, 4, 442-461, 1975.

Laughton, A.S., D.G.Roberts, and R.Graves, Bathymetry of the Northeast Atlantic : Mid-Atlantic ridge to Northwest Europe, Deep-Sea Res., 22, 791-810, 1975.

Le Pichon, X., and J.-C.Sibuet, Western extension of boundary between European and Iberian plates during the Pyrenean orogeny, Earth and Planet. Sci.Letters, 12, 83-88, 1971.

Le Pichon, X., J.-C.Sibuet, and J.Francheteau,

The fit of the continents around the North Atlantic ocean, Tectonophysics, 38, 169-209, 1977.

Mauffret, A., G.Boillot, J.-L.Auxiètre, and J.-P. Dunand, Evolution structurale de la marge continentale au Nord-Ouest de la Péninsule ibérique, Bull.Soc.Géol.Fr., in press, 1978.

Montadert, L., B.Damotte, J.-P.Fail, J.-R.Delteil, and P.Valery, Structure géologique de la plaine abyssale du golfe de Gascogne, in "Histoire structurale du golfe de Gascogne", vol.2, Technip, Paris, VI/14/1-VI/14/42, 1971.

Montadert, L., D.G.Roberts, et al., From Brest to Aberdeen. Glomar Challenger sails on Leg 47, Geotimes, December, 19-23, 1976.

Montadert, L., D.G.Roberts, G.-A.Auffret, W.Bock, P.-A.Dupeuble, E.A.Harlewood, W.Harrison, H. Kagami, D.N.Lumsden, C.Muller, D.Schnitker, R.W.Thompson, and P.P.Timofeef, Rifting and subsidence on passive continental margins in the North-East Atlantic, Nature, 268, 305-309, 1977.

Montadert, L., E.Winnock, J.-R.Delteil, and G.Grau, Continental margin of Galicia-Portugal and Bay of Biscay, in "The Geology of Continental Margins", Burk and Drake eds, Springer-Verlag, New-York, 3137-3180, 1974.

Mougenot, D., Géologie du plateau continental portugais entre le cap Carvoeiro et le cap de Sines, Thèse 3è cycle, Rennes, 76 p., 1976.

Olivet, J.-L., Nouveau modèle d'évolution de l'Atlantique nord et central, Thèse, Paris, 150 p., 1978.

Olivet, J.-L., J.Bonnin, and J.-M.Auzende, Manifestation des phases de compression tertiaire dans l'Atlantique du Nord-Est, 4è Réun.Ann.Sc. Terre, Paris, 1976.

Parga, J.R., Spätvariszische Bruchsysteme in Hesperischen Massiv, Geol.Rundsch., 59, 323-336, 1969.

Romalho, M., Contribution à l'étude micropaléontologique et stratigraphique du Jurassique supérieur et du Crétacé inférieur des environs de Lisbonne (Portugal), Mem.Serv.Geol.Portugal (nova ser.), 19, 16-212, 1971.

Rehault, J.-P., and A.Mauffret, Relationships between tectonics and sedimentation around the northwestern Iberian Margin, in Ryan W.B.F., J.-C.Sibuet, et al. "Initial reports of the deep-sea drilling project", Leg 47 B, in press, 1978.

Ryan, W.B.F., J.-C.Sibuet, et al., Passive continental margin, Geotimes, octobre, 21-24, 1976.

Searle, R.C., and R.B.Whitmarsh, The structure of King's Trough, Northeast Atlantic, from bathymetric, seismic and gravity studies, Geophys. J.R.Astr.Soc., 53, 259-287, 1978.

Sibuet, J.-C., and X.Le Pichon, Structure gravimétrique du golfe de Gascogne et le fossé marginal nord-espagnol, in "Histoire structurale du golfe de Gascogne", vol.2, Technip, Paris, VI/9/1-VI/9/18, 1971.

Wilson, R.C.L., Atlantic opening and Mesozoic continental margin basins of Iberia, Earth Planet. Sci.Letters, 25, 33-43, 1975.

Zbyszewski, G., and J.Barreto de Faria, O sal gemma em Portugal metropolitano : suas Jazidas, caracteristicas e approveitamento, Estud.Notas Trabalh.Serv.Fomento Mineiro, XX, 1/2, 5-106, 1971.

# NORTHEAST ATLANTIC PASSIVE CONTINENTAL MARGINS: RIFTING AND SUBSIDENCE PROCESSES

Lucien Montadert and Olivier de Charpal

Institut Français du Pétrole, 92506 Rueil, Malmaison, France

David Roberts

Institute of Oceanographic Sciences, Wormley, Surrey, England

Pol Guennoc and Jean-Claude Sibuet

Centre Océanologique de Bretagne, 29273 Brest, France

Abstract. From geophysical data and DSDP drilling results (Legs 47B and 48) in the NE Atlantic (Galicia-Portugal and Northern Bay of Biscay), a model for rifting, attenuation and subsidence of a passive continental margin is proposed.

## Introduction

The northern margin of the Bay of Biscay and the Galicia marginal plateau were selected for drilling during I.P.O.D., because they offer one of the unique areas in the Atlantic Ocean, where drilling could reach easily layers deposited during the early stages of the evolution of a passive continental margin. The four sites drilled, 398, 400, 401, 402 did not attain all the objectives ; nevertheless, complemented by intensive multichannel seismic reflection profiling and dredgings, they allowus to propose a model of evolution of a passive continental margin. The geological structure of this part of the N.E. Atlantic and of their continental margins is complex because it results not only from rifting and drifting of Europe, Iberia and North America, but also from convergence between Europe, Iberia and Africa. The age and kinematics of the opening of the Bay of Biscay is still matter of controversy. If one accepts identification of anomalies 33 - 34 following CANDE et al (1977), the creation of Oceanic Crust in Biscay finished before anomalies 33 - 34 or eventually terminated just after, if these anomalies are also recognized in the axis of the Bay (triple junction during anomalies 33 - 34, Williams, 1975). The beginning of accretion is most probably intra Aptian (see Section III). One must thus distinguish (MONTADERT et al, 1974) the western part of Galicia Bank area and the Northern Bay of Biscay margin with its onshore prolongation in the Aquitaine basin which remained essentially stable during their entire history, and the North Spanish margin including the northern part of Galicia bank which was active almost since the opening of the Bay of Biscay (Cenomanian movements recorded in the Pyrenées) and at least until the Eocene-Oligocene.

Bathymetry of the part of the Northeast Atlantic considered in this paper shows clearly different provinces (fig. 1, 2) (BERTHOIS et al 1966, 1968) :

1. From Nazare canyon to the latitude of Porto offshore from the Portugal sedimentary basin, the continental shelf 40 to 50 km wide is linked to the Iberian Abyssal Plain by a relatively narrow continental slope.

2. Farther North, all the way to Cape Finisterre, the continental shelf is about 30 km wide and is bounded in the East by the Hercynian basement of Galicia. In the West as opposed to the preceeding zone, it is prolonged for nearly 200 km by a marginal plateau. This plateau comprises the large Galicia Bank whose top is 600 m deep, and several other seamounts (Vigo, Vasco de Gama) ; it is separated from the shelf by an Interior Basin running in a North-South direction from the Biscay Abyssal Plain to Porto Seamount. DSDP site 398 is located 20 km to the South of Vigo Seamount (fig.1,2).

3. The northern steep margin of Spain which had been strongly affected by the Pyrenean orogeny.

4. The Armorican margin from Aquitaine to the western Approaches basin is narrow and steep and bounded to the west by the deep and thick Mesozoïc-Cenozoïc Armorican marginal basin. It corresponds on the shelf to a Hercynian basement covered by a thin wedge of sediments.

5. The Western Approaches margin is broader with several large topographic features e.g. the Meriadzek Terrace, the Trevelyan escarpment, the Shamrock Canyon. It intersects the NE-SW Western Approaches Mesozoic-Cenozoïc basin on the shelf. Its SE boundary with the Armorican margin is very sharp near the Black Mud Canyon and is controlled by a NE-SW fault zone known also on the shelf.

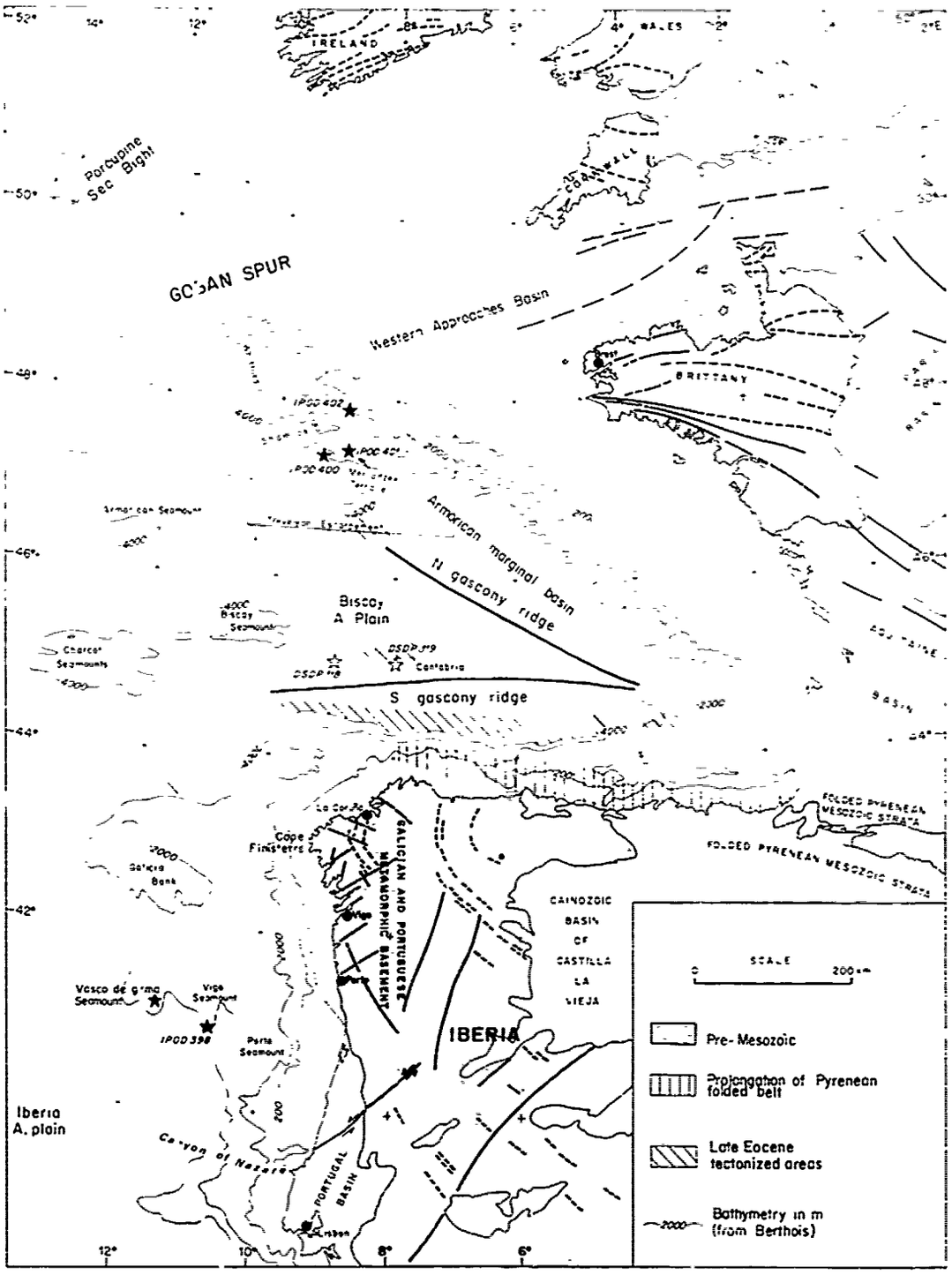


Fig. 1. General physography of SW Europe. Continental margins with DSDP drilling sites.

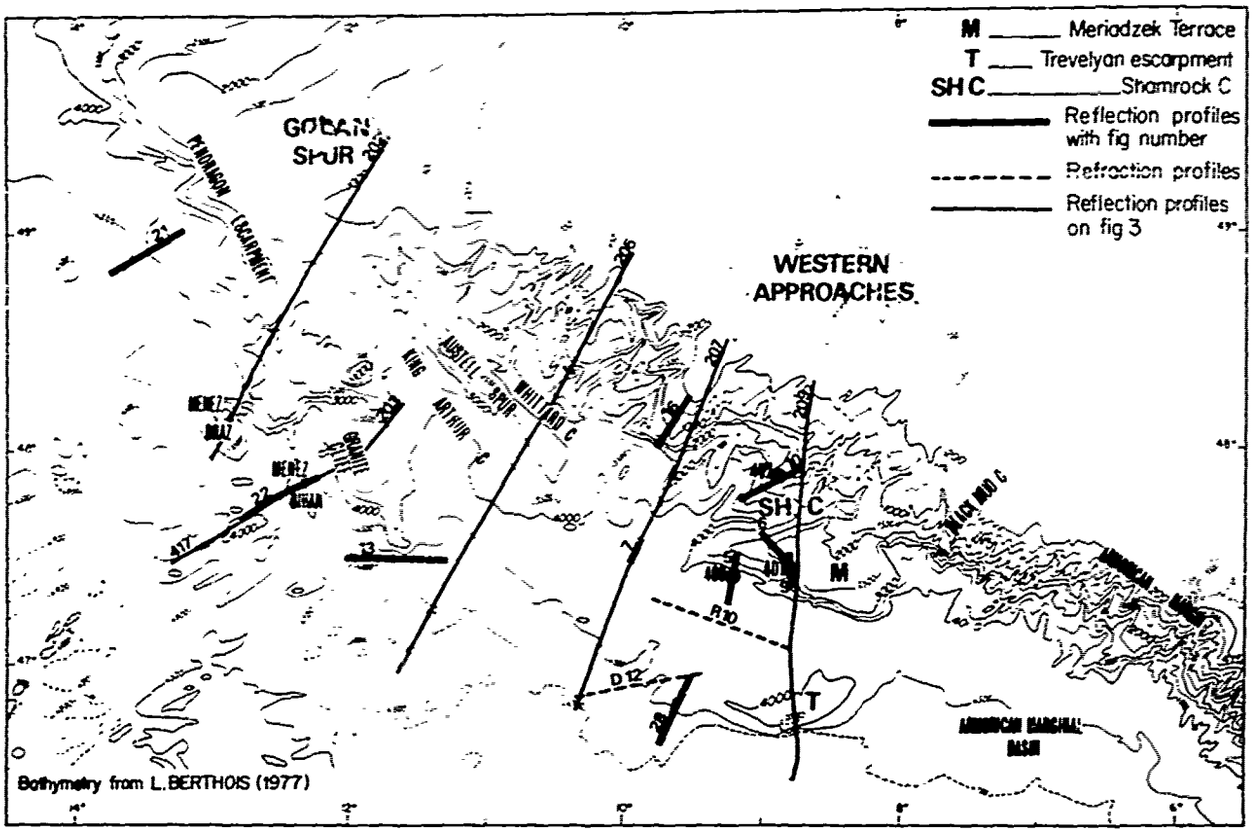


Fig. 2 A. Bathymetry and location of seismic profiles (N. Biscay margin).

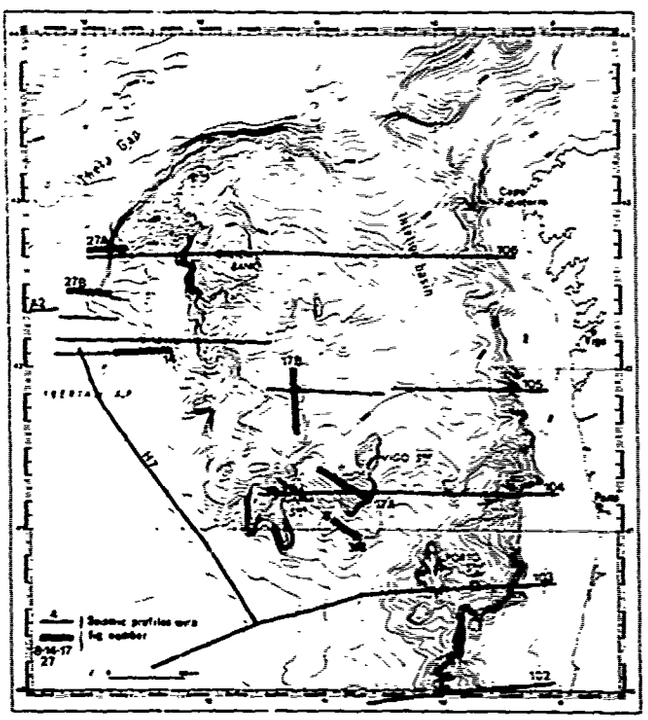

Fig. 2 B. Bathymetry and location of seismic profiles (W. Galicia margin).

6. The Goban Spur margin has a quite different physiography with a broad smooth rise relatively shallow (above 2000 m) deepening abruptly along the Pendragon escarpment. It intersects a basement high in the prolongation of Cornwall. The connection with the Western Approaches margin is marked by several topographic features like the Granite Cliff, and the Austell Spur separated by large canyons trending NW-SE.

7. The Porcupine Sea Bight is a depression corresponding to a thick Mesozoic-Cenozoic basin intersected by the margin.

The area considered in the Northern Biscay corresponds to the Western Approaches margin where sites 400 - 401 - 402 have been drilled, and the Goban Spur margin. Its detailed bathymetry by BERTHOIS is shown figure 2A.

Previous published seismic reflection data in these areas of drilling were scarce. In the Galicia Bank area, BLACK et al. (1964), FUNNEL et al. (1969) carried out geophysical surveys and got numerous dredge data. IFP-SNPA carried out a regional multi-

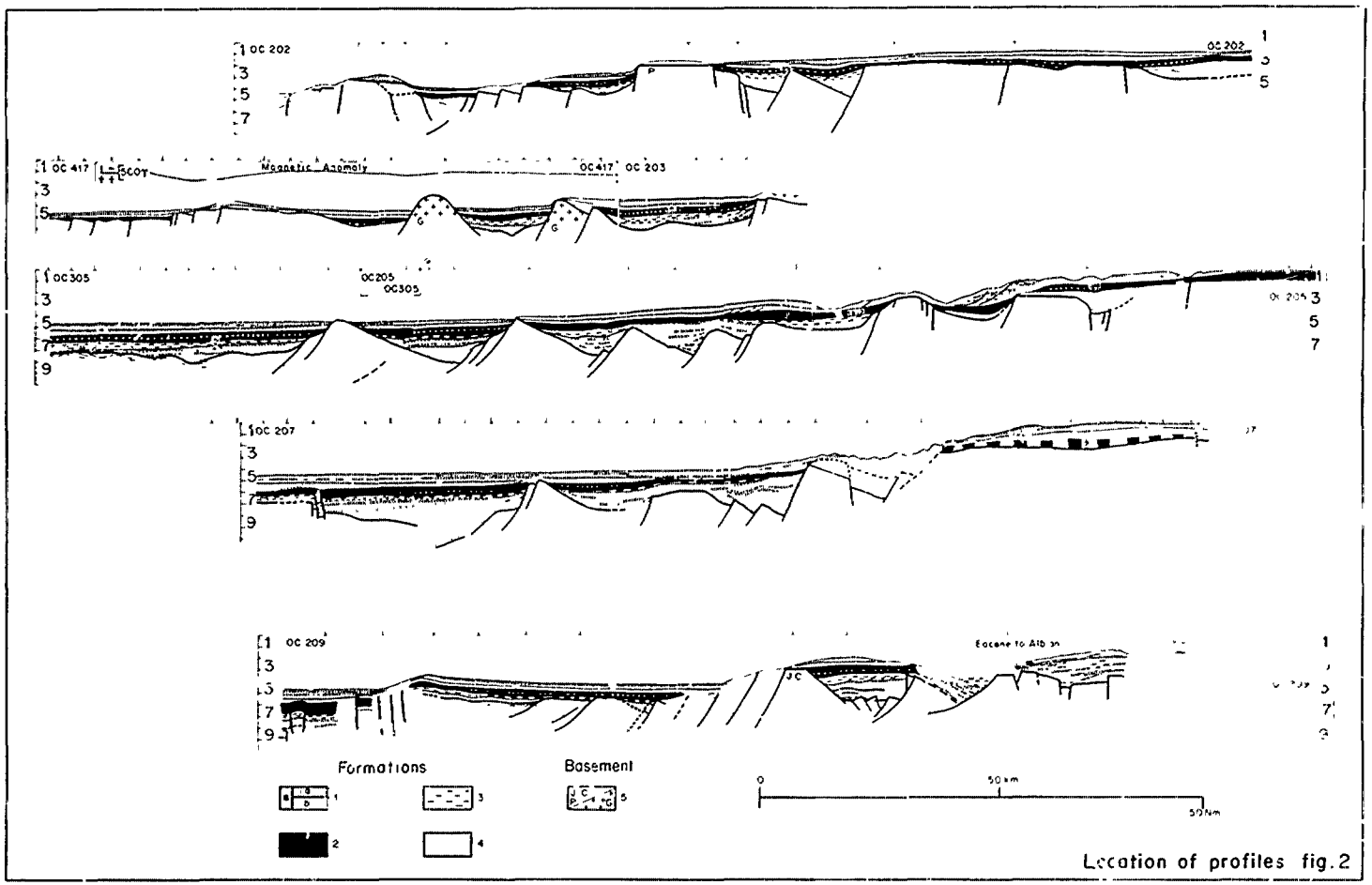


Fig. 3. Depth sections across N. Biscay margin.

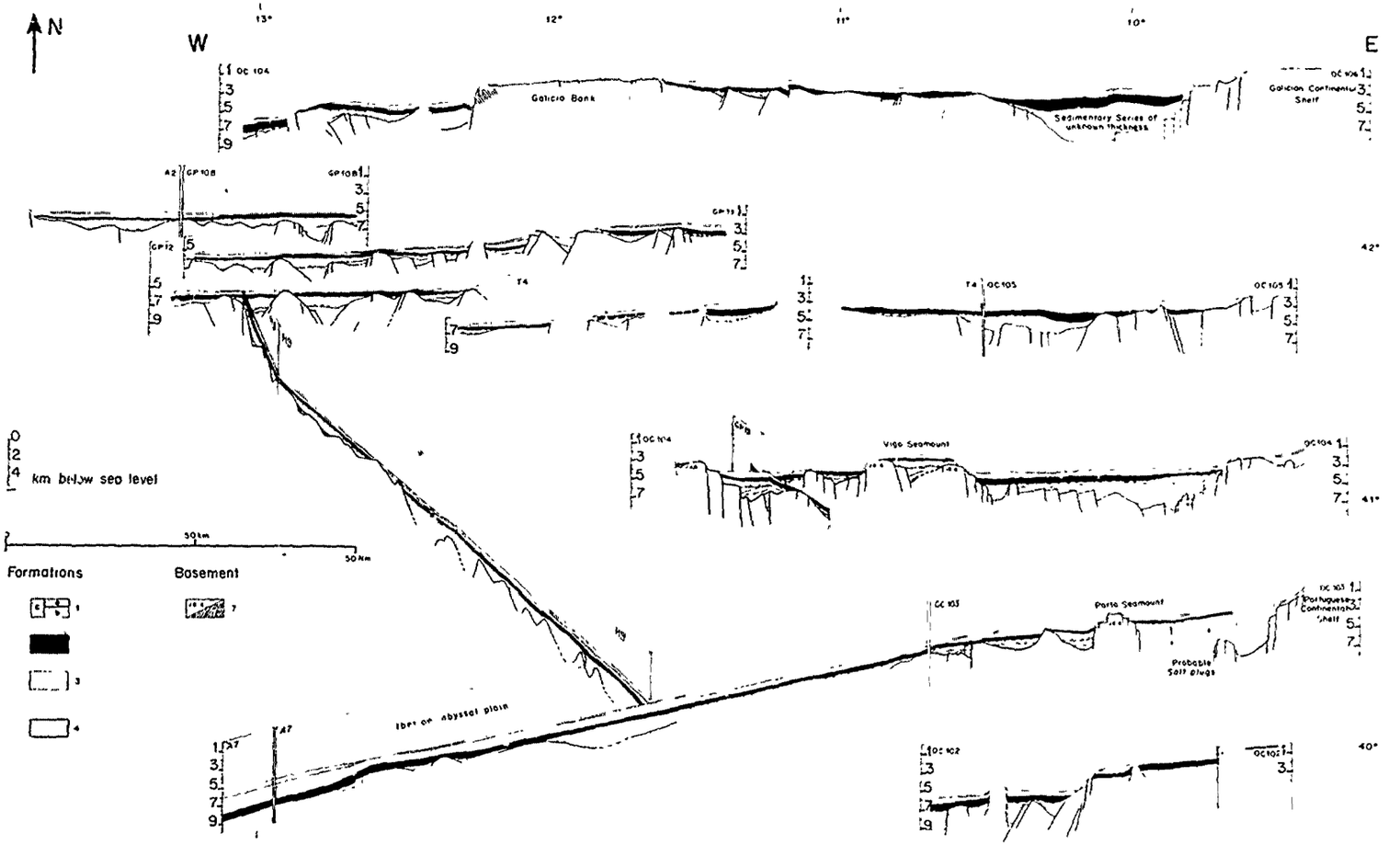


Fig. 4. Depth sections across W. Galicia margin

channel seismic reflection survey (MONTADERT et al., 1974). For the leg 47B (Groupe Galice, in press), CNEXO-IFP shot 2600 km of additional multichannel seismis reflection profiles while CNEXO and University of Paris (Laboratoire de Géologie Dynamique) carried out several cruises with single channel seismic reflection profiling (5800 km) and numerous dredgings. In northern Biscay, single channel profiles (STRIDE et al 1968, DINGLE and SCRUTTON 1977, C.O.B. unpublished profiles) and multichannel profiles (MONTADERT et al. 1971, 1974) have shown the existence of horst and graben structures and of Cenozoïc and Mesozoïc sediments. To prepare Leg 48 drilling sites, French institutions (Institut Français du Pétrole, CNEXO, CEPM) made 3600 km of multichannel seismic profiles. After the Leg, these institutions carried out a new survey with 1300 km of multichannel seismic profiles completed by high resolution multichannel seismic on the three sites. The Institut of Oceanographic Sciences (U.K.) made also about 2000 kms of multichannel seismic profiles in this area.

## Stratigraphy

This section will be devoted mainly to the seismic stratigraphy calibrated by boreholes and dredge data.

### Acoustic stratigraphy (Fig. 3 and 4)

The seismic sections show in most cases 4 main sedimentary units over an acoustic basement.

Acoustic basement. The "basement" is distinguished from overlying sediments either by its diffractive character or by dipping reflectors. Folding is present locally (Devonian, Carboniferous ?). A strong reflector defines the basement surface and is characterized by a strong relief consisting of sharp crests, undulations, flat horizontal surfaces that comprise the buried relief (fig. 3, 4). The basement itself appears to be divided by faults into blocks (horst and half grabens) of different heights, very frequently tilted along rotational faults (fig. 5). Where the "basement" is also composed of sedimentary rocks, their thickness may reach two seconds, or more than 3 kilometers assuming a mean sound velocity of 3,5 km/sec (fig. 5). In the Galicia area, where the acoustic basement is of sedimentary nature, it seems generally not so well layered (fig. 8) as in the upper part of the Biscay margin. The dips and faults show that it was fractured and displaced prior to the deposition of most of the overlying sedimentary cover.

Formation 4 (fig. 3, 4, 5, 6). Formation 4, which is a moderately to strongly layered formation, is separated from the overlying formation 3 by a strong reflector. Formation 4 lies in troughs between horsts and tilted blocks. Layering is quite conformable at the base with the top of the basement in the lowest part of the fills and at the top can be almost flat. This indicates that sedimentation occurred as basement blocks were being tilted.

Formation 3 (fig. 3, 4, 6). Formation 3 is in most cases transparent or slightly layered. It is thickest in the deep troughs between large tilted blocks (e.g. 800 m in Meriadzek) (fig. 6) but in the abyssal plain it appears as a thin continuous layer (about 200 m thick) overlying Formation 4 (fig. 7). Bedding may be slightly inclined in troughs and basins but dips are much less than in Formation 4. In general, the Formation appears to be absent on the structural highs, and its upper boundary lies well below the highs ; however very condensed equivalents may be present on some high points (site 401). Deposition of Formation 3 infilled the depressions between the fault blocks resulting in a subdued but not totally buried topography. Dips within Formation 3 between tilted blocks reflects only differential compaction. In contrast to Formation 4, deposition took place after the basement had ceased to move actively.

Formation 2 (fig. 3, 4, 5, 6, 7). The sequence above Formation 3 consists in several strong reflectors separated by finely layered strata. It cannot be considered as a single unit since a structural or erosional unconformity frequently occurs within the sequence. Its lower part has been called Formation 2 and is distinguished easily from the upper part called Formation 1b where these two units are unconformable (fig. 8). Elsewhere, the units are identified only on the basis of layer-to-layer correlation. Generally Formation 2 contains more reflectors than 1b, except in areas of thick distal deposition (the abyssal plain), where it may be the contrary. It should be noted that Formation 2 is layered in most areas. In those cases where post-rift deformation is observed, Formation 2 is always affected but not 1b. Thickness of Formation 2 is between 200 to 800 meters thick, reaching its maximum beneath the abyssal plain but it may be condensed into a single reflector. On Biscay margin (Meriadzek Terrace), it may be completly eroded (fig. 6).

Formation 1. Formation 1 is the most recently deposited sequence and is weakly layered. Often, it can be divided into two members, 1a and 1b, the latter one being more intensely layered. If high resolution seismic profiles are considered, a higher member of subunits can be locally distinguished but their correlation throughout the area is very difficult. The lower member 1b is often unconformable on Formation 2, but may be conformable over large areas. Member 1a is almost everywhere conformable with 1b. The whole Formation 1 is 600 to 900 meters thick, and its thickness is greatest beneath the abyssal plain and the Continental slope (1200 to 1400 m). This formation is characterized by large scale sedimentary features.

### Correlation of formations with the lithological units of the holes

Detailed correlations between seismic units and major lithologic changes on the holes are

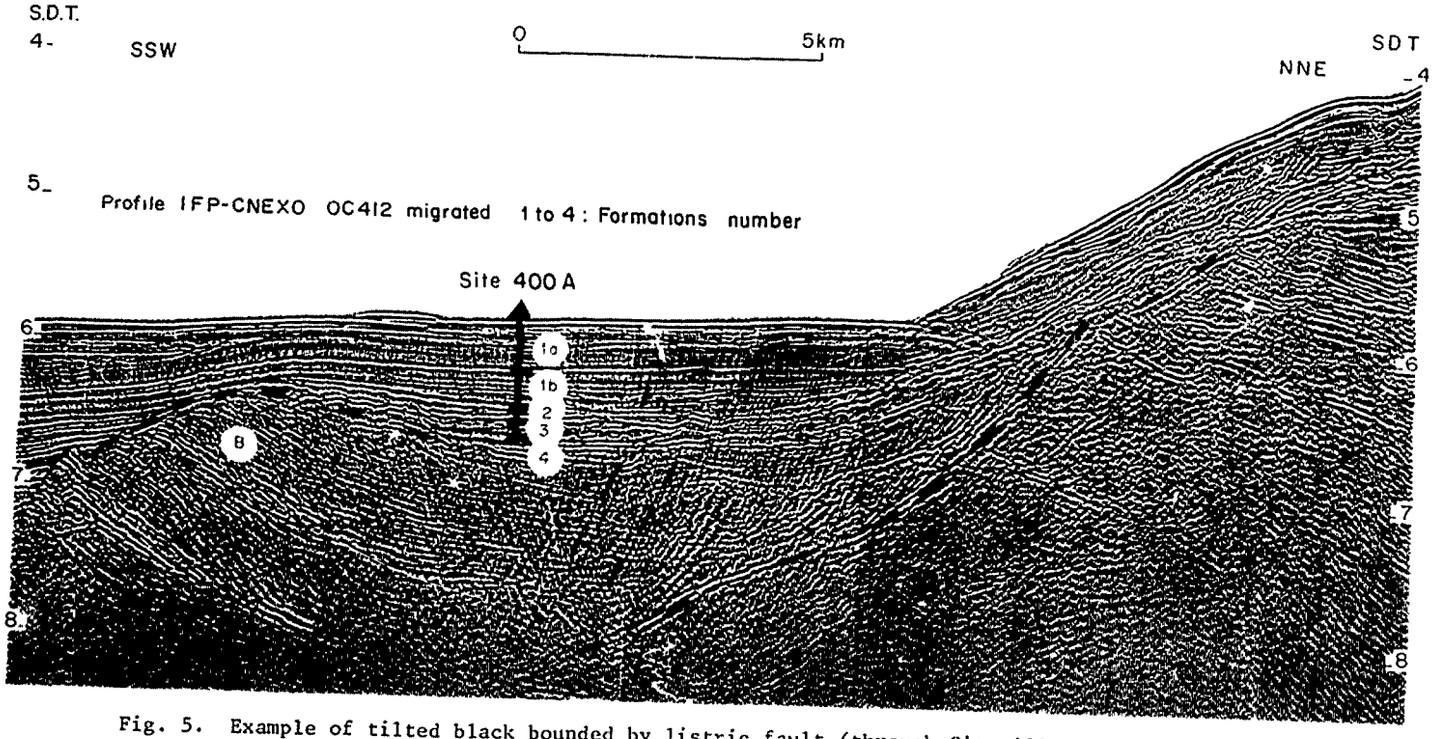


Fig. 5. Example of tilted black bounded by listric fault (through Site 400 A,N. Biscay margin)

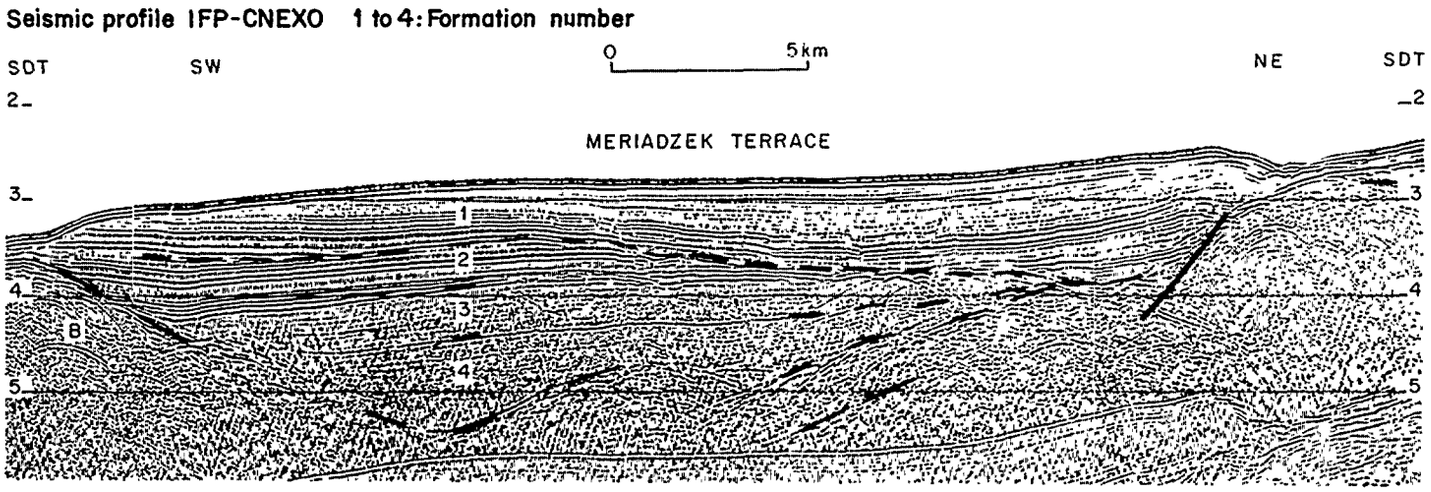


Fig. 6. Acoustic stratigraphy and unconformities on N. Biscay margin.

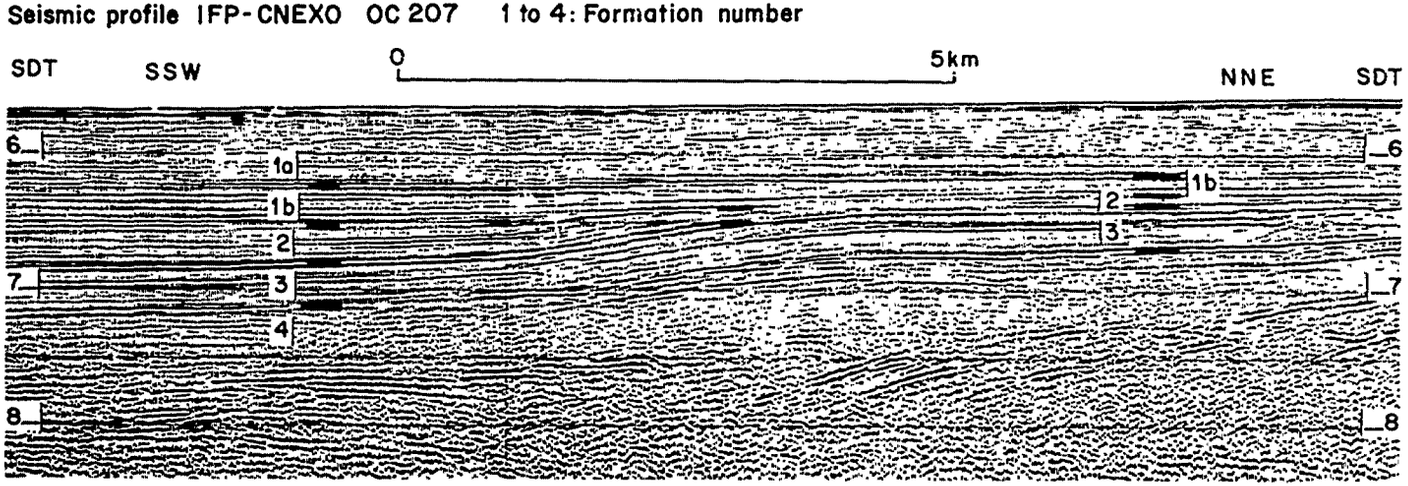


Fig. 7. Acoustic stratigraphy on the lower slopes of N. Biscay margin.

always one of the major problems for extending regionally results of DSDP holes. At site 398, correlations have been improved by computation of synthetic seismogram, using acoustic impedance values deduced from core measurements and computation of acoustic impedance pseudologs (BOUQUIGNY and WILLM, in press). In Biscay, density and velocity logging obtained in holes 401 and 402 permit a good correlation, especially because high resolution seismic reflection profiling have been carried out on the sites after leg 48. (Site chapters 401, 402, leg 48, in press). A summary of these correlations is given below :

Hole 398 (fig. 8) (Site chapter 398, leg 47B, in press, Groupe Galice, in press). Acoustic formation 1 is of Oligocene age to present and is essentially constituted by nanno ooze and chalk. Acoustic formation 2 corresponds to Senonian to Upper Eocene. It consists of two main lithological units : brown marly nanno chalk, calcareous mudstone, claystone and siliceous mudstone in the lower part which underlies siliceous marly nannochalk and mudstone interbedded with turbiditic sand-silt-marl sequences. Acoustic formation 3 corresponds to Lower Albian to Middle Cenomanian. At its base, Lower to Middle Albian laminated dark shales mostly of continental provenance are followed by interbedded dark shales and marlstones from Middle to Late Albian and by Late Albian to Middle Cenomanian redeposited marl and chalk of pelagic origin. Acoustic formation 4 corresponds to Late Barremian to Uppermost Aptian. It is constituted of sand-silt-clay graded sequences interbedded with thick (1 to 10 m) slumped beds of debris flows. A stratigraphical break exists in the Uppermost Aptian and corresponds both to a sharp lithological change and to a major reflector between formations 4 and 3. The acoustic basement is clearly of sedimentary origin on this profile. It is highly diffractive in most places and shows strong reliefs either as broad undulations or as sharp crests corresponding to buried highs. At hole 398, it consists of marlstone, siltstone and white indurated limestone of late hauterivian to early Barremian age.

Holes 400 - 400A (fig. 5) (400, Site Chapter, leg 48, in press). Formation 1a corresponds to Quaternary, Pliocene and Upper-Middle Miocene oozes and chalk. 1b is the underlying layered sequence whose base is the Oligocene/middle Eocene hiatus. This sequence is composed of an upper slightly layered member and a lower more strongly stratified member and corresponds to lower Miocene, Oligocene oozes, nannofossils chalks and marly chalks with mudstone layers. Although well defined in the Site 400 area, this sequence is not easily correlated far from the hole, because it is very similar in appearance to Formation 2 and the boundary between the two Formations may be not clear where the formations are conformable. In some cases, Formations 1b and 2 have not been distinguished. Formation 2 corresponds in the hole to the sequence defined at the top by the Oligocene/

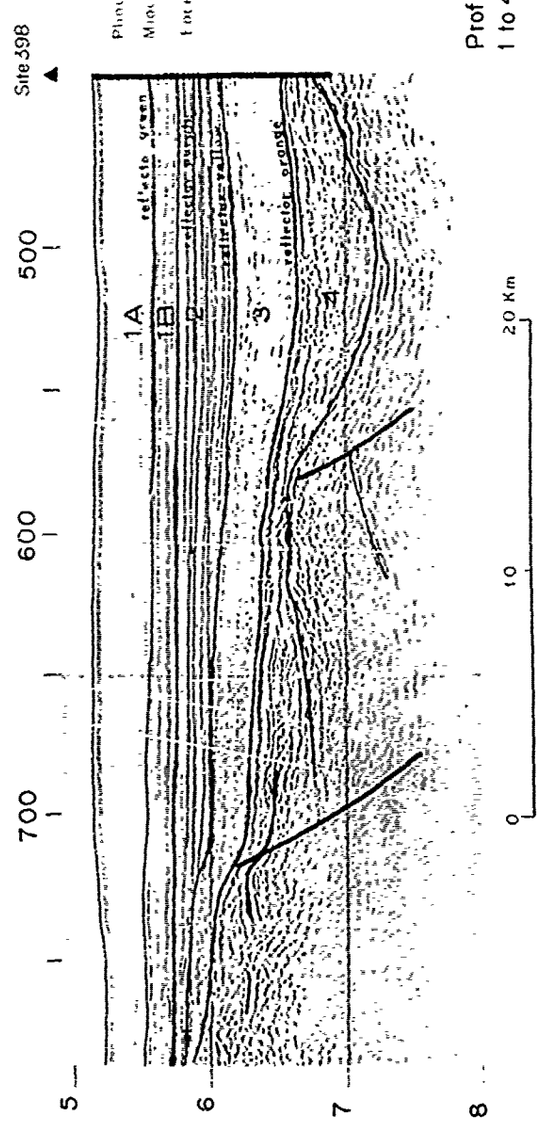


Fig. 8. Acoustic stratigraphy on W. Galicia margin through site 398.

middle Eocene hiatus and its base by the Upper/ Lower Cretaceous hiatus. This sequence is composed of alternating marly chalks and mudstones. Formation 3 was drilled in part and is composed of carbonaceous mudstones, marly chalks and limy claystones of Albian to Aptian age. This sequence is correlated with all the transparent or slightly layered sequences underlying Formation 2 observed on the profiles at depths below two and half seconds beneath sea level. In many places, these layers are characterized by low interval velocity although this is not the case at Site 400. Formation 4 was not reached and is assumed to be of pre-Aptian Early Cretaceous age.

Hole 401 (fig. 9) (401 Site Chapter, leg 48, in press). Formation 1 was partly drilled and corresponds with the Quarternary to Oligocene sequence. The top of Formation 2 has been correlated with the Late Eocene unconformity (Reflector 1 in the hole) that is clearly seen in the right part of the profile in fig. 9. Formation 2 is composed of siliceous nannochalk and marly nannochalk of Middle Eocene to late Cretaceous age. Formation 3 is not visible on the profiles near site 401, where very thin Upper Aptian chalks were drilled. It is well developped to the North of the site where it is characterized as elsewhere by weak layering and low sound velocity. The acoustic basement drilled at hole 401 consists of Late Jurassic to possible lowermost Cretaceous shelf bioclastic limestones.

Hole 402 (fig. 10) (402 Site Chapter, leg 48, in press). The upper formation 1 is constituted by Quaternary muds and oozes with ice-rafted pebbles. Neogene is very reduced. The layered sequence (formation 2) comprises late Eocene oozes and Middle Eocene siliceous nanno chalks and limestones, above a series of carbonaceous calcareous mudstones, and limestones of Albian and Aptian age (formation 3). The top of the almost transparent lower formation 4 has probably been attained (lower Aptian Nannoconus limestone). It must represent essentially pre-Aptian Early Cretaceous sediments contemporaneous with the rifting. The acoustic basement is interpreted as pre-rifting Mesozoic platform carbonates.

The stratigraphic controls provided by dredgings will be discussed later but generally support the seismic interpretation.

## The main unconformities

Several unconformities are observed on the North Biscay and Galicia continental margins. Some are related to tectonic movements, others to paleo-oceanographic events.

The first unconformity of structural origin separates the post-rifting sediments (formation 3) from the underlying sediments (formation 4 or

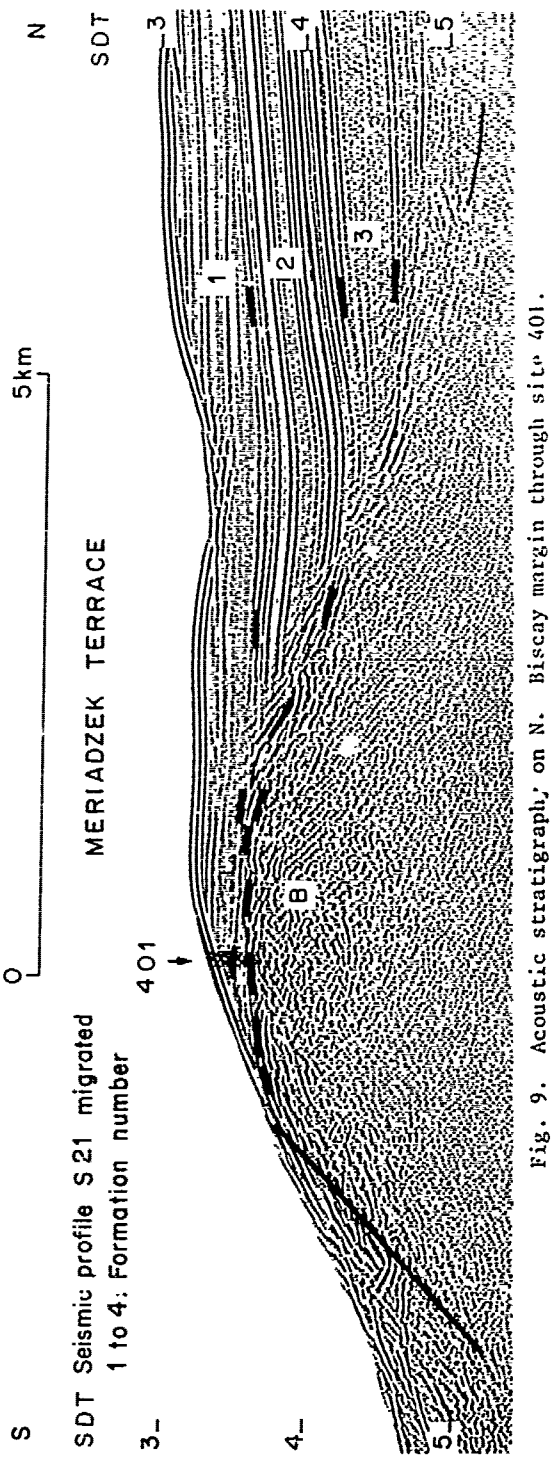


Fig. 9. Acoustic stratigraphy on N. Biscay margin through site 401.

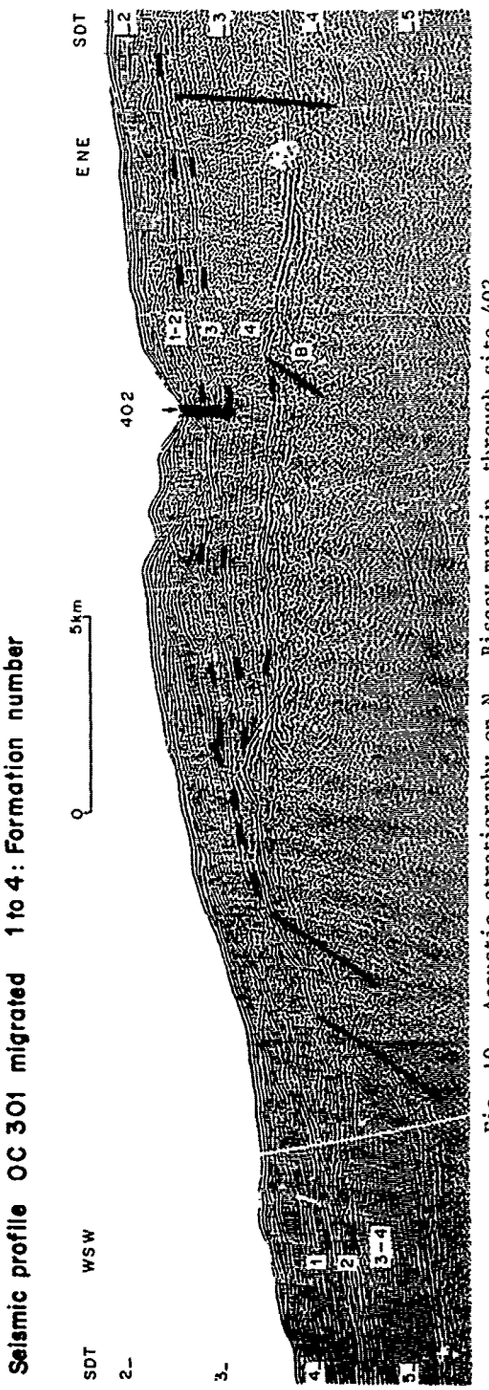


Fig. 10. Acoustic stratigraphy on N. Biscay margin through site 402.

acoustic basement) which were affected by rift tectonics. Since the paleotopography created by rifting was very pronounced (fig. 3, 4) and the post-rift sediments are very thin, every situation is present from no visible unconformity in a half graben to non deposition of post-rifting sediments on the crest of a tilted block ; fault block crests even outcrop on the sea bottom. However beneath large parts of the margin, the change in regime from rifting to subsidence occurred in deep waters so that deep syn-rift sediments grade without interruption to deep post-rift sediments in half grabens. In these cases one cannot observe a continuous break-up unconformity.

Another unconformity of structural origin is observed locally in areas which were affected by late Eocene compressional movements. This is particularly clear along the Trevelyan escarpment which was largely created at that time and along the northern flank of Galicia Bank (see last section).

Another unconformity separates the upper Cretaneous chalks from the Aptian-Albian "black shales". A large hiatus of Cenomanian to Santonian age in Biscay and of Mid Cenomanian to early Senonian in Galicia separates the two formations (389 Site chapter, leg 47B, in press). The unconformity is emphasized by the change of seismic facies between the transparent formation 3 and the strongly layered formation 2. Angular truncation of the black shales below formation 2 at the unconformity is due to differential compaction of the black shales in the half graben during a period of non deposition and bottom current activity. This hiatus is known in many parts of the Atlantic and is due to a major paleo-oceanographic event synchronous with the global Cenomanian-Turonian transgression.

Between Formation 2 (Upper Cretaceous to late Eocene) and Formation 1, an unconformity is also often visible and associated with strong erosion (fig. 6, 9). This event which occurred between the Late Eocene and Oligocene has not been dated with great precision, but it clearly post dates the middle Eocene paleo-oceanographic change that is marked by a sharp increase of silica production. This paleo-oceanographic event which resulted of a change in plate tectonic motions is linked to the onset of a strong bottom water circulation that caused erosion, sediment drift, dunes, sediment waves, resulting in a seismic facies very different from Formation 2 which is in contrast mainly characterized by pelagic draping. This event very probably affected the whole Atlantic and could be synchronous of the "great sculptural event" described on the western Atlantic margin (TUCHOLKE, 1978).

Formation 1 is also composed of different depositional sequences separated by unconformities

that are particularly visible on the upper slope, and possibly related to eustatic changes in sea level (VAIL et al., 1977). They are however difficult to pick on the whole margin.

## The structural evolution of the continental margin

### The rifting phase

Pre-rifting geology and beginning of rifting. In Biscay, seismic reflection profiles show that the fault blocks (fig. 3, 4, 5) contain either thick layered sediments whose parallel inclined reflectors are clearly seen in front of the Western approaches basin, or basement with a thin sedimentary cover in the area of Goban Spur. Data on the age and nature of these rocks are rather scarce. At Site 401, on Meriadzek Terrace, late Jurassic and possibly earliest Cretaceous calcarenites were penetrated below an horizontal erosional surface. These sediments may represent a pre-rift carbonate platform. Late Jurassic Calpionellid limestones dredged on the Meriadzek Terrace (PASTOURET et al., 1976) support this interpretation, but indicates also more open sea conditions. Since the exact age for beginning of the rifting phase is not known, an alternative hypothesis is that the late Jurassic shallow water Carbonates found at Site 401 are geographically restricted to the highest point of previously faulted blocks. Several dredges in the Goban Spur area, (Granite Cliff, Menez Bihan, fig. 2) recovered granitoïdes whose ages vary from 251 MY to 290 MY, indicating an hercynian basement (PAUTOT et al., 1976). Metamorphic rocks have also been dredged as well as sedimentary rocks as shallow water carbonate of probable Carboniferous age and sandstones (AUFFRET et al., in press). These lithologic data confirms the seismic reflection data, and demonstrate the existence of two geological provinces prior to rifting i.e. one with thick mesozoïc deposits in front of the western Approaches basin, and another on Goban Spur that corresponds to a regional basement high with a thin Mesozoïc sedimentary cover. These geological realms are known on the shelf as the western Approaches mesozoïc basin and the basement high running from Cornwall to Goban Spur and are intersected by the present margin and the initial rift.

On Galicia plateau, numerous dredges recovered schists, phyllads, gneiss, granulite and granite on the escarpments of Galicia Bank, Vigo Seamount and Vasco da Gama Seamount (DUPEUBLE et al., 1976) (Groupe Galice, in press) indicating the presence of a continental basement of probably same nature than known on land in Galicia. The oldest sedimentary rocks, obtained by dredgings on the continental slope and on the marginal banks of Vigo, Porto and Vasco da Gama, are bioclastic limestones with algae dated Late Kimeridgian to Berriasian and Calpionella pelagic micrites dated Late Tithonian to early Berriasian (Groupe Galice, in press). This means that at the end of Jurassic times there was a shallow epicontinental sea communicating with an open sea connected to the Mesogea. These samples seem to come either from the acoustic basement or perhaps from formation 4. There is no direct evidence on the margin of sedimentary rocks older than Late Jurassic but on the continental shelf of Portugal, a complete mesozoïc series exists including evaporites of Triassic age. Seismic reflection surveys in the deep basin between Porto Seamount and the continental shelf show diapiric structures, probably linked to these Triassic evaporites (MONTADERT et al. 1974). In the area of site 398 (fig. 8), the acoustic basement is constituted of tilted faulted blocks clearly of sedimentary origin. It has been proposed that the lowermost 73 meters were drilled in the acoustic basement (Site 398 chapter, in press). This lowermost section consists of a complex sequence of marlstone, siltstone and white indurated limestone of Late Hauterivian to Early Barremian age. The white indurated limestones were deposited under pelagic conditions whereas marlstones and siltstones could have been emplaced by low density turbidity currents in a very quiet environment. Limestones have been deposited at a depth shallower than the CCD but probably at depths reaching 2 kilometers at the site (site 398 chapter, in press). If this interpretation is correct, the initiation of rifting in this area would have been early Barremian. Nevertheless, the acoustic basement being steep and irregular, and taking in account the uncertainty of hole location with respect to the seismic profile, it is possible that site 398 did not penetrate in the pre-rift formations but bottomed in the syn-rift formations.

It is clear that pre-rifting geology in North Biscay and Galicia are similar. In both cases, rifting occurred on a pre-existing marine mesozoic basin.

The pre-rift paleogeography is still disputable because of the lack of deep stratigraphic data on the margins, and uncertainties on the pre-rift reconstructions of Biscay. The Hercynian basement was subjected to a first phase of tensional tectonics during Triassic-lower Liassic time with evaporite deposition that is well known in Aquitaine and part of Galicia-Portugal (WINNOCK 1971 - ROS ET et al., 1971 - MONTADERT et al., 1971 - 1974 - BRGM et al., 1974). The western Approaches basin could also have been initially structured by this distension. It is noteworthy that in the Aquitaine, the northern boundary of the thick Triassic deposits is a fault system (the Celtaquitaine flexure of WINNOCK, 1971) which is exactly in the prolongation of the present armorican continental margin. These tensional movements ceased in Aquitaine as well as in Galicia-Portugal during most of the Jurassic when marine epicontinental sediments were depo-

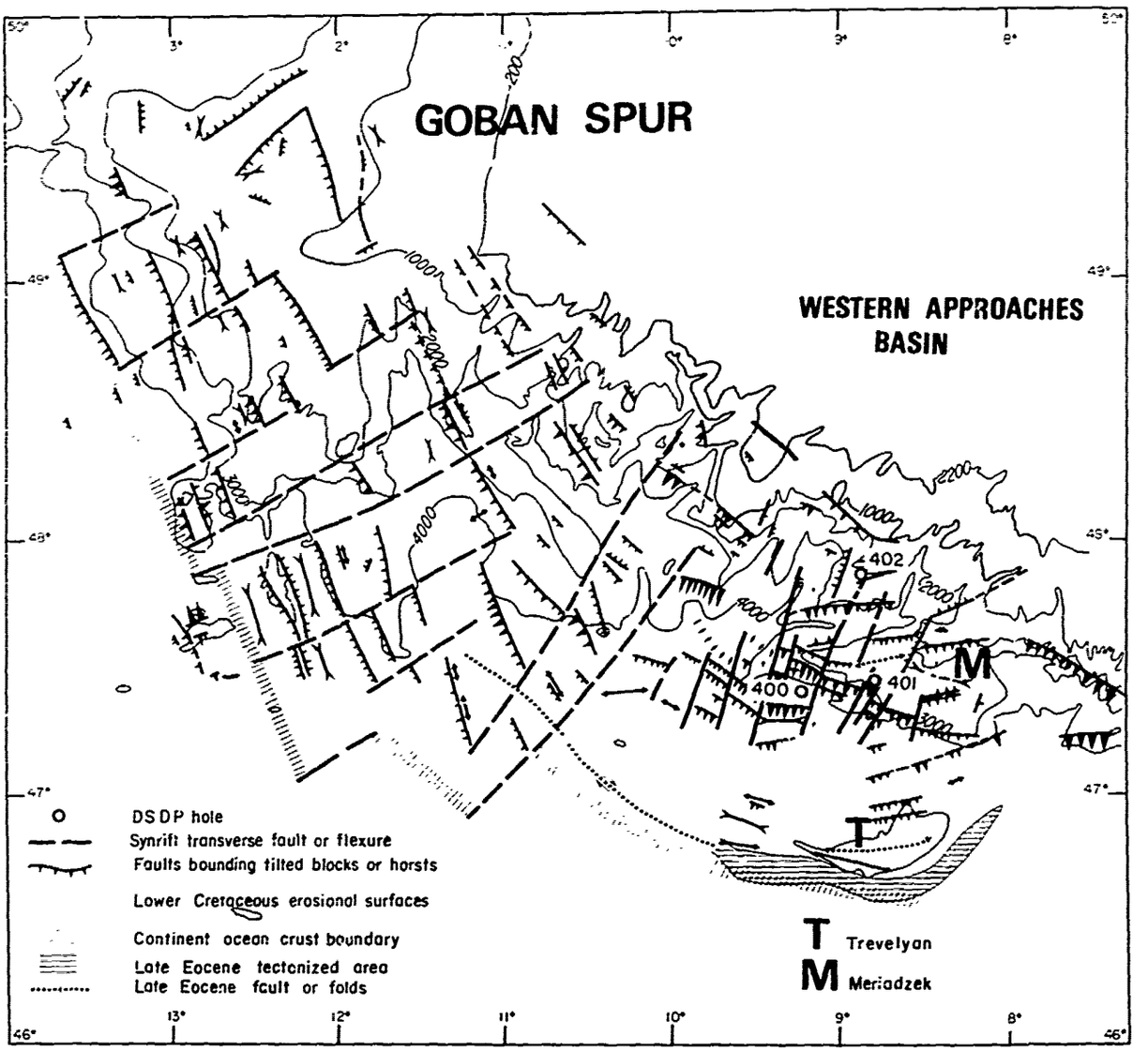


Fig. 11. Schematic tectonic pattern of the rift system on N. Biscay margin.

sited indicating an open sea. The bathymetry of this Mesozoïc sea is not well established offshore, but calpionellid limestones are known all around Biscay and Galicia. In northern Biscay, seismic reflection profiles consistently show a downslope facies variation of the pre-rift mesozoïc, with the developement of a well layered series perhaps indicating more basinal deposits. This change is examplified by figure 10 upslope and by figure 5 downslope. After this quiet Jurassic period, tensional tectonism occurred again at the end of the Jurassic all over the Europe-America plate, creating a complex system of rifts. Some of these subsequently aborted like in the North sea or in the Western Approaches but others evolved to form a passive continental margin with accretion of new oceanic crust. In Northern Biscay, the start of this rifting episode is not well documented. In the Western Approaches basin, results of the exploration wells have not been published but in the Celtic Sea the break up unconformity is of Aptian age. In Aquitaine it is particularly well documented for the Parentis Basin which opens directly westward into Biscay. Detailed maps based on drilling results (BRGM et al., 1974) indicate that the Parentis Basin is first identifiable in late Oxfordian time as an area of slightly more rapid subsidence. During the Neocomian the Parentis Basin became a large graben, indicating a period of active rifting. Since the northern boundary of the Parentis Basin is in continuity with the Armorican margin, the timing may

be extrapolated to the Northern Biscay and is not in contradiction with our observations. Site 398 results (see above) could indicate a starting of the rifting episode or an episode in the rifting process in Lower Barremian time.

It is thus concluded that in this part of the Northeast Atlantic, active rifting took place in Lower Cretaceous time, in a preexisting marine basin in contrast to other rift systems which were subaerial.

The tectonic style of the rift system. The tectonic style of rifting is examplified by several interpretative depth sections across both margins based on seismic reflection profiles (fig. 3, 4). The overall tectonic style is characterized by a series of tilted blocks bounded by faults which in many cases are clearly listric faults. These blocks delineate half grabens. True horsts are rare on the Biscay margin. Some of these blocks are cut by erosional surfaces, which on too highly exaggerated profiles give the misleading appearence of horsts. There is a clear polarity of the dip of faults towards the axis of the rift system in Northern Biscay and in the western part of the Galicia Plateau.

A schematic fault pattern of the rift system developped during lower Cretaceous has been mapped from the seismic profiles in North Biscay (fig. 11). The pattern is best documented in the area of Meriadzek where the spacing of the profiles is less than 10 km. However, delineation of fault trends is often uncertain and more so in the area of Goban Spur. Spacing between consecutive fault block crests varies from a few kilometers to 30 kilometers and the length of individual blocks is limited to between several and 20 - 30 kilometers by transecting normal faults that do not show horizontal displacement. These faults are often delineated by the lack of continuity of tilted blocks. The apparent throw can vary along these faults since crests and half grabens do not coincide on both sides. Comparable patterns have been described on intracontinental rift system such as the southern Ethiopian rift system (MOORE et al. 1978). The trend of the tilted blocks generally follows the strike of the margin and changes between the Goban Spur (150° E) and the Meriadzek area to more variable trends of 80° to 130° E. Transecting faults oriented almost perpendicular to the margin, vary in direction from 60° E in Goban Spur area to 15° - 30° E in the Meriadzek area where trends are again more variable. If, as is probable, faulting during rifting accomodated previous fractures or inhomogeneities in the Hercynian basement, the observed differences in fault orientation suggests that the Hercynian basement in the areas of Goban Spur and Meriadzek is different on both lithology and structure. In any case, the faults trending at 80° E in the Meriadzek area and controlling in particular the Shamrock

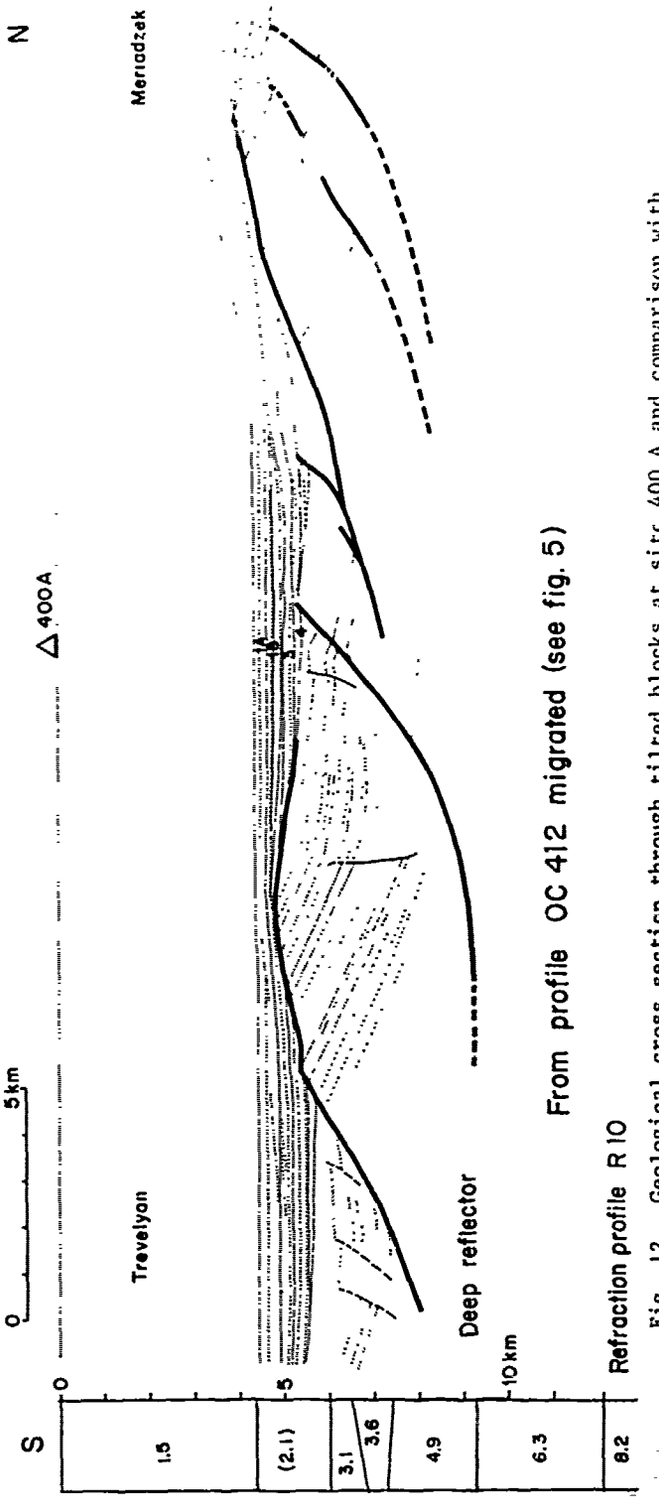


Fig. 12. Geological cross section through tilted blocks at site 400 A and comparison with seismic refraction data (N. Biscay margin).

canyon, have clearly the same orientation as the Hercynian shear zones of Brittany (fig. 1).

Of particular interest and significance for the rifting process is the nature of listric faults created during rotation of the blocks. The base of the syn-rifting sediments is a datum which allows determination of the throw of the faults. For listric faults this throw is a function of the amount of rotation of the block and of the width of the block. It may be as much as 3 to 4 kms for some large individual blocks. Tilting of the blocks involves their rotation about axes parallel to their strike. Depth reconstruction from seismic profiles (fig. 3, 4) show that rotation of the block is commonly 20° to 30°. The change of dip of the faults with depth which characterized listric faults is especially visible beneath the rise, where the faults become near horizontal with depths below the blocks. Figure 5 shows details of individual block with listric faults and figure 12 is a depth reconstruction of the same profile with the same horizontal and vertical scales. Such listric faults have been also described by BLAIR (1975) and BOWEN (1975) in the North Sea and postulated by LOWELL et al. (1972-1975) in the Red Sea and by GARFUNKEL and BARTOV (1977) in the Suez Rift. A reflector, often very strong, underlying the base of the listric faults is seen beneath the rise (fig. 13). Variations in travel time to this reflector are visible and shown as a "pull up" below the crest of the blocks due to the velocity difference between beds within the blocks and sediments infilling the adjacent half grabens. It may therefore be assumed that this reflector is relatively flat and thus independent of the tectonised layer above. An exactly similar feature (fig. 14) observed at the foot of the western escarpment of the Galicia Bank area (fig.2B) demonstrates that it is not of local origin. Such a strong reflector must correspond to a sharp contrast in acoustic impedance and should therefore correspond also to a refraction horizon. On the N. Biscay margin, refraction profile D12 of Ewing et al. (1959) is unfortunately located at the western end of Trevelyan (fig.2A) on both continental and oceanic crusts, thus making the results of little value in this respect. However a recent profile(n° 10) using O.B.S. parallel to the Meriadzek escarpment (fig.2A) (AVEDIK and HOWARD, in press) crosses the reflection profile shown figure 12. Below sediments with 2,1, 3,1 and 3,6 km/sec velocities there is a 2 km thick layer of 4,9 km/sec velocity whose base is situated near 9,500 km below sea level, almost exactly at the level where the listric faults become near horizontal. Below there is a 3 km thick layer with 6,3 km/sec velocity above the Moho discontinuity (8,2 km/sec) situated at 12 km below sea level. Computing vertical sound travel time from the seismic refraction data shows that the interface between 4,9 and 6,3 km/sec layers would lie at 9,2 sec two way travel time in good agreement with the observed travel time of the horizontal

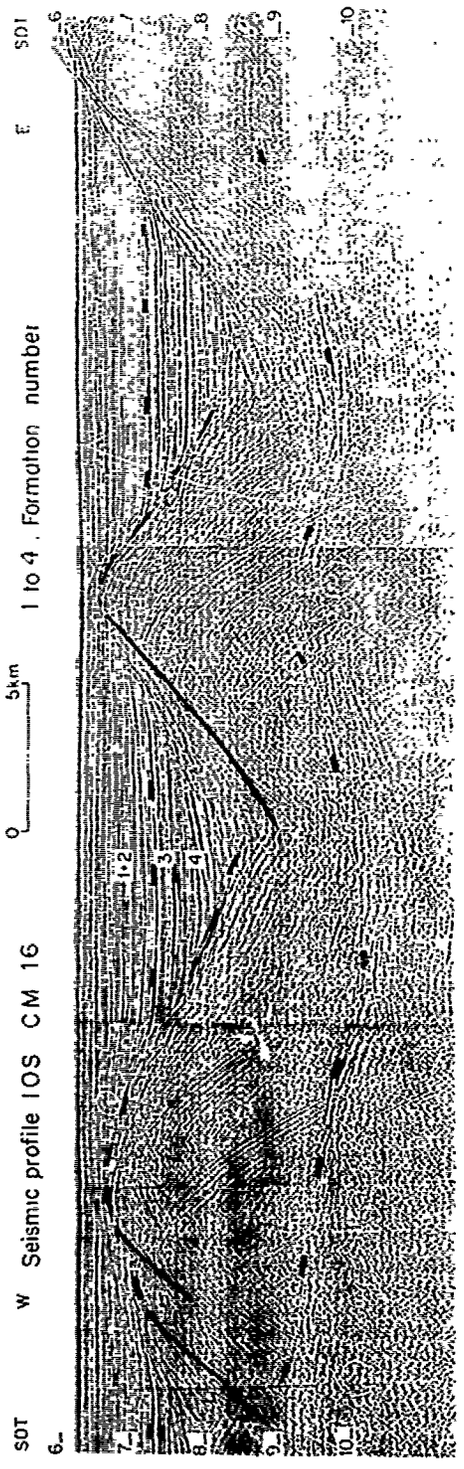


Fig. 13. Tilted blocks and the deep horizontal reflector below (South of Goban Spur - N. Biscay margin).

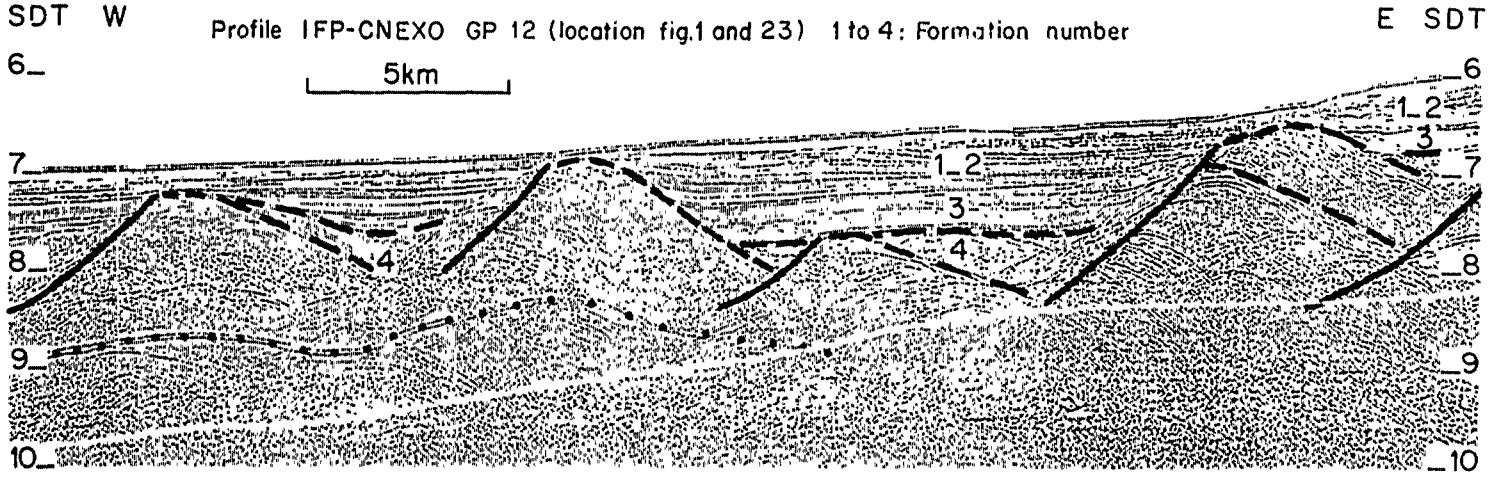


Fig. 14. Tilted blocks and the deep horizontal reflector below (S.W. of Galicia Bank).

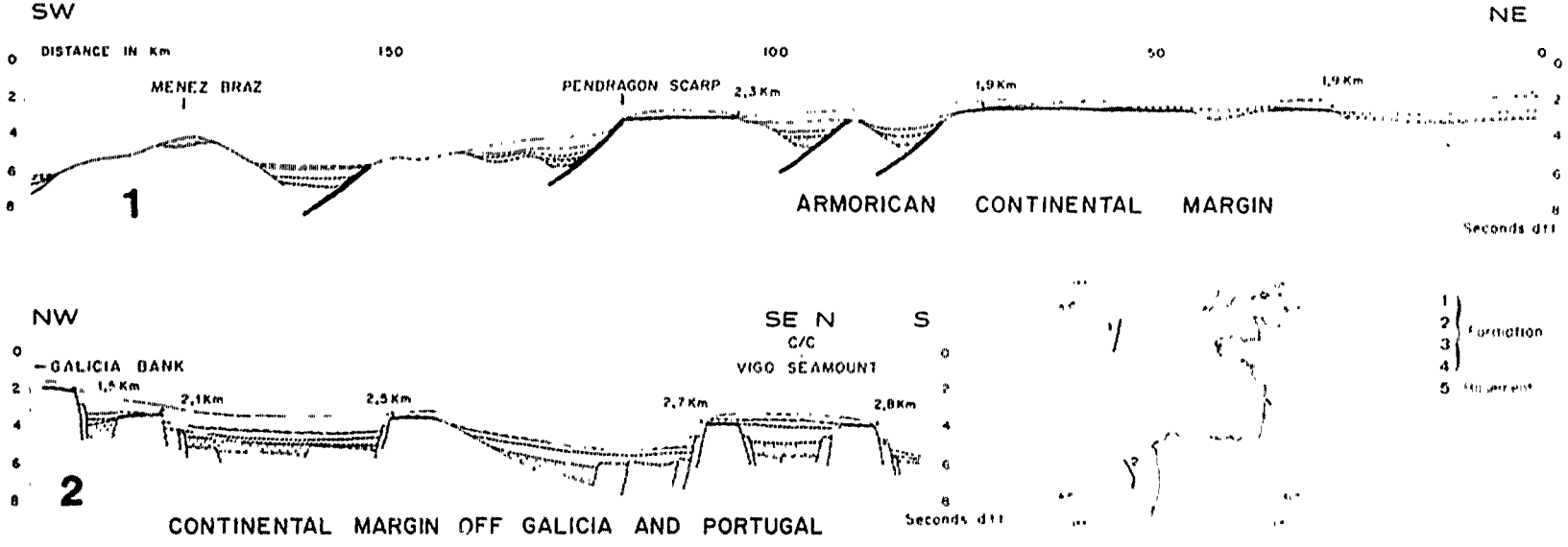


Fig. 15. Lower Cretaceous erosional surfaces truncating faulted blocks on N. Biscay and W. Galicia margins.

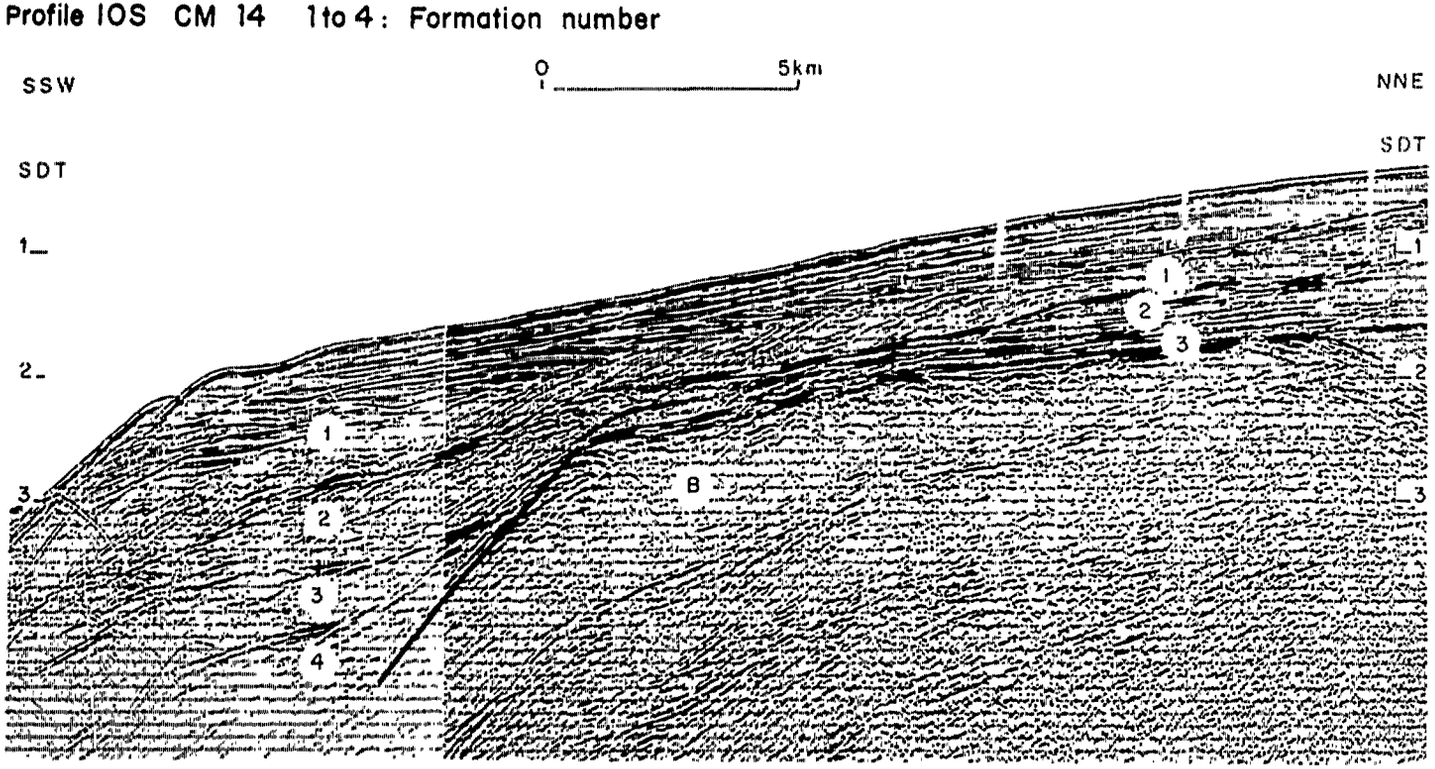


Fig. 16. Lower Cretaceous erosional surface truncating a tilted block on N. Biscay Upper slope.

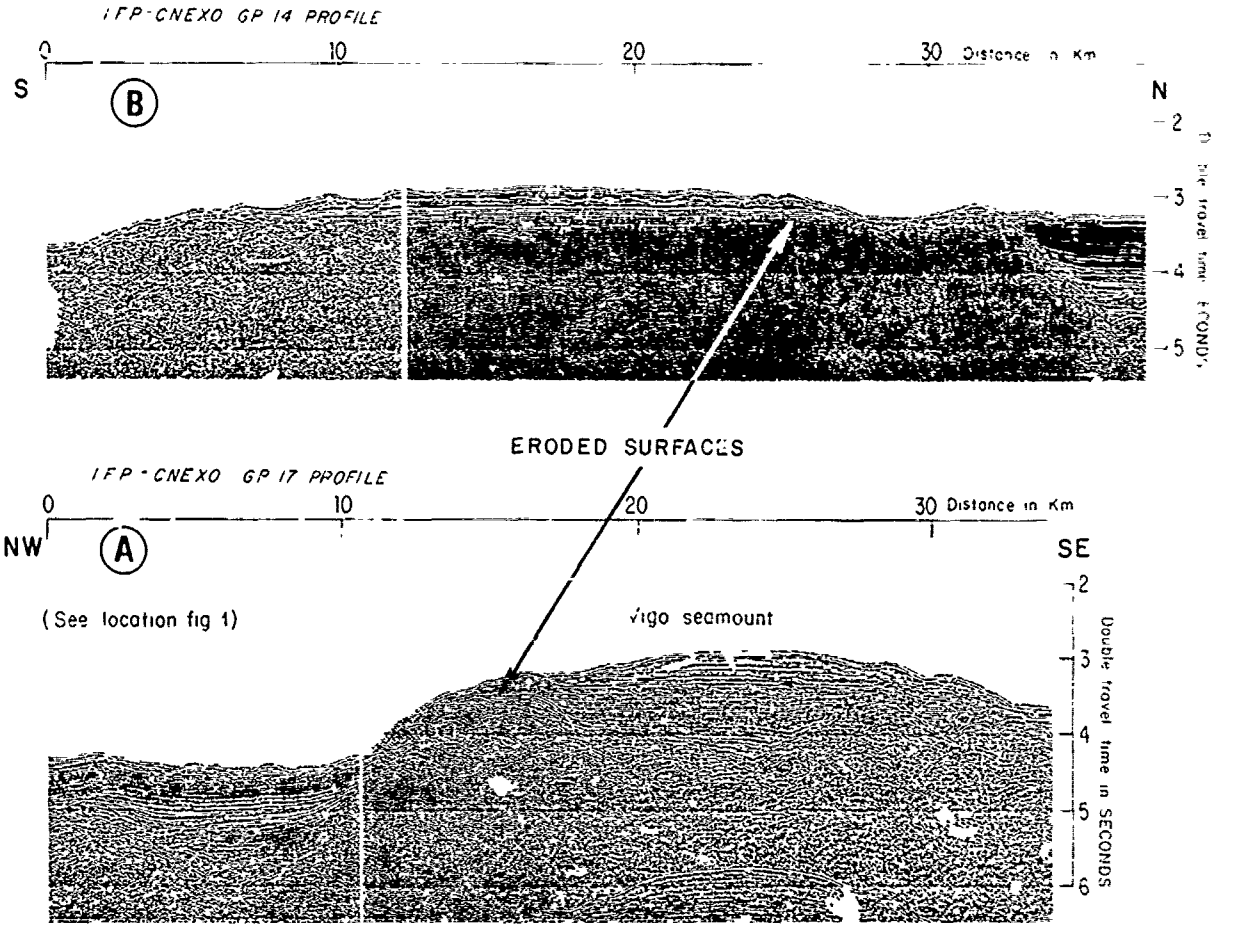


Fig. 17. Lower Cretaceous erosional surfaces truncating faulted blocks on W. Galicia margin.

reflector below the tilted blocks. Drill and dredge data show that tilted blocks include Mesozoic sediments, and others Hercynian basement showing that the tectonised layer includes continental basement as well as sedimentary rocks. The geological and refraction data thus show that the boundary defined by the near horizontal base of the listric faults and the reflector does not correspond to a particular geological horizon in sedimentary rocks allowing decollement but merely to a mechanical discontinuity within the upper part of the continental crust. This discontinuity which clearly existed at the time of rifting, was situated at around 6 to 8 km below sea level in the central part of the rift South of Meriadzek as calculated from the depth section (fig. 12).

The Syn-rifting sediments. Sediments deposited during rifting (Formation 4) are generally well characterized by convergence of the reflectors towards the crest of the block indicating contemporaneous deposition during tilting. Due to the complex fault block pattern the distribution of the syn-rifting sediments is complex and they may be thin or absent on top of the blocks, and very thick in the half grabens behind large tilted blocks. In some grabens the upper part of the syn-rifting sediments do not show any evidence of tectonic influence on their deposition and seems only to infill a pre-existing depression. This may indicate that rotation of the blocks could have stopped at different periods in different areas. Nevertheless, the latest activity which is probably intra-Aptian without precision in Biscay is very well defined in Galicia and dated latest Aptian (site 398 chapter, in press, SIBUET and RYAN, in press) (fig. 8).

No precise stratigraphic data are available in Northern Biscay because leg 48 drilling was not able to penetrate below the Aptian in a half graben. Some dredgings (AUFFRET et al., in press) found Barremian micritic limestones or marly chalks deposited at shelf or outer shelf depths in the Shamrock Canyon, and Valanginian to Barremian shallow water limestones or chalks on Meriadzek escarpment. On the contrary, in Galicia, the hole 398 penetrated a syn-rift section of sand-silt-clay graded sequences interbedded with thick (1 to 10 m) slumped beds or debris flows dated

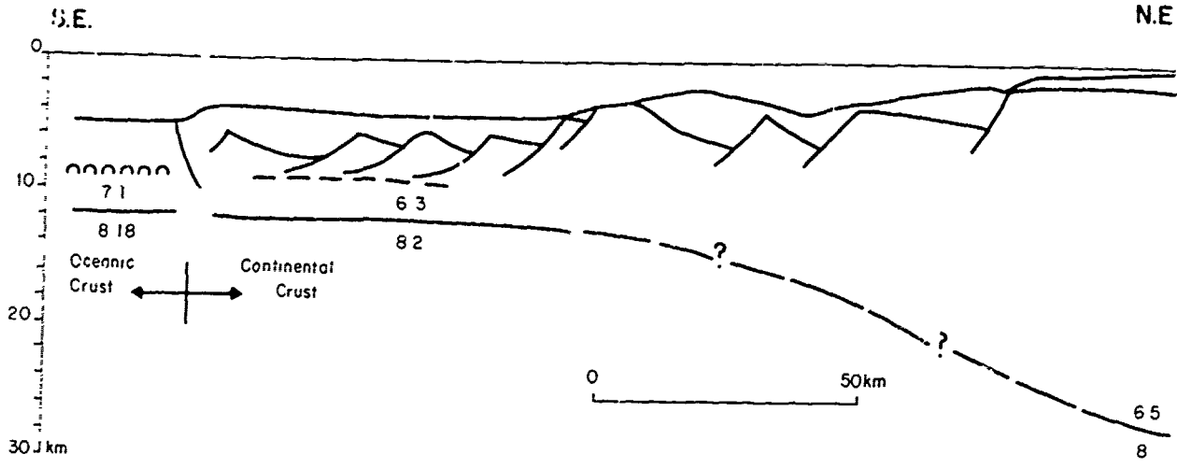


Fig. 18. Schematic crustal section through the N. Biscay continental margin.

Aptian and Barremian and a complex sequence of marlstone, siltstone, and white indurated limestones of Late Hauterivian to Early Barremian age.

The submarine topography at the end of rifting. In Biscay, the drill and dredge data and seismic reflection profiles allow reconstruction of the topography of the sea floor at the end of rifting in Aptian time.

The most striking feature allowing this reconstruction are horizontal planes which cut, in some areas, the crest of the tilted blocks (fig. 15), and indicate subaerial or shallow submarine erosion. These erosional surfaces are shown on fig. 11 in grey. They extend much closer to the ocean-continent boundary off Goban Spur than in the Meriadzek-Trevelyan area where the closest point to the boundary is near site 401.

The age of this erosional event is given by hole 401 and by data on the shelf. At site 401 (fig. 9) outershelf chalks of upper Aptian age rest above shallow water carbonates of late Jurassic and possibly lowermost Cretaceous age ; this demonstrates that erosion occurred during pre-Aptian time while rifting was active, i.e. while blocks were rotating. Near the shelf edge, (fig. 16) calibration of seismic lines from data of the western Approaches basin demonstrate also that the Aptian (pro-parte)-Albian rests on the erosional surfaces cutting the faulted blocks. The seismic profiles therefore delineate areas on the continental margin which were at zero level during rifting. Fig. 11 shows that a large part of the margin in front of the western Approaches basin was below this level. However results from dredging and hole 402 show areas where no erosion occurred but were nevertheless under shallow water during Aptian time. At site 402 Aptian-Albian black shales were deposited as a prograding shelf on a subsiding shallow platform. It appears that in front of the Aptian shelf, one or several isolated shallow banks existed in the area of Meriadzek. Outside these areas, water was deeper. At site 400A, Aptian-Albian sediments are interpreted as deep water sediments deposited not far above the CCD. Since post-rifting sediments including formation 3 are not faulted, the depth at which Aptian sediments were deposited at site 400 can be estimated from the throw of the faults along the Meriadzek escarpment, i.e. from the difference of altitude between the Aptian at site 401 and site 400. A depth of 1500-2000 m is indicated for the area of site 400A on Trevelyan plateau at the end of rifting. In front of the western Approaches basin, large areas of the submarine rift system were deep and a central trough existed of about 2000 m depth. At the same time most of the Goban Spur area was much shallower since erosional surfaces are observed relatively close to the continental-oceanic boundary (fig. 11). Only a narrow deep trough existed there at the end of rifting. This change of style between the two areas may be explained by the difference in nature of the pre-rift rocks. On Goban Spur rifting affected an hercynian granitic basement without sedimentary cover, but in the Meriadzek area rifting affected an hercynian basement probably of a different nature and covered by a thick mesozoïc sequence. This would suggest that the physiography of a rift system may be largely controlled by the nature of the pre-rift rocks.

In Galicia, the same erosional surfaces are observed (fig. 15, 17 ) but no hole had been drilled through. Hole 398 which was drilled in a low demonstrated that syn-rift sediments were deposited in a deep water environment above the CCD during Hauterivian and Lower Barremian and clearly beneath the CCD after Mid Aptian times. Even, if the CCD on margins could be different from oceanic basins, an estimate of water depth during Aptian time is given by several authors (LE PICHON et

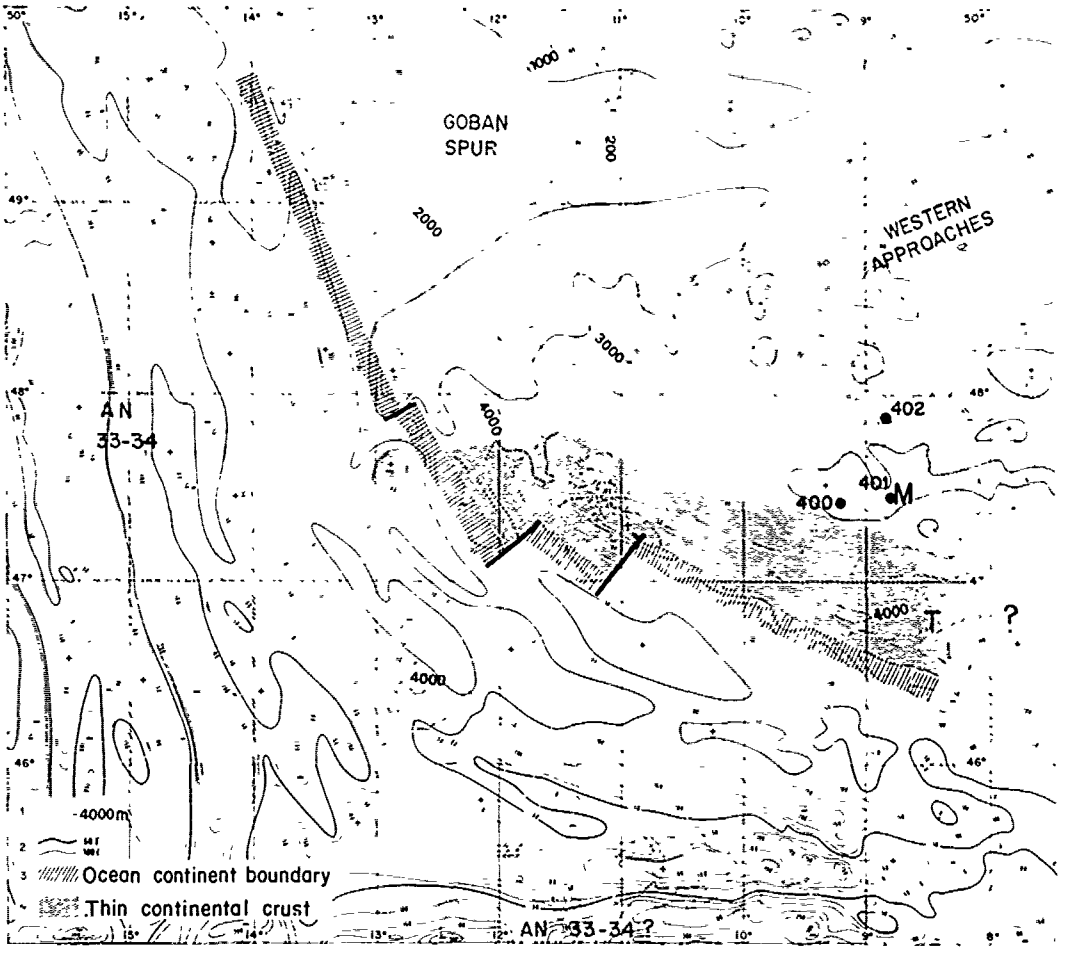


Fig. 19. Magnetic anomalies, and oceanic-continental crusts boundary (N. Biscay margin).

al. in press, VAN ANDEL et al. 1977) around 1500-2000 meters. An independent estimate of the water depth at the end of rifting is given by the difference of levels between the Aptian depth at site 398 and the erosional surface evidenced on Vigo Seamount and supposed to be of Lower Cretaceous age as in Biscay ; the value obtained is around 2500 meters. Such result is in a good agreement with the estimation made in Biscay (1500-2000 m). The higher value for Galicia is in agreement with the fact that there, the Aptian was deposited below CCD, while in Biscay at site 400 it was deposited slightly above. The major consequence of these observations is that on the Northeast Atlantic during Aptian, at the end of rifting, large submarine troughs as deep as 2500 m existed.

## Discussion on rifting and thinning of the crust

Although rift tectonics are relatively simple, there is continuing controversy about their nature and development. Structural models are based mainly on the studies of continental subaerial rift systems like the East African rifts, the Rhine Graben, the Suez rift,...

The different hypothesis. A common hypothesis is that intracontinental rifts are related to doming of the continental crust (CLOSS 1939) and the following stages have been recently proposed (NEUGEBAUER 1978) : 1. upwarping of the crust 2. incipient volcanic activity 3. formation of faults and increasing volcanic activity 4. subsidence of graben. BURKE and WHITEMAN (1973) considered also that rifts developed on crest of uplifts interpreted as isostatic responses to mass deficiencies produced by partial melting of the mantle above rising plumes at the base of the lithosphere. FREUND (1965) pointing out the difference in width between the different rifts, the presence or absence of a swell, proposed a necking hypothesis with thinning of the crust below accompanied by rising of the mantle. He also raised the question of the spatial and temporal relations between the rifts and the orogenies. ARTEMJEV and ARTYUSHKOV (1971) from a study of

the Baïkal rift proposed a mechanism resulting from crustal extension when neck shaped strains in the crust are developed. The lower part of the crust is plastically attenuated and faults occur in the upper layer of the crust where the viscosity is too high. FUCHS (1974) proposed a somewhat similar model for the Rhine Graben.

The cause of crustal extension is also a matter of controversy. HEISKANEN and VENING-MEINESZ (1958) proposed large scale movements in the mantle created by thermal convection, while ARTEMJEV and ARTYUSHKOV (1971) suggest gravity convection. Others relate rifting to the stress field existing inside plates as a consequence of collisions (ILLIES 1975 - GARFUNKEL and BARTOV 1977).

Data on rifting from the study of continental margins are relatively scarce because the rift structures are often covered by a very thick sedimentary overburden hiding the deep structures. This difficulty is partly overcome on the starved North Biscay and Galicia margins.

Rifting and attenuation in Biscay and Galicia. Legs 47B and 48 results and seismic reflection profiles demonstrated that on this area rifting was submarine (MONTADERT, ROBERTS et al. 1977, de Charpal et al. 1978) in contrast to many rifts and occurred on a pre-existing mesozoïc sedimentary basin perhaps shaped during an earlier Triassic tensional episode (WINNOCK, 1971). Although the onset of rifting is not well established, comparison with Aquitaine basins suggests it may have begun by late Jurassic but was probably mainly active during Neocomian. The end of rifting and the onset of spreading is very probably late Aptian. As demonstrated in the previous section, broad 2500 m deep troughs existed at that time. This fact and the tectonic style observed with tilted blocks including the upper part of the continental crust, bounded by listric faults, is characteristic of an extension of the crust with the synchronous development of a central trough. Under continuing extension the fault blocks can rotate only because the central trough is subsiding so that individual blocks dip away from the axis. In the trough, the continental crust affected by listric faults was about 6 to 8 km thick ; the rotation of the blocks reduced this thickness to about 4 - 5 kms (fig. 12).

We suggest that the mechanical discontinuity which controlled the level above which continental crust was faulted during rifting corresponds to the transition between the upper brittle and the lower ductile continental crust (GRIGGS, 1960).This boundary is close to a strong horizontal reflector situated at about 10 km below sea level. This reflector corresponds to an increase of velocities from 4,9 km to 6,3 km/sec as shown by refraction data (fig. 18). (AVEDIK and HOWARD, in press - BOTT and WATTS, 1971). The Moho discontinuity was determined at 12 km below sea level. These results demonstrate an almost complete thinning of the ductile continental crust, reduced to 3 km as a maximum, by some subcrustal process, while it was probably around 15 - 20 km away from the rift (fig. 18). Recent heat flow data obtained in North Biscay margin (FOUCHER and SIBUET, in press) support this mechanism of thinning of the ductile part of the continental crust. Phase changes or intrusion in the lower part of the ductile continental crust could be mechanisms which played a part in crustal attenuation. Nevertheless, as the layer affected by these processes does not contain radiogenic elements, it is still necessary to explain the amount of crustal attenuation and heat flow data, to invoke another process for thinning of the almost entire ductile crust.

The amount of horizontal extension can be estimated approximately for the upper part of the continental crust. For rotation of 20° to 30° of the blocks the extension of the area between the present shelf edge and the oceanic-continental crusts boundary is around 10 - 15 % of the previous width.

Also relevant to the rifting process is the fact that no erosion occurred before and during rifting in the central trough of the rift system. In this case rifting was not preceded by and therefore is not a consequence of a large doming. The same observation was made in the Rhine Graben and in the Suez rift where more or less complete pre-rift sedimentary layers are preserved. The uplifting of the shoulders of the rift there postdates the initiation of the graben. Such uplifting occurred also in Biscay away from the rift trough but is not expressed in the topography since erosion kept pace with the uplift and maintained the area at the level of the sea. The cause of the uplift of the shoulders of the rift could well be regional isostatic adjustment.

Speculation on the mechanism of rifting. From our observations, therefore, the most appealing mechanism for rifting would be stretching of the lithosphere as a response to intraplate stresses. These stresses could be due to the difference between the absolute velocities of plate boundaries or consequences of continental collisions. (FORSYTH and UYEDA, 1975). These stresses were applied to a crust made of two layers of completely different mechanical properties. As shown above, the extension is limited, but the thinning of the ductile part of the crust is much more important than the thinning of the brittle part by rotation of blocks. Rock mechanics experiments (POULET, 1976) show that strain of ductile material increases continuously when a certain level of stress is attained (viscous behavior). On the contrary, the continuous strain of brittle material is relatively limited for increasing stress until a fracture is created which releases the stress. One must therefore conclude that there was mechanical decoupling between the two sections of the crust. For this reason, it is quite possi-

ble that thinning of the ductile part of the crust began before the creation of the first fault in the brittle crust. Then speculating that tensile stresses are the same at the lateral boundaries of the whole lithosphere, the extension will be more important in the lower ductile part by continuous viscous flow starting at a low level of stress accumulation and stress relaxation by faulting until complete break up of the lithosphere. The continuous necking of the lower ductile part of the crust is accompanied by rising of the mantle and a depression in the upper brittle crust (the rift trough) which allows rotation of blocks along listric faults.

## The post rifting history

Complete rupture of the lithosphere occurred at the end of rifting in latest Aptian time and new oceanic crust accreted in deep waters along the young Continental margin which began to subside.

The different mechanisms for subsidence. Several mechanisms have been proposed for explaining this subsidence of the continental margins. SLEEP (1971, 1973), SLEEP and SNELL (1976) suggested that post-rifting subsidence could be related to thermal contraction of the lithosphere which occurred when the heat source moves away the margin after onset of spreading. BOTT (1971, 1973), BOTT and DEAN (1973) suggested that accompanying or following the thermal contraction of the lithosphere, subsidence could occur as an isostatic response to crustal thinning caused by hot creep of lower continental crustal material towards the suboceanic mantle. This would be due to instability of young continental margins because of gravitational energy associated with the junction between oceanic and continental crust that would create wedge subsidence in the upper brittle layer. Finally WALCOTT (1970 - 1972) explained subsidence of the continental margin under loading by sediments by flexure of the lithosphere.

On the starved North Biscay and Galicia margins, the post rifting sediments are so thin that the influence of loading or subsidence is negligible, so that the fundamental mechanism of subsidence of a passive continental margin can be directly studied.

Transition between continental and oceanic crusts. In Biscay, the transition between continental crust and oceanic crust is relatively well documented by geophysical data. The magnetic anomaly map of the total field (fig. 19) (SIBUET et al., in preparation) covers an area from the shelf of the western Approaches to the center of the Bay of Biscay. The continental shelf is characterized by strong amplitude anomalies (HILL and VINE, 1965 - SEGOUFIN, 1975 - LE BORGNE and LE MOUEL, 1970) which do not extend off the shelf break. On the continental slope, anomalies of generally small amplitude are oriented parallel to the margin with some transverse discontinuities which can be linked with transverse faults of the rift pattern. Northward, gravity and magnetic anomalies show the extension of the batholitic axis of SW England until the shelf break (HILL and VINE, 1965 - DAY and WILLIAMS, 1970 ; SIBUET, 1972). The map shows that this axis extends until the foot of the continental slope where a late hercynian granodioritic complex have been found by dredgings (PAUTOT et al. 1976). The oceanic domains of the Porcupine abyssal plain and of the Bay of Biscay are characterized by magnetic anomalies often of strong amplitude and small wave length, shown as well marked linerations respectively oriented SSE-NNW and E. - W. to ESE - WNW. In the Porcupine abyssal plain the first clearly identified anomalies may be anomalies 33 - 34 (CANDE and KRISTOFFERSEN, 1977) of late Upper Cretaceous age (VAN HINTE, 1976). Although interpretation of magnetic anomalies in Biscay is still under discussion, it seems that the central anomalies of the Bay, oriented E.W. and superimpose on the N. ans S CHARCOT and Biscay seamounts can be identified as anomalies 33 - 34 (CANDE and KRISTOFFERSEN, 1977 - SIBUET et al., in press). This would imply that a triple point was active during the last phase of opening of the Bay (WILLIAMS, 1975 - SIBUET et al., in preparation). However the Biscay seamounts are extensively tectonised and this interpretation may not be correct (ROBERTS, to be published). Lineations existing between the anomalies 33 - 34 and the margin indicate the existence of an oceanic crust of pre-Senonian age (An 34, 80 MY) (ALVAREZ et al., 1977 - Van HINTE, 1976). These lineations are not very continuous but they exist. They have been delineated mainly from the correlation between profiles of 3 small positive anomalies. These anomalies inside the "quiet zone" may be small reversals as observed for example in the Albian of Site 400 A (HAILWOOD et al., in press). This is in good agreement with geological data on the margin that indicates an Aptian age for the end of rifting. Nevertheless it must be pointed out that anomaly M0 of Aptian age is not found along the margin and accretion of new oceanic crust just after anomaly M0 cannot be excluded. At the foot of the margin the transition from continental crust to oceanic crust is delineated from the gravity and magnetic profiles (fig. 20) and from seismic reflection profiles (fig. 21, 22). In the NW part of the margin, this boundary follows the base of the continental slope from Porcupine Sea Bight as far as Southern end of Goban Spur. The boundary is linear and very sharp along Goban Spur (fig. 21). South of Goban Spur, the transition is also sharp (fig. 22) since Hercynian granites have been dredged on the last tilted block and oceanic crust is seen about 10 km to the SW. In this case, magnetic anomalies amplitude begin to increase already below the very attenuated continental crust. South eastwards, the boundary is shifted northward and it is close a localized positive magnetic anomaly and a strong amplitude (more than 400 γ). Along the Trevelyan

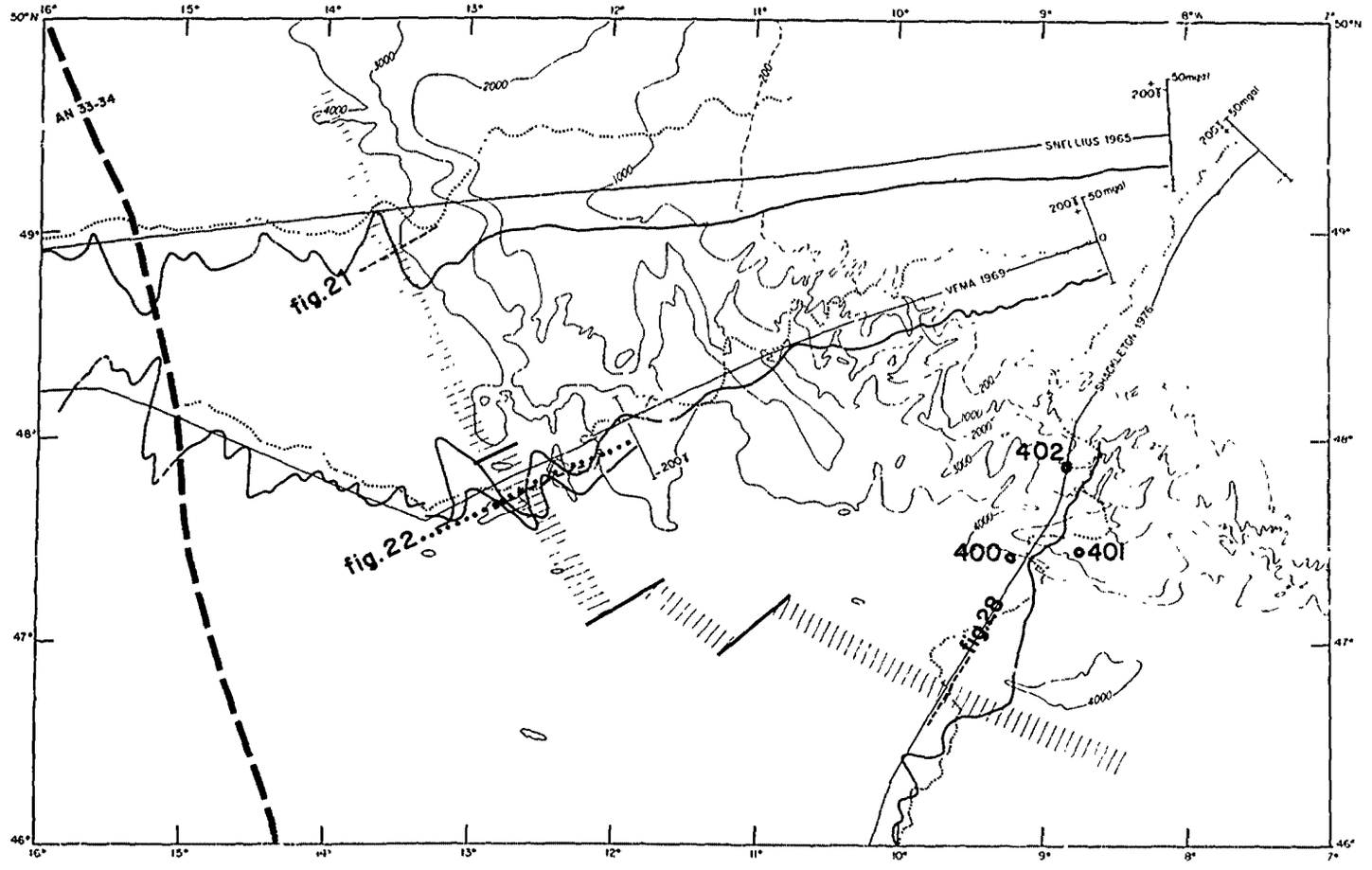


Fig. 20. Magnetic and gravity profiles through the continental-oceanic crusts boundary (N. Biscay margin).

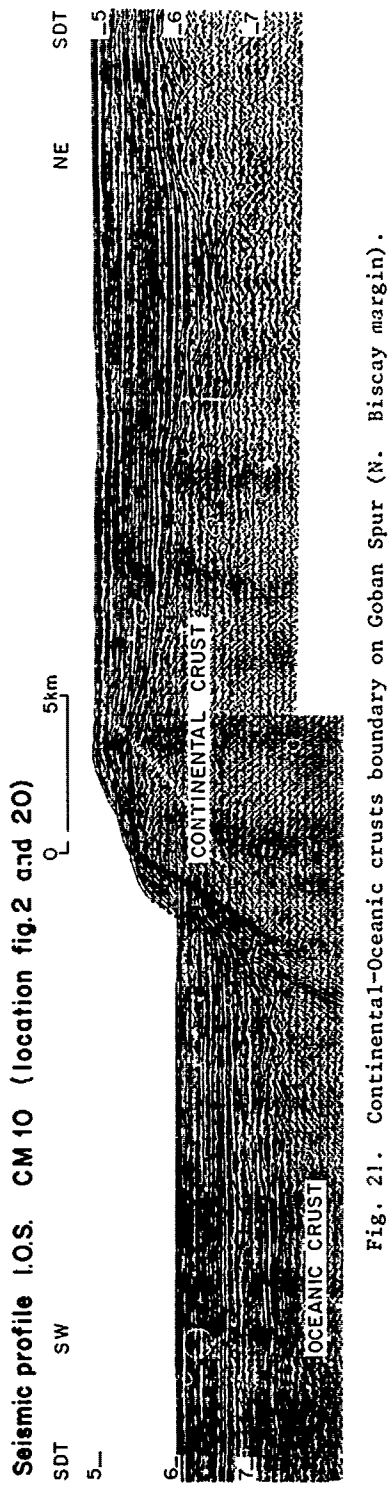


Fig. 21. Continental-Oceanic crusts boundary on Goban Spur (N. Biscay margin).

escarpment, it follows a large negative magnetic anomaly (250 γ) which extends far to the SE where it is superimposed on the north Gasgony ridge (GRAU et al., 1973 - MONTADERT et al., 1975) which is the Southern limit of the deep thick Armorican marginal basin. Seismic reflection data do not show evidence of formation 3 (Aptian-Albian) on the oceanic crust west of Goban Spur, but it is present along Trevelyan (fig. 27). This may indicate that the opening along Goban Spur was slightly younger than to the South. The nature and origin of the Armorican marginal basin north of the North Gasgony ridge is also raised by these results. It is either a piece of pre-Aptian oceanic crust covered by a thick mesozoïc sediment or it may be thinned continental crust as at Trevelyan covered by a much thicker layer of lower cretaceous sediments.

In the Galicia area, the magnetic anomaly map of the total field (fig. 23) (SIBUET et al., in preparation - Groupe Galice, in press) covering the western Iberian continental part of Galicia including Galicia bank, Vigo, Porto and Vasco de Gama Seamounts, is characterized by magnetic anomalies of ± 150 gammas without an obvious grain direction, typical of continental areas. Westwards, a north-south positive feature has been interpreted, South of 41°N, as the MO anomaly (Groupe Galice, in press). The MO anomaly cannot be traced northwards. Between MO and the well defined 34 anomalies exist a series of positive and negative anomalies of ± 150 gammas more or less continuous and similar to the magnetic quiet zone anomalies described in the Bay of Biscay. Some of these magnetic lineations correspond probably to an isochron in the quiet magnetic zone and could be associated with the small reversals observed by Hailwood et al. (in press). Northwards of 41°N, where the MO anomaly is not defined, the transition between continental and oceanic crusts is evidenced by steep gradients in magnetic anomalies and is well defined on seismic profiles as in North Biscay. Southwards of 41°N and East of anomaly MO, the Iberian abyssal plain has the same magnetic character than the surroundings continental area. It could be either oceanic crust older than Aptian either subsided thin continental crust. The beginning of oceanic crust formation is clearly dated Latest Aptian (MO anomaly) in perfect agreement with the age of the end of rifting phase of the margin as shown by site 398 results.

The post-rifting subsidence. Significant faulting of the post-rifting sediments is absent and only local cenozoïc deformations are observed. Post-rifting subsidence is thus characterized by an overall tilting of the margin in post Aptian time with coupling between the oceanic and continental crust. The absolute subsidence of the margin after rifting can be therefore estimated by the difference between the altitude of the Aptian horizon at the end of rifting and today.

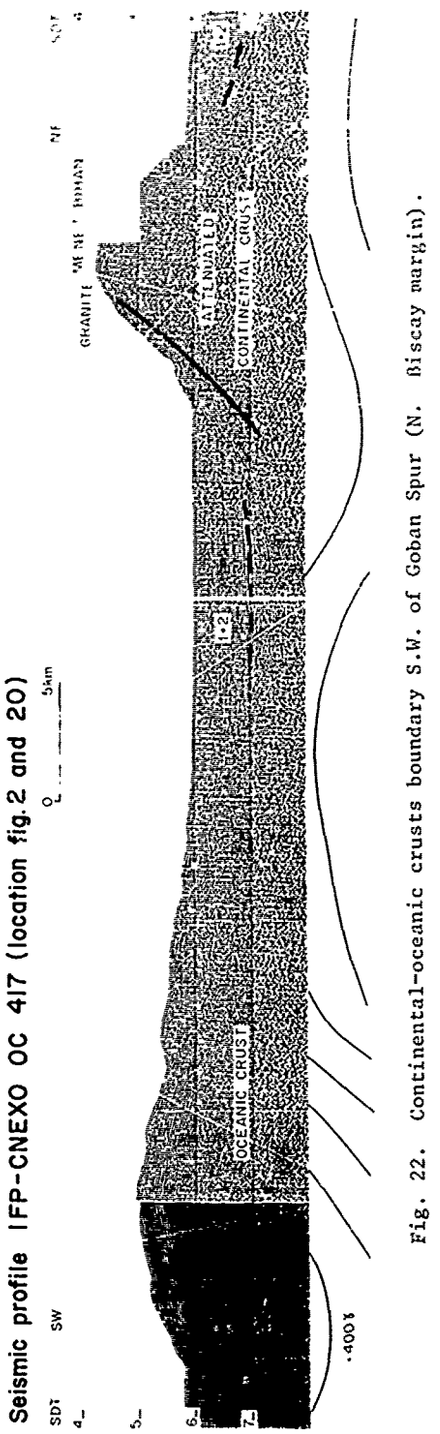


Fig. 22. Continental-oceanic crusts boundary S.W. of Goban Spur (N. Biscay margin).

In Galicia, subsidence cannot be determined on a transect of the margin by lack of data but can be estimated in the area of site 398 (SIBUET and RYAN, in press). Since at site 398 we have no precise paleodepths, we first determined the subsidence curve (fig. 24) of a subaerial early cretaceous erosional surface on the top of Vigo Seamount (fig. 15, 17) located 20 km north of the site. This surface which was at the sea-level at the end of rifting in Latest Aptian time is presently 2,5 km deep. We supposed that the subsidence is related to the thermal cooling of the lithosphere since the opening of the North Atlantic, and we have drawn (figure 24) a subsidence curve of exponential type. We have supposed that the same subsidence curve could be applied to the site area if the site location is 2 km deeper than the present depth of the erosional surface. Consequently, the paleodepth of the acoustic basement should be at about 2,5 kilometers in Lower Cretaceous time, which is compatible with the paleodepth of sediment emplaced at this time. The local isostatic readjustment has been calculated using shipboard density measurements. Compaction has been taken into accound to calculate the site 398 paleodepth. The CCD curve have been superimposed on the paleodepth curve. Extrema of the CCD curve are arbitrary.

On the contrary, in North Biscay, data from leg 48 drillings, dredgings and constraints from seismic reflection profiles allow reconstruction of the topography of the sea floor at the end of rifting, and by substraction of the present depth of Aptian calculation of the absolute subsidence along a transect trough the margin. The results are presented on a simplified section (fig. 25) through the best documented area of the margin from the shelf edge to the continental-oceanic crusts boundary. Although post-rifting sediments are only a few hundred meters thick, an isostatic correction has been applied to the Aptian horizon for a local loading on an Airy-type crust (see for example WATTS and RYAN, 1976).

From fig. 25, it is inferred that the present depth attained by a point on the margin depends on its altitude at the end of rifting and on its distance from the ocean-continent boundary, while the absolute value of subsidence depends only on the distance to the ocean-continent boundary. It should be noted that estimation of the subsidence of a margin requires knowledge of the topography at the end of rifting which may be difficult to determine. This diagram confirms that a good coupling existed between the continental and oceanic crusts since near the boundary, the continental crust subsided practically as much as the adjacent oceanic crust. SLEEP (1971) suggested that due to cooling of the lithosphere the subsidence rate would decay exponentially with time and that the time constant of subsidence would be similar to the time constant of subsidence of mid-ocean ridges, i.e. 50 M.Y. Fig. 25 shows that, for the

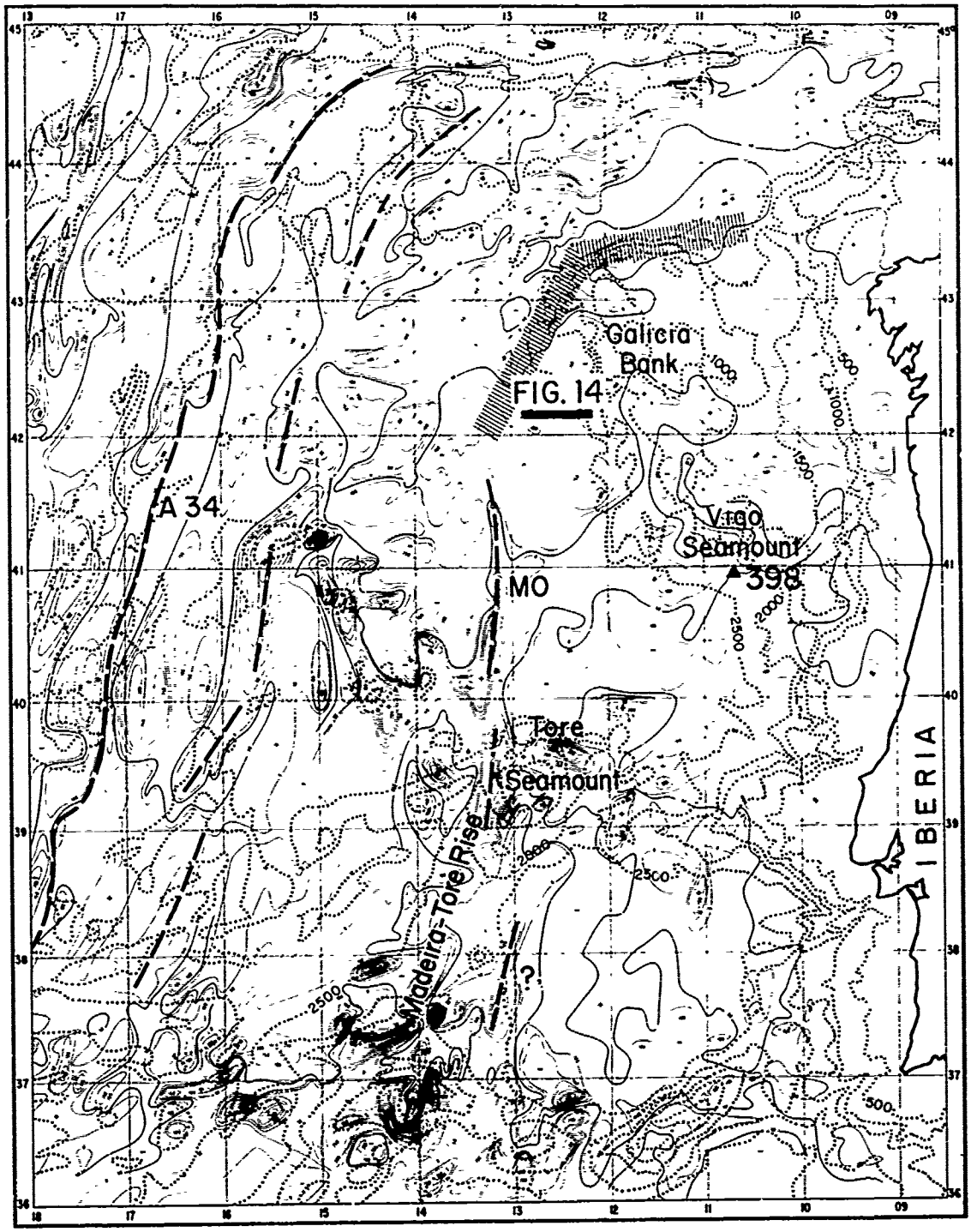


Fig. 23. Magnetic anomalies W. of Iberia.

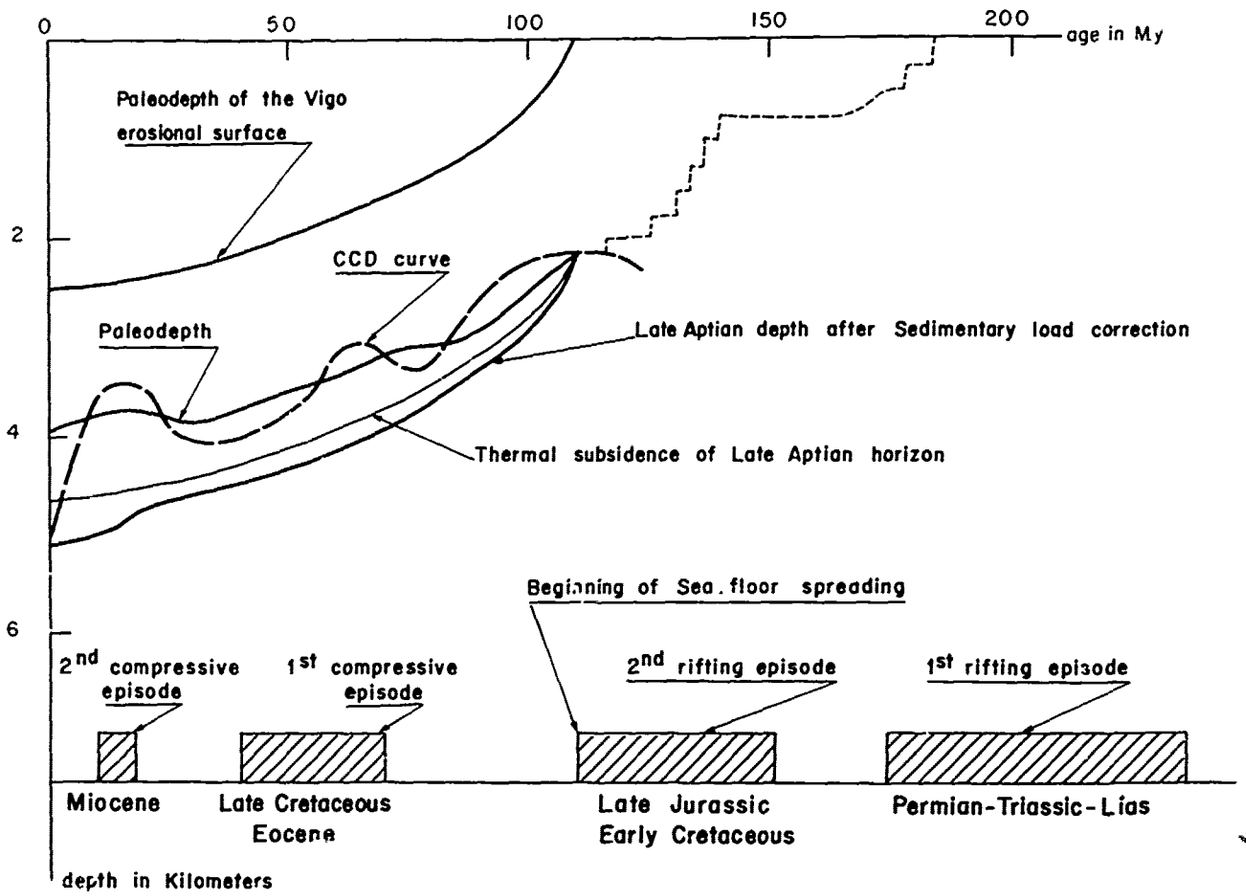


Fig. 24. Subsidence versus time curve at site 398 (W. Galicia margin).

same period of time, say 120 MY since Aptian, the amount of subsidence is not the same for every point of the margin, so that the time constant cannot be the same for the whole margin if subsidence decreased exponentially with time. Only in the lower part of the margin is the constant similar to the one of the oceanic crust. There is therefore not a single law that characterizes the subsidence of a whole margin but one law for each point.

The exponential decay of the subsidence rate with time for different points on the margin can can be checked from paleodepth estimate for different periods of time after Aptian. In the case of Biscay, these curves cannot be drawn with precision since paleodepth estimates from paleontological data are less and less precise for increasing water depths and for increasing ages. Paleodepths estimate for the Mesozoïc (DUPEUBLE, in press) and for Cenozoïc (SCHNITKER, in press - DUCASSE and PEYPOUQUET, in press) nevertheless support an exponential decay especially at site 401, although elsewhere there is no contradiction with the paleontological and sedimentological data (fig. 26).

In the lower part of the margin where the continental crust is very thin, the subsidence rate is not too different from the subsidence rate of the adjacent oceanic crust but towards the shelf, with increasing thickness of continental crust, the subsidence rate diminishes considerably. Changes of slope on the subsidence versus distance curve (fig. 25) reflect probably a sharper change in thickness of the continental crust (fig. 18). It is therefore suggested that post rifting subsidence without influence of loading is essentially an isostatic adjustment to cooling of the lithosphere in which the continental crust has been previously thinned during the rifting process. In that case, one can expect a relationship between the absolute subsidence of a point on a margin and the thickness of the continental crust.

The Cenozoic (Eocene) deformations. In N. Biscay, we observed that after rifting of the margin, subsidence occurred tilting regionally the margin. Rejuvenation of the rift faults is not observed during this period, although it may occur on other margins due to differential loa-

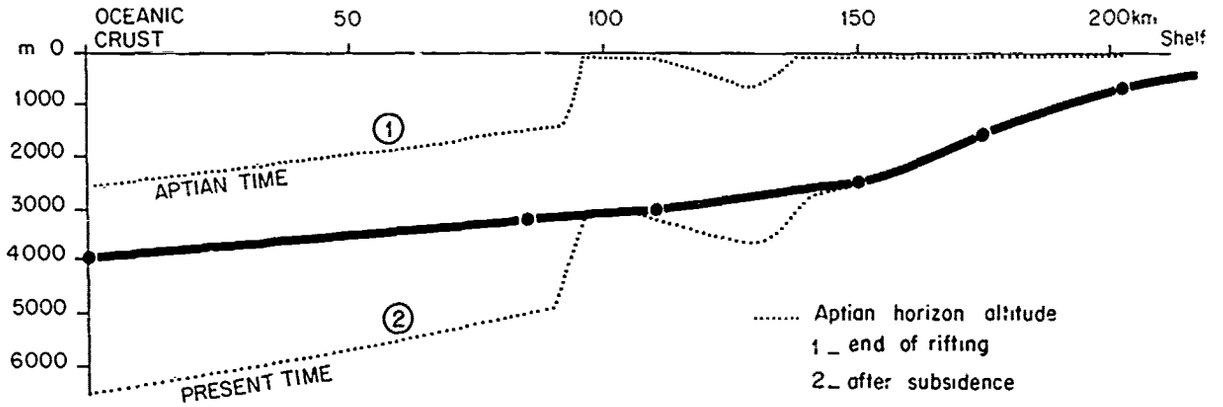


Fig. 25. Absolute amount of subsidence (full line) after rifting on a transect through N. Biscay margin.

ding under a thick sedimentary cover. The absence of tectonic activity is in good agreement with the position of the North Biscay margin within the European plate during Cenozoïc. Nevertheless to the South, the northern edge of Iberia including Galicia Bank area was a plate boundary where some subduction of Biscay oceanic floor occurred at least until late Eocene-Oligocene. Intense deformations linked to this compression phase occur all along the Northern boundary of Iberia and Galicia Bank area (Pyrenean foldings) (fig. 1). Eastwards, towards the Mediterranean area, Europe-Iberia was in collision with Africa. In such conditions, intraplate deformations can occur and indeed have been described both in the oceanic and continental parts of the European and Iberian plates. Moreover, South of Iberia along Betics and Magrebian ranges, intense early to middle Miocene tectonics occurred. Some deformations of this age can be observed northwards until the southern part of Galicia Bank area.

In the Galicia area (Groupe Galice, in press) the large faults which runs along the northwest edge of Galicia Bank continues in the southwest as a flexure which affects the Mesozoïc and Eocene layers without disturbing more recent deposits. Movements of the same age are also visible in the Interior basin. At the foot of the northwestern Galicia bank, the deformations are much more intense with clear reverse faults linked with some overthrusting of Galicia Bank over the oceanic crust (fig. 27).

Another way to quantify cenozoïc deformations on the continental margin is to follow the shape, slope and altitude of the lower Cretaceous erosional surfaces. Figure 17 shows significant difference in the altitude of these surfaces between the southern part (2,5 - 2,8 km) and the Galicia Bank (1,5 km). This could be explained by uplifting of Galicia Bank during the Eocene compressional events. Nevertheless, if one takes into account the relationship between subsidence and thickness of continental crust as established in N. Biscay, the higher level of the surface of Galicia Bank s.s. could be explained also by thicker continental crust there than southwards.

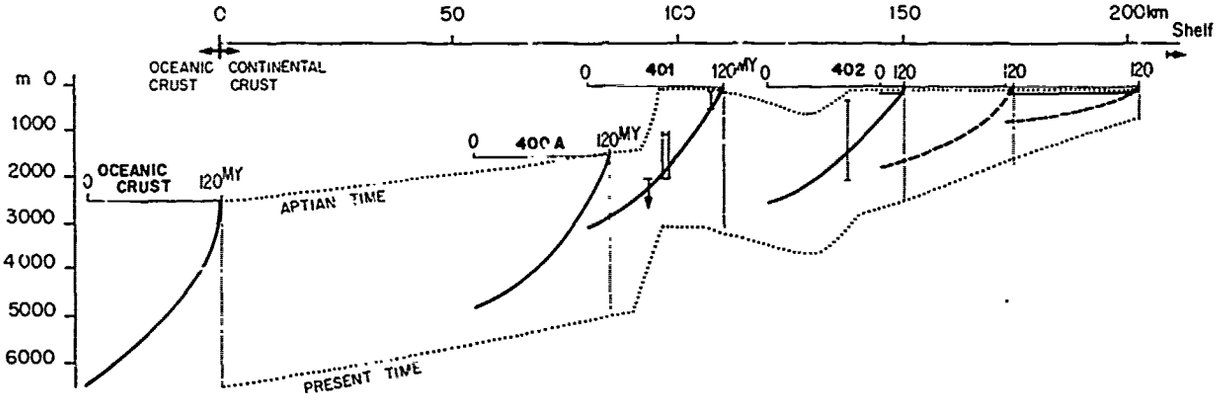


Fig. 26. Hypothetic subsidence versus time curves for different points on a transect through N. Biscay margin (compare with fig. 18).

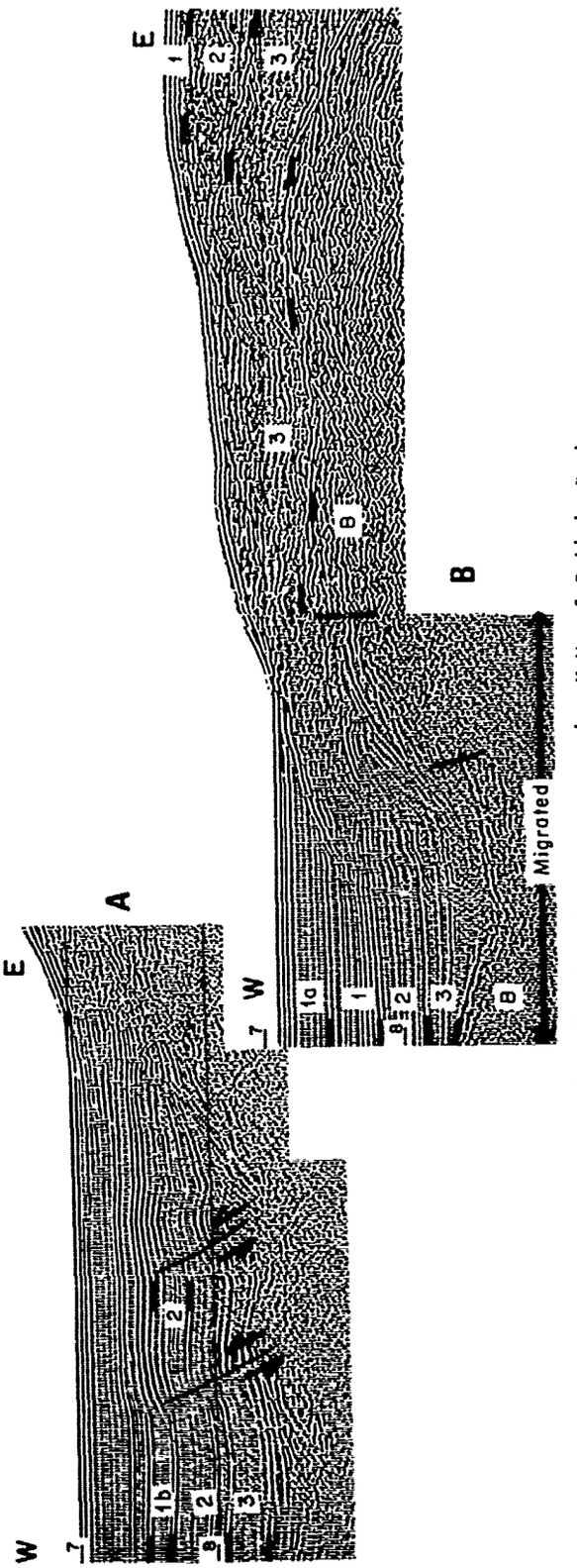


Fig. 27. Late Eocene compression N.W. of Galicia Bank.

In the oceanic area, to the north the tectonized area (fig. 1) along Iberia, numerous areas uplifted during late Eocene can be defined (MONTADERT et al., 1971 - GRAU et al., 1972 - MONTADERT et al., 1974) from seismic reflection and drilling. On uplifted areas, thin pelagic post Eocene sediments were deposited (DSDP site 119, LAUGHTON, BERGGREN et al., 1972) and are easily distinguished from turbidites deposited around the high points. Numerous faults of this age are also visible in the abyssal plain as well as on the continental margin. Their occurrence has led to overestimates of their role on the formation of the continental margin. On land, numerous studies show that deformation occurred in the whole continental domain at the same period (DE CHARPAL et al., 1974, TREMOLIERES, to be published) in France, England, Germany, linked to compression along a 10° - 20° E direction. Another compressional event occurred since Miocene time but seems to be restricted mainly to the Southeastern part of the Paris basin. The whole European plate was submitted during late Eocene-Oligocene to compression in the oceanic domain as well as in the continental one. Following orientation of the pre-existing structures, this compression created strike-slip faults. reverse faults, folds, etc...

On the North Biscay margin, the new seismic profiles allows a better estimate of the Cenozoïc deformations. Faults are relatively restricted to some areas (fig. 11) and the most striking features are observed along the Trevelyan escarpment. Along an E.W. belt, numerous faults, including reverse faults, affected the series including Formation 2 (fig. 28). The faulting caused uplift that created the Trevelyan escarpment. This strongly tectonized E.W. belt disappears progressively towards the N.W., as indicated by the disappearance of the escarpment, and merges into almost a single fault system oriented NW-SE which can be followed as far as the south of Goban Spur (fig. 11). This fault is interpreted as a strike slip fault because of absence of vertical throw and deformation of layers on both sides as in drag folds. Other effects of late Eocene deformations include maybe narrow elongated folds, broadly oriented EW, on top and along Trevelyan escarpment and Meriadzek escarpment. In a few cases, rejuvenation of rift faults is visible. The Cenozoïc deformations observed in this part of the margin accord with an almost N.S. direction of Eocene lateral compression as determined on land. Reverse faults and even some thrusting is observed when a pre-existing almost EW discontinuity existed in the basement. This is true for the Trevelyan escarpment which is situated at the junction between the oceanic-continental crusts boundary and the important structural boundary separating the western Approaches margin from the Armorican margin and the Armorican marginal basin (fig. 1). This is true also for the uplifted area oriented E.W. in the center of Biscay with some features like Cantabria Seamount, which are controlled by

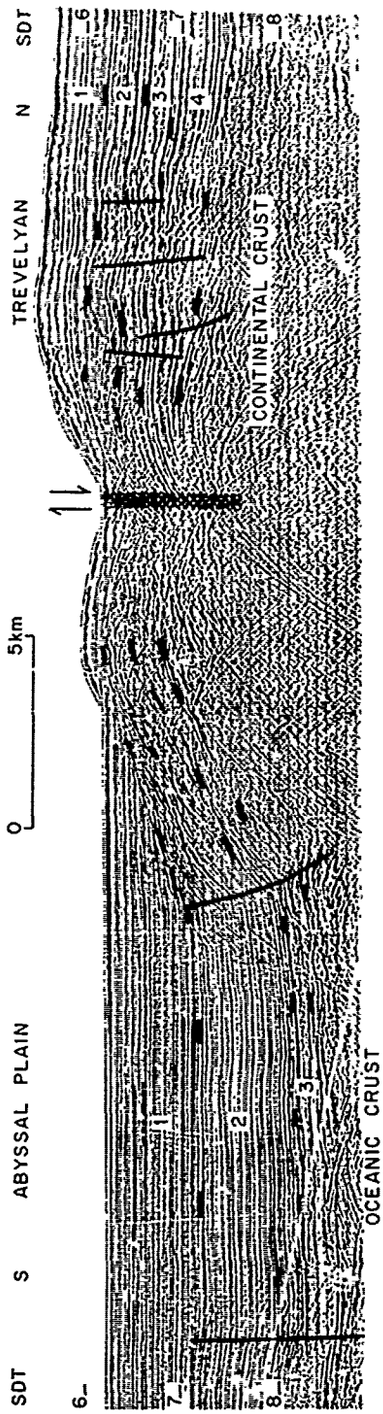


Fig. 28. Late Eocene compression along Trevelyan escarpment (N. Biscay margin) (see fig. 11).

a very sharp rise, oriented E.W., of the Ocean crust. When the discontinuities or inhomogeneities in the basement are oriented differently for example NW-SE like the North Biscay and Armorican margins or the North Gascony ridge in the central part of Biscay, the Eocene compression is marked essentially by faults with a strike slip component.

## Conclusion

A scheme of the structural evolution of a starved passive continental margin can be proposed from DSDP drilling results combined with intensive geophysical surveys. Environment and tectonics of the rifting phase has been established : active rifting took place in Lower Cretaceous time in a pre-existing marine basin and with no volcanic activity in contrast to many subaerial rift systems. The overall tectonic style is characterized by a series of tilted fault blocks bounded in many cases by listric faults. The rotation of the blocks (20-30°) along listric faults reduced the thickness of the upper continental crust from 6-8 km to 4-5 km. Close to the near horizontal base of the listric faults, a strong horizontal reflector corresponding to the 6,3-4,9 km/s refraction interface has been interpreted as the boundary between the upper brittle and the lower ductile continental crusts. The Moho discontinuity 25 km deep in the vicinity of the shelf break is 12 km deep in the lower part of the margin. In this area the ductile part of the crust (6,3 km/s) is only 3 km thick. Drill dredge and seismic reflection data allow to reconstruct the topography of sea floor at the end of rifting in Aptian time. In the axis of the rift system, submarine troughs 2,5 km deep existed. The thinning of the continental crust cannot be explained by the 10-15 % of extension estimated for the upper brittle part. One suggests that the ductile part of the crust is thinned by creep in response to tension in the continental plate. Rift would not be related to doming of the continental crust but merely to stretching of the lithosphere as a response to intraplate stresses. Knowing the topography of the sea-floor at the end of rifting and the present depth of the Aptian datum, one can determine the absolute amount of subsidence on a transect of the margin after the beginning of accretion (late Aptian time). This value decreased continuously from the oceanic-continental crust boundary (4000 m) to the shelf break. For each point of the margin, the subsidence versus time curve is an exponential whose time constant increases with depth. This suggests that post rifting subsidence was essentially an isostatic adjustment to cooling of the lithosphere in which the continental crust has been previously thinned during the rifting process.

Acknowledgments. L.M, D.G.R and J.C.S wish to acknowledge the U.S. National Science Foundation, the international JOIDES institutions and D.S.D.P-

IPOD who made legs 47B and 48 and their participation possible. L.M, O.C, P.G and J.C.S are indebted to Institut Français du Pétrole, CNEXO and CEPM (IFP, SNEA(P), CFP) which permitted the acquisition of data, and their participation to Leg 47B and 48 studies. They are particularly grateful to the geophysicists (J.P. FAIL, R. DONATIEN, J. CASSAND) and Crew of the M.S Florence of the Institut Français du Pétrole which collected the geophysical data in Galicia plateau and in the Bay of Biscay before and after Leg 47B and 48 of the Glomar Challenger. D.G.R. whishes to acknowledge the Department of Energy supporting acquisition of the seismic data after Leg 48 and his participation with Leg 48 studies. The authors are grateful to M. POULET (IFP) for his many helpful suggestions and discussions and to P. VAIL (Exxon Research) and J.GROW (U.S.G.S.) for their critical review of the manuscript.

## References

Alvarez W.A., Fisher A.G., Lowrie W., Napoleone G., Premoli Silva I., Roggenthen W.M. - Upper Cretaceous-Paleocene magnetic stratigraphy at Gubbio, Italy - V - Type section for the late Cretaceous-Paleocene magnetic time scale. Geol. Soc. America Bull, 88, 367-389, 1977.

Artemjev, M.E. and Artyushkov, E.V. Structure and isostasy of the Baikal rift and the mechanism of rifting. J. Geophys. Res., 76 : 1197-1211, 1971.

Auffret G.A., Pastouret L., Cassat G., de Charpal O., Cravatte J., Guennoc P. - Dredged rocks from the Armorican and Celtic Margins. In Initial Reports of the Deep Sea Drilling Project, volume 48, Washington (U.S. Government Printing Office). In press.

Avedik F., Howard D. - Preliminary results of a seismic refraction study in the Meriadzek - Trevelyan area, Bay of Biscay. In Initial Reports of the Deep Sea Drilling Project, volume 48, Washington (U.S. Government Printing Office). In press.

Berthois L. and Brenot R. - Cartes bathymétriques du talus du plateau continental en onze feuilles éditées par Berthois L. avec le concours du CNRS. 1966.

Berthois L., Brenot R. et Debyser J. - Remarques sur la morphologie de la marge continentale entre l'Irlande et le cap Finisterre. Rev. Inst. Franç. du Pétrole, vol. XXIII, n° 9, p. 1046-1049, 1968

Black M., Hill M.N., Laughton A.S., Matthews D.H. Three non magnetic seamounts off the Iberian coast. Geol. Soc. London Quart. Jour, v. 120, p. 477-517, 1964.

Blair D.G. - Structural styles in North Sea Oil and Gas Fields. In Petroleum and the continental shelf of North-West Europe. Vol. 1 Geology - Ed. A.W. Woodland. Applied Science Publishers Ltd 327-338, 1975.

Bott, M.H.P. - Evolution of young continental margins and formation of shelf basins - Tectonophysics, 11, 5, 319-327, 1971.

Bott, M.H.P. and Dean, D.S. - Stress systems at young continental margins. - Nature phys. Sci. 235, 23-25, 1972.

Bott, M.H.P. - Shelf subsidence in relation to the evolution of young continental margins. - In : Tarling, D.H. & Runcorn, S.K. (eds) : Implications of Continental Drift to the Earth Sciences. Academic Press, London, 2, 675-683, 1973.

Bott, M.H.P. and Watts A.B. - Deep structure of the continental margin adjacent to the British Isles. In : The Geology of the East Continental Margin - 2 - Europe. Ed. F.M. Delany Report n° 70/14 Institute of Geological Sciences - p. 93-109, 1971.

Bouquigny R. and Willm, C. - Tentative Calibration of Site 398 and special processing of part of lines GP19 and GP23. In Initial Reports of the Deep Sea Drilling Project, volume 47B. Washington (U.S. Government Printing Office), in press.

Bowen J.M. - The Brent oil field. In : Petroleum and the continental shelf of North-West Europe. Vol 1 Geology. Ed. A.W. Woodland. Applied Science Publishers Ltd 353-362, 1975.

BRGM - ELF Re - ESSO REP - SNPA - Géologie du Bassin d'Aquitaine. Editions : BRGM Paris, 1974.

Burke K. and Whiteman A.J. - Uplift, rifting and the break-up of Africa. In Implication of Continental drift to the earth Sciences, D.H. Tarling and S.K. Runcorn. Eds. V. 2, p. 735-756, 1973.

Charpal O. de, Trémolières P., Jean F. et Masse P.- Un exemple de tectonique de plate-forme. Les Causses majeurs. Rev. Inst. Franç. du Pétrole, XXIX-5, p. 715-732, 1974.

Charpal O. de, Guennoc P., Montadert L., Roberts D.G. Rifting, crustal attenuation and Subsidence in the Bay of Biscay. Nature. Vol. 275. n° 5682, 26 octobre 1978.

Cande S.C., and Kristoffersen Y. - Late Cretaceous magnetic anomalies in the North Atlantic. Earth Planet. Sci. Letters, 35, 215-224, 1977.

Cloos H. - Hebung - Spaltung - Vulkanismus. Geol. Rundsch., 30 : 405-527, 1939

Day G.A., Williams C.A. - Gravity compilation in the northeast Atlantic and interpretation of gravity in the Celtic Sea. Earth Planet. Sc. Letters, 8, 207, 213, 1970.

Dardel R.A., and Rosset R. - Histoire géologique et structurale du bassin de Parentis et de son prolongement en mer; in Histoire structurale du golfe de Gascogne. t. I-II : Paris, Ed. Technip p. IV.2-1-IV.2-28, 1971

Dingle R.V., Scrutton R.A. - Continental margin fault pattern mapped South West of Ireland. Nature vol. 268 - 25 Aug. 1977 p. 720-723, 1977.

Ducasse O., and Peypouquet J.P. - Cenozoïc Ostracoda : their importance for bathymetry, hydrology and biogeography. In Initial Reports of the Deep Sea Drilling Project, volume 48 - Washington (U.S. Government Printing Office). In press.

Dupeuble P. - Mesozoïc Foraminifera and microfacies from sites 400 A, 401 and 402 A of the DSDP Leg 48. In Initial Reports of the Deep Sea Drilling Project, volume 48 - Washington (U.S. Government Printing Office). In press.

Ewing J. and Ewing M. - Seismic refraction measurements in the Atlantic Ocean basins, in the Mediterranean Sea, on the Mid-Atlantic Ridge, and the Norwegian Sea, Bull. Geol. Soc. Am. 70, 291, 1959.

Forsyth D. and Uyeda S. - On the relative importance of the driving forces of the plate motion. Geophs. J.R. Astr. Soc. 43, p. 163-200, 1975

Foucher J.P. and Sibuet J.C. - Thermal regime of the Norchern Bay of Biscay Continental margin in vicinity of the DSDP sites 400 to 402. In Initial Reports of the Deep Sea Drilling Project, volume 48 - Washington (U.S. Government Printing Office). In press.

Freund R. - Rift Valleys. Can. Geol. Surv. Pap., Paper 64-14, p. 330-344, 1965.

Fuchs K. - Geophysical contributions to taphrogenesis. In : J.H. Illies and K. Fuchs (Editors), Approaches to Taphrogenesis. Schweizerbart, Stuttgart, p. 420-432, 1974.

Funnel, B.M., Friend J.K. and Ramsey A.T.S. - Upper Maestrichtian planktonic foraminifera from Galicia Bank, West of Spain, Paleontology, 12, part 1, 19-42, 1969.

Garfunkel Z., Bartov Y. - The Tectonics of the Suez Rift. Geol. Surv. Israel Bull n° 71, 1977.

Grau G., Montadert L., Delteil R., and Winnock E. - Structure of the European continental margin between Portugal and Ireland, from seismic data, in Mueller, S., ed., The structure of the earth's crust : Tectonophysics, v. 20, no. 1-4, p. 319-339, 1973.

Griggs D.T. and Handin J. (Editors) - Rock deformation. Geol. Soc. Am., Mem., 79 : 1-382, 1960.

Groupe GALICE. The continental margin off Galicia Bank and Portugal : acoustical stratigraphy and structural evolution. In Initial Reports of the Deep Sea Drilling Project, volume 47B, Washington (U.S. Government Printing Office), in press.

Hailwood E.A., Schnitker D., Bock W., Costa L., Muller C., and Dupeuble P.A. - Northeast Atlantic magnetobiostratigraphy. In Initial Reports of the Deep Sea Drilling Project, volume 48 - Washington (U.S. Government Printing Office), in press.

Heiskanen W.A. and Vening-Meinesz F.A. - The Earth and its Gravity Field. 470 pp. Mc Graw-Hill, New-York, 1958.

Hill M.N. and Vine F.J. - A preliminary magnetic survey of the western Approaches to the English Channel. Quart. Jl. Geol. Soc. London, 121, 463-465, 1965.

Illies J.H. - Recent and paleo-intraplate tectonics in stable Europe and the Rhine graben rift system. Tectonophysics, 29 - 251 - 264, 1975.

Laughton A.S., Bergen W.A., et al. - Initial reports of the Deep Sea Drilling Project, v. XII : Washington (U.S. Govt. Printing Office) Site 118 and 119, 1972.

Le Borgne E. and Le Mouël J. - Cartographie aéromagnétique du Golfe de Gascogne. C.R. Acad. Sc. Paris, 271 - D, 1167-1170.

Lowell J. and Genik G. - Sea-floor spreading and structural evolution of the southern Red Sea, Am. Ass. Petroleum Geol. Bull., 56, 247-59, 1972.

Lowell J.D., Genik G.J., Nelson T.H. and Tucker P.M. - Petroleum and plate tectonics of the southern Red Sea. In : Petroleum and Global Tectonics. Ed. A.G. Fischer and S. Judson. Princeton University Press. p. 129-153, 1975.

Montadert L., Damotte B., Delteil J.R., Valéry P. and Winnock E. - Structure géologique de la marge continentale septentrionale du golfe de Gascogne (Bretagne et Entrées de la Manche), in Histoire structurale du golfe de Gascogne, t. I-II: Paris, Ed. Technip, p. III. 2-1-III. 2-22, 1971).

Montadert L., Roberts D.G., Auffret G.A., Bock W.O., Dupeuble P.A., Hailwood E.A., Harrison W., Kagami H., Lumsden D.N., Muller C., Schnitker D., Thompson R.W., Thompson T.L., Timofeev P.P. - Glomar Challenger sails on Leg 48. Geotimes, 21, 12, 19-23, 1976.

Montadert L., Roberts D.G., Auffret G.A., Bock W.O., Dupeuble P.A., Hailwood E.A., Harrison W., Kagami H., Lumsden D.N., Muller C., Schnitker D., Thompson R.W., Thompson T.L., Timofeev P.P. - Rifting and subsidence on passive continental margins in the North East Atlantic. Nature vol. 268 n° 5618 p. 305-309, 1977.

Montadert L., and Winnock E. - L'histoire structurale du golfe de Gascogne, in Histoire structurale du golfe de Gascogne, t. I-II : Paris, Ed. Technip, p. VI.16-1-VI.16-18, 1971.

Montadert L., Winnock E., Delteil J.R., and Grau G. Continental Margins of Galicia - Portugal and Bay of Biscay. In the Geology of Continental Margins, C.A. Burk and C.L. Drake, eds.,Springer-Verlag, New-York, 323-342, 1974.

Montadert L., Roberts D.G., De Charpal O., Guennoc P. Rifting and Subsidence of the northern continental margin of the Bay of Biscay. In Initial Report of the Deep Sea Drilling Project, volume 48 - Washington (U.S. Government Printing Office), in press.

Moore J.M., Davidson A. - Rifting Structure on Southern Ethiopa. Tectonophysics 46 (1978) 159-173, 1978.

Neugebauer H.J. - Crustal doming and the mechanism of rifting Part I : Rift formation. Tectonophysics, 45. n° 2-3. 159-186, 1978.

Pastouret L., Auffret G.A. - Observations sur les microfaciès des roches sédimentaires prélevées sur la marge armoricaine. Rev. Inst. Français du Pétrole, vol. XXXI, n° 3, p. 401-425, 1976.

Pautot G., Renard V., de Charpal O., Auffret G.A., Pastouret L. - A granite cliff deep on the North Atlantic. Nature, 263, 1976, p. 669-672, 1976.

Poulet M. - Apport des expériences de mécanique des roches à la géologie structurale des bassins sédimentaires. Rev. Inst. Français du Pétrole. XXXI, n° 5 p. 781-822, 1976.

Schnikter D. - Cenozoic deep-water benthic Foraminifera. Bay of Biscay. In Initial Reports of the Deep Sea Drilling Project, volume 48 - Washington (U.S. Government Printing Office), in press.

Segoufin J. - Structure du plateau continental armoricain. In : A discussion on the geology of the English Channel. Phil. Trans. R. Soc. London, A 279 p. 109-121, 1975.

Sibuet J.C. - Contribution de la gravimétrie à l'étude de la Bretagne et du plateau continental adjacent. C.R. Somm. Soc. Geol. France, 24 avril 1972, 124-129, 1972.

Sibuet J.C., Ryan W.BF - Site 398 : Evolution of the West Iberian Passive Continental Margin in the framework of the early evolution of the North Atlantic Ocean - In Initial Reports of the Deep Sea Drilling Project, volume 47B - Washington (U.S. Government Printing Office), in press.

Site chapter 398 - In Initial Reports of the Deep Sea Drilling Project, volume 47B - Washington (U.S. Government Printing Office), in press.

Site chapters 400, 401, 402 - In Initial Reports of the Deep Sea Drilling Project, volume 48 - Washington (U.S. Government Printing Office) in press.

Sleep N.H. - Thermal effects of the formation of Atlantic Continental Margins by continental break-up. Geophys. J.R. Astron. Soc., 24, 325-350, 1971.

Sleep N.H. - Crustal Thinning on Atlantic Continental Margings : evidence from older margins. - In : Tarling D.H. & Runcorn S.K. (eds) : Implication of Continental Drift to the Earth Sciences. Academic Press, London, 2, 685-692, 1973.

Sleep N.H. and Snell N.S. - Thermal Contraction and flexure of Mid-Continent and Atlantic marginal basins. - Geophys. J.R. Astron. Soc., 45, 125-143, 1976.

Stride A.H., Curray J.R., Moore D.G. and Belderson R.H. - Marine geology of the Atlantic Continental margin of Europe, Phil. Trans. Roy. Soc. (London) A264 31, 1969.

Tremolieres P. - Les mécanismes de déformation à l'échelle d'un bassin. To be published.

Tucholke B.E., Mountain G.S. - Lithologic correlation and significance of major seismic reflectors in the Western North Atlantic. The 2d Ewing M. Memorial Symposium. March 19-25-1978, 1978.

Van Andel T.H., Thiede J., Sclater J.G., Hay W.W. Depositional history of the South Atlantic Ocean during the last 125 million years. J. of Geology, vol. 85 n° 6 Nov. 77 p. 651-699, 1977.

Van Hinte J.E. - A Cretaceous Time Scale. Am. Ass. Petr. Geol. Bull., 60, 4, 498-516, 1976.

Vening-Meinesz F.A. - Les "graben" africains, résultats de compression ou de tension dans la croûte terrestre. Bull. Inst. R. Colonial Belge, 21 : 539-552, 1950.

Walcott R.I. - Flexural rigidity, thickness and viscosity of the lithosphere - J. Geophys. Research, 75, 10, 3941-3954, 1970.

Walcott R.I. - Gravity flexure and the growth of sedimentary basins at a continental edge. - Bull. geol. Soc. Amer., 83, 6, 1845-1848, 1972.

Watts A.B. and Ryan W.B.P. - Flexure of the lithosphere and continental margins basins. Tectonophysics n° 36 p. 25-44, 1975.

Williams C.A. - Sea-floor spreading in the Bay of Biscay and its relationship to the North Atlantic. Earth Planet. Sci. Letters, 24, 440-456, 1975.

Winnock E. - Géologie succincte du Bassin d'Aquitaine (contribution à l'histoire du Golfe de Gascogne).In Histoire Structurale du Golfe de Gascogne, Technip, Paris, IV, 1, 1-30, 1971.

# GEODYNAMIC, SEDIMENTARY AND VOLCANIC EVOLUTION OF THE CAPE BOJADOR CONTINENTAL MARGIN (NW AFRICA)

Ulrich von Rad

Bundesanstalt für Geowissenschaften und Rohstoffe (BGR), 3000 Hannover 51, F.R. of Germany

Michael A. Arthur

Scripps Institution of Oceanography, Deep Sea Drilling Project, A-031, La Jolla, CA 92093, U.S.A.

Abstract. The geodynamic and sedimentary evolution of the Northwest African continental margin at Cape Bojador is well documented by a transect of DSDP sites, commercial wells, and seismic surveys (Fig.1-3). This evolution is mainly influenced by vertical tectonics (subsidence), sediment supply from the continent, volcanism of the Canary Islands, and global fluctuations of sea level, climate, and surface or deep-water circulation.

Jurassic shallow-water carbonates deposited on a steadily subsiding shelf are overlain by a very-thick Cretaceous Wealden-type deltaic sequence with an upward and seaward facies transition from continental clastics to lagoonal/intertidal deposits, delta front sediments, and laminated prodelta muds (Fig.5). Distal turbidites reached the Moroccan Basin and the deep-sea fan recorded in the flysch-type sediments of Fuerteventura. Many similar "Wealden-type" deltas were built out along the narrow Neocomian North Atlantic (Fig.4).

A conspicuous unconformity with a 100 m.y. hiatus cuts 1-3 km deep into the upper continental rise. This is the result of a major erosional event which removed about 7,500-15,000 km³ of lower slope and upper rise sediments (erosion rate >100 m/m.y.) and may have destroyed evidence of several previous hiatuses. The mid-Cenozoic slope rejuvenation was probably caused by the coincidence of a major regression with intensified bottom water circulation during late Oligocene to earliest Miocene times. The oversteepened escarpment was rapidly covered by early to middle Miocene gravitative sediments (debris flows, turbidites, slumps), derived primarily from the Cape Bojador margin and partly from more distant source areas (Fig.7). The slope was gradually stabilized and equilibrium conditions ensued (Fig.6). This thick flysch-type sediment sequence occurs in a "passive" margin setting with no obvious local tectonic deformation.

Early to middle Miocene debris flow deposited volcaniclastic sandstones and hyaloclastites evidence the evolution of the Canary Island uplift and volcanism from a submarine to a subaerial shield stage. Air-fall ash layers record the post-middle Miocene volcanic history of the individual islands (Fig.8).

In the uniformly subsiding, 12-15 km thick "Cape Bojador marginal basin" below the present shelf, slope and upper rise, the Jurassic subsidence rates were high (80-120 m/m.y.); they increased slightly during the Early Cretaceous (130-140 m/m.y.) and decreased more or less exponentially during the Late Cretaceous and Cenozoic to about 15 m/m.y. After mid-Cretaceous times, the accumulation rates lagged behind subsidence rates, causing a gradual deepening of the outer margin from a few hundred meters to its present depth.

## Introduction

During the past decade the Cape Bojador margin has become one of the best documented Atlantic-type continental margins. This is mainly due to detailed seismic surveys (e.g. Hinz et al., 1974; Seibold and Hinz, 1974; Uchupi et al., 1976; Lehner and De Ruiter, 1977; Vail et al., 1977; Hinz, in press; Wissmann, in press) in conjunction with Deep Sea Drilling on a transect from the outer and intermediate rise (Leg 14 Sites 138-140) to the uppermost rise (Leg 47A-Site 397: von Rad, Ryan et al., in press) and slope (Leg 41-Site 369: Lancelot, Seibold et al., 1977). Dredging and coring along lower slope canyons (von Rad et al., 1979), and several on- and offshore commercial boreholes in the Aaiun Basin (AUXINI, 1969; CONOCO, 1969) supplement this information and help to bridge the gap between the deep-sea record and the geology of the shelf and the adjacent coastal basin exposed on land (Ratschiller, 1970; Wiedmann et al., 1978).

Tentative syntheses on the evolution of the mature Northwest African passive margin are based on the information of DSDP Leg 14 (Berger and von Rad, 1972), Leg 41 (Lancelot and Sei-

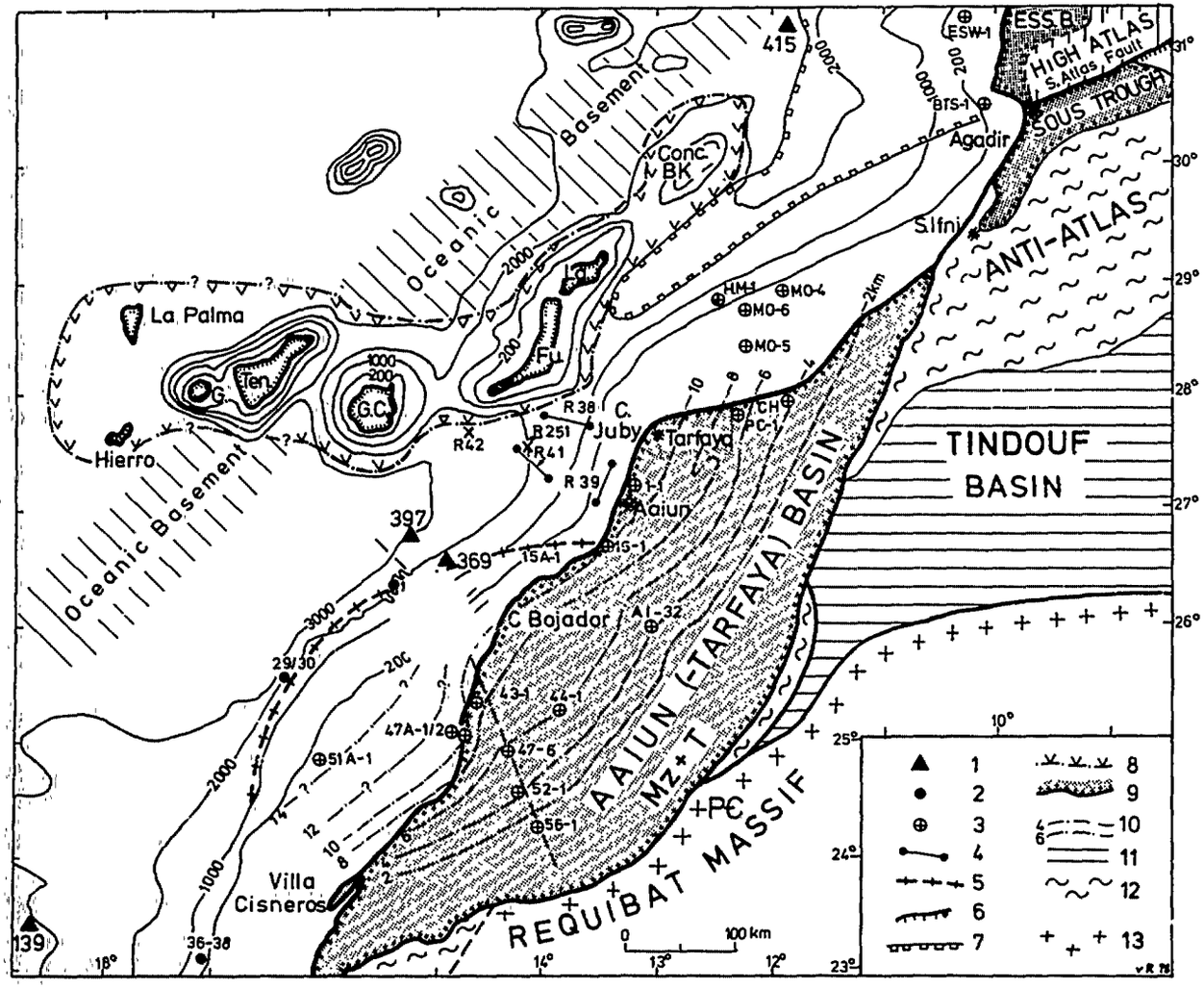


Figure 1. Sketch map of the Cape Bojador continental margin and its vicinity between the Aaiun-Tarfaya coastal basin and the Canary Islands. 1 = DSDP sites, 2 = selected dredge sites (von Rad et al., 1979), 3 = selected on-and offshore commercial wells, 4 = seismic refraction profiles (BGR), 5 = axis of "slope anticline" (Hinz et al., 1974), 6 = major fault, 7 = limit of offshore "salt basin" (Beck and Lehner, 1974), 8 = extent of "volcanic mass" around Canary Islands, 9 = unfolded Mesozoic-Cenozoic coastal basins with approximate isopachs in km (8 and 9 after G.Wissmann, personal communication) 10 = unfolded Paleozoic, 11 = Paleozoic rocks, folded during Hercynian orogenesis (Mauretanides), 12 = Precambrian crystalline massif.

bold, 1977), Leg 47A (e.g. Arthur et al., in press; Cita and Ryan, in press), Leg 50 (Winterer, in press), and on the geology of the coastal basins (Wiedmann et al., 1978).

The drilling and continuous coring of Site 397 at the uppermost rise off Cape Bojador has revealed an unexpectedly thick (1300 m), complex Neogene section directly overlying prodelta mudstones of Early Cretaceous (Hauterivian) age. In this paper, we summarize some of the outstanding Leg 47A results in the context of information from nearby drilling sites, offshore commercial wells, dredges and cores, and seismic records. We restrict ourselves to a brief discussion of the following topics, which are covered in more detail in the indicated publications: (1) the Early Cretaceous "Wealden-type" deltaic facies off Northwest Africa and around the North Atlantic (Einsele and von Rad, in press); (2) the massive mid-Cenozoic erosional event which stripped 1-3 km of Early Cretaceous to Paleogene sediments from the uppermost rise and lower slope (Arthur et al., in press); (3) the subsequent early Neogene sedimentation of predominantly allochthonous lithotypes which led to a gradual stabilization of the slope (Arthur and von Rad, in press); (4) the Neogene evolution of the Canary Island volcanism, inferred from the record of volcaniclastic debris flows and ash layers (Schmincke and von Rad, in press); and (5) the Mesozoic-Cenozoic evolution of paleobathymetry, sedimentation rates, and subsidence of the Cape Bojador continental margin recorded in drillsites from the present shelf, slope, and upper rise (von Rad and Einsele, in press).

## Geological Setting of the Cape Bojador Margin

The Northwest African margin has received considerable interest by the Deep Sea Drilling Project (DSLP) and International Phase of Ocean Drilling (IPOD). Between southern Portugal and the Cape Verde Islands 15 holes were drilled during Legs 2, 13, 14, 41, 47A, and 50, and additional sites are planned for IPOD II. Of special importance for our disscussion are the almost continuously cored Sites 369 (Leg 41) and 397 (Leg 47A) off Cape Bojador (Fig.1).

The Cape Bojador continental margin is the seaward extension of the Aaiun-Tarfaya coastal basin which is bounded on the east and south by the Paleozoic fold belt of the Mauretanides and the Precambrian Requibat Massif, and to the north by the Precambrian Antiatlas High and the South Atlas Fault. To the west, the coastal basin, which is filled by unfolded Mesozoic and Tertiary shallow-water sediments, extends far out onto the continental margin. Based on interval velocities in commercial multichannel seismic lines and an oceanic crust sloping towards the continental margin, the thickness of the basin fill reaches 12-15 km under the present shelf and slope (Fig.1 and 3A; cf. Wissmann in von Rad et al., 1979). During middle Tertiary times, the uplift of the Canary Archipelago and Conception Bank created a partly closed Neogene basin between Cape Bojador and the oldest eastern Canary Islands. The ocean/continent boundary probably lies close to the present lower continental slope. True oceanic basement is found seaward of Gran Canaria (Dash and Boshardt, 1969; Wissmann, personal communication).The extent of an early Jurassic offshore "salt basin" is recognized from diapiric structures and is restricted to an elongated area north of a line connecting the South Atlas Fault with the Canary Arch (Beck and Lehner, 1974; Wissmann, in press). The "slope anticline" (Hinz et al., 1974) is probably not a compressional feature, but was caused by differential sedimentation and subsidence between the coastal basin and the outer continental margin (Lancelot and Seibold, 1977) and/or flexural response (isostatic rebound) to the accentuated mid-Tertiary erosion of the lower slope and uppermost rise (Arthur et al., in press).

Figure 2 gives an overview of the lithostratigraphy of seven DSDP/IPOD sites across the Northwest African margin projected onto a west-east profile from the abyssal hills to the continental rise, slope and shelf off Cape Bojador. The commercial shelf well Spansah 51A-1 penetrated a 3.3 km thick, rather complete Early Cretaceous to Neogene section of the outer Aaiun Basin (CONOCO, 1969). The major depocenters off Northwest Africa are the "Cape Bojador marginal basin" (von Rad and Einsele, in press) between the shelf and the uppermost rise, and the Moroccan Basin. Unfortunately, a very large portion of the stratigraphic record is lost in those margin sites due to Late Cretaceous, early Tertiary and mid-Tertiary erosional events. Seaward, the thickness of the sediments, the sedimentation rates, and the hiatus durations decrease considerably.

Extremely thick terrestrial to marine deltaic sediments grading into a prodelta mud (397) and distal turbidite facies (416) characterize the Early Cretaceous record of the West African continental margin. Mid-Cretaceous sediments including organic-rich "black shales" are common under the present shelf (51A-1), slope (369) and upper rise (370/416), as well as in the deeper ocean (137,138). Late Cretaceous sediments are well preserved in the shelf well and, in part, in Site 369.

The Paleocene and Eocene is often separated from the Late Cretaceous record by an hiatus, and consists of limestones, marls and cherts in the shallower sites, and of more or less siliceous clays, when deposited below the CCD. Oligocene sediments are conspicuously missing on the shelf and in the rise Sites 140 and 397, whereas the Oligocene record is preserved in Sites 369 and 138. At the uppermost rise (Site 397), a 1300 m thick Neogene section overlies directly Hauterivian sediments. Also at the intermediate rise off Cape Blanc (Site 139) the

wells; 4 = seismic refraction profiles (BGR), 5 = axis of "slope anticline" (Hinz et al., 1974), 6 = major fault, 7 = limit of offshore "salt basin" (Beck and Lehner, 1974), 8 = extent of "volcanic mass" around Canary Islands, 9 = unfolded Mesozoic-Cenozoic coastal basins with approximate isopachs in km (8 and 9 after G.Wissmann, personal communication) 10 = unfolded Paleozoic, 11 = Paleozoic rocks, folded during Hercynian orogenesis (Mauretanides), 12 = Precambrian crystalline massif.

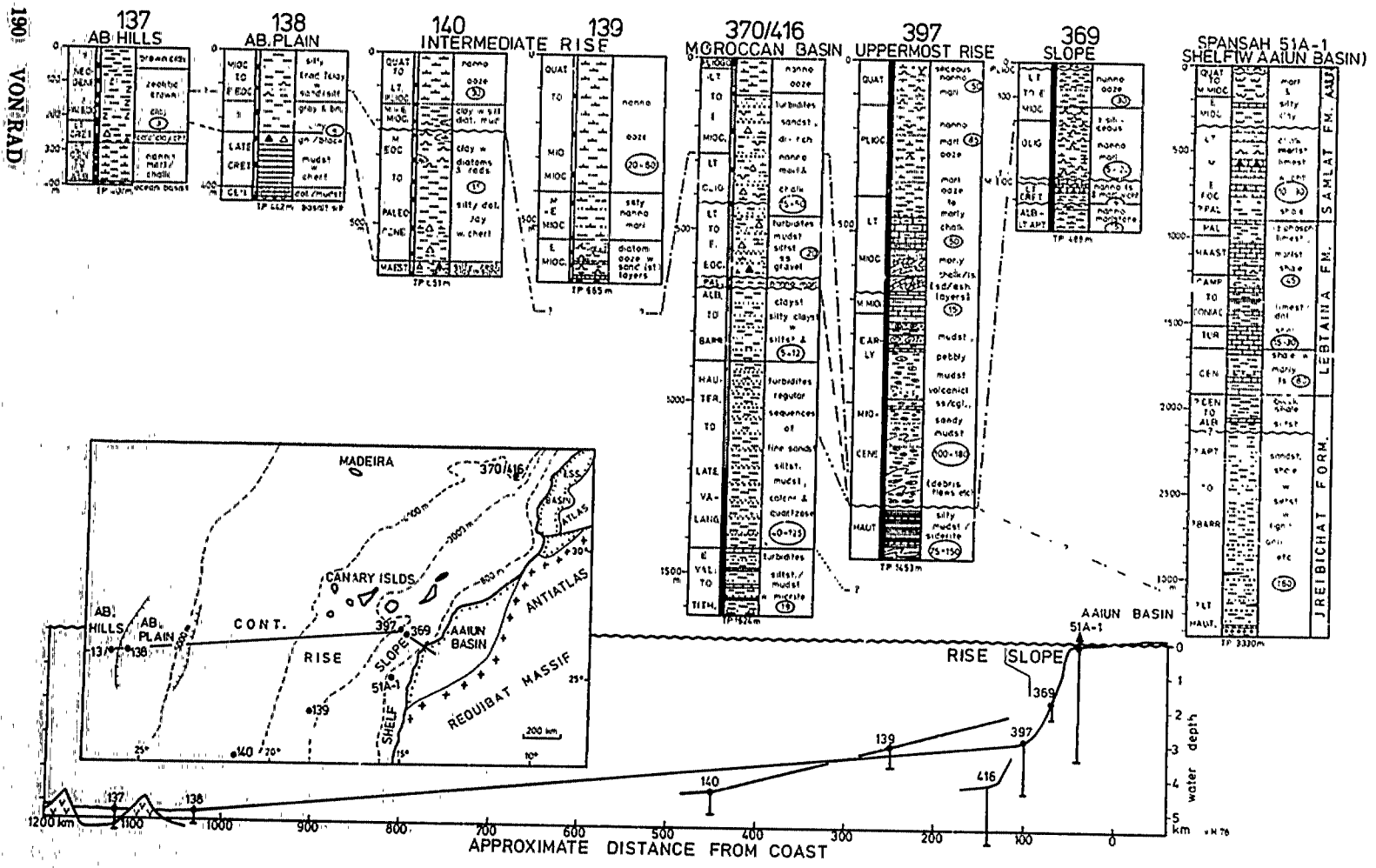


Figure 2. Generalized lithostratigraphy of DSDP sites across the Northwest African continental margin: Leg 14 Sites 137-140 after Berger and von Rad (1972), Leg 41 Site 369 after Lancelot, Seibold et al. (1977), Leg 47A-Site 397 after von Rad, Ryan et al. (in press), Leg 50-Site 416 after Shipboard Scientific Party (1977), Spansah 51A-1 well after CONOCO (1969; note different vertical scale for this well). Lithologic symbols equal those used in the Initial Reports of the Deep Sea Drilling Project. Encircled numbers indicate accumulation rates (m/m.y.).

Neogene section is comparatively thick (1100 m, Wissmann, personal communication).

Figure 3A shows a generalized cross-section across the Aaiun Basin and the continental margin off Cap Bojador, based on seismic reflection and refraction data, onshore commercial wells, two offshore shelf wells, and two DSDP Sites. Continental basement consisting of crystalline rocks of the Requibat Massif was reached at Well 56-1 and is estimated to lie 12-15 km below the present shelf and slope. The basement is overlain by possibly Triassic terrestrial sandstones and conglomerates (56-1) and by Jurassic evaporites, carbonates and clastics

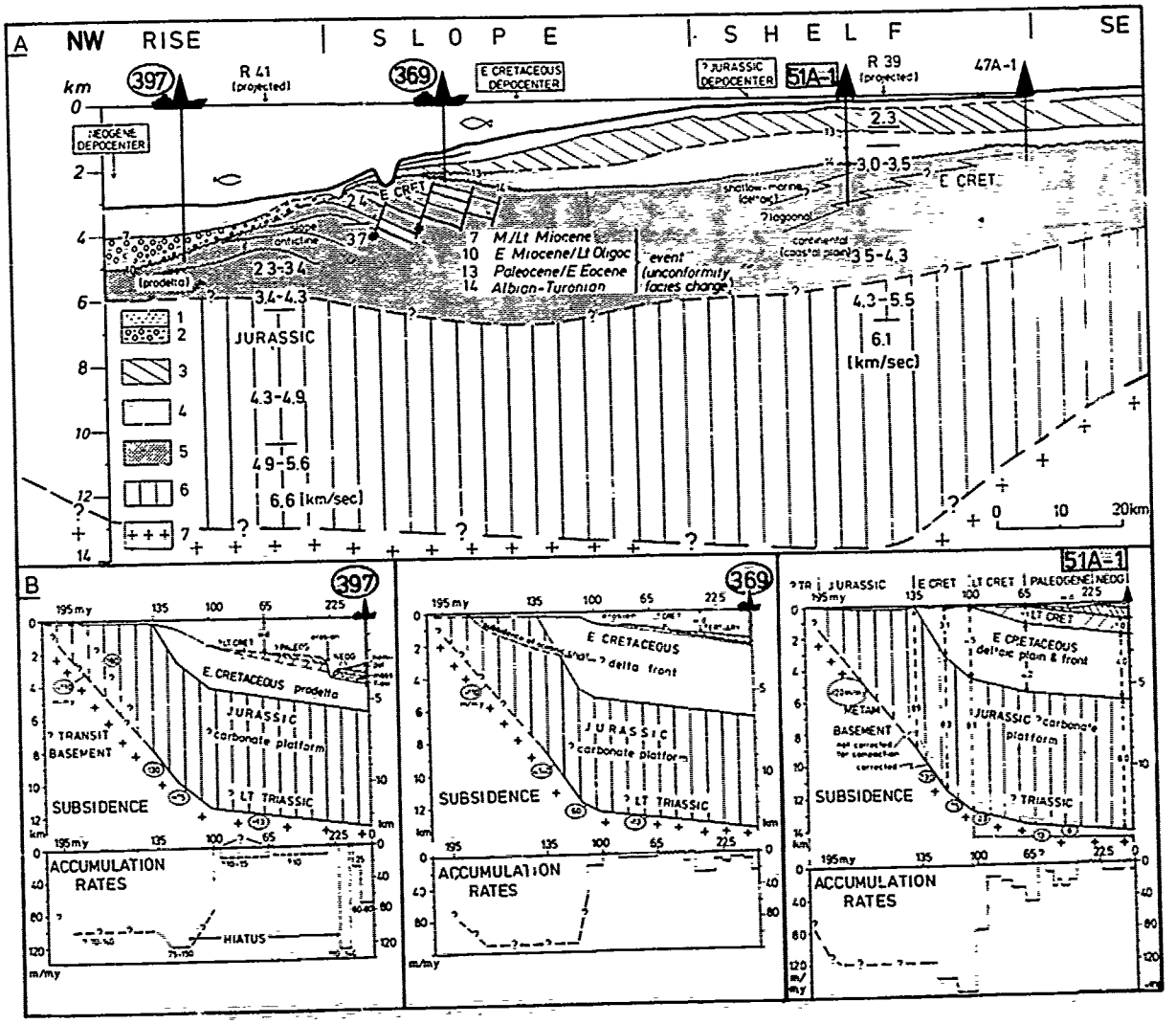


Figure 3. A: Highly generalized SE-NW cross-section from the outer Aaiun Basin to the upper rise off Cape Bojador. Location of profile and drilling sites indicated in Figure 1. Basement depth and Jurassic/Cretaceous boundary tentatively interpreted from refraction and multichannel seismic profiles (G. Wissmann, personal communication). 1 = Neogene (mainly hemipelagic), 2 = early Neogene on slope and rise (mainly allochthonous), 3 = Paleogene, 4 = Late Cretaceous, 5 = Early Cretaceous, 6 = Jurassic, 7 = "Basement" (Precambrian to Paleozoic continental basement, ?transitional to continental basement under slope and uppermost rise).
B: Mesozoic-Cenozoic subsidence rates (m/m.y.), changes in water depth and accumulation rates at three drilling sites from the shelf (51A-1), slope (369), and upper rise (397). A and B modified after von Rad and Einsele (in press).



after Berger and von Rad (1972), Leg 41 Site 369 after Lancelot, Seibold et al. (1977), Leg 47A-Site 397 after von Rad, Ryan et al. (in press), Leg 50-Site 416 after Shipboard Scientific Party (1977), Spansah 51A-1 well after CONOCO (1969; note different vertical scale for this well). Lithologic symbols equal those used in the Initial Reports of the Deep Sea Drilling Project. Encircled numbers indicate accumulation rates (m/m.y.).

of shallow-water origin. These sediments attain a thickness of up to 8 km, especially below the present shelf and upper slope.

The Early Cretaceous is represented by a very thick Wealden-type deltaic sequence of continental clastics (Well 43-1). Seawards, they grade into lagoonal to intertidal deposits (51A-1), into shallow-marine deltaic sediments (possibly below Site 369), and finally into distal prodelta muds (Site 397). The maximum sediment thickness of 4 km is reached in the inferred delta-front environmen below the present slope. Late Cretaceous sediments are much thinner and only preserved landward of the intermediate slope. Their thickness increases from 60 m in Site 369 (bounded by hiatuses) to 915 m in Site 51A-1. Only a few hundred meters of Paleogene sediments were deposited without any progradation. They were also erosionally truncated seaward of the intermediate slope.

The Neogene below the inner continental margin is extremely thin, because most sediment bypassed this area on its way to the rise and prevented any outbuilding of the slope. Below the uppermost rise and lower slope, however, the oversteepened pre-Miocene erosional surface is covered by thick, rapidly deposited early Neogene mass flow units They are followed by a thick drape of undisturbed middle Miocene to Quaternary hemipelagic deposits, which afford an unusually good resolution for magnetic, isotopic, biostratigraphic, and sedimentological studies.

## Early Cretaceous "Wealden" Facies

During latest Jurassic and earliest Cretaceous times the proto-Atlantic Ocean, as reconstructed by Sclater et al. (1977) and McCoy and Zimmerman (personal communication) was only 1000-1500 km wide, and not deeper than 4 km (Fig.4). Along the southeastern and northwestern margin of this narrow ocean, huge "Wealden-type" deltaic systems were built out, shedding large amounts of terrigenous clastic sediments onto alluvial plains and adjacent freshwater lakes, brackish seas, shelves, and slopes. The widespread development of a regressive deltaic facies around the North Atlantic coincides with a major global sea level lowstand during the Valanginian following a sea level fall about 132 m.y. ago (Vail et al., 1977). The earliest Cretaceous may be an "oligotaxic" period, characterized by relatively low marine temperatures, sharp latitudinal and vertical temperature gradients, intensified oceanic circulation, and global regression (Fischer and Arthur, 1977).

The "Wealden" (s.str.) is a facies designation for a 200-500 m thick sequence of fluviatile, lacustrine, or brackish, lignite-rich sandstones, siltstones, and shales which were deposited during the Berriasian to Barremian early-rift stages of the Northeastern Atlantic (Allen, 1959, 1975).

In the Aaiun Basin, a very thick (1-3 km) pile of deltaic sediments prograded over the Tithonian to Berriasian carbonate platform and produced a seaward thickening clastic wedge with a system of antithetic gravity faults (see Fig.3; Vail et al., 1977). In a generalized way, Figure 5 shows the vertical and horizontal facies changes after the formation of the widespread Early Cretaceous Wealden-type delta system detected off Cape Bojador (Einsele and von Rad, in press). This reconstruction represents the depositional environment between the shelf well 51A-1 (Fig.1,2) and the uppermost continental rise (Si-

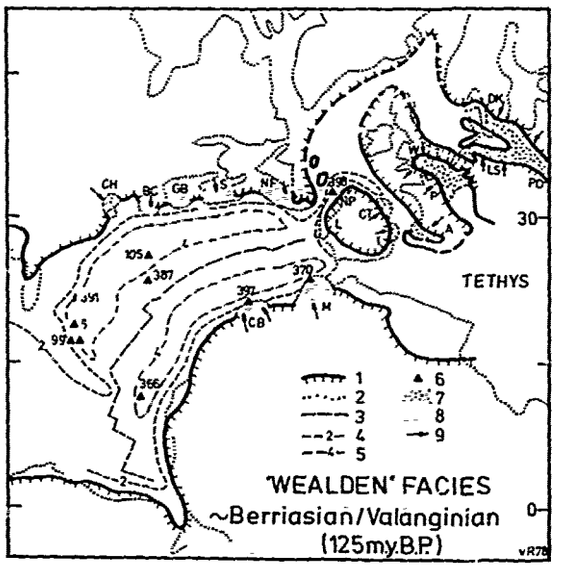


Figure 4. "Wealden"-Facies around the Early Cretaceous North Atlantic. Paleogeography and paleobathymetry modified from McCoy and Zimmerman (in preparation) and various other sources. 1 = paleo-coastline, 2 = present coastline, 3 = Mid-Atlantic Ridge, 4,5 = 2 km and 4 km isobath, 6 = DSDP Site, 7 = mainly nonmarine "Wealden"-type deposits (alluvial, fluviatile, lacustrine, estuaine, deltaic), 8 = nonmarine sediments, grading seaward into deltaic-marine (delta-front, prodelta etc) subenvironments, 9 = estimated directions of sediment supply. A = Aquitaine (Parentis and Adour Basins), BC = Baltimore Canyon Trough, CB = Cape Bojador marginal basin, CT = Cantabrian Trough, CH = Cheseapeake Bay (Potomac Formation), DK = eastern Denmark and southern Sweden, GB = Georges Basin, I = Iberic Ranges (Sierra de los Cameros, Maestrazgo Basin), LS = Lower Saxony and Central Germany, M = "Atlas Gulf" (Moroccan Basin), L = Lusitanian Basin, NF = eastern Newfoundland and Flemish Basins, NP = North-Portuguese-Galician Basin, P = northern France (Paris Basin), PO = Poland, S = Scotian Basin, W = Wealden of southeast England.

te 397) during Early and "middle" Cretaceous times. Overlying the fluvial delta plain sand with gravel and redbeds we observe a landward migration of lagoonal and tidal silts and clays. These sediments are overlain by sublittoral to inner shelf deposits (e.g. coquinas), indicating a relative sea level rise ("coastal onlap") during upper Early Cretaceous times. In front of large river mouths marine delta front sands (expected to underly Site 369; Fig.3) were deposited. This moved the shoreline seaward. Einsele and von Rad (in press) interpreted the finely laminated Hauterivian mudstones of Site 397 as distal prodelta muds which were rapidly (75-150 m /m.y.) deposited by turbid layer transport in an oxygen-depleted slope environment in

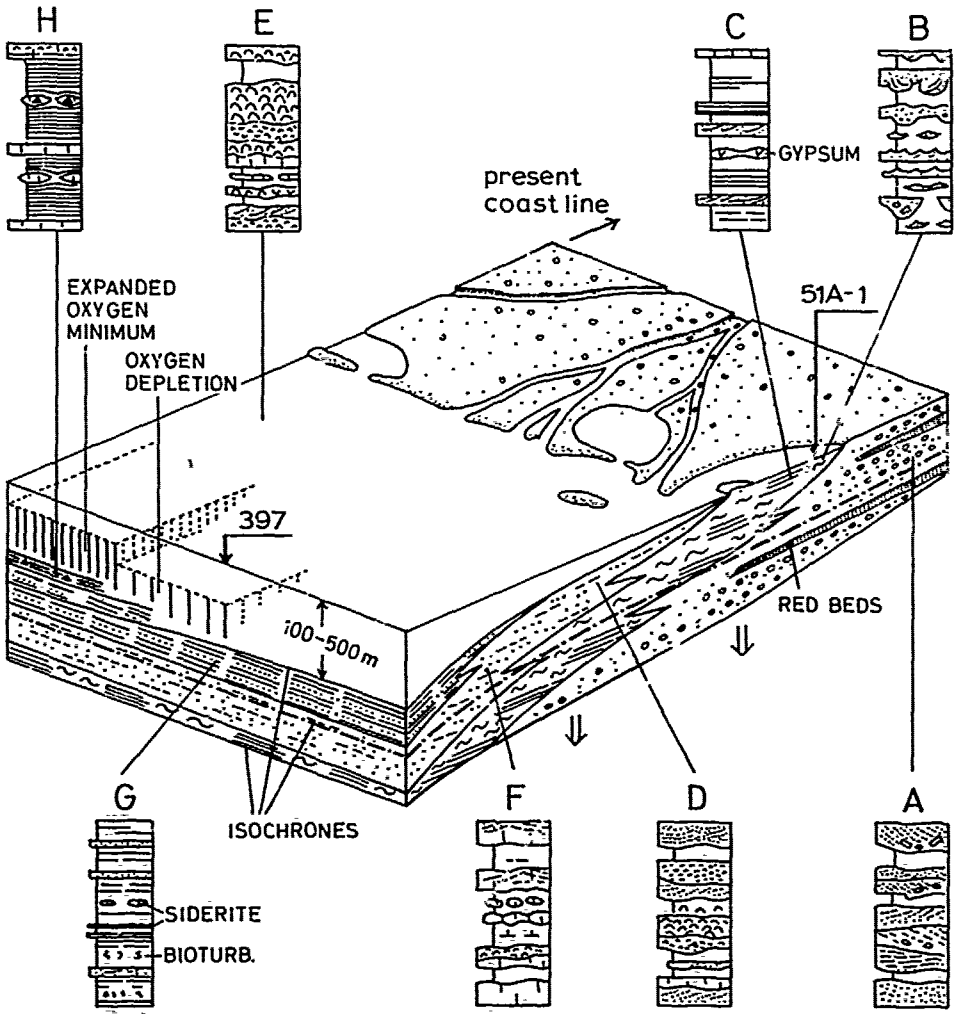


Figure 5. Block diagram showing facies model of the Early Cretaceous Wealden-type delta on the Northwest African continental margin between Site 397 and the Aaiun Basin (after Einsele and von Rad, in press). To characterize the various clastic subenvironments, typical generalized sections of on-and offshore wells and outcrops representing a sediment thickness of 1 to 3 m are shown: A = alluvial delta-plain sands, gravel and redbeds (Aaiun Basin); B = interdistributary lagoonal clays, silty slays, dolomitic silts, gypsiferous marls and limestones (Spansah 51A-1); C = intertidal muds and sands near Tarfaya; D = delta front sands and F = marly, bioclastic sands and shell beds of shelf adjacent to deltaic environment; G = prodelta silty clays and clayey silts (Site 397), H = dark bituminous well-laminated marls (Cenomanian-Turonian, Tarfaya).

a few hundred meters of water. The lithology, sparse fauna, and sedimentary fabric is comparable with that of fossil or recent prodelta muds (e.g. the Niger delta).

Later on, a distinct shelf edge and slope was created and deep oceanic circulation initiated. Thinly laminated bituminous marls with micritic limestones and cherts (Tarfaya Basin) accumulated in relatively deep water during late Cenomanian to Turonian times, probably under upwelling and expanded oxygen minimum conditions (see Fig.5; Einsele and Wiedmann, 1975). In the Aaiun Basin, the mid-Cretaceous transgression ended the Wealden-type phase of prograding deltas, and caused a landward facies migration, an upward decrease of terrigenous input, and an increase of biogenic carbonate sedimentation.

Mitchum and Vail (1977) described a similar facies transition from the Tan-Tan delta under the present shelf north of the northern Aaiun Basin. There Valanginian to Barremian nonmarine to shallow-marine sediments grade seaward into slope sediments with a downlap relationship to the lower boundary. The upper part of this sequence, however, shows a seaward progradation of shelf sediments over slope deposits.

We can study the seaward continuation of this facies in the Valanginian to Hauterivian (?) outcrops of the uplifted and deeply eroded oldest sediments of Fuerteventura, where flysch-like, cross-laminated siltstone/shale alternations with flute casts suggest a distal deep-sea fan or rise environment (D. Bernoulli, personal communication). The alternations of rapidly deposited (125 m/m.y.) late Valanginian to Hauterivian mudstones with thin fine-grained distal turbidites penetrated at Site 416 in the Moroccan Basin (Shipboard Scientific Party, 1977) indicate a comparable (? upper) rise environment.

Jansa and Wade (1975) described nonmarine to marine deltaic sequences from the Newfoundland and Nova Scotian shelves. There the Verril Canyon Member of the Berriasian to Barremian Missisagua Formation is very similar to the Hauterivian prodelta facies of Site 397. More than 1 km thick terrestrial to very shallow-water clastic sediments were also penetrated by the COST B-2 well in the Baltimore Canyon Trough off New Jersey (Scholle, 1977) and inferred for the Georges Bank Basin (Schlee et al., 1977).

## The Pre-Miocene Sculpturing of the Base-of-the-Slope

Drilling at Site 397 revealed that the complete Late Hauterivian through Oligocene sedimentary record is missing (Fig.3A,6). The gradient of this conspicuous base-of-slope unconformity which truncates strata of earliest to "middle" Cretaceous age decreases gradually from the lower slope (maximum: 7-15°) to the uppermost rise.

The timing of this large-scale erosional event at the foot of the continental slope can be attempted by seismic stratigraphy (Wissmann, in press) using control provided by the sequence drilled at the nearby slope Site 369, on- and offshore wells of the southern and central Aaiun Basin (AUXINI, 1969; von Rad and Einsele, in press) and the Tarfaya Basin northeast of Cape Juby (Vail and Mitchum, 1977), where the hiatus durations are much shorter. This information suggests that the 100 m.y. hiatus at Site 397 might include four consecutive erosional events: (1) an early Late Cretaceous event (? Turonian-Coniacian, Site 369); (2) an (? early) Paleocene erosion (e.g. Spansah 51A-1, Cape Jury sites, 370/416); (3) a late Eocene erosion (Site 369), coinciding with the beginning of the incision of submarine canyons (von Rad et al., 1979); and (4) a major (? late) Oligocene/earliest Miocene erosional event, which was restricted to parts of the lower slope and uppermost rise (Site 397, H.M.1), and wiped out most of the record of the previous unconformities.

Because of a predominantly synchronous reworking of sediments the mixing of lithologies and ages in the early Neogene mass flows is surprisingly small. However, a few pebbles of Aptian, Albian, Turonian-Coniacian and ? Eocene age were occasionally found in the debris flows and slumps at Site 397 (Arthur and von Rad, in press). These pebbles prove the existence of an escarpment with truncated lower Cretaceous to Paleogene strata exposed along the Cape Bojador slope prior and during the rapid early to middle Miocene sedimentation (cf. von Rad et al., 1979). Also during the late Pleistocene, huge sediment masses with a volume of at least 600 km$^3$ of translated [illegible]s slid off the gentle West Saharan lower slope (south of 26°N); on the adjacent upper and intermediate continental rise they were redeposited as several hundred km long tongues of debris flows and turbidites (Embley and Jacobi, 1977).

The interpretation of seismic reflection profiles (Hinz, in press: Wissmann, in press) and of vitrinite reflectance maturity data (Cornford et al., in press) suggests that roughly 1-2 km (or up to 3 km?) of sediments were eroded at Site 397 prior to the deposition of the early Miocene section (see also Fig.3). If we assume for this erosional scarp a width of 30 km and a length of 500 km (25°N to Cape Juby), a sediment volume of 7.500 to 15,000 km$^3$ must have been removed. If this erosion was restricted to a relatively brief time interval (e.g. 10 m.y.), we come to incredibly high erosion rates of 100 (to possibly 300) m/m.y.

At the present time, we can only speculate on the possible causes for the localized, but large-scale destruction of the lower Northwest African continental slope. The late Oligocene (Globorotalia opima zone) is characterized by the most accentuated global sea level fall (possibly 200 m) of the Tertiary (Vail et al., 1977), which surpassed the subsidence rate of the continental margin and moved the strandline beyond

the shelf edge. This favored the slumping of late Eocene to lower late Oligocene slope sediments (Site 369; lower slope canyons) and the generation of turbidity currents cutting deep canyons into the lower slope (von Rad et al, 1979).

At the same time, enhanced long-term geostrophic bottom currents helped to erode and steepen the lower slope by undercutting. Possibly an eastern boundary undercurrent originated from an intensified "pre-Antarctic Bottom Water" (pre-AABW) circulation in the South Atlantic which developed after the initiation of a globe-encircling circum-Antarctic current about 30-25 m.y. ago (Kennett, 1977; McCoy and Zimmerman, 1977). This northward flowing ancient geostrophic current was probably deflected by the Coriolis effect towards the Northwest African slope just as a presently much weaker (up to 10 cm/sec) semi-permanent northward-directed undercurrent along the upper slope (Mittelstaedt, 1976). During extended time intervals this current must have attained comparatively high velocities. Because the Oligocene record is not destroyed in Site 369, this current must have been restricted to water depths between 2 and 3 km along the lower slope and upper rise off Cape Bojador. A generally enhanced variable northward flow of AABW, which reached the Northeast Atlantic mainly through the Romanche and Vema Fracture Zones, has also been postulated for the latest Pliocene and pre-latest Pleistocene by Jacobi et al. (1975), von Stackelberg et al. (1976), Lowrie et al. (1978), and Cita and Ryan (in press). The velocity of this eastern boundary current might have been locally increased by the funneling effect between the Cape Bojador margin and the oldest submarine volcanoes of the Canary Archipelago which probably started to grow upward during late Oligocene to earliest Miocene times.

Apparently, the main causes for the mid-Cenozoic slope rejuvenation off Cape Bojador were the coincidence of a major regression with enhanced (pre-)AABW circulation and the beginning uplift of the Canary Islands during late Oligocene (to earliest Miocene) times. The interrelationship of these global and regional events is still poorly understood.

Along the eastern North American continental margin, a southwestward flowing Western Boundary Undercurrent (North Atlantic Deep Water) has been active since Late Eocene to Oligocene times and eroded the uppermost rise during the late Oligocene. Here, the slope was cut back for

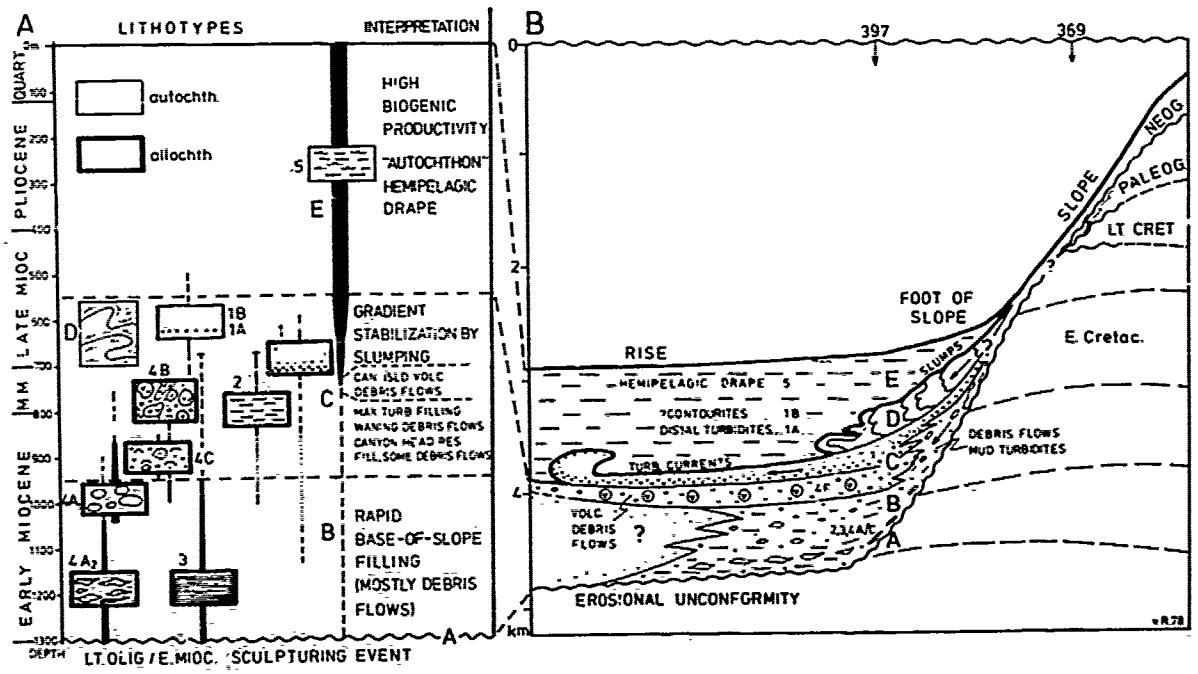


Figure 6. A: Schematic drawing showing vertical evolution of Neogene allocnthonous facies types (F-1,2, 3,4A,4B,4C) and hemipelagic sediments (F-5) on the upper continental rise at Site 397 (after Arthur and von Rad, in press).
B: Spatial and temporal evolution of gravitative sedimentation in a typical "base-of-slope environment" (modified after Kelling and Stanley, 1976, their Fig.31). A = major sculpturing event, B = rapid base-of-slope-filling stage, C = stage of gradual stabilization of slope, D = slump stage, E = hemipelagic drape.

20–30 km, mainly by headward canyon erosion in response to major regressions (Folger et al., 1978 . similar to offshore Cape Bojador.

## Early Neogene Gravitative Deposition

The large-scale sculpturing of the Cape Bojador margin caused an oversteepening of the slope gradient which then reached values of 7 (and locally 15) degrees. This triggered gravitative sedimentation mechanisms from the slope which deposited a great variety of displaced "flysch-type" lithofacies types (see Fig.6). These sediments make up 90% of the 540 m thick early to middle Miocene section of Site 397 and include the following lithofacies types: (1) pebbly mudstones with plastically deformed ($F\text{-}4A_2$) and undeformed clasts ($F\text{-}4A_1$), interpreted as debris flows (see Fig.6A); (2) dark olive-gray organic-rich silty claystones, transported from an oxygen-depleted upper slope environment by turbid layers or low-density turbidity currents; (3) poorly sorted quartz-granule-rich fossil hash derived from the shelf edge (F-4C); (4) volcaniclastic debris flows and turbidites from the Canary Islands (F-4B); and (5) graded turbiditic sandstones (F-1) Slumped hemipelagic sediments (D) overly these mass flows and grade upwards into undisturbed hemipelagic sediments of late Neogene age (E).

Figure 6b shows a simplified model of the evolution of gravitative sedimentation at relatively steep or rejuvenated slopes of passive margins. This model was first conceived by Kelling and Stanley (1976, their Fig.31) from the evidence of alpine flysch basins (e.g. the Grès d'Annot, Maritime Alps; Stanley, 1975).

We explain the horizontal (spatial) and vertical (temporal) change from a high-energy submarine canyon and base-of-slope to a lower-energy fan or rise facies by the gradual decrease of the gradient of a slope which was oversteepened by erosive geostrophic bottom currents (A). At the base of the sequence, we find rapidly deposited, chaotic debris or grain flows (B) which developed from slumps along the upper slope and grade seawards into turbidites. They were deposited at the abrupt decrease of the slope gradient along the base of the slope. Turbidity currents and other gravity-driven flows (C), and finally slumped hemipelagic sediments (D)follow these mass flows. By late Miocene times, the depositional conditions were stabilized and most coarse-grained terrigenous material bypassed the uppermost rise. Only occanionally and only in the lowermost part of the section, we find thin silt layers representing distal turbidites (facies 1A) or contourites (facies 1B) in the thick late Neogene hemipelagic drape (E). Thus typical sequences of thick sedimentary mélange ("wildflysch") or flysch-type sediments do occur in a "passive" margin setting without any obvious tectonic deformation, although ancient or recent flysch environments have mostly been attributed to subduction zones along active margins. Therefore, it is dangerous to infer the tectonic setting of an ancient flysch basin from the information on sedimentary sequences and composition alone. Commonly, major unconformities at the base of Atlantic-type continental margins are overlain by thick non-orogenic. redeposited sedimentary sequences ("flyschoid" sequences of Stanley, 1975). The failure of the slope sediment and the subsequent rapid gravitative sedimentation may have been triggered by an oversteepening of the lower slope which was undercut by erosive geostrophic currents; the mass wasting might have been also influenced by excessive sedimentation and overloading of the slope during low sea level stands, and by seismic activity during orogenic phases to the north (Atlas Mountains) or volcano-tectonic uplift of the Canary Archipelago (Arthur and von Rad, in press).

Figure 7 shows the source and transport direction of the allochthonous lithofacies in the South Canary Island Channel during early Neogene times. Most lithotypes (F-2, F-3, F4-A,C) belong to a more or less proximal facies, supplied as transversal fill from the adjacent slope and shelf off Cape Bojador. Schmincke and von Rad (in press) derive the volcaniclastic debris flows (F-4B) from the Canary Islands to the northeast, most probably from Fuerteventura; these debris flows can be traced on seismic records as a more than 200 km long, 10–25 km wide and 10–25 m thick tongue extending along the base of the slope to the SSW (G.Wissmann, personal communication 1978). Some well-sorted sand layers (F-1) might be distal turbidites, longitudinally introduced into this basin from more distant source areas to the east (shelf north of Cape Juby) or northeast (? Anti-Atlas or Atlas Mountains). At middle to early late Miocene times the predominantly gravitative redeposition from the Cape Bojador margin gave way to the undisturbed deposition of 700 m of late Miocene to Quaternary hemipelagic nanno marls.

## Evolution of Canary Island Volcanism

The evolution of the Canary Island volcanism can be inferred from the age and nature of the volcaniclastic debris flows and air-fall ash layers. The age of the formation of these islands increases from Tenerife to Gran Canaria and to Fuerteventura (Fig.8). In each of these islands a very brief (0.5–1 m.y.), but voluminous shield-building stage marked the beginning of subaerial island volcanism. This was known for Gran Canaria (McDougall and Schmincke, 1977), but Schmincke and von Rad (in press) now postulate a similar shield stage for the earliest volcanic history of Fuerteventura. The hyaloclastic composition (palagonitized siderome-lane shards) of the lower volcaniclastic debris flows(flows V-3 and V-4) of Site 397 suggests that a shallow-submarine shield-building stage

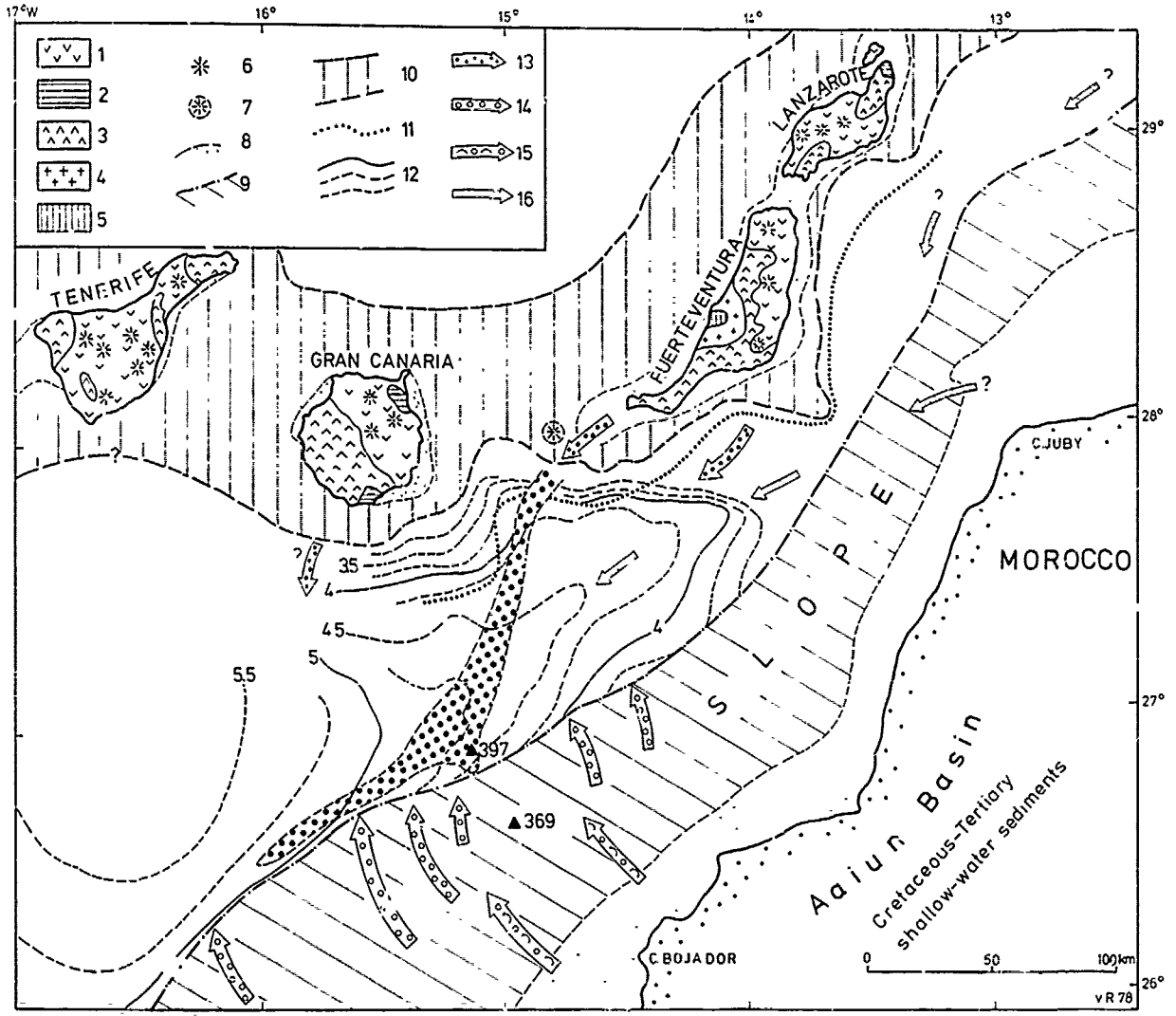


Figure 7. Provenance and dispersal of allochthonous lithofacies types in the South Canary Island Channel during early to middle Miocene times (modified from Arthur and von Rad, in press). 1-6 = generalized geology of the Canary Islands (see Schmincke and von Rad, in press), 7 = young submarine volcano; 8 = continental or island shelf with shelfbreak; 9 = base-of-continental-slope boundary; 10 = "volcanic mass" or "socle", partly overlain by young sediments and/or pyroclastics, 11 = seaward boundary of "volcanic apron", over- and underlain by sediments; 12 = depth contours of seismic reflector R-7 in seconds two-way travel time below sea level, indicating the approximate paleobathymetry during middle Miocene times. Arrows demonstrate inferred transport directions for: 13 = volcaniclastic debris flows (F-4B), dotted area = seismically detected extent; 14 = debris flows and mud turbidites (F-2,3,4A) from Cape Bojador slope (and outer shelf), 15 = distal turbidites (F-1), 16 = proximal shell and quartz-granule-rich debris flows (F-4C) from outer shelf. Source for 7,10,11,12,13: G. Wissmann (BGR, personal communication).

preceded the subaerial shield stage. This stage is represented by debris flows full of epiclastic fragments of tachylitic to crystallized basalt, trachyte, trachyandesite, and microgabbro (V-1, 1a,2). These thick volcaniclastic debris flows have a volume of about 50 km$^3$ and were deposited in the South Canary Island Channel (Fig.7) between about 17.5 and 15.5 m.y. ago. This is

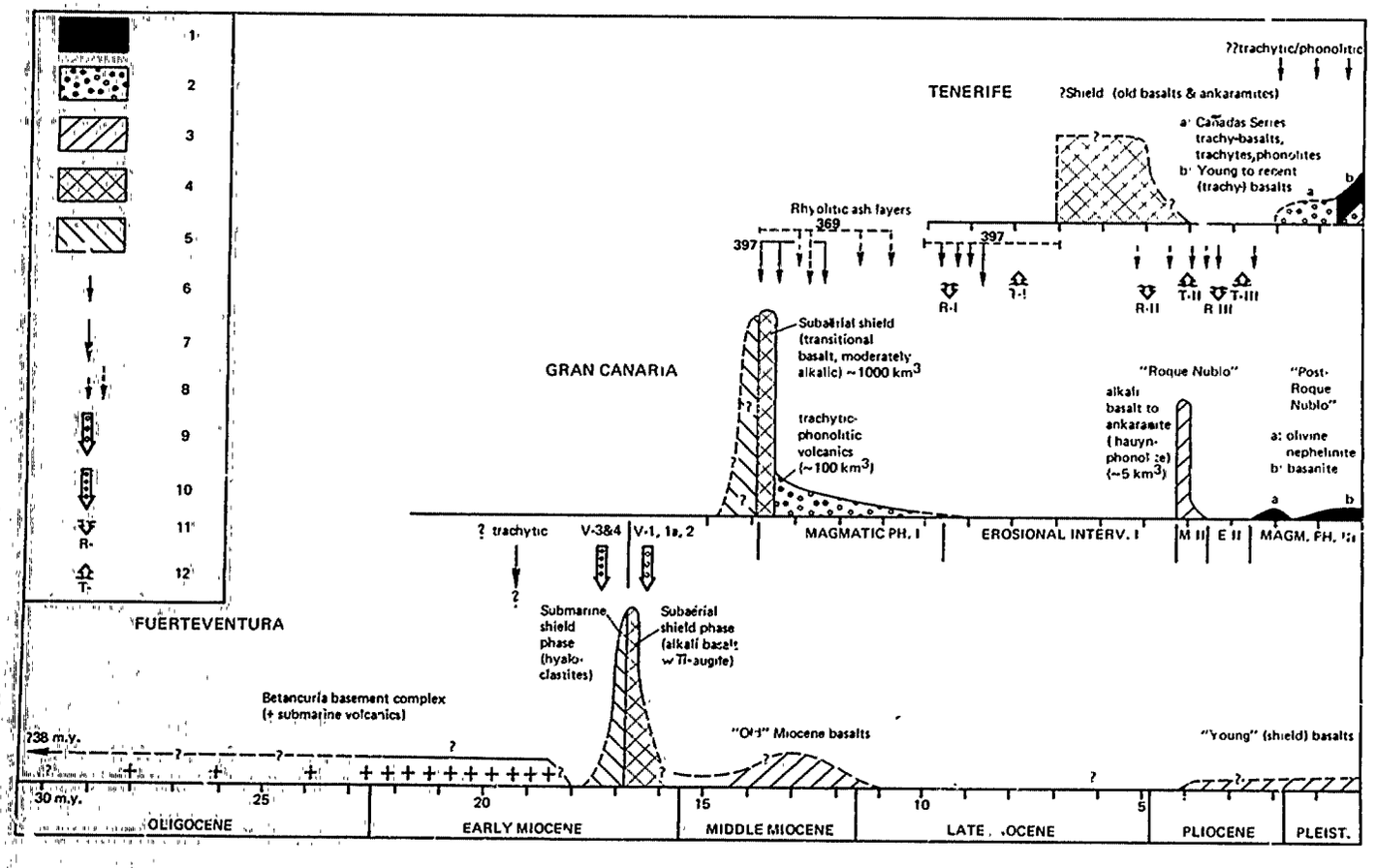


Figure 8. Schematic diagram showing generalized type, age, and duration of magmatic (M) and erosional (E) phases, transgressions (T), regressions (R) on Tenerife, Gran Canaria, and Fuerteventura (modified after McDougall and Schmincke, 1977, their Figures 5 and 6). Age and composition of volcaniclastic sandstones and ash layers found in Sites 369 and 397 (Schmincke and von Rad, in press) indicated in diagrams of those islands which are considered to be the source areas. 1 = extremely silica-undersaturated, alkalic magmas (nephelinite); 2 = trachyte, phonolite, etc.; 3 = alkali basalts, basanite; 4 = subaerial shield phase (moderately alkalic basaltic to mugearitic magmas, typical of all Canary Island shields (Schmincke, 1976) and inferred for Fuertenventura from Site 397; 5 = submarine shield phase (hyaloclastite; only inferred from Site 397 evidence for Fuerteventura); 6,7 = age and estimated composition of air-fall ash layers from Site 397 (7 = >10 cm thick); 8 = thin or thick air-fall ash layers, respectively, from Site 369; 9 = volcaniclastic sandstones/conglomerates (debris flows V-1, 1a, and 2; mainly subaerial source); 10 = hyaloclastites (debris flows V-3 and 4; mainly submarine source); 11,12 = regressions (R) and transgressions (T), after Lietz and Schmincke (1975, their Fig.4).

and estimated composition of air-fall ash layers from Site 397 (7 = > 10 cm thick); 8 = thin or thick air-fall ash layers, respectively, from Site 369; 9 = volcaniclastic sandstones/conglomerates (debris flows V-1, 1a, and 2; mainly subaerial source); 10 = hyaloclastites (debris flows V-3 and 4; mainly submarine source); 11,12 = regressions (R) and transgressions (T), after Lietz and Schmincke (1975, their Fig.4).

about 3 m.y. earlier than the well-dated formation of the subaerial shield of Gran Canaria, and much earlier than the oldest volcanics of the islands west of Gran Canaria (Schmincke, 1976). This age and the composition of the volcanic clasts suggest that Fuerteventura (or Lanzarote) were the source area of these debris flows.

Altered vitreous tuff layers of trachytic composition (Site 397) which are the product of large-scale explosive eruptions about 19-20 m.y. ago belong to the oldest, comparatively well-dated volcanic materials on or around the Canary Islands. This suggests that no subaerial "Canary Ridge" existed during Mesozoic to Eocene times, and that the growth and uplift of the oldest submarine Canary volcanoes did not begin before late Paleogene times. The occurence of deep-water pelagic Early Cretaceous (to Paleogene?) sediments on Fuerteventura (D.Bernoulli, personal communication) supports a relatively late initiation of the volcanic activity of the Canary Archipelago.The volcanism might have been triggered by the collision between the Eurasian and African plates during late Eocene to Oligocene times. The timing of this event is similar to that of the tectono-volcanic uplift of the Cape Verde Rise which in Site 368 contains 19 m.y. old basaltic sills and dates back also to Miocene times (Lancelot and Seibold, 1977).

A completely different process is responsible for the deposition of the middle Miocene to Quaternary ash layers of Sites 369 (Rothe and Koch, 1977) and 397. These ashes originated from highly explosive eruptions of more differentiated rhyolitic, trachytic and phonolitic magmas on the volcanic islands, and underwent lateral transport by high-altitude winds, and sedimentation by passive fall-out through the water column. Most ash layers of both sites are 7-14 m.y. old, i.e. their age coincides with that of Gran Canaria's most voluminous "Magmatic Phase I" (Lietz and Schmincke, 1975). A few 3.5-5 m.y. old ash layers might be attributed to Gran Canaria's second magmatic phase ("Roque Nublo Series"). The youngest late Pliocene to Pleistocene ashes might indicate explosive eruptions on Tenerife and the adjacent western Canary Islands.

## Paleobathymetry and Subsidence History

Figures 3A and B show a schematic cross-section of the passive continental margin at Cape Bojador together with subsidence-paleodepth-accumulation rate diagrams representing the tectonostratigraphic evolution during the past 200 m.y. at three characteristic sites below the present shelf, slope and upper rise (von Rad and Einsele, in press). These "geohistory diagrams" (Van Hinte, 1978) contain two types of stratigraphic information: (1) the cumulative thickness of sediments, deposited during a certain time interval (taken from biostratigraphical dating of drilled horizons or extrapolated from seismic evidence), and (2) the paleo-water depth, determined by bio- or lithofacies interpretation or by inference from comparable shallower-water sites. Because of the lack of stratigraphic detail, inaccuracy of biostratigraphic boundaries, uncertainties of their correlation with an absolute time scale, and ambiguities of paleo-water depth interpretations, these geohistory diagrams record only general trends in the geodynamic evolution of this margin. We define the term "subsidence" as the change of depth which a certain stratigraphic level undergoes during a given time with respect to the present sea level. The subsidence curves have been corrected for compaction (von Rad and Einsele, in press), but not for past sea level fluctuations, as attempted by Steckler and Watts (1978) for the continental margin off New York.

Since near the present coastline and on the shelf (well 51A-1) the water depth was probably never greater than 100-200 m during the past 200 m.y., we can directly deduce the subsidence rate during a given time from the thickness of sediment accumulated during that time. This exercise gives extremely high subsidence rates of 80-120 m/m.y. for the Jurassic and Early Cretaceous which decrease more or less exponentially to about 15 m/m.y. during Late Cretaceous to Tertiary times (Fig.3B). The Jurassic-Early Cretaceous subsidence rate is tentative, because it depends on the geophysical interpretation which defines the base of this sequence (G.Wissmann, personal communication). The beginning of subsidence is more or less arbitrarily placed at 200 m.y. If Triassic or even late Paleozoic sediments overly the "basement" (a possibility, suggested by P. Lehner, personal communication), subsidence rates become considerably smaller; if sedimentation began later than the onset of spreading about 165-180 m.y. ago, the rates would be somewhat greater.

If we assume continuous shallow-water conditions also for the slope and uppermost rise sites, then the enormous thickness of Jurassic sediments (7-8 km) must be attributed to a very high initial subsidence of the underlying basement. This subsidence was compensated by carbonate buildup after a rapid initial deposition of continental clastics, redbeds, and evaporites. During the Jurassic and earliest Cretaceous the water depth at the slope and rise sites remained close to sea level. At the beginning of the Cretaceous the water depth increased. Early Cretaceous subsidence rates were very high (130 m/m.y.); during middle Cretaceous to recent times, the rate of subsidence of the slope and upper rise slowed. Since the sedimentation rates, possibly influenced by the global Late Cretaceous rise in sea level, slowed even more, the sea floor continued to deepen.

To learn more about the history of subsidence since the earliest Cretaceous we had to apply the results from comparable shallow-water sites

and "backtrack" Sites 369 and 397 using the better established Late Cretaceous and Tertiary subsidence rates of the shelf and coast sites. This "continental margin backtracking method" is outlined in von Rad and Einsele (in press).

## Summary and Conclusions
## Geodynamic, Sedimentary and Volcanic Evolution of the Cape Bojador Continental Margin During the Past 200 m.y.

We can only speculate on the late Triassic and Jurassic early rift, drift, and subsidence stages of the 200 m.y. old, mature Cape Bojador margin. In the Aaiun (-Tarfaya) Basin (Fig.1) several exploration wells penetrated 1 to over 2 km thick sequences of middle to late Jurassic shallow-water limestones, marlstones and dolomites (von Rad and Einsele, in press). Similar Jurassic carbonate platforms were reported from dredging, drilling and seismic evidence below the shelf edges off Senegal (Lehner and De Ruiter, 1977) and off southern and central Morocco (Mitchum and Vail, 1978; Renz et al., 1975). Therefore, von Rad and Einsele (in press) have postulated Jurassic shallow-water limestones below the entire Cape Bojador continental margin which were deposited on a tectonically stable, slowly subsiding shelf. This hypothesis is supported by the comparatively shallow paleodepth inferred for the earliest Cretaceous prodelta mudstones and the extremely thick sequence of pre-Cretaceous carbonate (?) rocks under the present slope and uppermost rise.

A remarkable facies change from shallow-water carbonate to a more or less terrigenous facies took place in the Aaiun Basin during earliest Cretaceous times. A very thick sequence of continental clastics grades seawards into lagoonal, intertidal, delta plain, delta forset, and finally into distal prodelta muds (Fig.5), and constitutes a huge deltaic system with its maximum sediment thickness below the present slope (Fig.3A). For the Hauterivian prodelta mud environment under the present upper rise (at Site 397), Einsele and von Rad (in press) assumed a water depth of a few hundred to a maximum of 1000 meters. It is likely that not even the rapid accumulation rates (75-150 m/m.y.) of the Hauterivian sequence could keep pace with the subsidence of the outer margin. Similar Wealden-type deltaic facies developed at many places around the Early Cretaceous North Atlantic Ocean (Fig.4).

Late Early Cretaceous to Paleogene sediments which were eroded at Site 397, are partly preserved landward of the lower slope and seaward of the upper rise (Fig.3A). Aptian to Cenomanian organic-rich shales indicating restricted oceanic circulation and at least partly anaerobic conditions are present in the sites under the present shelf (51A-1), slope (369), and Moroccan Basin (370/416), as well as in the deeper ocean (137,138). In the outer Aaiun Basin laminated anaerobic marls of late Cenomanian to Turonian age suggest an expanded mid-water oxygen minimum zone and/or high-fertility (upwelling) conditions of the surface waters along the West African coast (Einsele and Wiedmann, 1975). A pronounced shelf edge developed during Cenomanian times and remained at this position (between Sites 51A-1 and 369) for the past 90 m.y.

During the last 100 m.y. the rates of accumulation at the present shelf, slope and rise were much lower (10-15 m/m.y.) than in Early Cretaceous times. Sedimentation was probably interrupted by periods of non-deposition or even erosion, especially during early Late Cretaceous, early Paleocene, and late Eocene to Oligocene times. Therefore the sea floor continued to deepen, even when subsidence rates decreased to 13 m/m.y. (Figure 3B; von Rad and Einsele, in press).

Probably during latest Eocene through middle Oligocene, geostrophic bottom currents (enhanced flow of "pre-Antarctic Bottom Water"?) cut several kilometers deep into the lower part of the continental margin at Site 397 (Fig.3B) and eroded all sediments of Paleogene through Hauterivian age. The oversteepening of the lower continental slope and a pronounced late Oligocene sea level fall triggered rapid redeposition of sediment from the slope during early Neogene time. This resulted in a deep-marine onlap of a thick redeposited sediment sequence at the foot of the slope. The predominantly allochthonous sediments buried the erosional scarp, diminished the water depth to its present value, and gradually reduced the slope gradient. This shifted the depocenter from its Jurassic and Early Cretaceous position below the present slope and shelf to the uppermost rise.

The early evolution of the Canary Island volcanism started in late Paleogene times and culminated in the inferred voluminous submarine and subaerial shield phase of Fuerteventura (about 17.5-15.5 m.y. ago) and the well known shield phase of Gran Canaria (about 14 m.y. ago). The early Neogene growth and uplift of the Canary Archipelago influenced the evolution of the Cape Bojador margin by earthquake activity related to volcanism which triggered some mass flows and deposited them as thick volcaniclastic debris flows and turbidites along the foot of the slope. The initiation of the Canary Island volcanism also caused an increase in the local geothermal gradient which is now 4°/100 m at Site 397 (Arthur et al., in press) and decreases towards the Aaiun Basin (P.Lehner, personal communication). This secondary heating might have caused an additional decrease in the local subsidence rate during the Neogene. At about 20 m.y. B.P., the uplift of the Cape Verde Rise and Canary Archipelago may have helped to cut off any large-scale erosion by geostrophic currents.

During the past 10 m.y., a thick sequence of undisturbed hemipelagic late Neogene sediments accumulated with high sedimentation rates on the uppermost continental rise. Frequent oscilla-

tions in climate and sea level changes, high plankton productivity (upwelling), some terrigenous and shallow-water sediment input, and minor pulses of $CaCO_3$ dissolution and sea floor scouring have left an important imprint on the late Neogene sediments.

The continental to transitional basement below the Cape Bojador margin has a similar depth of about 12-15 km below the present shelf, slope, and upper rise over a distance of 100 km (Fig.3A). Similar basement depths (10-14 km) were reported from the Baltimore Canyon Trough (Scholle, 1977) and the Blake-Bahama Basin (Sheridan, 1976). Thus the Cape Bojador margin constitutes a uniformly subsiding "marginal basin" with very high Jurassic and earliest Cretaceous subsidence rates which decreased more or less exponentially during the past 100-120 m.y. Not before Late Cretaceous to Tertiary times did the subsidence rate approach values similar to the ones known from the empirical cooling curve of oceanic crust (Fig.3B).

With the fragmentary stratigraphic and structural information at hand, it is impossible to answer the question of the driving forces responsible for the subsidence at the Cape Bojador margin. A simple thermal contraction plus loading model as suggested by Sleep (1971), Watts and Ryan (1976), Steckler and Watts (1978) seems insufficient to explain the extremely high initial subsidence rates at this margin (see Arthur et al., in press). Other driving mechanisms, such as an increase in the thickness or density of the crust, might have further influenced the subsidence of the basement below the Cape Bojador margin, especially during Jurassic and Early Cretaceous times.

Acknowledgements. We acknowledge with thanks the free exchange of data and ideas with all scientists who have participated in geological studies of Leg 47A material and whose results are published in the Initial Reports of the Deep Sea Drilling Project (vol.47). In particular, we are indebted to Gerhard Einsele (Tübingen) and Hans-Ulrich Schmincke (Bochum) with whom the senior author had a very close cooperation during the past two years. Thanks are also due to D.Bernoulli (Basel), F.W. McCoy (Palisades), P.Lehner (Den Haag), M.Sarnthein (Kiel), M.S. Steckler (Palisades), W.F.B.Ryan (Palisades), P.Vail (Houston) and G.Wissmann (Hannover) for valuable ideas and helpful comments.

## References

Allen,P., The Wealden environment, Anglo-Paris Basin, Phil. Trans. Royal Soc. (London), Ser. B, 242, 283-346, 1959.

Allen,P., Wealden of the Weald: a new model, Proceed. Geologists' Assoc. London, 86 (4), 389-437, 1975.

Arthur,M.A., U.von Rad, C. Cornford,F.W.McCoy, and M.Sarnthein, Evolution and sedimentary history of the Cape Bojador continental margin, NW Africa. In von Rad,U., W.B.F. Ryan, et al. Initial Reports Deep Sea Drilling Project,, 47 (1), in press.

Arthur,M.A. and U.von Rad, Early Neogene base-of-slope sedimentation at Site 397: sequential evolution of gravitative mass transport processes and redeposition along the NW African passive margin. In von Rad,U., W.B.F. Ryan, et al. Initial Reports Deep Sea Drilling Project 47 (1), in press.

AUXINI (Departamento de Investigaciones Petroliferas de AUXINI), Correlacion estratigraphica de los sondeos perforados en el Sahara espanol, Bol. Geol. Minero, Madrid, 83, 235-251, 1969.

Beck,R.H. and P.Lehner, Oceans, new frontier in exploration, Amer. Assoc. Petroleum Geologists, Bull., 58, 376-395, 1974.

Berger,W.H. and U.von Rad, Cretaceous and Cenozoic sediments from the Atlantic Ocean, In Hayes,D.E., A.C. Pimm et al., Initial Reports Deep Sea Drilling Project, 14, Washington (U.S. Government Printing Office). 787-954, 1972.

Cita,M.B. and W.B.F. Ryan, Late Neogene Paleoenvironment: part 4. Evolution of ocean paleoenvironment. Interpretation. In von Rad,U., Ryan W.B.F., et al., Initial Reports Deep Sea Drilling Project, 47 (1), in press.

CONOCO, Spansah 51A-1, offshore Spanish Sahara: Final Report by Continental Oil Company of Spain, Spanish Gulf Oil Company, Compania Espanol de Petroleas S.A. Exploration Department, unpublished report and logs, 1969.

Cornford,C., J. Rullkötter and D. Welte, Organic geochemistry of DSDP Leg 47a, Site 397, eastern North Atlantic: organic petrography and extractable hydrocarbons, In von Rad,U., Ryan W.B.F., et al., Initial Reports Deep Sea Drilling Project 47 (1), in press.

Dash,B.P. and E. Bosshardt, Seismic and gravity investigations around the western Canary Islands, Earth Planet. Science Letters, 7, 169-177, 1969.

Einsele,G. and U. von Rad, Facies and paleoenvironment of Early Cretaceous sediments in DSDP Site 397 and in the Aaiun Basin (NW Africa). In von Rad,U., W.B.F. Ryan, et al., Initial Reports Deep Sea Drilling Project, 47 (1), in press.

Einsele,G. and J. Wiedmann, Faunal and sedimentological evidence for upwelling in the Upper Cretaceous coastal basin of Tarfaya, Morocco, Ninth Internat. Congress of Sedimentology, Nice, theme 1, 67-72, 1975.

Embley,R.W. and R.Jacobi, Distribution and morphology of large submarine sediment slides and slumps on Atlantic continental margins, In: A.F.Richards (Ed.), Marine Slope Stability, Mar. Geotechn., 2, 205-228, 1977.

Fischer,A.G. and M.A.Arthur, Secular variations in the pelagic realm, In: H.E. Cook and P. Enos (Editors), Deep Water Carbonate Environ-

ments, Soc. Economic Paleontol. Mineralogists, Spec. Publ. 25, 19-50, 1977.
Folger,D.W , W.P.Dillon, J.A.Grow, K.D.Klitgord, and J.S.Schlee, Evolution of the Atlantic continental margin of the United States Abstracts, Second M.Ewing Symposium, March 19-25, 1978, Arden House, N.Y. 15-16, 1978.
Hinz,K., Seismic sequences off Cape Bojador, Northwest Africa, In: von Rad,U., Ryan,W.B.F., et al., Initial Reports Deep Sea Drilling Project, 47 (1), in press.
Hinz,K., E.Seibold, and G.Wissmann, Continental slope anticline and unconformities off West Africa, "Meteor" Forsch-Ergebnisse C, no. 17, 67-73, 1974.
Jacobi,R.D., P.D. Rabinowitz, and R.W. Embley, Sediment waves on the Moroccan continental rise, Marine Geol., 19, 61-68, 1975.
Jansa,L.F. and J.A. Wade, Geology of the continental margin off Nova Scotia and Newfoundland, Offshore Geology of Eastern Canada, Geol. Survey Canada, Paper 74-30, 2, 258 pp. 1975.
Kelling,G. and D.J. Stanley, Sedimentation in canyon, slope and base-of-slope environments, In Stanley, D.J. and D.J.P. Swift (Eds.), Marine sediment transport and environmental management (J.Wiley, Sons, Inc.), 379-435, 1976.
Kennett, J.P., Cenozoic evolution of Antarctic glaciation, the circum-Antarctic Ocean and their inpact on global paleooceanography, J. Geophys. Res., 82, 3843-3860, 1977.
Lancelot,Y. and E. Seibold, The evolution of the central northeastern Atlantic-Summary of results of DSDP Leg 41, In Lancelot,Y., E. Seibold, et al., Initial Reports Deep Sea Drilling Project, 41, 1215-1245, 1977.
Lancelot,Y., E.Seibold et al., Initial Reports Deep Sea Drilling Project, 41, Washington U.S. Government Printing Office), 1259 pp., 1977.
Lehner, P. and P.A.D. De Ruiter, Structural history of the Atlantic margin of Africa, Amer. Assoc. Petroleum Geol. Bull, 61, 961-981, 1977.
Lietz,J. and H.U. Schmincke, Miocene-Pliocene sea level changes and volcanic phases on Gran Canaria (Canary Islands) in the light of new K-AR ages, Palaeogeography, Palaeoclimatology, Palaeoecology, 18, 213-239, 1975.
Lowrie,A., J. Egloff and W.H. Jahn, Kane Seamount in the Cape Verde Basin, eastern Atlantic, Marine Geology, 26, M29-M35, 1978.
McCoy, F.W. and H.B. Zimmerman, A history of sediment lithofacies in the South Atlantic Ocean, In Supko, P.R., K. Perch-Nielsen, et al., Initial Reports Deep Sea Drilling Project, 39, 1047-1080, 1977.
McDougall, I. and H.U. Schmincke, Geochronology of Gran Canaria, Canary Islands: age of shield building volcanism and other magmatic phases, Bull. Volcanology, 40, 1-21, 1977.
Mitchum Jr., R.M. and P.R. Vail, Seismic stratigraphic interpretation, procedure, In Vail, P.R. et al., Seismic stratigraphy and global changes of sea level, Amer. Assoc. Petroleum Geol. Memoir 26, 135-144, 1977.
Mittelstaedt, E., On the currents along the Northwest African coast south of 22° north, Deutsch. Hydrogr. Zeitschr., 29 (3), 97-117, 1976.
Ratschiller, L.K., Lithostratigraphy of the northern Spanish Sahara, Memorie del Museo Tridentino di Scienze Naturali, Trento, 18, 9-84, 1970.
Renz, O., R. Imlay, Y. Lancelot, and W.B.F. Ryan Ammonite-rich Oxfordian limestones from the base of the continental slope off Northwest Africa, Eclogae geol. Helv., 68, 431-448, 1975.
Rothe, P. and R. Koch, Miocene volcanic glass from DSDP Sites 368, 369 and 370, In Lancelot Y., E. Seibold, et al., Initial Reports Deep Sea Drilling Project, 41, 1061-1064, 1977.
Schlee, J., J.C. Behrendt, J.M. Robb, R.E. Mattick, P.T. Taylor, and B.J. Lawson, Regional geologic framework off northeastern United States, Amer. Assoc. Petroleum Geol., Bull., 60, 926-951, 1976.
Schmincke, H.U., The geology of the Canary Islands. In Kunkel, G. (Ed.), Biogeography and ecology in the Canary Islands, The Hague (W.Junk), 67-184, 1976.
Schmincke, H.U. and U. von Rad, Neogene evolution of Canary Island volcanism inferred from ash layers and volcaniclastic sandstones of DSDP Site 397 (Leg 47A), In von Rad, U., Ryan W.F.B.,et al., Initial Reports D.S.D.P., 47 (1) in press.
Scholle, P.A. (Ed.), Geological Studies on the COST No. B-2 well, U.S. mid-Atlantic outer continental shelf area, U.S. Geol. Survey Circ. 750, 71 pp., 1977.
Sclater, J.G., St. Hellinger, and Ch. Tapscott, The paleobathymetry of the Atlantic Ocean from the Jurassic to the Present, J. Geol., 85, 509-552, 1977.
Seibold, E. and K. Hinz, Continental slope construction and destruction, West Africa, In C.A. Burk and Ch.L. Drake (Eds.), The Geology of Continental Margins, New York, Heidelberg, Berlin (Springer), 179-196, 1974.
Sheridan, R.E., Sedimentary basins of the Atlantic margin of North America, Tectonophysics, 36, 113-132, 1976.
Shipboard Scientific Party of DSDP Leg 50, In the Atlantic: documenting early riftling. Geotimes, 22 (April), 24-27, 1977.
Sleep, N.H., Thermal effects of the formation of Atlantic continental margins by continental break-up, Geophy. J. Royal astron. Soc., 24, 325-350, 1971.
Stanley, D.J., Submarine canyon and slope sedimentation (Grès d'Annot) in the French Maritime Alps, Ninth Internat. Congress of Sedimentology, Nice, Guidebook, 129 pp. 1975.

Steckler, M.S. and A.B. Watts, Subsidence of the Atlantic-type continental margin off New York, Earth Plan. Science Letters, 41, 1-13, 1978.

Uchupi, E., K.O. Emery, C.O. Bowin, and J.O. Phillips, Continental margin off Western Africa, Amer. Assoc. Petroleum Geologists, Bull., 60, 809-878, 1976.

Vail, P.P., R.M. Mitchum Jr., and S. Thompson III, Global cycles of relative changes of sea level. In Vail, P.R. et al., Seismic stratigraphy and global changes of sea level, Amer. Assoc. Petroleum Geol., Memoir 26, 83-98, 1977.

Van Hinte, J.E., Geohistory analysis-application of micropaleontology in exploration geology, Am. Assoc. Petroleum Geol. Bull., 62 (2), 201-222, 1978.

von Rad, U., P. Cepek, U. von Stackelberg, G. Wissmann, and B. Zobel, Cretaceous and Tertiary sediments from the Northwest African slope (dredges and cores supplementing DSDP results), Marine Geol., 29, 1979.

von Rad, U. and G. Einsele, Mesozoic - Cainozoic subsidence history and paleobathymetry of the Northwest African continental margin (Aaiun Basin to DSDP Site 397), Phil. Trans. Royal Soc. (London), in press.

von Rad, U., W.B.F. Ryan, et al., Initial Reports Deep Sea Drilling Project, 47 ,1), in press.

von Stackelberg,U., U. von Rad, and B. Zobel, Asymmetric distribution of displaced material in calcareous oozes around Great Meteor Seamount (North Atlantic), "Meteor" Forsch.-Ergebn., Reihe C, (25), 1-46, 1976.

Watts, A.B. and W.B.F. Pyan, Flexure of the lithosphere and continental margin basins, Tectonophysics, 36, 25-44, 1976.

Wiedmann J., A.Butt, and G. Einsele, Vergleich von marokkanischen Kreide-Küstenaufschlüssen und Tiefseebohrungen (DSDP): Stratigraphie, Paläoenvironment und Subsidenz an einem passiven Kontinentalrand, Geol. Rundsch., 67, 454-508, 1978.

Winterer, E.L., Sedimentary facies on the rise and slopes of passive continental margins, Phil. Trans. Royal Soc. (London), in press.

Wissmann, G., The Cape Bojador slope, an example for potential pitfalls in seismic interpretation without the information of outer margin drilling. In von Rad, U., Ryan, W.F.B., et al., Initial Reports Deep Sea Drilling Project, 47 (1),in press.

# SEISMIC REFLECTION RECONNAISSANCE OF THE ATLANTIC MARGIN OF MOROCCO

Joel S. Watkins
Gulf Science and Technology
11111 Wilcrest
Houston, Texas 77099

K. W. Hoppe
Gulf Oil Exploration and Production Company
2604 Gulf Building
Houston, Texas 77001

Abstract. Data from a seismic reconnaissance of the Atlantic margin of Morocco indicate that the continental margin, like onshore Morocco, exhibits a complex structural and depositional history. In the Rharb basin, the Prerif Nappe of Tortonian (Middle Miocene) age thrusts over faulted shelf and slope sediments. Post-nappe slope sediments are undeformed. Moderate deformation of post-nappe shelf sediments probably results from diapiric movement within the mobile core of the nappe.

The margin between the Canary Arch and Tarfaya basin has thick salt overlying inferred attenuated continental crust located between the present-day coast and the Canary Arch. The Canary Arch was first uplifted between Middle Cretaceous and Miocene. There is evidence of volcanism during and possibly prior to the Eocene. We find no evidence, however, for Tertiary movement along a supposed lineament extending from the South Atlas fault along the southern margin of the salt basin and into or south of the Canary Island axis.

Large scale mass transport of slope sediments by gravity gliding and debris flow accounts for a significant fraction of the sediment transport budget off Morocco. The subtle character of these flows on seismic sections suggests that gravity gliding and debris flow may be more important worldwide than previously recognized.

## Introduction

In 1969, the R/V GULFREX (named for Gulf Oil Research and Exploration) conducted a reconnaissance seismic reflection study of the Atlantic margin of northwest Africa. This report presents three seismic lines located between latitudes 24°-35°N (Figure 1). The lines cross the Moroccan continental margin west of the Rharb basin of northern Morocco, the Tarfaya basin - Canary Arch, and Villa Cisneros, the Spanish Sahara, in the vicinity of latitude 25°N. The Rharb basin line shows deformation of continental margin structure by Alpine tectonics. The Tarfaya basin-Canary Arch line shows salt structures of the Moroccan salt basin, and provides evidence of timing and effects of Canary Island uplift and volcanism. The line west of Villa Cisneros shows extensive buried olistostromes at the foot of the paleoslope.

Collectively, the structures of the region represent a moderately active margin.

## Rharb Basin

### Geologic Setting

The Rharb basin line shown in Figure 2 lies within the Rif structural province of northwestern Morocco. Major geologic features are shown in Figure 1. The Rif is the southern analog in time, structure and lithology to the Betic cordillera of southern Spain. Convergence of Europe and Africa during the Alpine orogeny resulted in compression, uplift, metamorphism and volcanism, and in northward thrusting or gravity gliding in Spain and similar southward displacements in Morocco.

Choubert and Marais (1952) separated the Rif into four zones: (1) an internal zone of Paleozoic rocks, (2) a Limestone Dorsal of dominantly Triassic, Jurassic and Cretaceous carbonates, (3) the Rif Nappe zone of dominantly marl and shale, and (4) the Prerif Nappe. These zones are shown in Figure 1.

According to Faure-Muret and Choubert (1971), the internal Paleozoic zone and Limestone Dorsal were compressed, folded and thrust southward during the Eocene and Oligocene. A flysch sequence overlying Paleozoic and Dorsal zones slid southward during upper Oligocene, stopping finally at the end of Middle Miocene. Fragments of this large flysch nappe overlap parts of the Rif Nappe zone. The sequence of deformation in the Rif and Prerif zones is not clear. According to Faure-Muret and Choubert, rocks outcropping in these zones were deposited in a trough bounded by the Paleozoic and Limestone Dorsal zones on the north and the Moroccan Meseta on the south. The Rharb Basin probably represents the relatively undeformed southern margin of the trough.

Rif zone rocks are dominantly marls and shales ranging in age from Triassic to Oligocene. In the southern part of the Rif zone, evaporites are the source of salt diapirs. Huge, exotic fragments of Liassic

limestone, Jurassic reef banks and Precambrian granite lie within the mobile matrix.

The Prerif Nappe consists mainly of muddy, highly mobile Cretaceous and Tertiary marls encasing more competent blocks of Mesozoic and Lower Tertiary ages. Fossils indicate that the Prerif Nappe was emplaced in the Middle Tortonian (Miocene) and during a short time interval.

Faure-Muret and Choubert note that stable bottom depths and lack of disturbance of microfaunal ecologies during emplacement suggest gravity gliding rather than thrust faulting as the mechanism of emplacement. According to them, the nappe appears to have slid gently off higher land to the north into the quiet waters of the Rharb Basin.

Further support for the gravity gliding emplacement mechanism comes from marine studies by Lajat et al. (1975). They observed that the leading edge of the Prerif Nappe can be traced in the form of a vast east-facing "U" on the floor of the Atlantic Ocean from Morocco to Spain. Lajat et al.'s seismic data further suggests an olistostromal origin for the nappe front.

In western Morocco, outcrops and drill hole data suggest division of the Prerif Nappe into inner and outer

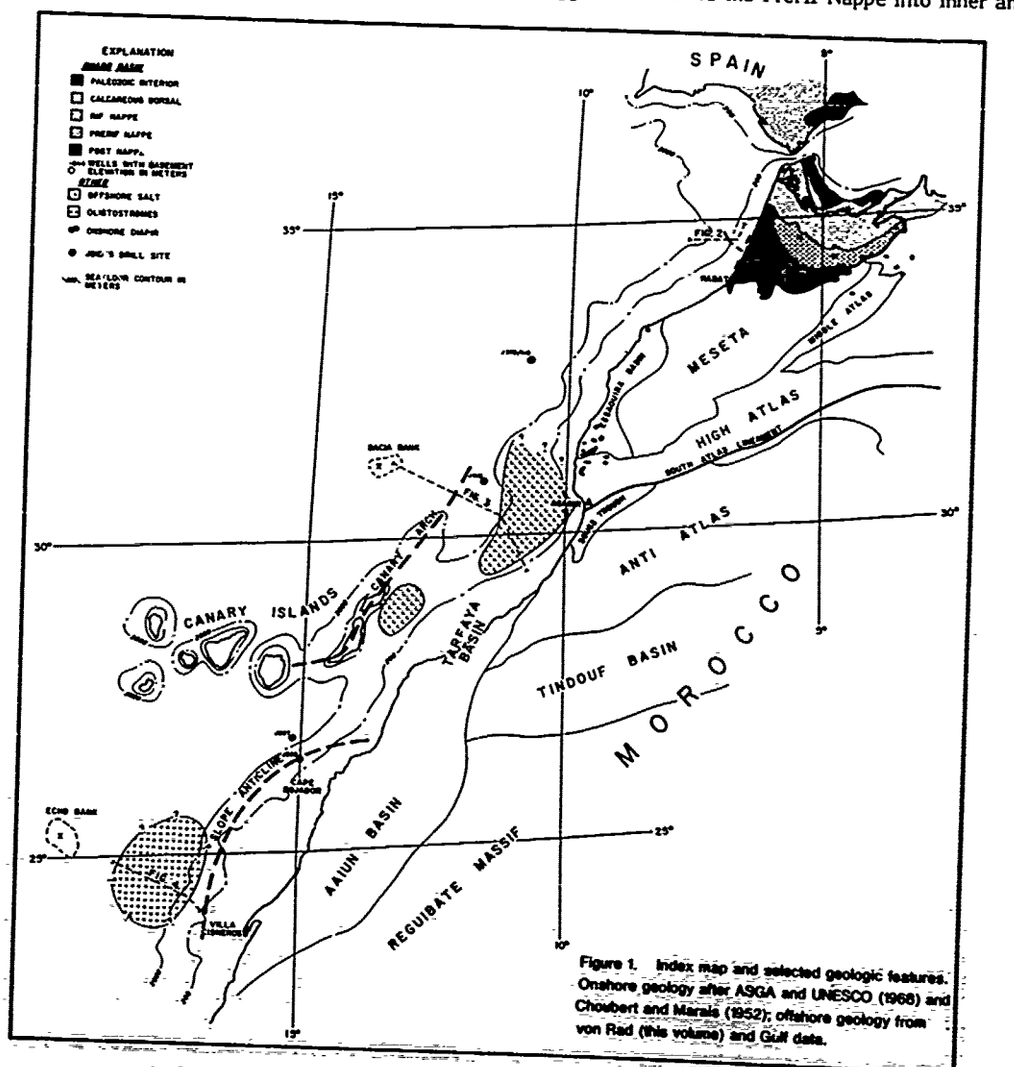


Figure 1. Index map and selected geologic features. Onshore geology after ASGA and UNESCO (1968) and Choubert and Marais (1952); offshore geology from von Rad (this volume) and Gulf data.

zones (G. Suter, quoted by Faure-Muret and Choubert, 1971). Inner zone rocks consist of a matrix of flysch and marl pierced by blocks and slices of more competent lithologies while outer zone rocks consist of a muddy, marly melange of Cretaceous and Tortonian age injected by Triassic gypsiliferous evaporites. Inner and outer zone rocks of the Prerif were folded in late Miocene and Pliocene (Faure-Muret and Choubert, 1971).

South of the Rharb, the subsurface extension of the Meseta served as a stable abutment against which the Rif structures were compressed, folded and thrust (Dillon and Sougy, 1974).

Little is known of the offshore geology of the Rharb basin. Data from the only well drilled here are unavailable to us at the present time. Although seismic reflection data from the southwestern Morocco offshore have been published, we are unaware of published seismic data from the Rharb margin.

## Discussion of Results

We have divided the Rharb basin seismic section into 5 units (Figure 2). Unconformities separate the upper 4 units and possibly the deepest 2 units as well but reflector resolution is too poor to unequivocally demonstrate the lowermost unconformity. From top to bottom, the units are as follows.

Unit 1. Post-nappe sediments of Plio-Pleistocene age. Within the unit, seismic signature and/or velocities distinguish four subunits, 1a, 1b, 1c, and 1d, some having both slope and shelf facies. Subunit 1a, the uppermost subunit, consists of flat-lying sediments on both slope and shelf; has a thickness of 200-500 milliseconds (msec) two-way travel time; and has interval velocities of 1.8-2.0 km/sec. We interpret this subunit as unconsolidated sediments of Pleistocene age.

Subunit 1b is a lens-shaped deposit located on the upper slope. The subunit has a maximum thickness of 250 msec and its interval velocity range is 2.0-2.2 km/sec. The lower boundary of this subunit is an erosional unconformity. The subunit appears to have filled a depression, possibly a slump scar, in the upper slope. Velocities indicate slightly compacted sediments.

Subunits 1c and 1d are distinguished on the basis of their interval velocities. Subunit 1c velocities range from 2.3-2.6 km/sec and subunit 1d velocities cluster near 2.7 km/sec. Subunit 1c overlies 1d with apparent comformity. Subunit 1d fills topographic lows in the upper surfaces of 2a and 3. Between SPs 2000 and 2100, subunit 1d pinches out against the flanks of a high in Unit 3, which allows 1c to lie directly on 3. The slope facies of subunits 1c and 1d are flat or nearly so while their shelf facies are undulating and faulted. The difference in aspect is probably due to movements within the shelf portion of Unit 2.

Unit 2. We correlate Unit 2 with the Prerif Nappe because of its allochthonous character and the location of its seaward edge close to the seaward projection of the nappe edge (Figure 1). Interval velocity data suggest division of the nappe into upper and lower subunits, 2a and 2b. Velocity data also indicate lateral differences within the Prerif Nappe (Figure 2). Velocities near the toe of the nappe range down to 2.5 km/sec. Throughout the remainder of the nappe they are no lower than 2.7 km/sec in the upper part and significantly higher in the deeper part. West of SP 1600, only subunit 2a can be distinguished with velocities of 2.7-3.1 km/sec except near the extreme western limit of the nappe. East and north of SP 1600, subunit 2b with velocities of 2.7-4.8 km/sec lies beneath 2a. The highest velocities within subunit 2b occur in the deeper part of the nappe beneath the present-day shelf. The higher velocities (ca. 4.0 km/sec) probably result from incorporation within the nappe of blocks of higher velocity material derived from the underlying unit 5.

The base of the nappe dips 12½° approximately N10°E.

Unit 3. This unit unconformably overlies Unit 4 and is restricted to the present-day slope and has velocities ranging from 2.4 to 2.7 km/sec. The basal plane of the Prerif nappe truncates this unit to the east. Missing portions of the eastward extension of Unit 3 have probably been incorporated within the nappe. The basal plane of the nappe also truncates Unit 4 beneath the present-day shelf edge.

Unit 4. The unit consists of 2 facies, the easternmost contains more-or-less flat reflectors exhibiting progressively steeper dips with depth. This fan-like reflector pattern strongly suggests deposition on a passive margin where the seaward edge is subsiding more rapidly than the landward edge. Seismic sections of the northeast coast of the United States (e.g. Schlee et al., 1976) and parts of West Africa (e.g. Vail et al., 1977, p. 80) commonly exhibit this type of reflector pattern. Velocities in the inferred shelf facies of Unit 4 range from 3.0-4.0 km/sec. Velocities tend to increase with depth in the unit.

The seaward facies of Unit 4 is thought to represent the anastomosing, lensoid reflector pattern caused by offlapping deposition on a continental slope such as that described by Mitchum et al. (1977, p. 119, fig. 2c). Subsequent faulting and possibly movement of the inferred underlying salt have disrupted to some extent the offlap pattern in Figure 2. The interval velocity range of the slope facies of Unit 4 is 3.3-4.3 km/sec. Velocities generally increase with depth in the unit.

Unit 5. This consists of two possibly diachronous facies. The western facies beneath the inferred slope facies of Unit 4 is defined on the basis of several strong, broadly convex upward reflectors. We suggest that these reflectors may represent tops of salt pillows, as salt of Triassic-Liassic age is known both onshore and offshore in the region (Figure 1). The base of the unit is undetermined. The eastern part of Unit 5 is bounded on the top by (1) a strong reflector forming acoustic basement beneath the shelf facies of Unit 4 and (2) the Prerif basal plane east and north of SP 1500. Precambrian basement and a limestone platform of Jurassic age underlie the onshore extension of the Prerif Nappe to the east. The acoustic-basement reflector may represent the upper surface of one or the other of these units.

## Interpretation

Data summarized above suggest the following evolution of the Rharb basin margin.

1. Rifting, deposition of salt and earliest clastic rocks during Triassic-Liassic, followed by drifting in

Liassic (?) or slightly earlier time. Unit 5 is thought to belong to this phase.

2. Development of a shelf and slope on a cooling, subsiding passive margin during Jurassic (?), Cretaceous and possibly earliest Tertiary. Unit 4, and possibly Unit 5, were deposited during this interval.

Velocities ranging up to and above 4.0 km/sec in lower parts of Unit 4 suggest carbonates. Onshore wells penetrated carbonates of Jurassic age in the Rharb basin and exotic carbonate blocks of Cretaceous age occur in the shale series and Prerif Nappe. We suggest, therefore, that Unit 4 consists for the most part of middle-to-late Mesozoic carbonates, part of what may have once been a continuous carbonate bank extending from southwest Morocco into the Rharb basin. This inferred platform was broken and fragmented during the Alpine orogeny. The velocities do not preclude evaporites in Unit 4.

3. Clastic deposition on the shelf and slope and minor faulting associated with the onset of Alpine deformation. Unit 3 was deposited during this phase.

Unit 4 appears to have been deformed somewhat, then dropped downward during early phases of the Alpine orogeny to allow the deposition of Unit 3. Greater magnitudes of fault movement along the upper surfaces of Unit 4 than Unit 3 suggest that deformation began after deposition of Unit 4 and continued through deposition of Unit 3. Unit 3 probably represents clastic sediments shed from the rising Paleozoic and limestone Dorsal sequences into the incipient Rharb basin during the early stages of Rif deformation. This would make the Unit 3-4 unconformity latest Cretaceous-Eocene in age.

4. Emplacement of the Prerif Nappe by thrust faulting in the Middle Miocene. Unit 2 belongs to this phase.

The character of the basal plane of the Prerif Nappe in Figure 2 suggests a thrust fault. Its northward dip of 12½° is too steep for gravity gliding. The basal plane truncates units 3 and 4; further, it is over 7 km deep and still dipping northward where the reflection is lost at SP 1330. These facts seem inconsistent with a gravity gliding origin.

On the other hand, evidence of gravitational gliding is strong on the Atlantic seafloor north and west of Figure 2 and on land east of Figure 2. The evidence for gravity gliding, however, tends to be restricted to the outer edge of the Prerif Nappe. We interpret the data to indicate the Prerif Nappe was initiated by southward-directed thrusting rooted well to the north of its present-day outcrop. The extremely mobile matrix of the upthrust block flowed outward toward the lower elevations during, or perhaps after, faulting. Flowage created structures observed in the Rharb Basin and in the Atlantic.

The data shown in Figure 2 also suggest an explanation for the inner - outer zonation of the Prerif Nappe described in Faure-Muret and Choubert (1971). Seismic velocities of inner zone flysch, marls and exotic blocks could match velocities of subunit 2b if the inner zone contained a sufficiently large fraction of high-velocity exotic blocks. Lower velocities of subunit 2a are appropriate for the muddy, marly melange of the outer zone. Thus, uplift, southward tilting and erosion of the nappe in Figure 2 might expose an outcrop sequence similar to that described by Suter.

5. Abrupt cessation of tectonic activity followed by deposition of post-nappe slope and shelf sediments.

The Unit 1 slope facies is undeformed and the Unit 1 shelf facies deformation is probably due to compaction and minor diapiric movements in the mobile subunit 2a. Unit 1 facies appear to be prograding slightly seaward, probably as a result of increased sediment flux from erosion of the uplifted Rif sediments.

## Aauin-Tarfaya Basin - Canary Arch

### Geologic Setting

The Aauin-Tarfaya basin is one of several basins formed along the coast of Northwest Africa by post-rift subsidence. Vail et al. (in press, figure 5) show the outer shelf of the Aauin-Tarfaya basin underlain by over two seconds of Jurassic and Cretaceous sediments covered by a Tertiary veneer. An additional two-plus seconds of Triassic and older (?) sediments lie beneath the Jurassic. Average sedimentary velocities for rocks of equivalent age and depth suggest a total section thickness in excess of 8 km. Tertiary deep-sea sediments lap up on the Cretaceous slope. Most pinch out but a few continue up onto the shelf with greatly decreased thicknesses.

In late Cretaceous, marine transgression into the region of the Souss Trough presaged the elevation and deformation of the Atlas during Pyreneic (post-Lutetian) phase in late Eocene time (Choubert et al., 1965). More intense folding of the Atlas followed during pre-Aquitanian compression at the Miocene-Oligocene boundary (Allard et al., 1958).

The South Atlas lineament (Figure 1) separates the High Atlas to the north from the Anti-Atlas to the south. Dillon and Sougy (1974) note that this controversial lineament (or fault?) marks the boundary between more or less unfolded miogeosynclinal Paleozoic rocks of the Tindouf basin and Anti-Atlas and Paleozoic eugeosynclinal facies in the High Atlas. Dewey et al. (1973) interpret it as a right-lateral transform fault active in early phases of opening of the Atlantic, but locked shut after Middle Jurassic. LePichon and Fox (1971) extend the lineament through the Kelvin Seamounts and connect it with the 40°N fault of the northeastern U. S. continental margin. The feature marks the southern limit of Alpine orogeny in north Africa (Choubert and Marais, 1952). Pliocene downwarping and sedimentation in the Souss Trough represent the latest major movement near the lineament. It is still seismically active.

Numerous investigators (e.g. Lehner and DeRuiter, 1977; LePichon and Fox, 1971) have remarked on the apparent alignment of the South Atlas lineament, the southern margin of the salt basin, and the southern limit of the Canary Islands. This alignment is suggested as evidence of a major fracture zone extending offshore at this point.

The location of the ocean-continent boundary in the Canary Island region is in dispute. Uchupi et al. (1976) concluded that existing evidence favored attenuated

continental crust underlying much of the region between the coast and the Canary Islands. Von Rad and Arthur (this volume) suggest the boundary lies beneath the lower continental slope. Thick salt deposits in the Red Sea and Gulf of Mexico lie on continental crust in those regions where subsalt crustal character can be determined. Thus, salt diapirism in the Canary gap would seem to support the existence of continental crust in the gap. Seismic refraction data from the gap (P. Goldflam, K. Hinz and W. Weigel, pers. comm.) are equivocal. They show about 8 km of 5.6 km/sec material overlying an unknown thickness of 7.3 km/sec material.

Oceanic rocks are included in the basement series of the Canary Islands (Uchupi et al., 1976). The seismic signature of the acoustic basement west of the Islands and linear seafloor-spreading magnetic anomalies indicate that oceanic crust extends into the Canary Arch from the west (Uchupi et al., 1976). Thus, the Canary Islands evidently formed on oceanic crust.

Initial uplift of the Canary Arch occurred not earlier than middle Cretaceous and not later than Miocene. Robertson and Stillman (1979) suggest an Albian age for initial uplift based on their studies of Fuerteventura sediments. They interpret the sedimentary sequence as indicating localized uplift in the Albian, followed successively by a hiatus, extrusion of alkalic submarine volcanic rocks, folding, and finally intrusion of a sheeted dike complex beginning in Eocene and ending in Mid-Miocene. This sequence of events suggests crustal uplift, compression and extension, all synchronous with High Atlas orogenic events.

Grunau et al. (1975) infer an Eocene-Middle Miocene age of the initial uplift based on K-Ar studies in Fuerteventura (Canary Islands), Maio (Cape Verde Islands), and Sao Tome (Gulf of Guinea). They interpret coincident ages of early magmatic phases in these localities as indicative of a change in the regional stress field of the crust, probably as a result of collision of African and Euro-Asian plates.

Von Rad and Arthur (this volume) conclude that no subaerial Canary Ridge existed during Mesozoic to Eocene times. They find the earliest datable volcanic event evidenced in Site 397 cores is a submarine shield-building stage of early Miocene age.

## Discussion of Results and Interpretation

Salt Basin. Seismic data show a moderately thick section of sediments intruded by numerous diapirs, probably salt. Correlation of deeper units in the center of the zone are necessarily uncertain as the diapirs disrupt the reflectors. We have more confidence in ages of units along the margins of the diapir zone where we are able to tie reflectors to wells. The slope data are tied to Exxon wells via proprietary and published (Vail et al., in press) data. Deep ocean data are tied to DSDP hole 415 via BGR line 3902 (H.-J. Dostmann, pers. comm.). Consequently, diapir zone units are only approximately time-equivalent to Canary Arch units.

In the Salt Basin (Figure 3), we recognize 6 units. Relatively flat-lying reflectors, broken across some but not all diapirs, characterize Unit 1 of Plio-Pleistocene age. Unit 1 rests unconformably on Unit 2 of probably Pliocene-Late Miocene age. Unit 2 thickens to a maximum of approximately 800 m or more under the lower rise, then thins toward the Canary Arch. S , of the Salt Basin, east of SP 1730, the base of Un. 2 lies in an erosional channel cut into the upper part Unit 3. An analogous channel may be responsible for the thickening of Unit 2 in the outer part of the zone.

Units 3 and 4 attain maximum thicknesses lo.. shore and Unit 5, as shown by Vail et al. (in press), attains its maximum thickness closer to shore than Units 3 and 4, indicating that the lower slope-upper rise has prograded seaward during the time interval represented by Units 3, 4, and 5. Units 3 and 4 are probably Miocene in age. The Oligocene unconformity underlies Unit 4. Unit 5 is thought to be mainly Lower Cretaceous in this section, and Unit 6 (whose base is not evident in Figure 3) is thought to be the Jurassic carbonate sequence.

Diapirs in Figure 3 are unusual in that they lack rim synclines indicative of salt withdrawal as are often seen in other areas such as Sigsbee Knolls of the Gulf of Mexico (see e.g. Watkins et al., 1976).

The Jurassic magnetic quiet zone north of the Canary Islands is wider than it is to the south of the Canary Islands (Dewey et al , 1973). This together with the termination of salt diapirs at approximately the same location as the change in width of the quiet zone, suggests that the diapirs derive from a thick salt layer deposited in a rift valley floored by thinned continental crust or possibly floored in part by early-formed oceanic crust destined to become an initial segment of the Atlantic Ocean. A transform fault probably terminated the rift valley south of the salt basin along the present day southern boundary of the Canary Islands.

Poor resolution of early Mesozoic reflectors prohibits drawing any inferences about the character of the South Atlas lineament within the diapir zone prior to Tertiary time. We see no evidence of tectonic activity attributable to movements along the South Atlas fault during the Alpine orogeny. Although the trace of a major fault could lie hidden within a diapir, significant movement should produce observable changes in the depositional patterns of the Tertiary sediments within the salt basin. Absence of marked changes in thickness and seismic character suggests that any genetic link between Alpine deformation in the Atlas Mountains and uplift and volcanism in the Canary Islands did not take the form of a connecting fracture zone.

Canary Arch. We divide the seismic section in this area into 7 units (Figure 3). Differences in seismic character suggest further division into eastern and western reflector facies. Reflectors in the facies east of the Arch are relatively flat, whereas reflectors west of the Arch are sinuous and sometimes discontinuous.

As mentioned earlier, reflectors have been tied to DSDP Hole 415 via R/V METEOR line 3902 shot by the Bundesanstalt fur Geowissenschaften und Rohstoffe (BGR - The Federal German Geological Survey). The connecting section of 3902 consists of single-channel analog data, and individual cycles cannot be followed everywhere. Hence, ties may be slightly in error. However, the pronounced character of reflectors in this area facilitates correlation and enhances our confidence in age attributions. The location of the intersection of METEOR line 3902 and the GULFREX line is shown in Figure 3.

The following table summarizes our attribution of unit ages.

The large number of unconformities, some representing sizeable gaps in time (Lancelot, Winterer, et al., 1977), the thick slide reported in Hole 415, slumps discussed later in this paper, and the buried channel in the vicinity of SP 1600 suggest that seafloor erosion has been active in this area at least throughout the Tertiary.

Patterns of erosion and deposition over the Canary Arch indicate that Canary Arch uplift is post-Middle Cretaceous and pre-Early Eocene. Unit 5, of predominantly Middle Cretaceous age, shows no effects of the uplift except for erosion of the upper surface of the unit. Reflector intervals thin uniformly seaward, passing over the Arch with no apparent change in rate of thinning. The top of Unit 5 is eroded, the largest amount of missing section occurring at the crest of the arch and the least amount occurring in the swale in the vicinity of SP 1600. This suggests that Unit 5 was uplifted and eroded during the time interval represented by the overlying unconformity, i.e. Late Cretaceous-Paleocene.

Sinuous, discontinuous reflectors within Units 5 and 6 (vicinity SP 0100) and the presence of magnetic anomalies suggest that igneous activity west of the Arch may have begun earlier than Eocene as suggested by Robertson and Stillman (1979). Alternatively the sinuous reflectors may represent oceanic basement or intrusives.

Unit 4 of inferred Eocene age thins perceptibly over the crest of the Arch, indicating that uplift began prior to deposition. Volcanics and volcaniclastics evident between SPs 0300 and 0430 indicate volcanic activity during the Eocene, coincident with results of Grunau et al. (1975) from other volcanic islands off northwest Africa. Seismic reflection data thus suggest that uplift of the Arch and volcanic activity began during or prior to Eocene time.

The top of Unit 4 - base of Unit 3 is thought to be equivalent to the BGR tan reflector, found in DSDP Hole 370/416 to be a late Oligocene unconformity. The tan reflector could not be followed from Hole 370/416 to Hole 415 (Lancelot, Winterer, et al., 1977) but drilling revealed an unconformity between units of Eocene and early Miocene age at an appropriate depth. Oligocene rocks in Hole 415 may have been missed due to the intermittent nature of core collection.

Unit 3 lies between the Oligocene unconformity and the BGR brown reflector of Middle Miocene age. No unconformity correlative with the brown reflector was found in Holes 370/416 and 415, nor was an unconformity noted at the Unit 1 - Unit 2 contact, whereas both are clearly unconformable in the seismic data, especially near SP 1600.

## Villa Cisneros

### Geologic Setting

Evidence of seafloor erosion in seismic sections is corroborated by DSDP Holes 369 (Lancelot, Seibold, et al., 1978) and 397 (Ryan, von Rad and Arthur, this volume) which penetrated unconformities representing major hiatuses off Cape Bojador. The largest hiatus identifed in the lower slope by Hole 397 ranged in age from Hauterivian to early Miocene and that found in Hole 369 from Maestrictian to middle Eocene. Von Rad and Arthur (this volume) observes that 4,000 - 15,000 $km^3$ of lower slope sediments were removed, probably during late Eocene-Miocene time. Numerous less dramatic unconformities also exist as noted in the above discussion. Vail et al. (in press) identify 28 major unconformities in the area ranging in age from basal Sinemurian through basal Messinian.

Much of the eroded material was transported into deeper waters of the Atlantic either grain by grain or as

TABLE 1

| Unit | Comment | Age |
|---|---|---|
| 1 | | Pleistocene |
| 2 | BGR brown refl. at base | Middle Miocene-Pliocene |
| 3. | BGR tan refl. at base Oligocene unc. | Early-Middle Miocene |
| 4 | BGR red refl. at base (near base Tertiary) | Early-Eocene |
| 5 | Base - Top L. Cretaceous | Middle Cretaceous |
| 6 | | Early Cretaceous and older |
| 7 | Acoustic basement | Variable, Cretaceous to Pre(?) Jurassic |

*BGR data published by Lancelot, Winterer, et al. (1977), referred to reflectors by a color scheme. The above notes how our data tie to BGR data.

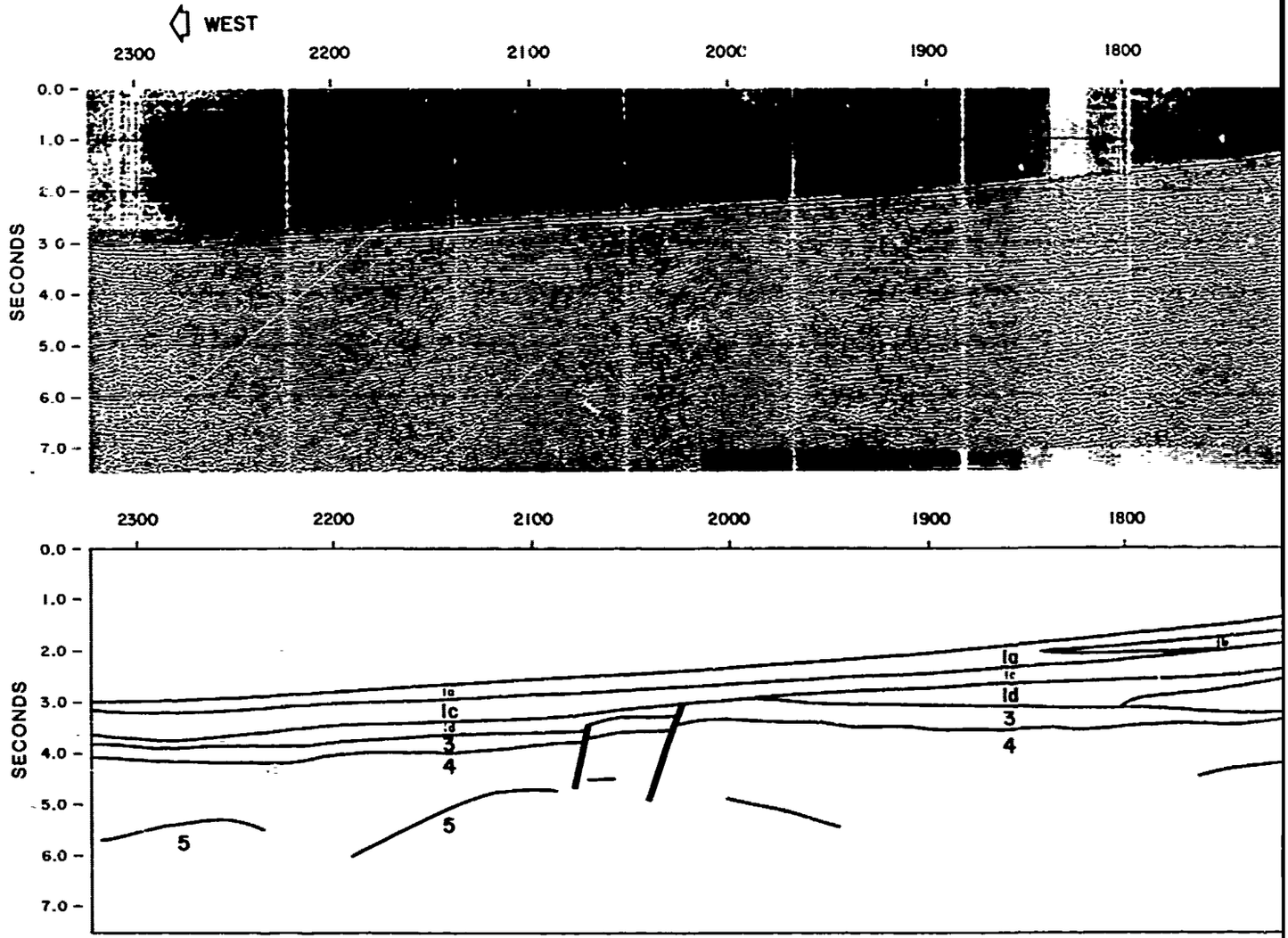


Figure 2. Seismic section and matching line drawing from offshore Rharb Basin. Units are as sediments, (1a) Vp = 1.8-2.0 km/sec, (1b) Vp = 2.0-2.2 km/sec, (1c) Vp = 2.3-2.6 km/sec, (1d) (Tortonian), (2a) Vp = 2.7-3.1 km/sec, except in western extremity where Vp = 2.5 km/sec, (2b Vp = 2.4-2.7 km/sec, (4) Paleo shelf (east) and slope (west) of Cretaceous (?) age, probably 3.3-4.3 km/sec (slope), (5) possibly Triassic-Liassic sal- in western part, Precambrian baseme

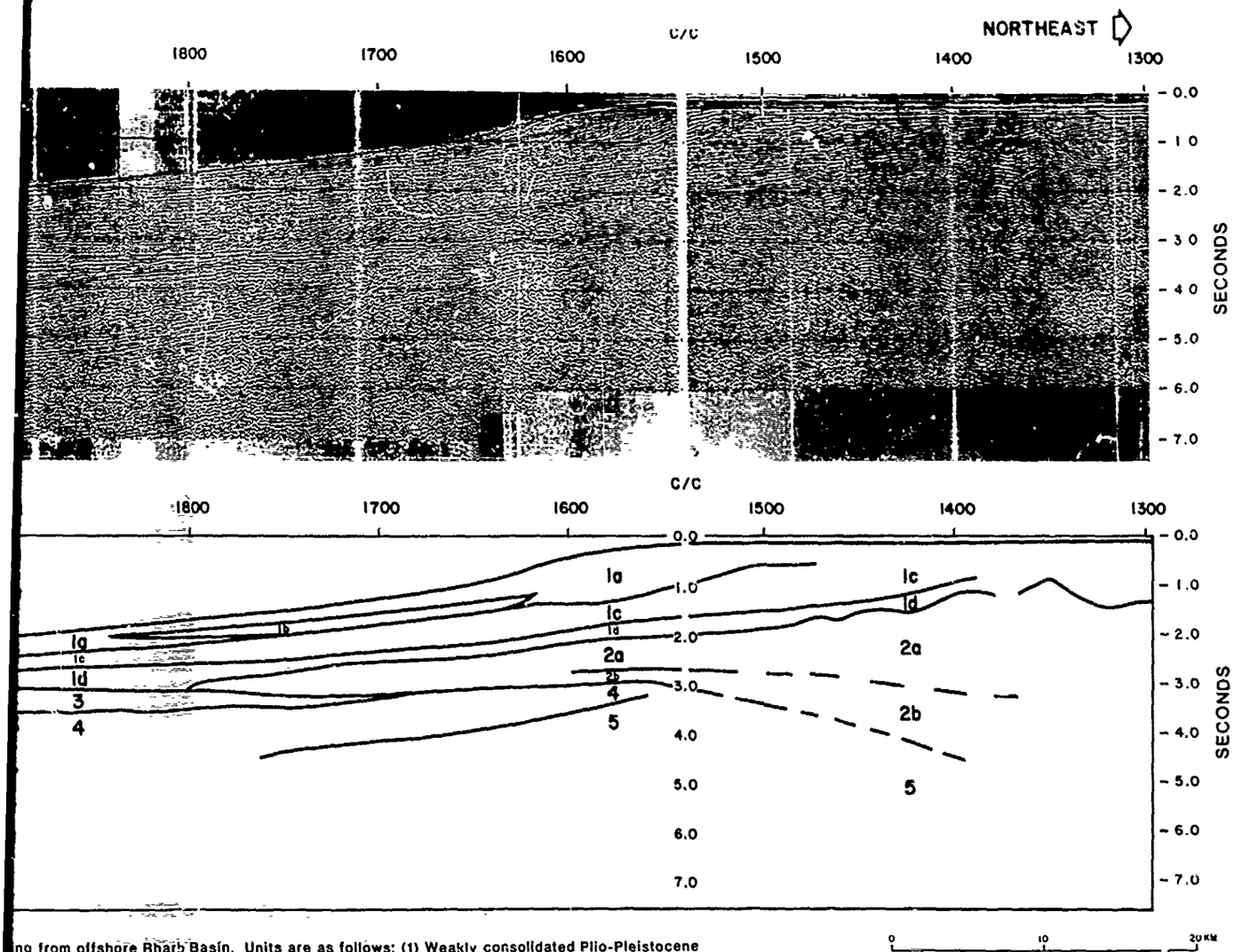


ng from offshore Rharb Basin. Units are as follows: (1) Weakly consolidated Plio-Pleistocene
-2.2 km/sec, (1c) Vp = 2.3-2.6 km/sec, (1d) Vp = 2.7 km/sec, (2) Prerif Nappe, Middle Miocene
estern extremity where Vp = 2.5 km/sec, (2b) Vp = 2.7-4.8 km/sec, (3) Lower Tertiary (?) clastics,
ope (west) of Cretaceous (?) age, probably mainly carbonates, Vp = 3.0-4.0 km/sec (shelf) and
sic salt in western part, Precambrian basement and/or Jurassic carbonates in eastern part.

2

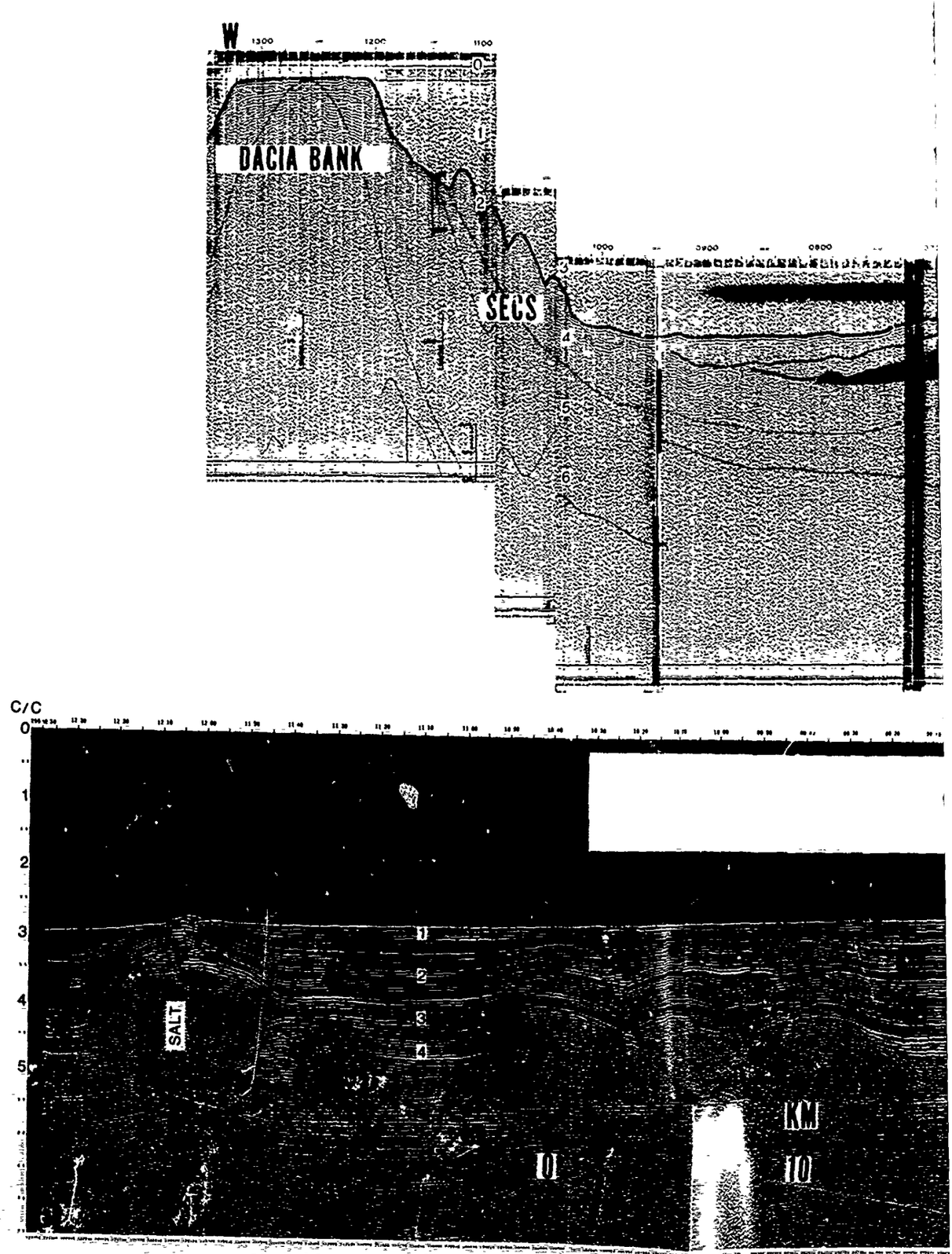


Figure 3. Seismic section fro northern Tarfaya basin to
ity at base (4). (5)probably L.wer Cretaceous and (6)prob
Paleocene-Eocene with base Ter iary unconformity at base
from Cretaceous to Jurassic a.d possibly older. "Meteor

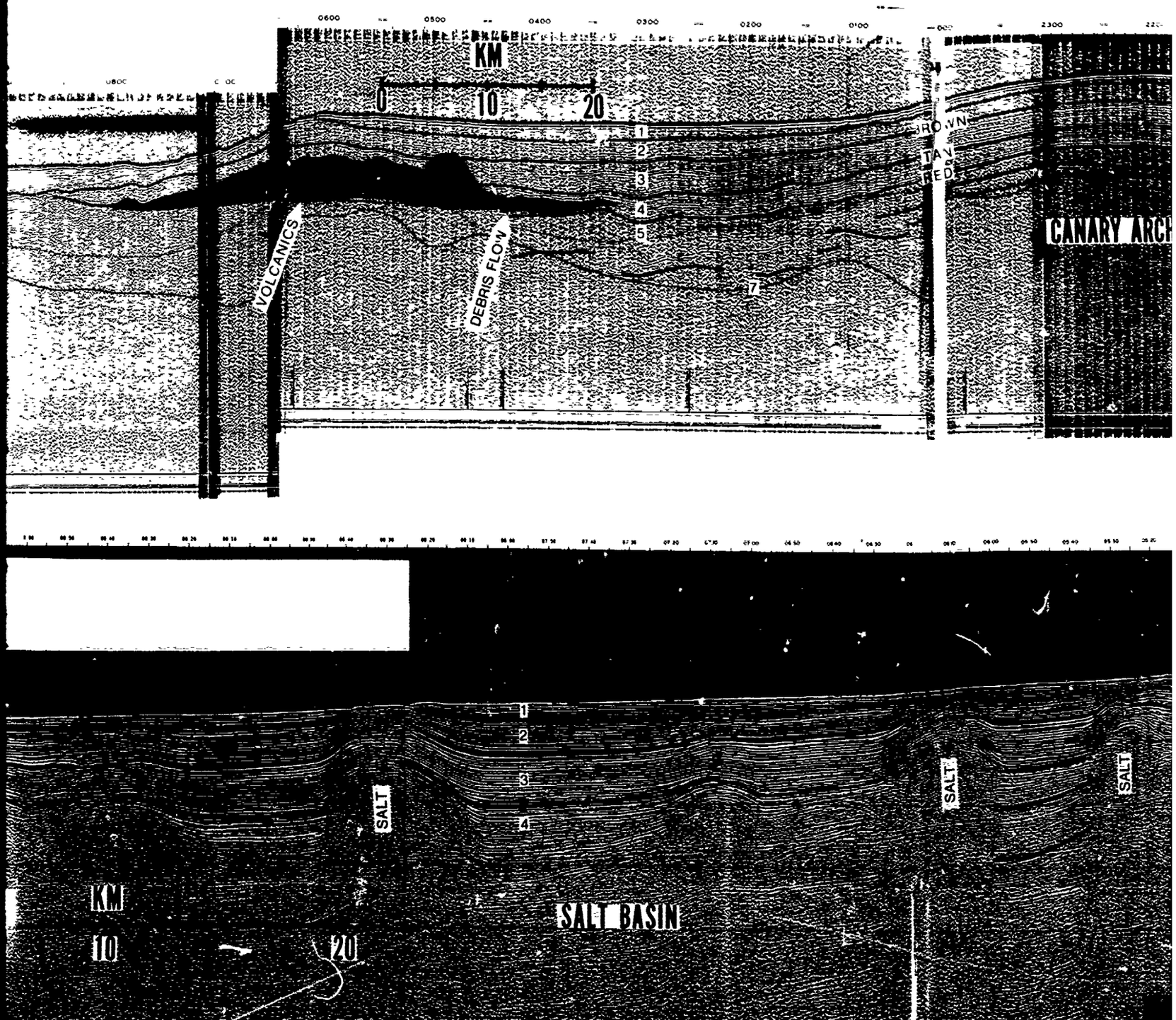





m northern Tarfaya basin to vicinity Dacia Bank. Salt basin. Ages of units are inferred as follows: (1) Plio-Pleistocene, (2) L
ower Cretaceous and (6) probably Jurassic carbonates. Canary Arch-Dacia Bank. (1) Pleistocene, (2) Middle Miocene-Pliocene, (3) Early
rtiary unconformity at base. Note this unit not equivalent to 4 in the Salt Basin, (5) Middle Cretaceous, Early Cretaceous and ol
nd possibly older. "Meteor 3902" indicates location of intersection with seismic section tying data to DSDP hole 415. Note chan

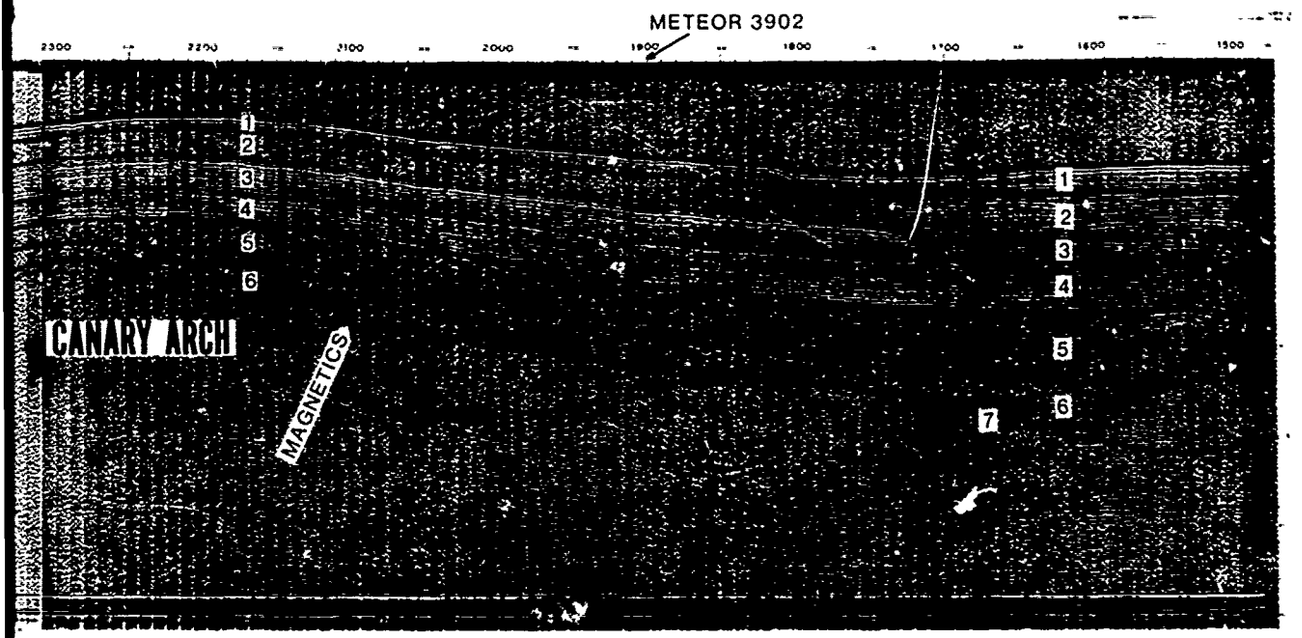


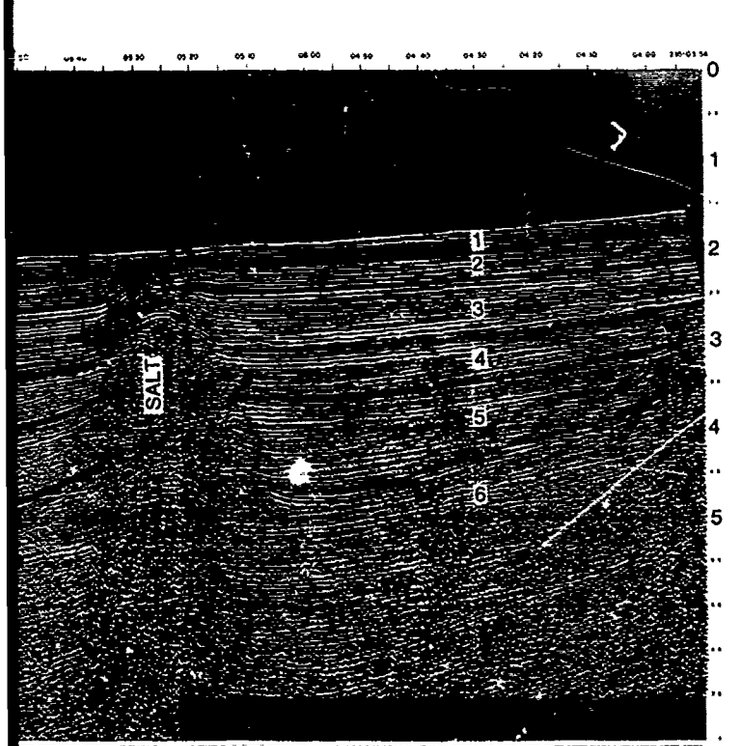


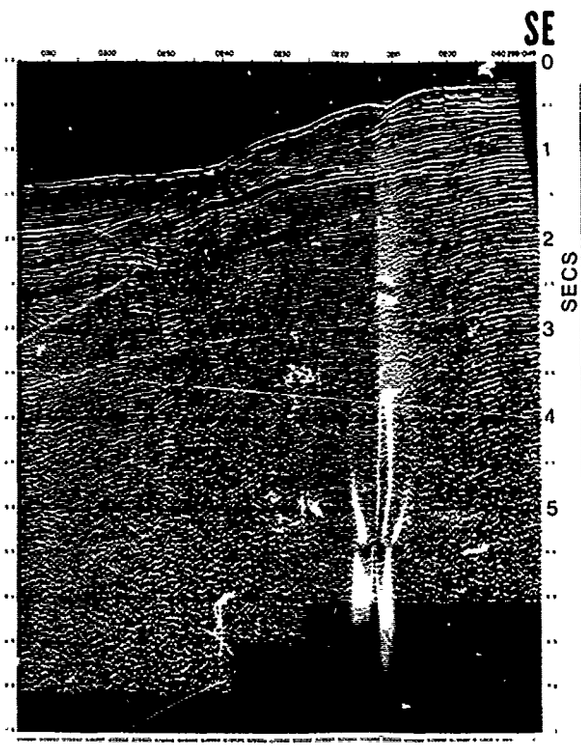


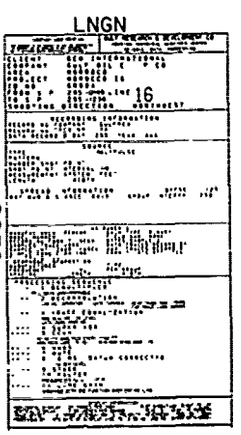


Pleistocene, (2)Late Miocene-Pliocene, (3)and(4)Miocene with Oligocene unconform-
iocene, (3)Early Middle Miocene with Oligocene unconformity at base, (4)
retaceous and older(?), (6)Middle Mesozoic, and (7)Basement, age ranges
415. Note change in horizontal scale on either side of course change at 12:38.

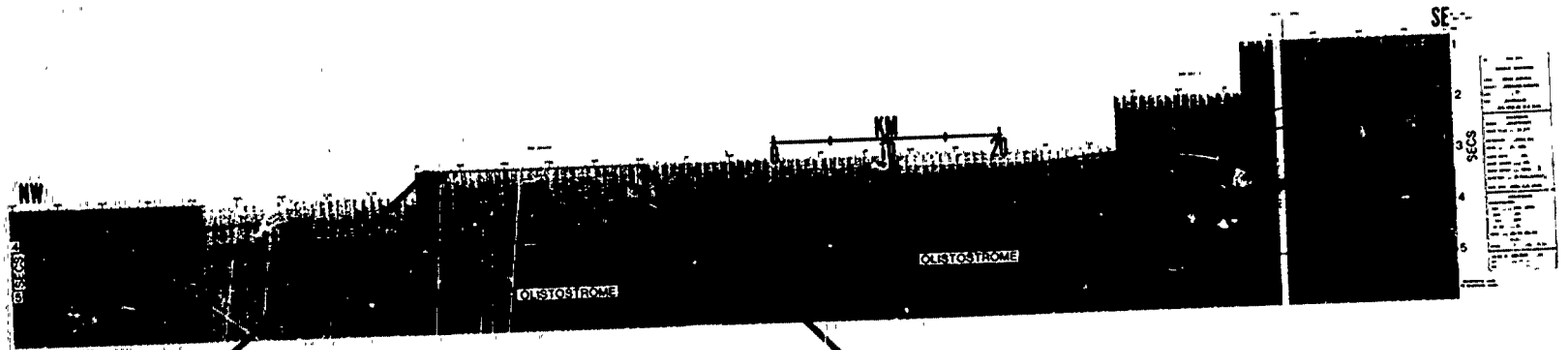


Fig. 4a

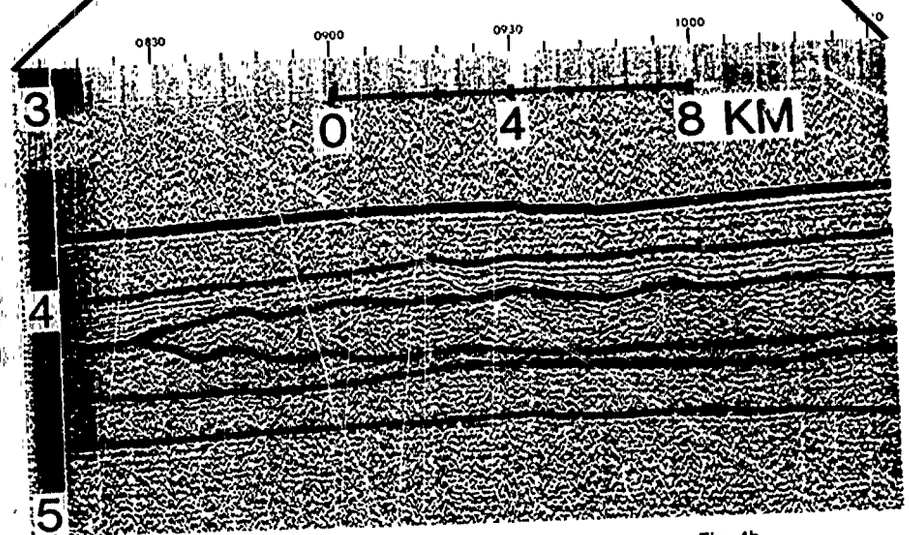


Fig. 4b

Figure 4. (4a) Interpreted section showing occurrence of olistostromes of Middle Tertiary (?) age deposited beneath the slope and rise seaward of Villa Cisneros; (4b) Seismic section showing distal edge of an olistostrome. Note ripply upper surface, scouring and erosion along base, and poor coherency of reflectors within the flow. Reflectors above and below tend to be subhorizontal except for thin zone on top of the flow.

part of turbidite flows, but some sediments were transported as olistostromes or debris flows.The "slope anticline" (Figure 1; Seibold and Hinz, 1974; Uchupi et al., 1976; Todd and Mitchum, 1977, Fig. 9, p. 157), especially the northern part, dramatically shows erosion and mass wasting, much of it by slumping. One such flow was reported from DSDP Hole 415 (Lancelot, Winterer, et al., 1977).

## Discussion of Results

The extreme eastern part of Figure 4a shows the outer edge of the slope anticline. Two major unconformities and faults at bases of prominent slumps are marked. Debris flows of varying magnitude, such as those of Figures 4a and 4b, can be seen in other seismic sections. A seismic line to the north of that shown in Figure 4 (see Figure 1) also shows flow units at the same depth that are probably extensions of those in Figure 4. The seismic data suggest that the aggregate volume of flows shown in Figures 1 and 4 is about $10^4$ $km^3$, which represents a significant fraction of material removed from the slope anticline (Hinz et al., 1974). Price (in press) shows data indicating that the volume of the flow found in DSDP Hole 415 was probably larger than that of the flows in Figure 4.

## Interpretation

We have been unable to obtain reliable ages for reflectors in Figure 4 by ties to DSDP holes, but if sedimentation rates are roughly equivalent to those observed in DSDP Holes 397, 415 and 370, the slumps are probably mid-Tertiary in age. Prominent Oligocene and Miocene unconformities on the slope are probably equivalent in age to these slumps. It is interesting that the slumps were emplaced with sufficient vigor to scour the underlying seafloor in places (Fig. 4b).

Gravity gliding, debris flows and turbidite flows are common off the Atlantic margin of northwest Africa. Possibly they were triggered to some extent by earthquakes as was the case during the 1929 Grand Banks earthquake off the eastern coast of North America. The large slumps appear as subtle features on seismic sections; the flow in DSDP Hole 415 was not recognized prior to drilling. This flow may be present in Figure 3, but we cannot conclusively identify it because of the poor resolution deeper in the section. We suggest, therefore, that gravity sliding, olistrostrome and coarse debris flow emplacement may be a more important mechanism of submarine deposition than generally recognized.

Acknowledgements: We gratefully acknowledge the contribution of Bundesanstalt fur Geowissenschaften und Rohstoffe, notably K. Hinz, H.-J. Dostmann, U. von Rad and G. Wissman, who provided seismic reflection data used in age correlations, and who also provided fruitful discussion of the geologic evolution of northwest Africa. William P. Dillon of U. S. G. S. and Bernard Biju-Duval of I. F. P. provided many worthwhile comments. P. Vail of Exxon contributed ideas regarding the seismic stratigraphy of the region. Our colleagues at Gulf contributed much during informal discussion. Gulf Oil Exploration and Production Corporation provided the data shown in Figures 2-4.

## References

Allard, P. L., E. Cochet, and F. Duffand, L'Oligocene dans le Haut Atlas Occidental, Notes Mem. Serv. Geol. Maroc, 143, 7-16, 1958.

Association des Services Geologiques Africains, and UNESCO, Carte tectonique internationale de l'Afrique, 1:5,000,000, general coordinator, G. Choubert, International Geological Congress, 1968.

Choubert, G., and J. Marais, Geologie du Maroc in 19th Intl. Geol. Cong., Rabat, Regional Mans., 3d Ser., Maroc. 6, Apercu Structural, pp. 1-73, 1952.

Choubert, G., M. Diouri, and A. Faure-Muret, Mesures geochronologiques recentes par la methode $A^{40}/K^{40}$ au Maroc, Notes Mem. Serv. Geol. Maroc, 183, 53-62, 1965.

Dewey, J. F., W. C. Pitman, III, W. B. F. Ryan, and J. Bonnin, Plate tectonics and the evolution of the Alpine System, Geol. Soc. Amer. Bull., 84, 3137-3180, 1973.

Dillon, W. P., and J. M. A. Sougy, Geology of West Africa and Canary and Cape Verde Islands in The Ocean Basins and Margins, Volume 2, the North Atlantic, edited by A. E. M. Nairn and F. G. Stehli, pp. 315-390, Plenum Press, New York, 1974.

Faure-Muret, A. and G. Choubert, Le Maroc. domaine rifain et atlasique in Tectonique de l'Afrique, Sciences de la terre (6), pp. 17-46, UNESCO, Paris, 1971.

Grunau, H. R., P. Lehner, M. R. Cleintaur, P. Allenbach, and G. Bakker, New radiometric age and seismic data from Fuerteventura (Canary Islands), Maio (Cape Verde Islands) and Sao Tome (Gulf of Guinea) in Progress in geodynamics, pp. 89-118, Roy. Soc. Neth. Acad. Arts and Sc., Amsterdam, 1975.

Hinz, K., E. Seibold, and G. Wissman, Continental slope anticline and unconformities off West Africa, METEOR Forschung Ergebnise, c-1, 67-73, 1974.

Lajat, D., B. Biju-Duval, R. Gonnard, J. Letouzey, and E. Winnock, Prolongement dans l'Atlantique de la partie externe de l'Arc betico-rifain, Bur. Serv. Geol. Fran., 17, 481-485, 1975.

Lancelot,Y., E. Seibold, et al., Site 369: continental slope off Cape Bojador Spanish Sahara in Initial Reports of the Deep Sea Drilling Project, vol. 41, pp. 327-420, U. S. Government Printing Office, Washington, D. C., 1978.

Lancelot, Y., E. L. Winterer, et al., Documenting early rifting, Geotimes, April, 24-27, 1977.

Lehner, P., and P. A. C. DeRuiter, Structural history of Atlantic margin of Africa, Amer. Assoc. Petrol. Geol. Bull., 61, 961-981, 1977.

LePichon, X., and P. J. Fox, Marginal offsets, fracture zones and the early opening of the North Atlantic, J. Geophys. Res., 76, 6294-6308, 1971.

Mitchum, R. M., P. R. Vail, and J. B. Sangree, Seismic stratigraphy and global changes in sea level, Part 6: Stratigraphic interpretation of seismic reflection patterns in depositional sequences in Seismic Stratigraphy - Application to Hydrocarbon Exploration, Amer. Assoc. Petrol. Geol. Mem. 26, edited by C. E. Payton, pp. 83-98, American Association of Petroleum Geologists, Tulsa, Oklahoma, 1977.

Price, E., Gravity tectonics on a passive margin: IPOD Site 415 in the light of regional seismic data in Initial Reports of the Deep Sea Drilling Project, vol. 50, U. S. Government Printing Office, Washington, D. C., in press.

Robertson, A. H. F., and C. J. Stillman, Late Mesozoic sedimentary rocks of Fuerteventura, Canary Islands: Implications for West African continental margin evolution, Jour. Geol. Soc. London, 136, in press.

Schlee, J., J. C. Behrendt, J. A. Grow, J. M. Robb, R. E. Mattick, P. T. Taylor, and B. J. Lawson, Regional geologic framework off northeastern United States, Amer. Assoc. Petrol. Geol. Bull., 60, 926-951, 1976.

Seely, D. R., P. R. Vail, and G. G. Walton, Trench slope model in The Geology of Continental Margins, edited by C. A. Burk and C. L. Drake, pp. 249-260, Springer-Verlag, New York, 1974.

Seibold, E., and K. Hinz, Continental slope construction and destruction, West Africa in The Geology of Continental Margins, edited by C. A. Burk and C. L. Drake, pp. 179-196, Springer-Verlag, New York, 1974.

Todd, R. G., and R. M. Mitchum, Seismic stratigraphy and global changes of sea level, Part 8: Identification of Upper Triassic, Jurassic and Lower Cretaceous seismic sequences in Gulf of Mexico and offshore West Africa in Seismic Stratigraphy-Applications to Hydrocarbon Exploration, Amer. Assoc. Petrol. Geol. Mem. 26, edited by C. E. Payton, pp. 145-163, American Association of Petroleum Geologists, Tulsa, Oklahoma, 1977.

Uchupi, E., K. O. Emery, C. O. Bowin, and J. D. Phillips, Continental margin off western Africa: Senegal to Portugal, Amer. Assoc. Petrol. Geol. Bull., 60, 809-878, 1976.

Vail, P. R., R. M. Mitchum, T. H. Shipley, and R. T. Buffler, Unconformities of the North Atlantic in the evolution of passive continental margins in the light of recent drilling results, Phil. Trans. Royal Soc., London, in press.

Vail, P. R., R. M. Mitchum, and S. Thompson, III, Seismic stratigraphy and global changes in sea level, Part 4: Global cycles of relative change in sea level in Seismic Stratigraphy-Applications to Hydrocarbon Exploration, Amer. Assoc. Petrol. Geol. Mem. 26, edited by C. E. Payton, pp. 145-163, American Association of Petroleum Geologists, Tulsa, Oklahoma, 1977.

Von Rad, U., and M. A. Arthur, Geodynamic, sedimentary and volcanic evolution of the northwest African margin (Cape Bojador-Canary Islands): paleoenvironment, slope rejuvenation and gravitative deposition in 2d M. Ewing Symp., this volume.

Watkins, J. S., J. W. Ladd, F. J. Shaub, R. T. Buffler, and J. L. Worzel, Seismic section WG-3, Tamaulipas shelf to Campeche Scarp, Gulf of Mexico, Amer. Assoc. Petrol. Geol., Seismic Section No. 1, 1976.

# SUBSIDENCE AND EUSTASY AT THE CONTINENTAL MARGIN OF EASTERN NORTH AMERICA

A. B. Watts and M. S. Steckler

Lamont-Doherty Geological Observatory and Department of Geological Sciences
of Columbia University, Palisades, New York 10964

Abstract. Biostratigraphic data from the COST B-2 well off New York and four deep commercial wells off Nova Scotia have been used to remove the effect of sediment loading at the Atlantic-type continental margin off the East Coast, North America. The resulting subsidence contains terms due to both "tectonic" and "eustatic" effects. By assuming the tectonic subsidence is thermal in origin these effects can be separated. The "eustatic" effects have been isolated by least squares fitting an exponential curve to the subsidence data. The resulting sea-level curve shows a maximum rise in sea-level during the Late Cretaceous (about 75-80 m.y.B.P.) which probably does not exceed 150 meters. The tectonic subsidence has been interpreted in terms of a simple thermal model for the cooling lithosphere. Based on this model the thermal thickness of the lithosphere and the total amount of crustal thinning are estimated. These estimates which are consistent with surface ship gravity and GEOS-3 altimeter measurements are used to define the structural elements which control the tectonic evolution of the margin.

## Introduction

The Atlantic-type continental margin off the East Coast of North America comprises a substantial thickness ($\gtrsim$ 12 km) of seaward dipping Mesozoic and Tertiary sediments (for example, Sheridan, 1974; Schlee et al., 1976; Jansa and Wade, 1974). Biostratigraphic data from deep commercial boreholes in the outer continental shelf (Scholle, 1977; Gradstein et al., 1975; Jansa and Wade, 1975) show that a large proportion of these sediments were deposited in shallow-water environments. Such large thicknesses of shallow-water sediments cannot be caused by the effects of sediment loading alone and other factors must contribute to the observed subsidence.

A number of authors (Sleep, 1971; Artemjev and Artyushkov, 1971, Bott, 1973; Falvey, 1974; McKenzie, 1978) have discussed the origin of the subsidence of Atlantic-type margins. A useful approach (Sleep, 1971; Watts and Ryan, 1976; Steckler and Watts, 1978) is to account quantitatively for the effect of sediment loading and isolate that part of the subsidence which is not caused by the weight of the sediments. Sleep (1971) corrected for sediment loading using stratigraphic data from more than 35 commercial boreholes in the U.S. coastal plain. He showed that the subsidence not caused by sediment loading was exponential in form and that it was probably thermal in origin. Watts and Ryan (1976) used biostratigraphic data from the Gulf of Lion in the western Mediterranean and showed that the subsidence was similar in form to the empirical ocean ridge curve, and Steckler and Watts (1978) used biostratigraphic data from the COST B-2 well off New York and showed that the subsidence could be interpreted in terms of a simple thermal model for the lithosphere.

In order to quantitatively evaluate and remove the effect of sediment loading two procedures should be followed (Steckler and Watts, 1978). First, use biostratigraphic data to reconstruct the sedimentary section during the development of the margin. Second, "backstrip" the sedimentary section to obtain the subsidence not caused by the weight of sediments.

The resulting subsidence of the margin, however, is affected by world-wide changes in sea-level through time. These changes act as an additional load of water on the basement. Sleep (1971) and Watts and Ryan (1976) did not correct for sea-level changes. Steckler and Watts (1978) corrected for sea-level changes using Pitman's (1978) curve, based on changes in ridge crest volumes and Vail et al. (1977) curve based on seismic stratigraphy. Steckler and Watts (1978) showed that this correction was large and that it significantly altered the shape of the subsidence curve.

There is a difficulty, however, in determining a sea-level curve because "tectonic" and "eustatic" effects cannot be easily separated (for example, Fairbridge, 1961; Hallam, 1963). For example, Pitman (1978) assumed a single, constant hypsometric curve for the continents through time. Differential changes in continental hypsometry, however, may have significantly altered this curve (Bond, 1978).

There is now good evidence that the subsidence of Atlantic-type margins not caused by the

effects of sediment loading is thermal in origin (Sleep, 1971; Watts and Ryan, 1976; Steckler and Watts, 1978). Thermal models predict that the subsidence is a function of age and is exponential in form. It should therefore be possible at a margin to separate the thermal or "tectonic" part of the subsidence and isolate that part caused by "eustatic" changes in sea-level.

The purpose of this paper is to use biostratigraphic data from five wells off the East Coast, North America (Fig. 1) to quantitatively understand the origin of the subsidence of Atlantic-type continental margins. By assuming the subsidence is thermal in origin we can separate "tectonic" and "eustatic" effects. The "eustatic" effects are interpreted in terms of a new sea-level curve and the "tectonic" effects in terms of a simple thermal model for the cooling lithosphere. This model is used to place constraints on the evolution of the margin.

## Data Reduction

Biostratigraphic data from the five wells off the East Coast, North America (Fig. 1) have been used to remove the effect of sediment loading at the margin. We have used the "backstripping" technique described by Steckler and Watts (1978) assuming the Airy model of isostasy. In this case "backstripping" each stratigraphic horizon can be summarized by the equation

$$Y = S^* \left[\frac{(\rho_m-\rho_s)}{(\rho_m-\rho_w)}\right] + W_d - \Delta SL \left[\frac{\rho_m}{(\rho_m-\rho_w)}\right] \quad (1)$$

where $\rho_m$ is the average mantle density, $\rho_w$ is the average water density, and $\rho_s$ is the average sediment density. Y is the depth to basement without sediment and water loads and represents the subsidence caused by "tectonic" effects. S* is the sediment thickness corrected for compaction, $W_d$ is the water depth at the time of deposition, and $\Delta_{SL}$ is the elevation of mean sea-level. The right hand term in equation 1 therefore represents the subsidence caused by "eustatic" effects.

The five wells (Fig. 1) are located in different tectonic settings along the margin (Jansa and Wade, 1975; Scholle, 1977). The Naskapi N-30 (Fig. 2) and Mohawk B-93 wells are located on the slowly subsiding La Have platform, and the Sable Island C-67 and COST B-2 (Fig. 2) wells are located in deep sedimentary troughs. The Oneida O-25 (Fig. 2) well is located near a hinge zone separating these two tectonic environments.

We summarize the stratigraphy of each of the five wells in Figure 3. The wells penetrated sediments which range in age from Middle to Latest Jurassic (Fig. 3; Williams, 1975; Smith et al., 1976). The sediments comprise a sequence of mainly sands and shales with only a small amount of carbonate rocks.

To correct for the effect of compaction (equation 1) we utilized downhole sonic and density logs for each well to determine the variation of porosity with depth (Fig. 4). For the COST B-2 well we used the sonic and density log porosity values tabulated in Rhodehamel (1977), and for wells off Nova Scotia we examined the original Schlumberger sonic and density logs. By assuming that the porosity versus depth curve has remained constant we calculated the thickness and average density of each horizon as it appeared through geologic time. In these calculations we used a uniform grain density of 2.70 g/cm$^3$ for the wells off Nova Scotia and 2.65 g/cm$^3$ for the COST B-2 well (Rhodehamel, 1977). We also assumed that the porosity values at the base of these wells could be extrapolated to great depth.

The paleo-water depths required for each well (equation 1) are summarized in Figure 5. Estimates of paleo-water depth for the COST B-2 well are based on dinoflagellates and benthonic foraminifera (Smith et al., 1976) and estimates for the wells off Nova Scotia are based on unpublished multidisciplinary studies (F.J. Paulus, personal communication).

We have not applied a correction for variations in water load due to changes in sea-level through time. Equation 1 can therefore be rewritten

$$Y' = Y + \Delta_{SL}\left[\frac{\rho_m}{(\rho_m-\rho_w)}\right] \quad (2)$$

where Y' is the depth to basement through time corrected for sediment loads, but still contains terms due to both "tectonic" and "eustatic" effects.

Figure 6 shows the total sediment accumulation and the calculated Y' for each of the wells through time. The dotted region represents that part of the subsidence caused by sediment loading and the hatched region represents that part caused by "tectonic" and "eustatic" effects. The relative smoothness of Y' shows that "backstripping" successfully removes variations in the total sediment accumulation through time that are due to changes in the supply of sediments and local sea-floor sedimentary processes.

## Eustasy

In order to examine the evolution of the margin it is necessary to separate the "tectonic" and "eustatic" effects from Y .

A number of studies have now been carried out (Sleep, 1971; Watts and Ryan, 1976; McKenzie, 1978; Steckler and Watts, 1978) that suggest the tectonic subsidence at margins is thermal in origin. Sleep (1971) has suggested the subsidence is caused by cooling of the lithosphere following uplift and sub-aerial erosion whereas McKenzie (1978) has postulated the subsidence is caused by cooling of the lithosphere following "stretching" and thinning at the time of initial rifting. McKenzie (1978) has shown, however, that for all thermal models the subsidence of the

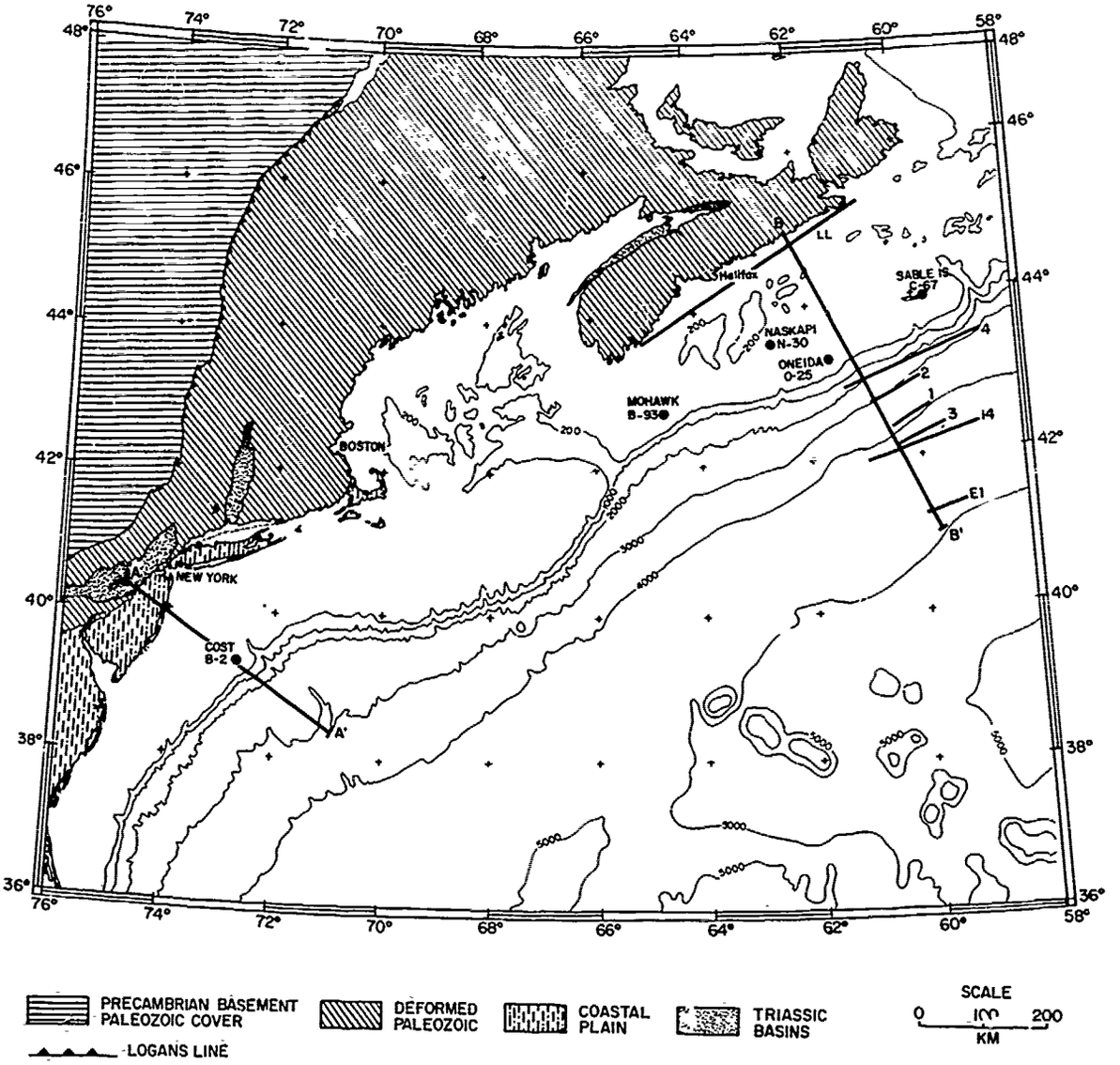


Figure 1. Location map of the COST B-2 well (Scholle, 1977) and the wells offshore Nova Scotia used in this study (Williams, 1975; Jansa and Wade, 1975; A. W. Bally, personal communication). The summary geology and generalized bathymetry are based on the tectonic map of North America (King, 1969). The heavy lines with bars indicate the location of the schematic geological structure sections of the margin shown in Figure 2 and the heavy lines without bars indicate the location of seismic refraction stations 1, 2, 3, 4 of Keen et al. (1975), E1 of Ewing and Ewing (1959), 14 of Keen and Loncarevic (1976) and LL of Barrett et al. (1964).

margin can be characterized by a simple exponential curve for ages greater than 20 to 30 m.y. after initial rifting.

These considerations suggest, therefore, that the "tectonic" and "eustatic" effects can be separated by fitting an exponential curve to Y' We then interpret the exponential component of the subsidence as the "tectonic" effect and the difference between the exponential and Y' as the "eustatic" effect. We fitted an exponential curve to the data within each well by least squares.

In addition, for the three wells which did not reach basement (Oneida O-25, Sable Island C-67,

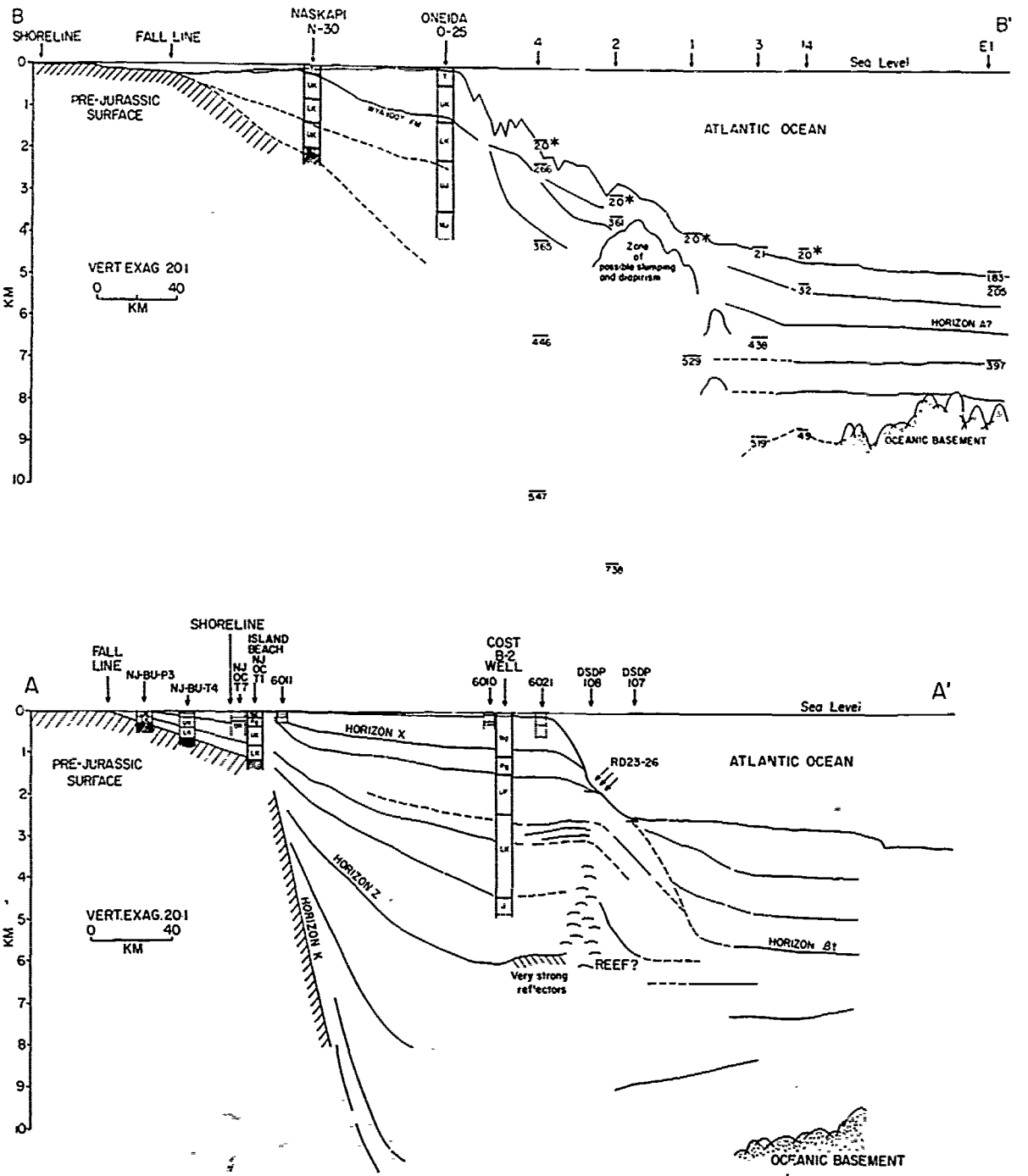


Figure 2. Summary geologic cross-section of the continental margin off New York (profile A-A', Fig. 1) and Nova Scotia (profile B-B', Fig. 1). The summary stratigraphy of COST B-2, Oneida O-25 and Naskapi N-30 wells is based on Scholle (1977) and Williams (1975). In profile A-A' the summary stratigraphy of other wells in the coastal plain is based on Maher and Applin (1971) and in the Outer Continental Shelf is based on Hathaway et al. (1976). Solid lines indicate prominent seismic reflectors identified on adjacent multi-channel seismic profiles based on Given (1977) and King and MacLean (1974) for profile B-B' and Grow et al. (lines 2 and 9; in press) for profile A-A'. The sources and location of seismic refraction profiles is given in Fig. 1.

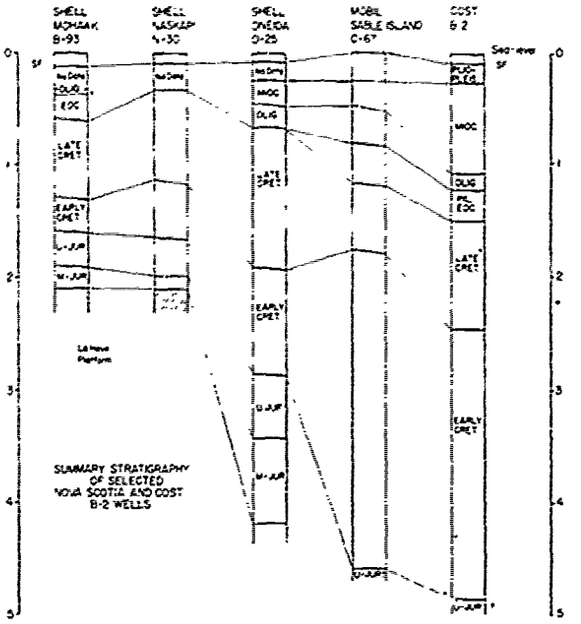


Figure 3. Generalized stratigraphy of the deep commercial wells which are used in this study (Fig. 1). The depth to stratigraphic horizons is based on Scholle (1977) for the COST B-2 well and on Williams (1975) for the wells off Nova Scotia. The slope of the horizons represents the uncertainty in its position.

COST B-2) we considered the effect of the additional data point at the base of the sediments beneath the well. Since this data point is at the time of initial rifting a complete thermal model must be used. For this point we assumed the cooling plate model of Parsons and Sclater (1977). As pointed out by McKenzie (1978) and Steckler and Watts (1978) the ocean ridge model may not strictly apply to a continental margin. At a margin the entire lithosphere has probably not been heated to the solidus temperature. A constraint on this data point is needed, however, in order to determine the long-term trend in sea-level.

In order to apply the model we made the following assumptions: 1) The depth to basement at the Oneida O-25 well is 5.3 km based on a nearby multi-channel seismic profile (Given, 1977), at the Sable Island C-67 well is 8.2 km based on the contours on basement map of the Scotian shelf (Geological Survey of Canada map 1400 A), and at the COST B-2 well is 12.8 km based on nearby multi-channel seismic profile USGS Line 2 (Schlee et al., 1976; Mattick, 1977). 2) The earliest sediments beneath the well were deposited at sea-level. 3) The subsidence of the margin began 195 m.y.B.P., corresponding to the time of extensive basaltic activity in the North Atlantic region at the Triassic-Liassic boundary (Van Houten, 1977).

The sea levels, $\Delta_{SL}$, required to explain the differences between these exponentials and Y' (equation 2) are shown in Figure 8. Figure 8a indicates the differences from an exponential curve least squares fitted to the data within the well and Figure 8b indicates the differences in which the additional data at the base of the well has been included. Since Mohawk B-93 and Naskapi N-30 both reached basement, the differences for these wells in Figure 8 are the same. Although there is scatter in the data, a similar pattern of sea-level changes can be distinguished for each well (Fig. 8). With the exception of the Sable Island C-67 well, sea-level appears to rise between the Early and Late Cretaceous and fall between Late Cretaceous and Miocene. A smaller, but rapid, rise in sea-level appears to occur during the Latest Jurassic. The shapes of the two sea-level curves are similar, therefore the sea-level curve is only weakly dependent on the time constant $\tau$ and the assumptions of the model.

The well data was then corrected for sea-level using the curve in Figure 8b (equation 2) and the previous procedure was repeated until the differences from the best fitting exponential were satisfactorily reduced. We chose the sea-level curve in Figure 8b because it includes the long-term trend in sea-level. Figure 9 shows the sea-level curve from Figure 8b and the "first estimate" of the sea-level curve derived after iteration. The sea-level curves in this figure have been plotted with present day sea-level as the origin.

The well data which includes the "first estimate" sea-level curve together with the best fitting exponential curves is shown in Figure 10. The inclusion of the sea-level correction has resulted in a noticeably improved fit of an exponential curve to the well data, as can be seen by comparing Figures 7 and 10. There are, however, departures from an exponential curve which cannot be explained by sea-level changes. We attribute these departures to local "tectonic" effects. Prior to the Late Cretaceous the Sable Island C-67 well departs from the curve. This well is located on a possible basement block (North Sable high, Jansa and Wade, 1975) as indicated by dip reversals on nearby seismic reflection profiles. There is also evidence on these profiles of salt diapirism. These factors indicate local tectonic activity which could have disturbed the lower part of the well. The COST B-2 well departs from the curve mainly during the Oligocene when extensive erosion of the shelf may have occurred (Grow et al., in press). The flexural effects of this erosion have been modeled by Steckler and Watts (1978) and can adequately account for the observed departures from the curve.

We compare in Figure 11 the "first estimate" curve to other sea-level curves. The fine solid line is the sea-level change based on the Schuchert-Wise percentage continental flooding estimates and the hypsometric curve for North America given by Wise (1974, fig. 5). The heavy

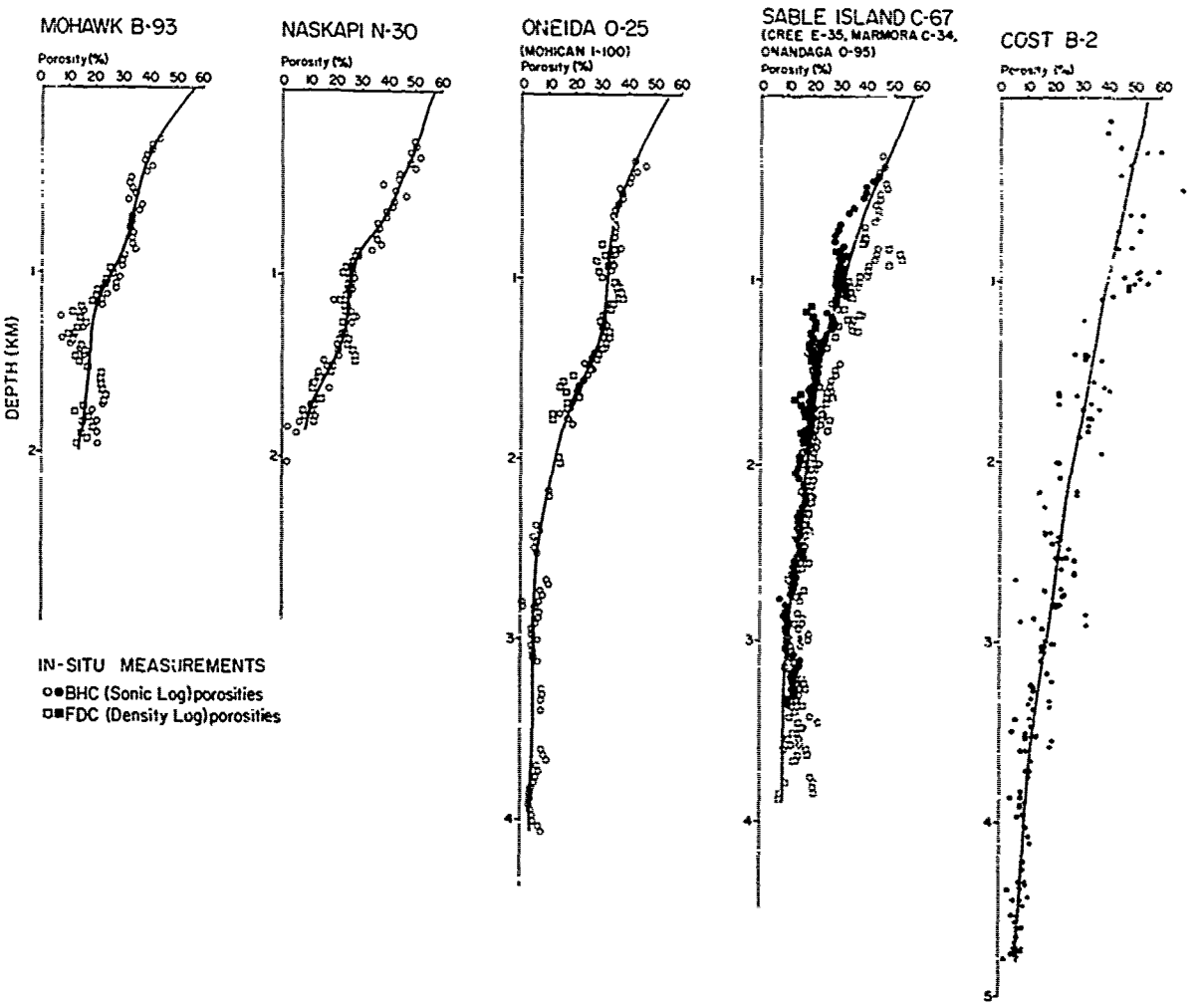


Figure 4. Porosity-depth curves for the five wells used in this study. The sources of the porosity data are discussed in the text. The porosity data for Oneida O-25 and Sable Island C-67 are based on the nearby well logs indicated in the figure. The solid lines indicate the curve used in the computation of the reconstructed sedimentary section.

dashed line is the adjusted sea-level curve of Bond (1978, fig. 4B) based on more recent percentage continental flooding estimates and different hypsometric curves for each continent. The discrepancies between Bond (1978) and Schuchert-Wise are caused by differences in the hypsometric curve assumed through time. There is good agreement that the maximum rise in sea-level in the Late Cretaceous based on estimates of percentage continental flooding and the "first estimate" sea-level curve is 100 to 150 meters. The dashed line with open circles is the sea-level change obtained by Pitman (1978) and Vail et al. (1977). The maximum rise in sea-level based on this curve is greater than 300 meters, which is significantly larger than the "first estimate" sea-level curve.

The differences between using the Pitman (1978) and Vail et al. (1977) sea-level curves and the "first estimate" curve are illustrated in Figure 12 for the Oneida O-25 well. The upper curve in this figure is Y' which includes the "tectonic" subsidence uncorrected for "eustatic" effects. The lower two curves in figure 9 show Y, the "tectonic" subsidence at the margin, calculated using Pitman (1978) and Vail et al. (1977) and the "first estimate" curve. This figure shows the "first estimate" curve successfully improves the fit of the tectonic subsidence to an exponential curve while the Pitman (1978) and Vail et al. (1977) curve implies a nearly linear tectonic subsidence. A

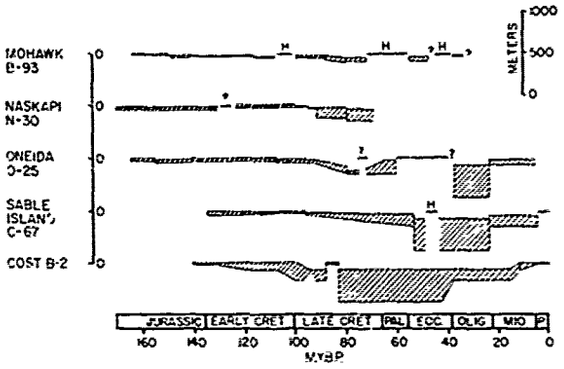


Figure 5. Estimates of the change in water depth of deposition for each of the wells through geological time. The sources of this data are discussed in the text. H indicates a hiatus in the stratigraphic record and S indicates subaerial deposition.

subsidence curve of this form cannot easily be explained by current tectonic models for the evolution of Atlantic-type continental margins.

## Thermal Parameters

We have used the "first estimate" sea-level curve to correct Y' and obtain Y, the tectonic subsidence at each well (Fig. 10). By comparing this subsidence to the cooling plate model, which Parsons and Sclater (1977) have shown explains the subsidence of oceanic crust out to ages of at least 160 m.y., the thermal parameters of the lithosphere beneath each well can be estimated. The advantage of this model is that the subsidence follows a relatively simple pattern. At first, the subsidence is proportional to $t^{\frac{1}{2}}$ and then, after a time dependent upon the thickness of the thermal lithosphere, the subsidence is arrested and decays exponentially to a constant value. The parameters that characterize the subsidence curve can be estimated by plotting the tectonic subsidence Y on two simple graphs, Y versus $t^{\frac{1}{2}}$ and log Y versus t. The rate of subsidence on a $t^{\frac{1}{2}}$ plot normalized to the total subsidence ($C_1/C_3$ of Parsons and Sclater,

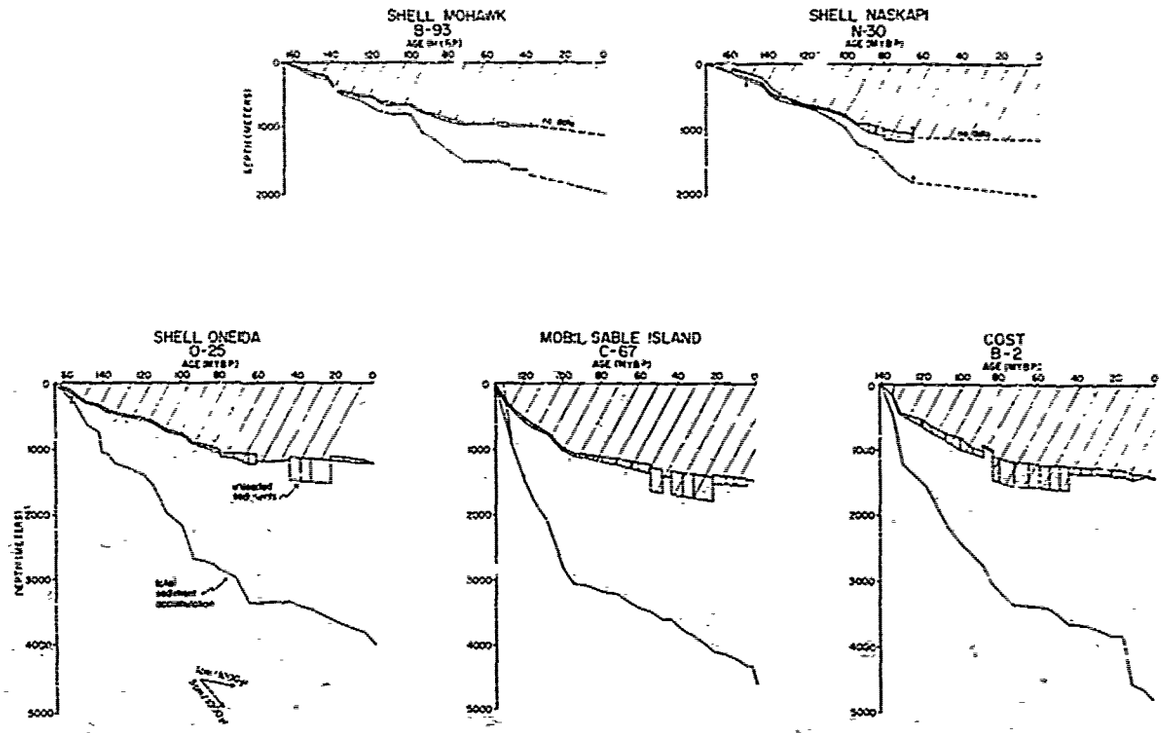


Figure 6. Plot of Y' and the total sediment accumulation through time for each of the wells (Fig. 1). The dotted region indicates that part of the subsidence caused by sediment loading and the hatched region indicates that part of the subsidence caused by other "tectonic" and "eustatic" effects. The range of Y' reflects uncertainties in the water depth (Fig. 5) and the position of individual stratigraphic horizons (Fig. 3).

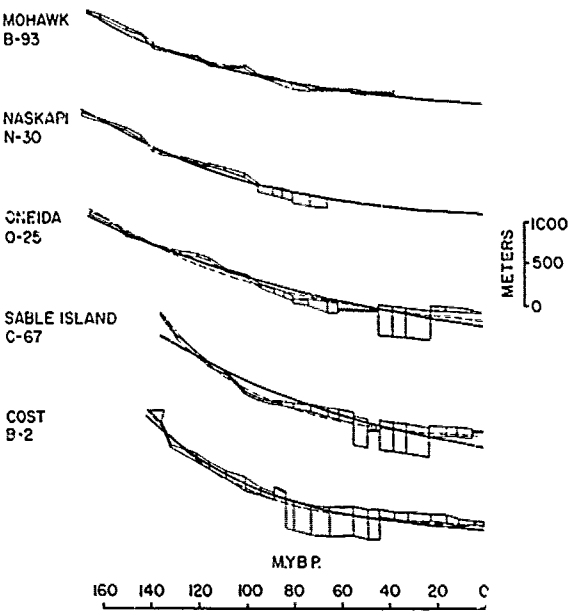


Figure 7. Plot of Y' (Fig. 6) compared to simple exponential curves. The dashed line represents an exponential curve least squares fitted to data within each well. The solid line represents an exponential curve obtained by a least squares fit to the observed data including the data point at the base of the sedimentary section.

1977), the breakdown of the linear part of Y versus $t^{\frac{1}{2}}$ ($C_2$), and the time constant of the exponential decay ($C_2'$) can be used to obtain independent estimates of the thermal thickness of the lithosphere. In addition, from simple isostatic considerations (Steckler and Watts, 1978), the total tectonic subsidence $D_o$ ($C_3$) can be used to estimate the total amount of crustal thinning that has occurred at the margin.

We have obtained estimates of the thermal parameters for the COST B-2 and the Oneida O-25 wells. These wells have been selected because they are considered the most reliable of the five wells studied. Both the Naskapi N-30 and Mohawk B-93 wells are located on relatively thin sedimentary sections (Fig. 3) which penetrated basement. The oldest sediments in these wells are of Middle Jurassic age and are significantly younger than the inferred age of the opening of the Atlantic. The Sable Island C-67 well was not considered because of the poor fit of the tectonic subsidence to an exponential curve (Fig. 10).

Figure 13 shows the plot of the tectonic subsidence Y against $t^{\frac{1}{2}}$ and log Y against t for the COST B-2 and Oneida O-25 wells. The linear part of the $t^{\frac{1}{2}}$ plot is generally well constrained for the Oneida O-25 well but poorly constrained for the COST B-2 well. The tectonic subsidence data for the COST B-2 well extends into only a small part of the linear portion of the plot. However, even with this uncertainty the tectonic subsidence for each well appears to deviate from a straight line. Thus estimates of the slope of the straight line ($C_1$) and the age of the departure from the straight line ($C_2$) can be determined for each well. The straight line in the plots of log Y against t was determined by a least squares fit to the tectonic subsidence using $D_o$ ($C_3$) as an independent parameter. The fit to a straight line is generally good and gives an estimate for the time constant of the exponential term ($C_2'$) and $D_o$ ($C_3$) for each well.

The estimates of the parameters obtained from the plots (Table 1) have been used to compute the thermal thickness of the lithosphere, a, and the amount of crustal thinning that has occurred beneath each well. The COST B-2 well, which is located in a deep sedimentary trough, yields a small estimate for the lithospheric thickness (108 to 130 km), and a large estimate for the amount of crustal thinning. The Oneida O-25 well, which is located just landward of the "hinge zone" (Fig. 2; Jansa and Wade, 1975) yields a large estimate for the lithospheric thickness (160 to 170 km) and a small estimate for the amount of crustal thinning.

## Lithospheric models

We have examined the validity of these estimates of the crustal thinning and thermal lithospheric thickness at the COST B-2 and Oneida O-25 wells by comparing their computed gravitational effect to observed surface-ship gravity data and GEOS-3 satellite radar altimeter measurements over the margin.

We constructed models for the crustal structure of the margin along profiles A-A' and B-B' (Fig. 1) which include the COST B-2 and Oneida O-25 wells and compared their gravitational effect to observed surface-ship gravity measurements (Fig. 14). The distribution of the sediments for each profile is based on nearby multi-channel seismic reflection data summarized in Figure 2. The sediment structure thus determined was held constant and only the configuration of the 'Moho' surface was varied between the models. In the upper models (Fig. 14), the 'Moho' is based on an Airy model of compensation for the bathymetry and sediments and an assumed compensation depth of 32 and 30 km for Nova Scotia and New York respectively. The crust and mantle densities assumed are the same as used in the "backstripping" calculations. There is generally a poor agreement between the computed gravity effect based on an Airy model and the observed profiles for each margin. In the lower models (Fig. 14), the 'Moho' surface was varied until a "best fit" was obtained between the computed and observed effects.

The dashed vertical line beneath the Oneida O-25 and COST B-2 wells in Figure 14 is the

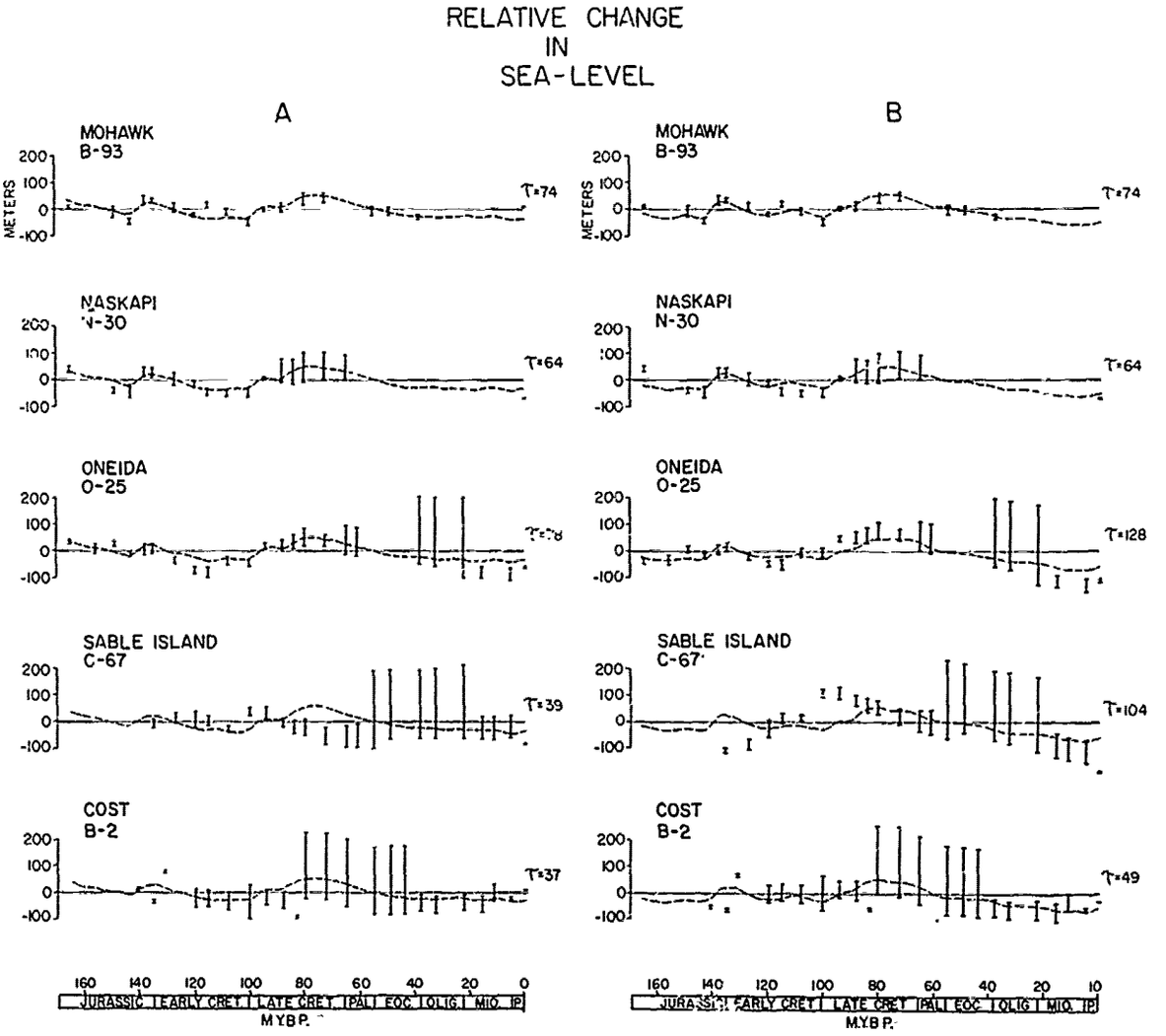


Figure 8. Differences between Y' and the simple exponential curves in Figure 7 expressed as relative changes in sea-level. Column A are the differences from an exponential curve based on data within each well. Column B are the differences from an exponential curve including the data point at the base of the sedimentary section. The dashed line is the average sea-level curve for each column. The time constant τ in m.y. is indicated to the right of each curve.

estimate of the crustal thickness based on thermal calculations (Table 1). This estimate was obtained by subtracting the assumed compensation depth from the amount of crustal thinning, based on $D_o$. Although gravity data cannot be used to uniquely determine the depth to 'Moho' beneath each well there is good agreement between the crustal thickness based on gravity and thermal modeling (Fig. 14). Thus gravity data are consistent with a small amount of crustal thinning beneath the Oneida O-25 well and a large amount of crustal thinning beneath the COST B-2 well.

Available seismic refraction measurements (Ewing and Ewing, 1959; Barrett et al., 1964; Keen and Loncarevic, 1966; Keen et al., 1975) do not constrain the crustal thickness beneath the Oneida O-25 and COST B-2 wells (Fig. 14). However, they are in agreement with the crustal structure determined in the models for the continental rise off Nova Scotia.

Although gravity data is a useful constraint on the shallow structure of the margin, it provides little information on the deep structure. Recent advances in satellite radar altimetry (Leitao and McGoogan, 1975; Martin and Butler,

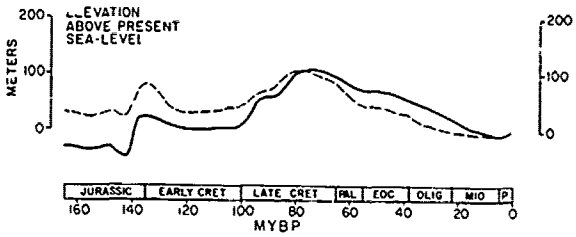


Figure 9. Elevation of sea-level above present day. The dashed line is the average sea-level curve from Figure 8B. The solid line is the "first estimate" sea-level curve determined by iteration. The origin is at present day sea-level.

1977) enable the height of the marine geoid above the reference ellipsoid to be determined to an accuracy of about one meter. The geoid is more sensitive than gravity to long wavelength features in the gravitational field and may therefore provide more information on deep structures. We have used recent determinations of the geoid height derived from GEOS-3 altimeter measurements over the margin off New York and Nova Scotia to better constrain our estimates of the thermal thickness of the lithosphere (Table 1).

The geoid height associated with the "best fit" gravity models in Figure 14 was computed and compared to the observed GEOS-3 geoid height (Fig. 15 a,b). There is an excellent agreement between the observed and computed geoid off New York, but a discrepancy of over 3 meters in the step in the geoid across the margin off Nova Scotia. We have found that reasonable variations in the density of the crust and upper mantle cannot explain this discrepancy, suggesting that its source is located deeper within the lithosphere.

The thermal models predict there may be a significant difference in the lithospheric thickness between the continental shelf (160-170km) and the ocean (128 km, Parsons and Sclater, 1977) off Nova Scotia but little or no difference in the corresponding region off New York (108-130 versus 128 km). To test this possibility we computed the geoid effect of a model which included these differences in the lithosphere for the margin off Nova Scotia. We used the cooling plate model to determine the temperature within the plate and then computed densities using $\rho = \rho_o (1-\alpha T(Z))$ where $\alpha$ is the coefficient of thermal volume expansion and T(Z) is the temperature as a function of depth. We assumed the same values of $\alpha$ and $T_m$, the temperature at the base of the plate, as those determined by Parsons and Sclater (1977). The lithospheric model was compensated by adjusting the 'Moho' surface in order to ensure a good fit to the gravity data. This procedure increased the relief of the 'Moho' slightly and increased the depth to the base of the crust from 32 to 33.2 km.

The geoid effect of the lithospheric model is compared to the observed geoid off Nova Scotia in Figure 15c. This figure shows the step in the computed geoid is about 5 to 6 meters, which is in good agreement with the observed geoid. Thus, GEOS-3 altimeter measurements are consistent with similar thermal thicknesses beneath the COST B-2 well and the oceanic lithosphere and with significant differences beneath the Oneida O-25 well and the oceanic lithosphere.

## Discussion

We have determined the tectonic subsidence at five deep wells in the Atlantic-type continental margin off the East Coast, U.S. The tectonic subsidence can be explained by simple models for the cooling of the lithosphere. The total amount of subsidence appears to be determined by the amount of heating and thinning that occurs during the rifting process. Therefore, the structural evolution of the margin is mainly controlled by the amount of initial thinning and the subsequent tectonic subsidence.

The pattern of crustal thinning appears to be similar for both the margin off New York and Nova Scotia (Fig. 14). In a seaward direction across the margin the continental crust gradually thins to a hinge zone. At the hinge zone, the crust thins rapidly to thicknesses similar to that of the oceanic crust. Off New York, the hinge zone corresponds to a major fault identified on multi-channel seismic reflection profile Line 2 (Schlee et al., 1976) as "Horizon K". The hinge zone off Nova Scotia, corresponds to a region of faults and flexures in the basement observed on multi-channel seismic reflection profiles (Jansa and Wade, 1975).

The crustal thinning also appears to be associated with a thinning of the entire lithosphere. Thermal calculations at the Oneida O-25 well, which is located just landward of the hinge zone, indicate a significantly larger thickness for the lithosphere than at the COST B-2 well, which is located seaward of the hinge zone.

A number of authors have discussed the origin of lithospheric thinning at Atlantic-type margins. Sleep (1971) and Turcotte et al. (1977) have suggested the thinning is caused by uplift and erosion. We have previously shown (Steckler and Watts, 1978) that this mechanism cannot satisfactorily explain the large amount of crustal thinning at the COST B-2 well. McKenzie (1978) has suggested the thinning is caused by "stretching" or "necking" of the lithosphere. There are two observations of basement structure which support the suggestion of regional extension at a margin. First, the presence of normal faulting at the young, starved margin of the Bay of Biscay (De Charpel et al., this volume). Second, the presence of extensive dyke intrusion in the Precambrian basement underlying the former continental shelf of the proto-Atlantic (Rast, in preparation).

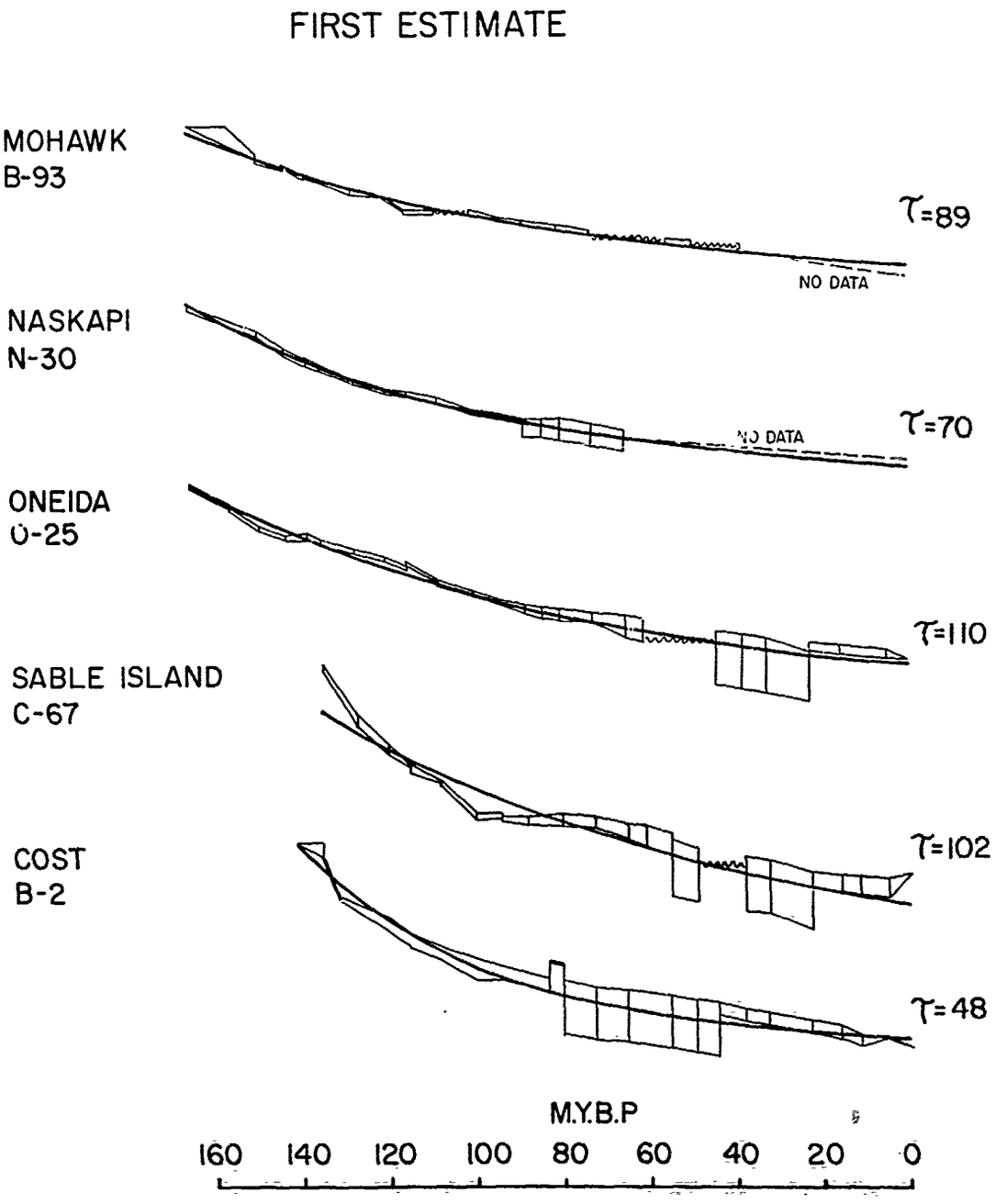


Figure 10. Tectonic subsidence Y of the margin at each well obtained by correcting Y' for "eustatic" effects using the "first estimate" sea-level curve (Fig. 9). The heavy line is the "best fit" exponential which describes the tectonic subsidence for each well.

The tectonic subsidence is a result of the cooling of the thinned lithosphere. As a margin subsides sediments accumulate so that the regions of largest crustal thinning are associated with the largest thickness of sediments. Although we have assumed a simple Airy model of loading in our "backstripping" calculations we would expect that the scheme of loading would change during

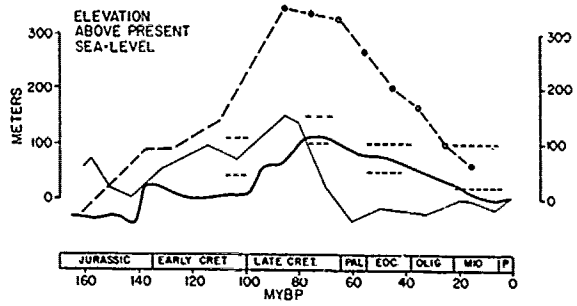


Figure 11. Comparison of recent estimates of sea-level elevations from the present to 165 m.y.B.P. The heavy line is based on the "first estimate" sea-level curve determined in this paper. The circles are from Pitman (1978) and the dashed line is a smoothed curve based on Vail et al. (1977). The fine line is from the Schuchert-Wise estimates of percentage flooding of North America and an hypsometric curve for North America (Wise, 1974). The dashed heavy line is from Bond (1978) and shows the range of sea-level elevations based on percentage continental flooding estimates with different hypsometric curves for each continent.

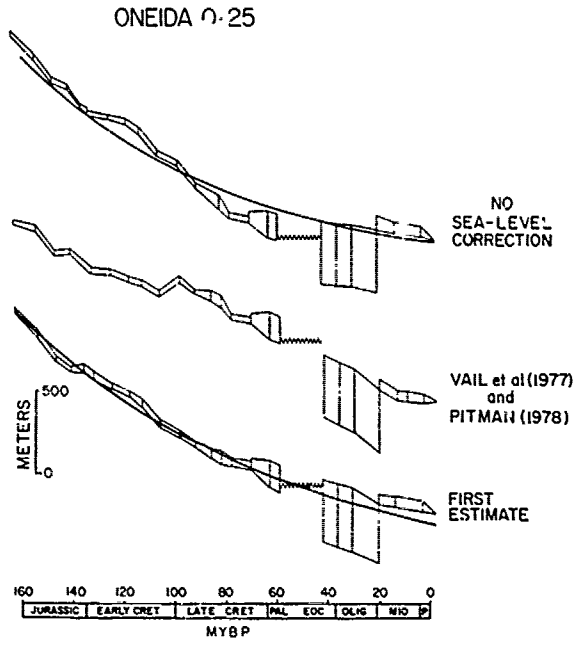


Figure 12. Comparison of the subsidence at the Oneida O-25 well with no sea-level correction curve (upper curve), the Pitman (1978) and Vail et al. (1977) sea-level curve (middle curve) and the "first estimate" sea-level curve (Fig. 9) (lower curve). The heavy lines on the upper and lower curve are the "best fit" exponentials.

the evolution of the margin. Initially, sediments load a relatively hot and weak lithosphere. Later in margin evolution the sediments load a relatively cool and rigid lithosphere. Thus the deposition of sediments landward of the hinge zone may be controlled more by lithospheric

TABLE 1. SUMMARY OF THERMAL PARAMETERS DETERMINED FOR THE ONEIDA O-25 AND COST B-2 WELLS

| CONSTANT | FORMULA (Parsons & Sclater, 1977) | ONEIDA O-25 | COST B-2 |
|---|---|---|---|
| Slope Depth vs $(Age)^{\frac{1}{2}}$ | $C_1 = \frac{2\rho_o \alpha T_m}{(\rho_o - \rho_w)}\left[\frac{K}{\pi}\right]^{\frac{1}{2}}$ | 172 M/$(M.Y.)^{\frac{1}{2}}$ | 512 M/$(M.Y.)^{\frac{1}{2}}$ |
| Asymptote of Depth vs $(Age)^{\frac{1}{2}}$, $D_o$ | $C_3 = \frac{\rho_o a \alpha T_m}{2(\rho_o - \rho_w)}$ | 2550 M. | 5280 M. |
| Breakdown of linear $(Age)^{\frac{1}{2}}$ relation | $C_2 = a^2/9K$ | 110-130 M.Y. | 70-80 M.Y. |
| Slope of log (elevation) vs age | $C_2' = \frac{a^2}{\pi^2 K}$ | 110 M.Y. | 38 M.Y. |
| Thickness of the lithosphere | a | 160-170 KM | 108-130 KM |
| Crustal thinning | $T_c = D_o \frac{(\rho_c - \rho_w)}{(\rho_o - \rho_c)}$ | 10 KM | 21 KM |

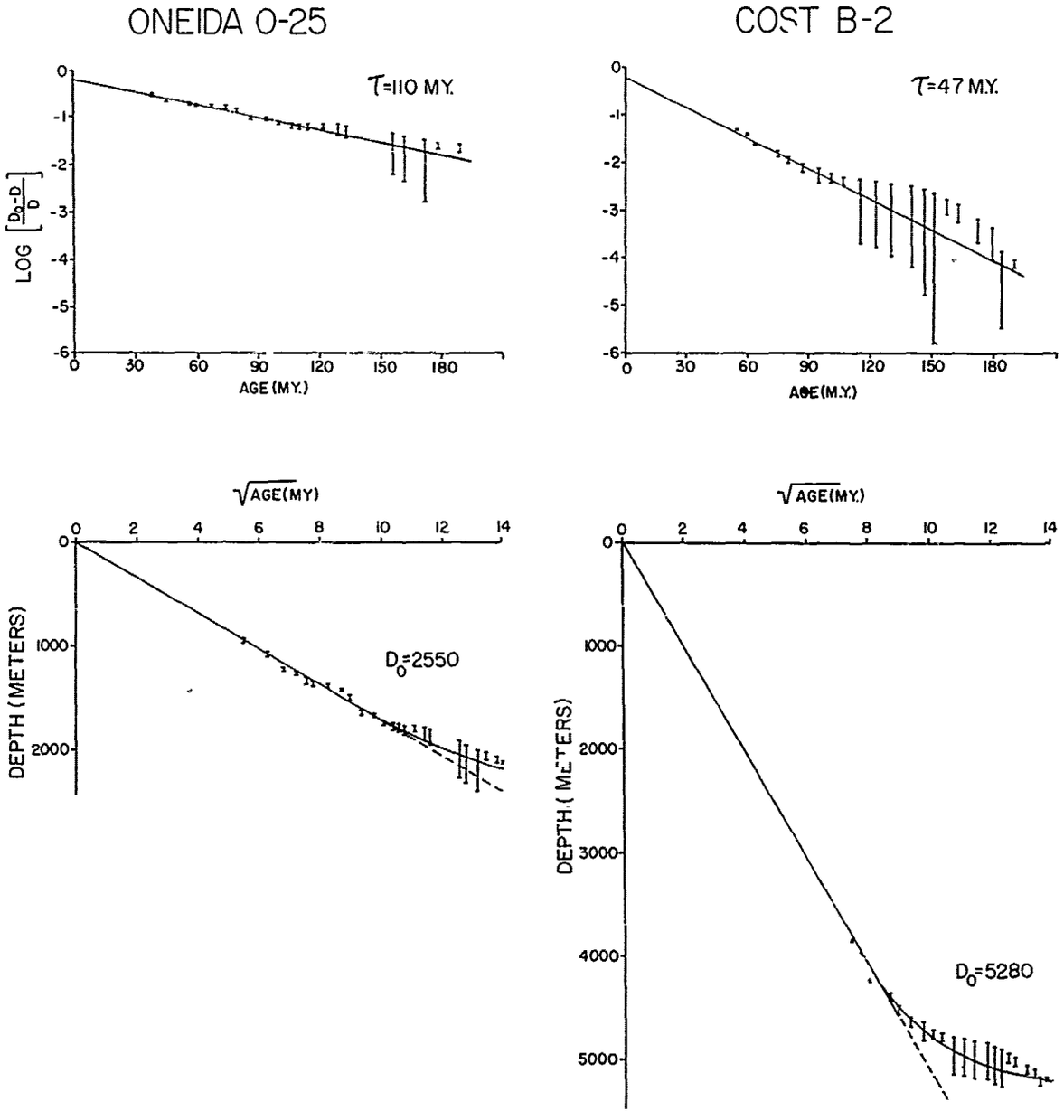


Figure 13. Plot of tectonic subsidence Y against age$^{\frac{1}{2}}$ and log Y against age for the Oneida O-25 and COST B-2 wells.



NEW YORK

NOVA SCOTIA

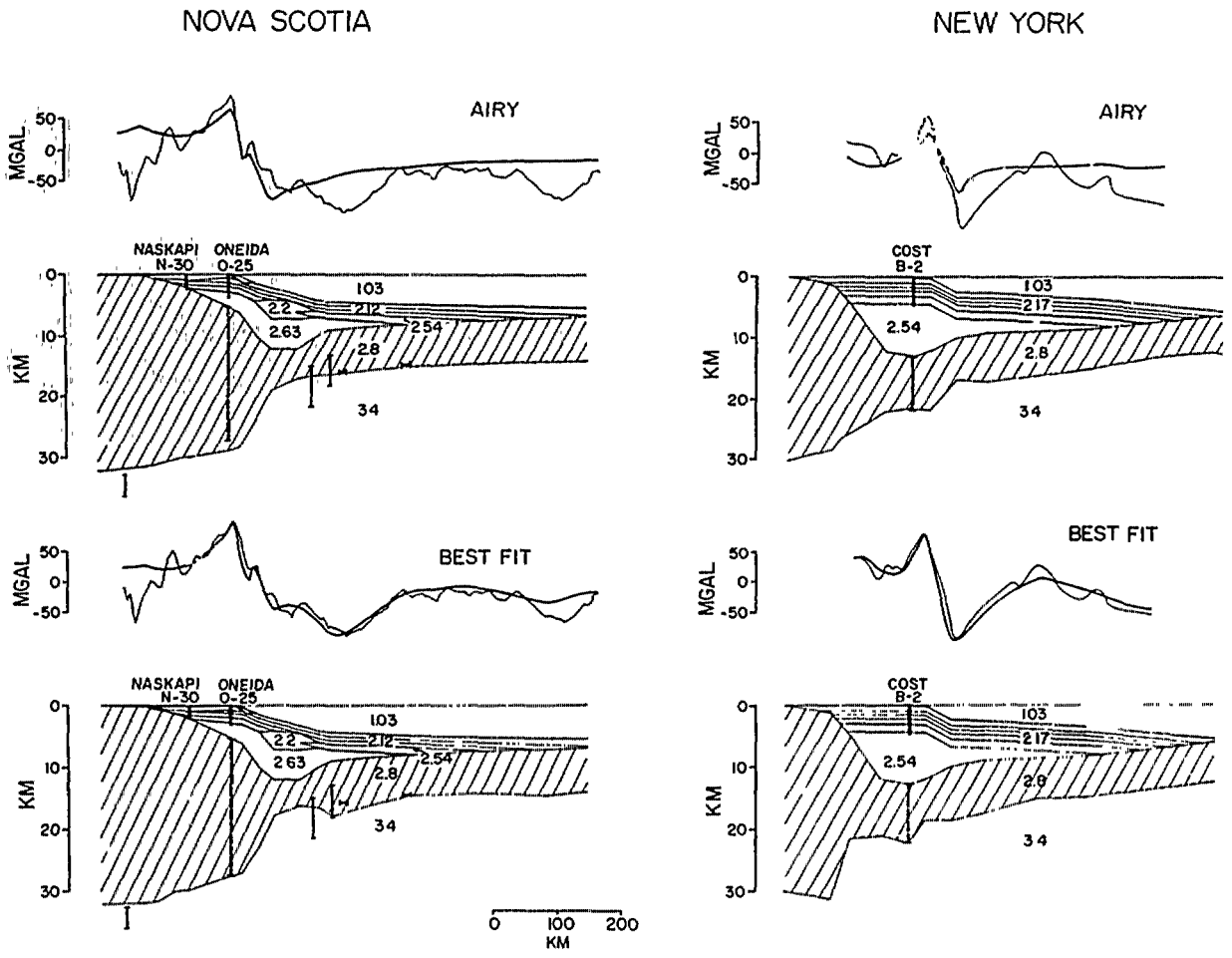


Figure 14. Computed gravity effect of simple models of the margin off New York and Nova Scotia compared to observed free-air gravity anomaly data. The data off Nova Scotia was obtained from R/V Vema cruise 23 and the data off New York was obtained from a map compiled by Ewing (1978). The upper model is based on Airy isostasy and lower model is based on a "best fit" model. The total mass is the same for the computed profiles of each margin. The solid vertical lines indicate the depth to 'Moho' from the seismic refraction lines in Fig. 1. The dashed vertical lines indicate estimates of the crustal thickness based on thermal calculations.

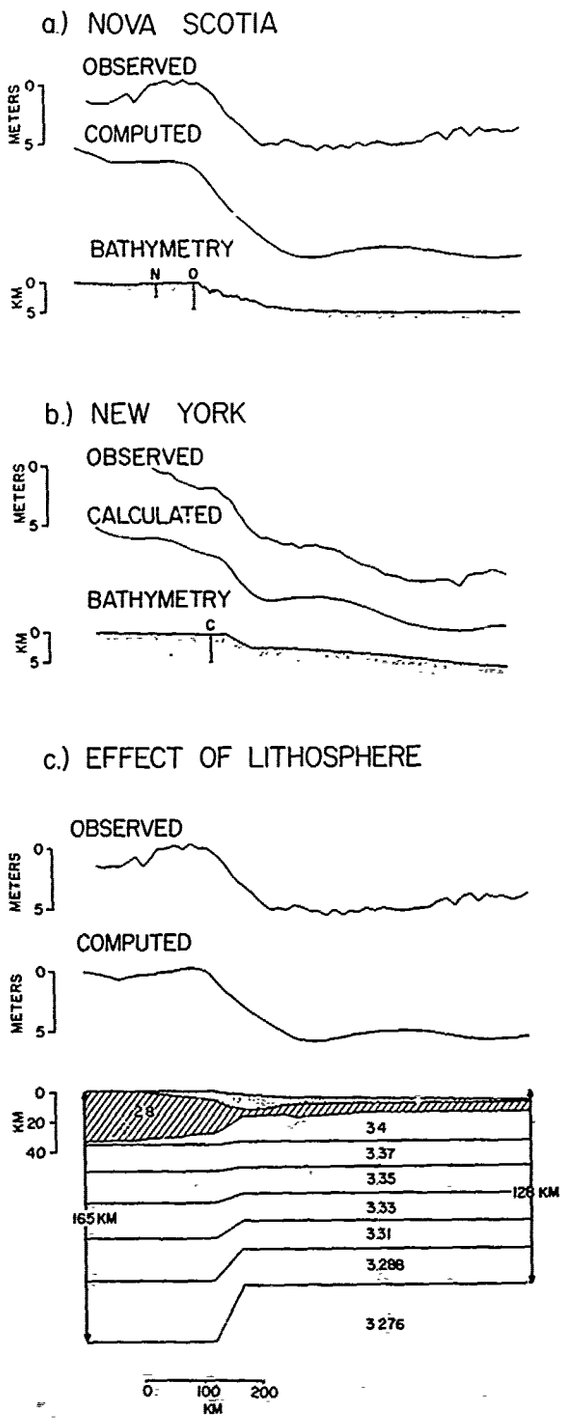


Figure 15. a) and b). Comparison of computed geoid heights associated with the "best fit" models in Figure 13 with observed geoid heights based on the GEOS-3 satellite radar altimeter. The profile off Nova Scotia was obtained on October 30th, 1975 during Orbit #2875 and off New York was obtained on August 9th, 1975 during Orbit #1724. Note that the fit for the New York profile which includes only the crustal structure is generally good but that the fit for the Nova Scotia profile is poor.
c). Comparison of computed geoid heights of a lithospheric model based on thermal calculations to observed geoid heights for the Nova Scotia margin. The fit for this profile, which includes the effect of the lithosphere, is greatly improved.

flexure than by crustal thinning. For example, at Naskapi N-30 and Mohawk B-93 sediments are not deposited until the Middle Jurassic.

The position of the present-day shelf edge does not appear to be controlled by the tectonic subsidence (Fig. 14). The margin off New York, has built out seaward of the maximum sediment thickness. Off Nova Scotia, however, the shelf edge has not built out as far and is located landward of the maximum sediment thickness. Furthermore, off Nova Scotia the trend of the shelf edge and of the locus of the maximum sediment thickness differ. Adjacent to the La Have platform the maximum sediment thickness occurs beneath the continental rise whi further to the northeast the maximum sediment thickness occurs beneath the outer continental shelf. These observations suggest the position of the shelf edge is not controlled by the tectonic subsidence; rather, it is probably controlled by the rate of sediment influx and near-bottom sedimentary processes.

In our models a major change in crustal thickness occurred at the hinge zone. It is not known whether the hinge zone represents the boundary between continental and oceanic crust. The crust beneath the COST B-2 well, for example, could be either oceanic, continental, or "transitional" in origin. The hinge zone does, however, represent the location of a major transition in the thermal and mechanical properties of the margin. It is the hinge zone, we believe, that has played the major role in controlling the structural evolution of the margin.

Acknowledgments. We are grateful to A.W. Bally of Shell Oil Company and F.J. Paulus of Superior Oil Company for help in providing down-hole geophysical logs and to W.B.F. Ryan for suggesting we use the well data to examine sea-level. Discussions with G. Karner, D.P. McKenzie and W.C. Pitman have been helpful. G. Bond, V. Ewing, and R. Fairbridge critically read the manuscript and made a number of helpful suggestions. This research was supported by National Science Found-

ation grant OCE 77-10647 and National Aeronautic and Space Administration grant NAS 6-2519.

Lamont-Doherty Geological Observatory Contribution Number 2802.

## References

Artemjev, M.E. and E.V. Artyushkov, Structure and isostasy of the Baikal rift and the mechanism of rifting, J. Geophys. Res., 76, 1197, 1971.

Barrett, D.L., M. Barry, J.E. Blanchard, M.J. Keen and R.E. McAllister, Seismic studies on the eastern seaboard of Canada: The Atlantic Coast of Nova Scotia, Can. J. Earth Sci. 1, 10-12, 1964.

Bond. G., Speculations on real sea-level changes and vertical motions of continents at selected times in the Cretaceous and Tertiary periods, Geology, 6, 247-250, 1978.

Bott, M.H.P., Shelf subsidence in relation to the evolution of young continental margins; in: Implications of Continental Drift to the Earth Sciences, v.2, D.H. Tarling and S.K. Runcorn, (eds.), Academic Press, London, 675-683, 1973.

DeCharpel, O., L. Montadart and D. Roberts, Rifting, subsidence and crustal attenuation in the N.E. Atlantic continental margins, in press, this volume.

Ewing, J. and M. Ewing, Seismic refraction measurements in the Atlantic Ocean Basins, Bull. Geolog. Soc. America, 70, 291-318, 1959.

Ewing, V., Free-air gravity map of the U.S. Atlantic margin, E.O.S. abstract, 59, 378, 1978.

Fairbridge, R.W., Eustatic changes in sea level, in: Physics and Chemistry of the Earth, L.H. Ahrens, F. Press, K. Rankama, S.K. Runcorn, (eds.), Pergamon Press, London, 4, 99-185, 1961.

Falvey, D.A., The development of continental margins in plate tectonic theory, APEA Bull., 58, 95-106, 1974.

Given, M.M., Mesozoic and Early Cenozoic geology, Bull. Can. Petrol. Geol., 25, 63-91, 1977.

Gradstein, F.M., G.L. Williams, W.A.M. Jenkins and P. Ascoli, Mesozoic and Cenozoic stratigraphy of the American continental margin, eastern Canada, in: Canada's Continental Margin and Offshore Petroleum Exploration, C.J. Yorath, E.R. Parker and D.J. Glass, (eds.), Can. Soc. Petrol. Geol. Memoir, 4, 103-130, 1975.

Grow, J.A., R.E. Mattick, J.S. Schlee, Multichannel seismic depth sections and interval velocities over Outer Continental Shelf and Upper Slope between Cape Hatteras and Cape Cod, in: Geological Investigations of Continental Margins, J.S. Watkins, L. Montadert and P.W. Dickerson, (eds.), A.A.P.G. Memoir, in press.

Hallam, A., Major epeieogenic and eustatic changes since the Cretaceous and their possible relationship to crustal structure, Amer. J. Sci., 261, 397-423, 1963.

Hathaway, J.C., J.S. Schlee, C.W. Poag, P.C. Valentine, E.G.A. Weed, M.H. Bothner, F.A. Kohut, F.T. Manheim, R. Schoen, R.E. Miller, and D.M. Schultz, Preliminary summary of the 1976 Atlantic margin coring project of the U.S. Geological Survey, U.S. Dept. Int. Geol. Surv. Open File Report 76-844.

Holmes, A., Principles of Physical Geology, Ronald Press, New York, 1288p, 1965.

Jansa, L.F. and J.A. Wade, Geology of the Continental Margin off Nova Scotia and Newfoundland, in: Offshore Geology of Eastern Canada, Geol. Surv. of Canada, paper 74-30, v.2, 51-105, 1975.

Keen, C.E., M.J. Keen, D.L. Barrett and D.E. Heffler, Some aspects of the ocean-continent transition at the continental margin of eastern North America, in: Offshore Geology of Eastern Canada, Geol. Surv. of Canada, paper 74-30, v.2, 189-197, 1975.

Keen, C.E. and B.D. Loncarevic, Crustal structure on the eastern seaboard of Canada: Studies on the Continental Margin. Can. J. Earth Sci., 3, 65-76, 1966.

King, L.H. and B. MacLean, Geology of the Scotian shelf and adjacent areas, Marine Sci. Paper series No. 7, G.S.C. Paper No. 74-31, 31p., 1976.

King, P.B., Tectonic map of North America, U. S. Geol. Survey, Dept. of Interior, Washington, D.C. #G67154, 1976.

Leitao, C.D. and J.T. McGoogan, Skylab Radar Altimeter: Short wavelength perturbations detected in ocean surface profiles, Science 186, 1028-1029, 1969.

Maher, J.C. and E.R. Applin, Geologic framework and petroleum potential of the Atlantic coastal plain and continental shelf, U.S. Geol. Survey Prof. paper 659, 98p, 1971.

Martin, C.F. and M.L. Butler, Calibration results for the GEOS-3 altimeter, NASA Contractor Rept. CR-141430, 86p., 1977.

Mattick, R.E., Geologic setting, in: Geological Studies on the COST B-2 well, U.S. Mid-Atlantic Outer Continental Shelf Area, P.A. Scholle, (ed.), Geol. Surv. Circ. 750, 4, 1977.

McKenzie, D.P., Some remarks on the development of sedimentary basins, Earth Planet. Sci. Lett., 40, 25-32, 1978.

Parsons, B. and J.G. Sclater, An analysis of the variation of ocean floor bathymetry and heat flow with age, J. Geophys. Res., 82, 803-827, 1977.

Pitman, W.C., III, The relationship between eustasy and stratigraphic sequences of passive margins, Bull. Geol. Soc. America, 89, 1389-1403, 1978.

Rast, N., Precambrian Meta-Diabases of southern New Brunswick, the opening of Iapetus Ocean?, in preparation.

Rhodehamel, E.C., Sandstone porosities, in:

Geological Studies on the Cost B-2 well, U.S. Mid-Atlantic Outer Continental Shelf Area, P.A. Scholle, (ed.), U.S. Geol. Survey Circ. 750, 23, 1977.

Schlee, J., J. C. Behrendt, J.A. Grow, R.M. Robb, R.E. Mattick, P.T. Taylor and B.A. Lawson, Regional geologic framework off northeastern United States, A.A.P.G. Bull. 60, 926-951, 1976.

Scholle, P.A., Geological studies on the COST B-2 well, United States Mid-Atlantic outer continental shelf area, in: Geological Studies of the COST B-2 well U.S. Mid-Atlantic Outer Continental Shelf Area, P.A. Scholle, (ed.), U.S. Geol. Surv. Circ. 750, 1-3, 1977.

Sheridan, R.E., Atlantic continental margin of North America, in: Geology of continental margins, C.A. Burk and C.L. Drake, (eds.), Springer-Verlag, New York, 391-407, 1974.

Sleep, N.H., Thermal effects of the formation of Atlantic continetal margins by continental breakup, Geophys. J.R.astr. Soc., 24, 325-350, 1971.

Smith, M.A., R.V. Amato, M.A. Furbush, D.M. Pert, M.E. Nelson, J.S. Hendrix, L.C. Tamm, G. Wood, Jr., and D.R. Shaw, Geological and operational summary, COST No. B-2 well, Baltimore Canyon trough area, Mid-Atlantic Outer-Continental Shelf (OCS), U.S. Geol. Surv. open file rept. 76-774, 79p. 1976.

Steckler, M.S. and A.B. Watts, Subsidence of the Atlantic-type continental margin off New York, Earth Planet. Sci. Lett. 41, 1-13, 1978.

Turcotte, D.L., J.L. Ahern and J.M. Bird, The state of stress at continental margins, Tectonophysics, 42, 1-28, 1977.

Vail, P.R., R.M. Mitchum Jr., and S. Thompson III, Part Four: Global cycles of relative changes of sea level, in: Seismic stratigraphy - applications to hydrocarbon exploration, A.A.P.G. Memoir 26, 83-98. 1977.

Van Houten, F.B., Triassic-Liassic deposits of Morocco and eastern North America: Comparison, A.A.P.G. Bull. 61, 79-99, 1977.

Watts, A.B. and W.B.F. Ryan, Flexure of the lithosphere and continental margin basins, Tectonophysics, 36, 25-44, 1976.

Williams, G.L., Dinoflagellate and Spore Stratigraphy of the Mesozoic-Cenozoic, Offshore Eastern Canada, in: Offshore Geology of Eastern Canada, Geol. Survey of Canada paper 74-30, v.2, 107-161, 1975.

Wise, D.U., Continental margins, freeboard and the volumes of continents and oceans through time, in: The Geology of Continental Margins, C.A. Burk and C.L. Drake, (eds.), Springer-Verlag, New York, 45-58, 1974.

# A QUANTITATIVE ANALYSIS OF SOME FACTORS AFFECTING CARBONATE SEDIMENTATION IN THE OCEANS

John G. Sclater, Edward Boyle, and John M. Edmond

Department of Earth and Planetary Sciences
Massachusetts Institute of Technology
Cambridge, Massachusetts 02139

Abstract. The calcite compensation depth (CCD), the carbonate compensation surface (CCS) and the carbonate line are useful statistical concepts with which to examine pelagic sedimentation in the deep ocean. There is evidence that since the cretaceous there is a large global component in the CCD variation in all the major ocean basins. A variety of possible explanations such as basin/deep sea fractionation, changes in shape of saturation profiles, variations in the amount of river input, fertility changes and bottom water flow have been suggested to explain this variation. Assuming a mass balance between carbonate supplied by weathering and deposition in the oceans we examine quantitatively, with simplified ocean sedimentation models, the effect on the CCD of basin/deep sea fractionation, changes in the hypsometric curve, variations in the shape of the saturation profiles and alterations in the river input. In this treatment we reverse the oceanic portion of the hypsometric curve and we introduce the concept of the mean rectangular ocean. Making reasonable assumptions about present day conditions we show that the CCD would be changed (a) 500 ~ 750 m by doubling the accumulation rate on the shelves, (b) 1 km by increasing the mean spreading rate of the oceans from 3 cm/yr to 6 cm/yr for 10 million years, (c) 350 m by altering the river input by 10% about the present value and (d) very little by varying the depth to the top of the lysocline. The effects of spreading rate change, shelf accumulation and river input all work in the same direction and could account for the 1.5 km increase in the CCD since the Cretaceous.

This is reasonable but, as yet, not overwhelming evidence for a correlation between mean spreading rate, Eustatic sea level and CCD. However, more observational work is needed to justify this correlation before a modified basin/shelf fractionation model can be unreservedly accepted as the explanation of the variation of the CCD. Also a more quantitative analysis is needed of the other explanations to examine whether or not they produce effects of sufficient magnitude to compete with our preferred model.

## Introduction

The existence of a calcite compensation level in the deep oceans is a consequence of the dissolution rate of calcite which increases with depth in response to increasing pressure and decreasing temperature. The depth at which calcite is totally dissolved is known as the calcite compensation depth (CCD). It varies as a function of water chemistry and productivity. To avoid problems associated with this loose definition we follow Berger and Winterer (1974) and define the surface traced out by the CCD in the water column as the carbonate compensation surface (CCS). Where this surface intersects the sea floor is known as the carbonate line. This line marks the boundary between predominantly calcareous ooze and sediments with only a few percent carbonate. In the present ocean it lies at an average depth of 4.7 kms and as a broad generalization spreading centers and aseismic ridges are covered by calcium and carbonate and the deep basins on either side consist mainly of red clay or radiolarian ooze.

Most of the calcium carbonate deposited in the oceans comes from the weathering of continental material. This carbonate is redistributed by deposition on the continental shelves, shallow seas and on the floor of the deep ocean. Globally the most important effect is the requirement for a mass balance between the calcium carbonate supplied by weathering and that deposited in the oceans. As there is a higher rate of accumulation in shallow water the amount of carbonate available for deposition in the deep sea is critically dependent upon the area of continental shelf and shallow seas. However, this shelf/deep sea fractionation effect is not the only factor controlling the accumulation of carbonate sediments in the deep sea. Berger and Winterer (1974) have reviewed

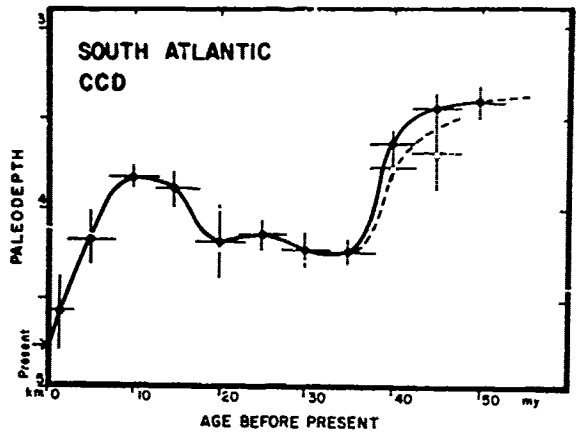


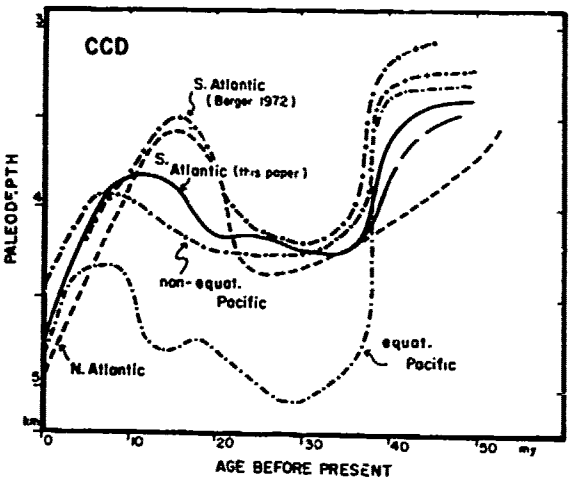


Fig. 1. Variation of calcite compensation depth (CCD) in the South Atlantic with time. Data points and error bars from van Andel et al., (1977). Bottom graph is a comparison of the CCD in the South Atlantic with that in other oceans (van Andel et al., 1977).

in a comprehensive manner the global and local factors affecting the depth of the mean carbonate compensation surface in the oceans. They show that the depth of this surface at any point in space and time results from the interaction of a variety of complex and poorly understood phenomena. As well as shelf/deep sea fractionation these include differences in saturation profiles, differences in shell properties, bottom water flow, changes in the hypsometric curve for the oceans, changes in the fertility of the ocean with time and space and finally differing rates of carbonate input from the continents.

All of these phenomena are related to sea floor spreading and the motion of continents though some more directly than others. For example, the amount of shelf available for carbonate deposition is increased by continental rifting and subsidence. Further, changes in the mean age of the ocean will affect sea level which will also alter in a dramatic fashion the amount of shelf available for deposition. Bottom water flow is also directly related to sea floor spreading and continental drift as it is the motions of the major plates which control the opening and closing of the major seaways. Causes which are less obviously related to plate motions are changes in the saturation profiles, differences in fertility and shell properties and changes in the basin input of carbonate to the oceans. However, ultimately all of these phenomena are affected by the position of the major continents within the global wind belts and within the major paths of ocean surface water circulation (Luyendyk et al., 1974).

Berger and Winterer (1974) have shown that it is useful to consider the carbonate compensation surface in a statistical manner. In their concept the CCS though it may change considerably over a short time period and local distances has a mean depth in a particular area which varies coherently on a time scale of the order of five million years. Accepting this concept it is possible to determine the depth of the CCS at a given point in the past by backtracking the type of sediment recovered in deep sea drilling cores along the depth versus age relation (Berger, 1972). Berger (1972) and Berger and von Rad (1972) used this technique and the assumption that to a first approximation the CCS would remain at a constant depth in any basin to determine the variation of CCD in the South and North Atlantic through the Tertiary. Van Andel (1975) making the same assumptions extended this analysis to all oceans through the Cretacecus (Figure 1.). He showed there were striking similarities in the variation of CCD with time in all basins. Ramsay (1977) applied the same analysis but allowed latitudinal variations within basins. He also found striking similarities for CCD variations with time since the Eocene.

The idea of a carbonate compensation surface which varies only slowly with time in an individual basin presents an interesting method for examinirg the distribution of sediments in the deep sea. If the distribution of this surface at a particular epoch is known then by matching this surface with the paleobathymetric contours it is possible to compute the carbonate line for the basin under consideration. This 'paleocarbonate line' marks the boundary between predominantly carbonate and other types of sediment. These ideas were first applied to the Indian Ocean by Thiede in Sclater et al., (1977) and then in more detail and greater care by Van Andel et al., (1977) to the South Atlantic. A feature of the latter study was the prediction of major changes in the surface distribution of carbonate versus non-carbonate sediments in the

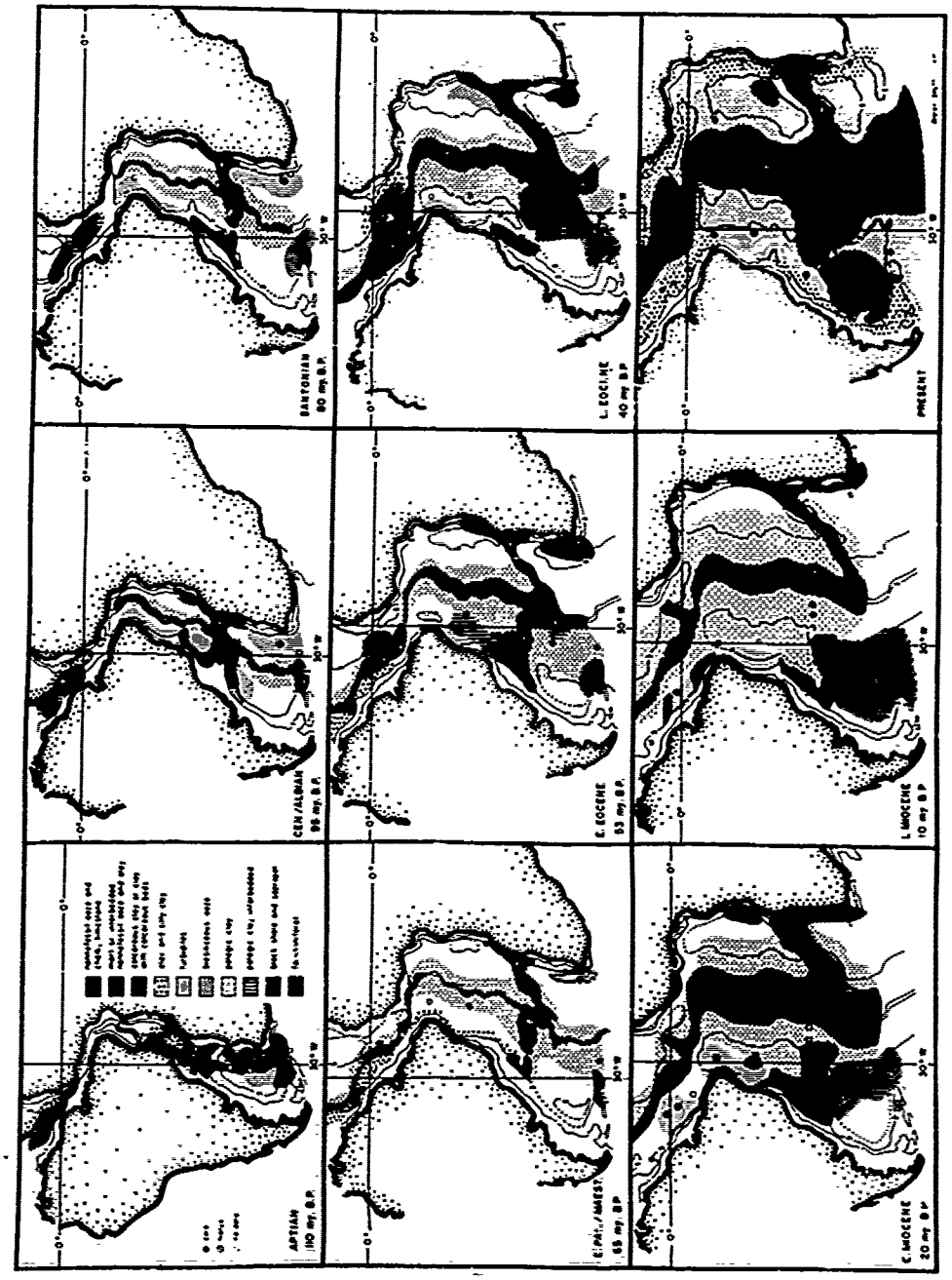


Fig. 2. Lithofacies sketch maps of the South Atlantic for five time slices from the early Eocene. (From van Andel et al., 1977).

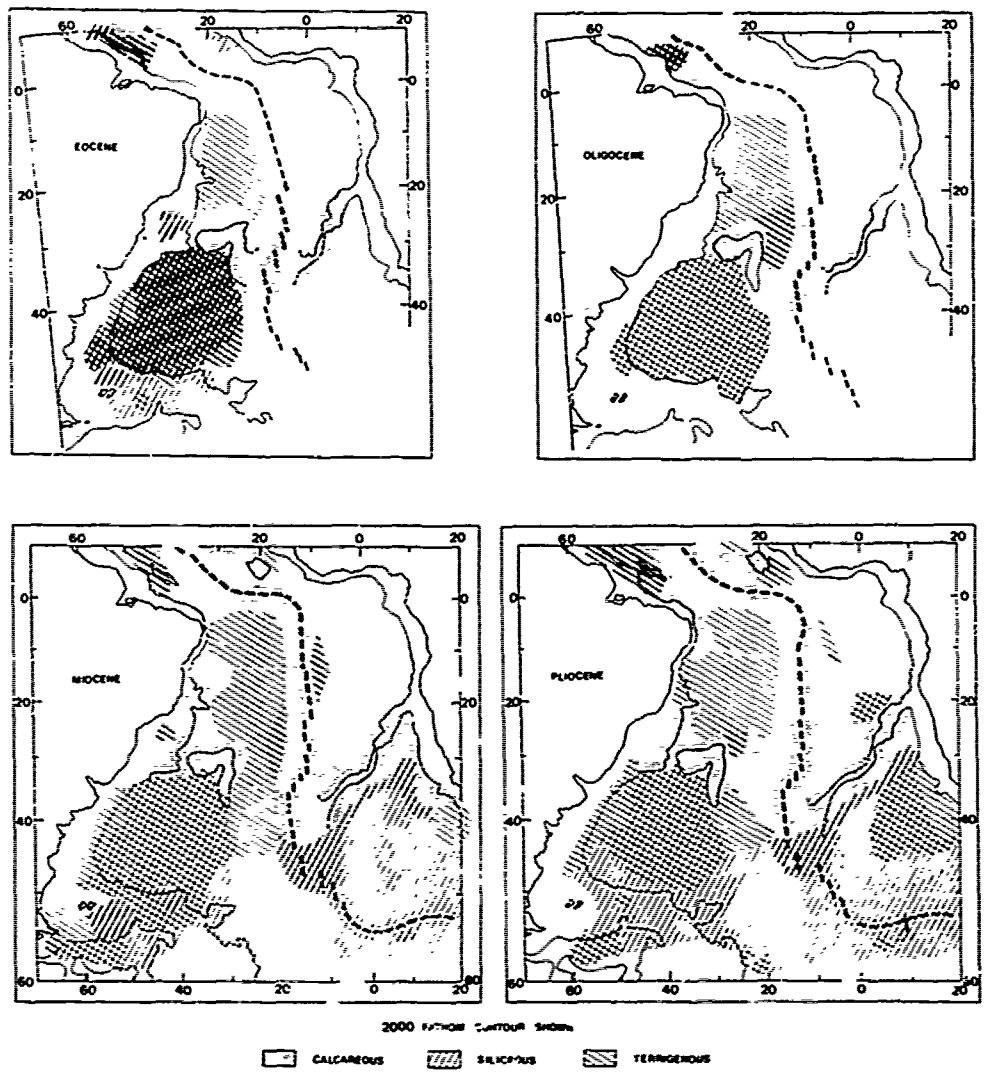


Fig. 3. Observed sediment distribution superimposed upon tectonic reconstructions of the South Atlantic at four time slices (from McCoy and Zimmerman, 1977).

South Atlantic between the late Eocene and present (Figure 2). Recently a complimentary study by McCoy and Zimmerman (1977) using only observational data and a data base amplified by cores from the Lamont-Doherty Geological Observatory gave carbonate line fluctuations very similar to those of Van Andel et al., (1977) (Figure 3).

These studies and that of Ramsay (1977) are evidence that the statistical concept of carbonate compensation surface is a useful idea with which to examine carbonate and non-carbonate deposition during the tectonic history of an ocean. We feel it is important now to extend the qualitative approaches of Berger and Winterer (1974) and Ramsay (1977) and to examine quantitatively some of the phenomena which might directly affect the depth of this surface. Some of these phenomena do not lend themselves to quantitative analysis. For example it is difficult to model fertility changes or changes in the dissolution rate of shells in the absence of any evidence constraining these parameters. Also it is not clear how to handle bottom water flow or the effect of temperature changes in the water column on the saturation curve. On the other hand four phenomena can be examined quantitatively. It is our objective in this paper to examine simplistically but quantitatively the

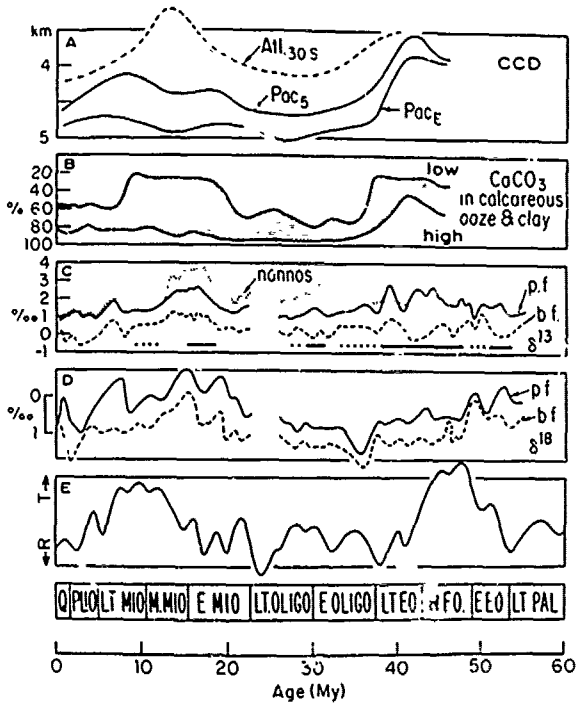


Fig. 4. Comparison of fluctuations in various parameters of the carbon system through the Cenozoic. (a) CCD fluctuations, (b) carbonate scatter (c) $\delta^{13}C$ in nannoplankton in planktonic and benthic foraminifera in DSDP sites 277, 279 and 281, (d) $\delta^{18}O$ in planktonic and benthic forams in same DSDP sites, (e) transgression and regression cycles (from Berger, 1977).

shelf/deep sea fractionation model and to extend it by stages to include the effects of changes in the hyposometric curve of the deep oceans, changes in the slope of the lysocline, and the rate of input of carbonate to the deep sea.

In our analysis we introduce the concept of a mean rectangular ocean and a potentially useful and quantitative method of examining the influence of various factors on ocean sedimentation. We believe the variation of the carbonate compensation surface in the deep ocean is global in nature. Though we do not think we have discovered the unique or even dominant explanation of this variation we feel it is necessary to treat each of the phenomena simplistically and to calculate the magnitude of the various effects under given assumptions. We believe that only by proceeding in this manner will it be possible to separate the basic signal from local geologic noise.

## Shelf Versus Deep Sea Fractionation

Van Andel (1975) has emphasized that the variation of CCD with age for the individual basins have two properties in common. First the CCD is about 1.5 kms deeper during the Quaternary than it was at the beginning of the Tertiary. Second all the profiles show a sharp drop at the beginning of the Oligocene, a general rise in the early to mid-Miocene followed by a sharp drop in the Pliocene (Figure 1). The first property appears true for all basins studied whereas for the second there is considerable variation between basins. The general similarity of the profiles is evidence of a world wide phenomenon. This is almost certainly the case for the general decrease since the late Cretaceous but it is not so convincingly documented for the Miocene shallowing of the CCD.

There are a variety of possible explanations for the observed variation of the CCD. Of these shelf versus deep sea fractionation is the most attractive. It is easy to understand how this explanation would have a world wide effect if the variations of surface area were large and synchronous. Also there is now increasing evidence from the literature for a world wide decrease in sea level since the late Cretaceous which correlates with observed change in CCD. Berger (1977) has demonstrated in a comparison of various parameters in the carbon cycle through the Cenozoic a close correspondence between fluctuations in the plots of CCD, carbonate scatter and eustatic sea level changes (Figure 4). Vail and Mitchum (1978) present additional support for the close correspondence of CCD and Eustatic sea level changes. They show from an analysis of seismic sections on continental shelves considerable evidence for a major fall in sea level since the Cretaceous and also possible evidence for a secondary rise in the Miocene (Figure 5). Though there are questions concerning the amplitude of the sea level changes and the explanation of the sharp nature of the regressions the shape of the CCD curve and a 'statistically-averaged' sea level curve are remarkably similar. High stand corresponds to a shallow CCD in the late-Cretaceous and Early Tertiary and low stand corresponds to a deep Quaternary CCD. We feel that this new evidence requires a more extensive investigation of some quantitative aspects of the shelf versus deep sea fractionation model than was attempted by Berger and Winterer (1974).

Carbonates accumulate more rapidly on continental shelves and in shallow seas than in the deep ocean (Milliman, 1974). If the total input from the rivers remains constant and there is an increase in the area of shelves and the shallow seas the supply of carbonate to the deep sea will drop. To compensate for this drop in supply the CCD will rise. To start our investigation we took the simplest model possible made some very general assumptions and estimated under these assumptions how far the CCD would rise under varying conditions of deposition on the shelves.

Our basic assumptions are that (a) the river

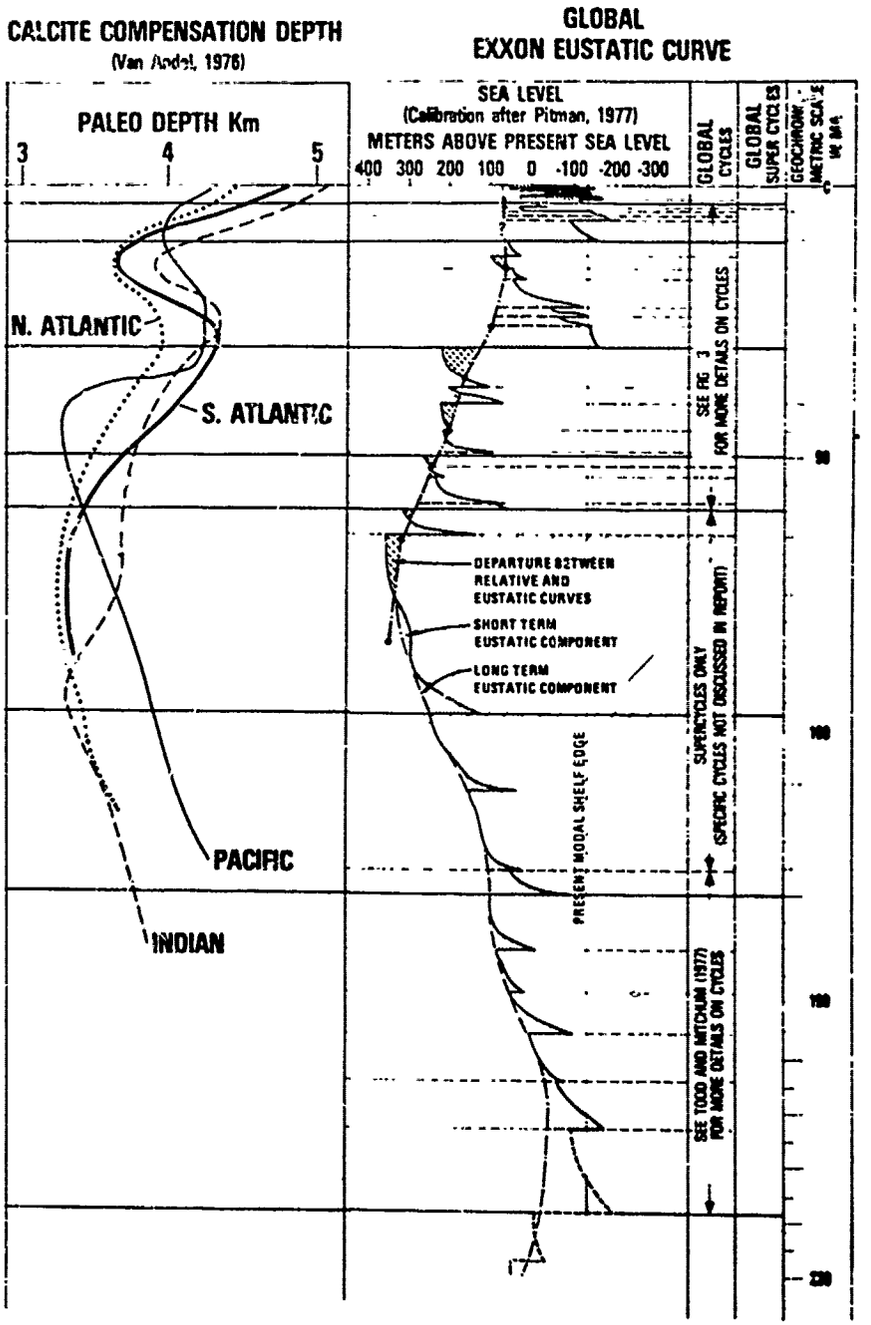


Fig. 5. A direct comparison of the global CCD variation and the Exxon Eustatic sea level curve (from an early version of Vail and Mitchum, 1978).

input equals the sum of the deposition in the shallow seas and in the deep ocean, (b) this input remains constant with time and finally (c) that the deposition in the shallow seas and deep oceans above the CCD is constant and linear and hence is only a function of time. (We will show later that a more realistic non-linear deposition model produces substantially similar results.) These are gross assumptions and are not true in detail (c.f. Berger and Winterer,

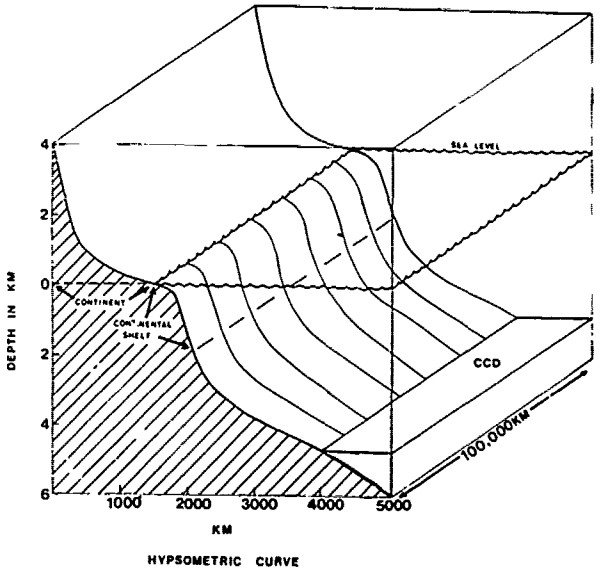


Fig. 6. Hypsometric curve from Kossina (1921).

1974, p. 15) but they suffice for this stage of our treatment. We will neglect recycling within the oceans and ocean sediments. Further we know that the present average CCD is at 4.7 kms and that the area above the CCD represents 61% of the deep ocean. Our only major unknown is the amount of carbonate being deposited in the shallow seas relative to that going into the deep oceans.

To carry out the computations we take the hypsometric curve for both the land and the sea (Figure 6) and tabulate the area of ocean as a cumulative percentage above a certain depth (Table 1). Then, starting with three different assumptions for the present calcareous deposition between the deep ocean and the shelves we change the percentages deposited on the shelves and in the deep sea and compute the effective rise in the CCD. In case 1, we assume all the carbonate is deposited in the deep sea and none on the shelf and ask the question what area is required if we increase the percentage deposition on the shelf to 25%, 50% and 75% and decrease the deposition in the deep sea by the equivalent amount. The area of deep sea involved decreases by 15%, 30% and 46% (i.e., 1/4 of 61%, 1/2 of 61% or 3/4 of 61%). We return to the hyposometric curve and evaluate what depth lies above this calculated percentage of the area. This gives the CCD for the assumed increase in deposition on the shelf. For example, if the area of deep sea necessary is reduced to 46% the CCD goes to 4.0 km or is raised by 0.7 km (Table 2). We considered two other cases, 25% and 50% of present day carbonate accumulation occurring on the shelf, and carried out similar estimates of the change in the CCD with increasing shelf deposition. At present we think that about a quarter to one third of all carbonate is deposited on the shelves and that in the late Cretaceous sea level was 200 to 300 m higher than at present. With these assumptions, Case 2 of Table 2, with a doubling of the shelf area and a consequent doubling of the carbonate accumulation on the shelf we compute that the CCD will rise to 3.7 kms. Thus a 250 to 300 m rise in sea level could raise the CCD by 1 km. This figure is close to that calculated by Berger and Winterer (1974) from a similar but independent line of reasoning.

## Varying the Mean Age of the Ocean

In the simplistic model considered in the previous section we assumed a constant hypsometric curve. This is an unjustified assumption as changes in the mean age of the ocean will cause variations in the volume of the mid-ocean ridges which will in turn alter sea level (Hallam, 1963, Russel, 1968; Menard, 1969 and Valentine and Moores, 1972). As this results in a considerable variation in the amount of shelf flooded (Hays and Pitman, 1973; Pitman, 1978) it is necessary to consider the effects of ridge volume changes and the increased area of the shelf in combination.

In order to compute the effects of ocean volume changes we have redrawn the standard hypsometric curve for oceans and continents. We assumed that all depths shallower than 2.5 km are continent and that all deeper depths are oceans. We split the standard hypsometric curve at this boundary and inverted the oceanic section (Figure 7). The equivalent one-sided rectangular world is 100,000 km in length with 3,100 km of ocean, 500 km of shelf and 1500 km of continent. Making the mean rectangular ocean symmetric reduces the ridge axis length to 50,000 km (close to that observed in the present oceans) and doubles the width of the ocean, shelf and continent. The redrawn hypsometric curve resembles one side of a cross section of the Atlantic.

Next we found a uniform spreading rate ocean

TABLE 1. Oceans Cumulative Area

| Depth (kms) | Cumulative Percentage* Above the Depth |
|---|---|
| .2 | 7.5 |
| 1.0 | 11.9 |
| 2.0 | 16.0 |
| 3.0 | 25.0 |
| 4.0 | 46.0 |
| 5.0 | 77.0 |
| 6.0 | 99.0 |

*(after Menard and Smith, 1966)

TABLE 2. Estimation of Changes in the Mean Calcite Compensation Depth for the Oceans After Varying the Percentage Deposited on the Shelves and in the Deep Sea For Three Different Assumptions About Present Day Conditions.

| | Calcareous Deposition Area Shallow Sea | Deep Sea | Area Required | Depth CCD kms |
|---|---|---|---|---|
| Case 1* | 0% | 100% | 61% | ≤4.7 |
| | 25% | 75% | 46% | ≤4.0 |
| | 50% | 50% | 31% | ≤3.5 |
| | 75% | 25% | 15% | ≤2.0 |
| Case 2 | - | 100% | 81% | ≤5.0 |
| * | 25% | 75% | 61% | ≤4.7 |
| | 50% | 50% | 40% | ≤3.7 |
| | 75% | 25% | 21% | ≤2.5 |
| Case 3 | - | 100% | - | - |
| | 25% | 75% | 91% | ≤5.5 |
| * | 50% | 50% | 61% | ≤4.7 |
| | 75% | 25% | 31% | ≤3.5 |

that gives a reasonable match between the real (Table 3) and theoretical relation between area and age. We chose 3 cm/yr for 100 m.y. for our mean rectangular ocean. Thus our theoretical rectangular world has an ocean area of $300 \times 10^6$ sq. kms and combining this with $50 \times 10^6$ sq. kms for the shelves and $150 \times 10^6$ sq. kms for the oceans (Figure 8) we have numbers that are close to the actual areas involved and also easy to handle (Table 4). Our mean rectangular ocean (Table 5) matches the observed (Table 3) well out to 50 Ma. Thereafter the theoretical is compressed relative to the real world. Using the actual area above given depths we plotted the actual hypsometric curve over our mean rectangular ocean. Then we compared this with a curve where the depths are constrained to follow the relation between depth and age from Parsons and Sclater (1977). The difference between the percent of area actually above a given depth and that predicted from the depth versus age relation is due to the effects of sedimentation, residual depth anomalies and the compression in the older section of theoretical ocean. From the calculations of Berger and Winterer (1974, Figure 11) sediments probably account for about half the difference. For our calculations we ignore any changes in the amount of sediment or in the residual depth anomalies and we assume that this difference remains constant with time. We also ignore the effects of trenches (Pitman, 1978). It is possible to make more exact computations of the effect of spreading rate changes on the actual ocean that we have made here (c.f., Berger and Winterer, 1974; Pitman, 1978). We have chosen our approach of a mean equivalent rectangular ocean because (a) it is very simple (b) it is easy to comprehend exactly what is happening (c) it is easy to compute the actual increase in volume of the ridges and (d) introduces errors that are sufficiently small to be unimportant at our level of argument. It is important to point out that increases in spreading rate are not the only way to decrease the mean age of the ocean. Other possible mechanisms are continental thickening and/or changes in the overall length of the ridge axis. We prefer increasing the mean spreading rate because there is some evidence that it occurs and also because it leads to very easy calculations.

We are now in the position to calculate the affect of varying the spreading rate on the mean volume of the oceans. For these calculations we considered two cases, doubling the spreading rate for 10 million years and doubling it for 50 million years (curves 2 and 3, Figure 8). We assumed no increase in the mean sedimentary fill of the ocean or in the residual depth anomalies. Thus we adjusted the theoretical depth by varying the mean spreading rate and added the constant value representing the sediment and depth anomalies. The difference between the hypsometric curves in the two cases and the present gives the increase in ridge volume as a function of distance from the ridge axis ( H, Figure 8). We averaged this difference to obtain the mean change in ocean

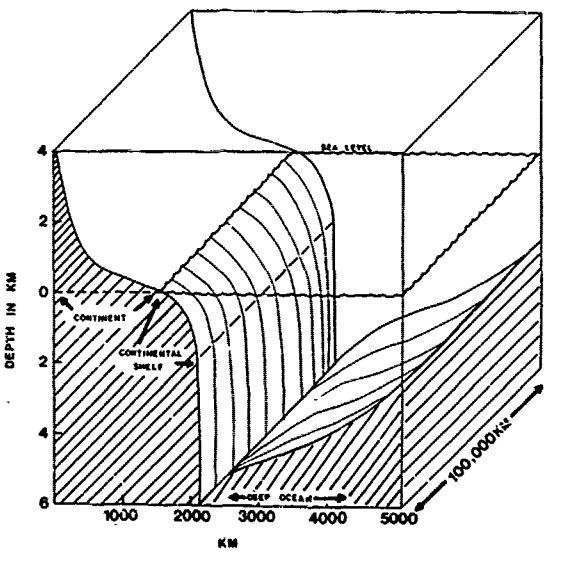


Fig. 7. Alternate presentation of the hypsometric curve to show the creation of sea floor at spreading centers.

TABLE 3. Cumulative Area in $10^6$ sq. kms and Percent for Ocean Crust Younger Than a Given Age.

| Age Ma | Area* x $10^6$ sq. kms | % | Depth+ kms |
|---|---|---|---|
| 4 | 14 | 5 | 3 |
| 20 | 66 | 21 | 4 |
| 35 | 108 | 35 | |
| 52 | 145 | 47 | 5 |
| 65 | 176 | 57 | |
| 80 | 213 | 69 | |
| 95 | 241 | 78 | |
| 110 | 266 | 86 | |
| 125 | 281 | 91 | 6 |
| 140 | 298 | 96 | |
| 160 | 306 | 99 | |
| 180 | 309 | 100 | |

*Area versus age from Sclater et al., (in press).

+Predicted depth from the relation between depth and age from Parsons and Sclater (1977).

volume and muliplied this by .7 to obtain the effective change in freeboard (Table 6).

For the two cases, assuming a given ratio of carbonate on the shelves to that in the deep oceans for the present, it is possible to calculate the relative change in CCD. As before, we determine the percentage increase in shelf area and decrease in area for carbonate deposition in the deep sea. The CCD is found by matching this area with the adjusted hypsometric curve. In the case where we doubled the mean spreading rate for 10 million years and we assume between one quarter and one third of all carbonate is deposited on the shelves the CCD rises by 0.8 to 1.4 km. Doubling the mean rate of spreading for all the ocean with the same two assumptions about present conditions raises the CCD 1.4 to 1.8 km. This last estimate of the changes in mean spreading rate is probably

TABLE 4. Comparison of Actual Area of Continents and Oceans With Asymmetric Rectangular Ocean With 50,000 kms of Ridge Axis Spreading at 3 cm/yr for 100 Million Years.

| | $10^6$ sq. kms | |
|---|---|---|
| | Observed World | Mean Rectangular |
| Continental Area | 149 | 150 |
| Continental Shelf | 52 | 50 |
| Oceans | 309 | 300 |
| Total | 510 | 500 |

TABLE 5. Cumulative Area in Percent For Ocean Crust Younger Than a Given Age For An Ocean Spreading at 3 cm/yr For 100 Million Years.

| Age Ma | Area % | Depth Predicted* | Percent Observed Area Above Given Depth+ |
|---|---|---|---|
| 4 | 4 | 3 | 6 |
| 20 | 20 | 4 | 30 |
| 35 | 35 | | |
| 52 | 52 | | |
| 65 | 65 | 5 | 70 |
| 80 | 80 | | |
| 95 | 95 | | 98 |
| 100 | 100 | 6 | |

*Depth predicted from depth/age relation (Parsons and Sclater, 1977)

+Observed area above a given depth assuming upper 2.5 kms all on continental shelf (from Table 1).

much too great. On the other hand, Pitman (1978) has estimated that in the Cretaceous changes in ridge volume gave rise to about a 300 m change in freeboard which has steadily decreased since then. If our assumptions are valid such a change in freeboard would raise the CCD between 1 and 1.5 km. Thus changes in ocean volume, that are within reasonable limits, clearly have the potential to explain most if not all of the decrease in the CCD since the Cretaceous.

### Relation Between Lysocline, Rate of Input, Hypsometric Curve and CCD

In the previous two sections we have assumed that the accumulation of carbonate in deep sea is a linear function of supply and area. This is overly simplistic as has been pointed out by Berger and Winterer (1974) and in fact their major objection to this model is that it assumes there is no dissolution in areas above the CCS, an assumption that is demonstrably false. In this section we extend our arguments of the previous two sections to include variable dissolution above the CCD. In the process we develop a simple relation between varying the lysocline, the rate input and the oceanic hypsometric curve and the CCD.

Since the dissolution rate of calcium carbonate increases with increasing undersaturation (and therefore with increasing depth, due to the pressure effect on the solubility), carbonate sediments accumulate above the CCD and quantitatively balance the net input to the deep ocean. If an imbalance in the input/output relation occurs, the resulting excess sedimentation/redissolution alters the saturation state of seawater so as to shift the CCD to a

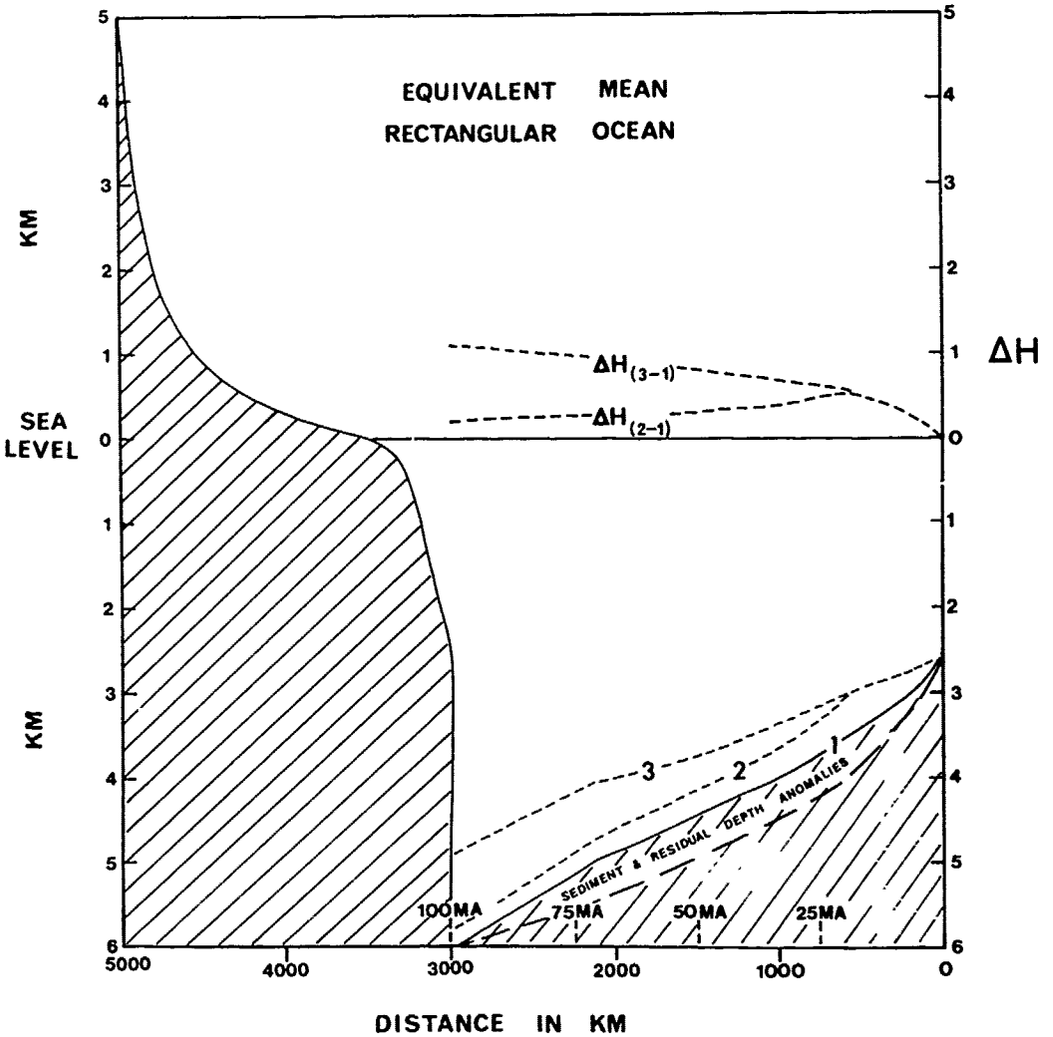


Fig. 8. Equivalent mean rectangular ocean assuming 50,000 kms of ridge axis. 1 represents present hypsometric curve; 2, curve for doubling mean rate of 10 million years and 3, curve for doubling mean spreading rate for 50 million years. Dashed line beneath 1 is the hypsometric curve from age and depth versus age relation. ΔH is the change in sea level associated with changing the mean spreading rate.

level where the area of sedimentation matches the new input.

Using the uniform linear rectangular ocean model this balance can be written

$$Ri - Rss = \int R_s(z)\, A'(z)dz \qquad (1)$$

where Ri is the river input of calcium carbonate and Rss is the rate of sedimentation on the shelf and shallow seas. z is depth in the ocean, $R_s$ is the net sedimentation rate as a function of depth and A'(z) is the first derivative of the area/depth relation of the ocean, A(z). The variation in carbonate sedimentation with depth is a function of the near-bottom carbonate saturation. In the present ocean the transition from supersaturation to undersaturation varies from a few hundred meters to several kilometers (Edmond, 1974) and always increases with depth. For reasons of simplicity, we will parameterize $R_s$ using a hinged 'lysocline' model (Heath and Culberson, 1970), where there is no dissolution down to a depth $Z_o$ and a linearly increasing rate to the CCD

TABLE 6. Computation of Changes in the CCD For Two Different Mean Spreading Rates on the Ocean Floor.

| | Present | Double Rate 50 Ma | Double Rate 10 Ma |
|---|---|---|---|
| Mean Rise in Ridge Volume | - | 750 M[1] | 350 M[2] |
| Mean Change in Sea Level | - | 530 M | 250 M |
| Area Increase For Shelves | - | 250% | 200% |
| Case 1 | | | |
| Carbonate on Shelves | 25% | 62.5% | 50% |
| Carbonate in Deep Sea | 75% | 37.5% | 50% |
| Area of Ocean Above CCD | 61% | 30% | 40% |
| Depth of CCD in Km | 4.7 | 3.3 | 3.9 |
| Case 2 | | | |
| Carbonate on Shelves | 33% | 83% | 67% |
| Carbonate in Deep Sea | 67% | 17% | 33% |
| Area of Ocean Above CCD | 61% | 14% | 27% |
| Depth of CCD | 4.7 | 2.9 | 3.3 |

[1]Mean of ΔH(3-1) Figure 8

[2]Mean of ΔH(2-1) Figure 8

$$Rs = Rp \frac{(z_{CCD}-z)}{(z_{CCD}-z_o)} \quad \text{for} \quad (z_{CCD}>z>z_o) \qquad (2)$$

where Rp is the uniform surface carbonate productivity.

A(z) below 2 km can be approximated by a parabolic fit

$$A(z) = a_o + a_1 z + a_2 z^2 \qquad (3)$$

so that $A'(z) = a_1 + 2a_2 z$ (4)

Thus (1), (2) and (4) can be combined to give

$$\frac{Ri - Rss}{Rp} = A(\leq 2) + \int_2^{z_o} (a_1+2a_2 z)dz +$$

$$\int_{z_o}^{Z_{CCD}} \frac{(Z_{CCD}-z)}{(Z_{CCD}-z_o)} (a_1+2a_2 z)dz \qquad (5)$$

$$= (A(\leq 2)-2a_1-4a_2) + a_2(z_o^2+z_{CCD}^2+z_o z_{CCD})$$

$$+ \frac{a_1}{2}(z_{CCD}+z_o) - \frac{2a_2}{3}\left(\frac{z_{CCD}^3-z_o^3}{z_{CCD}-z_o}\right) \qquad (6)$$

Let $A = A(2)-2a_1-4a_2$ and $R = \frac{R_i-R_{ss}}{R_p}$.

Multiplying through by $(z_{CCD}-z_o)$ and rearranging terms:

$$(A-R)Z_o + \frac{a_1}{2} Z_o^2 + \frac{a_2}{3} Z_o^3 = (A-R)Z_{CCD}$$

$$+ \frac{a_1}{2} Z_{CCD}^2 + \frac{a_2}{3} Z_{CCD}^3$$

This simple cubic equation in $Z_{CCD}$ (neglecting the false root $Z_{CCD} = Z_o$) can be used to investigate the effect of changes in the net deep ocean input, the area versus depth relation and $z_o$ on the CCD.

We examined this system assuming the present day CCD is 4.7 km and that A(z) as a percentage of total area was given by the following relation (after Menard and Smith, 1966)

$$A(z) = 14.6\% \quad (z \leq 2)$$

$$A(z) = 23.2 - 13.9z + 4.8z^2(\%) \quad (z \geq 2)$$

Using values for $z_o$, the depth of the lysocline, of 3.5, 3.0 and 2.5 km requires Rp values of 2.11, 2.36, and 2.68 times the net input $(R_i - R_{ss})$ respectively. Doubling the spreading rate for 10 million years (the first case considered in the previous section) gives an A(z) in present form Figure 8 of

$$A(z) = 15\% \quad (z \leq 2)$$

$$A(z) = -2.6 + 2.6Z + 3.0Z^2(\%),$$

$$(z \geq 2)$$

This bathymetric distribution was used with the above paired $Z_o$ and Rp values, and the results of these investigators together with the critical depth CCD models discussed earlier are presented in graphical form (Figure 9).

Several features are immediately obvious from the graphs. The critical depth and lysocline models differ little in their prediction for the change in the CCD versus change in the net input, for small perturbations about the present-day input (<25%). The variation of lysocline depths (and thus variation of dissolution gradients, Heath et al., 1977) does not significantly affect the results. It appears that the depth variations of the CCD with changing input are relatively insensitive to the model chosen; in all cases the gradient is approximately 0.35 km per 10 percent change in net input.

It appears that the effect of changing the bathymetric distribution is quite significant: a change in the spreading rate of a factor of two for 10 m.y. will raise the CCD by 0.8 km in the absence of any net input changes. Since

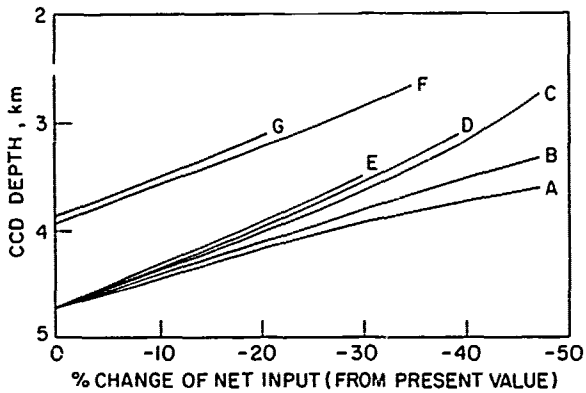


Fig. 9. CCD changes associated with changing the depth of the lysoline $z_o$ and varying the percent change of river input from present.
A: case 1 from Table 2 ("critical depth" CCD), present-day bathymetry
B: case 2 from Table 2 ("critical depth" CCD), " "
C: hinged lysocline model, $z_o$ = 2.5 km, present-day bathymetry
D: " " " $z_o$ = 3.0 km, " "
E: " " " $z_o$ = 3.5 km, " "
F: " " " $z_o$ = 2.5 km, 10 m.y. spreading-rate doubling
G: " " " $z_o$ = 3.0 km, " " "

the accompanying extensive shallow sea formation should decrease the net input, a combined model for the change in CCD suggests that a relatively modest decrease of -20% from the present-day net input can combine with the effect of the changing bathymetry to produce the observed 1.4 km shift in the CCD between the Cretaceous and the present.

Although these models differ from reality in several features, the insensitivity of the calculations to the two quite different representations of the CCD suggests that improvements in the realism of the models probably will not alter the results substantially. This observation does not deny the influence of other variables on the CCD; rather it implies that the effects of changing bathymetry and net input can account for much of the observed variability.

## Conclusions

The analysis of Berger and Winterer (1974) and the attempts to interpret sediment distribution in the Atlantic and Indian Oceans by Van Andel et al., (1977), McCoy and Zimmerman (1977) and Sclater et al., (1977) have shown that the carbonate compensation surface (CCS) and the 'carbonate line' are useful concepts when viewed in a statistical manner over 5 million years. Particularly revealing is the evidence presented by Van Andel (1975) that the calcite compensation depth has a uniform variation for all ocean basins since the Late Cretaceous. Recently Vail and Mitchum (1978) have shown that changes in the global height of sea level have the same shape and the correct sense to account for the variations in the CCD.

We show that the ocean volume changes necessary to explain the decrease in Eustatic sea level since the Late Cretaceous (Pitman, 1978) would have a major effect on the CCD. For example three effects, changing hypsometry, increased surface area and hence deposition on the shelf and reduced input all affect the CCD in the same direction. This coupled with the observation that the major shelves were in a more southerly latitude in the Cretaceous all make shelf/deep sea fractionation a most attractive explanation of gross CCD changes in the ocean.

Two other lines of evidence also support this explanation of the general decrease in the depth of the CCD since the late Cretaceous. First Hallam (1977) has estimated that as much as 50 x $10^6$ sq. km of present continental area were flooded in the late Cretaceous and since this area has decreased relatively uniformly. This figure is very close to that used in our analysis of the effect of increasing the spreading rate by a factor of two for 10 million years. Second, Davies et al., (1977) have demonstrated a net decrease in carbonate accumulation in the ocean between the present and the Paleocene. Such a decrease is totally consistent with a lack of input due to steadily increasing accumulation in the shelf during the early Tertiary transgression.

Though this shelf/deep sea explanation is the most attractive, there are still some unresolved problems. First, the observational basis for the correlation between CCD variations and changes in Eustatic sea level is not overwhelming. The curves of Van Andel (1975) are preliminary and there are questions concerning the amplitude of the changes in sea level noted by Vail and Mitchum (1978). Second, compilation of global oceanic sedimentation rates show lower values during the Oligocene than in the Eocene. This is in direct conflict with the prediction of the basin/deep sea fractionation model where high rates would be predicted during a regression and a deep CCD. Finally, third, a dramatic drop of about 1 km is observed in the late Eocene for the CCD in all basins (Figure 1). Ocean volume changes associated with decreasing the mean age of the ocean are not sufficiently fast to explain such a rapid change.

The above points demonstrate that considerably more work is needed to resolve the enigma

of CCD variations in the deep sea. This is particularly true because the implications of the possible explanations are important for geology and geophysics as well as micropaleontology.

If it can be shown that both the CCD and the eustatic sea level curve can be related to changes in ocean volume over the past 50 million years, then variations in these curves can be used to investigate changes in ocean volume throughout the geologic record. As these changes result from variations in the rate of heat loss of the earth, the CCD and eustatic curves may enable us to examine these variations as a function of time (Turcotte and Burke, 1978). This information would be invaluable for models of thermal convection and global heat loss. Because this problem is of such potential importance we feel more effort should be placed to justify the observational basis of the correlations we have assumed to exist in this paper and further careful quantitative analysis should be made of explanations such as fertility and deep sea currents which we have not considered. The preliminary approach of Ramsay (1977) to hiatuses appears to have considerable potential for the quantitative analysis of the effects of deep sea currents, and internal recycling of carbonates within the ocean.

Acknowledgements

We would like to thank Colin Summerhayes, Wolfgang Berger, Ross Heath, and Taro Takahashi for help, suggestions and criticism in the initial stages of this manuscript. The work was supported by the Office of Naval Research.

References

Berger, W.H., Deep-sea carbonates: dissolution facies and age-depth constancy, Nature 236, 392-395, 1972.

Berger, W.H., Carbon dioxide excursions and the deep-sea record: aspects of the problem, in Fate of Fossil Fuel $CO_2$, N.R. Anderson and A. Malahoff, (eds.) Plenum, NY, 505-542, 1977.

Berger, W.H., and U. Von Rad, Cretaceous and Cenozoic sediments from the Atlantic Ocean, in Hayes, D.E., Pimm, A.C., et al., Initial Reports of the Deep Sea Drilling Project, Vol. XIV, Washington, DC (U.S. Government Printing Office), p. 787-954, 1972.

Berger, W.H. and Winterer, E.L., Plate stratigraphy and the fluctuating carbonate line: International Association of Sedimentology, Spec. Publ. Vol. 1, p. 11-48, 1974.

Davies, T., et al., Science, 1 July 1977, 197, p. 55, 1977.

Edmond, J.M., On the dissolution of carbonate and silicate in the deep ocean, Deep Sea Res., 21, 455, 1974.

Hallam, A., Major epeirogenic and eustatic changes since the Cretaceous and their possible relationship to crustal structure, Amer. J. Sci., 261, 397-423, 1963.

Hallam, A., Secular changes in marine inundation of USSR and North America through the Phanerozoic, Nature, 269, 769-772, 1977.

Hays, J.D. and W.C. Pitman, Lithospheric plate motion, sea level changes and climatic and ecological consequences, Nature, 246, 18-12, 1974.

Heath, G.R., T.C. Moore, Jr., and T.H. Van Andel, Carbonate accumulation and dissolution in the equatorial Pacific during the past 15 million years, in The Fate of Fossil Fuel $CO_2$ (eds. N. Andersen and A. Malahoff), Plenum, NY, pp. 627-640, 1977.

Kossina, E., Die Tiefen des Weltmeers, Meeresk. Geogr. Natuno. 9, 70 pp., 1921.

Luyendyk, B.P., D. Forsyth, and J.D. Phillips, An experimental approach to the paleocirculation of the oceanic surface waters, Bull. Geol. Soc. Amer., 83, 2649-2664, 1972.

McCoy, F.W. and H.B. Zimmerman, A history of sediment lithofacies in the South Atlantic, in P. Supko and K. Perch-Nielson, et al., Initial Reports of the Deep Sea Drilling Project, Vol. XXXIX, Washington, DC (U.S. Government Printing Office), 1977.

Menard, H.W. and S.M. Smith, Hypsometry of ocean basin provinces, J. Geophys. Res., 71, 4305-4326, 1966.

Menard, H.W., Elevation and subsidence of oceanic crust, Earth Planet. Sci. Lett., 6, 275-284, 1969.

Milliman, J.D., Marine Carbonates, Springer-Verlag, Berlin, pp. 206-222, 1974.

Parsons, B. and J.G. Sclater, An analysis of the variation of ocean floor bathymetry and heat flow with age, J. Geophys. Res., 82, 5, 803-827, 1978.

Pitman, W.C., Relationship between Eustacy and stratigraphic sequences of passive margins, Bull. Geol. Soc. Amer., 89, 1389-1403, 1978.

Ramsay, A.T.S., Sedimentological clues to Paleo-oceanography in Oceanic Micropaleontology, A.T.S. Ramsay, ed., 1371-1453, Academic Press, New York, 1977.

Sclater, J.G., D. Abbott, and J. Thiede, Paleobathymetry and sediments of the Indian Ocean, in Indian Ocean Geology and Biostratigraphy, Studies Following DSDP Legs 22-29, edited by J.R. Heirtzler et al., AGU Monograph, 1977.

Sclater, J.G., C. Jaupart, and D. Galson, The heat flow through oceans and continents, submitted to Rev. of Geophys., 1978.

Turcotte, D.L. and K. Burke, Glacial sea-level changes and the thermal structure of the earth, Earth Planet. Sci. Lett., 41, 341-346, 1978.

Vail, P.R., R.M. Mitchum, Jr. and S. Thompson, III, Seismic stratigraphy and global changes of sea level in Payton, C., ed., Stratigraphic

Interpretation of Seismic Data, Amer. Assoc. of Pet. Geol., Memoir 26, 83-97, 1976.

Valentine, J.W., and E.M. Moores, Global tectonics and the fossil record, J. Geol., 80, 167-184, 1972.

van Andel, Tj. H., Mesozoic-Cenozoic calcite compensation depth and the global distribution of calcareous sediments, Earth Planet. Sci. Lett., 26, 187-194, 1975.

van Andel, Tj. H., G.R. Heath, and T.C. Moore, Cenozoic history and paleoceanography of the central equatorial Pacific Ocean, Geol. Soc. Amer., Memoir, 143, 1-134, 1975.

van Andel, Tj. H., J. Thiede, J.G. Sclater, and W.H. Hey, Depositional history of the South Atlantic Ocean during the last 125 million years, J. Geology, 85, 5, 509-552, 1977.

# PALEOCEANOGRAPHIC IMPLICATIONS OF ORGANIC CARBON AND CARBONATE DISTRIBUTION IN MESOZOIC DEEPSEA SEDIMENTS

Hans R. Thierstein

Scripps Institution of Oceanography, University of California, San Diego,
La Jolla, California 92093

Abstract. Depositional environments in the deep Atlantic, Pacific and Indian Ocean underwent large changes from 140 m.y. to 60 m.y. ago. The bathymetric and chronologic distribution patterns of organic carbon and carbonate suggest strong basin-basin fractionation of abyssal waters. A model of salinity-stratified deep waters in topographically restricted basins is proposed to explain occurrence and timing of Cretaceous anoxic events and the peculiarities of Mesozoic carbonate versus depth profiles.

## Introduction

Recent success in the recovery of Mesozoic deep-sea sediments by Glomar Challenger of the Deep Sea Drilling Project (DSDP) has made it obvious that depositional oceanic environments in the past must have been very different from today's. The evidence includes widespread intermittent occurrence of mid-Cretaceous black shales (recently reviewed by Ryan and Cita (1977)), and the rapid fluctuations of the carbonate compensation depth (CCD) observed in the major ocean basins during the Cretaceous (Thierstein and Okada, in press). Potential variables to be examined in an attempt to understand past changes in ocean circulation and climate are paleogeography, paleobathymetry, distribution, preservation, geochemistry and accumulation rates of sediment components, and evolution and diversity of organisms. Among these parameters the stratigraphic and paleobathymetric distributions of carbonate and organic carbon through the Mesozoic are analyzed and interpreted in the framework of a dominantly salinity-stratified world ocean with topographically isolated basins leading to repeated basin-basin deep-water fractionation.

## Data Base and Data Treatment

### Time Scale

The accuracy of the time scale used in paleooceanographic reconstructions deserves critical evaluation, since it is important in several aspects. Biostratigraphy places the sediments from different paleoenvironments into a relative time-framework. Knowledge of the present depth and absolute age of deposition of a sediment sample, and of the absolute age of the emplacement of the underlying oceanic crust allows the depositional paleodepth to be determined (Berger, 1972). Because oceans are dynamic systems, they are characterized by processes which vary through space and time. Past changes in such processes can only be unraveled if various sedimentary constituents (grain size, biological, mineralogical, and chemical components) are interpreted with respect to rates of accumulation or dissolution.

While late Cretaceous biostratigraphic, magnetic and radiometric time scales are reasonably well established, the correlation and absolute ages of pre-Cenomanian magnetic reversals and biostratigraphic events is still controversial. Uncertainty on the absolute length of the Albian stage, for instance, is over 50%, if the time scales proposed by van Hinte (1976a) and Thierstein (1976) are compared with the biostratigraphically correlated radiometric K/Ar ages given by Obradovich and Cobban (1975); age estimates based upon the magnetic reversal time-scale by Larson and Pitman (1972) and van Hinte (1976a,b) differ by as much as 13 million years (Berggren et al., 1975)!

In the absence of direct radiometric measurements, dating of the Mesozoic magnetic anomaly sequence is almost exclusively done via the oldest nannofossil assemblages overlying basaltic basements (Larson and Chase, 1972; Larson and Pitman, 1972; Larson and Hilde, 1975). These nannofossil assemblages are in turn correlated with the assemblages observed in Cretaceous stratotypes (Manivit, 1971; Sissingh, 1977; Thierstein, 1973, 1975, 1976). All presently available radiometric ages in the late Jurassic and early Cretaceous are correlated with the stratotypes by independent paleontologic evidence. A number of DSDP sites drilled on

Mesozoic magnetic anomalies do allow correlation of the magnetic and biostratigraphic time scales: anomaly M-0 has been dated as late Aptian at Site 417 (Donnelly et al., 1977), anomaly M-4 as Hauterivian to Barremian at Site 303 (Larson, Moberly et al., 1975; personal observation), the interval between anomalies M-7 and M-8 as Hauterivian at Site 166 (Thierstein, 1976), anomaly M-9 as middle to late Valanginian at Site 304 (Larson, Moberly et al., 1975; personal observation), and the interval between anomalies M-15 and M-16 as early Valanginian at Site 387 (Okada and Thierstein, in press). These correlations required only minor adjustments to be made to the correlation of the Cretaceous magnetic reversal sequence with biostratigraphy proposed by Thierstein (1976). This adjusted Cretaceous time-scale has been used to assign absolute ages to magnetically dated basement and biostratigraphically dated sediments. Age estimates of Jurassic magnetic anomalies and sediment samples are averages of the absolute time-scales proposed by van Hinte (1976b) and Thierstein (1976). The absolute ages of those cores which contained no biostratigraphic boundaries or were barren of any fossils were interpolated from the age of the closest underlying and overlying fossiliferous cores.

## Paleobathymetry

All DSDP sites that were drilled on Mesozoic crust during legs 1 through 53 and whose basement ages are known or can be reasonably well estimated (Table 1) have been backtracked from their present depth along the empirical subsidence curve given by Berger and Winterer (1974). Their paleogeographic distribution is shown in Figures 1 - 3 (after Smith and Briden, 1977; Sclater, Abbott and Thiede, 1977; Lancelot, 1978). Parsons and Sclater (1977) have recomputed an empirical subsidence curve which includes recently drilled sites on old basement. Their curve indicates that our paleodepth estimates for the older parts may be too shallow by up to 100 m. Computed paleodepositional depths were corrected for the thickness and the isostatic effect of sediments deposited since ("back-stripping" of Watts and Ryan, 1976) by applying a correction factor of 50% (Berger, 1972) (Figure 4 - 7). More recently an isostatic correction of one third of the sediment thickness was used by van Andel et al. (1977), which would result in a paleodepositional estimate 200 m deeper than ours for a sediment load of 1 km. These possible errors, together with those caused by uncertainties of the absolute age of magnetic anomalies and biostratigraphic events, are systematic and may be analysed at all sites. Additional errors are introduced by the uncertain position of a sediment sample within a biostratigraphic zone or by uncertainty of depth determination in DSDP holes (van Andel, 1972; for discussion and review see also Thierstein and Okada, in press). We estimate that our paleodepth determinations are generally within ± 200 m and, particularly in the early part of the subsidence history of a site, within ± 300 m of the true paleodepth. This also applies to sites drilled on aseismic ridges and near continental margins since their subsidence appears to closely follow, after correction for sediment loading, the lithospheric cooling curve of mid-oceanic ridges (Sleep, 1971; Watts and Ryan, 1976; Detrick, Sclater and Thiede, 1977).

## Organic Carbon and Carbonate Data

All carbonate and organic carbon measurements made on Mesozoic and early Paleocene sediments recovered during the first 52 legs of the Deep Sea Drilling Project were obtained from the DSDP data bank. Additional carbonate measurements of late Cretaceous sediments from Sites 192, 199 and 289 were made in our laboratory and incorporated into the data base. For each measured sample an estimate of the time of deposition, based on its fossil content, and an estimate of the paleodepth of deposition, based on the subsidence curve, were made. Data for each major ocean basin were then plotted by computer on an age versus paleodepth diagram with a grid resolution of one million years and 200 m depth. Four plots per run were produced, one showing the number of over-lapping data points per grid point (Figures 8 - 11) and one each showing the minimum, maximum and averaged organic carbon and carbonate values encountered at each grid point. The values were then contoured by hand.

Considerable variability of carbonate and organic carbon values in any one grid point or of neighboring grid points were occasionally encountered. The variability was analyzed in each instance for its possible cause, such as provenance from different geographic areas for samples with similar ages and paleodepths, or dilution by detritus, or rapidly alternating lithology as encountered frequently in the transitional interval from early Cretaceous well-oxygenated chalks and limestones into middle Cretaceous black shales (e.g. DSDP Sites 105, 384, 367). Within these intervals of a highly variable CCD, contouring average, rather than minimum carbonate contents appears to be the most sensible way to interpret the data, since frequent carbonate content excursions over short time intervals are far beyond the biostratigraphic and plotting resolution and, occasionally, might even be due to local displacement. Organic carbon contents are contoured around the maximum values encountered. When averaged, most of these values decrease to below one percent and only high, isolated values remain. Such a plot thus would contain a strong sample density bias.

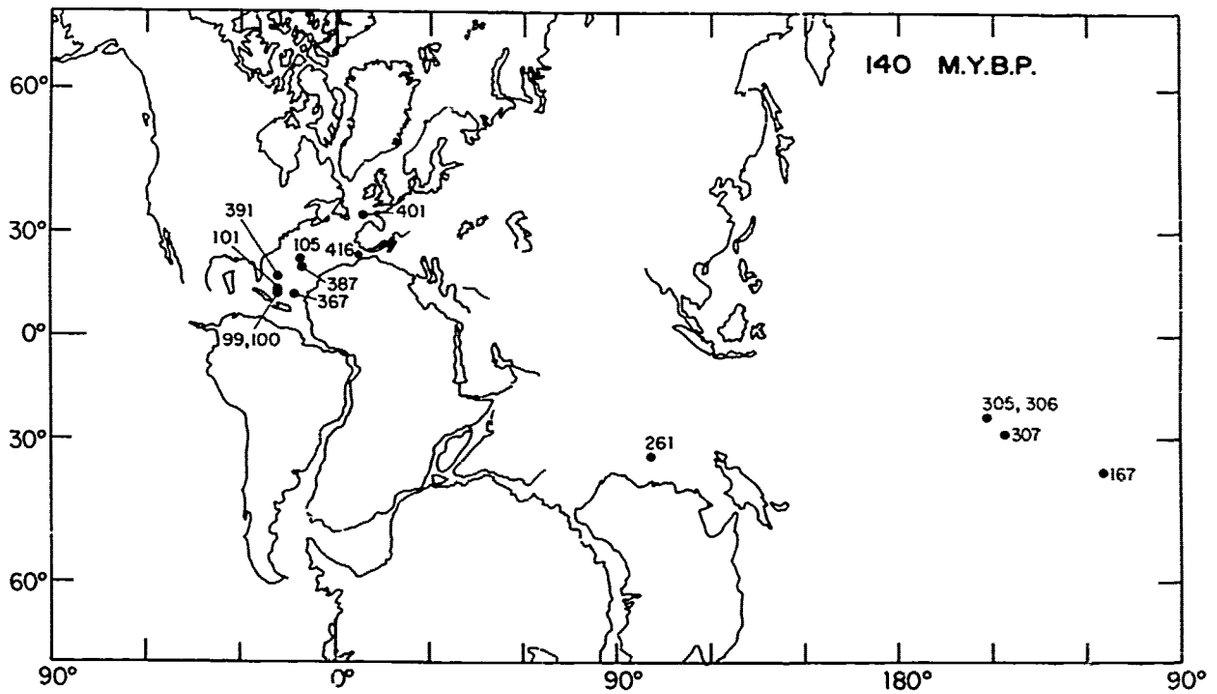


Figure 1. Paleogeography and paleoposition of DSDP sites 140 million years ago.

### Distribution of Organic Carbon

Increasing attention is being given to the unique organic carbon preservation in Mesozoic black shale deposits recovered from all ocean basins by the Deep Sea Drilling Project (see reviews by Schlanger and Jenkyns, 1976, and Ryan and Cita, 1977) in an attempt to understand the paleoceanographic and economic implications of widespread oxygen depletion of deep ocean waters (Fischer and Arthur, 1977; Thiede and van Andel, 1977; Arthur and Schlanger, in press). Although the provenance of the preserved organic compounds is still being established (Tissot, this volume), the fact that organic carbon of pelagic or detrital origin has never been preserved since, and possibly never prior to the middle Cretaceous, in such quantities (Irving et al., 1974) warrants a careful review of the stratigraphic and paleobathymetric distribution of organic carbon in Mesozoic sediments.

#### North Atlantic

The highest organic carbon contents measured in Mesozoic sediments of the North Atlantic are shown in Figures 12 - 14. In the western North Atlantic (Figure 9) organic carbon contents (in weight percent of dry bulk sample) increase above one percent in the earliest Berriasian (Nannoconus colomi Zone) at Site 391C (Wind, in press) and in the late Berriasian to early Valanginian (Cretarhabdus angustiforatus Zone) at Site 387 (Okada and Thierstein, in press). Values above three percent occur from the early Hauterivian onwards (Sites 105, 387 and 391). The highest organic carbon contents in the western Atlantic are observed in the late Cenomanian at Sites 386 (11.5%) and 387 (11.3%). One odd value of 4.0% occurs in late Campanian chalks at Site 10, and two measurements of less than 1.3% were made in early Paleocene sediments at Site 387.

In the eastern North Atlantic basin (Figure 13) the earliest organic carbon contents above one percent occur in the Hauterivian at Sites 367 and 416 (Cepek, 1978; and pers. comm.). Highest values have been observed in the late Albian to earliest Turonian at Site 367 and the Albian at Site 369. The maximum organic carbon content (28.0% in 367-18-2, 34 cm) appears also to be the youngest one measured in the deep North Atlantic. In the site report (Lancelot, Seibold et al., 1978) the age of Core 18 is indicated as Cenomanian or younger, based on foraminifera and nannoplankton. Cepek (1978), however, claims a Coniacian age for Core 18, the evidence being the occurrence of Lucianorhabdus cayeuxii as the only species present in the core

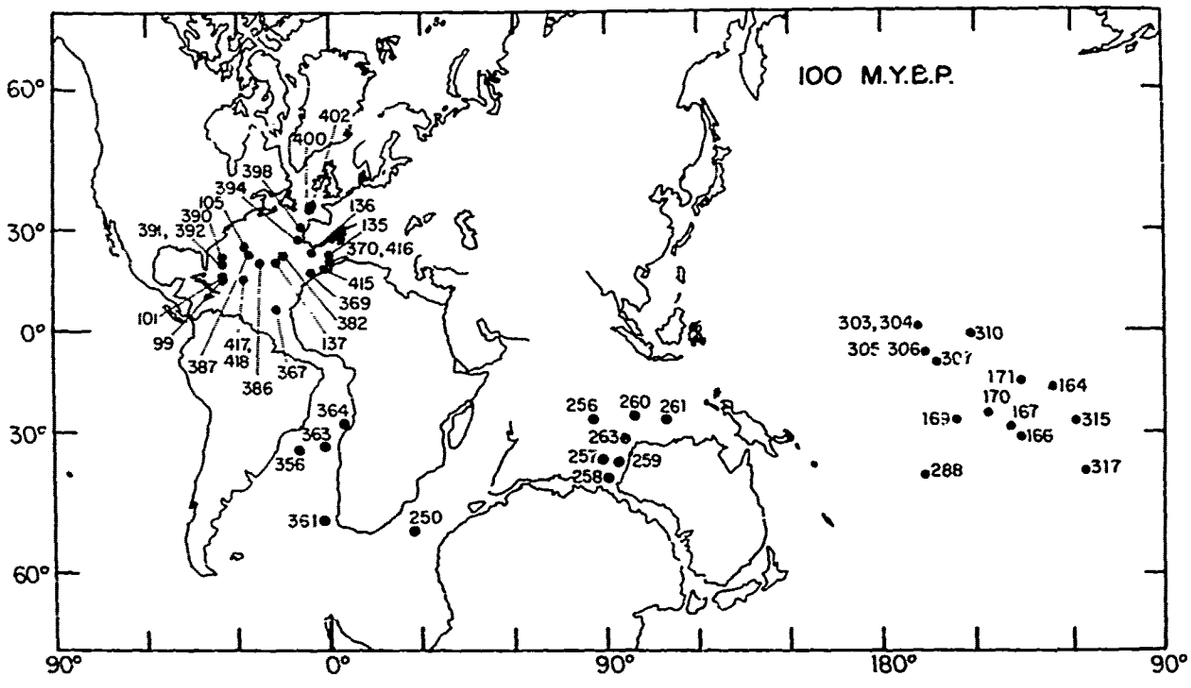


Figure 2. Paleogeography and paleoposition of DSDP sites 100 million years ago.

catcher sample. L. cayeuxii s.l., however, has been observed in the Turonian type area by Manivit (1971), Thierstein (1976), Sissingh (1977) and Verbeck (1977). Reexamination of nannofossils in 16 samples from Core 18 yielded a late Cenomanian to early Turonian age (with Podorhabdus albianus, Gartnerago obliquum, G. nanum present and no Vagalapilla octoradiata, Eiffellithus augustus, Micula staurophora, Corollithion exiguum or Kamptnerius spp. present). Core 19, recovered immediately below, contains Cenomanian planktonic foraminifera. Organic carbon accumulation in the deep North Atlantic therefore appears to have ceased by the early Turonian. Early and middle Cretaceous organic carbon accumulations in the North Atlantic are highest in the deeper parts of the basins and are not concentrated along the continental margins (Figure 14). The distribution pattern may have been somewhat different during late Cretaceous in the southwestern North Atlantic and in the Caribbean, because unknown basement ages or poor biostratigraphic control have so far prevented incorporation of the following organic carbon measurements exceeding 1% into our interpretation:

Eastern North Atlantic

Site 138, Core 6, 16.8% organic carbon, 1 sample, unknown age

Site 368, Core 60, 3.3% organic carbon, 1 Turonian sample

Site 368, Core 63, 7.6% organic carbon, 1 Cenomanian sample

Southwestern North Atlantic

Site 144, Core 4, 6.5% and 10.3% organic carbon, 2 Cenomanian samples

Site 144, Core 5A, 11.1% organic carbon, 1 Coniacian-Santonian sample

Caribbean

Site 150, Core 9, 3.1% organic carbon, 1 Coniacian-Santonian sample

Site 151, Core 12, 4.2% and 4.7% organic carbon, 2 Santonian samples

Site 153, Core 16, 1.9% to 6.2% organic carbon, 3 Coniacian samples

Site 153, Core 17, 4.2% organic carbon, 1 Turonian-Coniacian sample

South Atlantic

The history of organic carbon deposition in

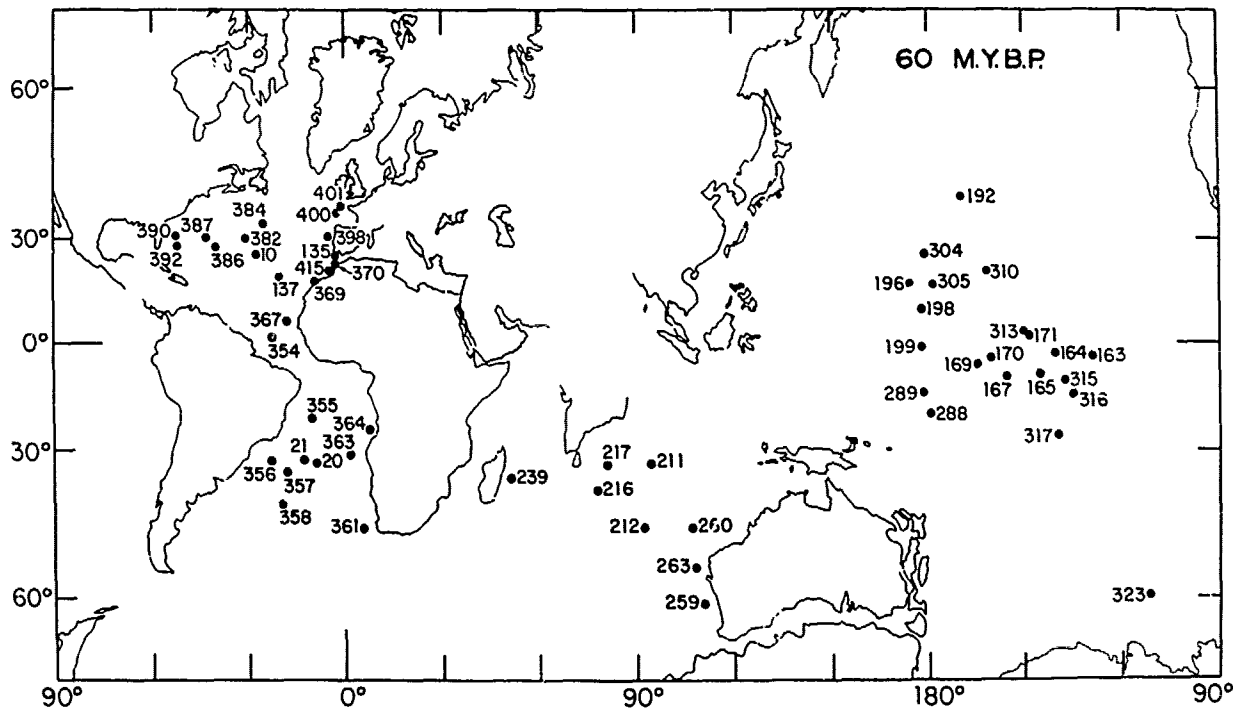


Figure 3. Paleogeography and paleoposition of DSDP sites 60 million years ago.

the South Atlantic is shown in Figure 15. The oldest recovered sediments are of early Aptian age (Proto Decima et al., 1978) at Site 361 in the Cape Basin, where the highest organic carbon values range from 13.7% in the early Aptian to 14.6% in the late Aptian. In Albian through Santonian sediments from the Cape Basin, organic carbon accumulations never exceed 2% and those from post-Santonian time remain below 1%, as do those from the Argentine Basin. Oxygen deficiency apparently persisted longer north of the Rio Grande-Walvis sill. A maximum of 22.5% organic carbon occurs in late Aptian sediments from Site 364 off the Angolan coast, values below 2% occur in samples of middle Albian and younger age. A single early Santonian sample at Site 364 with 21.3% organic carbon marks the end of oxygen deficiency in the South Atlantic. Occurrences of organic carbon from the Brazil basin are limited to less than 4.8% and were found at Site 356 in sediments of Turonian to Coniacian age (Supko, Perch-Nielsen, et al., 1977). The available evidence from the South Atlantic is not sufficient to show whether the late Cretaceous oxygen deficiency in the northern part or the South Atlantic was due to stagnation or an intensification of an intermediate oxygen minimum layer (Thiede and van Andel, 1977). The high late Cretaceous organic carbon contents north of the Rio Grande-Walvis sill are in the deepest sediments recovered so far within that topographically restricted basin and can not reasonably be compared with Site 361 on the south side of the shallow sill, where high organic carbon accumulations are limited to the early Cretaceous.

The following organic carbon contents in excess of 1% have been measured at other South Atlantic DSDP sites of unknown paleodepths:

Northern Brasil Basin

Site 24, Core 3, 1.2% organic carbon, 1 late Cretaceous sample

Falkland Plateau

Site 327A, Cores 22 - 25, 1.1% to 3.5% organic carbon, 3 Aptian samples

Site 327A, Cores 26, 27, 1.4% and 2.6% organic carbon, 2 Berriasian-Hauterivian samples

Site [illegible], Core 3, 5.8% organic carbon, [illegible]ian sample

Site 330, Core 4, 5.3% organic carbon, 1 Berriasian-Hauterivian sample

Site 330, Cores 5 - 13, 1.2% to 4.4% organic carbon, 28 Oxfordian samples

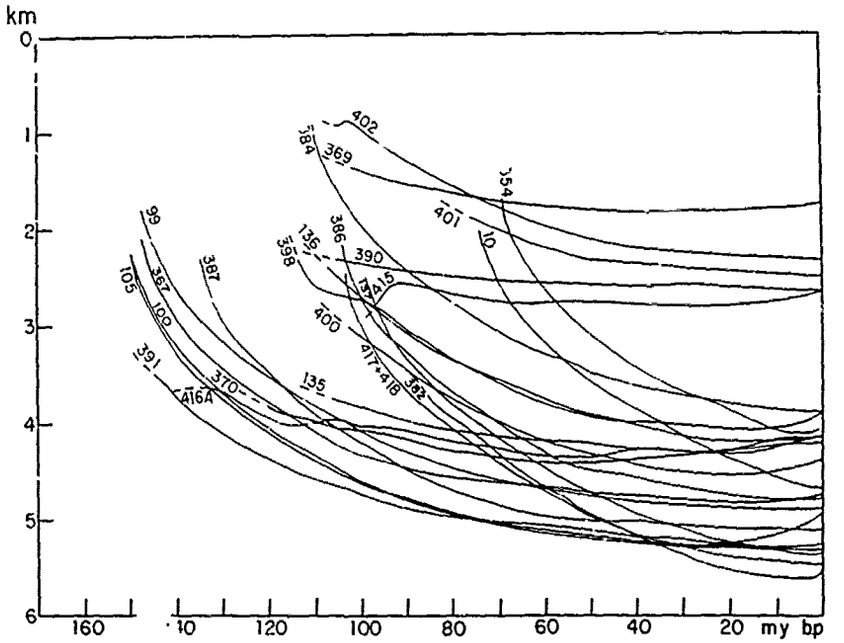


Figure 4. Backtracking of DSDP sites in the North Atlantic

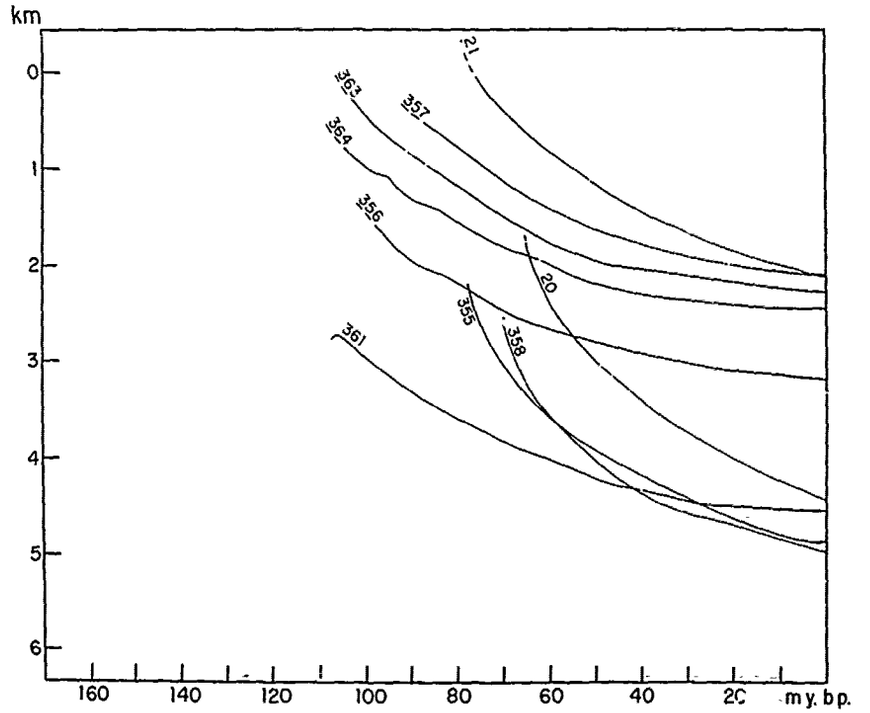


Figure 5. Backtracking of DSDP sites in the South Atlantic

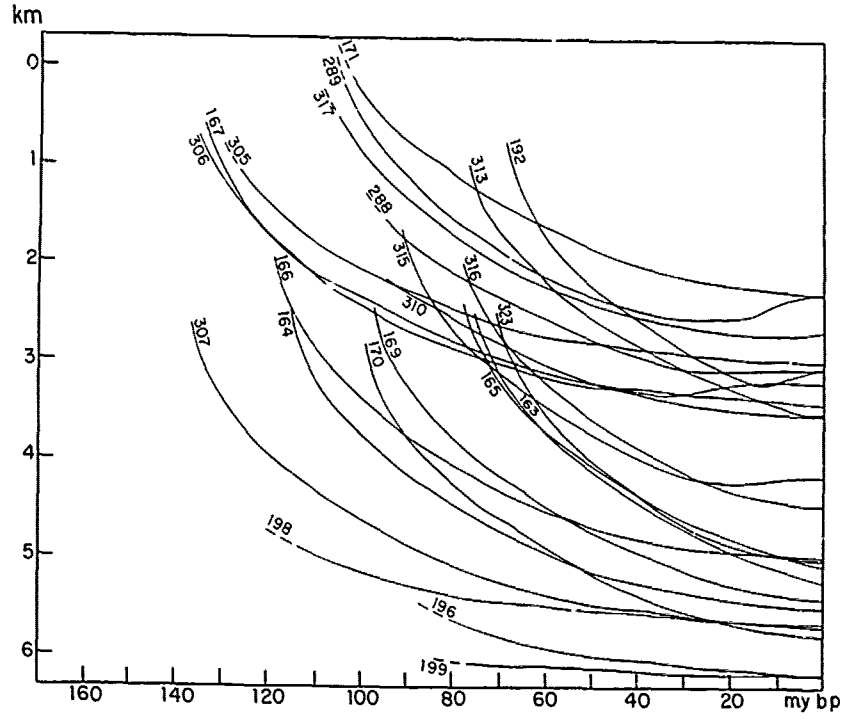


Figure 6. Backtracking of DSDP sites in the Pacific.

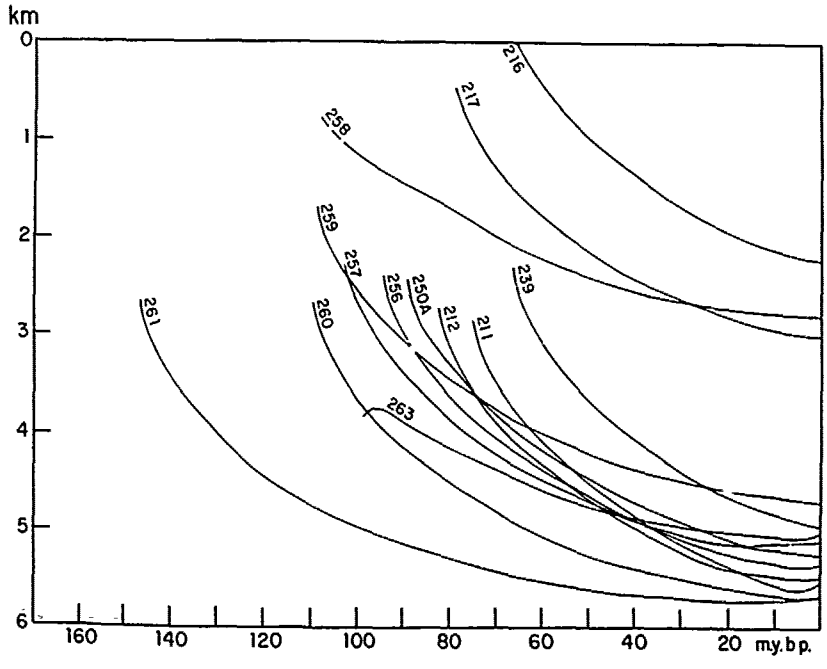


Figure 7. Backtracking of DSDP sites in the Indian Ocean.

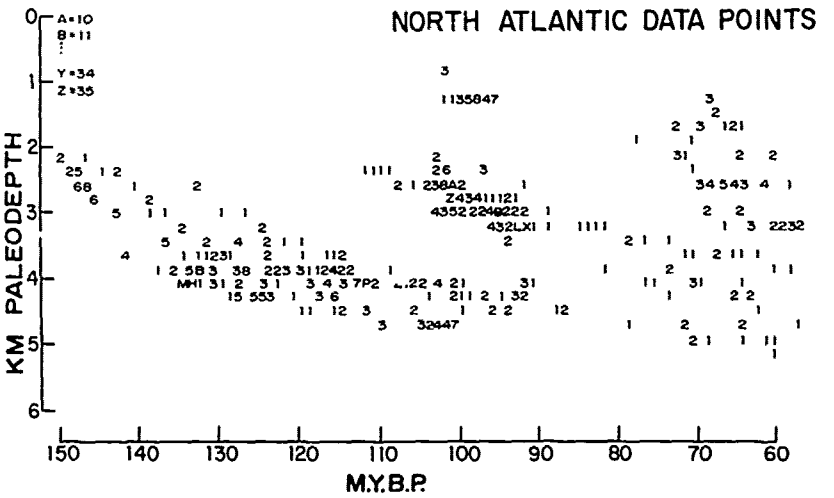


Figure 8. Data point density in the North Atlantic, showing number of overlying carbonate and organic carbon measurements.

Pacific

Significant accumulations of organic carbon in the Mesozoic Pacific are limited to paleodepths of less than 2 km (Figure 16). There is one sample with 1.2% organic carbon of late Valanginian age at Site 306, one sample with 28.7% of Barremian to Aptian age at Site 317, and two samples with 2.3% and 2.8% of Turonian age at Site 171. Although documentation of Mesozoic sediments in the deep Pacific is still very poor (Figure 10), well oxygenated sediments of Valanginian, Barremian, Aptian and Turonian age were recovered from paleodepths in excess of 2 km at Sites 164, 166, 167, 170, 288, 306 and 307. The possibility that short intervals of oxygen depletion in the deep Pacific have occurred and have so far been missed by drilling due to spot coring and poor recovery cannot be ruled out, but appears rather unlikely.

No organic carbon contents in excess of 1% have been reported from any other sites drilled in the Pacific on Paleocene or older crust.

Indian Ocean

Despite the widespread occurrence of black shale facies in the Cretaceous sediments of the Indian Ocean, measured organic carbon contents never exceeded 2.8% (Figure 17). Values in excess of 1% are limited to middle and late Albian occurrences at Sites 258, 261 and 263 with the exception of two Santonian samples of 1.2% organic carbon each at Site 258 and two early Paleocene samples of less than 2% at Site 259.

At site 249, drilled on the Mozambique Ridge, organic carbon contents between 1% and 2% are observed from the Aptian through the Campanian. Although the subsidence history of the Mozambique Ridge is not known, Site 249 probably always was at paleodepths less than 2 km. One organic carbon content of 2.0% was measured in late Cretaceous (Turonian?) sediments at Site 241, located in the Somali Basin on basement of unknown age.

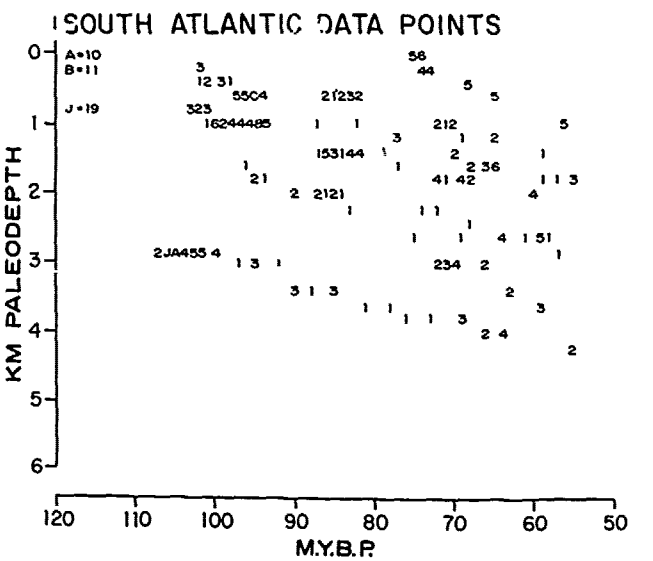


Figure 9. Data point density in the South Atlantic, showing number of overlying carbonate and organic carbon measurements.

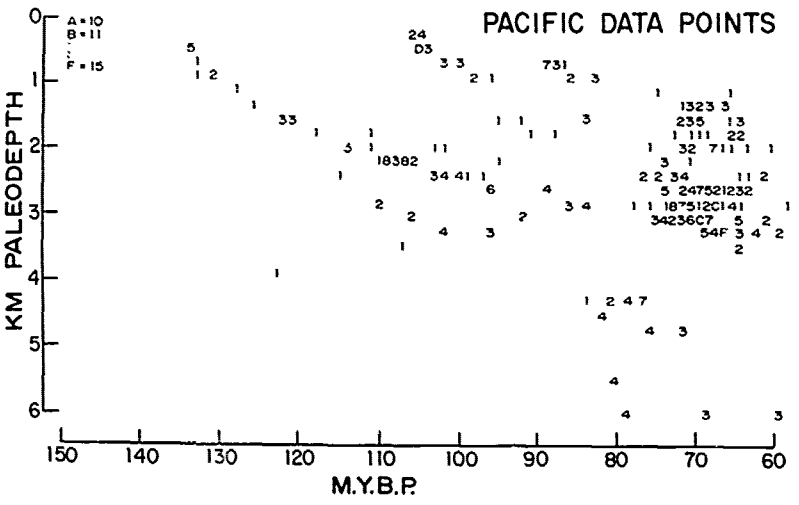


Figure 10. Data point density in the Pacific, showing number of overlying carbonate and organic carbon measurements.

## Distribution of Carbonate

Since the pioneering work of Bramlette (1961), Peterson (1966), Berger (1967), Ruddiman and Heezen (1967), and others, geologists have successfully used carbonate distribution patterns in deep-sea sediments for interpreting the chemistry, circulation, and watermass distributions of the present-day oceans and of those in the past (for a recent review see Berger, 1977). The amount of carbonate buried in deep-sea sediments is the final product of the interacting processes of surface fertility, fecal transport, dissolution, benthic burrowing, lateral transport, and diagenesis. The effects of these contributing mechanisms are being studied intensively, primarily in recent sediments, and the emerging results may greatly enhance our capability of interpreting the oceanographic signals preserved in ancient sediments. It has been shown convincingly, however, that some basic information on the chemistry, fertility, and circulation patterns of the oceans may be gained from an analysis of sediment composition alone (e.g. Berger, 1972; Lisitzin, 1972; Berger, Adelseck, and Mayer,

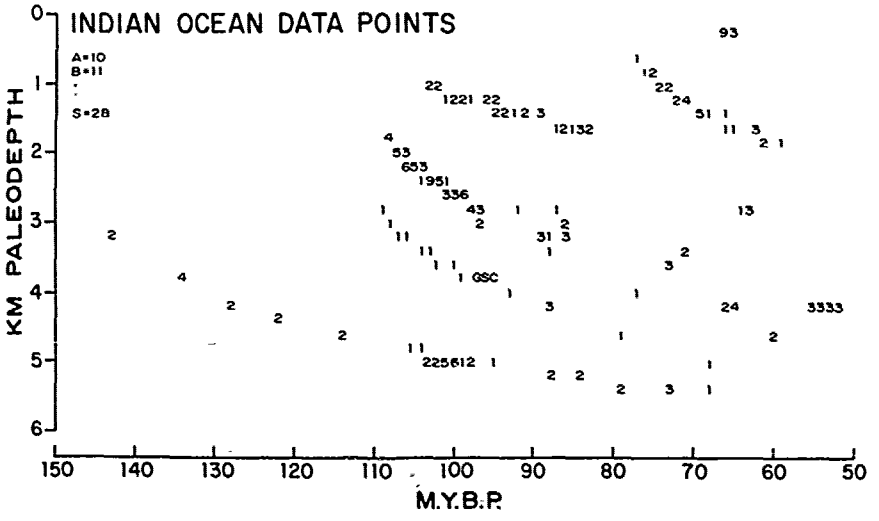


Figure 11. Data point density in the Indian Ocean, showing number of overlying carbonate and organic carbon measurements.

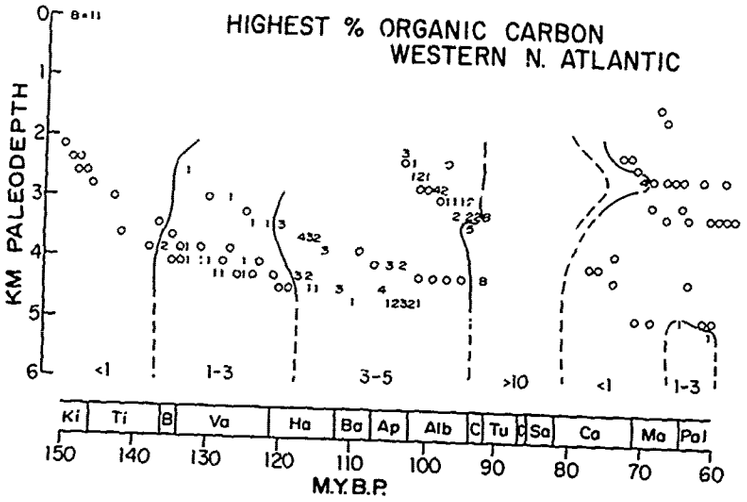


Figure 12. Distribution of highest organic carbon contents in western North Atlantic.

1976; Biscaye, Kolla, and Turekian, 1976; Kolla, Bé and Biscaye, 1976; Ramsay, 1977; and references therein).

Given the rather poor recovery of Mesozoic deep-sea sediments until quite recently, previous attempts have concentrated on delineating changes in the depth position of the lysocline and CCD (in various definitions) through time (Hay, 1970; Berger and von Rad, 1972; van Andel, 1975; Ramsay, 1977; Sclater, Abbott and Thiede, 1977; van Andel et al., 1977). Drilling by Glomar Challenger into Mesozoic sediments during the past few years has permitted a considerable refinement of the pre-Cenozoic oceanic carbonate history, particularly in the North Atlantic (Thierstein and Okada, in press). A reassessment of the subsidence history and biostratigraphy of the various Mesozoic DSDP sites in conjunction with the measured carbonate contents reveals rather variable patterns of carbonate deposition in the different Mesozoic ocean basins, which are discussed below.

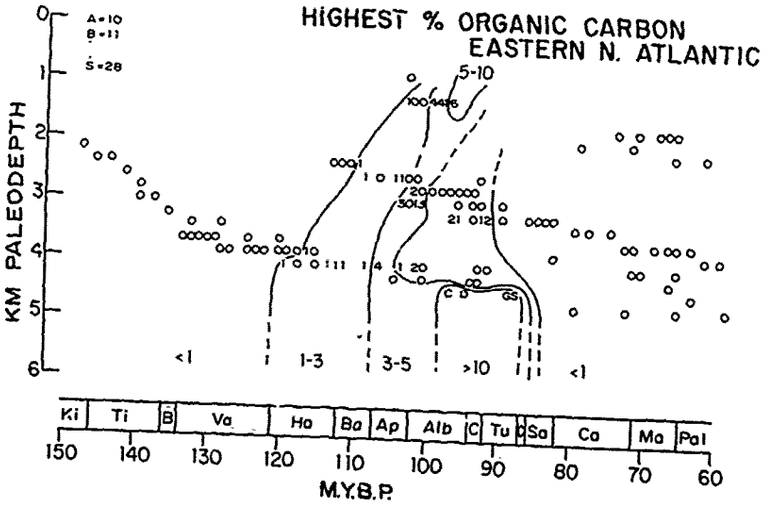


Figure 13. Distribution of highest organic carbon contents in eastern North Atlantic.

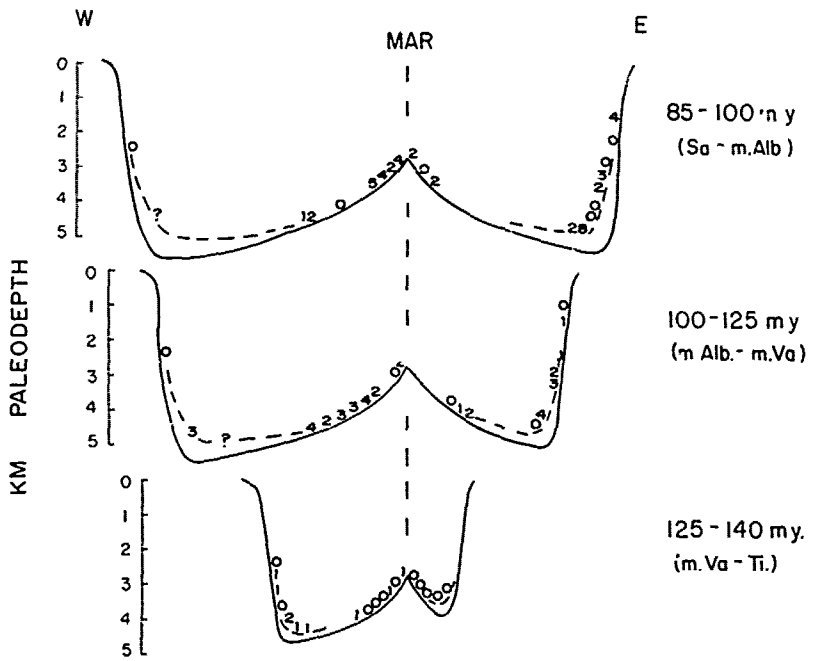


Figure 14. Distribution of highest organic carbon contents in the Mesozoic North Atlantic. Values projected laterally onto paleoprofiles (Georgia-Senegal) constructed from paleobathymetric maps given by Sclater, Hellinger and Tapscott (1977). Note location of highest values [12% (11.5% measured) at Sites 386 and 387; 28% at Site 367].

North Atlantic

The bathymetric distribution of late Mesozoic carbonate deposits in the North Atlantic is characterized by repeated fluctuations across a depth range of more than 2 km (Figure 18). Late Jurassic sediments have carbonate contents of generally less than 60% on both sides of the North Atlantic (Sites 100, 105, and 367). A well-defined Jurassic CCD cannot be documented, but if present, appears to have been at depths greater than 3 - 4 km. High carbonate values predominate in Berriasian through late Berremian sediments at Sites 99, 100, 105, 367, 387 and 398. Lower values occur in the detrital-rich flysch deposits at Sites 370 and 416A (Lancelot, Seibold et al., 1978; Lancelot, Winterer et al., 1977). A sharp decrease of carbonate contents near the Barremian/Aptian boundary is documented at Sites 105, 367, 387, and 398D and is equivalent to a sudden rise of the CCD of more than 2 km. Low-carbonate black shale facies are documented at numerous sites and lasted from Aptian through Cenomanian time. A gradual descent of carbonate deposition to greater paleodepths in the late Albian and early Cenomanian was reversed in the late Cenomanian as is evident at Sites 137, 386, and 398D. There are at present no data points available from shallower parts of the North Atlantic from the Turonian

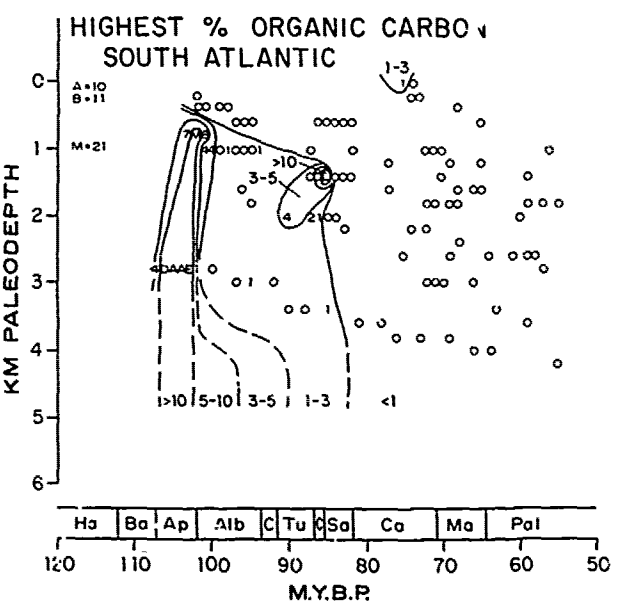


Figure 15. Distribution of highest organic carbon contents in the South Atlantic. Sites from north and south of the Rio Grande-Walvis sill plotted together.

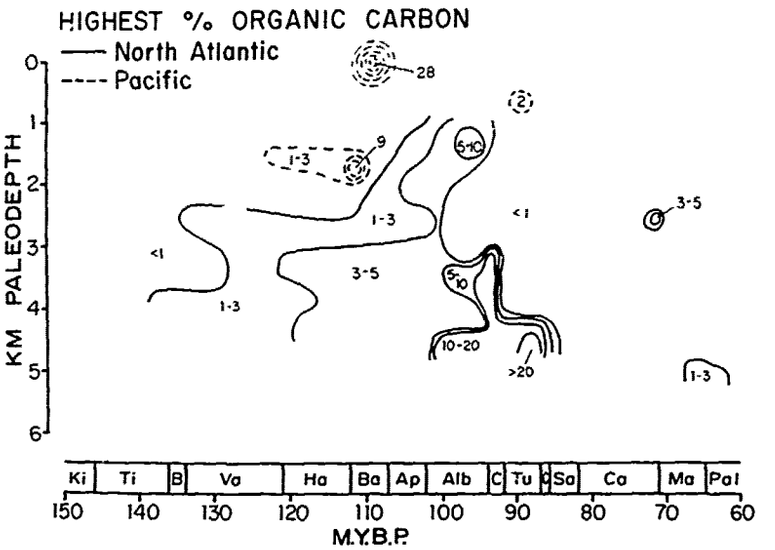


Figure 16. Distribution of highest organic carbon contents in the Pacific (dashed contours) and in the North Atlantic (eastern and western basins combined, solid contours).

through the Santonian (Figure 8). Another carbonate excursion of more than 2 km into the deep North Atlantic from the middle Maastrichtian to the earliest Danian is manifested at Sites 370, 386, 387, 398 and 400A.

South Atlantic

Documentation of the history of carbonate deposition in the South Atlantic (Figure 19) is based on less evidence than that of the North

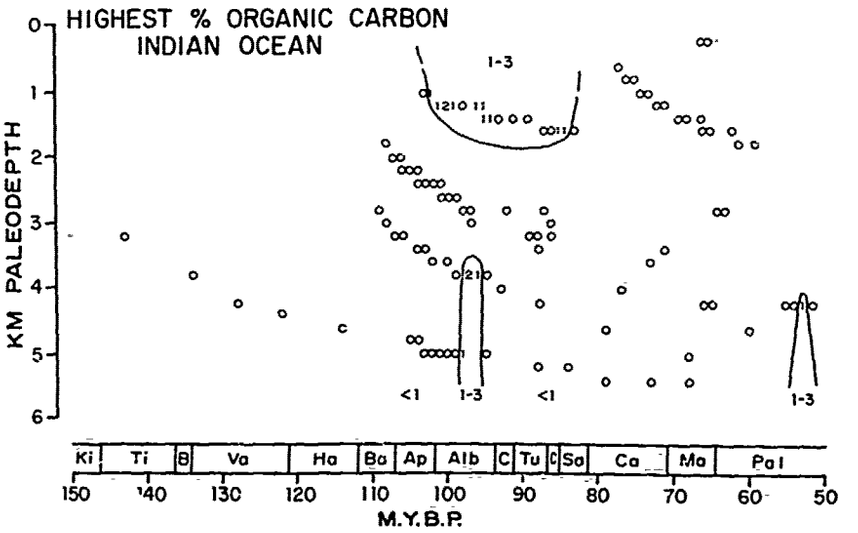


Figure 17. Distribution of highest organic carbon contents in the Indian Ocean.

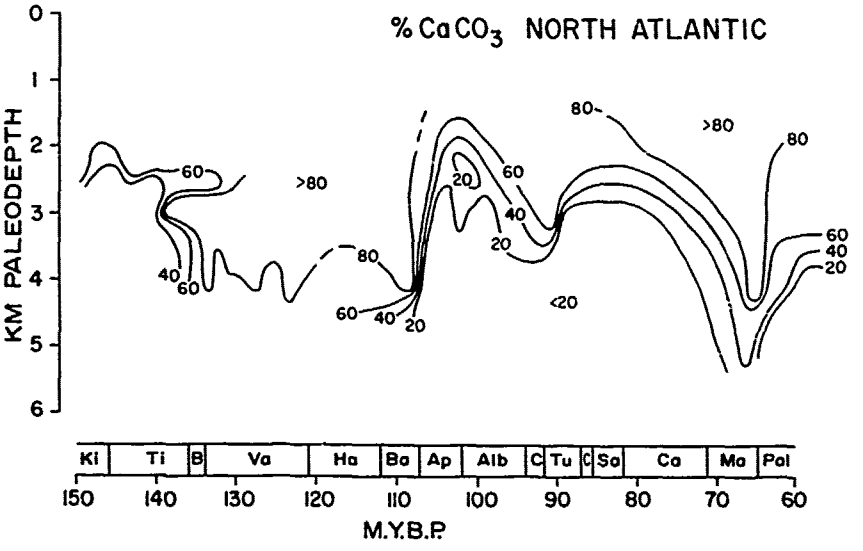


Figure 18. Distribution of average carbonate contents in the North Atlantic.

Atlantic (Figures 8 and 9). No pre-Aptian early Cretaceous marine sediments have been recovered so far from the deep sea (McCoy and Zimmerman, 1977) or from the surrounding continents (Bertels, 1977). The CCD can only be documented by a comparison of sites from north of the Walvis-Rio Grande sill with the deeper sites (i.e. 358 and 361) in the south, except for the Turonian shallowing of the CCD preserved at Site 356. A late Campanian to early Maastrichtian dissolution pulse is manifested at Sites 356, 358, and 364.

The average late Cretaceous carbonate contents in the South Atlantic are considerably lower than those in the North Atlantic.

Pacific

The bathymetric changes in carbonate contents of late Mesozoic sediments in the Pacific are shown in Figure 20. The extremely poor coverage of abyssal pre-Campanian sediments (Figure 10) is mainly due to spot coring and poor recovery in the cherty sequences drilled at Sites 198 and 307 and to uncertainties and difficulties in biostratigraphically dating the recovered cores. Low carbonate contents at paleodepths greater than 2 km in the early Cretaceous have been documented at Sites 164, 166, 170, 198 and 307. A decrease in carbonate contents near the Barremian/Aptian boundary is observed at Sites 166 and 305. Considerably higher carbonate values than in the Atlantic are observed in the late Aptian and Albian at paleodepths between 2 and 3 km. A Coniacian to Santonian dissolution pulse occurs at Sites 167 and 317A. Increased carbonate contents in the early Campanian sediments at Sites 167 and 170 indicate a CCD excursion into the deep Pacific, that extended down to 6 km paleodepth in the late Campanian to early Maastrichtian Tetralithus trifidus Zone at Site 199. The presence of a middle Maastrichtian to early Paleocene hiatus at the same site and reworking of late Maastrichtian and early Danian nannofossils into middle Danian sediments (Chiasmolithus danicus Zone) has been discussed by Thierstein and Okada (in press). The deepest and possibly continuous sediment record across the Cretaceous/Tertiary boundary was recovered at Site 305 at a paleodepth of about 2700 m, and shows carbonate contents of over 90%. A middle Maastrichtian drop in carbonate contents is documented at Site 163 (3400 m paleodepth), Site 315A (3230 m paleodepth) and Site 316 (2940 m paleodepth). Carbonate deposition in the deep Pacific may have resumed shortly after the beginning of the Paleocene as evidenced by the recovery of middle Danian (C. danicus Zone) limestones and chalks at Sites 199 (transported from shallower areas), 316 and 317A.

The observed depth fluctuations of the carbonate contents through the Mesozoic appear to go in opposite directions in the Pacific and North Atlantic oceans (compare Figures 18 and 20) except for the global dissolution pulses occurring in the Aptian and Turonian-Coniacian intervals.

TABLE 1 Deep Sea Drilling Sites Considered

| Site | Leg | Latitude | Longitude | Water depth (m) | Depth to oldest recovered sediment (m) | Basement age (m.y.) | Remarks: +/- basement reached/not reached; P/M basement dated paleontologically/magnetically |
|---|---|---|---|---|---|---|---|
| North Atlantic | | | | | | | |
| 10 | 2 | 32°37'N | 52°20'W | 4712 | 453 | 74 | + P,M |
| 99A | 11 | 23°41'N | 73°51'W | 4914 | 248 | 148 | - M |
| 100 | 11 | 24°41'N | 73°48'W | 5325 | 317 | 150 | + P,M |
| 101 | 11 | 25°12'N | 74°27'W | 4868 | 691 | 153 | - M no carbon/carbonate data |
| 105 | 11 | 34°54'N | 69°10'W | 5251 | 623 | 150 | + P,M |
| 135 | 14 | 35°21'N | 10°26'W | 4152 | 689 | 159 | - M age extrapolated |
| 136 | 14 | 34°10'N | 16°18'W | 4169 | 313 | 122 | + P age extrapolated |
| 137 | 14 | 25°56'N | 27°04'W | 5361 | 397 | 99 | + P |
| 354 | 39 | 05°54'N | 44°12'W | 4052 | 886 | 68 | + P, K/Ar |
| 367 | 41 | 12°29'N | 20°03'W | 4748 | 1146 | 148 | + P |
| 369A | 41 | 26°36'N | 14°59'W | 1752 | 489 | 167 | - M age extrapolated |
| 370 | 41 | 32°50'N | 10°47'W | 4214 | 1177 | 165 | - M age extrapolated |
| 382 | 43 | 34°25'N | 56°32'W | 5526 | 521 | 95 | - M age extrapolated |
| 384 | 43 | 40°22'N | 51°40'W | 3909 | 325 | 110 | + M age extrapolated |
| 386 | 43 | 31°11'N | 64°15'W | 4782 | 964 | 104 | + P |
| 387 | 43 | 32°19'N | 67°40'W | 5117 | 792 | 135 | + P,M |
| 390A | 44 | 30°09'N | 76°07'W | 2670 | 143 | 185? | - M age extrapolated |
| 391C | 44 | 28°14'N | 75°37'W | 4963 | 1412 | 157 | - M age extrapolated |
| 392 | 44 | 29°55'N | 76°11'W | 2607 | 349 | 175? | - M no carbon/carbonate data |
| 398D | 47 | 40°58'N | 10°43'W | 3910 | 1740 | 118 | - M age extrapolated |
| 400A | 48 | 47°23'N | 9°12'N | 4399 | 778 | 120 | - M age extrapolated |
| 401 | 48 | 47°24'N | 8°49'W | 2495 | 341 | 125 | - M age extrapolated |
| 402 | 48 | 47°53'N | 8°50'W | 2340 | 137 | 125 | - M age extrapolated |

TABLE 1 (continued)

| Site | Leg | Latitude | Longitude | Water depth (m) | Depth to oldest recovered sediment (m) | Basement age (m.y.) | Remarks<br>+/- basement reached/not reached<br>P/M basement dated paleontologically/magnetically |
|---|---|---|---|---|---|---|---|
| *415A* | *50* | *31°02'N* | *11°39'W* | 2817 | 1080 | 165 | - M age extrapolated |
| 416A | 50 | 32°50'N | 10°48'W | 4203 | *1624* | *165* | - *M* age extrapolated |
| *417A, D* | *51* | *25°07'N* | *68°03'W* | 5479 | 343 | 105 | + P,M |
| 418A | 52 | 25°02'N | 68°03'W | 5519 | 324 | *105* | + *P,M* |
| South Atlantic | | | | | | | |
| 20C | 3 | 28°32'S | 26°51'W | 4484 | 72 | 65 | + P |
| 21 | 3 | 28°35'S | 30°36'W | 2102 | 131 | 82 | - P |
| 355 | 39 | 15°43'S | 30°36'W | 4886 | 449 | 78 | + P, K/Ar |
| 356 | 39 | 28°17'S | 41°05'W | 3175 | 741 | 110 | - M age extrapolated |
| 357 | 39 | 30°00'S | 35°34'W | 2086 | 797 | 97 | - M age extrapolated |
| 358 | 39 | 37°40'S | 35°58'W | 4990 | 842 | 70 | - M |
| 361 | 40 | 35°04'S | 15°27'E | 4549 | 1314 | 112 | - M |
| 363 | 40 | 19°39'S | 9°03'E | 2248 | 715 | 107 | - M |
| 364 | 40 | 11°34'S | 11°58'E | 2448 | 1086 | 112 | - M |
| Pacific | | | | | | | |
| 163 | 16 | 11°15'N | 150°18'W | 5230 | 276 | *75* | + *P* |
| 164 | 17 | 13°12'N | 161°31'W | 5499 | 265 | 115 | + P,M M extrapolated |
| 165 | 17 | 8°11'N | 164°52'W | 5053 | 480 | 73 | + P |
| 166 | 17 | 3°46'N | 175°05'W | 4962 | 307 | 119 | + P,M |
| 167 | 17 | 7°04'N | 176°50'W | 3176 | 1168 | 135 | + P |
| 169 | 17 | 10°40'N | 173°33'E | 5407 | 233 | 97 | + P |
| 170 | 17 | 11°48'N | 177°37'E | 5792 | 192 | 99 | + P |
| 171 | 17 | 19°08'N | 169°28'W | 2290 | 479 | 108 | + P age extrapolated |
| *192A* | *19* | *53°01'N* | *164°42'E* | 3014 | 1044 | 69 | + P |
| 196 | 20 | 30°07'N | 148°35'E | 6184 | 623 | 140 | - M |
| 198 | 20 | 25°50'N | 154°35'E | 5848 | 251 | 160 | - M age extrapolated no carbon/carbonate data |
| 199 | 20 | 13°31'N | 156°10'E | 6090 | 566 | 160 | - M age extrapolated |
| 288A | 30 | 5°59'S | 161°50'W | 3030 | 989 | 107 | - P age extrapolated |
| 289 | 30 | 0°30'S | 158°31'E | 2224 | 1263 | 107 | + P |
| 303 | 32 | 40°49'N | 154°27'E | 5609 | 285 | 115 | + P,M no carbon/carbonate data |
| 304 | 32 | 39°20'N | 155°04'E | 5640 | 334 | 125 | + P,M no carbon/carbonate data |

TABLE 1 (continued)

| Site | Leg | Latitude | Longitude | Water depth (m) | Depth to oldest recovered sediment (m) | Basement age (m.y.) | Remarks: +/- basement reached/not reached; P/M basement dated paleontologically/magnetically |
|---|---|---|---|---|---|---|---|
| 305 | 32 | 32°00'N | 157°51'E | 2921 | 641 | 136 | - M age extrapolated |
| 306 | 32 | 31°52'N | 157°29'E | 3416 | 475 | 136 | - M age extrapolated |
| 307 | 32 | 28°35'N | 161°00'E | 5696 | 300 | 137 | + M |
| 310+A | 32 | 36°52'N | 176°54'E | 3524 | 353 | 109 | - P age extrapolated |
| 313 | 32 | 20°11'N | 170°57'W | 3484 | 594 | 76 | + P |
| 315A | 33 | 4°10'N | 158°32'W | 4152 | 996 | 91 | + P age extrapolated, K/Ar |
| 316 | 33 | 0°05'N | 157°08'W | 4451 | 847 | 77 | - P age extrapolated |
| 317A | 33 | 11°00'S | 162°16'W | 2622 | 905 | 110 | + P age extrapolated |
| 323 | 35 | 63°41'S | 97°60'W | 4993 | 683 | 71 | + P,M age extrapolated |
| Indian Ocean | | | | | | | |
| 211 | 22 | 9°47'S | 102°42'E | 5535 | 428 | 75 | + P,K/Ar |
| 212 | 22 | 19°11'S | 99°18'E | 5500 | 516 | 82 | + See Thierstein and Okada (in press) |
| 216 | 22 | 1°28'N | 90°12'E | 2237 | 457 | 66 | + P |
| 217 | 22 | 8°56'N | 90°32'E | 3010 | 615 | 79 | - P age extrapolated |
| 239 | 25 | 21°18'S | 51°41'E | 4971 | 320 | 66 | + P,M |
| 250A | 26 | 33°28'S | 39°22'E | 5119 | 725 | 89 | + P age extrapolated |
| 256 | 26 | 23°27'S | 100°46'E | 5361 | 251 | 94 | + P,K/Ar |
| 257 | 26 | 30°59'S | 108°21'E | 5278 | 262 | 102 | + P |
| 258+A | 26 | 33°48'S | 112°28'E | 2793 | 445 | 115 | - P age extrapolated |
| 259 | 27 | 29°37'S | 112°42'E | 4712 | 304 | 109 | + M |
| 260 | 27 | 16°09'S | 110°18'E | 5702 | 323 | 110 | + P age extrapolated |
| 261 | 27 | 12°57'S | 117°54'E | 5667 | 532 | 147 | + P,M |
| 263 | 27 | 23°19'S | 110°59'E | 5048 | 746 | 122 | - See Veevers and Cotterill (1978) |

Table 1. Deep Sea Drilling Sites considered

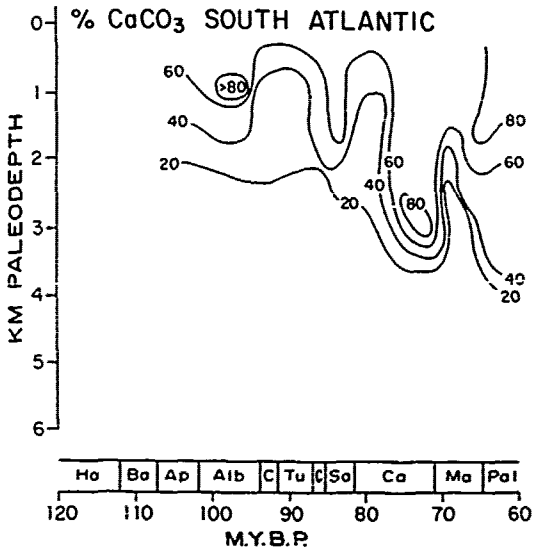


Figure 19. Distribution of average carbonate contents in the South Atlantic.

## Indian Ocean

Mesozoic sediments from the Indian Ocean (Figure 21) are characterized by low carbonate contents prior to the Turonian. A gradual descent of the CCD can be distinguished from about 1 km depth in the Cenomanian (Site 258) to 3.5 km in the early Maastrichtian (Sites 211 and 259) and to more than 4.5 km in the late Maastrichtian (Site 212, paleodepth of sediment source area used). Low carbonate values are measured in the early Paleocene sediments from Sites 239, 259 and 263.

Occasional early Cretaceous occurrences of carbonate values up to 70% at Sites 259, 260 and 261 were found in sediments often containing mixed nannolith assemblages and shallow water benthic foraminifera (Bartenstein, 1974; Scheibnerova, 1974 and 1977), and must therefore be considered allochthonous. This, together with the inclusion of the source of the Maastrichtian carbonates preserved at Site 212, leads to a somewhat different interpretation of the carbonate history in the Indian Ocean than those given previously by van Andel (1975) and Sclater, Abbott and Thiede (1977).

## Oceanic Circulation and the Mesozoic Deep Sea Record

A globally-observed deficiency of preserved carbonate in middle Cretaceous deep-sea sediments is correlative with the accumulation and preservation of large amounts of organic carbon. A general descent of carbonate deposition to abyssal depths through the late Cretaceous is observed in all four major ocean basins. This global dichotomy between middle and late Cretaceous sedimentation patterns can be attributed to either changes in fertility, terrigenous dilution, or basin-shelf fractionation of lime related to transgressive-regressive cycles, or to a combination of these.

### Basin-Basin Fractionation

A strong, rapidly reversing basin-basin fractionation of carbonate is evident in the offset timing of several dissolution and preservation intervals, especially between the Pacific and North Atlantic. In the early part of the early Cretaceous the deep North Atlantic appears to have acted as a carbonate trap. The fractionation of lime during the middle Cretaceous is observed mainly in reciprocal changes of carbonate percentages at shallow to intermediate depths in the Pacific and North Atlantic oceans, rather than in obvious depth fluctuations of the CCD. The most striking carbonate excursions are observed near the Cretaceous-Tertiary boundary. In the Pacific, carbonate deposits are preserved down to paleodepths of more than 6 km in the late Campanian and early Maastrichtian. A widespread hiatus of only a few million years duration is observed at several sites from intermediate depths in the Pacific in which carbonate sedimentation resumed in the early Paleocene. A brief abyssal erosion event is suggested by the presence of reworked latest Cretaceous and earliest Danian planktonic foraminifera and nannoliths in middle Danian carbonate sediments at Site 199 (Krasheninnikov and Hoskins, 1973; Thierstein and Okada, in press). A very sharp depression of carbonate dissolution levels in the deep North Atlantic, however, is observed in the late Maastrichtian and earliest Danian. The latest Cretaceous carbonate record of the South Atlantic follows the Pacific pattern, whereas the carbonate history of the Indian Ocean resembles that of the North Atlantic. These differences in the abyssal depositional patterns of the major ocean basins indicate that bottom water interchange may still have been restricted in the earliest Tertiary by topographic sills between North and South America and Africa and South America.

Topographic restriction of deep water in the Atlantic basins during the middle Cretaceous is strongly suggested by the bathymetric distribution of preserved organic carbon. Sediments recovered so far from the deep Cretaceous Pacific are all considerably more oxydized than those from comparable depths in the Atlantic and Indian Oceans. A maximum depth of 2 km for the hypothetical "Panama" barrier is indicated by the apparent lack of exchange of the oxygen-deficient deep Atlantic waters with those of the better ventilated deep Pacific. A temporary intensification of a shallow oxygen minimum layer in the

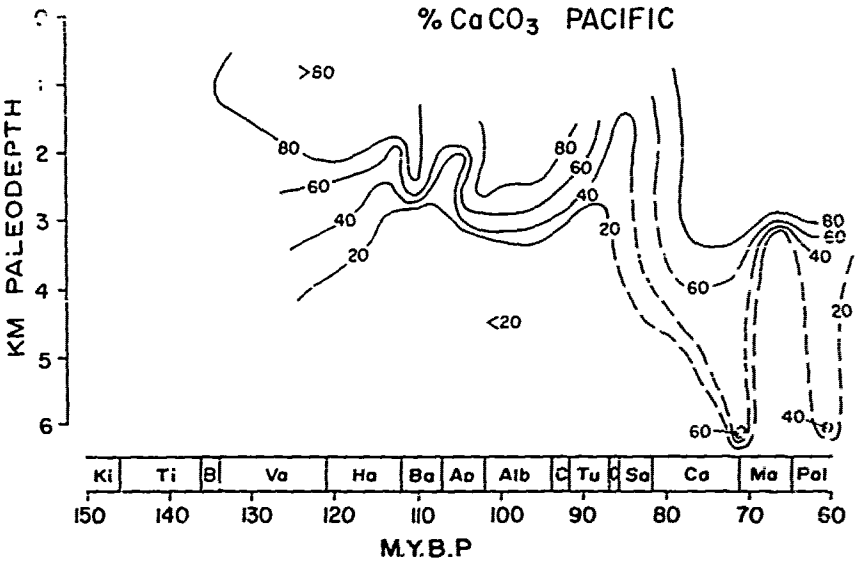


Figure 20. Distribution of average carbonate contents in the Pacific.

middle Cretaceous, suggested by the paleobathymetric distribution of organic carbon in the Pacific (Schlanger and Jenkyns, 1976), might be confirmed by an analysis of contemporaneous supply and dissolution rates. The presently available data on the Pacific mid-Cretaceous anoxic events and the rather imprecise dating of the extinction and drowning of Cretaceous reefs on numerous guyots in the western Pacific (Heezen et al., 1973) do not allow to establish or disclaim any causal relationship between the two events.

The observed carbonate distribution patterns in any of the major deep ocean basins are not readily correlated with published transgression-regression cycles (Kauffman, 1977; Vail et al., 1977) and do not seem to be due entirely to repeated trapping of carbonate on shelves and in marginal seas during transgressions.

## Deep Water Structure in the Mesozoic Oceans

The organic carbon and carbonate contents measured in over 1700 samples from Mesozoic and early Paleocene sediments show a strong negative correlation which is not only the result of dilution of organic carbon by carbonate (Figure 22). An increase of preserved organic carbon relative to the non-carbonate sediment-fraction indicates either higher planktic productivity, or higher detrital organic carbon supply, or lowered dilution by non-carbonate detritus or siliceous skeletons. The concurrent decrease of carbonate needs to be explained by enhanced dissolution or lowered production of carbonate tests. Dissolution of carbonate may have occurred during settling through anoxic deep water with lowered pH. Such a mechanism has been proposed to account for the negative correlation of organic carbon and carbonate contents in late Quaternary anoxic sediments deposited in isolated stagnate basins (Ross and Degens, 1974; Degens and Stoffers, 1976). Dissolution of carbonate after settling through an increase of carbon dioxide by oxidation (chemical or bacterial) of organic matter appears to be indicated by the occurrence of coccolith imprints found in early Aptian sapropelic clays in the South Atlantic by Noël and Melguen (1978). Repeated alternation of layers with well preserved calcareous tests and layers with strongly etched or completely dissolved calcareous tests have been observed in numerous black shale sequences from the deep sea. They may reflect changes of the diagenetic chemical interface between poorly aerated and completely anoxic sediments with enhanced carbonate preservation, which was observed in recent sediments of the Santa Barbara Basin by Berger and Soutar (1970), and which has been linked to the thermodynamics of diagenetic redox reactions by Berner (1972). Sholkovitz (1973) concluded that the diagenesis of carbonates in the Santa Barbara Basin is extremely sensitive to small changes in the oxygen content of sea water in the range of 0.4 ml/l to 0.1 ml/l of $O_2$.

In contrast, organic carbon contents deposited below today's oceanic high productivity areas are positively correlated with carbonate contents and become oxidized with increasing age and burial depth (Stackelberg, 1972; Heath, Moore and Dauphin, 1977).

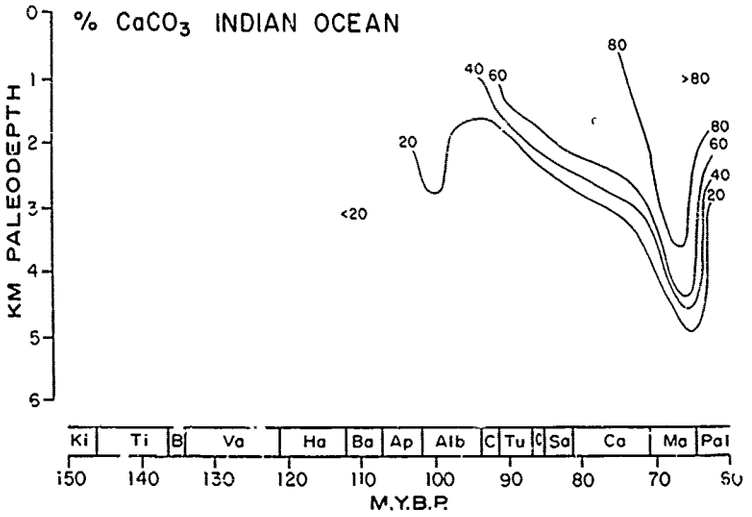


Figure 21. Distribution of average carbonate contents in the Indian Ocean.

More detailed information on the source of the organic material, preservation of carbonate tests and accumulation rates of different sediment components is clearly needed for an understanding of the underlying mechanisms of black shale deposition.

Lithologic cycles have been observed frequently in mid-Cretaceous black shale deposits from the deep sea (Lancelot, Hathaway and Hollister, 1972; Berger and von Rad, 1972; Jansa, Gardner and Dean, 1978; McCave, in press). These cycles range from limestone/black shale and limestone/marlstone couplets, mainly in the early part of the black shale sequence, to black shale/green shale couplets near the younger end of the black shale interval. Bioturbation appears to be associated with limestone and green clays, whereas black shales usually are finely laminated (Hollister, Ewing et al., 1972; Lancelot, Seibold et al., 1978). The causes for the occurrence of these cycles may be related to periodic local oxygen deficiency in the sediments, intermittent stagnation of the entire basin leading to completely anoxic deep waters, and later lly transported carbonate (Berger and von Rad, 1972; Dean et al., 1978; Jansa, Gardner and Dean, 1978; McCave, in press). All these explanations require repeated rapid changes in the chemistry of the depositional environment. How could such drastic changes come about? Why are they not observed in present-day abyssal environments?

The carbonate distribution in today's oceans has been mapped and studied intensively. Although the kinetics of carbonate dissolution are still controversial (Li, Takahashi, Broecker, 1969; Ingle et al., 1973; Berner and Morse, 1974; Berner, 1977, Broecker and Takahashi, 1977), the effects of changing supply and of various dissolution rate profiles or oceanic carbonate distribution have been discussed by Heath and Culberson (1970), Berger (1971, and in press), Berger, Adelseck and Mayer (1976), and Dean et al. (1978). The slope of the decreasing carbonate percentages with depth can be explained as the result of the slope of the dissolution rate versus depth curve and the initial carbonate/noncarbonate ratio (Figure 23). The loss of carbonate through solution (L), if measured against the insoluble fraction is $L=100(1-R_o/R)$, where $R_o$ is the percentage of insolubles in the supply, and R is the percentage of insolubles after dissolution. The carbonate versus paleodepth distributions in the North Atlantic and Pacific Oceans in the middle Cretaceous are shown in Figure 24. Compared to carbonate distribution patterns observed in the present oceans (e.g. Berger, Adelseck and Mayer, 1976; Broecker and Takahashi, 1977) the middle Cretaceous distribution patterns are peculiar in their great variability of the measured carbonate contents and in the rather linear decrease of the maximum values between 2 km and 4.5 km paleodepth in the North Atlantic and considerably shallower in the Pacific. The maximum carbonate values could be accounted for by a dissolution rate profile as shown on the right-hand graph in Figure 23. The dissolution rate below the lysocline (knick-point in carbonate content curve ($R_o$= 10) at about 3 km depth) would have to be very low to keep the carbonate content decrease linear. This may be quite feasible in a stagnating North Atlantic, since carbonate preservation under strongly

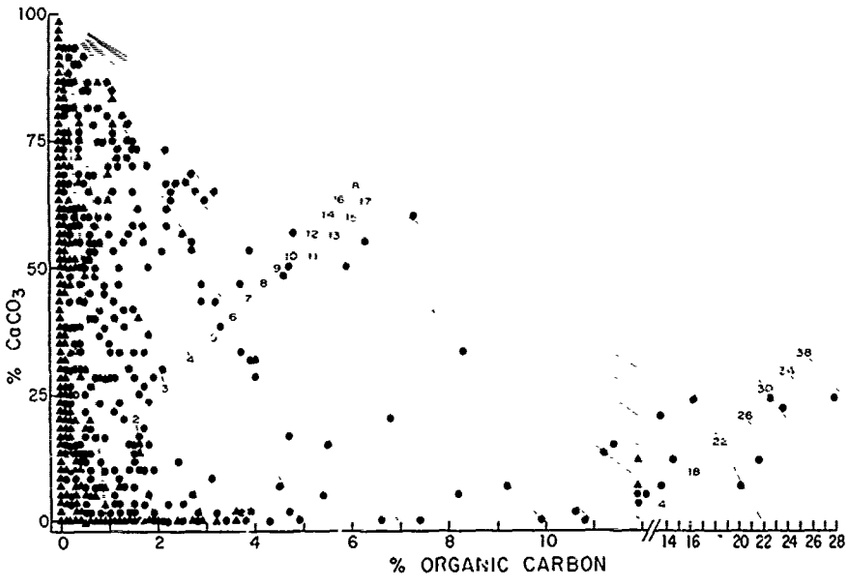


Figure 22. Organic carbon and carbonate contents (in percent of dry bulk weight on Cartesian coordinates) measured in 1766 Mesozoic and early Paleocene DSDP sediment samples considered in this study (dot for one measurement, triangle for two or more overlying measurements). Diagonal lines indicate organic carbon content in percent of non-carbonate fraction (i.e. without dilution by carbonate) for a sample of given carbonate content.

anoxic conditions may be exceptionally good and include aragonite (Berger and Soutar, 1970; Jung, 1973). In the Pacific, the highest carbonate contents may be explained by a linear dissolution rate model (Figure 23, middle) with a CCD around 2.5 km paleodepth. The low carbonate values encountered at relatively shallow paleodepths must be due to intermittently decreased supply of carbonate either by low productivity, or very strong dissolution in the uppermost few hundred meters of the water column, similar to the dissolution of aragonite today (Berner, 1977), or increased supply of noncarbonate detritus. To dilute the supply from 90% carbonate to 50% carbonate, however, a nine-fold increase of the noncarbonate flux would be necessary, which seems indeed rather unlikely (Dean et al., 1978).

Repeated large changes in the supply of carbonate might be due to intermittent nutrient starvation in the photic zone. There is, however, little indication of exceptional environmental stress preserved in the plankton assemblages from the Middle Cretaceous, such as monospecific blooms, patchyness of assemblage distributions, or exceptionally high evolutionary rates. It appears likely that oxygen deficiency may have reached into rather shallow depths at times, thus increasing the dissolution gradient in near surface waters tremendously, which may be interpreted as equivalent to a decreased supply rate in the models of Figure 23. Dissolution pulses and carbonaceous black shale deposition are indeed observed in shallower environments, such as the Aptian "marnes bleues" in southeastern France and the Mowry shale in the Western Interior. Today large scatter of carbonate contents is observed in some areas in the Pacific Ocean, where it has been attributed to high relief by Berger, Adelseck and Mayer (1976). The occurrences of scattered carbonate contents and indications of more gradually decreasing carbonate contents with increasing depth seem to be located dominantly under the subtropical gyres in the North and South Pacific, which are characterized by low surface productivity. A lowered carbonate productivity in surface waters in pre-Cenozoic oceans, possibly related to the evolution of calcareous plankton, was inferred from mass-balance estimates by Southam and Hay (1977).

Ryan and Cita (1977), using the Black Sea and the Pleistocene Mediterranean as a model, suggested increased surface water run-off together with low thermal gradients as a cause for stronger water stratification. The widespread occurrence of shallow water organisms considered to be stenohaline (e.g. corals, rudists, orbitolinas, ammonites, bryozoans) in the Tethyan middle Cretaceous indicates that no significant freshening of surface waters may have occurred. Nevertheless it seems likely

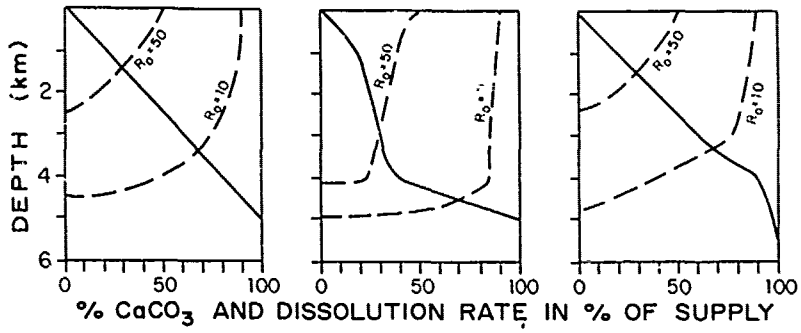


Figure 23. Three models showing expected carbonate distributions (dashed lines) versus depth as a result of different dissolution rate profiles (solid lines) for 50% and 90% carbonate supply ($R_o$ = % insolubles of supply). Left: Linear dissolution rate model (after Berger, 1971). Middle: Lysocline model (after Berger, 1970a). Right: Middle Cretaceous model. Note that the change in supply has a much larger effect on the depth of the CCD in the linear and Mesozoic models, than in the lysocline model.

that an increased stratification of the deep waters was caused by salinity differences. In view of the fact that even at today's large thermal gradients, the relatively warm but saline Mediterranean outflow forms a widely recognizable deep water contributor in the Atlantic Ocean, topographic isolation of water bodies in areas with high evaporative loss appears to be a very feasible mechanism to produce high salinity deep water in a latitudinally restricted Tethys and Atlantic (Chamberlin, 1906; Burke, 1975; McCoy and Zimmerman, 1977). The distribution of evaporite deposits in the Cretaceous given by Lotze (1964) is characterized by their proximity to the ocean, suggesting evaporite formation in lagoonal settings, possibly behind rudistid reefs (Roth, in press). The low solubility of oxygen in marine brines (Berger, 1970b; Kinsman et al., 1974) by itself would have fostered abyssal anaerobism. Climatically or tectonically controlled changes in the sill depths of the lagoonal inlets may have been the cause of repeated brine injections leading temporarily to increased stratification and stagnation of deep waters. The sudden rise of the CCD in the North Atlantic and the dissolution pulse in the Pacific in the early Aptian coincide with salt deposition in the South Atlantic. Brine injections into the North Atlantic may have occurred through tectonically controlled rift elevations between North and South Atlantic from the early Aptian onwards, leading to repeated anoxic events (Schlanger and Jenkyns, 1976; Arthur and Schlanger, in press). The presence of Tethyan nannoconids in Aptian sediments in the South Atlantic at Sites 327A (Wise and Wind, 1977), 363, and 364 (Protc Decima et al., 1978) also indicates the existence of at least a temporary shallow water connection between the North and South Atlantic in Aptian times. Migration through the Atlantic seems necessary because no nannoconids have been found in any middle Cretaceous samples from the western Indian Ocean, South Africa or the Wharton Basin (Thierstein, 1977). Injections of saline, oxygen-depleted deep waters from the South Atlantic into the North Atlantic over a deepening sill might have continued at depth beyond the Aptian, allowing plankton and nekton migration in the surface waters (Fö ter, 1978).

A world-wide rise of the CCD of comparable magnitude and improved preservation of organic carbon is also observed in the Miocene (Berger, 1972; van Andel et al., 1977; Ryan, von Rad et al., in press), again synchronous to the isolation of a low latitude ocean basin, i.e. the western Tethys, which started in the Burdigalian and culminated in the Messinian evaporite event (Berggren, 1972; Hsu et al., 1973).

In the middle Cretaceous spills of highly saline deep waters would have acted as triggers for periodic increased deep-water stratification in an already sluggishly circulating ocean. Partial oxygen depletion and carbon dioxide enrichment at intermediate depths leading to linear dissolution rate profiles, together with lowered surface fertility is suggested for the pre- late Cretaceous oceans by the gradual increase of organic carbon contents in the North Atlantic from the late Jurassic onwards, as well as by the large scatter of carbonate contents in middle Cretaceous sediments of the Pacific and North Atlantic.

The dissolution rate profiles and supply rates in all oceans appear to have stabilized by the end of the Cretaceous as evidenced by the carbonate versus depth distribution patterns in the North Atlantic and Pacific (Figure 25). Preliminary calculations of accumulation rates of carbonate in a number of DSDP sites, using

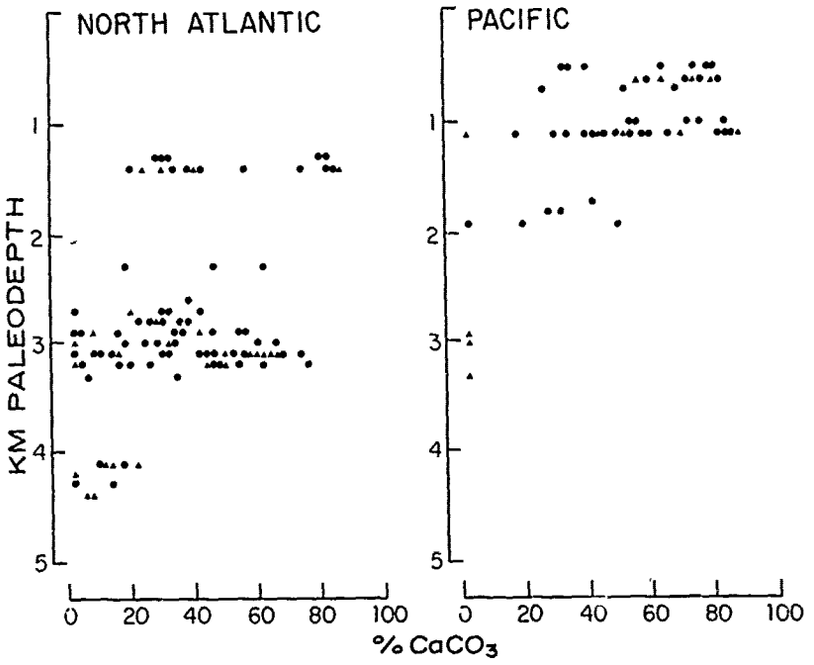


Figure 24. Carbonate contents in middle Cretaceous (90 - 100 m.y.) DSDP samples versus paleodepth. Dot = one measurement, triangle = two or more measurements.

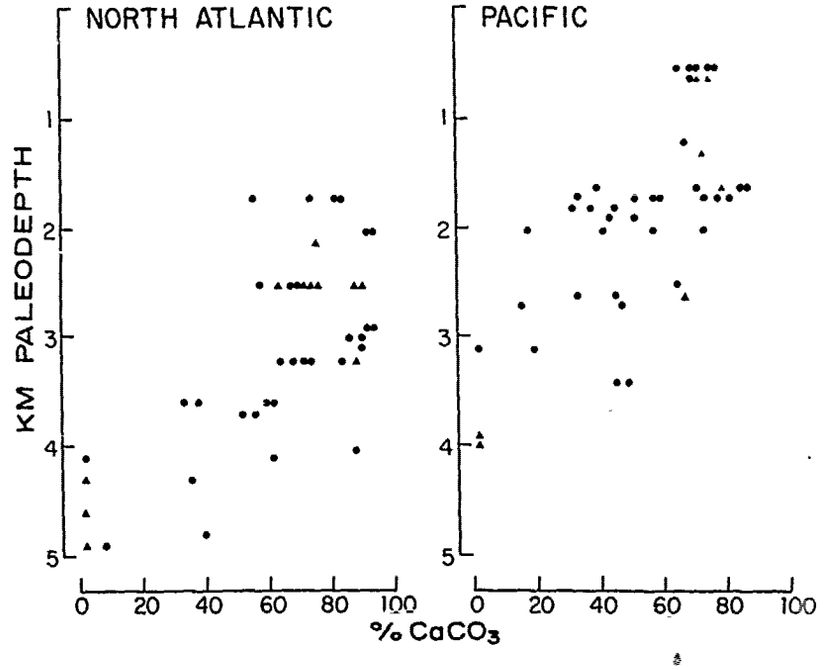


Figure 25. Carbonate contents in Maastrichtian and Danian (60 - 70 m.y.) DSDP samples versus paleodepth. Dot = one measurement, triangle = two or more measurements.

nannofossil biostratigraphy as time control, show that the rates in the late Cretaceous central Pacific were at least twice as high as those in the Atlantic. This factor must be a minimum estimate, since the carbonate preservation at comparable paleodepths in the Atlantic cores is far superior to that in the Pacific cores. It is evident that the next step in our struggle to understand the sedimentation processes in the Mesozoic deep oceans will have to come through an improvement of the chronostratigraphic control -- only then will we be able to transform measured concentrations into the paleoceanographic Rosetta stone of accumulation- and dissolution rates.

Acknowledgments. Sediment samples were obtained from the DSDP curator, and sedimentological data were provided by P. Woodbury of the Deep Sea Drilling Project, which is sponsored by NSF. Research supported by the National Science Foundation under Grant No. OCE76-22150. Sample preparation by Carmen Chavez and computer-programming by Mike Coryell are acknowledged. Rachel Haymon helped computing sample bathymetry. Discussions with M. Arthur, W. Berger, I. Premoli-Silva, P. Roth, M. Kastner and W. Sliter were beneficial and are greatly appreciated. Reviews by W. H. Berger, T. A. Davies and F. W. McCoy are appreciated.

## References

Arthur, M.S. and S.O. Schlanger, Cretaceous "oceanic events" as causal factors in development of giant oil fields, Geophysics (in press).

Bartenstein, H., Upper Jurassic-Lower Cretaceous primitive arenaceous foraminifera from DSDP Sites 259 and 261, eastern Indian Ocean. In: Veevers, J.J., Heirtzler, J.R., et al., Init. Rep. Deep Sea Drilling Project, vol. 27, Washington (U.S. Government Printing Office), 683-695. 1974.

Berger, W.H., Foramin[illegible]ooze: solution at depths, Science, 156, 383-385, 1967.

Berger, W.H., Planktonic foraminifera: Selective solution and the lysocline, Mar. Geol., 8, 111-138, 1970a.

Berger, W.H., Biogenous deep-sea sediments: Fractionation by deep-sea circulation, Geol. Soc. Am. Bull., 81, 1385-1402, 1970b.

Berger, W.H., Sedimentation of planktonic foraminifera, Mar. Geol., 11, 325-328, 1971.

Berger, W.H., Deep sea carbonates: Dissolution facies and age-depth constancy, Nature, 236, 392-395, 1972.

Berger, W.H., Carbon dioxide excursions and the deep-sea record: Aspects of the problem. In: N.R. Andersen and A. Malahoff (eds.), The Fate of Fossil Fuel $CO_2$ in the Oceans (Plenum Publish. Corp., N.Y.), 505-542, 1977.

Berger, W.H., Sedimentation of deep-sea carbonate: Maps and models of variations and fluctuations, J. Foram. Res. (in press).

Berger, W.H., C.G. Adelseck, Jr., and L.A. Mayer, Distribution of carbonate in surface sediments of the Pacific Ocean, J. Geophys. Res., 81, 2617-2627, 1976.

Berger, W.H. and A. Soutar, Preservation of plankton shells in an anaerobic basin off California, Geol. Soc. Am. Bull., 81, 275-282, 1970.

Berger, W.H. and U. von Rad, Cretaceous and Cenozoic sediments from the Atlantic Ocean. In: D.E. Hayes, A.C. Pimm et al., Init. Rep. Deep Sea Drilling Project, Vol. 14, Washington (U.S. Government Printing Office), 787-954, 1972.

Berger, W.H. and E.L. Winterer, Plate stratigraphy and the fluctuating carbonate line, Spec. Publs. Int. Assoc. Sedimentologists, 1, 11-48, 1974.

Berggren, W.A., A Cenozoic time-scale -- some implications for regional geology and paleobiogeography, Lethaia, 5, 195-215, 1972.

Berggren, W.A., D.P. McKenzie, J.G. Sclater and J.E. van Hinte, World-wide correlation of Mesozoic magnetic anomalies and its implication: Discussion, Geol. Soc. Am. Bull., 86, 267-269, 1975.

Berner, R.A., Principles of chemical sedimentology (McGraw-Hill, N.Y.), 240 pp, 1972.

Berner, R.A., The solubility of calcite and aragonite in sea water at atmospheric pressure and 34.5°/$_{oo}$ salinity, Am. J. Sci., 276, 713-730, 1976.

Berner, R.A., Sedimentation and dissolution of pteropods in the Ocean. In: N.R. Andersen and A. Malahoff (eds.), The Fate of Fossil Fuel $CO_2$ in the Oceans (Plenum Press, N.Y.), 243-260, 1977.

Berner, R.A. and J.W. Morse, Dissolution kinetics of calcium carbonate in sea water IV. Theory of calcite dissolution, Am. J. Sci., 274, 108-134 1974.

Bertels, A., Cretaceous Ostracoda -- South Atlantic. In: F.M. Swain (ed.), Stratigraphic Micropaleontology of Atlantic Basins and Borderlands, Developments Paleont. Stratigr., 6 (Elsevier Sci. Publ. Co., Amsterdam), 271-304, 1977.

Biscaye, P.E., V. Kolla and K.K. Turekian, Distribution of calcium carbonate in surface sediments of the Atlantic Ocean, J. Geophys. Res., 81, 2595-2603, 1976.

Bramlette, M.N., Pelagic sediments. In: M. Sears (ed.), Oceanography, (Am. Assoc. Adv. Sci., Washington, D.C.), 345-366, 1961.

Broecker, W.A. and T. Takahashi, Neutralization of fossil fuel $CO_2$ by marine calcium carbonate. In: N.R. Andersen and A. Malahoff (eds.), The Fate of Fossil Fuel $CO_2$ in the Oceans, (Plenum Press, N.Y.), 213-241, 1977.

Burke, K., Atlantic evaporites formed by evaporation of water spilled from Pacific, Tethyan, and Southern oceans, Geology, 3, 613-616, 1975.

Čepek, P., Mesozoic calcareous nannoplankton of the eastern North Atlantic. In: Y. Lancelot, E. Seibold et al., Init. Rep. Deep Sea Drilling Project, vol. 41, Washington (Government Printing Office), 667-687, 1978.

Chamberlin, T.C., On a possible reversal of deep-sea circulation and its influence on geologic climates, J. Geology, 14, 363-373, 1906.

Dean, W.E., J.V. Gardner, L.F. Jansa, P. Čepek and E. Seibold, Cyclic sedimentation along the continental margin of Northwest Africa. In: Y. Lancelot, E. Seibold et al., Init. Rep. Deep Sea Drilling Project, Vol. 41, Washington (U.S. Government Printing Office), 965-989, 1978.

Degens, E.T. and P. Stoffers, Stratified waters as a key to the past, Nature, 263, 22-27, 1976.

Detric , R.S., J.G. Sclater and J. Thiede, The subs lence of aseismic ridges, Earth Planet. Sci. Lett., 34, 185-196, 1977.

Donnelly, T.W. et al., Mid-ocean ridge in the Cretaceous, Geotimes, 22, 21-23, 1977.

Fischer, A.G. and M.A. Arthur, Secular variations in the pelagic realm. In: H.E. Cook and P. Enos (eds.), Deep-water Carbonate Environments, Soc. Econ. Paleontol. Mineral., Spec. Pub. No. 25, 19-50, 1977.

Förster, R., Evidence for an open seaway between northern and southern proto-Atlantic in Albian times, Nature, 272, 158-159, 1978.

Hay, W.W., Sedimentation rates. In: W.E. Benson, R.D. Gerard, W.W. Hay, Summary and Conclusions. In: R.G. Bader, et al., Init. Rep. Deep Sea Drilling Project, Vol. 3, Washington (U.S. Government Printing Office), 668-670, 1970.

Heath, G.R. and C. Culberson, Calcite degree of saturation, rate of dissolution, and the compensation depth in the deep oceans, Geol. Soc. Am. Bull., 81, 3157-3160, 1970.

Heath, G.R., T.C. Moore and J.P. Dauphin, Organic carbon in deep-sea sediments. In: N.R. Andersen and A. Malahoff (eds.), The Fate of Fossil Fuel $CO_2$ in the Ocean (Plenum Press, N.Y.), 605-625, 1977.

Heezen, B.C. et al., Western Pacific guyots. In: B.C. Heezen, I.D. MacGregor et al., Init. Rep. Deep Sea Drilling Project, Vol. 20, Washington (U.S. Government Printing Office), 653-702, 1973.

Hollister, C.D., J.I. Ewing et al., Init. Rep. Deep Sea Drilling Project, Vol. 11, Washington (U.S. Printing Office), 1077 pp, 1972.

Hsu, K.J., W.B.F. Ryan, M.B. Cita, Late Miocene desiccation of the Mediterranean, Nature, 242, 240-244, 1973.

Ingle, S.E., C.H. Culberson, J.F. Hawley, and Pytcowicz, The solubility of calcite in sea water at atmospheric pressure and 35°/oo salinity, Mar.Chem., 1, 295-307, 1973.

Irving, E., F.K. North and R. Couillard, Oil, climate and tectonics, Can. J. Earth Sci., 11, 1-15, 1974.

Jansa, L., J.V. Gardner, and W.E. Dean, Mesozoic sequences of the central North Atlantic. In: Y. Lancelot, E. Seibold et al., Init. Rep. Deep Sea Drilling Project, Vol. 41, Washington (U.S. Government Printing Office), 991-1010, 1978.

Jung, P., Pleistocene pteropods -- Leg 15, Site 147, Deep Sea Drilling Project. In: T.N. Edgar, J.B. Saunders et al., Init. Rep. Deep Sea Drilling Project, Vol. 15, Washington (U.S. Government Printing Office), 753-767, 1973.

Kauffman, E.G., Geological and biological overview: Western interior Cretaceous basin, The Mountain Geologist, 14, 75-99, 1977.

Kinsman, D.J.J., M. Boardman and M. Borcsik, An experimental determination of the solubility of oxygen in marine brines. In: A.H. Coogan (ed.), Fourth Symposium on Salt (Northern Ohio Geol. Soc. Inc., Cleveland), Vol. 1, 325-327, 1974.

Kolla, V., A.W.H. Bé, and P.E. Biscaye, Calcium carbonate distribution in the surface sediments of the Indian Ocean, J. Geophys. Res., 81, 2605-2616, 1976.

Krasheninnikov, V. and R. Hoskins, Late Cretaceous, Paleogene and Neogene planktonic foraminifera. In: B.C. Heezen, I.D. MacGregor et al., Init. Rep. Deep Sea Drilling Project, Vol. 20, Washington (U.S. Government Printing Office), 105-203, 1973.

Lancelot, Y., Relations entre évolution sédimentaire et tectonique de la plaque pacifique depuis le Crétacé inférieur. Thèse, Univ. Pierre et Marie Curie, Paris, 1978.

Lancelot, Y., J.C. Hathaway and C.D. Hollister, Lithology of sediments from the western North Atlantic, Leg 11 of the Deep Sea Drilling Project. In: C.D. Hollister, J.I. Ewing et al., Init. Rep. Deep Sea Drilling Project, Vol. 11, Washington (U.S. Government Printing Office), 901-949, 1972.

Lancelot, Y., E. Seibold et al., Init. Rep. Deep Sea Drilling Project, Vol. 41, Washington (U.S. Government Printing Office), 1259 pp, 1978.

Lancelot, Y., E.L. Winterer et al., Documenting early rifting, Geotimes, 22, 24-27, 1977.

Larson, R.L. and C.G. Chase, Late Mesozoic evolution of the western Pacific Ocean, Geol. Soc. Am. Bull., 83, 3627-3644, 1972.

Larson, R.L. and T.W. Hilde, A revised time scale of magnetic reversals for the early Cretaceous and late Jurassic, J. Geophys. Res., 80, 2586-2594, 1975.

Larson, R.L., R. Moberly et al., Init. Rep. Deep Sea Drilling Project, Vol. 32, Washington (U.S. Government Printing Office), 980 pp, 1975.

Larson, R.L. and W.C. Pitman III, World-wide correlation of Mesozoic magnetic anomalies, and its implications, Geol. Soc. Am. Bull., 83, 3645-3662, 1972.

Li, Y.H., T. Takahashi and W.S. Broecker, Degree of saturation of $CaCO_3$ in the Oceans, J. Geophys. Res., 74, 5507-5525, 1969.

Lisitzin, A.P., Sedimentation in the world ocean, Soc. Econ. Paleontol. Mineral., Spec. Publ., 17, 218 pp, 1972.

Lotze, F., The distribution of evaporites in space and time. In: A.E.M. Nairn, Problems in Paleoclimatology (Interscience Publ., London), 491-506, 1963.

Manivit, H., Les Nannofossiles calcaires du Crétacé francais (de l'Aptien au Danien). Essai de biozonation appuyée sur les stratotypes, Thèse. Fac. Sci., Univ. de Paris, 1971.

McCave, I.N., Depositional features of organic-carbon-rich black and green mudstones at DSDP Sites 386 and 387, western North Atlantic. In: B.E. Tucholke, P. Vogt et al., Init. Rep. Deep Sea Drilling Project, Vol. 43, Washington (U.S. Government Printing Office) (in press).

McCoy, F.W. and H.B. Zimmerman, A history of sediment lithofacies in the South Atlantic Ocean. In: J.R. Supko, K. Perch-Nielsen et al., Init. Rep. Deep Sea Drilling Project, Vol. 39, Washington (U.S. Government Printing Office), 1047-1079, 1977.

Noël, D. and M. Melguen, Nannofacies of Cape Basins and Walvis Ridge sediments, Lower Cretaceous to Pliocene (Leg 40). In: H.M. Bolli, W.B.F. Ryan et al., Init. Rep. Deep Sea Drilling Project, Vol. 40, Washington (U.S. Government Printing Office), 487-524, 1978.

Obradovich, J.D. and W.A. Cobban, A time scale for the Late Cretaceous Western Interior of North America, Geol. Assoc. Canada, Spec. Pap., No. 13, 31-54, 1975.

Okada, H. and H.R. Thierstein, Calcareous nannoplankton -- Leg 43, Deep Sea Drilling Project. In: B.E. Tucholke, P. Vogt et al., Init. Rep. Deep Sea Drilling Project, Vol. 43, Washington (U.S. Government Printing Office) (in press).

Parsons, B. and J.G. Sclater, An analysis of the variation of ocean floor heat flow and bathymetry with age, J. Geophys. Res., 82, 803-827, 1977.

Peterson, M.N.A., Calcite: Rates of dissolution in a vertical profile in the central Pacific, Science, 154, 1542-1544, 1966.

Proto-Decima, F., F. Medizza and L. Todesco, Calcareous nannofossils: Southeastern Atlantic. In: H.M. Bolli, W.B.F. Ryan et al., Init. Rep. Deep Sea Drilling Project, Vol. 40, Washington (U.S. Government Printing Office), 571-634, 1978.

Ramsay, A.T.S., Sedimentological clues to paleo-oceanography. In: A.T.S. Ramsay (ed.), Oceanic Micropaleontology, Vol. 2, (Academic Press, London), 1371-1453, 1977.

Ross, D.A. and E.T. Degens, Recent sediments of Black Sea. In: E.T. Degens and D.A. Ross (eds.), The Black Sea -- Geology, Chemistry, and Biology, Am. Assoc. Petr. Geol., Mem. 20, 183-199, 1974.

Roth, P.H., Cretaceous nannoplankton biostratigraphy and paleoceanography of the northwestern Atlantic. In: W.E. Benson, R.E. Sheridan et al., Init. Rep. Deep Sea Drilling Project, Vol. 44, Washington (U.S. Government Printing Office) (in press).

Ruddiman, W.F. and B.C. Heezen, Differential solution of planktonic foraminifera, Deep-Sea Res., 14, 801-808, 1967.

Ryan, W.B.F., U. von Rad et al., Init. Rep. Deep Sea Drilling Project, Vol. 47, Washington, (U.S. Government Printing Office) (in press).

Ryan, W.B.F. and M.B. Cita, Ignorance concerning episodes of ocean-wide stagnation, Mar. Geol., 23, 197-315, 1977.

Scheibnerova, V., Aptian-Albian benthonic foraminifera from DSDP Leg 27, Sites 259, 260, and 263, eastern Indian Ocean. In: J.J. Veevers, J.R. Heirtzler et al., Init. Rep. Deep Sea Drilling Project, Vol. 27, Washington (U.S. Government Printing Office), 697-741, 1974.

Scheibnerova, V., Synthesis of the retaceous benthonic foraminifera recovered by the Deep Sea Drilling Project in the Indian Ocean. In: J.R. Heirtzler et al. (eds.), Indian Ocean Geology and Biostratigraphy, (Am. Geophys. Union, Washington), 585-597, 1977.

Schlanger, S.O. and H.C. Jenkyns, Cretaceous oceanic anoxic events: Causes and consequences, Geologie en Mijnbouw. 55, 179-184, 1976.

Sclater, J.G., D. Abbott and J. Thiede, Paleobathymetry and sediments of the Indian Ocean. In: J.R. Heirtzler et al. (eds.), Indian Ocean Geology and Biostratigraphy, (Am. Geophys. Union, Washington), 25-59, 1977.

Sclater, J.G., S. Hellinger and C. Tapscott, The paleobathymetry of the North Atlantic Ocean from the Jurassic to Present, J. Geology, 85, 509-522, 1977.

Sholkovitz, E., Interstitial water chemistry of the Santa Barbara Basin sediments, Geochim. Cosmochim. Acta, 37, 2043-2073, 1973.

Sissingh, W., Biostratigraphy of Cretaceous calcareous nannoplankton, Geologie en Mijnbouw. 56, 37-65, 1977.

Sleep, N.H., Thermal effects of the formation of Atlantic continental margins by continental break up, Geophys. J.R. Astr. Soc. 24, 325-350, 1971.

Smith, A.G. and J.C. Briden, Mesozoic and Cenozoic paleocontinental maps (Cambridge University Press), 63 pp, 1977.

Southam, J.R. and W.W. Hay, Time scales and dynamic models of deep-sea sedimentation, J. Geophys. Res. 82, 3825-3842, 1977.

Stackelberg, U.v., Faziesverteilung in Sedimenten des indisch-pakistanischen Kontinentalrandes (Arabisches Meer), "Meteor" Forsch.-Ergebnisse, Reihe C, No. 9, 1-73, 1972.

Supko, P.R., K. Perch-Nielsen et al., Init. Rep. Deep Sea Drilling Project, Vol. 30, Washington (U.S. Printing Office), 1139 pp, 1977.

Thiede, J. and T.H. van Andel, The paleoenvironment of anaerobic sediments in the late Mesozoic Atlantic Ocean, Earth Planet. Sci.

Lett., 33, 301-309, 1977.
Thierstein, H.R., Lower Cretaceous calcareous nannoplankton biostratigraphy, Abh. Geol. B.A. Wien, 29, 52 pp, 1973.
Thierstein, H.R., Calcareous nannoplankton biostratigraphy at the Jurassic-Cretaceous boundary. In: Colloque sur la limite Jurassique-Crétacé, Lyon, Neuchâtel, Sept. 1973, Memoires du B.R.G.M., 86, 84-94, 1975.
Thierstein, H.R., Mesozoic calcareous nannoplankton biostratigraphy of marine sediments, Mar. Micropaleontol., 1, 325-362, 1976.
Thierstein, H.R., Mesozoic calcareous nannofossils from the Indian Ocean, Deep Sea Drilling Project Legs 22 to 27. In: J.R. Heirtzler et al. (eds.), Indian Ocean Geology and Biostratigraphy, (Am. Geophys. Union, Washington), 339-351, 1977.
Thierstein, H.R. and H. Okada, The Cretaceous/Tertiary boundary event in the North Atlantic. In: B.E. Tucholke, P. Vogt et al., Init. Rep. Deep Sea Drilling Project, Vol. 43, Washington (U.S. Government Printing Office) (in press).
Vail, P.R., R.M. Mitchum and S. Thompson III, Global changes of sea level from seismic stratigraphy. In: C.E. Payton (ed.), Seismic stratigraphy -- applications to hydrocarbon exploration, Am. Assoc. Petrol. Geol. Mem., 26, 83-97, 1977.
van Andel, T. H., Establishing the age of the oceanic crust, Comments on earth sciences: geophysics, 2, 157-168, 1972.
van Andel, T.H., Mesozoic/Cenozoic calcite compensation depth and the global distribution of calcareous sediments, Earth Planet. Sci. Lett., 26, 187-194, 1975.
van Andel, T.H., J. Thiede, J.G. Sclater and W.W. Hay, Depositional history of the South Atlantic Ocean during the last 125 million years, J. Geology, 85, 651-698, 1977.
van Hinte, J.E., A Cretaceous time scale, Am. Assoc. Petrol. Geol. Bull., 60, 498-516, 1976a.
van Hinte, J.E., A Jurassic time scale, Am. Assoc. Petrol. Geol. Bull., 60, 489-497, 1976b.
Veevers, J.J. and D. Cotterill, Western margin of Australia: Evolution of a rifted arch system, Geol. Soc. Am. Bull., 89, 337-355, 1978.
Verbeek, J.W., Calcareous nannoplankton biostratigraphy of middle and upper Cretaceous deposits in Tunesia, southern Spain and France, Utrecht Micropal. Bull., 16, 157 pp, 1977.
Watts, A.B. and W.B.F. Ryan, Flexure of the lithosphere and continental margin basins, Tectonophysics, 36, 25-44, 1976.
Wind, F., Western North Atlantic late Jurassic calcareous nannofossil biostratigraphy. In: W.E. Benson, R.E. Sheridan et al., Init. Rep. Deep Sea Drilling Project, Vol. 44, Washington (U.S. Government Printing Office) (in press).
Wise, S.W. and F.H. Wind, Mesozoic and Cenozoic calcareous nannofossils recovered by Deep Sea Drilling Project Leg 36 drilling on the Falkland Plateau, Southwest Atlantic sector of the southern Ocean. In: P.F. Barker, I.W.D. Dalziel et al., Init. Rep. Deep Sea Drilling Project, Vol. 36, Washington (U.S. Government Printing Office), 269-491, 1977.

# HISTORY OF THE NORTH ATLANTIC OCEAN: EVOLUTION OF AN ASYMMETRIC ZONAL PALEO-ENVIRONMENT IN A LATITUDINAL OCEAN BASIN.

Jörn Thiede

Department of Geology, University of Oslo,
P.O. Box 1047, Blindern, Oslo 3, Norway

Abstract. The Atlantic is the only ocean connecting both polar hydrospheres. Its edges consist almost entirely of passive continental margins of the American and Eurafrican land masses, but they are interrupted by the tectonically unstable regions of the Caribbean and Mediterranean Seas which trace the ancient mobile circum-equatorial Tethys belt. The opening and evolution of the Atlantic during the last 160-180 myrs had profound consequences both for the paleo-oceanography of the world ocean and for the geology of the adjacent continents where vast basins developed. The dominant portion of the global land area drain today therefore directly or indirectly into the Atlantic Ocean. The main North Atlantic basin was part of the circum-equatorial Tethys Ocean from its early mid-Jurassic formation until the late Cretaceous when the South Atlantic with its connection to the Southern Ocean opened wide enough to allow the exchange of surface and deep water masses. The opening of the Norwegian-Greenland Sea during late Paleocene and early Eocene created a pathway for the exchange of water between the Arctic and North Atlantic Oceans. The subsidence of the main platform of the aseismic Iceland-Faeroe Ridge with a deep channel at its southeastern end during middle Miocene allowed deep water from the Norwegian-Greenland Sea to enter the main North Atlantic basin. The stepwise evolution of the ocean basin including the history and final closure of the circum-equatorial seaway during the late Tertiary, the waxing and waning of epicontinental seas and marginal basins, and the evolution of the paleoclimate, had a dominating influence on the paleo-oceanography and thereafter on the pelagic lithofacies through time. The spatial and temporal distribution of pelagic sediments display a zonation and a latitudinal asymmetry which were more intense during times of steep paleoclimatic and paleo-oceanographic gradients than in periods of relatively uniform and less intensively zoned atmosphere and surface water masses. Both the North and the South Atlantic oceans are subdivided into smaller basins due to the presence of the mid-ocean ridge and the development of large aseismic structural highs. Sediments from the flanks of the Iceland-Faeroe Ridge (as well as from the Rio Grande Rise and Walvis Ridge) also allow a description of the paleo-oceanography of the intermediate water masses of the adjacent ocean basins. They reveal evidence of subsidence and allow reconstruction of the evolution of deep channels which intersect these barriers and which have acted as passages for the deep water circulation during the geologic past.

## Introduction

The Atlantic Ocean is a latitudinal ocean basin connecting the polar regions of both the northern and southern hemispheres. This was not always so. Information collected by the Deep Sea Drilling Project over the past 10 years has allowed us to draw a detailed picture of the paleogeographic and paleobathymetric evolution of this ocean. We can also see how the depositional environment reacted to changes in physiography, although many details cannot be resolved at present because some of the pertinent data are not available. Sedimentation in the Atlantic Ocean is controlled by a complicated network of boundary conditions because this latitudinal ocean basin crosses all climatic zones of the modern world as it has probably done throughout its geologic past.

This paper will emphasize the North Atlantic Ocean, which today is probably the best studied part of the world ocean. It is also a very complex part of the world ocean. It is composed of various basins which, with the exception of the Caribbean and possibly the southern Bay of Biscay, are surrounded by passive continental margins. The North Atlantic includes some of the world's oldest crust of the present ocean basins (Hayes and Rabinowitz, 1975, Rabinowitz, 1974). Shortly after the initial opening during the mid-Jurassic, its main basin became part of the circum-equatorial Tethys Ocean, which had an important impact on the North

Atlantic paleo-environment throughout the Mesozoic (Bernoulli, 1972). The opening of the Norwegian-Greenland Sea during the Cenozoic (Talwani and Eldholm, 1977) created the first deep connection between the Arctic Ocean and the main North Atlantic basins. The generation of a latitudinal ocean had profound consequences for the water mass structure of the entire Atlantic basin; this can be seen from the distribution of the North Atlantic Deep Water, which can be traced from the Norwegian-Greenland Sea throughout the entire Atlantic (Wüst, 1935). I will combine geologic and geophysical data to reconstruct the origin and physiographic evolution of this important ocean basin, and subsequently show how changes in the physiography of the North Atlantic and in the paleoenvironment result in depositional regimes which are different from basin to basin.

## Tectonic and physiographic evolution of the North Atlantic

The North and South Atlantic oceans have a Mesozoic and Cenozoic history, but originated from rifting in cratonic regions of widely different character (Beurlen, 1974). The South Atlantic and the southern North Atlantic separated old shield areas of western Africa and eastern South America during Jurassic and Cretaceous times by cutting across largely Precambrian fold belts (Martin, 1976). The North Atlantic cut through mobile belts of Paleozoic and Mesozoic to Cenozoic age (Fitch et al., 1974). It presently consists of a complex assemblage of basins underlain by oceanic crust which started to develop between the Jurassic and Paleogene (Hayes and Rabinowitz, 1975, Vogt et al., 1971, Vogt and Einwich, 1978) and which followed belts of structural weakness along parts of the Caledonian, Variscan and Alpine (Bay of Biscay) mountain chains (Figure 1). The central North Atlantic split parts of the Variscan and Caledonian orogenes and the Norwegian-Greenland Sea split only parts of the Caledonian orogene. Remnants of these Paleozoic mountain chains are found on either side of the North Atlantic (Dewey, 1974), but in many areas these ancient mobile belts have been divided asymmetrically.

Magnetic anomalies in the South Atlantic provide evidence of the evolution of an ocean basin due to sea floor spreading of a two-plate system. Its mid-ocean ridge, which is offset by many transform faults in the equatorial Atlantic continues into the North Atlantic Ocean. However, the pattern of spreading north of Gibraltar on the eastern side and north of the northern tip of South America on the western side is much more complicated than that in the South Atlantic. In the North Atlantic the tectonic system is composed of a variable number of plates and spreading axes which cut the early Mesozoic Laurasian continent (Dietz and Holden, 1970) into a complex jigsaw puzzle. This complexity made it extremely difficult to reconstruct the outline of the original rift through Laurasia and to reassemble it into a single piece of continental crust (Le Pichon et al., 1977). The crust below the North Atlantic and the surrounding continents belongs to a number of different plates which have a complex relationship to each other and whose spatial arrangement has changed several times during the past 150 yrs.

The opening of the North and South Atlantic oceans had profound consequences for the geology of the surrounding land masses of the American, African, and European continents. The large basins which today drain the dominant portion of all continental areas directly or indirectly into the Atlantic Ocean, did not exist before this ocean had evolved. The present drainage patterns on these land masses may well be the indirect result of the extensional plate movements along the rifting and spreading axes (dominantly latitudinal structural elements) or of compressional tectonic movements along the ancient mobile Tethys belt (dominantly longitudinal structural elements).

Important structural highs subdivide the eastern and western basins in both the South and North Atlantic oceans. The Walvis Ridge and Rio Grande Rise separate the Argentine and Cape basins from the Brazil and Angola basins, and have controlled the exchange of bottom as well as surface water masses between these basins since late Mesozoic time when they were large subaerial volcanic massifs (Thiede, 1977). The Iceland-Faeroe Ridge covers the most important portion of a structural high which separates the Cenozoic Norwegian-Greenland Sea from the Mesozoic North Atlantic basin.

## An attempt to reconstruct the physiography of the North Atlantic

The physiographic-tectonic events in the evolution of the North Atlantic are discussed only insofar as they are pertinent to Mesozoic and Cenozoic paleo-oceanography. In this context, I analyze the events which established the physiographic framework for the hydrographic regime of the entire ocean, describe major epicontinental seas around it, discuss the opening and closure of pathways for surface and deep water circulation, and point out important remaining problems of paleogeography and paleobathymetry. Three types of data are used to reconstruct trends of the physiographic evolution of the North Atlantic. They are 1) the linear magnetic anomalies which are commonly observed in regions underlain by oceanic crust (Figure 2), 2) the depth vs. age relationship of the ocean floor based on the information of the sites of the Deep Sea Drilling Project (Figure 3), and 3) the extent of the epicontinental seas on the adjacent continents. With

Figure 1. Tectonic development of the North Atlantic Ocean during Bathonian, Hauterivian, Cenomanian, Danian, Oligocene and present times (after Sclater et al., 1977, Beurlen, 1974, Fitch et al., 1974). The pairs of maps sketch the arrangement of plates with their accreting and transform margins, and the locations of remains of Paleozoic and Mesozoic-Cenozoic ancient mobile belts.

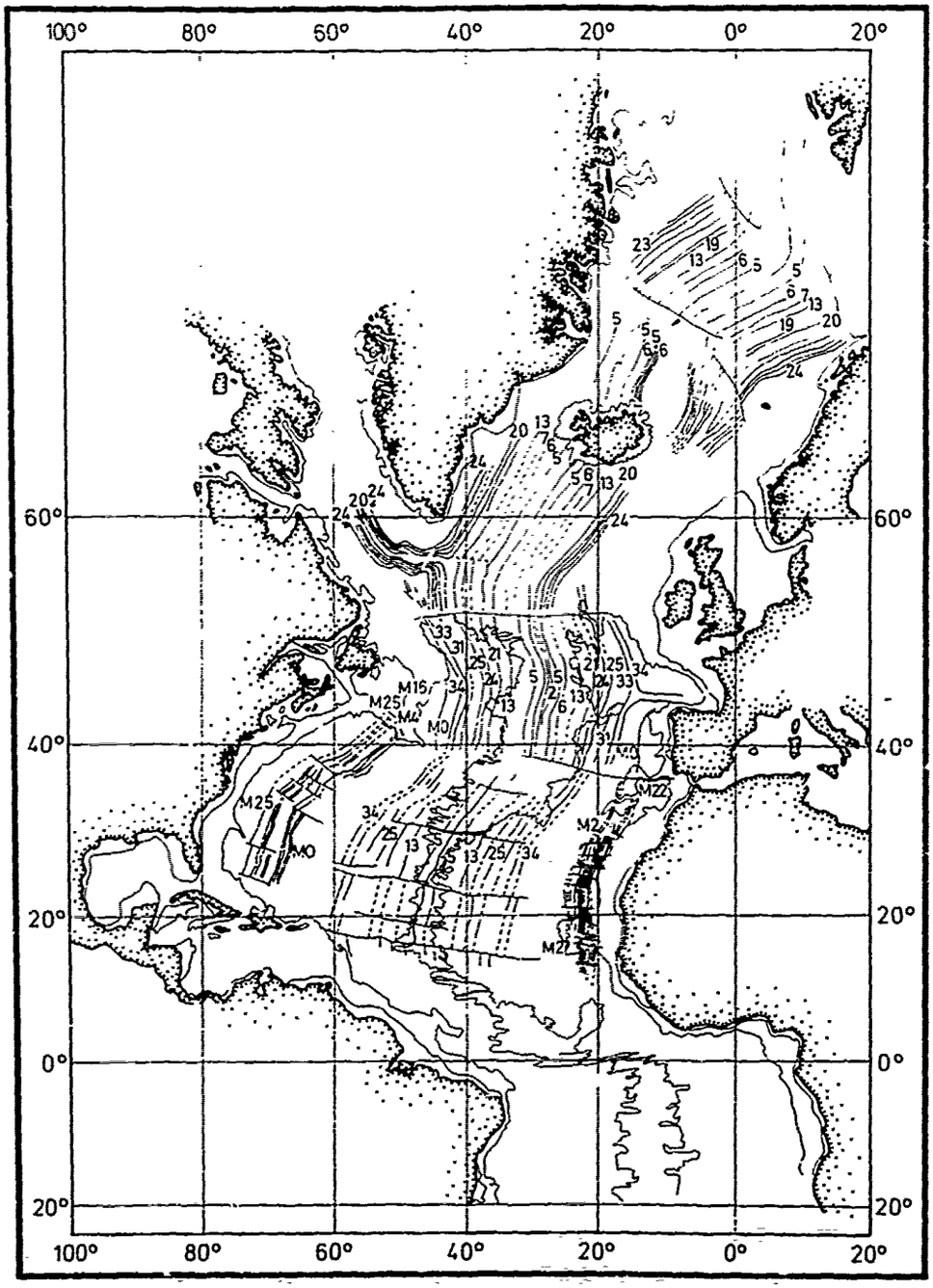


Figure 2. Distribution of magnetic anomalies in the North Atlantic (compiled from various sources as discussed in the text).

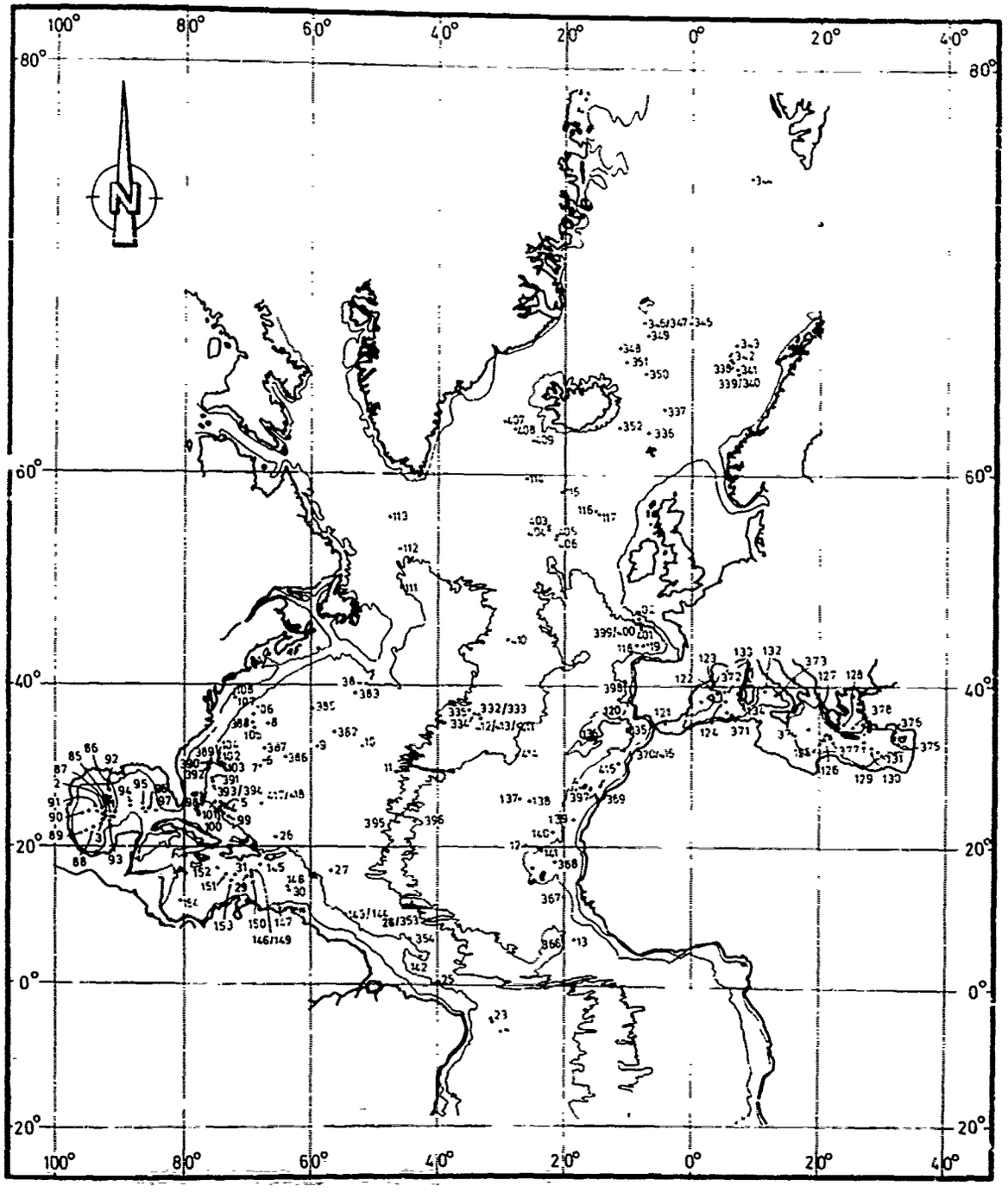


Figure 3. Distribution of Deep-Sea Drilling Project sites in the North Atlantic and its marginal ocean basins. Compiled after the Initial Reports of the Deep-Sea Drilling Project and the "Geotimes" cruise reports.

respect to plate rotations and paleobathymetry of the ocean basins proper, the data published by Sclater et al. (1977) have been used. The time scales of van Hinte (1976, a and b) have been accepted for the Mesozoic ages, and those of Berggren (1972) for the Cenozoic ages.

The distribution of linear magnetic anomalies and their correlation to an absolute time scale allow a reconstruction of the horizontal component of the growth of the parts of the basins that are underlain by oceanic crust. The magnetic anomalies (Figure 2) have been mapped over major parts of the North Atlantic (Pitman and Talwani, 1972, Laughton, 1975), although details of their correlations are disputed in many regions. The data illustrated in Figure 2 have been pieced together from several sources. Jurassic magnetic anomalies (Hayes and Rabinowitz, 1975, Rabinowitz, 1974) indicate that the oldest North Atlantic basins should be sought along the northwestern African and southeastern North American continental margins. The oldest magnetic anomalies between Ireland and Newfoundland (Kristoffersen, 1978, Cande and Kristoffersen, 1977) and in the Bay of Biscay (Sibuet et al., 1978, Williams, 1975, Williams and McKenzie, 1971) are of Late Cretaceous age. The Labrador Sea began to open during the late Cretaceous, but concluded its evolution during the early Tertiary (Kristoffersen and Talwani, 1977, Srivastava, 1978). Rockall Plateau, which represents a small piece of continental crust and which is probably surrounded by ocean floor (Roberts, 1975), is situated close to the Iceland-Faeroe Ridge, whose age structure has yet to be resolved in sufficient detail (Talwani and Udintsev, 1976). The first rift in the Norwegian-Greenland Sea did not appear before Paleocene (Talwani and Eldholm, 1977); the repetition of the Magnetic anomaly pattern north and northeast of the Iceland-Faeroe Ridge suggests jumping of the Tertiary spreading center.

The subsidence of oceanic crust with time as a consequence of its thermal history provides the vertical component of the physiographic evolution of an ocean basin (Sclater et al., 1971). This concept of subsidence has been developed in the Pacific where in many areas only a thin veneer of sediments overlies the oceanic basement. In the Atlantic Ocean, however, because of the weight of thick sediments, corrections for the isostatic response (Ewing et al., 1973) have to be carried out individually for the single site which was occupied by the Deep Sea Project (Figure 3) and where age and depth of basement are approximately known.

According to the model of Sclater et al. (1971) spreading centers are situated approximately 2.7 km below the sea surface. Ocean crust subsides about 1 km during the first 10 myrs after its formation, another kilometer during the next 30 myrs, and an additional kilometer during the following 40-50 myrs. Subsidence also continues afterwards, although at a reduced pace. This process has a controlling influence on the shape of the ocean basin, because young regions, with certain unique exceptions such as in the Arctic Ocean (Vogt and Avery, 1974 a), are considerably shallower than old ones. It also explains the position of the Atlantic Ocean's deep basins along the continental rises where the oldest oceanic crust has been preserved. Under ideal conditions this process would lead to a rather simple morphology of the ocean basins. The deep eastern and western North Atlantic basins are therefore subdivided by a relatively shallow mid-Atlantic Ridge. Bottom water exchange between these basins is largely confined to regions where the continuity of this ridge system is interrupted due to the presence of deep channels along fracture zones, for example along the Charlie-Gibbs Fracture Zone in the North Atlantic (Uchupi, 1971). Vertical tectonic movements, however, are believed to affect the oceanic crust close to fracture zones in a hitherto poorly understood manner (Bonatti, 1978) so that it is impossible to reconstruct the physiographic evolution of such areas quantitatively.

Fracture zones also can be traced as narrow elongate morphologic irregularities of the seafloor across the basins. Seamount chains along fracture zones usually contain wide and deep gaps between the single seamounts, but they have grown into a massive transverse ridge along an old plate boundary off Gibraltar (Laughton and Whitmarsh, 1974). This ridge prevents Arctic polar bottom water from flowing from the Tagus Abyssal Plain into the deep basins of the southeastern North Atlantic Ocean (Wüst, 1935).

Parts of the Greenland-Scotland Ridge (Bott, 1974) presently control the water exchange between the Norwegian-Greenland Sea and the main North Atlantic basin (Vogt, 1972). It probably prevented this water exchange almost entirely during Paleogene times because it can be shown that aseismic ridges subside in a fashion similar to the surrounding oceanic crust (Detrick et al., 1977) after the volcanic activity giving rise to these structural highs has ceased and after they have reached isostatic equilibrium with the surrounding oceanic crust. The Iceland-Faeroe Ridge has probably impeded the circulation of surface water during times of low eustatic sea levels because of its shallow main platform rises to 400-600 m water depth. The only passage is a narrow 800-900 m deep channel southeast and south of the Faeroe Islands. Talwani et al. (1976 a) have documented the volcanic origin of the Iceland-Faeroe Ridge from basalts encountered under late Eocene sediments at Site 336. A volcanic origin had been presumed for many years and this aseismic ridge had therefore been believed to be part of the Thulean basalt province that stretches from Baffin Island to the Fennoscandian border zone and whose origin had been linked to the existence of a hot spot since the Jurassic (Vogt, 1974).

The Iceland-Faeroe Ridge links the volcanic rocks of Iceland, which are middle Miocene to Recent in age (Piper, 1973), with the Faeroe Islands, which were built by early Tertiary subaerial basaltic volcanism (Noe-Nygaard, 1974). The Faeroe Islands, however, are situated to the northeast of Rockall, and this had led to considerable discussion concerning their continental or oceanic origin (Bott, 1974). At Site 336 northwest of the Faeroe Islands, basaltic rocks have been obtained with compositions resembling mid-ocean ridge tholeiites (Talwani et al., 1976 a). Their age has been dated as $43.4 \pm 3.3$ myrs B. P., which corresponds to the late Eocene red clayey soil overlying them (Nilsen, 1978). The subsidence of this site (Thiede, 1978) suggests that it sank below sea level during the late Eocene, that it crossed a neritic environment during the Oligocene and that it did not reach water depths of around 1000 m before the Plio-Pleistocene.

The subsidence of an elongate aseismic ridge can only be described completely through a whole family of different subsidence curves whose length and shape is dependent upon the age of the underlying oceanic crust. This age cannot be assessed properly at the present time because of the complicated and in part unresolved spreading history of the ocean basins north and south of the Iceland-Faeroe Ridge (Talwani and Eldholm, 1977). However, from the subsidence of Site 336, which is situated on the north flank of this structural high, it can be deduced that the main ridge platform, which towers some 400-600 m above the basement at Site 336 did not sink below sea level before middle Miocene. The last peaks, which lie almost 1 km above the basement at this site, did not submerge before the Pliocene. Thus, results from Site 336 support the idea of a large subaerial aseismic ridge of volcanic origin separating the Norwegian-Greenland Sea from the main North Atlantic for a long period during early and late Cenozoic. A primordial Iceland must have existed at least twice as long as had been previously assumed (Laughton, 1975, Talwani and Eldholm, 1977). The idea first postulated at the beginning of this century of a Tertiary land bridge between North America and Europe (Strauch, 1970; McKenna, 1972) can therefore be revived (Eldholm and Thiede, 1978).

The Yermak Plateau north of Svalbard and the Morris Jessup Rise north of Greenland which have separated from each other as a result of late Tertiary spreading along Gakkel Ridge, might have controlled the water exchange between the Arctic Ocean and the Norwegian-Greenland Sea. Both features rise to approximately 500 m water depth (Herman, 1974 a) and both are situated adjacent to the oldest Cenozoic oceanic crust of the Eurasian Basin of the Arctic Ocean. Although they have never been sampled it has been suggested (Le Pichon et al., 1977) that they contain oceanic features which subsided in a fashion similar to other aseismic ridges (Detrick et al., 1977).

The North Atlantic also includes a fair number of microcontinents (Orphan Knoll, Flemish Cap, Galacia Bank, Rockall Plateau, Jan Mayen Ridge). As can be shown by means of benthic fossil assemblages sampled at their flanks (Berggren, 1974), these fragments of continental crust have undergone considerable subsidence since their separation from the continents on either side of the North Atlantic. It has been impossible to reconstruct detailed histories of their subsidence because of the lack of suitable data. However, because of their generally small size it can be assumed that they are of minor importance for the reconstruction of the physiography of the North Atlantic, with the possible exception during its rifting stage.

Passive continental margins undergo vertical tectonic movements during their evolution from the boundary of a juvenile rift to that of a mature ocean basin (Curray, 1978). Although it is clear from the establishment of the present drainage pattern around the Atlantic that its continental margins have undergone considerable subsidence, a generally applicable model which would explain this subsidence, quantitatively has yet to be found (Watts and Ryan, 1976). The depth contours along the continental margins, except the coast lines as shown on the paleogeographic reconstructions of the North Atlantic (Figures 4 a and b), therefore must be viewed with some caution because they largely represent the depth contours of the modern continental margins.

The present coastline, seen on the "Recent" map (Figure 4 b) as a stippled line, is also given as a reference on the maps illustrating the older time slices. The fossil coastlines have been added to mark the outline of the paleophysiography of the North Atlantic Ocean. The bulk of the paleogeographic information published about this region has been averaged over long intervals (in general over whole epochs, such as Paleocene, Eocene, etc.) because inadequate stratigraphic information resulted in a reduced regional resolution. The most complete source of information for the Caribbean region, the Gulf of Mexico, northern South America and North America, including its northern continental margins with the Canadian Arctic islands and Greenland, is found in Cook and Bally (1975). The questionable paleodepth information available from many of the continental margins and from the epicontinental seas around the North Atlantic during the Mesozoic and Cenozoic has resulted in only the former coastline, the 2 and 4 km contours being marked on the historic time slices (Figures 4 a and b).

The physiography of the Mesozoic and Cenozoic North Atlantic is shown in 12 time slices spanning the time interval from Jurassic to Recent (Figures 4 a and b). Its evolution has gone through a number of specific settings and

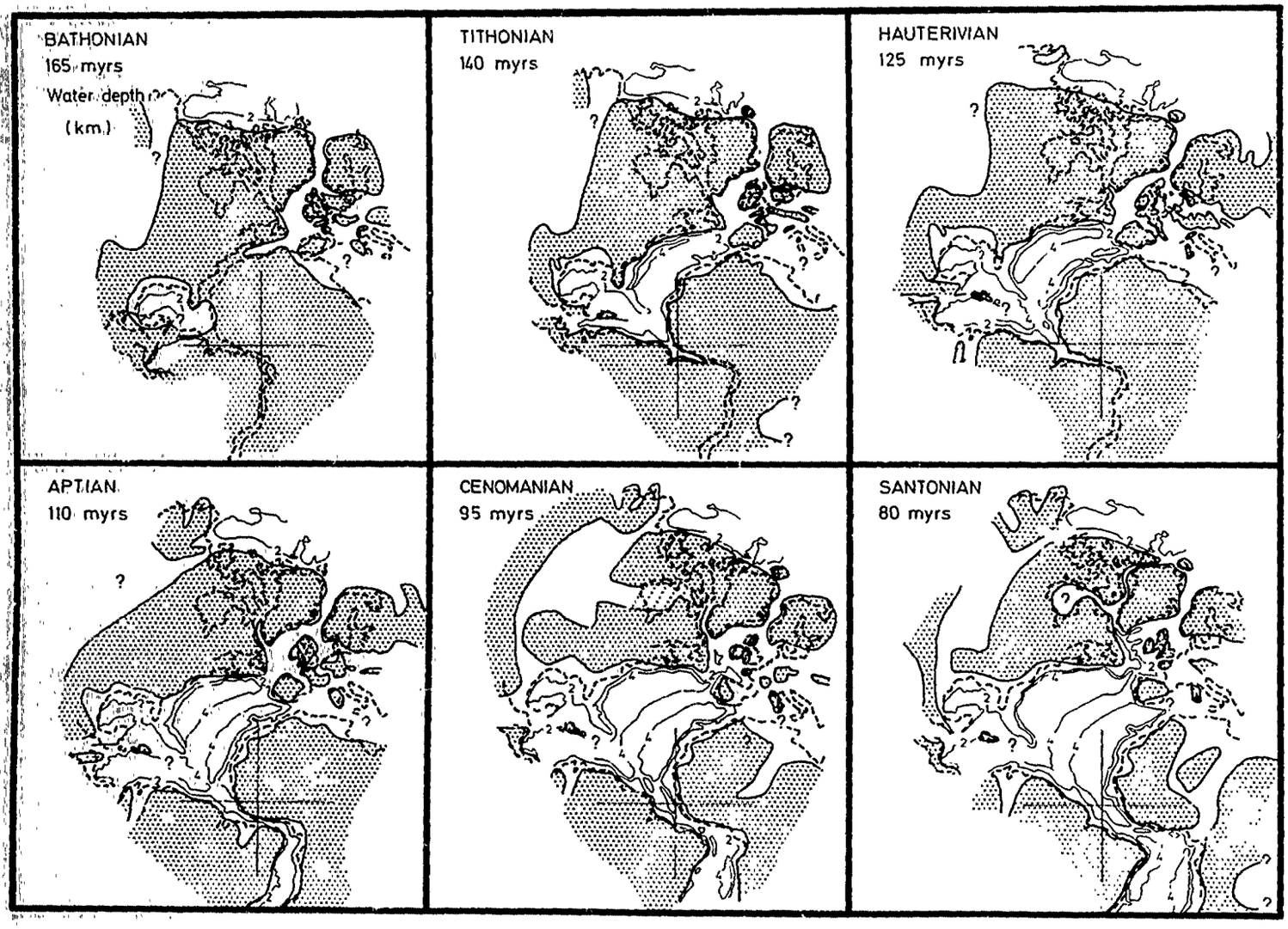


Figure 4 a. Figure 4 a and b. Paleogeography and paleobathymetry of the Mesozoic (a) and Cenozoic (b) North Atlantic. Depth contours are given for the 2, 4 and 6 km isobaths. The paleogeography of the epicontinental seas along the adjacent continents is overlain on the outline of the present land areas whose modern coasts are marked for reference by a stippled line.

depth contours are given for the 2, 4 and 6 km isobaths. The paleogeography of the epicontinental seas along the adjacent continents is overlain on the outline of the present land areas whose modern coasts are marked for reference by a stippled line.

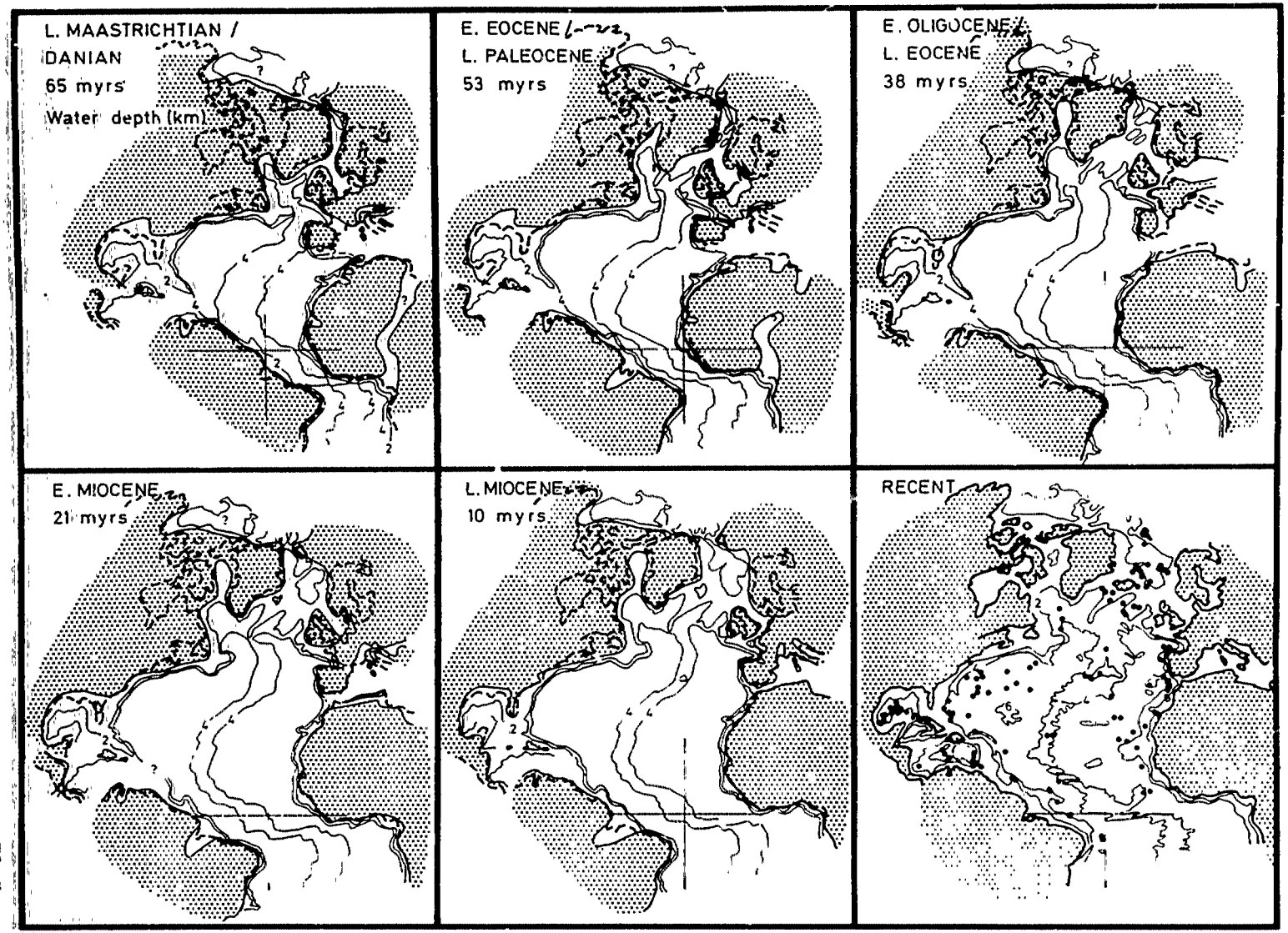


Figure 4 b.

events which control the hydrographic regime of the ancient North Atlantic Ocean (Table 1). The earliest steps of this development are still hidden deeply beneath the continental margins because it is not clear precisely where the boundary between oceanic and continental basement is situated, nor when the oldest oceanic crust was formed (Hayes and Rabinowitz, 1975).

## Physiography of the Mesozoic North Atlantic

The oldest part of the main North Atlantic basin opened during the middle and late Jurassic. The earliest stages of the North Atlantic during the mid-Jurassic are not well understood (Manspeizer et al., 1978), and the age and nature of basement under the Gulf of Mexico are unknown (Martin and Case, 1975). Evaporitic lithofacies in central America, and along the western African and northwestern American continental margins, point to the existence of troughs that were isolated from the world ocean by important sills, and that were probably fed with salt water from the Pacific and Tethys (Burke, 1975). The timing of salt deposition off western Africa and North America is particularly difficult to determine, but it seems to be of early, or possibly middle Jurassic age (Lehner and de Ruiter, 1977, Keen, 1974). Western Europe was covered during that time by a complicated network of land areas and epicontinental seas (Hallam, 1971, Ziegler, 1975 and 1977). Our knowledge of seaways between Scandinavia and Greenland and the British Isles-western Europe and southwestern Greenland-northwestern North America is patchy at best (Hallam, 1971). Sublittoral sediments of Jurassic age in eastern Greenland suggest a transgression from the south (Birkelund et al., 1974).

During the Tithonian (approximately 140 myrs ago) a small deep basin had developed in the North Atlantic. It was not part of a latitudinal ocean basin but rather part of a circumequatorial seaway which consisted of the Pacific, Caribbean, the North Atlantic/the Tethys (Biju-Duval et al., 1977). To the north this ocean was attached to the epicontinental seas which extended across central and eastern Europe. This configuration existed essentially throughout the following 30 myrs. The sediments which were deposited during this early stage of the North Atlantic resemble Mediterranean (=Tethyan) Mesozoic lithofacies (Bernoulli, 1972).

Throughout the early Cretaceous the North Atlantic basin was continuously widening and deepening, and a clearly defined mid-ocean ridge is believed to have separated a northwestern and southeastern deep basin. A narrow gulf apparently existed between the continental margins of northwestern South America and western Africa. After the connection to the southern South Atlantic had broken through during the mid-Cretaceous (van Andel et al., 1977, Ponte and Asmus, 1978) the North Atlantic became part of a north-south trending ocean basin which was connected to the Pacific and Tethys realms, but which was virtually closed on the north because the Norwegian-Greenland Sea had yet to open, with the possible exception of a narrow and shallow epicontinental seaway (Dalland, 1975, Harland, 1969, Frebold, 1930). Oceanographically the mid- to late Cretaceous North Atlantic might have resembled today's northern Indian Ocean with its characteristic mid-water oxygen minimum.

A shallow and narrow seaway connected the North and South Atlantic oceans during Aptian (110 myrs ago) times (Ponte and Asmus, 1978). Restricted depositional environments in the Atlantic during this interval suggest the presence of important obstacles for the free bottom water exchange between the Southern Ocean and the South Atlantic as well as between the North and South Atlantic oceans. However, the restricted depositional environments during this part of the Cretaceous are not just an Atlantic phenomenon, but appear to be global (Schlanger and Jenkyns, 1976), and they seem to be due to large scale climate fluctuations on our globe (Fischer and Arthur, 1977) rather than to a specific physiographic tectonic setting. Albian ammonite faunas on Svalbard (Nagy,1970) suggest close affinities with those of western Europe, northern North America and eastern Greenland which were probably connected by shallow epicontinental seas.

During the time span from Aptian to Cenomanian (approximately 95 myrs ago) the paleogeography of the North Atlantic underwent major changes when transgressions flooded large parts of the adjacent continents, and when new seaways across continental regions created pathways for faunal migrations (Schott, 1967). By this time the wide and deep North Atlantic basin was slowly extending further to the north, the South Atlantic was widening, and deep troughs appeared between western Africa and South America. During Santonian (approximately 80 myrs ago) a deep water connection between the South and North Atlantic had been firmly established (van Andel et al.,1977). Despite this deep water connection sediments indicative of restricted depositional environments during this time span have been found along South Atlantic continental margins and flanks of aseismic ridges (Thiede and van Andel, 1977). A trans-Saharan sea connected the northern South Atlantic to the Tethys realm (Machens, 1973). Wide areas of Europe and North America were flooded by shallow seas, and marine sediments in western Greenland (Birkelund, 1965. Rosenkrantz and Pulvertaft, 1969, Noe-Nygaard, 1974) suggest the existence of a narrow seaway bypassing Greenland. However, it remains to be seen how and where this seaway connected to the North Atlantic and to the ancient Arctic basin

Table 1

PHYSIOGRAPHIC-TECTONIC EVENTS CONTROLLING THE MESOZOIC AND CENOZOIC PALEO-OCEANOGRAPHY OF THE NORTH ATLANTIC OCEAN

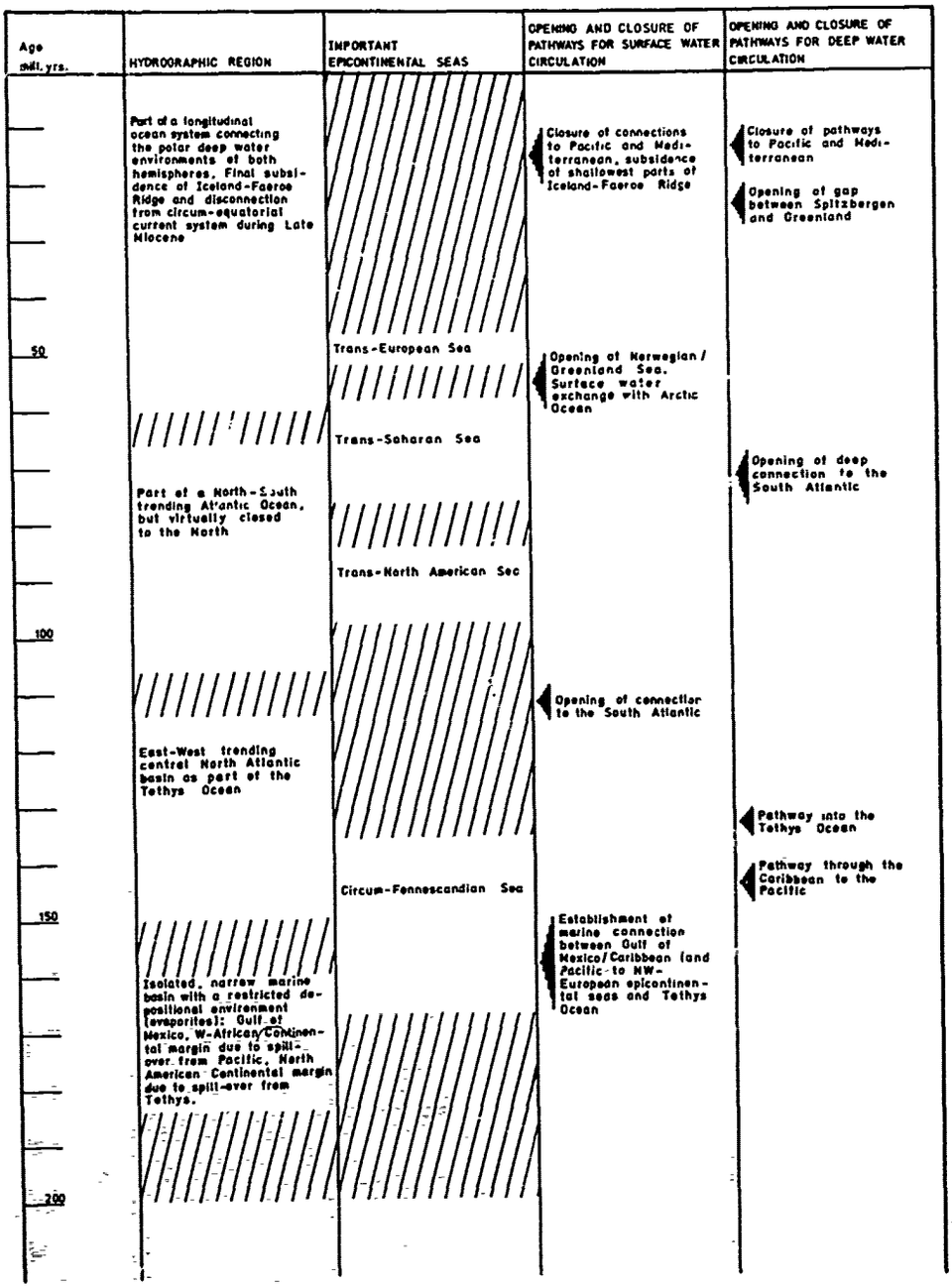

across the North American continent (Williams and Stelck, 1975). One possible connection existed through the Labrador Sea and Baffin Bay which had begun to open (Keen et al., 1972).

## Physiography of the Cenozoic North Atlantic

At the end of the Mesozoic Era the North Atlantic comprised an ocean basin which was several thousand kilometers wide. The floor of the eastern and western basins had subsided to more than 5 km water depth (Sclater et al., 1977). A deep water connection to the South Atlantic had probably been established during late Cretaceous times, 70-80 myrs ago (van Andel et al., 1977). During that time an opening in the east and west to a circum-equatorial seaway also existed (Laubscher and Bernoulli, 1977, Donelly, 1975). However, the temporal and spatial history of these openings, especially their width and water depth, and the impact of the addition of the circumglobal equatorial surface current system to the paleo-oceanography of the Cenozoic North Atlantic, are not understood at present (Berggren and Hollister, 1974 and 1977). The main developments of the Cenozoic North Atlantic consist of the breakup and widening of the Norwegian Greenland Sea during the Paleocene to Eocene, the establishment of a deep water connection to the Arctic Ocean during the Oligocene to Miocene, the closure of the circum-equatorial Tethys seaway between Europe and Africa and between both Americas, and major changes of the paleo-geography of the epicontinental seas in western Europe, western Africa and in the southern part of North America.

The early Paleocene deep North Atlantic consisted of eastern and western basins divided by the mid-ocean ridge (Figure 4 b). The deep water environment continued as a relatively narrow appendage to the north branching into the late Cretaceous Labrador Basin (Laughton, 1975, Vogt and Avery, 1974 b) and into the late Jurassic-early Cretaceous Rockall Trough (Roberts, 1975). A shallow shelf sea probably covered a relatively narrow corridor between Europe and Greenland, and the North Sea was attached to this seaway (Pegrum et al., 1975). The Mediterranean exchanged its water masses with the North Atlantic via the Aquitanian Basin, through a gap between Africa and Europe and by way of a much disputed shelf sea across the central Sahara (Machens, 1973, Reyment et al., 1976, Kogbe, 1972, Murat, 1972). The Caribbean and the Gulf of Mexico were open to the southwestern North Atlantic (Cook and Bally, 1975). The extent of the early Paleocene deposits along the Brazilian continental margin is not known in great detail, but the major sedimentary basins contain early Tertiary sediments that were deposited in an open marine environment (Asmus and Ponte, 1973, Ponte and Asmus, 1976). The Amazon Basin was a limnic-continental paleo-environment during that time (Bigarella, 1973).

During late Paleocene and early Eocene (approximately 53 myrs ago) the Labrador Sea was widening as spreading continued. The Rockall Trough had attained roughly its present shape and size after the spreading axis had shifted to the northwest of the Rockall Plateau during Paleocene times, separating Greenland and Rockall (Laughton,1975). Talwani and Eldholm, 1977, suspected that spreading started briefly prior to that time in the Norwegian-Greenland Sea generating the first deep marine troughs between Scandinavia and Greenland. Late Paleocene-early Eocene faunas on Svalbard (Livsič, 1974) prove the existence of a seaway connecting the Arctic Ocean with the growing Norwegian-Greenland Sea and through them with the North Atlantic Ocean. Although their semi-consolidated sediments have been reported from the Barents Sea (Sundvor, 1975), their exact age is not known. The North Sea was invading the central part of northwestern Europe and it was probably connected to the Bay of Biscay while the pathways between the North Atlantic and the Mediterranean narrowed. The trans-Saharan seaway had ceased to exist shortly after the early Palocene (Reyment et al., 1976). Following its widest extension over the continental shelf in the Gulf of Mexico during early Paleocene, the sea started to withdraw, first from the shallow carbonate platforms in Yucatan and later in Florida.

The Labrador Basin attained its present size during the late Eocene to early Oligocene. The youngest magnetic anomalies found in this area suggest that its active spreading ridge ceased about 47 myrs (Le Pichon et al., 1971) or 38 myrs ago (Kristoffersen and Talwani, 1977). The widening of the Norwegian-Greenland Sea continued and provided growing space to an oceanic paleo-environment which has been documented through the presence of pelagic microfossils in Eocene sediments from the Vøring Plateau (Bjørklund and Kellogg, 1972) and from the Lofoten Basin (Talwani et al., 1976 b). A predecessor of the Iceland-Faeroe Ridge existed during that time. The coastline around the Norwegian-Greenland Sea probably followed the modern continental margin, possibly with the exception of the Barents Sea. In western and central Europe an extension of the North Sea transgressed over wide regions establishing a seaway to the eastern European epicontinental seas. A narrow channel which connected northwestern Europe with the Alpine-Mediterranean realm, however, existed only for a short time during mid-Oligocene (Papp, 1959). The pathways from the Mediterranean to the eastern North Atlantic continued to narrow, and the Bay of Biscay was finally separated from the Tethys. Marine sediments of late Eocene (?) and Oligocene age mark the beginning of a transgression over parts of the Amazon Basin where the sea remained until the end of the Tertiary (Bigarella, 1973).

The style of spreading in the North Atlantic varied between the late Eocene to early Oligocene and Recent times because the spreading axis shifted and the direction of spreading changed pronouncedly in the region adjacent to Iceland (Laughton, 1975). How these changes influenced the morphologic evolution of the growing ocean basin is not quite clear because of the exceptionally shallow depth of the oceanic basement in this region.

The early Miocene (approximately 21 myrs ago) coastline seems to have followed rather closely the continental margin along the eastern North Atlantic, with exception of the shrinking North Sea (Spjeldnaes, 1975) and relatively small epicontinental seas in western France. Both the outlet from the Mediterranean (Dewey et al., 1973) and the pathway to the tropical Pacific (Malfait and Dinkelman, 1972, Weyl, 1973) had become relatively narrow by that time, although the ostracodes observed in the western Mediterranean Oligocene strata indicate that the passage was over 2 km deep (Benson, 1976). The marine transgression in the Amazon Basin continued and the appearance of planktonic foraminifers in the sediments suggests an open connection to the southwestern North Atlantic (Bigarella, 1973).

During the late Miocene (approximately 10 myrs ago) the North Atlantic and the Norwegian-Greenland Sea had attained roughly their present size, shape and depth. The pathways of the circum-equatorial seaway were virtually closed, although foraminiferal data (Keigwin, 1978) suggest that the Isthmus of Panama has not been closed completely before the Pliocene. The Mediterranean experienced partial desiccation with evaporite deposition for a brief period during late Miocene (Hsü et al., 1973). A deep water connection between the Arctic Ocean and the Norwegian-Greenland Sea had finally been established and it continued to widen until Recent times (Talwani and Eldholm, 1977). The Iceland-Faeroe Ridge, as a major barrier, inhibited the deep water exchange between the Norwegian-Greenland Sea and the main North Atlantic basin, and Iceland is believed to have existed at least for the last 16 myrs years (Laughton, 1975, Piper, 1973). The epicontinental seas in western Europe had approximately the same size as during early Miocene; the North Sea had attained roughly its present shape and continued its regression by withdrawing from the present northwestern European coastlines during Pliocene times. Minor epicontinental basins still existed in southwestern Europe and along the African continental margin. A shallow sea covered the outer part of the Amazon Basin, which has been filled by fluvial Quaternary deposits.

After opening of the Norwegian-Greenland Sea in the late Paleocene (Talwani and Eldholm, 1977), after the final subsidence of the Iceland-Faeroe Ridge and after the disconnection from the circum-equatorial current system during Miocene, the North Atlantic is today part of a latitudinal ocean basin which connects the cold polar water masses of both the northern and southern hemispheres. The hydrography of the dominant portion of the water masses in the entire Atlantic Ocean is therefore controlled to a high degree by the climatic conditions in the polar realms, although the outflow from the Mediterranean, which had been refilled from the Atlantic after the late Miocene desiccation event, has an important impact on the hydrography of the intermediate water masses in the North Atlantic.

## Important remaining problems of the physiographic evolution of the North Atlantic

The main physiographic-tectonic events during the evolution of the North Atlantic (Table 1) help to define a number of important remaining problems. The tectonic history of aseismic ridges has recently been studied (Detrick et al., 1977, Thiede, 1977), but major problems usually arise if the timing of the origin, the nature and morphology of the underlying volcanic edifice, and the destruction and subsidence histories of the ridge are not known. This problem is particularly pertinent to the Cenozoic North Atlantic because the dominant structural high comprising the aseismic Iceland-Faeroe Ridge has been inhibited the exchange of the surface and bottom water masses between the Norwegian-Greenland Sea and the main North Atlantic basin troughout the Cenozoic (Vogt, 1972 and 1974). The complex evolution of the Caribbean region and the paleogeography of the middle-American region (Weyl, 1973) pose a special problem to the reconstruction of the North Atlantic paleo-environments because only a very small portion of the geologic history of this region - temporally as well as spatially - has been preserved because of the nature of the plate tectonic processes in this mobile area (Malfait and Dinkelman, 1972). Similar difficulties are encountered when trying to understand the evolution of the ancient mobile Tethys belt in the Mediterranean area (Biju-Duval et al., 1977, Laubscher and Bernoulli, 1977).

During the late Mesozoic the North Atlantic was virutally closed to the north because the Norwegian-Greenland Sea did not exist as a deep ocean basin during that time. Althoug marine Mesozoic rocks deposited close to the former coastlines have been found along the continental margins of Norway (Dalland, 1975), eastern Greenland (Birkelund et al., 1974) and western Greenland (Birkelund, 1965), neither the width nor the extent of these shallow shelf seas, nor their connection to the late Mesozoic North Atlantic or Arctic oceans are known (Hallam, 1971 and 1975).

The growth of the Arctic Ocean during the Cenozoic a long Gakkel Ridge (Vogt and Avery, 1974 a) has been documented through the presence of linear magnetic anomalies; however, the age of the Amerasia Basin of the Arctic Ocean (Sweeney et al.,

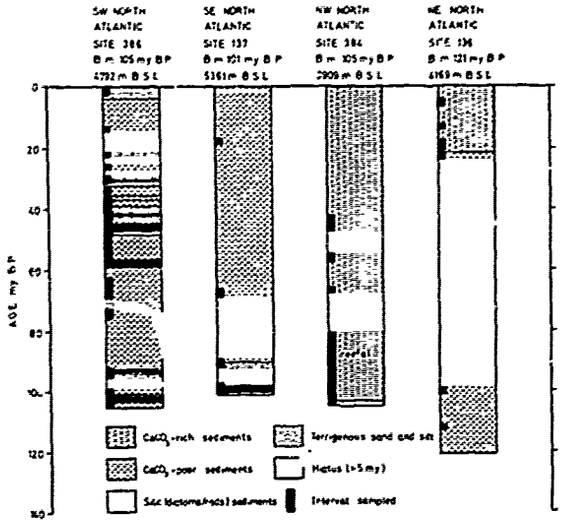


Figure 5. Simplified lithology of drill sites in the SW, SE, NW and NE North Atlantic (after Hayes, Pimm et al., 1972, Tucholke, Vogt et al., 1975). B.S.L. = below sea level, B.m. = basement age.

1978) as well as the nature and origin of the Alpha Mendeleev and Lomonossov Ridges has not been resolved (Pitman and Herron, 1974). The extent of the primordial Mesozoic predecessor of the modern Arctic Ocean can therefore only be a matter for speculation. Although marginal marine basins are of minor importance around the South Atlantic, epicontinental seas have at times covered wide regions of the land masses around the North Atlantic. The most important events of flooding of continental areas around the North Atlantic (Table 1) are the evolution of a circum-Fennoscandian sea during late Jurassic, the development of a trans-North American sea during mid-Cretaceous , of a trans-Saharan sea during late Cretaceous and very early Tertiary, and of a trans-European sea during mid-Tertiary. It is important to note that these trans-continental seas did not occur simultaneously, at least in terms of the time slices shown in Figure 4. It is therefore difficult to explain these transgressions and regressions entirely with eustatic sea level fluctuations as Vail et al. (1978) have suggested, but they might rather be used to infer major time-transgressive changes of the continental hypsometries (Bond, 1978) caused by isostatic movements of the continental crust (Reyment and Mörner, 1977).

## Aspects of the Mesozoic and Cenozic North Atlantic paleo-environment

The physiographic evolution of the North Atlantic and the establishment of the drainage basins on the surrounding continents since middle to late Jurassic must have had an important impact on the deep-sea deposits of this ocean basin. This study will concentrate on drill sites from three areas: Norwegian-Greenland Sea, the northern part of the main North Atlantic basin and the basins of the central Atlantic. The sites selected have been drilled during Deep Sea Drilling Project Legs 1, 2, 11, 12, 13, 14, 37, 38, 41, 43, 44, 44A, 46, 47A, 49, 50, and 51-53. Only a few selected aspects of the sediment cover found in these three regions will be used in this discussion of latitudinal as well as longitudinal distribution patterns of various deep-sea sediment facies. The sediment data used for this discussion can be found either in the Initial Reports of the Deep Sea Drilling Project or in the respective "Geotimes" articles about the above listed cruises.

The sediments preserved in the North Atlantic reveal that almost every individual basin has its own depositional history, probably because the controlling boundary conditions are different from basin to basin. This is most easily observed if comparing sediment sections from some of the basins in the main North Atlantic (Figure 5). In these sections as well as in those used in Figures 6 and 7, sediment data have been plotted against a time scale. The detailed lithologies of these sites have also been simplified considerably to show only $CaCO_3$-rich, $CaCO_3$-poor, silica-rich, and terrigenous sediments, volcanic

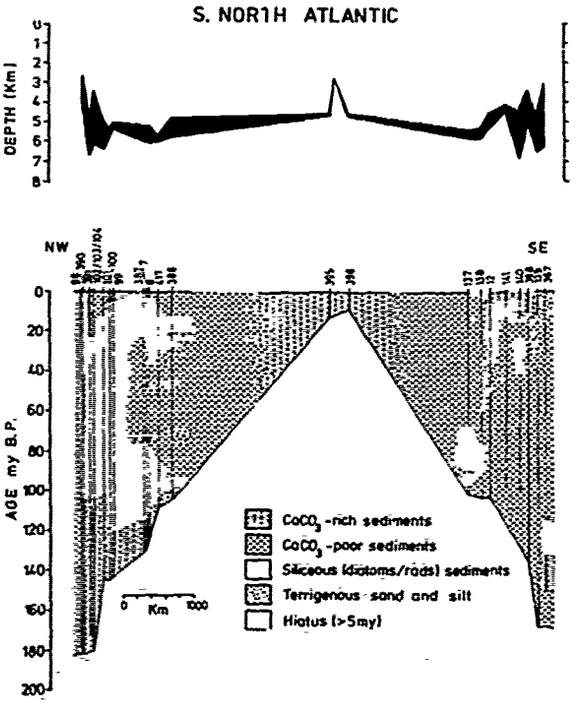


Figure 6. Distribution of sediments across the S part of the main North Atlantic basin.

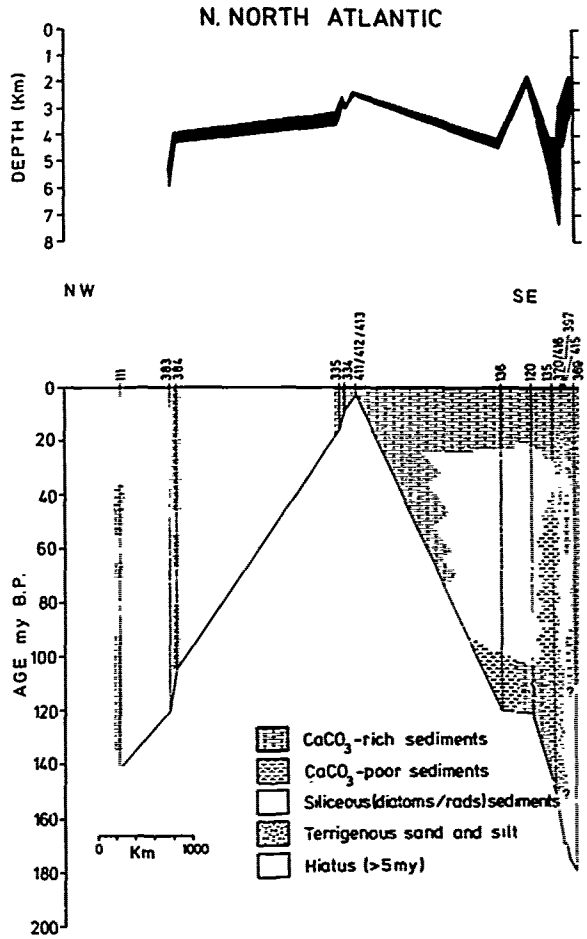


Figure 7. Distribution of sediments across the N part of the main North Atlantic basin.

rocks and hiatuses which cover more than 5 myrs. It is difficult to find sites which come from physiographically comparable depositional environments. The four sites shown in Figure 5 are strikingly dissimilar although they have penetrated sediment sections which reach 100-120 myrs back in time. Other pairs of drill sites from either side of the mid-ocean ridge in the North Atlantic showed characteristic dissimilarities too, and it was soon obvious that a symmetrical evolution of the depositional environment as conceived by Jansa et al., 1977 does not explain the actually observed sediment data satisfactorily.

## Major asymmetries between eastern and western basins of the North Atlantic

Important differences of the sediment volume between the eastern and western basins which have been mapped by means of geophysical methods (Ewing et al., 1973) disappear if the lithologies of the drill sites are plotted against a time scale However, the thick sediment cover up to 10 k- .Emery et al., 1970) which has deeply bur' . the crustal rocks of the western North Atlantic continental margin, opposes a starved passive continental margin along the eastern North Atlantic seaboard (Montadert et al., 1977, Curray, 1978) where sialic continental basement rocks have been dredged from several kilometers of water depth. These asymmetries are also enhanced by the abyssal plains, which are much larger in the western North Atlantic than in its eastern basins (Davies and Laughton, 1972).

The previously mentioned differences can be better understood when projecting a number of sites into two profiles across the southern and northern parts of the main North Atlantic basin. The data have been plotted into age versus distance from mid-ocean ridge crest diagrams (Figures 6 and 7); water depth and actual sediment thickness have been sketched in the upper part of these two figures. The northwestern North Atlantic is not well presented because too few sites were situated close to the chosen profile. The Norwegian-Greenland Sea sites drilled during Leg 38 encountered largely terrigenous deposits. Uneven site distribution does not allow an evaluation of comparable asymmetries north of the Iceland-Faeroe-Ridge although the hydrographic gradients and the asymmetric ice cover on the adjacent continents suggest large differences in the depositional environment on the east and west side of this subpolar ocean basin. The differences between the depositional environment in the northeastern, southeastern and southwestern North Atlantic are particularly evident in the proportions of calcareous material deposited and in the spatial as well as temporal extent of hiatuses in these basins. The oldest crust in the southwestern North Atlantic is largely covered by calcareous deposits which resemble isochron lithofacies of the Tethyan paleo-environment (Bernoulli, 1972) supporting the idea of a circum-equatorial ocean which incorporated the Mesozoic North Atlantic. However, the deposition of calcareous material apparently decreased drastically (except in the immediate vicinity of the carbonate platforms along the adjacent continental margins (Stehli, 1974) with the development of a large and long lasting hiatus approximately 120 myrs ago. This hiatus (Figure 6) which is confined to the abyssal plain and the foot of the continental rise and slope, and which can be traced throughout the last 120 myrs, reveals two pulses of particularly wide regional extent; the older one approximately 100 myrs ago, the younger one 20 myrs ago. These events coincide with important hiatuses mapped in the entire Atlantic (Moore and Heath, 1978). The coherence of this long lasting hiatus also suggests that the hydrographic regime generating it was a spatially and tempo-

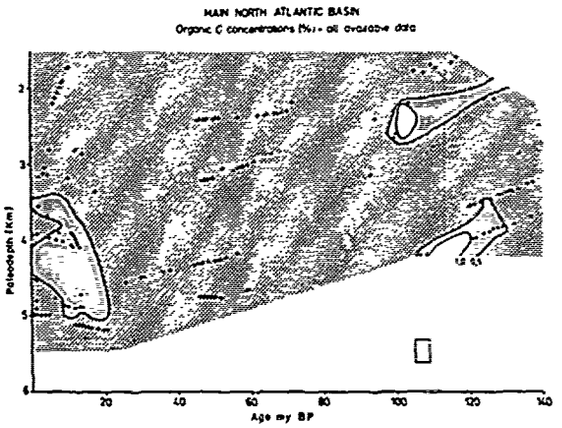


Figure 8. Organic carbon concentrations (in percent of bulk sediment) in the main North Atlantic basin (excluding the Norwegian-Greenland Sea). Data have been backtracked to their paleodepth of deposition following the method of Berger and von Rad, 1972. Data are available for each sample point, but they have been averaged over 300 m and 4 myrs intervals for contouring.

rally stable feature of the deep southwestern North Atlantic from late Cretaceous.

The southeastern North Atlantic basin received far less calcareous deposits than the southwestern North Atlantic during the Mesozoic, and the sedimentation of calcareous components increased only during the last 20 myrs (cf. Berger and von Rad, 1972, Lancelot and Seibold, 1977). Except for relatively short and regionally not very extensive hiatuses, sedimentation appears to have been continuous from late Mesozoic times in the southeastern North Atlantic. This basin has been protected against vigorous bottom water currents because of the presences of the structural high west of Gibraltar, of Walvis Ridge in the South Atlantic, and of the mid-Atlantic Ridge to the west.

The northeastern North Atlantic apparently received relatively little terrigenous input throughout the last 130-140 myrs because wide epicontinental seas in Europe acted as depocenters for the terrigenous components before they were able to reach the ocean. The sediments in the northeastern North Atlantic are therefore largely calcareous (Figure 7). The hiatus off Gibraltar is difficult to explain, but is seems to be an important coincidence that sedimentation in this region resumed in the early Miocene when the deep water passage into the Mediterranen (Benson 1976) became shallower. Important hiatuses have also been observed along the northern continental margin of the Bay of Biscay where they have been explained by vigorous bottom currents associated with the "Cenomanian" transgression (Montadert et al., 1977). After mapping the spatial and temporal extent of hiatuses regionally in the South Atlantic (van Andel et al., 1977), it is now clear that the processes generating gaps in the lithologic succession of deep-sea sediments can selectively affect certain depth intervals. Some hiatuses extend over almost the entire ocean basin, some are restricted to the deep basins and others are confined to relatively shallow water depths. None has yet been explained satisfactorily.

## Distribution patterns of characteristic sediment components in the North Atlantic

The distributions of calcareous sediments and of organic carbon in the North Atlantic are illustrated in Figures 9 and 10. The available data have been backtracked to their paleodepth of deposition following the method described by Berger and von Rad, 1972. Since both data sets revealed a wide scatter I have averaged the data from the main North Atlantic basin (Figures 8 and 9) over 300 m depth and 4 myrs time intervals for contouring. These data reveal a clear zonation of the North Atlantic Cenozoic paleo-environment because virtually no calcareous components have been deposited in the Norwegian-Greenland Sea (Figure 10) behind the Iceland-Faeroe- Ridge whose function as a barrier is also expressed in the strong Paleogene faunal and floral gradients between the Norwegian-Greenland Sea and the main North Atlantic basin (Talwani et al., 1976

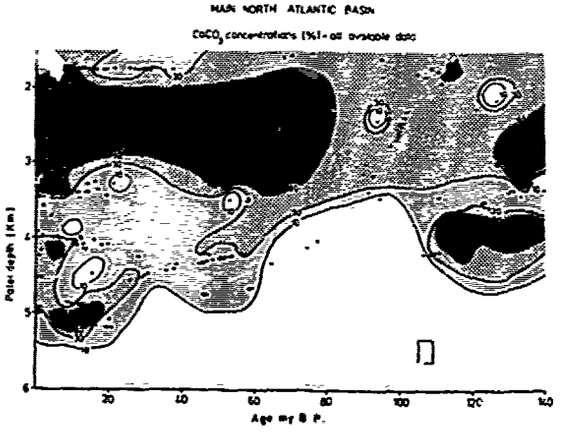


Figure 9. Distribution of calcium carbonate concentrations (in percent of bulk sediment) in the main North Atlantic basin (excluding the Norwegian-Greenland Sea). Data have been backtracked to their paleodepth of deposition following the method of Berger and von Rad, 1972. Data are available for each sample point, but they have been averaged over 300 m and 4 myrs intervals for contouring.

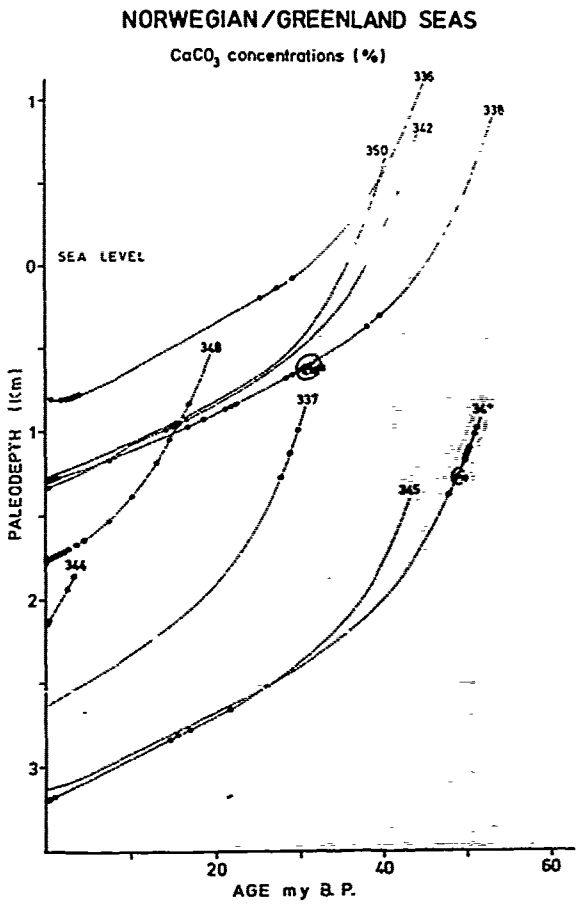


Figure 10. Calcium carbonate concentrations (in percent of bulk sediment) in Norwegian-Greenland Sea sediments. Data have been backtracked to their paleodepth of deposition following the method of Berger and von Rad, 1972.

Organic carbon. The average organic carbon concentrations in the bulk sediment have been contoured at the 0.5 and 1.0 % isopleths. Three areas of high concentrations appear on the diagram. An early Cretaceous maximum close to the former bottom of the basin supports the suggestions of an anoxic depositional environment (cf. Lancelot and Seibold, 1977). In other sites it has been observed that anaerobic sediments immediately overlie the oceanic basement (McCave, 1978). A mid- to late Cretaceous maximum just below the 2 km paleo-water depth, however, migh indicate a radical change of the oxygen deficient depositional environment because this maximum is over- and underlain by oxygenated sediments. This situation might more easily be explained by an oceanic mid-water oxygen minimum (Schlanger and Jenkyns, 1976, Thiede and van Andel, 1977). Higher values than normal have also been observed in samples from 3.5 - 5 km paleo-water depth which have been deposited during the last 20 myrs. They seem to correlate to carbonate-poor fine-grained terrigenous muds (cf. figures 8 and 9) deposited in the deep basin at the foot of the continental margins. Favourable conditions for the preservation of organic carbon are a prerequisite for the accumulation of high organic carbon concentrations. But it seems disputable if the modern analogs such as the northern Indian Ocean with its well developed mid-water oxygen minimum or the Black Sea with its euxinic conditions are suitable models for the late Mesozoic oxygen-poor depositional environments.

Calcium carbonate. The calcium carbonate concentrations (Figure 9) from the North Atlantic have been treated the same way as the organic carbon data (figure 8), but they have been contoured at 10, 30 and 60% isopleths. It is important to note that the Norwegian-Greenland Sea (Figure 10) is almost entirely void of calcareous material. Well preserved calcareous fossils, however, have been observed in the Norwegian-Greenland Sea and in Arctic Ocean deep-sea sediments (Herman, 1974 b) although they were deposited in water depths similar to those of the North Atlantic main basin. The concept of a calcite compensation depth (=CCD) shoaling towards the polar regions as invoked by Ramsay, 1978 and others is not supported by the North Atlantic data.

The samples from the main North Atlantic basin provide us with a variety of scenarios revealing that the definition of the CCD, which is usually done by plotting $CaCO_3$-concentrations against water depth, is disputable at best, and that accumulation rates should be used (van Andel et al., 1975). However, even though the original data were averaged considerably, the values above the 10% isopleths are scattered over a wide range (Figure 9). One can discern Jurassic through early Cretaceous, and late Cretaceous through Cenozoic phases of carbonate sedimentation in the North Atlantic which are interrupted by a mid- to late Cretaceous event of low carbonate concentrations and probably considerable shoaling of the CCD. This event coincided with epicontinental seas flooding wide areas of the adjacent continents. While the early Tertiary shoaling of the CCD has been observed by previous authors (e.g. Berger and von Rad, 1972) the data reported here do not support a comparably shallow CCD 10-20 myrs ago.

Two levels of high carbonate concentrations occur during both phases of carbonate deposition, but are particularly well developed during the late Cenozoic. An upper an very dominant level is observed at 2-3 km water depth (Figure 9), which probably represents the sedimentation of normal pelagic calcareous oozes. The deep level at 4-4.5 km is suggestive of

calcareous material displaced into the deep basins, as has been observed in the South Atlantic (van Andel et al., 1977). Obviously, such patterns can also be due to the injection of large amounts of non-calcareous terrigenous components into the main North Atlantic, but the evaluation of this problem will have to wait until further data from this basin are available.

## Conclusion

The evolution of the North Atlantic (Sclater et al., 1977) and its surrounding epicontinental seas through time can now be translated into a list of important events (Table 1) controlling the hydrography of the North Atlantic water masses (Berggren and Hollister, 1974 and 1977). These physiographic-tectonic events illustrate the development of the ancient North Atlantic Ocean from a narrow latitudinal tropical sea as part of the Tethys Ocean during the Mesozoic, to a wide latitudinal basin which, as part of the Atlantic Ocean, connects both polar oceans and whose water masses thereby carry important hydrographic characteristics from the Arctic and Antarctic realms (Wüst, 1935). However, it has to be remembered that these events provide us with only one set of physical boundary conditions which constrain the surface and deep water circulations of this ocean basin.

With respect to the surface water circulation these events are: 1) The establishment of a marine connection from the northwestern European epicontinental seas-Tethys realm to Gulf of Mexico-Caribbean area and through that to the Pacific during early Late Jurassic; 2) A surface water pathway to the South Atlantic opened during mid- to late Cretaceous (van Andel et al., 1977); 3) A seaway through the Norwegian-Greenland Sea to the Arctic Ocean was established during early Tertiary (Talwani and Eldholm, 1977) although it may have been in existence during the Mesozoic as part of a narrow epicontinental basin; 4) The passage through the Caribbean realm to the Pacific and the gap between the Iberian Peninsula and northern Africa was closed during late Tertiary; and 5) The Iceland-Faeroe Ridge did not entirely subside before late Miocene.

To understand the sediment distribution in this growing ocean basin, it is probably even more important to consider the passages for the deep-water circulation. Deep-water connections to the Pacific and Tethys oceans probably existed from the late Jurassic and early Cretaceous to late Tertiary time. A deep basin connected the North and South Atlantic Oceans since late Cretaceous, while a deep Norwegian-Greenland Sea passage to the Arctic Ocean broke through only during Miocene. It is unclear, and probably not resolvable by means of methods used in this paper, when deep and narrow channels through fracture zones allowed an exchange of bottom water masses between the eastern and western basins of the North Atlantic.

Distribution of deep-sea sediments have been used to evaluate the impact of the changing physiography of the North Atlantic on the late Mesozoic and Cenozoic paleo-environment. The dominant components of these deposits are terrigenous non-calcareous and calcareous material whose concentrations reflect a wide range of temporal and spatial fluctuations of the CCD (Figure 9). Although the North Atlantic is fairly well documented by now, it is difficult to depict well defined variations in CCD with time. Particularly high contributions of displaced calcareous components seem to depress the lower limit of the CCD to considerably deeper water depths than previously suspected (Berger and von Rad, 1972). A period of deep-sea sedimentation with relatively low carbonate concentrations during mid-Cretaceous (approximately 80 to 110 myrs ago) throughout the entire North Atlantic is indicative of the contribution of large volumes of fine-grained terrigenous sediments. It is interesting to note that this interval coincides with the mid-Cretaceous anaerobic depositional environments in both the South and North Atlantic oceans as well as in the Indian and Pacific oceans (Fischer and Arthur, 1977). The concentrations of calcareous particles and organic carbon in North Atlantic deep-sea sediments also reveal an important zonation because both are virtually missing from the Norwegian-Greenland Sea, whose deposits have been dominated by the high terrigenous influx into the basin throughout the 50-60 myrs.

Profiles across the northern and southern main North Atlantic basin reveal major asymmetries in the depositional environments between the eastern and western basins which seem closely related to the hydrographic regime of the evolving ocean basin (Berggren and Hollister, 1974). The asymmetries involve the sedimentation pattern or major sediment components along the continental margins and in the deep-sea basins, as well as the distribution and extent of hiatuses. These data allow us to show how the temporal and spatial evolution of the North Atlantic physiography (Sclater et al., 1977) and of the epicontinental seas on the adjacent continents has interacted with the paleo-oceanography of the pelagic water masses and with the paleoclimate over this part of the northern hemisphere in generating depositional environments which are different from basin to basin. The ever increasing volume of sedimentary data available from Deep Sea Drilling Project sites in the North Atlantic will soon help us refine the recognition of these depositional environments and to quantify the interaction of the plate tectonic processes with the motion of the ocean and of the atmosphere over the North Atlantic.

Acknowledgments. This work has been supported by a grant from the Norwegian Petroleum Directorate (Stavanger). I have been assisted in this study by J.E. Strand and T. Agdestein. The main data base for this study has been assembled by the shipboard scientific parties of D/V GLOMAR CHALLENGER under the auspices of the Deep Sea Drilling Project and of the International Program of Ocean Drilling (IPOD). I have benefited from the comments of T. Vallier (USGS, Menlo Park), N. Dean (USGS, Denver), O. Eldholm (Univ. Oslo) and two anonymous reviewers whose help was very much appreciated.

## References

Asmus, H.E., and F.C. Ponte, The Brazilian marginal basins, in The ocean basins and margins. Vol. 1. The South Atlantic, ed. by A.E.M. Nairn and F.G. Stehli, (Plenum) New York, pp. 87-133, 1973.

Benson, R.H., Miocene deep-sea ostracodes of the Iberian portal and the Balearic basin, Marine Micropal., 1, 249-262, 1976.

Berger, W.H., and U. von Rad, Cretaceous and Cenozoic sediments from the Atlantic Ocean, Init. Rep. Deep-Sea Drill. Proj., 14, 787-954, 1972.

Berggren, W.A., A Cenozoic time scale, Some implications for regional geology and paleobiogeography, Lethaia, 5, 195-215, 1972.

Berggren, W.A., Late Paleocene, Early Eocene benthonic foraminiferal biostratigraphy and paleoecology of Rockall Bank, Micropaleontology, 20, 426-448, 1974.

Berggren, W.A., and C.D. Hollister, Paleogeography, paleobiogeography and the history of circulation in the Atlantic Ocean, Soc. Econ. Paleon. Miner. Spec. Publ., 20, 126-186, 1974.

Berggren, W.A., and C.D. Hollister, Plate tectonics and paleocirculation-commotion in the ocean, Tectonophysics, 38, 11-48, 1977.

Bernoulli, D., North Atlantic and Mediterranean Mesozoic facies: A comparison, Init. Rep. Deep-Sea Drill. Proj., 11, 801-871, 1972.

Beurlen, K., Die geologische Entwicklung des Atlantischen Ozeans. Geotekt. Forsch., 46, 1-69, 1974.

Bigarella, J.J., Geology of the Amazon and Parnaiba Basin, in The ocean basins and margins Vol. 1, The South Atlantic, ed. by A.E.M. Nairn and F.G. Stehli, (Plenum) New York, pp. 25-86, 1973.

Biju-Duval, B., J. Dercourt, and X. Le Pichon, From the Tethys Ocean to the Mediterranean Seas: A plate tectonic model of the evolution of the western Alpine system, in Structural history of the Mediterranean Basins, ed. by B. Biju-Duval, and L. Montadert, (Technip) Paris, pp. 143-164, 1977.

Birkelund, T, Ammonites from the upper Cretaceous of West Greenland, Medd. Grønland, 179, 192 pp., 1965.

Birkelund, T., K. Perch-Nielsen, D. Bridgewater, and A.K. Higgins, An outline of the geology of the Atlantic coast of Greenland, in The ocean basins and margins, Vol. 2, The North Atlantic, ed. by A.E.M. Nairn, and F.G. Stehli, (Plenum) New York, pp. 125-159, 1974.

Bjørklund, K.R., and D.E. Kellogg, Five new Eocene radiolarian species from the Norwegien Sea, Micropaleontology 18, 386-396, 1972.

Bonatti, E., Vertical tectonism in oceanic fracture zones, Earth Planet. Sci. Lett., 37, 369-379, 1978.

Bond, G., Speculations on real sea-level changes and vertical motions of continents at selected times in the Cretaceous and Tertiary periods, Geology, 6, 247-250, 1978.

Bott, M.H.P., Deep structure, evolution and origin of the Icelandic transverse ridge, in Geodynamics of Iceland and the North Atlantic area, ed. by L. Kristjansson, (Reidel) Dordrecht, pp. 33-47, 1974.

Burke, K., Atlantic evaporites formed by evaporation of water spilled from Pacific, Tethyan and Southern Oceans, Geology, 3, 613-616, 1975.

Cande, S.C., and Y. Kristoffersen, Late Cretaceous magnetic anomalies in the North Atlantic, Earth Planet. Sci. Lett. 35, 215-224, 1977.

Cook, T.D., and A.W. Bally, Stratigraphic atlas of North and Central America, (Princeton Univ. Press) Princeton, 272 pp., 1975.

Curray, J.R., The IPOD programme on passive continental margins, Phil. Trans. R. Soc. London, (in press), 1978.

Dalland, A., The Mesozoic rocks of Andøy, northern Norway, Norges geol. unders., 316, 271-287, 1975.

Davies, T.A., and A.S. Laughton, Sedimentary processes in the North Atlantic, Init. Rep. Deep-Sea Drill. Proj., 12, 905-934, 1972.

Detrick, R.S., J.G. Sclater, and J. Thiede, Subsidence of aseismic ridges, Earth Planet. Sci. Lett., 34, 185-196, 1977.

Dewey, J.F., The geology of the southern truncation of the Caledonides, in The ocean basins and margins, Vol. 2, The North Atlantic, ed. by A.E.M. Nairn, and F.G. Stehli, (Plenum) New York, pp. 205-231, 1974.

Dewey, J.F., W.C. Pitman, W.B.F. Ryan, and J. Bonnin, Plate tectonics and the evolution of the Alpine system, Geol. Soc. Amer. Bull., 84, 3137-3180, 1973.

Dietz, R.S., and J.C. Holden, Reconstruction of Pangaea: Breakup and dispersion of continents, Permian to Present, J. Geophys. Res., 75, 4939-4956, 1970.

Donelly, T.W., The geological evolution of the Caribbean and Gulf of Mexico -some critical problems and areas, in The ocean basins and margins, Vol. 3, The Gulf of Mexico and the Caribbean, ed. by A.E.M. Nairn, and F.G. Stehli, (Plenum), New York, pp. 663-689, 1975.

Eldholm, O., and J. Thiede, Cenozoic continental separation between Europe and Greenland, Geol. Soc. Amer. Abstr. Progr., 10 (7), 396, 1978.

Emery, K.O., E. Uchupi, J.D. Phillips, C.O. Bowin, E.T. Bunce, and S.T. Knott, Continental rise

of eastern North America, Amer. Assoc. Petrol. Geol. Bull., 54, 44-108, 1970.
Ewing, M., C. Carpenter, C. Windisch, and J.I. Ewing, Sediment distribution in the oceans: The Atlantic, Geol. Soc. Amer. Bull., 84, 71-88, 1973.
Fischer, A.G., and M.A. Arthur, Secular variations in the pelagic realm, Soc. Econ. Paleont. Miner. Spec. Publ., 25, 19-50, 1977.
Fitch, F.J., J.A. Miller, D.M. Warrel, and S.C. Williams, Tectonic and radiometric age determinations, in The ocean basins and margins, Vol. 2, The North Atlantic, ed. by A.E.M. Nairn, and F.G. Stehli, (Plenum), New York, pp. 485-538, 1974.
Frebold, H., Verbreitung und Ausbildung des Mesozoikums in Spitzbergen, Skr. Svalbard Ishavet, 31, 126 pp., 1930.
Hallam, A., Mesozoic geology and the opening of the North Atlantic, J. Geol., 79, 129-157, 1971.
Hallam, A., Jurassic environments, (Cambridge Univ. Press), 269 pp., 1975.
Harland, W.B., Contribution of Spitzbergen to understanding of tectoni evolution of North Atlantic region, Amer. Assoc. Petrol. Geol. Mem., 12, 817-851, 1969.
Hayes, D.E., A.C. Pimm et al., Initial Reports of the Deep Sea Drilling Project, Vol. 14, (U.S. Government Printing Office), Washington, D.C., 975 pp., 1972.
Hayes, D.E., and. P.D. Rabinowitz, Mesozoic magnetic lineations and the magnetic quiet zone off northwest Africa, Earch Planet. Sci. Lett., 28, 105-115, 1975.
Herman, Y., Topography of the Arctic Ocean, in Marine geology and oceanography of the Arctic Seas, ed. by Y. Herman, (Springer) New York, pp. 73-81, 1974 a.
Herman, Y., Arctic Ocean sediments, microfauna, and the climatic record in late Cenozoic time, in Marin geology and oceanography of the Arctic Seas, ed. by Y. Herman, (Springer), New York, pp. 283-348, 1974 b.
Hsü, K.J., W.B.F. Ryan, and M.B. Cita, Late Miocene desiccation of the Mediterranean, Nature, 242, 240-244, 1973.
Jansa, L., J.V. Gardner, and W.E. Dean, Mesozoic sequences of the central North Atlantic, Initial Rep. Deep Sea Drill. Proj., 41, 991-1031, 1977.
Keen, C.H., D.L. Barrett, K.S. Manchester, and D.I. Ross, Geophysical studies in Baffin Bay and some tectonic implications, Can. J. Earth Sci., 9, 239-256, 1972.
Keen, M.J., The continental margin of eastern North America, Florida to Newfoundland, in The Ocean Basins and Margins, Vol. 2, The North Atlantic, ed. by A.F.M. Nairn, and F.G. Stehli, (Plenum), New York, pp. 41-78, 1974.
Keigwin, L.D., Pliocene closing of the Isthmus of Panama, based on biostratigraphic evidence from nearby Pacific Ocean and Caribbean Sea cores, Geology, 6, 630-634, 1978.
Kogbe, C.A., Preliminary study of the geology of the Nigerian sector of the Iullemeden Basin, in African geology, ed. by T.F.J. Dessauvagie, and A.J. Whiteman, (Dept. Geol., Univ. Ibadan) Ibadan, pp. 219-227, 1972.
Kristoffersen, Y., Sea-floor spreading and the early opening of the North Atlantic, Earth Planet. Sci. Lett., 38, 273-290, 1978.
Kristoffersen, Y., and M. Talwani, Extinct triple junction south of Greenland and the Tertiary motion of Greenland relative to North America, Geol. Soc. Amer. Bull., 88, 1037-1049, 1977.
Lancelot, Y., and E. Seibold, The evolution of the central northeastern Atlantic - Summary of results of DSDP Leg 41, Init. Rep. Deep-Sea Drill. Proj., 41, 1215-1245, 1977.
Laubscher, H., and D. Bernoulli, Mediterranean and Tethys, in The ocean basins and margins, Vol. 4A, The eastern Mediterranean, ed. by A.E.M. Nairn, W.H. Kanes, and F.G. Stehli, (Plenum), New York, pp. 1-28, 1977.
Laughton, A.S., Tectonic evolution of the north-east Atlantic Ocean; a review, Norges geol. unders., 316, 169-193, 1975.
Laughton, A.S., and R.B. Whitmarsh, The Azores-Gibraltar plate boundary, in Geodynamics of Iceland and the North Atlantic area, ed. by L. Kristjansson, (Reidel) Dordrecht, pp. 63-81, 1974.
Lehner, P., and. P.A.C. de Ruiter, Structural history of Atlantic margin of Africa, Amer. Assoc. Petrol. Geol. Bull, 61, 961-981, 1977.
Le Pichon, X., R. Hyndman, and G. Pautot, Geophysical study of the opening of the Labrador Sea, J. Geophys. Res., 76, 4724-4743, 1971.
Le Pichon, X., J.-C. Sibuet, and J. Francheteau, The fit of the continents around the North Atlantic Ocean, Tectonophysics, 38, 169-209, 1977.
Livsic, J.J., Paleogene deposits and the platform structure of Svalbard, Norsk Polarinst. Skr., 159, 51 pp. 1974.
Machens, E., The geologic history of the marginal basins along the north shore of the Gulf of Guinea, in The ocean basin and margins, Vol. 1, The South Atlantic, ed. by A.E.M. Nairn, and F.G. Stehli, (Plenum), New York, pp. 351-390, 1973.
Malfait, B.T., and M.G. Dinkelman, Circum-Caribbean tectonic and igneous activity and the evolution of the Caribbean plate, Geol. Soc. Amer. Bull., 83, 251-272, 1972.
Manspeizer, W., J.H. Puffer, and H.L. Cousminer, Separation of Morocco and eastern North America, A Triassic-Liassic Stratigraphic record, Geol. Soc. Amer. Bull., 89, 901-920, 1978.
Martin, H., A geodynamic model for the evolution of the continental margin of southeastern Africa, An. Acad. bras. Ciênc., 48 (Supl.), 169-177, 1976.
Martin, R.G., and J.E. Chase, Geophysical studies in the Gulf of Mexico, in The ocean basins and margins, Vol. 3, The Gulf of Mexico and the Caribbean, ed. by A.E.M. Nairn, and F.G. Stehli, (Plenum), New York, pp. 65-106, 1975.

McCave, I.N., Depositional features of organic-rich black and green mudstones at DSDP sites 386-387 in the western North Atlantic, Init. Rep. Deep-Sea Drill. Proj., 43 (in press).
McKenna, M.C., Eocene Final Separation of the Eurasian and Greenland-North American Landmasses, 24. Internat. Geol. Congr. (Montreal) 7, 275-281, 1972.
Montadert, L., D.G. Roberts et al., Rifting and subsidence on passive continentalmargins in the North East Atlantic, Nature, 268, 305-309, 1977.
Moore, T.C., and G.R. Heath, Survival of deep-sea sedimentary sections, Earth Planet. Sci. Lett., 37, 71-80, 1977.
Murat, R.C., Stratigraphy and paleogeography of the Cretaceous lower Tertiary in southern Nigeria, in African geology, ed. by T.F.J. Dessauvagie, and A.J. Whiteman, (Dept. Geol.,Univ., Ibadan) Ibadan, pp. 251-266, 1972.
Nagy, J., Ammonite faunas and stratigraphy of lower Cretaceous (Albian) rocks in southern Spitzbergen, Norsk Polarinst. Skr., 152, 58 pp., 1970.
Nilsen, T.H., Lower Tertiary laterite on the Iceland-Faeroe Ridge and the Thulean land bridge, Nature, 274, 786-788, 1978.
Noe-Nygaard, A., Cenozoic to Recent volcanism in and around the North Atlantic basin, in The ocean basins and margins, Vol. 2, The North Atlantic, ed. by A.E.M. Nairn, and F.G. Stehli, (Plenum), New York, pp. 391-443, 1974.
Papp, A., Tertiär, Grundzüge regionaler Stratigraphie, Handbuch der stratigraphischen Geologie, Vol. 3 (1), ed. by F. Lotze, (Enke) Stuttgart, 411 pp., 1959.
Pegrum, R.M., G. Rees, and D. Naylor, Geology of the north-west European continental shelf, Vol. 2, The North Sea, (Graham Trotman Dudley Ltd.), London, 255 pp., 1975.
Piper, J.D.A., History and mode of crustal evolution in the Icelandic sector of the mid-Atlantic Ridge, in Implications of continental drift to earth sciences, Vol. 2, ed. by D.H. Tarling, and S.K. Runcorn (Academic Press), London, pp. 635-647, 1973.
Pitman, W.C., and E.M. Herron, Continental drift in the Atlantic and the Arctic, in Geodynamics of Iceland and the North Atlantic area, ed. by L. Kristjansson, (Reidel), Dordrecht, pp. 1-15, 1974.
Pitman, W.C., and M. Talwani, Sea-floor spreading in the North Atlantic, Geol. Soc. Amer. Bull., 83, 619-646, 1972.
Ponte, F.C., and H.E. Asmus, The Brazilian marginal basins, current state of knowledge, An Acad. bras. Ciênc.,48 (Supl.), 215-239, 1976.
Ponte, F.C., and H.E. Asmus, Geological framework of the Brazilian continental margin, Geol. Rundsch., 67, 201-235, 1978.
Rabinowitz, P.D., The boundary between oceanic and continental crust in the western North Atlantic, in The Geology of Continental Margins, ed. by C.A. Burk, and C.L. Drake, (Springer), Berlin, pp. 391-408, 1974.
Ramsay, A.T.S., Sedimentological clues to paleooceanography, in Oceanic micropaleontology, Vol. 2, ed. by A.T.S. Ramsay, (Academic Press), London, pp. 1372-1453, 1977.
Reyment, R.A., P. Bengtson, and E.A. Tait, Cretaceous transgressions in Nigeria and Sergipe-Alagoas (Brazil), An Acad. Brasil. Ciênc., 48 (Supl.), 253-264, 1976.
Reyment, R.A., and N.-A. Mörner, Cretaceous transgressions and regressions exemplified by the South Atlantic, Paleont. Soc. Japan Spec. Pap., 21, 247-261, 1977.
Roberts, D.G., Marine geology of the Rockall Plateau and trough, Phil. Trans. R. Soc. London, A278, 447-509, 1975.
Rosenkrantz, A. and T.C.R. Pulvertaft, Cretaceous-Tertiary stratigraphy and tectonics in northern West-Greenland, Amer. Assoc. Petrol. Geol. Mem., 12, 883-898, 1969.
Schlanger, S.O., and H.C. Jenkyns, Cretaceous oceanic anoxic events, causes and consequences, Geol. Mijnb., 55, 179-184, 1976.
Schott, W., Palaogeographischer Atlas der Unterkreide von Nordwest-Deutschland, (Bundesanst. Bodenforsch.), Hannover, 289 pp., 1967.
Sclater, J.G., R.N. Anderson, and M.L. Bell, The elevation of ridges and the evolution of the central eastern Pacific, J. Geophys. Res., 76, 7888-7915, 1971.
Sclater, J.G., S. Hellinger, and C. Tappscott, The paleobathymetry of the Atlantic Ocean from the Jurassic to Present, J. Geol., 85, 509-552, 1977.
Sibuet, J.C., W.B.F. Ryan et al., Deep drilling results of Leg 47B (Galicia Bank area) in the framework of the early evolution of the North Atlantic Ocean, Phil. Trans. R. Soc. London (in press), 1978.
Spjeldnaes, N., Palaegeography and facies distribution in the Tertiary of Denmark and surrounding areas, Norges geol. unders., 316, 289-311, 1975.
Srivastava, S.P., Evolution of the Labrador Sea and its bearing on the evolution of the North Atlantic, Geophys. J.R.A.S. , 52, 313-351, 1978.
Stehli, F.G., The geology of the Bahama-Blake Plateau region, in The ocean basin and margins, Vol. 2, The North Atlantic, ed. by A.E.M. Nairn, and F.G. Stehli, (Plenum) New York, pp. 15-39, 1974.
Strauch, F., Die Thule-Landbrücke als Wanderweg und Faunenscheide zwischen Atlantik und Skandik im Tertiär, Geol. Rundsch., 60, 381-417, 1970.
Sundvor, E, Thickness and distribution of sedimentary rocks in the southern Barents Sea, Norges geol. unders., 316, 237-240, 1975.
Sweeney, J.F., E. Irving, and J.W. Geuer, Evolution of the Arctic Basin, Arctic Geophys. Rev., Pub. Earth Phys. Br., 45 (4), (in press), 1978.
Talwani, M., and O. Eldholm, Evolution of the

Norwegian-Greenland Sea, Geol. Soc. Amer. Bull., 88, 969-999, 1977.

Talwani, M., and G. Udintsev, Tectonic synthesis, Init. Rep. Deep-Sea Drill. Proj., 38, 1213-1242, 1976.

Talwani, M., G. Udintsev et al., Sites 336 and 332, Init. Rep. Deep-Sea Drill. Proj., 38, 23-116, 1976 a.

Talwani, M., G. Udintsev et al., Sites 338-343, Init. Rep. Deep-Sea Drill. Proj., 38, 151-387, 1976 b.

Thiede, J., The subsidence of aseismic ridges: Evidence from sediments on Rio Grande Rise (SW Atlantic Ocean), Amer. Assoc. Petrol. Geol. Bull., 61, 929-940, 1977.

Thiede, J., Palaeo-oceanography, margin stratigraphy, and palaeophysiography of the Tertiary North Atlantic and Norwegian-Greenland Seas, Phil. Trans. R. Soc. London (in press), 1978.

Thiede, R., and. T.H. van Andel, The paleoenvironment of anaerobic sediments in the Late Mesozoic South Atlantic Ocean, Earth Planet. Sci. Lett., 33, 301-309, 1977.

Tucholke, B., P. Vogt et al., Glomar Challenger drills in the North Atlantic, Geotimes, 20 (12), 18-21, 1975.

Uchupi, E., Bathymetric atlas of the Atlantic, Caribbean, and Gulf of Mexico, Woods Hole Oceanogr. Inst. Ref. No. 71-72, Woods Hole, 1971.

Vail, P.R., R.M. Mitchum, and S. Thompson, Seismic stratigraphy and global changes of sea level, Parts 3 and 4, Amer. Assoc. Petrol. Geol. Mem., 26, 63-97, 1978.

van Andel, T.H., G.R. Heath, and T.C. Moore, Cenozoic history and paleoceanography of the central equatorial Pacific, Geol. Soc. Amer. Mem., 143, 134 pp., 1975.

van Andel, T.H., J. Thiede, J.G. Sclater, and W.W. Hay, Depositional history of the South Atlantic Ocean during the last 125 years, J. Geol., 85, 651-698, 1977.

van Hinte, J.E., A Jurassic time scale, Amer. Assoc. Petrol. Geol. Bull., 60, 489-497, 1976 a.

van Hinte, J.E., A Cretaceous time scale, Amer. Assoc. Petrol. Geol. Bull., 60, 498-516, 1976 b.

Vogt, P.R., The Faeroe-Iceland-Greenland aseismic ridge and the western boundary undercurrent, Nature, 239, 79-81, 1972.

Vogt, P.R., The Iceland phenomenon: Imprints of a hot spot on the ocean crust, and implications for flow below the plates, in Geodynamics of Iceland and the North Atlantic area, ed. by L. Kristjansson, (Reidel), Dordrecht, pp. 105-126, 1974.

Vogt, P.R., C.N. Anderson, and D.R. Bracey, Mesozoic magnetic anomalies, sea-floor spreading and geomagnetic reversals in the southwestern North Atlantic, J. Geophys. Res., 76, 4796-4823, 1971.

Vogt, P.R., and O.E. Avery, Tectonic history of the Arctic Basin: Partial solutions and unsolved mysteries, in Marine geology and oceanography of the Arctic Seas, ed. by Y. Herman, (Springer), Berlin, pp. 83-117, 1974 a.

Vogt, P.R., and O.E. Avery, Detailed magnetic surveys in the northeast Atlantic and Labrador Sea, J. Geophys. Res., 79, 363-389, 1974 b.

Vogt, P.R., and A.M. Einwich, Magnetic anomalies and sea-floor spreading in the western North Atlantic, and a revised calibration to the Keathley (M) geomagnetic revised chronology, Init. Rep. Deep-Sea Drill. Proj., 43 (in press), 1978.

Watts, A.B., and W.B.F. Ryan, Flexure of the lithosphere and continental margin basins, Tectonophysics, 36, 25-44, 1976.

Weyl, R., Die paläogeographische Entwicklung Mittelamerikas, Zentralbl. Geol. Paläont., Pt. I (1973) 5/6, 432-466, 1973.

Williams, C.A., Sea-floor spreading in the Bay of Biscay and its relationship to the North Atlantic, Earth Planet. Sci. Lett., 24, 440-456, 1975.

Williams, C.A., and D. McKenzie, Evolution of the northeast Atlantic, Nature, 232, 168-173, 1971.

Williams, G.D., and C.R. Stelck, Speculations on the Cretaceous paleography of North America, Geol. Assoc. Canada Spec. Pap., 13, 1-20, 1975.

Wüst, G., Blockdiagramme der Atlantischen Zirkulation auf Grund der Meteor-Ergebnisse, Kieler Meeresforsch., 7, 24-34, 1935.

Ziegler, P.A., North Sea basin history in the framework of northwestern Europe, in Petroleum and the continental shelf of NW Europe, 1. Geology, ed. by A.W. Woodland, (Applied Sci. Publ. ), London, pp. 131-148, 1975.

Ziegler, P.A., Geology and hydrocarbon provinces of the North Sea, GeoJournal, 1, 7-32, 1977.

# IMPACT OF DEEP-SEA DRILLING ON PALEOCEANOGRAPHY

W. H. Berger

Scripps Institution of Oceanography, La Jolla, California 92093

Abstract. Paleoceanography - the history of circulation, chemistry, fertility, and biogeography of the oceans - initially took a back seat in the objectives of deep-sea drilling, due to the sudden emergence of the theory of sea floor spreading. Within a few years, however, paleoceanographic goals achieved high priority, in a fusion of geophysical, geochemical, and paleontological concepts and approaches. The paleoceanographic research associated with deep-sea drilling has laid the groundwork for a global stratigraphy, by establishing relationships between changes in circulation and stratification of the ocean, and the evolution of climate and marine plankton. Focal points of interest are fluctuations of sea level and of productivity, and the circumstances of dramatic change of the oceanic environment, that is, the causes of epoch boundaries.

## Introduction

Ten years ago, on August 18, 1968, the GLOMAR CHALLENGER departed from Galveston, Texas, to drill in the Gulf of Mexico and off the East Coast during the first leg of a long series of drilling expeditions into the ocean's past. The chief scientist on this first leg was Maurice Ewing. The Initial Report on Leg One appeared within a year after the cruise (Ewing et al., 1969).

Since then, some forty volumes have been published, each covering a two-month long leg. In almost all of these volumes biostratigraphy and paleoceanography occupy a prominent place in the quantity and significance of results reported. The associated journal literature indicates the emergence of a global stratigraphy of ocean-atmosphere and ocean-biosphere interaction, as a result of deep-sea drilling. We are witnessing a quantum jump in the evolution of the earth sciences reminiscent of that brought about by the geophysical exploration of the ocean floor in the fifties and early sixties. Paleoceanography - the history of circulation, chemistry, fertility, and biogeography of the oceans - is a key ingredient of this quantum jump.

In the present essay I attempt to trace in broad brush fashion, and from a rather personal viewpoint, the development and application of paleoceanographic concepts in the context of deep sea drilling. For background, I have consulted the proposals of JOIDES to the National Science Foundation (Nierenberg, 1965, 1969; Nierenberg and Peterson, 1971; Peterson, 1973, 1977) and the scientific prospectus for each leg, in addition to the Initial Reports of the Deep Sea Drilling Project (Volumes 1 to 43), and the journal literature. Some suggestions as to how paleoceanographic research might be usefully focused are appended.

## Paleoceanography as an Objective of Deep Sea Drilling

### Priorities and Sea Floor Spreading

The spectacular growth of paleoceanography in the wake of GLOMAR CHALLENGER and the prominent place of biostratigraphy - the mother science of paleoceanography - in the Initial Reports might suggest that paleoceanography and deep-sea drilling co-evolved in a symbiotic relationship from the start. This is in fact not so, for one simple reason: the stuff of paleoceanography is sediments, and the recovery of sediments did not enjoy a high priority in the scientific objectives of the early phases of the Deep-Sea Drilling Project. The resulting frustration of the biostratigraphers was forcefully expressed by Moore (1972) who complained that too much material had been flushed from the drill holes, material that holds the geological record of the oceans.

It seems surprising that this complaint arose at all. The JOIDES Project originated from the idea of a broad investigation of the sedimentary layer of the oceans following the Project MOHOLE (which was to penetrate the crust). Significantly, early initiatives for such a sediment-centered program came from the paleoceanographer Cesare Emiliani of the University of Miami (fide van Andel, 1968, p. 1420). The initial plans took shape in 1964, under the leadership of Fritz F. Koczy, a chemical oceanographer. The other planning committee members were Charles L. Drake, J. Brackett Hersey, William R. Riedel, and Tjeerd H. van Andel.

There were several reasons why the priorities of

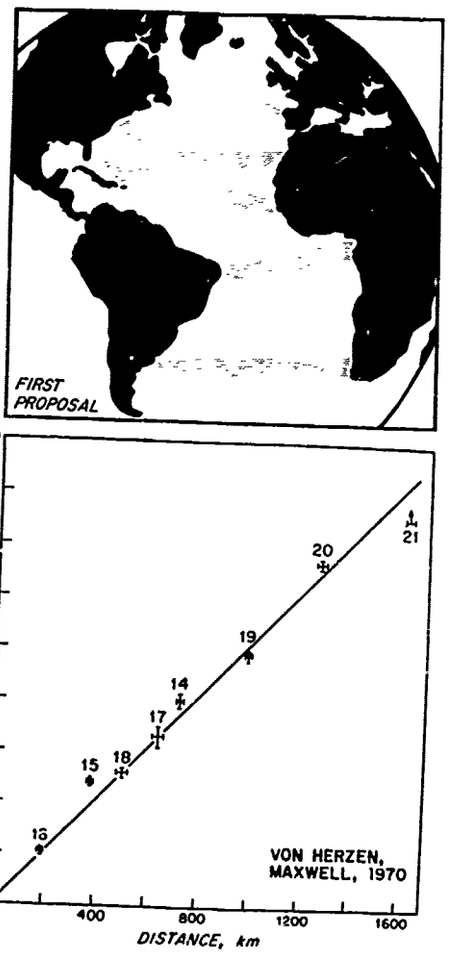


Fig. 1. Upper: Proposed general drilling pattern in the Atlantic (Nierenberg, 1965), across the Mid-Atlantic Ridge. Lower: Results of DSDP Leg 3; basal age of sediments (from biostratigraphy) plotted against distance from ridge crest(von Herzen and Maxwell, 1970).

deep-sea drilling were subsequently formulated in terms of geophysics rather than geochemistry and biostratigraphy. The chief reason was the new Theory of Sea Floor Spreading which completely captured the imagination of marine geologists and geophysicists, including sedimentologists. The Atlantic drilling pattern set forth in the first JOIDES proposal to NSF (July, 1965) was designed to test sea floor spreading, and a widely acclaimed achievement of the early Atlantic legs was the discovery of the regular age progression of basal sediment dates (Figure 1). By the time these results were published, in 1970, sea floor spreading was a reigning theory solidly based on geophysical evidence from magnetic lineations (Vine, 1966; Heirtzler et al., 1968) and from seismology (Isacks, Oliver, and Sykes, 1968). Further testing seemed unnecessary. However, in the meantime drilling for basal sediment had become important for checking on the dating of magnetic anomalies. Thus, it retained a high priority for the next several years.

In contrast to the Atlantic drilling pattern of the first JOIDES proposal, the Pacific pattern emphasized paleoenvironment as the chief scientific goal (Figure 2). Equatorial sedimentation had been the subject of considerable paleoceanographic study based on piston cores (Arrhenius, 1952; Riedel and Funnell, 1964) and the intriguing carbonate cycles promised that there would be a close relationship between stratigraphy

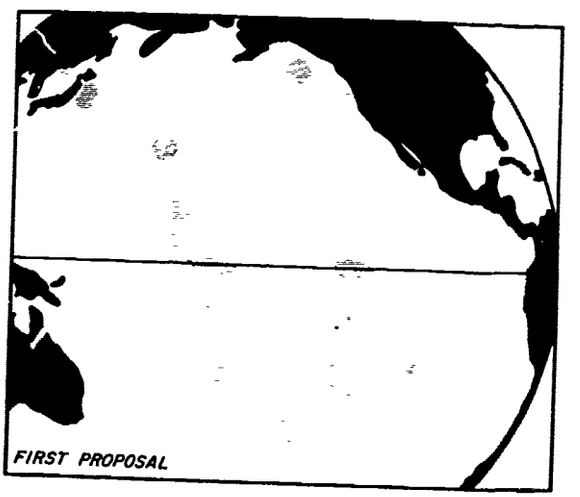


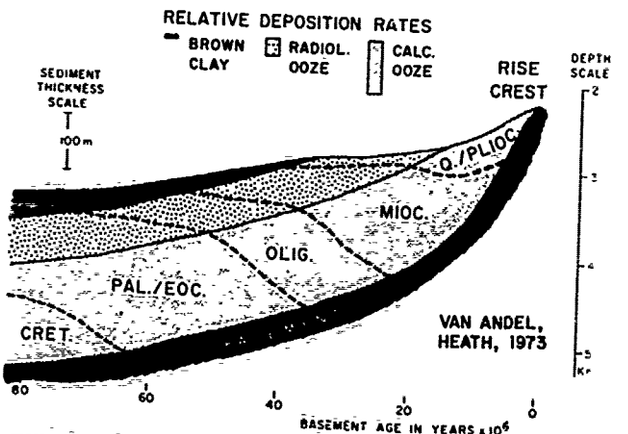


Fig. 2. Upper: Proposed general drilling pattern in the Pacific (Nierenberg, 1965), across the Equator. Lower: Plate stratigraphic sedimentation model of van Andel and Heath (1973), DSDP Leg 16.

and global climatic change. As a consequence of the initial emphasis on sedimentation, recovery was much better in the Pacific than in the Atlantic during the first several years (Moore, 1972). However, regardless of the amount of sediment recovered (which was excellent in a number of the early legs, including Leg 3 in the South Atlantic and several legs in the equatorial Pacific), the focus of research was by 1970 entirely on the New Global Tectonics.

General stratigraphy was chiefly used as a tectonic tool just as biostratigraphy was largely seen as a means to date basement and also acoustic reflectors, which in turn could be used to elucidate regional tectonics. In the resulting stratigraphic models, sedimentation patterns tended to be seen as static, as exemplified in a number of early syntheses (Hsü and Andrews, 1970; van Andel and Heath, 1973; Winterer, 1973; Berger, 1973). An extreme example of this approach to deep-sea stratigraphy is the "kinematic model" proposed by Leg 20 scientists (Heezen et al., 1973) which derives a hypothetical sedimentary sequence of the North Pacific from supposed present-day sedimentation patterns assumed to persist over a hundred million years on the moving Pacific Plate.

## Emergence of Paleoceanography

The effects of plate motion on sediment patterns had to be determined before the next step could be taken, that is, the reconstruction of environmental changes. To define change, to find the amplitudes, rates, phase relationships, and the regional extent of change, one needs continuous and well-dated stratigraphic sequences. Priorities having been set with the focus on tectonics, the interests of paleoceanography were initially represented mainly by the biostratigraphers, who insisted on the value of continuous coring.

Biostratigraphers maintained the focus on environmental change: changes in water temperature at the surface and at depth (Douglas and Savin, 1971), changes in carbonate chemistry (Hay, 1970, 1971), changes in faunal assemblages and diversity (Berggren, 1971; Cita, 1971). As the importance of their contributions became evident, and as they acquired the language of geochemistry and climatology, their constituency broadened and support for paleoceanographic goals grew.

Beginning with the fourth year of deep-sea drilling, and even before Moore's (1972) complaint about the flushing away of ocean history, virtually every leg had a significant amount of continuous recovery for biostratigraphic and paleoceanographic purposes. In some of the legs paleoceanography actually had the highest priority. Instead of meekly delivering dates for geophysical purposes, biostratigraphers began to incorporate geophysical and geochemical methods to provide a comprehensive view of the evolution of the deep sea environment and the life within it.

Conversely, instead of focusing entirely on sea floor motions, or on regional tectonics and morphology, marine geologists became interested in the history of oceanic circulation and chemistry. The forced fusion of the various subdisciplines of marine geology, geophysics, and stratigraphy: this is the impact of deep sea drilling on paleoceanography.

The results of the merger process are exemplified in the memoir on "Cenozoic History and Paleoceanography of the Central Equatorial Pacific Ocean" by van Andel, Heath, and Moore (1975), and in the numerous syntheses of drilling results published last year (Berger, 1977; Berggren and Hollister, 1977; Davies et al., 1977; Fischer and Arthur, 1977; Heath, Moore, van Andel, 1977; Heirtzler et al., 1977; Kennett, 1977; Moore and Heath, 1977; Ryan and Cita, 1977; Savin, 1977; van Andel et al., 1977). These syntheses have to cope with an extraordinary amount of new and unusual information.

The trends and events in a changing ocean, as seen through the conceptual instruments of the practicing paleoceanographers may be termed the "paleoceanographic inventory". Its results are presented as facts. The underlying assumption is that such "facts" represent meaningful patterns in terms of identifiable causes. This assumption may not always hold up. For example, "factual" sedimentation rate changes may incorrectly summarize apparent rates of entirely different facies deposited at systematically differing elevations; "factual" fluctuations of the carbonate compensation depth may include redeposition events and missing sections to unknown and varying degrees; hiatus stratigraphy may mix apples and oranges by including the effects of non-deposition, mechanical erosion, carbonate dissolution, and systematic coring difficulties (e.g. in chert) under one common label.

With this note of caution, let us accept the inventory and proceed from there.

## Trends and Events: Inventory of the Cenozoic Ocean

### The Cenozoic Temperature Decline

An overall cooling of surface temperatures on Earth from Late Cretaceous time to the Quaternary is part of textbook geology, and also a warming during the Eocene and during the Miocene superimposed on this trend.

The response of the deep ocean waters to the cooling trend had been sketched by Emiliani (1954) on the basis of a few chance samples from the deep sea floor. He suggested that the oxygen isotope composition of deep sea benthic forams reflects the high latitude temperature at the sites of bottom water production, and the planktonic foraminifera reflect the surface temperature. The difference between the two then reflects the overall planetary temperature gradient. The development of this gradient, as cooling progressed through

the Cenozoic, can be seen in the extensive oxygen isotope work of Douglas and Savin (1975) and of Shackleton and Kennett (1975) (Figure 3).

Clearly, the familiar cooling trend is largely a high latitude phenomenon. Except for the Oligocene, low latitude surface waters remain about as warm as they were in the latest Cretaceous, especially when considering that the oxygen isotope values are depressed to the heavy side by ice formation in the late Cenozoic. Recent CLIMAP results provide an analogue to this observation: even during maximum glaciation, tropical temperatures drop but little, except where disturbed by influx from cold ocean currents (CLIMAP, 1976; Cline and Hays, 1976). The apparent coolness of the Oligocene tropics and the associated drought (Davies et al., 1977) is a major problem. One possible mechanim to hinder establishment of a warm tropical surface layer during the Oligocene is mid-ocean overturn due to low stability of the water column, with a negative salinity-depth gradient counteracting the temperature gradient, in mid- and low latitudes.

The high latitude cooling as reflected in the benthic foraminifera is a combination of the general trend and several rather discrete events of

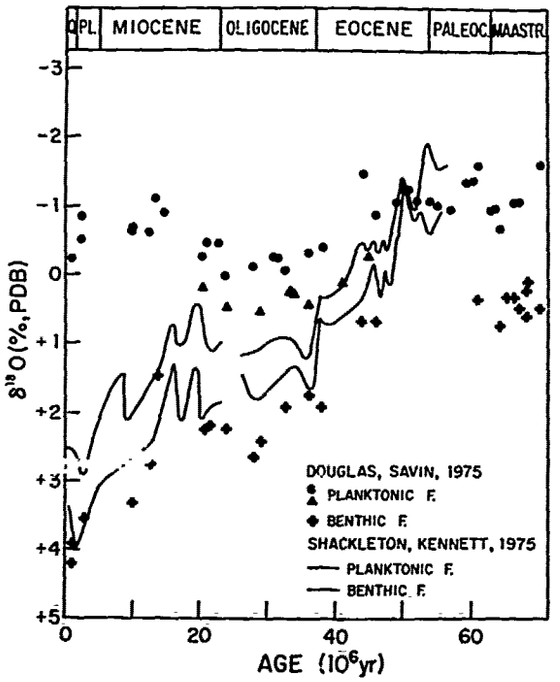


Fig. 3. Oxygen isotope stratigraphy of calcareous foraminifera in Pacific sediments. Data from Douglas and Savin (1975), DSDP Leg 32 (low latitudes) and from Shackleton and Kennett (1975), DSDP Leg 29 (high southern latitudes). Note the narrow range of values in the early Eocene, and increasing separation since.

which the Eocene-Oligocene drop is the most striking. The fact that planktonic isotopic values for high latitudes are lighter than tropical ones in the Eocene indicates low salinities of high latitude surface waters. Presumably, rain belts reached farther poleward than today. To the degree that rain belts moved equatorward during the course of cooling, the post-Eocene isotopic signal from high latitudes, including deep sea benthics, reflects both cooling and a decrease in (isotopically light) precipitation.

The overall trend, presumably, is a function of the change of arrangements of continents -- leading to thermal isolation of Antarctica and of the Arctic, as proposed by Ewing and Donn (1956) -- as well as the overall regression since the Late Cretaceous, which increased albedo, since land reflects incoming radiation more than water.

The discrete events are more difficult to explain. The remarkable drop of isotopic temperature near the Eocene-Oligocene boundary apparently took place within 100,000 years or less (Kennett and Shackleton, 1976). It is not at all clear whether this event was brought about by a profound change in the circulation system (the opening of a passage between Antarctica and Australia) or by an internal feedback mechanim triggered by regression (such as continuous albedo increase due to progressive drought), or to a combination of these or neither. Talwani and Edlholm (1977) show the Norwegian-Greenland Sea opening at this time. The possibility of establishing a new bottom water source in this area must be considered, as well as exchange with Arctic low salinity waters (Thierstein and Berger, 1978). Both of these phenomena could change the oceanographic setting and result in a new type of ocean stratification and circulation.

Perhaps the simplest hypothesis is that falling temperatures on Antarctica reached a critical value - that of freezing - with concomitant albedo increase of this continent, causing extension and intensification of the polar high. The extended polar high, in turn, would have moved the rainbelt off the coast and away from the shelves of Antarctica, allowing cooling (and sinking) of waters of normal salinity.

The Mid-Miocene event is marked by a distinct and rapid change of oxygen isotope composition of benthic foraminifera, toward heavier values. Both a temperature drop at the bottom water source, and a glacial effect due to rapid ice expansion on Artarctica are invoked to explain this change in isotopes (Savin, Douglas, Stehli, 1975; Shackleton and Kennett, 1975). From the data (Figure 3) it appears that the event starts during a warming period in the tropics. In fact, a correction for the glacial effect would intensify the apparent warming. Why should Antarctic glaciation proceed concomitantly with a warming of the tropics? And why so suddenly and rapidly? Again, two approaches to an explanation can be considered: a change of the entire system of circulation, or a triggering effect starting a cascade of feedback

processes in a metastable system, or both. For the first type of answer, the opening of Drake Passage provides a convenient explanation. Sufficient separation of South America from Antarctica allows circumpolar flow and hence promotes the isolation of the tropics from the high latitude areas. Interaction between warm, humid air masses and cold polar ones provides for formation of snow and ice. The resulting increase in albedo in high latitudes then intensifies the temperature drop there. Alternatively, the Miocene transgression warms the tropics and ends an Oligocene drought, decreasing the tropical albedo. The resulting intensified tropical warming provides for transport of moisture to high latitudes, with albedo-feedback via snow cover, which greatly increases the planetary temperature gradient. In the absence of an exact date for the opening of Drake Passage, and of climatic models for the presumed warm-cold interaction, of course, such "explanations" remain mere scenarios -- it could have happened this way.

The final major event seen in the oxygen isotope stratigraphies is the sudden change to heavier oxygen values in the upper Pliocene, interpreted as the onset of northern continental glaciation. The same event is dramatically recorded in the onset of terrigenous sedimentation at Site 116 in the North Atlantic (Berggren, 1972). One can hardly invoke a radical change in the geologic setting of the system at exactly 3 million years ago: everything was much in the same place as before. The Panama Isthmus had been closed for some time. Thus, climatic deterioration from whatever source, presumably from mountain building, apparently reached a threshold at which positive feedback mechanisms could greatly enhance the effects from minor causes, such as Milankovitch irradiation fluctuations, or volcanic activity. Evidence for increasing volcanic activity in Late Neogene time comes from the abundance of ash layers in DSDP sites (Kennett and Thunell, 1975).

The search for the explanations for the striking events seen in the oxygen isotope records remains a major challenge.

## Cenozoic CCD Fluctuations

That the CCD fluctuated during the Cenozoic was first proposed by Bramlette (1961), who also defined the term "carbonate compensation depth" as a facies boundary between calcareous and non-calcareous sediments. Bramlette suggested that the CCD in the Pacific was lower than today in the mid-Tertiary, as did Heath (1969). Before this suggestion could be evaluated, the subsidence of the sea floor had to be accounted for, using age-depth plots (Sclater, Anderson, Bell, 1971) and assuming that the present age-depth relationships are valid for the geologic past (Berger, 1972; 1973). As it turned out, the CCD stood indeed low in the Oligocene, not only in the Pacific, but also in the Atlantic (Berger and Winterer, 1974; van Andel, 1975). CCD fluctuations also were proposed by Tappan (1968), Peterson et al. (1970), Hay (1970), and Worsley (1971), and by Ramsay, Schneidermann and Finch (1973).

Today's CCD is near 4500 m on the average. It is indistinct in the North Pacific, where it rises to above 4000 m, and it is rather more distinct in the North Atlantic where it descends to 5500 m. Its position is a function of supply rate and dissolution rate, which in turn depend on fertility of upper waters, on the state of saturation of deep waters (alkalinity, $CO_2$ content) and on the rate of flow of the water across the sediment interface (for reviews see Berner, 1974; Broecker, 1974; Broecker and Takahashi, 1978; Edmond, 1974). The position of the present CCD has not yet been modelled from first principles, and it is therefore unlikely that this can be done for ancient oceans. Nevertheless, the changes in the CCD and the associated carbonate sedimentation patterns provide clues to the chemistry and fertility of the ocean which are of great interest.

An initial attempt to correct for sea floor subsidence in describing carbonate sedimentation patterns was based on Leg 3 data in the South Atlantic; additional information has now become available (Figure 4). The CCD is seen to drop at the end of the Eocene and to reach a maximum in the mid-Oligocene. The CCD starts to rise at the beginning of the Miocene, reaches a peak in middle to late Miocene time, and drops dramatically starting about 10 million years ago. The depth gradient of sedimentation rates (and hence the dissolution rate gradient) tends to increase from the Oligocene to the Pleistocene.

The interpretation of this pattern assumed an increasing role of corrosive Antarctic Bottom Water, entering with the start of the Miocene, and reaching a peak 10 million years later (Berger, 1972). Ten million years ago the production of North Atlantic Deep Water was assumed to set in. The isolation of North Atlantic Waters due to gradual emergence of the Panama Isthmus presumably led to increased salinities, and the subsequent cooling of the saline waters led to deep water production. The North Atlantic Deep Water then started to drive back the Antarctic Bottom Water, as is the case today. Carbonate could then be sedimented above the boundary of the two abyssal water masses.

Although this scenario still seems attractive, the overall parallelism of the Atlantic and Pacific CCD requires that global effects be taken into account, rather than solely Atlantic circulation patterns or exchange patterns with the Pacific (Figure 4). This realization rests especially on the reconstruction of the extra-equatorial Pacific CCD, by van Andel and Moore (1974). One possibility for a global explanation is that the CCD rose during transgressions, when carbonate was locked up on shelves, and fell during regressions, when carbonate was transferred from the shelves to the deep sea (Berger and Winterer, 1974; van Andel, 1975). Unfortunately, sedimentation rate patterns

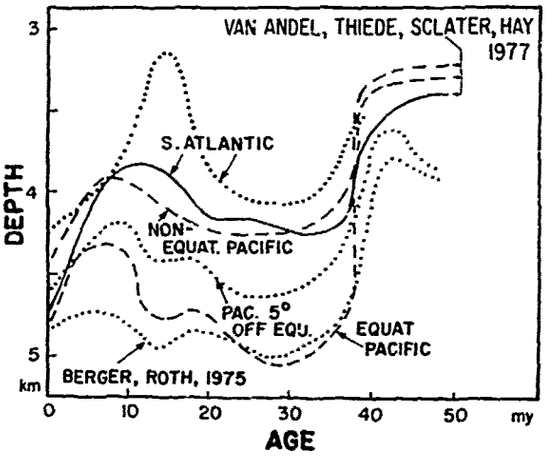


Fig. 4. Various reconstructions of CCD variations through Cenozoic time. Heavy lines: from van Andel et al. (1977), incorporating data from van Andel and Moore (1974), and van Andel, Heath, Moore (1975). Stippled: from Berger and Roth (1975), based on data in Berger (1972, 1973). The differences between reconstructions reflect to some degree an increase in information, but also largely differences in interpretation of data.

do not support this simple picture (Figure 5). According to the compilation by Davies et al. (1977), in the Oligocene, when the CCD stood low, there was actually less carbonate being sedimented than during the Miocene when it stood high. This is also indicated in the sedimentation rate patterns of Leg 3 (Berger, 1972) and in those of the central Pacific (van Andel, Heath, Moore, 1975).

The fluctuations in the depth gradient of dissolution rates calculated by Heath et al. (1977) for the central Pacific contain the clue to this seeming paradox (Figure 6). The sharp increase in gradient since the beginning of the Miocene is remarkable, and suggests control of carbonate patterns by increasing chemical erosion from Antarctic Bottom Waters (with increasing deposition in areas above the Bottom Water) as well as increasing fertility (to provide the high carbonate sedimentation rates above the CCD). In this sense, the high supply - high erosion CCD of the Neogene differs in fundamental ways from the "near-equilibrium" CCD of the Paleogene.

The increasing dissolution gradients in the Neogene imply considerable erosion, not only of contemporaneous carbonate but also of older carbonates which were deposited during times of a deep CCD or which became available for dissolution through subsidence. Such recycling of older carbonates increases sedimentation rates in the Neogene. The problem has been discussed at length by Moore and Heath (1977) who compiled the frequency of missing sections for the world ocean. Their compilation is essentially a mirror image of that of Davies et al. (1977) (Figure 5), with the exception of the middle Miocene. Apparently the supply of sediments essentially controls the abundance of hiatus development, in addition to general recycling (Moore and Heath, 1977). The middle Miocene (which was seen earlier to be characterized by extensive Antarctic glaciation and presumably by large-scale formation of Antarctic Bottom Water) presents a special case of both increased erosion and sedimentation. At this time the shallowness of the CCD combined with a strong dissolution gradient provides an excellent opportunity for widespread chemical erosion of older sediments. In contrast, the oft-repeated notion of widespread Oligocene erosion appears unfounded: if much sediment was eroded in the Oligocene, it should have been redeposited in the Oligocene. Where then is this sediment?

In summary, Cenozoic CCD fluctuations are highly complex phenomena. The CCD drops at the end of the Eocene, concomitant with a temperature drop (showing that bottom water temperature per se is unimportant). It stays deep during the Oligocene, but sedimentation rates are low. Thus, less carbonate is actually being deposited during the low

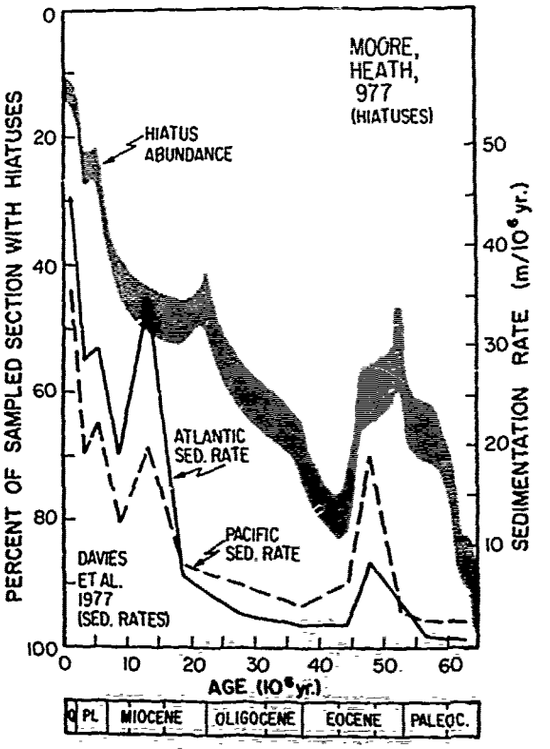


Fig. 5. Comparison of hiatus abundance in the world ocean (Moore, Heath, 1977) and total sedimentation rates in Atlantic and Pacific (Davies, Hay, Southam, Worsley, 1977).

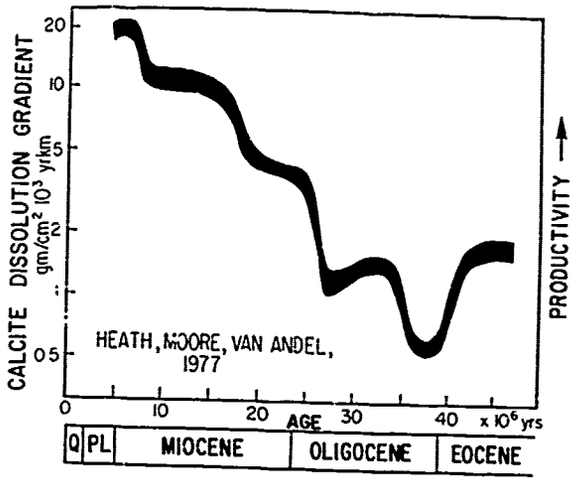


Fig. 6. Cenozoic fluctuations of the vertical gradient of the calcium carbonate dissolution in the equatorial Pacific, according to Heath, Moore, van Andel (1977).

stand than before or after. Essentially this suggests the existence of a "near-equilibrium" ocean in the Oligocene, with low fertility and hence little "excess precipitation" that would drive the ocean to undersaturation. Surprisingly, there is little supply from the continents, presumably due to widespread dry conditions (Davies et al., 1977) and to trapping of sediments on the continent. The CCD rises in the Miocene in response to increased fertility and hence "excess supply" of carbonate to the sea floor which drives the ocean toward undersaturation (Berger and Winterer, 1974). The onset of large scale production of Antarctic Bottom Water at the beginning of the Neogene provides a sharp deep boundary for carbonate sedimentation in much of the ocean. At the same time total sedimentation increases, both because of greatly increased supply from land (beginning about 10 million years ago) and because of internal recycling of older sediments.

## The Search for Correlations

The fluctuations of temperature patterns, as recorded by oxygen isotopes in foraminifera, and the fluctuations of carbonate saturation patterns, as recorded in preservation stratigraphy (CCD, dissolution gradients, fragmentation of foraminifera) describe different aspects of the same system which changes through time. To define these changes correctly, they must be seen simultaneously. To find the driving forces, the independent environmental variables must be found and correlated with the dependent ones. To understand how these forces work, interactions have to be modelled from first principles. Failing that, plausible analogues whose workings are reasonably familiar must be found.

The present emphasis in the search for dynamics is in finding correlations (Haq, 1973; Berger and Roth, 1975; van Andel, 1975; Berger, 1977; van Andel et al., 1977). The prime example of this approach is the stimulating paper by Fischer and Arthur (1977). So far, little use has been made of Quaternary analogues, and virtually none of physical models, in trying to explain the trends and events in Cenozoic temperature and carbonate patterns.

One type of correlation which goes back to geologic antiquity is the one between temperature and sea level change. Times of transgression are known to be warm and equitable, those of regression are associated with cooling. Within the Cenozoic, sea level stood high in the Eocene and Miocene, and these are indeed the times when tropical planktonic foraminifera show low $\delta^{18}O$ values, that is warming (Figure 3).

Changes in carbon isotopic composition of calcareous plankton and benthos also are correlated with sea level change. In principle, there are three main factors to be considered when interpreting the carbon isotope fluctuations: (1) a change in the composition of oceanic $CO_2$, due to a shift in the input/output relationships of the sedimentary reservoirs (carbonate and organic carbon); (2) a change in the composition of $CO_2$ within the particular water masses within which the shells grow, that is, fractionation within the ocean; (3) a change in the "vital effect", that is, the difference to equilibrium precipitation, due to a change in metabolic activity of the shell-making organisms. In general, transgression corresponds to carbonates rich in $^{13}C$ and vice versa. This corresponce presumably arises because of preferential deposition of organic matter (low in $^{13}C$) during transgression (Tappan, 1968). In addition, the magnitude of the planktonic-benthic difference in carbon isotopes tends to go parallel to that in oxygen isotopes. Both differences appear to reflect the degree of density stratification. In a stably stratified ocean upper waters tend to become depleted in $^{12}C$. This will increase $^{13}C$ values in the planktonic carbonate (Kroopnick et al., 1977).

As mentioned previously, sea level changes bear on the patterns of carbonate sedimentation rates. The fact that the overall CCD variation looks somewhat like the Cenozoic transgression-regression curve is certainly suggestive of the commonly postulated shelf-basin fractionation. The fact that this notion fails to explain things has been discussed above. While the fractionation is not denied, more subtle mechanisms are at work also. Sea level, through its effect on stability of the water column and "age" of deep waters (hence $CO_2$ content) determines the amount of $CaCO_3$ the ocean can hold in solution and the shape of the saturation profile. Furthermore, sea level may affect productivity which in turn is crucial to the understanding of CCD fluctuations (Li, Takahashi, Broecker, 1969; Fischer and Arthur, 1977).

Productivity of the pelagic ocean, as measured

by maximum pelagic sedimentation rates, more or less parallels the general trends, being high when sea level is high and the CCD is shallow. The tie-in betweeen productivity and CCD variation is given by the notion of "excess supply". "Excess supply" is the amount of sediment falling on the seafloor which is not balanced by input from weathering or volcanism. It is that portion of the supply which has to be redissolved for material balance. The "excess supply" is responsible for the overall undersaturation of the ocean with the biogenic substance in question. An increase in "excess supply", therefore, leads to an increase in undersaturation. Thus, the CCD should rise when carbonate is being supplied to the seafloor in increasing amounts, without concomitant increase of supply from outside the ocean (continental erosion, ridge crest reactions, or volcanism). The apparent relationship between productivity and the CCD can be rationalized in this manner.

Any effects of sea level changes on productivity of the ocean are not readily apparent. Fundamentally, productivity is tied to the availability of nutrients and to the stability of the uppermost water column, allowing the planktonic algae to stay in the photic zone (Sverdrup, 1953). The two requirements are antagonistic. Best results, therefore, should be achieved by frequent alternation between stratification and mixing during the seasonal cycle. The intermittent action of strong winds on a well stratified ocean would produce such an effect. The increasing planetary temperature gradient increasingly produces both stable stratification and strong winds during the Neogene. In turn, the high fertility of the Neogene results in an increase of maximum sedimentation rates (above the lysocline) and an increase in undersaturation and hence dissoluton rates (below the lysocline). The end effect is a strong increase in the depth gradient of the dissolution rate (van Andel et al., 1975: see Figure 6).

At other times transgressions may not necessarily go parallel with high pelagic productivity. The notion that they do (Tappan, 1968) is based on setting diversity equal to productivity and on length-of-food-chain arguments. Both arguments do not work in the present ocean: the pelagic realm has low fertility, high diversity, and long food chains, compared with the coastal ocean. Thus the co-occurrence of high pelagic diversity with transgressions and warm climate (Frerichs, 1971; Haq, 1973; Roth, 1974) could be used to argue lowered fertility (but high stability) for such times, in the pelagic realm.

Sea level change is not the only apparent driving force for paleoceanographic trends. The marked changes in the composition of pelagic sediments from one epoch to the next (Davies and Supko, 1973) would seem to require additional factors, besides fractionation of lime from silica between basins and between deep ocean and shelf seas. Varying intensity of volcanism or varying intensity and type of continental erosion must be considered, as well as variations in detrital recycling of marine sediments (erosional fractionation between geologic periods). It has been suggested that the high silica content of Eocene and Miocene sediments reflects volcanic ash (Bramlette, 1946; Gibson and Towe, 1971), and this is in accord with the abundance of ash and other indicators in deep-sea sediments (Kennett and Thunnell, 1975; Karig, 1975, Leg 31). Karig's (1975) suggestion that arc volcanism is roughly proportional to subduction rates implies a correlation between volcanism and age of seafloor, and hence elevation of sea surface. The co-occurrence of high sea level, high volcanic activity (and hence $CO_2$ supply), shallow CCD, and deposition of siliceous sediment has to be contemplated from this viewpoint as well.

## The Cretaceous Challenge: A Different Kind of Ocean

### Significance of a reduced temperature gradient

The present ocean can be described as a two-layer system, with a 1-km thick upper layer (the thermocline) and a 3-km thick deep layer of polar waters (Munk, 1966). In addition, there is a thin (100 m) mixed layer whose thickness just about corresponds to the photic zone. The mixed layer is depleted in nutrients because the thermocline forms a barrier to diffusion of nutrients from below. Leakage occurs around the continents, where the barrier breaks down. The circulation is largely wind-driven in the upper layer, and density-driven below, with roughly 80% of the drive derived from temperature gradients and 20% from differences in salinity (Wyrtki, 1961).

Cretaceous oceans must have been entirely different, and many of the concepts appropriate for the present ocean - thermocline, oxygen minimum, upwelling, bottom water, perhaps even "mixed layer" - do not apply or must be drastically redefined. The chief characteristic of Cretaceous oceans is the reduced temperature gradient, horizontally and vertically. The difference in oxygen isotope values of planktonic coccoliths and benthic forams shown by Douglas and Savin (1975, Leg 32) is on the order of 1.6 $^{o}/_{oo}$, corresponding to less than 10°C. Our own results for the Cenomanian of Site 137 (Berger and Eicher, unpublished) show a similarly low difference of 1.5 $^{o}/_{oo}$ between planktonic and benthic foraminifera, as well as a difference of only 0.6 $^{o}/_{oo}$ for $\delta^{13}C$. Compared with the Neogene ocean ($\Delta\delta^{18}O$: 3 to 5 $^{o}/_{oo}$, $\Delta\delta^{13}C$: 1-2 $^{o}/_{oo}$), these differences are distinctly reduced and suggest that stratification was much less stable in the Cretaceous than in the Neogene ocean.

The overall temperature gradient on the planet (which represents the maximum the ocean can attain) is on the order of 15°C in the Cretaceous (Bowen, 1966; Kauffman, 1978). This means that bottom water temperatures could not drop far below 15°C. Under these conditions, salinity distributions

must have played an important role in driving deep circulation (Chamberlin, 1906; Berger, 1970b). In principle, this type of circulation requires sinking of waters in the subtropics and rising of waters in high latitudes. The sources of deep saline water are not readily apparent, since many of the large epicontinental seas appear to have had slightly brackish surface waters (Kauffman, 1978). The most likely sources are indentations of the subtropical Tethys, modern analogues being the Red Sea and the Persian Gulf. At the present time also, deep water formation depends to a considerable extent on evaporation in the subtropics, and on the cooling of saline waters thus produced, after moving them to high latitudes. The equability of the Cretaceous climate suggests that there was, in addition to a high latitude fog blanket, an efficient transfer of heat by atmospheric moisture from low latitudes to high, which would have counterbalanced the density increase of surface waters from cooling in high latitudes. This situation probably dominated throughout the Mesozoic, the stability of the water column depending largely on salinity stratification.

In this view, the early Tertiary may be seen as a time of transition between salinity-dominated and temperature-dominated stratification. Under certain conditions the competition between these mechanisms would lead to low stability and hence to open-ocean overturn. This has been shown to occur in the Mediterranean (Anati and Stommel, 1970) which is in other respects also an attractive source of analogues for ancient oceans, due to warm deep water and low stability, low fertility, and occasional development of oxygen deficiency during periods of high fresh water input.

Evidence for open-ocean overturn may exist in the Paleogene nannoplankton blooms recorded from various parts of the ocean (Roth, 1974; Haq, Premoli-Silva, Lohmann, 1977). The prime example is the Braarudosphaera-chalk of Leg 3 (Wise and Kelts, 1972). This chalk shows unusually heavy (="cold") $\delta^{18}O$ values (Wise and Hsü, 1971) which would be appropriate for mid-ocean "upwelling". Open-ocean overturn would produce a very thick "mixed layer", with essentially unfavorable conditions for algal production and hence for the entire food chain. Open ocean overturn also would bring intermediate waters to the surface - waters that quite possibly had low salinity, being produced in high latitude rainbelts and deriving their ability to sink from low temperature. Intermediate water salinities of 30 $^{o}/_{oo}$ or less, in the bloom areas, are compatible with the available isotope data.

Foraminiferal production is generally extremely low in Cretaceous oceans compared with the present: typical sand content of calcareous ooze is 1 percent or less compared with 10 to 30 percent in Neogene oozes. In addition, overall pelagic sedimentation rates also seem lower, although this is difficult to establish since the duration of zones is unknown. The low fertility of the Cretaceous ocean, which is reflected in the patterns of preservation of phosphatic sediments and other precipitates (Berger and Roth, 1975; Fischer and Arthur, 1977) is essentially still a mystery. Presumably, a low oxygen content of deep waters played a role, in slowing decay of organic matter and hence the recycling of nutrients.

## Oxygen deficiency and calcite preservation

Black shales on the deep-sea floor of the North Atlantic were first discovered in piston cores aimed at outcrops of Cretaceous sediments (Habib, 1969). Subsequently deep-sea drilling showed that black shales rich in organic carbon are widespread in mid-Cretaceous deep sea sediments of the North Atlantic (Lancelot, Hathaway, Hollister, 1972, Leg 11). The occurrence of the shales was interpreted as indicating a stagnant ocean basin, that is, oxygen deficiency of abyssal waters. Black, finely laminated clays were found again in mid-Cretaceous sediments of Leg 14. Backtracking of Site 137 showed that the organic-rich sediments were deposited on the ridge crest, and that oxidized sediments were deposited on the ridge flank. This distribution suggested a deep-reaching oxygen minimum intersecting the ridge crest (Berger and von Rad, 1972). The contemporaneous black shale in Site 138 was interpreted as hemipelagic sedimentation with redeposited organic matter creating a strong oxygen deficiency near the sea floor.

The two scenarios of oxygen deficiency, the "Stagnant Basin" and the "Deep Oxygen Minimum" type, have dominated recent discussions of mid-Cretaceous deep-sea sedimentation (Schlanger and Jenkyns, 1976; Ryan and Cita, 1977; Fischer and Arthur, 1977; Thiede and van Andel, 1977). Other scenarios also are conceivable, including the ridge crest as a barrier to deep oxygenation, and multiple low oxygen layers, due to inter-layering of cool and salty deep water layers derived from various deep water sources (Figure 7). The available information, so far, does not allow a clear choice between these models, nor is such a choice necessarily the most pressing task in assessing the importance of oxygen deficiency for Cretaceous oceanography.

Fundamentally, the preservation of organic carbon, whether from plankton sources or from continental sources, is a matter of the low initial dissolved oxygen content ("oxyty") of a warm Cretaceous ocean, combined with local imbalance of oxygen supply and demand. The evidence for poorly aerated seas in the Cretaceous has been at hand for some time. As Kauffman (1978) points out, over large areas and through thick stratigraphic sections, Cretaceous marine sediments on the shelves are characterized by well laminated, dark organic-rich shales and pelagic carbonates, and by glauconitic sand. In the absence of a strong polar drive for deep circulation (which would introduce cold, oxygen-rich bottom waters) the type of water associated with this neritic facies is similar to the one that provides a

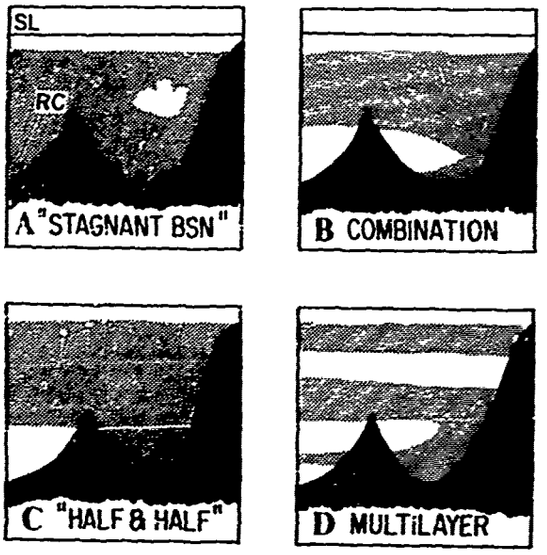


Fig. 7. Some possible configurations of conditions of oxygen deficiency, SL, sea level: RC, ridge crest. "Combination": deep oxgyen minimum plus oxygen deficiency on continental slope area. "Half and Half": deep oxygen minimum on one side of ridge, stagnant basin on the other. Other configurations also can be envisaged (see Schlanger and Jenkyns, 1976; Ryan and Cita, 1977; Thiede and van Andel, 1977).

large part of the deep waters of the ocean. It is already comparatively oxygen-poor when arriving at depth, with perhaps one-half of the oxyty of today's deep waters (Berger, 1970b). Today, if there were only 2 ml per liter less oxygen in deep waters below 1 km, much of the present Pacific would be anaerobic down to 2000 m depth. With 3 ml per liter less, an oxygen deficient layer would reach below the ridge crest in both the Pacific and the Indian Oceans. In the Atlantic the oxygen deficiency would reach to 1500 meters. Black sediments would develop over depth ranges larger than this, because of the oxygen loss in interstitial waters. The reduction in oxygen content could be derived simply from warming the water, reducing oxygen solubility, without any recourse to "sluggish circulation" or "poor ventilation".

The most interesting aspect of the oxygenation of Cretaceous oceans is that it is delicately balanced. This allows small fluctuations in regional productivity and circulation to result in great changes in living conditions and in preservation of organic carbon and shell carbonates. Consider, for example, the organic carbon contents in deep sea sediments of the Cretaceous South Atlantic. In the middle Cretaceous, this ocean was in the early stages of opening. It had a sill to the south (Rio Grande-Walvis Ridge) and a slowly opening seaway to the north (Förster, 1978). The local supply of organic carbon, planktonic and terrigenous, provided sufficient oxygen demand for temporary anaerobism (Figure 8).

The data compiled by Thiede and van Andel (1977) show that carbon preservation fluctuated considerably at all depths, suggesting a fluctuation of oxygen content around a ow, critical level. Presumably, changes in deep circulation pattern (estuarine versus anti-estuarine) in the South Atlantic Bight could have produced such patterns. Incidentally, the data are compatible with the multiple oxygen minimum concept (Figure 7).

Analogous fluctuations - in this case expressed as alternations of greenish and reddish clays and marls - are also seen in Cenomanian ridge crest sediments of the North Atlantic (Site 137, Leg 14) and in late Aptian to Turonian hemipelagic sediments of Site 367, Leg 41 (Dean et al., 1978). A delicate balance between oxygen supply and demand is indicated. The effects of such a balance on carbonate preservation have been discussed by Berger and von Rad (1972) who postulated that the CCD was tied to the fluctuating lower limit of a deep oxygen minimum.

The relationship between oxygenation and carbonate preservation can be generalized from a selection of present-day analogues (Figure 9). The extremely rapid change of preservation seen

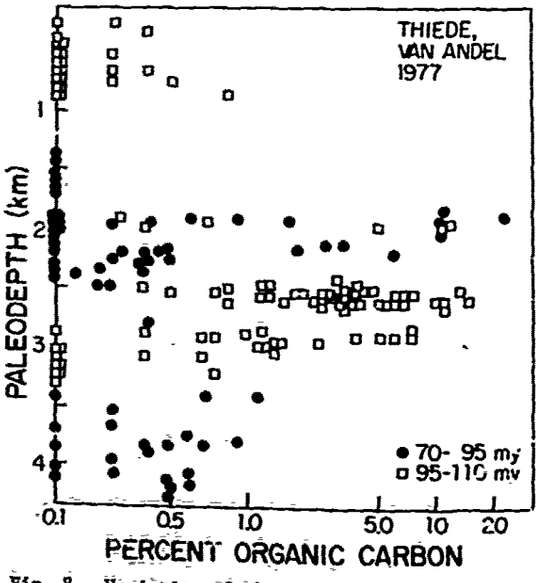


Fig. 8. Variation of the organic content of South Atlantic sediments, as a function of paleodepth, for two time periods in the Cretaceous, according to Thiede and van Andel (1977). Note the large range of carbon values within each depth interval.

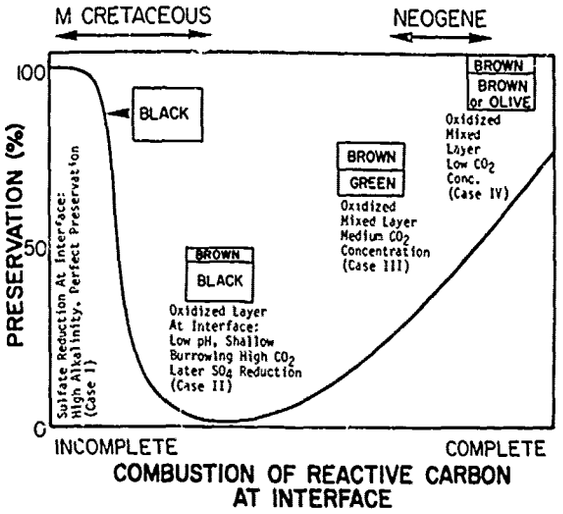


Fig. 9. Proposed relationship between the combustion of organic matter and the preservation of calcareous shells, at depths above the oceanic lysocline. Analogues: Case I, Santa Barbara Basin (Berger and Soutar, 1970); Case II, Kiel Bay, Baltic Sea (Wefer, 1976); Cases III and IV, present-day continental slope and deep-sea floor (Berger, 1970a).

in Cretaceous deep-sea sediments from Site 137 and also reported from other sites and from epicontinental seas, can be explained by a flip-flop situation involving the exact level, within the sediment, of sulfate reduction. If sulfate reduction takes place on the surface of the sediment, the associated increase in alkalinity can preserve carbonate on the sediment surface. If sulfate reduction takes place below the interface, the increase in alkalinity may come too late to prevent dissolution at the interface. In contrast, the Neogene setting makes for much gentler transitions between well and poorly preserved shell carbonate.

The fundamental difference of the Neogene CCD (the phenomenon on which the CCD concept is based) and the Cretaceous "CCD" derives from the great importance of temperature stratification in the Neogene ocean, and of oxygenation in the Cretaceous ocean (Fig. 10). When mapping carbonate preservation patterns in the Cretaceous, therefore, a strong depth gradient cannot be assumed a priori. A statement that the CCD rose to the surface, for example, is not necessarily meaningful in the Cretaceous setting: dissolution can occur in shallow waters while carbonate deposition proceeds at depth.

If the delicate balance of oxyty in Cretaceous oceans holds the key to sedimentation patterns, we should ask how this balance is brought about. Why not widespread anaerobism?

The oxygen content of the water may be expressed as follows

$$x = x_o - A\,dx/dt \qquad (1)$$

where $x_o$ is the initial oxygen content, dx/dt is the rate of combustion, and A is the age of the water, that is the time span since it last equilibrated with the atmosphere. $x_o$ for Mid-Cretaceous deep waters may be taken as near 5 ml per liter of oxygen, assuming saturation. There is strong negative feedback on changes in A and dx/dt. The quotient dx/dt depends on the supply of organic carbon, which in turn depends on the rate of recycling of nutrients, which depends on the average value of A and on rates of decay. For large A, the quotient dx/dt becomes small: this is the first feedback mechanism tending to maintain a balance. Also, rates of decay decrease as x becomes small. A itself tends toward an equilibrium: at times of low circulation drive, stability also is low, and vice versa. Another important feedback mechanism involves sedimentation. If oxyty drops, organic matter is locked up in sediments together with nutrients (Broecker, 1969). Thus, dx/dt drops and oxygen depletion is retarded. Complete oxygen deficiency, therefore, is always a local or regional phenomenon involving nutrient influx (or carbon influx) from outside the system under study. The one exception to this rule is a temporary imbalance on the time scale of a few times A. A sudden increase of nutrient input, or of low salinity or high salinity water could create such an imbalance. This would happen if the ocean connects up to a previously closed basin such as the South Atlantic in the mid-Cretaceous or the Arctic at the end of the Cretaceous, by tectonic events.

If oxygen supply and oxygen uptake are indeed balanced so that overall anaerobism does not develop, we get

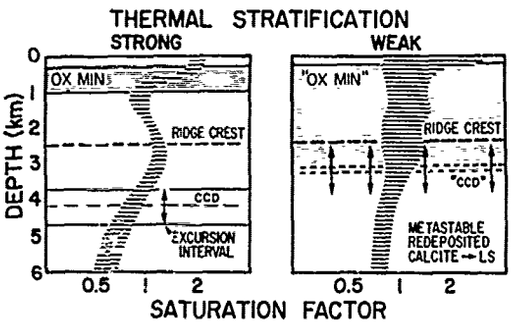


Fig. 10. Sketch of suggested general ranges of saturation profiles, in Neogene (left) and in mid-Cretaceous (right) time. Neogene characterized by high oxygen concentrations, upwelling at margins, high fertility, relatively stable CCD, high rates of chemical erosion, high rate of deposition. Mid-Cretaceous characterized by low oxyty, propensity for mid-ocean overturn, low fertility, unstable "CCD", low rates of chemical erosion, low rates of deposition. (Horizontally ruled area indicates general range of saturation profiles.)

$$x_o > A\ dx/dt, \quad \text{and } dx/dt < x_o/A$$

If A tends to equilibrium, while $x_o$ varies with temperature, the effect is that warming of an ocean will decrease the maximum possible productivity of the ocean, as reflected in dx/dt.

## A Focus for Paleoceanography

### The History of Productivity

According to A. Defant the central problem of oceanography is the circulation of the ocean, while according to G. G. Simpson the central problem of earth sciences is surely the evolution of life. Paleoceanography embraces both these viewpoints: the simple equation just discussed relates the fertility and chemistry to the physics of the ocean, and these, to paraphrase G. E. Hutchinson, provide the ecologic theater within which the drama of evolution can unfold.

There are two aspects to this drama, which are inherent in the earlier discussions of "trends" and "events". They are the general setting and its gradual change on the one hand, and the drastic revolutions in regimes on the other.

As regards the setting, the fertility of the ocean is the central problem of paleoceanography. This was recognized by Bramlette (1965) and emphasized especially by Tappan (1968). The history of the ocean must be read from the preserved record of shells, organic matter, and authigenic minerals. The fertility of the ocean is the primary agent responsible for the aspects and distribution of these deposits. The fertility gradient – together with the depth gradient – therefore provides a convenient way to classify marine sediments other than clastics (Olausson, 1966; Berger, 1976). The fertility level strongly influences the overall geochemical and biological activity. A low level allows the development of near-equilibrium ("Sillén Ocean"), while a high fertility level provides for disequilibrium ("Harvey Ocean"). On the whole, Neogene oceans represent the Harvey type, while Cretaceous oceans are close to the Sillén type (Figure 11). The Paleogene oceans represent a transition period.

The fundamental differences between a Sillén Ocean and a Harvey Ocean lie in the near-saturation with bio-substances (carbonate, silica, nutrients) in the former, and the pronounced undersaturation with bio-substances in the latter (Berger and Roth, 1975). Saturation favors preservation of precipitated matter and undersaturation favors redissolution (and hence reprecipitation).

In the Harvey Ocean, redissolution and reprecipitation allow for fractionation of carbonate from silica, phosphate and organic carbon. Consequently, in the Neogene, the different facies are nicely separated. In the Sillén Ocean, there is a tendency for biogenic precipitates to stay where they fell. This makes for interesting interlayering of carbonate, black shale and siliceous deposits.

Many of the Cretaceous marine deposits on land and in the deep ocean appear to be of a rhythmic or cyclic nature. Presumably this is a sign of amplification of small quasi-periodic disturbances in the chemistry and fertility of the ocean. In the absence of ice sheets or large land areas with their albedo feedback mechanisms, it is not immediately obvious how small input signals can be amplified. Variations in fertility -- increased productivity raises the albedo -- and associated changes in oxygenation and $pCO_2$ could provide such an amplification system.

### The Times of Crisis

The other, equally important aspect of evolution of the ocean and of its life is the punctuation of the marine record by major crises. On land, these times of crisis generally tend to be marked by hiatuses, a fact which originally facilitated the drawing of boundaries between the segments of Earth history. The true nature of the boundaries can best be determined in continuous sections from the deep sea.

Although all boundaries between the traditional Mesozoic and Cenozoic periods are worthy of scrutiny, the Cretaceous-Tertiary boundary has received the most attention. It is beyond the scope of this paper to review the evidence pertaining to this major break in evolution, and the wealth of arguments and speculations brought to bear on the problem. Here I wish merely to emphasize that purely oceanographic considerations can provide a testable hypothesis for this event as well as similar ones before and after.

The Cretaceous-Tertiary boundary was recently penetrated at two sites in the South Atlantic, apparently with recovery of a continuous record in both cases (Site 356, Leg 39, Premoli-Silva and Boersma, 1977; Perch-Nielsen, 1977; Site 384, Leg 43, Thierstein and Okada, in press). The boundary is characterized by wholesale extinction of a diverse calcareous nannofossil assemblage and replacement by a low diversity flora dominated by neritic forms (Thoracosphaera, and subsequently Braarudosphaera), as previously noted by Bramlette (1965). As is well known, and much discussed, all other plankton is greatly affected by the boundary event, as well as a host of marine and terrestrial creatures, from ammonites to dinosaurs (Béland et al., 1977).

The evidence from deep-sea drilling shows that the plankton extinction occurs within a very short time (Thierstein and Okada, in press), which makes Bramlette's (1965) starvation mechanism unattractive other than as an overall conditioning factor. The same criticism applies to all other gradualist explanations, such as changes in shelf area and other geographic configurations.

We are faced, then, with the necessity of explaining a geologically short, essentially catastrophic event.

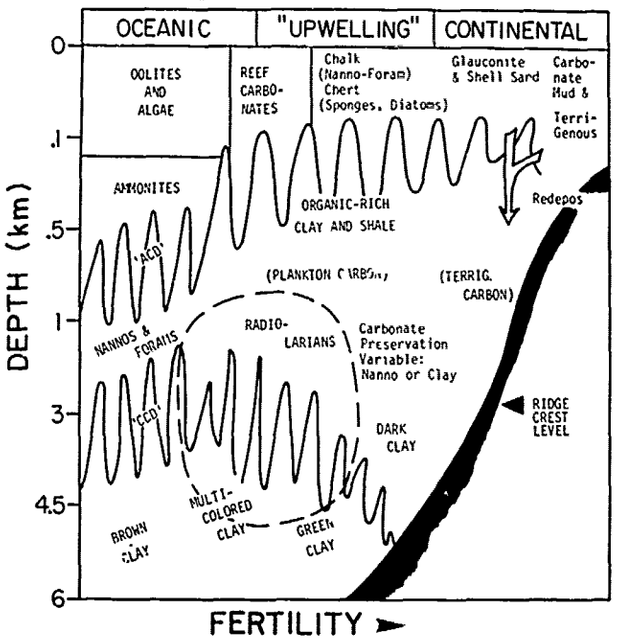


Fig. 11. Sketch of facies distribution in mid to late Cretaceous time, in a fertility-depth frame. Compiled and generalized from various sources.

How can a sudden global change be provided through a purely oceanographic mechanism, without resorting to extraterrestrial events? The most obvious way of changing the oceanographic setting rather quickly is to open or to close a passage between different ocean basins (Berggren and Hollister, 1974, 1977). To bring about a catastrophe for living things, however, the waters of one basin must be incompatible with the organisms in the other. We are looking, then, for an isolated basin which will swamp the global ocean with "bad" water.

There is, at the end of the Cretaceous, only one good candidate: the Arctic Basin. According to the reconstructions of Smith and Briden (1977), this basin was closed to the Atlantic and may have been closed to the Pacific at least below shelf depth. Also, according to Smith and Briden (1977), the Labrador Sea opened an access between the North Atlantic and the Arctic Sea during the latest Cretaceous and earliest Tertiary (Figure 12).

The implications of a geologically sudden opening of a seaway to a previously isolated Arctic have been pointed out by Gartner and Keany (1978a, b) and are discussed in some detail by Thierstein and Berger (1978). The following line of reasoning closely parallels their arguments.

The Arctic, as today, was in a position beyond the polar circle. The equability of late Cretaceous and early Tertiary climates excludes widespread ice formation, and demands transport of large amounts of heat into the area by the latent heat of precipitation, no strong ocean currents being available for heat transport. Thus, the surface waters of the Arctic had low salinity. Assume the Arctic was cut off from both the Pacific and the Atlantic, even briefly, during the latest Cretaceous regression. The Arctic would have developed into a freshwater lake. Its area presumably was about the same as now (Smith and Briden, 1977). If its volume also was the same, about 1.3 percent of the water of the oceans would have resided in a fresh water body (Sverdrup, Johnson, Fleming, 1942). If this water had been instantaneously available, say, within a few hundred years, it would have provided a thick layer of diluted seawater on the world ocean.

Assume the water has to be diluted to well below normal salinity, but not below 20 per mil or so, to allow survival of coastal forms of calcareous nannoplankton, as today in the Black Sea (Bukry, 1974). Assume further that this dilution has to include the photic zone, about 150 meters in clear ocean waters. An addition of 50 meters worth of fresh water, mixing to 150 meters, could produce the observed effects on oceanic plankton. The effect can be stretched out over several thousand years by providing only a small breach to begin with, with mixed fresh and saline waters entering

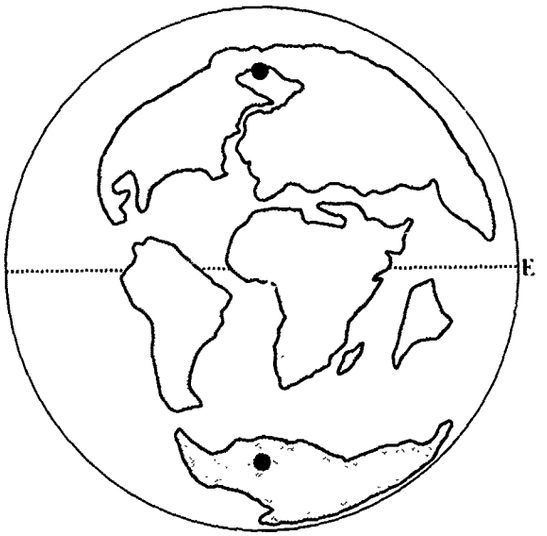


Fig. 12. Continental positions in early Paleocene, showing conditions favorable for isolation of the Arctic Ocean. From Smith and Briden (1977), simplified.

the Atlantic and using up part of the reservoir. Repeated isolation also would be possible. The crisis would come when the breach is wide and deep enough for catastrophic replacement of Arctic waters, by deep saline inflow from the Atlantic.

The effects on open ocean plankton from such an inflow of fresh water would be devastating, but not on coastal forms. Benthic organisms below the mixed layer would be unaffected, as observed (Douglas, 1973; L. Tjalsma, ps. comm., June, 1978). A strong oxygen minimum would develop ("boundary shale" of Percival and Fischer, 1977) and $CO_2$ would build up in the ocean as well as decrease in the atmosphere, as postulated for the deglaciation event (Berger, 1978). A strong warming in the tropics might be expected from the presence of a thin layer of water thermally isolated from the deep ocean, but a strong cooling, lasting perhaps no longer than a few hundred years, would be expected from a subsequent reduction of atmospheric $CO_2$. The ocean eventually would turn over and after another warming event (from addition of the $CO_2$ stored in deep waters, to the atmosphere), things would be much like before - except for exchange with the Arctic.

If the "extinction-by-low salinity" model should prove to be attractive - and the stable isotope record suggests that this is the case (Thierstein and Berger, 1978) - it will be worth considering the Eocene-Oligocene boundary under a similar aspect. Talwani and Eldholm (1977) show the Greenland Sea opening just about at boundary time, while the Labrador Passage had closed in the Eocene, according to Smith and Briden (1977). Within the Noegene, there is another analogous event, in this case involving an isolated saline basin (Hsü, Cita, Ryan, 1973; Cita and Ryan, 1973). Again, exchange with the world ocean of this isolated basin marks the end of a geologic period (the Miocene), again a fall of sea level appears to have triggered isolation (Adams et al., 1977). Taking this line of reasoning even further one might investigate the possibility that the major Phanerozoic mass extinctions, beginning with the Permian Termination were associated with injection of "bad" water from temporarily isolated basins (Berger and Thierstein, 1979).

Charting the productivity of the oceans through time, and defining in detail the exact sequence of events at the boundaries between the major segments of ocean history, is a major challenge. It is a challenge that needs to be taken up if we are to understand ocean circulation, ocean chemistry, the food chain structure, and the evolution of life in the sea and ultimately on the entire planet.

Acknowledgements. I thank M. Talwani and W. B. F. Ryan for inviting me to the second Maurice Ewing Symposium, which provided the opportunity for stimulating exchange of ideas with many fellow paleoceanographers. Concerning Cretaceous oceans, I profited greatly from discussions with H. R. Thierstein, D. Eicher, S.Gartner, E. Kauffman, and E. Stenestad.

Erle Kauffman's insistence on a "delicate balance" between oxygen supply and demand in shallow seas greatly strengthened my belief that a similar situation holds over large areas of the deep ocean. Erik Stenestad, several years ago, gave me a personal guided tour of the type-Danian and the Cretaceous-Tertiary boundary at Stevn's Klint. He introduced me to the mysterious "fiskeler", the phosphatic and pyritiferous clay which marks the boundary, and which calls for a major short-lived change in oceanographic conditions. The concept of Arctic injection during the terminal Cretaceous derives from Steve Gartner's suggestion, at the Maurice Ewing Symposium, that the Cretaceous-Tertiary nannofossil record in the North Sea region indicates repeated large-scale invasion of low salinity water from the Arctic. The ensuing discussion with Gartner on the significance of a global low salinity layer as a possible cause for extinction of ocean plankton and other marine life, prompted me to pursue the matter. The expansion of the injection concept to a general mechanism for boundary events, and the exploration of the various analogies between the (hypothetical) deglacial meltwater event, and the (hypothetical) Arctic injection events are a result of collaboration with H. R. Thierstein. Thanks are due also to Tj. H van Andel, J. Thiede, and H. R. Thierstein for reading the manuscript in draft, and for making much appreciated suggestions for improvement.

Last, but not least, I thank all those col-

leagues who have labored hard in and out of committee to make deep-sea drilling a reality. Without their devotion there would be nothing to talk about.

## References


Adams, C. G., R. H. Benson, R. B. Kidd, W. B. F. Ryan, and R. C. Wright, The Messinian salinity crisis and evidence of late Miocene eustatic changes in the world ocean, Nature, 269, 383-386, 1977.

Anati, D., and H. Stommel, The initial phase of deep water formation in the Northwest Mediterranean, during MEDOC '69, on the basis of observations made by "Atlantis II", Cahiers Oceanographiques, 22, 343-351, 1970.

Arrhenius, G., Sediment cores from the East Pacific: Rept. Swedish Deep-Sea Exped. 1947-1948, v.5 1-228, 1952.

Béland, P., P. Feldman, J. Foster, D. Jarzen, G. Norris, K. Pirozynski, G. Reid, J.-R. Roy, D. Russell, and W. Tucker, Cretaceous-Tertiary extinctions and possible terrestrial and extraterrestrial causes, Nat. Mus. Canada, Syllogeus, No. 12, 162, 1977.

Berger, W. H., Planktonic foraminifera: selective solution and the lysocline, Marine Geology,8, 111-138, 1970a.

Berger, W. H., Biogenous deep-sea sediments: fractionation by deep-sea circulation, Geol. Soc. Amer. Bull., 81, 1385-1402, 1970b.

Berger, W. H., Deep-sea carbonates: dissolution facies and age-depth constancy, Nature, 236, 392-395, 1972.

Berger, W. H., Cenozoic sedimentation in the eastern tropical Pacific, Geol. Soc. Amer. Bull., 84, 1941-1954, 1973.

Berger, W. H., Biogenous deep-sea sediments: production, preservation and interpretation, In, Treatise on Chemical Oceanography, v. 5, pp. 265-388, (J. P. Riley and R. Chester, Eds.) Academic Press, London, 1976.

Berger, W. H., Carbon dioxide excursions and the deep sea record: aspects of the problem, In The Fate of Fossil Fuel $CO_2$ in the Oceans, pp. 505-542 (N. R. Andersen and A. Malahoff, Eds.) Plenum Press, New York, 1977.

Berger, W. H., Oxygen-18 stratigraphy in deep-sea sediments: additional evidence for the deglacial meltwater effect, Deep-Sea Res., 25, 473-480, 1978.

Berger, W. H., and P. H. Roth, Oceanic micropaleontology: progress and prospect, Review Geophys. Space Phys., 13, 561-585, 624-635, 1975.

Berger, W. H., and A. Soutar, Preservation of plankton shells in an anaerobic basin off California, Geol. Soc. Amer. Bull., 81, 275-282, 1970.

Berger, W. H., and H. R. Thierstein, On Phanerozoic mass extinctions, Naturwissenschaften, in press, 1979.

Berger, W. H., and U. von Rad, Cretaceous and Cenozoic sediments from the Atlantic Ocean, Initial Repts. Deep Sea Drilling Proj., v. 14, pp. 787-954, U.S. Gov. Printing Office, Washington, D. C., 1972.

Berger, W. H., and E. L. Winterer, Plate stratigraphy and the fluctuating carbonate line, In, Pelagic sediments on land and under the sea Spec. Pub. Internat. Assoc. Sediment., v. 1, pp. 11-48, (K. J. Hsü and H. Jenkyns, Eds.) 1974.

Berggren, W. A., Paleogene planktonic foraminifera faunas on Legs I-IV (Atlantic Ocean), JOIDES Deep Sea Drilling Program; a synthesis, 2nd Internat. Conf. Planktonic Microfossils, Proc. V. 1, 57-66, 1971.

Berggren, W. A., Late Pliocene-Pleistocene glaciation. Init. Repts. Deep Sea Drilling Proj., v. 12, pp. 953-963, U. S. Gov. Printing Office, Washington, D. C., 1972.

Berggren, W. A., and C. D. Hollister, Paleogeography, paleobiogeography and the history of circulation in the Atlantic Ocean, In Studies in paleo-oceanography, Soc. Econ. Paleont. Mineral, Spec. Publ. 20, pp. 126-186 (W. W. Hay, Ed.), 1974.

Berggren, W. A., and C. D. Hollister, Plate tectonics and paleocirculation - commotion in the ocean, Tectonophysics, 38, 11-48, 1977.

Berner, R. A., Physical chemistry of carbonates in the oceans, In, Studies in Paleo-oceanography, Soc. Econ. Paleont. Mineral Spec. Publ., 20, pp. 37-43 (W. W. Hay, Ed.) 1974.

Bowen, R., Paleotemperature analysis, 265 pp., Elsevier, Amsterdam, 1966.

Bramlette, M. N., The Monterey Formation of California and the origin of its siliceous rocks. U. S. Geol. Surv. Prof. Paper 212, 1-57, 1946.

Bramlette, M. N., Pelagic sediments, In, Oceanography, 345-366 (M. Sears, Ed.), Amer. Assoc. Advancement of Sci. Publ. No. 67, 1961.

Bramlette, M. N., Massive extinctions in biota at the end of Mesozoic time, Science, 148, 1696-1699, 1965.

Broecker, W. S., Why the deep sea remains aerobic, Geol. Soc. Amer. Program with Abstracts 1969, 20, 1969.

Broecker, W. S., Chemical Oceanography, 214 pp., Harcourt, Brace, Jovanovich, New York, 1974.

Broecker, W. S., and T. Takahashi, The relationship between lysocline depth and in situ carbonate ion concentration, Deep-Sea Res, 25, 65-95, 1978.

Bukry, D., Coccoliths as paleosalinity indicators - evidence from the Black Sea, In, The Black Sea. Its Geology, Chemistry and Biology: Am. Assoc. Pet. Geol., Mem. 20, pp. 353-363 (E. T. Degens and D. A. Ross, Eds.), 1974.

Chamberlin, T. C., On a possible reversal of deep-sea circulation and its influence on geologic climates, Jour. Geology, 14, 363-373, 1906.

Cita, M. B., Paleoenvironmental aspects of DSDP Legs I-IV: Planktonic Conf., Proc. No. 2, v. 1, 251-275, 1971.

Cita, M. B., and W. B. F. Ryan, Time scale and

general synthesis, Init. Repts. Deep Sea Drilling Proj., 13, pp. 1405-1415, U. S. Gov. Printing Office, Washington, D. C., 1973.

CLIMAP Project Members, The surface of the Ice-Age Earth, Science, 191, 1131-1137, 1976.

Cline, R. M., and J. D. Hays, (Eds.), Investigation of Late Quaternary Paleoceanography and Paleoclimatology, Geol. Soc. Amer. Memoir 145, 1-464, 1976.

Davies, T. A., and P. R. Supko, Oceanic sediments and their diagenesis: some examples from deep sea drilling, J. Sediment. Petrol, 3, 381-390, 1973.

Davies, T. A., W. W. Hay, J. R. Southam, and T. R. Worsley, Estimates of Cenozoic oceanic sedimentation rates, Science, 197, 53-55, 1977.

Dean, W. E., J. V. Gardner, L. F. Jansa, P. Cepek, and E. Seibold, Cyclic sedimentation along the continental margin of Northwest Africa, Init. Repts. Deep Sea Drilling Proj., 41, 965-989, U. S. Gov. Printing Office, Washington, D. C., 1978.

Douglas, R. G., Benthonic foraminiferal biostratigraphy in the central North Pacific, Leg 17, DSDP, Init. Repts. Deep Sea Drilling Project, 17, 607-672, U. S. Gov. Printing Office, Washington, D. C., 1973.

Douglas, R. G., and S. M. Savin, Isotopic analysis of planktonic foraminifera from the Cenozoic of the Northwest Pacific, Leg 6, Init. Repts. Deep Sea Drilling Project, v. 6, 1123-1127, U. S. Gov. Printing Office, Washington, D. C., 1971.

Douglas, R. G., and S. M. Savin, Oxygen and carbon isotope analyses of Tertiary and Cretaceous microfossils from Shatsky Rise and other sites in the North Pacific Ocean, Init. Rept. Deep Sea Drilling Proj, v. 32, 509-520, U. S. Gov. Printing Office, Washington, D. C., 1975.

Edmond, J. M., On the dissolution of carbonate and silicate in the deep ocean, Deep-Sea Res., 21 455-480, 1974.

Emiliani, C., Temperatures of Pacfiic bottom waters and polar superficial waters during the Tertiary, Science, 119, 853-855, 1954.

Ewing, M. and W. L. Donn, A theory of ice ages, Science, 123, 1061-1066, 1956.

Ewing, M., J. L. Worzel, A. O. Beall, W. A. Berggren, D. Bukry, C. A. Burk, A. G. Fischer, and E. A. Pessagno, Initial Repts. of the Deep Sea Drilling Proj., v. 1, 672 pp., U. S. Gov. Printing Office, Washington, D. C., 1969.

Fischer, A. G., and M. A. Arthur, Secular variations in the pelagic realm, SEPM Special Publ. 25, 19-50, 1977.

Förster, R., Evidence for an open seaway between northern and southern proto-Atlantic in Albian times, Nature, 272, 158-159, 1978.

Frerichs, W. E., Evolution of planktonic foraminifera and paleotemperatures, Jour. Paleo, 45, 963-968, 1971.

Gartner, S., and J. Keany, The terminal Cretaceous event: an oceanographic solution for a geological puzzle, Geol. Soc. Amer. Abstr. w. Programs, 10, 406, 1978a.

Gartner, S., and J. Keany, The terminal Cretaceous event: a geologic problem with an oceanographic solution, Geology, 6, 708-712, 1978b.

Gibson, T. G., and K. M. Towe, Eocene volcanism and the origin of Horizon A, Science, 172, 152-154, 1971.

Habib, D., Middle Cretaceous palynomorphs in a deep-sea core from the seismic reflector Horizon A outcrop area, Micropaleontology, 15, 85-101, 1969.

Haq, B. U., Transgressions, climatic changes and the diversity of calcareous nannoplankton, Marine Geology, 15, 25-30, 1973.

Haq, B. U., I. Premoli-Silva, and G. P. Lohmann, Calcareous plankton paleobiogeographic evidence for major climatic fluctuations in the early Cenozoic Atlantic Ocean, J. Geophys. Res., 82, 3861-3876, 1977.

Hay, W. W., 1970, Calcium carbonate compensation: Initial Repts. Deep Sea Drilling Proj., v. 4, 669 and 672, U. S. Gov. Printing Office, Washington, D. C., 1970.

Hay, W. W., Calcareous nannofossils - Legs I-IV-Deep Sea Drilling Proj., 2nd Planktonic Conf. Proc., Roma, 1970, Edizione Tecnosienza, 607-609, 1971.

Heath, G. R., Carbonate sedimentation in the abyssal Equatorial Pacific during the past 50 million years, Geol. Soc. Amer. Bull., 80, 689-694, 1969.

Heath, G. R., T. C. Moore, and T. H. van Andel, Carbonate accumulation and dissolution in the equatorial Pacific during the past 45 million years, In, The Fate of Fossil Fuel $CO_2$ in the Oceans, pp. 627-639 (N. R. Andersen and A. Malahoff, Eds) Plenum Press, New York, 1977.

Heezen, B. C., I. D. MacGregor, H. P. Foreman, G. Forristal, W. Hekel, R. Hesse, R. H. Hoskins, E. J. W. Jones, A. Kaneps, V. A. Krasheninnikoy, H. Okada, and M. H. Ruff, Diachronous deposits: a kinematic interpretation of the post-Jurassic sedimentary sequence on the Pacific plate, Nature, 241, 25-32, 1973.

Heirtzler, J. R., G. O. Dickson, E. J. Herron, W. C. Pitman, and X. Le Pichon, Marine magnetic anomalies, geomagnetic field reversals, and the motions of the ocean floor and continents, J. Geophys. Res., 73, 2119-2136, 1968.

Heirtzler, J. R., H. M. Bolli, T. A. Davies, J. B. Saunders, and J. G. Sclater (eds.), Indian Ocean Geology and Biostratigraphy, American Geophys. Union, Washington, D. C. 616 pp., 1977

Hsü, K. J., and J. E. Andrews, History of South Atlantic Basin, Init. Rept. Deep Sea Drilling Proj, v. 3, 464-467, U. S. Gov. Printing Office, Washington, D. C., 1970.

Hsü, K. J., M. B. Cita, and W. B. F. Ryan, The origin of the Mediterranean evaporites, Init. Repts. Deep Sea Drilling Proj. v. 13, 1203-1231, U. S. Gov. Printing Office, Washington, D. C., 1973.

Isacks, B., J. Oliver, and L. R. Sykes, Seismology

and the new global tectonics, J. Geophys. Res., 73, 5855-5899, 1968.

Karig, E. D., Basin genesis in the Philippine Sea, Init. Repts. Deep Sea Drilling Proj. v. 31, 857-879, U. S. Gov. Printing Office, Washington, D. C., 1975.

Kauffman, E., Cretaceous: Treatise on Invertebrate Paleontology, Pt. A., Univ. of Kansas Press and Geol. Soc. America, in press.

Kennett, J. P., Cenozoic evolution of Antarctic glaciation, the Circum-Antarctic Ocean, and their impact on global paleoceanography, J. Geophys. Res., 82, 3843-3860, 1977.

Kennett, J. P., and N. J. Shackleton., Oxygen isotopic evidence for the development of the psychrosphere 38 m.y. ago, Nature, 260, 513-515, 1976.

Kennett, J. P., and R. C. Thunnell, Global increase in Quaternary explosive volcanism, Science, 187, 497-504, 1975.

Kroopnick, P. M., S. V. Margolis, and C. S. Wong, $\delta^{13}C$ variations in marine carbonate sediments as indicators of the $CO_2$ balance between the atmosphere and oceans, in, The Fate of Fossil Fuel $CO_2$ in the Oceans, pp. 295-321 (N. R. Andersen and A. Malahoff, Eds) Plenum Press, New York, 1977.

Lancelot, Y., J. C. Hathaway, and C. D. Hollister, Lithology of sediments from the western North Atlantic, Leg XI, Deep Sea Drilling Project, Init. Repts. Deep Sea Drilling Proj., v. 11, 901-949, U. S. Gov. Printing Office, Washington, D. C., 1972.

Li, Y.-H., T. Takahashi, and W. S. Broecker, Degree of saturation of $CaCO_3$ in the oceans. J. Geophys. Res., 74, 5507-5525, 1969.

Moore, T. C., Deep Sea Drilling Project: successes, failures, proposals, Geotimes, 17, 27-31, 1972.

Moore, T. C., and G. R. Heath, Survival of deep-sea sedimentary sections, Earth Planet. Sci. Letters, 37, 71-80, 1977.

Munk, W. H., Abyssal recipes, Deep-Sea Res., 13 707-730, 1966.

Nierenberg, W. A. (Investigator), Drilling of sediments and shallow basement rocks in the Pacific and Atlantic Oceans and adjacent seas. Proposal for Research to the National Science Foundation, University of California, San Diego, UCSD 1581 (open file, DSDP), 1965.

Nierenberg, W. A. (Investigator), Drilling of sediments and shallow basement rocks in the Pacific and Atlantic Oceans and adjacent seas. Proposal for Research to the National Science Foundation, University of California, San Diego, UCSD-2854, (open file, DSDP), 1969.

Nierenberg, W. A., and M. N. A. Peterson (Investigators), Drilling of sediments and shallow basement rocks in the Pacific and Atlantic Oceans and Adjacent Seas. Proposal for Research to the National Science Foundation, University of California, San Diego, UCSD-4405 (open file, DSDP), 1971.

Olausson, E., Calcareous oozes, In, The Encyclopedia of Oceanography, pp. 76-78, (R. W. Fairbridge, Ed.), Reinhold, New York, 1966.

Perch-Nielsen, K., Albian to Pleistocene calcareous nannofossils from the western South Atlantic, DSDP Leg 39, Init. Repts. Deep Sea Drilling Proj., v. 39, 699-823, U. S. Gov. Printing Office, Washington, D. C., 1977.

Percival, S.F., and A. G. Fischer, Changes in calcareous nannoplankton in the Cretaceous-Tertiary biotic crisis at Zumaya, Spain, Evol. Theory, 2, 1-35, 1977.

Peterson, M. N. A. (Investigator), Drilling of sediments and shallow basement rocks in the Pacific and Atlantic Oceans, and Adjacent Seas. Proposal for Research to the National Science Foundation, University of California, San Diego, UCSD-6297 (open file, DSDP), 1973.

Peterson, M. N. A. (Investigator), Drilling of sediments and shallow basement rocks in the Atlantic Ocean and adjacent seas. Proposal for Research to the National Science Foundation, University of California, San Diego, UCSD-0862 (open file, DSDP), 1977.

Peterson, M. N. A., N. T. Edgar, C. C. von der Borch, and R. W. Rex, Cruise leg summary and discussion, Init. Repts. Deep Sea Drilling Proj., v. 2, 413-427, U. S. Gov. Printing Office, Washington, D. C., 1970.

Premoli-Silva, I., and A. Boersma, Cretaceous planktonic foraminifers - DSDP Leg 39 (South Atlantic), Init. Repts. Deep Sea Drilling Proj., v. 39, 615-641, U. S. Gov. Printing Office, Washington, D. C., 1977.

Ramsay, A. T. S., N. Schneidermann, and J. W. Finch, Fluctuations in the past rates of carbonate solution in Site 149: a comparison with other ocean basins and an interpretation of their significance, Init. Repts. Deep Sea Drilling Proj., v. 15, 805-811, U. S. Gov. Printing Office, Washington, D. C., 1973.

Riedel, W. R., and B. M. Funnell, Tertiary sediment cores and microfossils from the Pacific Ocean floor, Quat. J. Geol. Soc., London, 120, 305-368, 1964.

Roth, P. H., Calcareous nannofossils from the northwestern Indian Ocean, Leg 24, Deep Sea Drilling Project, Init. Repts. Deep Sea Drilling Proj., 24, 969-994, 1974.

Ryan, W. B. F., and M. B. Cita, Ignorance concerning episodes of ocean-wide stagnation, Marine Geology, 23, 197-215, 1977.

Savin, S. M., The history of the Earth's surface temperature during the past 100 million years. Ann. Rev. Earth Planet. Sci., 5, 319-355, 1977.

Savin, S. M., R. G. Douglas, and F. G. Stehli, Tertiary marine paleotemperatures. Geol. Soc. Amer. Bull., 86, 1499-1510, 1975.

Schlanger, S. O., and H. C. Jenkyns, Cretaceous oceanic anoxic events: causes and consequences. Geologie en Mijnbouw, 55, 179-184, 1976.

Sclater, J. G., R. N. Anderson, and M. L. Bell, Elevation of ridges and evolution of the central eastern Pacific, Jour. Geophys. Res., 76, 7888-7915, 1971.

Shackleton, N. J., and J. P. Kennett, Paleotempera-

ture history of the Cenozoic and the initiation of Antarctic glaciation: oxgyen and carbon isotope analyses in DSDP Sites 277, 279, and 281. Init. Repts. Deep Sea Drilling Proj., v. 29, 743-755, 1975.

Smith, A. G., and J. C. Briden, Mesozoic and Cenozoic Paleocontinental Maps, 66 pp., Cambridge Univ. Press, Cambridge, 1977.

Sverdrup, H. U., On conditions for the vernal blooming of phytoplankton, J. Cons. Int. Explor. Mer, 18, 287-295, 1953.

Sverdrup, H. U., M. W. Johnson, and R. H. Fleming, The oceans, their physics, chemistry, and general biology, 1087 pp., Prentice-Hall, Englewood Cliffs, N. Y., 1942.

Talwani, M., and O. Eldholm, Evolution of the Norwegian-Greenland Sea, Geol. Soc. Amer. Bull., 88, 969-999, 1977.

Iappan, H., Primary production, isotopes, extinctions and the atmosphere, Paleogeogr. Paleoclimatol. Paleoecol., 4, 187-210, 1968.

Thiede, J., and T. H. van Andel, The paleoenvironment of anaerobic sediments in the Late Mesozoic South Atlantic Ocean, Earth Planet. Sci. Letters, 33, 301-309, 1977.

Thierstein, H. R., and W. H. Berger, Injection events in ocean history, Nature, 276, 461-466, 1978.

Thierstein, H. R., and H. Okada, The Cretaceous/Tertiary boundary event in the North Atlantic, Init. Repts. Deep Sea Drilling, v. 43, in press.

van Andel, T. H., Deep-sea drilling for scientific purposes: a decade of dreams, Science, 160, 1419-1424, 1968.

van Andel, T. H., Mesozoic/Cenozoic calcite compensation depth and the global distribution of calcareous sediments, Earth Planet. Sci. Letters, 26, 187-194, 1975.

van Andel, T. H., and G. R. Heath, Geological results of Leg 16: the Central Equatorial Pacific west of the East Pacific Rise, Init. Repts. Deep Sea Drilling Proj., v. 16, 937-949, 1973.

van Andel, T. H., and T. C. Moore, Cenozoic calcium carbonate distribution and calcite compensation depth in the central equatorial Pacific, Geology, 2, 87-92, 1974.

van Andel, T. H., G. R. Heath, and T. C. Moore, Cenozoic history and paleo-oceanography of the Central Equatorial Pacific Ocean, Geol. Soc. Am. Memoir 143, 1-134, 1975

van Andel, T. H., J. Thiede, J. G. Sclater, and W. W. Hay, Depositional history of the South Atlantic Ocean during the last 125 million years, J. Geology, 85, 651-698, 1977.

von Herzen, R. P., and A. E. Maxwell, Sea floor spreading, Init. Repts. Deep Sea Drilling Proj., v. 3, 459-464, U. S. Gov. Printing Office, Washington, D. C., 1970.

Vine, F. J., Spreading of the ocean floor: new evidence, Science, 154, 1405-1415, 1966.

Wefer, G., Umwelt, Produktion und Sedimentation benthischer Foraminiferen in der westlichen Ostsee, Dissertation, Universität Kiel, 104 pp, 1976.

Winterer, E. L., Sedimentary facies and plate tectonics of Equatorial Pacific, Amer. Assoc. Petrol. Geol. Bull., 57, 265-282, 1973.

Wise, S. W., and K. J. Hsü, Genesis and lithification of a deep sea chalk, Eclogae Geological Helvetiae, 64, 273-278, 1971.

Wise, S. W., and K. R. Kelts, Inferred diagenetic history of a weakly silicified deep sea chalk, Gulf Coast Assoc. Geol. Soc. Trans., 22, 177-203, 1972.

Worsley, T. R., The terminal Cretaceous event, Nature, 230, 318-320, 1971.

Wyrtki, K., The thermohaline circulation in relation to the general circulation in the oceans, Deep-Sea Res., 8, 39-64, 1961.

# SILICA DIAGENESIS IN THE ATLANTIC OCEAN: DIAGENETIC POTENTIAL AND TRANSFORMATIONS

Volkher Riech and Ulrich von Rad

Bundesanstalt für Geowissenschaften und Rohstoffe (Federal Institute for Geosciences and Natural Resources), D 3000 Hannover 51, F.R. Germany

Abstract. We studied biosiliceous and volcanogenic sediments in all Atlantic DSDP sites and the decrease of their diagenetic potential during the transformations of skeletal opal and volcanic glass into authigenic silica and silicates in response to age, burial depth, and lithofacies.

The distribution of biogenic and authigenic silica in Early Cretaceous to Neogene sediments (Fig. 5) is mainly controlled by variations of basin geometry (sea floor spreading), paleocirculation (upwelling) and paleoclimate.

High plankton productivity and sedimentation rates favor the preservation of biogenic opal and later diagenetic transformations after the dissolution of the skeletons. The intensity of the dissolution of biogenic opal correlates often positively with the proportion of authigenic silica and silicates. In Atlantic sediments, clinoptilolite and opal-CT (disordered low-temperature cristobalite/tridymite) are associated with siliceous organisms, whereas the alteration of volcanic glass leads to the precipitation of authigenic smectite and phillipsite and not to the formation of porcellanites. Opal-CT which crystallizes from solution during intermediate diagenesis after an early calcite cement generation is always the first authigenic silica phase formed during silicification. At the same time accessory quartz is directly precipitated in porcellanites and fills voids or replaces calcitic fossils. Genuine quartz cherts were never formed without an opal-CT precursor.

In general, silica diagenesis proceeds as a maturation from biogenic opal (opal-A)→opal-CT→quartz. This is supported by the lack of quartz cherts in post-Eocene sediments and by pseudomorphs after opal-CT spherules in quartz cherts. The rate of these transformations depends mainly on the rate of dissolution of biogenic opal which controls the concentration of dissolved interstitial silica and on the rate of solid-state structural ordering of opal-CT which promotes the reorganization to quartz.

In general, the transition from opal-A to opal-CT goes through a solution step. On the other hand, opaline skeletons may also be transformed *in situ* into opal-CT. Quartz, however, appears to be formed from opal-CT by a "quasi-solid-solid" microstructural conversion. This is evident from well-preserved quartz-replaced opal-CT spherules and skeletons.

Although age/burial depth diagrams (Fig.10,11) show a wide overlap of the stability fields of opal-A, opal-CT and quartz, a general positive correlation of the "maturity" of the silica phases with those parameters is indicated. Surprisingly, primary opal-A, opal-CT and quartz occur together in Paleocene/Eocene sediments. In the Pacific the overlap of opal-CT porcellanites and quartz cherts is more distinct than in the Atlantic. This marked discontinuity of silica diagenesis (i.e. the alternation of opal-A sediments and porcellanites or of porcellanites and quartz cherts) resembles carbonate diagenesis, where local reversals in the degree of lithification with increasing burial depth are a common phenomenon.

The youngest opal-CT occurs sporadically in diatomaceous and ashy sediments of Pliocene and Miocene age. However, silicification becomes more significant in 30-40 m.y. old rocks. The conversion of biogenic opal to authigenic opal-CT is slightly accelerated in carbonate host rocks, whereas clayey facies retards the opal-CT→quartz transformation considerably. But in many cases the mode and rate of silica transformations cannot be sufficiently explained by the factors time, burial depth, temperature, and host rock facies alone.

## Introduction

The detailed study of Deep Sea Drilling samples during the past decade has yielded many new insights into silica diagenesis which could not be gained from investigations of silicified sediments exposed on land.

As age, burial depth or temperature, pore water chemistry and lithofacies of these deep-sea sediments vary widely, all progressive diagenetic conversion stages of the original unstable biogenic or volcanogenic silica to porcellanites and authigenic silicates, and finally

Table 1. Mineralogical and genetic classification of silicified sediments. Transitions between A,B, and C are common.

| |
|---|
| A. "IMMATURE" WEAKLY SILICIFIED ("PORCELLANEOUS" SEDIMENTS: < 50% authigenic $SiO_2$, generally opal-CT >> quartz<br>opal-A : siliceous fossils partly preserved<br>opal-CT : impregnation or replacement of matrix, pore filling, in situ transformation of siliceous skeletons<br>diag.qtz: mostly replacing foraminifera, not in matrix |
| B. PORCELLANITES: > 50% $SiO_2$<br>opal-CT >> quartz<br>opal-A : dissolved and/or replaced by opal-CT (in situ)<br>opal-CT : predominant (in matrix and pores)<br>diag.qtz: minor amounts, filling and replacing fossils |
| C. "MATURE" QUARTZ CHERTS<br>>> 50% authigenic silica:<br>quartz >> opal-CT; no opal-A. |

to quartz cherts can be investigated under the widest possible range of natural conditions. During this process the "diagenetic potential" (Schlanger and Douglas, 1974) decreases from a maximum value (e.g. in siliceous oozes) to zero (in quartz cherts).

Diagenesis complicates the interpretation of the depositional conditions of sedimentary sequences, because it destroys paleoenvironment indicators and leads to the formation of new minerals and rock types. Hence, the investigation of these neoformations is directed towards (1) the recognition of the silica sources, (2) the relationship of the depositional paleoenvironment (e.g. siliceous oozes under upwelling conditions) and the present " diagenetic facies", and (3) the nature and causes of the silicification processes.

One of the major controversies in this field is the role that the lithofacies of associated sediments may play in determining the nature and rate of diagenetic silica transformations.

Publications on biogenic and authigenic silica in the Pacific and Indian Oceans are numerous (e.g. Heath and Moberly, 1971; Weaver and Wise, 1972; Heath, 1973; Lancelot, 1973; Leclaire, 1974; Johnson, 1974; Keene, 1975; Garrison et al., 1975; Kelts, 1976; Hein et al., 1978), and Keene (1976) has written a very complete synthesis on silica diagenesis in the Pacific Basin. The literature on the Atlantic Ocean, however, is very scattered (e.g. Calvert, 1971; 1974; 1977; Berger and von Rad, 1972; Wise et al., 1972; Greenwood, 1973; von Rad and Rösch, 1974; Wise and Weaver, 1974).

Therefore, we have attempted to summarize in this paper the results of our own petrographical and mineralogical investigation of 34 North Atlantic DSDP Sites from Legs 1-3. 11-14 (von Rad and Rösch,1974, and unpublished data), 41 (von Rad et al., 1977), 43 (Riech and von Rad, in press), 47 (Riech, in press(1)) and 50 (Riech, in press (2)). We have discussed and synthesized also the published data from the remaining 54 Atlantic DSDP Sites containing authigenic and/or biogenic silica (Fig. 5, Table 2).

Whereas our petrographical approach to silica diagenesis is strictly empirical, other researchers have investigated selected chemical and physical properties and diagenetic factors (e.g. time, temperature, pore water chemistry) by experiments (e.g. Hurd and Theyer, 1977; Ernst and Calvert, 1969; Stein and Kirkpatrick, 1976; Flörke et al., 1975; and especially Kastner et al., 1977). Only a combination of these efforts will help to solve the open questions in this field.

## Analysis and Classification of Silicified Sediments

The three principal pure silica phases present in deep-sea sediments are (1) amorphous opal-A, (2) metastable opal-CT (disordered low-temperature cristobalite/tridymite), and (3) stable quartz (nomenclature after Jones and Segnit, 1971). Figure 1 shows typical SEM photos of the three modifications and describes their mineralogy, ultrastructure, and genesis. We did not identify an inorganic $SiO_2$-phase "opal-A'" (Hein et al., 1978).

The silica varieties were determined by optical, scanning electron microscope (SEM) and X-ray diffraction analyses (XRD), described in von Rad and Rösch (1974) and von Rad et al. (1977). Since it is difficult to distinguish by XRD opal-A from other X-ray amorphous matter, the mineralogical composition of siliceous skeletons was studied by measuring refractive indices.

Our classification of silicified sediments (Table 1) is mainly based on a semiquantitative estimate of silica mineralogy by optical and/or XRD analysis. Genetically, we differentiate between "bedded" varieties in clayey or siliceous environments, and "nodular" types (or "flints"), characteristic for calcareous sediments. In agreement with Calvert (1971, 1977), we use the term "porcellanite" strictly in a mineralogical sense (silica content > 50% with opal-CT > quartz), and not as a field term for a siliceous rock which is less hard, dense, and vitreous than chert (Bramlette, 1946; Keene, 1976).

## Source Material

Figure 2 shows the cycle of dissolved silicon in the oceans (Calvert, 1974; Heath, 1974). The main input of dissolved silicon comes from the continents or as reflux from the interstitial waters into the overlying water column. Volcanic

Table 2. Distribution, abundance and burial depth of biogenic silica, volcanic debris, and authigenic silica and silicates (accessory opal-CT, porcellanites, quartz cherts, zeolites) of all silica-bearing DSDP Sites in the Atlantic Ocean (Legs 1-51). * = Sites investigated by the authors; data for other sites compiled from the Initial Reports and Initial Core Descriptions of the Deep Sea Drilling Project. CA= Caribbean; GM= Gulf of Mexico; NW,NE,SW= Northwest, Northeast, Southwest Atlantic. b.d. = burial depth of authigenic silica (in meters), opal-CT= accessory opal-CT, porc. = porcellanites, silicified r. = silicified rocks (porcellanite and/or quartz chert), sp.sp.= sponge spicules, volc. mat. = volcanic material.

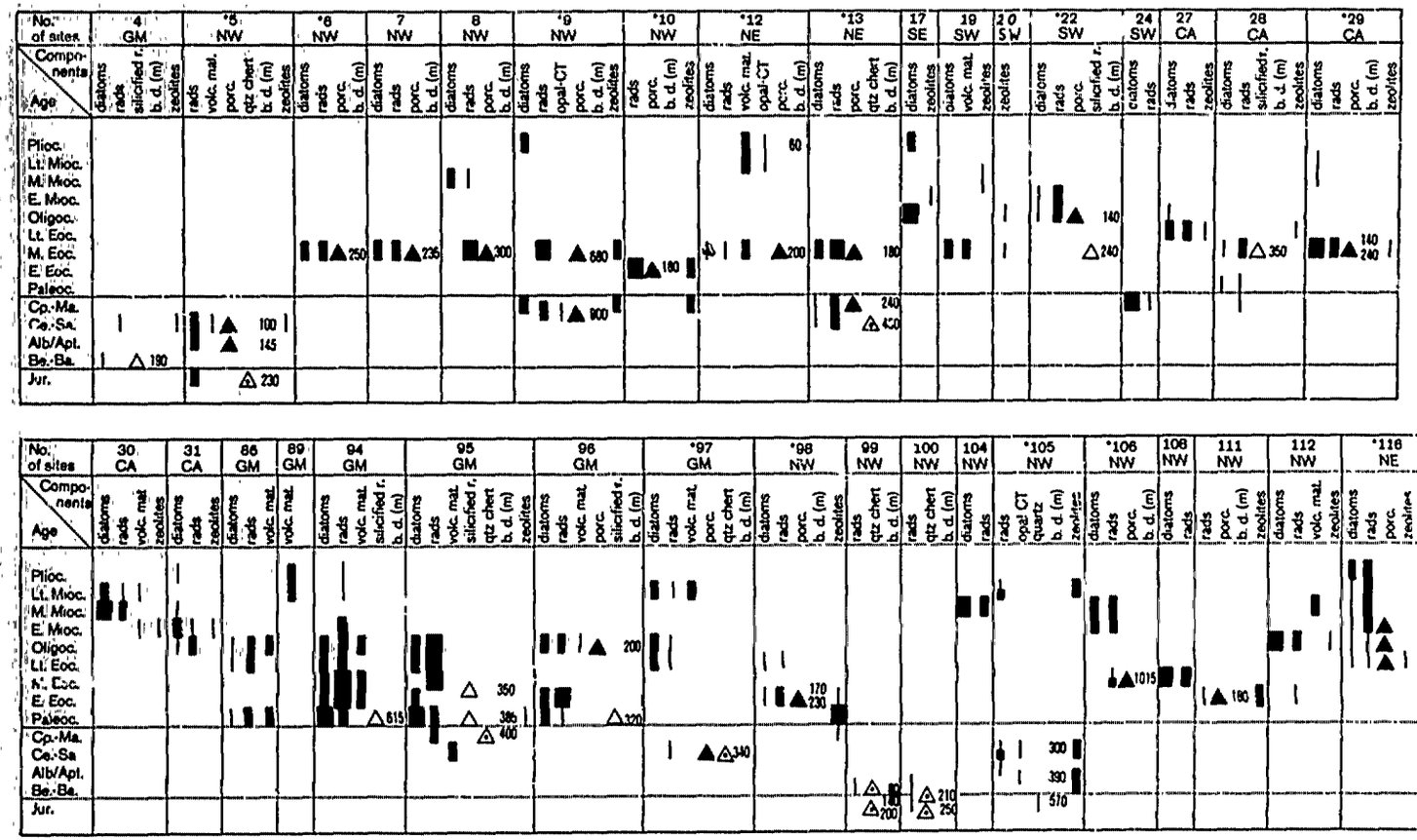

Table 2 - Continued

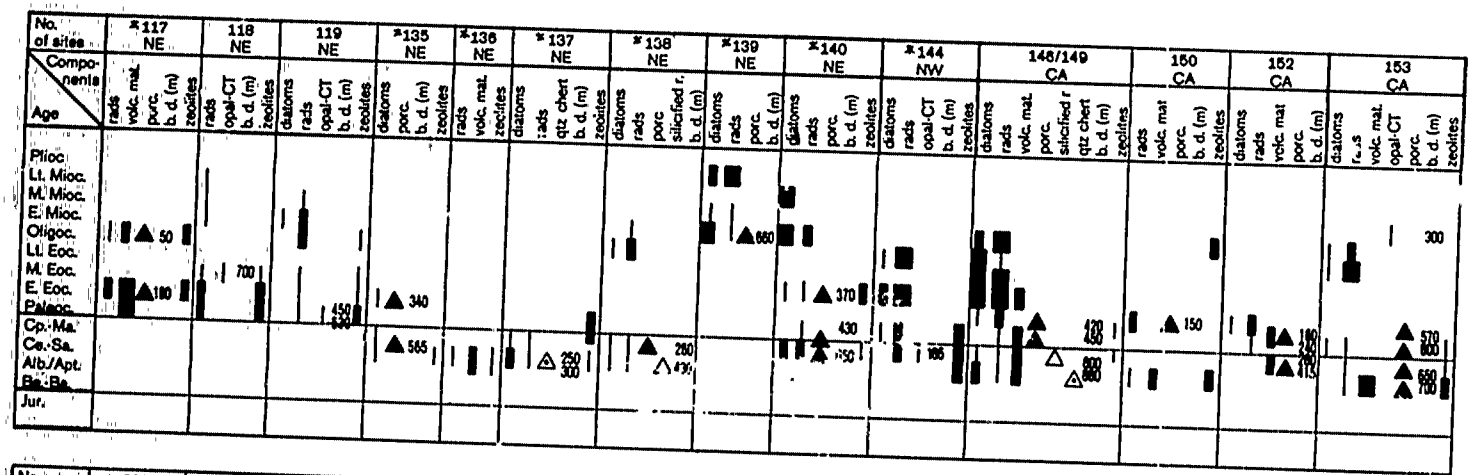


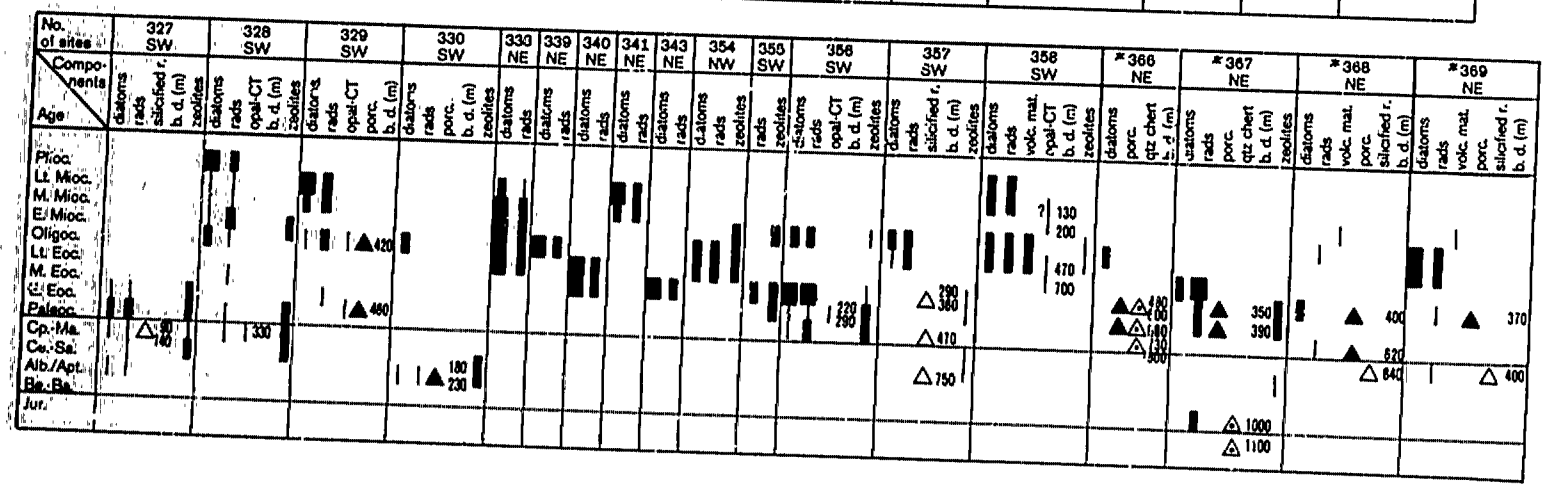

Table 2 – Continued

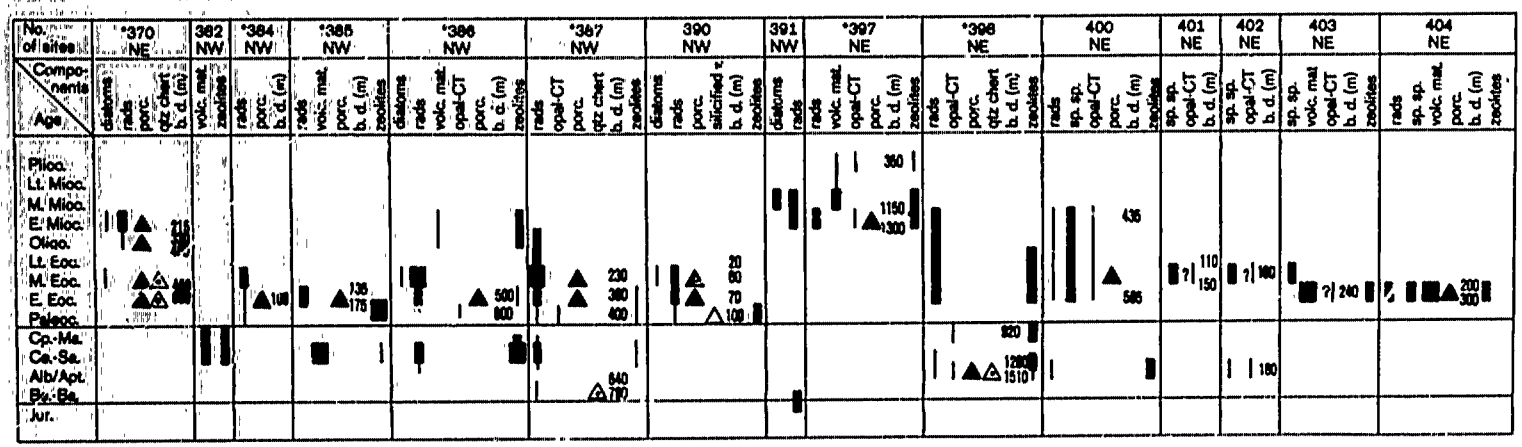


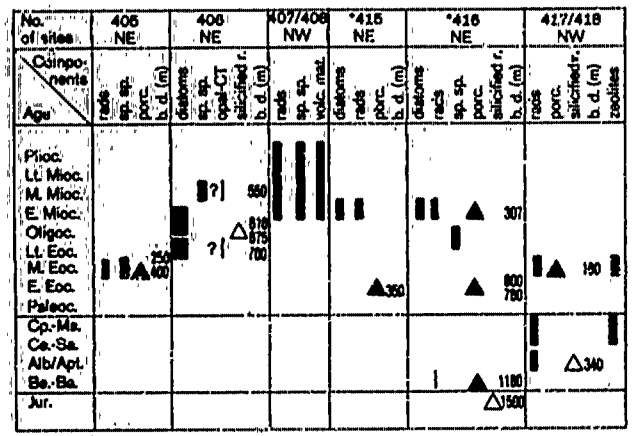


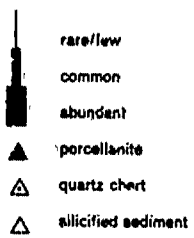

sources (halmyrolysis of basalt, devitrification of ashes, or hydrothermal solutions) are of minor importance. Other sources, such as clay minerals which can release adsorbed silica, are neglected in the following discussion. Most of the dissolved silica is fixed as skeletal opal by siliceous organisms in the photic zone. Post mortem, this silica is recycled by oxidative regeneration (i.e. opal dissolution during protoplasma oxidation)and inorganic dissolution of skeletons in the lower part of the water column and at the sediment/water interface. This increases the silica and the phosphate content of the upwelling waters. Only about 2% of the siliceous organisms living in the high-productivity surface waters are permanently removed from the oceanic silica cycle and enter the geological record.

Diagenesis is mainly controlled by the original distribution of opaline skeletons and volcanic glass in the sediments. Siliceous organisms are a much more abundant source than volcanic material, especially in sediments of Cenozoic age (Fig.3). Also the "diagenetic potential", indicated by the increase in the ratio of diagenetic products versus source material, decreases with time; this ratio is slightly greater than 1 for Eocene sediments, for which we note the well-known absolute maximum for authigenic silica; the ratio increases progressively for the Paleocene to Early Cretaceous formations.

Figure 4 shows the correlation of authigenic silica and silicates with the cooccuring biosiliceous or volcanogenic material. In many samples, authigenic silica occurs together with remains of siliceous organisms, but only in a few samples the volcanic material (e.g. volcanic glass) could have caused the precipitation of opal-CT. Our investigations from Site 397 near the Canary Islands indicate that diagenetic alteration of volcanic ash results mainly in the formation of phillipsite and smectite (Riech, in press (1)). Massive porcellanites are unknown in volcanogenic horizons lacking opaline skeletons, although accessory opal-CT does occur. With increasing age and maturity of the silicified sediments, the relationship between the products of silica diagenesis and their source materials becomes more and more obliterated (Fig.4.).

## Deposition and Preservation of Siliceous Sediments

Upwelling of nutrient-rich waters in the subarctic, subantarctic, equatorial, or eastern boundary current belts results in high plankton productivity in surface waters and an increased sedimentation rate and preservation of siliceous organisms. Thus even in Eocene to Oligocene sediments the delicate tests of diatoms are well preserved (Plate 1: Fig.1). The first steps of diagenetic alteration are the incipient corrosion of siliceous skeletons (Plate 1: Fig.2) or an "aging" of the opal-A surface ("globulose" appearance; see Plate 1: Fig.3). The bulk of opaline tests was dissolved before or during deposition (Fig.2), as nowhere the ocean water is more than one-tenth saturated with respect to amorphous silica. The concentration of dissolved silica in pore waters of deep-sea sediments is higher than in the corresponding bottom waters (Johnson, 1974,1976). This is due to a further dissolution of opaline skeletons after burial. Part of the dissolved silica is returned from the surface sediments back to the ocean (Fig.2). Johnson (1976), however, assumes that only little of the $Si(OH)_4$ can escape from sediment depths greater than 15 cm into the overlying bottom water.

The interstitial waters are strongly oversaturated with respect to quartz and are also saturated with respect to a wide range of silicates, such as smectite and phillipsite.

Bergren and Hollister (1974) connect the dissolution of siliceous organisms and the genesis of porcellanite with periods of erosion and non-deposition (e.g. the wide-spread Horizon-A chert in the western North American Basin). Our data and the differentiation between an $A^c$-reflector (Eocene cherts) and an $A^u$ Horizon (late Eocene-Oligocene continental margin unconformity) by Tucholke and Mountain (1978) do not support this hypothesis. The formation of opal-CT is only possible, if a considerable proportion of the siliceous organisms is not dissolved until after burial. Thus the preservation of biogenic silica and its later mobilization and reprecipitation as thick porcellanite beds is favored by increased, not lowered, rates of (hemi)pelagic sedimentation (Riech and von Rad, in press).

## Distribution of Biogenic and Authigenic Silica in the Cretaceous to Tertiary Sediments of the Atlantic Ocean

Today, the Atlantic is a $CaCO_3$-rich and silica-poor "lagoonal" basin which loses its nutrient-rich deep waters to the Pacific in exchange for surface waters which are stripped of silica by opal-secreting plankton (Berger, 1970; Heath, 1974). However, in the past "thalassocratic" or "polytaxic" times alternated with "epeirocratic" or "oligotaxic" periods (Berger and Roth,1975; Fischer and Arthur, 1977). During "polytaxic times" the eustatic sea level was high, and a warm, uniform climate with low vertical and horizontal temperature gradients produced widespread anaerobism, continuous pelagic deposition, and a sluggish circulation of silica-rich bottom waters (Fischer and Arthur, 1977). Such conditions prevailed 105 m.y. (Aptian/Albian), 75 m.y. (Campanian), 45 m.y. (middle Eocene), and 15 m.y. ago (middle Miocene). This permitted the preservation of siliceous tests in the sediments over a wider area of the deep ocean floor than during "oligotaxic" periods (e.g. Oligocene; Holocene) with their extensive regressions, lower marine temperatures, intensified

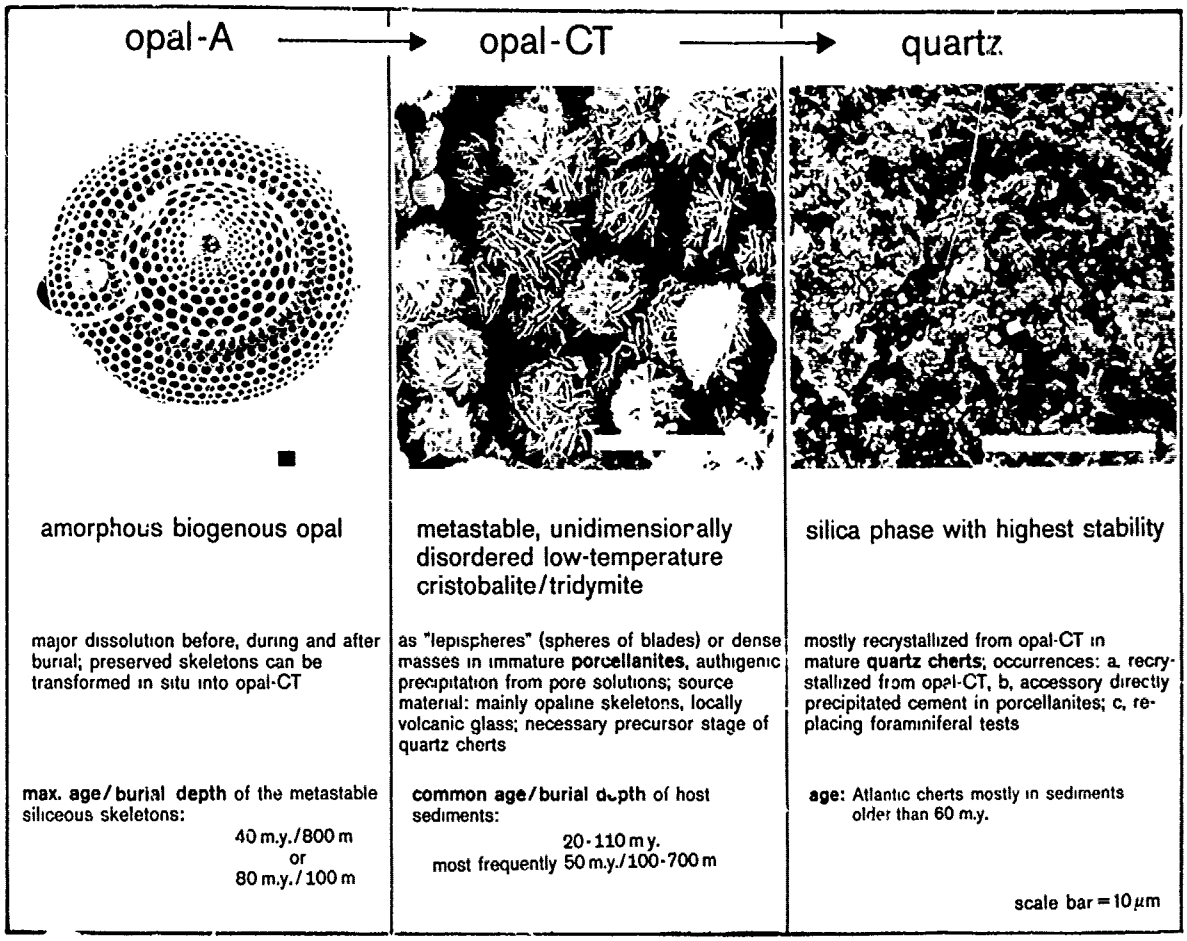


Figure 1. Mineralogy and ultrastructure of silica phases ocurring in deep-sea sediments.

circulation, and more efficient oxygenation of deep waters.

Figure 5 shows the distribution of siliceous organisms, volcanic debris, zeolites, porcellanites, and cherts in the Atlantic DSDP Sites (see also Table 2). We distinguish four time slices representing the paleogeography and paleobathymetry of the Atlantic Ocean during the deposition of these sediments. We will briefly discuss the impact of the paleogeographic and paleoceanographic setting of the Atlantic on the regional distribution and preservation of siliceous sediments and the successive silica diagenesis following Ramsay (1973), Bergren and Hollister (1974), van Andel et al. (1977), Sclater et al. (1977), and McCoy and Zimmerman (1977). Lack of authigenic silica in many DSDP sites may be due to (1) lack of siliceous organisms (e.g. in the Southeast Atlantic), (2) insufficient burial depth of siliceous sediments (e.g. Norwegian Sea), or (3) retarded silica diagenesis.

During Late Jurassic times (not shown in Fig.5) a narrow proto-Atlantic ocean connected the Tethys with the Pacific. Siliceous pelagic sediments (now converted to quartz cherts) were deposited in the eastern (Sites 367 and 416) and western (Sites 5 and 99) tropical North Atlantic.

The Early Cretaceous South Atlantic was a narrow "Mediterranean"-type marginal sea, connected with the Southern Ocean. Only the Cape Basin received bottom waters from the south; siliceous sediments (now porcellanites) are restricted to the Falkland Plateau (subantarctic belt, Site 330). The North Atlantic Basin was part of the circumequatorial sea connecting the Pacific and the Tethys Ocean. South of paleolatitude 32°N, siliceous sediments occur along the eastern and western continental margins parallel to a postulated broad clockwise gyre of fertile surface waters. The restricted mid-Cretaceous circulation is characterized by black shales which are often associated with chert (e.g. Sites 5, 137, 138, and 16).

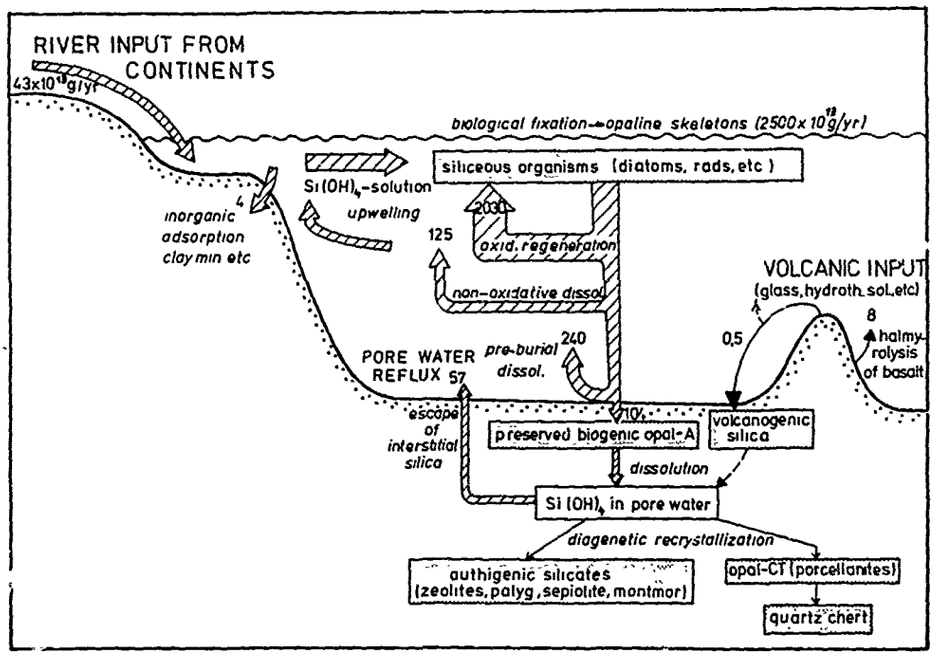


Figure 2. The cycle of dissolved silica in the oceans (modified from Heath, 1974, Fig.7). All numbers represent magnitudes of dissolved silica in $10^{13}$ g $SiO_2$/year (estimates by Heath, 1974, Table 2). Silica sources in capitals; transformations (cycling) in italics; solid biogenic, volcanogenic, or authigenic silica phases are stippled.

At the beginning of Late Cretaceous times, a fully developed North Atlantic Ocean was connected for the first time with a narrow South Atlantic permitting a longitudinal surface water mass and faunal exchange. In the South Atlantic, siliceous oozes (now cherts) are restricted to the Falkland Plateau (Site 327) and Rio Grande Rise (Site 357) in the west. The North Atlantic (including the Caribbean Sea and Gulf of Mexico) was open to equatorial surface water masses from the Pacific and Tethys. Because no cold bottom waters reached the basin from the Arctic or Antarctic, the Late Cretaceous North Atlantic (south of 30°N) developed as a subtropical carbonate province with intermittent explosive blooms of siliceous plankton (now mainly diatoms), especially during Campanian to Maastrichtian times (e.g.Sites 13,369,95,146,152). During Late Cenomanian to Turonian times, laminated bituminous marls (rich in radiolarian chert nodules) along the Northwest African coast suggest the initiation of upwelling conditions during the development of a modern North Atlantic circulation pattern (Wiedmann et al., 1978). Below the CCD, radiolarian mudstones were deposited (e.g.Sites 140,368).

During Eocene times (about 50 m.y. ago), the Falkland Plateau and the Rio Grande Rise had subsided sufficiently to allow the invasion of cold "pre-Antarctic Bottom Water" (McCoy and Zimmermann, 1977) into the Argentine, Brazil, and Cape Basins. Occurrences of siliceous sediments in the western South Atlantic indicate the influence of subantarctic nutrient-rich waters, whereas the Southwest African margin is devoid of siliceous oozes.

In the North Atlantic, silica-rich surface waters flowed directly from the Pacific into the Caribbean, Gulf of Mexico and the Atlantic via an open Isthmus of Panama; they produced a continuous high-fertility belt of biosiliceous sediments in connection with equatorial and coastal upwelling (Ramsay, 1973). The tropical Atlantic was also connected with the Tethys. Production of siliceous organisms along the eastern and western ocean margins reached its absolute maximum during the (late) early and (early) middle Eocene. The northernmost late Eocene occurrences (Sites 116,340,338) reflect the influx of cold Arctic bottom water after the opening of the Norwegian Sea between Greenland and Europa. A shallow CCD, high plankton fertility and an equable warm climate with silica-rich sluggish bottom waters helped to increase silica deposition and preservation (Fischer and Arthur, 1977). Although Eocene volcanism appears to have been common throughout the Atlantic and especially in the Caribbean (Gibson and Towe, 1971; Mattson

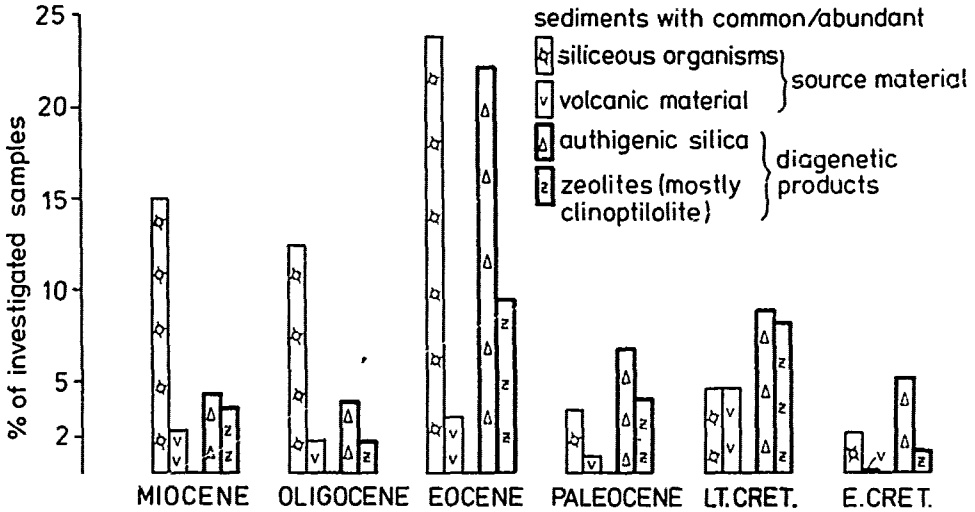


Figure 3. Age distribution of Atlantic sediments with common to abundant proportions of siliceous organisms, volcanic material, authigenic silica and zeolites. Each sample represents the average sediment composition for the selected time slice at each site. 100% = 230 "samples" from all Atlantic sites, which contain one or more of the four specified components (see Table 2).

and Pessagno, 1971), submarine and subaerial volcanism has probably contributed very little to the silica budget of the oceans (see Fig.2; Heath, 1974).

Similar to today, the deep water circulation pattern at the Oligocene/Miocene boundary (about 22 m.y. ago) was dominated by a cold circumpolar source of surface water. Subsidence of the southwestern Atlantic and the invasion of Antarctic Bottom Water (AABW) following the establishment of a circum-Antarctic Current caused deposition of siliceous oozes in the Argentine Basin

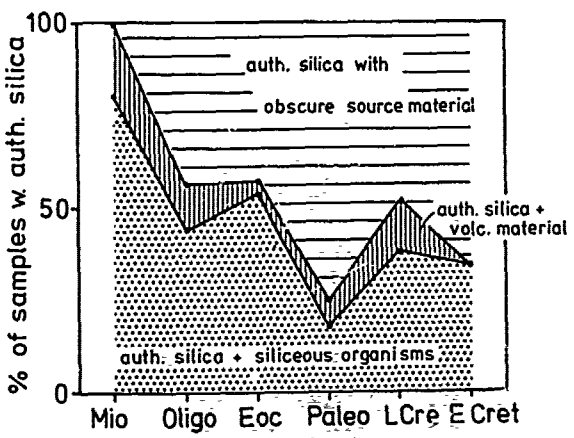


Figure 4. Co-occurrence of authigenic silica with biosiliceous or volcanogenic material (100 % = all samples containing authigenic silica, "samples" being defined as in Fig.3).

(Site 358). Late Oligocene siliceous oozes in the Angola Basin reflect surface fertility connected with coastal upwelling. In the North Atlantic there are three zones with comparatively high silicoplankton productivity: (1) the northeast Atlantic margin (Sierra Leone Rise to Biscay), where the eastern boundary (Canary) current and upwelling cause high plankton production; (2) the subarctic Atlantic (Labrador Sea to Norwegian Sea) and (3) the (sub)-tropical western North Atlantic (south of 30°N), probably influenced by nutrient-rich equatorial Pacific waters. The lack of Neogene porcellanites in siliceous sediments off northeastern America and in the Norwegian Sea is conspicuous.

## Formation of Weakly Opal-CT Cemented Sediments and Porcellanites

In general, post-burial dissolution of siliceous skeletons (Plate 1: Fig.9) provides the silica source for the formation of opal-CT and clinoptilolite (Plate 1:Fig.4). This important causal relationship is proven by the positive correlation of the intensity of opal dissolution with the quantity of authigenic silica and silicates present in these sediments (e.g. Leg 43: Riech and von Rad, in press; Leg 47A: Riech, in press (1)). Considering this, the absence of siliceous microfossils in some silicified rocks is not surprising (Fig.4 and 6).

Porcellanites or weakly opal-CT cemented sediments occur in all facies types. The authigenesis of opal-CT requires higher silica concentrations in pore waters than the precipitation of quartz (Kastner et al., 1977). The precipitation

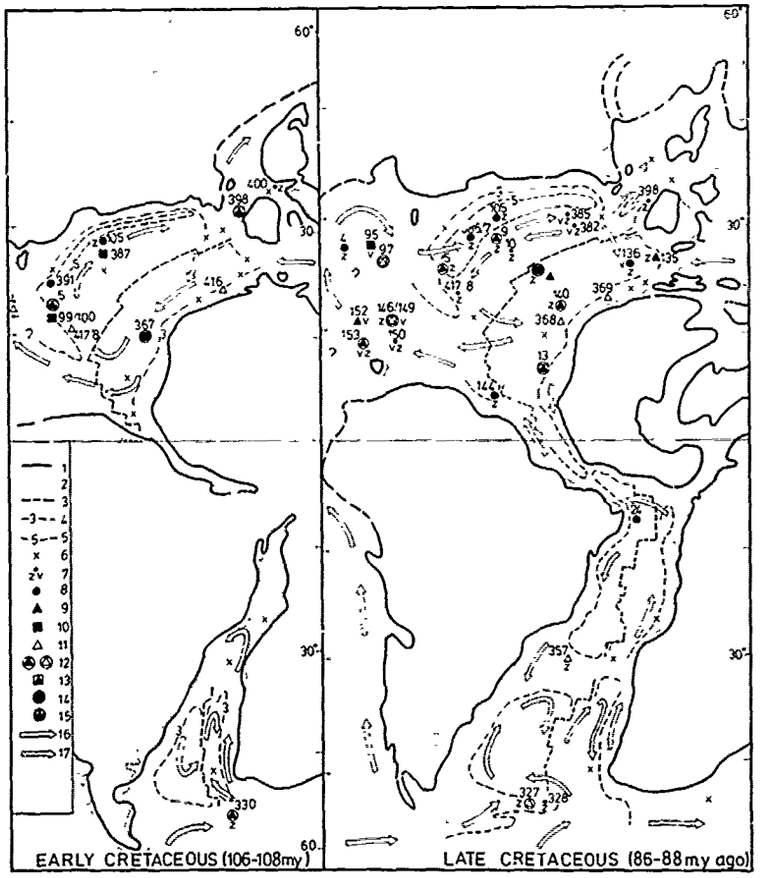


Figure 5. Regional distribution of siliceous organisms, silicified sediments, zeolites, and volcanic debris in Atlantic DSDP sites averaged for sediments of four time intervals (Table 2). Approximate paleo-position of DSDP sites, paleogeography and paleobathymetry simplified after McCoy and Zimmerman (in preparation) and Sclater et al. (1977). Paleoposition of the Gulf of Mexico and Caribbean sites highly speculative. For the northern North Atlantic the paleocoastlines of mid-Eocene times (45 m.y. ago) are shown. Note that the depicted standardized sediment parameters cover a wider age range (e.g. the Late Cretaceous) than the paleogeographic maps (e.g. "Turonian/Coniacian", 86-88 m.y. ago). Paleocurrent directions highly speculative and adapted from Ramsay (1973), Bergren and Holliste (1974), and McCoy and Zimmerman (1977). Explanation of symbols: 1= paleocoastline towards the Atlantic, including epicontinental seas, 2= present outline of continents, 3= spreading center (Mid-Atlantic Ridge etc.), 4= 3 km paleoisobath (not shown where it parallels the Mid-Atlantic Ridge), 5= 5 km paleo-isobath, 6= selected DSDP sites without biogenic or authigenic silica, 7= DSDP site with zeolites (z) and/or volcanic debris (v), 8= DSDP site with siliceous organisms, 9= porcellanite, 10= quartz chert, 11= silicified sediment (porcellanite and/or quartz chert), 12= porcellanite or silicified sediment + siliceous organisms, 13= porcellanite + quartz chert, 14= quartz chert + siliceous organisms, 15= siliceous organisms + porcellanite + quartz chert, 16= paleo-surface current, 17= paleo-bottom currents.

Figure 5 - Continued

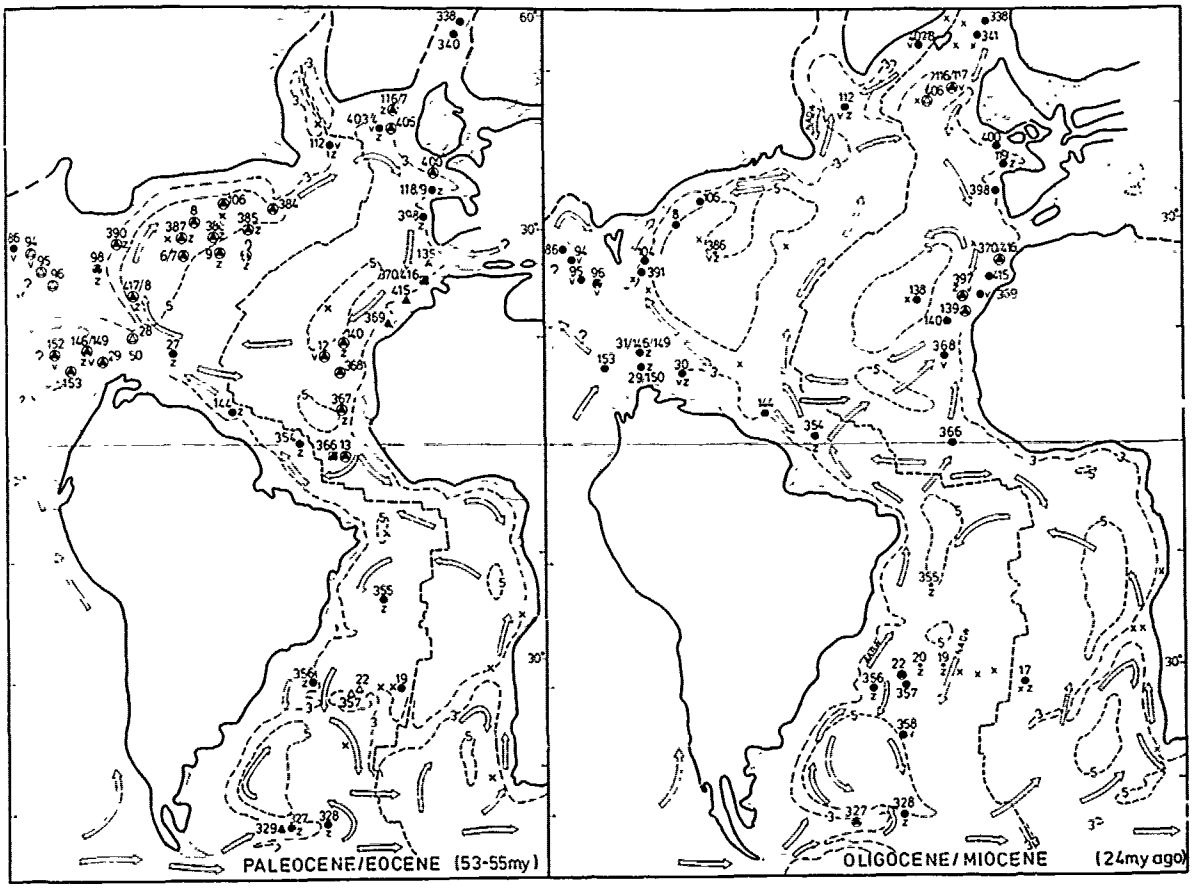


of opal-CT precedes that of quartz, since opal-CT has a higher nucleation and growth rate. According to experiments by Kastner et al. (1977), the nucleation of opal-CT is aided by the precipitation of magnesium hydroxide.

Figure 6 shows schematically the early-diagenetic transformations occurring in siliceous sediments. Opal-CT precipitation leads either to the formation of massive porcellanites (B and D in Fig.6), or to less spectacular, weakly silicified "porcellaneous" sediments (Plate 3: Fig. 1-3). Porous sediments are first cemented, and later more or less completely replaced by opal-CT. In some weakly consolidated carbonates, a patchy silicification may be observed with opal-CT impregnating the calcareous matrix in a diffuse manner (Riech and von Rad, in press). This contrasts with the sharp chalk/porcellanite/chert boundaries, so typical for flints all over the world (Plate 3: Fig.6). In some Leg 43 sites, the thickness of the porcellanite horizons correlates positively with the sedimentation rates.

No appreciable mobilization of biogenic silica takes place, if siliceous organisms are converted directly into opal-CT without having passed through a dissolution stage (Fig.6:A; Plate 1: Fig.5-7). The walls of the radiolarian skeletons are thickened by active outward growth of opal-CT.

If biogenic silica is completely dissolved and the interstitial waters are undersaturated with respect to opal-CT, authigenic zeolites, phyllosilicates and quartz can be precipitated instead of opal-CT (Fig.6:C).

In open cavities opal-CT forms spherical aggregates, so-called "lepispheres" (Plate 2: Fig.2,3; Plate 3: Fig.2,3,7). Isolated blades occur in the initial stage (Plate 3: Fig.1). The conspicuous "cardhouse"-structure of lepispheres is characterized by the constancy of angles (70°) between opal-CT blades. This intergrowth can be explained by the twinning laws of tridymite (see Flörke et al., 1976). On progressive silicification, the lepispheres grow together

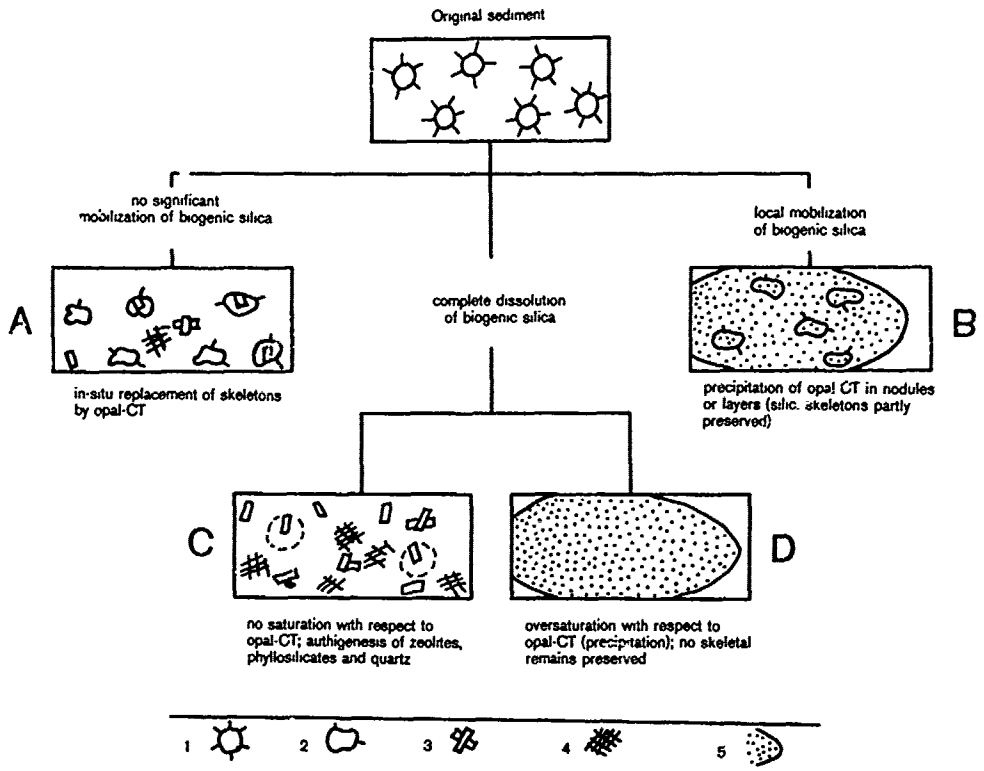


Figure 6. Schematic sketch of early diagenetic transformations in siliceous sediments. 1= unaltered siliceous organisms (opal-A), 2= siliceous organisms, transformed into opal-CT, 3= authigenic zeolites, 4= authigenic clay minerals, 5= nodular porcellanite. A,B,C,D = silicification stages (explanation in text).

and gradually reduce the pore space (Plate 2: Fig.3). Finally, the spherical aggregates may completely disappear: this results in a dense matrix of massive opal-CT. Massive opal-CT may also completely fill the interior of the planktonic foraminifera, including the delicate wall pores (Plate 2: Fig.1).

According to our experience, opal-CT is always the first silica phase during silicification. Apparently, this confirms Ostwald's step rule stating that an unstable phase (opal-A) usually passes through one or more intermediate phases before becoming structurally transformed into a stable phase (quartz). A comparatively small amount of quartz formed prior to the late-diagenetic conversion of opal-CT into quartz indicating a change in pore water chemistry towards decreasing silica contents. Accessory quartz which commonly replaces the calcitic foraminiferal tests and fills the open pores (cf. Heath and Moberly, 1971) does not contradict Ostwald's rule.

## Formation of Authigenic Silicates

Authigenic silicates, such as zeolites, palygorskite, sepiolite, and smectite are formed if sufficient aluminum, alkali, and alkali - earth ions are available in the pore water and if the silica concentration is below the saturation for opal-CT. Although less conspicuous than silicified rocks, occurrences of disseminated zeolites are more widespread in the Atlantic than are the porcellanites and cherts. Because this low silica level was often reached due to the precipitation of opal-CT, euhedral clinoptilolite prisms usually constitute the latest phase filling the foraminiferal tests after the formation of an (1), early-diagenetic calcite cement and (2 the second generation of opal-CT lepispheres (Plate 2: Fig.2,3). Clinoptilolite can also form during an increase of interstitial silica concentration before opal-CT precipitation. In a manner similar to opal-CT, massive clinoptilolite can also completely fill out foraminiferal chambers, including the delicate wall pores (Plate 2: Fig.5,6). In the Atlantic sediments, clinoptilolite is associated more frequently with partially dissolved siliceous remains than with volcanogenic parent material. On the other hand, authigenic smectite and phillipsite occur commonly as alteration products of volcanic glass and other pyroclastics. In general, this agrees with the results of Stonecipher (1976) who

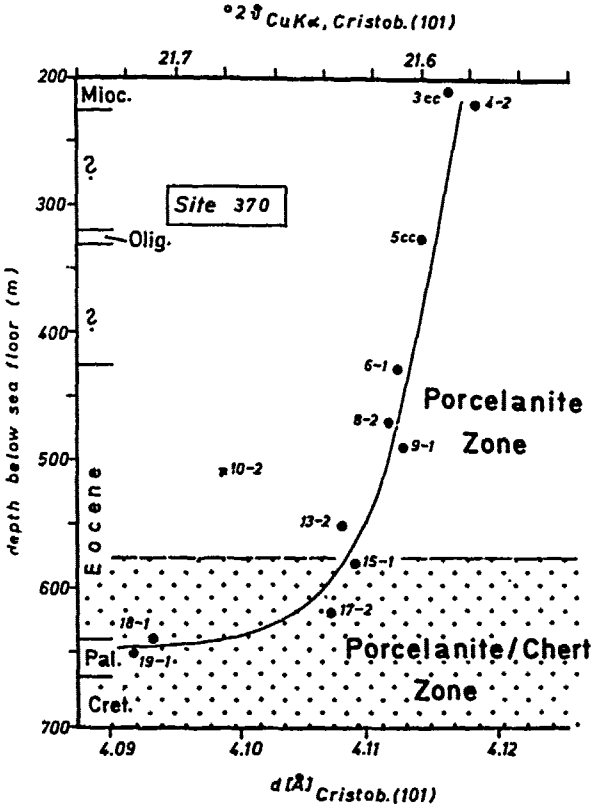


Figure 7. Maturation and re-ordering of the opal-CT structure as a function of burial depth (temperature) in DSDP Site 370 (Moroccan Basin) using the precise position of the d (101)- cristobalite XRD peak near 4.1 Å (from von Rad et al., 1977). Note exponential decrease of the d (101) spacing in the porcelanite/chert zone below 550 m.

found that phillipsite is usually associated with comparatively young, slowly deposited clayey or volcanic sediments, whereas clinoptilolite occurs commonly in older calcareous sediments and at greater burial depths. Our results from Leg 47A, however, indicate that phillipsite is stable also in middle Miocene to Pliocene air fall ash layers at burial depths of 300-800 m which are intercalated between quickly deposited calcareous oozes (Riech, in press (1)). Authigenic phillipsite forms with a much higher nucleation rate (Plate 2: Fig.4) than clinoptilolite (Plate 2: Fig.3).

Although smectite is mainly of detrital origin in deep-sea sediments, authigenic montmorillonite occurs locally as alteration product of volcanogenic sediments. Plate 2 (Figure 8) shows an authigenic montmorillonite formed in a foraminiferal chamber. The complete filling of the delicate wall pores by smectite (Plate 2: Fig.8) suggests actual cementation of the cavities, rather than a mechanical introduction of clay minerals during sedimentation.

Palygorskite and sepiolite-rich, more or less silicified sediments are abundant in the Late Cretaceous and Paleogene sections of many West African coastal basins (Millot, 1970), in the central Atlantic off West Africa between 12° and 34°N (Berger and von Rad, 1972; von Rad et al., 1977), in the Gulf of Mexico, in the Northwest Atlantic (Riech and von Rad, in press), and in the coastal basins of the southeastern U.S (Weaver and Beck, 1977). Several authors (e.g. Chamley and Millot, 1975; Weaver and Beck, 1977) postulate that most of the palygorskite and sepiolite along the West African margin was not precipitated during diagenesis from silica-, Mg- and Al-rich alkaline solutions in the deep-sea environment (von Rad and Rösch, 1974), but was recycled by river or wind transportation from brackish sediments deposited along Northwest Africa under (sub)tropical conditions. On the other hand, distinctly authigenic palygorskite of hydrothermal origin or from the diagenetic alteration of pyroclastics or montmorillonite formed under low temperatures in the deep

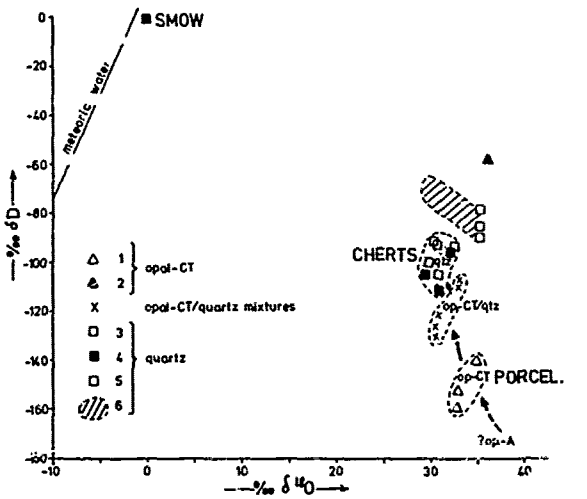


Figure 8. Isotopic composition of authigenic opal-CT (porcellanites), opal-CT/quartz mixtures, and quartz (cherts) from DSDP Sites 366 (middle to early Eocene, 537-595 m burial depth) and 367 (Oxfordian to Hauterivian, 1000-1130 m burial depth). $\delta^{18}O = {}^{18}O/{}^{16}O$ ratio of total oxygen in silica phase (silica + water); $\delta D$= D/H ratio of water extracted from opal-CT or quartz; SMOW= Standard Mean Ocean Water; measurements by Dr. H. Friedrichsen (Tübingen). 1= pure opal-CT (Site 366), 2= opal-CT (Site 356; Knauth and Epstein, 1975), 3= pure quartz from immature porcellanites (Site 366), 4= pure quartz from mature quartz cherts (Site 367), 5= quartz cherts (Sites 64, 70, 356; Knauth and Epstein, 1975), 6= cherts, more or less in equilibrium with ocean water (Knauth and Epstein, 1976).

sea (Bonatti and Joensuu, 1968; Couture, 1978).

Independent of its origin, the palygorskite in deep-sea sediments has been at least partly influenced by diagenesis (Plate 2: Fig.9). Thin-sections of these sediments commonly show a uniform extinction of the total matrix under crossed nicols (see also Keene, 1976; von Rad et al., 1977).

## Transformation of Porcellanite into Chert

With increasing age and burial depth, the metastable opal-CT of the "immature" porcellanites is gradually transformed into quartz. Before this transformation is achieved, a "maturation" (ordering) of the opal-CT structure takes place (Fig.7). This is demonstrated by a progressive shift of the 4.1.Å peak of opal-CT towards smaller values for increasing burial depths or temperatures (cf. Murata and Nakata, 1974; Murata and Larson, 1975). We have observed the first transitional stages between porcellanites and true cherts in Eocene host rocks (von Rad et.al., 1977). In thin-section, this transition is indicated by the presence of many light-colored nuclei of microcrystalline quartz within a matrix of very fine-grained, almost isotropical opal-CT (Plate 3: Fig.5,6). In zoned porcellanite nodules the quartzification starts from the center, where the oldest opal-CT is present. The mature end product of this process is a vitreous chert which consists mainly of non-clastic microcrystalline (Plate 3: Fig.6) to chalcedonic quartz. In our

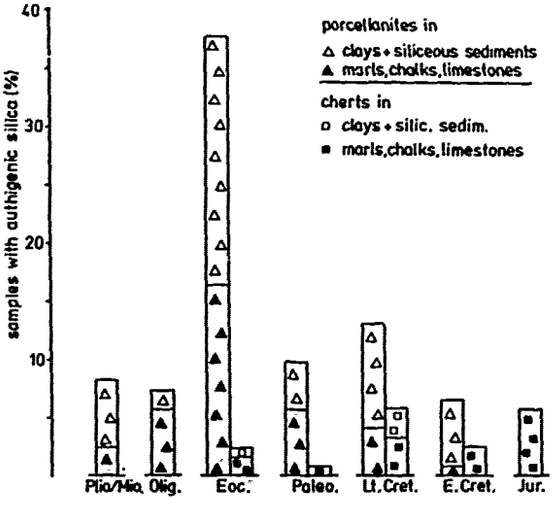


Figure 9. Distribution of porcellanites and quartz cherts in the Atlantic Ocean (122 samples = 100 %) as a function of age and host rock rock lithology. Note that porcellanites are present in Eocene to Pliocene carbonate and clayey sediments. There are no quartz cherts in post-Eocene sediments.

Cretaceous to Tertiary samples, the crystallinity of quartz is not improved with increasing age and burial depth (or temperature) of the cherts (H. Rösch, pers. comm.) as found by Murata and Norman II (1976).

Indications of all transformation steps from opal-A via opal-CT to quartz can be seen in a quartz-replaced sponge spicule which still shows the characteristic interpenetration of the original opal-CT blades (Plate 1: Fig.7). Well-preserved quartzified radiolarians (Plate 1: Fig.8) indicate in situ transformation of the same type. This is also documented by quartz-replaced lepispheres which still possess the gross ultramorphology of the opal-CT precursor stage (Plate 3: Fig.8 and 9).

Our data confirm that typical quartz cherts were never formed directly from silica solutions without an intermediate opal-CT stage. Prior to chertification, the direct precipitation of quartz is restricted to the local filling of open pores or to the replacement of foraminiferal tests.

According to Stein and Kirkpatrick (1976) and Kastner et al. (1977), opal-CT is transformed to quartz by nucleation and growth of quartz, i.e. by a dissolution/reprecipitation mechanism, and not by a zero-order solid-solid conversion (Ernst and Calvert, 1969; Heath and Moberly, 1971). However, quartz-replaced lepispheres, radiolarians and sponge spicules (i.e. quartz pseudomorphs after opal-CT) show still the original ultrastructure of opal-CT, and quartz cherts are formed only after the opal-CT structure has been progressively reordered. This proves that in these cases the transformation must have occured within the opal-CT lattice. Such a quasi-solid-solid microstructural conversion is more likely for the replacement of opal-CT by quartz than the complete dissolution of opal-CT, followed by the reprecipitation of quartz from a silica solution.

## Diagenetic Maturation with Respect to Age, Burial Depth (Temperature) and Host Rock Lithology

We investigated the isotopic composition of opal-CT and quartz, in order to learn more about the origin and thermal history of these silica phases during diagenesis (cf. also Knauth and Epstein, 1975, 1976; Murata et al., 1977). Independent of age and burial depth, opal-CT and pure diagenetic quartz occupy discrete areas in the $\delta D/\delta^{18}O$ diagram (Fig.8), with the mixed opal-CT/quartz samples lying in between. According to these and other authors, the isotopically heavier opal-CT suggests lower formation temperatures (25-50°C?) than the cooccuring isotopically lighter quartz in cherts (60-80°C?). Our preliminary data, however, suggest that both silica phases might possess different fractionation factors. Therefore it might be impossible to correlate the $\delta^{18}O$-values of quartz with those of coexisting opal-CT, and to derive "paleo-formation temperatures" directly from them.

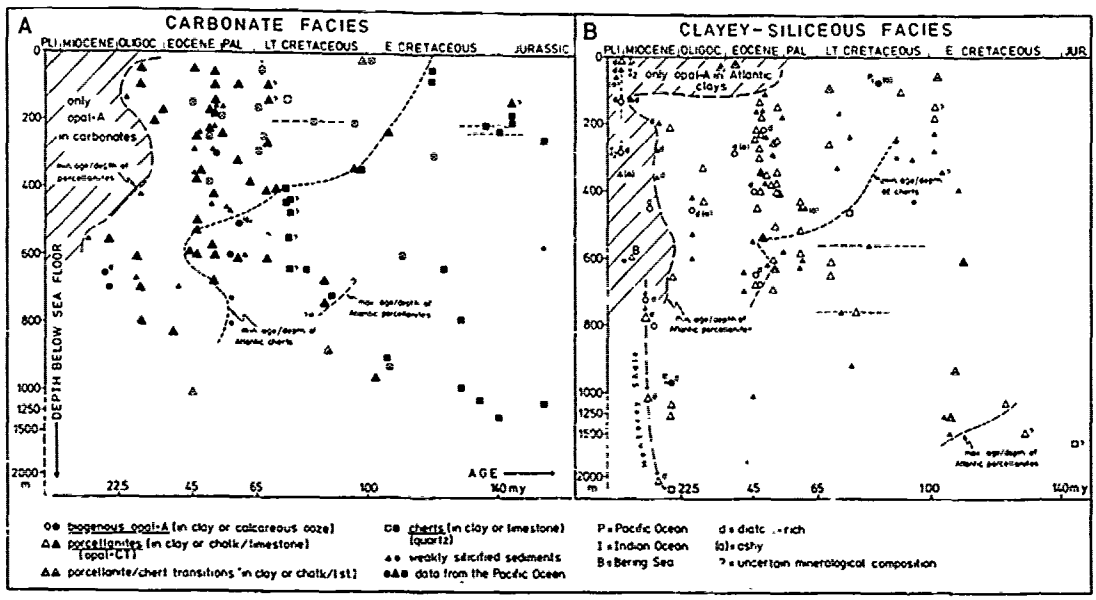


Figure 10. Mineralogy of biogenic and authigenic silica as a function of sample age, burial depth (temperature), and host rock facies. Note that Pacific quartz cherts occur in the field of Atlantic porcellanites (Fig.10A) and porcellanites from the Indian and Pacific Ocean and Bering Sea in the field of Atlantic opal-A (Fig.10B). Only selected samples are shown for opal-A to define the opal-A/opal-CT boundary. Selected data from the Pacific Ocean after Keene (1975) and other sources.
$P_1$= Site 61.0, $P_2$= Site 438B, $I_1$= Eltanin core 47-15, $I_2$= Site 238; Monterey Shale after Murata and Larson (1975), Bering Sea after Hein et al. (1978).

In addition to time and temperature which is usually inferred from burial depth and the present geothermal gradient, the chemical composition of the interstitial solutions and host sediments also control the rates of the transformation from opal-A to opal-CT and from opal-CT to quartz (Keene, 1976; Kastner et al., 1977). Therefore, we studied the distribution of porcellanites and quartz cherts in the Atlantic as a function of age and host rock lithology (Fig.9.). About 40% of the silicified Atlantic sediment samples are of Eocene age (predominantly porcellanites); the youngest quartz cherts are Eocene and the oldest porcellanites Early Cretaceous in age. The main causes for the global abundance of Eocene porcellanites are: (1) maximum productivity of siliceous organisms, (2) good preservation of skeletal opal in the surface sediments, and (3) optimal time/burial depth frame (40-50 m.y.; more than a few hundred meters) for the diagenetic silicification processes (Fig.12).

Independent of their ages, porcellanites occur both in the clayey and carbonate environments, although for the Cretaceous they are more common in the clayey facies. Although quartz cherts are more commonly associated with carbonate rocks, they also occur in Late Cretaceous and Eocene clayey or siliceous sediments. Keene (1976) proposed a model which predicts the fastest opal-A→opal-CT and opal-CT→quartz conversi . for diatom-rich calcareous oozes deposite under high heat-flow conditions (e.g. for Quaternary diatomites in the Gulf of California). According to experimental data of Kastner et al. (1977) opal-A is much faster transformed into opal-CT in carbonates than in clays. Our results from the Atlantic do not fully agree with that concept: in at least 20 DSDP sites no opal-A→opal-CT conversion was noted, although these sites contained calcareous and opaline-rich (partly diatomaceous) sediments of Paleocene to Miocene age.

Figures 10 and 11 show the mineralogy of biogenic and authigenic silica as a function of sample age, burial depth, and host rock lithology. It is obvious from these graphs that in general the stability of all silica phases is dependent on the age and burial depth. These two parameters are inversely correlated. On the other hand, there are no clearly defined stability fields for any of the three silica polymorphs: The opal-A field overlaps much of the area of opal-CT and even a small part of that of quartz; opal-CT is spread out over a very wide age/depth range and the youngest opal-CT occurrences do not follow the inverse age/depth regression. Therefore the Atlantic porcellanites cannot be decribed

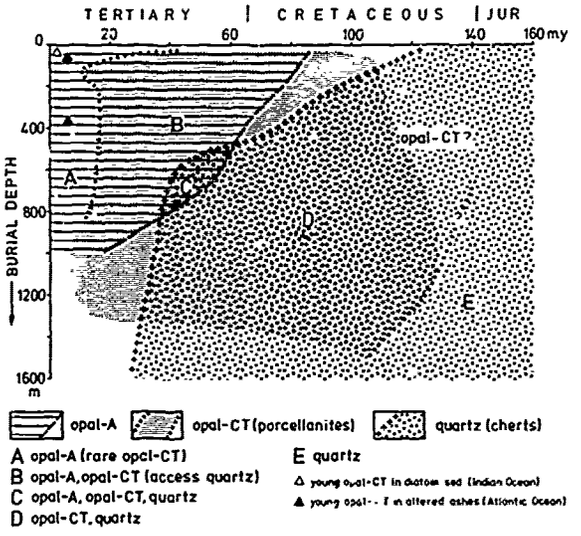


Figure 11. Graph summarizing the data of Fig. 10A+B showing occurrence and stability fields of opal-A, opal-CT and diagenetic quartz in the age-depth diagram. Note the overlapping of the maximum age/depth of unaltered biogenous opal and the minimum age/depth of mature quartz cherts in Eocene and Paleocene from the Atlantic Ocean.

by a simple linear time-temperature (burial depth) relationship. The influence of lithofacies is especially marked at the lower boundary of the opal-CT field, where the opal-CT→quartz conversion is retarded in clayey host sediments (Fig.10: A+B).

Opal-A appears to be completely missing in pre-Late Cretaceous sediments, while unaltered opal-A is present in Miocene diatom claystones at burial depths of nearly 1000 m (see $P_2$ in Fig.10,B). The transformation of biogenic opal into authigenic opal-CT, however, is not a continuous process. In the Monterey Shale, this conversion takes place below 700 m (Murata and Larson, 1975), in the Bering Sea at about 600 m (in late Miocene sediments), corresponding to in situ temperatures of 35-50°C (Hein et al., 1978). In the Atlantic, Pliocene opal-CT is very rare; in the Miocene, this mineral becomes more common at depths greater than 200 m. Some extremely young (Pliocene) opal-CT occurrences (burial depth only 6-38 m) from the Kerguelen Plateau and the Central Indian Ridge (Wise and Weaver, 1974; see $I_1$ and $I_2$ in our Fig. 10,B) have been interpreted as the result of "high heat flow" (Keene, 1976). This is difficult to imagine, as thick opal-A sediments are present below these porcellanites.

Surprisingly, the minimum age and depth of quartz cherts and the maximum age and depth of unaltered biogenic opal overlap (Fig. 11). This indicates that all stages of diagenesis can be present in the Paleogene sediments of the Atlantic. In the Pacific, quartz cherts appear to occur already at significantly lower burial depths than in the Atlantic (Fig.10,A).

## Conclusions: Diagenetic Potential and Transformations

By the transformation of skeletal opal-A into opal-CT and by the conversion of opal-CT into quartz the diagenetic potential of siliceous sediments is progressively reduced (Fig.12). Opal-A is abundant in Recent to Eocene sediments and very rare in the upper Cretaceous. Opal-CT occurs in Pliocene to lower Cretaceous deposits with accessory quartz from the Miocene downward. Genuine quartz cherts are very rare in the Eocene (Sites 366 and 370, ≥ 500 m burial depth) and are mostly restricted to Mesozoic sediments. We distinguish three diagenetically significant time intervals:

(1) about 10-65 m.y. after deposition of the siliceous sediments: silicification by precipitation of opal-CT during early and intermediate diagenesis Post-Miocene porcellanites are extremely rare and have not been found in the

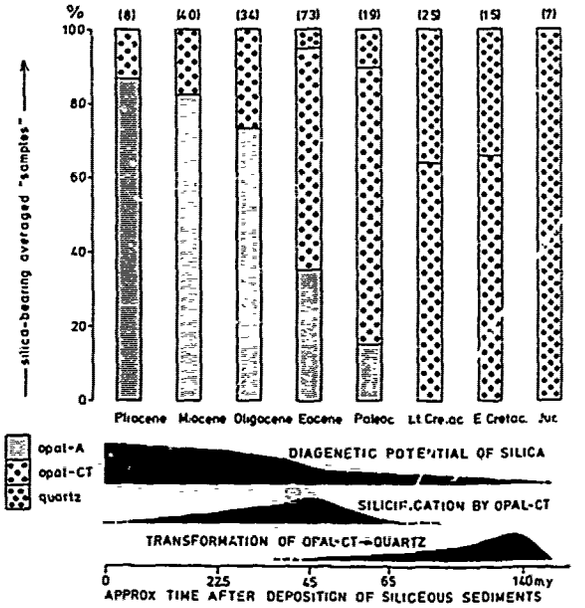


Figure 12. Distribution of the principal silica phases in selected time intervals and decrease of the diagenetic silica potential with time by the opal-CT silicification and opal-CT→quartz transformation (100 % = all investigated silica-bearing samples of that time interval). In pre-Early Cretaceous sediments the diagenetic potential approaches zero, since no significant diagenetic changes of the quartzified sediments can be expected.

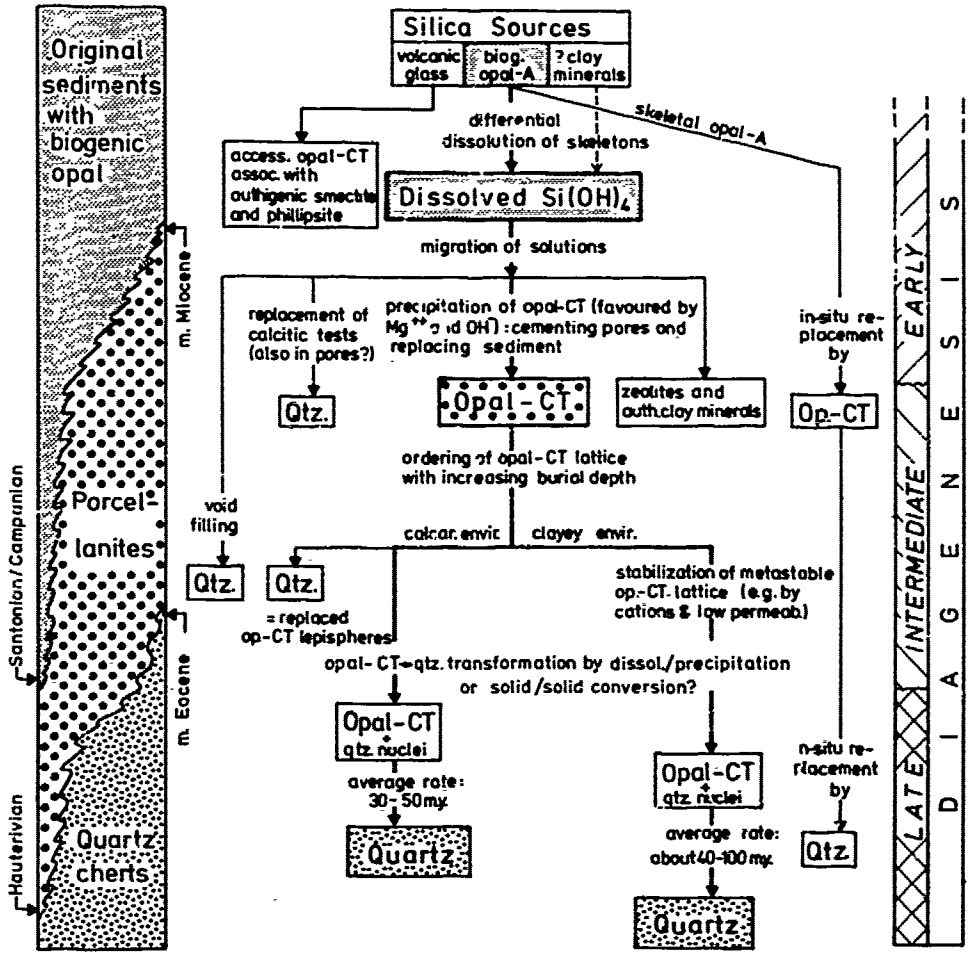


Figure 13. Schematic diagram showing the age-, burial depth, and facies-dependent diagenetic transformations from opal-A to opal-CT and quartz in the Atlantic Basin. Modified from von Rad et al. (1977) using interpretations from Heath and Moberly (1971), Lancelot (1975), Keene (1976), and Kastner et al. (1977).

Atlantic. After 40 m.y., about 50% of the siliceous sediments have been transformed into porcellanites. After 65 m.y. no further precipitation of opal-CT occurs because essentially no source material (opal-A) is left.
(2) 50-140 m.y. after deposition: late-diagenetic opal-CT→quartz transformation.
(3) Older than 140 m.y.: all siliceous sediments deposited near the Cretaceous/Jurassic boundary have been transformed into stable quartz cherts.

Figure 13 summarizes our knowledge on the diagenetic transformations from the deposition and early diagenesis of siliceous skeletons (opal-A) via the intermediate porcellanite stage (opal-CT) to late diagenetic quartz cherts. In our view, only accessory opal-CT, associated with phillipsite and authigenic smectite, is formed from volcanic parent material. Without any mobilization of silica, siliceous organisms can be transformed in situ, into opal-CT and later into quartz. The differential dissolution of opaline skeletons leads to $Si(OH)_4$-rich interstitial solutions. Depending on the silica, $Mg^{++}$, $(OH)^-$ and other metal ion concentrations in these solutions the following minerals can be precipitated during early to intermediate diagenesis: (1) primary quartz filling voids or replacing calcitic fossil tests, (2) zeolites (clinoptilolite) and authigenic smectites, (3) opal-CT, forming weakly silicified (porcellaneous) sediments and bedded or nodular porcellanites. Under "normal" deep-sea conditions (average heat flow), this step does not take place earlier than 20 m.y. after deposition and at burial depths less than about 200 m.

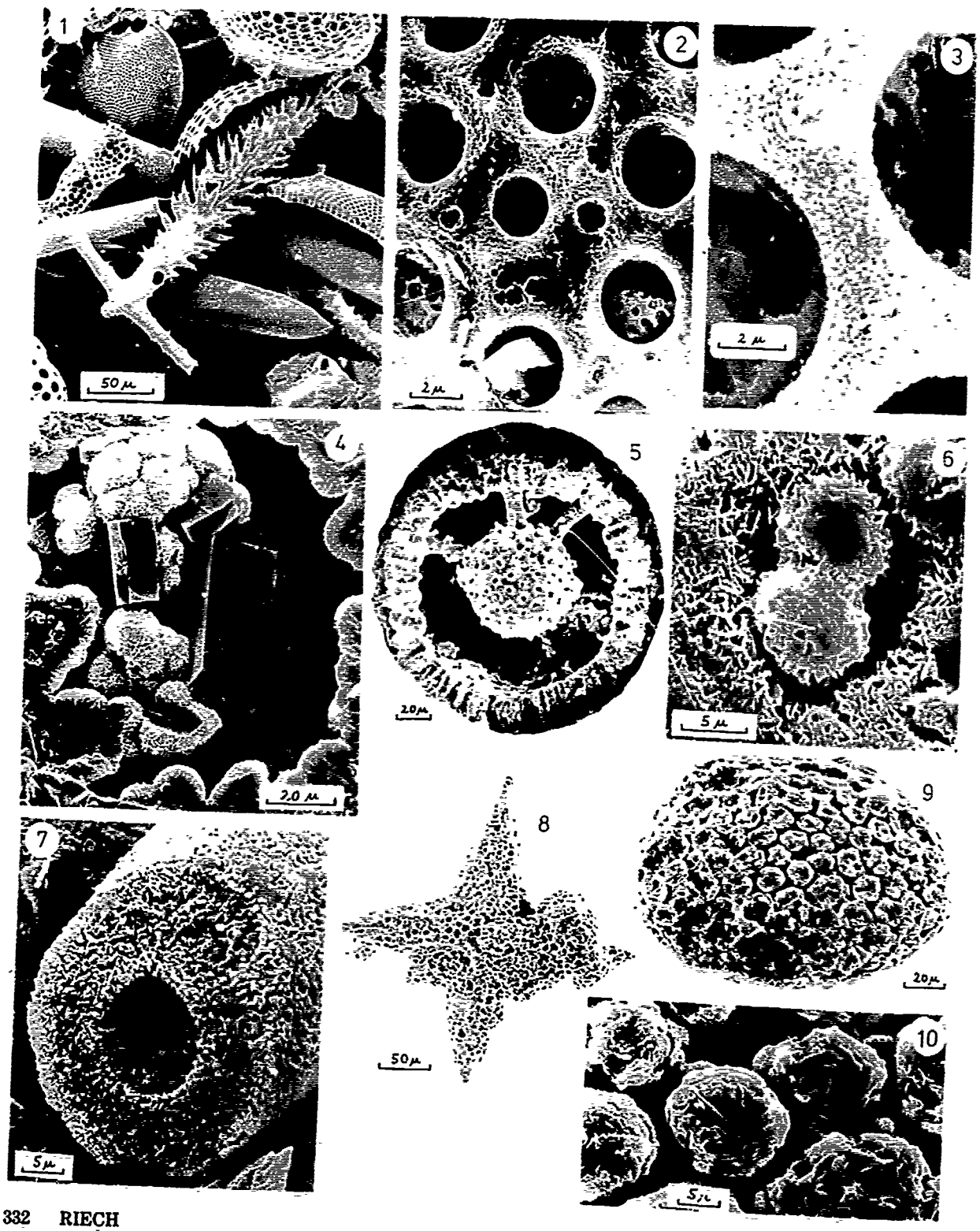
1
50 μ
2
2 μ
3
2 μ
4
20 μ
5
20 μ
6
5 μ
7
5 μ
8
50 μ
9
20 μ
10
5 μ

with increasing burial depth and temperature, the opal-CT attains a higher degree of structural order.

Age/burial depth diagrams of the silica phases (Fig. 10,11) indicate a significant influence of those parameters for the diagenetic evolution from biogenic opal to porcellanites and cherts. There is a wide overlap of the stability fields of the three silica modifications. This is due to the different rates at which the transformation processes take place. Clayey facies, especially, retards the conversion of opal-CT to quartz. Up to now, we have no explanation for the very different transformation rates of biogenic opal-A into the metastable silica varieties (see opal-A/opal-CT boundary in Fig.10,B).

According to our results, genuine cherts, in which the matrix consists completely of quartz, were never precipitated directly from silica solutions without a preceding opal-CT phase. The nature of the opal-CT→quartz transformation is still poorly understood, although most authors now favor a dissolution/reprecipitation mechanism. Quartz-replaced lepispheres, radiolarians, and sponge spicules in which the quartz was transformed in situ from an opal-CT precursor, however, suggest some kind of a "quasi solid-solid" microstructural conversion. The average rate of this transformation is ower (40-100 m.y.?) in the clayey environment than in calcareous facies (30-50 m.y.).

The source material, the silica phases and the diagenetic processes are now comparatively well known. However, up to now we have only studied a few simple factors influencing silica diagenesis, namely, time, temperature (usually inferred from burial depth and geothermal gradient), and the facies of the associated sediments. These parameters are not sufficient to explain the discontinuous silica diagenesis, i.e. the alternation of porcellanites and cherts with original opal-A bearing sediments. Probably the variable physico-chemical stability of biogenic opal as a function of species properties (specific surface, water and trace metal content; Hurd and Theyer, 1977) and of paleo-ecological and -oceanographic conditions should also be considered as important parameters (Goll and Bjørklund, 1972).

---

Plate 1. Preservation and filling of siliceous organisms.

Figure 1. Unaltered skeletal opal-A (sponge spicules, radiolarians, diatoms). Late Eocene-early Oligocene sample from New Zealand, kindly contributed by Dr. H.-J. Schrader (SEM photo 793/3).

Figure 2. Etched radiolarian skeleton (opal-A) with solution pits. Sample DSDP 43-386-16-3, 120-122 cm (middle Eocene, SEM 907/4).

Figure 3. Slightly altered diatom skeleton with globulose structure of aged opal-A (SEM 792/4). Same sample as Figure 1.

Figure 4. Relic of dissolved radiolarian ("ghost") filled with opal-CT lepispheres and euhedral clinoptilolite crystals. DSDP 43-386-30-2, 95 cm (Eocene, SEM 387/1).

Figure 5. Opal-CT replaced, well-preserved radiolarian skeleton. DSDP 41-366-23-1, 42-44 cm (middle Eocene, SEM 643/7, HCl-residue of a limestone).

Figure 6. Detail of central area of Figure 5 showing network of regularly intertwinned opal-CT blades and lepispheres on the surface of the central capsule (SEM 344/5).

Figure 7. Quartz-replaced sponge spicule in opal-CT cemented turbiditic arenite (spiculite). HCl and $H_2SiF_6$- treated sample DSDP 43-387-17-2, 56-58 cm (? early Eocene, SEM 788/8). The characteristic interpenetration of quartz crystallites at the surface suggests (1) early-diagenetic in situ replacement of the original skeletal opal-A by opal-CT and (2) later in situ replacement of bladed opal-CT by quartz without intermediary dissolution steps.

Figure 8. Quartz-replaced radiolarian with overgrowth. Sample DSDP-43-386-43-3, 50-52 cm (late Cenomanian, SEM 923/2).

Figure 9. Radiolarian cast consisting of amorphous silicates and montmorillonite. DSDP 47A-397A-23-3, 8-10 cm (early Miocene, "radiolarian dissolution facies", SEM 904/8).

Figure 10. Detail of Figure 9 showing opal-CT blades and lepispheres where the original siliceous skeleton was dissolved. Flaky smectite forming "blossom"-like structures (SEM 904/7).

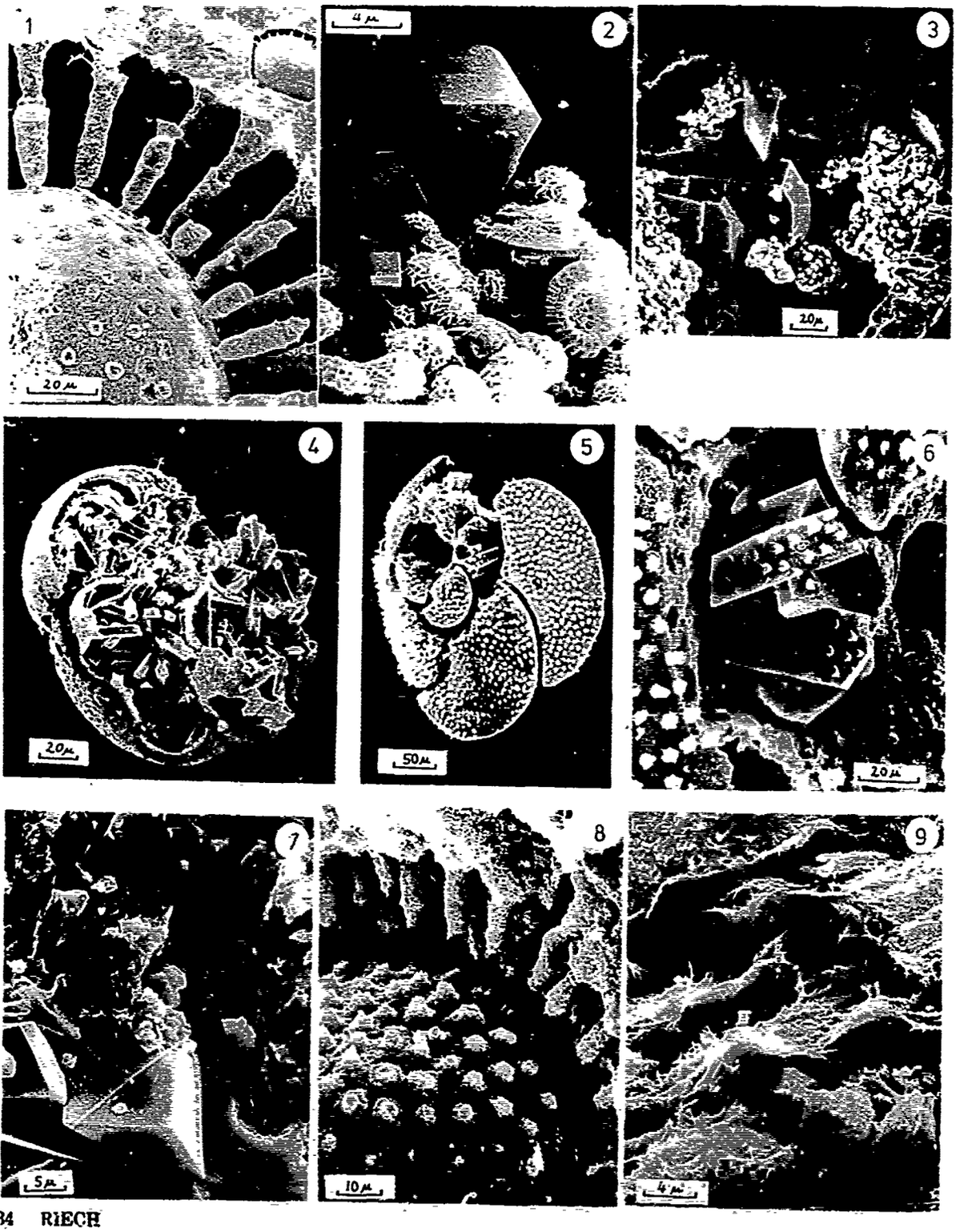
1
20 µ
2
4 µ
3
20µ
4
20µ
5
50µ
6
20µ
7
5µ
8
10µ
9
4µ

Plate 2. Opal-CT and authigenic silicates filling fossils and open voids in silicified chalks, porcellanites, and cherts.

Figure 1. Detail of opal-CT filled planktonic foraminifer (calcitic test dissolved by HCl) within opal-CT cemented arenite. Chamber filling, diagenetically thickened wall pores and surrounding matrix, all consist of "massive" opal-CT. Compare pore diameter of central foraminifer (4-8 μ) with that of small (? benthonic) foraminiferid in upper right. DSDP 43-387-17-2, 56-58 cm (? early Eocene, SEM 791/6).

Figure 2. Clinoptilolite and opal-CT lepispheres filling fossil pore in silicified marlstone. Opal-CT surrounds and partly replaces coccoliths; euhedral clinoptilolite is last cavity-filling generation. DSDP 14-144-3-2, 103-104 cm (Campanian-Maastrichtian, SEM 702/3).

Figure 3. Small opal-CT lepispheres and large clinoptilolite crystals filling foraminiferal chamber in "radiolarian dissolution facies". Note small nucleation rate for zeolites which formed later than the opal-CT. Sample DSDP-47A-397A-23-3, 8-10 cm (early Miocene, SEM 905/6).

Figure 4. Phillipsite-filled foraminiferal chamber in altered volcanic ash. Note high nucleation rate for the zeolite. DSDP 47A-397-34-2, 130-132 cm (Pliocene, SEM 906/4).

Figure 5. Clinoptilolite cast of planktonic foraminifer (calcite dissolved by HCl). Note massive zeolite completely filling the interior of most chambers and casting wall pores (now cylinder-like "spines") and euhedral zeolite (open cavity growth) in center. DSDP 47A-397-77-3cc (middle Miocene, SEM 924/12).

Figure 6. Detail showing center of Figure 5 (SEM 924/11).

Figure 7. Part of foraminiferal chamber in weakly silicified chalk. Hemispheres of ± massive opal-CT (center) grow on the interior wall of the foraminiferid (upper right). The opal-CT in turn is overgrown by late diagenetic calcite cement (note negative of lepisphere at lower right). Sample DSDP 41-366-29-1, 59-61 cm (early Eocene, SEM 625/3).

Figure 8. Foraminiferal chamber in clayey foraminiferal arenite, filled by authigenic silicates (montmorillonite and X-ray amorphous silicates.) The perfect casting of foraminiferal chamber and wall pores proves in situ growth of the smectite connecting the foraminiferal fill with the surrounding clayey matrix. Sample DSDP 47A-397A-2-2, 24 cm (early Miocene, SEM 927/3).

Figure 9. Bedded porcellanite with structureless opal-CT (top left), a few clinoptilolite crystals and early diagenetic palygorskite mats oriented parallel to void (diameter of individual fibers: 0.1-0.3 μ). Sample DSDP 41-367-14-4, 14-16 cm (early Eocene, SEM 727/3).

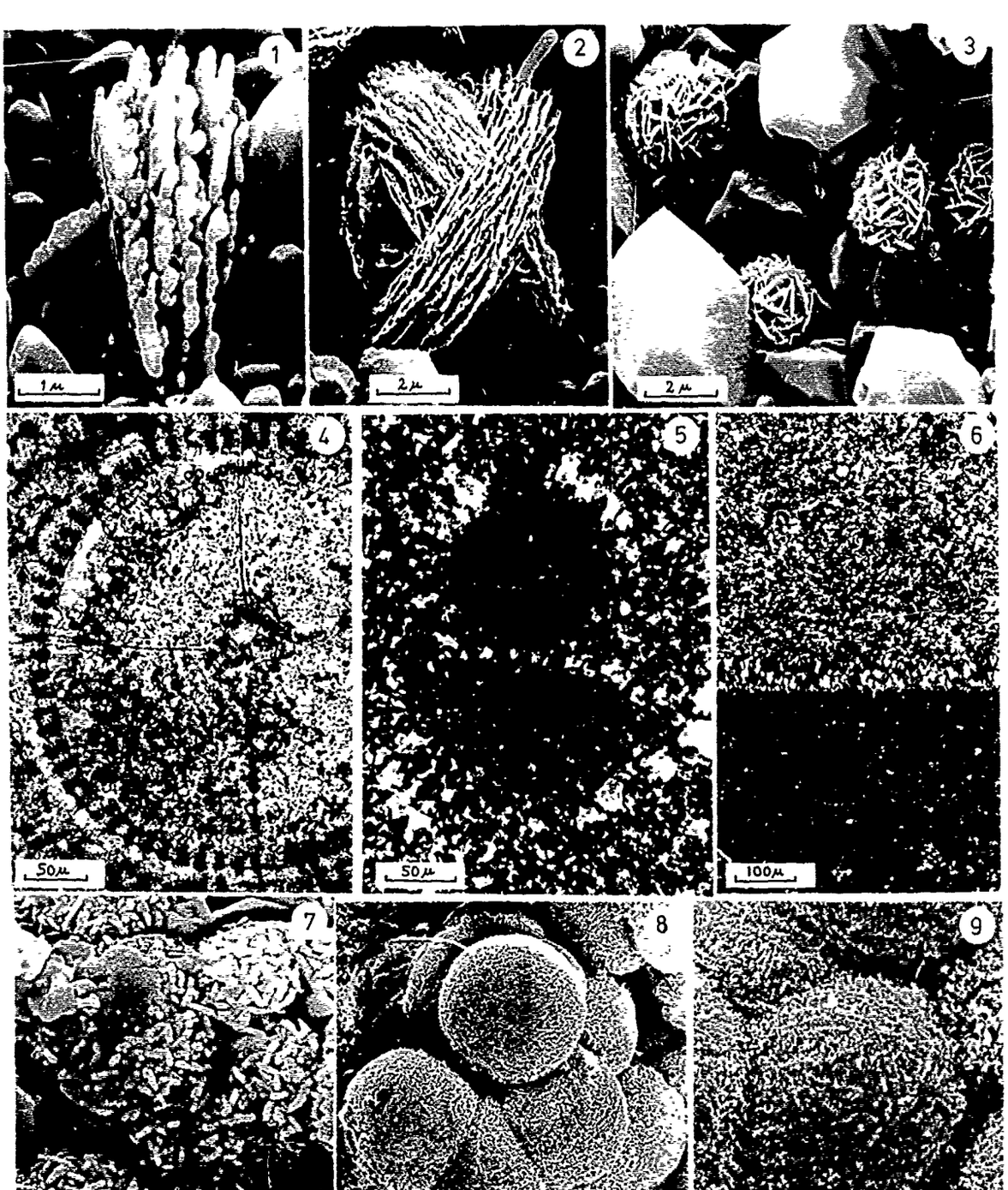
1
1 μ
2
2 μ
3
2 μ
4
50 μ
5
50 μ
6
100 μ
7
1 μ
8
10 μ
9
10 μ

Plate 3. Opal-CT lepispheres, porcellanite and quartz chert.

Figure 1. Individual opal-CT blades (0.2 μ thick) with irregular ragged edges. Sample DSDP 11-98-10-1, 70-73 cm (late Paleocene to early Eocene; SEM 492/8).

Figure 2. Well developed large bladed lepisphere showing groups of opal-CT blades intergrown according to the twinning laws of tridymite (note 70° or 180°-70° angle). Lepisphere grows on calcite cement in the interior of the foraminiferal chamber. Porcellanite nodule (same sample as Figure 1, SEM 492/3).

Figure 3. Moderately silicified Maastrichtian chalk with a few small, early-diagenetic, individual lepispheres growing on euhedral calcite crystals and coccoliths. Sample DSDP 14-144-3-2, 103-104 cm (Campanian-Maastrichtian; SEM 502/9).

Figure 4. Well preserved (opal-A?) radiolarian in early Eocene calcareous porcellanite with chert bands, filled by (a) structureless opal-CT replacing nanno ooze with relic coccoliths (center right); (b) well developed opal-CT lepispheres (open-cavity growth, center left); (c) quartz (remaining pore space, upper left). Sample DSDP 41-366-31-4, 91-93 cm.

Figure 5. Incipient quartzification in early Eocene, zoned chalk-porcellanite-chert nodule. Ghost of foraminiferid is filled by opal-CT (black) with scattered distinct nuclei of quartz crystals (light-colored spots), whereas the matrix consists already mostly of microcrystalline quartz. DSDP 41-366-29-1, 50 cm (X nicols).

Figure 6. Well defined boundary between porcellanite (black) with scattered quartz nuclei (white) and microcrystalline quartz chert (top). Quartz-filled vein at contact. DSDP 41-370-15-2, 139-141 cm (middle Eocene, X nicols).

Figure 7. Ghost of radiolarian filled by ellipsoidal, spherical and coalescent "stubby" or "nubby" lepispheres. Individual "blades" are thicker (0.1-0.2 μ) and shorter (0.5-1 μ) than in normal lepispneres. Tridymite-type twinning is less evident. Oligocene-Miocene clayey radiolarian porcellanite (DSDP 11-106B-7-1, 13-14 cm; SEM 494/11).

Figure 8. Quartz-replaced lepispheres with well preserved gross morphology from the original opal-CT stage. Sample DSDP 41-367-31-1, 64-66 cm (Berriasian, SEM 729/3).

Figure 9. Quartzified lepisphere with relic surface structure indicative of an opal-CT precursor stage (interpenetration twins; SEM 631/9). Same sample as Figure 8.

Acknowledgements. This study on silica diagenesis in the North Atlantic Basin was supported by the German Research Society (DFG grant Ra 191/4-7) for a number of years. We are indebted to Dr. H.Rösch (Hannover) for the quantitative X-ray diffraction analyses, to Professor H.Friedrichsen (Tübingen) for measuring oxygen and hydrogen isotope ratios of opal-CT and quartz samples, and to Professor O.W.Flörke (Bochum) for his comments on the opal-CT/quartz conversion. Thanks are also due to Mr. E.Knickrehm (Hannover) for operating the SIEMENS (ETEC) Autoscan electron microscope. All samples studied were kindly supplied by the Deep Sea Drilling Project (La Jolla), financed by the National Science Foundation (U.S.A.). We are very grateful to Dr.H.Rösch and to the reviewers for their comments and constructive criticism.

## References

Berger, W.H., Biogenous deep-sea sediments: fractionation by deep-sea circulation, Bull. Geol. Soc. America, 81, 1385-1401, 1970.

Berger, W.H. and P.H.Roth, Oceanic micropaleontology: progress and prospect, Reviews of Geophys.and Space Phys., 13, 561-653, 1975.

Berger, W.H. and U. von Rad, Cretaceous and Cenozoic sediments from the Atlantic Ocean, In Hayes, D.E., Pimm, A.C., et al., Initial Reports Deep Sea Drilling Project, 14, 787-954 1972.

Bergren, W.H. and C.D. Hollister, Paleogeography, paleobiography and the history of circulation in the Atlantic Ocean, In W.W. Hay (Ed), Studies in paleooceanography, Soc. Econ. Paleont. Mineral., Spec. Publ. 20, 126-186, 1974.

Bonatti, E. and O. Joensuu, Palygorskite from Atlantic deep sea sediments, Am. Mineralogist., 53, 975-983, 1968.

Bramlette, M.N., The Monterey Formation of California and the origin of its siliceous rocks, Prof. Pap. U. S. Geol. Surv., 213, 57 pp,1946.

Calvert, S.E., Composition and origin of North Atlantic deep sea cherts, Contrib. Mineral. Petrol., 33, 273-288, 1971.

Calvert, S.E., Deposition and diagenesis of silica in marine sediments, In K.J. Hsü and H.C. Jenkyns (Eds.) Pelagic Sediments: on Land and under the Sea, Spec. Publs. int. Ass. Sediment. 1, 273-299, 1974.

Calvert, S.E., Mineralogy of silica phases in deep-sea cherts and porcelanites, Phil. Trans. Royal Soc. London (A), 286 (1336), 239-252, 1977.

Chamley, H. and G. Millot, Observations sur la répartition et la genèse des attapulgites plio-quaternaires de Mediterranée, Compt. rend. hebd. Séanc. Acad. Sci. Paris (D), 281 (17), 1215-1218, 1975.

Couture, R.A., Comments on: Miocene of the S.E. United States: A model for chemical sedimentation in a peri-marine environment (Weaver and Beck), Sed. Geol., 21, 149-154, 1978.

Ernst, W.G. and S.E. Calvert, An experimental study of the recrystallization of porcelanite and its bearing on the origin of some bedded cherts, Am. J. Sci. (Schairer Vol.), 267A, 114-133, 1969.

Fischer, A.G. and M.A. Arthur, Secular variations in the pelagic realm, In Cook, H.E. and P. Enos (Eds.) Deep Water Carbonate Environments, Soc. Econ Paleont. Mineral., Spec. Publ. 25, 19-50, 1977.

Flörke, O.W., R. Hollmann, U. von Rad, and H. Rösch, Intergrowth and twinning in opal-CT lepispheres, Contr. Mineral. Petrol., 58, 235-242, 1976.

Flörke, O.W., J.B. Jones and E.R. Segnit, Opal-CT crystals, Neues J. Miner. Mh., 8, 369-377, 1975.

Garrison, R.E., St. M. Rowland, I.J. Horau and J.C. Moore, Petrology of siliceous rocks recovered from marginal seas of the western Pacific, Leg 31, Deep Sea Drilling Project, In Karig, D.E., J.C. Ingle et al., Initial Reports Deep Sea Drilling Project, 31, 519-529, 1975.

Gibson, T.G. and K.M. Towe, Eocene volcanism and the origin of Horizon A, Science, 172, 152-153, 1971.

Goll, R.M. and K.R. Bjorklund, Radiolaria in surface sediments of the North Atlantic Ocean, Micropaleontology, 17 (4), 434-454, 1972.

Greenwood, R., Cristobalite: its relationship to chert formation in selected samples from the Deep Sea Drilling Project, J. Sedim. Petrol., 43, 700-708, 1973.

Heath, G.R., Cherts from the eastern Pacific, In Van Andel, T.H., G.R. Heath et al., Initial Reports Deep Sea Drilling Project, 16, 609-613, 1973.

Heath, G.R., Dissolved silica and deep-sea sediments, in W.W. Hay (Ed.), Studies in Paleo-Oceanography, Soc. Econ. Paleontol. Mineral., Spec. Publ. 20, 77-93, 1974.

Heath, G.R. and R. Moberly, Cherts from the western Pacific, Leg 7, Deep Sea Drilling Project, In E.L. Winterer, W.R. Riedel et al., Initial Reports Deep Sea Drilling Project, 7, 991-1008, 1971.

Hein, J.R., D.W. Scholl, J.A. Barron, M.J. Jones, and J. Miller, Diagenesis of late Cenozoic diatomaceous deposits and formation of the bottom simulating reflector in the southern Bering Sea, Sedimentology, 25, 155-181, 1978

Hurd, D.C. and F. Theyer, Changes in the physical and chemical properties of biogenic silica from the central equatorial Pacific: Part II Refractive index, density and water content of acid-cleaned samples, Amer. J. Science, 277, 1168-1202, 1977.

Johnson, Th.C., The dissolution of siliceous microfossils in surface sediments of the eastern tropical Pacific, Deep-Sea Research, 21, 851-864, 1974.

Johnson, Th.C., Biogenic opal preservation in pelagic sediments of a small area in the eastern tropical Pacific, Geol. Soc. Amer. Bull., 87., 1273-1282, 1976.

Jones, J.B. and E.R. Segnit, The nature of opal.

I. Nomenclature and constituent phases, J. Geol. Soc. Australia, 18, 57-68, 1971.

Eastner, M., J.B. Keene, and J.M. Gieskes, Diagenesis of siliceous oozes. I. Chemical controls on the rate of opal-A to opal-CT transformation - an experimental study, Geochim. Cosmochim. Acta, 41, 1041-1059, 1977.

Keene, J.B., Cherts and porcellanites from the North Pacific, Deep Sea Drilling Project Leg 32, In Larson R.L., R. Moberly et al., Initial Reports Deep Sea Drilling Project, 32, 429-507, 1975.

Keene, J.B., The distribution, mineralogy and petrography of biogenic and authigenic silica from the Pacific Basin, Ph.D. Thesis, Scripps Inst. Oceanogr., Univ. Cal. San Diego, 264 pp., 1976.

Kelts, K., Summary of chert occurrences from Line Island Sites 314,315,316, DSDP-Leg 33, In Schlanger, S.O., E.D. Jackson, et al., Initial Reports Deep Sea Drilling Project, 33, 855-863, 1976.

Knauth, L.P. and S. Epstein, Hydrogen and oxygen isotope ratios in silica from the JOIDES Deep Sea Drilling Project, Earth Plan. Science Letters, 25, 1-10, 1975.

Knauth, L.P. and S. Epstein, Hydrogen and oxygen isotope ratios in nodular and bedded cherts, Geochim. Cosmoch. Acta, 40, 1095-1108, 1976.

Lancelot, Y., Chert and silica diagenesis in sediments from the central Pacific, In E.L. Winterer, J.I. Ewing et al., Initial Reports Deep Sea Drilling Project, 17, 377-405, 1973.

Lancelot, Y., J.C. Hathaway and C.D. Hollister, Lithology of sediments from the Northwest Atlantic Leg 11, Deep-Sea Drilling Project, In Hollister, C.D., J.E. Ewing et al., Initial Reports Deep Sea Drilling Project, 11, 901-949, 1972.

Leclaire, L., Late Cretaceous and Cenozoic pelagic deposits - paleoenvironment and paleooceanography of the central western Indian Ocean, In Simpson, E.S.W., R. Schlich, et al., Initial Reports Deep Sea Drilling Project, 25, 481-513, 1974.

Mattson, P.H. and E.A. Pessagno, Caribbean Eocene volcanism and the extent of Horizon A, Science, 174, 138-139, 1971.

McCoy, F.W. and H.B. Zimmerman, A history of sediment lithofacies in the South Atlantic Ocean, In Supko, P.R., K. Perch-Nielsen et al., Initial Reports Deep Sea Drilling Project, 39, 1047-1080, 1977.

Millot, G., Geology of clays, Springer (Masson & Cie, Chapman & Hall), New York, Heidelberg, Berlin, 429 pp, 1970.

Murata, K.J., Friedman, I., and Gleason, J.D., Oxygen isotope relations between diagenetic silica minerals in Monterey shale, Temblor Range, California, Amer. J. Science, 227, 259-272, 1977.

Murata, K.J. and R.R. Larson, Diagenesis of Miocene siliceous shales, Temblor Range, California, J. Research U. S. Geol. Surv., 3 (No.5), 553-566, 1975.

Murata, K.J. and J.K. Nakata, Cristobalitic stage in the diagenesis of diatomaceous shale, Science, 18, 567-568, 1974.

Murata, K.J. and M.B. Norman II, An index of crystallinity for quartz, Amer. J. Science, 276, 1120-1130, 1976.

Ramsay, A.T.S., A history of organic siliceous sediments in oceans, In Hughes, N.F. (Ed.) Special papers in Paleontology, 12, Paleont. Assoc. London, 199-234, 1973.

Riech, V., Diagenesis of silica, zeolites and phyllosilicates in Sites 397 and 398, In U. von Rad, W.B.F. Ryan et al., Initial Reports Deep Sea Drilling Project, 47 (1), in press (1).

Riech, V., Diagenesis of siliceous sediments, porcellanites, and cherts of the Moroccan Basin (Sites 370,415 and 416), In Y. Lancelot, E.L. Winterer et al., Initial Reports Deep Sea Drilling Project, 50, in press (2).

Riech, V. and U. von Rad, Eocene porcellanites and Early Cretaceous cherts from the western North Atlantic, In B. Tucholke, P.R.Vogt et al., Initial Reports Deep Sea Drilling Project, 43, in press.

Schlanger, S.O. and R.G. Douglas, Pelagic ooze-chalk -limestone transition and its implications for marine stratigraphy, In Hsü, K.J. and Jenkyns, H.C. (Eds) Pelagic sediments: on Land and under the Sea, Spec. Publs. int. Ass. Sediment, 1, 117-148, 1974.

Sclater, J.G., St. Hellinger and Ch. Tapscott, The paleobathymetry of the Atlantic Ocean from the Jurassic to the Present., J. Geol., 85, 509-552, 1977.

Stein, C.L. and R.J. Kirkpatrick, Experimental porcelanite recrystallization kinetics: A nucleation and growth model, J. Sed. Petrol, 46, 430-435, 1976.

Stonecipher, Sh. A., Origin, distribution and diagenesis of phillipsite and clinoptilolite in deep-sea sediments, Chem. Geol., 17, 307-318, 1976.

Tucholke, B.E. and G.S. Mountain, Lithologic correlation and significance of major seismic reflectors in the Western North Atlantic, Abstracts, Second M. Ewing Symposium, Arden House, Harriman, N.Y., 40-41, 1978.

Van Andel, Tj.H., J. Thiede, J.G. Sclater, and W.W. Hay, Depositional history of the South Atlantic Ocean during the last 125 million years, J. Geol., 85, 651-698, 1977.

von Rad, U., V. Riech and H. Rösch, Silica diagenesis in continental margin sediments off Northwest Africa, In Y. Lancelot, E. Seibold et al., Initial Reports Deep Sea Drilling Project, 41, 879-905, 1977.

von Rad, U. and H. Rösch, Petrography and diagenesis of deep-sea cherts from the Central Atlantic, In K.J. Hsü and H.C. Jenkyns (Eds.) Pelagic Sediments: on Land and under the Sea, Spec. Publs. int. Ass. Sediment., 1, 327-347, 1974.

Weaver, Ch.E. and K.C. Beck, Miocene of the S.E. United States: a model for chemical sedimenta-

tion in a peri-marine environment, Sedim. Geol., 17, 1-234, 1977.
Weaver, F.M. and S.W. Wise, Jr, Ultramorphology of deep sea cristobalitic chert, Nature Phys. Sci., 237, 56-57, 1972.
Wiedmann, J., A. Butt and G. Einsele, Vergleich von marokkanischen Kreide-Küstenaufschlüssen und Tiefseebohrungen (DSDP): Stratigraphie, Paläoenvironment und Subsidenz an einem passiven Kantinentalrand, Geol. Rdsch., 67, 454-508, 1978.
Wise, S.W., Jr., B.F. Buie, and F.M. Weaver, Chemically precipitated sedimentary cristobalite and the origin of chert, Eclog. Geol. Helv., 65, 157-163, 1972.
Wise, J.W., Jr. and F.M. Weaver, Chertification of oceanic sediments, In K.J. Hsü and H.C. Jenkyns (Eds.) Pelagic Sediments: on Land and under the Sea, Spec. Pubis. int. Ass. Sediment., 1, 301-326, 1974.

# NORTH ATLANTIC CLAY SEDIMENTATION AND PALEOENVIRONMENT SINCE THE LATE JURASSIC.

Hervé Chamley

Sédimentologie et Géochimie, Lille I University,
B.P. 36, 59650 Villeneuve d'Ascq, France.

Abstract. The large abundance of clay particles in ancient marine sediments raises the question of their origin. Detailed mineralogical, chemical and lithological investigations on numerous DSDP Mesozoic and Cenozoic sediments of the North Atlantic margins point to insignificant contribution of autochthonous sources compared to continental detrital supply. Thus the clay sediments strongly reflect the continental environmental variations in the geological past, rather than the present marine environment. Selected examples show how mineralogical changes may contribute to explaining major geographical events : 1) Climate : Cretaceous and Paleogene smectite chiefly inherited from hydromorphic soils of low-relief areas under hot temperature and contrasting humidity ; irregular increase of primary minerals in Cenozoic rocks due to a world-wide cooling associated with more regular rainfall. 2) Tectonics : strong supply and rapid accumulation of a mixture of primary and pedogenic minerals in the NW Atlantic during the middle-late Jurassic, related to ocean initiation and continental drift. 3) Physiography : detrital attapulgite (palygorskite) in Albian time, and attapulgite and sepiolite in Early Eocene time, indicators of closed or semi-closed marginal basins, in which fibrous minerals formed under warm and confined conditions. 4) Currents and global tectonics : strong increase of primary minerals in the upper Cretaceous, probably induced by the onset of longitudinal deep-water circulation at the time of the NW Atlantic widening. A tentative chronological and geographical interpretation of clay mineral variations in marine deposits is proposed which takes into account the highly variable train of environmental factors.

## Introduction

One of the most obvious facts arising from the survey of deep sea drilling materials is the abundance of clay-rich sedimentary rocks. Well known for the recent sediments of the world ocean (Lisitzin, 1972), this fact is also particularly clear for the Mesozoic and Cenozoic sediments of the North Atlantic ocean. For instance the proportion of claystone, mudstone, marl, clayey chalk from Legs 47, 48 and 50 of the Glomar Challenger is about 75 % of the whole sedimentary sequence since the late Jurassic (see Ryan, von Rad et al., in press ; Ryan, Sibuet et al., in press ; Montadert, Roberts et al., in press ; Lancelot, Winterer et al., in press).

The nature of the clay fractions and the significance of their high proportion in past sediments are important to determine for they may contribute to the reconstruction of paleoenvironments. For some authors North Atlantic ancient marine clays are chiefly autochthonous and reflect the volcanogenic and diagenetic history of marine sediments (Kossowskaya et al., 1975 ; Lomova, 1975). For some others the marine clay could be the result of both diagenetic-volcanogenetic and alluvial processes and have a complex significance (Berger and Von Rad, 1972 ; Lancelot et al., 1972). In recent Atlantic sediments the clay fraction is mainly detrital and expresses continental environments and the influence of currents (Biscaye, 1965 ; Griffin et al., 1968).

Our purpose is to consider the nature, distribution and behaviour of clays in North Atlantic DSDP cores in order to understand their origin and signification. About 1.500 original samples have been studied by x-ray diffraction on non-calcareous, less than 2 µm particles, complemented by electro-microscopic observations, differential thermal analyses and various chemical analyses. 25 drill sites of the East and West North Atlantic margins are considered, originating from Legs 11, 14, 44, 47A, 47B, 48 and 50 of the Deep Sea Drilling Project (Fig. 1). The data and discussions are presented here in a generalized manner, detailed considerations being published elsewhere (Chamley and Giroud d'Argoud, in press ; Chamley et al., in press ; Chamley and Diester-Haass, in press ; Debrabant et al., in press ; Diester-Haass and Chamley, in press ; Pastouret et al., in press).

## Origin of Marine Clays

In most parts of the world ocean, modern clay minerals show a general latitudinal zonation (Biscaye, 1965 ; Griffin et al., 1968 ; Rateev

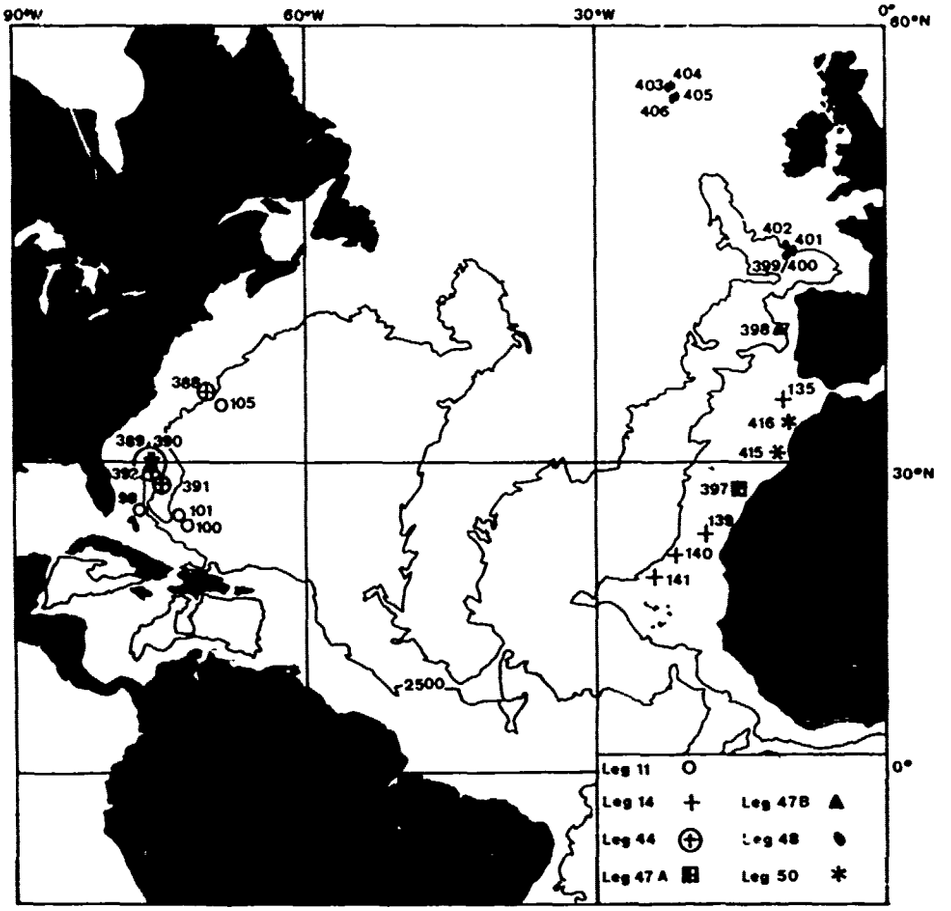


Figure 1. Location map.

et al., 1969), which approximately reproduces the continental pedogenic zonation (Millot, 1964 ; Pédro, 1968). This is especially the case in the Atlantic ocean and in all basins located in the vicinity of land masses. The large variety of clay species and associate small-sized minerals (quartz, feldspars, amphiboles, ...) chiefly reflects the diversity of continental sources and the main supply form soils and other surficial alterations. There are no structural changes of minerals either when clay passes from continental water to marine water (i.g. Gibbs, 1977), nor when it is deposited. Now the question arises what happened during past geological times.

## Diagenesis With Depth of Burial

Clay species are the same in ancient and recent sediments. Their variety and variability are large in both cases, as shown for instance by the succession of Cretaceous and Cenozoic assemblages recovered off the Iberian margin in Site 398, which reached a depth of 1 740 m (Fig. 2). Minerals such as chlorite and illite, inherited from crystalline rocks (≈ "primary" minerals), occur as well as smectite, fibrous clays (attapulgite ≈ palygorskite, sepiolite), kaolinite and irregular mixed-l. rs (chiefly of illite-smectite and chlorite-smectite types), the later group being formed and stable under low temperature and pressure conditions (Millot, 1964). There is no progressive and continuous change with increasing depth in cores, neither in the relative abundance, crystallinity and morphology of minerals (Fig. 2, Fig. 3), nor in the chemistry of major and minor elements. Rare earth elements associated with clay minerals, especially with smectite, do not show any change such as an equilibration with sea water, from early Cretaceous to present time (Courtois and Chamley, 1978). Thus there is no appreciable sign of diagenesis with depth of burial in the Mesozoic and Cenozoic deposits of the North Atlantic margins.

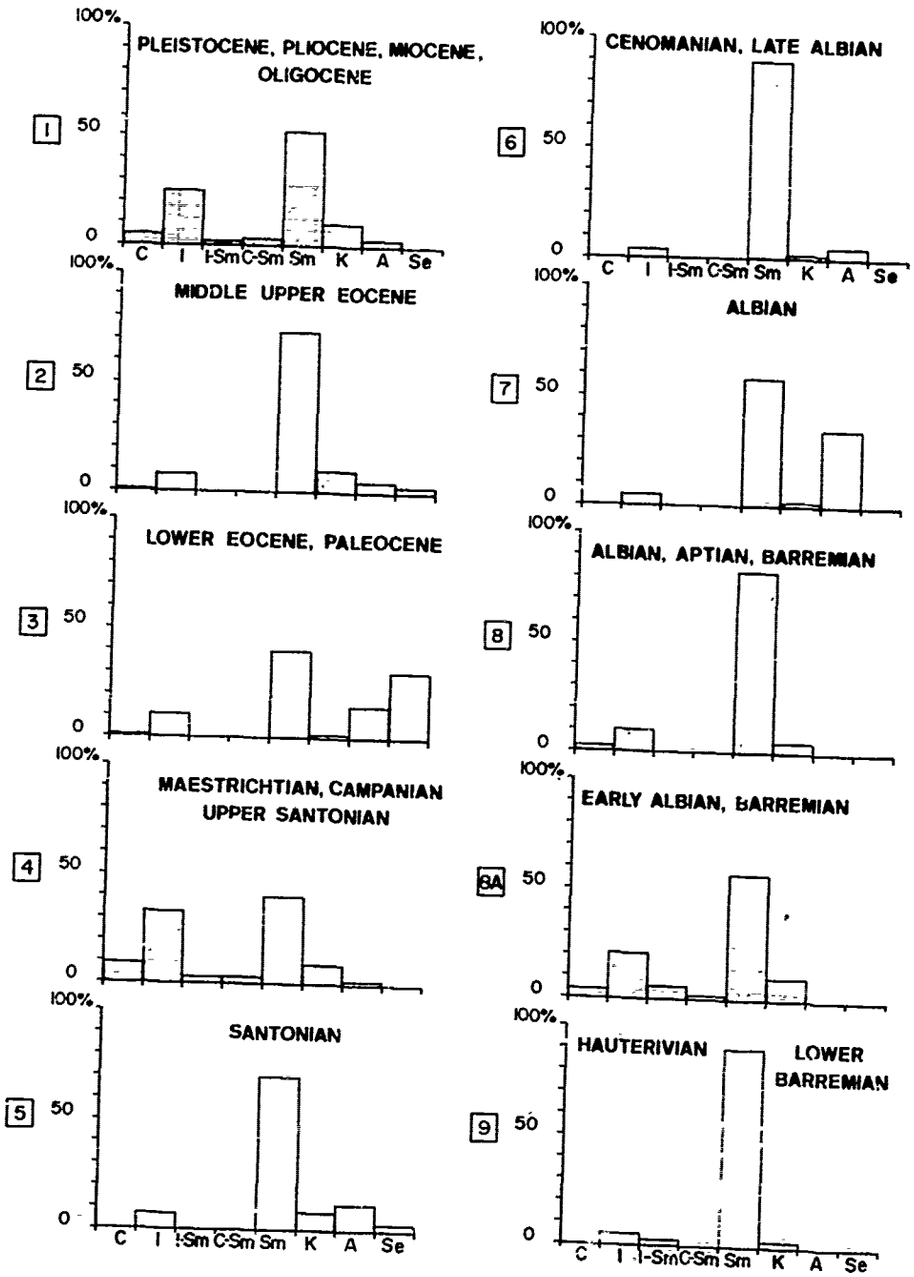


DSDP Leg 47B_MINERALOGICAL ZONATION OF SITE 398.

Figure 2. Site 398, Leg 47 B. Mineralogical zonation (average data). Legend : C, chlorite. I, illite. I-Sm, illite-smectite irregular mixed-layers. C-Sm, chlorite-smectite irregular mixed-layers. Sm, smectite. K, kaolinite. A, attapulgite (= palygorskite). S, sepiolite.

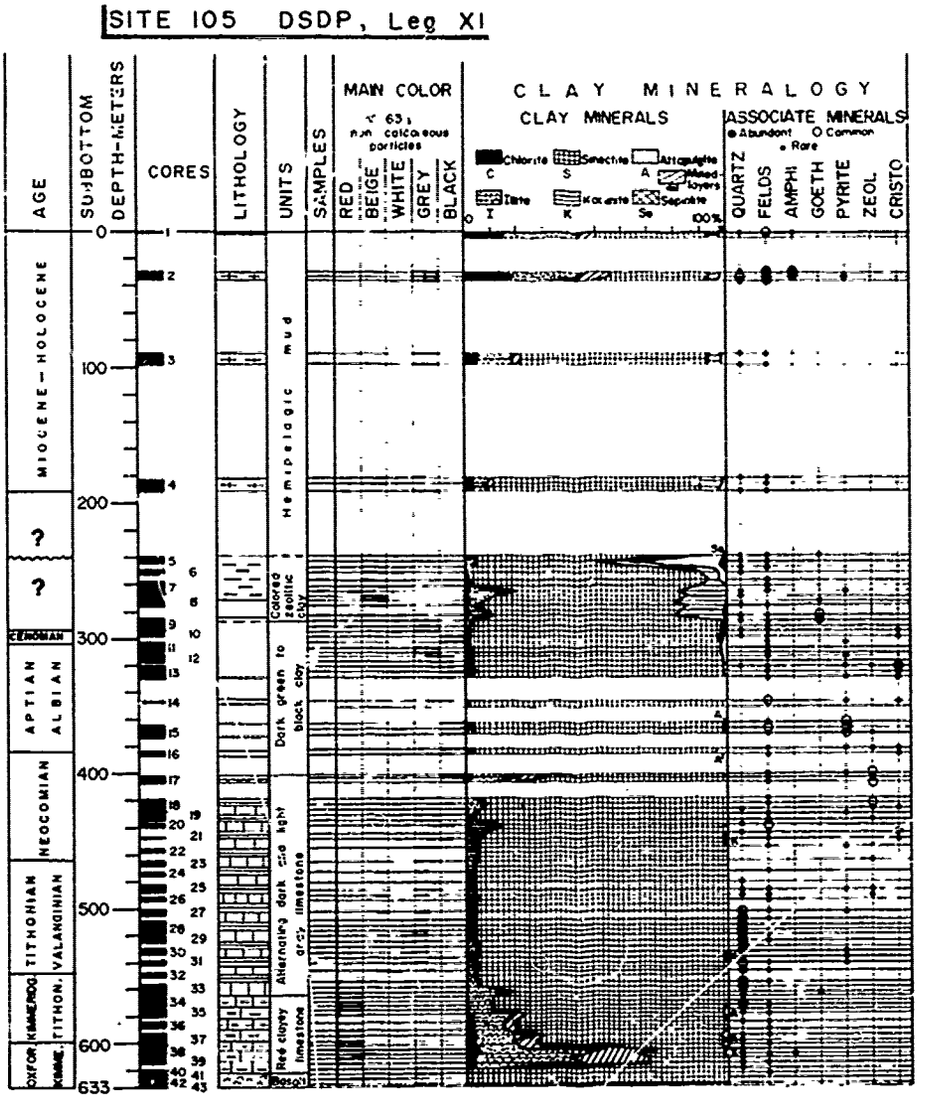


Figure 3. Site 105, Leg 11, Clay mineralogy (unpublished data).

Local Diagenesis

Although common sediments do not show any evidence of clay diagenesis along the sedimentary column, such phenomena could affect local deposits or periods. The organic-rich, black shale facies, widely distributed in the Atlantic Cretaceous (Ryan and Cita, 1977), especially in the Barremian- Cenomanian interval, generally contains clay assemblages similar to those found in oxidized sediments. Smectite, whose high exchange properties favor interlayer and structural degradation, generally does not show any significant alterations in black layers (Fig. 4, lower part), comparable to those observed in Plio-Pleistocene Mediterranean sapropels (Sigl et al., 1978). The chemical composition is similar in dark and light levels, except for manganese or iron complexes, which are pecularly sensitive to reducing environments. The same results characterize the organic-rich stages of Cape and Angola basin sediments in the South Atlantic (Leg 40 DSDP ; Robert et al., in press). In a general way, there is no noticeable diagenesis in organic environment. Only a few early Cretaceous organic-rich levels deposited off the Iberian margin (Site 398) show a decrease of smectite and an increase of irregular mixed-layers and more resistant illite and chlorite. This may indicate a local and minor *in situ* degradation by organic acids in confined reducing conditions.

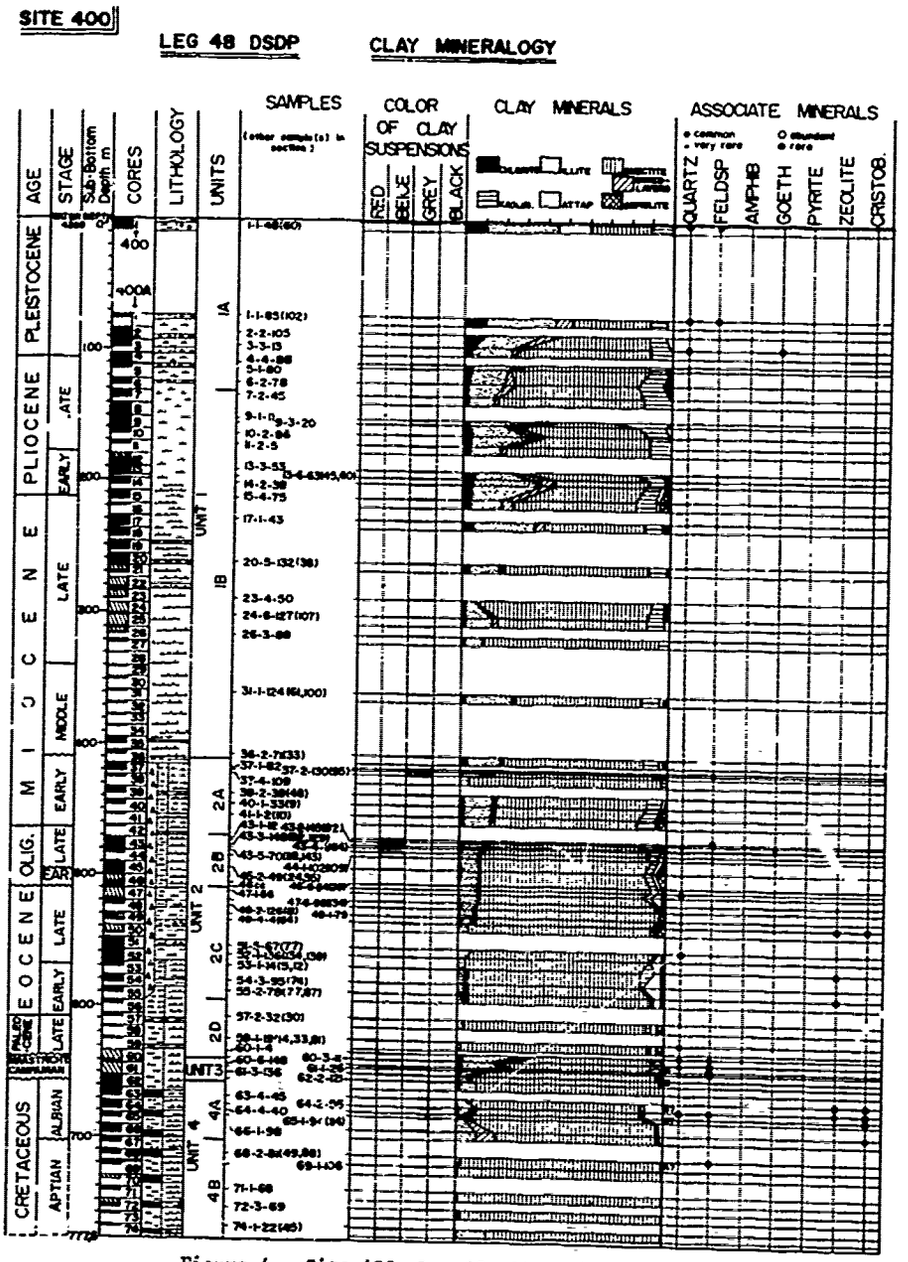


Figure 4. Site 400, Leg 48. Clay mineralogy.

Several periods are characterized by high amounts of fibrous clays - sepiolite and/or attapulgite (Fig. 2 to 4 ; see also Peterson et al., 1970 ; Berger and von Rad, 1972 ; Mélières, 1978). These reputed fragile minerals are not restricted to any particular lithological facies such as clayey chalks or limestones where they typically formed (Millot, 1964 ; Trauth, 1974 ; Weaver and Beck, 1977). On the contrary sepiolite and playgorskite here are abundant in heterogeneous, reworked, often turbiditic clastic sediments, as it is the case loca[illegible] recent sediments (Chamley and Millot, 19[illegible] ; [illegible]get and Chamley, 1977). The fibers are sometimes broken, sometimes not, but intimately dispersed among other clay minerals, some of them being typically detrital (illite, chlorite, kaolinite). Thus there is no evidence of clay diagenesis in calcareous alkaline environment, and

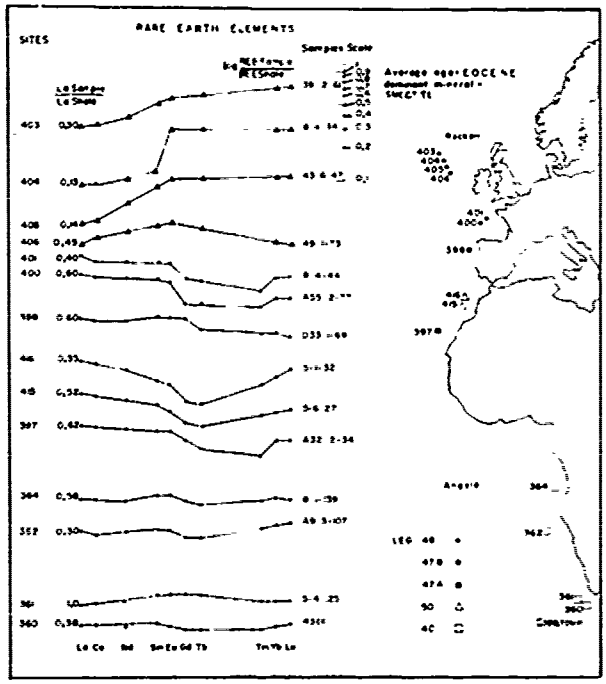


Figure 5. Distribution of rare earth elements in Eocene smectite-rich sediments of the East Atlantic margins (after Courtois and Chamley, 1978).

other possibilities are questionable (Timofeev et al., 1978).

As a general statement the clay mineralogy along the cores does not depend on the lithologic and petrographic variations, which stands in opposition to the hypothesis of noticeable *in situ* influence.

## Influence of Volcanism

Smectite is generally widely distributed in older sediments of the North Atlantic, especially in the late Jurassic and Cretaceous ones, when the ocean was narrower than today and crustal rifting and volcanism were very active. To correlate the genesis of the mineral with volcanism contemporary to the ocean initiation is enticing, for smectite formation is often correlated to volcano-hydrothermal mechanisms (in Millot, 1964; Grim and Güven, 1978). The same possibility exists for fibrous clays (Bonatti and Joensuu, 1968 ; Hathaway, 1972 ; Lomova, 1975). Nevertheless several data indicate that in most cases such hypotheses are not supported by the facts.

Smectite abundance is not systematically connected with the presence of volcanic materials or typical volcanic-derived minerals. Smectite often is very abundant in series devoid of volcanic manifestations (most Cretaceous sediments) or frequently is moderately represented in sediments marked by noticeable volcanic contributions (late Miocene to Pleistocene, Site 397, South of Canary Islands). The siliceous minerals (opal CT) occurring in numerous Cretaceous and Paleocene-Eocene deposits probably result from a diagenetic formation (Riech and von Rad, this vol.), as do some zeolites of the clinoptilolite family. These minerals chiefly form from biogenic silica and do not necessarily depend on volcanogenic supplies.

In Sites 105 and 100 located off the coast of United States, the Jurassic clayey limestones immediately overlying the basaltic basement are poor in smectite, which is there a badly crystallized mineral accompanied by detrital chlorite, illite, irregular mixed-layers, quartz and feldspars (Fig. 3) ; the rare earth composition of bulk sediment and clay fraction is that of land-derived material. If smectite is rare very close to the oceanic crust when the ocean was narrow and the ridge activity high, what about later periods such as late Cretaceous or Paleogene when the ocean was broad and the ridge influence far away from the drill sites ?

Most of smectite-rich Atlantic sediments are of an aluminous-iron type with associate V and Li, a composition not representative of volcanogenic contributions. The rare earth association of smectitic clays points to a detrital continental supply with a relative enrichment in light elements (La, Ce, Nd, Sa) (Courtois and Chamley, 1978 ; Fig. ). On the Rockall Plateau only (Sites 403 to 406) the heavy rare earth elements (Eu, Gd, Tm,

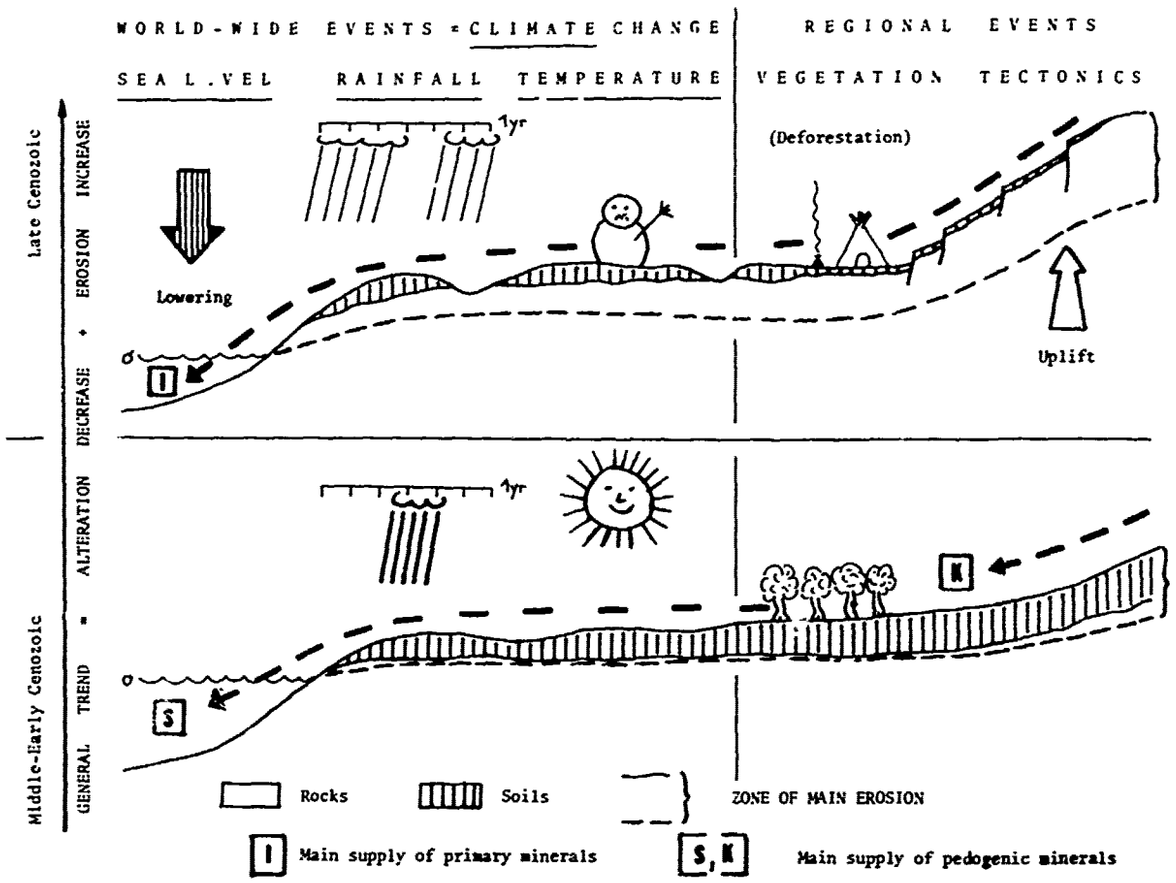


Figure 6. Schematic evolution of detrital supply to ocean since the middle Paleogene.

Yb, Lu) are relatively abundant, indicating a smectite formation from alteration of tholeiitic basalts, as does the abundance of Fe, Mg and Ti. But even in this case the alteration of basaltic rocks seems to have been aerial or subaerial (absence of negative anomaly of Ce, an indicator of sea water influence), which agrees with recent hypotheses on the subaerial rifting of the Rockall Plateau (Montadert, Roberts et al., in press).

Thus the most probable origin of smectite occuring in old sediments is a terrigenous supply, and not a submarine transformation of volcanic material. The same conclusion is valid as far as fibrous clays are concerned, as shown by their preferential occurrence in clastic and reworked sediments (see above, and also Timofeev et al., 1978). An autochthonous genesis of these minerals does exist locally (Riech and von Rad, this vol., op. cit. ; see also sepiolite in Core 43, Site 105, Fig. 3), but it seems to be restricted to very closed environments or near the volcanic sources, and to have a minor quantitative importance.

## Detrital Supply

The above discussion points to the essentially terrigenous origin of the diverse clay minerals identified in the Mesozoic and Cenozoic sediments deposited on the North Atlantic margins and on the adjacent basins. Diagenetic influences are local or insignificant compared to continental influences. This main result is in agreement with data on sedimentary organic matter which is mostly of a terrestrial origin (Habib, this vol. ; Tissot, this vol.) and closely related to clay. As the mineralogical and geochemical changes after deposition are very weak, we can conclude that the high amounts of clay contained in past marine sediments are not able to provide noticeable information about the marine diagenetic environments. On the contrary, Atlantic clays appear to be of significant interest in reconstructing the environmental history of adjacent land masses and the conditions of deposit, as they do in recent sediments. Moreover, as today clays minerals chiefly proceed from soil erosion, we can

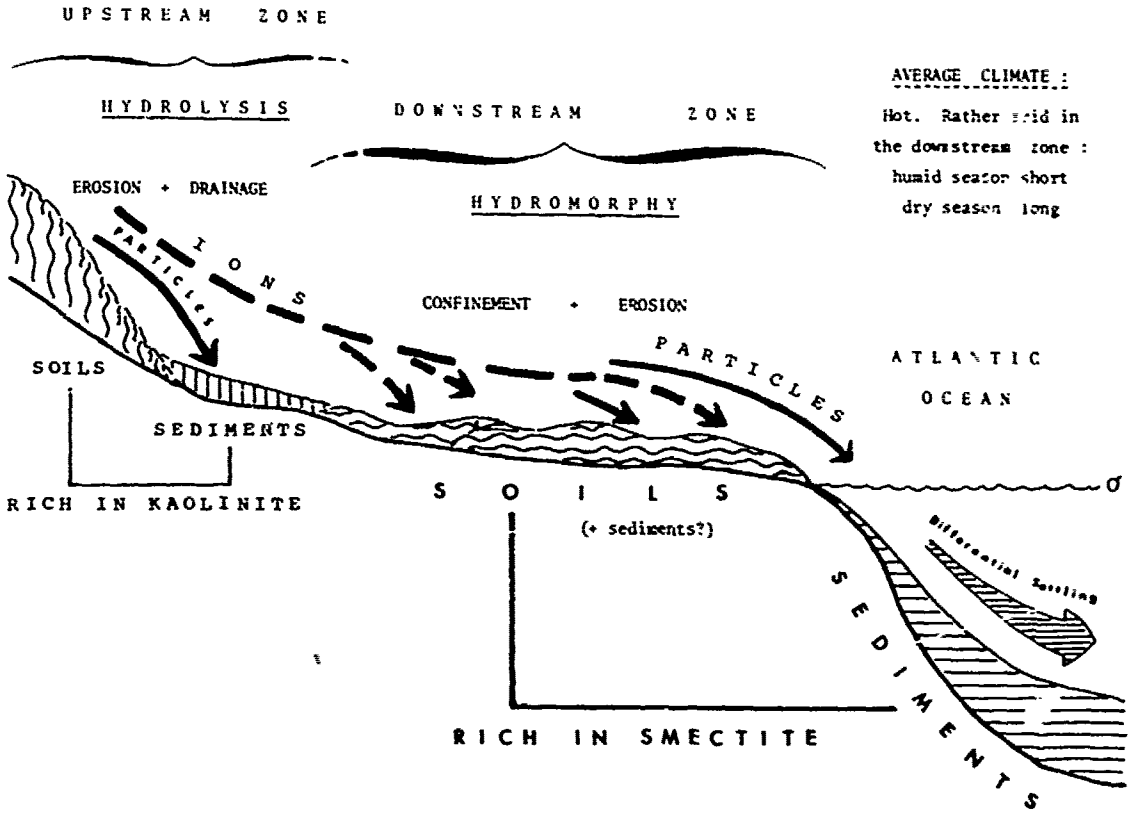


Figure 7. Possible origin of smectite in Cretaceous and Paleogene Atlantic sediments.

assume that soil-derived detritus were of a predominant importance in the sediment constitution during past geological time.

## Significance of Marine Clays

Several examples of the use of marine clays in reconstructing paleoenvironments are considered. They relate to four main topics : climate, regional tectonics, physiography, currents/global tectonics.

### Climate

All the Cenozoic sequences recovered show from the uppermost Eocene to the late Pleistocene an irregular increase of primary minerals (chlorite, illite), associated with poorly crystallized mixed-layers, quartz, feldspars and sometimes amphiboles (Fig. 3, Fig. 4). In the same time the smectite concentration decreases. Progressively the mineralogical composition of sediments becomes comparable to that of present sediments, marked by mixed supplies from soils and rocks (Griffin et al., 1968). This evolution is interpreted as a consequence of irregular world cooling combined with an increased deep circulation (Tucholke and Mountain, this vol.), that developed since the middle Paleogene (Frakes and Kemp, 1973 ; Shackleton and Kennett, 1975). Its onset is marked by the first setting up of ice caps in southern hemisphere (Kennett, 1975). The cooling was responsible for the progressive diminution of continental chemical weathering processes, leading to a lesser development of soils : hydrolyses were insufficient to permit the development of kaolinite and smectite, and allowed only a moderate degradation of primary minerals into mixed-layers. At the same time the direct physical erosion of rocks increased (illite, chlorite, quartz, feldspars), because of both a diminution of soil thickness and the lowering of the sea-level. In some areas the erosion processes increased due to alpine and post-alpine tectonics (Fig. 6).

There are many variations in this general evolution according to time and geography. For instance the cooling presents two major episodes (Fig. 11). The first one during late Miocene corresponds to the growth of the Antarctic ice-sheet and the Mediterranean dessication (Kennett and Brunner, 1973). The second one during the Plio-Pleistocene represents the development of the Arctic ice-cap (Blank and Margolis, 1975) and then the alpine glacial system. The cooling expressed by clayey sediments appears more marked towards high latitudes, in the

vicinity of glaciers and ice-rafting, than in temperate areas (Fig. 12).

Numerous other climatic data are suggested by variations in the clay mineralogy along DSDP cores, as proposed on figure 11. The most important mineralogical event extends from at least Biscay Bay (Leg 48) to Cape Basin (Leg 40 ; Robert et al., in press) and covers at least the late Jurassic-late Paleogene interval, independently of lithology. It consists of a generally high content of well-crystallized smectite (Fig. 3, Fig. 4). The mineral, which we believe to be of terrigenous detrital origin (see discussion above), is similar to the pedogenic smectite formed today in restricted peri-african areas marked by hot climate and season-contrasted humidity (Paquet, 1969). The late Mesozoic and early Cenozoic interval is known to have been characterized by warm temperature averages (Furon, 1972) ; until the late Cretaceous there was a wide extension of low relief areas on african and western european land masses (i.e. Nairn and Stehli, 1974). These climatic and topographic conditions favoured the development of hydromorphic soils in the downstream areas of river basins, leading to the pedogenic genesis of smectite. The ionic supply issued from upstream areas where hydrolyses were strong and kaolinite formed. This implies, for the entire considered period, generally hot climate, marked by fairly strong contrasts in the seasonal humidity (strong and short humid season, rather long dry season). These considerations on Cretaceous and Paleogene climate, topography, pedogenesis, erosion and sedimentation are summarized on figure 7.

## Regional Tectonics

During Leg 11 of the DSDP basaltic rocks of middle-late Jurassic age were reached, which probably represent the uppermost part of the oceanic crust (Hollister, Ewing et al., 1972). The clay fraction of basaltic alterations and of interbedded clayey limestones contains either smectite or smectite and sepiolite (Fig. 3). The petrographical, mineralogical and chemical data indicate for these minerals an alteration of tholeiitic material. Immediately overlying the basalts, Oxfordian-Kimmeridgian red clayey limestones show a typical detrital assemblage of minerals. More or less altered illite and chlorite are accompanied by irregular mixed-layers, poorly crystallized smectite, quartz and feldspars. Such an assemblage suggests a strong erosion of both rocks and little evolved soils. The rare earth composition, marked by a relative enrichment in light elements, characterizes continental supplies (comm. C. Courtois). There is no sign of any influence of crust on the formation of sedimentary clays. Such a strong and fairly short event is interpreted as an evidence of a major tectonic event in North East America, where continental rocks outcrop widely and are rich in primary minerals (continental crust, old sedimentary deposits). The cause of the tectonic event is probably one of the first stages of North Western Atlantic opening during the middle-late Jurassic (Hollister, Ewing et al., 1972). The way in which the clay fraction of first marine sediments could express such a pheromenon is schematically illustrated on figure 8. After the rift initiation accompanied only by local and minor formation of volcanogenic clay minerals (smectite, fibrous clays, ...) the collapse of the oceanic crust led to heat transfers in direction of adjacent continental crust. The result was an uplift of the margins and a correlative erosion of continental crust and old sedimentary blanket, with a detrital supply in the young ocean of moderately-degraded primary minerals. Afterwards the marginal topography progressiveiy became more equilibrated and allowed the formation of coastal soils rich in smectite, which was supplied during the following periods (Fig. 3, Tithonian-Valanginian). Note that in a strong volcanic environment, when old continental sediments and crust are poorly represented, the initiation of ocean may be characterized by strong supplies of smectite derived of the alteration of volcanic rocks. An example of such conditions is given by the Rockall Plateau, which formed during early Paleogene in the volcanic environment of the South Iceland sea (Fig. 5, Fig. 12). In all these cases the first stages of the ocean formation appear to be marked by a high erosion of emerged land-masses, clearly expressed by clay assemblages. The regional tectonic influence on clay mineralogy is preponderant and does not permit to identify possible climatic effects during these periods.

Similar mineralogical changes as those described above occurred elsewhere in late Jurassic, Cretaceous and early Paleogene of the North Atlantic, probably indicating a succession of stages of rifting, of sea-floor spreading and consequent marginal reactions, followed by stages of relaxation (Sibuet et al., in press). A preliminary interpretation of these changes is proposed on figure 11. Note that off the Morocco (Leg 50) the strong supply of primary minerals concerns almost all uppermost Jurassic and early Cretaceous time, possibly pointing to continuous active tectonic on the north-western African margin (Lancelot, Winterer et al., in press).

## Physiography

Detrital fibrous clays are common, although in low amounts in the Mesozoic and Cenozoic series drilled on both Atlantic margins. A few periods however show a strohg increase of these minerals in marine sediments (Fig. 2, Fig. 3). It is the case on north-eastern margins at least in Albian time, marked by numerous broken fibers of attapulgite (palygorskite) dispersed among other detrital minerals. It is also the case in Paleogene and mostly early Eocene times on all Atlantic margins, characterized by sepiolite in very long and flexuous fibers, and attapulgite in free fibers or as outgrowths at the edge of smectite sheets. Another attapulgite major stage occurs during Oxfordian-Kimmeridgian time off the north-west margin at

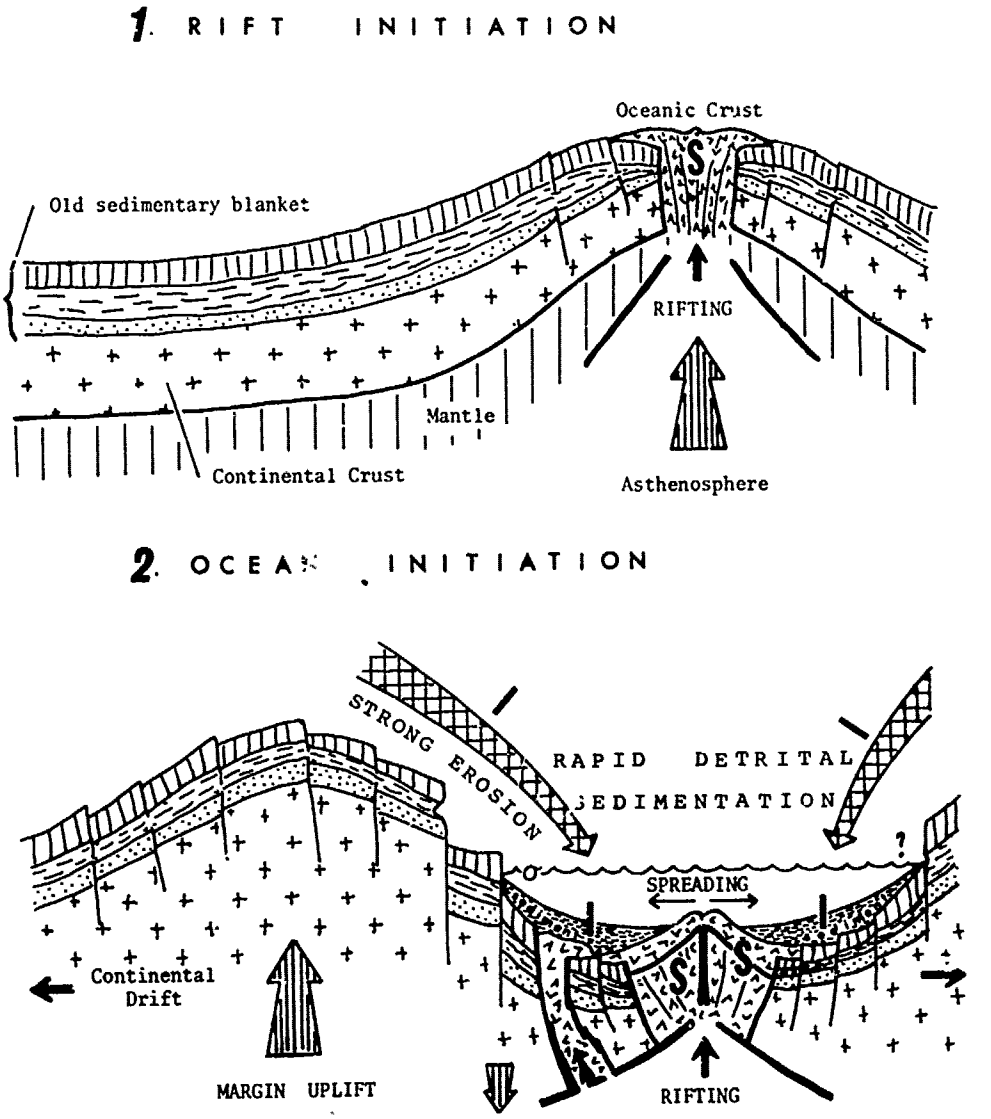


Figure 8. Influence of the ocean initiation on the clay sedimentation in a strong continental environment.

least (Leg 11, Site 100 ; see also Zemmels and Cook, 1972).

Fibrous clays occurring in marine sequences studied here are essentially detrital, but they formed in peculiar sedimentary or pedogenic environments before their erosion and reworking (Millot, 1964 ; Millot et al., 1969 ; Trauth, 1974 ; Weaver and Beck, 1977). The climate was marked by a contrasting alternation of humid and hot episodes allowing upstream hydrolysis and ionic mobilization with arid episodes allowing down-stream crystallization. Climatic parameters, however, were not sufficient for providing the alkaline chemical conditions needed for the massive genesis of aluminous-magnesian fibrous clays. A very important factor was the presence of restricted areas where ionic supplies were trapped and crystallization occurred. This supposes the existence of enclosed or semi-closed marginal basins, at least temporarily isolated from open sea, in which evaporitic

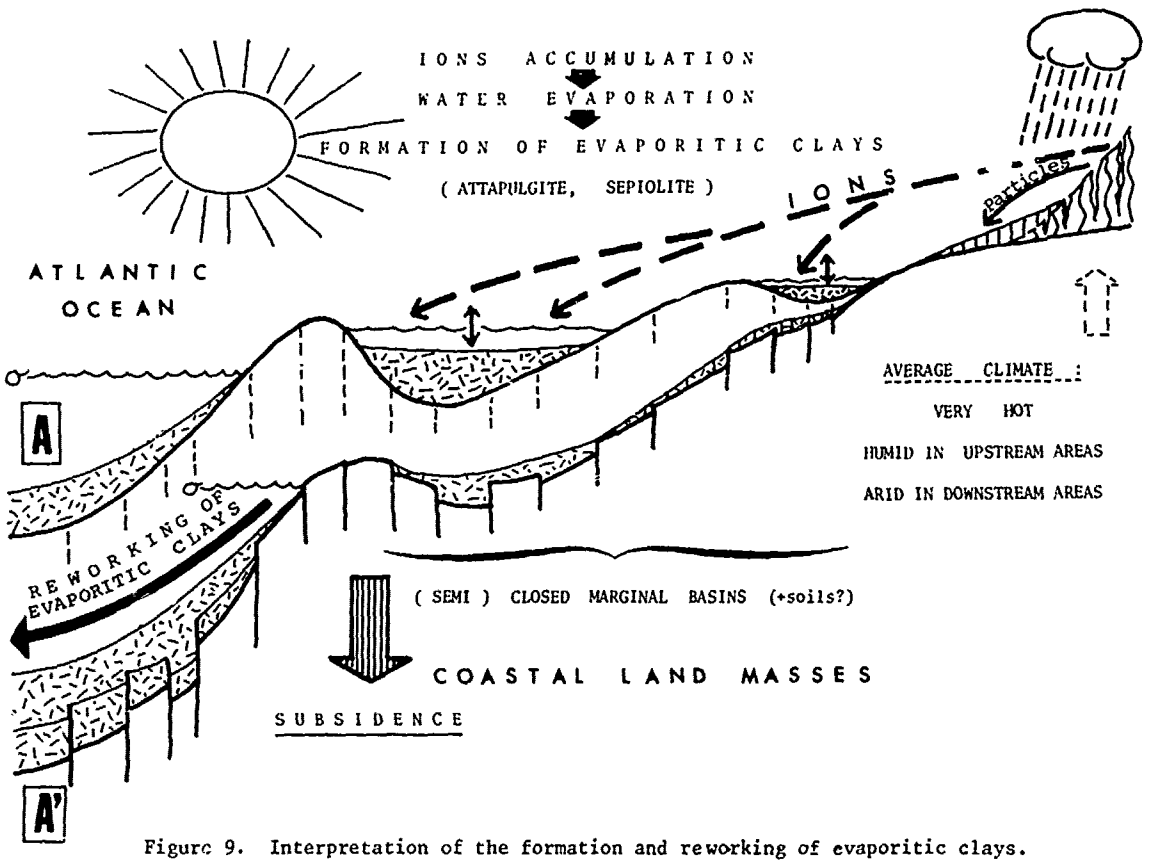


Figure 9. Interpretation of the formation and reworking of evaporitic clays.

clays such as sepiolite and attapulgite formed in sediments and/or calcareous crusts. Thus the main conditions responsible for the formation of large amounts of fibrous clays appears to be of a physiographic nature, namely the development of confined basins all along the Atlantic margins at some privileged periods (Fig. 9, A ; Fig. 11). An argument for the secondary importance of climatic factors compared to topographic ones consists in the local development of evaporitic clays in brackish or lacustrine basins until the late Miocene, when world-wide cooling was starting since a long time (i.e. South of United States, Weaver and Beck, 1977 ; South of France, Chamley, Roux and Colomb, unpubl.). Note that such restricted conditions locally permitted, especially during Paleocene-Eocene (Millot, 1964 ; in Chamley, 1971), the development not only of fibrous clays but also of smectite, zeolites (clinoptilolite), opal CT, sometimes phosphate or hydrocarbon deposits (Millot, 1964 ; Sommer, 1972 ; Lucas and Prévôt, 1975 ; Trauth, 1974 ; Weaver and Beck, 1977).

The presence of large amounts of fibrous clays in open marine sediments results from the instability of Atlantic margins at Cretaceous and Paleogene times, when the ocean widened in irregular steps. The reworking in debris flows, turbidites, slumps, and other massive displaced deposits was determined by the marginal subsidence (Fig. 9, A'). In some cases the formation and strong reworking of fibrous clays seem to be sub-contemporaneous, as suggested by the large extension of the phenomenon (form North of France to Cape Town basin at early Eocene time) and by the only local presence of these minerals in continuously reworked sediments (Albian of west european margin). The reworking of fibrous clays continued in a decreased way after the periods of their formation, as it is the case for all minerals supplied from old rocks and soils (Fig. 2 to 4).

To summarize, the periodic development of sepiolite and attapulgite in marine sediments at different Mesozoic and Cenozoic stages reflects the temporary existence of a peculiar physiography on the Atlantic margins (confined basins), combined with contrasted climate responsible for the latitudinal zonation of the phenomenon (Fig. 12) and with tectonic instability responsible for the detrital supply of evaporitic clays in the open ocean.

## Currents - Global Tectonics

Off the Iberian peninsula (Leg 47B, Site 398) a gap exists in the sedimentation which includes most of Cenomanian, Coniacian and part of Santo-

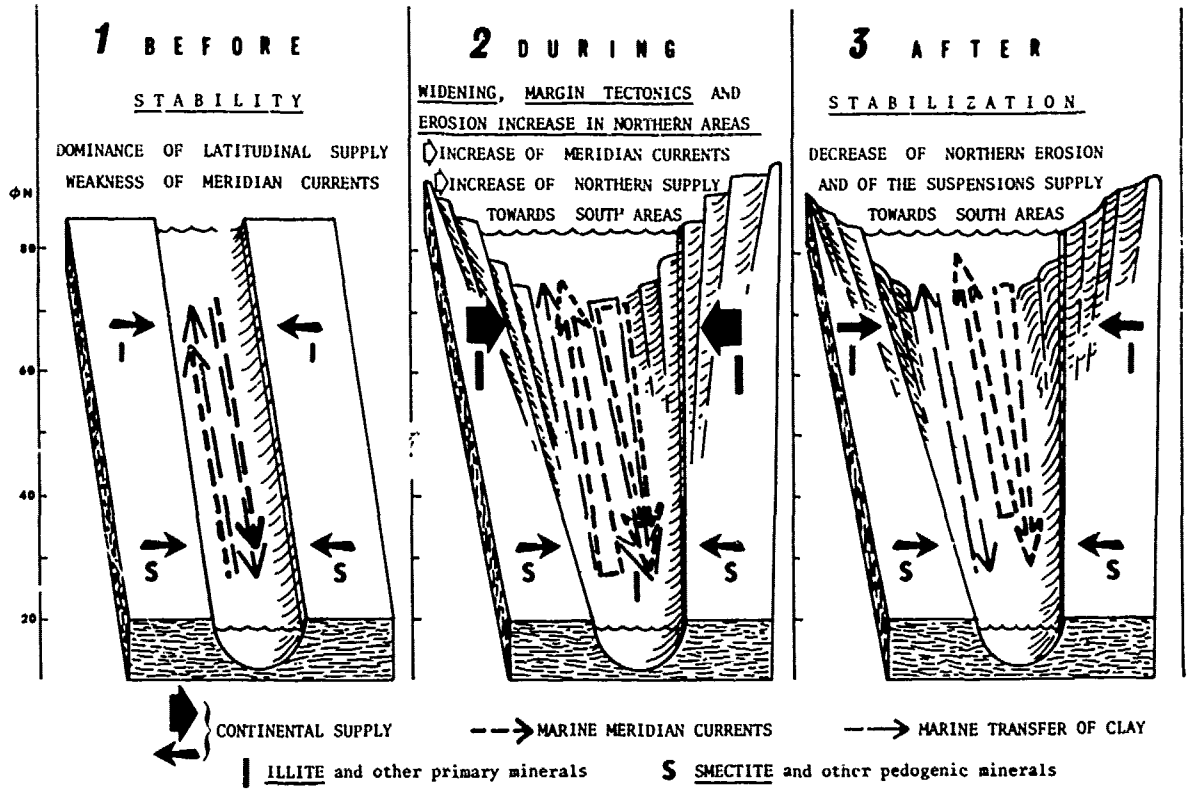


Figure 10. Continental drift, oceanic widening and meridian currents. Influence on the clay sedimentation.

nian time. The immediately overlying deposits, from late Santonian to Maastrichtian, show a peculiar clay mineralogy (Fig. 2). Succeeding to smectite-rich gray and then reddish sediments, red calcareous marls occur containing much illite and associated minerals (chlorite, quartz, feldspars), and also increased amounts of kaolinite and mixed-layers. On the other hand smectite and fibrous clays are present in lesser amounts or are missing. A simple explanation would be to relate this temporary fact to the initiation of Pyrenees mountains (Boillot and Capdevila, 1977). Such a tectonic rejuvenation would easily justify the strong erosion of both rocks and soils outcropping on the Iberia peninsula.

But the mineralogical event disappeared at the beginning of the Tertiary (Paleocene), just before the major stages of Pyrenees formation took place. Moreover the mineralogical event has a wide extension for it is recognized off the old and rather stable Armorican margin (Leg 48, Fig. 4) as well as off the north-east American margin (Leg 11, Fig. 3). Thus the mineralogical change is difficult to correlate with a regional tectonical activity. It more probably proceeds from a major opening stage of the North Atlantic ocean, allowing the setting-up of strong North-South marine currents. Note that strong currents are recognized on the Blake Plateau starting just before the Campanian (Sheridan, this vol.). The primary clay species (illite, chlorite) and associated minerals, largely outcropping in northern areas (Biscaye, 1965 ; Griffin et al., 1968 ; Kolla et al., in press), could have been transported towards the middle latitudes at that moment, in the same time as other minerals such as mixed-layers derived of low alteration processes (Chamley, 1975) and kaolinite contained in old sedimentary rocks (Darby, 1975). The cause of the major current event is probably the separation of Canada and Greenland at late Cretaceous time (Berggren and Hollister, 1975), inducing marginal tectonics, large meridian water exchanges and displacement of mineral suspensions (Fig. 10). The cause cannot be a widening of the North East Atlantic, for the Norvegian Sea and the South Iceland Sea formed at the Paleocene-Eocene time only (Talwani, Udinstev, et al., 1976 ; Montadert, Roberts et al., in press).

In the most complete sequence recovered (Site 398) the mineralogical evolution shows two successive stages interrupted by a short increase of smectite content. This could express an ocean enlarging in two steps. The progressive increase of smectite supply in sediments after the Maastrich-

NE ATLANTIC MARGIN
MINERALOGY during TIME
AGE
M.Y
S CANARY DSDP 47A
W MOROCCO DSDP 50
W IBERIA DSDP 47B
N BISCAY
ROCKALL
DSDP 48
PLEISTOCENE
PLIOCENE
MIOCENE
OLIGOCENE
EOCENE
PALEOC.
EARLY
LATE
MID.
EAR.
CHLORITE
ILLITE
IRREGULAR MIXED-LAYERS
SMECTITE
KAOLINITE
ATTAPULGITE
SEPIOLITE
QUARTZ
FELDSPARS
AMPHIBOLES
GOETHITE
CLINOPTILOLITE
CRISTOBALITE
PYRITE
CLAY FRACTION
INTERPRETATIONS
CLIMATE
very high
high
mean
low
Humidity
Temperature
TECTONICS
Spreading
Rifting
Subsidence
Uplift
OTHERS
Normal Interstitial
Reducing
Volcanic
Marginal basins

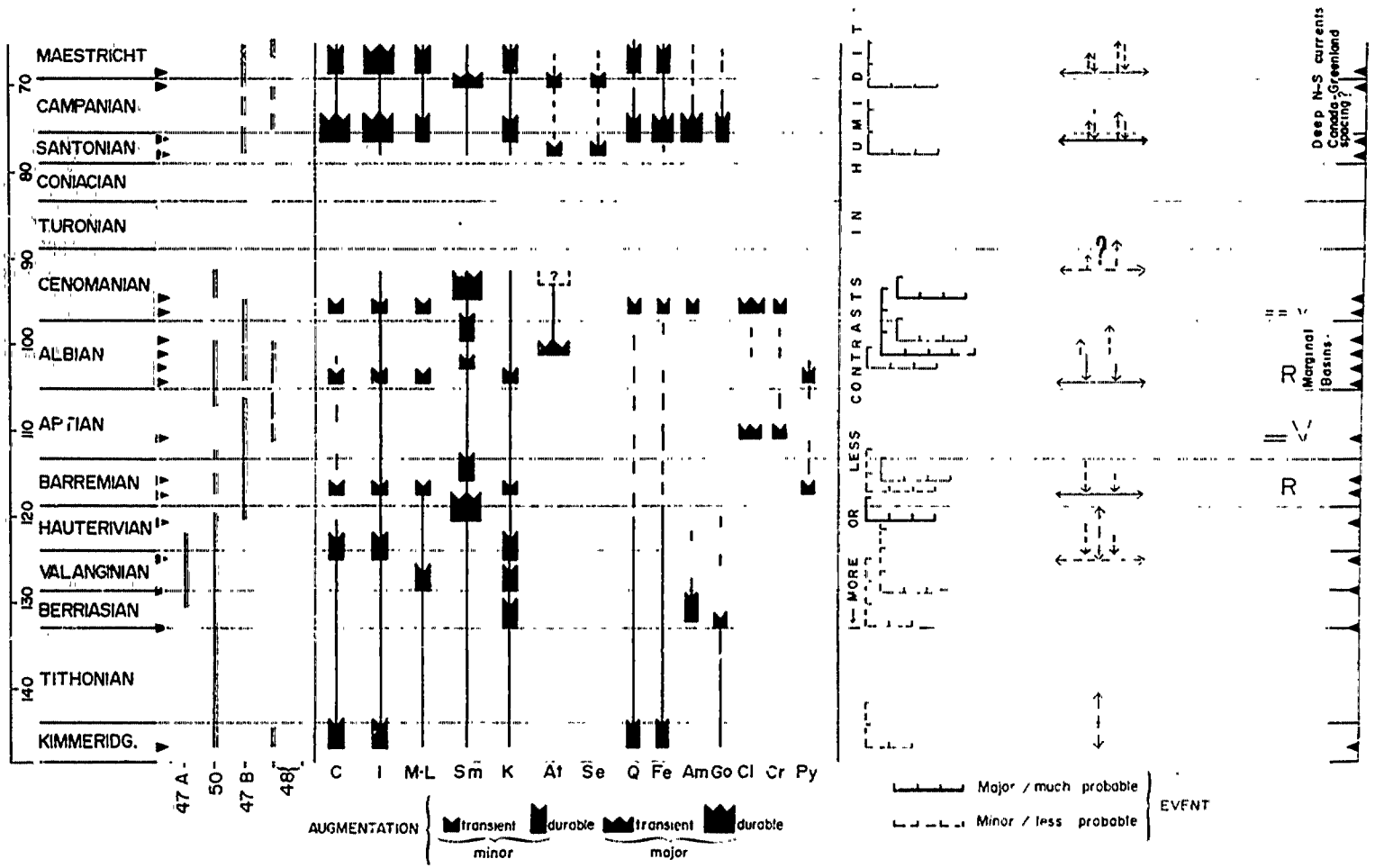


Figure 11. North East Atlantic Ocean. Successive mineralogical events and interpretations.

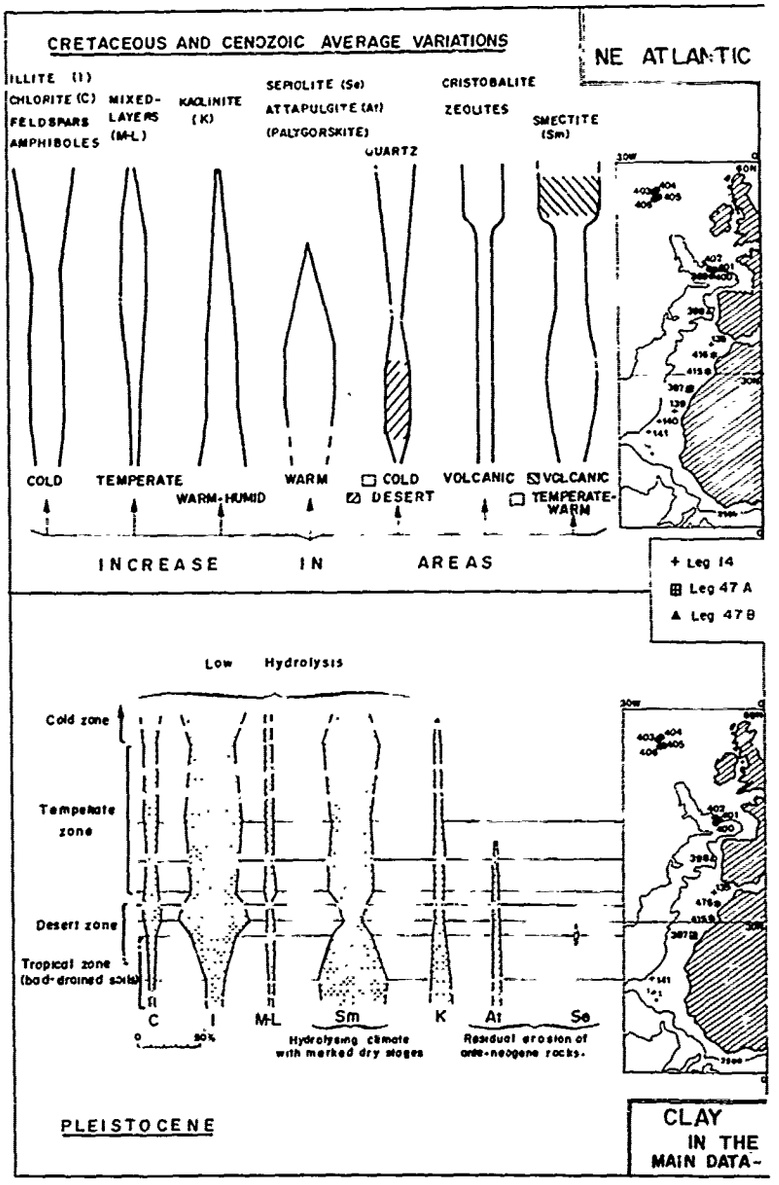


Figure 12. North East Atlantic Ocean. Geographical changes of clay mineralogy. Main trends and first reconstructions.

tian probably results of the diminution of erosion processes on the northern margins and the decreased strength of North-South currents after they are set up. The consequence would be an equilibration between distant and local supply. The interpretation of this evolution is sketched on figure 10.

Other current events, generally not connected with tectonics, are recognized in DSDP cores (op. cit.). For instance differential settling mechanisms exist on the Armorican margin (Leg 48) during the late Cretaceous and Paleogene, favouring the deposition toward the open sea of smaller and less floculable minerals (smectite, fibrous clays) compared to micas, chlorite, kaolinite and coarser minerals (quartz, feldspars). Off North West Africa (Legs 14 and 47A) the comparative data of late Cenozoic clay and sand particles show variations in water and wind energy due to climatic changes on the nearby continent (op. cit.).

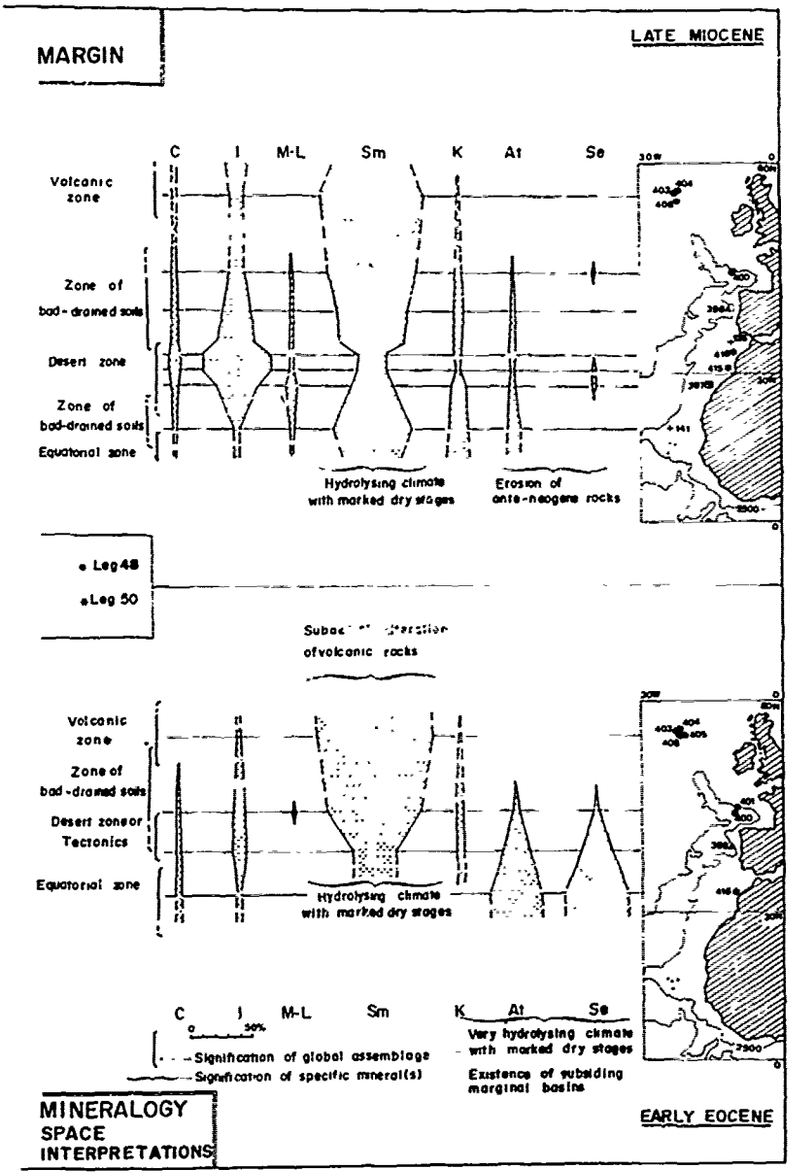


## Conclusions

The examples exposed in this paper merely intend to propose a use of the clay fractions of sediments for reconstructing past continental and depositional environments. The data base utilized in this study does not allow to present a synthesis on the subject. It is necessary to develop these studies in a large way, from most of available drill sites. Nevertheless an attempt at interpreting the data is presented here, for the late Mesozoic and Cenozoic interval of the North East Atlantic.

## Clay Sedimentation and Chronology (Fig. 11)

Twenty-six mineralogical events have been identified from the late Kimmeridgian to the Pleistocene (Legs 47A, 47B, 48, 50), and are interpreted in terms of climate and tectonics, with indications on physiography, marine currents and local diagenesis. The most important events, summarized on Table I and discussed in the text above, show the predominant influence of climate, tectonics and sometimes physiography on composition and variations of clay assemblages. Each of these fac-

Table I. Chains of causes responsible for some of mineralogical events recognized in North Atlantic sediments.

| PERIOD | REGION | MINERALOGICAL EVENT | MAIN CAUSE | SECONDARY POSSIBLE CAUSES | | |
|---|---|---|---|---|---|---|
| | | | CLIMATE | CURRENTS | TECTONICS | PHYSIOGRAPHY |
| Middle-early Paleogene to Pleistocene | Everywhere | Irregular increase of Illite, Chlorite, Quartz, Feldspars, mixed-layers | (World cooling ; less seasonal contrasts in humidity ; sea-level lowering) | (increase of deep-sea meridian circulation) | (relief rejuvenation) | (vegetation partial denudation) |
| Early Eocene | NE Atlantic (at least) | Appearance and increase of Sepiolite and Attapulgite (Palygorskite) | PHYSIOGRAPHY (closed or semi-closed marginal basins) | CLIMATE (hot ; strong contrasts in humidity) | TECTONICS (marginal instability) | CURRENTS (local - turbidites) |
| Santonian to Maastrichtian | NE Atlantic (at least) | Strong increase of Primary Minerals : Illite and associate Minerals | TECTONICS (global event ; separation of Canada and Greenland?) | CURRENTS (general ; meridian circulation of sea-water masses) | CLIMATE (cooler under northern latitudes) | PHYSIOGRAPHY (continental geological environment) |
| Albian | NE Atlantic (at least) | Sudden appearance of Attapulgite (Palygorskite) | PHYSIOGRAPHY (closed or semi-closed marginal basins) | CLIMA: (hot ; contrasts in continental humidity) | TECTONICS (marginal instability) | CURRENTS (local ; differential settling or turbidites) |
| Most of Cretaceous and Paleogene | Everywhere | Large abundance of well-crystallized Smectite | CLIMATE (warm ; rather arid with short humid seasons) | PHYSIOGRAPHY (large extension of flattened continental areas ; hydromorphic soils) | TECTONICS (marginal instability) | CURRENTS (local ; differential settling) |
| Middle upper Jurassic | NW Atlantic | Strong and fast supply of Minerals inherited from rocks and soils (mineralogical mixture) | TECTONICS (oceanic initiation) | PHYSIOGRAPHY (continental geological environment) | CURRENTS (local) | (CLIMATE?) (temperate and humid?) |

tors may at times become dominant and can determine the main character of the clay sedimentation. The different causes of changes recorded in deep sea sediments, however, are generally interconnected and constitute sorts of chains, the first link of which is variable according to time and space. Such a deciphering of the respective importance of each factor, from an analysis of the clay facies, represents a new approach to paleoenvironmental interpretation.

Clay Sedimentation and Geography (Fig. 12)

The comparison of data available for all drill sites for a given time slice allows the establishment of paleomineralogical maps and their interpretion. After collecting and interpreting the average Cretaceous and Cenozoic variations of different mineralogical groups compiled in sections located from off West-Africa (Leg 14) to South Iceland (Leg 48) (Fig. 12, left above), the main latitudinal variations are summarized as a first attempt for early Eocene (right below), late Miocene (right above) and Pliocene (left below). The principal factor responsible for the geographical changes is climate and the information concerns the latitudinal distribution and extension of paleoclimatic belts. The large development of smectite-rich deposits at Cretaceous and Paleogene time contrasts with the well defined zonation of climatic belts (cold, temperate, desertic, tropical) in recent ages, indicating a complication of the world zonation due to Cenozoic coolings. Further steps are envisaged such as the recognition of migration of the "continental" climatic Equator in the course of time, related to the plate motion and the establishment of oceanic currents. Other informations (Table I, Fig. 12) concern distinctions between regional and global tectonics, identification of alluvial petrographic provinces, and relative importance of rock and soil detrital supplies into the ocean.

Acknowledgments. I am grateful to the National Science Foundation (USA) for authorizing a large sampling of materials from Deep Sea Drilling Project This work was supported by grants n° 76/5320 and 77/5489 of CNEXO (France). Its realization was made possible thanks to discussions and common works with numerous scientists, especially C. Courtois, P. Debrabant, J. Debyser, L. Diester-Haass, J. Foulon, G. Giroud d'Argoud, Y. Lancelot, H. Maillot M. Melguen, L. Pastouret, C. Robert, W.B.F. Ryan and J.-C. Sibuet. G. Giroud d'Argoud, M. Acquaviva, F. Dujardin and C.H. Froget are gratefully acknowledged for technical assistance. I friendly acknowledge P.E. Biscaye and Y. Lancelot for carefully and usefully reviewing the manuscript.

References

Berger, W.H., and U. von Rad, Cretaceous and Cenozoic sediments from the Atlantic ocean, in Hayes, D.E., Pimm, A.C., et al., Init. Rep. Deep Sea Drill. Proj., (U.S. Gov. print. off.), 14, 787-954, 1972.

Berggren, W.A., and C.D. Hollister, Paleogeography, paleobiogeography and the history of circulation in the Atlantic region, in Hay, W.W., Ed., Studies in Paleoceanography, Soc. Ec. Petr. Min., sp. publ. 20, 126-186, 1974.

Biscaye, P.E., Mineralogy and sedimentation of recent deep-sea clay in the Atlantic ocean and adjacent seas and oceans, Geol. Soc. Amer. Bull., 76, 803-832, 1965.

Blank, R.G., and S.V. Margolis, Pliocene climatic and glacial history of Antarctica, as revealed by south-east Indian ocean deep-sea cores, Geol. Soc. Amer. Bull., 86, 1058-1066, 1975.

Boillot, G., and R. Capdevilla, The Pyrenees : subduction and collision ?, Earth Plan. Sci. Lett., 35, 151-160, 1977.

Bonatti, E., and O. Joensuu, Palygorskite from Atlantic deep-sea sediments, Amer. Min., 53, 975-983, 1968.

Chamley, H., Recherches sur la sédimentation argileuse en Méditerranée, Sci. Géol., Strasbourg, Mém. 35, 1-225, 1971.

Chamley, H., Remarques sur la sédimentation argileuse quaternaire en mer de Norvège, Bull. Un. Ocean. France, 7, 15-20, 1975.

Chamley, H., P. Debrabant, J. Foulon, G. Giroud d'Argoud, C. Latouche, N. Maillet, H. Maillot, and F. Sommer, Mineralogy and geochemistry of Cretaceous and Cenozoic Atlantic sediments off the Iberian peninsula (Site 398, Leg 47B DSDP), in Ryan, W.B.F., Sibuet, J.-C., et al., Init. Rep. Deep Sea Drill. Proj. (U.S.Gov. print. off.), 47B (in press).

Chamley, H., and L. Diester-Haass, Upper Miocene to Pleistocene climates in North-west Africa deduced from terrigenous components of Site 398 sediments (DSDP Leg 47A), in Ryan, W.B.F., von Rad, U., et al., Init. Rep. Deep Sea Drill. Proj., (U.S. Gov. print. off.) 47A (in press).

Chamley, H., and G. Giroud d'Argoud, Clay mineralogy of Site 397, South of Canary islands (DSDP Leg 47A), in Ryan, W.B.F., von Rad, U., et al., Init. Rep. Deep Sea Drill. Proj. (U.S. Gov. print. off.), 47A (in press).

Chamley, H., G. Giroud d'Argoud, and C. Robert, Clay mineralogy of Cretaceous and Cenozoic sediments off the Morocco margin (Leg 50 DSDP), in Lancelot, Y., Winterer, E.L., et al., Init. Rep. Deep Sea Drill. Proj. (U.S. Gov. print. off.), 50 (in press).

Chamley, H., and G. Millot, Observations sur la répartition et la genèse des attapulgites plio-quaternaires de Méditerranée, C.R. Acad. Sci., Paris, D, 281, 1215-1218, 1975.

Courtois, C., and H. Chamley, Terres Rares et minéraux argileux dans le Crétacé et le Cénozoïque de la marge atlantique orientale, C.R. Acad. Sci., Paris, D, 286, 671-674, 1978.

Darby, D.A., Kaolinite and other clay minerals in Arctic Ocean sediments, J. Sedim. Petr., 45, 272-279, 1975.

Debrabant, P., H. Chamley, J. Foulon, and H. Maillot, Mineralogy and geochemistry of upper Cretaceous and Cenozoic sediments from North Biscay Bay and Rockall Plateau (Eastern North

Atlantic), DSDP Leg 48, in Montadert L.C., Roberts D.G., et al. Init. Rep. Deep Sea Drill. Proj. (U.S. Gov. print. off.), 48 (in press).
Diester-Haass, L., and H. Chamley, Neogene paleoenvironment off NW Africa based on sediments from DSDP Leg 14, J. Sedim. Petr., 48, 879-896, 1978.
Frakes, L.A., and E.M. Kemp, Paleogene continental position and evolution of climate, in Tarling, D.H., and Runcorn, S.K., Implications of continental drift to the earth sciences, Academic press, 1, 539-558, 1973.
Froget, C., and H. Chamley, Présence de sépiolite détritique dans les sédiments récents du golfe d'Arsew (Algérie), C.R. Acad. Sci., Paris, D, 285, 307-310, 1977.
Furon, R., Eléments de Paléoclimatologie, Vuibert, Paris, 1-216, 1972.
Gibbs, R.J., Clay mineral segregation in the marine environment, J. Sedim. Petr., 47, 237-243, 1977.
Griffin, J.J., H. Windom, and E.D. Goldberg, The distribution of clay minerals in the world ocean, Deep-Sea Res., 15, 433-459, 1968.
Grim, R.E., and N. Güven, Bentonites, Elsevier, 1-260, 1978.
Habib, D., Origin and distribution of palynofacies in Cretaceous carbonaceous sediments of the North Atlantic (this vol.).
Hathaway, J.C., X-ray mineralogy studies, Leg 11, in Hollister, C.D., Ewing, J.T., et al., Init. Rep. Deep Sea Drill. Proj. (U.S. Gov. print. off.), 11, 729-789, 1972.
Hollister, C.D., J.T. Ewing, et al., Initial Reports of the Deep Sea Drilling Project (U.S. Gov. print. off.), 11, 1-1977, 1972.
Kennett, J.P., and C.A. Brunner, Antarctic late Cenozoic glaciation. Evidence for initiation of ice rafting and inferred increased bottom-water activity, Geol. Soc. Amer. Bull., 84, 2043-2052, 1973.
Kolla, V.R., P.E. Biscaye, and A.F. Hanley, Distribution of quaternary in late Quaternary Atlantic sediments in relation to climate, Quat. Res. (in press).
Kossowskaya, A.G., E.B. Gushina, W.A. Drits, A.L., Dmitrik, O.S. Lomova, N.D. Serobronnikova, Mineralogy and genesis of Meso-Cenozoic deposits of the Atlantic based on materials of Deep Sea Drilling Project, Leg 2, Akad. Nauk SSSR, Litol. Pol. Isk., 6, 12-26, 1975.
Lancelot, Y., J.C. Hathaway, and C.D. Hollister, Lithology of sediments from the Western North Atlantic, Leg 11, Deep Sea Drilling Project, in Hollister, C.D., Ewing, J.T., et al., Init. Rep. Deep Sea Drill. Proj. (U.S. Gov. print. off.), 11, 901-949, 1972.
Lancelot, Y., E.L. Winterer et al., Initial Reports of the Deep Sea Drilling Project (U.S. Gov. print. off.), 50 (in press).
Lisitzin, A.P., Sedimentation in the world ocean, Soc. Ec. Pal. Min. sp. publ. 17, 1-218, 1972.
Lomova, O.S., Palygorskite clays of East Atlantic and their genetic relationship with alkaline volcanism, Akad. Nauk SSSR, Litol. Pol. Isk., 4, 10-27, 1975.
Lucas, J., and L. Prévôt, Les marges continentales pièges géochimiques ; l'exemple de la marge atlantique de l'Afrique à la limite Crétacé-Tertiaire, Bull. Soc. géol. France, 17, 496-501, 1975.
Mélières, F., X-ray mineralogy studies, Leg 41, Deep Sea Drilling Project, Eastern North Atlantic ocean, in Lancelot, Y., Seibold, E., et al., Init. Rep. Deep. Sea Drill. Proj. (U.S. Gov. print. off.), 41, 1065-1086, 1978.
Millot, G., Géologie des argiles, Masson, Paris, 1-499, 1964.
Millot, G., H. Paquet, and A. Ruellan, Néoformation de l'attapulgite dans les sols à carapaces calcaires de la Basse Moulouya (Maroc oriental), C.R. Acad. Sci., Paris, D, 268, 2771-2774, 1969.
Montadert, L.C., D.G. Roberts, et al., Initial Reports of the Deep Sea Drilling Project (U.S. Gov. print. off.), 48 (in press).
Nairn, E.M., and F.C. Stehli, Ed., The ocean basins and margins, 2, The North Atlantic, Plenum, 1-598, 1974.
Paquet, H., Evolution géochimique des minéraux argileux dans les altérations et les sols des climats méditerranéens et tropicaux à saisons contrastées, Mém. Serv. Carte géol. Als. Lorr., Strasbourg, 20, 1-212, 1969.
Pastouret, L., G.-A. Auffret, and H. Chamley, Microfacies of some sediments from the Western North Atlantic : paleoceanographic implications (Leg 44 DSDP), in Benson, W.E., Sheridan, R.E., et al., Init. Rep. Deep Sea Drill. Proj. (U.S. Gov. print. off.), 44 (in press).
Pédro, G., Distribution des principaux types d'altération chimique à la surface du globe. Présentation d'une esquisse géographique, Rev. Géogr. phys. Géol. dyn., Paris, 10, 457-470, 1968.
Peterson, M.N.A., et al., Initial Reports of the Deep Sea Drilling Project (U.S. Gov. print. off.), 2, 1-1131, 1970.
Ratcev, M.A., Z.N. Gorbunova, A.P. Lisitzin, and G.I. Nosov, Climatic zonality of the argillaceous minerals in the world ocean sediments, Okeanology, 18, 283-311, 1968.
Riech, W., and U. von Rad, Silica diagenesis in the North Atlantic basin : diagenetic potential and transformations (this vol.).
Robert, C., J.-P. Herbin, G. Giroud d'Argoud, and H. Chamley, Evolution de l'Atlantique Sud au Crétacé d'après l'étude des minéraux argileux et de la matière organique (Leg 39 et 40 DSDP), Oceano. Acta, (in press).
Ryan, W.B.F., and M.B. Cita, Ignorance concerning episodes of ocean-wide stagnation, Mar. Geol., 23, 197-215, 1977.
Ryan, W.B.F., U. von Rad, et al., Initial Reports of the Deep Sea Drilling Project (U.S. Gov. print. off.), 47A (in press).
Ryan, W.B.F., J.-C. Sibuet, et al., Initial Reports of the Deep Sea Drilling Project (U.S. Gov. print. off.), 47B (in press).
Shackleton, N.J., and J.P. Kennett, Paleotempera-

ture history of the Cenozoic and the initiation of Antarctic glaciation : oxygen and carbon analyses in DSDP Sites 277, 279 and 281, in : Kennett, J.P., R.E. Houtz, et al., Init. Rep. Deep Sea Drill. Proj. (U.S. Gov. print. off.), 29, 743-755, 1975.

Sheridan, R.E., P. Enos, and T. Freeman, Stratigraphic evolution of the Blake Plateau based on a decade of drilling (this vol.).

Sibuet, J.-C., W.B.F. Ryan, et al., Deep drilling results of leg 47 B (Galicia bank area) in the framework of the early evolution of the North Atlantic Ocean, Phil. Trans. Roy. Soc. London (in press)

Sigl, W., H. Chamley, F. Fabricius, G. Giroud d'Argoud, and J. Müller, Sedimentology and environmental conditions of sapropels, in Hsü, K.J., Montadert, L.C., et al., Init. Rep. Deep Sea Drill. Proj. (U.S. Gov. print. off.), 42, I, 445-465, 1978.

Sommer, F., Néogenèse de clinoptilolite dans l'Eocène et l'Oligocène de Casamance (Sénégal) : Sci. géol. Bull., Strasbourg, 25, 251-258, 1972.

Talwani, M., G. Udintsev, et al., Initial Reports of the Deep Sea Drilling Project (U.S. Gov. print off.), 38, 1-1256, 1976.

Timofeev, P.P., V.V. Eremeev, and M.A. Rateev, Palygorskite, sepiolite, and other clay minerals in Leg 41 oceanic sediments : Mineralogy, facies and genesis, in Lancelot, Y., Seibold, E. et al., Init. Rep. Deep Sea Drill. Proj. (U.S. Gov. print off.), 41, 1087-1101, 1978.

Tissot, B., Organic matter in Cretaceous sediments of the North Atlantic : contribution to sedimentology and paleogeography (this vol.).

Trauth, N., Argiles évaporitiques dans la sédimentation carbonatée tertiaire. Bassin de Paris, de Mormoiron et de Salinelles (France) ; Jbel Ghassoul (Maroc), Thèse, Sci. nat., Strasbourg, 1-309, 1974.

Tucholke, B.E., and G.S. Mountain, Lithologic correlation and significance of major seismic reflectors in the Western North Atlantic (this vol.).

Weaver, C.E., and K.C. Beck, Miocene of the S.E. United States : a model for chemical sedimentation in a peri-marine environment, Sedim. Geol., 17, 1-234, 1977.

Zemmels, I., and H.E. Cook, X-ray mineralogy studies, Leg 11, in Hollister, C.E., Ewing, J.T., et al., Init. Rep. Deep Sea Drill. Proj. (U.S. Gov. print. off.), 11, 729-789, 1972.

# ORGANIC MATTER IN CRETACEOUS SEDIMENTS OF THE NORTH ATLANTIC: CONTRIBUTION TO SEDIMENTOLOGY AND PALEOGEOGRAPHY

B. Tissot, G. Deroo, and J. P. Herbin

Institut Français du Pétrole, BP 311, 92506 Rueil-Malmaison Cedex, France

Abstract. Concentrations of organic matter have been widely observed in Cretaceous marine sediments of the Atlantic. However, they are related to several different sources and/or conditions of preservation. The three basic types of organic sedimentation in marine environments are (A) organic matter of marine origin deposited in a reducing environment (B) terrestrial organic matter transported and incorporated in the sediment with a moderate degradation (C) residual organic matter of terrestrial origin, which has been highly degraded in subaerial soils prior to transportation. This kind of degradation may have affected contemporaneous and/or recycled organic matter. In addition to that, there are mixtures of different sources.

Conditions of preservation may be the controlling factor for organic sedimentation of marine origin. Terrestrial organic matter is mainly controlled by climate and land physiography. Residual organic matter may be spread over wide areas, regardless of the local environment. The occurrences of dark or carbonaceous shales and mudstones in the North Atlantic are considered in the light of the successive stages of ocean evolution and interpreted in terms of origin of the organic input and environment of deposition.

## 1. Introduction

Accumulations of organic matter as great as 30% of the sediment have been reported in many cores of Cretaceous shales, mudstones and marls from various locations in the Atlantic Ocean. Such organic rich beds are frequently found in Aptian-Albian or Cenomanian to Coniacian beds, although they may occur in other horizons (Schlanger and Jenkyns, 1976 ; Thiede and Van Andel, 1977 ; Ryan and Cita, 1977).

Several hypotheses have been considered with respect to the paleogeography of these sediments. In fact, geochemical analyses show that different types of organic matter are involved (Berger and Von Rad, 1972 ; Ryan and Cita, op. cit.). Thus it is necessary to first determine the type and origin of the organic matter, before conclusions are reached in terms of environment of deposition.

## 2. Types of organic matter

The insoluble fraction of the organic matter (usually called kerogen) generally amounts to ca. 95-99% of the total organic matter in Cretaceous beds of the Atlantic. Kerogen may be studied directly on the rock by pyrolysis (Espitalié et al, 1977) or after destruction of the mineral matrix (Tissot et al, 1974). Pyrolysis is usually performed as a scanning method. For shallowly buried sediments the results of pyrolysis allow one to distinguish the different types of organic matter, and subsequently to process a limited number of samples for kerogen isolation. In turn, kerogen analyses are used to check the organic type assigned from pyrolysis data. Furthermore, elemental analysis of kerogen and infrared spectrometry provide informations on the chemical composition of the organic matter. For instance high values of the H/C atomic ratio (ca. 1.5) mean a low aromaticity and a large abundance of saturated chains and cycles. The relative proportion of these groups can also be evaluated by using the ratios of certain bands of infrared absorption, like $K_{2900}/K_{1630}$ and $K_{1455}/K_{1630}$. The absorptions at 2900 and 1455 cm-1 are related to saturated $CH_2$ and $CH_3$ groups, whereas the absorption at 1630 cm-1 comprises in particular the effect of the aromatic nuclei. The $K_{2900}/K_{1710}$ ratio indicates the relative contribution of saturated $CH_2$ and $CH_3$ groups (2900 cm-1 band) versus oxygenated functional groups (1710 cm-1 band). Finally optical examination by transmitted and reflected light provides information on the origin of the organic constituents, and also on the stage of thermal matura-

tion. In particular, the reflectance of huminite-vitrinite, one of the main macerals of coals also occurring in shales, is one of the best maturation parameters (Hood and Castano, 1974 ; Dow , 1977). Reflectances below 0.3% are indicative of very immature organic material. The analytical data related to legs 41, 44, 47, 48, 50 and 51 to 53 have been reported by Deroo et al (Initial Reports of DSDP, in press).

Table I and fig. 1 and 2 show some significant data related to the kerogen of eight samples of Cretaceous carbonaceous shales or mudstones. Five of them ($A_2$, $B_2$, $C_2$, $D_1$ and $D_2$) originate from the North Atlantic, and three ($A_1$, $B_1$, $C_1$) from the South Atlantic. The four pairs of samples, $A_1$-$A_2$, $B_1$-$B_2$, $C_1$-$C_2$ and $D_1$-$D_2$ are representative of the most frequent situations met in the Atlantic cores, although all transitions can be observed. The various parameters shown in table I can be compared with the values observed on well known series of organic matter (Tissot et al, 1974 ; Robin, 1975). For the sake of comparison, it should be noted that the eight samples belong to the immature stage of the thermal evolution of the organic matter (diagenesis) : depths of burial range from 365 to 1636 m ; huminite reflectances measured on contemporaneous, non-reworked material, are lower than 0.25%.

a) Kerogens of samples $A_1$-$A_2$ are hydrogen rich ($1.3 \leqslant H/C \leqslant 1.5$) and their oxygen content is low to moderate. Infrared and elemental analyses show an abundance of aliphatic structures, whereas aromatic nuclei and oxygenated functional groups are only subordinate (fig. 2). These various data can be compared with the characters of kerogen type II (Tissot et al., op. cit.), e.g. Lower Toarcian shales of the Paris Basin or Silurian shales of Algeria and Libya. The organic matter can be considered as derived from marine (or lacustrine) organisms (phyto-and zooplankton) deposited in a reducing environment. This type of organic matter is commonly referred to as "sapropelic". However we shall avoid this nomenclature, because the same word is frequently used to describe an amorphous organic matter on optical examination by transmitted light. Although sample $A_1$ contains almost 100% amorphous organic matter (fig. 3 and 4), the same optical character may be found in other types of kerogen, e.g. terrestrial organic matter, under certain circumstances.

b) Kerogens of samples $B_1$-$B_2$ contain less hydrogen than $A_1$-$A_2$ and more oxygen, despite a comparable degree of immaturity shown by their burial depths and huminite reflectances. The relative abundance of aliphatic structures is somewhat lower in samples $B_1$-$B_2$, as compared to aromatic and functional groups. This fact is clearly shown by the values of H/C, $K_{2900}/K_{1630}$ and $K_{2900}/K_{1710}$ ratios, which are lower than the values measured in samples $A_1$-$A_2$. The organic matter of samples $B_1$-$B_2$ can be considered as a mixture of kerogen type II (planktonic) and III (terrestrial), according to the same nomenclature (op. cit.). All ratios of mixture seem to exist : the proportion of type II kerogen is high in sample $B_1$, whereas type III predominates in sample $B_2$. The admixture of terrestrial material is corroborated by optical examination (presence of vegetal or coaly debris).

c) Kerogens of samples $C_1$-$C_2$ are hydrogen poor ($H/C < 1$) and oxygen rich. The relative abundance of aliphatic structures is low, as compared to aromatic and oxygenated functional groups : the $K_{2900}/K_{1630}$ and $K_{2900}/K_{1700}$ ratios are lower than 1. The data shown in table I can be compared with the characters of kerogen type III (op. cit.), e.g. Upper Cretaceous shales of Douala Basin. The organic matter is considered as terrestrial, mostly derived from higher plants and moderately degraded. The important contribution of lignin is probably responsible for the abundance of oxygen and aromatic rings. The major participation of terrestrial organic matter is confirmed by the high percentage of vegetal plus coaly debris, on optical examination by transmitted light. Furthermore these observations have shown that the terrestrial organic matter comprises mainly contemporaneous material (e.g. huminite with 0.17% reflectance in sample $C_1$) and also a certain fraction of recycled material (marked by a wide spectrum of vitrinite with different reflectances).

d) Kerogens of samples $D_1$-$D_2$ are also hydrogen poor or very poor (H/C = 0.58 in $D_2$) but the abundance of oxygen is abnormally high (O/C = 0.28 and 0.26). In particular, the H/C ratios observed in $D_1$ (H/C = 0.80) and in $D_2$ (H/C = 0.58) would correspond to O/C ratios lower than 0.2 and 0.1, respectively, along a normal evolution path : fig. 1. It can be observed that some Cretaceous samples of legs 47B and 48 are so hydrogen poor and oxygen rich that they fall outside of the usual field of kerogens, when plotted on the Van Krevelen diagram of fig. 1. Furthermore elemental and infrared analyses suggest that aliphatic structures are almost absent, whereas aromatic nuclei and oxygenated functional groups are abundant (fig. 2). These data can be related to the contribution of terrestrial organic matter which has suffered an intense weathering and oxidation in subaerial soils. This kind of degradation may have affected contemporaneous and/or recycled organic matter. For instance $D_1$ contains a huminite fraction with a reflectance of 0.22%, which is obviously contemporaneous, together with dark or coaly debris, which is probably oxidized and/or recycled : fig. 5. Sample $D_2$ shows a wide spectrum of reflectance values (Cornford, pers. comm.) that are a characteristic of this kind of organic matter : 90% of the vitrinite of this sample is probably recycled, with a maximum frequency corresponding to 1% reflectance. This particular type of kerogen, resulting from deep weathering and oxidation of contemporaneous and/or recycled organic matter, will be called residual kerogen in this paper. The importance of weathering and oxidation is confirmed by the percentage of inertinite measured in reflected light : 30% of the total organic matter and 65% of the particulate organic matter in sample $D_1$.

TABLE 1. Examples of kerogen analyses

| | $A_1$ | $A_2$ | $B_1$ | $B_2$ | $C_1$ | $C_2$ | $D_1$ | $D_2$ |
|---|---|---|---|---|---|---|---|---|
| (IFP sample number) | 23845 | 23233 | 23773 | 23118 | 23786 | 21532 | 23350 | 24174 |
| Leg | 40 | 41 | 40 | 41 | 40 | 44 | 47 B | 48 |
| Site | 364 | 367 | 361 | 367 | 361 | 391 C | 398 | 402 A |
| Core, section | 45-2 | 18-2 | 33-3 | 23-2 | 41-3 | 10-3 | 127-5 | 25-1 to 5 |
| Subbottom depth (m) | 1100 | 658 | 1100 | 777 | 1165 | 905 | 1636 | 365 |
| Organic carbon (%) | 26 | 32 | 7.2 | 4.0 | 2.9 | 2.7 | 1.8 | 1.3 |
| Elemental analysis | | | | | | | | |
| Atomic ratio H/C | 1.4 | 1.4 | 1.2 | 1.1 | 0.81 | 0.84 | 0.80 | 0.58 |
| Atomic ratio O/C | 0.07 | 0.12 | 0.13 | 0.18 | 0.18 | 0.22 | 0.28 | 0.26 |
| Infrared spectrometry | | | | | | | | |
| $K_{2900}/K_{1630}$ | 5.2 | 3.9 | 1.7 | 1.2 | 0.6 | 0.4 | $<0.2$ | $<0.2$ |
| $K_{1455}/K_{1630}$ | 0.74 | 0.55 | 0.38 | 0.15 | 0.15 | 0.10 | 0.09 | 0.06 |
| $K_{2900}/K_{1710}$ | 5.4 | 3.6 | 2.4 | 1.3 | 1.0 | 0.6 | $<0.4$ | $<0.4$ |
| Optical examination (reflected light) | | | | | | | | |
| Inertinite : | | | | | | | | |
| % of particulate OM | 10 | | 0 | | 38 | | 65 | |
| % of total OM | 5 | | 0 | | 23 | | 29 | |
| Huminite reflectance | 0.06 | | 0.08 | | 0.17 | | 0.22 | |

Nota $K_{2900}$ and $K_{1455}$ are related to the absorption by saturated $CH_2$ + $CH_3$ groups, at 2900 and 1455 cm-1 respectively. $K_{1710}$ is related to the absorption by $C^3$= O groups at 1710 cm-1 and $K_{1630}$ is related to a more complex absorption band at 1630 cm-1 comprising in particular aromatic nuclei (Robin, 1975).

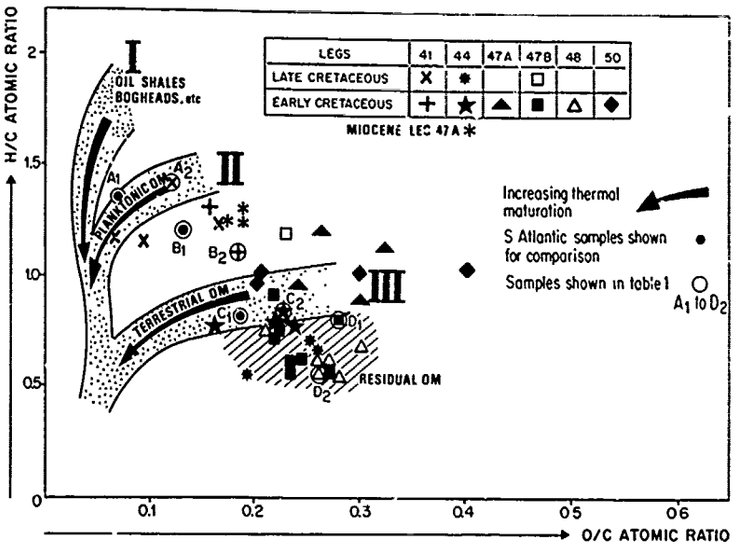


Fig. 1 Elementary composition of kerogens from North Atlantic (Van Krevelen diagram). Three samples from South Atlantic ($A_1$, $B_1$, $C_1$) are shown for comparison. Samples marked $A_1$ to $D_2$ are also shown in Table I.

3. Distribution of the organic matter in Cretaceous cores of the North Atlantic

The abundance of organic matter in Cretaceous cores varies widely. Frequently a background of terrestrial and/or residual organic matter is found at a level of 0.3 or 0.5% organic carbon (by weight of dry rock). We shall consider as "accumulations" of organic matter the abundances over 1% organic carbon by weight. Such accumulations may reach 30% in the case of marine kerogen (type II), in Cretaceous cores of the North Atlantic. The maximum values found for terrestrial (type III) and residual organic matter are ca. 8% and 3% respectively. In the following paragraphs, only accumulations of organic matter with more than 1% organic carbon are discussed.

During Lower Cretaceous time, accumulations of pure marine organic matter (type II) over a continuous section is only known in the Southeastern part of the North Atlantic basin : Cape Verde Basin (Albian, site 367), continental slope off Western Sahara (Aptian-Albian site 369, fig. 6. Discrete beds containing marine organic matter are found in the deep basin off Morocco (Aptian-Albian, Sites 370, 416 and possibly 135) and on the Blake Plateau (Barremian to Albian, Site 390). Admixture of marine and terrestrial (type III) organic matter occurs in the Cape Verde Basin (Neocomian to Aptian, Site 367) in the abyssal plain south of Bermuda (Aptian-Albian, Sites 417/418) and in the basin off Morocco where terrestrial organic matter is predominant (Neocomian to Albian, sites 370 and 416). Elsewhere terrestrial organic matter (type III) is the main source of kerogen accumulations during Lower Cretaceous, with some admixture of residual kerogen. This situation is found in several places off United States and Bermuda (sites 391, 105 and 368). Towards the northeastern end of the Atlantic, the residual kerogen is the main organic input in Aptian or Albian time (site 398 off Portugal, sites 400 and 402 in the Bay of Biscay).

During Upper Cretaceous, accumulations of pure marine organic matter (type II) continues through Cenomanian to Coniacian in the Cape Verde Basin (site 367) and is also known over approximately the same period on the Cape Verde and Demerara rises (sites 368 and 144) : fig. 7. Discrete beds (1) containing marine organic matter and/or admixtures of marine and terrestrial kerogen are known in many places in the North Atlantic, mainly during Cenomanian : off Western Sahara (Coniacian-Santonian, site 369 ; Cenomanian, site 138), off Morocco (Cenomanian, site 415 and possibly 135), off Portugal (Cenomanian under unconformity, site 398) off United States and Bermuda (Cenomanian, sites 105, 386, 387, and 417/418). However, the terrestrial input is generally

(1) in some instances the discrete character may be due to discontinuities in the availability of cores.

the main source of organic accumulations in the rest of Upper Cretaceous with the exception of the Cape Verde and Demerara areas. Terrestrial, including residual, organic matter is also responsible for the very lean organic material spread over the North Atlantic during the late part of Cretaceous.

The distribution of the organic matter in the Cretaceous of the North Atlantic appears rather different from the distribution observed in the South Atlantic by Deroo et al (1978). There accumulation of organic rich beds occurs over a continuous section covering Aptian and sometimes part of Albian and Neocomian, in the Angola Basin (planktonic), in the Cape Basin and on the Falkland Plateau (alternation and mixture of planktonic and terrestrial). This situation can only be compared with that found in the Southeastern part of North Atlantic, from Cape Verde to Morocco. The second accumulation of planktonic organic matter during Cenomanian-Turonian reported in the Angola Basin (op. cit.) can be paralleled with the situation in the Demerara and Cape Verde areas, and also with the discrete beds containing marine organic matter observed during Cenomanian, in many places of the North Atlantic.

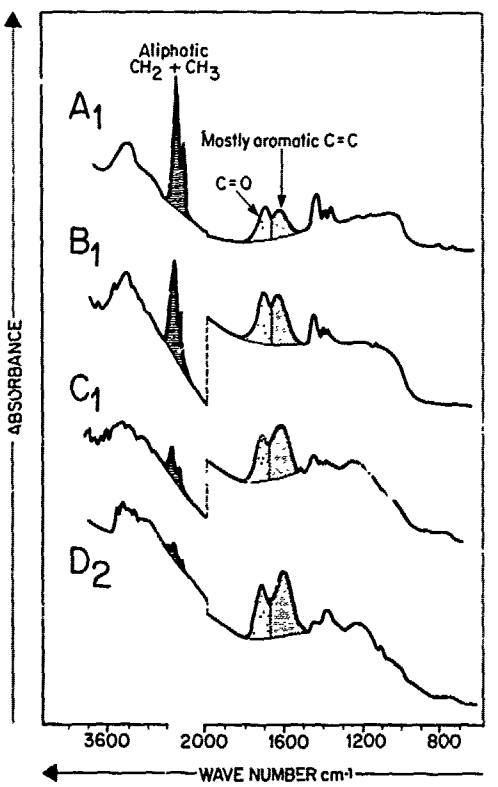


Fig. 2 Infrared spectrometry of four typical kerogens. The symbols refer to samples shown in table I and fig. 1.

Fig. 3 Flakes of amorphous organic matter (type II) : leg 40 site 364, core 45-2.

4. Environments responsible for the accumulation of organic matter

The various types of organic matter presented above require rather different climatic, physiographic and oceanologic conditions for their production, preservation and accumulation. These conditions are schematically presented on fig. 8. A special consideration will be given to accumulation of organic matter under deep water conditions, as paleobathymetric reconstructions (Sclater et al, 1977) suggest that most organic rich Cretaceous sediments of the North Atlantic have been deposited under water depths of ca. 1500 to 5000 m. In the South Atlantic, Thiede and Van Andel (1977) showed that comparable sediments were deposited under water depths ranging from less than 500 m to more than 3000 m.

The typical habitat for accumulation of the marine organic matter (type II) is a sea where the primary productivity of phytoplankton is abundant (e.g. along continental margins and especially in areas of upwelling) and where a substantial part of the planktonic material is preserved (fig. 8). The main factors of destruction of this material are feeding by heterotrophic animals and biochemical degradation by aerobic bacteria.

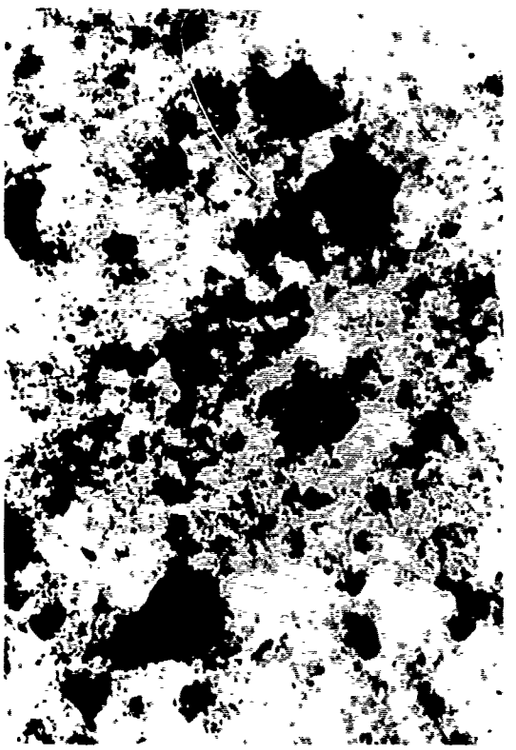

Fig. 4 Dispersed and flaky amorphous organic matter (type II) : same core as fig. 3.

This happens mainly during the slow fall of the dead organisms from the surface waters to the bottom of the sea. Thus, the residence time of the organic particles in the oxygen containing water column is of great importance. This time is obviously limited in shallow waters, and the wide occurrences of black shales in the Jurassic of W. Europe, e.g., Lower Toarcian of France and W. Germany, were probably deposited under shallow waters. In deep seas, degradation is also prevented if there is a stratified water column, where free oxygen is restricted to the surface water layer and absent in most of the underlying waters. Organic accumulation presently occurs at great depth in the Black Sea and in the Cariaco Trench under these conditions. Oxygen depletion is due to restrictions to the circulation of deep oceanic waters, and stratification of the water layers. The conditions may range from an extended anoxic layer, starting at shallow depth and spreading over most of the water column, to a completely barred or confined basin, such as the Black Sea, where the whole water column is anoxic below 175-200 m depth.

Preservation of marine organic matter may eventually occur in open oceanic conditions, without restriction to water circulation. Local or seasonal conditions (important upwelling, phytoplankton blooms) may generate a surplus of productivity, as compared to heterotrophic fauna and destructive microbes. Thus a fraction of the organic matter is still preserved, e.g. in places along the present western margin of continents. Associated mechanisms for preservation of organic matter in open oceanic conditions, are the deposition as fecal pellets and/or the existence of reverse currents which greatly shorten the transit time.

A special question is whether the water-sediment interface has to be anoxic. From observations made by Pelet (1977, 1978) on recent deep sea sediments of the ORGON cruises, it appears that at great water depth microbial activity is usually much reduced and organic material suffers little change over the first meters of burial. Thus, once organic material has been preserved during the transit through the deep water column, it can accumulate even in places where the bottom water is not strictly anoxic.

The typical habitat for the accumulation of moderately degraded terrestrial organic matter (type III) can be described as follows (fig. 8).

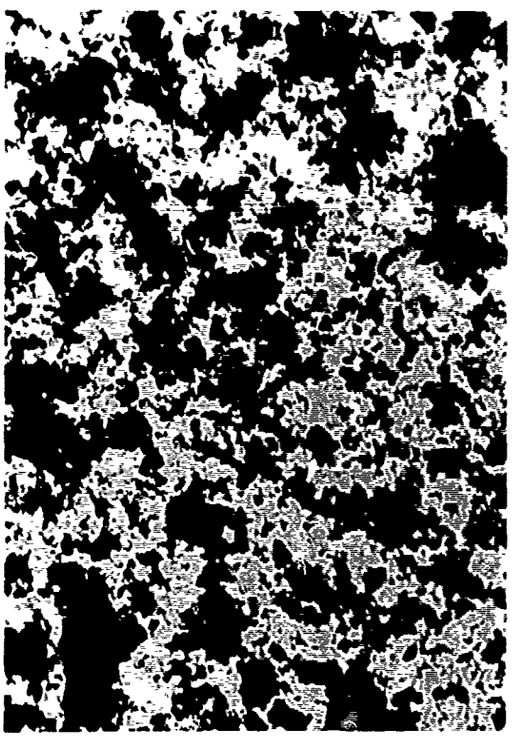

Fig. 5 Finely disseminated organic matter, with some ligneous debris and about 50% of dark or coaly debris which are probably oxidized and/or recycled : leg 47 B, site 398 core 125-5.

On land there is an abundant development of higher plants under humid climate, either temperate or tropical. The organic material is collected and transported by rivers to the basin of deposition. A part of the organic input is laid down in coastal areas, where appropriate conditions for preservation are found in peat swamps and deltas. Another fraction of the organic input is carried away by currents into the deep sea. Compared to marine organic matter, a specific aspect of the terrestrial organic input is the association with detrital mineral particles due to a common terrestrial origin, comparable particle size and/or adsorption on clay minerals. This association is an important factor of preservation by shortening the transit time in oxygenated oceanic waters and protecting the organic constituents by adsorption on clays. Thus preservation and accumulation of terrestrial organic matter is much less dependent on an oxygen depletion than accumulation of marine organic matter.

Furthermore, contemporaneous shallow organic deposits may also be retransported by sliding and turbidity currents, particularly onto the base of the continental slope. A quasi-instant burial would protect the organic matter associated with the turbidites against any further degradation on the site of re-deposition. This situation is rather common with respect to terrestrial organic matter, but it may occasionally affect marine organic beds of the slope : this was suggested by Deroo et al (op. cit.) with respect to the origin of Miocene black shales of site 397.

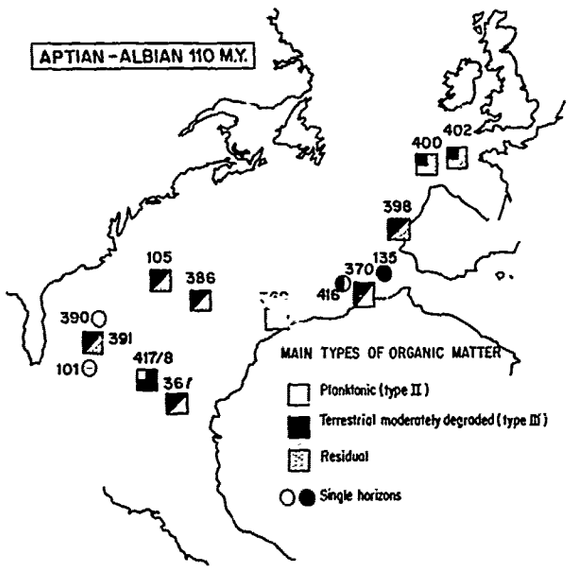


Fig. 6 Main types of organic matter observed in the Albian and/or Aptian of the North Atlantic (position of the continents is only approximate at 110 m.y.).

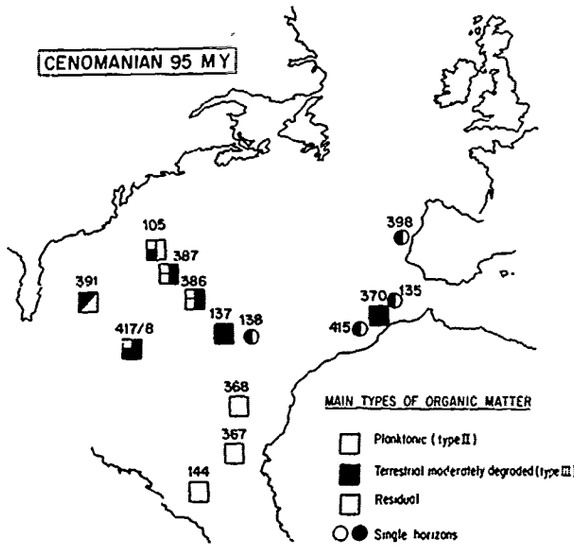


Fig. 7 Main types of organic matter observed in the Cenomanian and/or Turonian of the North Atlantic (position of the continents is only approximate at 95 m.y.).

An extreme case of the terrestrial input is the "residual" organic matter, as examplified by samples $D_1$ and $D_2$ in table I. Such organic material has probably been deeply degraded in subaerial conditions and cannot be degraded any more. Thus residual organic matter is no more sensitive to the specific conditions of deposition and can be found in any location from the shelf, through the oxygen minimum layer, down to the deep oxygenated oceanic basins. The occurrence of residual organic matter has little value in terms of paleoenvironment. For example, sites 400 and 402 of leg 48 are closely spaced, but they differ by about 2000 m of water depth. From sedimentological and paleontological studies they are considered to have been in the same relative position during Early Cretaceous time. (Montadert et al, 1977). Despite this important difference of paleobathymetry, the same residual organic matter is present in both sites over most of the Aptian and Albian section (Deroo et al, op. cit.), even if the vertical distributions are different.

## 5. Paleoenvironment of the North Atlantic

The distribution of the organic matter may be interpreted in terms of environment of deposition, climate, and land physiography.

a) Environment of deposition (fig. 9 and 10)

Rifting and spreading of the central North Atlantic during Late Jurassic had already resulted in two elongated basins in existence during

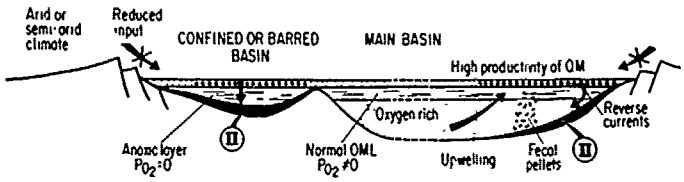


TYPICAL HABITAT OF MARINE OM

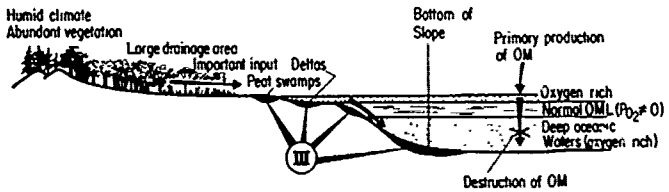


TYPICAL HABITAT OF MODERATELY DEGRADED TERRESTRIAL OM

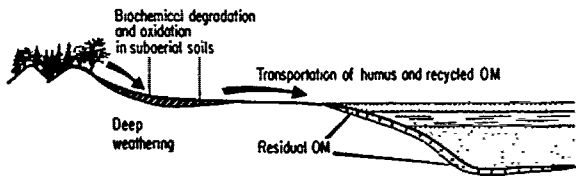


WIDESPREAD OCCURRENCE OF RESIDUAL OM

Fig. 8 Principal environment of deposition of the main types of organic matter.

Lower Cretaceous and later : the western basin extending off North America from Bahamas to New England and the eastern basin extending off North West Africa. In turn two areas can be distinguished in the eastern basin. The northern part, off Western Sahara and Morocco, and the southern part (Cape Verde) with a more complex physiography due to many fractures and to the relatively late connection with the South Atlantic. The Demerara area may to some extent be linked to this southern part. In addition to that, a younger northern embayment progressively develops between Portugal and Grand Banks and in the Bay of Biscay.

A general feature of the western basin and of the northern embayment is the predominant terrestrial character of the organic fraction, which is commonly composed of an alternation, or a mixture, of terrestrial moderately degraded (type III) and residual organic matter. The scarcity of marine organic matter (type II) suggests the absence of a generalized or extended oxygen depletion in the western basin of North Atlantic and in the northern embayment. There is no reason to reject the existence of an oxygen minimum layer at that stage, but its value above zero and vertical extension should have been comparable to what is presently observed in the oceans. Thus most of the water column above the deep sea floor contained free oxygen and did not favour a preservation of the planktonic material. This interpretation suggests that a good connection was established with the Pacific, probably allowing circulation of deep oceanic waters into the western basin. Furthermore, the sites of the Northern embayment (Vigo, Bay of Biscay) which appear from current paleogeographic reconstruction to be rather isolated during Aptian-Albian time, have mainly shown residual organic matter derived

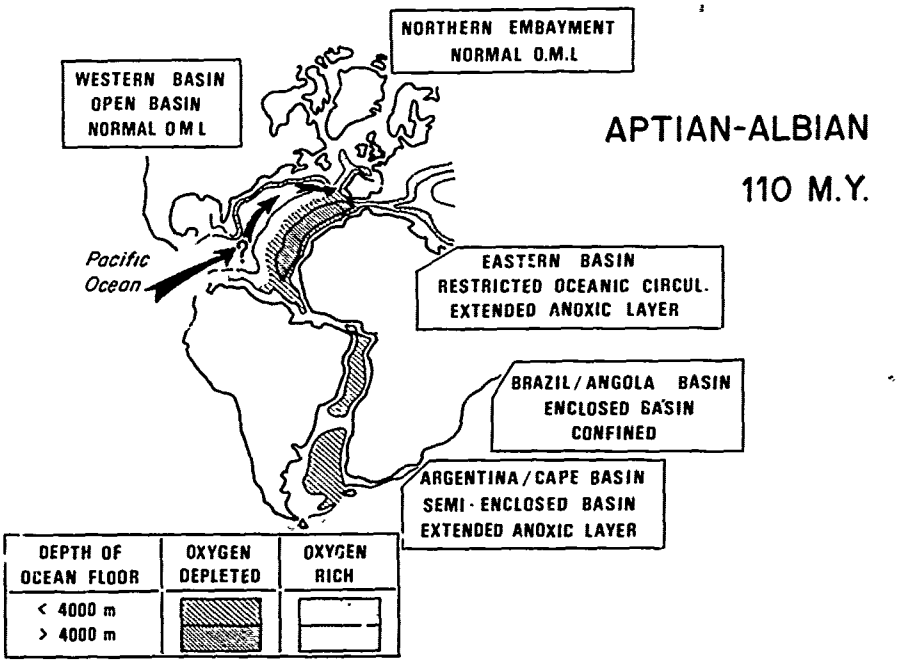


Fig. 9 Distribution of the depositional environments during Lower Cretaceous (Aptian-Albian) Position of the continental masses at 110 m.y. and depth of Atlantic ocean floor according to Sclater et al (1977) and Thiede and Van Andel (1977) with minor changes. Contours for Tethys and Mesogea inferred from Biju Duval et al. (1977). Contours for Carribean are purely hypothetical. Shallow epicontinental seas are not shown.

from the continent. This fact points to the absence of a "barren basin", despite adequate physiography in this area. In addition to that, the terrestrial input was considerable, as shown by the high rate of sedimentation.

A few exceptions to this situation are known in the western basin, mainly in Cenomanian time, where some beds containing marine (type II), or alternations of marine and terrestrial, organic matter have been found on the Bermuda and continental rises and in the abyssal plain (sites 105, 387, 386 and 417-418). These facts suggest a temporary reduction of deep oceanic circulations (from and to the Pacific ?) and a related, possibly cyclic, extension of an anoxic layer. Other isolated occurrences of marine organic matter, e.g., a single bed in the Aptian-Albian of the Blake Plateau, may be explained by local variations.

The situation is rather different in the eastern basin where some accumulations of mixed or terrestrial organic matter are found in the Neocomian-Barremian beds. They change to accumulations of marine or mixed organic matter in Aptian-Albian time (Cape Verde basin, continental slope off Western Sahara, deep basin off Morocco). Later, important accumulations of marine organic matter occur in the southern part of the eastern basin (Cape Verde basin and rise) and also on the Demerara rise. This feature extends from Cenomanian to Coniacian. The organic carbon content may reach values as high as 15% in the Cenomanian and 34% in the Coniacian of the Cape Verde basin. A few discrete occurrences of marine or mixed organic matter have also been found in Cenomanian beds off Morocco and Vigo.

These data suggest the existence of an extended anoxic layer in the eastern basin during part of the Lower Cretaceous, and mainly during Albian-Aptian. Restrictions to oceanic circulation may be due to a narrow and relatively shallow connection with the Tethys and Mesogea (Biju Duval et al, 1977), and to the absence of any deep connection across the ridge to the western basin. During Cenomanian the anoxic layer possibly extended periodically to the western basin, e.g., Bermuda area.

After Cenomanian time the connection of the eastern basin with Tethys and Mesogea becomes progressively wider and deeper. Furthermore, high latitude, cold waters probably entered the North Atlantic basins between Labrador and Greenland and/or between Greenland and Rockall. Thus, there is no more anoxic layer during the late part of Cretaceous, with the exception of the Southern end of the eastern basin. There, a confined basin persists through Cenomanian to Coniacien in the

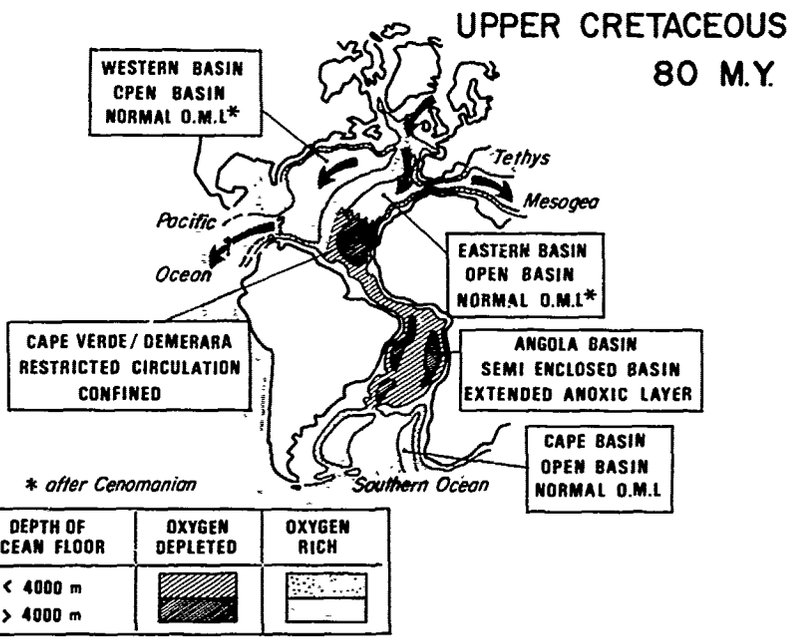


Fig. 10 Distribution of the depositional environments during Upper Cretaceous. Position of the continental mass at 80 m.y. and depth of Atlantic ocean floor according to Sclater et al (1977) and Thiede and Van Andel (1977) with minor changes. Contours for Tethys and Mesogea inferred from Biju Duval et al (1977). Contours for Carribean are purely hypothetical. Shallow epicontinental seas are not shown.

Cape Verde area and extends over Demerara, thus providing the highest accumulations of organic matter. It is not clear whether this feature is due to abnormally high productivity (upwelling) or to a local restriction of oceanic circulation (fracture zone, early existence of the Canary Arch ?)

A comparison of the data from North and South Atlantic shows that the accumulation of marine organic matter has been more continuous and considerably more important in the South Atlantic. There, the absence of deep oceanic connection either to the North Atlantic or to the Southern Ocean prevented the entry of deep oxygenated oceanic waters into the Angola and Cape Basins during Lower Cretaceous until M. Albian time (Deroo et al. op. cit.). Thus a wide vertical extension of an anoxic layer can be postulated, allowing abundant preservation of the planktonic input (Schlanger and Jenkyns, 1976 ; Thiede and Van Andel, 1977). This situation could be compared only with the environment of the eastern basin of North Atlantic but it is quite different from the western basin and the northern embayment.

During Upper Cretaceous, an anoxic environment prevailed again in the Angola Basin (Cenomanian-Turonian), whereas a broader opening of the Cape Basin towards the Southern Ocean allowed the entry of deep oceanic water. As a result, the anoxic layer disappeared or was considerably diminished, and all sites of the Falkland Plateau and Cape Basin are marked by a terrestrial organic input (Deroo et al, op. cit.). The southern part of the eastern basin (Cape Verde, Demerara) may be considered during Upper Cretaceous as a North Atlantic equivalent of the Angola Basin, whereas the northern part and the western basin are generally comparable to the Cape Basin.

b) Climate

The considerable input of terrestrial organic matter in the North Atlantic suggests a humid climate for most of the surrounding lands. First, the abundance of contemporaneous terrestrial organic matter shows that onland productivity of plants was quite high. Then the widespread occurrence of recycled organic matter points to an active erosion. Both require that transportation by surface waters to the basin of sedimentation was reasonably efficient. An alternation of dense vegetal coverage, rock weathering and soils erosion may be suggested.

Rifting and separation between North America, Africa and Europe did not start in a massive emergent land, but mainly in epicontinental seas. This is particularly evident for the northern embayment where separation occurred in Lower Cretaceous between Iberia and North America, and also in the Bay of Biscay (Montadert et al, 1977). The continental

masses surrounding the narrow oceanic belt, during Aptian-Albian and Late Cretaceous times, were in fact composed of several emergent lands and shallow seas (fig. 11). Following the Purbeck semi-arid period, the climate is likely to have been under marine influence during a large part of Cretaceous and to range from tropical humid to temperate oceanic. Under those conditions terrestrial vegetation was probably abundant. The climate and abundant vegetation are corroborated by carbonaceous deposits, including lignite and coal, known in Europe and North America. Erosion was also active as proven by the Wealden deposits (Allen, 1975) and also by the important rate of terrigenous sedimentation found in the Bay of Biscay and off Portugal (25 to 50 m per m.y.).

A comparable situation is possibly found at the extreme south of the Atlantic, where a progressive widening of the Cape Basin during Cretaceous probably increased the oceanic influence on the climate. Again, the terrestrial organic input is important and terrigenous sedimentation rate is high : more than 100 m per m.y. in the Cape Basin during Aptian-Albian time (Van Andel et al., 1977).

This type of landscape contrasts with the situation observed between South America and central or western Africa, at the end of Lower Cretaceous. There, planktonic organic matter is either the only or predominant source in the Angola and Cape Verde Basins. The initial rifting and separation started there under mid-continental conditions. The land bordering the young and narrow basins formed a massive emergent continent, remnant of the ancient Gondwana land. Under tropical or subtropical latitudes, the climate was possibly comparable to that of the present Central Asia, i.e. acid and semi-desertic. Another comparison would be the present shores of the young Red Sea, although the surrounding land masses were more important in Africa-South America during Early Cretaceous. This climatic hypothesis is supported by occurrences of red beds and sometimes gypsum on lands during the late Jurassic-Lower Cretaceous (Sahara, Amazon Basin, Eastern Andes). Thus the terrestrial organic and mineral input was probably very low and marine or lacustrine plankton was the main source of organic matter.

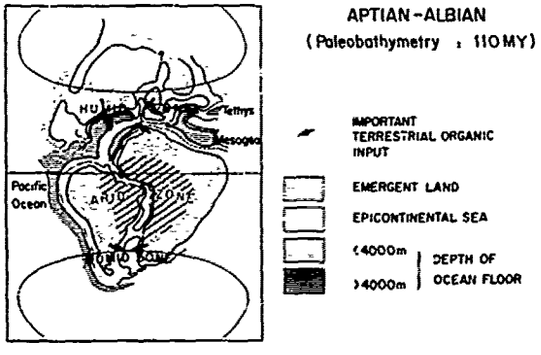


Fig. 11 Approximate paleogeography of Lower Cretaceous. Position of continents and depth of ocean floor as in fig. 9. Extension of emergent land and seas according to Pomerol (1975), Van Andel et al (1977) and the authors own work.

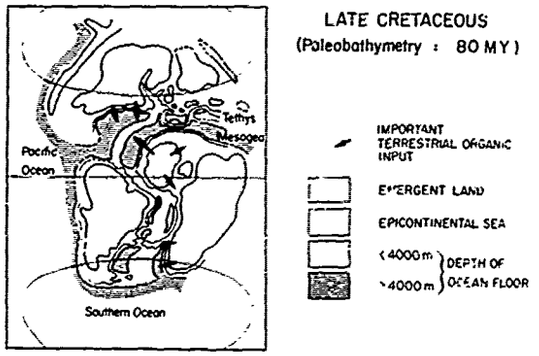


Fig. 12 Approximate paleogeography of Upper Cretaceous. Position of continents and depth of ocean floor as in fig. 10. Extension of emergent land and seas according to Pomerol (1975), Van Andel et al. (1977) and the authors own work.

The climate probably changes in Cenomanian, when a large transgression by shallow sea connected the Tethys with the South Atlantic (fig. 12) and changed the West African and the Hoggar massives into islands covered with trees which are now fossilized in Upper Cretaceous sediments (Pomerol, 1975). A humid climate in late Cretaceous is also supported by Senonian coals in Nigeria.

c) Land physiography

The hydrographic pattern on lands surrounding the North Atlantic Ocean directed an important terrestrial input (organic and mineral) towards most of the ocean : western basin, northern embayment and northern part of the eastern basin. This feature may be contrasted with the reduced terrestrial input in the Cape Verde and Demerara areas, and also in the Angola Basin (fig. 11).

This contrast is possibly due to submarine versus subaerial rifting. Between South America and Africa, the rifting phase may have created an arch, comparable to the present Sudan - S.W. Arabia, resulting in a much reduced area of drainage towards the new ocean. The major hydrographic pattern was probably directly towards the other side of the continents, e.g. Amazon river flowing into the Pacific, or towards continental lowlands, marked by terrestrial sediments with gypsum (Sahara). With reference to a previous comparison, this type of drainage and sedimentation could resemble the present situation in the Balkach and other lake basins of Central Asia.

On the contrary, submarine rifting between Europe and North America prevented land rising around the new ocean : the drainage pattern was not affected, allowing transportation of an impor-

tant terrestrial organic contribution. Furthermore, Ryan and Cita (1977) emphasized the widespread outpouring of clastic wedges in North America, Western Europe and Morocco.

## 6. Conclusion

1. Geochemical studies of the black and carbonaceous shales found in the Cretaceous of the North Atlantic have shown that different types of organic matter are involved. In particular the concepts of "black shale" and "marine organic matter deposited in a reducing environment" are not necessarily associated.

2. Three main types of organic matter have been distinguished : planktonic (marine or lacustrine) ; terrestrial moderately degraded (higher plants) ; residual, which comprise contemporaneous oxidized and older recycled organic material.

3. Conditions of preservation and accumulation may be different according to the type of organic matter. Their study provides information on the aquatic environment of deposition and also on the surrounding continents.

4. The major controls on organic sedimentation are climate and oceanic circulation. Terrestrial organic matter is mainly influenced by climate, whereas marine organic matter is mainly controlled by oceanic circulation.

5. Lower Cretaceous and the older part of Upper Cretaceous appear to be a unique episode in the history of the Atlantic for preservation and accumulation of the planktonic organic matter to an unusual extent. The high organic content, the size of the areas concerned, and the accumulation under deep oceanic conditions are the main characteristics of this event. It can be explained firstly by the poor connection of some of the new basins with other oceanic masses (Pacific, Tethys, Southern Ocean) and also between them. Additionally, the land physiography and an arid climate over part of South America and Africa restricted the terrestrial input in this area.

6. Once deep oceanic connections were established between North and South Atlantic basins, and also with other oceans, these conditions no longer existed. Thus, no massive accumulation of planktonic organic matter has been reported in the Tertiary beds. The only exception would be the early Miocene black shales found in the Tarfaya Basin off Morocco (site 397). Their organic matter belongs to type II and is considered to be marine and deposited in a reducing environment. However Deroo et al (D.S.D.P. Initial Report, op. cit.) suggested that the Miocene black shales may be partly composed of reworked material slumped off the edge of the continental shelf during Neogene time.

7. A contrast is observed at certain ages (fig. 9 and 10) between the western basin (normal) and the eastern basin (with an extended anoxic layer) of the North Atlantic. It is suggested that the mid-Atlantic ridge possibly acted as a barrier to oceanic circulation. Considering the high rate of organic preservation, the top of the anoxic level in the eastern basin may have been relatively shallow for some time. Thus the crest of the ridge might have been, at certain ages, less deep than generally accepted.

Acknowledgements. The authors thank the National Science Foundation for making the core samples available through the Deep Sea Drilling Project.

The authors are indebted to J. Roucaché for pyrolysis and kerogen analyses, H. Castex for infrared spectrometry, J. Bellet and J.L. Pittion for optical examination of the organic matter. Valuable discussions and suggetions were made by R. Pelet and L. Montadert.

They also thank Chevron Overseas Petroleum Inc., Compagnie Française des Pétroles, Société Nationale Elf-Aquitaine, and Petrofina S.A. for partial financial support.

## References

Allen P., Wealden of the Weald : a new model. Proc. Geol. Ass. 86 (4), 389-437, 1975.

Berger W.H., and Von Rad U., Cretaceous and Cenozoic sediments from the Atlantic Ocean floor : Initial Reports Deep Sea Drilling Project, 14, 787-954, 1972.

Biju-Duval B., Dercourt J. and Le Pichon X., From the Tethys Ocean to the Mediterranean seas : a plate tectonic model of the evolution of the Western Alpine system : International Symposium on the structural history of the Mediterranean basins, Technip, Paris, 143-164, 1977.

Deroo G. and Herbin J.P., Paleogeographic assay in South Atlantic Ocean during the Cretaceous period deduced from an organic matter sedimentological study (in preparation), 1978.

Deroo G., Herbin J.P., Roucaché J. and Tissot B., in : Initial Reports Deep Sea Drilling Project, legs 41, 44, 47, 48, 50, 51 to 53 (in press).

Dow , W.G., Kerogen studies and geological interpretations. J. Geochem. Explor. 7, 79-99 (1977).

Espitalié J., Madec M., Tissot B., Mennig J.J. and Leplat P., Source rock characterization method for petroleum exploration. Offshore Technology Conference, Houston, Paper OTC 2935, 1977.

Hood A., Castano J.R., Organic metamorphism Its relationship to petroleum generation and application to studies of authigenic minerals. Coordinating Comm. Offshore Prospecting Techn. Bull. 8, 85-118 (1974).

Pelet R., Géochimie organique des sédiments marins profonds de la mer de Norvège. Vue d'ensemble. in : Géochimie organique des sédiments marins profonds, Orgon I, Mer de Norvège, Centre National de la Recherche Scientifique, Paris, 281-296, 1977.

Pelet R., Géochimie organique des sédiments marins profonds de l'appareil détritique

de l'Amazone et du bassin de Cariaco : vue d'ensemble. in : Géochimie organique des sédiments marins profonds, Orgon II. Centre National de la Recherche Scientifique, Paris (in press), 1978.

Pomerol C., Stratigraphie et Paléogéographie, II-Ere mésozoïque. Doin, Paris, 383 pp., 1975.

Robin P., Caractérisation des kérogènes et de leur évolution par spectrométrie infrarouge. Thesis, Univ. of Louvain, 162 pp., 1975.

Ryan W.B.F. and Cita M.B., Ignorance concerning episodes of ocean-wide stagnation Marine Geology, 23, 197-215, 1977.

Schlanger S.O. and Jenkyns H.C., Cretaceous oceanic anoxic events : causes and consequences. Geologie en Mijnbouw, 55, (3-4) 179-184, 1976.

Sclater J.G., Hellinger S., Tapscott C., The paleobathymetry of the Atlantic Ocean from the Jurassic to present. Journal of Geology, 85 (5) 509-552, 1977.

Thiede J. and Van Andel T.H., The paleoenvironment of anaerobic sediments in the late Mesozoic South Atlantic Ocean. Earth and Planetary Science Letters, 33, 301-309, 1977.

Tissot B., Durand B., Espitalié J. and Combaz A., Influence of the nature and diagenesis of organic matter in formation of petroleum, Bull. Amer. Assoc. Petrol. Geol., 58, (3) 499-506, 1974.

Van Andel T.H., Thiede J., Sclater J.G., Hay W.W., Depositional history of the South Atlantic Ocean during the last 25 million years. Journal of Geology, 85, (6), 651-698, 1977.

pscott C., The
lantic Ocean from
Journal of
1977.
The paleoenviron-
s in the late
ean. Earth and
33, 301-309,

J. and Combaz A.,
d diagenesis of
n of petroleum,
Geol., 58, (3)

er J.G.,
of the South
last 125 million
85, (6), 651-

# CARBONACEOUS SEDIMENTS IN THE NORTH AND SOUTH ATLANTIC: THE ROLE OF SALINITY IN STABLE STRATIFICATION OF EARLY CRETACEOUS BASINS

Michael A. Arthur and James H. Natland

Geologic Research Division, Scripps Institution of Oceanography, La Jolla, California 92093

Abstract. Early to middle Cretaceous sediments rich in organic carbon have been recovered at many North Atlantic and South Atlantic DSDP sites. Those in the North Atlantic show many of the consequences of that basin having been less restricted with a relatively more vigorous circulation than that of the coeval South Atlantic.

The Angola-Brazil Basin in the South Atlantic was tectonically restricted by continental land masses to the north and the Walvis-São Paulo Ridge system to the south until late Albian time. Evaporites were deposited in this basin until the early-late Aptian, but a dense, saline water mass probably persisted through the latest Albian. Carbonaceous mudstones were deposited in anoxic deep water masses until mid-Albian time. The deep Cape-Argentine Basin was stagnant during most of Aptian time as a result of partial restriction behind the Falkland Plateau and overflow of dense brines from the Angola-Brazil Basin. Upon further opening of the South Atlantic, the Cape Argentine Basin became oxygenated while intermittent salinity stratification and anoxic episodes continued in the more restricted Angola-Brazil Basin from late Albian through Coniacian time.

Sediment of virtually all paleodepths in the central North Atlantic reflect conditions of intermittent anoxia and generally low oxygen content in deep water masses from at least Hauterivian through Cenomanian time. There is a high proportion of terrigenous organic matter in the carbonaceous sediment during Hauterivian through early Albian time, but marine organic matter was also preserved at times, especially after the middle Albian. Cenomanian and Turonian mudstones contain exceptionally high amounts of marine organic matter in the eastern central North Atlantic, probably reflecting conditions of upwelling and high surface productivity there. The remainder of the post-Cenomanian central North Atlantic apparently was characterized by well-oxygenated deep waters. The northern North Atlantic may have been partially restricted behind the J-anomaly ridge and the southeast Newfoundland Ridge until late Albian time, leading to mildly stagnant conditions with high rate of terrigenous clastic and organic input.

The stratification and oxygen contents of the deep waters in the central North Atlantic may have been influenced by intermittent spillage of waters of different salinities from the more restricted high latitude northern North Atlantic and the saline, restricted Angola-Brazil Basin, as well as by sinking of more saline shelf waters from evaporative settings such as broad Bahamian platforms.

## Introduction

The recovery of lower to middle Cretaceous "black clay", "black shale" or "sapropel" facies sediments in the North and South Atlantic during a number of Deep Sea Drilling Project legs has greatly altered our conception of the early evolution of ocean basins, paleocirculation, and the relative importance of influx of terrigenous matter with respect to marine organic matter in the generation of organic-carbon rich marine facies. The occurrence of these deposits over much of the North and South Atlantic ocean basins has led a number of workers to speculate on their origin and possible global significance (e.g., Schlanger and Jenkyns, 1976; Ryan and Cita, 1977; Fischer and Arthur, 1977). Other workers have leaned more heavily on hypotheses related to knowledge of local occurrences or have attempted to synthesize individual basins (e.g., Lancelot, et al., 1972; Berger and von Rad, 1972; Thiede and van Andel, 1977; McCoy and Zimmerman, 1977; Natland, 1978; McCave, in press; Kendrick, in press; Dean, et al., 1978; Gardner, et al., 1978; Arthur, in press). It is clear, however, that organic-carbon rich facies are very widely distributed from roughly Hauterivian through Cenomanian and locally Turonian time in the North Atlantic, and Oxfordian through Cenomanian and locally even Coniacian time in the South Atlantic, regardless of their lithologic attributes or origin.

Our purpose in presenting results from both the North and South Atlantic is to outline a descriptive model for the deposition of carbonaceous marine sediments. This involves differentiating between the earliest occurrences of such sediments in narrow, nascent ocean basins, when

anoxic conditions are persistent and oceanic circulation can be much restricted as in the early Cretaceous South Atlantic (Fig. 1), and deposition of such sediments in older, wider, and deeper basins with less restricted circulation but periodic density stratification as in the early Cretaceous central North Atlantic. The latter situation results in rhythmic intermittent patterns of anoxia, the origin of which we do not yet understand well. The earlier (South Atlantic-type) phases of carbonaceous sediment deposition associated with evaporite formation could well apply to older (Triassic-early Jurassic), as yet uncored, continental margin sediments of the North Atlantic. These could be important hydrocarbon sources, for the South Atlantic sediments we shall describe have higher average organic carbon contents than most of the rhythmic North Atlantic carbonaceous facies recovered so far. The relative importance of rapid burial of organic carbon, oxygen minima, and salinity stratification in producing the organic-carbon rich sediments must be considered.

We propose that young, widening ocean basins can progress through a sequence wherein salinity stratification initially is most important (as outlined recently by Kinsman, 1975) allowing preservation of organic carbon in sediments regardless of its rate of supply from rivers or surface productivity. The effects of salinity stratification diminish as the basin widens and barriers to effective circulation subside; organic carbon preservation can then be modulated by other factors of variable local or regional extent.

Especially important might be the spillage of waters of high salinity from restricted basins into less restricted ones causing short term stable stratification and inducing anoxia. We suggest this as the cause of episodes of stagnation in the Aptian Cape-Argentine basin and in the Aptian-Albian central North Atlantic; dense saline waters from the highly restricted Angola basin may have topped the basin margins and sunk to become bottom water in both settings. Saline waters formed in evaporative shelf settings also may have become North Atlantic bottom water. Partial restriction of the northern North Atlantic may have allowed a less saline low-density "lid" to form over most of that basin, occasionally spilling into the central North Atlantic. This could also have helped to establish stably stratified water masses in the central North Atlantic.

In detail, many of the occurrences of organic-carbon rich facies to be discussed here are neither "black shales" (s.s.) nor wholly composed of organic-carbon rich strata. In this paper, the term "carbonaceous mudstone" will be used in a general sense to refer to relatively organic-carbon rich dark colored (dark gray, greenish black, and black) mudstone and marlstone which may or may not be "shale" in the classical sense. These sediments are typified by above-average contents of organic carbon (>0.5% $C_{org}$) when compared with marine sediments of all ages (McIver, 1975). We shall also use the informal terms early and middle Cretaceous to refer to the periods Valanginian through Albian, and Cenomanian-Turonian respectively.

## Regional Setting of South Atlantic DSDP Sites During the Cretaceous

Organic-carbon rich Mesozoic sediments have been recovered at six sites in the South Atlantic. When carbonaceous sediments were deposited during the early Cretaceous, the locations of the sites spanned over 20° of latitude, and the sediments were deposited in a much narrower, more recently opened ocean basin than contemporaneous sediments in the North Atlantic (Fig. 1). The age distribution of organic-carbon rich facies in the South Atlantic sites is listed on Table 1 and a summary of their organic carbon content and composition on Tables 1 and 2.

At the north end of the South Atlantic, the bulge of West Africa and what is now the Amazon coast of Brazil prevented major exchange between the North and South Atlantic until probably late Albian time (Francheteau and LePichon, 1972; Kennedy and Cooper, 1975; Petters, 1978; Forster, 1978; Evans, 1978). Only cold-water planktonic and benthic foraminifers reached even tropical South Atlantic waters until that time and these came in from the south (Premoli-Silva and Boersma, 1977; Caron, 1978; Scheibnerova, 1978; Beckmann, 1978). The climate at the northern end of the South Atlantic was harsh and arid as indicated by a low diversity of palynomorphs in the carbonaceous sediments of Site 364 (Morgan, 1978) and by the presence of evaporites in the marginal coastal basins (e.g., Evans, 1978). The Angola and Brazil salt deposits are known to be Aptian in age from continental occurrences (Asmus and Ponte, 1973; Brink, 1974).

At the southern end of the South Atlantic (Fig. 1), the Falkland Plateau was moving past the southern tip of the landmass of Africa along the Agulhas Fracture Zone (Dingle and Scrutton, 1974). Sites 327 and 330 were located close together on the Falkland Plateau. Site 327 bottomed in Aptian carbonaceous sediments, but Jurassic carbonaceous sediments at Site 330 overlie terrestrial fluvial sediments and a Paleozoic granitic-gneissic basement (Barker, Dalziel, et al., 1977; Beckinsdale, et al. 1977; Tarney, 1977). Passages for sea water between the Antarctic-Indian Ocean and the South Atlantic thus had to pass over a shallow sill until at least Albian time.

The South Atlantic was divided into the Cape-Argentine, and the Angola-Brazil Basins by the Walvis-São Paulo Ridge complex (Fig. 1). Site 363, on Walvis Ridge, verified that during the Aptian the ridge was a highstanding feature, perhaps with islands (Bolli, Ryan, et al., 1978).

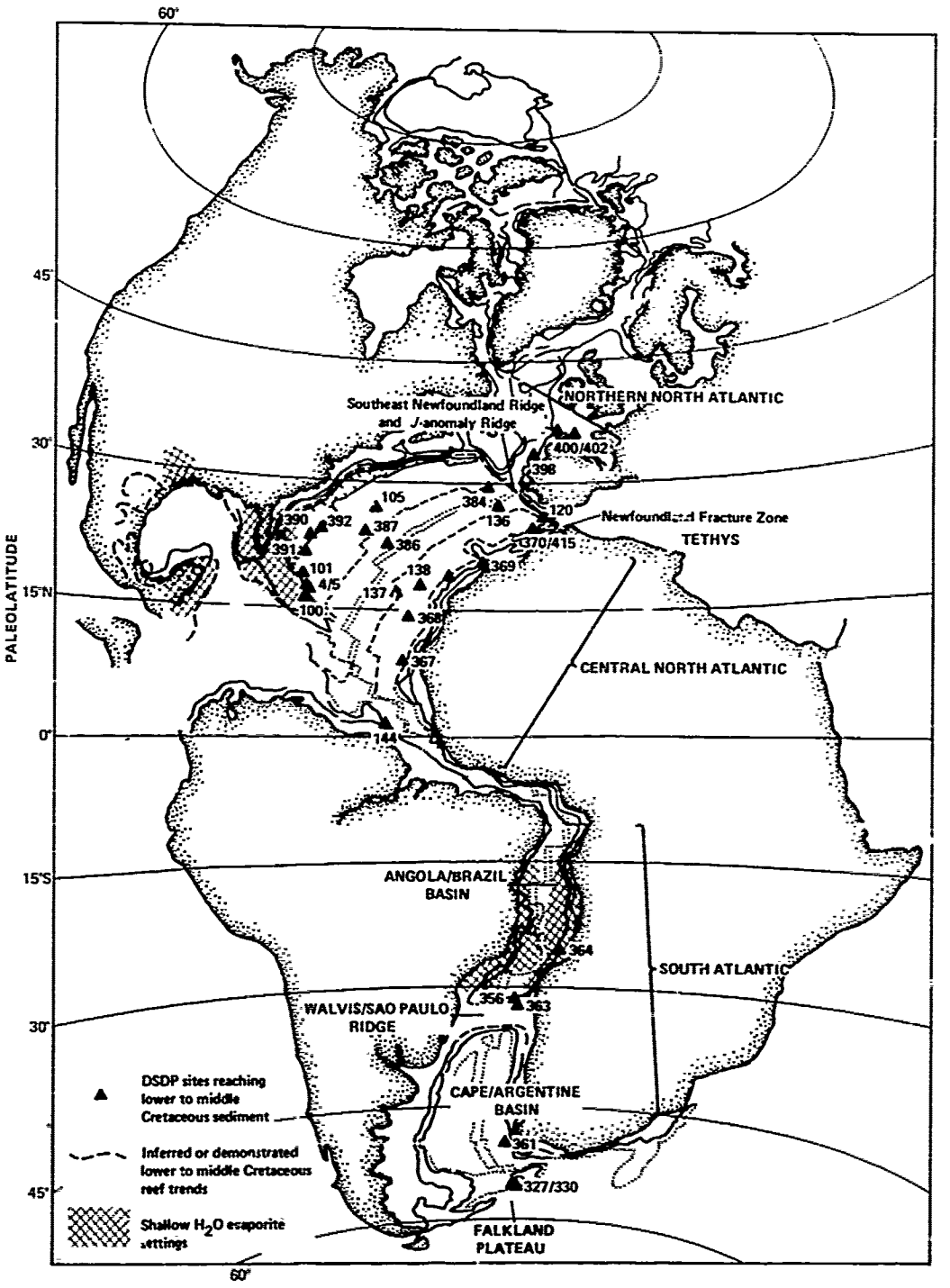


Fig. 1. Index map of paleogeography around North and South Atlantic Oceans at about 95 MA, modified after Sclater et al., 1977. This shows major physiographic features and location of DSDP sites discussed in text. Note location of major evaporite provinces of early to middle Cretaceous age.

TABLE 1. Organic Carbon Content and Compositions: In The South Atlantic

| Site | Facies | Age | Mean or Highest $C_{org}$[1] | $\delta C13$ (PDB) (Range) | Inferred $C_{org}$ Sources | Basis |
|---|---|---|---|---|---|---|
| 327/ 330 | Carbonaceous Mudstone | Oxfordian-Early Albian | 3.29 ±0.85 (25) | | Terrestrial and Marine | Lithology |
| 361 | Carbonaceous Mudstone<br>Sandy Mudstone<br>Sandystone<br>Marly Nanno-fossil Chalk | Aptian to Early Albian | 3.69 ±2.23% (38)<br>2.69 ±2.70 (35)<br>0.65% (2)<br>8.6% (1)<br>3.1% (mean for entire unit) | -24.7 to -27.7 | Terrestrial and Marine | Lithology<br>$\delta C^{13}$ (PDB) |
| 356 | Carbonaceous Mudstones interbedded with marly chalks and clay-pebble conglomerates | Turonian-Coniacian Santonian | 12.61% (highest of 7) | -23.6 to -27.4 | Terrestrial and Marine | Lithology and<br>$\delta C^{13}$ (PDB) |
| 363 | Limestones<br>Marly limestone<br>Calcareous Mud-stone<br>Carbonaceous Mudstone | Latest Albian (perhaps Cenomanian) | -<br>-<br>1.0% (highest of 2) | - | ? | ? |
| 364 | Chalk or Lime-stone (I-III)<br>Marly Chalk or Limestone (I-III)[2]<br>Calcareous Mudstone (I-III)[2]<br>Carbonaceous Mudstone (I and III)[2]<br>Dolomite or Dolomitic Limestone (III)[2] | Early and Mid. Albian<br>then again<br>Late Albian to<br>Coniacian-Santonian | (see Table 1)<br><br>5.97 ±1.5% (mean for all of sub-division III) | -27.7 to -30.4 (I)[2]<br>-24.9 to -28.2 (III)[2] | Terrestrial and Marine | Lithology<br>$\delta C^{13}$ (PDB)<br>Alkanes in lipids |

[1]Number of measurements in parentheses.
[2]$C_{org}$ subunits of Table 2.

Data Sources:
Lithology: Bolli, Ryan et al. (1978) for Sites 361, 363 and 364; Supko, Perch-Nielsen et al. (1977) for Site 356; Barker, Dalziel et al. (1977) for Sites 327 and 330.
$C_{org}$: Foresman (1978) for Sites 356, 361, 363 and 364; Bolli, Ryan et al. (1978) for Sites 361, 363 and 364; Cameron (1977) and Commer and Littlejohn (1977) for Sites 327 and 330; Scott (1977) for Site 356; Kendrick et al. (1978) and Hunt (1978) for Sites 361 and 364.
$\delta C^{13}$ (PDB): Foresman (1978) Sites 356, 361 and 364.

TABLE 2. Average Organic Carbon in South Atlantic Facies

Site 361

| | | Average $C_{org}$ (%) in Lithologic Types (±σ) |
|---|---|---|
| Sediment Type | Sandstone | 0.625(2) |
| | Sandy mudstone | 2.95 ±2.70(35) |
| | Carbonaceous mudstone | 3.69 ±2.23(38) |
| | Marly nannofossil chalk | 8.6(1) |
| | Mean $C_{org}$ accumulation rate $g/cm^2/m.y.$[3] | 258 |
| | | In 11 m.y., 2837 $g/cm^2$ of $C_{org}$ accumulated[3] |

Site 364

| | | Average $C_{org}$ (%) in Lithologic Types (±σ) | | |
|---|---|---|---|---|
| | $C_{org}$ Subunits[2]: | I (Cores 20-29) | II (Cores 30-37) | III (Cores 38-46) |
| Sediment Type | Chalk or limestone | .1 | .45 ±.47(12) | 3.88 ±5.00(14) |
| | Marly chalk or limestone | .1 | 1.10 ±.37(4) | 6.40 ±6.70(9) |
| | Mudstone | .1 | 1.75 (est.) | - |
| | Carbonaceous mudstone | 14.62 ±4.91(6) | - | 12.60 ±8.46(8) |
| | Dolomite or dolomitic limestone | - | - | 2.47 ±2.82(3) |
| | Mean $C_{org}$ accumulation rate $g/cm^2/m.y.$[3,4] | 20 ±28(16 m.y.) | 28 ±20(8 m.y.) | 504 ±128(4 m.y.) |
| | | In 28 m.y., 2560 $g/cm^2$ of $C_{org}$ accumulated[3] | | |

[1]Number of measurements in parentheses, 76 total for Site 361, 89 total for Site 364.
[2]$C_{org}$ subunits defined on discrete changes in typical $C_{org}$ in limestone or marly limestone facies.
[3]Accumulation rates and total $C_{org}$ accumulated determined from $C_{org}$ abundances per core, and total sediment accumulation rate curves in Bolli, Ryan et al. (1978).
[4]Means ± standard deviations computed over number of cores in $C_{org}$ subunits.

Shallow water algal limestones, calcarenites produced in a high-energy near-shore environment, shallow-water benthic foraminifers, and phosphorite were recovered in the deepest cores of the site. Site 356, on the São Paulo Ridge, is located just south of the diapir margin of the Brazil salt plateau (Supko, Perch-Nielsen, et al., 1977). The ridge, which bounds the salt plateau, has a south-facing scarp (Gamboa and Kumar, 1977) whereas north of Site 363, Walvis Ridge has a north-facing scarp (Barnaby, 1974). These could represent the trace of the fracture zone that separated the Walvis and São Paulo Ridges, (Bolli, Ryan, et al., 1978, p. 232). A reconstruction of the position of the Brazil and Angola salt plateaus in Albian time (Bolli, Ryan, et al., 1978, Chapter 3, Fig. 36, based on a figure in Leyden, et al., 1976; see also Fig. 1) shows that Site 356 and a lobe of the Brazil salt plateau, as well as the São Paulo Ridge, lay between Site 363 and the Angola salt plateau at that time.

Two sites, 361 in the Cape Basin and 364 on the Angola margin salt plateau, provide the most significant evidence for restricted circulation in these basins in Aptian and Albian times. In each, hundreds of meters of organic-carbon rich sediments were penetrated.

Site 361 is located on magnetic anomaly M-4 (estimated Barremian age) of the Cape sequence (Larson and Ladd, 1973). Over 300 meters of lower Albian and Aptian carbonaceous and interbedded turbiditic sandstones were penetrated at this site. Lowermost Aptian carbonaceous sediments recovered in the deepest core here are estimated to be within only tens of meters of basement, considered to be oceanic crust (Bolli, Ryan, et al., 1978, p. 68). At the time of deposition of these sediments (about anomaly M-1 time), the crest of the Mid-Atlantic Ridge was about 120 km to the southwest, paralleling fracture zones (Bolli, Ryan, et al., 1978, chapter 2, Fig. 5). The sediments were thus deposited in the deepest part of the Cape Basin, between the elevated ridge crest to the west, and the continental margin sediment prism rising gently to the east. In the Aptian, Site 361 was northwest of Sites 327 and 330 which were on the much shallower Falkland Plateau (Fig. 1).

Site 364 is located in the Angola Basin above the marginal salt plateau, which is about 2 km thick and underlain by highly magnetized presumed oceanic crust (Emery et al., 1975). High pore-water salinities (up to 74 °/oo) in the lowest cores of Site 364 (Sotelo and Gieskes, 1978) and nearly complete penetration of the acoustic unit above the principal salt reflector (Bolli, Ryan, et al., 1978, p. 382) verified the proximity of the salt body. Carbonaceous mudstone deposition was most pronounced in the late Aptian and early Albian, and was intermittent from late Albian to Turonian times (Bolli, Ryan, et al., 1978).

The South Atlantic was thus a unique pair of narrow, linked, and highly restricted ocean basins, constricted at the middle by the Walvis-São Paulo Ridge complex, and supplied sea water across a high sill from only the southern end. Though few in number, the sites reaching Mesozoic carbonaceous sediments in the South Atlantic are in critical locations for evaluating its oceanographic history. The cores from the sites contain evidence for the gradual ventilation of the South Atlantic. Consistent with the initial supply of sea water only from the south, the degree of circulation in the Cape Basin kept one step ahead of that in the Angola Basin as the South Atlantic widened (Bolli, Ryan et al., 1978). When the Cape Basin was anoxic, the Angola Basin was evaporitic (Fig. 2A). When anoxic conditions ceased in the Cape Basin, the Angola Basin, too, was less restricted and become anoxic without accompanying evaporite deposition (Fig. 2B). Finally, it, too, achieved sufficient circulation to become oxygenated for good in the Late Cretaceous when surface and deep water connections were made from both north and south (Fig. 2C). Throughout this time, circulation developed in response to climatically induced sinking of dense saline waters formed primarily in the low-latitude, nearly land-locked, arid Angola-Brazil Basin (Natland, 1978). Anoxia was the result of stable salinity stratification in which dense, saline waters were trapped behind high sills, first in both basins, then only in the Angola-Brazil Basin (Fig. 2). Sediments deposited in the basins at these times are distinctive because they have the imprint of both anoxia and elevated salinity. Such sediments have not been recovered from the North Atlantic, and because their characteristics are not widely known, we have here integrated organic carbon and lithologic data for them in some detail.

## Organic Carbon in South Atlantic Cretaceous Carbonaceous Sediments

There is far more organic carbon ($C_{org}$) data through thicker sequences of sediments at Sites 361 (Cape Basin) and 364 (Angola Basin) than for the other South Atlantic sites. These have been used to determine accumulation rates of organic carbon in each basin (Figs. 3 and 4; Table 2). The average $C_{org}$ for the section at Site 361 weighted to lithology (3.1%) is very close to that calculated for the much more uniformly deposited largely synchronous carbonaceous mudstones of Site 330 (3.3%). Figure 4 shows that there were two distinctly different periods of organic carbon preservation at Site 364 separated by an interval of non-preservation of $C_{org}$. In the lower and middle Albian, $C_{org}$ is high in all lithologies whereas in the later Cretaceous it was preserved only in the carbonaceous mudstones. Hence, though individual $C_{org}$ values are as high in the later period as in the earlier, the accumulation rate weighted to litho-

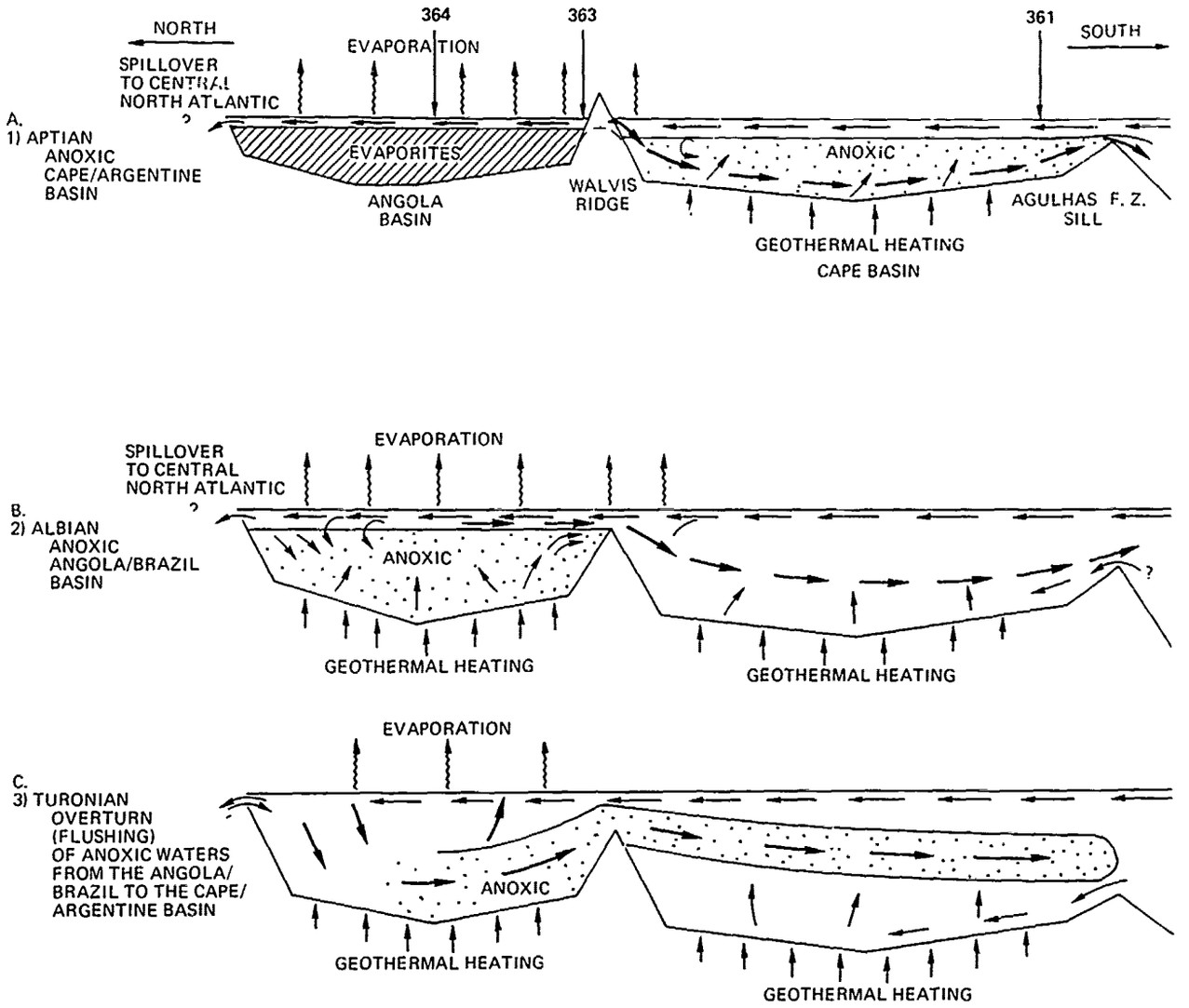


SCHEMATIC THERMOHALINE
CIRCULATION IN THE SOUTH ATLANTIC
DURING THE CRETACEOUS

Fig. 2. Schematic cross-section of South Atlantic and suggested circulation patterns for (A) Aptian, (B) Albian, and (C) Turonian time, after Natland (1978).

logies is much lower. In the lower-middle Albian sediments, the average $C_{org}$ weighted to lithologies is 5.97 ±1.5%, higher than all but 27 of $C_{org}$ measurements in the North Atlantic, and much higher than averages by stage for the North Atlantic shown in Table 3.

Preserved marine organic matter is the most positive indication that conditions in the water column rather than high terrigenous influx alone contributed to the high organic carbon in sediments. Marine organic carbon can be detected using carbon isotope data (Table 1), and conditions of deposition (marine versus terrigenous). For sites where carbon isotope data exists, $\delta^{13}C$ (PDB) values in the lower to middle -20's, indicate a significant marine component, whereas values from -28 to -30 imply a major terrigenous source (Degens, 1969). At Site 364, much of the $C_{org}$ is terrestrial, but the proportion of marine $C_{org}$ appears to increase with depth, inasmuch as $\delta^{13}C$ (PDB) in general decreases from -28.2 to -24.9 downhole in the lower to middle Albian (Foresman, 1978). Simoneit (1978) also reports that lipids from one lower Albian sample were derived from both marine and terrigenous sources based on alkane distribution.

Lithologic indicators that much organic carbon was deposited as a pelagic component are present

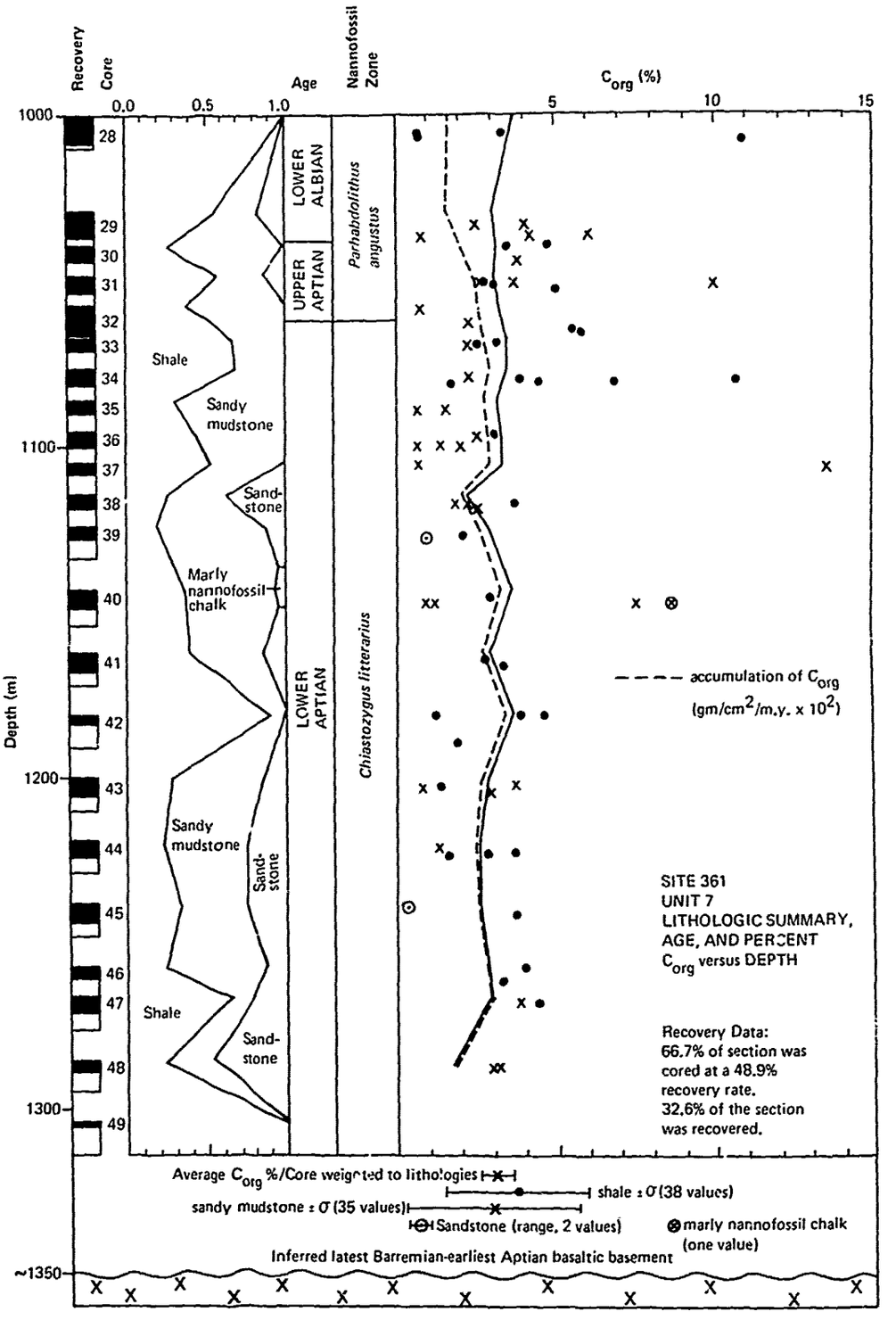


Fig. 3. South Atlantic Site 361, Unit 7: lithologic summary, age, and precent $C_{org}$ versus depth. Average $C_{org}$ per core shown by solid line; accumulation rate of $C_{org}$ per core by dashed line, computed from bulk sediment accumulation rate curve (Bolli, Ryan, et al., 1978, p. 64).

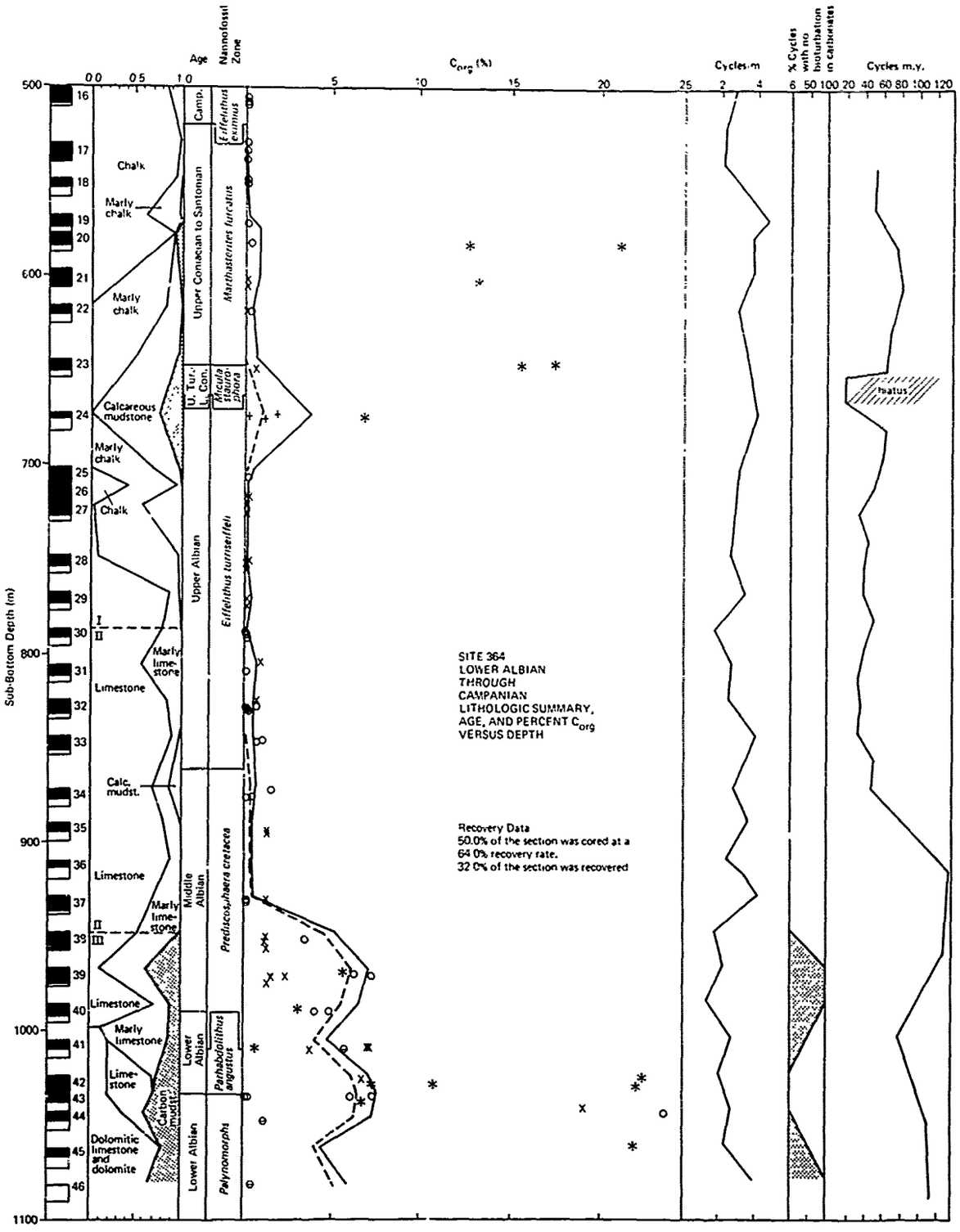


Fig. 4. South Atlantic Site 364: lithologic summary, age, percent $C_{org}$, and frequency of carbonate cycles versus depth (lower Albian through Campanian). Average $C_{org}$ per core shown by solid lines, accumulation rate of $C_{org}$ per core by dashed line, computed from bulk sediment accumulation rate curve (Bolli, Ryan et al., 1978, p. 381). $C_{org}$ symbols are *, carbonaceous mudstone; o, chalk and limestone; x, marly limestone, θ, dolomitic limestone and dolomite.

TABLE 3. Organic Carbon North Atlantic[1]

| Cretaceous Stage | Number Measurements[2] | Average Organic Carbon | |
|---|---|---|---|
| Maestrichtian | 33 | 0.08 | organic matter predominantly marine |
| | 9 | 0.62 | |
| Campanian | 12 | 0.04 | |
| | - | - | |
| Santonian | - | - | |
| | 3 | 3.7 | |
| Coniacian | 1 | 0.10 | |
| | 4 | 0.25 | |
| Turonian | 1 | 0.70 | |
| | 3 | 6.4 | |
| Cenomanian | 45 | 1.0 | |
| | 24 | 1.0 | |
| Albian | 82 | 0.82 | |
| | 14 | 0.57 | organic matter predominantly terrigenous |
| Aptian | 43 | 0.92 | |
| | 7 | 1.4 | |
| Barremian | 4 | 0.30 | |
| | 22 | 0.98 | |
| Hauterivian | 22 | 0.77 | |
| | 17 | 0.72 | |
| Valanginian | 12 | 0.24 | |
| | 33 | 0.55 | |
| Berriasian | 6 | 0.10 | |
| [3]upper Cretaceous | 48 | 0.50 | |
| lower Cretaceous | 60 | 1.23 | |

[1]Data from DSDP Legs 1, 11, 12, 14, 41, 43, 44, 47, 48; LECO determinations by DSDP Sediment Lab courtesy of DSDP computer group.

[2]Note: there may be an over-representation of organic carbon rich layers which are more likely to be sampled. Also, values noted between stages are those which fall either into the latter part of the stage below or the early part of the stage above (e.g., late Albian-early Cenomanian).

[3]Average of samples which could only be assigned to either lower or upper Cretaceous.

at all sites in the South Atlantic. At Sites 327 and 330, where there is no carbon isotope data, $C_{org}$ was deposited very uniformly in mudstones interbedded with minor limestones (one sideritic). The limestones imply deposition in a marine environment (Barker, Dalziel, et al., 1977). Limestones are also interbedded with carbonaceous mudstones at Sites 356 (Supko, Perch-Nielsen, et al., 1977). Similarly at Site 364, even though carbon isotopes indicate that much of the organic carbon is terrigenous, especially higher in the section, the site was far off shore, and the carbonaceous sediments are interbedded with tranquilly deposited chalks and limestones. Morgan (1978) concluded that Cretaceous palynomorphs at Site 362 were wind-borne for these reasons. Thus, even though the terrestrial organic carbon component is high, it was not the result of rapid deposition and burial.

At Site 361, most of the carbonaceous mudstones and sandstones are parts of graded turbidite sequences, and much of the $C_{org}$ had a terrigenous source since coarse coalified wood fragments (up to 8 cm long) and plant debris are abundant (Bolli, Ryan, et al., 1978). The sandy mudstones in fact include soft lithic grains of carbonaceous mudstone ripped from previous sites of deposition and incorporated into debris flows or turbidites (Natland, 1978; Kagami, 1978). The matrix of sandy mudstones largely consists of carbon-rich argillaceous material compressed between sand grains. Many carbonaceous mudstones, however, were deposited tranquilly and are not part of turbidite sequences. These are finely laminated, and some contain literally hundreds of millimeter-thin nannofossil layers, some monospecific, others containing plates of individual coccospheres in small heaps around their site of deposition (Noël and Melguen, 1978). Even in carbonate-free laminated mudstones, scanning electron microscope observations reveal impressions of coccoliths, with all calcium carbonate removed diagenetically (Noël and Melguen, 1978). These authors concluded that when these sediments were deposited, most of the water column was both anoxic and limpid. In the entire sequence at Site 361, there are no bioturbated intervals. The anoxic water mass persisted without significant turnover for at least eight million years.

## Sedimentary Indicators of Anoxic and Hypersaline Water Masses

Several lines of evidence suggest that deep water masses in the Angola and Cape basins were hypersaline in addition to being anoxic during Aptian and most of Albian times. These are carbonate-mudstone rhythms, dolomite chemistry, and zeolite mineralogy. All three pertain to Site 364, but only arguments concerning zeolite mineralogy apply to Site 361.

Sediments from Site 364 exhibit a marked rhythmic variation between mudstones (carbonaceous or otherwise) and chalks or limestones (some marly) similar to that occurring in many North Atlantic sites discussed below. Data on these rhythms are plotted versus depth (Fig. 4). The number of rhythms per meter shows no relationship to the occurrence of carbonaceous mudstone layers, but the frequency of rhythms per million years is about a factor of two higher in the lower-middle Albian sequence than in the upper Cretaceous. At one rhythm every 7-12,000 years, this is a frequency five times greater than typical rates in the North Atlantic. Anoxic conditions seem to have been superposed on an already established rhythmic pattern, one that persisted in the interim between anoxic intervals as well. In the upper Cretaceous sediments, most of the rhythms consist of interbedded chalks or limestones (some marly) and oxidized (red) mud-

stones. Only individual cores or portions of cores contain carbonaceous mudstone (black)-carbonate rhythms. These are more typically interbedded with pale gray green carbonates, whereas carbonates interbedded with reddish brown mudstones are generally tan or pale brown. Therefore, the carbonates associated with carbon-rich sediments, though bioturbated and thus not deposited in anoxic waters, nevertheless also appear to have had a more limited supply of oxygen than those associated with redder mudstones.

Downhole in Site 364, evidence for even scattered cycles of modest bottom-water oxygen levels disappears. Many rhythmic intervals of lower to middle Albian age have no bioturbation (Fig. 4) and consist of finely laminated mudstone and carbonate (Fig.5). The high $C_{org}$ in the marly carbonate portion of the rhythm lies in the high $C_{org}$ of dark laminae between carbonate laminae. Thus here, as in the upper Albian-Cenomanian, there is no relation between rhythmicity and preservation of organic carbon.

The origin of carbonate in the lower and middle Albian of Site 364 is enigmatic. Most of it is now dolomite (Fig. 4), and devoid of planktonic or benthonic calcareous microfossils (Beckmann, 1978; Bolli, 1978). The composition of the mineral dolomite changes from iron-rich to sodium rich with depth in the site (Matsumoto, et al., 1978), apparently reflecting simple anoxia (in which $Fe^{2+}$ was not oxidized and thus was available to enter the carbonate lattice) in the younger sediments, and anoxia plus hypersalinity in the sediments deposited just after

LOWER CRETACEOUS NORTH ATLANTIC OXIDATION/REDUCTION CYCLES COMPARED WITH CYCLE IN LAMINATED POST-EVAPORITE. CARBONACEOUS DOLOMITES OF ANGOLA BASIN, SOUTH ATLANTIC.

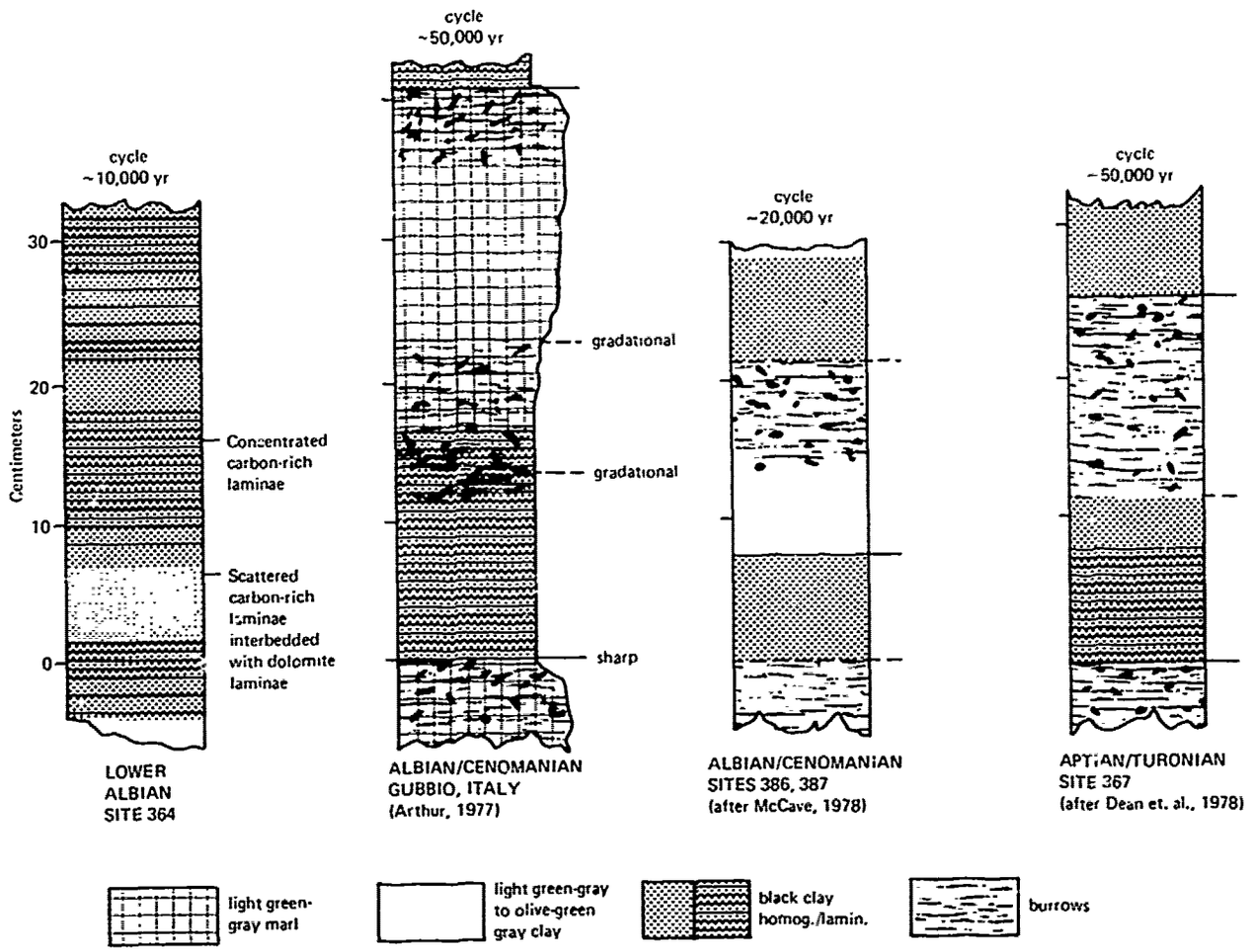


Fig. 5. Examples of early to middle Cretaceous oxidation-reduction rhythms in multicolored clays from the South Atlantic, North Atlantic, and Gubbio, Italy.

cessation of evaporitic conditions. Since much of the dolomitized carbonate was deposited as fine, almost varve-like laminae, its preservation is puzzling given the extensive evidence for diagenetic dissolution and reprecipitation of carbonate laminae at Site 361 already mentioned. Dissolution there resulted from the effects of acids produced during breakdown of organic matter and in the formation of sulfides, (Nöel and Melguen, 1978), and from the necessity to maintain pore-water alkalinity during diagenetic formation of clay minerals and zeolites (Natland, 1978). Since these effects probably also acted at Site 364, it is not clear how such delicate carbonate laminae were preserved in sediments containing so much organic carbon. Natland (1978) proposed that the carbonates in this interval were primarily chemical precipitates, analogous to Friedman's (1972) Red Sea "deep water" evaporite facies. In the Red Sea gypsum reaching the sea floor on the continental shelves can be bacterially converted to nearly pure calcium carbonate. The carbonates at Site 364 have been largely dolomitized, but such a mechanism would explain both the preservation of fine carbonate laminae and the absence of microfossils. The high carbonate/mudstone rhythm frequency and the abrupt drop in rhythm frequency in the middle Albian could be related to the chemical, rather than biological, origin of the carbonate. Site 364 sediments thus show evidence for restricted environment of deposition during the early and middle Albian which became progressively better ventilated and less saline through late Albian time. The lower carbonaceous mudstone sequence in particular is best described as transitional to an evaporite facies.

The distribution of dolomites at Sites 356, 363, and 364 suggests that anoxic and/or hypersaline waters swept across the Walvis-São Paulo Ridge complex during Albian to perhaps Cenomanian time. The proportion of dolomite increases in the lower (Albian) cores of both Sites 356 and 363, and at Site 363 the mineral dolomite is poorly ordered and iron-rich, approaching calcian ankerite in composition, similar to the iron-rich dolomite of Site 364 (Matsumoto et al., 1978). This dolomite is in part associated with the only small beds of latest Albian moderately carbonaceous mudstone recovered at Site 363 (all in a single core). This is also the time of greatest evidence for currents at Site 363 where the section is considerably shortened by erosion. The sediment mineralogy and lithology is most simply explained by passage of anoxic and perhaps hypersaline waters over Walvis-São Paulo Ridge from the Angola/Brazil to the Cape/Argentine Basin (Fig. 2). At Site 356, the succession from dolomitic limestones to carbonaceous mudstones has been compared to similar sequences in the Red Sea where anoxic episodes are related to salinity stratification similar to that proposed here (Supko and Perch-Nielsen, 1977).

The silicate authigenic mineral assemblage at Sites 361, 364 and possibly 363 also suggests conditions of heightened salinity in bottom waters in Aptian into Albian times. X-ray diffraction studies show that phillipsite, kaolinite and "illite" (hydromica) occur in the carbonaceous sediments of Sites 361 and 364, and in the marly dolomitic limestones of Site 363 (Siesser and Bremner, 1978; Matsumoto, et al., 1978). The presence of phillipsite, rather than clinoptilolite, was a surprise since there is little or no associated montmorillonite or mixed-layer clay, and since phillipsite normally requires a basaltic precursor (Stonecipher, 1976). Natland (1978) showed that the sandstones and mudstones of Site 361 have an almost entirely granitic provenance, and presented scanning electron photomicrographs revealing extensive dissolution of quartz and feldspar grains to form the authigenic mineral assemblage kaolinite (present both as dickite and halloysite), "illite", and phillipsite. Hess (1966) demonstrated that phillipsite could be stable in association with kaolinite and "illite" at elevated salinities, consistent with the presence of phillipsite and these clay minerals in siliceous tuffs in saline lakes (Hay, 1966). On this basis, Natland (1978) ascribed the authigenic clays and phillipsite at Sites 361 and 364 to heightened bottom water salinity during and after deposition. A similar inference for Site 363 is a little less certain because some montmorillonite and clinoptilolite occur in the phillipsite-bearing sediments. But Stonecipher (1976) has shown that phillipsite formed under normal marine conditions with a basaltic precursor has not persisted at all in any sediments older than Eocene age or buried more deeply than 600 meters recovered by the Deep Sea Drilling Project. Heightened salinity is thus also the probable cause for the preservation of phillipsite in Aptian and Albian sediments at Site 363.

## Age-Depth Relationships and the Linkage of Oceanographic Events in the Cretaceous South Atlantic

Figure 6 summarizes age-depth relationships in the South Atlantic based on subsidence curves determined by Thiede and van Andel (1977) and Melguen (1978). Since these two papers disagree in important ways on the subsidence history of Sites 361 and 364, the alternatives we most favor are indicated by solid lines, others by dashed lines on Figure 6. Melguen (1978), for example, back-tracked Site 361 from its present depth, giving an unusually shallow initial depth for a site on oceanic crust. We favor an initial depth nearer that typical of oceanic spreading centers and the present South Atlantic Mid-Atlantic Ridge (2700 meters), in agreement with Thiede and van Andel (1977). We suggest Paleogene uplift of the southwest African continental margin (Dingle and Scrutton, 1974;

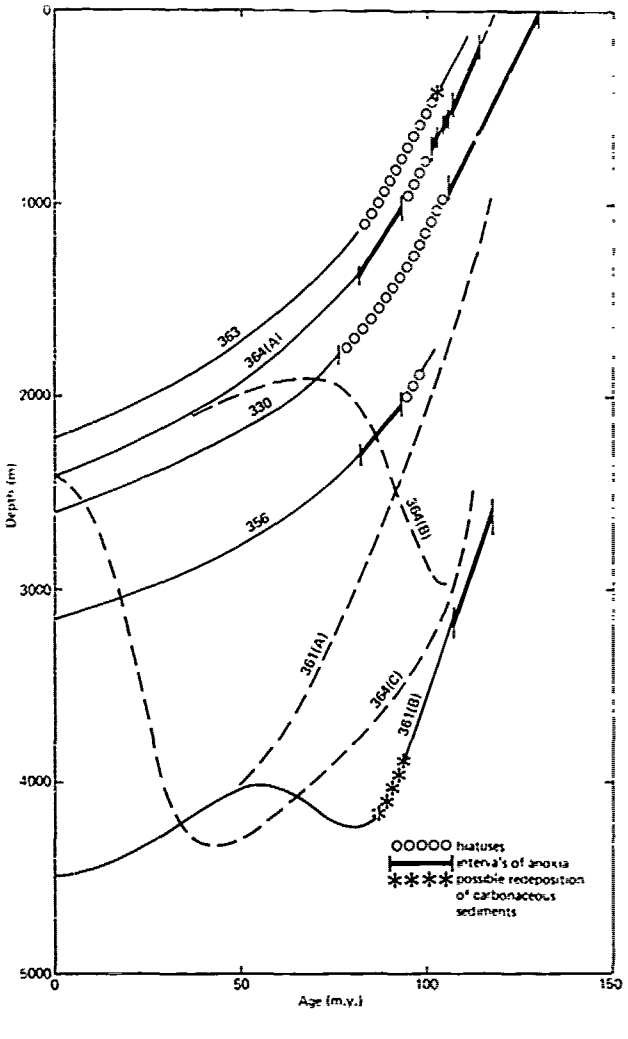


Fig. 6. Age-depth relation for South Atlantic DSDP sites reaching sediment of Cretaceous age. Modified after Thiede and van Andel (1977) and Melguen (1978). Alternative age-depth relations suggested by these authors shown by dashed lines. Intervals of anoxia shown on favored curves (solid lines).

Bolli, Ryan, et al., 1972, p. 69) to explain the present unusually shallow depth of Site 361. Thiede and van Andel (1977) and van Andel, et al. (1977), on the other hand, presumed an initial near ridge-crest depth for Site 364 and proposed that halokinetic flow uplifted the Angola marginal plateau either in the Late Cretaceous (between the two major intervals of anoxia), or perhaps in the Tertiary (both alternatives are shown on Fig. 6). But at Site 364, benthic foraminifers of Turonian to Maestrichtian age appear to have ranged between shelf depths and the deeper parts of the continental slope (200-2000 meters; Beckman, 1978). Deeper in the hole, Albian ammonites suggest inner shelf to epicontinental environments (Matsumoto, 1978). These, and lithologic evidence that the lower carbonaceous facies is transitional to an evaporite facies, imply that the site was quite shallow at times much earlier than that suggested by van Andel, et al. (1977).

The age-depth relationship for Site 330, on continental crust on the Falkland Plateau, is derived simply from knowledge of its present depth, and from the fact that it was subaerial in Jurassic times (Barker, Dalziel, et al., 1977). An oceanic subsidence curve has been applied in view of the lack of knowledge of the subsidence behavior of continental crust. Since we are here interested only in the general relationship of this site to Site 361, this is probably an adequate assumption.

All other sites are on oceanic crust, or aseismic ridges which follow oceanic subsidence paths (Detrick, et al., 1977). But they also are near continental margins, hence their early subsidence may have been accelerated by the landward piling up of salt (Site 364) or thick sediment prisms (Watts and Ryan, 1977). We are fortunate to have lithologic evidence for early shallow water histories of Sites 330, 363, and 364 to verify or to anchor the shallow ends of their subsidence curves.

On all curves on Figure 6, we have indicated when anoxia occurred, and the extent of hiatuses (based on nannofossil stratigraphy and the zonal-age scheme used in Bolli, Ryan, et al., 1978). Important aspects of the history of anoxia in the South Atlantic are apparent from this diagram. For example, Sites 330 and 361, though only a short distance apart in the Aptian (Fig. 1), spanned a water depth of over 2000 meters from the top of the Falkland Plateau to the deepest part of the Cape Basin. Accumulation of this basin was abrupt, inasmuch as the topmost carbonaceous sediments occur in the same nannofossil zone (*Parhabdolithus angustus*) at both sites. There can be little doubt that the Falkland Plateau dammed a basin-filling anoxic water mass which produced the high organic-carbon content of Aptian sediments at both sites (Fig. 2).

The northern South Atlantic sites, although all shallow in the Early Cretaceous, have overlapping periods of anoxia consistent with their close geographic proximity at the time, and with the presence of a dense saline mass of water trapped in the Angola-Brazil Basin behind the Walvis-São Paulo Ridge. Hiatuses and intervals of redeposition indicated on Figure 6 are critical to development of a circulation model for the South Atlantic (Fig. 2). For example, Natland (1978) inferred that spillover of dense, saline, episodically anoxic water from the Angola Basin to the Cape Basin persisted until late in the Cretaceous (Fig. 2, B and C) because of the evidence for erosion at Site 363 (indicated in part by the extended hiatus shown on Fig. 6), and because Site 361 contains evi-

dence for currents and a persistent basaltic component in its provenance throughout this time. The basaltic component probably was transported to the south by currents sweeping the Orange River delta (the river then as now drained the Karroo Basin with its abundant Stormberg basalts). It should also be noted that hiatuses could represent intervals of anoxia and in fact, at Sites 363 and 364, the Cenomanian marker fossil *Lithraphidites alatus* could be missing for ecological reasons (Proto-Decima, et al., 1978).

It is doubtful that southward flowing thermohaline currents in the Cape Basin could have existed without supply of dense, saline waters from the Angola Basin across Walvis-São Paulo Ridge. When deep passages opened to the North Atlantic and along Walvis-São Paulo Ridge by Campanian times, erosion on Walvis Ridge (Site 363), evidence for currents in the southern Cape Basin (Site 361), and anoxia in the Angola Basin (Site 364) all ceased. The consequence of completely ventilating the South Atlantic, paradoxically, was dramatically to slow down thermohaline circulation throughout the ocean. Vigorous bottom currents (sufficient to cause erosion) did not again develop until the formation of Antarctic deep cold-water currents late in the Tertiary (Kennett, et al., 1972; McCoy and Zimmerman, 1977; Melguen, 1978; Siesser, 1978). Turning the argument around, during its earlier, more restricted phases, deep currents in the South Atlantic had to form solely within its two basins. This must have been by sinking and flow of dense, more saline waters; there was no other way to produce them. With the evidence that such currents existed through much of the Late Cretaceous, it is likely that the intermittent anoxia in the Angola-Brazil Basin through much of this time resulted from episodic salinity stratification and overturn, as shown on Figure 2. Other explanations (such as an oxygen minimum) are inadequate to explain all aspects of South Atlantic circulation, although they may be permissable on lithologic grounds. It is also possible that the intermittence of anoxia at Site 364 in the Late Cretaceous merely reflects fluctuations in the top of a more persistent dense anoxic water mass. Therefore, no great stock should be placed in the precise timing or duration of anoxic events recorded at Site 364, since they are only the minimum possible for the Angola-Brazil Basin as a whole.

We have gone into some detail here on the South Atlantic to illustrate the variety of lithologic, chemical, mineralogic, and stratigraphic evidence needed to develop a wholly consistent model for paleocirculation and Cretaceous anoxic events, and because we believe that the South Atlantic, specifically the Angola-Brazil Basin, also influenced the central North Atlantic during perhaps Albian through Coniacian times in ways similar to that described for the Cape Basin. The complete story for the North Atlantic, though, is more involved than for the South Atlantic, and anoxic events there cannot be tied to a single mechanism.

## North Atlantic Carbonaceous Sediments - Regional Setting

Carbonaceous sediment of early to middle Cretaceous age has been recovered in the majority of Deep Sea Drilling sites reaching rocks of this age in the North Atlantic. These sites are located in both the eastern and western basins of the central North Atlantic which initially opened in early Jurassic (~180 m.y.B.P.) time (Pittman and Talwani, 1972; see Van Houten, 1977, for discussion of geological evidence) and lay in low to mid-latitudes during the early Cretaceous (Fig. 1). Carbonaceous sediment was also recovered in the northern North Atlantic Basin (north of the Newfoundland Fracture Zone), which opened much later, probably in Barremian-Aptian time (Ryan, Sibuet, et al., in press) and occupied a higher paleolatitude (~40°) during the early Cretaceous.

The central North Atlantic was already over 2500 km wide by Aptian-Albian time (Sclater, et al., 1977; see Fig. 1). Surface water exchange probably occurred with Tethys, the Pacific, and the northern North Atlantic; however, it is not clear whether efficient deep water exchange occurred with any of these ocean basins. Saunders, et al. (1975) suggest that a Panamanian submarine ridge formed a barrier to circulation from the Pacific through the Caribbean and North Atlantic during much of middle to late Cretaceous time. It is likely that some inflow to the North Atlantic occurred there. Continuity and similarity of pelagic deep-water facies in Tethyan settings with those of the North Atlantic basins (e.g., Bernoulli, 1972; Bernoulli and Jenkyns, 1974) suggests through-circulation between these oceans in Cretaceous time. Surface water connections were established with the South Atlantic Ocean by late Albian time (Petters, 1978; Forster, 1978) while deep water exchange was probably possible by Cenomanian time. The northern North Atlantic may have been at least partially restricted at its south end by the J-anomaly ridge and the southeast Newfoundland Ridge (e.g. Sibuet et al., in press; Tucholke and Vogt, in press) such that deep-water circulation was not possible to the rest of the North Atlantic until after mid-Albian time.

The age range of carbonaceous sediment in North Atlantic sites is generally Hauterivian through Cenomanian and locally early Turonian (Fig. 7). The carbonaceous sediment generally consists of interbedded dark-colored and lighter-colored claystone, marlstone and limestone. Interbedded sandy and silty layers are present in the Hauterivian through Aptian interval in a number of sites along the west African continental margin (e.g., Sites 370, 397, and 415) and off Portugal (Site 398). More calcareous facies are found in the pre-Aptian intervals of many

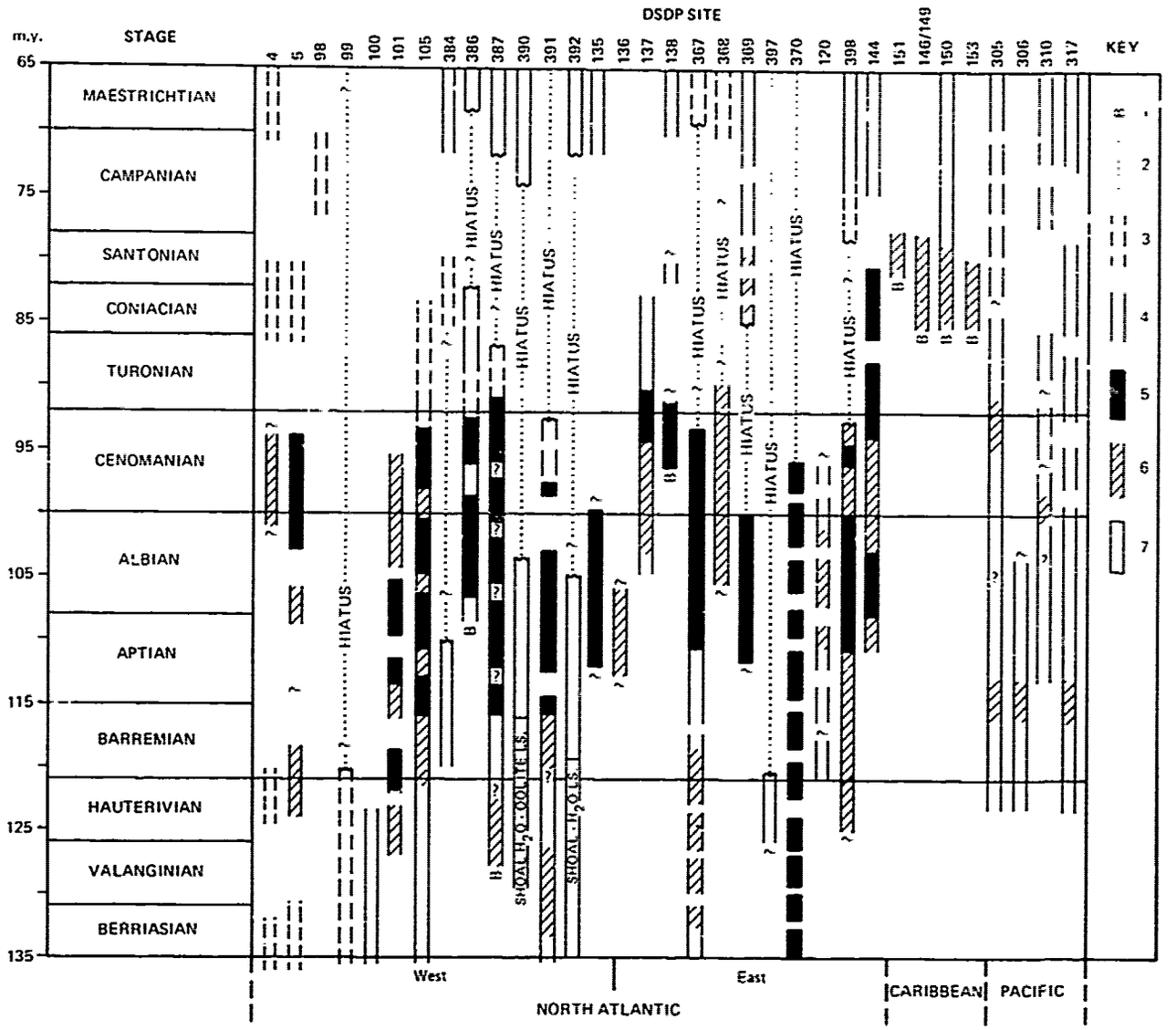


Fig. 7. Summary of ages of Cretaceous carbonaceous mudstone or other organic carbon rich facies in North Atlantic, Caribbean, and selected Pacific JOIDES-DSDP drill sites. Note concentration within Hauterivian through Cenomanian interval. Compiled from numerous sources.

Symbols:

1) site reached basement
2) hiatus
3) age uncertain or inferred
4) cored interval with age documented
5) primarily dark-colored, relatively organic rich sediment showing evidence of anoxic or very low oxygen condition
6) primarily dark-colored, organic carbon rich sediment showing evidence of low oxygen to oxygenated conditions
7) sediment evidencing well-oxygenated conditions

sites and in some sites occupying shallower paleodepths during Aptian-Albian time (e.g., Sites 144 and 369). At any rate, organic carbon-rich sediment has been recovered at sites of virtually all paleodepths (Fig. 8) except very shallow ones such as Sites 390 and 392 on the western margin of the central North Atlantic (see Benson, Sheridan, et al., 1978).

## Organic Matter in North Atlantic Sediment

Total organic carbon, palynological, vitrinite reflectance, pyrolysis, carbon isotope, and other studies of kerogen and extractable organic matter must be used to evaluate the paleoenvironmental conditions of preservation and extent of diagenesis of organic compounds (Didyk, et al., 1978). A more thorough discussion of studies of organic matter of Cretaceous age can be found in Tissot et al. (this volume).

Although North Atlantic carbonaceous sediments are mostly early and middle Cretaceous in age, organic-carbon rich facies persist into late

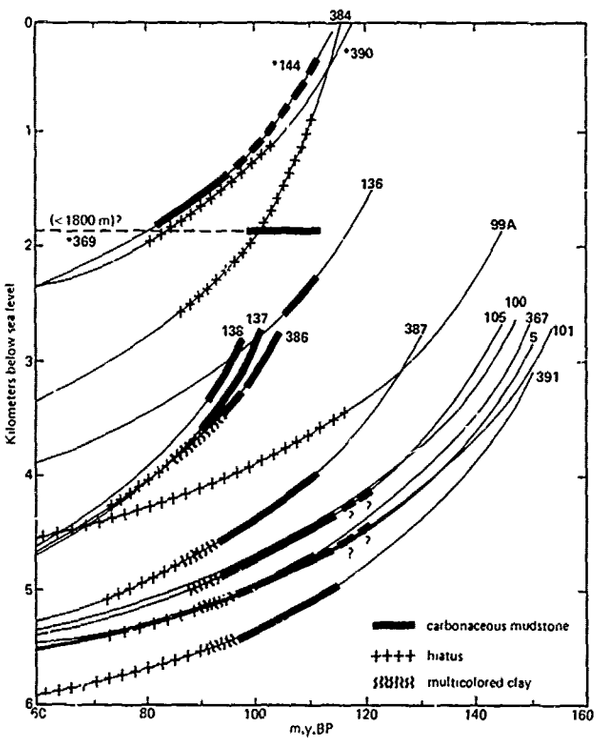


Fig. 8. Age-depth relation for selected central North Atlantic DSDP sites during Cretaceous time. Data modified from Sclater, et al., 1977; timing of carbonaceous muds, multicolored clay, and mid-Cretaceous hiatus shown at each site. Note that sites in the eastern basin are marked by slightly longer duration of carbonaceous mudstone deposition (138, 137, 367, 144).

Cretaceous time in some parts of the eastern and southern North Atlantic (e.g., Sites 144, 367) and through the Caribbean Sea (Edgar, Saunders, et al., 1973). Tethyan sections from southern France (de Boer, et al., 1978) and Italy (Arthur, unpublished data) show best development of black shale facies during Aptian-Albian time, but thin carbonaceous mudstones are interbedded with pelagic limestones as old as Hauterivian in age and again in Cenomanian-Turonian time. Patterns of organic carbon concentration in many DSDP sites and at Gubbio, Italy are similar but absolute values of organic carbon vary regionally (Fig. 9). Highest values occur in Cenomanian to earliest Turonian carbonaceous mudstones, and the lowest values occur in interbedded limestones and light-colored mudstone of all ages. Table 3 shows average values for organic carbon in the North Atlantic by stage from all DSDP sites through Leg 48. Note the high Hauterivian through Cenomanian averages.

Mixtures of marine and terrigenous or predominantly terrigenous organic matter are common in sediment of pre-late Albian age and the marine organic component dominates from late Albian onward at many sites. The details vary from region to region and according to analytical techniques used (see Tissot, et al., this volume; Simoneit et al., 1972, 1973; Dow, 1978; Kendrick, et al., 1978; Deroo, et al., 1978; Simoneit, 1978; Kendrick, et al., 1978; Cardoso et al., 1978; Erdman and Schorno, in press; Stuermer and Simoneit, 1978). For example, at Site 398 (Fig. 9C) terrigenous organic matter predominates until late Albian time in the northern North Atlantic, and significant marine-derived organic matter appears from late Albian through early Cenomanian time (e.g., Deroo, et al., in press; see Arthur, in press, for summary). Site 386 in the western central North Atlantic basin is characterized by the presence of both marine and terrigenous organic matter in carbonaceous clays of Aptian through lower Cenomanian age (Kendrick, et al., in press; Deroo et al., in press). Typical Aptian-Cenomanian black clay layers at Site 367 in the Cape Verde Basin of the east-central North Atlantic also contain marine planktonic organic matter (Deroo, et al., 1978). However, terrigenous organic matter is preserved in many muddy turbiditic layers (Lancelot and Seibold, 1978). Note that values or organic carbon are typically much higher in the eastern basin than the western basin of the central North Atlantic (Fig. 9A, B).

Deposition of many of the organic carbon rich layers probably occurred under anoxic conditions, based on sedimentary and geochemical criteria (e.g., Simoneit, 1977; Lancelot and Seibold, 1978; Kendrick, in press; McCave, in press) although there remains some debate about this (Gardner et al., 1978; Montadert, Roberts, et al., 1976). The intensity and duration of intervals of oxygen depletion in the water column also probably varied with time, stability of

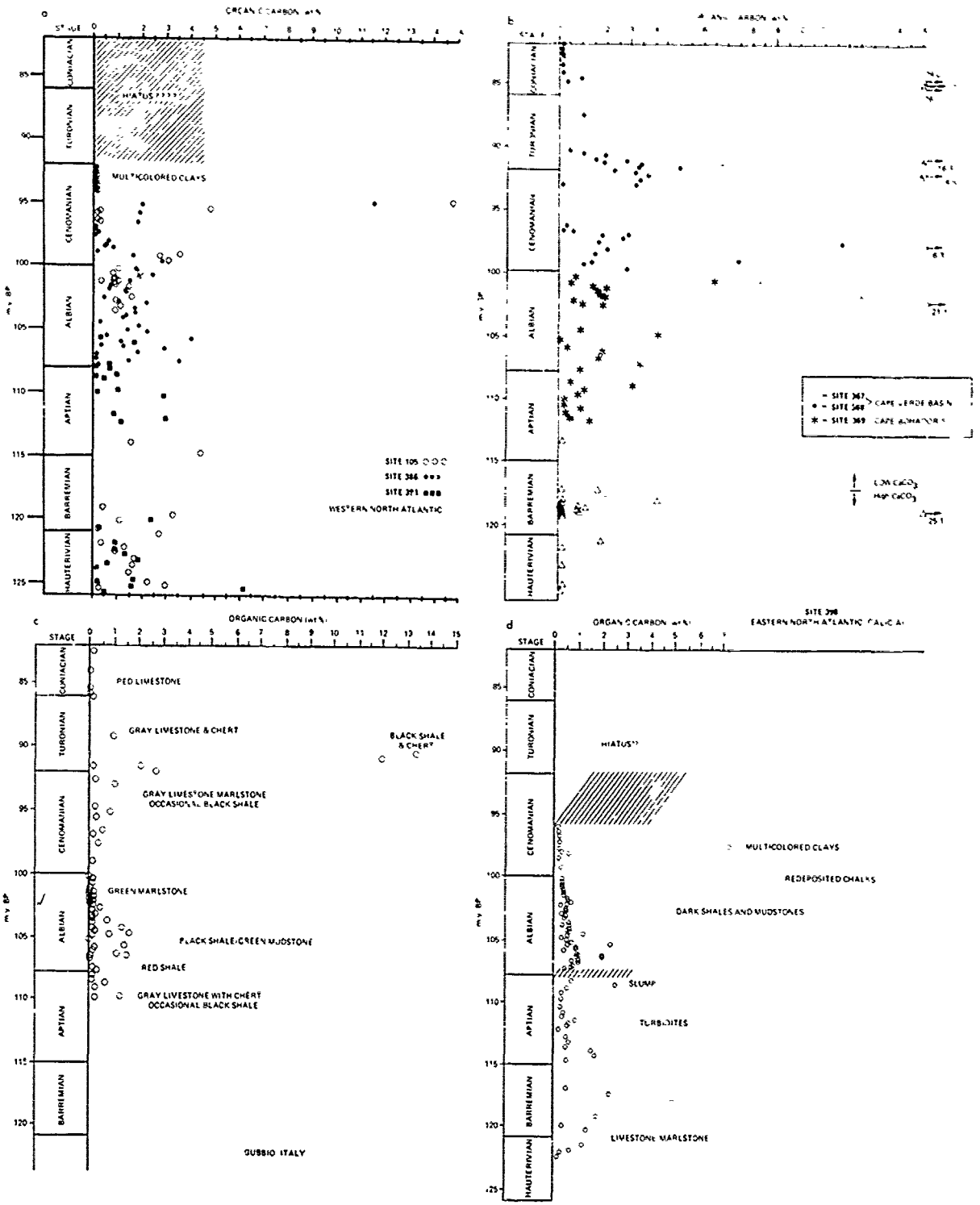


Fig. 9. Measurements of organic carbon content in lower to middle Cretaceous sediment from selected North Atlantic DSDP sites and from Gubbio, Italy to illustrate general trends. A) Western central North Atlantic: data and ages from Hollister, Ewing et al., 1972 (Site 105); Tucholke, Vogt et al., in press, (Site 386); and Benson, Sheridan et al., in press, (Site 391). B) Eastern central North Atlantic: data and ages from Lancelot, Seibold et al., 1978. C) Gubbio, Italy: data from Arthur (unpublished). D) Site 398, northern North Atlantic: data and ages from Ryan, Sibuet et al., in press.

stratification, and local rates of organic carbon supply. Sedimentation rates in many of these sequences were relatively low (usually less than 15-20 m/m.y.) except in sites located near continental margins and active deltas or deep-sea fans (e.g., Site 398 in northern North Atlantic and Site 370 in the Moroccan Basin). The large amount of terrigenous organic matter in the sediment of Hauterivian through Albian age is most likely the result of input from deltas fringing both sides of the Atlantic during early Cretaceous time (e.g., Jansa and Wade, 1975; Einsele and von Rad, 1978; Wiedmann, et al., 1978; Ryan and Cita, 1977).

The preservation of this material under at least partly anoxic conditions is not unlike that of the Black Sea, where terrigenous lipids (Simoneit, 1977) comprise most of the organic matter in sediment deposited during a period of intense anoxia existing during the last 7000 years (Degens and Ross, 1974). The contribution of marine organic matter to black shales in any one site is a function of contemporaneous sea-surface productivity over the site and extent of anoxia in the water column.

## Lithology of Carbonaceous Sediment in the North Atlantic

The details of lithology, sedimentary structures, and variations in organic carbon content of carbonaceous mudstones will not be presented here; they can be found in the appropriate Initial Reports of the Deep Sea Drilling Project and in some of the other papers which have discussed the early to middle Cretaceous "black shale" phenomenon (Lancelot et al., 1972; Berger and von Rad, 1972; Schlanger and Jenkyns, 1976; Ryan and Cita, 1977; Fischer and Arthur, 1977; Dean et al., 1978; Gardner, et al., 1978; McCave, in press; Arthur, in press).

A conspicuous feature of nearly all carbonaceous mudstone sections in the North Atlantic (and in post-middle Albian sediments of the Angola Basin) is rhythmically interbedded light and dark colored sediment. This rhythmicity is generally expressed as an alternation of dark gray to black, homogeneous to laminated, organic-carbon rich clay or mudstone and light greenish gray to blue-gray, burrow-mottled mudstone, marlstone, or limestone (Fig. 5). The carbonate content depends on age and depth of deposition, and on amount of terrigenous dilution: Neocomian rhythms generally consist of marl-limestone couplets while Aptian-Albian rhythms are generally more carbonate depleted. This is inferred to reflect a relatively shallow CCD level (i.e., less than 3000 meters) in the North Atlantic during post-Barremian through much of Late Cretaceous time (e.g., Tucholke and Vogt, in press). These marl-shale couplets or similar rhythmically interbedded light and dark-colored clays seem to be present at nearly all paleodepths sampled in the North Atlantic (from shallower Sites 144 and 369 to deepest levels during Aptian-Albian time at Sites 105, 386, 387 and 391) and in Tethyan sections such as Vergons, France (de Boer et al., 1978; personal observation) and Gubbio, Italy (Arthur and Fischer, 1977). McCave (in press) and Dean et al. (1978) have discussed exemplary lower Cretaceous sediments of the western and eastern central North Atlantic basins respectively.

Estimates of the periodicity of these oxidation-reduction rhythms are subject to several assumptions, but suggested periods range from 20,000 to 100,000 yrs./rhythm with an average of about 50,000 yrs. being the best estimate (Arthur and Fischer, 1977; Dean, et al., 1978). The estimated 20,000 yrs./rhythm for similar middle and late Cretaceous sediments in the Angola Basin already discussed is comparable to the lowest estimates for the North Atlantic. This type of rhythmicity with approximately the same period is seen to some extent in the lower Cretaceous section at Site 398 in the northern North Atlantic (Arthur, in press), especially within sediment of Hauterivian and of Albian-Cenomanian age; it has also been reported from Sites 400 and 402 along the Bay of Biscay margin in both shallow and deep water carbonaceous mudstone settings (Montadert, Roberts, et al., 1976).

The lithic expression of the cycles varies somewhat as shown in Figure 5. In more pelagic sequences, the passage from the underlying light colored portion of the cycle to black clay or mudstone above may be transitional to sharp, while the contact between dark colored mudstone and overlying lighter colored marl is also sharp to transitional. The original nature of this contact can be blurred by bioturbation (as at Gubbio, Fig. 5) but McCave (in press) has shown it to be often very sharp. In contrast, the cycles in more rapidly deposited sediment with a pronounced high terrigenous input generally show sharp contacts between light colored, more calcareous layers and overlying dark colored, relatively organic-carbon rich layers (Dean, et al., 1978; Arthur, in press). The passage from dark to light layers is generally more transitional. In oxidation-reduction rhythms from all settings, bioturbation is usually confined to the light colored, sometimes relatively carbonate-rich and organic carbon depleted intervals; dark gray to black layers are often organic carbon rich, relatively carbonate-poor and are homogeneous to finely laminated.

Many Aptian-Albian carbonaceous mudstone sequences are typified by abundant diagenetic minerals such as pyrite, siderite, and zeolites (particularly clinoptilolite) which are intimately related to the chemical conditions of anoxia. The zeolitic minerals are often associated with intervals containing abundant siliceous microfossils. Radiolarite or radiolarian bearing sediment is interbedded with black and gray mudstone at some sites in Albian-Cenomanian time

(e.g., Sites 105, 138, 144, 386, 387, 398). Turbiditic muddy silts and sands are common in some sequences of Hauterivian-Albian age as well, especially in the northern North Atlantic (Site 398) and the Moroccan Basin (Site 370).

## Saline Spillover: Intermittent Anoxia and Other Indicators

The rhythm described above for the central North Atlantic may represent periodicity in renewal of oxygen to bottom water, possibly by climatically-induced sinking of saline surface waters from evaporative shelf settings such as in the Florida-Bahamas region and the Aaiun Basin (see Fig. 1) (Arthur, in press) or in Albian and later time from adjacent restricted basins such as the Angola-Brazil Basin discussed above. Depletion of oxygen by organic metabolism after such a pulse of bottom water renewal would occur gradually so that the transition from burrowed light colored portions of cycles to dark-colored, typically unburrowed and organic carbon-rich portions would be transitional; following this nearly total depletion of oxygen might ensue for several thousand years. The oxygenation pulse would be expected to be fairly rapid, hence a sharp upper contact to the black clay part of the cycle (Fig. 5). However, later bioturbation may alter these contact relationships. Alternations in carbonate preservation would be enhanced during the oxygenated pulse where saline waters of high carbonate alkalinity sink to the bottom. During progressive oxygen depletion, $CO_2$ would be produced and the pH would be expected to fall within the sediment, resulting in dissolution of carbonate until saturation was again reached. Spillover from the saline Angola-Brazil Basin in the South Atlantic (see discussion above; Ryan, Bolli, et al., 1978) might also enhance stable density stratification and induce periodic anoxia. This may be an explanation for the presence of sometimes abundant dolomite and siderite (Berger and von Rad, 1972) in parts of many cycles where the saline waters react with carbonate phases in the sediment to produce these diagenetic minerals. These pulses may have influenced especially the east central Atlantic where saline waters overflowing the Angola-Brazil Basin could have mixed with east central North Atlantic deep waters during Albian through perhaps Coniacian time. This is the same period during which periodic anoxia occurred in the Angola-Brazil Basin (Fig. 10). Cyclic anoxia or low oxygen conditions occurred prior to known connections between the North and South Atlantic, as well as after the end of known large-scale evaporite formation. Cyclic fluctuations in surface productivity (McCave, in press) and in input of terrigenous organic matter (Dean, et al., 1978) cannot be excluded as a cause of some of the rhythmicity.

## Evolution of Carbonaceous Sediment Deposition in the Northern North Atlantic

Carbonaceous mudstones were deposited in the northern North Atlantic (cored at Site 398 of Leg 47B and Sites 400 and 402 of Leg 48) at water depths ranging from less than 200 meters (Montadert, Roberts, et al., 1976) to over 4000 meters. Organic carbon contents in these sequences are generally low for carbonaceous mudstones (Fig. 4) and consist nearly entirely of land-derived higher plant debris (e.g., Deroo, et al., in press; Habib, in press; Montadert, Roberts, et al., 1976) except within late Albian and Cenomanian strata. High sedimentation rates of terrigenous detritus (25 to 100 m/m.y.) and reducing conditions within the sediment column prevailed during most of early Cretaceous time (Ryan, Sibuet, et al., in press); conditions were also periodically anoxic or very oxygen-depleted with deeper waters of the basin.

The following factors probably led to the development of a carbonaceous mudstone facies in the northern North Atlantic: tectonic restriction (bounded by continents and possibly partially restricted by a high sill at the southeast Newfoundland Ridge and J-anomaly ridge; Sibuet, et al., in press) and an uplifted hinterland (Wilson, 1975) with adjacent coastal vegetation belts resulting in outpourings of terrigenous clastics and land plat detritus. This is the waning stage of the large Wealden deltaic episode of Early Cretaceous time (Allen, 1959, 1975; Jansa and Wade, 1974). Not all occurrences of carbonaceous sediment can be explained by the terrigenous influx model (cf., Montadert, Roberts, et al., 1976; Habib, in press; Tissot, this volume).

## Evolution in the Central North Atlantic

In the eastern and western basins early to middle Cretaceous sedimentation developed in three stages:

1) intercalations of dark, laminated carbonaceous mudstone and occasional thin sands or silts within light-colored, typically bioturbated pelagic limestone of Valanginian-Hauterivian and Barremian age. Sedimentation of pelagic carbonate declined at most sites as they subsided below the CCD and as the CCD apparently abruptly rose in Barremian time (e.g., Tucholke and Vogt, in press);

2) development of typical carbonaceous mudstone facies in Barremian through middle Albian time with an obvious terrigenous imprint mainly the result of lack of dilution by pelagic carbonates, but also the outbuilding of submarine fans at some points along continental margins. Limestones are generally absent except at much shallower sites (e.g., 144 and 369, 390, 392). Variations in sedimentation rate, the amount of

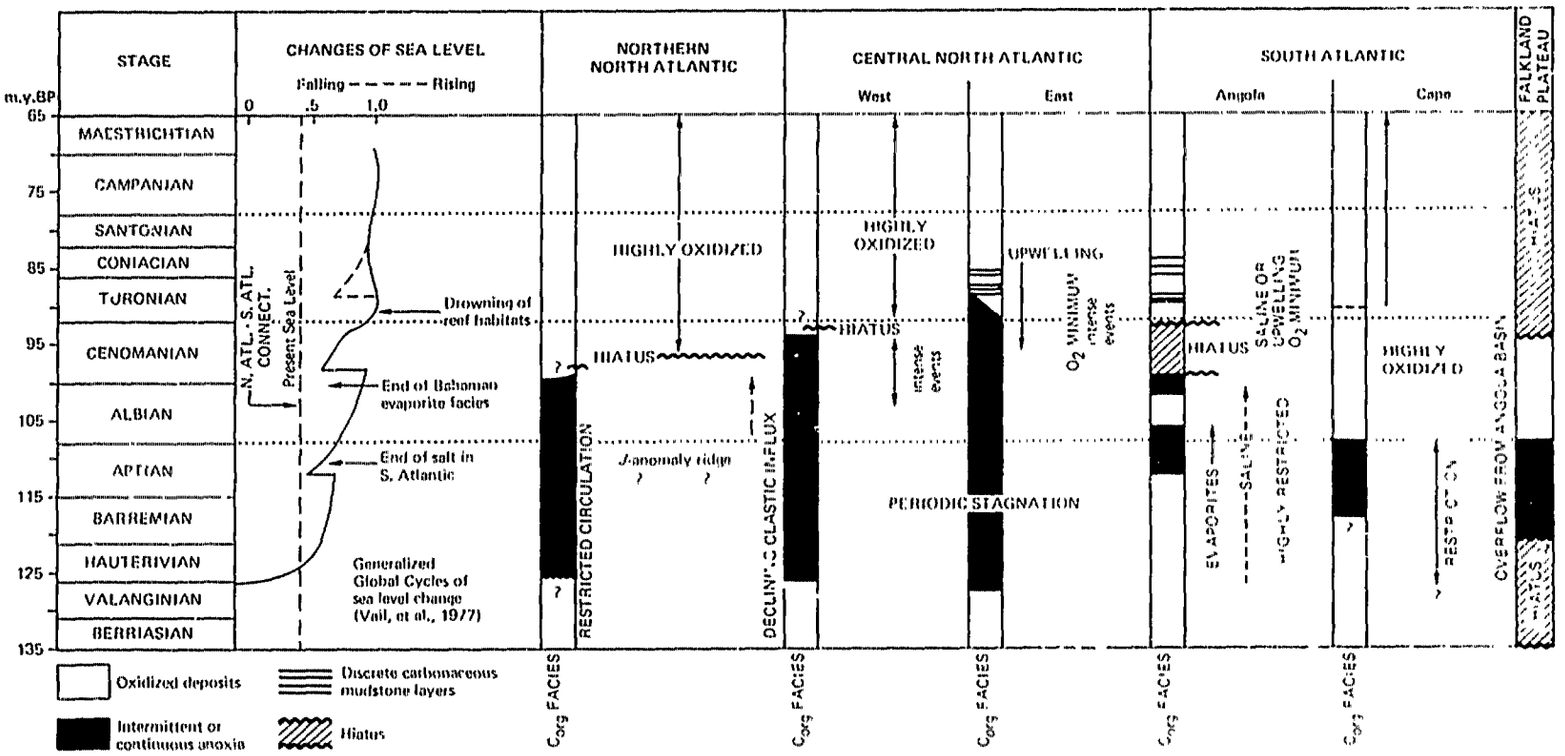


Fig. 10. Summary of timing of evaporite deposition, deposition of carbonaceous mudstone, and major circulation, sea level and tectonic events for Cretaceous time in the North and South Atlantic Oceans. Data from sources cited in text.

terrigenous detritus, and the ratio of terrigenous versus marine organic matter depended on paleodepth, proximity to deltaic influx, and local sea surface fertility. Anoxic or near anoxic conditions in the water column were periodic throughout most of the North Atlantic. Analogous Tethyan examples are common;

3) late Albian through Cenomanian carbonaceous mudstones or multicolored clays typified by primarily marine organic matter preserved in black mudstone layers and interbedded oxidized pelagic carbonates, mudstones, and radiolarian sands. This implies overturn of deep water masses, nutrients and increased sea surface productivity over much of the North Atlantic and a distinct waning of the terrigenous input. Periodic anoxia still occurred in deep water masses.

Hiatuses and/or condensed sedimentation of oxidized red or multicolored clays characterize post-Cenomanian upper Cretaceous sediments at most North Atlantic sites even those in central portions of the basin where slumping has not been significant (Figs. 7 and 10). Sea floor erosion or low rates of deposition and well-oxygenated conditions were probably related to the destruction of stable stratification and increased circulation, overturn, and oxygenation of deep waters. A Cenomanian sea level rise (Fig. 10) led to entrapment of terrigenous material in shallow shelf seas and possibly resulted in the destruction of sites of production of dense saline sea water by drowning of rudistid reef complexes and associated shallow water evaporite settings (e.g., Matthews, et al., 1974). The cessation of formation of saline water in the South Atlantic (Natland, 1978) in the late Cretaceous also probably led to more efficient mixing and oxygenation of deep waters. Upwelling of nutrient-rich waters and overflow of saline waters from the Angola-Brazil Basin probably continued along the coast of west Africa and northern South America and led to organic carbon-rich sediment of Turonian and possibly Coniacian age there (Berger and von Rad, 1972; Lancelot, Seibold, et al., 1978; Einsele and Wiedman, 1975).

## Conclusions

Stable water-mass stratification is necessary for establishment of deep water anoxia and for preservation of unusual amounts of organic matter in deep sea sediments; this is a function of salinity and temperature which may vary latitudinally and regionally. Salinity and temperature depend on such factors as average air temperature, the balance of evaporation versus precipitation over a sea and adjacent land areas, and the amount of restriction of an ocean basin (landlocked, silled or open to adjacent basins). The rate of input and burial of organic matter and sources of this material (terrigenous-derived versus marine) will influence organic matter preservation.

Restricted high latitude ocean basins having an excess of precipitation over evaporation can develop a stable salinity stratification with a low salinity surface water layer, especially if deep waters are derived from exchange with surface waters of adjacent more saline basins. A modern example of this is the Black Sea (e.g. see Ryan and Cita, 1977). Organic productivity in surface waters within such a restricted basin may be relatively low; anoxic or near anoxic conditions may develop in deep waters of the basin, but mainly terrigenous-derived organic matter will be preserved in sediments possibly because more easily degraded marine organic matter is rapidly utilized by micro-organisms and is primarily responsible for oxygen draw down in deeper water masses. Organic material is derived mostly through river deltas and low-lying coastal plains in this climatic regime (Habib, in press; Simoneit, 1977). This is probably an explanation for the origin of the carbonaceous mudstones in the northern North Atlantic (Fig. 1) and similar to the situation described by Kauffman (1975) and Scholle and Kauffman (1977) for the early Cretaceous western interior seaway of North America.

Another end-member of stably stratified basin types is a tectonically restricted low latitude basin where evaporation exceeds precipitation. In this type of basin, a stable salinity stratification develops by sinking of dense, saline surface or shelf waters. Again carbonaceous mudstones would result as anoxic conditions developed because of the low initial oxygen solubility in high salinity waters (Kinsman, et al., 1973) and long residence times of bottom water. These mudstones occur possibly in association with evaporites (Natland, 1978). Both terrigenous and marine organic matter could be preserved in such a basin. The early Cretaceous Angola-Brazil Basin of the South Atlantic is an example of this.

An intermediate situation can develop in sluggishly circulating but more open basins. Anoxic or low oxygen conditions may develop in deep waters due to a density stratification and low latitudinal thermal gradients. Such basins, in this case the early Cretaceous central North Atlantic and the Cape Basins (see Figs. 2 and 10) may be influenced by events in adjacent restricted basins. Dense, more saline sea water produced by evaporation in low latitude marginal coastal basins, on broad shoal water platforms, and in restricted low latitude oceanic basins such as the Angola-Brazil Basin may spill into adjacent, somewhat stably stratified basins causing even more stable stratification (in the absence of the great volume of cold dense deep water of today) thus enhancing anoxia. The high latitude restricted basin discussed above may have a similar effect in that less dense or brackish surface waters may periodically overflow into adjacent basins thus providing a "lid" for stable salinity stratification. These

spills, which may be climatically modulated, could be an explanation for the intermittent but apparently rhythmic anoxia in the larger ocean basins.

Variations on the oxygen minimum model (Schlanger and Jenkyns, 1976; Thiede and van Andel, 1977; Fischer and Arthur, 1977) can be applied to the vertical oxygen distribution in some open basins (e.g., early Cretaceous equatorial Pacific, Indian and middle Cretaceous North and South Atlantic Oceans). Enhanced overturn of deep waters, upwelling and high productivity may extend the record of carbonaceous sediment near and along continental margins after the major anoxic episodes have ceased due to the establishment of effective circulation (Fig. 10). This is suggested as one possible origin of Cenomanian-Turonian and Coniacian-Santonian organic-carbon rich sediment along northwest Africa (Einsele and Wiedmann, 1975; Wiedmann, et al., 1978) through the Caribbean region (see Edgar, Saunders, et al., 1973) and perhaps in parts of the South Atlantic (Thiede and van Andel, 1976; Supko, Perch-Nielson, et al., 1977).

Intensity, duration, and depth distribution of anoxia depends on the size of the basin, age and sources of bottom water, upwelling and fertility and therefore the amount of degradable organic matter entering the system. The early Cretaceous central North Atlantic Basin was probably intermittently anoxic or nearly so throughout its depth. These periodic oxygen-depleted intervals led to the preservation of both marine (phytoplanktic) and terrigenous (higher plant) organic matter in the carbonaceous mudstones. Deltaic systems added sediment and organic material to the northern and central North Atlantic (Jansa and Wade, 1975; Einsele and von Rad, 1978; Wiedmann, et al., 1978) during much of the early Cretaceous, and to the Aptian Cape Basin (Ryan, Bolli, et al., 1978). Marine organic matter in lower to middle Cretaceous carbonaceous mudstones resulted from enhanced preservation under areas of upwelling of nutrient-rich deep water such as around the continental margin of Africa and along oceanic divergences.

More detailed studies of carbonaceous mudstones are certainly necessary. Some promising areas of research seem to be: (1) continued characterization or organic matter with regard to its origin (terrigenous vs. marine) and degree of preservation, especially as an indication that anoxic conditions may have existed in the water column (see Didyk, et al., 1978). Care should be taken to note the lithology of samples taken for organic geochemical studies and examination of all lithologies should be made for comparison since the complexity of these sequences require study of more than the normal few samples; (2) geochemistry of certain mineral phases including carbonate (e.g., siderite, dolomite, ankerite), sulfide and zeolite minerals should be examined; the total sedimentary sulfide content and trace element associations may be a clue to the degree of establishment of anoxia in deep water above the sediment-water interface (e.g., Kendrick, in press), while the cation compositional variations in carbonate phases may indicate degree of salinity and alkalinity of deep waters in contact with sediment, hence possible sources of those water masses; (3) oxygen isotope studies of carbonate may give some information on paleosalinities, while carbon isotope analysis can possibly indicate trends in fractionation of carbon species with time, including the rate of preservation and burial of organic matter through time (e.g , Scholle and Arthur, 1976); (4) Finally, as has been attempted here, comparison of conditions of deposition, paleoenvironments and precise timing of events in adjacent basins should be made in order to establish possible links between anoxic stratified water masses in one basin, and evidence for currents or cyclic anoxic patterns in adjacent basins.

Acknowledgments. We would like to thank the convenors of the Second Maurice Ewing Symposium for inviting one of us (M.A.A.) to participate in the symposium and to contribute to this volume. We are indebted to many colleagues with whom we have had free exchange of data and ideas concerning the evolution of the Cretaceous North and South Atlantic Oceans, especially the shipboard parties of DSDP Legs 40 (J.H.N.) and 47 (M.A.A.) on which we participated and A.G. Fischer, Kerry Kelts, I.N. McCave, Greg Mountain, Peter Scholle, J.C. Sibuet, and Brian Tucholke. We are especially grateful to W.B.F. Ryan, Co-Chief Scientist on both Legs 40 and 47, for providing a stimulating intellectual environment and for his constant encouragement. The manuscript was greatly improved by thoughtful reviews of A.G. Fischer, Kerry Kelts, Floyd McCoy, and Brian Tucholke. Thanks are due the DSDP Production Department, particularly Kathleen Sanderson, for careful preparation of illustrations.

## References

Allen, P., the Wealden environment, Anglo Paris Basin, *Phil. Trans. Royal Soc. (London), Ser. B, 242,* 283-346, 1959.

Allen, P., Wealden of the Weald: a new model, *Proceed. Geologist's Assoc. London, 86 (4),* 389-437, 1975.

Arthur, M.A., North Atlantic Black Shales: the record at Site 398 and a brief comparison with other occurrences, *in* Ryan, W.B.F., Sibuet, J.C. et al., *Initial Reports of the Deep Sea Drilling Project, 47, (2),* Washington (U.S. Government Printing Office), in press.

Arthur, M.A. and Fischer, A.G., Upper Cretaceous-Paleocene magnetic stratigraphy at Gubbio, Italy: I. Lithostratigraphy and sedimentology, *Geol. Soc. Am. Bull., 88,* 367-389, 1977.

Asmus, H.E. and Ponte, F C., The Brazilian marginal basins, *in* Nairn, A.E.M. and Stehli,

F.G., (eds.), *The ocean basins and margins, Volume I: The South Atlantic*, New York (Plenum), 87-134, 1973.

Barker, P.F., Dalziel, I.W.D., et al., *Initial Reports of the Deep Sea Drilling Project, 36*, Washington (U.S. Government Printing Office), 1079, 1977.

Barnaby, A.M., *The structure of the eastern Walvis Ridge and the adjacent continental margin*, Unpublished M. Sc. thesis, University of Cape Town, Cape Town, South Africa, 1974.

Beckinsdale, R.D., Tarney, J., Darbyshire, D.P.F. and Humm, M.J., Rb-Sr and K-Ar age determinations on samples of the Falkland Plateau basement at Site 330, DSDP, *in* Barker, P.F., Dalziel, I.W.D. et al., *Initial Reports of the Deep Sea Drilling Project, 36*, Washington (U.S. Government Printing Office), 923-928, 1977.

Beckmann, J.P., Late Cretaceous smaller benthic foraminifers from Sites 363 and 364, DSDP Leg 40, Southeast Atlantic Ocean, *in* Bolli, H.M., Ryan, W.B.F. et al., *Initial Reports of the Deep Sea Drilling Project, 40*, Washington (U.S. Government Printing Office), 759-782, 1978.

Benson, W.E., Sheridan, R.E., et al., *Initial Reports of the Deep Sea Drilling Project, 44:* Washington (U.S. Government Printing Office), 1005 p., 1978.

Berger, W.H. and von Rad, U., Cretaceous and Cenozoic sediments from the Atlantic Ocean, *in* D.E. Hayes, A.C. Pimm and others, *Initial Reports of the Deep Sea Drilling Project, 14:* (U.S. Government Printing Office), Washington, D.C., 787-954, 1972.

Bernoulli, D., North Atlantic and Mediterranean Mesozoic facies: a comparison, *in* Hollister, C.D. and Ewing, J.I. et al., *Initial Reports of the Deep Sea Drilling Project, 11*: Washington (U.S. Government Printing Office), 801-871, 1972.

Bernoulli, D. and Jenkyns, H.C., Alpine, Mediterranean, and Central Atlantic Mesozoic facies in relation to the early evolution of the Tethys, *Soc. Econ. Paleont. and Mineral Spec. Publ. no. 19*, 129-160, 1974.

Bolli, H.M., Synthesis of the Leg 40 biostratigraphy and paleontology, *in* Bolli, H.M., Ryan, W.B.F. et al., *Initial Reports of the Deep Sea Drilling Project, 40*: Washington (U.S. Government Printing Office), 1063-1068, 1978.

Bolli, H.M., Ryan, W.B.F. et al., *Initial Reports of the Deep Sea Drilling Project, 40*: Washington (U.S. Government Printing Office), 1079 p., 1978.

Brink, A.H., Petroleum Geology of the Gabon Basin: *Am. Assoc. Petroleum Geol. Bull., 58*, 216-235, 1974.

Cameron, D., Grain-size and carbon-carbonate analyses, Leg 36, *in* Barker, P.F., Dalziel, I.W.D., et al., *Initial Reports of the Deep Sea Drilling Project, 36*: Washington (U.S. Government Printing Office), 1047-1050, 1977.

Cardoso, J.N., Wardroper, A.M.K., Watts, C.D., Barnes, P.J., Maxwell, J.R., Eglinton, G., Mound, D.G. and Speers, G.C., Preliminary organic geochemical analyses, Site 391, Leg 44 of the Deep Sea Drilling Project, *in* Benson, W.E., Sheridan, R.E., et al., *Initial Reports of the Deep Sea Drilling Project, 44:* Washington (U.S. Government Printing Office), 617-625, 1978.

Caron, M., Cretaceous planktonic foraminifers from DSDP Leg 40, southeastern Atlantic Ocean, *in* Bolli, H.M., Ryan, W.B.F. et al., *Initial Reports of the Deep Sea Drilling Project, 40*: Washington (U.S. Government Printing Office), 651-678, 1978.

Comer, J.B. and Littlejohn, R., Content, composition, and thermal history of organic matter in Mesozoic sediments, Falkland Plateau, *in* Barker, P.F., Dalziel, I.W.D. et al., *Initial Reports of the Deep Sea Drilling Project, 36*: Washington (U.S. Government Printing Office), 941-944, 1977.

Dean, W.E., Gardner, J.V., Jansa, L.F., Cepek, P., and Seibold, E., Cyclic sedimentation along the continental margin of northwest Africa, *in* Lancelot, Y., Seibold, E., et al., *Initial Reports of the Deep Sea Drilling Project, 41:* Washington (U.S. Government Printing Office), 965-989, 1978.

de Boer, P., de Leeuw, J., and Schlanger, S.O., Sedimentology and organic geochemistry of Aptian-Albian "Marnes Noires", Vergons, Alpes Maritimes, France, Abstract, *Xth Congress of International Association of Sedimentologists, Israel*, 1978.

Degens, E.T., Biogeochemistry of stable carbon isotopes, *in Handbook of Geochemistry*, Eglinton, G. and Murphy, M.T.J., (eds.) New York (Springer-Verlag), 304-329, 1969.

Degens, E.T. and Ross, D.A. (eds.), The Black Sea - geology, chemistry and biology, *Am. Assoc. Petroleum Geol., 20*, 633, 1974.

Deroo, G., Herbin, J.P., Roucache, J., Tissot, B., Albrecht, P., and Schaeffle, J., Organic geochemistry of some Cretaceous black shales from Sites 367 and 368; Leg 41, Eastern North Atlantic, *in* Lancelot, Y., Seibold, E. et al., *Initial Reports of the Deep Sea Drilling Project, 41*: Washington (U.S. Government Printing Office), 865-871, 1978.

Deroo, G., Herbin, J.P., Roucache, J. and Tissot, B., Organic geochemistry of some Cretaceous black shales from Sites 386 and 387, Leg 43, *in* Tucholke, B., Vogt, P., et al., *Initial Reports of the Deep Sea Drilling Project, 43*: Washington (U.S. Government Printing Office), in press.

Deroo, G., Herbin, J.P., Roucache, J., Tissot, B., Albrecht, P., and Schaeffle, J., Organic geochemistry of some Cretaceous black shales from Site 398, Leg 47B, *in* Ryan, W.B.F., Sibuet, J.C. et al., *Initial Reports of the Deep Sea Drilling Project, 47, II:* Washington (U.S. Government Printing Office), in press.

Detrick, R.S., Sclater, J.G., and Thiede, J., The subsidence of aseismic ridges, *Earth Planet. Sci. Lett., 34,* 185-196, 1977.

Didyk, B.M., Simoneit, B.R.T., Brassell, S.C. and Eglinton, G., Geochemical indicators of paleoenvironmental conditions of sedimentation, *Nature, 272,* 216-222, 1978.

Dingle, R.V. and Scrutton, R.A., Continental breakup and the development of post-Paleozoic sedimentary basins around southern Africa, *Geol. Soc. Am. Bull., 85,* 1467-1474, 1974.

Dow, W.G., Contact metamorphism of kerogen in sediments from Leg 41: Cape Verde Rise and Basin, *in* Lancelot, Y., Seibold, E., et al., *Initial Reports of the Deep Sea Drilling Project, 41:* Washington (U.S. Government Printing Office), 821-824, 1978.

Edgar, N.T., Saunders, J.B., et al., *Initial Reports of the Deep Sea Drilling Project, 15:* Washington (U.S. Government Printing Office), 1137 p., 1973.

Einsele, G. and von Rad, U., Facies and paleoenvironment of Early Cretaceous (Late Hauterivian) sediments in DSDP Site 397 and in the Aaiun Basin, *in* Ryan, W.B.F., von Rad, U. et al., *Initial Reports of the Deep Sea Drilling Project, 47, I:* Washington (U.S. Government Printing Office), in press.

Einsele, G. and Wiedmann, J., Faunal and sedimentological evidence for upwelling in the upper Cretaceous coastal basin of Tarfaya, Morocco, *Publ. IXth Intern. Cong. on Sedimentology, Nice, 1975, Theme 1,* 67-72, 1975.

Emery, K.O., Uchupi, E., Philips, J., Bowin, C.O., and Mascle, J., Continental margin off western Africa: Angola to Sierra Leone, *Am. Assoc. Petroleum Geol. Bull., 59,* p. 2209, 1975.

Erdman, J.G. and Schorno, K.S., Geochemistry of carbon: Deep Sea Drilling Project, Leg 43, *in* Tucholke, B. and Vogt, P., et al., *Initial Reports of the Deep Sea Drilling Project, 43:* Washington (U.S. Government Printing Office), in press.

Evans, R.E., Origin and significance of evaporites in basins around Atlantic margin, *Am. Assoc. Petroleum Geol. Bull., 62 (2),* 223-234, 1978.

Fischer, A.G. and Arthur, M.A., Secular variations in the pelagic realm, *in* Cook, H.E. and Enos, P. (eds.), *Deep water carbonate environments, SEPM Spec. Publ. 25,* 19-50, 1977.

Foresman, J.B., Organic geochemistry DSDP Leg 40, continental rise of southwest Africa, *in* Bolli, H.M., Ryan, W.B.F. et al., *Initial Reports of the Deep Sea Drilling Project, 40:* Washington (U.S. Government Printing Office), 557-558, 1978.

Forster, R., Evidence for an open seaway between northern and southern proto-Atlantic in Albian times, *Nature, 272,* 158-159, 1978.

Francheteau, J., and LePichon, X., Marginal fracture zones as structural framework of continental margins in the South Atlantic Ocean, *Am. Assoc. Petroleum Geol. Bull., 56,* 991-1007, 1972.

Friedman, G.M., Significance of the Red Sea in the problem of evaporites and basinal limestones, *Am. Assoc. Petroleum Geol. Bull., 56,* 1072-1086, 1972.

Gamboa, L.A.P. and Kumar, N., Synthesis of geological and geophysical data in a 1° square area around Site 356, Leg 39, DSDP, *in* Supko, P., Perch-Nielsen, K., et al., *Initial Reports of the Deep Sea Drilling Project, 39:* Washington (U.S. Government Printing Office), 947-954, 1977.

Gardner, J.V., Dean, W.E. and Jansa, L., Sediments recovered from the northwest African continental margin, Leg 41, DSDP, *in* Lancelot, Y., Seibold, E. et al., *Initial Reports of the Deep Sea Drilling Project, 41:* Washington (U.S. Government Printing Office), 1121-1134, 1978.

Habib, D., Palynology of lower Cretaceous sediments of Site 398, *in* Ryan, W.B.F., Sibuet, J.C. et al., *Initial Reports of the Deep Sea Drilling Project, 47, (2):* Washington (U.S. Government Printing Office), in press.

Hay, R.L., Zeolites and zeolitic reactions in sedimentary rocks, *Geol. Soc. Am. Spec. Paper 85,* 1-129, 1966.

Hess, P.C., Phase equilibrium of some minerals in the $K_2O$-$Na_2O$-$Al_2O_3$-$SiO_2$-$H_2O$ system at 25°C and 1 atm., *Am. J. Sci., 264,* 289-309, 1966.

Hunt, J.M., Light hydrocarbons in Holes 361 and 364, Leg 40, *in* Bolli, H.M., Ryan, W.B.F., et al., *Initial Reports of the Deep Sea Drilling Project, Vol. 40 Supplement:* Washington (U.S. Government Printing Office), 649-650, 1978.

Jansa, L.F. and Wade, J.A., Geology of the continental margin off Nova Scotia and Newfoundland, *in Offshore Geology of Eastern Canada, Geol. Surv. Can. Pap. 74-30, 2,* 51-105, 1975.

Kagami, H., Sedimentary features of Cape Basin and Angola Basin sediments, DSDP Leg 40, *in* Bolli, H.M., Ryan, W.B.F., et al., *Initial Reports of the Deep Sea Drilling Project, 40:* Washington (U.S. Government Printing Office), 525-540, 1978.

Kauffman, E., Dispersal and biostratigraphic potential of Cretaceous benthonic bivalvia in the western interior, *Geol. Assoc. Canada Spec. Pap. 13,* 163-194, 1975.

Kendrick, J.W., Geochemical studies of black claystones from Leg 43, Deep Sea Drilling Project, *in* Tucholke, B., Vogt, P., et al., *Initial Reports of the Deep Sea Drilling Project, 43:* Washington (U.S. Government Printing Office), in press.

Kendrick, J.W., Hood, A., and Castano, J.R., Petroleum-generating potential of sediments from Leg 40, Deep Sea Drilling Project, *in* Bolli, H.M., Ryan, W.B.F., et al., *Initial Reports of the Deep Sea Drilling Project, Vol. 40 Supplement:* Washington (U.S. Government Printing Office), 671-676, 1978a.

Kendrick, J.W., Hood, A., and Castano, J.R., Petroleum-generating potential of sediments from Leg 44, Deep Sea Drilling Project, *in* Benson, W.E., Sheridan, R.E., et al., *Initial Reports of the Deep Sea Drilling Project, 44:* Washington (U S. Government Printing Office), 599-603, 1978b.

Kendrick, J.W., Hood, A., and Castano, J.R., Petroleum-generating potential of sediments from Leg 41, Deep Sea Drilling Project, *in* Lancelot, Y., Seibold, E., et al., *Initial Reports of the Deep Sea Drilling Project, 43:* Washington (U.S. Government Printing Office), 817-819, 1978c.

Kennedy, W.J. and Cooper, M., Cretaceous ammonite distribution and the opening of the South Atlantic, *Jour. Geol. Soc. London, 131,* 283-288, 1975.

Kennett, J.P., Burns, R.E., Andrews, J.E., Churkin, M., Davies, T.A., Dumitrica, P., Edwards, A.R., Galehouse, J.S., Packham, G.H. and van der Lingen, G.J., Australian-Antarctic continental drift, paleocirculation changes and Oligocene deep-sea erosion, *Nature Phys. Sci., 239,* 51-53, 1972.

Kinsman, D.J.J., Salt floors to geosynclines, *Nature, 255,* 375-378, 1975.

Kinsman, D.J.J., Boardman, M., and Borcsik, M., An experimental determination of the solubility of oxygen in marine brines, *in* Coogan, A.H. (ed.), *Fourth Symposium on Salt, 1,* The Northern Ohio Geol. Soc., Inc., Cleveland, 325-328, 1973.

Lancelot, Y., Hathaway, J.C. and Hollister, C.D., Lithology of sediments from the western North Atlantic, Leg 11, DSDP, *in* Hollister, C.D., Ewing, J.I. et al., *Initial Reports of the Deep Sea Drilling Project, 11:* Washington (U.S. Government Printing Office), 901-949, 1972.

Lancelot, Y. and Seibold, E., The evolution of the central northeastern Atlantic: summary of results, *in* Lancelot, Y., Seibold, E., et al., *Initial Reports of the Deep Sea Drilling Project, 41:* Washington (U.S. Government Printing Office), 1215-1245, 1978.

Larson, R.L., and Ladd, J.W., Evidence for the opening of the South Atlantic in the Early Cretaceous, *Nature, 246,* 209-212, 1973.

Leyden, R., Asmus, H., Zembruscki, S., and Bryan, G., South Atlantic diapiric structures, *Am. Assoc. Petroleum Geol. Bull., 60,* 196-212, 1976.

Matsumoto, R., Utada, M., and Kagami, H., Sedimentary petrology of DSDP cores from Sites 362 and 363, the Walvis Ridge, and Site 364, the Angola Basin, drilled on Leg 40, *in* Bolli, H.M., Ryan, W.B.F., et al., *Initial Reports of the Deep Sea Drilling Project, 40:* Washington (U.S. Government Printing Office), 469-486, 1978.

Matthews, J.L., Heezen, B.C., Catalano, R., Coogan, A., Tharp, M., Natland, J., and Rawson, M., Cretaceous drowning of reefs on Mid-Pacific and Japanese guyots, *Science, 184,* 462-464, 1974.

McCave, I.N., Depositional features of organic-rich black and green mudstones at DSDP Sites 386 and 387, western North Atlantic, *in* Tucholke, B., Vogt, P., et al., *Initial Reports of the Deep Sea Drilling Project, 43:* Washington (U.S. Government Printing Office), in press.

McCoy, F.W., and Zimmerman, H.B., A history of sediment lithofacies in the South Atlantic Ocean, *in* Perch-Nielsen, K. and Supko, P., et al., *Initial Reports of the Deep Sea Drilling Project, 39:* Washington (U.S. Government Printing Office), 1047-1079, 1977.

McIver, R.D., Hydrocarbon occurrences from JOIDES Deep Sea Drilling Project, *Ninth World Pet. Cong. Proceedings, 12,* 269-280, 1975.

Melguen, M., Facies evolution, carbonate dissolution cycles in sediments from the eastern South Atlantic (DSDP Leg 40) since the early Cretaceous, *in* Bolli, H.M., Ryan, W.B.F., et al., *Initial Reports of the Deep Sea Drilling Project, 40:* Washington (U.S. Government Printing Office), 981-1024, 1978.

Montadert, L., Roberts, D., et al., *Glomar Challenger* sails on Leg 48, *Geotimes, 21,* 19-22, 1976.

Morgan, R., Albian to Senonian palynology of Site 364, Angola Basin, *in* Bolli, H.M., Ryan, W.B.F., et al., *Initial Reports of the Deep Sea Drilling Project, 40:* Washington (U.S. Government Printing Office), 915-952, 1978.

Natland, J.H., Composition, provenance, and diagenesis of Cretaceous clastic sediments drilled on the Atlantic continental rise off Southern Africa, DSDP Site 361 - implications for the early circulation of the South Atlantic, *in* Bolli, H.M., Ryan, W.B.F., et al., *Initial Reports of the Deep Sea Drilling Project, 40:* Washington (U.S. Government Printing Office), 1025-1062, 1978.

Noël, D., and Melguen, M., Nannofacies of Cape Basin and Walvis Ridge sediments, Lower Cretaceous to Pliocene, *in* Bolli, H.M., Ryan, W.B.F., et al., *Initial Reports of the Deep Sea Drilling Project, 40:* Washington (U.S. Government Printing Office), 487-524, 1978.

Petters, S.W., Stratigraphic evolution of the Benue Trough and its implications for the upper Cretaceous paleogeography of West Africa, *Jour. Geol., 86,* 311-322, 1978.

Pittman, W.C., III, and Talwani, M., Sea-floor spreading in the North Atlantic, *Geol. Soc. Amer. Bull., 83,* 619-646, 1972.

Premoli-Silva, I., and Boersma, A., Cretaceous planktonic foraminifers - DSDP Leg 39 (South Atlantic), *in* Supko, P., Perch-Nielsen, K., et al., *Initial Reports of the Deep Sea Drilling Project, 39:* Washington (U.S. Government Printing Office), 615-642, 1977.

Proto-Decima, F., Medizza, F., and Todesco, L., Southeastern Atlantic Leg 40 calcareous nannofossils, *in* Bolli, H.M., Ryan, W.B.F., et al., *Initial Reports of the Deep Sea Drilling Pro-*

*ject, 40:* Washington (U.S. Government Printing Office), 571-634, 1978.
Ryan, W.B.F. and Cita, M.B., Ignorance concerning episodes of ocean-wide stagnation, *Mar. Geol., 23,* 197-215, 1977.
Ryan, W.B.F., Sibuet, J.C. et al., *Initial Reports of the Deep Sea Drilling Project, 47, (2):* Washington (U.S. Government Printing Office), in press.
Saunders, J.B., Edgar, N.T., Donnelly, T.W., and Hay, W.W., Cruise synthesis, *in* Edgar, N.T., Saunders, J.B. et al., *Initial Reports of the Deep Sea Drilling Project, 15:* Washington (U.S. Government Printing Office), 1077-1111, 1973.
Scheibnerova, V., Aptian and Albian foraminifers of Leg 40, Sites 363 and 364, Southern Atlantic, *in* Bolli, H.M., Ryan, W.B.F., et al., *Initial Reports of the Deep Sea Drilling Project, 40:* Washington (U.S. Government Printing Office), 741-758, 1978.
Schlanger, S.O. and Jenkyns, H.C., Cretaceous oceanic anoxic events: causes and consequences, *Geologie en Mijnbouw, 55,* 179-184, 1976.
Scholle, P.A. and Arthur, M.A., Carbon-isotopic fluctuations in upper Cretaceous sediments: an indication of paleo-oceanic circulation, *Geol. Soc. Amer. Abstr. with Prog., 8, (6),* 1089, 1976.
Scholle, P.A. and Kauffman, E.G., Paleoecological implications of stable isotope data from Upper Cretaceous limestones and fossils from the U.S. western interior, *Abstr. North Amer. Paletontol. Conv. II, Jour. of Paleont., 51, supplement (2),* 24, 1977
Sclater, J.G., Hellinger, S., and Tapscott, C., The paleobathymetry of the Atlantic Ocean from the Jurassic to the present, *Jour. Geol., 85,* 509-552, 1977.
Scott, E., Grain-size and carbon-carbonate analyses, Leg 39, *in* Supko, P., Perch-Nielsen, K. et al., *Initial Reports of the Deep Sea Drilling Project, 39:* Washington (U.S. Government Printing Office), 501-504, 1977.
Sibuet, J.C., et al., Deep sea drilling results of Leg 47B (Galicia Bank area) in the framework of the early evolution of the North Atlantic Ocean, *Phil. Trans. Roy. Soc., London,* in press.
Siesser, W.G., Leg 40 results in relation to continental shelf and onshore geology, *in* Bolli, H.M., Ryan, W.B.F., et al., *Initial Reports of the Deep Sea Drilling Project, 40:* Washington (U.S. Government Printing Office), 965-980, 1978.
Siesser, W.G., and Bremner, X-ray mineralogy of cores from Leg 40, Deep Sea Drilling Project, *in* Bolli, H.M., Ryan, W.B.F., et al., *Initial Reports of the Deep Sea Drilling Project, 40:* Washington (U.S. Government Printing Office), 541-548, 1978.
Simoneit, B.R.T., The Black Sea, a sink for terrigenous lipids, *Deep-Sea Res., 24,* 813-830, 1977.
Simoneit, B.R.T., Lipid analyses of sediments from Site 364 in the Angola Basin, DSDP Leg 40, *in* Bolli, H.M., Ryan, W.B.F., et al., *Initial Reports of the Deep Sea Drilling Project, Vol. 40 Supplement:* Washington (U.S. Government Printing Office), 659-662, 1978.
Simoneit, B.R., Scott, E.S., and Burlingame, A.L., Preliminary organic analyses of DSDP cores, Leg 16, Atlantic Ocean, *in* van Andel, T.H., Heath, G.R., et al., *Initial Reports of the Deep Sea Drilling Project, 16:* Washington (U.S. Government Printing Office), 575-600, 1973.
Simoneit, B.R., Scott, E.S., Howells, W.G. and Burlingame, A.L., Preliminary organic analyses of the Deep Sea Drilling Project cores from Leg 11, *in* Hollister, C.D., Ewing, J.I., et al., *Initial Reports of the Deep Sea Drilling Project, 11:* Washington (U.S. Government Printing Office), 1013-1035, 1973.
Sotelo, V., and Gieskes, J.M., Interstitial water studies, Leg 40: shipboard studies, *in* Bolli, H.M., Ryan, W.B.F., et al., *Initial Reports of the Deep Sea Drilling Project, 40:* Washington (U.S. Government Printint Office), 549-554, 1978.
Stonecipher, S.A., Origin, distribution and diagenesis of phillipsite and clinoptilolite in deep-sea sediments, *Chem. Geol., 17,* 307-318, 1976.
Stuermer, D.H. and Simoneit, B.R.T., Varying sources for the lipids and humic substances in Site 44-391, Blake-Bahama Basin, *in* Benson, W.E., Sheridan, R.E., et al., *Initial Reports of the Deep Sea Drilling Project, 44:* Washington (U.S. Government Printing Office), 587-592, 1978.
Supko, P.R. and Perch-Nielsen, K., General synthesis of Central and South Atlantic drilling results, Leg 39, Deep Sea Drilling Project, *in* Supko, P.R., Perch-Nielsen, K., et al., *Initial Reports of the Deep Sea Drilling Project, 39:* Washington (U.S. Government Printing Office), 1099-1132, 1977.
Supko, P., Perch-Nielsen, K., et al., *Initial Reports of the Deep Sea Drilling Project, 39:* Washington (U.S. Government Printing Office), 1139 p., 1977.
Tarney, J., Petrology, mineralogy, and geochemistry of the Falkland Plateau basement rocks, Site 330, Deep Sea Drilling Project, *in* Barker, P.F., Dalziel, I.W.D., et al., *Initial Reports of the Deep Sea Drilling Project, 36:* Washington (U.S. Government Printing Office), 893-922, 1977.
Thiede, J., and van Andel, Tj. H., The paleoenvironment of anaerobic sediments in the Late Mesozoic South Atlantic Ocean, *Earth Planet. Sci. Lett., 33,* 301-309, 1977.
Tucholke, B. and Vogt, P., Synthesis of Leg 43 and evolution of the western North Atlantic: *in* Tucholke, B., Vogt, P., et al., *Initial Reports of the Deep Sea Drilling Project, 43:* Washington (U.S. Government Printing Office),

in press.
Vail, P.R., Mitchum, R.M., Jr., and Thompson, S., Seismic stratigraphy and global changes of sea-level, Part 3: Relative changes of sea level from coastal onlap, *Am. Assoc. Petroleum Geol.*, *26*, 63-98, 1977.
van Andel, Tj. H., Thiede, J., Sclater, J.G., and Hay, W.W., Depositional history and paleo-oceanography of the South Atlantic during the last 125 million years, *Jour. Geol.*, *85*, 651-698, 1977.
van Hinte, J.E., A Cretaceous time scale, *Amer. Assoc. Petroleum Geol. Bull.*, *60*, 498-516, 1976.
van Houten, F.B., Triassic-Liassic deposits of Morocco and eastern North America: comparison, *Am. Assoc. Petroleum Geol. Bull.*, *61*, *(1)*, 79-99, 1977.
Watts, A.B., and Ryan, W.B.F., Flexure of the lithosphere and continental margin basins, *Tectonophysics*, *36*, 25-44, 1976.
Wiedmann, J., Butt, A., and . G., Vergleich von morokkanischen Fr stanaufschliissen und Tiefsee bohrunge DP Stratigraphie, Paleoenvironment und Subsidenz einem passiven Kontinentalrand), *Geologische Rundschau*, *67*, (2), 454-508, 1978.
Wiedmann, J. and Neugebauer, J., Low Cretaceous ammonites from the South Atlantic, Leg 40 (DSDP), their stratigraphic value and sedimentological properties, *in*: Bolli, H.M., Ryan, W.B.F., et al., *Initial Reports of the Deep Sea Drilling Project, Vol. 40 supplement*: Washington (U.S. Government Printing Office), 709-734, 1978.

# LACUSTRINE AND HYPERSALINE DEPOSITS IN THE DESICCATED MEDITERRANEAN AND THEIR BEARING ON PALEOENVIRONMENT AND PALEO-ECOLOGY

Marie Bianca Cita

Department of Geology and Paleontology, University of Milano, Italy

Abstract. The isolation of the Mediterranean from the world oceans brought about by plate motions by the end of the Miocene resulted in evaporitic draw-down and eventual desiccation which had catastrophic effects on the marine faunas and floras which populated the Mediterranean waters before the salinity crisis. The evaporites represent an essentially abiotic environment and are usually barren; being basin-wide in extent, they document a kind of sterilization underzone by the Mediterranean. Exceptions are represented by algal stromatolites, which are common in the Mediterranean record, as related to the extraordinary development of unusual "intertidal" conditions.

Sediments associated with the evaporites are occasionally fossiliferous. When it can be proved that fossils are in situ (reworking is common) they generally indicate salinities different from normal marine. Of special interest in the eastern Mediterranean record is the late Messinian "lagomare" faunal assemblage of caspi-brackish affinity. Capture of the high standing lakes of the Paratethys is postulated, possibly through subterraneous aquifers. This kind of fauna was not recorded in the deep western Mediterranean basins, whereas it is present in peripheral or satellite basins of the Mediterranean. Sills had to play a major role in the distribution of this fauna, but dissemination through land is not impossible.

The repopulation of the Mediterranean resulting from the early Pliocene flooding was almost instantaneous, and essentially from the west (from the Atlantic). Shallow sills separating the western from the eastern Mediterranean resulted in (a) marked difference in bottom current activity, the eastern basins being less well ventilated than the western basins, and (b) slower repopulation of the former by bottom living animals, with species having a shallow upper bathymetric limit coming first.

The response of the world ocean to the Mediterranean salinity crisis is seen as a disturbance in the pelagic realm, detectable in the carbonate content of deep-sea sediments, and also recorded by the isotopic signal. The subtraction of over $1 \times 10^6$ km$^3$ of salts in a time span of less than $1 \times 10^6$ y indeed lowered the salinity of the world ocean by 6%.

This disturbance could be studied carefully in the eastern North Atlantic (DSDP Site 397) where a continuously cored succession of hemipelagic sediments deposited at an unusually high sedimentation rate offered the opportunity to calibrate with accuracy by means of micropaleontology and of paleomagnetic stratigraphy the Messinian event, and to clarify its climatic implications.

## Mediterranean Salinity Crisis

Two legs of the GLOMAR CHALLENGER in the Mediterranean (Ryan, Hsü et al, 1973; Hsü, Montadert et al, 1978) demonstrated beyond any doubt that Messinian age evaporites are basin-wide in extent. Indeed, of the twenty-two Mediterranean drillsites, the only ones which did not recover evaporites and/or associated clastic sediments are those indicated by an arrow in Figure 1, located on submarine volcanoes (DSDP Site 123) or seamounts (DSDP Site 373); those which did not penetrate beyond the Quaternary in the Nile Cone area (DSDP Sites 130 and 131), and those from the Hellenic Trench (DSDP Sites 127 and 128) which reached melange in a subduction zone.

Evaporites are the sedimentary expression of an essentially abiotic environment.

Evaporitic facies recorded from various Mediterranean basins (Alboran, Balearic, Tyrrhenian, Ionian, Levantine, Aegean) include dolomitic marls, selenitic gypsum, nodular or "chicken-wire" anhydrite, finely laminated ("balatino" facies) gypsum and/or anhydrite, and halite. Some of these facies are illustrated in Figures 2 and 3. Detailed investigations on their structural features, diagenetic characteristics, and environmental significance have been carried out since Leg 13 (Hsü et al, 1973; Schreiber, 1973; Friedman, 1973) and again after Leg 42A which provided a variety of evaporitic facies from the Ionian, Levantine and Aegean basins of the Eastern Mediterranean (Garrison et al, 1978).

In most cases evaporites are sterile. This basin-wide sterilization resulted in the anni-

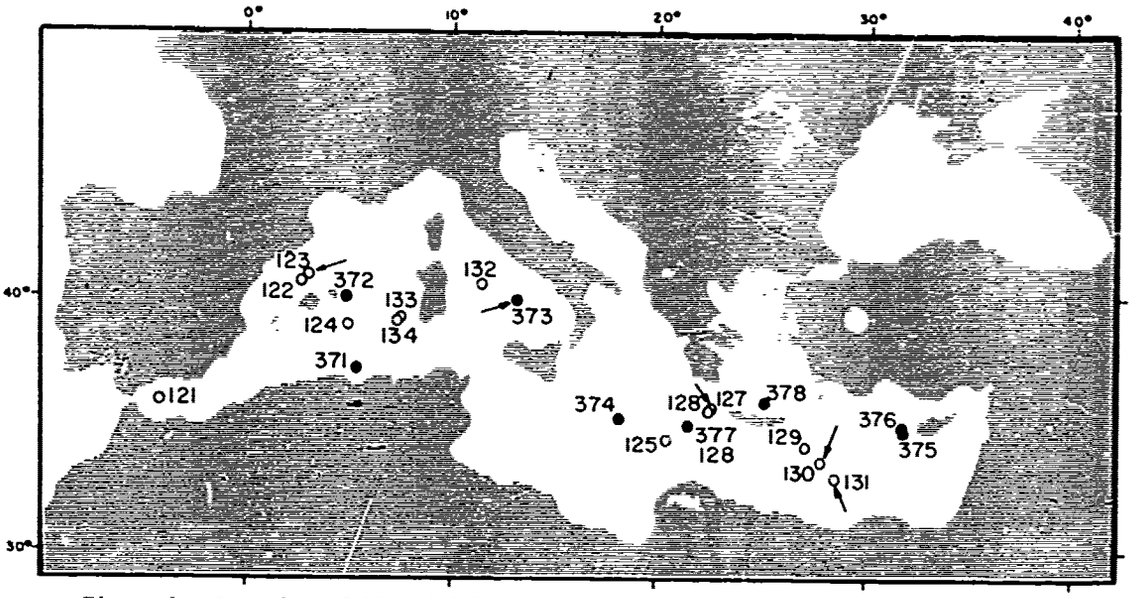


Figure 1 - Location of DSDP drillsites drilled in 1970 (open circles) and in 1975 (solid circles) during Leg 13 and 42A respectively. Arrows point to the locations where Messinian age evaporites have not been recovered.

hilation of the entire marine fauna which populated the Mediterranean waters prior to the salinity crisis (Cita, 1976).

Associated with the evaporites, algal stromatolites (see Figure 3C) are common in the record of both the Western and Eastern Mediterranean. They document a peculiar inter-tidal environment developed in a tideless sea, where water-level fluctuations were dynamically controlled by the evaporative power of the sun instead of the gravitational attraction of the moon, which resulted in extensive wandering of the paleo-strandlines (Ryan, Hsü et al, 1973, p. 161).

Non-evaporitic sediments associated with the evaporites include diatomites whose diatoms indicate salinities ranging from 0 to 10°/oo in the Eastern Mediterranean (Schrader and Gersonde, 1978) and from 15 to 20°/oo in the Western Mediterranean (Hajos, 1973; Schrader and Gersonde, 1978). They also include silts yielding rich palynological assemblages (Bertolani Marchetti and Cita, 1975) and laminites like those recovered at DSDP Site 372 in the Western Balearic Basin, where monospecific populations of Ammonia beccarii are suggestive of hypersaline waters, a few tens of meters deep, and where monospecific coccolith blooms and strange nannofossils interpreted as fungi have been discovered in the white laminae (Figure 4; see also cita et al, 1978).

Some pyritic marls yield dwarfed foraminiferal faunas whose paleoenvironmental significance is still poorly understood. They could be autochthonous faunas, dwarfed in response to stress conditions, or reworked and selected by size. A discrimination is neither easy, nor sure and convincing (Cita et al, 1978).

## Invasion of Paratethyan Immigrants

Of special interest in the deep-sea record from the Eastern Mediterranean is the Messinian "lago-mare" faunal assemblage dominated by the ostracod genus Cyprideis (Ruggieri, 1967). This genus is euryhaline, and may constitute a significant part of the benthic biomass of brackish water, or hypersaline or alkaline, calcium-rich lagoons and inland seas or lakes (Benson, 1973). The importance of Cyprideis as contributor of the fossil record of the Paratethys during the Pannonian is well known (Benson, 1972). Biometrical analysis by Wright (in Cita et al, 1978) could demonstrate that the rich populations are in place, since different instars have been found to co-occur (Figure 5).

A capture of the high standing lakes of the Paratethys was postulated by Cita and Ryan (1973) on the basis of Leg 13 results (Figure 6) and strongly supported by the new findings of Leg 42 A.

Figure 7 shows the distribution in Mediterranean peripheral basins and in DSDP drillsites of ostracods of Paratethyan affinity, with special reference to the genus Cyprideis, and depicts the probable immigration routes according to Sissingh (1976). It also shows the distribution of the mollusc Congeria, another immigrant from the Paratethys.

The "lago-mare" biofacies is typical of the latest Messinian and is limited to it. I insist on this point, which is important in order to understand the response of the open ocean to the Mediterranean salinity crisis. In the central Sicilian basin the "lago-mare" is recorded in

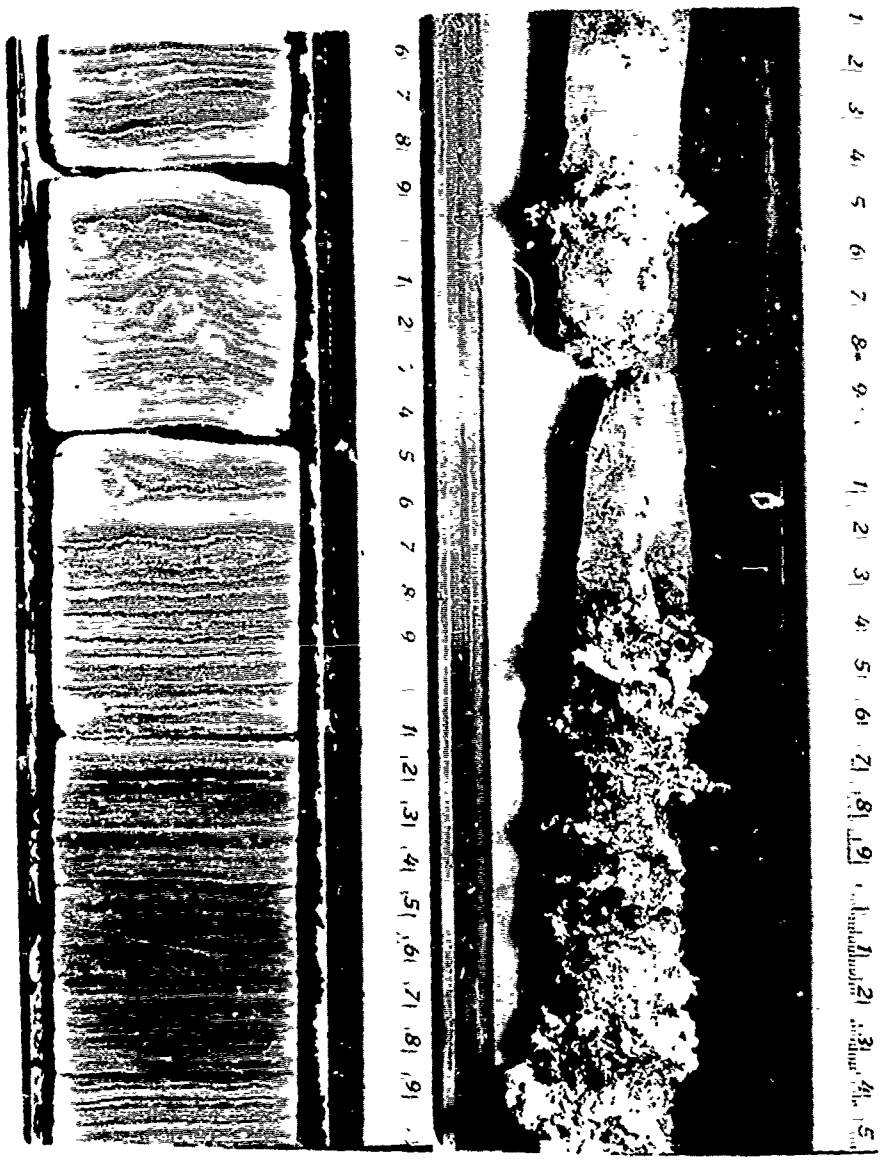

Figure 2 - Evaporitic facies indicative of subaqueous conditions recovered during Leg 42A of the Deep Sea Drilling Project. A is a finely laminated ("balatino") facies characterized by cyclically repeated alternances of gypsum and micritic carbonate. Cyclothemes are interpreted as annual. Site 372, Core 8, Section 2. Balearic Basin. B is clear halite associated with kainite and polyhalite. Site 374, Core 22, Section 3. Ionian Basin.

the marls intercalated in between the gypsum layers of the upper evaporitic series ("Gessi di Pasquasia" in Decima and Wezel, 1973), see Figure 8. In the Levantine Basin (DSDP Sites 375 and 376) it is recorded beneath the Early Pliocene oozes, but above the massive evaporites. In a locality of the Crotone basin of Calabria, southern Italy (Figure 9) near Zinga, we found marls with Cyprideis, Ammonia beccarii tepida and Limnocardium immediately overlying a 40 cm thick gypsiferous sand capping outcropping halite. This finding demonstrates that the invasion of the Paratethyan fauna in this central part of the Mediterranean (location 12 of Figure 7) post-dated the salt deposition.

Seismic reflection profiles across the major Mediterranean basins clearly show a tripartition of the Messinian age evaporites, with a lower layered sequence followed by the thick salt layer ("couche fluante") and by the upper layered sequence (see Ryan, Hsü et al, 1973, p. 136). The "lago-mare" biofacies was never recorded from

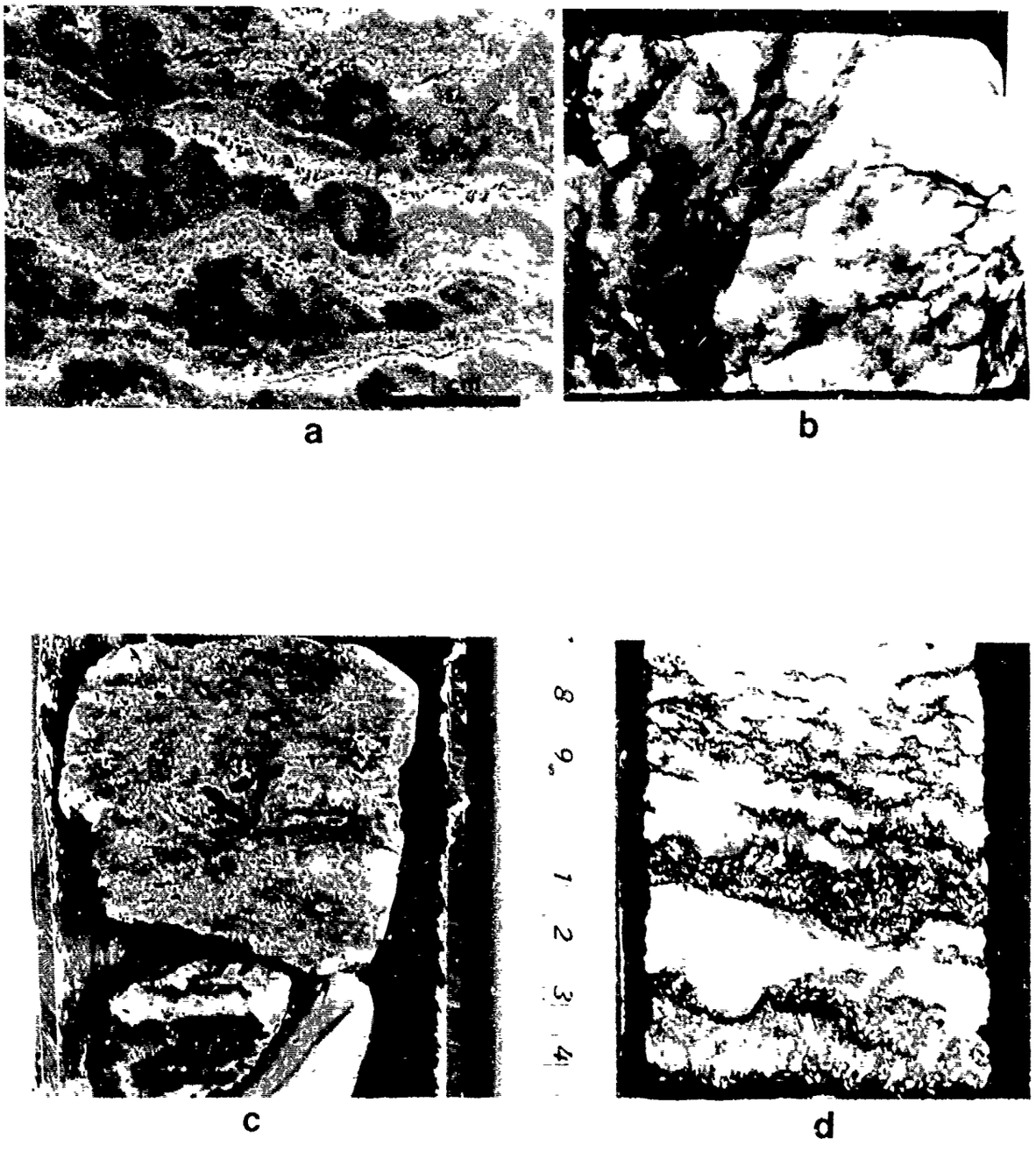


Figure 3 - Evaporitic facies indicative of intertidal (A, D?) and supratidal (B, C) conditions. A is a banded gypsum with wavy laminations suggestive of stromatolites, strongly diagenized. Site 132, Core 27, Section 2. B is a nodular anhydrite with "chickenwire" structure, interpreted as resulting from early diagenesis in a supratidal environment (tidal flats). Site 124, Core 10, Section 1. C is a banded brown to gray anhydrite with vugs. Site 374, Core 21, Section 1, from the Messina abyssal plain of the Ionian Sea.

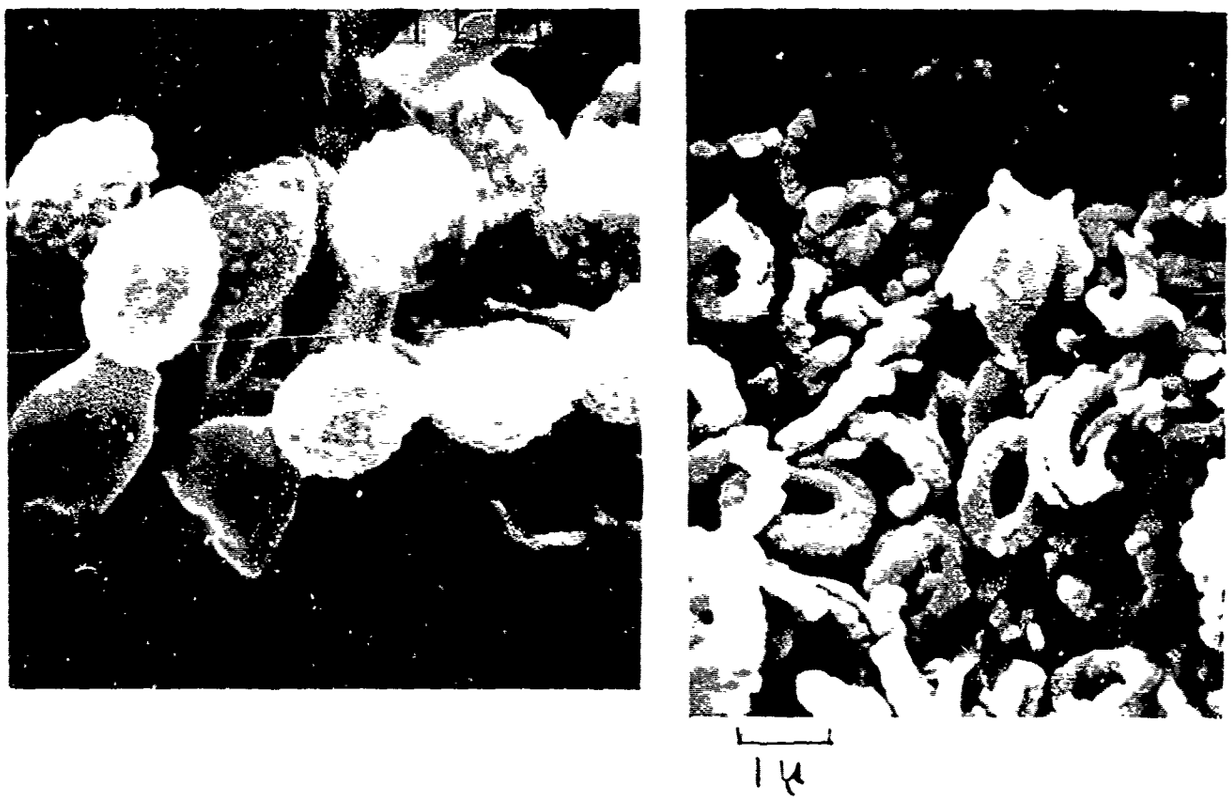

Figure 4 - Nannofossils from the white laminae of a finely laminated sediment recovered at Site 372, Section 2 of Core 9, at the base of the locally truncated evaporitic succession. A is an assemblage of fossil (?) fungi. B is a monospecific assemblage of Reticulofenestra sp.

the marly intercalations of the pre-salt evaporites (see Figure 8).

## Re-establishment of Open Marine Conditions in the Mediterranean

The ecologic niches at the bottom of endoreic, depressed water bodies occupied by the Paratethyan immigrants were destroyed by the invasion of Atlantic water masses at the beginning of the Pliocene (see Figure 6, below). A normal marine, stenohaline, deep-water fauna was re-introduced into the Mediterranean (Hsü et al, 1973; Cita and Ryan, 1973).

The Miocene/Pliocene boundary, identified with the termination of the salinity crisis and with the re-establishment of open marine conditions in the Mediterranean, is recorded with dramatic abruptness in the deep-sea record and on land (Cita, 1973, 1976).

Shallow sills separating the Western from the Eastern Mediterranean resulted in marked differences in bottom current activity, the eastern basins being less well ventilated than the western basins (see Figure 6, bottom). The finding, during Leg 42A, of thick organic-rich sapropels of earliest Pliocene age (Sphaeroidinellopsis Acme-zone) in basinal settings (DSDP Site 374, Messina abyssal Plain and DSDP Site 376, Antalya Basin plain) strongly support the assumption of high standing barriers, so that the Eastern Mediterranean became periodically stagnant almost immediately after the Pliocene flooding.

Phyletic lineages of planktonic foraminifera were interrupted in the Mediterranean by the Messinian salinity crisis (Figure 10). The bloom of Globorotalia margaritae in the Early Pliocene, and its great morphological variability are interpreted as a response to the lack of competitors in the water column, since the salinity crisis prevented their phyletic evolution in the Mediterranean (Cita, 1976).

## Response of the Open Ocean to the Mediterranean Salinity Crisis

So far I touched some critical paleoenvironmental aspects of the salinity crisis in the Mediterranean.

Which kind of response in the open ocean can we expect from the subtraction of approximately

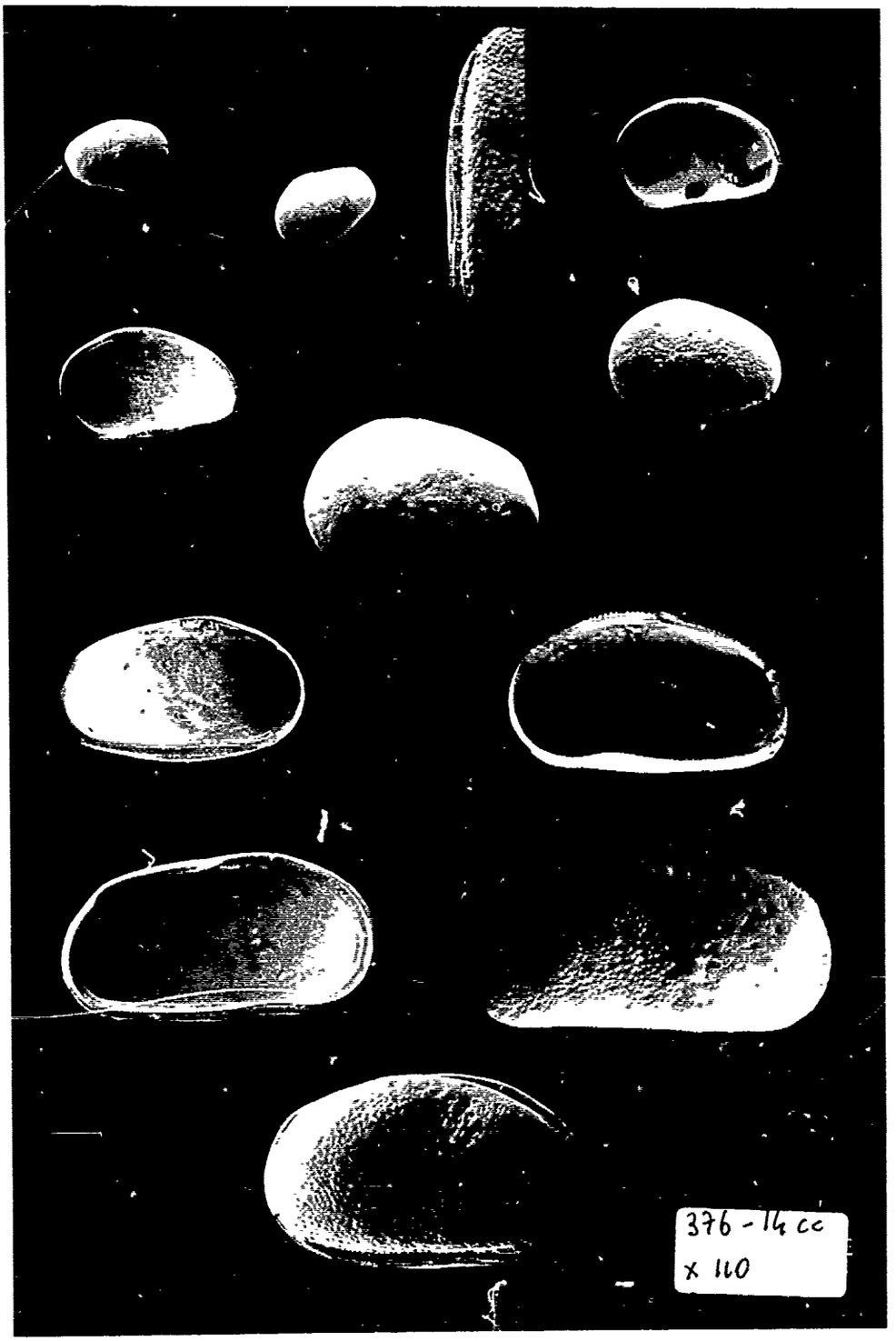


Figure 5 - Various instars of Cyprideis agrigentina Decima recorded in Core 14 CC of Site 376, west of Cyprus. The genus Cyprideis is the most prominent constituent of the "lago-mare" biofacies from the deep-sea record.

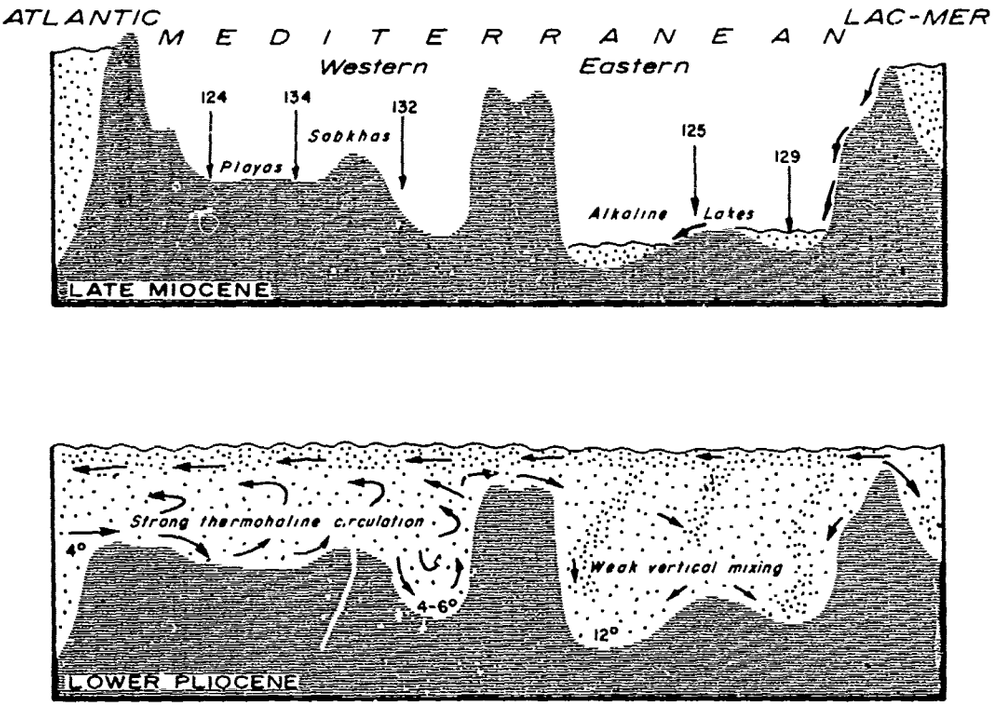


Figure 6 - Idealized cross-sections of the Mediterranean during the late Messinian dessication (above) and immediately after the re-establishment of open marine connections with the Atlantic (below). After Cita and Ryan (1973).

one million cubic kilometers of salt (Ryan, 1973) in less than one million years? If the salt removal is not accompanied by a contemporary diminishment of biological productivity, one should expect a brief upward excursion of the Calcite Compensation Depth, an expectation which seems to be supported by a sudden drop in carbonates recorded in the Godra Ridge of the North-Eastern Pacific, in the Cape Verde Basin and in the Columbia Basin, as well as by a considerable decrease in carbonate content in the equatorial Pacific, all these episodes being calibrated biostratigraphically at 5 to 5.5 m.y. approximately (Ryan et al, 1974).

Other climatically induced changes, involving a world-wide recognizable regression (Adams et al, 1977) will be discussed later.

## Importance of the Cape Bojador Record (DSDP Site 397)

A unique opportunity of testing our models was provided by the continuously cored Section penetrated off Cape Bojador, at DSDP Site 397. In an upper continental rise setting, at a water depth of 2900 m (well above CCD), we recovered an undisturbed, monotonous succession of hemipelagic sediments deposited at an unusually high sedimentation rate (Ryan, von Rad et al, in press).

For the first time in the history of the Deep Sea Drilling Project we had the opportunity to work out paleomagnetic stratigraphy directly on the ship (Hamilton, in press) so that the stratigraphic progression could be followed step by step with both biologic and magnetic techniques.

The biostratigraphic and paleomagnetic calibrations for the interval under discussion are presented in Figure 11. The lower and upper boundaries of the Messinian are correlated biostratigraphically on the basis of calcareous nannofossils (Mazzei et al, in press). They fall respectively at the middle of Epoch 6 (interpolated age 6.2 m.y.) and at the top of Epoch 5 (interpolated age 5.2 m.y.).

For correlating the onset of evaporitic conditions in the Mediterranean we have a datum plane (coiling change of Globorotalia acostaensis from sinistral to dextral) which seems highly reliable and has been calibrated in the North Atlantic (DSDP Site 397, see Salvatorini and Cita, in press) and in the equatorial Pacific (Saito et al, 1975) at the base of paleomagnetic Epoch 5 with an interpolated age of approximately 5.8

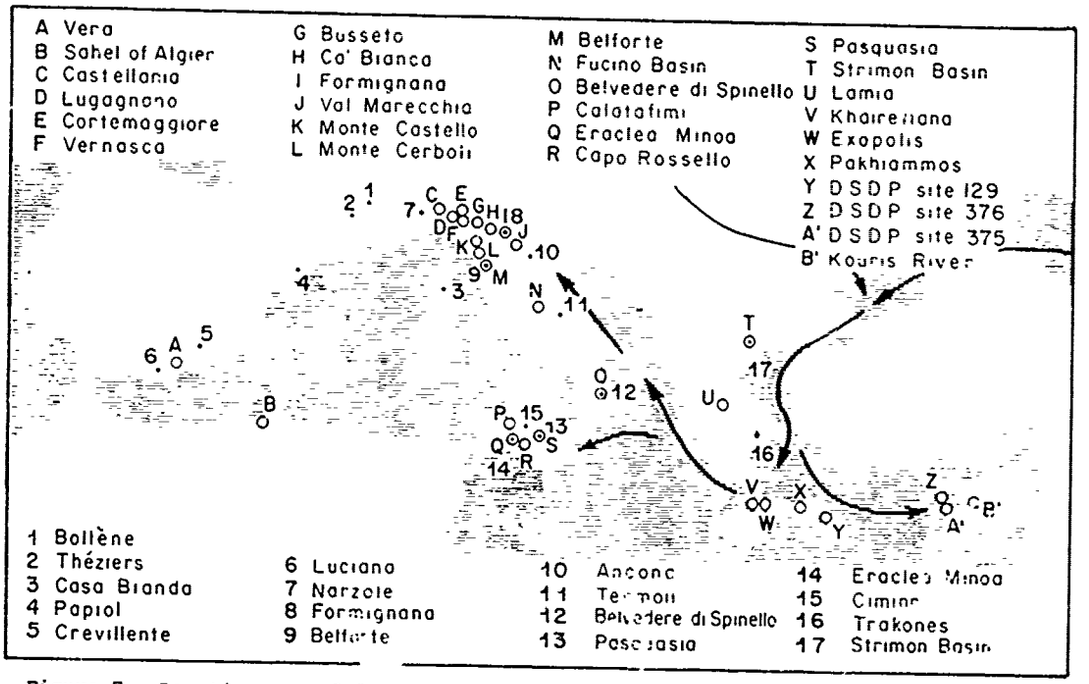


Figure 7 - Location map of faunas of Late Messinian age with definite Paratethyan affinity, compiled from various sources, essentially after Sissingh (1976) and Archimbault-Guezou (1976). Open circles and letters refer to ostracod populations; points and numbers refer to mollusks. Arrows indicate the inferred patterns followed by Paratethyan immigrants, according to Sissingh.

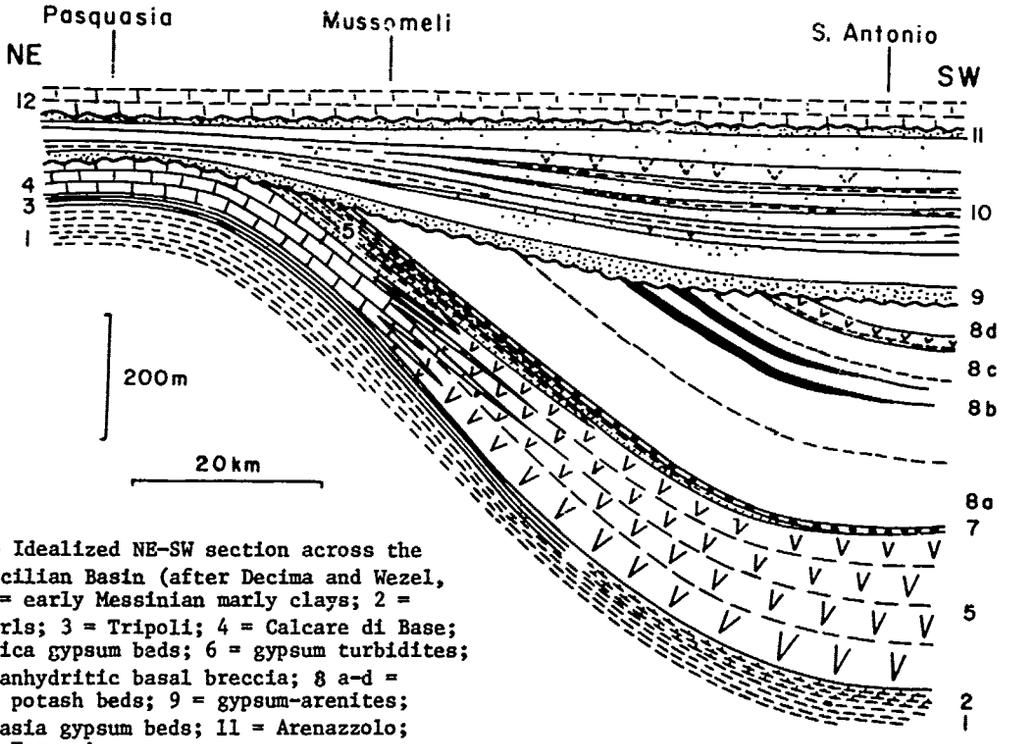


Figure 8 - Idealized NE-SW section across the central Sicilian Basin (after Decima and Wezel, 1973). 1 = early Messinian marly clays; 2 = whitish marls; 3 = Tripoli; 4 = Calcare di Base; 5 = Cattolica gypsum beds; 6 = gypsum turbidites; 7 = marly-anhydritic basal breccia; 8 a-d = halite and potash beds; 9 = gypsum-arenites; 10 = Pasquasia gypsum beds; 11 = Arenazzolo; 12 = Trubi Formation.

m.y. This biostratigraphic datum has been recorded in Sicily in the Tripoli diatomites (Stainforth et al, 1975) which immediately underlie the "Calcare di base" materializing the first (earliest) desiccation phase.

One more very useful biostratigraphic horizon, also calibrated at exactly the same paleomagnetic position at Site 397 in the North Atlantic and in Core RC 12-66 in the equatorial Pacific is the first evolutionary appearance of Globorotalia margaritae at the middle of Epoch 5, with an interpolated age of 5.5 m.y. Unlike the Gacostaensis datum, this datum is not recorded in the Mediterranean, which was dry at that time.

Physical measurements carried out on these cores, insuring a data point every approximately 20,000 years, show a disturbance in the pelagic realm (Figure 12). The parameters considered from left to right are (a) sediment fraction greater than 200 microns, that is to say abundance of large-sized, entire tests of planktonic foraminifers with minor benthic forms, the sediment fraction being essentially biogenic, (b) carbonate content and (c) isotopic ratio $^{16}O/^{18}O$, all calculated from the same set of s[illegible] (after Cita and Spezzi Bottiani, in press and after Schackleton and Cita, in press). The isotopic curve has a higher number of data points, additional measurements having been made in order to clarify the record.

Cycles have amplitudes comparable to those recorded at the same drillsite for the late Pleistocene (Brunhes Epoch) as shown in the lower part of the figure, but are off in scale. As in the late Pleistocene, the three parameters vary sympathetically.

This disturbance is considered as the response of the open ocean to the Mediterranean salinity crisis. In detail, we see that cycles (two complete cycles are visible, with durations of the order of 100,000 years, but they could be more) start to appear in Core 44, after the first evolutionary appearance of G. margaritae, that is to say - and with reference to the paleomagnetic

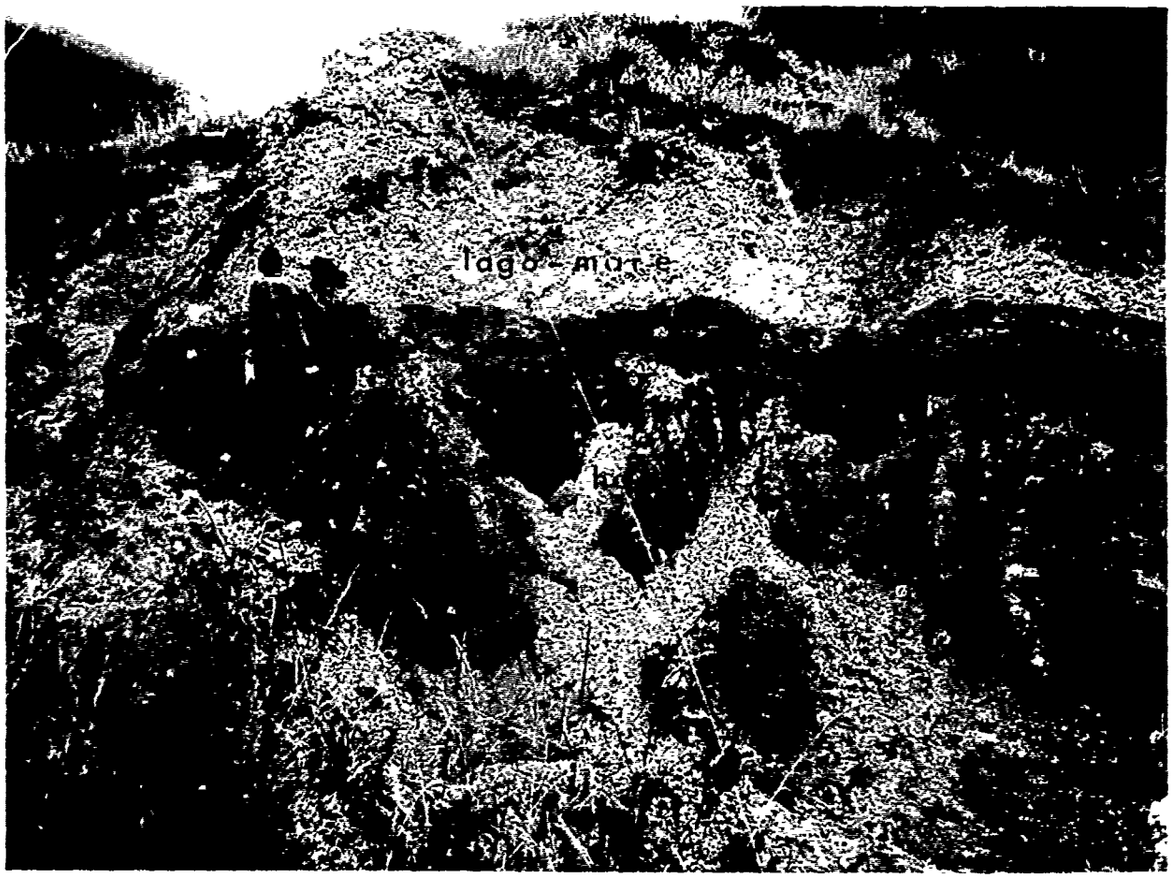


Figure 9 - Upper contact of outcropping halite formation near Zinga (Calabria, Italy). A rich population of Molluscs, ostracodes and foraminifera of Paratethyan affinity is present immediately above the salt.

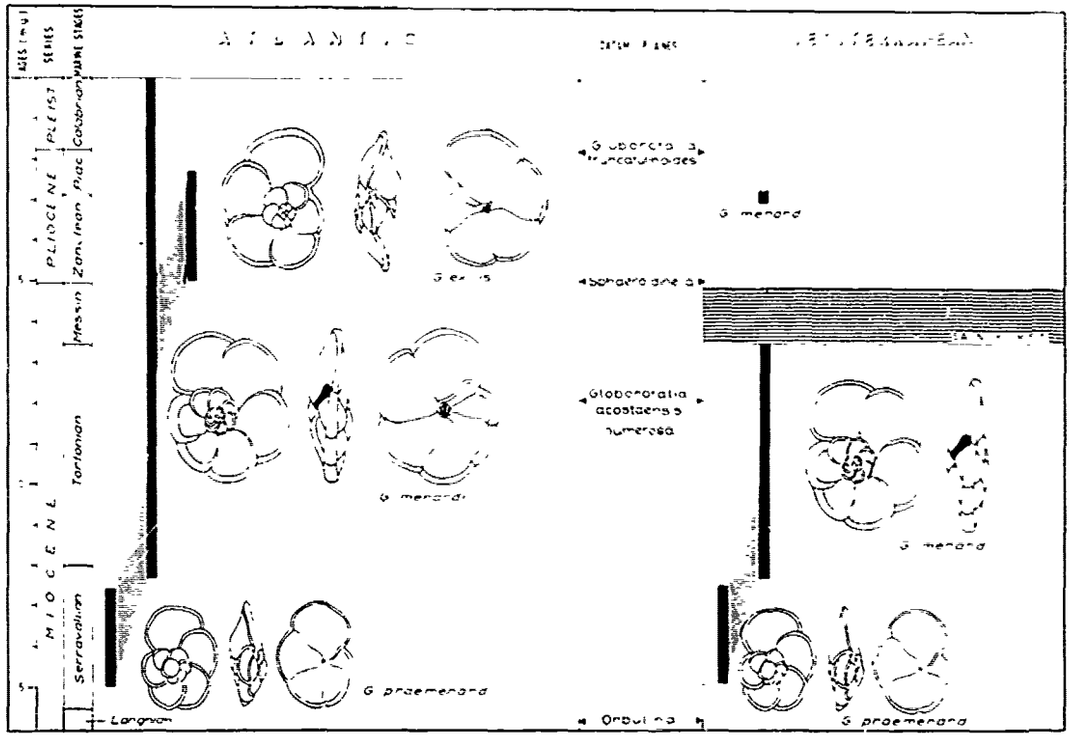


Figure 10 - Schematic development of the phyletic lineage of Globorotalia menardii as recorded in the open ocean (left column) and in the Mediterranean (right column). In the latter basin the destructive effects of the Messinian salinity crisis interrupted the phylum. Calibration of datum planes in the central column is after Ryan et al (1974).

calibration - approximately half way through the duration of the salinity crisis.

Background Discussion

The interpretation of these parameters, and of the variations recorded in this particular time-span, require some background explanation:

(1) Mediterranean-type marginal basins, landlocked and subject to excess evaporation, are considered the principal source of dense, salty water to the abyssal circulation (Rooth, 1978). The disconnection of the Mediterranean from the world ocean during the salinity crisis (Hsü et al, 1973) deprived the North Atlantic of its main source of dense, warm deep water. The expected consequences of this paleogeographic event include (a) cooling of deep water masses in the Atlantic and (b) enhancement of the North-South thermal gradient in the superficial water masses.

(2) Models proposed for the origin of Messinian age evaporites in the Mediterranean include a brine reflux model (Selli, 1973; Sonnenfeld, 1974; Debenedetti, 1978) and a multistep model with an early reflux stage (van Couvering et al, 1976). However, we have shown that desiccation, involving complete disconnection from the open ocean, occurred right from the beginning of the salinity crisis (see Ryan et al, 1974; Cita et al, 1978; Ryan and Cita, 1978) because (a) evidence of subaerial exposure is recorded in the stratigraphically lowermost evaporitic rocks (Schreiber, 1973) and (b) erosional surfaces recorded on the Mediterranean basin margins and extending towards the center of the major basins are developed beneath the main salt layer (Ryan and Cita, 1978; Ryan, 1978).

(3) The salt extraction in the Mediterranean was very rapid, as shown by the occurrence of annual cycles up to 30 cm thick recorded in halite from the central Sicilian Basin (Decima, 1978) Geochemical investigations on the salts recovered during DSDP Leg 42A (McKenzie and Ricchiuto, 1978; Pierre and Fontes, 1978) revealed that some of these salts are recycled as are the uppermost salts of the central Sicilian Basin, where the bromine content is minimal (Decima, 1978). These latest salts were probably deposited when the Mediterranean was completely cut off from the Atlantic, and exclusively continental conditions prevailed.

(4) The volume of the Mediterranean Evaporite, calculated at 1 million cubic kilometers (Ryan, 1973) (1) lowered the salinity of the world ocean by 6%. This decrease in salinity should have had important climatic repercussions, as discussed by Ryan et al (1974), such as raising the freezing point of sea-water, increasing the extension of sea-ice, increasing the albedo of the earth and thus impeding the transfer of heat into the atmosphere (Weyl, 1968). This effect is similar to that discussed under (1) and results in climatic deterioration.

(5) The existence of a Late Miocene cooling phase in the Southern hemisphere has been recognized paleontologically for some time (Bandy, 1966). The Kapitean stage of New Zealand documents a regression at that time (Kennett, 1967) and drilling in the Ross Sea with the GLOMAR CHALLENGER in 1973 provided new supportive data (Hayes, Frakes et al, 1975). A definite regressive cycle is also recorded in the generalized curve of Vail and Mitchum (1978), and corresponds to a change in diagentic potential detected

(1) The original calculation was based on seismic reflection profiles with great penetration available from the Western Mediterranean (Ryan, personal communication 1978) and extrapolated to the Eastern Mediterranean. This estimate was fully supported by independent calculations on seismic profiles different from those used by Ryan (E. Purdy, personal communication 1975). The volume of one million cubic kilometers concerns only evaporites buried beneath the abyssal plains of the Mediterranean. Evaporites outcropping on land or buried in the subsurface have not been included in the calculations. Therefore the volume of salts subtracted from the world oceans by the Mediterranean salinity crisis is certainly greater than $1 \times 10^6$ km$^3$.

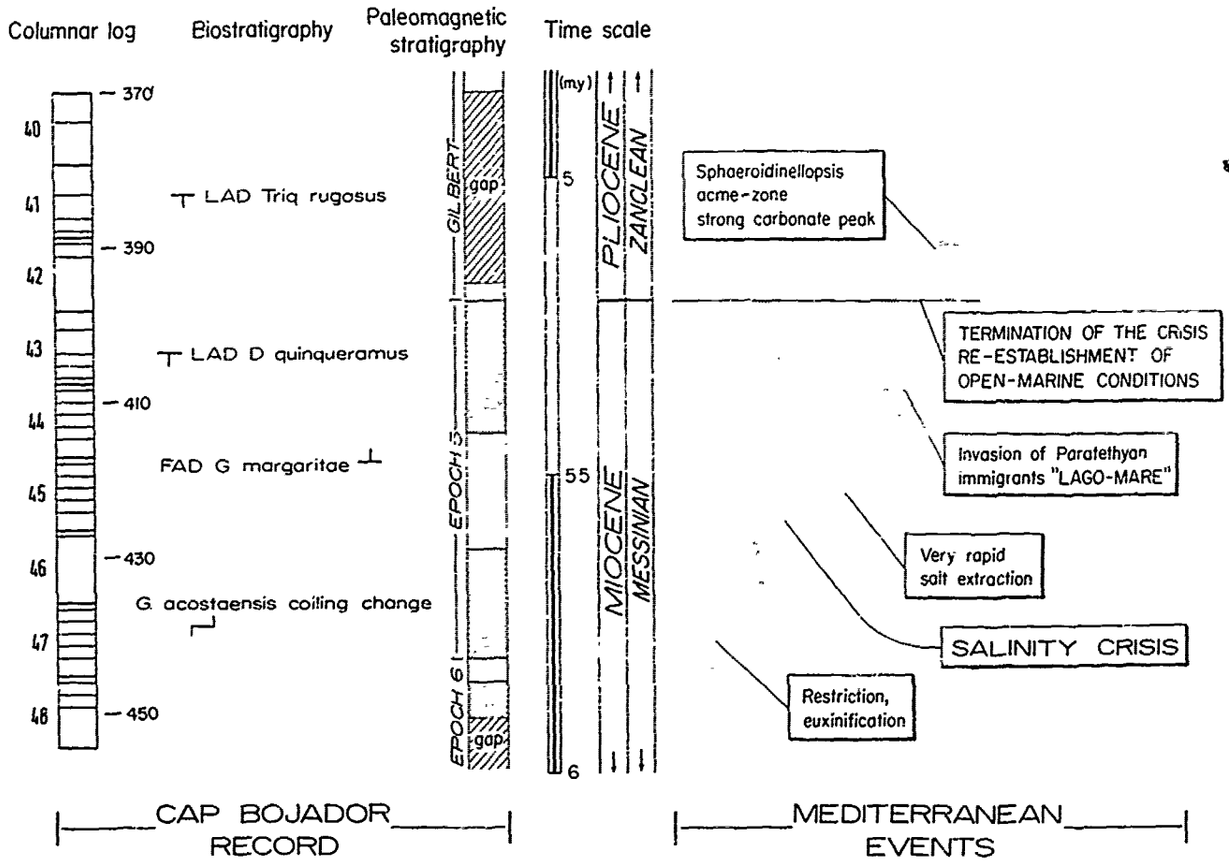


Figure 11 - Calibration of foraminiferal and nannofossil datum planes recorded at DSDP Site 397 with the magnetic reversals. The time-scale in the middle of the figure is based essentially on the interpreted paleomagnetic stratigraphy. It allows dating, with a certain accuracy, a number of Mediterranean events whose chronological succession is well established after recent studies in the Mediterranean area.

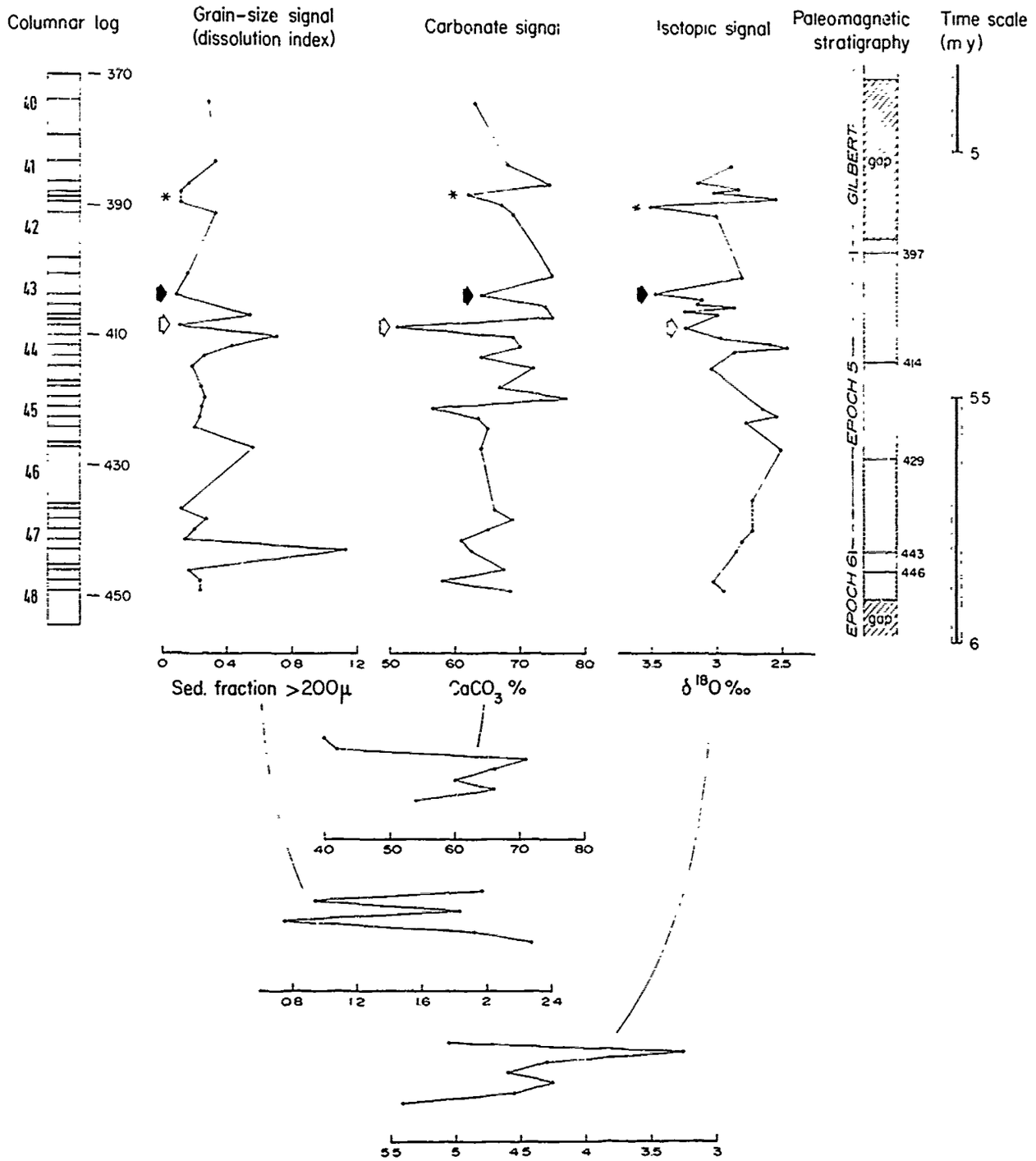


Figure 12 - Variations recorded in physical parameters in Cores 40-48, DSDP Site 397. In order to evaluate the amplitutde of cycles recorded in the latest part of the Messinian, late Pleistocene cycles recorded in the same parameters, at the same drill-site, are plotted in the lower part of the figure. The strong diminishment of grain-size (column to the left) is accounted to incipient diagenesis. The transition between marl-ooze and marl-chalk is recorded at approximately 300 m subbottom.

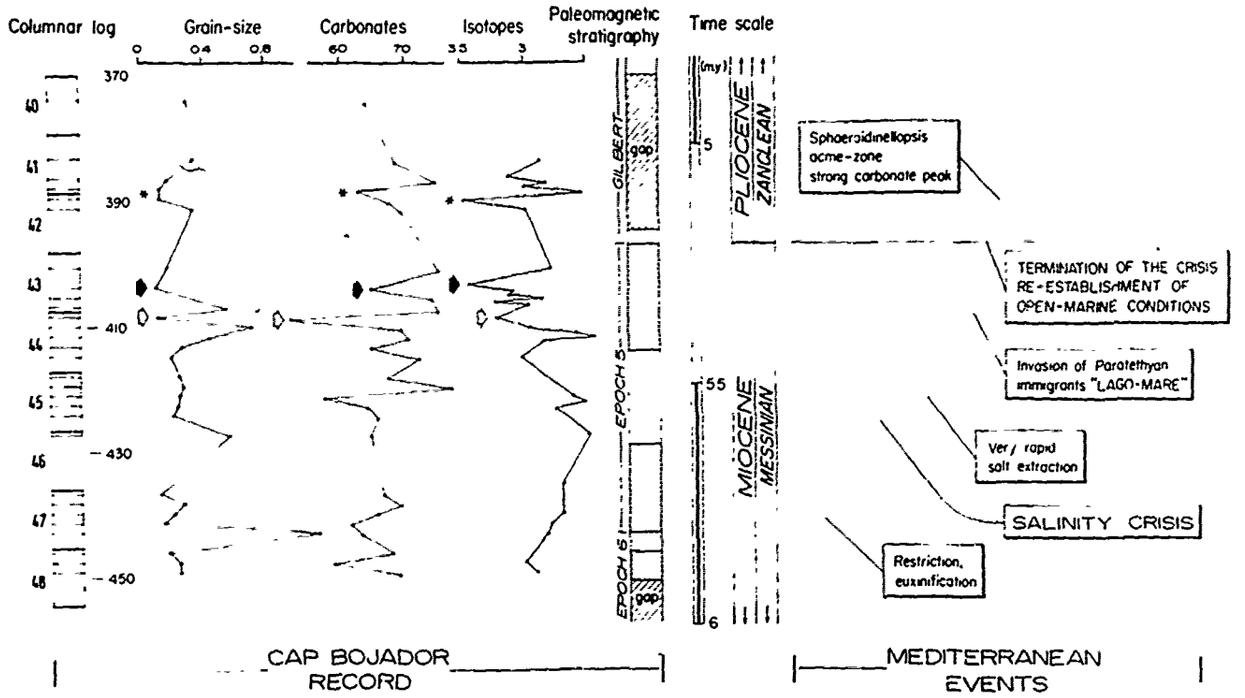


Figure 13 - Correlation of the physical parameters recorded at DSDP Site 397 with Mediterranean events, as discussed in the text.

in the equatorial Pacific deep-sea record ("b" reflector of Schlanger and Douglas, 1974).

In most cases, however, the Late Miocene regressive phase is not really well dated (Adams et al, 1977). Among the best dated regressive phases are those recorded in land sections facing the Eastern North Atlantic: in the Andalusian stratotype section Berggren and Haq (1976) documented a glacio-eustatically induced lowering of sea-level estimated at 50 m approximately, whereas in the Bou Reg Reg section of Morocco Cita and Ryan (in press) described climatically modulated cycles post-dating the first evolutionary appearance of Globorotalia margaritae, accompanied by evidence of a marked cooling.

## Climatic Interpretation

Most of the authors involved in the Messinian debate, from Bandy (1973, 1975) to Nesteroff (1973), see also Nesteroff and Glaçon,(1977), from Selli (1973) to van Couvering et al (1976) noted the coincidence of the Mediterranean salinity crisis and acme of Antarctic glaciation. A glacio-eustatically induced lowering of sea-level should have resulted in restriction of the Atlantic portal and eventually in the final cut-off of the Mediterranean. Van Couvering et al (1976) used the expression "temperate tail of the polar dog" in this context.

An alternative explanation was that the cut-off of the major source of warm, dense water to the deep ocean, accompanied by the subtraction of 1 million cubic kilometers of salts (representing 6% of the salinity of the world ocean) in such a short time span should have had important climatic repercussions, as discussed previously under (1) and (4). According to this latter model, first presented by Dreyfus and Ryan at the IGC at Montreal (1972), then elaborated by Ryan (1973) and further developed by Ryan et al (1974), the cause-to-effect relationships are exactly the opposite of that supposed by the other authors. Paleomagnetic calibrations available in 1974 seemed to support the relative timing of the two events, that is to say the Mediterranean salinity crisis predated the final glacial expansion in Antarctica.

Does our North Atlantic test-area offer the possibility to discriminate between the two alternatives?

The isotopic curve to the right of Figure 13 clearly shows a trend towards lighter isotopic values (warming trend) followed upwards by a trend towards heavier isotopic values (cooling trend). The turning point marking the climatic reversal is recorded at the top of Core 46, which correlates with the beginning of the rapid salt extraction in the Mediterranean. If our correlations are correct, models which attribute the Mediterranean salinity crisis (with or without disiccation) to glacio-eustatic lowering of sea-

level induced by the expansion of continental ice in Antarctica (Bandy, 1973; Nesteroff and Glacon, 1977; Sonnenfeld, 1974; Selli, 1973) should be rejected. Indeed, no cooling trend is detectable in Shackleton's curve prior to the middle part of paleomagnetic Epoch 5 characterized by a reversed polarity, which means over one hundred thousand years after the onset of evaporitic conditions in the Mediterranean.

The marked cycles indicated by short arrows in Figure 13 correlate with the latest part of the Messinian, when the Eastern Mediterranean endoreic, depressed alkali lakes (see Figure 6 above) were invaded by a peculiar shallow-water euryhaline fauna immigrated from the Paratethys (Ruggieri, 1967; Sissingh, 1975; Cita et al, 1978). The maximum excursion recorded in the isotopic cycle terminating at the point shown by the open arrow in Figure 13, a cycle which is well controlled with six date points, is of such a magnitude (0.8‰) as to represent about 80m sea-level equivalent in stored ice, following Shackleton and Opdyke (1977, p. 218).

A climatic message seems to be imprinted also in the isotopic signal of Carbon (Figure 14, after Schackleton and Cita, in press). Though the climatic interpretation of Carbon isotopes is still poorly understood (Cita et al, 1977; Vergnaud-Grazzini et al, 1977; Berger et al, 1978 inter alias) and the recorded changes are so small as to be strongly influenced by errors of measure, it seems sufficiently proved, at least for the Late Pleistocene, that isotopically heavy values correlate with periods of dryness, accompanied by a diminishment of forestation, whereas isotopically light values correlate with an increase in humidity.

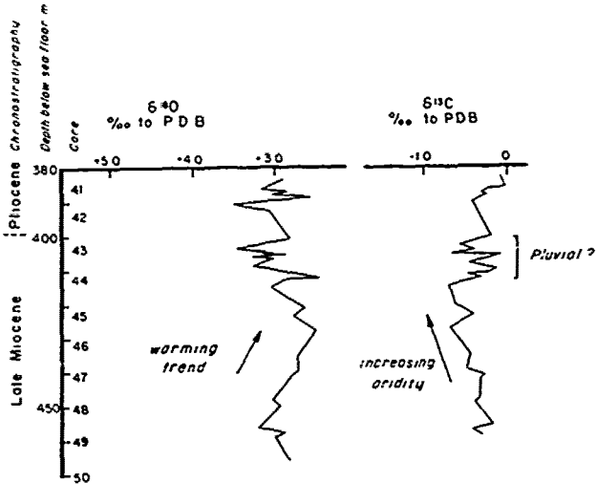


Figure 14 - Changes in the Isotopic composition of Oxygen (left) and of Carbon (right) as recorded by Shackleton through Cores 40-50 of DSDP Site 397, based on measurements carried out on monospecific assemblages of large-sized benthic foraminifera. The climatic interpretation is discussed in the text.

The curve represented in Figure 14 shows isotopically heavy values (arid? dry?) in the earlier part of the salinity crisis, extending upwards to encompass the salt extraction stage. This period of inferred dryness is followed upwards by an isotopically lighter period (wet? humid?) which correlates with the "lago-mare" stage. The recorded isotopic change reaches 0.8‰ in the terminal part of the Mediterranean salinity crisis, see Figure 14.

A discussion of the Mediterranean interactions is now required. At DSDP Site 376 West of Cyprus, see Figure 1, where coring was continuous from the sea-bottom, we recorded the Miocene/Pliocene boundary in Core 6, and the top of the evaporites in Core 15. Evaporites included intertidal, subtidal and supertidal facies with definite evidence of subaerial exposure, whereas the overlying 86.5m thick "lago-mare" facies sediments were deposited under permanent subaqueous conditions.

In the subsurface of the Po Plain in Northern Italy, where the stratigraphic control is provided by hundreds of deep wells by the Italian Oil Company (Rizzini and Dondi, 1978) in the depocenter of the rapidly subsiding Apennine foredeep, the Late Messinian sediments, deposited under subaqueous continental conditions, exceed 1 km in thickness (Cita et al, in press). How could these endoreic basins permanently keep their water under dry climatic conditions? A capture of the high standing Paratethyan lakes does not seem sufficient: pluvial conditions are required.

The termination of inferred pluvial climate occurs at the top of Core 43 (see Figure 14). Here we located the Miocene/Pliocene boundary by multiple biostratigraphic correlations with reference to the Miocene/Pliocene stratotype defined in Sicily (Cita, 1975) at the base of the Trubi Formation, in coincidence with the re-establishment of open marine conditions after the salinity crisis. The isotopic change recorded in the Carbon signal at this point of the curve (0.8‰ is comparable in magnitude to the 0.7‰ change recorded by Berger et al (1978) at the transition from the Late Glacial (= pluvial) to the Holocene (= arid) off NW Africa.

One more signal which is here interpreted as a response to a Mediterranean event is that indicated by an asterisk in Figure 13. It occurs in the earliest part of the Pliocene, at the base of the Gilbert Epoch, in Core 41. It is a short easily detectable cycle and of the same sign in the three parameters considered (grainsize, carbonate content and isotopic ratio of Oxygen). This cycle, suggestive of a short duration "cooling" of the North Atlantic, correlates with the Sphaeroidinellopsis Acme-zone of the Mediterranean (Cita, 1973), where the highest carbonate contents of the entire Early Pliocene are recorded (Figure 13).

The Sphaeroidinellopsis Acme-zone represents

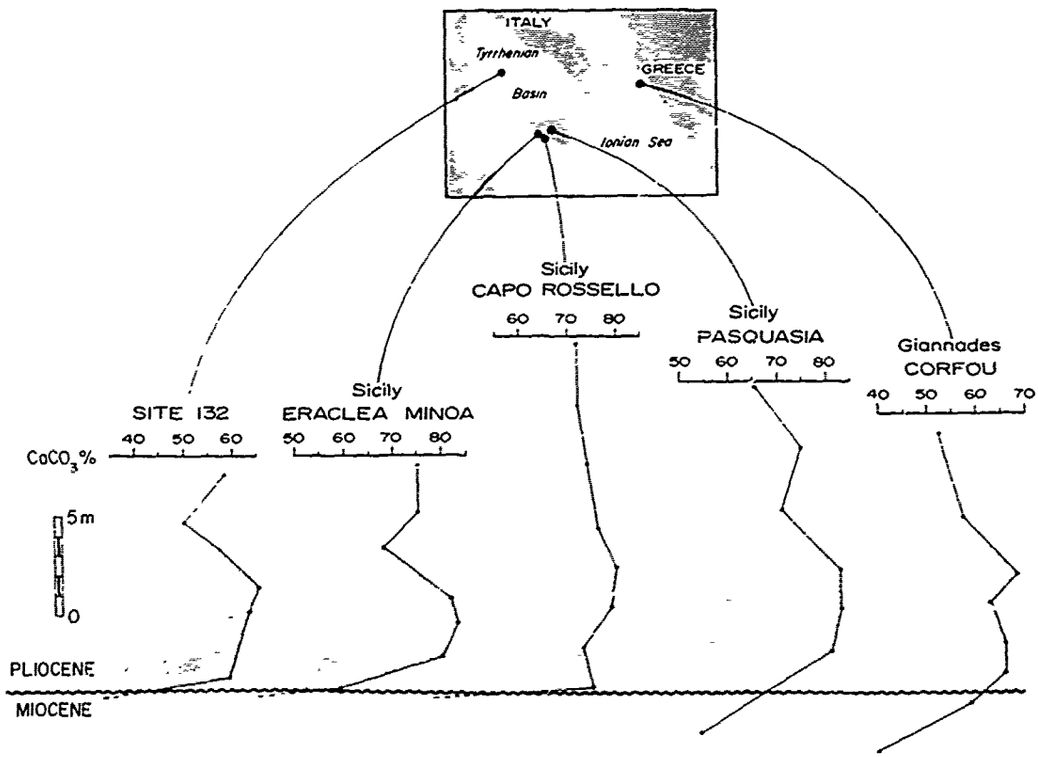


Figure 15 - Correlation of carbonate curves obtained in several Mediterranean stratigraphic sections straddling the Miocene/Pliocene boundary. Definite carbonate peaks are recorded in all the sections in the basal Pliocene, Sphaeroidinellopsis Acme-zone (shaded area).

the sedimentary expression of the final flooding of the Mediterranean basins by deep and cold Atlantic water masses. Vertical mixing was so strong as to result in an almost identical isotopic composition recorded in benthic and planktonic foraminifers at DSDP Site 132 (van Donk et al, 1973).

The Mediterranean (essentially the Western Mediterranean Basin) had a deep communication with the North Atlantic in the Early Pliocene (Figure 6, above) unlike in later times. The communication was sufficiently deep as to permit the re-immigration of psychrosphaeric ostracods (Benson, 1973). Consequently, the Mediterranean could not be considered at that time as the principal source of dense, salty water to the Atlantic Ocean (Rooth, 1978).

The short duration cycle discussed above could be the physically detectable response of the North Atlantic to the re-establishment of a permanent, deep-water connection with the Mediterranean after its isolation.

## Concluding Remarks

As a conclusion of this discussion, it appears quite clearly that the salinity crisis suffered by the Mediterranean at the end of the Miocene has a physically detectable response in the open ocean.

We should look in the open ocean record for similar signals in response to salt extraction in Mediterranean-type satellite basins or marginal seas in different parts of the geologic column.

Acknowledgments. The data, and interpretations, presented in this paper arise from my participation in Legs 13, 42A and 47A of the Deep Sea Drilling Project. I gratefully acknowledge the management of the Project for offering the opportunity to study an extremely stimulating scientific problem. I also thank the organizing Committee of the Second Maurice Ewing Symposium for the invitation to present this paper, and the several collegues and friends who contributed with their studies to the understanding of the multiple and complicated effects of the Mediterranean salinity crisis.

Discussions with Bill Ryan, Ken Hsü, Nick Shackleton, Wolf Berger, Michael Sarnthein have been of great benefit.

A careful revision of the text by D. Bernoulli and R. Wright is gratefully acknowledged and

special thanks for typing assistance to Ann Burns. Financial support was provided by CNR through Grant 78.00795.89. Technical assistance was offered by S. Antico, A. Malinverno and C. Secchi. This is Contribution no. of IGCP Project no. 96 "Messinian Correlation and Publication no. of CNR, Progetto Finalizzato GEODINAMICA.

## References


Adams, C.G., Benson, R.H., Kidd, R.B., Ryan, W.B. F., and Wright, R.C., The Messinian Salinity Crisis and Evidence of Late Miocene Eustatic Changes in the World Ocean, Nature, 269, 5627, 383-386, 1977.

Bandy, O.L., Faunal Evidence of Miocene-to-Recent Paleoclimatology in Antarctic, Bull.Am.Assoc. Petr.Geol., 50, 643-644, 1966.

Bandy, O.L., Chronology and Paleoenvironmental Trends, Late Miocene-Early Pliocene, Western Mediterranean. In: Messinian Events in the Mediterranean (C.W. Drooger Editor), 21-25, 1973.

Bandy, O.L., Messinian Evaporite Deposition and the Miocene/Pliocene boundary, Pasquasia-Capodarso Section, Sicily. In: Late Neogene Epoch Boundaries (T. Saito and L.H. Burckle Editors) Micropaleontology Press Spec. Publ. 1, 49-63, 1975.

Benson, R.H., Ostracodes as Indicators of Threshold Depth in the Mediterranean During the Pliocene. In: The Mediterranean Sea. A Natural Sedimentation Laboratory (D.J. Stanley Editor), 63-74, 1972.

Benson, R.H., Psychrospheric and Continental Ostracoda from Ancient Sediments in the Floor of the Mediterranean. Init.Reports DSDP, 13. 2, 1002-1008, 1973.

Berger, W.H., Diester-Haass, L. and Killingley, J.S., Upwelling off North-West Africa: the Holocene Decrease as Seen in Carbon Isotopes and Sedimentological Indicators, Oceanologica Acta, 1, 1, 3-8 1978.

Berggren, W.A. and Haq, B., The Andalusian Stage (Late Miocene): Biostratigraphy, Biochronology and Paleoecology, Paleogeogr., Paleo-climatol., Paleoecol., 20, 67-129, 1976.

Bertolani Marchetti, D. and Cita, M.B., Palynological Investigations on Late Messinian Sediments Recorded at DSDP Site 132 (Tyrrhenian Basin) and Their Bearing on the Deep Basin Desiccation Model, Riv.Ital.Paleont., 81, 281-308, 1975.

Cita, M.B., The Pliocene Record in Deep-Sea Mediterranean Sediments. 1. Pliocene Biostratigraphy and Chronostratigraphy. Init.Reports DSDP, 13, 2, 1343-1379, 1973.

Cita, M.B., The Miocene/Pliocene Boundary. History and Definition. In: Late Neogene Epoch Boundaries (T.Saito and L.H.Burckle Editors) Micropaleontology Press Spec. Publ. 1, 1-30, 1975.

Cita, M.B., Biodynamic Effects of the Messinian Salinity Crisis on the Evolution of Planktonic Foraminifera in the Mediterranean, Paleogeogr., Paleoclimatol., Paleoecol., 20, 23-42, 1976.

Cita, M.B., Follieri, M., Longinelli, A., Mazzei, R., d'Onofrio, S., and Bossio, A., Revisione di alcuni pozzi profondi della Pianura Padana nel quadro del significato geodinamico della crisi di salinita del Messiniano. Boll. Soc., Geol. Ital., in press.

Cita, M.B. and Ryan, W.B.F., The Pliocene Record in Deep-Sea Mediterranean Sediments. 5. Time-Scale and General Synthesis. Init. Reports DSDP, 13, 2, 1405-1416, 1973.

Cita, M.B. and Ryan, W.B.F., The Late Neogene Section of Bou Reg Reg, N.W. Morocco: Evidence, Timing and Significance of a Late Miocene Regressice Phase, Riv. Ital. Paleont., in press.

Cita, M.B. and Spezzi Bottiani, G., Late Neogene Paleoenvironment: Studies on Carbonate Content, Grain Sizes, and Dissolution, Cores 1-57 (DSDP Site 397). Init. Reports DSDP, 47A, in press.

Cita, M.B., Vergnaud-Grazzini, C., Robert, C., Chamley, H., Ciaranfi, N., d'Onofrio, S., Paleoclimatic Record of a Long Deep Sea Core from the Eastern Mediterranean. Quaternary Research, 8, 205-235, 1977.

Cita, M.B., Wright, R.H., Ryan, W.B.F. and Longinelli, A., Messinian Paleoenvironments, Init. Reports DSDP, 42A, 1978.

Debenedetti, A., Messinian Salt Deposits in the Mediterranean: Evaporites or Precipitrates? Boll. Soc. Geol. Ital., 95, 5, 941-950, 1978.

Deciman, A., Initial Data on the Bromine Distribution in the Miocene Salt Formation of Southern Sicily. Mem. Soc. Geol. Ital., 16, 39-43, 1978.

Deciman, A. and Wezel, F.C., Late Miocene Evaporites in the Central Sicilian Basin, Italy, Init. Reports DSDP, 13, 2, 1234-1240, 1973.

Friedman, G.M., Petrographic Data and Comments on the Depositional Environment of the Miocene Sulphates and Dolomites at Sites 124, 132 and 134, Western Mediterranean Sea., Init. Reports DSDP, 13, 2, 695-708, 1973.

Garrison, R., Schreiber, B.C., Bernoulli, D., Fabricius F., Kidd, R.B. and Melieres, F., Sedimentary Petrology and Structures of Messinian Evaporitic Sediments in the Mediterranean Sea, Leg 42A, DSDP. Init. Reports DSDP, 42A, 1978.

Hajos, M., The Mediterranean Diatoms, Init. Reports DSDP, 13, 2, 944-970, 1973.

Hamilton, N., A Paleomagnetic Study of Sediments from Site 397, NW African Continental Margin. Init. Reports DSDP, 47A, in press.

Hayes, D.E., Frakes, L.A. et al, Initial Reports of the Deep Sea Drilling Project, v. 28. 1-1007, U.S. Government Printing Office, Washington, D.C., 1974.

Hsü, K.J., Cita, M.B. and Ryan, W.B.F., The Origin of the Mediterranean Evaporites, Init. Reports DSDP, 13, 2, 1203-1231, 1973.

Hsü, K.J., Montadert, L. et al, Initial Reports of the Deep Sea Drilling Project, v. 47A, U.S. Government Printing Office, Washington, D.C., 1978.

Kennett, J.P., Recognition and Correlation of

the Kapitean Stage (Upper Miocene), New Zealand, New Zealand Journ. Geol. Geophys., 70, 4, 1051-1603, 1967.

Mazzei, R., Raffi, I., Rio, D., Hamilton, N. and Cita, M.B., Calibration of Late Neogene Calcareous Plankton Datum Planes with the Paleomagnetic Record of Site 397 and Correlation with Moroccan and Mediterranean Sections, Init. Reports DSDP, 47A, in press.

McKenzie, J. and Ricchiuto, A., Stable Isotopic Investigations of Carbonate Samples Related to the Messinian Salinity Crisis from DSDP Leg 42A, Mediterranean Sea, Init. Reports DSDP, 42A, p. 650-655, 1978.

Nesteroff, W.D., Mineralogy, Petrography, Distribution, and Origin of the Messinian Mediterranean Evaporite. Init. Reports DSDP, 13, 2, 673-694, 1973.

Nesteroff, W.D. and Glacon, G., Le caractere rythmique des evaporites messiniennes en Mediterranee orientale (coupe d'Eraclea Minoa, Sicile). Bull. Soc. Geol. France 7, 19, 3, 489-500, 1977.

Pierre, C. and Fontes, J.C., Isotope Composition of Messinian Sediments from the Mediterranean Sea as indicators of Paleoenvironments and diagenesis, Init. Reports DSDP, 42A, p. 635-650.

Rizzini, A. and Dondi, L., Erosional Surface of Messinian Age in the Subsurface of the Lombardian Plain. In: Messinian Erosional Surfaces in the Mediterranean (M.B. Cita and W.B.F. Ryan Editors), Marine Geology, 27, 303-325, 1978.

Rooth, C., Hydrology and Ocean Circulation. Some Possible Paleo-Oceanographic Scenarios. The Ewing Symposium, Abstracts, 29, 1978.

Ruggieri, G., The Miocene and Later Evolution of the Mediterranean Sea. Systematics Assoc. Publ. 7. In: Aspects of Tethyan Biogeography (C.G. Adams and D.V. Ager Editors), 283-290, 1967.

Ryan, W.B.F., Geodynamic Implications of the Messinian Crisis of Salinity. In: Messinian Events in the Mediterranean (C.W. Drooger Editor), 26-38, 1973.

Ryan, W.B.F., Messinian Badlands on the Southeastern Margin of the Mediterranean Sea. In: Messinian Erosional Surfaces in the Mediterranean (M.B. Cita and W.B.F. Ryan Editors), Marine Geology, 27, 349-367, 1978.

Ryan, W.B.F., Cita, M.B., Dreyfus Rawson, M., Burckle, L.H. and Saito, T., A Paleomagnetic Assignment of Neogene Stage Boundaries and the Development of Isochronous Datum Planes between the Mediterranean, the Pacific and Indian Oceans in Order to Investigate the Response of the World Ocean to the Mediterranean "Salinity Crisis". Riv. Ital. Paleont., 80, 4, 631-688, 1974.

Ryan, W.B.F. and Cita, M.B., The Nature and Distribution of Messinian Erosional Surfaces. Indicators of a Several-Kilometer-Deep Mediterranean in the Miocene. In: Messinian Erosional Surfaces in the Mediterranean (M.B. Cita and W.B.F. Ryan Editors), Marine Geology, 27, 193-230, 1978.

Ryan, W.B.F., Hsü, K.J. et al, Initial Reports of the Deep Sea Drilling Project, v. 13, 1-1447, U.S. Government Printing Office, Washington, D.C., 1973.

Ryan, W.B.F., von Rad, U. et al, Initial Reports of the Deep Sea Drilling Project, v. 47A U.S. Government Printing Office, Washington, D.C., in press.

Saito, T., Burckle, L.H. and Hays, J.F., Late Miocene to Pleistocene biostratigraphy of equatorial Pacific sediments, In: Late Neogene Epoch Boundaries (T. Saito and L.H. Burckle Editors) Micropaleontology Press Spec. Publ. 1, 226-244, 1975.

Salvatorini, G. and Cita, M.B., Miocene foraminiferal Biostratigraphy, DSDP Site 397. Init. Reports DSDP, 47A, in press.

Schlanger, S.O. and Douglas, R.G., The Pelagic Ooze-Chalk-Limestone Transition and its Implications for Marine Stratigraphy, Spec. Publ. IAS, 1, 117-148, 1974.

Schrader, H.J. and Gersonde, R., Messinian Diatoms, Leg 42A and their Paleoenvironmental Significance, Init. Reports DSDP, 42A, 1978.

Schreiber, B.C., Survey of the Physical Features of Messinian Chemical Sediments. In: Messinian Events in the Mediterranean (C.W. Drooger Editor), 101-110, 1973.

Selli, R., Il Mediterraneo nel Miocene superiore: un mare sovrasalato, Le Scienze, 56, 20-21, 1973.

Schackleton, N.J. and Cita, M.B., Oxygen and Carbon Isotope Stratigraphy of Benthonic Foraminifera in Site 397: Fine-Structure of Climatic Change in the Late Neogene, Init. Reports DSDP, 47A, in press.

Shackleton, N.J. and Opdyke, N.D., Oxygen-Isotope and Paleomagnetic Evidence for Early Northern Hemisphere Glaciation, Nature, 270, 216-219, 1977.

Sissingh, W., Aspects of the Late Cenozoic Evolution of the South Aegean Ostracode Fauna, Paleogeogr., Paleoclimatol., Paleoecol, 20, 131-145, 1976.

Sonnenfeld, P., The Upper Miocene Evaporite Basins in the Mediterranean Region, a Study in Paleo-Oceanography. Geol. Rundschau, 63, 1133-1172, 1974.

Stainforth, R.M., Lamb, J.L., Lutherbacher, H.P., Beard, J.H. and Jeffords, R.M., Cenozoic Planktonic Foraminiferal Zonation and Characteristic of Index Forms, The University of Kansas Paleont. Contrib., 62, 1-425, 1975.

Vail, P.R. and Mitchum, R.M., North Atlantic Sea-Level Changes, The Ewing Symposium, Abstracts, 41-42, 1978.

Van Couvering, J.A., Berggren, W.A., Drake, R.E., Aguirre, E. and Curtis, G.H., The Terminal Miocene Event, Marine Micropal., 1, 3,

263-286, 1976.
Van Donk, J., Saito, T., Shackleton, N.J., Oxygen Isotopic Composition of Benthonic and Planktonic Foraminifera of Earliest Pliocene Age at Site 132, Tyrrhenian Basin. Init. Reports DSDP, 13, 2, 798-800, 1973.
Vergnaud-Grazzini, C., Ryan, W.B.F. and Cita, M.B., Stable Isotopic Fractionation, Climate Change and Episodic Stagnation in the Eastern Mediterranean During the Late Quaternary, Marine Micropal., 2, 4, 353-370, 1977.
Weyl, P.K., The Role of the Oceans in Climatic Change: A Theory of the Ice Ages, Meteorological Monographs, 8, 30, 37-60, 1968.

# SEDIMENTARY ORIGIN OF NORTH ATLANTIC CRETACEOUS PALYNOFACIES

Daniel Habib

Department of Earth and Environmental Sciences
Queens College, Flushing, New York 11367

Abstract. Carbonaceous particles of terrestrial and marine origin are used to define four sedimentary palynofacies in Cretaceous sections cored in the North Atlantic. The exinitic facies contains sporomorph assemblages and structured palynodebris compositionally close to those in coeval fluviodeltaic sediments on continents bordering the North Atlantic, and it is concluded that they were deposited by turbidity currents near a deltaic source. The tracheal facies is of similar origin, except that marine currents sorted sporomorph species and admixed dinoflagellates prior to deposition. Both the xenomorphic and micrinitic facies contain dinoflagellates, bisaccate pollen, Classopollis and abundant amorphous palynodebris. Xenomorphic palynodebris is unknown palynologically, but is associated with pelagic lithology. Micrinitic palynodebris is considered to be the carbonized (fusinized?) woody tissue of land plants which were carried into offshore areas of the Cretaceous North Atlantic. The micrinitic facies in black shales reflects the much diminished supply of terrigenous organic detritus, most of which is micrinitic palynodebris.

The stratigraphic distribution of palynofacies is compared with published organic carbon data. Higher carbon percentages are associated with the exinitic and tracheal facies, which indicates that the increased carbon content was derived from land plants during episodes of increased deltaic activity. The occurrence of dinoflagellates in the latter palynofacies requires the admixture of marine carbon, however. The darker color of the black shales may be due to the nature of the micrinitic palynodebris rather than total carbon content alone.

Evidence is presented for episodes of increased deltaic activity during the Valanginian, Barremian-early Aptian, and late Aptian/early Albian.

## Introduction

Detrital carbonaceous particles are common in sections of Early Cretaceous-Cenomanian age drilled in the North Atlantic by the Deep Sea Drilling Project. They include the fragmented and dispersed materials of land plants, organic-walled cysts produced by marine microflora, and amorphous particles. Palynological study of the section recovered at D.S.D.P. site 398, located near the eastern margin of the North Atlantic (Figure 1), showed that it differed from that reported from sections in the western North Atlantic (Habib, in press). The purpose of this study is to re-examine two sections drilled near the western margin, at D.S.D.P. sites 105 and 391, so that the distribution of palynomorphs and palynodebris at the three sites can be explained in terms of sedimentary processes.

## Stratigraphy

Site 398 was drilled in the Galicia Region adjacent to the Iberian Peninsula, just south of Vigo Seamount. The investigated section is 795 meters thick and, on the basis of Foraminifera (Sigal, in press) and nannofossils (Blechschmidt, in press), ranges in age from late Hauterivian to Cenomanian. According to Ryan, Sibuet, et al., (in press) limestones were deposited during the Hauterivian on a seafloor of moderate depth, onto which there were periodic contributions of terrigenous mud and carbonaceous debris. Sedimentation rates of approximately 10 meters/million years are consistent with the pelagic setting of this environment. Turbiditic mudstones, siltstones, and sandstones were deposited during the Barremian-early Aptian in response to prodeltaic or submarine fan processes. The decrease in grain size of terrigenous sediment above the turbidite sequence reflects the waning of turbidity current activity during the late Aptian. Sedimentation rates for the Barremian-Aptian interval are estimated on the order of 100 meters/million years (Ryan, Sibuet et al., in press). They were still high during the early and earlier middle Albian when dark laminated shales were deposited, which may represent cycles of turbiditic sedimentation. In the middle Albian and Cenomanian the proportion of terrigenous clay and silt decreased so that by late Albian calcareous sediments were predominant and the rate of sedimentation was reduced to approximately 15.5 meters/million years.

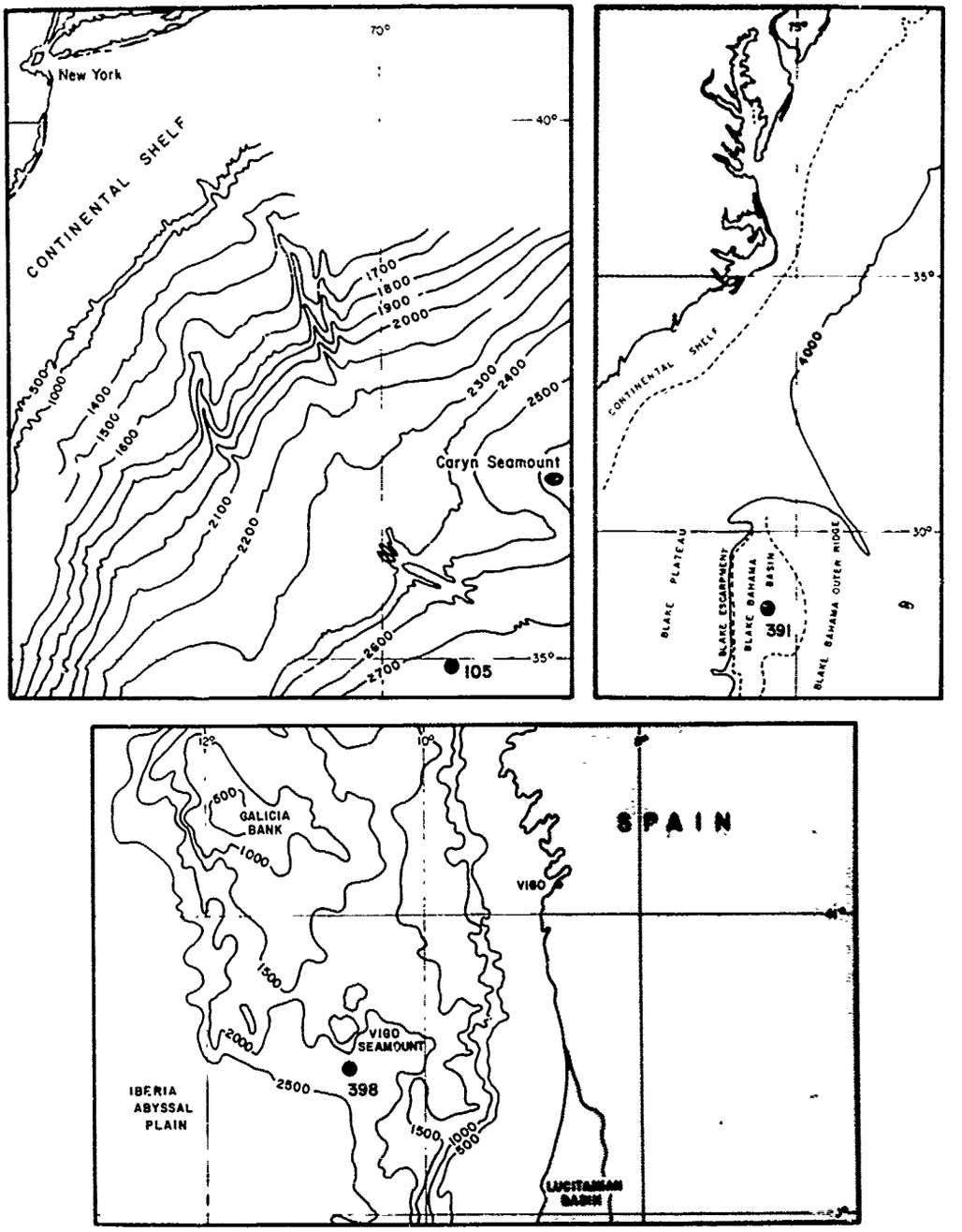


FIGURE 1 - GEOGRAPHIC LOCATIONS OF SITES 105, 391, AND 398.

The sedimentary history of the western North Atlantic sections differs from that described for site 398. In these sections, dated on the basis of dinoflagellate stratigraphy, middle Cretaceous black shales overlie Neocomian nannofossil limestones; evidence of the large scale and rapid sedimentation found at site 398 is lacking. Site 391 was drilled in the Blake-Bahama Basin (Figure 1). The investigated part of the section is 579 meters thick and ranges in age from Berriasian to late Albian. According to Benson, Sheridan, et al., (1978) Berriasian and early Valanginian bioturbated calcilutites and clays were deposited on a well-oxygenated seafloor. Later in the Neo-

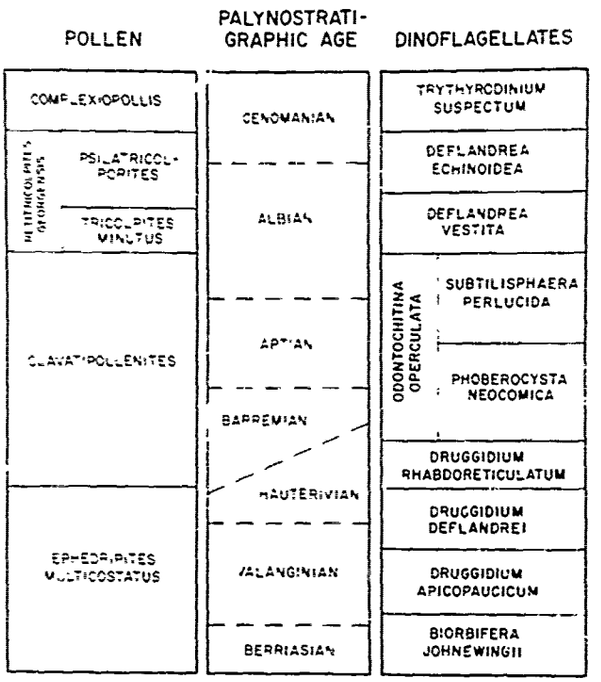


FIGURE 2 - PALYNOSTRATIGRAPHIC AGE OF PALYNOMORPH ZONATIONS IN THE WESTERN NORTH ATLANTIC (after Habib, 1977)

comian, calcareous sediments accumulated which included black clay laminites suggesting a periodicity in terrigenous sedimentation. In the Barremian-early Aptian interval thin, black, cross-laminated, terrigenous turbidites were deposited along with turbiditic limestones containing ooliths derived from a carbonate shelf. Nannofossils were deposited through the late Aptian-early Albian in calcareous claystones. These dark gray to black sediments indicate the increase of turbidity current deposition, and include thin intervals of cross-laminated mudstones. The calcareous claystone interval is transitional from the older, primarily calcareous, sediments to the Albian time of blackish claystones which lack carbonates.

Average sedimentation rates for the Berriasian-Albian sequence at site 391 are estimated to range from 28 meters/million years in the Neocomian to 11 meters/million years in the middle Cretaceous (Benson, Sheridan, et al., 1978).

Site 105 was drilled in the Lower Continental Rise hills at their margin with the Hatteras Abyssal Plains (Hollister, Ewing, et al., 1972). The investigated section is 245 meters thick, which is less than half as thick as that at site 391, and ranges in age from Berriasian to Cenomanian. Middle Cretaceous black shales grade abruptly to Neocomian clayey limestones (Lancelot et al., 1972). The sedimentary history of section 105 is essentially the same as that of section 391C. Bioturbated white limestones were deposited on a well-oxygenated seafloor during the Berriasian and Valanginian. Organic-rich clay laminae alternated with limestones and became progressively more frequent through the Early Cretaceous, during which the periodicity of these deposits became well-defined. During the Barremian-early Albian (Odontochitina operculata Zone of Figure 2), the carbonaceous layers became more abundant and graded through a sharp transition zone (Lancelot et al., 1972) to black shales of Albian and Cenomanian age. Sediments accumulated at rates ranging from 8 meters/million years in the Neocomian to 5 meters/million years in the middle Cretaceous.

## Palynology

The palynology of sections cored at six sites in the western North Atlantic was studied previously to correlate palynostratigraphic zonations of Early Cretaceous-Cenomanian age (Habib, 1977). The zonations are illustrated on Figure 2, and were used to date the sections from sites 391 and 105 (Figures 4 and 5).

Dinoflagellate cysts are numerous and diverse through most of the sections in the western North Atlantic. Sporomorphs are equally abundant, and even more so in some samples, but are not as diversified. Rather, the coniferous pollen Classopollis, Pinuspollenites, and Alisporites are dominant through most of each section. In contrast, the section at site 398 contains a rich and diversified sporomorph flora, including many species of fern and other pteridophyte spores in addition to coniferous pollen, and generally few dinoflagellates. However, dinoflagellates are abundant in samples of late Hauterivian age in section 398D (Figure 3). In the Albian-Cenomanian part of the section, dinoflagellates occur in a number of species. Each species is represented by only a few specimens, however.

Description of Palynofacies. One hundred and forty-two samples were macerated. Each sample was treated with hydrochloric and hydrofluoric acids to remove the mineral sediment, and subsequently with nitric acid to partially oxidize the organic matter. The residue was treated so that the number of specimens per gram of sediment was calculated (Habib, in press). The darker-colored lithologies were macerated for the most part. These included the black laminated layers in the Neocomian-Aptian nannofossil limestones, the Albian-Cenomanian black shales, and the turbiditic sequence at site 398.

The organic contents were examined to determine the stratigraphic variation of their constituent particles. These included the spores and pollen grains (sporomorphs) and cuticles and tracheids (structured palynodebris) of land plants, the dinoflagellate cysts and small acritarchs representing marine organic-walled phytoplankton, and

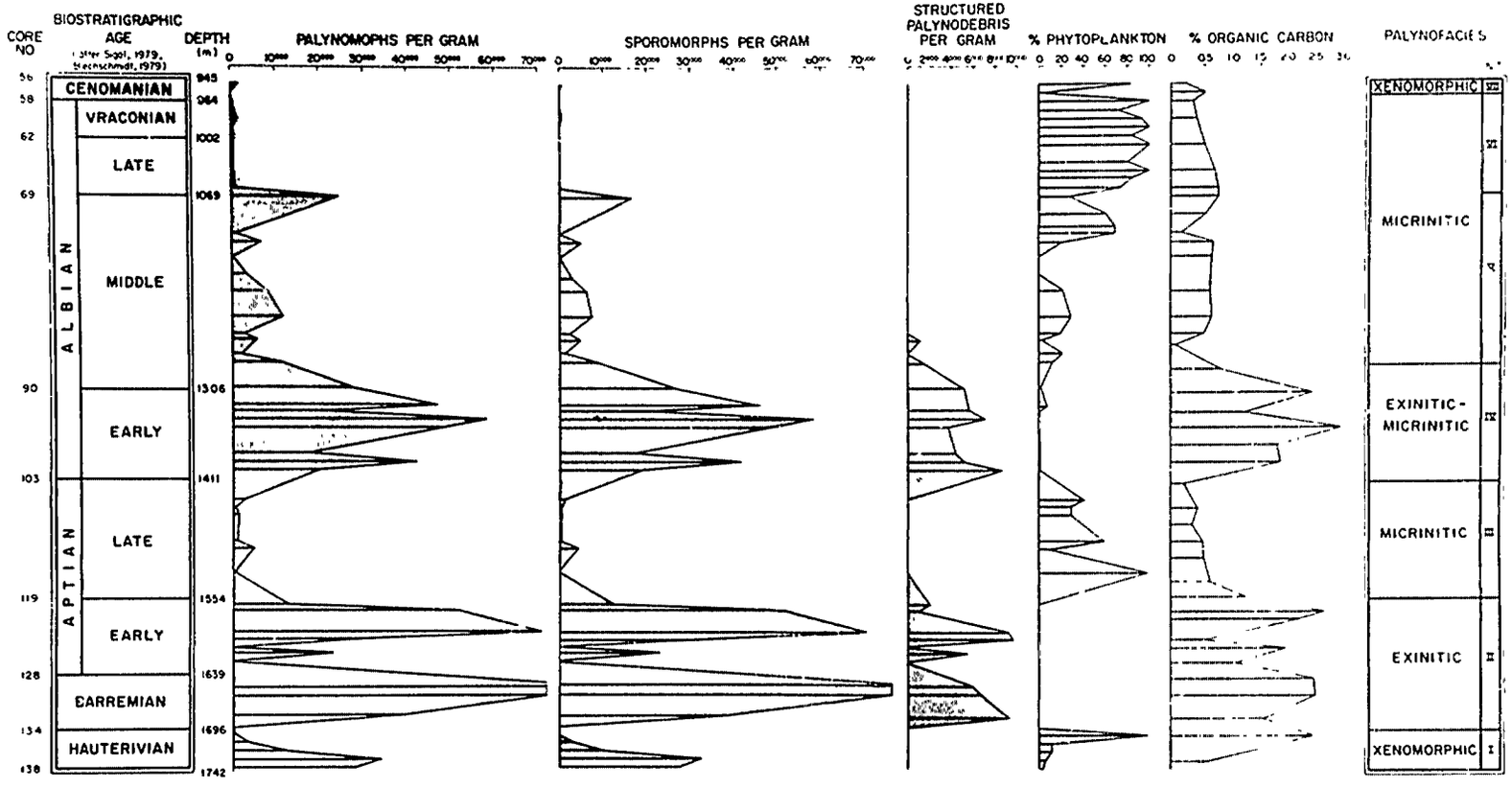


FIGURE 3 - DISTRIBUTION OF PALYNOMORPHS AND PALYNODEBRIS AT SITE 398

GALICIA REGION

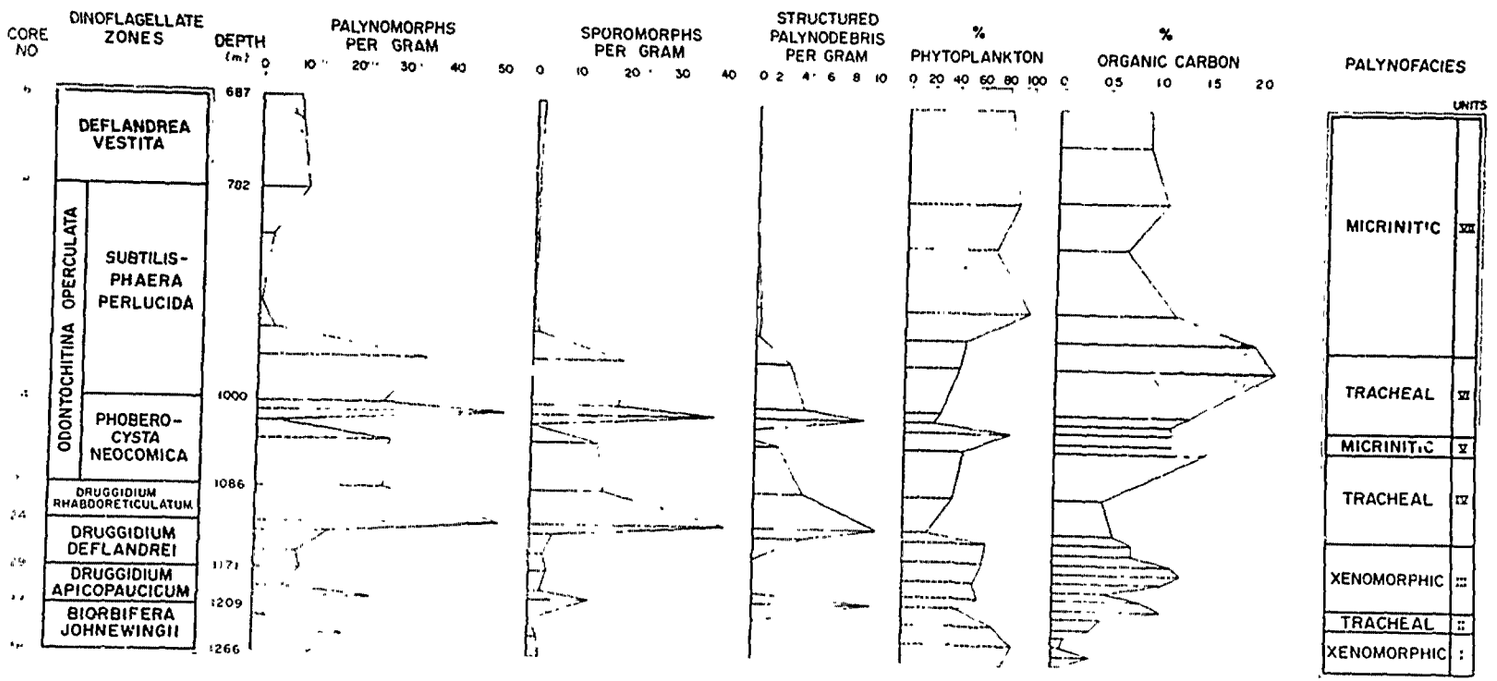


FIGURE 4 — DISTRIBUTION OF PALYNOMORPHS AND PALYNODEBRIS AT SITE 391
BLAKE-BAHAMA BASIN

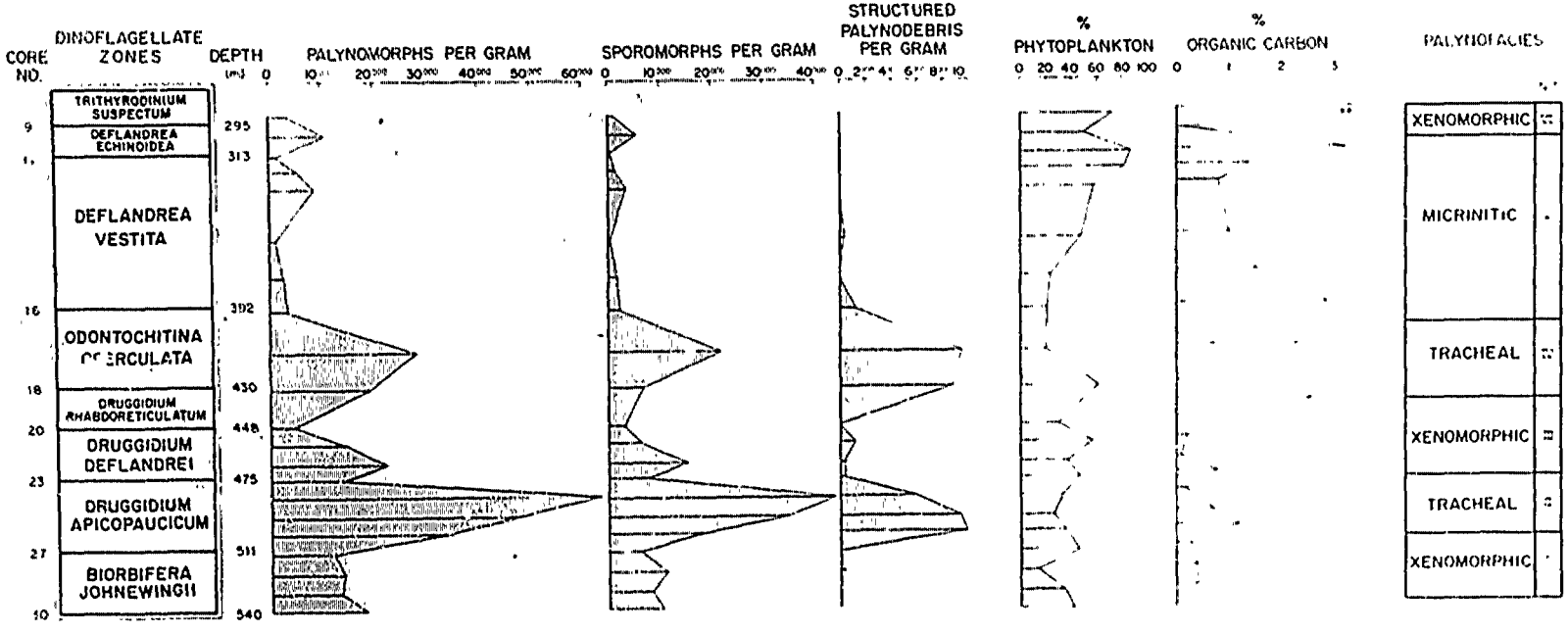


FIGURE 5 – DISTRIBUTION OF PALYNOMORPHS AND PALYNODEBRIS AT SITE 105
LOWER CONTINENTAL RISE HILLS

amorphous organic particles (amorphous palynodebris). Amorphous palynodebris is usually the most abundant organic constituent in the samples where it occurs.

Figures 3-5 show the stratigraphic distributions of all palynomorphs (sporomorphs + phytoplankton), sporomorphs, and structured palynodebris on the basis of specimens per gram of dried sediment calculated for each sample. These profiles are compared with the percentage of phytoplankton determined from the total palynomorphs, and the weight percentage of organic carbon. The organic carbon profiles were derived from data contained in the Initial Reports volumes published for sites 105, 391, and 398. Where there were a number of samples analyzed from a single core, the two highest values were averaged and plotted.

The discrete particles comprising the organic residues are not randomly distributed in the investigated sections but rather are distributed in assemblages forming palynofacies (Combaz, 1964), which were deposited by marine currents (cf. Manum, 1976). Four such palynofacies are distinguished. These are named exinitic, tracheal, micrinitic, and xenomorphic.

The exinitic facies is defined by the abundance and diversity of sporomorphs and structured palynodebris in the sediments, and the absence or extreme paucity of marine phytoplankton (Plate 1, Figures 1,3,6). There are many sporomorph species in the assemblages, which are characterized by striate schizaeaceous spores and other relatively large and well-ornamented pteridophyte species (Plate 2, Figures 1-4, 6,7,9). Plant cuticles and tracheids are also diverse and, together with the sporomorphs, are well-preserved.

The tracheal facies is similar to the exinitic facies, insofar as both contain numerous sporomorphs and structured palynodebris (Plate 1, Figures 7-8). The palynomorph assemblages of the tracheal facies differ in two important respects, however.

First, the marine phytoplankton are always well-represented. They never comprise less than 16% of the palynomorphs, and reach as high, in one sample from site 105, as 60%. Second, although sporomorphs are almost always more abundant than phytoplankton they are dominated by relatively few species, principally Classopollis torosus Reissinger and bisaccates in Pinuspollenites and Alisporites. The larger and well-ornamented pteridophyte spores characteristic of the exinitic facies are very rare or absent.

The xenomorphic facies is characterized by the abundance of amorphous palynodebris with neither visible internal structure nor consistent external form, but which is optically translucent and which stains in red safranin solution. Two kinds of xenomorphic debris occur in the samples; globular particles of which most are larger than 50 microns in diameter and which occur typically in the Cenomanian black shales at sites 105 and 398 (Plate 1, Figure 4), and smaller (less than 15 microns) particles with an irregular shredded appearance and which are typical of the clays within the Neocomian nannofossil limestones (Plate 1, Figure 5). The number of palynomorphs per gram of sediment is variable. The palynomorph assemblages are dominated by dinoflagellates, small acritarchs, Classopollis and the bisaccate genera Pinuspollenites and Alisporites (Plate 2, Figures 5 and 8). The xenomorphic facies is similar to the tracheal facies, especially in those samples where palynomorphs are abundant. It differs by its lack of structured palynodebris and by its abundance of amorphous (xenomorphic) palynodebris. It differs from the exinitic facies by its lack of a diverse sporomorph flora, occurrence in all the samples of relatively high percentages of marine phytoplankton, absence of structured palynodebris, and abundance of xenomorphic palynodebris.

The micrinitic facies is defined by the overwhelming abundance of amorphous palynodebris (Plate 1, Figure 2) and meager palynomorph assemblages dominated by Classopollis and/or species of bisaccate pollen. The principal characteristic of this facies is the occurrence of numerous, relatively small, apparently structureless, black or dark brown, opaque or semi-opaque particles without consistent external form but of which some at least have a polygonal outline with sharp corners. The palynofacies is otherwise similar to those samples of the xenomorphic facies containing few palynomorphs.

The micrinitic facies differs from the three other palynofacies in another respect. Palynomorphs are fairly well-preserved in the exinitic, tracheal, and xenomorphic facies. In the micrinitic facies, there is almost always a portion of each palynomorph assemblage consisting of badly corroded or otherwise poorly preserved specimens. Samples containing the micrinitic facies can usually be recognized when they are being prepared for examination with the microscope because of the dark color the micrinitic palynodebris imparts on the glass microscope slides.

## Section 398D

Section 398D is characterized by major fluctuations in the abundance of palynomorphs, most of which are the pollen grains and spores of land plants (Figure 3). In the highly palynifercus samples, palynomorphs are represented almost exclusively by numerous specimens and species of sporomorphs. It is only in those samples where palynomorphs are fewest that there are high relative percentages of dinoflagellate cysts and small acritarchs. Sporomorphs are abundant within palynostratigraphic units I (xenomorphic facies), and II and IV (exinitic facies). They are relatively few in the micrinitic facies of unit VI and the xenomorphic facies of unit VII. The exinitic and micrinitic facies form recurrent palynostratigraphic sequences in the interval dated as Barremian-middle Albian. The first exinitic-micrinitic cycle is represented in units II and

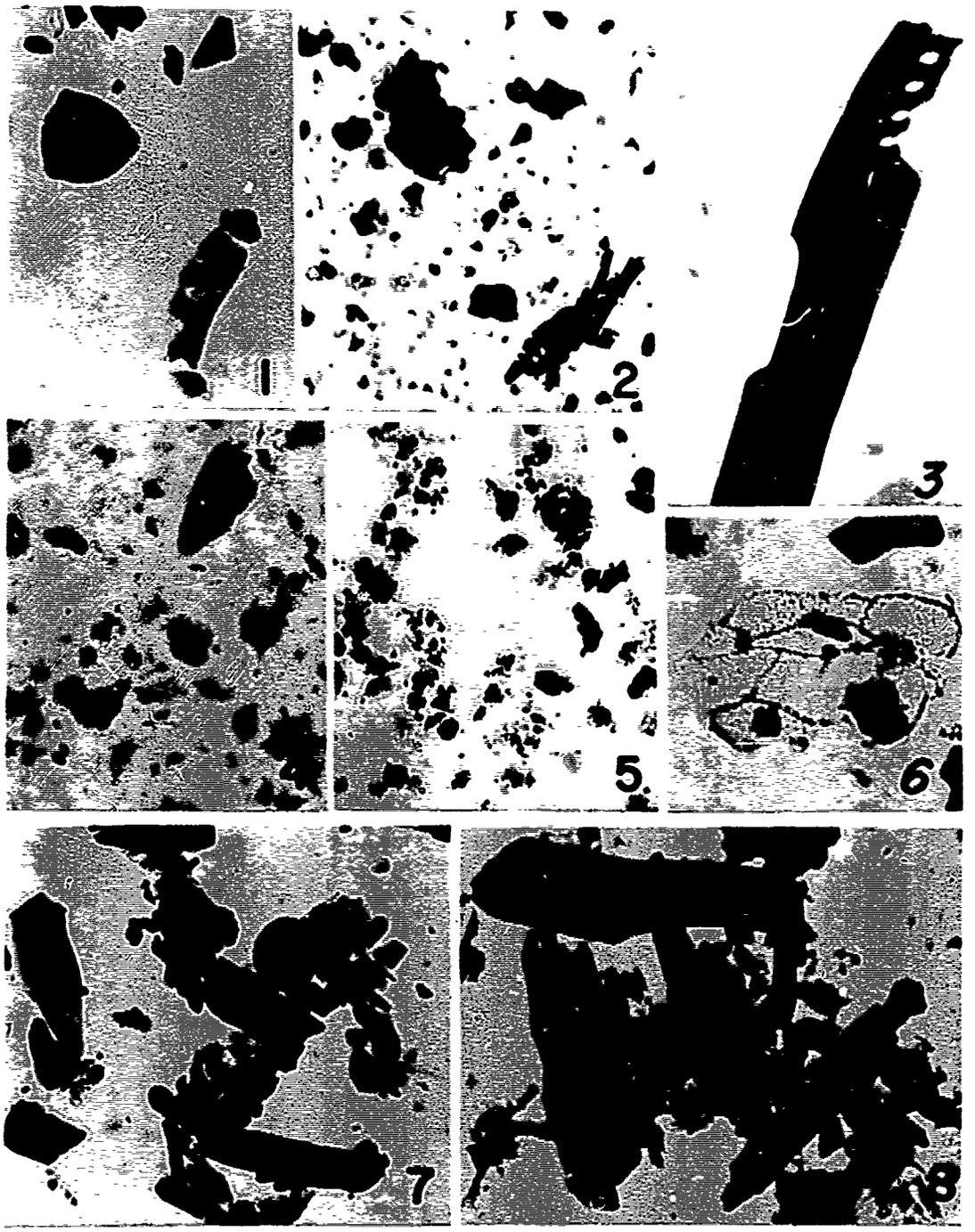


PLATE I

Plate 1. Palynofacies. Exinitic facies. Figure 1, schizaeaceous fern spore and tracheid with bordered pits. Figure 3, tracheid. Figure 6, plant cuticle. Micrinitic facies. Figure 2, black angular, amorphous palynodebri . Carbonized tracheid (?) in lower right corner. Xenomorphic facies. Figure 4, globular amorphous palynodebris. Figure 5, shredded amorphous palynodebris. Tracheal facies. Figure 7, tracheids and specimen of sporomorph genus Classopollis. Figure 8, numerous tracheids.

III of Barremian-Aptian age, and is followed by the second cycle in units IV and V of early Albian-middle Albian age. In units VI and VII of late Albian-Cenomanian age, palynomorphs are very few, and the assemblages are composed of between 68% and 100% phytoplankton regardless of the type of amorphous palynodebris. The xenomorphic facies of the late Hauterivian unit I is unique for section 398D, as it contains an abundant Classopollis- bisaccates sporomorph flora as well as a diverse and abundant dinoflagellate flora.

The xenomorphic facies in section 398D is characterized by the abundance of xenomorphic palynodebris of two types. The lower part of unit I contains an abundance of relatively small (15 microns), shredded, xenomorphic palynodebris and abundant palynomorphs. Palynomorphs vary between 3,586 and 34,943 specimens/gram and are dominated by Classopollis torosus, Alisporites bilateralis Rouse, and species of Pinuspollenites, which together comprise between 67% and 74% of the assemblages. The assemblages also contain a number of dinoflagellate species, small acritarchs, and other, smaller, sporomorphs occurring in minor percentages throughout the section, such as Cyathidites minor Couper, Exesipollenites tumulus Balme, Ginkgocyadophytus nitidus (Balme), Ephedripites multicostatus (Brenner), and Eucommiidites minor Groot and Penny, for example. The xenomorphic facies of the upper part of unit I and of unit VII differs in the overwhelming abundance of the larger, globular appearing, xenomorphic palynodebris and the paucity of palynomorphs. Palynomorphs vary from 0 (none observed) to 153 specimens/gram in the upper part of unit I, of which all are small acritarchs. Palynomorphs are very few in unit VII as well, averaging 764 specimens/gram, and composed mostly of phytoplankton which range between 68% and 100%.

The bulk of section 398D is composed of the exinitic and micrinitic facies (Figure 3). The exinitic facies is represented in units II and IV. Unit II contains the greatest number of sporomorphs, sporomorph species, and structured palynodebris in the section. An average of 48, 636 sporomorphs/gram was calculated for this interval, with a maximum number of 88,485/gram. Tracheids and cuticles vary between 945 and 9,625 specimens/gram but average as high as 6,100. The assemblages contain Classopollis and bisaccates, which range between 26% and 43%, but are distinguished by a large number of sporomorph species of pteridophyte spores. Between 39 and 50 sporomorph species were found in the samples, including as examples Densoisporites microrugulatus Brenner, Trilobosporites marylandensis Brenner, Dictyophyllidites equiexinus (Couper), Concavissimisporites punctatus (Delcourt and Sprumont), Pilosisporites trichopapillosus (Thiergart), and Converrucosisporites exquisitus Singh, as well as species of Murospora, Aequitriradites, Neoraistrickia, Foveotriletes, and Microreticulatisporites among others, which are generally absent in the section outside of the exinitic facies. As an example, the striated schizaeaceous fern spores Cicatricosisporites, Costatoperforosporites, and Appendicisporites alone account for an average of 28% of all sporomorph species in the samples.

In addition to the abundance and diversity of sporomorphs and structured palynodebris, there is also the increased occurrence of fungal spores, multicellular fossils of possible algal origin, and tetrads of Classopollis and Leptolepidites. Marine phytoplankton are virtually absent in this interval; a single specimen of Druggidium deflandrei (Millioud) was recorded.

Within unit II there are several samples containing xenomorphic palynodebris. Several samples contain abundant amorphous palynodebris and no palynomorphs.

The exinitic facies of unit IV is essentially the same as that of unit II, except that the total number of specimens/gram is somewhat less, and there is an interval within the unit characterized by the micrinitic facies. For example, sporomorphs average 27,449 per gram, and reach a high of 58,990. Pteridophyte spores and structured palynodebris are still important elements in the assemblages, and marine phytoplankton are virtually absent.

The micrinitic facies is distributed through units III, V, and VI. Micrinitic palynodebris is the single-most abundant organic constituent of the three intervals. Palynomorphs are relatively few in the samples, averaging 1803 per gram in unit III, 7050 in unit V, and 505 in unit VI. For the majority of samples, palynomorphs are fewer than 1,000 specimens per gram. However, in one sample the number of 24,900 specimens per gram was calculated. The assemblages are characterized by higher percentages of phytoplankton and a sporomorph flora dominated by Classopollis and bisaccate pollen. Other sporomorphs include species of Cyathidites, Ginkgocycadophytus, Eucommiidites, Exesipollenites, and others distributed sporadically through the section and, in units V and VI, minor amounts of triaperturate angiosperm pollen. In those samples where palynomorphs are more frequent, there is a larger proportion of sporomorphs; where they are the fewest, phytoplankton predominate. The micrinitic facies characterizes both of the stratigraphically contiguous units V and VI. They are separated on the basis of the greater numerical occurrence of sporomorphs in the lower unit. Sporomorphs are extremely rare in unit VI, where phytoplankton form between 67% and 100% of the very few palynomorphs present, and average 89%.

## Sections 391C and 105

The palynostratigraphy of sections 391C and 105 are similar with respect to the sequence of palynofacies (Figures 4 and 5). Both show an alternation of xenomorphic and tracheal facies in the lower part, an interval above where the tracheal facies is especially well-represented, and an

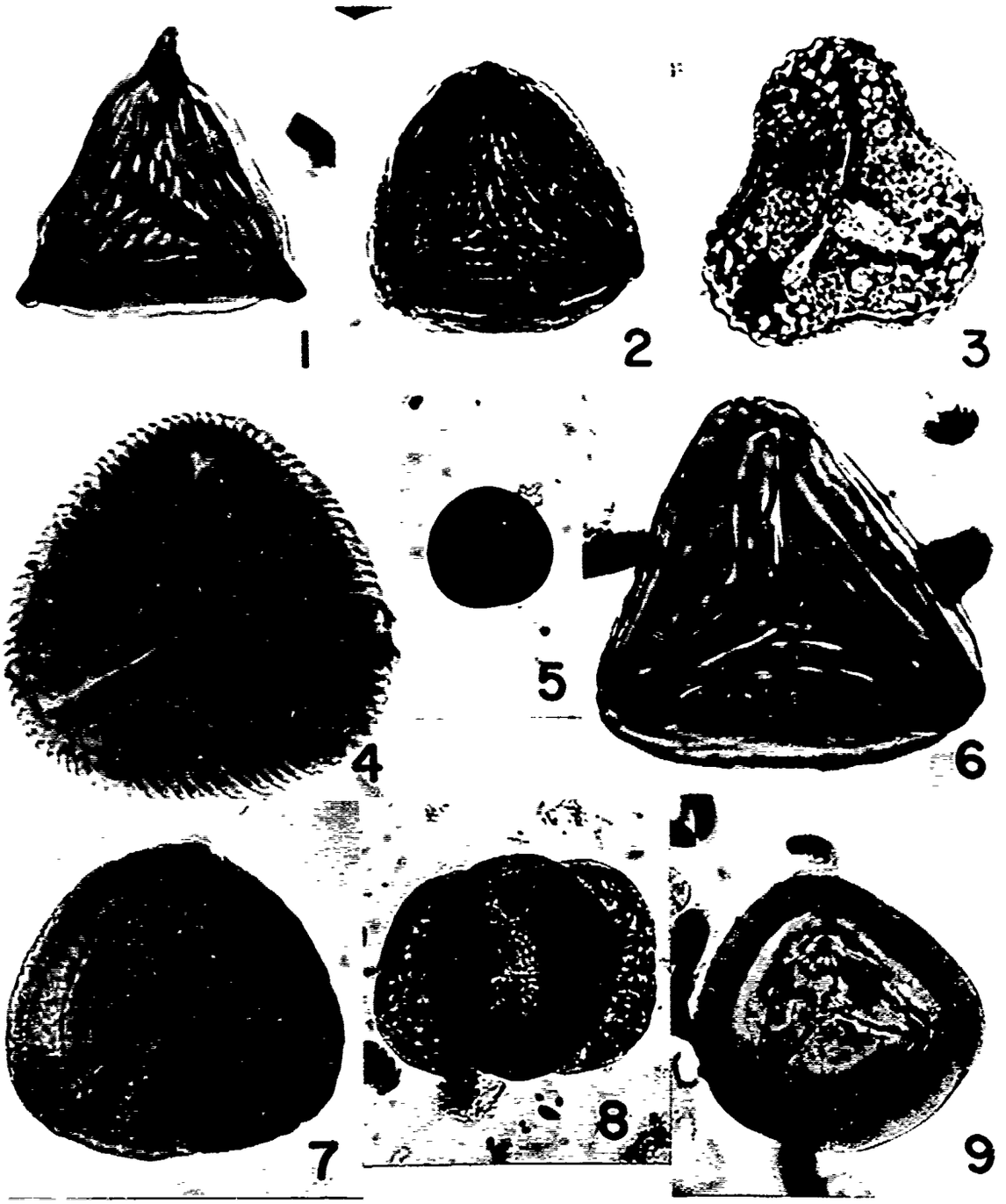


PLATE 2

Plate 2. Sporomorphs. Lower vascular plant spores characteristic of exinitic facies. Figures 1, 2, 4, 6, spores attributed to fern family Schizaeaceae. Figure 3, fern spore. Figures 7 and 9, spores attributed to the club mosses (Microphyllophyta). Pollen grains representative of the xenomorphic, micrinitic, and tracheal facies. Figure 5, specimen of Classopollis. Figure 8, bisaccate pollen genus Pinuspollenites.

overlying micrinitic interval. Section 105 differs in that it contains an additional younger interval (Deflandrea echinoidea and Trithyrodinium suspectum zones) characterized by the xenomorphic facies. Both sections also show major fluctuations in the abundance of palynomorphs, which is similar to that of section 398D. The western North Atlantic sites differ from site 398 markedly, however, in two important respects. First, they virtually lack the abundance and diversity of the larger and well-ornamented pteridophyte spores which characterize the exinitic facies of section 398D. Although there are intervals, e.g., tracheal facies, containing abundant sporomorphs and structural palynodebris in parts of these sections, two parameters which correlate it with the exinitic facies of section 398D, the sporomorph dominance is caused by increased numbers of Classopollis and bisaccate pollen rather than by the pteridophyte spores. Consequently, there are fewer sporomorph species in the tracheal facies, approximately one-half the number occurring in the exinitic facies. Second, in contrast to the palynology of site 398, marine phytoplankton are well-represented in all samples at sites 391 and 105. In most samples, they comprise between 40% and 100% of the palynomorph assemblages, and in only a few do they fall below 20%. The dinoflagellate flora is especially well-represented. Most of the dinoflagellate species have previously been described from Cretaceous epeiric and marginal marine facies on continents bordering the North Atlantic.

Both sections possess a rather monotonous and long-ranging sporomorph flora dominated by Classopollis and bisaccates, with subordinate percentages of other gymnospermous pollen and smaller pteridophyte spores distributed sporadically through the sections. Only a few of these species, e.g., Exesipollenites tumulus, Cyathidites minor, become relatively abundant in isolated smaples. Triaperturate angiosperm pollen grains occur in the higher parts of the sections. Striate schizaeaceous spores are extremely rare or absent. Within section 391C only two species, Cicatricosisporites hughesii Dettmann and C. potomacensis Brenner, are rare but stratigraphically persistent. In general, the palynology of section 391C appears to be more diverse than that of 105. There are both more sporomorph species and dinoflagellate species on the average. For example, the ceratioid dinoflagellates Muderongia, Phoberocysta, and Pseudoceratium are present in section 391C but not in 105.

Sporomorphs tend to be more numerous in the highly palyniferous samples of both sections. The phytoplankton occur in highest percentages in those samples containing fewest palynomorphs.

Section 391C. Seven palynostratigraphic units were distinguished in section 391C, based on the sequence of palynofacies (Figure 4). The xenomorphic facies occurs within units I and III. It is characterized by the shredded variety of amorphous palynodebris in both intervals. In unit I, palynomorphs average 10,533 specimens/gram, ranging from a low value of 1,783 to the maximum of 18,050. Despite the variation in numbers of palynomorphs, they are always dominated by marine phytoplankton which comprise between 73% and 89% of the assemblages. The number of palynomorph species in unit I is small, between 10 and 14, of which the number of dinoflagellate species is always the largest. The palynology of unit III is essentially the same. The average abundance is 9,689 palynomorphs/gram, of which between 58% and 68% are dinoflagellates and small acritarchs. The number of species per sample is higher, however, ranging from 8 to 20. Sporomorphs are better represented also, most of which are specimens of Classopollis torosus.

The tracheal facies is represented by a single core, 391C-32, producing the thin interval of unit II, and through the much larger collective interval of units IV and VI. In unit II, 23,369 palynomorphs/gram was calculated. Twenty-three species were counted of which 16 sporomorph species accounted for 54% of all palynomorphs. Classopollis-bisaccates comprise 38% of all palynomorphs. The most striking feature of unit II, however, is the abundance and diversity of structured palynodebris. Relatively large and well-preserved cross-pitted tracheids occur together with several varieties of cuticle. The structured palynodebris was calculated at 10,224 specimens/gram, but because of the prominence of the larger tracheids, appeared more numerous than the palynomorphs. Some fine xenomorphic palynodebris was also observed, but in very small amounts.

The tracheal facies of units IV and VI are very similar in both the composition and abundance of palynomorphs and palynodebris. Units IV and VI are separated by the very thin interval of unit V containing the micrinitic facies. Collectively, the interval of units IV-VI occupies approximately 180 meters in thickness, or approximately 31% of the investigated section. Both units IV and VI are characterized by the largest amounts of both palynomorphs and structured palynodebris in their lowest parts. For example, in unit IV the average number of palynomorphs/gram is 33,903, but the largest number calculated is in the lowest sample, with 48,994 palynomorphs/gram. Structured palynodebris averages 7,212 per gram, but again reaches a maximum in this sample of 9,612 per gram. The same is evident for other parameters. Although the number of palynomorph species remains constant through unit IV, between 20 and 21, the number of sporomorphs is the highest, where they comprise 80% of all palynomorphs. In the other samples, they range between 53% and 57% of palynomorphs. Classopollis and bisaccate pollen comprise 68% of all palynomorphs in the lowest sample, and are approximately 40% in the remainder. In addition, the lower part of unit IV is devoid of shredded xenomorphic material, whereas in the upper part it occurs in small amounts.

In unit VI, the number of palynomorphs/gram averaged 36,101 but, again, the highest value, 49,317 palynomorphs/gram, was recorded from the lowest sample. The number of palynomorph species ranges from 21 to 25 through this unit, although the largest proportion of sporomorphs, 75% of the assemblage, was recorded from the lowest sample. Classopollis-bisaccates comprise 54% of the assemblage in this sample, and range between 37% and 41% in the other samples. The structured palynodebris shows the same trend. As many as 8,612 specimens/gram occur in the lowest sample, with the average for the unit being 5,200/gram. Also, xenomorphic material was observed in the upper part of the unit only.

In both units IV and VI, other sporomorphs include the sporadically distributed smaller pteridophyte spores and gymnospermous grains. The dinoflagellate flora of both units is represented by a number of species, each represented by few specimens.

The micrinitic facies in section 391C is represented in units V and VII (Figure 4). Unit V is represented by a single sample. Of the 4,190 palynomorphs/gram in this sample, 96% are marine phytoplankton. Ten species were found in the palynomorph assemblage, of which eight are phytoplankton. The only sporomorph species encountered were Classopollis torosus and Alisporites bilateralis. The residue is otherwise characterized by abundant micrinitic palynodebris.

Unit VII is the thickest single palynostratigraphic interval within the section. It contains abundant micrinitic palynodebris and relatively few palynomorphs. The number of palynomorphs/gram averages 5,137 and ranges from 484 to 9,348. Although the abundance of palynomorphs increases towards the top of unit VII, and thus towards the top of the investigated section, they are dominated by marine phytoplankton throughout. The phytoplankton range between 72% and 100%, but average 87%. The number of species observed is also small, between 2 and 14.

Section 105. Six palynostratigraphic units were distinguished in section 105 (Figure 5). The xenomorphic facies is distributed through units I, III, and VI. Unit I is characterized by abundant xenomorphic palynodebris of the shredded kind. Palynomorphs range from 12, 320 to 18,156 specimens/gram and average 14,617. The palynomorph flora is dominated by very high percentages of Classopollis, bisaccates, and marine phytoplankton. Although the phytoplankton average only 40% in the assemblages, Classopollis, Pinuspollenites, and Alisporites collectively average an additional 53% of all palynomorphs. The number of palynomorph species ranges between 14 and 17. The palynofacies of unit III very closely resembles that of unit I. In unit III, for example, the amount of palynomorphs averages 14,273 per gram although there is a larger range, from 4,857 to 24,344. Palynomorph species range in the samples from 8 to 18. Like unit I, the assemblages are dominated by marine phytoplankton and Classopollis-bisaccates, which together range from 81% to 90% of all palynomorphs. In both units I and III the dinoflagellate flora is diverse, although there are relatively few specimens of each species. The sporomorph flora contains species such as Ephedripites multicostatus, Exesipollenites tumulus, and Gleicheniidites senonicus which range in low percentages through most of the section.

In contrast to units I and III, unit VI possesses a xenomorphic facies composed of abundant globular amorphous palynodebris. The abundance of palynomorphs varies between 3,264 and 10,710 specimens/gram of which between 48% and 71% are phtoplankton and between 5% and 41% are species of bisaccate pollen. No specimens of Classopollis were counted. The number of species ranges from 10 to 16; this includes a number of angiosperm pollen.

The tracheal facies occurs in units II and IV. In both units, it is characterized by numerous palynomorphs of which the larger proportions are sporomorphs, abundant structured palynodebris, and minor amounts of shredded xenomorphic palynodebris. Unit II contains the largest number of specimens in section 105. Palynomorphs average 50,349 per gram, with a maximum value of 68,765. There is also a larger number of palynomorph species, between 25 and 29. The assemblages are dominated by sporomorphs, which account for between 64% and 73% of all palynomorphs. Classopollis-bisaccates comprise between 44% and 55% of all palynomorphs; with marine phytoplankton comprising another 27%-36%. The palynomorph assemblages contain a rich dinoflagellate flora, and most of the smaller sporomorph species which range through much of the section. Despite the abundance of sporomorphs, striate schizaeaceous spores and other larger and/or well-ornamented species of pteridophyte spores are absent. For example, of the 1,958 specimens counted on the slides only one specimen of Cicatricosisporites hughesii and one of Dictyophyllidites equiexinus were found. Structured palynodebris is also abundant and diverse. This palynodebris averages 7,100 specimens/gram in the samples.

The tracheal facies of unit IV contains fewer specimens, fewer species, and a greater proportion of marine phytoplankton than that of unit II, but contains about as much structured palynodebris. In the lower part of unit IV, there are 19,200 palynomorphs/gram of which only 34% or 6,528 are sporomorphs. However, it also contains 8,412 specimens of cuticles and tracheids per gram. The dinoflagellates and small acritarchs are represented by seven species, and the sporomorph by ten. Classopollis, bisaccate pollen, and marine phytoplankton together account for 92% of all palynomorphs. In the upper part, there are 28,307 palynomorphs/gram, of which 78% are sporomorphs, and 9,400 specimens/gram of structured palynodebris. There are 22 palynomorph species in an assemblage dominated by

Classopollis, bisaccates, marine phytoplankton and the less prominent pollen and spores. Unit IV is devoid of any of the more structured pteridophyte spores.

The micrinitic facies occurs within a single palynostratigraphic unit which is the thickest in section 105. Unit V is similar to the others containing this palynofacies. It contains abundant micrinitic palynodebris and few palynomorphs, most of which are marine phytoplankton. Palynomorphs average only 3,810 per gram in the samples, and range from a low of 1,124 specimens/gram to a high of 8,976 per gram. There are fewer palynomorphs and a larger proportion of sporomorphs in the lower part of unit V. Towards the top, palynomorphs become more numerous, most of which are marine phytoplankton.

## Conclusions

Section 398D. Except for the xenomorphic facies, there is a close correspondence among the distributions of palynofacies, predominant lithologies, and organic carbon percentages in section 398D (Figure 3). In the Barremian-middle Albian part of the section, the distribution of numerous sporomorphs and structured palynodebris in the exinitic facies corresponds with high rates of sedimentation of terrigenous mineral sediment and with higher percentages of organic carbon. This palynofacies is expressed best in the terrigenous turbidite sequence of Barremian-early Aptian age (unit II) and less so in the terrigenous shales of early-Albian age. On the other hand, the fewer sporomorphs and higher relative percentages of marine phytoplankton of the micrinitic facies correlate with smaller amounts of terrigenous sediment and lower organic carbon percentages. Deroo et al., (in press) showed the close correspondence between the sporomorph abundance curve and organic carbon curve in the interval dated Barremian-Albian; pyrolysis of the organic matter of this age indicates that it is primarily issued from terrigenous detrital material.

The xenomorphic facies shows little or no correspondence with predominant lithology or with organic carbon content. In the late Hauterivian interval, very few sporomorphs are associated with high organic carbon; in the Cenomanian they are associated with low carbon percentages. Also, in the older unit the predominant lithology is limestone, whereas in the Cenomanian it is black clay.

Sections 391C and 105. There are similarities in the sequences of palynofacies, major lithologies, and percentage organic carbon distributions between sections 391C and 105, which suggest a contemporaneity in the sequence of similar events (Figures 4 and 5). Both sections show an alternation of xenomorphic and tracheal facies in predominantly calcareous sediments of early Early Cretaceous age and a thick micrinitic facies in black shales of largely Albian age. The tracheal facies occurs in the first black laminites, of Valanginian age (Druggidium apicopaucicum Zone), in both sections, and also in cross-laminated terrigenous turbidites of Hauterivian/Barremian-early Albian age (Odontochitina operculata Zone). They are expressed to different degrees, however. The Valanginian palynofacies is expressed best in Unit II of section 105. Conversely, in section 391C the Hauterivian/Barremian-early Albian interval is expressed better than in section 105.

In section 391C there are two distinctive pulses, within units IV and VI, of Hauterivian/Barremian-Aptian and late Aptian/early Albian ages, respectively, which was not found in section 105. This may be explained in part by the difference in thicknesses of sections 391C and 105. Section 105 is considered a condensed section when compared with sections 391C and 398D. For about the same time interval, it is roughly one-half the thickness of section 391C, and much thinner than section 398D. Nevertheless, most of the dinoflagellate zones in section 105 are almost as thick or at least proportionately thinner than in section 391C. However, it is the much thinner Odontochitina operculata zone at site 105 which is responsible to a large extent for the difference in thickness between the two sections. It is within the Odontochitina operulata zone in the western North Atlantic that the major change in lithofacies occurs, e.g., between the older nannofossil limestones and the younger black shales. The thinner zone at site 105 may be the result of an erosional unconformity between the two major lithologies. For example, the "transitional calcareous claystones" described by Benson, Sheridan, et al., 1978 occurs within the stratigraphic interval of the Subtilisphaera perlucida Subzone of section 391C, which is characterized by the tracheal facies (unit VI). This lithostratigraphic interval is apparently absent in section 105 where, according to Lancelot et al., 1972, nannofossil limestones grade rather abruptly within a single core to black shales.

Another factor which must be considered in comparing the Barremian-Albian tracheal facies of the two sections is the difference in number of cores available for sampling. Only two cores, 105-18 and 105-17, were available for the description of this palynofacies in section 105, which does not provide the stratigraphic resolution desired for unit IV.

Except for the thin interval containing micrinitic palynodebris within the predominantly tracheal interval in section 391C, the micrinitic facies is distributed in the same manner in both sections. Palynostratigraphic units VII in section 391C and V in section 105 extend from the upper part of the Odontochitina operculata zone through the Deflandrea vestita zone, and are considered to be largely, if not entirely, of Albian age. In both palynostratigraphic units, dinoflagellates increase in amounts and percentages of palynomorphs toward the top. Both units are also closely correlated with black shale lithology.

The palynostratigraphic units containing the

xenomorphic facies are also time-correlative in the two sections. The xenomorphic facies of palynostratigraphic unit VI of section 105 was not found in section 391C because of the lack of sediments of Vraconian-Cenomanian age there, e.g., the lack of the Deflandrea echinoidea and Trithyrodinium suspectum zones in section 391C.

The organic carbon profiles of sections 391C and 105 are similar, but do not show the close correlation with the distribution in abundance of sporomorphs that is evident in section 398D. In section 105, there is a correlation between increased organic carbon percentages and the distribution of the tracheal facies. However, in section 391C although there are also higher percentages of carbon in the tracheal facies of units II and VI, there are lower percentages in unit IV. The xenomorphic facies does show the same lack of correlation found in section 398D, where organic carbon percentages may be low or high within this palynofacies in both sections 105 and 391C. As an example, the highest percentages of carbon in section 105 occur in the xenomorphic facies of Cenomanian age, and the lowest in the same palynofacies of Berriasian/early Valanginian (Biorbifera johnewingii zone) age. The micrinitic facies in sections 105, 391C, and 398D all show reduced organic carbon percentages.

There is also a contemporaneity evident between the western North Atlantic sections and section 398D in the eastern North Atlantic. Sporomorphs and structured palynodebris are more abundant in the Barremian-early Albian time interval of all three sections. Where stratigraphic resolution permits, as in sections 391C and 398D, two episodes of increased terrigenous organic detritus are also correlative in this interval between the sequence of palynostratigraphic units II and IV in section 398D and units IV and VI in section 391C. In both sequences, also, the units characterized by these particles are separated by a unit with abudant micrinitic palynodebris. There is also a general correlation between increased organic detritus and increased organic carbon, with the exception of unit IV in section 391C. In all three sections, there is a subsequent reduction in the organic carbon percentages in the micrinitic facies in Albian black shales. In all three sections, dinoflagellates become prominent towards the top of the Albian units containing the micrinitic facies. In sections 105 and 398D, there is a xenomorphic facies of Cenomanian black clays, with the highest organic carbon percentages recorded in the section.

## Sedimentary Origin of Palynofacies

### Review of the Literature.

The sedimentological interpretation of palynomorphs and palynodebris is based on published studies concerning their distribution in modern environments. Cross et al., (1966) presented data on the distribution of palynomorphs, cuticles, tracheids, and other organic detritus in bottom surface sediments in the Gulf of California. They showed that the distribution of organic matter is similar to patterns of terrigenous and biogenic sedimentation. Sporomorphs are most abundant in the silt-clay fraction at delta mouths, where the assemblages are also most diversified, and in some submarine channels through which they were carried into deeper offshore areas and accumulated in submarine fans. According to Cross et al. (1966), the pollen of pine is the most abundant sporomorph type in the Gulf. It remains numerically abundant in offshore areas despite the decrease, in specimens per gram of sediment, of total sporomorphs. Other arboreal pollen types have more restricted patterns of distribution; they are concentrated closer to sources of terrigenous influx and consequently increase the diversity of sporomorph assemblages closer to the shore.

Bisaccate pine pollen is well-suited for selective transportation. Its air sacs permit it to be more buoyant than other types of sporomorphs, and thereby remain suspended in the water column for longer periods of time. In the study of the palynology of the Great Bahama Bank, Traverse and Ginsburg (1966) showed that pine pollen is distributed according to sedimentation patterns, especially those at the site of deposition. Proximity to source vegetation is not a primary factor in controlling its sedimentation on the Bahama Bank.

In the Gulf of California, cuticles and tracheids are concentrated in deltas. They are most abundant towards the shore in silty clays and also in deeper water where, along with abundant pine pollen and abundant very small carbonized particles, they were carried down through submarine canyons.

Dinoflagellate cysts and a palynomorph described as an unknown entity by Cross et al., (1966, Plate 1, figures 16, 18-19), but which possesses the same gross morphology as the small acritarchs of this study, become more numerous offshore and are similar in general distribution to other planktonic microfossils.

Palynologists have long noticed the co-occurrence of dinoflagellates and sporomorphs in marine muds and shales. It is the dinoflagellate cyst that is fossilized, and the vast majority of marine species which produce cysts today are confined to continental margins in estuarine and neritic assemblages (cf. Wall et al., 1977). With the exception perhaps of a few species which apparently are confined to the North Atlantic Cretaceous, most dinoflagellates have been described from relatively shallow marine sediments on the continents. For example, Williams (1975) recorded a large number of the species common to the investigated sections from Cretaceous inner neritic shelf assemblages along the continental margin of Canada, as has Millioud (1969) from Lower Cretaceous type sections in southern Europe. The facies of the western North Atlantic sections

is paleobathymetrically deep (Benson, Sheridan et al., 1978; Hollister, Ewing, et al., 1972) and it is likely that at least the majority of cysts in the samples have been displaced from a shelf environment into deeper water.

Relatively little research has been undertaken concerning the sedimentology of modern dinoflagellate cysts, although an important contribution by Dale (1976) has recently become available. Based on extensive data concerning the distribution of this microflora in the water column of Norwegian fjords, it was shown that dinoflagellate cysts, including those with a gross morphology similar to that of small acritarchs, accumulate in the bottom sediments over a period of years and are displaced into deeper water where they concentrate in fine silt detritus. Thus, it is evident that although they represent different source environments and different source vegetation, once in the marine environment both dinoflagellate cysts and sporomorphs may disperse as sedimentary particles which sediment in a similar fashion.

The palynofacies of this study are considered to have formed largely as the consequence of the sedimentary processes discussed above. However, before interpretations can be made, it is important to consider the composition and distribution of palynomorph assemblages in Lower Cretaceous sequences on the continents, particularly those of non-marine origin. Large and diverse assemblages of sporomorphs are distributed throughout the known Lower Cretaceous of the Atlantic Coastal Plain of the United States. Brenner (1963) described the assemblages of the fluviodeltaic Potomac Group of Maryland and stated that throughout the interval he dated as Barremian-Albian, they are dominated by pteridophyte spores, especially those attributed to the fern family Schizaeaceae, and the gymnosperm pollen Classopollis torosus and bisaccates. They are numerous throughout the Potomac Group but decrease in percentage towards the top with the concomitant appearance of triaperturate angiosperm pollen. Brenner (1963) did not include observations on the occurrence of palynodebris in his study. However, based on samples of the Potomac Group provided in the past by G. J. Brenner (State University of New York, New Paltz) cuticles and tracheids are known to be common in the residues, some of which also contain larger fragments of amorphous carbonized material assigned to micrinitic palynodebris, as well as structured fragments resembling fusinized tracheids. Wolfe and Pakiser (1971) directed particular attention to the distribution of striate schizaeaceous spores in the Potomac Group stating that there are 75 species present which compares favorably with the diversity of schizaeceous foliage in the megafossil flora. According to Wolfe and Pakiser (1971) these spores range into the Raritan Formation of Cenomanian age but are less diverse. The reduced number of striate species in the Raritan Formation (Woodbridge Clay member) may be due to the fact that marine sediments comprise this unit.

Williams (1975) proposed a formal palynostratigraphic zonation from wells drilled on the Scotian Shelf and Grand Banks of the Canadian continental margin. During the Early Cretaceous, depositional environments ranged from continental (Missisauga Formation) to marine inner neritic. According to Jansa and Wade (1975) the Missisauga Formation is a diachronous deltaic sequence ranging in different wells from Neocomian to early Aptian. A slow regional transgression began in the Aptian and culminated in the Late Cretaceous. The marine transgression during the Cenomanian was extensive producing an outer neritic and possibly farther offshore environment in the area of study. Williams (1975) reported a diverse sporomorph flora from the Missisauga Formation, including striate schizaeaceous spores. Striate spores dominate the sporomorph flora of the formation. In zones dated Aptian-Cenomanian by Williams (1975) diverse dinoflagellate assemblages are evident in the palynoflora which, however, still include elements of pteridophyte spores, e.g., Trilobosporites, Appendicisporites.

Sporomorph assemblages in the Neocomian Weald delta of England are dominated by the larger pteridophyte spores, including the Schizaeaceae (Couper, 1958). Batten (1973) described seventeen assemblage types in the Wealden. In his study of the total organic content of his residues he used preservation, abundance of cuticles and wood (tracheids), and size and diversity of spores to delineate his assemblage types. The record of assemblage type shows a correspondence between a variety of the pteridophyte spores (Trilobosporites, Verrucosisporites, Pilosisporites, Cicatricosisporites), tetrads, and structured palynodebris. Batten (1973, plate 1, figures 1-9) illustrates excellent examples of the cuticles and tracheids which characterize the exinitic and tracheal facies of this study. Hughes and Moody-Stuart (1967) attempted to reconstruct the sedimentological parameters governing the distribution of palynomorphs in the Weald delta of England, for the purpose of correlation across palynofacies. Larger fern spores are correlated with larger mineral grain size; Classopollis and minor marine phytoplankton are correlated with smaller grain size. Hughes and Moody-Stuart hypothesized that the larger fern spores are sedimented first, in the "upstream" direction in the delta.

It is evident that the well-ornamented and generally larger pteridophyte spores are numerous and are important components, along with structured palynodebris, Classopollis and other elements, in fluviodeltaic and deltaic sediments throughout Early Cretaceous age on the continental margins bordering the North Atlantic. The general absence of these pteridophyte spores, and the abundance of structured palynodebris in only the tracheal facies in the western North Atlantic, can thus be interpreted in terms of sedimentary processes.

## Conclusions

The palynofacies distributed through the investigated sections are interpreted to have formed from marine processes depositing carbonaceous detritus of terrestrial and marine origin. Residues containing abundant and diverse palynomorphs (particularly sporomorphs, sporomorph tetrads, and megaspores), tracheids, and cuticles are palynologically poorly sorted and are considered to have been deposited directly as the result of the rapid influx of terrigenous sediments, within prodeltaic sediments. These residues form the exinitic facies in section 398D, which reflect the dispersed and fragmented materials of land plants to the almost total exclusion of marine representatives. They are compositionally very close to the residues occurring in Early Cretaceous fluviodeltaic sediments on the adjacent continents, and it is concluded that marine currents did very little to modify the composition of the carbonaceous detritus that was discharged into the oceans. Support for this interpretation is taken from the association of the exinitic facies in section 398D with terrigenous mineral sediment and high rates of sedimentation.

The association of the conifer pollen genera Pinuspollenites, Alisporites, and Classopollis, and marine phytoplankton, is taken as evidence of the sorting of the land-derived sporomorph species and displacement of the dinoflagellate flora by marine currents prior to deposition. Pinuspollenites and Alisporites closely resemble the pollen grains of modern pine and, in the possession of air bladders which made them buoyant, are considered to have been dispersed and sedimented in a like manner. Their association in higher percentages with dinoflagellates in the micrinitic, xenomorphic, and tracheal facies in the North Atlantic also compares favorably with the co-occurrence of dinoflagellates and higher percentages of pine pollen in offshore areas of the Gulf of California. Habib (in press) presented the argument that Classopollis was also selectively transported and concentrated in sediments away from areas of major terrigenous influx, based on its ubiquitous distribution in high percentages in the Lower Cretaceous, regardless of the number of palynomorphs per gram, and also on the basis of its morphology. Classopollis torosus is a small, spheroidal pollen species. The genus is known to have been produced by a group of Jurassic and Cretaceous conifers and is abundant in the Lower Cretaceous terrestrial sporomorph flora (Brenner, 1963) as well as in marine sediments. Its abundance in nonmarine facies may reflect the larger amount of vegetation from which it was dispersed or perhaps, similar to present-day anemophilous conifers like pine, it was produced in larger numbers by individual trees for the purpose of wind dispersal and was thus over-represented in the sporomorph flora accumulating on the Cretaceous land surface. Whichever was the significant factor, it is believed that on the basis of its smaller size and spheroidal shape, and also on its association with the bisaccate genera, once it entered the North Atlantic it was transported more easily and farther than most other pollen grains and spores.

The fluctuation in numerical abundance of Classopollis and bisaccate conifers is also considered an important sedimentary parameter. These sporomorphs are numerically most abundant, and are proportionately more abundant than phytoplankton, in samples containing the tracheal facies where they are associated with structured palynodebris. The sporomorph flora is sorted and is associated with diverse dinoflagellates, but its increased abundance in the sediments and its association with numerous cuticles and tracheids indicate increased terrigenous influx of carbonaceous materials relative to the xenomorphic and micrinitic facies. This palynofacies is considered to reflect the increase of deltaic sedimentation discharging sporomorphs and structured palynodebris onto a shelf environment, where the sporomorph flora was sorted and mixed with dinoflagellates and subsequently displaced into deeper water. It is compared with the data published by Cross et al., (1966) which showed abundant pine pollen and structured palynodebris in offshore environments.

With few exceptions, palynomorphs are fewest in the micrinitic facies, despite the highest percentages of phytoplankton which are associated with bisaccates and Classopollis. This palynofacies is considered to represent, together with those samples of the xenomorphic facies containing few palynomorphs most of which are phytoplankton, the deposition of palynomorphs and amorphous palynodebris by currents of the least competence. The small opaque, generally black, amorphous particles which define the micrinitic facies are considered to be the carbonized, comminuted fragments of land plants, probably fragmented fusinized woody tissues, which when once formed became relatively resistant in the various sedimentary environments compared with other plant materials. Palynodebris of this type occurs in carbonaceous sediments (including coals) of terrestrial origin of various ages ranging from Carboniferous to Holocene, where it is commonly associated with larger fragments some of which are identifiable as carbonized tracheal elements. The concentration towards the small-sized particles in micrinitic facies is considered to be the result of sorting in the marine environment. Cross et al., (1966) distinguished two size classes of tracheids, much of it carbonized, in the Gulf of California, and stated that the larger fragments (larger than 50 microns) carried far seaward, presumably along with the smaller (5-50 microns) particles.

The origin of the amorphous palynodebris which characterizes the xenomorphic facies is not known palynologically. It may be of plant or animal origin, or an admixture of both, and may be terrestrial and/or marine. It tends to be

associated with lithologies of pelagic marine origin. It is possible also that it is related to the maceration process, which included partial oxidation of carbonaceous matter. In general, the shredded variety was observed in samples containing the more numerous palynomorphs and the globular variety was observed in those containing the fewer, but this was not always the case.

## Summary

As revealed in sections 391C and 105, the xenomorphic facies was formed during the Berriasian-early Valanginian in bioturbated limestones deposited on a well-oxygenated seafloor. Well-preserved and diverse dinoflagellate cysts were displaced from shelf environments into deeper water along with a sorted terrigenous sporomorph flora of variable abundance. In the Valanginian there was an episode of increased terrigenous influx of carbonaceous detritus, including Classopollis-bisaccate pollen, tracheids, and cuticles which produced the tracheal facies. The Valanginian/Hauterivian of sections 391C and 105, and late Hauterivian of section 398D, record the recurrence of organic sedimentation in the xenomorphic facies, similar to that of the earlier interval. However, during the interval dated Barremian-early Albian in section 398D and Hauterivian/Barremian-early Albian in the western North Atlantic, there were episodes of pronounced terrigenous sedimentation of carbonaceous detritus. Comparison of sections 391C and 398D indicates two distinctive pulses of terrigenous organic sedimentation, during the Barremian-early Aptian and early Albian in both sections, which are penecontemporaneous across the North Atlantic. In section 398D it is expressed in the sequence of exinitic-micrinitic-exinitic facies (units II-IV) reflecting fluctuations of direct terrigenous sedimentation in a prodeltaic environment and in section 391C (and as a single episode in the stratigraphically condensed or otherwise incomplete 105 section) in the sequence tracheal-micrinitic-tracheal (units IV-VI) which is considered to represent coeval episodes of terrigenous influx of organic detritus which then were partially sorted and displaced from a shelf environment into deeper water where it contributed to cross-laminated turbiditic layers.

The correspondence in time between episodes of increased terrigenous organic detritus in sections 391C and 398D indicates that time periods of increased deltaic sedimentation may have been the same at both western and eastern margins of the North Atlantic.

During the Albian, terrigenous sedimentation was sharply reduced and provided fewer palynomorphs to the black shales preserved in the three investigated sections but contributed a large amount of terrigenous micrinitic palynodebris. The increase in percentage of dinoflagellates in section 398D and in amounts as well in sections 391C and 105 towards the close of the Albian reflect the decrease in terrigenous sedimentation. During the Vraconian-Cenomanian in section 105 and Cenomanian in 398D, few palynomorphs were delivered to the North Atlantic in the xenomorphic facies.

Organic carbon content is closely related to sporomorph abundance in the exinitic and micrinitic facies of Barremian-middle Albian age in section 398D and is considered to be terrigenous and phytogenic. In the micrinitic facies of late Albian, including Vraconian, age marine phytoplankton occur in high relative percentages among very few palynomorphs and low organic carbon percentages, which pyrolysis (Deroo et al., in press) indicates is of pelagic marine origin. Organic carbon percentages show little relation to the palynology of the xenomorphic facies. In the Cenomanian, palynomorphs are very few in this palynofacies, most of which are dinoflagellates. The xenomorphic facies of late Hauterivian age differs in that sporomorphs are abundant where organic carbon percentages are lower. The palynology would indicate an admixture of terrigenous and pelagic carbon because of the abundance of sporomorphs and diverse dinoflagellates.

The distribution of organic carbon at sites 105 and 391 is similar to that at site 398, except that there is not the close correspondence with sporomorph abundance that was found in the eastern North Atlantic. This may be due to the greater occurrence of the xenomorphic facies than in section 398D, which shows the same lack of correspondence with organic carbon content. Outside of the xenomorphic facies, however, the tracheal (except unit IV in section 391C) facies shows higher organic carbon and the micrinitic facies shows lower carbon content, which follows the organic carbon curve and is thus similar to that of section 398D, which suggests that the carbon of these facies is largely terrigenous and phytogenic. The carbon of the tracheal facies may not be as highly terrigenous as that of the exinitic facies because of the occurrence of phytoplankton which are virtually absent in the exinitic facies. Marine phytoplankton increase in numbers of specimens per gram towards the top of the micrinitic facies of Albian age in sections 391C and 105 which suggests, like that of 398D, that the carbon in this part of the section is pelogic marine. The xenomorphic facies of Cenomanian age in section 105 has the highest organic carbon percentage of the three sections. It contains very few palynomorphs, mostly dinoflagellates, and thus may be marine.

The organic carbon curve is generally the same for each of the sections in the intervals dated Barremian-Albain. It is highest in the Barremian-early Albian interval and lowers in the middle/late Albian in black shales. It is difficult to relate the darker color of these shales to reduced carbon content. The darker color of this fine-grained lithology may be the result of the occurrence of abundant black micrinitic palynodebris, rather than total carbon content alone.

Acknowledgments. Sheldon Nelson prepared the samples for study. The organic carbon data were taken from volumes 11, 44, and 47 (part 2) of the Initial Reports of the Deep Sea Drilling Project. This study was supported by a grant from the National Science Foundation, NSF-OCE76-14619.

## References

Batten, D.J., Use of palynologic assemblage types in Wealden correlation, Palaeontol., 16, p. 1-40, 1973.

Benson, W.E., R.E. Sheridan, et al., Initial Reports of the Deep Sea Drilling Project, 44, 1978.

Blechschmidt, G., Calcareous nannofossil biostratigraphy of the Cretaceous-Cenozoic at site 398, in: Ryan, W.B.F., J.C. Sibuet, et al., Initial Reports of the Deep Sea Drilling Project, 47, in press.

Brenner, G.J., The spores and pollen of the Potomac Group of Maryland, Maryland Dept., Mines, Water Resources, Bull. 27, 215 p., 1963.

Combaz, A., Les palynofacies, Rev. Micropaleontol., 7, p. 205-218, 1964.

Couper, R.A., British Mesozoic microspores and pollen grains, Palaeontograph., 103, B, p. 75-179, 1958.

Cross, A.T., G.G. Thompson, and J.B. Zaitzeff, Source and distribution of palynomorphs in bottom sediments southern part of Gulf of California, Marine Geol., 4, p. 467-524, 1966.

Dale, B., Cyst formation, sedimentation, and preservation: factors affecting dinoflagellate assemblages in Recent sediments from Trondheimsfjord, Norway, Rev. Palaeobot., Palynol., 22, p. 39-60, 1976.

Deroo, G., P.C. deGraciansky, D. Habib, and J.P. Herbin, L'origine de la matiere organique dans les sediments Cretaces du site 398 (Haut Fond de Vigo): correlations entre les donnes de la sedimentologie, de la geochimie organique, et de la palynologie, Bull. Geol. Soc. France, in press.

Habib, D., Comparison of Lower and Middle Cretaceous palynostratigraphic zonations in the western North Atlantic, in: Stratigraphic Micropaleontology of Atlantic Basins and Borderlands, ed. F.M. Swain, Elsevier, p. 341-367, 1977.

Habib, D., Palynostratigraphy of the Lower Cretaceous section at D.S.D.P. site 391, Blake-Bahama Basin, and its correlation in the North Atlantic, in: Benson, W.E., R.E. Sheridan, et al., Initial Reports of the Deep Sea Drilling Project, 44, 1978.

Habib, D., Sedimentology of palynomorphs and palynodebris in Cretaceous carbonaceous facies south of Vigo Seamount, in: Ryan, W.B.F., J.C. Sibuet et al., Initial Reports of the Deep Sea Drilling Project, 47, in press.

Hollister, C.D., J.I. Ewing, et al., Initial Reports of the Deep Sea Drilling Project, 11, 1972.

Hughes, N.F., and J.C. Moody-Stuart, Palynological facies and correlation in the English Wealden, Rev. Palaeobot. Palynol., 1, p. 259-268, 1967.

Jansa, L.F., and J.A. Wade, Geology of the continental margin off Nova Scotia and Newfoundland, Geol. Surv. Canada, paper 74-30, 2, p. 51-105, 1975.

Lancelot, Y., J.C. Hathaway, and C.D. Hollister, Lithology of sediments from the western North Atlantic: in: Hollister, C.D., J.I. Ewing, et al., Initial Reports of the Deep Sea Drilling Project, 11, p. 901-949, 1972.

Manum, S.B., Dinocysts in Tertiary Norwegian-Greenland Sea sediments (D.S.D.P. Leg 38), with observations on palynomorphs and palynodebris in relation to environment: in: Talwani, M., G. Udintsev, et al., Initial Reports of the Deep Sea Drilling Project, 38, p. 398-419, 1976.

Millioud, M.E., Dinoflagellates and acritarchs from some western European Lower Cretaceous type localities, Internat. Conf. Planktonic Microfossils, Geneva, 1967, Proc., p. 420-434, 1969.

Ryan, W.B.F., J.C. Sibuet, et al., Initial Reports of the Deep Sea Drilling Project, 47, in press.

Sigal, J., Chronostratigraphy and ecostratigraphy of Cretaceous formations at site 398, D.S.D.P. Leg 47B, in: Ryan, W.B.F., J.C. Sibuet, et al., Initial Reports of the Deep Sea Drilling Project, 47, in press.

Traverse, A., and R.N. Ginsburg, Palynology of the surface sediments of Great Bahama Bank, as related to water movement and sedimentation, Marine Geol., 4, p. 417-459, 1967.

Wall, D., B. Dale, G.P. Lohmann, and W.K. Smith, The environmental and climatic distribution of dinoflagellate cysts in modern marine sediments from regions in the North and South Atlantic Oceans and adjacent seas, Marine Micropaleontol., 2, p. 121-200, 1977.

Williams, G.L., Dinoflagellate and spore stratigraphy of the Mesozoic-Cenozoic, offshore eastern Canada, Geol. Surv. Canada, Paper 74-30, 2, p. 107-161, 1975.

Wolfe, J.A., and H.M. Pakiser, Stratigraphic interpretations of some Cretaceous microfossil floras of the Middle Atlantic States, U.S. Geol. Surv. Prof. Paper 750-B, p. B35-B47, 1971.